

## 1.01 Catenated Compounds – Group 13 (Al, Ga, In, Tl)

G Linti, Ruprecht-Karls-Universität Heidelberg, Heidelberg, Germany

© 2013 Elsevier Ltd. All rights reserved.

<b>1.01.1</b>	<b>Introduction</b>	1
<b>1.01.2</b>	<b>Chain and Ring Compounds with Direct E–E–Single Bonds</b>	2
1.01.2.1	Synthesis and Structures of Compounds with Solitary E <sub>2</sub> -Units	2
1.01.2.1.1	Trielhalides	2
1.01.2.1.2	E <sub>2</sub> R <sub>4</sub> compounds	3
1.01.2.1.3	Lewis acidity – higher coordination numbers	6
1.01.2.1.4	Heteroleptic compounds	7
1.01.2.2	Synthesis and Structure of Compounds with E <sub>3</sub> -Units	11
1.01.2.3	Synthesis and Structure of Compounds with Higher E <sub>n</sub> -Units	13
1.01.2.3.1	Subhalides	13
1.01.2.3.2	Nonhalide derivatives	14
1.01.2.4	Synthesis and Structure of Compounds with E–E' Bonds	19
<b>1.01.3</b>	<b>Polyhedral Cluster Compounds</b>	22
1.01.3.1	Tetrahedral E <sub>4</sub> R <sub>4</sub> Cluster Compounds and Derivatives	22
1.01.3.1.1	Synthesis and structures	22
1.01.3.1.2	Bonding	23
1.01.3.1.3	Reactivity	26
1.01.3.2	Higher [E <sub>n</sub> R <sub>n</sub> ] <sup>X–</sup> Cluster Compounds	26
1.01.3.3	Aromaticity of [E <sub>n</sub> R <sub>n</sub> ] <sup>X–</sup> Cluster Compounds	30
<b>1.01.4</b>	<b>Element-Rich Cluster Compounds</b>	32
1.01.4.1	Introduction	32
1.01.4.2	Aluminum Cluster Compounds	34
1.01.4.3	Gallium Cluster Compounds	36
1.01.4.3.1	Ga <sub>8</sub> , Ga <sub>9</sub> , and Ga <sub>10</sub> clusters	36
1.01.4.3.2	Ga <sub>11</sub> and Ga <sub>13</sub> clusters	40
1.01.4.3.3	Ga <sub>16</sub> , Ga <sub>18</sub> , and Ga <sub>19</sub> clusters	40
1.01.4.3.4	Ga <sub>22</sub> clusters	40
1.01.4.3.5	Ga <sub>23</sub> and higher clusters	42
1.01.4.4	Indium Cluster Compounds	44
<b>1.01.5</b>	<b>Conclusion</b>	44
<b>References</b>		45

### Abbreviations

dipp 2,6-<sup>i</sup>Pr<sub>2</sub>C<sub>6</sub>H<sub>3</sub>

do Donor

<sup>R</sup>nacnac [NRCR']<sub>2</sub>CH

Sep Skeletal electron pairs

tmp 2,2,6,6-Tetramethylpiperidino

trip 2,4,6-<sup>i</sup>Pr<sub>3</sub>C<sub>6</sub>H<sub>2</sub>

xyl 3,5-Me<sub>2</sub>C<sub>6</sub>H<sub>3</sub>

### 1.01.1 Introduction

This chapter describes chain, ring, and cluster compounds of the triel elements (E) aluminum, gallium, indium, and thallium. This means bonds between the metal atoms have to be joined and oxidation states lower than +III are adopted. The story of metal–metal bonded compounds in group 13 started about 20 years ago with the pioneering work on ditriellanes E<sub>2</sub>R<sub>4</sub> by Uhl et al.<sup>1,2</sup> In the following years, a variety of low oxidation state compounds of these elements were prepared and characterized, including chains, rings, and polyhedral

clusters. A series of triel-rich clusters with unprecedented and fascinating structures resembling sections of triel element structures show interesting properties. Very large clusters with up to 84 triel atoms were obtained.<sup>3</sup> For these clusters, Schnöckel created the nomenclature 'metalloid' clusters.<sup>4–7</sup> This rapidly developing and fruitful chapter in chemistry has been reviewed several times since then.<sup>3,7–18</sup> Most of these reports focus on aspects of one class of compounds and describe these aspects in detail. Here the development of oligotriels, from dinuclear to higher species, is described, with special focus on developments during the past decade.

The metal–metal interactions in electron precise oligomers  $E_mR_n$  ( $n > m$ ) are described as  $2c2e$  bonds. Electron-deficient species  $[E_mR_n]^x$  ( $n \leq m$ ,  $x = 0, -1, -2$ ) form clustered structures with multicenter bonds. For cluster compounds, electron counting rules, for example, the Wade–Williams–Rudolph–Mingos rules, can be applied.<sup>19–25</sup>

The  $2c2e$  bond between heavier triel atoms is a very soft one, meaning the bond length is largely influenced by substituents. For example a typical gallium–gallium single bond can adopt values between 235 and 256 pm in length. It has been demonstrated that changes in bond length have little influence on the bonding energy. The difference is only a few kilojoules per mole if the bond length changes by  $\pm 10$  pm.<sup>26,27</sup> Formation of multiple bonds between group 13 elements is a special and intensively discussed topic, which will be treated in detail in **Chapter 1.10** of this book.

Such oligotrirel compounds can be either molecular compounds or parts of solid-state structures. This chapter deals only with molecular compounds. For the interesting field of solid-state structures with Zintl-type ions of triels, refer to **Chapter 1.09**.

## 1.01.2 Chain and Ring Compounds with Direct E–E Single Bonds

Triple coordinated compounds of group 13 elements are generally strong Lewis acids because of the electron sextet. The same is valid if one or more of the substituents are triel elements. This allows for the design of multiple Lewis acidic compounds on the one hand and on the other, these compounds tend to get stabilized either by adduct formation or cage formation. To prevent the latter, that is, to form chains or rings with triel centers, it is necessary to fill the electron sextet of the triel atoms or prevent the formation of multicenter bonded cluster structures by appropriate substituents. Bearing this in mind, a number of electron-precise compounds could be examined, which will be discussed according to the number of triel atoms involved.

### 1.01.2.1 Synthesis and Structures of Compounds with Solitary $E_2$ -Units

Compounds with metal–metal bonds attract special interest, because while speaking of metals, delocalized bonding in the solid is the first thought that occurs. Isolation of compounds with direct metal–metal bond of d-metals in the 1950s initiated a fruitful chemistry in this area.<sup>28,29</sup>

In the gas phase,  $E_2$  molecules have been studied with weak E–E bonds ( $D_{298}$  in  $\text{kJ mol}^{-1}$ : E = Al  $133 \pm 5.8$ , Ga  $114.5 \pm 4.9$ , In  $78.1 \pm 5.7$ , Tl 59).<sup>30–38</sup> The binary compounds  $E_2H_4$ , as the most simple compounds, are only stable under matrix-isolation condition for E = Al, Ga, In, Tl.<sup>39–41</sup> The E–E bonded structure  $H_2E-EH_2$  was shown by quantum chemical calculations to be the minimum structure only for boron.<sup>42–48</sup> The heavier congeners show a minimum on the hypersurface corresponding to a dimer  $E(\mu_2-H_3)EH$ . This is also formulated as  $E^+ [EH_4]^-$ . That means, triel(II) compounds with E–E bonds tend to disproportionate into triel(I) and triel(III) compounds. For a successful preparative access to ditrirelanes(4)  $R_2E-ER_2$

the influence of the substituents R, its bulk and electronic properties are very important. For the control of E–E bond formation versus charge separation also, the influences of solvents are effective.<sup>43,49–51</sup>

One can conclude that electron-withdrawing groups R will increase partial positive charges on the triel centers and thus will weaken E–E bonds. In contrast, ligation of additional groups will enforce E–E bonds. Steric demanding substituents will favor E–E bonded systems against bridging ones of type  $E(\mu_2-R_3)ER$ . This is the case for donor adducts of triel dihalides  $X_2(\text{do})E-EX_2(\text{do})$  or bulky substituted ditrirelanes(4)  $R_2E-ER_2$ .

Data for those compounds indicate weak E–E bonds, which are estimated to be 69–258  $\text{kJ mol}^{-1}$  for the ditrieltetrahalides  $E_2X_4$ . The bond strength decreases from aluminum to thallium and is much lower than for boron compounds (389–454  $\text{kJ mol}^{-1}$ ).<sup>52</sup> Keeping this in mind, ditrirelanes are discussed.

#### 1.01.2.1.1 Trieldihalides

Compounds with direct E–E bonds of type  $R_nE_2$  ( $n = 2, 3, 4, 5, 6$ , E = Al, Ga, In, Tl) were synthesized by various methods. While for E = Ga and In, the element(II) halides  $X_4E_2 \cdot 2\text{do}$  (X = Cl, Br, I) (**Tables 1–3** give an overview of available compounds prepared during the past 20 years) are easily prepared from subhalides with appropriate donors, corresponding  $Al_2X_4 \cdot 2\text{do}$  compounds were only accessible via metastable aluminum(I) halide solutions, which are obtained from AlX vapors by condensation with solvents.<sup>12,75–77</sup> For thallium no such derivatives are known. A rare example is a  $Tl_2^{4+}$  as structural motif in a phase  $Tl_{0.8}Sn_{0.6}Mo_7O_{11}$ .<sup>78</sup>

$EX_2$  compounds are diamagnetic and were postulated to have  $X_2E-EX_2$  molecules with E–E single bonds.<sup>79</sup> Crystallographic and spectroscopic data proved ionic structures of type  $E^+ [EX_4]^-$  (E = Ga, In; X = Cl, Br, I).<sup>80–87</sup> For molecular boron, diborontetrahalides  $B_2X_4$  exist; for aluminum, no compounds of stoichiometry  $AlX_2$  are known.<sup>88</sup> The  $E[EX_4]$  salts with  $E^{+1}$  and  $E^{+III}$  ions comproportionate under the influence of donors.

Especially for gallium, a large variety of derivatives  $Ga_2X_4 \cdot 2\text{do}$  has been characterized with donors such as ethers, amines, phosphanes, halides, and others.

Common to all is a Ga–Ga bond of 239–247 pm, depending on the size of the donor (do) and the electronegativity of X. A special derivative is  $(Et_3NH^+)_2 [(HexPGa_2I_4)_2]^{2-}$ <sup>(67)</sup> where two  $Ga_2I_4$  units are linked by two phosphide groups forming a six-membered ring. For halides as donor groups, several anionic derivatives  $E_2X_6^{2-}$  have been obtained. Examples such as  $[Ga(\text{dmf})_6]_2[Ga_2Br_6]_2$ <sup>59</sup> and  $(Me_4N_2CH)_2(Ga_2I_6)$ <sup>89</sup> are summarized in **Table 4**.

**Table 1**  $X_4Al_2 \cdot 2\text{do}$  compounds

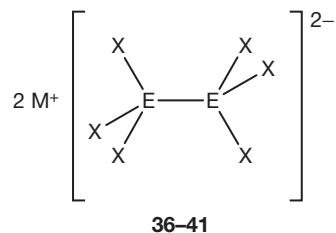
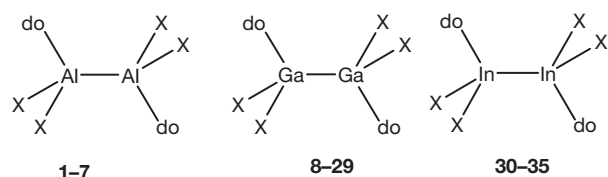
	X	do	$d_{Al-Al}$ (pm)	References
1	Cl	N(SiMe <sub>3</sub> )Me <sub>2</sub>	257.3	53
2	Br	N(SiMe <sub>3</sub> )Me <sub>2</sub>	256.4	53
3	Br	NEt <sub>3</sub>	257.1	54
4	Br	O(Me)Ph	252.7	55
5	I	Et <sub>2</sub> O	252	53
6	I	thf	252	56
7	I	PEt <sub>3</sub>	254.6	53

**Table 2**  $X_4Ga_2$ -2do compounds

	<i>X</i>	<i>do</i>	$d_{Ga-Ga}$ (pm)	References
<b>8a</b>	Cl	Dioxane	240.6	57
<b>B</b>	Cl	Dioxane (polymer)	238.3	58
<b>9a</b>	Cl	NEt <sub>3</sub>	244.7	59
<b>9b</b>	Cl	NMe <sub>3</sub>	242.1	60
<b>10</b>	Cl	OP(NMe <sub>2</sub> ) <sub>3</sub>	239.2	61
<b>11</b>	Cl	NC <sub>5</sub> H <sub>4</sub> (4-Me)	241.4	62
<b>12</b>	Cl	NC <sub>5</sub> H <sub>3</sub> (3,5-Me <sub>2</sub> )	240.0	63
<b>13</b>	Cl	PEt <sub>3</sub>	242.7	64
<b>14</b>	Br	Et <sub>3</sub> N	245.3	59
<b>15</b>	Br	thf	241.2	59
<b>16</b>	Br	NHEt <sub>2</sub>	243.5	59
<b>17</b>	Br	NC <sub>5</sub> H <sub>4</sub> (4- <sup>t</sup> Bu)	241.9	59
<b>18</b>	Br	PEt <sub>3</sub>	242.7	64
<b>19</b>	I	NH <sub>2</sub> ( <sup>c</sup> Hex)	242.9	65
<b>20</b>	I	NH <sub>2</sub> ( <sup>t</sup> Bu)	242.4	65
<b>21</b>	I	NH( <sup>c</sup> Hex) <sub>2</sub>	246.5	65
<b>22</b>	I	NEt <sub>3</sub>	249.8	66
<b>23</b>	I	( <sup>P</sup> Hex) <sup>2-</sup>	245.0	67
<b>24</b>	I	PH( <sup>c</sup> Hex) <sub>2</sub>	243.7	65
<b>25</b>	I	PH( <sup>t</sup> Bu) <sub>2</sub>	244.5	65
<b>26</b>	I	PEt <sub>3</sub>	243.6	68
<b>27</b>	I	PPH <sub>3</sub>	244.4	68
<b>28</b>	I	AsEt <sub>3</sub>	242.8	69
<b>29</b>	I	I, C[N(dipp)CH] <sub>2</sub> <sup>a</sup>	247.4	65

<sup>a</sup>cation:[HC(N(dipp)CH)<sub>2</sub>]<sup>+</sup>**Table 3**  $X_4In_2$ -2do compounds

	<i>X</i>	<i>do</i>	$d_{In-In}$ (pm)	References
<b>30</b>	Cl	thf	271.5	70
<b>31</b>	Br	C[N(Mes)CH] <sub>2</sub>	274.4	71
<b>32</b>	Br	tmeda	276.1	72
<b>33</b>	3Br, I	tmeda	277.5	73
<b>34</b>	I	<sup>P</sup> Pr <sub>3</sub>	274.5	74
<b>35</b>	I	tmeda	279.2	71



### 1.01.2.1.2 $E_2R_4$ compounds

#### 1.01.2.1.2.1 Synthetic pathways

Those  $E_2X_4(do)_2$  compounds are valuable starting materials for the synthesis of derivatives  $E_2R_4$  via substitution reactions. Uhl

**Table 4** Survey of compounds containing  $E_2X_6^{2-}$  units

	<i>E</i>	<i>X</i>	$M^+$	$d_{E-E}$ (pm)	References
<b>36</b>	Ga	Cl	[PPh <sub>3</sub> ] <sup>+</sup>	240.4, 240.7	90
<b>37</b>	Ga	Br	[PPh <sub>3</sub> ] <sup>+</sup>	241.0	90
<b>38</b>	Ga	Br	[Ga(dmf) <sub>6</sub> ] <sup>3+</sup>	242.0	59
<b>39</b>	Ga	I	[PPh <sub>3</sub> ] <sup>+</sup>	241.4	90
<b>40</b>	Ga	I	[(Me <sub>2</sub> N) <sub>2</sub> CH] <sup>+</sup>	242.3	89
<b>41</b>	In	Cl	[Ph <sub>4</sub> P] <sup>+</sup>	272.7	91

succeeded in 1989 in the synthesis of a series of  $E_2[(CH(SiMe_3)_2]_4$  compounds with  $E = Ga$  (45),  $In$  (55).<sup>1,2</sup> This method (eqn [1]) was also useful for other derivatives with various types of substituent  $R$  (Table 5).<sup>95</sup> Nevertheless, disproportionation of the triel compounds in oxidation state +II into element(III) compounds and compounds with triel atoms in oxidation states <+II are possible alternative reaction paths in these reactions. One example is the preparation of 51 from  $Ga_2Cl_4 \cdot 2dioxane$  and  $[LiN(SiMe_3)CH_2]CMe_2$ , where formation of elemental gallium and  $Li(thf)Ga[N(SiMe_3)CH_2]CMe_2]_2$  is observed as a side reaction.<sup>100</sup>

The corresponding Al compound  $Al_2[(CH(SiMe_3)_2]_4$  42 was prepared by reduction of the corresponding diorganoaluminumdihalide with potassium (eqn [2]).<sup>110</sup> In an earlier report <sup>t</sup>Bu<sub>2</sub>Al-Al<sup>t</sup>Bu<sub>2</sub> was obtained only in solution.<sup>111</sup>

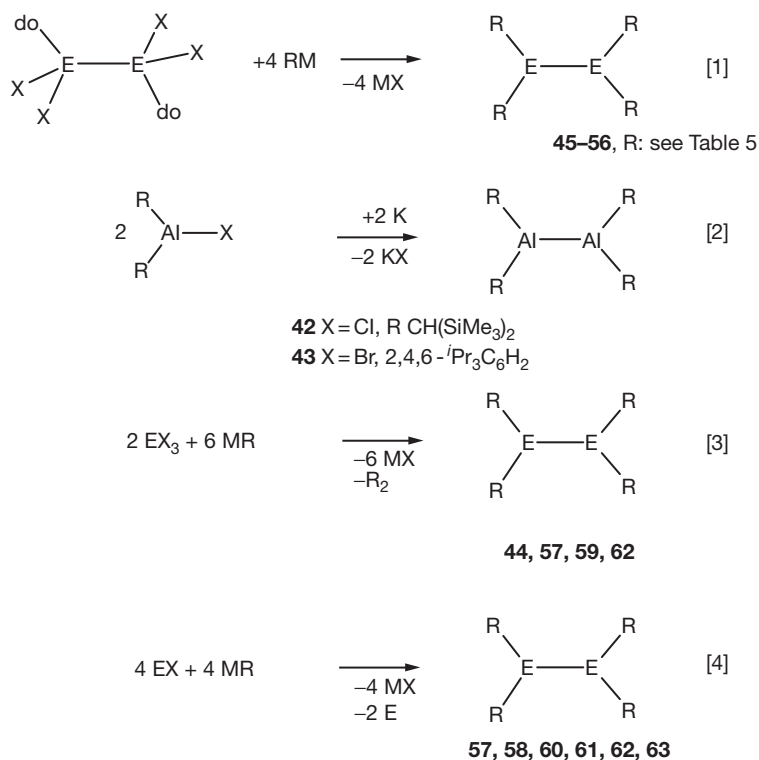
Alternative routes are the reactions of trihalides with reducing alkali metal silanides (eqn [3]) or redox disproportionation of EX ( $X = \text{halide}, N(SiMe_3)_2, Cp^*$ ) with RM reagents (eqn [4]). Through these routes, several ditrielanenes with various substituents were accessible (Table 5).

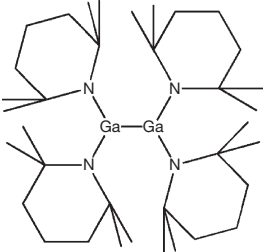
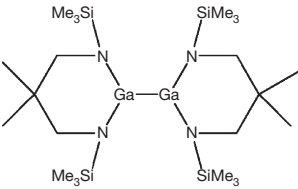
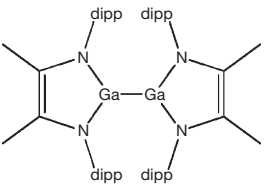
#### 1.01.2.1.2.2 Structural features

Most of these compounds exhibit monomeric  $E_2R_4$  molecules with planar three coordinate triel atoms. The  $ER_2$  units can be oriented coplanar or twisted, with torsion angles between 0° and 90°. The ideal staggered conformation is adopted for the silyl-substituted derivatives. The alkyl-substituted ones have nearly planar  $C_2E-EC_2$  arrangements. This was explained with hyperconjugative interactions between the empty p-orbital at the triel atoms and the filled  $\sigma$ -orbitals of the  $\alpha$ -C-Si bonds. Alternatively, or in addition, the ideal packing of the planar molecules in the crystal and subsequent ideal orientation of the R groups for the hyperconjugative interaction were used as explanation. In solution, no rotational barriers were detected by low temperature NMR experiments.<sup>1,92,112</sup> The tetraryl derivatives have conformations with torsion angles of approximately 45°.

The E-E bond seems to be the chromophore of ditrielanenes, the absorption maxima of which are influenced by the substituents. While the alkyl derivatives are yellow (Al) to orange (In), the silyl-substituted ones are described as dark-green to red. Bathochromic shifts in UV-Vis spectra are observed with increasing ordinal number and increasing torsion angles.

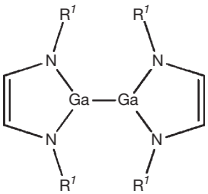
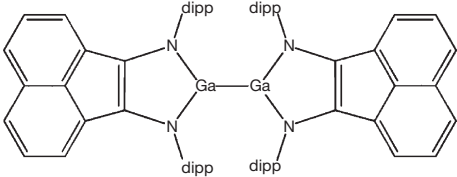
The largest number of these compounds was prepared with  $E = Ga$ . Here the Ga-Ga bond varies from 234 to 260 pm with the steric demand of the substituents. The longest bond was observed for the bulky silyl derivative  $[(Me_3Si)_3Si]_2Ga-Ga[Si(SiMe_3)_3]_2$  48. This dependence of the substituents is

**Table 5** Monomer ditrirelanes E<sub>2</sub>R<sub>4</sub> with three-coordinate triel atoms

		<i>d<sub>E-E</sub></i> (pm)	References
42	[(Me <sub>3</sub> Si) <sub>2</sub> CH] <sub>2</sub> Al–Al[CH(SiMe <sub>3</sub> ) <sub>2</sub> ] <sub>2</sub>	266.0	92
43	Trip <sub>2</sub> Al–AlTrip <sub>2</sub> <sup>a</sup>	264.7	93
44	( <sup>t</sup> Bu <sub>3</sub> Si) <sub>2</sub> Al–Al(Si <sup>t</sup> Bu <sub>3</sub> ) <sub>2</sub>	275.1	94 95
45	[(Me <sub>3</sub> Si) <sub>2</sub> CH] <sub>2</sub> Ga–Ga[CH(SiMe <sub>3</sub> ) <sub>2</sub> ] <sub>2</sub>	254.1	2
46	Trip <sub>2</sub> Ga–GaTrip <sub>2</sub>	251.5	96
48	[(Me <sub>3</sub> Si) <sub>3</sub> Si] <sub>2</sub> Ga–Ga[Si(SiMe <sub>3</sub> ) <sub>3</sub> ] <sub>2</sub>	259.9	97
49	( <sup>t</sup> Mes) <sub>2</sub> Ga–Ga( <sup>t</sup> Mes) <sub>2</sub> <sup>b</sup>	247.9	98 99
50		252.5	26
51		238.5	100
52		236.3	101

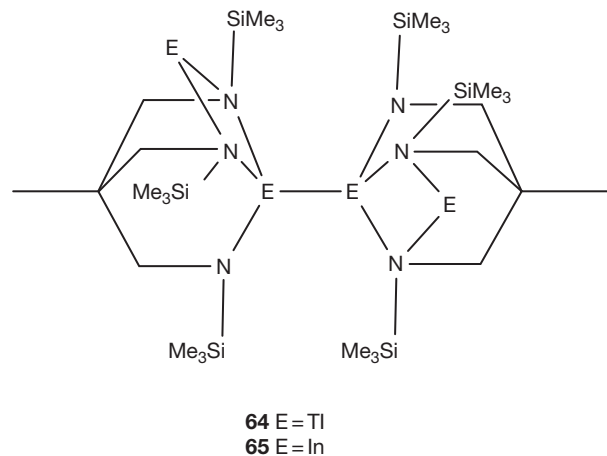
(Continued)

Table 5 (Continued)

		$d_{E-E}$ (pm)	References
53	 <p><math>R' = {}^t\text{Bu}, \text{dipp}, 2,6\text{-Et}_2\text{C}_6\text{H}_3</math></p>	233.1, 234.8, 235.9	102–104
54		236.0	102
55	$[(\text{Me}_3\text{Si})_2\text{CH}]_2\text{In-In}[\text{CH}(\text{SiMe}_3)_2]_2$	282.8	1
56	$\text{Trip}_2\text{In-InTrip}_2$	277.5	105
57	$({}^t\text{Bu}_3\text{Si})_2\text{In-In}(\text{Si}^t\text{Bu}_3)_2$	292.8	94 106
58	$({}^t\text{Bu}_2\text{PhSi})_2\text{In-In}(\text{Si}^t\text{Bu}_2\text{Ph})_2$	293.8	94
59	$[(\text{Me}_3\text{Si})_3\text{Si}]_2\text{In-In}[\text{Si}(\text{SiMe}_3)_3]_2$	286.8	107
60	$({}^f\text{Mes})_2\text{In-In}({}^f\text{Mes})_2$ <sup>b</sup>	274.4	98
61	$[(\text{Me}_3\text{Si})_3\text{Si}]_2\text{Tl-Tl}[\text{Si}(\text{SiMe}_3)_3]_2$	291.5	108
62	$({}^t\text{Bu}_3\text{Si})_2\text{Tl-Tl}(\text{Si}^t\text{Bu}_3)_2$	288.1	94
63	$({}^t\text{Bu}_2\text{PhSi})_2\text{Tl-Tl}(\text{Si}^t\text{Bu}_2\text{Ph})_2$	296.2	94,106,109

<sup>a</sup>2,4,6-<sup>c</sup>Pr<sub>2</sub>C<sub>6</sub>H<sub>2</sub>, <sup>b</sup>FMes = 2,4,6-(CF<sub>3</sub>)<sub>3</sub>C<sub>6</sub>H<sub>2</sub>

demonstrated with tetra(amino)digallanes. In  $\text{tmp}_4\text{Ga}_2$  **50** the molecule parts are twisted by 31° and the Ga–Ga bond length is 252.5(1) pm. The less steric demanding diamine residue  $\text{Me}_2\text{C}[\text{CH}_2\text{N}(\text{SiMe}_3)]_2$  leads to an orthogonal orientation of the GaN<sub>2</sub> planes in **51** and a short Ga–Ga bond of 238.5(1) pm. With diazabutadienediide substituents  $[\text{CHN}(\text{R})]_2$  (R = <sup>t</sup>Bu, 2,6-<sup>i</sup>Pr<sub>2</sub>C<sub>6</sub>H<sub>3</sub>, 2,6-Et<sub>3</sub>C<sub>6</sub>H<sub>3</sub>) similar short Ga–Ga bonds are observed in **52–54**. Dialanes have longer E–E bonds than digallanes, because of the smaller covalent radius of gallium.



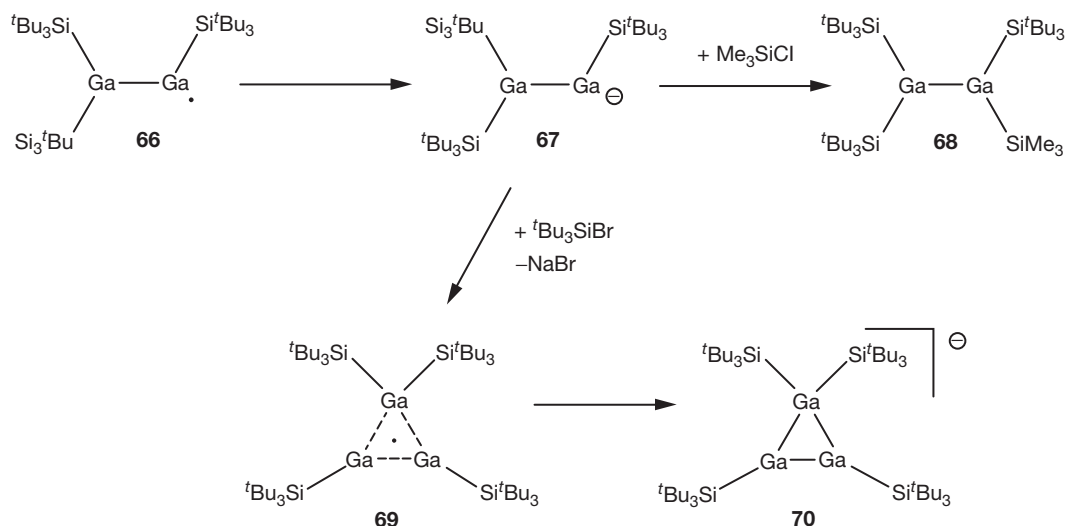
#### 1.01.2.1.2.3 Thallium–thallium interactions

For thallium  $[(\text{Me}_3\text{Si})_3\text{Si}]_2\text{Tl-Tl}[\text{Si}(\text{SiMe}_3)_3]_2$  **61**, prepared by the reaction of  $\text{RbSi}(\text{SiMe}_3)_3$  and  $\text{TlN}(\text{SiMe}_3)_2$ , is a rare

example with a thallium–thallium bond.<sup>108</sup> Thallium–thallium interactions are also present in a thalliumtripod complex **64**.<sup>113</sup> Here, additional thallium(I) cations coordinate to the tripod ligand. The thallium–thallium bond ( $d_{\text{Tl-Tl}} = 273.4$  pm) is even shorter than in the indium analog **65**.<sup>113</sup> A series of thallium(I) complexes with tripod ligands<sup>113–117</sup> and diamido ligands<sup>118,119</sup> also show Tl–Tl contacts.<sup>120,121</sup> Such interactions between closed shell s<sup>2</sup>-thallium(I) cations are also observed in other classes of compounds and are usually weak (370–>400 pm).<sup>120,122–126</sup>  $\text{Tl}_2[\text{RN}]_2\text{BPh}$  (R = <sup>i</sup>Pr, <sup>t</sup>Bu) aggregates to chains, where dithallium units interact with a thallium ion of the next unit, leading to infinite chains of edge-sharing triangles ( $d_{\text{Tl-Tl}} = 295.0$  and 300.4 pm).<sup>127</sup>

#### 1.01.2.1.2.4 Bulky silanide derivatives

Using the bulky silanide <sup>t</sup>Bu<sub>3</sub>SiNa, the corresponding tetrasilylditrialane, indane, and thallane are accessible. For aluminum and gallium the trihalides are reduced during the reaction (eqn [3]) and the indium and thallium derivatives are accessible via the monohalides, respectively (eqn [4]). Only for gallium, the smallest atoms in this row Al–Tl, the tetrasilyldigallane  $({}^t\text{Bu}_3\text{Si})_4\text{Ga}_2$  **47** was not stable under the reaction conditions, but lost one equivalent of <sup>t</sup>Bu<sub>3</sub>Si to afford the radical  $({}^t\text{Bu}_3\text{Si})_3\text{Ga}_2$  **66** ( $d_{\text{Ga-Ga}} = 242.3$  pm).<sup>128</sup> Reduction of this radical afforded  $[({}^t\text{Bu}_3\text{Si})_3\text{Ga}_2]^- (\text{Na}(\text{thf})_3)^+$  **67** ( $d_{\text{Ga-Ga}} = 237.9$  pm),<sup>128</sup> which can be used for nucleophilic substitution reactions, that is, against trimethylchlorosilane to **68**, or can be oxidized with <sup>t</sup>Bu<sub>3</sub>SiBr to a cyclotrigallane **69**, which then can be reduced to **70** (Scheme 1). Compound **44** decomposes on



**Scheme 1** Reactivity of supersilyl-substituted oligogallanes.

heating to 373 K within 10 h via the dialanylradical  $(\text{tBu}_3\text{Si})_3\text{Al}_2$ , an analog to **66**, to  $(\text{tBu}_3\text{Si})_4\text{Al}_3$ , which itself is an analog to **69** (see **Chapter 1.13**). The gallium ring compound was not formed on heating of  $(\text{tBu}_3\text{Si})_3\text{Ga}_2$ . The three-membered ring compounds of aluminum and gallium transform to give cluster compounds  $(\text{tBu}_3\text{Si})_4\text{E}_4$  ( $\text{E}=\text{Al}, \text{Ga}$ ) and others on heating. Similarly,  $(\text{tBu}_3\text{Si})_4\text{In}_2$  decomposes to a higher indium cluster (vide infra), which might also be the case for the thallium homolog. But here only an undefined black precipitate has been obtained so far.

#### 1.01.2.1.2.5 Cycloaddition products of ditrielenes

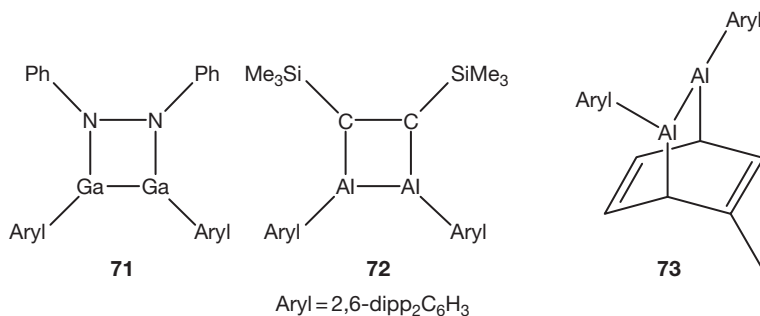
A special derivative is the cycloaddition product  $\text{ArylGa}(\text{NC}_6\text{H}_5)_2\text{GaAryl}$  **71** ( $\text{Aryl}=2,6\text{-dipp}_2\text{C}_6\text{H}_3$ ) of a corresponding digallene with a diazene. Compound **71** contains a  $\text{Ga}_2\text{N}_2$ -ring with a  $\text{Ga}_2$ -unit.<sup>129</sup> The corresponding  $\text{Aryl}_2\text{Al}_2$ -unit is part of an  $\text{Al}_2\text{C}_2$ -ring of  $\text{ArylAl}[\text{C}(\text{SiMe}_3)]_2\text{AlAryl}$  **72**<sup>130</sup> and is present in  $(\text{ArylAl})_2(\text{C}_6\text{H}_5\text{Me})$  **73**, the cycloaddition product of toluene and  $\text{Aryl}_2\text{Al}_2$ .<sup>131</sup> The latter is only one representative of a class of ditrielenes REER ( $\text{E}=\text{Al}$ ,<sup>132</sup>  $\text{Ga}$ ,<sup>133,134</sup>  $\text{In}$ ,<sup>135,136</sup>  $\text{Tl}$ <sup>137-139</sup>), which have been prepared in the last few years. They can be potentially looked upon as doubly bonded systems. Nevertheless, their long EE bonds indicate otherwise. On reduction, dianionic species  $[\text{REER}]^{2-}$  are obtained. The bonding situation of these compounds was discussed controversially. A triple bond as well as a single bond is an extreme description of

these compounds.<sup>134,140-142</sup> This will be discussed in detail in **Chapter 1.10**. One-electron reduction of ditrielenes **42**, **43**, **44**, and **46** gave the radical ions  $[\text{R}_4\text{E}_2]^-$  with a bond order of 1.5, showing that the additional electron fills the empty p-orbitals of the  $\text{E}_2$ -unit.<sup>93,96,143-147</sup>

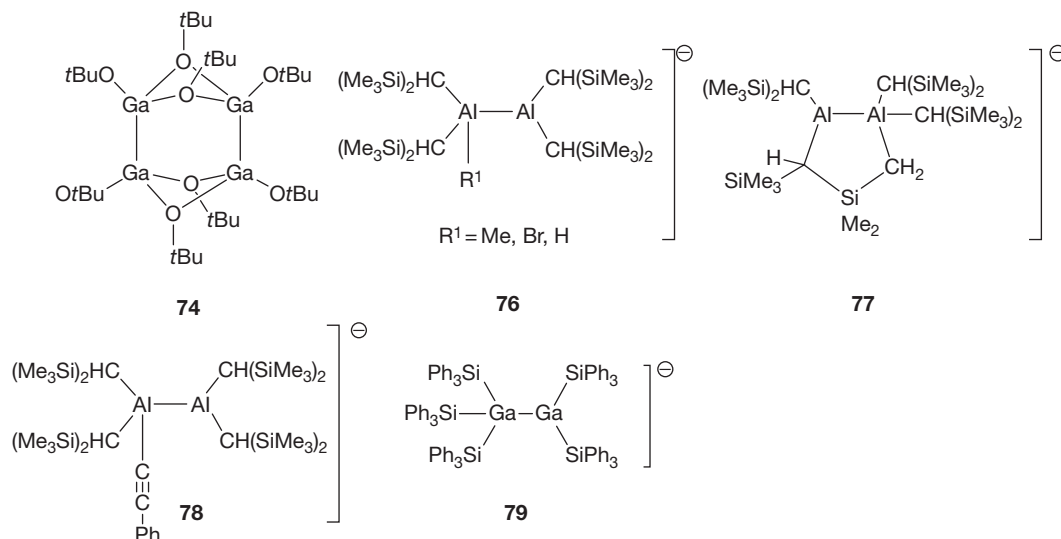
#### 1.01.2.1.3 Lewis acidity – higher coordination numbers

Chalcogenide substituents were rarely used in this kind of chemistry. The *tert*-butoxy-substituted digallane **74** forms a dimer with two parallel Ga–Ga bonds, which are linked via *tert*-butoxy bridges.<sup>100,148</sup> The isostructural aluminum alkoxide was prepared from  $\text{AlBr}$  solutions. The formation of these dimers shows that the triel atoms in ditrielenes(4) are still Lewis acidic.<sup>149</sup>

$\text{Al}_2(\text{P}^t\text{Bu}_2)_4$  **75**<sup>149</sup> is also formally an  $\text{Al}_2\text{R}_4$  derivate. It is obtained as two isomers **75a** and **75b**, depending on reaction conditions (**Scheme 2**). Compound **75a** is prepared by reaction of  $\text{AlX}$  solutions in toluene/ $\text{Et}_2\text{O}$  with  $\text{LiP}^t\text{Bu}_2$ . This  $\text{Al}_2\text{P}_2$  ring compound is a diradical without an Al–Al bond [ $d_{\text{Al}-\text{Al}}=350.8$  pm] (see **Chapters 1.13** and **1.14**). From solutions that contain no or only a little amount of donor solvents, **75b** with a Al–Al-bond [ $d_{\text{Al}-\text{Al}}=258.7$  pm] crystallizes. The difference has been explained by disproportionation of the  $\text{AlX}$  solutions, which proceed via  $\text{Al}_2\text{X}_4 \cdot 2\text{do}$  in the latter or via  $\text{Al}_5\text{Br}_5 \cdot 4\text{do}$  in the former case (see **Section 1.01.2.3**). Dimerization of **75a** would probably result in a structure analog to **74**.



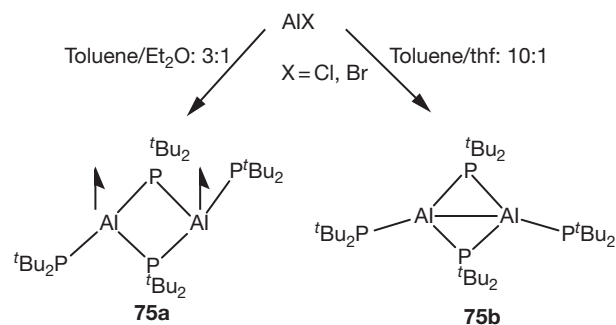




The Lewis acidic character of ditriellane(4) compounds can be used to prepare ditriellanes with five and six substituents, so-called ditriellanes(5) or ditriellanes(6). Thus,  $[(\text{Me}_3\text{Si})_2\text{CH}]_2\text{Al}-\text{Al}[\text{CH}(\text{SiMe}_3)_2]_2$  **42** reacts with  $\text{LiR}^1$  ( $\text{R}^1 = \text{Me}, \text{Br}$ ) to form  $[\text{R}^1[(\text{Me}_3\text{Si})_2\text{CH}]_2\text{Al}-\text{Al}[\text{CH}(\text{SiMe}_3)_2]_2]^- [\text{Li}(\text{tmeda})_2]^+$  **76**.<sup>150,151</sup>  $^t\text{BuLi}$  and  $\text{EtLi}$  react under  $\beta$ -H-elimination to give the hydrides ( $\text{R}^1 = \text{H}$ ).  $\text{LiCH}(\text{SiMe}_3)_2$  deprotonates to give a ring compound **77**.<sup>152</sup>

$[(\text{Me}_3\text{Si})_2\text{CH}]_2\text{Ga}-\text{Ga}[\text{CH}(\text{SiMe}_3)_2]_2$  reacts with  $\text{LiCCPh}$  under formation of an adduct **78**, for example.<sup>153</sup> A homoleptic  $\text{Ga}_2\text{R}_5$  compound is the anion  $[\text{Ga}_2(\text{SiPh}_3)_5]^-$  **79** ( $d_{\text{Ga}-\text{Ga}} = 254.6 \text{ pm}$ )<sup>154</sup> with three and a tetracoordinated gallium atom. Interestingly, the Ga–Si bonds of the three coordinate gallium atoms are longer than those of the tetracoordinate, one. This was explained by hyperconjugative effects. Higher coordination numbers at the gallium atoms are achieved by multipodal nitrogen ligands (**80**, **81**),<sup>155,156</sup> with a carboranate dianion (**82**) ( $d_{\text{Ga}-\text{Ga}} = 234.0 \text{ pm}$ )<sup>99</sup> as a substituent or in phthalocyanate complexes of  $\text{Ga}_2$  units.<sup>157–159</sup> A  $\text{TiCp}^*\text{N}$ -cage (**83**) ( $d_{\text{Ga}-\text{Ga}} = 239.7 \text{ pm}$ )<sup>160</sup> and P–S-ligands (**84**) ( $d_{\text{Ga}-\text{Ga}} = 238.3 \text{ pm}$ )<sup>161</sup> have been used for stabilization of  $\text{Ga}_2$ -units also.

The dialane(6)  $[\text{tBu}_3\text{Al}-\text{Al}^t\text{Bu}_3]^{2-}$  was obtained by reduction of  $^t\text{Bu}_3\text{Al}$  with potassium.<sup>162</sup> Even more easy is the adduct formation with diindanes, which is due to the larger radius of indium atoms compared to the lighter homologs.



**Scheme 2** Aluminum–aluminum bond formation from AIX solutions.

#### 1.01.2.1.4 Heteroleptic compounds

The gallium and indium compounds of type  $(\text{REX})_4$  **85a–e** (**Table 6**) adopt a  $D_{2d}$ -symmetric structure, where two  $\text{E}_2$ -units are linked via four halide bridges. The cage formed resembles the Realgar-structure ( $\text{As}_4\text{S}_4$ ). With the smaller  $(\text{Me}_3\text{Si})_2\text{CH}$ -substituent, a trimeric fluoride derivative **86a** and the hydroxide **86b** were obtained by treatment of digallane **45** with  $\text{HF}$  or  $\text{H}_2\text{O}$ , respectively. In these compounds three Ga–Ga bonds are in parallel arrangement.<sup>166</sup>

With more bulky substituents, monomeric derivatives  $\text{R}_2\text{E}_2\text{X}_2$  **87a–f** (**Table 7**) with three coordinate triel atoms were synthesized.

With bidentate substituents, a series of heteroleptic ditriellanes **88–93**<sup>170–178</sup> with tetracoordinate gallium atoms could also be obtained.

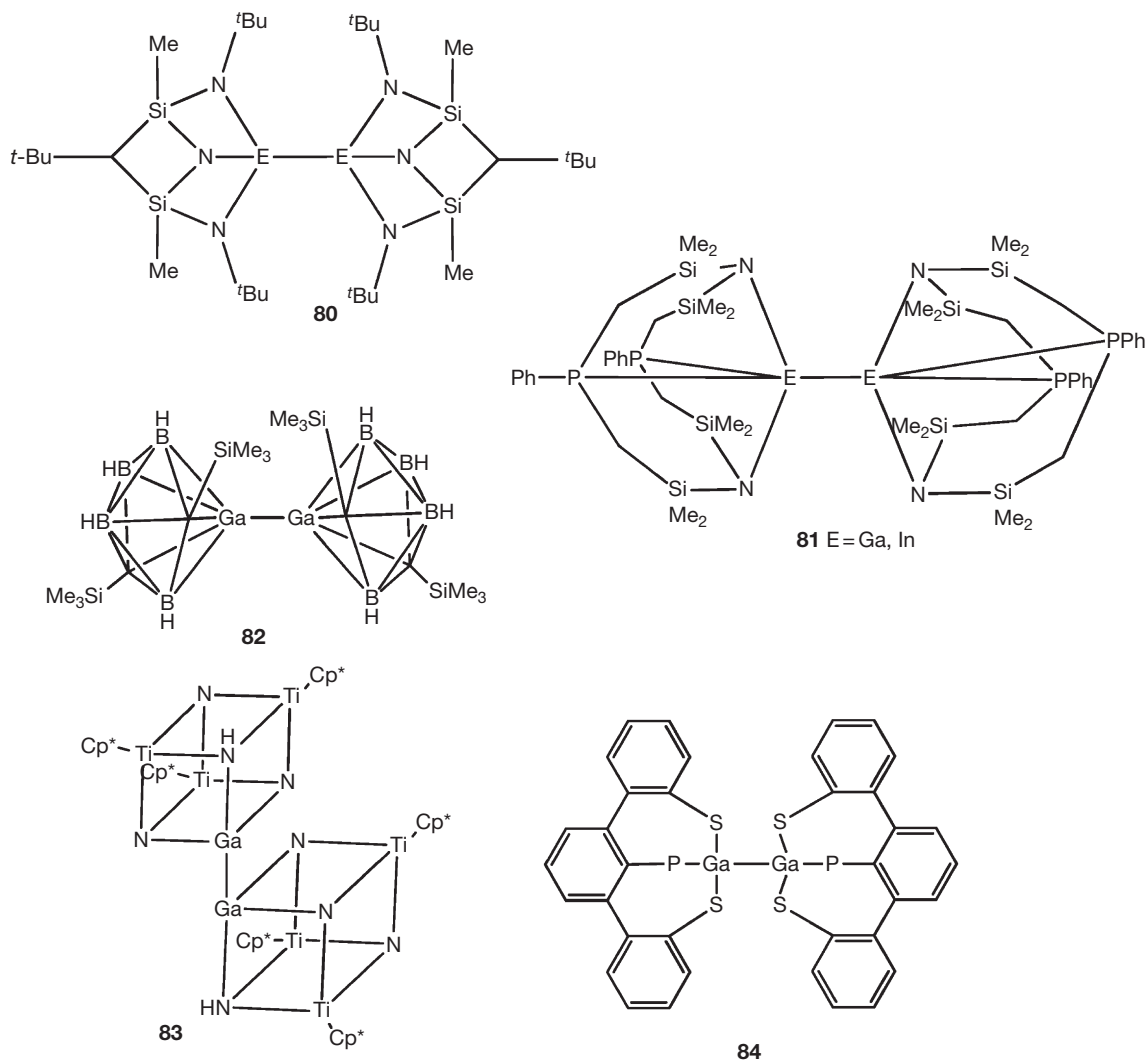
Biradical ditriellanes **94a–c** are products of reactions of 'Gal' or  $\text{InCl}$  with diazabutadienes (see **Chapter 1.13**),<sup>179–181</sup> while **94d** was isolated from an obscure reaction.<sup>180</sup>

**Table 6**  $D_{2d}$  symmetric  $(\text{REX})_4$  compounds

<b>85</b>	<i>E</i>	<i>R</i>	<i>X</i>	References
<b>a</b>	Ga	$\text{Si}(\text{SiMe}_3)_3$	Cl	97
<b>b</b>	Ga	$\text{Si}(\text{SiMe}_3)_3$	Br	163
<b>c</b>	Ga	$\text{Si}^t\text{Bu}_3$	Cl	164
<b>d</b>	In	$\text{C}(\text{SiMe}_3)_3$	Cl	165
<b>e</b>	In	$\text{C}(\text{SiMe}_3)_3$	Br	165

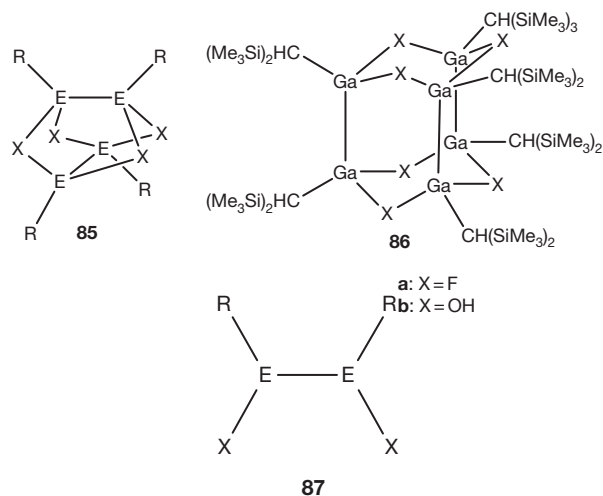
**Table 7** Monomeric  $\text{R}_2\text{E}_2\text{X}_2$  compounds

<b>87</b>	<i>E</i>	<i>R</i>	<i>X</i>	References
<b>a</b>	Al	Dipp	I	131
<b>b</b>	Ga	$\text{C}(\text{SiMe}_3)_3$	Br	167
<b>c</b>	Ga	$\text{C}(\text{SiMe}_3)_3$	I	168
<b>d</b>	Ga	2,4,6- $^t\text{Bu}_3\text{C}_6\text{H}_2$	Cl	169
<b>e</b>	Ga	2,6-dipp $_2\text{C}_6\text{H}_3$	I	133
<b>f</b>	Ga	2,6-tripp $_2\text{C}_6\text{H}_3$	I	134

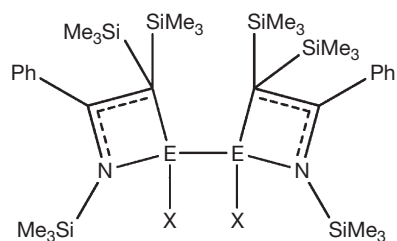


These types of functional digallanes  $[R_2E_2X_2]_n$  ( $n = 1, 2, 3$ ) normally do not undergo simple substitution reactions, which might offer a broad potential to the synthesis of heterocyclic compounds with Ga–Ga-units. Mostly, redox disproportionation or reduction by the nucleophile was observed. For example, **85a** reacts with Collman's reagent to a gallium-iron cluster **95**. Here,  $GaSi(SiMe_3)_3$  groups substitute for bridging CO-ligands in  $Fe_2(CO)_9$  (eqn [5]).<sup>182</sup> Similarly, other ER groups are versatile ligands (for reviews see, e.g., Baker and Jones,<sup>11</sup> Linti and Schnöckel,<sup>12</sup> Fischer and Weiß,<sup>183</sup> Gemel et al.,<sup>184</sup> Vidovic and Aldridge,<sup>185</sup> Whitmire<sup>186</sup>).

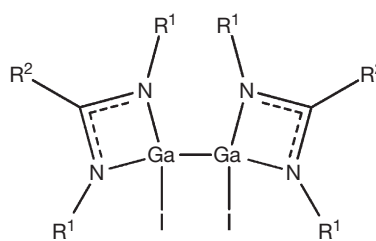
On the other hand, by reaction of  $Ga_2[CH(SiMe_3)_2]_4$  **45** with Brønsted acids of various types, a large variety of heteroleptic digallanes are accessible.<sup>187</sup> The large number of compounds available cannot be discussed here fully. The principle is shown in the reaction of **46** with a carboxylic acid to form **96** (eqn [6]). Here two alkyl ligands are protonated off and the carboxylate groups are bridging the intact  $Ga_2$ -unit. For the homologous aluminum and indium compounds, the protolysis reactions proceed in a different way, to produce **97** and **98**, where the E–E bond is cleaved.<sup>188</sup> Corresponding



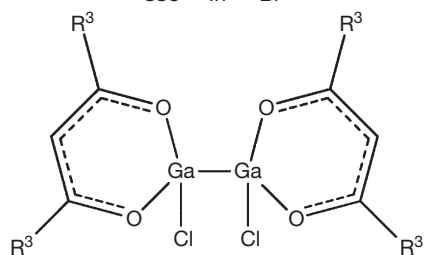




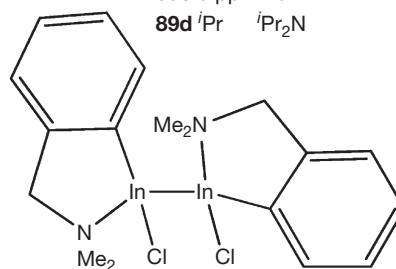
**88a** Al Cl  
**88b** Ga Cl  
**88c** In Br



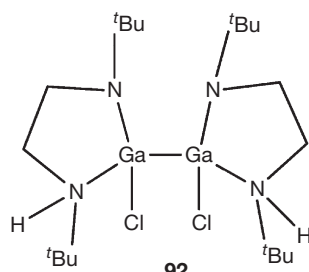
**89a** dipp H  
**89b** dipp <sup>t</sup>Bu  
**89c** dipp Me  
**89d** <sup>i</sup>Pr <sup>i</sup>Pr<sub>2</sub>N



**90a** Me  
**90b** <sup>t</sup>Bu

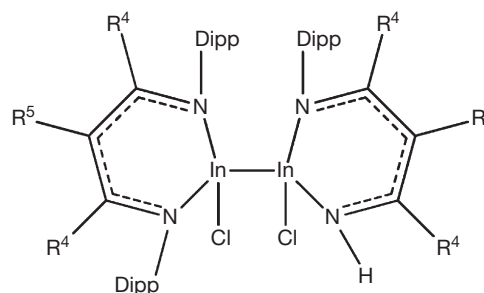


**91**

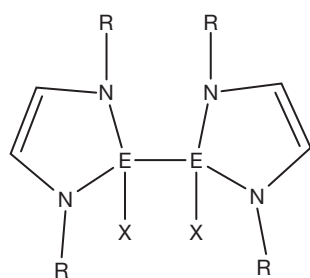


**92**

Dipp = 2,6-<sup>i</sup>Pr<sub>2</sub>C<sub>6</sub>H<sub>3</sub>



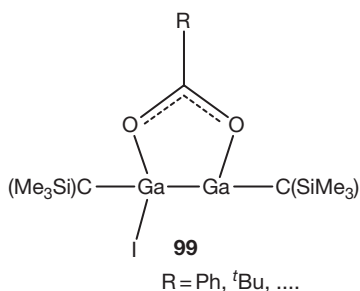
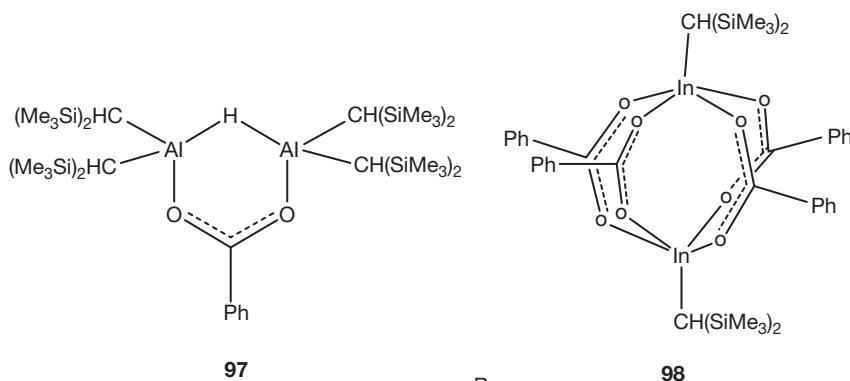
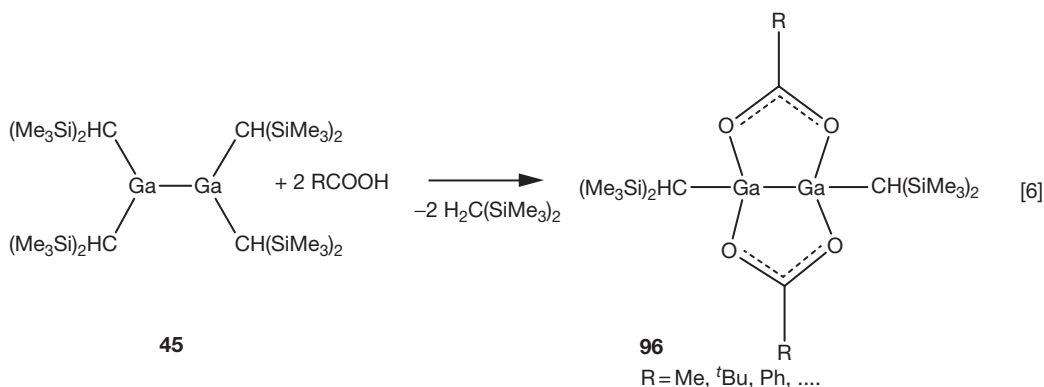
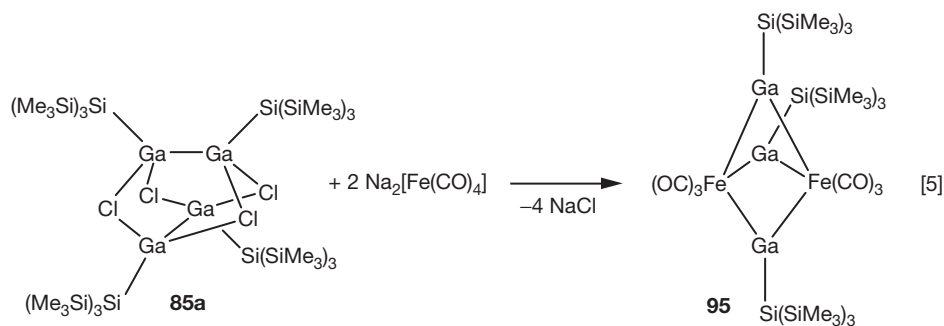
**93a** H Ph  
**93b** Me H



**94a** Ga <sup>t</sup>Bu I  
**94b** Ga dipp I  
**94c** In dipp Cl  
**94d** Ga dipp Br

indium(II) carboxylates were prepared from **85d** by reaction with silver or lithium carboxylates.<sup>189,190</sup> Reaction of [(Me<sub>3</sub>Si)<sub>3</sub>CGa]<sub>2</sub> **87c** with lithiumcarboxylates gave unsymmetrical substituted derivatives **99**.<sup>191</sup>

The stability of the Ga<sub>2</sub>-unit was used to arrange up to six Ga<sub>2</sub>-bonds in supramolecular aggregates using dicarboxylic acids. Flexible spacers allow dimeric species **100**.<sup>192</sup> 1,4-Butane-, 1,6-hexane-, 1,6-cyclohexane-, and 1,4-dimethylbenzenedicarboxylic acid have been used as flexible spacers. Rigid spacers such as ferrocenedicarboxylic acid, naphthalenedicarboxylic acid, or muconic acid allow higher nuclear derivatives **101a**,<sup>193</sup> **101b**,<sup>194</sup> and **101c**.<sup>195</sup> Here, carboxylates can either bridge a Ga<sub>2</sub>-unit (e.g., **101**) or link two Ga<sub>2</sub>-bonds (e.g., **102**). With benzotriazol-5-carboxylic acid six Ga<sub>2</sub>[CH(SiMe<sub>3</sub>)<sub>2</sub>] units get linked to form the cage **103**.<sup>196</sup> Hereby cavities of up to 1.5 nm diameter are formed, which can contain solvent molecules. Squaric acid reacts similarly to form a tetramer aggregate **104**,<sup>195</sup> while tropolone reacts with **45** to the monomeric digallane **105**.<sup>197</sup>

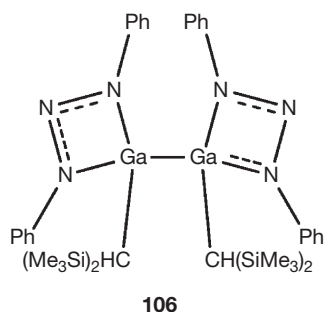
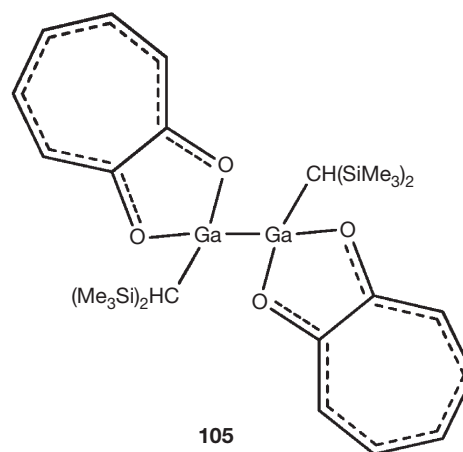
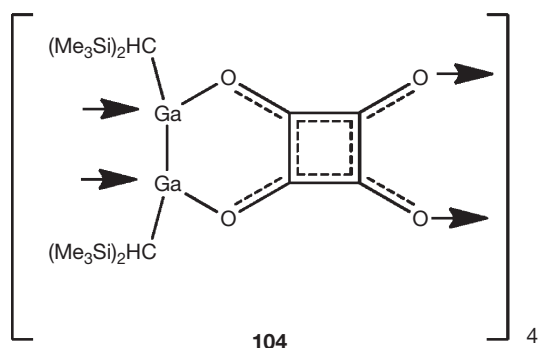
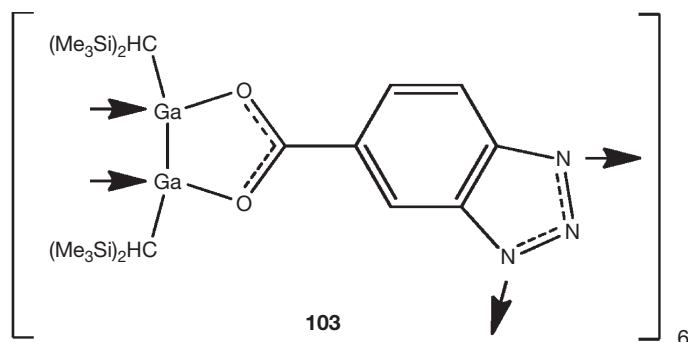


Those heteroleptic digallanes are themselves valid starting materials. Thus, reaction of  $[(\text{Me}_3\text{Si})_2\text{CH}]_2\text{Ga}_2(\text{O}_2\text{CMe})_2$  **96** with lithiumdiphenyltriazenide afforded the triazenido-substituted digallane **106**.<sup>198</sup> This is built analogous to amidinato-substituted digallanes with the triazenido ligand bonded in terminal positions, not in a bridging one like the carboxylate. This has been explained with the larger flexibility of the NNN angle compared to the OC(Me)O angle.

In addition, other types of protonic acids have been applied for reactions in analogy to eqn [6]. Imido-tetraphenyldiphosphinic acid and imido-tetraphenylthiodiphosphinic acid form the digallanes **107** and **108**, with a different coordination mode of oxygen and thioligands.<sup>199</sup>

Similarly, acetylacetonato derivatives of digallanes **109** are prepared by reaction of either the neutral acetylacetonones<sup>200,201</sup> or the lithium acetylacetonates with digallium





The Ga–Ga bond lengths of trigallanes **112**–**114** are in the range of 241–246 pm. That is comparable to the bond lengths observed for comparably substituted digallanes.

Reaction of the anionic gallium heterocycle  $[\text{Ga}[\text{N}(\text{dipp})\text{CH}]_2]^-$ <sup>181,204</sup> with donor-stabilized gallane  $[\text{GaH}_3 \cdot \text{donor}]$  (donor = quinuclidine) affords the anionic trigallanate  $[[\text{CHN}(\text{dipp})]_2\text{Ga}-\text{GaH}_2-\text{Ga}[\text{N}(\text{dipp})\text{CH}]_2]^-$  **115**. This is described as a donor–acceptor adduct of the anionic  $[\text{Ga}[\text{N}(\text{dipp})\text{CH}]_2]^-$  rings to a  $\text{GaH}_2^+$  cation.<sup>205</sup>

Oxidative addition reactions of  $\text{GaX}_3$  ( $X = \text{Cl}, \text{Me}$ ) to the gallium(I) bisketoimidinate  $\text{Ga}(\text{nacnac})$ <sup>204</sup> produced the trigallanes  $(\text{nacnac})\text{Ga}(\text{X})\text{Ga}(\text{X})\text{Ga}(\text{X})(\text{nacnac})$  **116a,b**.<sup>206</sup>

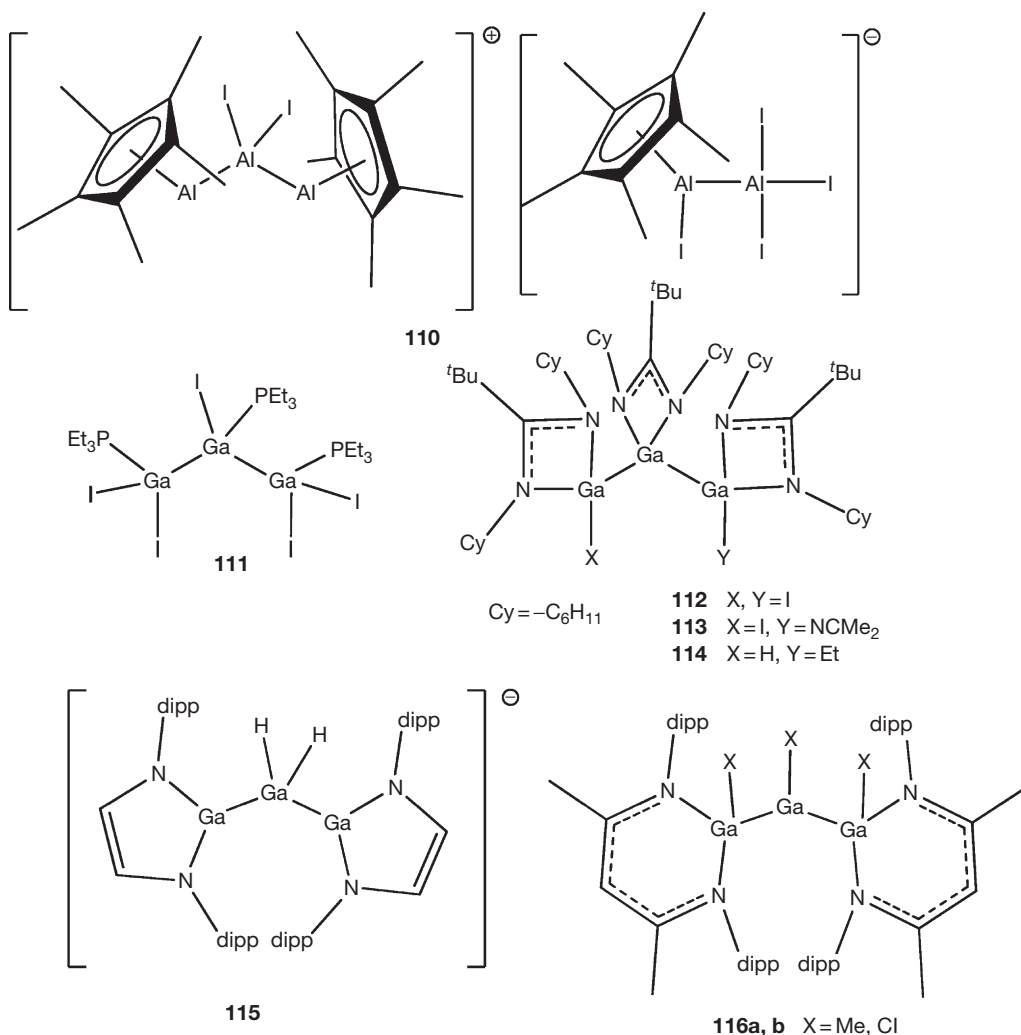
With a tris(imidazolinato)borate ligand (L) the ionic  $\text{Ga}_3$ -compounds  $[\text{L}_2\text{Ga}_3\text{I}_2]^+$  **117** ( $d_{\text{Ga}-\text{Ga}} = 245.86(5)$  pm) and  $[\text{LGa}_2\text{I}_5]^-$  **118** ( $d_{\text{Ga}-\text{Ga}} = 240.6(3)$  and 241.2(2) pm), as well as the corresponding digallanes  $[\text{L}_2\text{Ga}_2]^{2+}$  ( $d_{\text{Ga}-\text{Ga}} = 241.2(3)$  pm)

and  $\text{LGaGaX}_3$  ( $X = \text{Cl}, \text{I}$ ) ( $d_{\text{Ga}-\text{Ga}} = 241.4(4)$  pm) are accessible via reaction of the potassium or thallium derivative of the ligand and 'Gal'.<sup>207</sup> The Ga–Ga bonds are in the typical range known from other oligogallanes.

Starting from 'Gal' or GaBr-solutions a  $\text{Ga}_3\text{R}_5$  derivative **119** ( $\text{R} = \text{N}(\text{SiMe}_3)_2$ ) with three coordinate gallium atoms in an angled chain can be prepared. The Ga–Ga bonds ( $d_{\text{Ga}-\text{Ga}} = 252.8$  pm) are relatively long, comparable to those in digallanes with bulky substituents.<sup>208,209</sup>

A formal  $\text{R}^-$ -adduct of a  $\text{Ga}_3\text{R}_5$  derivative is  $[\text{Ga}_3\text{R}_6]^-$  **120** ( $\text{R} = \text{GePh}_3$ ). This trigallanate, as well as the indium analog  $[\text{In}_3(\text{SiPh}_3)_6]^-$  **121**, are isolated as alkali metal salts. The cations are coordinated by thf molecules and are separated from the anions in the crystal. Compounds **120** and **121** have linear  $\text{E}_3$ -units. These are described as double Lewis-base adducts of  $\text{E}^-$  to two  $\text{ER}_3$  groups according to **122**.





$\text{Al}_5\text{Br}_7(\text{thf})_5^{56}$  is an ionic compound composed of  $[\text{Al}[\text{AlBr}_2(\text{thf})_2]_2]_2[\text{Al}[\text{AlBr}_2(\text{thf})_2]_4]^+$  cations and  $[\text{Al}[\text{AlBr}_2(\text{thf})_2]_4]^-$  anions.

Octamer and decamer gallium(I) halides **136**<sup>66</sup> and **137**<sup>228</sup> were obtained. The core of **136** is a planar eight-membered ring, where six gallium atoms bear an iodine atom and a phosphane ligand. The remaining two gallium atoms are bridged by two iodine atoms.

Compound **137** exhibits a six-membered gallium ring in a flat chair conformation, where the two gallium atoms Ga(1) and Ga(4) are connected to two terminal  $\text{GaBr}_2(4\text{-}^t\text{Bu-pyridine})$  groups. From GaI-solutions with triethylamine, a partial oxidized product **138** was crystallized, built from two five-membered  $\text{Ga}_4\text{O}$  rings that are dimerized by two GaO-contacts.<sup>229</sup>

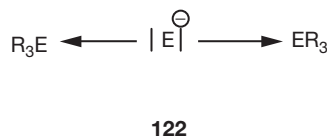
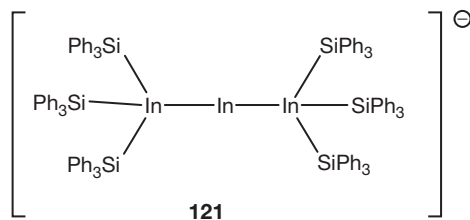
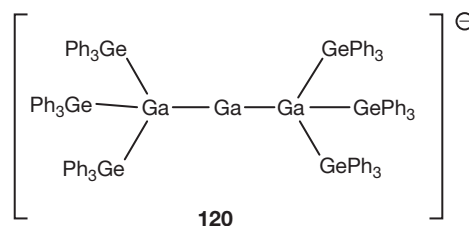
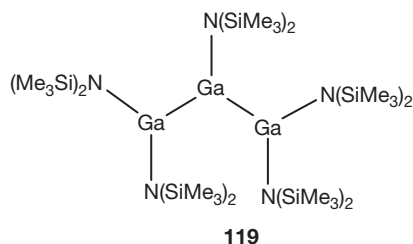
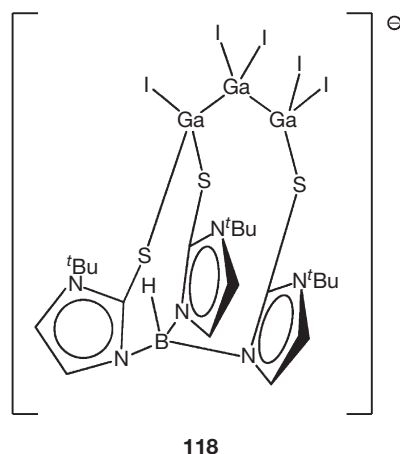
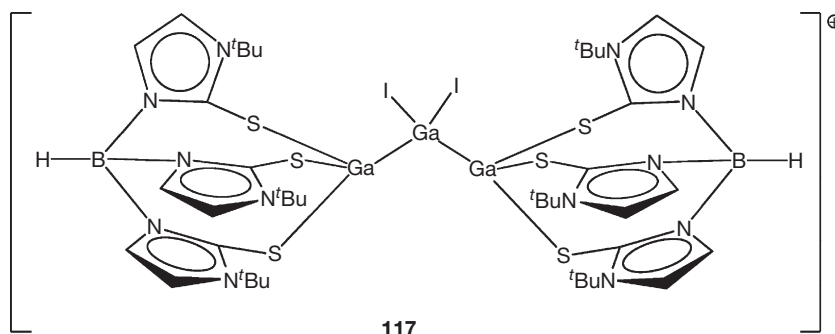
Starting from these GaX-solutions or alternatively sonochemically prepared 'GaI,' several chain and ring compounds with four or more gallium atoms have been prepared. Very common are  $\text{Ga}_5$ -derivates, which contain tetrahedral  $\text{GaGa}_4$ -cores **139**.<sup>56,230-233</sup> The terminal gallium atoms are either part of  $\text{GaX}(\text{do})_2$  or  $\text{GaX}_2(\text{do})$  groups. Thus, a central  $\text{Ga}^0$  atom is surrounded by  $\text{Ga}^{\text{I}}$  and  $\text{Ga}^{\text{II}}$  centers. Homologous  $\text{InIn}_4$  derivatives are also known. These are the ammonium salts  $[\text{In}[\text{InX}_2(\text{do})]_4]^- \text{Hdo}^+$  (**140a**: X = Cl,<sup>72</sup> **140b**: X = Br,<sup>234</sup> do =  $\text{N}(\text{CH}_2\text{CH}_2)_3\text{CH}$ ).

### 1.01.2.3.2 Nonhalide derivatives

Such a  $\text{GaGa}_4$  core of type **139** is also present in the salt-like compound  $[\text{Ga}_6\text{Cp}^*_2(\text{triflate})_6 \cdot 2\text{toluene}]$  **141** (triflate =  $\text{CF}_3\text{SO}_3$ ). Here the cation is a  $\text{Ga}^+$  ion coordinated by two toluene molecules and the anion can be described as a  $(\text{triflate})_3\text{Ga-Ga-Ga}(\text{triflate})_3$  chain, where two  $\text{GaCp}^*$  groups coordinate with the central gallium atoms. Compound **140** is obtained from protolysis of  $\text{GaCp}^*$  with trifluoromethanesulfonic acid together with **142** and several gallium(III) products. Compound **142** is a tetragallane, which can be described as a double  $\text{GaCp}^*$  adduct of the digallane  $\text{Ga}_2(\text{triflate})_4$ . Consequently, here the sequence  $\text{Ga}^{\text{I}}-\text{Ga}^{\text{II}}-\text{Ga}^{\text{II}}-\text{Ga}^{\text{I}}$  makes **142** an analog to  $\text{Ga}_2\text{Cl}_4 \cdot 2\text{dioxane}$ , where the gallium(I) compound  $\text{GaCp}^*$  adopts the role of the donor molecule.

A tetragallane with an inverse  $\text{Ga}^{\text{II}}-\text{Ga}^{\text{I}}-\text{Ga}^{\text{I}}-\text{Ga}^{\text{II}}$  arrangement is present in the galliumamidinate **143**.<sup>235</sup> With more steric demanding amidinates, only digallanes and trigallanes were accessible. The Ga-Ga bonds ( $d_{\text{Ga-Ga}} = 245.3(1)$  and  $245.5(1)$  pm) are slightly longer than in amidinato-substituted trigalliumiodides **112** and digalliumiodides **89**. This is in line with Bent's rule and the substitution pattern of the neighboring gallium atoms.



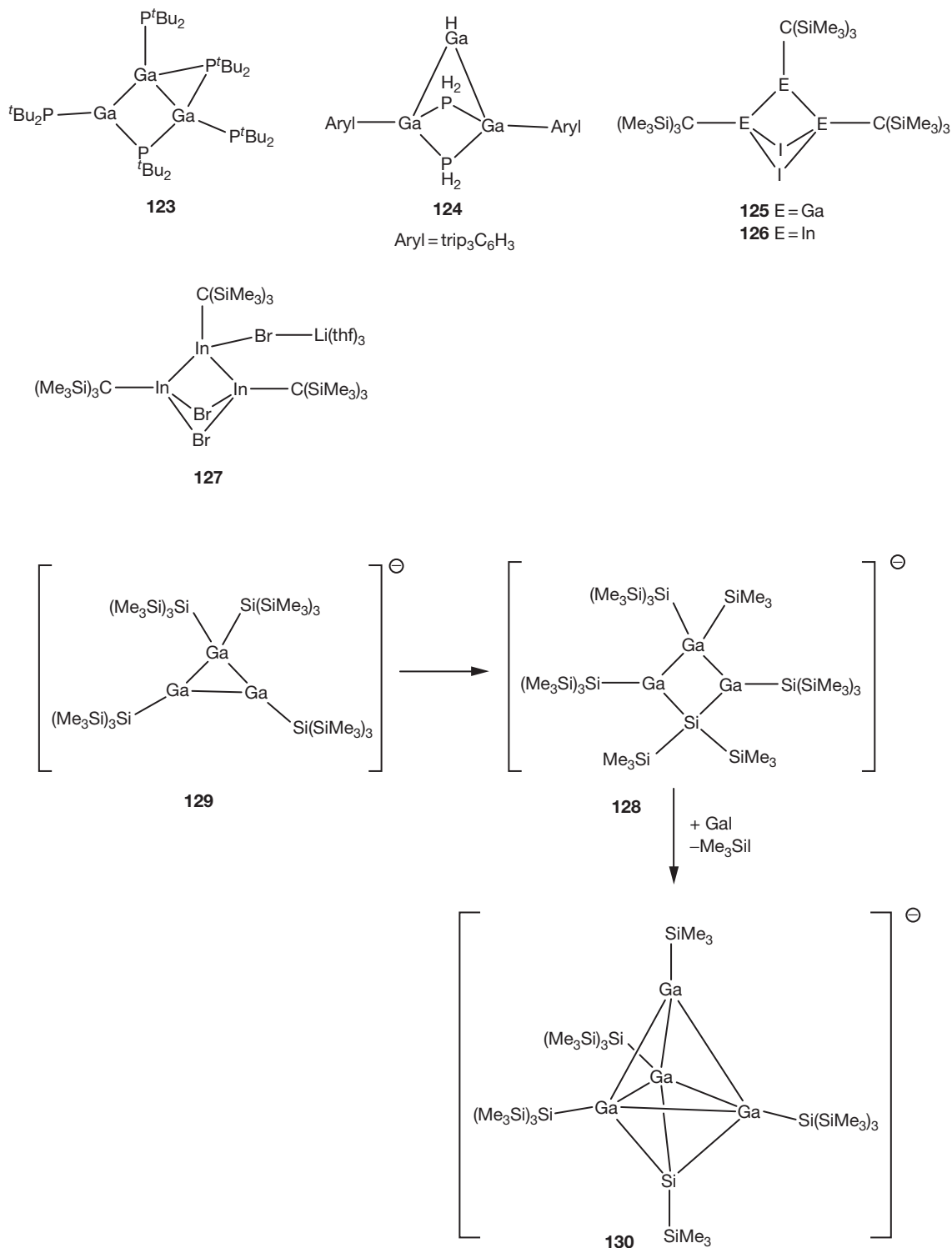


The hexagallanate **144**<sup>236</sup> is also based on a tetrahedral GaGa<sub>4</sub>-core. Here a tetrahedral GaGa<sub>3</sub>(Ga<sub>2</sub>) core is present, where the central gallium atom is bonded to three single gallium atoms and one digallium unit. One of the single gallium atoms bears two amide groups and the others are linked to an additional iodine or oxo group, respectively. The gallium atoms of the Ga<sub>2</sub> unit are bonded to one amide group each. The iodine atom and the oxygen atom are in bridging positions, thus forming a Ga<sub>5</sub>OI cage. Compound **144** forms

during the reaction of 'GaI' with LiN(SiMe<sub>3</sub>)<sub>2</sub> in low yields instead of an anticipated gallium(I) amide.

An analogous In<sub>6</sub>-core is present in [In<sub>6</sub>I<sub>8</sub>(tmeda)<sub>4</sub>]<sup>145</sup> (tmeda = tetramethylethylenediamine).<sup>71</sup> Two In(tmeda)I, one In(tmeda)<sub>2</sub>, and an In<sub>2</sub>-In<sub>2</sub>(tmeda) group are attached to the central indium atom. Thus, tetra- and penta-coordinate indium atoms are part of this molecule.

A structural related anion [Ga<sub>8</sub>O[N(SiMe<sub>3</sub>)Dipp]<sub>8</sub>(Ndipp)<sub>2</sub>[N(H)dipp]<sub>4</sub>]<sup>2-</sup> **146**<sup>233</sup> is obtained as lithium salt

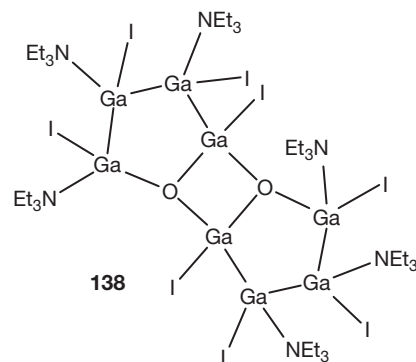
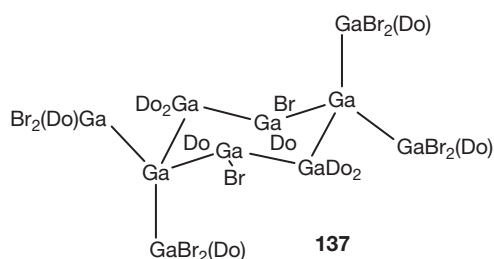
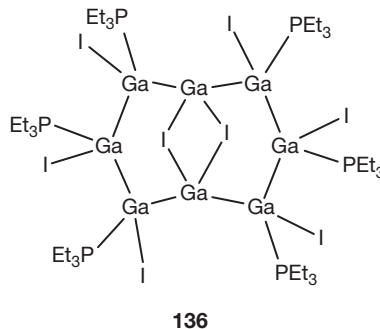
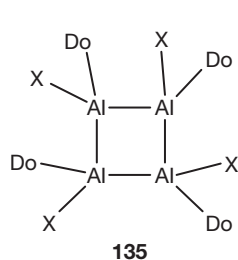
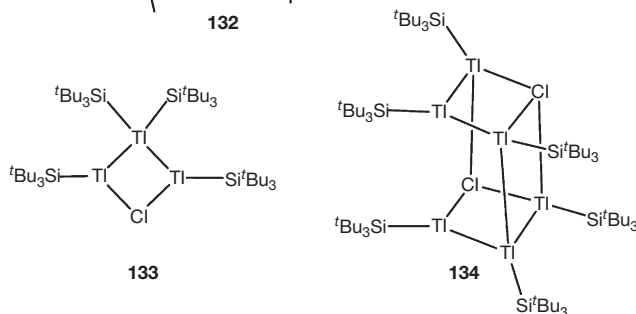
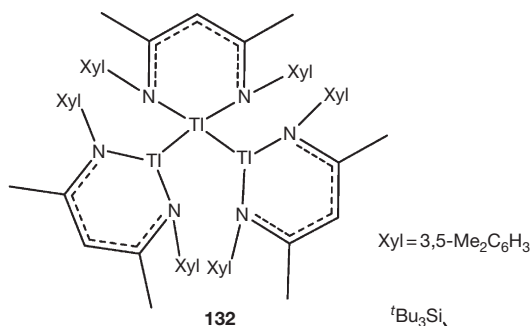
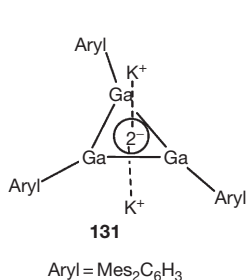


**Scheme 3** Formation of gallium-silicon ring compounds **128–130**.

from the reaction of  $\text{LiN}(\text{SiMe}_3)\text{dipp}$  with  $\text{GaCl}$  solutions at ambient temperature, that is, in a temperature region where gallium(I) chloride solutions are mostly disproportionated into gallium and halides of higher oxidation states. Here two  $\text{GaGa}_4$  units are joined via a common gallium atom.

Two imide groups  $\text{dippN}$  and one oxo atom close three  $\text{Ga}_4\text{X}$  rings, which are arranged in a 3,3,3-propellane type structure.

Compounds with a branched  $\text{Ga}_4$  chain were obtained starting from  $\text{Ga}_2\text{trip}_4$  [ $d_{\text{Ga-Ga}} = 251.5 \text{ pm}$ ].<sup>237</sup> While careful reduction with lithium metal (**Scheme 4**) produced the radical

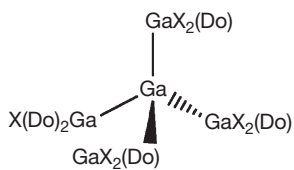


anion [trip<sub>4</sub>Ga<sub>2</sub>]<sup>-</sup> **147** [*d*<sub>Ga-Ga</sub> = 234.3 pm], reduction with an excess of sodium in trimethylamine led to the formation of dianionic [(trip)<sub>2</sub>Ga<sub>3</sub>Ga]<sup>2-</sup> **148**, with a planar GaGa<sub>3</sub> core. The short gallium-gallium distances [*d*<sub>Ga-Ga</sub> = 238.9 pm] are in accordance with two delocalized π-electrons in the gallium core. The neutral GaGa<sub>3</sub> compound **149** was obtained by oxidation of **148** with dry oxygen. The gallium-gallium bonds are elongated upon this oxidation [*d*<sub>Ga-Ga</sub> = 246.5–248.1 pm]. The indium analog of **150** has also been prepared.<sup>105</sup>

The monoanionic compound **151** of type [RGa(GaR<sub>2</sub>)<sub>3</sub>]<sup>-</sup> has a pseudotetrahedral Ga<sub>4</sub> core, where the edges of the Ga<sub>3</sub> base are bridged by iodine atoms.<sup>238</sup> The resulting cage is

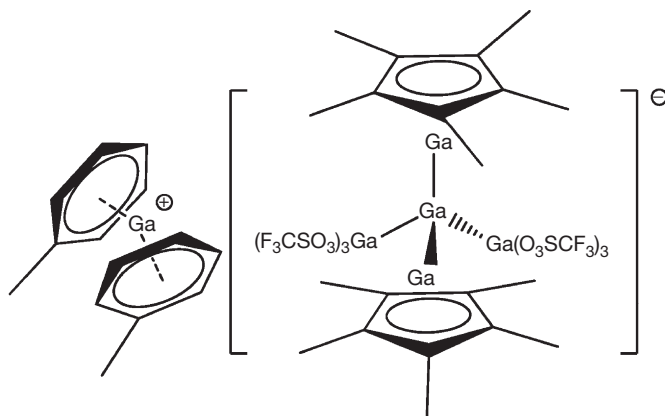
described as a cube with a missing corner. The long Ga-Ga distances [*d*<sub>Ga-Ga</sub> = 253.5 pm] are in line with the bulky silyl groups at the gallium atoms.

Cyclic Ga<sub>4</sub> derivatives are known as M<sub>2</sub>[Ga<sub>4</sub>Aryl<sub>2</sub>] **152** (Aryl = 2,6-trip<sub>2</sub>C<sub>6</sub>H<sub>3</sub>, **a**: M = Na, **b**: M = K,<sup>134,239</sup> and Na<sub>2</sub>[Ga<sub>4</sub>(Si<sup>t</sup>Bu<sub>3</sub>)<sub>4</sub>] **153**.<sup>164</sup> Compounds **152a,b** are obtained by reduction of ArylGaCl<sub>2</sub> with the respective alkali metals and show a planar, metalloaromatic Ga<sub>4</sub> ring with formally two π-electrons. The metal ions coordinate to the gallium-π-system and the π-system of the trip-rings. **153** is prepared by reduction of the gallatetrahedrane Ga<sub>4</sub>(Si<sup>t</sup>Bu<sub>3</sub>)<sub>4</sub>. It has a butterfly-type Ga<sub>4</sub>-core with a delocalized 2π system.

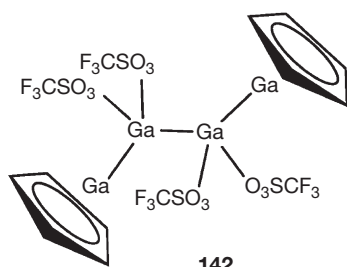


139

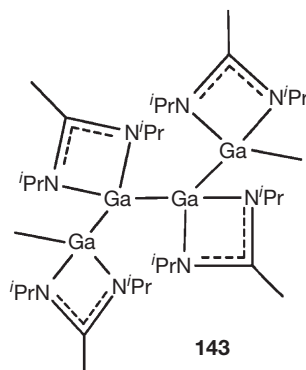
X Do  
Cl Et<sub>2</sub>O  
Cl thf  
Cl NHEt<sub>2</sub>  
Br NHEt<sub>2</sub>



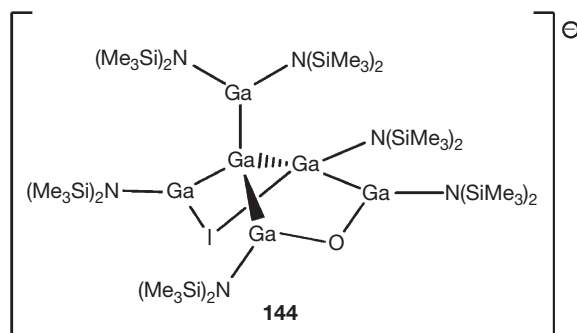
141



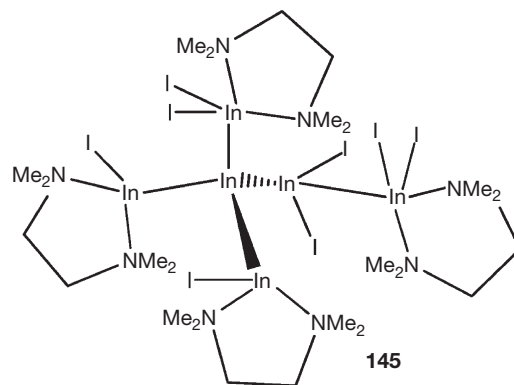
142



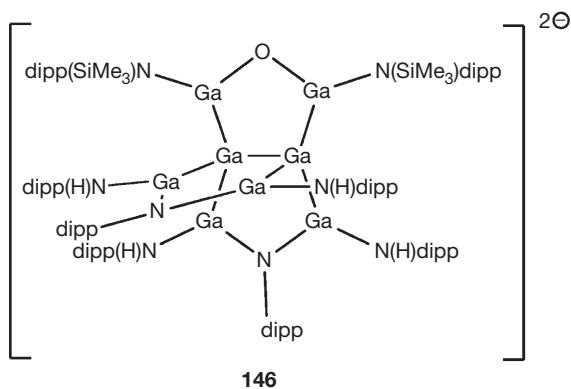
143



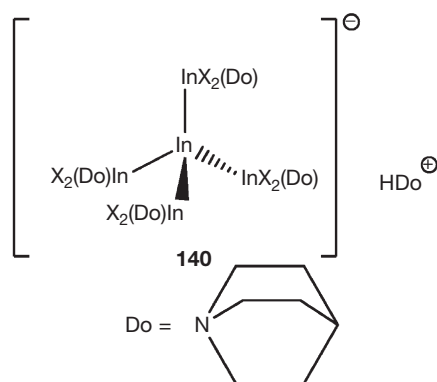
144



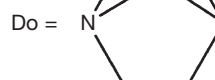
145

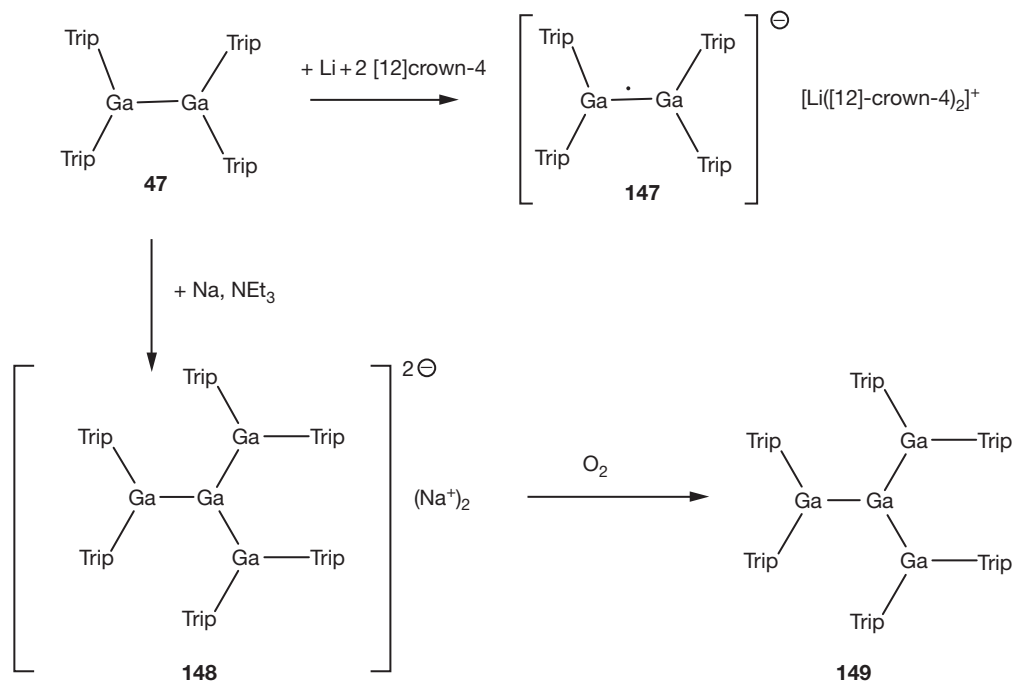


146

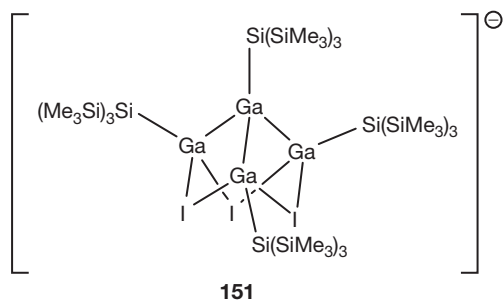


140





**Scheme 4** Redox chemistry with  $\text{Ga}_2\text{trip}_4$  **47**.



$[\text{Ga}_6(\text{SiPh}_2\text{Me})_8]^{2-}$  **154**, isolated as lithium salt, shows an unusual planar arrangement of six gallium atoms.<sup>240</sup> Formally it is derived by dimerization of two equivalents of a compound of type **122** with loss of four substituents. The delocalized bonding in **154** brings this compound to the border with cluster compounds and is discussed later.

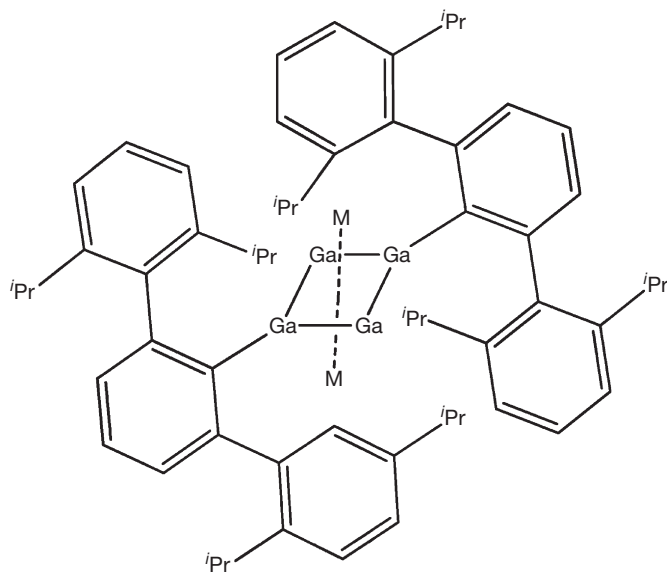
An unique example of a linear six-membered chain compound of triel elements is  $\text{In}_6\text{I}_2(\text{xy}^{\text{l}}\text{nacnac})_6$  **155** [ $\text{xy}^{\text{l}}\text{nacnac} = [\text{N}(3,5\text{-dimethylphenyl})\text{C}(\text{Me})_2\text{CH}]_2$ ;  $d_{\text{In-In}} = 282.2\text{--}285.4$  pm].<sup>241</sup> Compound **155** is obtained from indium(I) iodide and the potassium salt of  $\text{xy}^{\text{l}}\text{nacnac}$ . The bond lengths are similar to those in  $\text{nacnac}$ -substituted diindiumhalides [ $(\text{dipp}^{\text{nacnac}})\text{InCl}_2$  **156a** [ $d_{\text{In-In}} = 282.4$  pm]<sup>178</sup> and [ $(\text{Ph}^{\text{nacnac}})\text{InCl}_2$  **156b** [ $d_{\text{In-In}} = 275.7$  pm].<sup>177</sup> [ $(\text{xy}^{\text{l}}\text{nacnac})\text{In}_2$  **157** as an example of a dimeric indium(I) derivative has a longer indium-indium bond [ $d_{\text{In-In}} = 334.0$  pm], despite the fact that a double bond may be formulated here.<sup>242</sup> For a more detailed discussion see **Chapter 1.10**.

Reaction of  $\text{GaX}$ -solutions<sup>243</sup> with alkali metal phosphanides yields oligomeric gallium phosphanides  $\text{Ga}_8(\text{P}^t\text{Bu}_2)_8\text{Cl}_2$  **158**,<sup>233</sup>  $\text{Ga}_8(\text{P}^t\text{Pr}_2)_8\text{Cl}_2$  **159**,<sup>233</sup> and  $\text{Ga}_{12}(\text{P}^t\text{Bu}_2)_6(\text{Pr}^{\text{H}}\text{C}=\text{P}^{\text{H}}\text{Bu}_3)_3\text{Br}_2$

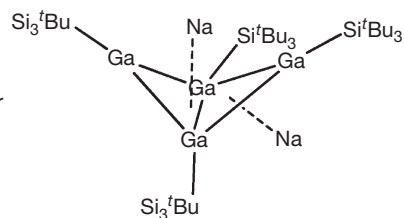
**160**<sup>244</sup> as well as higher cluster compounds.<sup>245</sup> Compounds **158** and **159** are octagallium derivatives with complicated oligocyclic structures. The central  $\text{Ga}_8$ -core of **158** is described as two distorted edge-sharing  $\text{GaGa}_4$  tetrahedra, where the terminal gallium atoms are bridged by phosphanido groups. The diisopropylphosphanido derivate **159** has an oligocyclic structure with attached  $\text{Ga}_2$  units. The unusual  $\text{Ga}_{12}$  compound **160** forms by reaction of metastable  $\text{GaI}$  solutions<sup>243</sup> with  $\text{LiP}^t\text{Bu}_2$  and  ${}^n\text{Pr}(\text{H})\text{C}=\text{P}^n\text{Bu}_3$ . It has a cluster core consisting of three nearly planar  $\text{Ga}_4$  rings. A related  $\text{In}_9$  compound [ $\text{In}_3(\text{In}_2)_3(\text{PhP})_4(\text{Ph}_2\text{P})_3\text{Cl}_7(\text{PEt}_3)_3$ ] featuring  $(\text{In}^{\text{II}})_2$  units as well as  $\text{In}^{\text{III}}$  units was prepared, starting from indiumtrichloride and silylated phenylphosphanes. Redox reactions are responsible for indium-indium bond formation here.<sup>246</sup>

#### 1.01.2.4 Synthesis and Structure of Compounds with E-E' Bonds

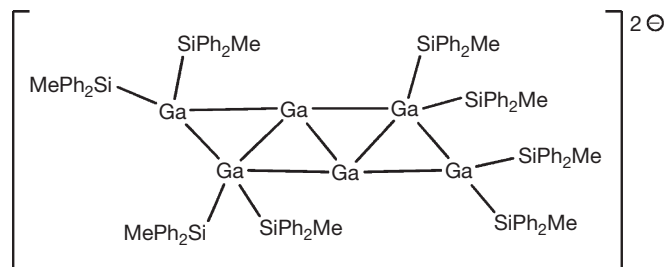
The availability of Lewis basic triel(I) derivatives  $\text{ECp}^*$ ,<sup>247,248</sup>  $\text{E}(\text{nacnac})$ ,<sup>204</sup>  $[\text{E}(\text{N}(\text{dipp})\text{CH})_2]^{-163,181,249,250}$  and  $\text{EL}$  ( $\text{L} =$  substituted pyrazolylborato)<sup>251</sup> offers the possibility for the preparation of mixed E-E' compounds.<sup>252</sup> We have already discussed donor-acceptor compounds of  $\text{AlCp}^*$  and  $\text{GaCp}^*$  for structures **110**, **115**, and **142**, involving  $\text{E}^{\text{+I}}$  and  $\text{E}^{\text{+II}}$  centers. The combination of  $\text{E}^{\text{+I}}$  and  $\text{E}^{\text{+III}}$  is realized in  ${}^t\text{Bu}_3\text{pzGa-GaI}_3$ ,  ${}^t\text{Bu}_3\text{pzIn-InI}_3$  ( ${}^t\text{Bu}_3\text{pz} = \text{tris-3,5-ditertbutylpyrazolyl}$ )hydroborate<sup>251,253-256</sup> and  $\text{XIn}[[18]\text{-crown-6}]\text{-InX}_3$  **161** [ $d_{\text{In-In}} = 268.2$  ( $\text{X} = \text{Cl}$ ),  $270.7$  ( $\text{X} = \text{Br}$ ),  $272.5$  ( $\text{X} = \text{I}$ )].<sup>257,258</sup> Compound **161** is obtained from  $\text{InCp}^*$  by protolysis with triflic acid and subsequent reaction with indiumtrihalides. The trend in bond lengths is as expected from Lewis acidities of  $\text{InX}_3$  and the steric demand of the halides.



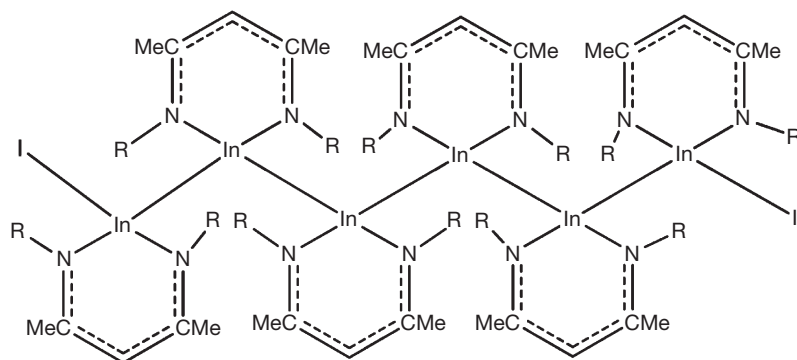
152a, b M = Na, K



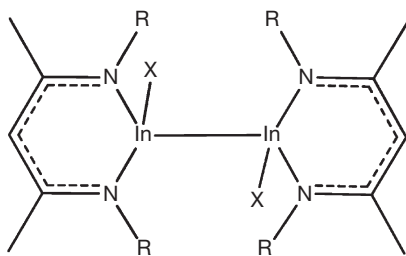
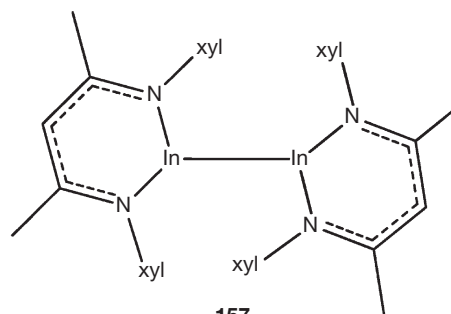
153



154

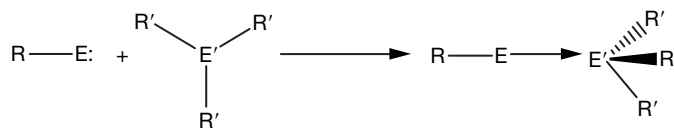
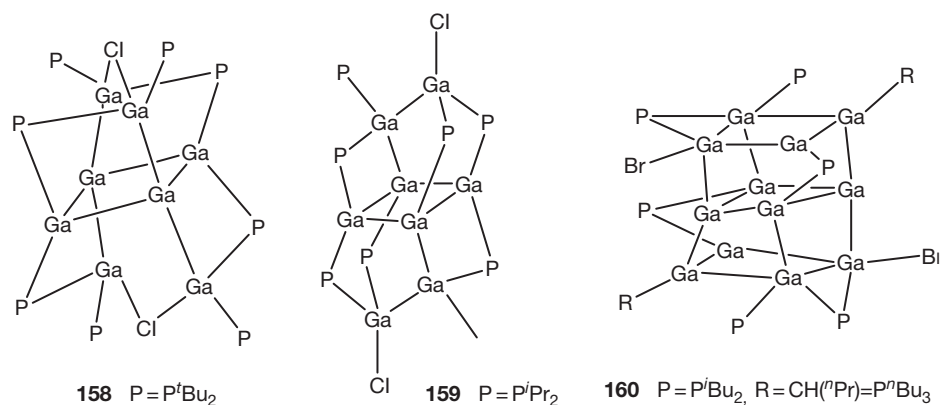


155 R = xyl

R = dipp  
156a  
Ph 156b

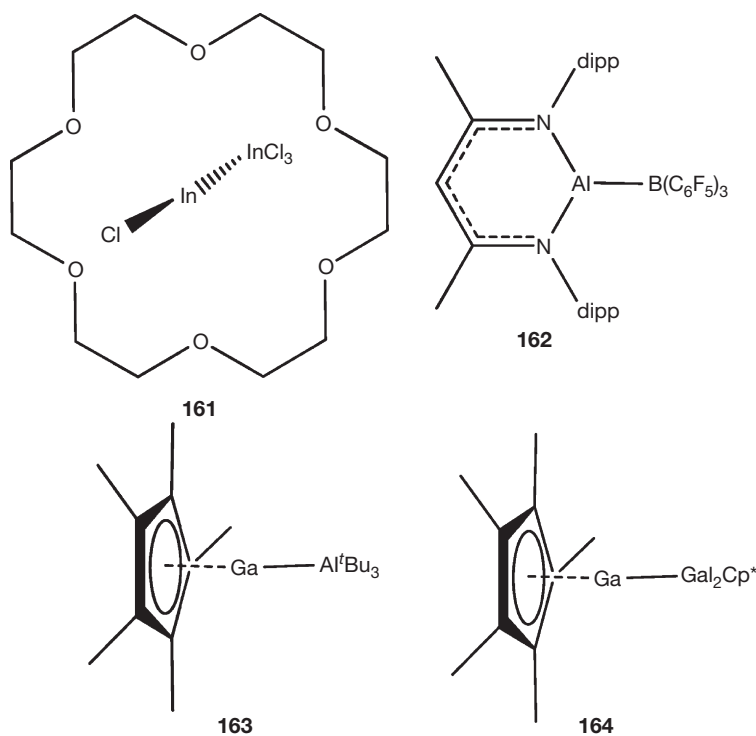
157





R, R': see Table 8

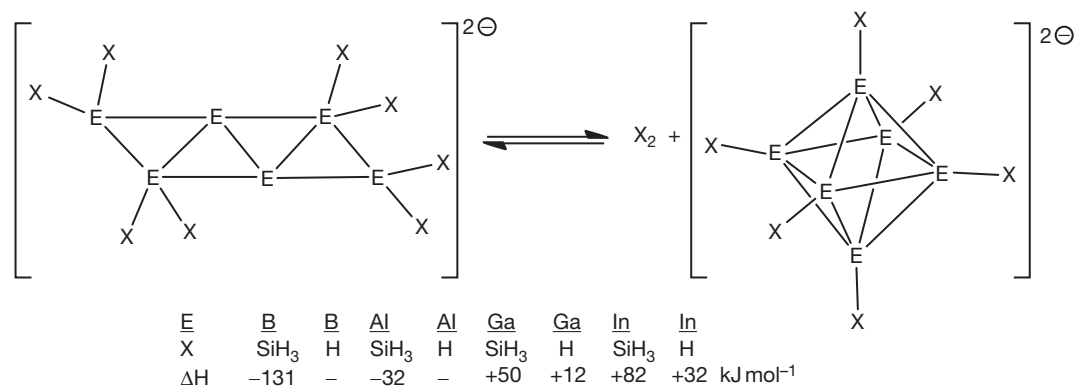
**Scheme 5** Principle of the formation of  $RE^{+1}-E'R'_3$  complexes.



**Table 8** Overview of  $RE^{+1}-E'R'_3$  complexes

$d_{E-E'}$ (pm)	$AlCp^*$	$GaCp^*$	$InCp^*$	$Alnacac$
$B(C_6F_5)_3$	216.9 <sup>265</sup>			218.3 <sup>266</sup>
$Al(C_6F_5)_3$	259.1 <sup>267</sup>			
$Al^tBu_3$	268.9 <sup>268</sup>	262.9 <sup>232,268,269</sup>	284.3	
$Ga^tBu_3$	262.0 <sup>252</sup>		284.5	
$GaCl_2Cp^*$		242.5		
$Gal_2Cp^*$		243.7		

ECp\* compounds form a variety of complexes with transition metal fragments<sup>183,259–264</sup> and main group Lewis acids. With the latter, redox reactions often occur (see e.g., 110, but with appropriately substituted acids,  $E^{+1}-E'^{+III}$  complexes are obtained (Scheme 5, Table 8).<sup>232,268,269</sup> Two examples are 162 and 163, prepared from the triel(I) compound. Compound 164 is a product of the reaction of Cp\*Li with 'Gal' and can be reduced with alkali metals to Cp\*Ga.<sup>261</sup> The bond lengths of an E–E' pair seem to be dependent on the Lewis acidity of the E'R'<sub>3</sub> part.



**Scheme 6** Possible formation of a polyhedral cluster from  $[E_6X_8]^{2-}$ .

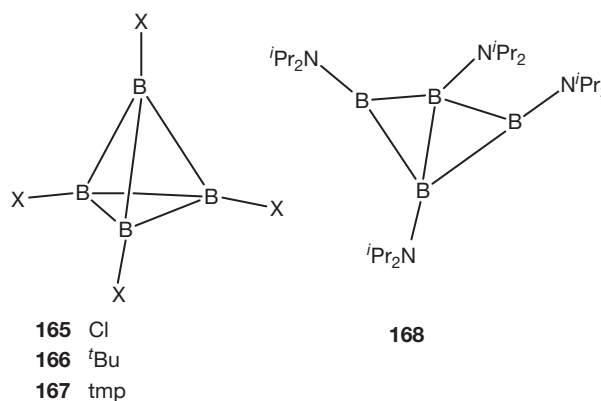
### 1.01.3 Polyhedral Cluster Compounds

With few exceptions, all ring and chain compounds described so far in this chapter are electron-precise, which means that a description with  $2c2e$  bonds is valid. **154**, of type  $[R_8Ga_6]^{2-}$ , is an electron-deficient molecule. While only ten electrons are available for Ga–Ga bonds, nine such contacts are present. A bonding description of **154** needs to make use of multicenter bonds. DFT calculations have been made for **154** and its other triel homologs  $[E_6X_8]^{2-}$  to examine a possible transfer into a polyhedral, here octahedral *closo*-cluster-ion  $[E_6X_6]^{2-}$  by loss of  $X_2$  (**Scheme 6**).<sup>240,270</sup> For the lighter homologs boron and aluminum, the polyhedral cluster is preferred, while for gallium and indium the equilibrium should be on the side of **154**. The calculations were made for SiH<sub>3</sub> and H as substituents, and it was observed that the type of substituents is of large influence. This will be demonstrated by the polyhedral clusters of these elements in this section.

Looking at  $Al_4X_4$ ·4do, for example, removal of the donor molecules would leave an  $Al_4X_4$  ring with electron sextets at the aluminum atoms. Here, formation of a tetrahedral cluster  $Al_4X_4$  would allow fulfilling the octet rule by multicenter bonds. Polyhedral cluster compounds of the triel elements are described here. The synthetic methods to prepare them and their structures are also described. For a discussion of the bonding in clusters, how electron bookkeeping according to the Wade–Williams–Rudolph rules<sup>19–21,271</sup> is applicable is examined.

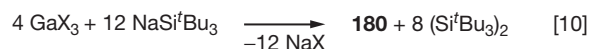
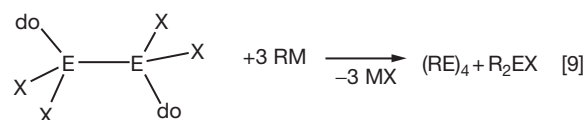
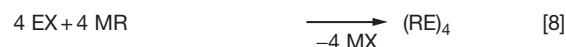
#### 1.01.3.1 Tetrahedral $E_4R_4$ Cluster Compounds and Derivatives

The most common cluster compounds for the triels aluminum to thallium are tetrahedral  $E_4R_4$  clusters. These are known for all triels. The chemistry of these clusters has been reviewed extensively.<sup>4,7,12,49,137,243,272–281</sup> For boron, the subhalide  $B_4Cl_4$  (**165**) as well as  $B_4^tBu_4$  (**166**) possess a tetrahedral core. In the case of boron,  $B_4R_4$  compounds can also adopt ring structures. For amino-substituted derivatives, BN- $\pi$ -bonding is an alternative for the boron atoms to achieve an electron octet. **167** with the bulky tetramethylpiperidino groups is tetrahedral, while **168** with  $R = N^iPr_2$  has a butterfly type ring structure.<sup>282</sup>



##### 1.01.3.1.1 Synthesis and structures

The heavier congeners are prepared by reduction of  $REX_2$  (eqn [7]), substitution reactions at triel(I) compounds ( $X = \text{halide, triflate, amide, Cp}^*$ ) (eqn [8]) or disproportionation reactions of  $E_2X_4$ ·2do upon substitution (eqn [9]).



For aluminum,  $(AlCp^*)_4$  **169** and several derivatives (**Table 9**) have been prepared by routes according to eqns [7] and [8]. All of these crystallographically characterized derivatives are stabilized by bulky substituents.  $[Al(CH_2^tBu)]_4$  was reported only in solution, and was found to be tetramer by molecular weight determinations.<sup>289</sup>  $Al_4[N(SiMe_3)dipp]_4$  (**174**), the only tetramer aluminum(I) amide, is prepared in a reaction according to eqn [7].<sup>287</sup>  $Al_4Cp^*_3[N(SiMe_3)_2]$  (**175**) is

prepared from **169** and  $\text{LiN}(\text{SiMe}_3)_2$ ,<sup>288</sup> and is a unique example of a mixed substituted cluster. The Al–Al distances in these tetrahedranes cover a wide range from 259.2 to 277.8 pm. The longest bonds are observed for Cp\* and other carbon-based substituents and the shortest for silyl groups. Intriguingly, in **175**, long Al–Al distances between the Cp\*-substituted atoms and short distances between the amido-substituted ones are observed.

Most of these tetramers dissociate in solution. The degree of monomerization is correlated with the strength of the Al–Al interactions in the cluster. Thus, those with short Al–Al bonds, that is, the silyl-substituted ones, show no tendency to dissociation.  $\text{Al}_4\text{Cp}^*_4$ , on the other hand, is a monomer in solution. This was also confirmed by <sup>27</sup>Al NMR spectroscopy, where tetramers show chemical shifts of  $\delta = -62$  to  $-111$  ppm and monomer AlR compounds those of  $\delta = -150$  to  $-168$  ppm.<sup>94,290</sup> Obviously, short Al–Al distances in tetramers are related to stronger bonding in the cluster. This difference in the stability of the tetramers depending on the type of substituents was also confirmed by quantum chemical calculations (see below). In addition, the color of these clusters is dependent on the type of substituents and thus of the Al–Al distances. Compound **169** is yellow, **171** orange, and **172** violet.

For gallium(I) compounds of type  $\text{R}_4\text{Ga}_4$ , originally the disproportionation reaction of  $\text{Ga}_2\text{Cl}_4 \cdot 2$ dioxane according to eqn [9] was applied. This was successful with various substituents R. More economically these clusters are prepared by reduction of gallium(III) derivatives, either by metals or by using the nucleophile MR (M = Li, Na) itself as reducing agent (eqn [10]). This was the case with  $\text{R} = \text{Si}^t\text{Bu}_3$ . An alternative (eqn [9]) is the use of formal gallium(I) halides, either sonochemically prepared 'GaI'<sup>291</sup> or metastable GaX solutions obtained by high-temperature routes.<sup>243</sup>

With more bulky substituents, monovalent gallium(I) species are realized. Thus the amide  $\text{GaN}(\text{SiMe}_3)\text{aryl}$  **183** ( $\text{aryl} = \text{C}_6\text{H}_3-2,6-(\text{C}_6\text{H}_2-2,4,6-\text{Me}_3)$ ) is monomer even in solid

state, while other gallium(I) compounds, which are monomeric in gas phase or solution, associate in the solid state.<sup>292</sup>

An overview on tetrahedral gallium species is in Table 10.

Indium derivatives  $\text{In}_4\text{R}_4$  **184–186** (Table 11) are prepared via indium(I) compounds InI or  $\text{InCp}^*$  (eqn [8]). The use of indium(I) halides was not successful for silyl-substituted tetrahedranes, because disproportionation to indium and indium(III) derivatives  $\text{R}_2\text{InX}_2(\text{Li}(\text{thf})_2)$  was observed.

For thallium the  $\text{C}(\text{SiMe}_3)_3$ -substituted tetrahedrane **187** has a severely distorted core. The compound is very sensitive to temperature and light. The tripod ligand-substituted  $\text{Tl}_5$  compound **188** also contains a severely distorted tetrahedron of thallium atoms ( $d_{\text{Tl-Tl}} = 340.9\text{--}380.0$  pm). An additional thallium atom is attached in a terminal position ( $d_{\text{Tl-Tl}} = 340.3$  pm).<sup>113</sup>

For aluminum the tetramer  $\text{Al}_4\text{Cp}^*_4$  is a prominent example of a tetrahedral cluster compound. For the heavier congeners gallium, indium, and thallium no such tetramer cyclopentadienyl derivatives are known. There are monomer  $\text{Cp}^x\text{E}$  compounds ( $\text{Cp}^x = \text{Cp}^*$ ,  $\text{C}_5\text{H}_2(\text{SiMe}_3)_3$ ,  $\text{C}_5\text{H}_4^t\text{Bu}$ ,  $\text{C}_5(\text{CH}_2\text{Ph})_5$ ,  $\text{C}_5\text{Me}_4\text{Ph}$ ,  $1,2,4\text{-P}_3\text{C}_2^t\text{Bu}_2$ ,  $\text{PC}_4\text{H}_2\text{-}2,4\text{-}^t\text{Bu}_2$ )<sup>300–303</sup> in solution or gas phase, while in the solid state most of them are loosely aggregated.  $\text{Cp}^*\text{Ga}$  and  $\text{Cp}^*\text{In}$  form hexamers with very long E–E distances. Those for gallium ( $d_{\text{Ga-Ga}} = 412.2$  pm)<sup>248,300,304,305</sup> are even longer than those for indium ( $d_{\text{In-In}} = 395$  pm).<sup>306,307</sup> These hexamers are not regarded as E–E bonded systems, but are held together by CH–CH van der Waals interactions.

### 1.01.3.1.2 Bonding

Comparing tetrahedral clusters in the row boron to thallium, there are remarkable differences. The E–E distances increase from boron to aluminum and gallium to thallium. The Ga–Ga distances are shorter than the Al–Al ones. This is in line with

**Table 9** Survey on compounds  $\text{Al}_4\text{R}_4$

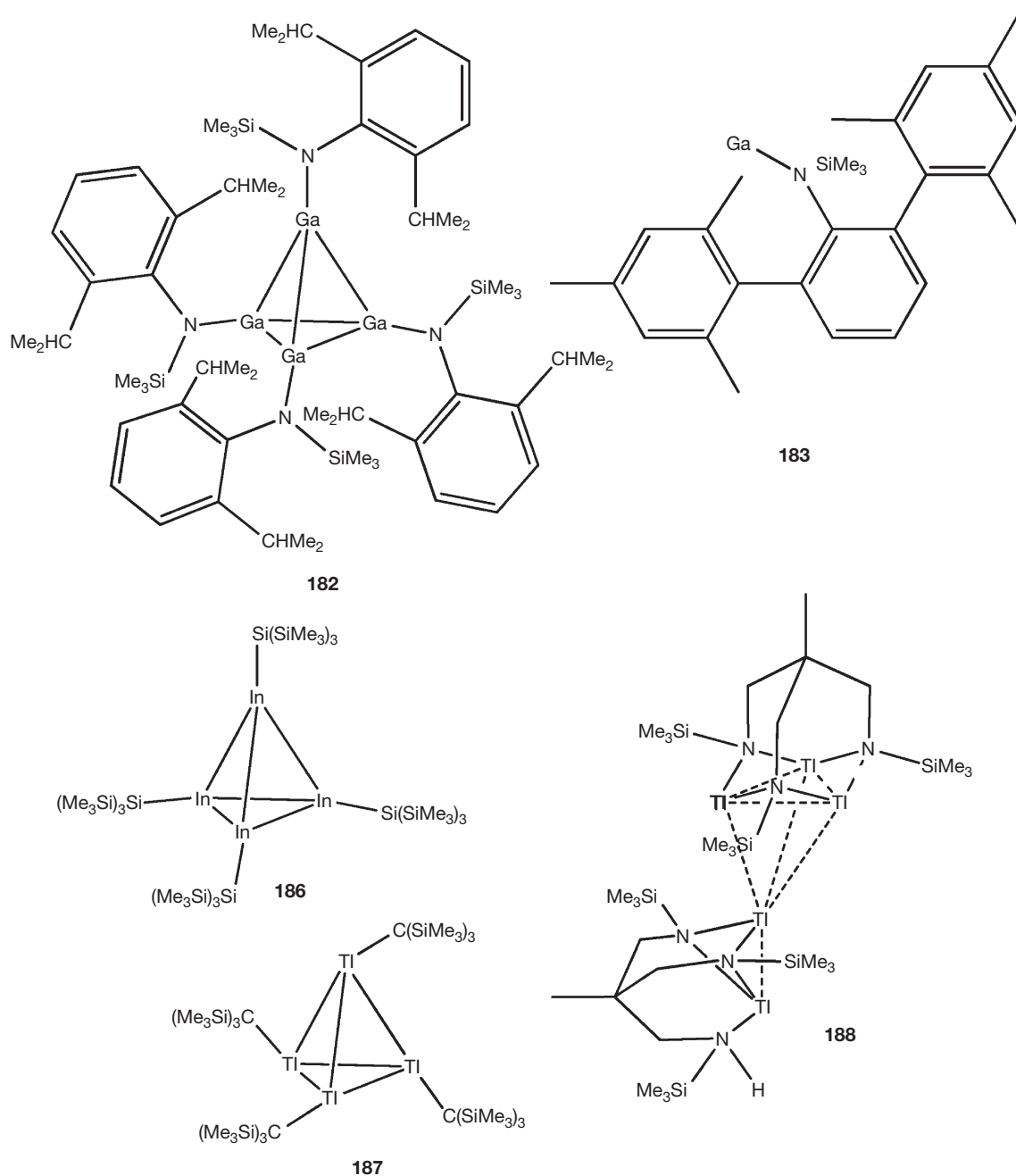
		$d_{\text{Al-Al}}$ (pm; mean)	References
<b>169</b>	$\text{Al}_4\text{Cp}^*_4$	277.0	247,283
<b>170</b>	$\text{Al}_4(\text{C}_5\text{Me}_4\text{H})_4$	271.4	283
<b>171</b>	$\text{Al}_4[\text{C}(\text{SiMe}_3)_3]_4$	274.0	284
<b>172</b>	$\text{Al}_4(\text{Si}^t\text{Bu}_3)_4$	260.6	285
<b>173</b>	$\text{Al}_4[\text{Si}(\text{SiMe}_3)_3]_4$	260.2	286
<b>174</b>	$\text{Al}_4[\text{N}(\text{SiMe}_3)\text{dipp}]_4$	261.8	287
<b>175</b>	$\text{Al}_4\text{Cp}^*_3[\text{N}(\text{SiMe}_3)_2]$	263.2–276.2	288

**Table 10** Overview on tetrahedral gallium species  $\text{Ga}_4\text{R}_4$

		$d_{\text{Ga-Ga}}$ (pm; mean)	Method	References
<b>176</b>	$\text{Ga}_4[\text{C}(\text{SiMe}_3)_3]_4$	268.8	Eqns [7]–[9]	135
<b>177</b>	$\text{Ga}_4[\text{C}(\text{SiMe}_3)_2\text{R}]_4$ (R = Me, Et)	271.1	Eqn [7]	136
<b>178</b>	$\text{Ga}_4[\text{Si}(\text{SiMe}_3)_3]_4$	258.2	Eqns [8] and [9]	293
<b>179</b>	$\text{Ga}_4[\text{Ge}(\text{SiMe}_3)_3]_4$	258.7	Eqn [9]	294
<b>180</b>	$\text{Ga}_4(\text{Si}^t\text{Bu}_3)_4$	257.2	Eqn [10]	295
<b>181</b>	$\text{Ga}_4\text{tmp}_4$	258.6(1)–268.5(1)	Eqn [9]	236
<b>182</b>	$\text{Ga}_4[\text{N}(\text{SiMe}_3)\text{dipp}]_4$	258.4(1)–264.2(1)	Eqn [9]	236

**Table 11** Overview on tetrameric species  $\text{In}_4\text{R}_4$  and  $\text{Tl}_4\text{R}_4$

		$d_{\text{E-E}}$ (pm; mean)	Method	References
<b>184</b>	$\text{In}_4[\text{C}(\text{SiMe}_3)_3]_4$	300.2	Eqn [8]	296
<b>185a</b>	$\text{In}_4[\text{C}(\text{SiMe}_3)_2\text{Et}]_4$ (R = Et)	300.4	Eqn [8]	297
<b>185b</b>	$\text{In}_4[\text{C}(\text{SiMe}_3)_2\text{Et}_2]_4$	300.6–304.0	Eqn [8]	297
<b>185c</b>	$\text{In}_4[\text{C}(\text{SiMe}_3)_2^i\text{Pr}]_4$	315.2	Eqn [8]	297
<b>186</b>	$\text{In}_4[\text{Si}(\text{SiMe}_3)_3]_4$	289.3	Eqn [8]	298
<b>187</b>	$\text{Tl}_4[\text{C}(\text{SiMe}_3)_3]_4$	332–364	Eqn [8]	299



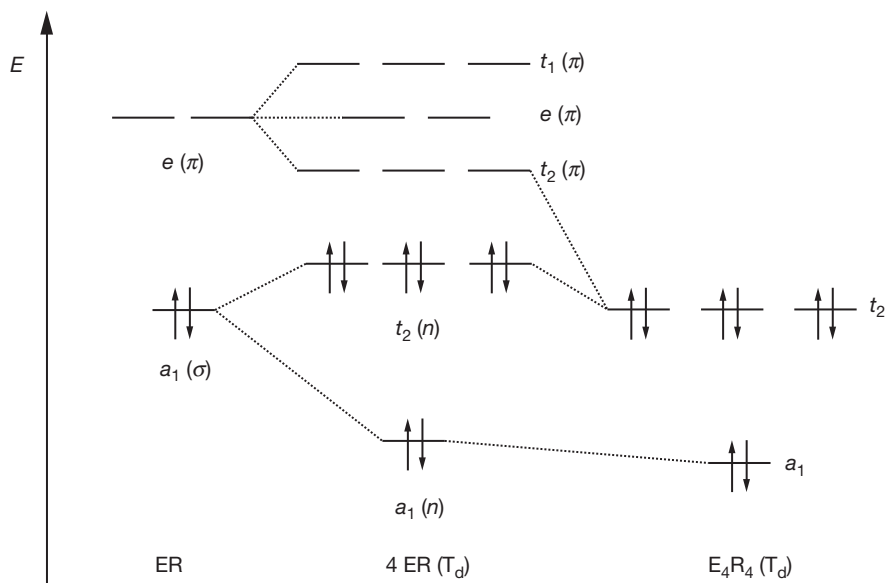
the smaller covalent radius of gallium atoms compared to aluminum.

$\text{Ga}_4[\text{C}(\text{SiMe}_3)_3]_4$  and  $\text{Ga}_4[\text{Si}(\text{SiMe}_3)_3]_4$  are, at first glance, two very similar compounds, but even the color is different, it changes from red (176) to violet (178). The Ga–Ga distances of the silyl-substituted compound are shorter by approximately 10 pm. Comparable differences are observed for the Al and In derivatives, respectively. This hints of a stronger bonding in the silyl-substituted cluster molecules compared to alkyl-substituted ones. This is obvious in the behavior in the solution and gas phases. Compound 176 monomerizes in solution and in the gas phase the structure of the monomer could be determined by electron diffraction.<sup>308</sup> The Ga–C distance in

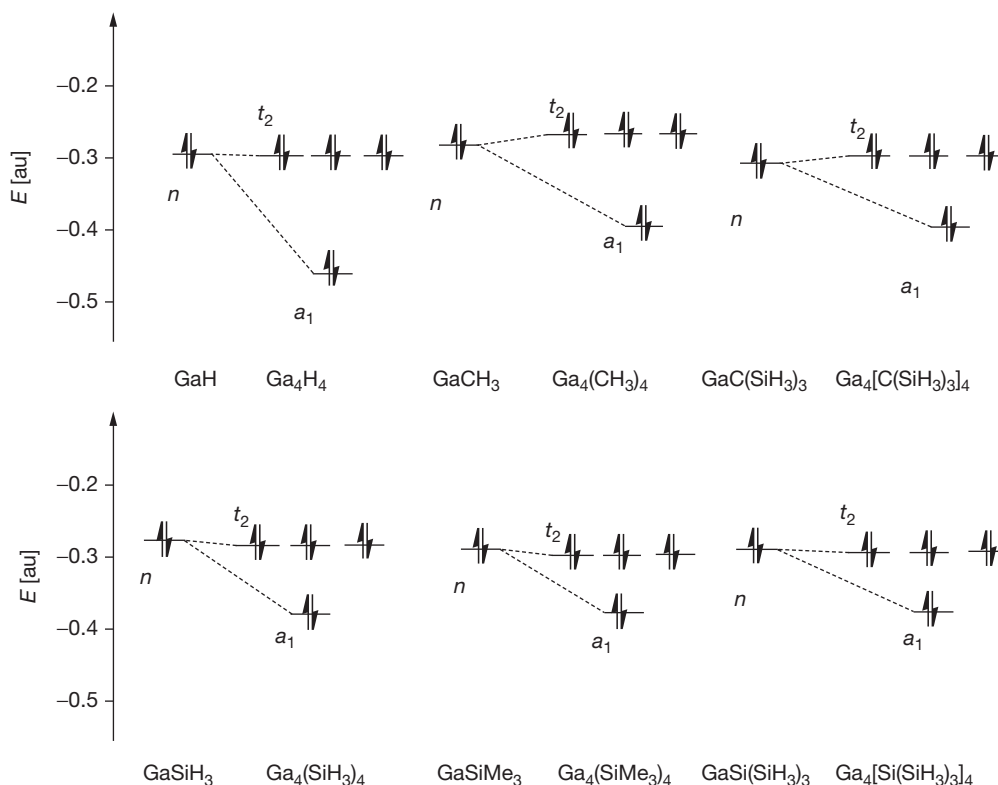
the monomer is drastically longer than in 176. Compound 178 remains tetramer under these conditions.

Looking at the bonding of these tetrahedral clusters, four skeletal electron pairs (sep) are counted, which makes them different from carbatetrahedranes or  $\text{P}_4$  with 6 sep, for example. In the latter, six 2c2e bonds can be assumed and for triel clusters, four 3c2e bonds on the four faces of the tetrahedral. Building the clusters from monomers ER, with a lone pair of electrons and two vacant p-type orbitals, linear combination gives the cluster orbitals (Figure 1).

The energy of the triply degenerate HOMO is largely influenced by the type of R for a given triel E (Figure 2). Silyl groups lead to stabilization of the HOMO compared to alkyl

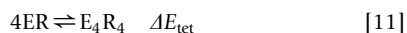


**Figure 1** Qualitative MO scheme for triel clusters  $E_4R_4$  in  $T_d$  symmetry. Reproduced with permission from Linti, G.; Schnöckel, H.; Uhl, W.; Wiberg, N. In *Molecular Clusters of the Main Group Elements*; Driess, M., Nöth, H., Eds.; Wiley-VCH: Weinheim, 2004; pp 126–168. Copyright Wiley-VCH Verlag GmbH & Co. KGaA.



**Figure 2** Change of the HOMO energies with R for triel clusters  $E_4R_4$  in  $T_d$  symmetry.

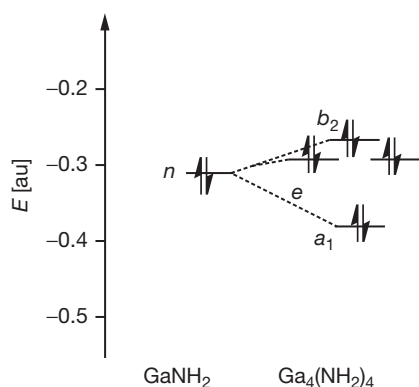
substituents. Consequently, large differences in tetramerization energies  $\Delta E_{tet}$  are observed (Table 12, eqn[11]). This is reflected in the experimental findings on dissociation of the clusters.



For amido-substituted tetrahedranes, a modified picture is valid. Due to the lower symmetry of the substituents, the HOMO is now a nondegenerate one, which is energetically near the doubly degenerate HOMO-1 (Figure 3). This also explains the less regular structures of the tetramers and might

**Table 12** Tetramerization energies of  $E_4R_4$  calculated according to eqn[11]

	$\Delta E_{tet} (kJ mol^{-1})$	Method	References
$B_4H_4$	-1153	MP2	309,310
$Al_4H_4$	-571	MP2	309,310
$Ga_4H_4$	-556	MP2	293
$In_4H_4$	-337	MP2	297
$Ga_4H_4$	-424	DFT (RI; BP86; def-SV(P))	311
$Ga_4[C(SiMe_3)_3]_4$	-197	DFT (RI; BP86; def-SV(P))	311
$Ga_4[Si(SiMe_3)_3]_4$	-419	DFT (RI; BP86; def-SV(P))	311
$Ga_4[Si(CMe_3)_3]_4$	-499	DFT (RI; BP86; def-SV(P))	311
$Ga_4[Ge(SiMe_3)_3]_4$	-365	DFT (RI; BP86; def-SV(P))	311
$Ga_4[NH_2]_4$	-56	DFT (RI; BP86; def-SV(P))	236
$Ga_4[NMe_2]_4$	-50	DFT (RI; BP86; def-SV(P))	236
$Ga_4[N(SiMe_3)dipp]_4$	-150	DFT (RI; BP86; def-SV(P))	236
$Ga_4[tmp]_4$	-173	DFT (RI; BP86; def-SV(P))	236

**Figure 3** Qualitative MO scheme for triel clusters  $E_4(NR_2)_4$  in  $D_{2d}$  symmetry.

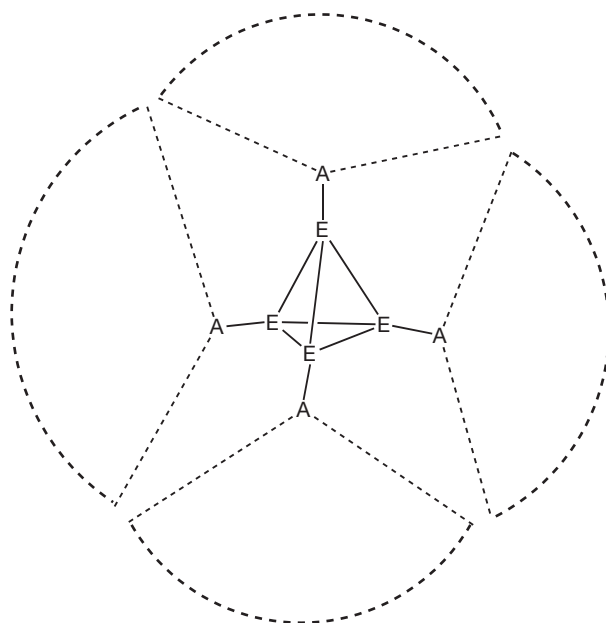
be viewed upon as tendency to open up the cage to a butterfly type structure as is observed for  $B_4(N^iPr_2)_4$ .

The E–X bonds shorten upon cluster formation from the monomers to tetramers, which is against the normal trend for bond lengths and coordination numbers. The lone-pair orbital of the monomers has a high s-character and is regarded as slightly antibonding for the E–X bond. On cluster formation, it gets involved in cluster bonding and loses its antibonding character.<sup>236</sup>

In addition to these electronic arguments, simple steric ones are applicable. Thus, in 176 and 178, the four monomers ( $Me_3Si$ )<sub>3</sub>AGa (A=C, Si) form a cavity of a given size, determined by the size of the substituents (Figure 4). The gallium atoms attached come nearer together if the Ga–A bonds are longer. Here, the gallium–carbon and gallium–silicon have an approximately 30 pm difference in length.

### 1.01.3.1.3 Reactivity

The cluster compounds of type  $E_4R_4$  have proved to be valuable starting materials for transition metal complexes, where ER groups are terminal or bridging ligands. This is described in Chapter 1.17. Oxidation of tetrahedral clusters with chalcogens gives heterocubanes (REY)<sub>4</sub> 188<sup>147,164,296,312–317</sup> or hexagonal prismatic cages (REY)<sub>6</sub> 189,<sup>317–321</sup> where all E–E bonds are broken. Careful oxidation of 184 with a thiirane afforded a

**Figure 4** Schematic representation of the steric requirements for  $Ga_4$ -clusters.

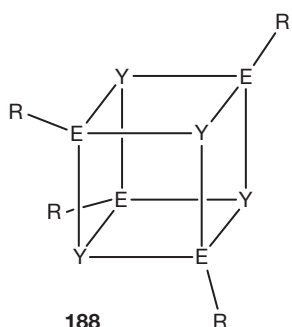
partially oxidized product  $R_4In_4S$  190.<sup>322</sup> The  $Ga_4$  core was retained in partial oxidation with halogens. For examples see Section 1.01.2.3.

$E_4$  cores are also present in  $[(ER)_3(ESiMe_3)Si(SiMe_3)]^-$  191 (E=Al)<sup>323</sup> and 192 (E=Ga, R=Si(SiMe<sub>3</sub>)<sub>3</sub>)<sup>215</sup> with trigonal bipyramidal  $E_4Si$  cores. Six sep make them *closo*-clusters according to the Wade rules. An alternative description as heterobicyclopentanes is not in agreement with delocalized bonding confirmed by quantum chemical calculations. These show extensive 3c2e bonds on the  $E_3$ -faces of the cage and significant bonding interactions between the equatorial triel atoms. These clusters are obtained from AlX solutions or 'Gal' with  $Li(thf)_3Si(SiMe_3)_3$ .

### 1.01.3.2 Higher $[E_nR_n]^{x-}$ Cluster Compounds

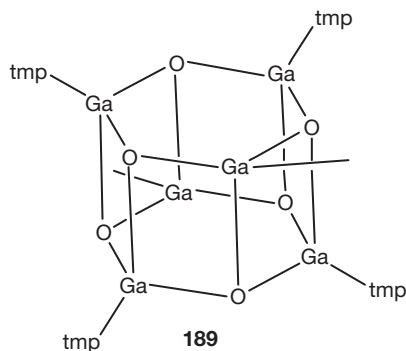
Only the  $[Al_6R_6]^-$  ion is described for hexaaluminum clusters as a radical ion. The compound is characterized on the basis of



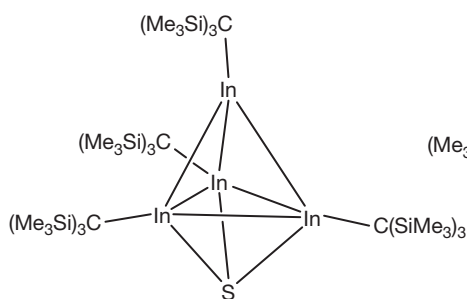


188

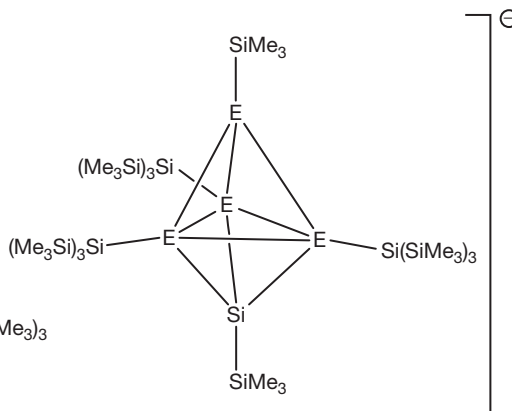
E = Al, Ga, In  
 Y = O, S, Se, Te  
 R = C(SiMe<sub>3</sub>)<sub>3</sub>, Si(SiMe<sub>3</sub>)<sub>3</sub>,  
 Si<sup>i</sup>Bu<sub>3</sub>, tmp, ...



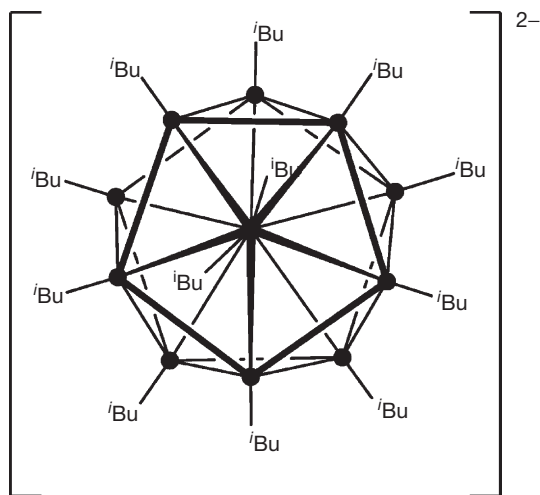
189



190



191 E = Al  
 192 E = Ga



193

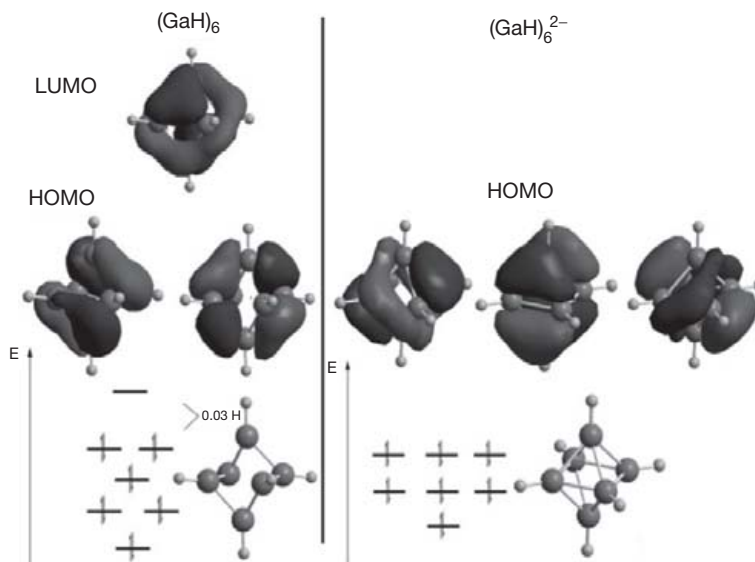
● = Al

its EPR spectrum, which exhibits the expected 31 lines by hyperfine coupling with six equivalent <sup>27</sup>Al nuclei.<sup>324</sup> The icosahedral cluster [Al<sub>12</sub><sup>i</sup>Bu<sub>12</sub>]<sup>2-</sup> 193<sup>325</sup> was obtained and structurally characterized [*d*<sub>Al–Al</sub> = 267.9–269.6 pm] at the beginning of the investigations on aluminum and gallium cluster compounds. It fulfills the Wade rules for a *closo* cluster and is a homolog to the *closo* boranate [B<sub>12</sub>H<sub>12</sub>]<sup>2-</sup>.

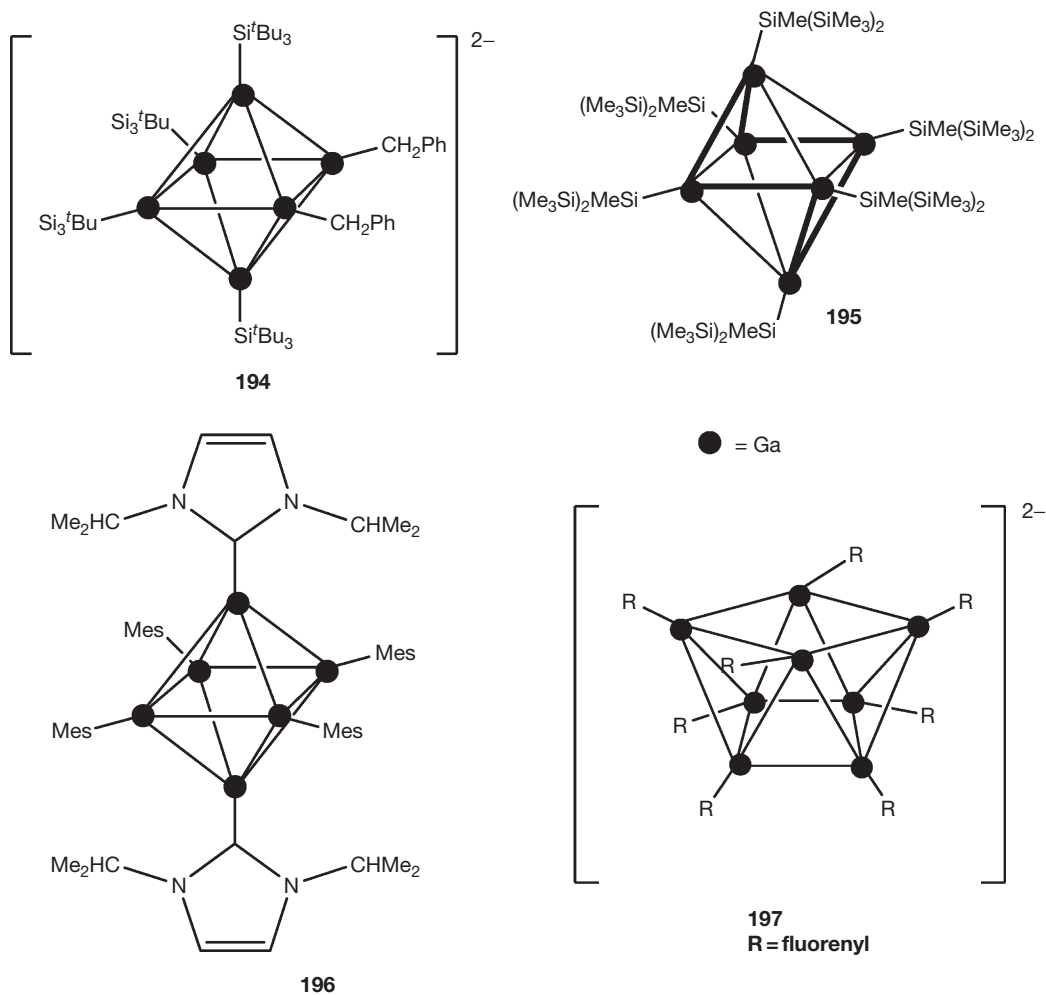
For gallium, a hexagallate [Ga<sub>6</sub>(SiPh<sub>2</sub>Me)<sub>4</sub>(CH<sub>2</sub>Ph)<sub>2</sub>]<sup>2-</sup> 194<sup>326</sup> features a nearly octahedral cluster core, as is expected for a *closo* cluster. The gallium–gallium distances are in line with a nearly regular octahedron (*d*<sub>Ga–Ga</sub> = 252.7–263.9 pm).

The neutral [Ga<sub>6</sub>(Si(SiMe<sub>3</sub>)<sub>2</sub>Me)<sub>6</sub>] 195<sup>326</sup> has only six sep and is regarded as a hypercloso cluster. As it becomes obvious from the MO scheme for octahedral clusters (Figure 5), with only 12 cluster electrons, a distorted structure is expected. This is realized for 195 as a distorted octahedron with six long (296 pm) and six short (251 pm) bonds. The triple degenerate HOMO in the *closo*-cluster [Ga<sub>6</sub>H<sub>6</sub>]<sup>2-</sup> is completely occupied. On oxidation to [Ga<sub>6</sub>H<sub>6</sub>] only four electrons are in these orbitals, which give rise to a distortion towards a structure with only a double degenerate HOMO. An alternative distortion would be the transition to a capped trigonal bipyramid, as observed for transition metal clusters [Os<sub>6</sub>(CO)<sub>18</sub>]<sup>29</sup> or predicted by DFT calculations for nonexistent B<sub>6</sub>H<sub>6</sub>.<sup>327</sup> DFT calculations on [Ga<sub>6</sub>H<sub>6</sub>] show the capped trigonal bipyramidal structure to be more stable by only 5 kJ mol<sup>-1</sup> than the observed distorted octahedral structure for 193. Here, the influence of the steric demanding substituents seems to be important.

A remarkable approach to gallium cluster R<sub>4</sub>Ga<sub>6</sub>(L)<sub>2</sub> 196 was recently reported.<sup>328–330</sup> The neutral cluster was obtained by reduction of the complex [GaCl<sub>2</sub>(Mes)L] (Mes = 2,4,6-Me<sub>3</sub>C<sub>6</sub>H<sub>2</sub>, L = 1,3-diisopropyl-4,5-dimethylimidazol-2-ylidene) with potassium in toluene. The six gallium atom



**Figure 5** Schematic representation of the MO- scheme for distortion of  $[\text{Ga}_6\text{H}_6]^{n-}$  ( $n=0, 2$ ). Reproduced with permission from Linti, G.; Coban, S.; Dutta, D. Z. *Allg. Anorg. Chem.* **2004**, 630, 319. Copyright Wiley-VCH Verlag GmbH & Co. KGaA.



adopts a slightly distorted octahedral structure ( $d_{\text{Ga-Ga}} = 251.1\text{--}259.1$  pm). Four RGa groups and two LGa units provide seven sep for this *closo*-cluster. This approach of reducing NHC-stabilized compounds was applied for successful preparation of compounds containing B<sub>2</sub>, Si<sub>2</sub>, and P–P bonded units (see also Chapter 1.16).<sup>331–334</sup>

Such discrepancies between expected structures from application of the Wade rules and realized ones in triel chemistry are quite common. [Ga<sub>8</sub>(fluorenyl)<sub>8</sub>]<sup>2-</sup> **197**<sup>335</sup> adopts a square antiprismatic structure and not the expected disphenoidal one, which is found for the octaboranate [B<sub>8</sub>H<sub>8</sub>]<sup>2-</sup>.<sup>336</sup> Even B<sub>8</sub>Cl<sub>8</sub> with only eight sep has a disphenoidal structure.<sup>337,338</sup>

The octaindium clusters [In<sub>8</sub>(SiPh<sub>3</sub>)<sub>8</sub>] **198a** and [In<sub>8</sub>(SiPh<sub>3</sub>)<sub>8</sub>]<sup>2-</sup> **198b** are obtained from InCp\* by reaction with MSiPh<sub>3</sub> (M = Li(thf)<sub>3</sub>, Na(thf)<sub>n</sub>) (eqn [12]). Compound **198a** has a ‘snub disphenoidal’ In<sub>8</sub> core,<sup>339</sup> which shows a transition to distorted square antiprismatic (**198b**) upon two electron reduction.<sup>270</sup> DFT calculations (BP86-functional, def-SV(P)-base) show the square antiprismatic structure to be more favorable for anionic clusters of indium and gallium and disphenoidal for neutral ones.

Each of the indium atoms in **198a** is bonded to a triphenylsilyl group with indium–silicon distances of 260 pm on an average [ $d_{\text{In-Si}} = 257.0(5)\text{--}262.2(5)$  pm]. This is shorter than those in clusters with the more bulky tri(*tert*-butyl)silyl groups as substituents [ $d_{\text{In-Si}} = 265$  pm (**239**), 268 pm (**206**)]. The indium–indium distances in the cluster vary between 285.5 and 328.2 pm. The deviation of ideal D<sub>2d</sub> symmetry is significant. This spreading is comparable to that in other indium clusters (vide infra). For the tetrahedral cluster **186** indium–indium distances of 290 pm are observed. On reduction to **198b** the distances change. Overall, a shrinking of the indium–indium distances is observed.

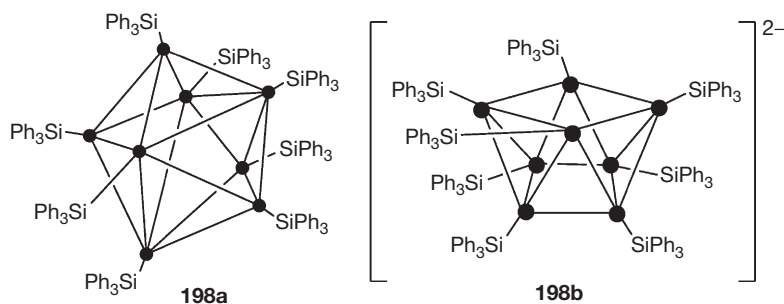
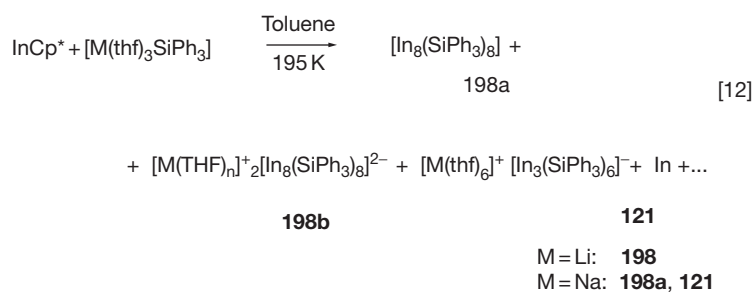
A nonagallane cluster [Ga<sub>9</sub><sup>+</sup>Bu<sub>9</sub>] **199** was obtained as dark green crystals as byproduct of the large-scale preparation of Ga<sup>+</sup>Bu<sub>3</sub>.<sup>297,340</sup> The gallium atoms are at the corners of a tricapped trigonal prism. Here, short Ga–Ga distances

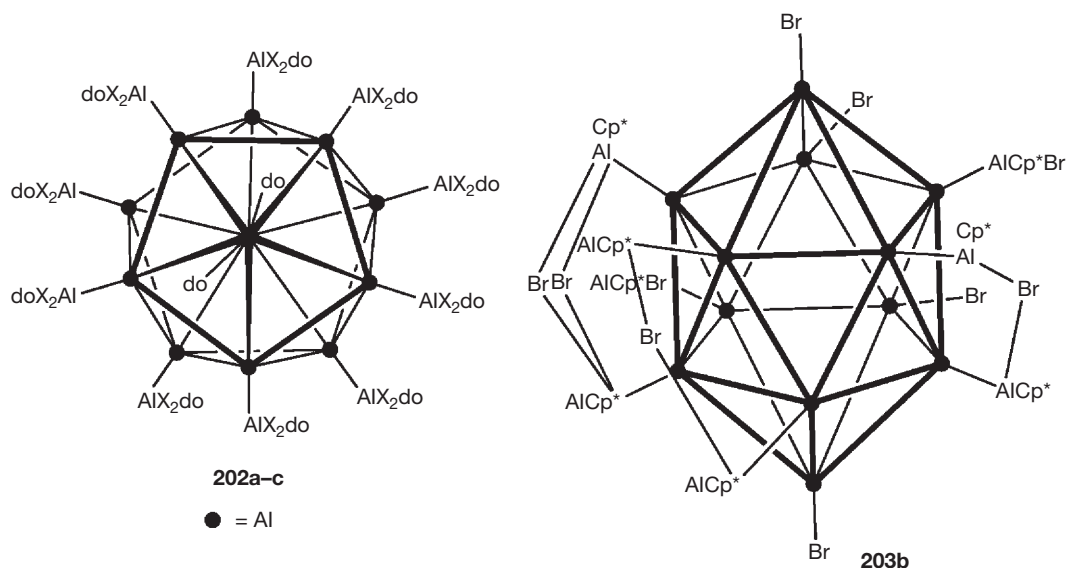
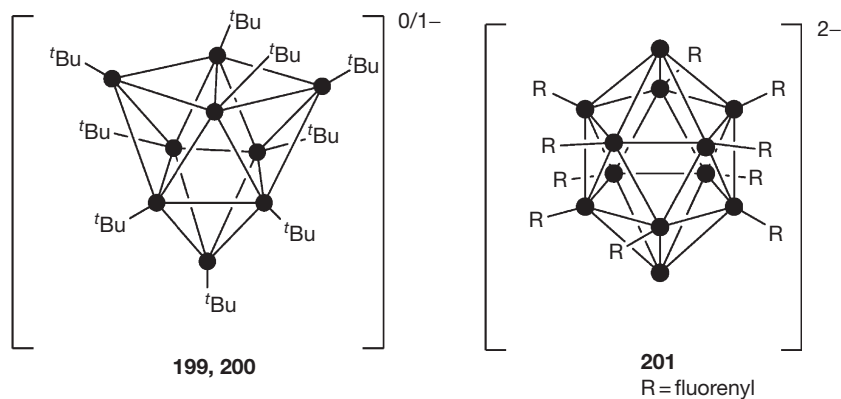
( $d_{\text{Ga-Ga}} = 259$  pm) are observed for the capping gallium atoms, and longer ones (up to  $d_{\text{Ga-Ga}} = 299$  pm) parallel to the threefold axis of the cluster. This makes the structure near a mono-capped square antiprism, which is the expected structure for an E<sub>9</sub> cluster with nine sep. A reversible one-electron reduction of **199** was demonstrated by cyclic voltammetric studies ( $E^0 = -1.74$  V against FeCp<sub>2</sub>]<sup>0/+1</sup>). On a preparative scale **199** was reduced to **200** by CoCp\*<sub>2</sub>. The radical anion **200** has a very similar structure to the neutral compound **199**, only the Ga–Ga distances parallel the threefold axis shrink by 17 pm.

Icosahedral clusters of type [E<sub>12</sub>R<sub>12</sub>]<sup>2-</sup> are only realized for aluminum with **193**. The cluster was obtained in small amounts by reduction of <sup>t</sup>BuAlCl<sub>2</sub> with potassium. [Ga<sub>12</sub>(fluorenyl)<sub>10</sub>]<sup>2-</sup> **201** is similar, and also has an icosahedral cluster core.<sup>341</sup> The formal oxidation of this cluster to a [Ga<sub>12</sub>R<sub>12</sub>]<sup>2-</sup> cluster is hindered by the unfavorable energy of the HOMO as quantum chemical calculations indicate.

In Section 1.01.2.3 electron-precise aluminum subhalides of type Al<sub>4</sub>X<sub>4</sub>·4do are described as crystallized products from metastable aluminum monohalide solutions. Under varied conditions (type of donor, concentration) higher subhalides of type Al<sub>22</sub>X<sub>20</sub>·12do (do = thf, thp = tetrahydropyrene) **202a–c** are obtained.<sup>226,227</sup> Compounds of type **202** show icosahedral Al<sub>12</sub> cores, where ten aluminum atoms bear AlX<sub>2</sub>(do) substituents. The apical aluminum atoms are each ligated by one donor molecule. Thus, the *closo*-Al<sub>12</sub> core has 13 sep, 10 × 2 electrons from 10 Al[AlX<sub>2</sub>(do)] groups and 2 × 3 electrons from the two Al(do) fragments.

An icosahedral Al<sub>12</sub> core is also present in Al<sub>20</sub>Cp\*<sub>8</sub>X<sub>10</sub> (X = Cl, Br) **203a,b**.<sup>54</sup> Here, six aluminum atoms of the icosahedral core are bonded to AlCp\*(X) substituents, two to AlCp\* groups. These aluminum atoms are joined, in addition, by bridging halides. The remaining four cluster aluminum atoms are part of AlBr groups. Thus, electron bookkeeping for the Al<sub>12</sub> cluster core makes 4 × 2 (AlBr) + 2 × 3 (AlAlCp\*) + 6 × 2 (AlAlCp\*X) = 26 electrons necessary for an icosahedral *closo*-polyhedron.





Several related  $\text{Ga}_{22}$  clusters with icosahedral cores are known and are described in [Section 1.01.4.3](#).

### 1.01.3.3 Aromaticity of $[\text{E}_n\text{R}_m]^{x-}$ Cluster Compounds

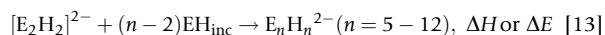
Various concepts have been introduced to explain the structures and stoichiometry of main group cluster compounds. The most commonly known are the Wade–William–Rudolph rules.<sup>22,271,342</sup> For higher, conjugated clusters, they were modified by Jemmis.<sup>343,344</sup> Element-rich clusters  $[\text{E}_n\text{R}_m]^{x-}$ , especially the heavier elements of group 13, were classified as metalloids (see [Section 1.01.4.1](#)).<sup>13,275</sup>

Cluster compounds such as the polyhedral boranates  $[\text{B}_n\text{H}_n]^{2-}$  have been discussed as three-dimensional aromatic systems.<sup>345–347</sup> A diatropic ring current is the most typical property of an aromatic molecule.<sup>348</sup> For endohedral fullerenes, it was proved that chemical shifts for atoms in endohedral and exohedral positions behave similar to shifts of atoms in and out of the ring plane of an aromatic hydrocarbon, respectively.<sup>349</sup> Quantification of aromaticity by the calculated magnetic shielding constants at selected regions of a molecule, where no atoms reside, was suggested. The resulting nuclear-independent shifts (NICS) are negative (diatropic) for

aromatic molecules, positive (paratropic) for antiaromatic ones and approximately zero for nonaromatic molecules.<sup>348</sup>

The skeletal number of electrons, as well as the substituents of boron cluster compounds, influence the NICS values in the center of clusters.<sup>350</sup>  $\text{B}_8\text{Cl}_8$  and  $\text{B}_9\text{Cl}_9$  are well-known compounds,<sup>351</sup> but it was not possible to prepare  $\text{B}_8\text{H}_8$  and  $\text{B}_9\text{H}_9$ .  $\text{B}_9\text{F}_9$  as well as  $[\text{B}_8\text{H}_8]^{2-}$ <sup>(338)</sup> and  $[\text{B}_9\text{H}_9]^{2-}$ <sup>(336)</sup> are aromatic according to NICS values in the cluster center. Only the last one is a *closo*-cluster compound by the Wade-rules.  $\text{B}_9\text{H}_9$ , in contrast, is paratropic, that is, anti-aromatic. Similarly,  $\text{B}_4\text{F}_4$  is classified as aromatic and nonexistent  $\text{B}_4\text{H}_4$  as antiaromatic.<sup>352</sup> Various criteria of aromaticity are fulfilled for the icosahedral *closo*-boranate  $[\text{B}_{12}\text{H}_{12}]^{2-}$ . Its NICS value is diatropic.<sup>353–355</sup> The isoelectronic  $\text{Si}_{12}^{2-}$  and  $\text{Ge}_{12}^{2-}$  follow the Wade rules, obviously. Nevertheless, paratropic NICS values are obtained for these Zintl ions. This was explained by the different influence of hydrogen atoms and lone pairs on the cluster molecule orbitals. Naked cluster ions of heavier group 13 elements of type  $\text{E}_4^{2-}$  and  $[\text{E}_2\text{X}_2]^{n-}$  [ $\text{E} = \text{Al, Ga, In}$ ;  $\text{X} = \text{Na, Si, Ge}$ ], with planar rings, have also been characterized as aromatic compounds.<sup>356–368</sup> A  $2\pi$ -metalloaromatic ring is present in  $\text{Na}_2[\text{Ga}_3\text{Aryl}_3]$  [ $\text{Aryl} = 2,4,6\text{-}t\text{Bu}_3\text{C}_6\text{H}_2$ ].<sup>369</sup> For example, a NICS value of  $-45$  ppm has been calculated for the model compound  $[\text{Ga}_3\text{H}_3]^{2-}$ .<sup>142,345</sup>

A detailed study on aromaticity of *closo*-boranates  $[B_nH_n]^{2-}$  ( $n=5-12$ ) by Schleyer et al.<sup>354</sup> uses geometrical and energetic criteria as well as NICS values. A reaction (eqn[13]), describing the formation of *closo*-clusters  $[E_nH_n]^{2-}$  ( $n=5-9$ ; E=B, Al, Ga, In) from an ethyne analog  $[E_2H_2]^{2-}$  and an appropriate number of incremental EH units, is used as energetic criterion. The formation energy increases with growing cluster size; therefore,  $\Delta H/n$  as averaged bonding energy of each EH vertex is used as a criterion. Plotting  $\Delta H/n$  against  $n$ , Schleyer observed local minima for clusters with highest symmetry  $[B_6H_6]^{2-}$  und  $[B_{12}H_{12}]^{2-}$ , which means that all other cluster sizes are less stabilized.



A classical criterion for aromaticity is equalization of bond lengths, for which the deviation  $\Delta R$  is a measure.

Polyhedral cluster ions  $[E_nH_n]^{2-}$  (E=B, Al, Ga, In;  $n=5-9$ ) were investigated by the means described above.<sup>354,370,371</sup> The results are summarized in Table 13. Inspecting the change of the values  $\Delta E/n$  against the number of cluster atoms  $n$  (Figure 6) reveals a special stabilization of octahedral clusters for boron and aluminum, while octanuclear bisphenoidal gallium and indium clusters are preferred. In fact, 197 and 198 have a square antiprismatic structure, which demonstrates this stabilization of  $E_8$ -clusters even more. In the case of aluminum and gallium, the curves between values for  $[E_6H_6]^{2-}$  to  $[E_8H_8]^{2-}$  are flat, showing that in this region, cluster size is not determined electronically but might be influenced by the steric demand of the substituents.

**Table 13** Results for *closo*-cluster  $[E_nH_n]^{2-}$  (E=B, Al, Ga, In;  $n=5-9$ )

	$\Delta E/n^a$	$\Delta R^b$	NICS <sup>c</sup>	NICS <sup>d</sup>
$[B_5H_5]^{2-}$	-96.47	0.139	-24.8	
$[B_6H_6]^{2-}$	-123.35	0.002	-29.9	
$[B_7H_7]^{2-}$	-117.07	0.168	-23.4	
$[B_8H_8]^{2-}$	-109.00	0.281	-20.0	
$[B_9H_9]^{2-}$	-109.87	0.260	-22.9	
$[Al_5H_5]^{2-}$	-111.62	0.301	-7.7	
$[Al_6H_6]^{2-}$	-131.17	0.004	-24.3	
$[Al_7H_7]^{2-}$	-130.32	0.299	-22.1	
$[Al_8H_8]^{2-}$	-129.58	0.302	-18.3	
$[Al_9H_9]^{2-}$	-127.85	0.290	-14.2	
$[Ga_5H_5]^{2-}$	-88.17	0.393	0.7	-1.7
$[Ga_6H_6]^{2-}$	-103.06	0.021	-24.3	-22.5
$[Ga_7H_7]^{2-}$	-104.03	0.424	-22.1	-20.5
$[Ga_8H_8]^{2-}$	-105.19	0.618	-16.8	-16.1
$[Ga_9H_9]^{2-}$	-99.49	0.311	-12.1	-13.0
$[In_5H_5]^{2-}$	-75.51	0.531		9.7
$[In_6H_6]^{2-}$	-86.26	0.147		-15.4
$[In_7H_7]^{2-}$	-88.72	0.683		-13.0
$[In_8H_8]^{2-}$	-92.83	0.774		-17.5
$[In_9H_9]^{2-}$	-85.93	0.309		-7.6

<sup>a</sup>Electronic energy in a.u., BP86/def-SV(P); averaged electronic energy per EH unit energy ( $\Delta E/n$ , kJ mol<sup>-1</sup>) according to eqn[13].

<sup>b</sup>Relative electronic ( $\Delta E$ , kJ mol<sup>-1</sup>). Deviation of bond lengths ( $\Delta R$ , Å).

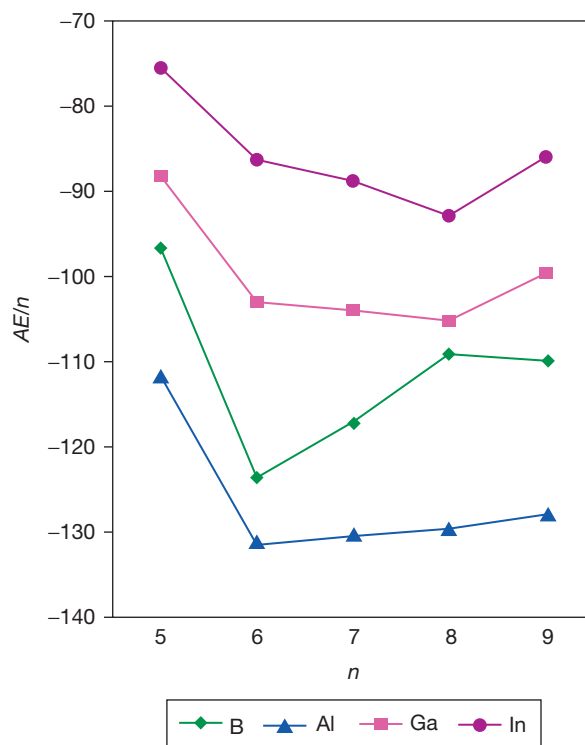
<sup>c</sup>Nucleus-independent chemical shifts (NICS, ppm), Functional: B3LYP, Base set: 6-311 G\*\*.

<sup>d</sup>Nucleus-independent chemical shifts (NICS, ppm), Functional B3LYP, Base set LANL2DZ with Huzinaga polarization.

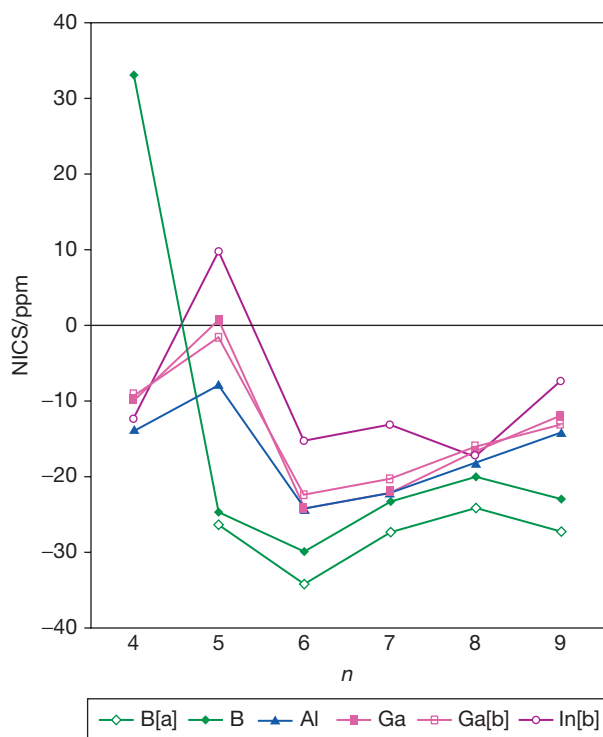
The deviation in bond lengths with cluster size is not really dependent on  $E$ . Nearly ideal octahedral structures with a  $\Delta R$  near zero are calculated for  $[E_6H_6]^{2-}$ . For  $[E_8H_8]^{2-}$ , the deviation is largest for all elements. Overall, in the homolog row from boron to indium, the deviation of  $\Delta R$  increases.

The discussion of aromaticity of  $[E_nH_n]^{2-}$  molecules (Figure 7, Table 14) on the basis of NICS values is confined here primarily to those in the cluster centers. Because the NICS values directly on triangular cluster faces are usually negative, it is important to take into account their change on a trajectory to the cluster center. The problem is shown for  $[B_5H_5]^{2-}$ . Of  $[E_5H_5]^{2-}$  cluster ions, a largely negative value classifies only the pentaboranate as an aromatic system. For all other group 13 elements, the trigonal-bipyramidal cluster should be classified as nonaromatic. NICS values 1 Å above a B<sub>3</sub>-face in  $[B_5H_5]^{2-}$  are -16.7 ppm. The center of a face is only 0.57 Å off the center, and the cluster center itself is part of a three-membered ring, with a distance of only 0.53 Å from edge to center. This means the influence of the electron densities on edges and faces sums up to a highly negative NICS value in the center. As a consequence, Aihara classified  $[B_5H_5]^{2-}$  as nonaromatic.<sup>347</sup>

A fusion of two tetrahedra via a common face is not allowed for boron<sup>372</sup>. Similarly, in  $[Al_5H_5]^{2-}$ , the influence of the electron density on the faces, which are only 0.86 Å distant from the center, sums up to a negative NICS in the cluster. Thus, based on geometrical, energetic, and magnetic criteria, *closo*-cluster compounds  $[E_5H_5]^{2-}$  (E=B, Al, Ga, In) are



**Figure 6** Averaged relative energy per EH unit  $\Delta E/n$  against number of cluster atoms  $n$  in  $[E_nH_n]^{2-}$ . Reproduced with permission from Linti, G.; Bühler, M.; Monakhov, K.; Zessin, T. In *Modeling of Molecular Properties*; Comba, P., Ed.; Wiley-VCH: Weinheim, 2011; p 455. Copyright Wiley-VCH Verlag GmbH & Co. KGaA.



**Figure 7** NICS values in cluster center of  $E_4H_4$  and *closo*-clusters  $[E_nH_n]^{2-}$  ( $E = B, Al, Ga, In; n = 5-9$ ) (B3LYP-functional, 6-311 G\*\* base for B, Al, Ga and [b] LANL2DZ base with Huzinaga polarization for Ga, In). [a] NICS values from literature<sup>354</sup> for *closo*-boranates  $[B_nH_n]^{2-}$  ( $n = 5-9$ ). Reproduced with permission from Linti, G.; Bühler, M.; Monakhov, K.; Zessin, T. In *Modeling of Molecular Properties*; Comba, P., Ed.; Wiley-VCH: Weinheim, 2011; p 455. Copyright Wiley-VCH Verlag GmbH & Co. KGaA.

nonaromatic. This is a possible explanation for why it has not been possible till now for clusters of this to be synthesized. Only derivatives<sup>322,348,373,374</sup> such as, for example, carbaboranes and a silagallanate  $[Me_3SiSi(GaR)_3GaSiMe_3]^-$  ( $R = Si(SiMe_3)_3$ )<sup>215</sup> are known.

All higher clusters have negative NICS values for all elements examined. For octahedral boron, aluminum, and gallium clusters, the NICS values are most negative, for indium the octanuclear cluster is the extreme.

Here, it has to be noted that for tetrahedral cluster compounds  $E_4H_4$ , only the borane cluster has a positive NICS value; the higher homologs exhibit negative ones. According to Schleyer<sup>352</sup>  $B_4H_4$  is antiaromatic.

Compared to *closo*-boranates, central NICS values are smaller for heavier homologs. Together with highly negative NICS on the faces, these clusters are only weak three-dimensional aromatic molecules. It may be seen as an accidental coincidence that for indium, aromaticity criteria show octaindium clusters  $[In_8R_8]^{2-}$  the most stable, which are the only one prepared, so far.

## 1.01.4 Element-Rich Cluster Compounds

### 1.01.4.1 Introduction

Reactions of triel subhalides, that is,  $Ga_2X_4 \cdot 2$ dioxane, 'Gal' metastable EX solutions ( $E = Al, Ga$ ),  $InX$  often proceed with

redox disproportionation. Thus, compounds with triel atoms in oxidation state +III and elemental triels  $E^0$  result. But the latter is not a necessity. It was observed that  $E^0$  can be incorporated in ER cluster frameworks to produce element-rich clusters  $[E_mR_n]^{x-}$  ( $m > n; x = 0, -1, \dots$ ). For those clusters, where naked triel atoms are bonded only to other triel atoms, the term metalloid was created.<sup>4-7</sup> More specifically, metalloid here means that the triel cores of the clusters resemble sections of structural features of the elements. But this is not necessarily the case for all element-rich clusters described in this section. For example, clusters of type  $[Ga_9R_6]^-$  and  $Ga_{10}R_6$  are element-rich but their structure can be described on the basis of polyhedral descriptions, while an  $Al_7R_6$  built from two fused tetrahedral was discussed as a section of a close-packed structure. This also shows that a definition of metalloid is not sharp and cannot generally be related to special bonding situations. We will use the term element-rich as the more general one, and will confine metalloid to those clusters where element-structure relationships are obvious.

Mixed oxidation states are assigned to the building metal atoms in these cluster types. They average to values  $0 < x < 1$ . This makes them different from polyhedral clusters  $[E_nR_m]^{x-}$  ( $m \geq n$ ), where the Wade rules are valid and can be used for structure elucidation by electron bookkeeping.

For element-rich or metalloid clusters, they often fail or the counting has to be modified. Special types of cluster compounds are naked metal clusters, prepared and observed in the gas phase. For example, mass spectrometry revealed the special stability of sodium clusters of defined size. The so-called Jellium model was used to explain stability islands of clusters with 8, 20, 40, 58, and 70 electrons.<sup>375-377</sup> Such pure metal clusters are not discussed here, but this model was successfully applied for some metalloid clusters.


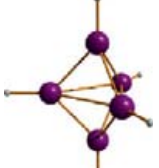

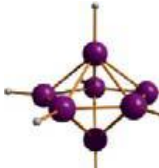
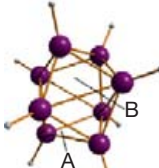
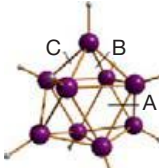
Most of the clusters described in this section are nanoscaled cluster molecules and some of them have fascinating properties. Beginning from  $Ga_{26}$  clusters, the crystals are metallic lustrous and for a  $Ga_{84}$  cluster, crystals are superconducting at low temperatures. Nevertheless, the complicated synthesis and in many cases the sensitivity against air and moisture give them drawbacks compared to noble metal clusters and salt-like clusters, which are sections of semiconductor material frameworks.

Preparation of these element-rich clusters starts from subhalides of the triels, normally. Monohalides are prepared by a combination of high temperature and cryo techniques. Aluminum or gallium is reacted with gaseous hydrogen halides  $HX$  ( $X = Cl, Br, I$ ) at 1100–1300 K in vacuo ( $10^{-1}$  mbar).<sup>7,12,75-77,243,378</sup> The resulting diatomic monohalides are trapped at low temperatures (100 K) together with appropriate solvents, for example a toluene/thf mixture. This is done in a condensation apparatus, described elsewhere.<sup>7,12,76,77,243,378,379</sup> On warming up, metastable solutions of the monohalides are obtained, which can be stored at 195 K for months.

For gallium, sonochemically initiated reaction of the elements gallium and iodine (1:1 ratio) in toluene leads to 'Gal', a greenish, amorphous substance, which reacts in many reactions as expected from a monohalide. Raman investigations revealed  $Ga_4I_6$  as one of the possible components (Figure 8).<sup>380</sup>



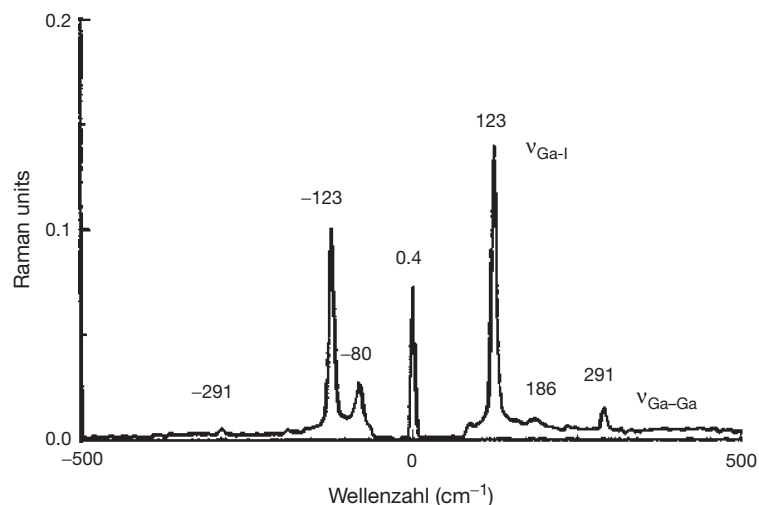
**Table 14** NICS (ppm) of  $E_4H_4$  and of the *closo*-Wade cluster  $[E_nH_n]^{2-}$  ( $E = B, Al, Ga, In; n = 5-9$ )

	NICS							
	Center	Face	1 Å above face					
$E_4H_4$								
	$B_4H_4$	33.0	25.5	-7.7				
	$Al_4H_4$	-13.9	-15.7	-13.2				
	$Ga_4H_4$	-10.0	-13.5	-12.3				
	$Ga_4H_4$	-9.2	-12.6	-12.8				
	$In_4H_4$	-12.7	-15.6	-13.3				
$[E_5H_5]^{2-}$								
	$[B_5H_5]^{2-}$	-24.8	-32.7	-16.7				
	$[Al_5H_5]^{2-}$	-7.7	-11.3	-8.2				
	$[Ga_5H_5]^{2-}$	0.7	-6.8	-6.5				
	$[Ga_5H_5]^{2-}$	-1.7	-8.5	-8.0				
	$[In_5H_5]^{2-}$	9.7	2.9	-1.2				
$[E_6H_6]^{2-}$								
	$[B_6H_6]^{2-}$	-29.9	-43.6	-14.4				
	$[Al_6H_6]^{2-}$	-24.3	-26.7	-14.1				
	$[Ga_6H_6]^{2-}$	-24.3	-31.0	-16.5				
	$[Ga_6H_6]^{2-}$	-22.5	-29.0	-16.1				
	$[In_6H_6]^{2-}$	-15.4	-20.9	-13.5				
$[E_7H_7]^{2-}$								
	$[B_7H_7]^{2-}$	-23.4	-37.8	-13.8				
	$[Al_7H_7]^{2-}$	-22.1	-24.8	-13.3				
	$[Ga_7H_7]^{2-}$	-22.1	-27.8	-14.9				
	$[Ga_7H_7]^{2-}$	-20.5	-26.2	-14.9				
	$[In_7H_7]^{2-}$	-13.0	-23.6	-14.9				
	$[E_8H_8]^{2-}$	NICS						
		Center	Face A	Face B	1 Å above face A	1 Å above face B		
	$[B_8H_8]^{2-}$	-20.0	-34.9	-36.1	-10.3	-13.4		
	$[Al_8H_8]^{2-}$	-18.3	-21.8	-22.7	-10.7	-11.2		
	$[Ga_8H_8]^{2-}$	-16.8	-26.5	-23.3	-11.7	-11.5		
	$[Ga_8H_8]^{2-}$	-16.1	-25.7	-22.5	-12.2	-12.1		
	$[In_8H_8]^{2-}$	-17.5	-24.3	-21.7	-12.8	-12.2		
	$[E_9H_9]^{2-}$	NICS						
		Center	Face A	Face B	Face C	1 Å above face A	1 Å above face B	1 Å above face C
	$[B_9H_9]^{2-}$	-22.9	-35.9	-37.4	-42.6	-14.4	-9.9	-10.9
	$[Al_9H_9]^{2-}$	-14.2	-18.3	-17.5	-20.1	-7.6	-7.9	-11.2
	$[Ga_9H_9]^{2-}$	-12.1	-19.5	-20.0	-21.0	-15.5	-8.9	-11.2
	$[Ga_9H_9]^{2-}$	-13.0	-20.1	-20.3	-21.7	-9.6	-9.6	-12.0
	$[In_9H_9]^{2-}$	-7.6	-15.0	-13.6	-13.6	-7.0	-7.5	-9.9

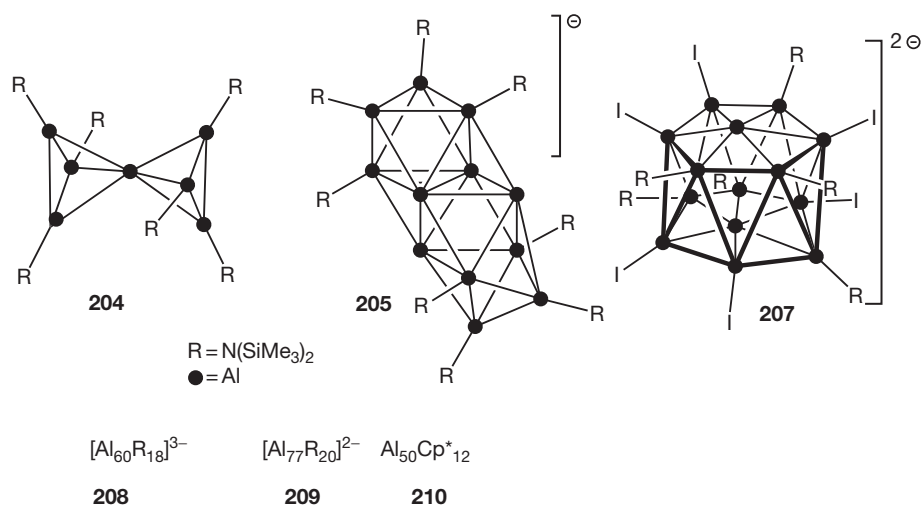
(B3LYP-functional, 6-311 G\*\*-base set for boron, aluminum, gallium; LANL2DZ-base set with Huzinaga polarization for gallium and indium). Figures show structures of indium cluster compounds.

Reproduced with permission from Linti, G.; Bühler, M.; Monakhov, K.; Zessin, T. In *Modeling of Molecular Properties*; Comba, P. Ed.; Wiley-VCH: Weinheim, 2011; p. 455. Copyright Wiley-VCH Verlag GmbH & Co. KGaA.





**Figure 8** FT-Raman spectrum of 'Gal' showing characteristic bands for  $\text{Ga}_4\text{I}_6$ .



**Figure 9** Overview of element-rich aluminum cluster types.

The behavior of 'Gal' against donor solvents like thf is different to metastable Gal solutions, obtained via the high-temperature route. It does not dissolve, but disproportionation occurs into gallium metal and gallium triiodide. With some donor molecules, intermediate oxidation states were trapped (e.g., 26, 111). Alternatively 'GaOSO<sub>2</sub>CF<sub>3</sub>' prepared from GaCp\* and HOSO<sub>2</sub>CF<sub>3</sub> was used in cluster synthesis.<sup>381</sup>

Indium halides often show disproportionation as the preferred reaction pathway on attempted substitution reactions. Better results are obtained by the use of InCp\* and reacting it with nucleophiles MR under elimination of MCp\* (M = Li, Na, K).

The chemistry of metalloid aluminum and gallium clusters was reviewed several times (see, e.g., Schnöckel,<sup>9,10</sup> Linti and Schnöckel,<sup>12</sup> Linti et al.<sup>275</sup>). Therefore, here a brief overview of the structural variety and relationships between cluster types will be given, rather than a complete treatment of all details of synthesis and structures. Due to significant differences, a separate description by elements will be applied.

#### 1.01.4.2 Aluminum Cluster Compounds

Cluster sizes range from Al<sub>7</sub> to Al<sub>77</sub> (Figure 9). [Al<sub>7</sub>R<sub>6</sub>]<sup>−</sup> 204 [R = N(SiMe<sub>3</sub>)<sub>2</sub>] consists of two corner-sharing aluminum tetrahedral, with staggered orientation of the two Al<sub>3</sub>R<sub>3</sub> rings.<sup>6</sup> The Al–Al distances are about 260 pm in the Al<sub>3</sub>R<sub>3</sub> rings and up to 20 pm longer for the other distances. Therefore, an ionic description consisting of two metalloaromatic [Al<sub>3</sub>R<sub>3</sub>]<sup>2−</sup> rings coordinating a central cation Al<sup>3+</sup> was suggested, but is not consistent with results of DFT calculations, which predict no significant charge differences on the aluminum atoms. The Al<sub>7</sub> core of 204 is viewed upon as a section of a close-packed aluminum structure, where six neighbors of the central aluminum atom are missing.

[Al<sub>12</sub>R<sub>8</sub>]<sup>−</sup> 205 [R = N(SiMe<sub>3</sub>)<sub>2</sub>] represents a larger section of the close packing of elemental aluminum.<sup>382</sup> Topologically, it can be described as a reduced dimer of two distorted octahedral Al<sub>6</sub>R<sub>4</sub> fragments, where dimerization occurs through linkage of octahedral faces. This results in a cluster core of three

penetrating octahedral and allows description as *conjuncto*-alane.

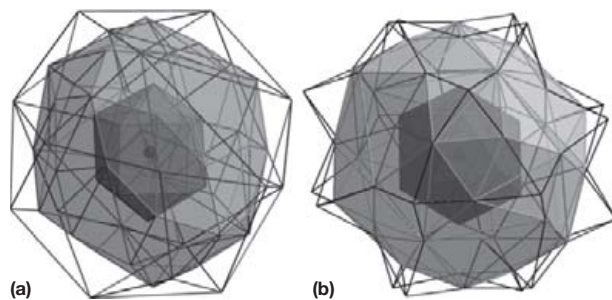
A similar structure is observed for  $\text{In}_{12}(\text{Si}^t\text{Bu}_3)_8$  **206**, obtained by thermolysis of  $\text{In}_2(\text{Si}^t\text{Bu}_3)_4$ .<sup>383</sup> The *conjuncto*-cluster description is also in accordance with a postulated pathway of formation, starting from  $\text{In}_2(\text{Si}^t\text{Bu}_3)_4$ , which might proceed via  $\text{In}_6(\text{Si}^t\text{Bu}_3)_4$  with elimination of  $(\text{Si}^t\text{Bu}_3)_2$ .

For the aluminum cluster, the formation is thought to be a growth process initiated by disproportionation and the clusters are intermediates on the way to the metal. But both ideas need not be exclusive. Thus, description of **205** and **206** as metalloid clusters and as *conjuncto*-clusters, in analogy to *conjuncto*-boranes, is possible. The application and limits of electron counting rules will be discussed later in this chapter.

An even larger cluster,  $[\text{Al}_{14}\text{R}_6\text{I}_6]^{2-}$  **207** [ $\text{R}=\text{N}(\text{SiMe}_3)_2$ ], has a skeleton of two staggered aluminum-centered  $\text{Al}_6$ -rings, where the ring aluminum atoms are bonded to iodine or  $\text{N}(\text{SiMe}_3)_2$  groups. The naked aluminum atoms are slightly above the planes of the rings. Thus, a flattened  $\text{Al}_{14}$  polyhedron, a bicapped hexagonal antiprism, results. **207**, by common counting rules, has eight sep, which are necessary for a *closo*-cluster. A 14-vertex polyhedron, as bicapped hexagonal antiprism, is observed for metallocarboranes, for example.<sup>384</sup> The flattening observed for **207** might be reasonable by partial participation of the aluminum lone pairs and formation of a bonding interaction between the apical aluminum atoms. Such a flattening was discussed for certain indium and gallium clusters, too.<sup>385,386</sup> Thus,  $\text{In}_{11}^{7-}$ , present in a Zintl phase, has three flattened vertices, which allow for 12 sep, required for a *closo*-cluster. In line with this description are the results of quantum chemical calculations, which show a regular  $\text{Al}_{14}$  polyhedron as energetically unfavorable.

On the other hand, **207** is described as a typical metalloid cluster because the core structure of two-centered  $\text{Al}_6$  rings can be transformed by rotation and a translational shift into a section of the structure of metallic aluminum.

With  $\text{R}=\text{N}(\text{SiMe}_3)_2$  as substituent, the largest aluminum clusters have been obtained (Figure 10). Cores of 69 (**208**) and 77 (**209**) aluminum atoms are surrounded by 18 or 20 R groups, respectively.<sup>387,388</sup> Both clusters are built up in shells, where a central aluminum atom is surrounded by 12 atoms, as inner building unit. These  $\text{Al}@\text{Al}_{12}$  ( $\text{Al}_{13}$ ) cores are



**Figure 10** Cluster cores of **208** and **209**. Dark gray: central  $\text{Al}@\text{Al}_{12}$  core; light gray: shell of 38 and 44 naked Al atoms, respectively; lines:  $\text{Al}[\text{N}(\text{SiMe}_3)_2]$  shell. Reproduced with permission from Linti, G.; Schnöckel, H.; Uhl, W.; Wiberg, N. In *Molecular Clusters of the Main Group Elements*; Driess, M., Nöth, H., Eds.; Wiley-VCH: Weinheim, 2004; pp 126–168. Copyright Wiley-VCH Verlag GmbH & Co. KGaA.

the center of two more shells of aluminum atoms, 38 atom and 18 atom shells in **208** and a 44 atom and outer 20 atom shell in **209**. The aluminum atoms of the outer shells are each bonded to terminal R groups. According to this, the aluminum–aluminum distances decrease from the inner ( $d_{\text{Al-Al}}=278$  pm on an average) to the outer shells ( $d_{\text{Al-Al}}=268$  pm on an average), indicating a transition from a metal-type bond to more localized bonding modes between the aluminum atoms. The distances of the central Al atom to the surrounding 12 Al atoms are nearly identical to those in the shell.

Describing this in more detail, the  $\text{Al}_{13}$  cores are different for **208** and **209**. The  $\text{Al}_{69}$  cluster has a distorted decahedral core,<sup>389</sup> based upon a  $D_{5h}$  symmetric structure, whereas in the  $\text{Al}_{77}$  cluster, the  $\text{Al}_{13}$  core is nearly icosahedral.

These huge main group clusters are often compared to noble metal cluster compounds such as  $\text{Au}_{55}(\text{PPh}_3)_{12}\text{Cl}_6$ <sup>390</sup> or  $\text{Pd}_{145}(\text{CO})_{60}(\text{PR}_3)_{30}$ .<sup>391</sup> For the gold cluster, a central  $\text{Au}_{13}$  core with either an icosahedral or cuboctahedral structure was postulated. No crystal structure is available till now. Thirty-seven naked gold atoms are present. In the larger, structurally characterized  $\text{Au}_{102}$  cluster, 39 naked gold atoms form the cluster core.<sup>392</sup> The  $\text{Pd}_{145}$  cluster has a filled icosahedral  $\text{Pd}@\text{Pd}_{12}$  core, where the distances of the central palladium atom to the shell are shorter than those in the shell. Obviously, the structures of the cores of these clusters ( $\text{Al}_{69}$ ,  $\text{Al}_{77}$ ,  $\text{Pd}_{145}$ ) deviate from those of the bulk metals. On the one hand, the distances between the metal atoms are different and on the other, the normal cuboctahedral environment of atoms in a close cubic packing is not exactly realized in the clusters. Nevertheless, the term metalloid is useful in this case of cluster compounds, making it clear that small metal particles are embedded in a shell of ligands. The type of ligands obviously influences the details of the structures such as inter-atom distances.

The central  $\text{M}_{13}$  cores of these clusters resemble a naked  $\text{Al}_{13}$  cluster ion, prepared in a mass spectrometer. Its chemistry has been studied in the gas phase.<sup>392–397</sup> Its reactions with HI and  $\text{I}_2$ , especially, gave rise to the name of this  $\text{Al}_{13}$  cluster ion as superhalide, which should not be confused with the classic pseudo halides. This  $\text{Al}_{13}^-$  ion has an icosahedral structure, even according to quantum chemical calculations. Electron counting results in 40 electrons for this cluster, which is in accordance with the Jellium model (see above).

Isolation of **210** demonstrates that stabilization of large aluminum clusters is not confined to hexamethylsilazido substituents. This  $\text{Al}_{50}\text{Cp}^*_{12}$  cluster<sup>378,398</sup> is built around a central square antiprismatic  $\text{Al}_8$  unit ( $d_{\text{Al-Al}}=266$  pm). This resembles structures found for  $[\text{Ga}_8\text{fluorenyl}]_8^{2-}$  and  $[\text{In}_8(\text{SiPh}_3)_8]^{2-}$ . This core is surrounded by a shell of 30 aluminum atoms ( $d_{\text{Al-Al}}=281$  pm), which are arranged in an icosidododecahedron with 12 pentagonal and 20 trigonal faces. The pentagonal faces are capped by 12  $\text{AlCp}^*$  groups, where the 12 aluminum atoms are arranged icosahedrally ( $d_{\text{Al-Al}}=570$  pm). The 60 methyl groups of the  $\text{Cp}^*$  rings are arranged in a fivefold symmetric manner, with distances between the methyl groups governed by van der Waals contacts between them. An intriguing idea is that these 12  $\text{AlCp}^*$  groups form a sort of bag with a defined volume, in which the remaining 38 aluminum atoms are filled.

Model calculations on the DFT level suggest a stabilization of approximately  $11\,000$  kJ mol<sup>-1</sup> for a reaction of 38

aluminum atoms in the gas phase with 12 AlCp\* groups. By the way, cluster **210** with its shell of 60 carbon atoms and 60 methyl groups has a volume five times larger than C<sub>60</sub> fullerene.

Three aluminum clusters are described, having not an aluminum but a silicon atom as the central atom. Clusters **211–213** are obtained from metastable AlX solutions and SiCp\*<sub>2</sub> or SiCl<sub>4</sub>/AlCp\* for **211**<sup>399</sup> and LiN(dipp)SiMe<sub>3</sub> for **212**<sup>400</sup> and **213**.<sup>401</sup> As silicon source for the latter, decomposition of the amide LiN(dipp)SiMe<sub>3</sub> was claimed. For the SiAl<sub>14</sub>R<sub>6</sub> compounds **211** and **212**, the structure is described as a body-centered Si@Al<sub>8</sub> cube, where six AlR groups cap the faces of the cube. SiAl<sub>56</sub>R<sub>12</sub> has a shell structure consisting of a central Si@Al<sub>44</sub> core capped by 12 AlR groups. The problems of assigning the correct stoichiometry by x-ray crystal structure analysis for those compounds become obvious after FT mass spectrometric analysis using MALDI of **211**. These investigations show Si<sub>2</sub>Al<sub>13</sub>Cp<sub>6</sub>Cl as an additional cluster, present to approximately one-third in the crystals of **211**.

#### 1.01.4.3 Gallium Cluster Compounds

For gallium, an even larger variety of element-rich or metalloid clusters is known than for aluminum (Figure 11). Similar principles of understanding the structures, either deriving the cluster structures from polyhedral assemblies or describing them as metalloid, are useful. Gallium seems to be special in providing several element modifications with a diversity of structural motifs. These range from digallium units in  $\alpha$ -gallium over icosahedral substructures in  $\delta$ -gallium to nearly close-packed structures in high pressure modifications gallium-III and -IV.<sup>15,275</sup> The clusters, ordered by increasing numbers of gallium atoms, are discussed.

##### 1.01.4.3.1 Ga<sub>8</sub>, Ga<sub>9</sub>, and Ga<sub>10</sub> clusters

Ga<sub>8</sub>R<sub>6</sub> is the general formula for element-rich octagallium clusters. **214** [R=C(SiMe<sub>3</sub>)<sub>3</sub>] is obtained from metastable GaBr solutions and LiC(SiMe<sub>3</sub>)<sub>3</sub>. Molecules of **214** consist of two R<sub>3</sub>Ga<sub>4</sub> tetrahedra linked by a gallium–gallium bond ( $d_{\text{Ga-Ga}} = 261.4$  pm).<sup>402</sup> Similarly, as for Al<sub>7</sub>R<sub>6</sub>, an ionic complex involving aromatic [Ga<sub>3</sub>R<sub>3</sub>]<sup>2-</sup> rings and a Ga<sub>2</sub><sup>4+</sup> cation might be discussed. But two tetrahedra with four sep each (see Section 1.01.3.1), with MOs of types a<sub>1g</sub> and t<sub>2u</sub> seem more reasonable. The other Ga–Ga distances are in the range of 260.5–264.8 pm. This is shorter than in **176** ( $d_{\text{Ga-Ga}} = 268.3$  pm). This can be explained by less steric strain in substituting one C(SiMe<sub>3</sub>)<sub>3</sub> group in **176** for a Ga<sub>4</sub>[C(SiMe<sub>3</sub>)<sub>3</sub>]<sub>3</sub> residue. With this structural change, the color varies from red for **176** to black for **214**. This shift is in line with a change in the energetic level of HOMO and LUMO, which is sensitive to the electronegativity of the substituents and the Ga–Ga distances (Section 1.01.3.1). It was mentioned that this is a hint for a metalloid character of **214**. Here, the Ga<sub>2</sub> unit in the center is a section of  $\alpha$ -gallium, where each of the gallium atoms is bonded only to other gallium atoms. Thus, **214** with all gallium atoms in formal oxidation state +I differs from digallanes R<sub>4</sub>Ga<sub>2</sub>, where three- or four-coordinate gallium(II) atoms are connected to heteroatoms. The situation that gallium atoms of a digallane are part of a cluster is realized also in the carborane-substituted digallane **82**. Here, an extremely

short gallium–gallium bond is observed, a fact which can be explained by steric arguments. Model calculations on analogs to **214** with less bulky substituents also indicated short gallium–gallium bonds.<sup>402</sup> Thus, **214** can be regarded as a molecule of fundamental interest, because it includes a pure metal–metal bond, free of the influences of directly bonded substituents.

An isomer **215** (R=Si<sup>t</sup>Bu<sub>3</sub>) is obtained by thermolysis of the cyclic trigallane R<sub>4</sub>Ga<sub>3</sub> in heptane together with Ga<sub>2</sub>R<sub>3</sub> and Ga<sub>4</sub>R<sub>4</sub>.<sup>403</sup> The structure of **215** is completely different from **214** and the octagallium cluster [Ga<sub>8</sub>(fluorenyl)<sub>8</sub>]<sup>2-</sup>. It has a distorted octahedral R<sub>4</sub>Ga<sub>6</sub> core with an RGa–GaR unit attached to two neighboring gallium atoms.

This means, looking upon the RGa–GaR substituent as a two electron donating one, cluster **215** has six sep. So **215** is a *preclso* cluster for which a face-capped trigonal bipyramid is expected. Here an alternative distortion of the octahedron into a trigonal bipyramid with one edge bridged by an RGa unit is realized. The gallium–gallium distances along the edges cover a range from 251.9 to 292.5 pm. The distances of the RGa–GaR unit to the cluster core atoms are relatively short (240.6, 244.6 pm). The RGa–GaR ( $d_{\text{Ga-Ga}} = 251.9$  pm) is in the typical range for silyl-substituted digallanes. Bond **215** can easily be reduced to the dianionic cluster [R<sub>6</sub>Ga<sub>8</sub>]<sup>2-</sup> **216**, where the arrangement of the gallium atoms is nearly the same as in **215**, with the octahedron being more regular ( $d_{\text{Ga-Ga}} = 255.1$ – $268.5$  pm). The bonds of the RGa–GaR substituent get longer on reduction ( $d_{\text{Ga-Ga}} = 245.3, 246.6, 253.5$  pm, respectively). This is in line with **216** having seven sep, as required for a *clso* cluster. A similar relation between an octahedral *clso* and a distorted octahedral *preclso* cluster is known for **194** and **195**. The sodium atoms are attached to the dianionic cluster core bridging two gallium–gallium edges neighboring the RGa–GaR unit ( $d_{\text{Ga-Na}} = 300$  pm). This indicates, as for the metalloaromatic rings **131**, that the sodium atoms might be regarded as part of the cluster.

One might ask at this point, whether those element-rich cluster compounds are metalloid. **215** as well as **216** show a planar Ga<sub>6</sub>R<sub>4</sub> arrangement as a feature of their cluster cores, where two GaR residues are attached from top and bottom. Thus some resemblance to [Ga<sub>6</sub>R<sub>8</sub>]<sup>2-</sup> **154** exists, whose core can be related to gallium atom sheets in  $\beta$ -gallium.<sup>240</sup>

Later on, it will be seen that an In<sub>8</sub>R<sub>6</sub> cluster adopts a totally different structure.<sup>404</sup>

Using 'Gal' as the source for gallium in low oxidation state, several gallium-rich cluster compounds can be obtained. Due to the insolubility of 'Gal,' variation of reaction conditions cannot be achieved by changing the concentration of the gallium source. But a possible tool is to change the ratio of gallium to iodine in preparation of 'Gal,' which in principle can be from 2:1 to 1:3, meaning formally 'Ga<sub>2</sub>I' and GaI<sub>3</sub> as products. For cluster synthesis reaction mixtures 2:1 up to 1:1.5 are useful. These gallium subiodides are then treated in a heterogeneous reaction in toluene with a slight excess of the metallated substituent MR (M=Li, Na, K).

One of the products is [Li(thf)<sub>4</sub>]<sup>+</sup>[Ga<sub>9</sub>R<sub>6</sub>]<sup>-</sup> (R=Si(SiMe<sub>3</sub>)<sub>3</sub>) **217**.<sup>238</sup> A pentagonal bipyramid with two RGa groups in apical and two RGa groups and three naked gallium atoms in equatorial positions make up the cluster core ( $d_{\text{Ga-Ga}} = 242.5$  and 289.8 pm). The two gallium–gallium bonds of the Ga<sub>3</sub> unit of

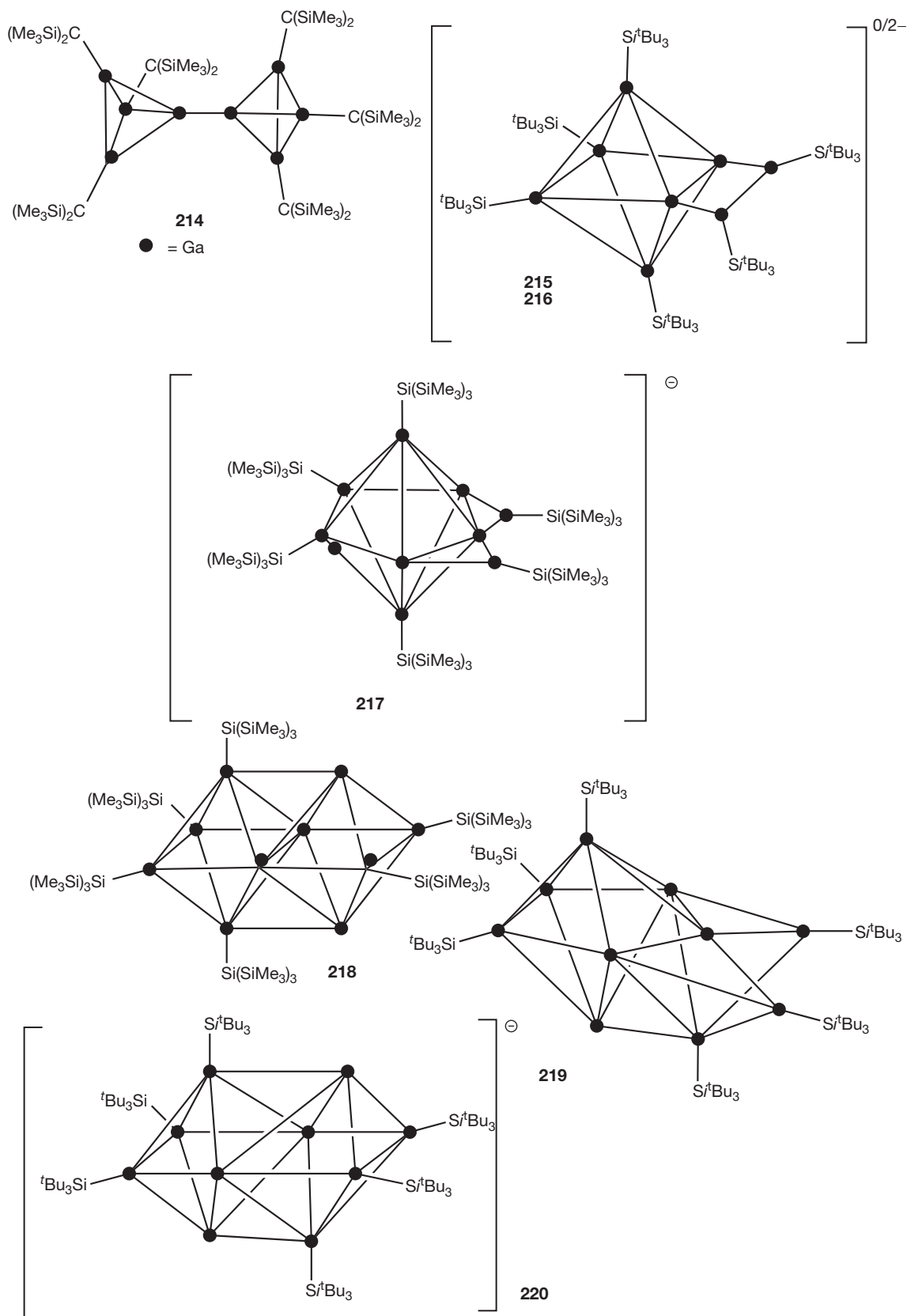
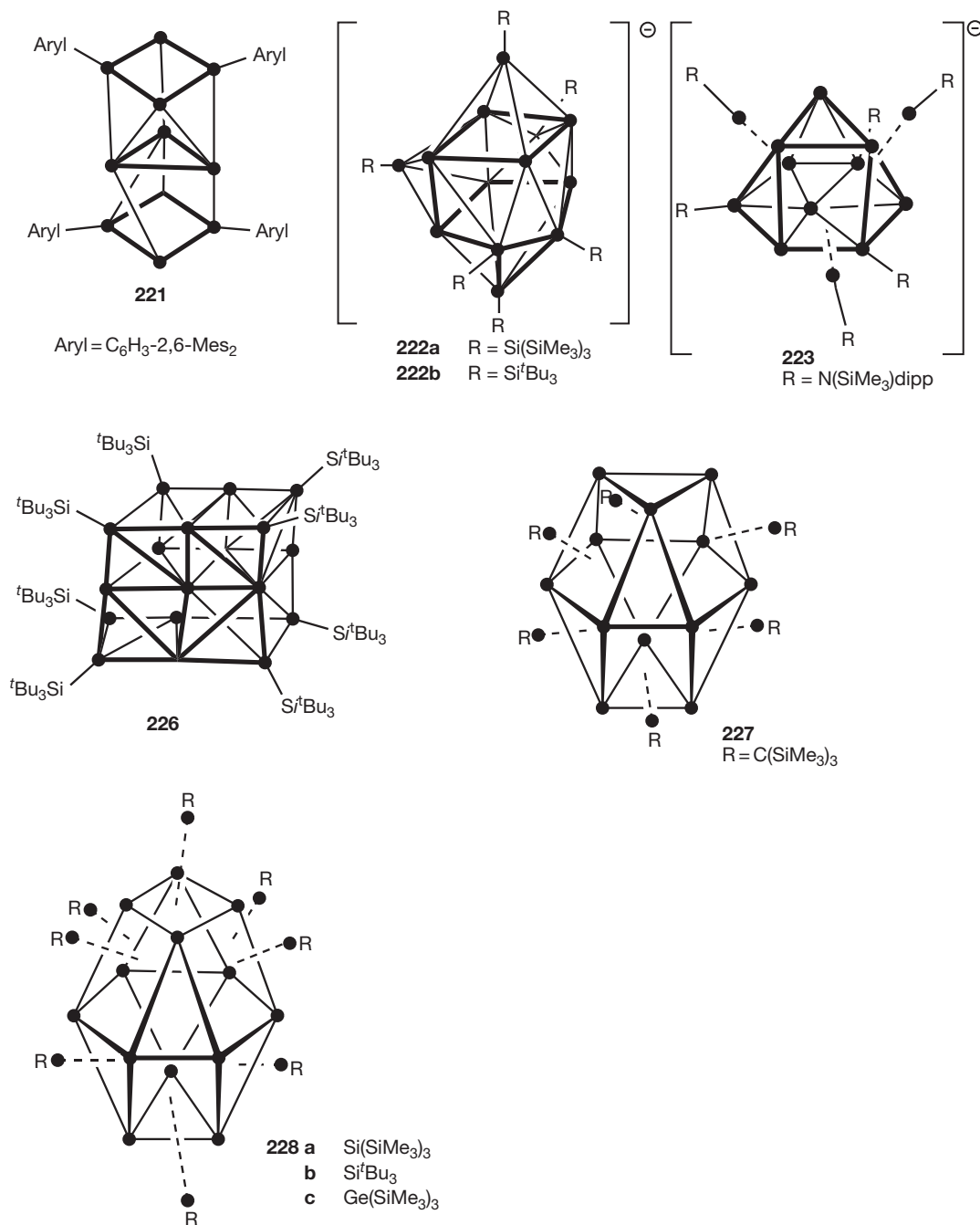


Figure 11 (Continued)



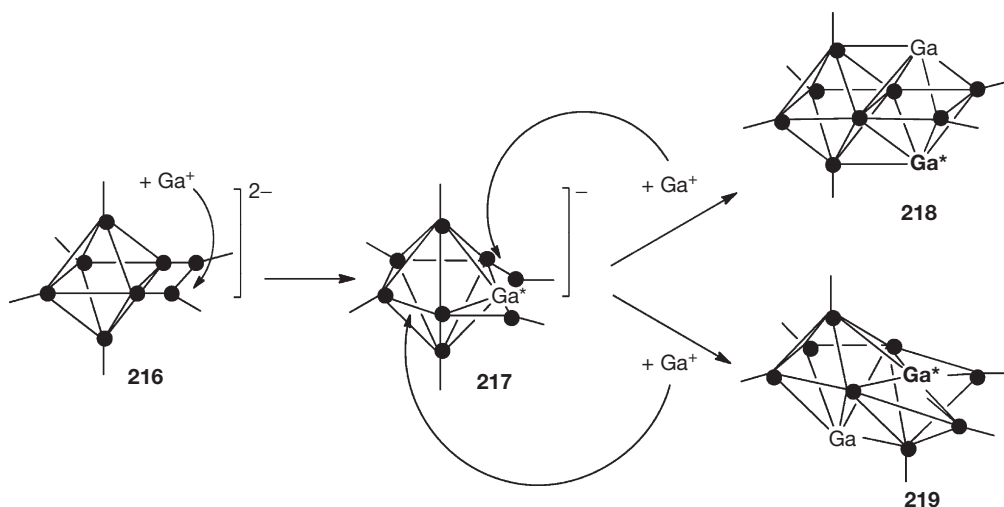
**Figure 11** Overview of types of element-rich gallium clusters (Ga<sub>8</sub> to Ga<sub>22</sub>).

naked gallium atoms are bridged by RGa groups ( $d_{\text{Ga-Ga}} = 234.4$  and  $237.7$  pm). Considering these bridging RGa groups as two-electron substituents, meaning the cluster is built up from four RGa and a (RGa)<sub>2</sub>Ga<sub>3</sub> unit, delivering two and seven electrons each, leaves a Ga<sub>7</sub> cluster with eight sep, classifying it as a *closo*-cluster. Alternatively, if all nine gallium atoms are considered as cluster atoms, these eight sep for a nine vertex cluster stand for a bicapped pentagonal bipyramid. The capping in this case is restricted to bridging two edges. This might be due to steric requirements of the bulky silyl groups. This distinction seems to be a semantic one, leading to the same

result, which is on the basis of a MO description of the cluster eight binding molecular orbitals for the cluster core.

Compound 217 is structurally closely related to the octagallium clusters 215 and 216. Formally, regardless of the different substituents, addition of a Ga<sup>+</sup> cation to the RGa-GaR bridge in 216 widens the Ga<sub>6</sub> plane to a Ga<sub>7</sub> plane (Scheme 7).

Further incorporation of a Ga<sup>+</sup> cation into 217 produces the decagallium clusters 218 and 219.<sup>313,386</sup> Attacking the gallium cation at the central atom of the naked Ga<sub>3</sub> unit leads to cluster 218. Here the gallium atom marked Ga\* moves out of the original Ga<sub>7</sub> plane. If the gallium cation attacks via a Ga<sub>3</sub>R<sub>3</sub>



**Scheme 7** Cluster relations of **216–219** regardless of different substituents.

face of **217**, one of the original RGa groups moves toward the Ga\* atoms forming cluster **219**.

Compound **218** is built from two fused octahedra, meaning a  $R_4Ga_6$  and a  $R_2Ga_6$  cluster fragment fuse via a common edge ( $d_{Ga-Ga} = 298.3$  pm), which is the longest of all neighboring gallium atoms in this cluster. On the other hand, the tops of the octahedra have short distances ( $d_{RGa-Ga} = 254$  pm). The other gallium–gallium bond lengths in **218** range from 258 to 279 pm. This is in the same range as observed in gallium modifications.

As indicated, only six gallium atoms bear  $Si(SiMe_3)_3$  groups, four of them in the  $Ga_6$  base plane of the cluster. One of the octahedra carries four bulky substituents and the other one only two. The gallium–silicon bond lengths are influenced by this imbalance of crowding in the molecule. Longer gallium–silicon bonds ( $d_{Ga-Si} = 244.3$ – $246.8$  pm) are found in the sterically more strained part of the molecule than in the other ( $d_{Ga-Si} = 240.5$  pm). Also, the average gallium–gallium distances in the  $Ga_6R_4$  part of the molecule are 4.6 pm longer than in the  $Ga_6R_2$  part. At first glance, the seemingly unfavorable distribution of the substituents in **218** is surprising, but it is in line with a proposed formation (Scheme 7).

Compound **219**, which is obtained co-crystallized with the tetragallane **180**, has a more fancy structure. The core of **219** is a flat pentagonal bipyramid of gallium atoms. Three RGa groups ( $R = Si^iBu_3$ ) form one of the trigonal faces, the other four core atoms are naked gallium atoms.

The equatorial plane has three rather short ( $d_{Ga-Ga} = 253.1$ – $256.9$  pm) and two long Ga–Ga distances ( $d_{Ga-Ga} = 284.0$ ,  $306.0$  pm), which are bridged by gallium atoms ( $d_{Ga-Ga} = 244.1$ – $253.3$  pm). One of the bridging gallium atoms is part of an RGa group, the other of an RGa–GaR unit ( $d_{Ga-Ga} = 246.6$  pm). This broad distribution of Ga–Ga distances is typical for gallium-rich cluster compounds. The Ga–Si distances also vary over a broad range. The gallium–silicon bonds [ $d_{Ga-Si} = 240.9$ – $245.5$  pm] to the bridging gallium atoms are shorter than the gallium–silicon bonds of the bipyramidal core atoms [ $d_{Ga-Si} = 246.9$ – $250.2$  pm], but comparable to those in **218**.

Alternatively, **219** is described as a fused cluster of a  $Ga_8$  and a  $Ga_4$  polyhedron, sharing a  $Ga_3R$  face. DFT calculations, which indicate a large three-center bonding contribution for the Ga–Ga(R)–Ga bridge, support a description of the cluster as a bridged pentagonal bipyramid.

The bipyramid is quite flat, as mentioned. The Ga–Ga distance ( $d_{Ga-Ga} = 295.3$  pm) between the apical atoms, an RGa and a naked gallium atom, is similar to the lengths of edges in this cluster. For comparison, the assumed parent cluster of type **217** has a height of 344 pm. This suggests an additional interaction between the apical gallium atoms, which is consistent with the results of DFT calculations.

A discussion of electron counting for clusters **218** and **219** is now appropriate.

If **218** is looked upon as a *conjuncto*-cluster of two octahedral, the Jemmis rules,<sup>343,344,405</sup> developed for *conjuncto*-boranes on basis of the Wade rules, might be applicable.<sup>352,406</sup> Here, for a *conjuncto*-cluster of  $m$  fused polyhedral ( $2n + 2m$ ) skeletal electrons ( $n$ , number of cluster atoms;  $m$ , number of polyhedral) are necessary. Therefore, **218** would need 24 electrons to fill the bonding cluster molecular orbitals. Six RGa groups mean 12 electrons and so the four naked gallium atoms have to contribute three electrons each. This is not unambiguous, because quantum chemical calculations for **218** suggest lone pairs at the apical, naked gallium atoms.<sup>313</sup>

For **219**, the short distance between the apical gallium atoms through the cluster make it possible that the bare vertex atom contributes not only one but three electrons and four orbitals to the cluster bonding. This should be the case for two of the other naked gallium as well. That makes 11 sep for **219**, as required for a fused polyhedron of a  $Ga_8$  (9 sep) and a  $Ga_4$  (4 sep) polyhedron.

The structures and electron count in bare indium clusters in Zintl phases have been discussed similarly. The flattening of vertices is deduced as a result of the contribution of four orbitals to cluster bonding by some of the vertex atoms.<sup>407,408</sup> Thus,  $In_{11}^{7-}$ , has three flattened vertices, which results in 12 sep, required for a *closo*- $E_{11}$ -cluster, if some indium atoms contribute more than one electron to cluster bonding.<sup>385</sup>



Obviously, counting rules give only rough explanations for the structure of these hypoelectronic clusters but are near their limits. Therefore, a forecast of structures on this basis is not possible at all.

A third  $\text{Ga}_{10}$  cluster is  $[\text{Ga}_{10}\text{R}_6]^-$  ( $\text{R}=\text{Si}^t\text{Bu}_3$ ) **220**, isolated as black crystals together with a  $\text{Ga}_{13}$  cluster **222a**. Counterion is  $[\text{Na}(\text{thf})_6]^+$ . The six GaR groups are distributed more regularly over the cluster and form a trigonal prism, elongated along the  $C_3$  axis. A four-membered ring of naked gallium atoms is embedded between the two  $\text{Ga}_3\text{R}_3$  rings. As a consequence of the  $C_3/C_4$  symmetry mismatch of the cluster-building units, the four-membered ring is disordered over three equivalent positions. The range of gallium–gallium distances is similar to that in **218** ( $d_{\text{Ga-Ga}}=245.3\text{--}288.0$  pm). This arrangement of three-membered rings and embedded triel fragments is realized in **204** and **214**, which are prototypes of metalloid clusters.

Another view of the structure of **220** emphasizes the similarity to **218**. Here, shortening of the bridging edge and elongation of the distance of the tops of the fused octahedra bring the structures together.

DFT calculations on isomers of  $\text{Ga}_{10}(\text{SiMe}_3)_6$  revealed a structure analog to **218** as more stable by  $56.6$  kJ mol $^{-1}$  than a **219** based one. On reduction, both isomers undergo a structural change to that of type **220**.

#### 1.01.4.3.2 $\text{Ga}_{11}$ and $\text{Ga}_{13}$ clusters

$\text{Ga}_{11}\text{aryl}_4$  **221** with bulky aryl substituents consists of two  $\text{Ga}_4\text{R}_2$  rings interconnected by a  $\text{Ga}_3$  unit.<sup>134</sup> The paramagnetic cluster was obtained from ‘Gal’ and Li-aryl ( $\text{aryl}=2,6\text{-Me}_2\text{C}_6\text{H}_3$ ). The EPR spectrum of **221** confirmed a radical with one unpaired electron. The gallium–gallium distances in the four-membered ring part (255 pm) are shorter than in the  $\text{Ga}_3$  unit (266 pm). It has to be noted that  $[\text{Ga}_4\text{R}_2]^{2-}$  and  $[\text{Ga}_3\text{R}_3]^{2-}$  rings have been isolated and characterized as metalloaromatic with contacts to alkali metal ions.<sup>134,216</sup> Whether in **220** and **221** the central  $\text{Ga}_4$  or  $\text{Ga}_3$  rings take the role of the cations might be considered. On the other hand, the structure of this  $\text{Ga}_{11}$  cluster core has some resemblance to that of the metalloid  $[\text{Al}_{12}[\text{N}(\text{SiMe}_3)_2]_8]^-$  cluster.<sup>382</sup>

The  $\text{Ga}_{12}$  cluster **160**, already mentioned, can be described by three nearly planar four-membered rings of gallium atoms, where eight of the ten substituents (2 Br, 6  $\text{P}^t\text{Bu}_2$ , 2 ylid ligands) are bonded to the outer rings. The connection to the central ring is made by gallium–gallium interactions and phosphide bridges. The  $\text{Ga}_{12}$  core has some resemblance of the  $\text{Ga}_{11}$  core of **221**.

The  $[\text{Ga}_{13}\text{R}_6]^-$  cluster ions are obtained as alkali metal salts from ‘Gal’ and MR (**222a**:  $\text{M}=\text{Li}$ ,  $\text{R}=\text{Si}(\text{SiMe}_3)_3$ <sup>409</sup>; **222b**:  $\text{M}=\text{Na}$ ,  $\text{R}=\text{Si}^t\text{Bu}_3$ <sup>313</sup>). Here a pseudo-cuboid core is present, where seven naked gallium atoms are at the corners of a cube, and the eighth corner is occupied by a  $\text{Ga}_3\text{R}_3$  ring. The three complete square faces of the cube are capped by RGa units. The structure has some features of that of the silicon-centered  $\text{Si}@\text{Al}_{14}$  clusters.

Another type of a  $[\text{Ga}_{13}\text{R}_6]^-$  cluster **223** is obtained with an amido substituent ( $\text{R}=\text{N}(\text{SiMe}_3)\text{dipp}$ ).<sup>410</sup> The framework of **223** is comprised of two stapled  $\text{R}_3\text{Ga}_6$  rings, one of which is gallium-centered. This means nine of these atoms form a part of a cuboctahedron, where one of the  $\text{Ga}_3$  units is missing.

The remaining three GaR groups cap the  $\text{Ga}_4$  faces of the cuboctahedral trunk. This structural feature makes the metalloid character of **223** more obvious than it is for the isomers **222**.

#### 1.01.4.3.3 $\text{Ga}_{16}$ , $\text{Ga}_{18}$ , and $\text{Ga}_{19}$ clusters

In  $\text{Ga}_{16}(\text{P}^t\text{Bu}_2)_{10}$  **224** a totally different structural motif is present. In the clusters discussed so far, often planar four-membered  $\text{Ga}_4$  rings occurred. In **224**, a tetrahedral  $\text{Ga}_4$  core is at the center of the structure, around which a  $\text{Ga}_{12}(\text{P}^t\text{Bu}_2)_{10}$  framework of phosphido bridged gallium atoms is built.<sup>411</sup> This framework can be described as based on an adamantoid  $\text{Ga}_4\text{P}_{10}$  cage.

$[\text{Ga}_{18}(\text{P}^t\text{Bu}_2)_{10}]^{3-}$  **225**<sup>245</sup> and the silyl-substituted cluster  $[\text{Ga}_{18}(\text{Si}^t\text{Bu}_3)_8]$  **226**<sup>412</sup> are obtained from metastable GaBr solutions and  $\text{LiP}^t\text{Bu}_2$  or  $\text{NaSi}^t\text{Bu}_3$ , respectively. The structure of the metalloid core of **225** is compared to that of the high pressure gallium modification Ga(II), where the gallium atoms have coordination number 10 on an average.<sup>413,414</sup>

Compound **226** has a core of three stapled  $\text{Ga}_6$  layers, which resemble the  $\text{Ga}_6$  core of **154**. Thus, the structure can be described as a section of  $\beta$ -gallium.

$[\text{Ga}_{19}[\text{C}(\text{SiMe}_3)_3]_6]^-$  **227** is a metalloid cluster with a central gallium atom surrounded by twelve others in a distorted cuboctahedral manner.<sup>5</sup> This typical structural feature of a cubic close-packed metal is here wrapped into a shell of six  $\text{GaC}(\text{SiMe}_3)_3$  groups, which cap rectangular faces.

Compound **227** is also prepared via metastable GaX solutions. The cluster is unique because in contrast to most other gallium-rich clusters, it is soluble in organic solvents. Therefore, a  $^{71}\text{Ga}$  NMR spectrum can be measured. The shift for the central atom ( $\delta=-134$  ppm) is different from those calculated for naked gallium metal clusters and suggests a different electronic situation.<sup>415,416</sup> Compound **227** is also special because in mass spectrometric experiments (ESI, laser desorption/ionization) not only can the molecule ion of this metalloid cluster be detected, but the collision-induced six GaR groups can also be degraded stepwise, resulting in a  $\text{Ga}_{13}^-$  ion.

This fragmentation by sequentially removing RGa units confirms the point of view that these carbenoid units are a protecting shell for the central  $\text{Ga}_{13}^-$  core. This is comparable to CO ligands shielding a metal cluster core in transition metal clusters. The analogy of GaR and CO is discussed for  $[\text{M}]-\text{GaR}$  complexes as well.

This  $\text{Ga}_{13}^-$ -cluster ion was calculated to be very stable and the corresponding neutral  $\text{Ga}_{13}$  cluster has a very high electron affinity of 3.35 eV. This is similar to that of a fluorine atom and gives some justification to the term superhalide, which has been given to the  $\text{Al}_{13}^-$  cluster ion. It was noted that these results stand for the electron deficiency of metalloid clusters of aluminum and gallium and make them different from  $\text{Ga}_n$ -Zintl ions, which are of polyhedral type.<sup>417–420</sup> This is discussed in detail in another chapter.

#### 1.01.4.3.4 $\text{Ga}_{22}$ clusters

For  $\text{Ga}_8$ ,  $\text{Ga}_{10}$ , and  $\text{Ga}_{13}$  clusters, structural isomers for the cluster cores are observed. The same is true for  $\text{Ga}_{22}$  clusters **228–231**.  $\text{Ga}_{22}\text{R}_8$  ( $\text{R}=\text{Si}(\text{SiMe}_3)_3$  **a**,<sup>163</sup>  $\text{Ge}(\text{SiMe}_3)_3$  **b**,<sup>294</sup>  $\text{Si}^t\text{Bu}_3$  **c**<sup>412</sup>) **228a–c** are prepared by reaction of metastable GaBr solutions (**a**, **c**) or ‘Gal’ (**b**) with the metallated substituent R. All of the three clusters are isostructural (**Figure 12**).  $\text{Ga}@\text{Ga}_{13}$

cores ( $d_{\text{Ga-Ga}}=287$  pm) are surrounded by eight GaR units, capping  $\text{Ga}_4$  faces ( $d_{\text{Ca-Ca}}=267$  pm). The eight GaR units are at the corners of an Archimedes' antiprism, with distances of  $\sim 500$  pm between the gallium atoms. The  $\text{Ga}@_{\text{Ga}_{13}}$  core is a gallium-centered, widened cuboctahedron, which means that one of the triangular faces is enlarged to a  $\text{Ga}_4$  ring. Thus a 4-6-3 polyhedron with layers of  $\text{Ga}_4$ ,  $\text{Ga}_6$  and  $\text{Ga}_3$  rings is formed. Thus, somehow a metal packing is evident in this cluster core. Electron counting results in  $22 \times 3 - 8 \times 1 = 58$  electrons for these clusters, which is in accordance with the Jellium model.

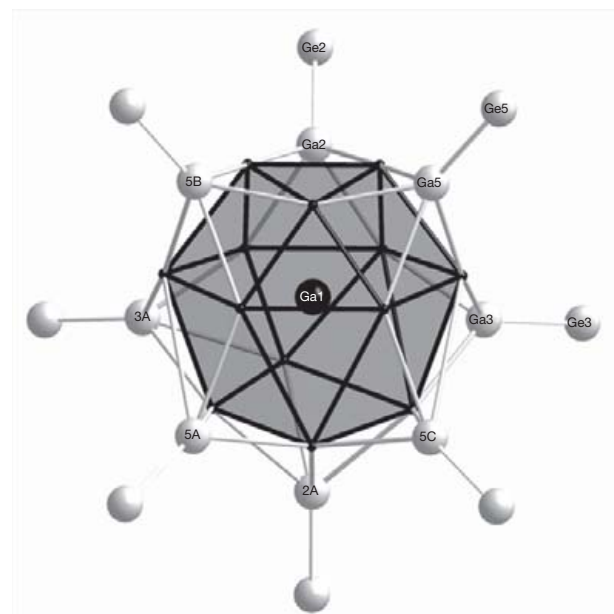
Applying the classic counting scheme of the Wade rules, the cluster is separated into a  $\text{Ga}_{14}$  core and eight GaR groups, which deliver 16 electrons for cluster bonding. Adding the 14 gallium atoms, counted as contributing one electron each, a total of 15 sep result for the  $\text{Ga}_{14}$  core, making it a specially

filled  $\text{Ga}_{13}$ -*closo*-polyhedron. This filled polyhedron might be due to the size of the cavity defined by the eight RGa residues.

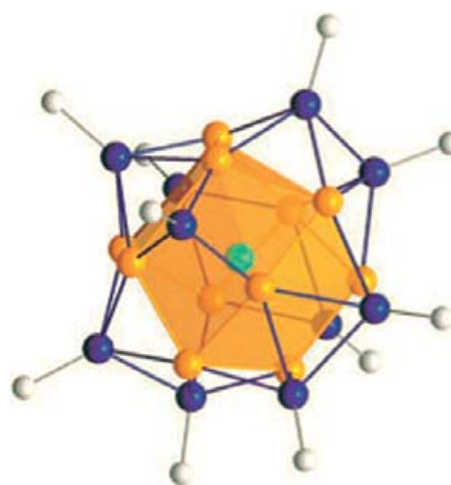
Cluster 226 is regarded as a section of  $\beta$ -gallium in metalloid terms. Similarly, the  $\text{Ga}_{22}$  clusters 228 can be looked upon as derived from gallium(III), with an additional atom in the coordination sphere of the central gallium atom (Figure 13).

The anionic cluster  $[\text{Ga}_{22}[\text{N}(\text{SiMe}_3)_2]_{10}]^{2-}$  229 (Figure 14) has two more substituents, which are attached to gallium atoms of the naked gallium shell.<sup>421</sup> Thus, only a  $\text{Ga}@_{\text{Ga}_{11}}$  core, with irregular structure results, is capped by 10 RGa groups.

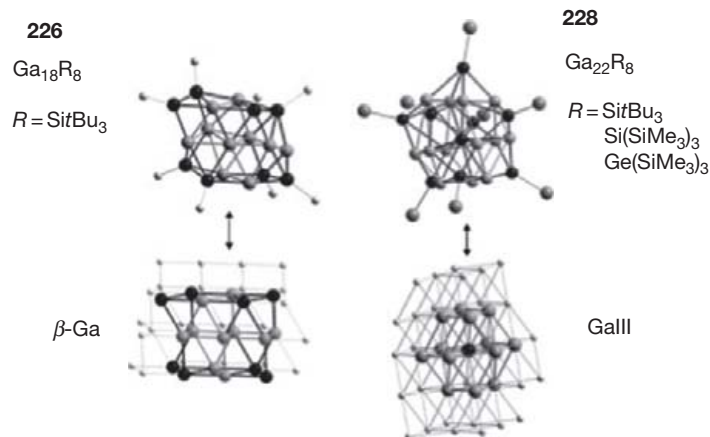
The clusters  $[\text{Ga}_{22}\text{R}_{10}\text{Br}_{11}]^{3-}$  230 and  $[\text{Ga}_{22}\text{R}_{10}\text{Br}_{12}]^{2-}$  231 [ $\text{R}=\text{N}(\text{SiMe}_3)_2$ ], with a higher ratio of gallium:substituents, have empty icosahedral gallium cores.<sup>422</sup> The remaining ten gallium atoms are attached to the icosahedron with covalent 2c2e bonds ( $d_{\text{Ga-Ga}}=240$  pm), such that the fivefold



**Figure 12** View of  $\text{Ga}_{22}[\text{Ge}(\text{SiMe}_3)_3]_8$  228b (SiMe<sub>3</sub> groups omitted for clarity).

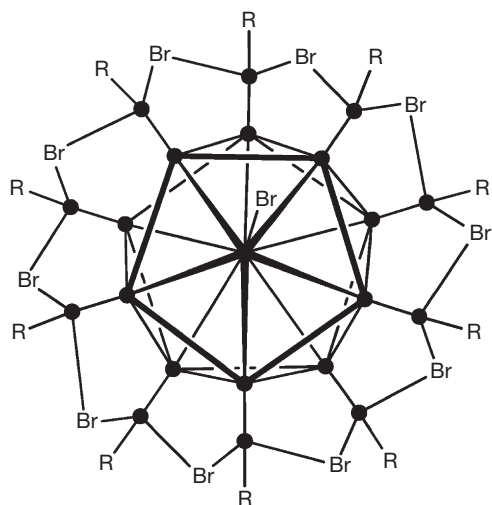


**Figure 14** View of  $[\text{Ga}_{22}[\text{N}(\text{SiMe}_3)_2]_{10}]^{2-}$  anion 229 (SiMe<sub>3</sub> groups omitted for clarity; Ga atoms: gray shade; N atoms: light gray). Reproduced with permission from Linti, G.; Schnöckel, H.; Uhl, W.; Wiberg, N. In *Molecular Clusters of the Main Group Elements*; Driess, M., Nöth, H., Eds.; Wiley-VCH: Weinheim, 2004; pp 126–168. Copyright Wiley-VCH Verlag GmbH & Co. KGaA.



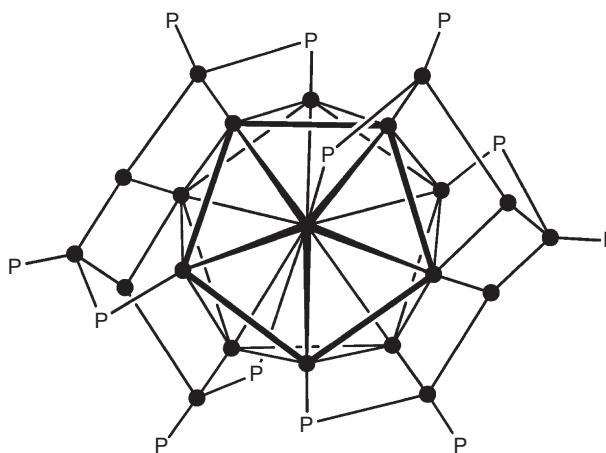
**Figure 13** Relationships of clusters 226 and 228 to gallium modifications. Reproduced with permission from Linti, G.; Schnöckel, H.; Uhl, W.; Wiberg, N. In *Molecular Clusters of the Main Group Elements*; Driess, M., Nöth, H., Eds.; Wiley-VCH: Weinheim, 2004; pp 126–168. Copyright Wiley-VCH Verlag GmbH & Co. KGaA.





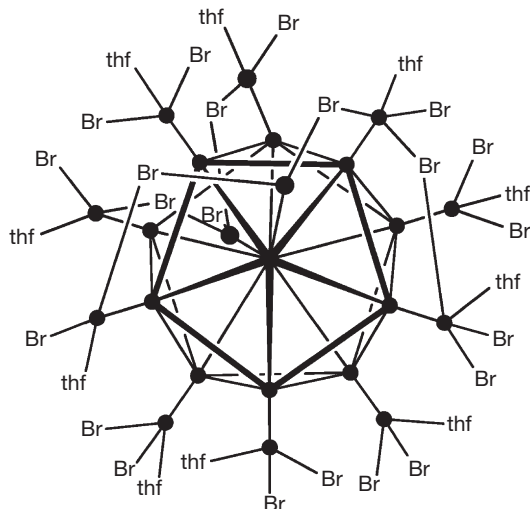
230

● = Ga  
R = N(SiMe<sub>3</sub>)<sub>2</sub>



232

● = Ga  
P = P<sup>t</sup>Bu<sub>2</sub>



234

● = Ga

symmetry of the icosahedron is retained. One of the free apical gallium atoms of 230 bears a bromine atom. In 231, two GaBr groups are present. Thus, 231 is a regular icosahedral *closo*-[E<sub>12</sub>X<sub>12</sub>]<sup>2-</sup> cluster, with ten Ga(R)Br and two Br substituents. An electron count for 230 reveals it as a cluster with 13 sep, if the naked apical gallium atom retains its lone pair and contributes one electron and three orbitals to cluster bonding. The Al<sub>22</sub>X<sub>20</sub> clusters 202 have related structures.

Ga<sub>22</sub>(P<sup>t</sup>Bu<sub>2</sub>)<sub>12</sub> 232 also has an icosahedral core.<sup>423</sup> The other ten gallium atoms form Ga<sub>5</sub> chains wrapped around the core and attached to it via three phosphide-bridges and two gallium–gallium bonds.

These icosahedra-based structures are metalloids with regard to δ-gallium. This modification is a network of fused, filled gallium icosahedra. The Ga<sub>12</sub> core together with the two Ga<sub>5</sub> chains now represent one of these icosahedra elements, with parts of the next ones.

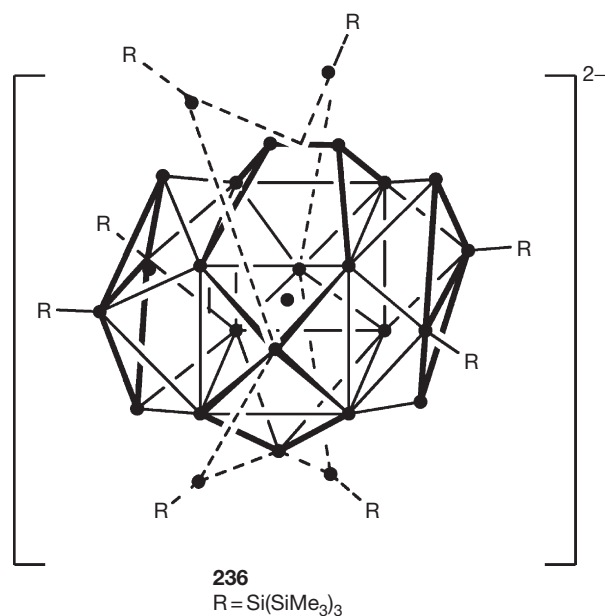
#### 1.01.4.3.5 Ga<sub>23</sub> and higher clusters

Ga<sub>23</sub>R<sub>11</sub> 233 [R = N(SiMe<sub>3</sub>)<sub>2</sub>] has a body-centered core of 12 naked gallium atoms.<sup>424</sup> This is capped by 11 GaR groups. The structure is similar to that of dianionic 229. In both clusters, the central gallium atom is surrounded by 11 naked gallium atoms. The shell of GaR groups in 233 contains one more group, but the number of cluster electrons of dianionic 229 and neutral 233 is the same. This might mean that the number of electrons is more important for the central cluster core than the number of shell atoms.

The gallium subhalides [Ga<sub>24</sub>Br<sub>22</sub>(thf)<sub>10</sub>] 234<sup>425</sup> and [Ga<sub>24</sub>Br<sub>18</sub>Se<sub>2</sub>(thf)<sub>10</sub>] 235<sup>426</sup> are obtained from GaBr solutions with low thf content upon slow warming up to room temperature. In the case of 235 Se(SiMe<sub>3</sub>)<sub>2</sub> was added. The clusters are of the same type as 230, meaning they have a central, nonfilled icosahedron of gallium atoms. The gallium–gallium distances indicate a slight distortion ( $d_{\text{Ga-Ga}} = 255\text{--}267$  pm). Attached to

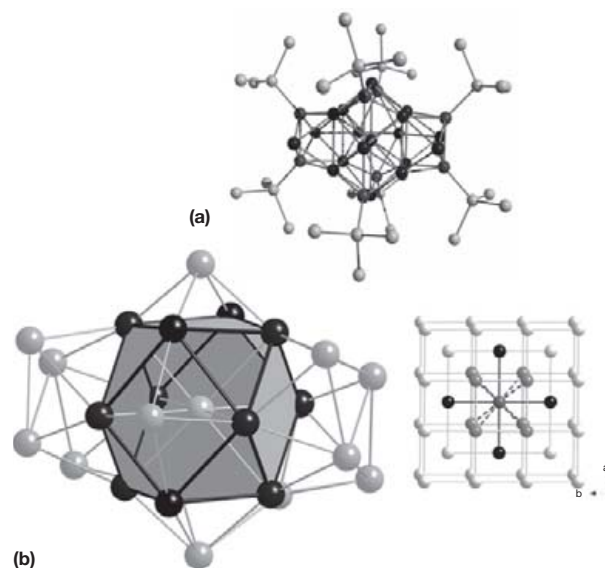
the polyhedral atoms are terminal  $\text{GaBr}_x$  units ( $x=1, 2$ ), two gallium dibromide and ten gallium monobromide groups, which are interconnected by bromine bridges. Due to coordinated thf molecules, the exopolyhedral gallium atoms are surrounded tetrahedrally. Those  $2c2e$  gallium–gallium bonds are significantly shorter ( $d_{\text{Ga-Ga}}=240$  pm) than the bonds in the icosahedron, as expected. In 235 four bridging bromine atoms are substituted for two selenium atoms, which are threefold capping three gallium atoms, which remain tetra coordinated. The cluster structure is not changed very much by this. A special feature is the packing of 235 in the crystal. Here, Se–Se contacts (409 pm) arrange the clusters in chains. The Se–Se contacts are longer than in GaSe (385 pm), but lead to a closer contact between clusters for 235 than it is in crystals of 234. Thus, a chain of  $\text{Ga}_{24}$ -‘superatoms’ is formed and is used as a model for the photovoltaic properties of GaSe or selenium itself.

The largest gallium clusters prepared so far are  $[\text{Ga}_{26}[\text{Si}(\text{SiMe}_3)_3]_8]^{2-}$  236,<sup>427</sup>  $[\text{Ga}_{51}(\text{P}^t\text{Bu}_2)_{14}\text{Br}_6]^{3-}$  237,<sup>428</sup> and  $[\text{Ga}_{84}[\text{N}(\text{SiMe}_3)_2]_{20}]^{x-}$  ( $x=3, 4$ ) 238.<sup>3,17</sup> 236 is obtained via ‘GaI,’ the others only via metastable GaX solutions.



In 236 a central gallium atom is surrounded by eight gallium atoms, which are at the corners of a distorted cube.<sup>427</sup> Two opposite faces are capped by butterfly-shaped  $\text{Ga}_4\text{R}_2$  rings. Three single gallium atoms and a  $\text{Ga}_2$  dumbbell cap the other faces. Bridging between these five naked gallium atoms are four GaR groups. Ignoring the  $\text{Ga}_4\text{R}_2$  and GaR groups, the  $\text{Ga}_{14}$  core has a central gallium atom with coordination number  $8+3+2=13$ , which was found in other clusters as well. Taking the dumbbell as one coordinating neighbor, the coordination number ( $8+4$ ) resembles the environment in the high-pressure modification Ga(III) (Figure 15).

Electron counting rules after Wade or Jemmis have been applied for element-rich clusters. For  $\text{Ga}_{10}\text{R}_6$  and  $\text{Ga}_{22}\text{R}_8$ , the counting of bare gallium atoms as one or three electron donating cluster atoms was ambiguous. For  $[\text{Ga}_{26}[\text{Si}(\text{SiMe}_3)_3]_8]^{2-}$  a multiple capped polyhedron is expected.



**Figure 15** (a) View of the cluster ion  $[\text{Ga}_{26}[\text{Si}(\text{SiMe}_3)_3]_8]^{2-}$  236 (methyl groups omitted) and (b) relation of the cluster core to the gallium modification III.

At this point, an alternative way of interpreting cluster structures is introduced. Schleyer suggested that a special class of boranes, the so-called ‘sea urchin’ boranes that are stable clusters with triangular, rectangular and pentagonal faces, capped on all faces larger than triangular by ER fragments, need special electron counts. He postulated a  $6m+2n$  counting rule to fit the number of cluster valence electrons less the pairs for bonding of R groups. Here,  $m$  is the number of capped faces and  $n$  the number of triangles.<sup>429</sup>

For 236 with 88 cluster valence electrons this rule was applied recently.<sup>430</sup> The centered 13 vertex polyhedron has eight triangles, four rectangles, and two pentagons. Two rectangles and the pentagons are capped. The other rectangles are not isolated, but fused to fragments of bicapped trigonal prisms. That means two triangles and two rectangles have to be added. The third rectangle is out of count, because it is needed for fusion. Thus we calculate  $2 \times 8$  for triangles,  $6 \times 4$  for capped faces,  $16 \times 2$  for complex caps and  $2 \times 8$  for R groups, which totals to 88 cluster valence electrons. Whether this approach, which is not really straightforward, has generality has to be proved in future. At least the structure of 227 has been rationalized, using this approach.<sup>430</sup>

$[\text{Ga}_{51}(\text{P}^t\text{Bu}_2)_{14}\text{Br}_6]^{3-}$  237 has a metalloid structure of a filled cuboctahedron surrounded by 38 gallium atoms, which make bonds to gallium, phosphorus, or bromine.

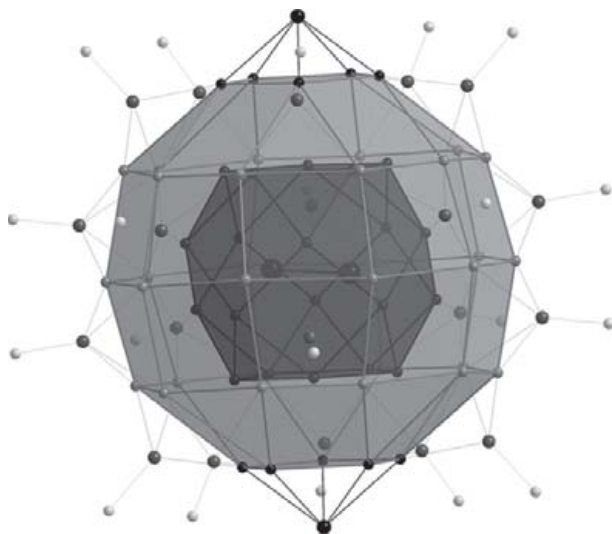
$[\text{Ga}_{84}[\text{N}(\text{SiMe}_3)_2]_{20}]^{4-}$  238<sup>3</sup> is the largest main group cluster prepared and structurally characterized up to now. A  $\text{Ga}_{84}^{3-}$  cluster with the same cluster structure was also obtained.<sup>17</sup>

In 238 (Figure 16) a central  $\text{Ga}_2$ -unit ( $d_{\text{Ga-Ga}}=234$  pm) is surrounded by 62 naked gallium atoms, to which 20 GaR groups are attached. The short bond length of the  $\text{Ga}_2$  dumbbell is comparable to that in a molecule with a formal gallium–gallium triple bond.<sup>141</sup> The 62 naked gallium atoms can be subdivided into two shells. An inner  $\text{Ga}_{32}$  shell with the shape of a football with icosahedral caps is surrounded by a belt of 30 gallium atoms.

Crystals of **238** show a metallic luster, which was also observed for  $\text{Ga}_{26}$  cluster crystals (**236**). In addition, electric conductivity and even supraconduction (7 K) was observed for **238**. This was explained with the packing of the cluster molecules which are aligned in chains, where the naked tops of the  $\text{Ga}_{32}$  shell are oriented to one another.<sup>431–434</sup>

#### 1.01.4.4 Indium Cluster Compounds

Several tetrahedral cluster compounds  $\text{In}_4\text{R}_4$  **184–185**<sup>296,297,340</sup> were prepared from the reaction of lithium organyls with indium(I) halides. Silyl-substituted  $\text{In}_4[\text{Si}(\text{SiMe}_3)_3]_4$  **186**<sup>298</sup> was accessible via elimination of  $\text{LiCp}^*$  ( $\text{Cp}^* = \text{C}_5\text{Me}_5$ ) from  $\text{InCp}^*$ <sup>307</sup> with  $\text{Li}(\text{thf})_3\text{Si}(\text{SiMe}_3)_3$ .  $\text{NaSi}^t\text{Bu}_3$  ( $\text{NaR}^*$ ) reacted



**Figure 16** View of the  $\text{Ga}_{84}$  cluster ion **238** showing the layered structure (Ga atoms: dark to middle gray; N atoms of R groups: light gray). The football/belt description is rationalized by viewing the three middle layers of the middle gray shaded shell as belt and the remaining gallium atoms, which are not GaR units as capped football. Reproduced with permission from Linti, G.; Schnöckel, H.; Uhl, W.; Wiberg, N. In *Molecular Clusters of the Main Group Elements*; Driess, M., Nöth, H., Eds.; Wiley-VCH: Weinheim, 2004; pp 126–168. Copyright Wiley-VCH Verlag GmbH & Co. KGaA.

with  $\text{InCp}^*$  to produce indium-rich cluster compounds  $\text{In}_8\text{R}^*_6$  **239**<sup>404</sup> and  $\text{In}_{12}\text{R}^*_8$  **206**,<sup>383</sup> demonstrating the stronger reducing abilities of this silanide. With  $\text{M}(\text{thf})_3\text{SiPh}_3$  ( $\text{M} = \text{Li}, \text{Na}$ ) two polyhedral octaindane cluster compounds **198a** and **198b** were obtained.<sup>270</sup>

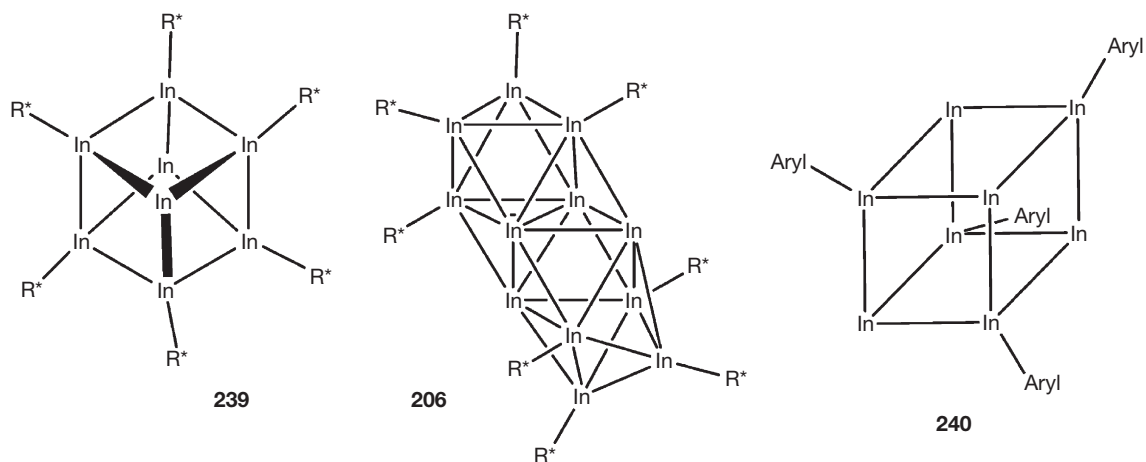
Compound **239** has a cube of eight indium atoms lengthened along one space diagonal, where the two opposite indium atoms are ligand-free. Electron counting gives seven sep, allowing apostroph **239** as a *hypoprecloso* cluster. Thus, it is described as a two-capped  $\text{In}_6\text{R}^*_4$  octahedron with two naked indium atoms at opposite vertices.

In **206** the 12 indium atoms form a section from a distorted close packing, which is similar to that in  $[\text{Al}_{12}\{\text{N}(\text{SiMe}_3)_2\}_6]^-$  **205**.<sup>382</sup>

$\text{In}_8(\text{C}_6\text{H}_3-2,6-\text{Mes}_2)_4$  **240** ( $\text{Mes} = \text{C}_6\text{H}_2-2,4,6-\text{Me}_3$ )<sup>435</sup> was prepared from  $\text{InCl}$  and  $\text{LiC}_6\text{H}_2-2,4,6-\text{Me}_3$ . The core is a distorted cubic array of indium atoms where only the four indium atoms, located at the corners of a tetrahedron, are part of  $\text{In}(\text{aryl})$  groups. Thus the well-known  $\text{E}_4\text{R}_2$  fragments are present again.

#### 1.01.5 Conclusion

The chemistry of element-rich and polyhedral clusters of the heavier triel elements has been established during the past two decades. Several synthetic pathways are available now, but none that allows for a planned synthesis of a specific new cluster. The complex structures stress classic bonding concepts. For smaller clusters, concepts developed for boron cluster compounds are applicable. Therefore this chapter has focused on rationalizing structures by topology and attempted application of well-known electron counting rules. The higher clusters are too complex to be described by a simple rule. Gallium as an element adopts various allotropic modifications, which are stable at different temperature ranges and pressure. It seems that the high pressure necessary for some modifications can be modeled by a shell of substituents. Their steric demand and electronic properties influence cluster cores, but a real understanding of the effects is far from complete. Aluminum, which has a typical metal lattice, has modified structures in the nano-scale cluster cores. With indium, which has the higher stability



of oxidation state one, compared to aluminum and gallium, only a few element-rich clusters could be obtained.

A topic of special interest was and is the formation of bonds between triel atoms in the low oxidation state, where the range is from 2c2e bonds to multiple bonds and multicenter bonds. The properties of these metal–metal bonded systems including the nanoscale clusters, being described as intermediate between dissolved metals and bulk material, have begun to be investigated and offer interesting perspectives.

## References

- Uhl, W.; Layh, M.; Hiller, W. *J. Organomet. Chem.* **1989**, *368*, 139–154.
- Uhl, W.; Layh, M.; Hildenbrand, T. *J. Organomet. Chem.* **1989**, *364*, 289–300.
- Schnepf, A.; Schnöckel, H. *Angew. Chem. Int. Ed. Engl.* **2001**, *40*, 711.
- Schnöckel, H.; Schnepf, A. *Angew. Chem. Int. Ed.* **2002**, *41*, 3532–3552.
- Schnepf, A.; Stoesser, G.; Schnöckel, H. *J. Am. Chem. Soc.* **2000**, *122*, 9178.
- Purath, A.; Köppe, R.; Schnöckel, H. *Angew. Chem. Int. Ed.* **1999**, *38*, 2926.
- Schnöckel, H.; Schnepf, A. *Adv. Organomet. Chem.* **2001**, *47*, 235–281.
- Driess, M.; Nöth, H., Eds.; In *Molecular Clusters of the Main Group Elements*; Wiley-VCH: Weinheim, New York, 2004.
- Schnöckel, H. *Dalton Trans.* **2008**, 4344.
- Schnöckel, H. *Chem. Rev.* **2010**, *110*, 4125–4163.
- Baker, R. J.; Jones, C. *Coord. Chem. Rev.* **2005**, *249*, 1857–1869.
- Linti, G.; Schnöckel, H. *Coord. Chem. Rev.* **2000**, *206–207*, 285–319.
- Schnöckel, H. *J. Chem. Soc. Dalton Trans.* **2005**, *19*, 3131–3136.
- Pardoe, J. A. J.; Downs, A. J. *Chem. Rev.* **2007**, *107*, 2–45.
- Schnepf, A.; Schnöckel, H. *Angew. Chem. Int. Ed.* **2002**, *41*, 3533.
- Schnepf, A.; Schnöckel, H. *ACS Symp. Ser.* **2002**, *822*, 154.
- Schnepf, A.; Jee, B.; Schnöckel, H. *Inorg. Chem.* **2003**, *42*, 7731–7733.
- Köppe, R.; Schnöckel, H. *Angew. Chem. Int. Ed.* **2004**, *43*, 2170.
- Wade, K. *Adv. Inorg. Chem. Radiochem.* **1976**, *18*, 1.
- Williams, R. E. *Adv. Inorg. Chem. Radiochem.* **1976**, *18*, 67.
- Rudolph, R. W. *Acc. Chem. Res.* **1976**, *9*, 446.
- Mingos, D. M. P. *Nature* **1972**, *236*, 99.
- Burgert, R.; Stokes, S. T.; Bowen, K. H.; Schnöckel, H. *J. Am. Chem. Soc.* **2006**, *128*, 7904.
- Burgert, R.; Schnöckel, H.; Grubisic, A.; Li, X.; Stokes, S. T.; Bowen, K. H.; Ganteför, G. F.; Kiran, B.; Jena, P. *Science* **2008**, *319*, 438.
- Burgert, R.; Schnöckel, H. *Chem. Comm.* **2008**, 2075.
- Linti, G.; Frey, R.; Schmidt, M. Z. *Naturforsch. B* **1994**, *49b*, 958–962.
- Downs, A. J.; Himmel, H.-J. In *The Group 13 Metals Aluminium, Gallium, Indium and Thallium*; Aldridge, S., Downs, A. J., Eds.; Wiley: New York, 2011; p 1.
- Wilson, F. C.; Schoemaker, D. P. *Naturwissenschaften* **1956**, *43*, 57.
- Elschenbroich, C. H. *Organometallics*, 4th ed.; Teubner: Stuttgart, 2003.
- Lide, D. R., Ed.; In *Handbook of Chemistry and Physics*, CRC Press: Boca Raton, FL, 2009–2010.
- Himmel, H.-J.; Manceron, L.; Downs, A. J.; Pullumbi, P. *Angew. Chem. Int. Ed.* **2002**, *41*, 796.
- Himmel, H.-J.; Manceron, L.; Downs, A. J.; Pullumbi, P. *J. Am. Chem. Soc.* **2002**, *124*, 4448.
- Huber, K. P.; Herzberg, G. *Molecular Spectra and Molecular Structure IV, Constants of Diatomic Molecules*. Van Nostrand: Reinhold, New York, 1979.
- Fu, Z.; Lemire, G. W.; Bishea, G. A.; Morse, M. D. *J. Chem. Phys.* **1990**, *93*, 8420.
- Balducci, G.; Gigli, G.; Meloni, G. *J. Chem. Phys.* **1998**, *109*, 4384.
- Fang, L.; Davis, B. L.; Lu, H.; Lombardi, J. R. *Spectrochim. Acta A* **2001**, *57*, 2809.
- Himmel, H.-J.; Gaertner, B. *Chem. Eur. J.* **2004**, *10*, 5936.
- Martienssen, W. *Landolt-Börnstein: Numerical Data and Functional Relationships in Science and Technology*; Springer: Heidelberg, 1974; Vol. 1982 Continuation of: Landolt-Börnstein: Zahlenwerte und Funktionen aus Physik, Chemie, Astronomie, Geophysik und Technik - 6. Auflage ed., 1983, 1992, 1995; II/6, II/14a, II/14b, II/19a, II/19d-1.
- Andrews, L.; Wang, X. *Angew. Chem. Int. Ed.* **2004**, *43*, 1706.
- Wang, X.; Andrews, L. *J. Phys. Chem. A* **2004**, *108*, 4440.
- Wang, X.; Wolfe, B.; Andrews, L. *J. Phys. Chem. A* **2004**, *108*, 5169.
- Aldridge, S.; Downs, A. J. *Chem. Rev.* **2001**, *101*, 3305.
- Pardoe, J. A.; Downs, A. J. *J. Chem. Rev.* **2007**, *107*, 2.
- Lammertsma, K.; Güner, O. F.; Drewes, R. M.; Reed, A. E.; Schleyer, P. v. R. *Inorg. Chem.* **1989**, *28*, 313.
- Lammertsma, K.; Leszczynski, J. *J. Phys. Chem.* **1990**, *94*, 5543.
- Lammertsma, K.; Ohwada, T. *J. Am. Chem. Soc.* **1996**, *118*, 7247.
- Himmel, H.-J.; Schnöckel, H. *Chem. Eur. J.* **2002**, *8*, 2397.
- Morrison, J. A. *Chem. Rev.* **1991**, *91*, 35.
- Downs, A. J. *Chemistry of Aluminium, Gallium, Indium and Thallium*. Blackie Academic Press: Glasgow, 1993.
- Tuck, D. G. *Polyhedron* **1990**, *9*, 337.
- Tuck, D. G. *Coord. Chem. Rev.* **1992**, *112*, 215.
- Szabó, A.; Kovács, A.; Frenking, G. *Z. Anorg. Allg. Chem.* **2005**, *631*, 1803.
- Ecker, A.; Baum, E.; Friesen, M. A.; Junker, M. A.; Üfing, C.; Köppe, R.; Schnöckel, H. *Z. Anorg. Allg. Chem.* **1998**, *624*, 513–516.
- Vollet, J.; Burgert, R.; Schnöckel, H. *Angew. Chem. Int. Ed.* **2005**, *44*, 6956–6960.
- Mocker, M.; Robl, C.; Schnöckel, H. *Angew. Chem. Int. Ed. Engl.* **1994**, *33*, 862–863.
- Klemp, C.; Stöber, G.; Krossing, I.; Schnöckel, H. *Angew. Chem. Int. Ed.* **2000**, *39*, 3691–3694.
- Beamish, J. C.; Small, R. L. H.; Worrall, I. J. *Inorg. Chem.* **1979**, *18*, 220–223.
- Wei, P.; Li, X.-W.; Robinson, G. H. *Chem. Commun.* **1999**, 1287.
- Duan, T.; Schnöckel, H. *Z. Anorg. Allg. Chem.* **2004**, *630*, 2622–2626.
- Pashkov, A. Y.; Belsky, V. K.; Butychev, M.; Zvukova, T. M. *Russ. Chem. Bull.* **1996**, *45*, 1973–1976.
- Rickard, C. E. F.; Taylor, M. J.; Kilner, M. *Acta Crystallogr. C* **1999**, *55*, 1215–1216.
- Gordon, E. M.; Hepp, A. F.; Duraj, S. A.; Habash, T. S.; Fanwick, P. E.; Schupp, J. D.; Eckles, W. E.; Long, S. *Inorg. Chim. Acta* **1997**, *257*, 247–251.
- Nogai, S. D.; Schmidbaur, H. *Organometallics* **2004**, *23*, 5877–5880.
- Nogai, S.; Schmidbaur, H. *Inorg. Chem.* **2002**, *41*, 4770–4774.
- Baker, R. J.; Bettentrop, H.; Jones, C. *Eur. J. Inorg. Chem.* **2003**, *2003*, 2446–2451.
- Doriat, C. U.; Friesen, M.; Baum, E.; Ecker, A.; Schnöckel, H. *Angew. Chem. Int. Ed. Engl.* **1997**, *36*, 1969–1971.
- Baker, R. J.; Bettentrop, H.; Jones, C. *Inorg. Chem. Commun.* **2004**, *7*, 1289–1291.
- Schnepf, A.; Doriat, C. *Chem. Commun.* **1997**, 2111–2112.
- Beagley, B.; Godfrey, S. M.; Kelly, K. J.; Kungwankunakorn, S.; McAuliffe, C. A.; Pritchard, R. G. *Chem. Commun.* **1996**, 2179–2180.
- Gabbai, F. P.; Schier, A.; Riede, J.; Schmidbaur, H. *Inorg. Chem.* **1995**, *34*, 3855–3856.
- Green, S. P.; Jones, C.; Stasch, A. *Angew. Chem. Int. Ed.* **2007**, *46*, 8618–8621.
- Green, S. P.; Jones, C.; Stasch, A. *Chem. Commun.* **2008**, 6285–6287.
- Khan, M. A.; Peppe, C.; Tuck, D. G. *Canadian J. Chem.* **1984**, *62*, 601–605.
- Godfrey, M. S.; Kelly, J. K.; Kramkowski, P.; McAuliffe, A. C.; Pritchard, G. R. *Chem. Commun.* **1997**, 1001–1002.
- Tacke, M.; Schnöckel, H. *Inorg. Chem.* **1989**, *28*, 2895.
- Schnöckel, H.; Klemp, C. In *Inorganic Chemistry Highlights*; Meyer, G., Naumann, D., Wesemann, L., Eds.; Wiley-VCH: Weinheim, 2002; p 245.
- Schnöckel, H.; Köppe, R. In *Silicon Chemistry*; Jutzki, P., Schubert, U., Eds.; Wiley-VCH: Weinheim, 2003; p 20.
- Dronskowski, R.; Simon, A. *Angew. Chem. Int. Ed.* **1989**, *28*, 758–760.
- Klemm, W.; Tilk, W. *Z. Anorg. Allg. Chem.* **1932**, *207*, 175.
- Garton, G.; Powell, H. M. *J. Inorg. Nucl. Chem.* **1957**, *4*, 84.
- Corbett, J. D.; Hershaff, A. *J. Am. Chem. Soc.* **1958**, *80*, 1530.
- McMullan, R. K.; Corbett, J. D. *J. Am. Chem. Soc.* **1958**, *80*, 4761.
- Woodward, L. A.; Greenwood, N. N.; Hall, J. R.; Worrall, I. *J. Chem. Soc.* **1958**, 1505.
- Clark, R. J.; Griswold, W.; Kleinberg, J. *J. Am. Chem. Soc.* **1958**, *80*, 4764.
- Schmidbaur, H.; Nowak, R.; Bublak, W. *Z. Naturforsch. B* **1987**, *42b*, 553.
- Hönle, W.; Simon, A.; Gerlach, G. *Z. Naturforsch. B* **1987**, *42b*, 546.
- Khan, M. A.; Tuck, D. G. *Inorg. Chim. Acta* **1985**, *97*, 73.
- Massey, A. G. *Adv. Inorg. Chem. Radiochem.* **1983**, *26*, 1.
- Tian, X.; Pape, T.; Mitzel, N. W. *Z. Naturforsch. B* **2004**, *59*, 1524–1531.
- Khan, M. A.; Tuck, D. G.; Taylor, M. J.; Rogers, D. A. *J. Chem. Cryst.* **1986**, *16*, 895–905.
- Bubenheim, W.; Frenzen, G.; Müller, U. *Acta Crystallogr. C* **1995**, *C51*, 1120–1124.
- Uhl, W. *Z. Naturforsch. B* **1988**, *43*, 1113.
- Wehmschulte, R. J.; Ruhlandt-Senge, K.; Olmstead, M. M.; Hope, H.; Sturgeon, B. E.; Power, P. P. *Inorg. Chem.* **1993**, *32*, 2983–2984.
- Wiberg, N.; Blank, T.; Amelunxen, K.; Nöth, H.; Schnöckel, H.; Baum, E.; Purath, A.; Fenske, D. *Eur. J. Inorg. Chem.* **2002**, *2002*, 341–350.



95. Wiberg, N.; Amelunxen, K.; Blank, T.; Nöth, H.; Knizek, J. *Organometallics* **1998**, *17*, 5431.
96. He, X.; Bartlett, R. A.; Olmstead, M. M.; Ruhlandt-Senge, K.; Sturgeon, B. E.; Power, P. P. *Angew. Chem. Int. Ed. Engl.* **1993**, *32*, 717–718.
97. Linti, G.; Köstler, W. *Angew. Chem.* **1996**, *108*, 593–595.
98. Schluter, R. D.; Cowley, A. H.; Atwood, D. A.; Jones, R. A.; Bond, M. R.; Carrano, C. J. *J. Am. Chem. Soc.* **1993**, *115*, 2070–2071.
99. Saxena, A. K.; Zhang, H.; Maguire, J. A.; Hosmane, N. S.; Cowley, A. H. *Angew. Chem. Int. Ed. Engl.* **1995**, *34*, 332–334.
100. Linti, G.; Köstler, W.; Rodig, A. Z. *Anorg. Allg. Chem.* **2002**, *628*, 1319–1326.
101. Baker, R. J.; Jones, C.; Mills, D. P.; Pierce, G. A.; Waugh, M. *Inorg. Chim. Acta* **2008**, *361*, 427–435.
102. Fedushkin, I. L.; Lukoyanov, A. N.; Ketkov, S. Y.; Hummert, M.; Schumann, H. *Chem. Eur. J.* **2007**, *13*, 7050–7056.
103. Brown, D. S.; Decken, A.; Cowley, A. H. *J. Am. Chem. Soc.* **1995**, *117*, 5421–5422.
104. Pott, T.; Jutzi, P.; Schoeller, W. W.; Stammler, A.; Stammler, H.-G. *Organometallics* **2001**, *20*, 5492–5494.
105. Power, P. P.; Brothers, P. J.; Hübler, K.; Hübler, U.; Noll, B. C.; Olmstead, M. M. *Angew. Chem. Int. Ed. Engl.* **1996**, *35*, 2355–2357.
106. Wiberg, N.; Amelunxen, K.; Nöth, H.; Schmidt, M.; Schwenk, H. *Angew. Chem. Int. Ed. Engl.* **1996**, *35*, 65–67.
107. Wochele, R.; Schwarz, W.; Klinkhammer, K. W.; Locke, K.; Weidlein, J. Z. *Anorg. Allg. Chem.* **2000**, *626*, 1963–1973.
108. Henkel, S.; Klinkhammer, K. W.; Schwarz, W. *Angew. Chem. Int. Ed. Engl.* **1994**, *33*, 681–683.
109. Wiberg, N.; Amelunxen, K.; Blank, T.; Lerner, H.-W.; Polborn, K.; Nöth, H.; Littger, R.; Rackl, M.; Schmidt-Amelunxen, M.; Schwenk-Kircher, H.; Warchold, M. Z. *Naturforsch. B* **2001**, *56*, 634–651.
110. Baker, R. J.; Jones, C.; Kloth, M.; Platts, J. A. *Organometallics* **2004**, *23*, 4811–4813.
111. Hoberg, H.; Krause, S. *Angew. Chem. Int. Ed. Engl.* **1976**, *15*, 694.
112. Uhl, W.; Layh, M.; Hildenbrand, T. J. *Organomet. Chem.* **1989**, *364*, 289–300.
113. Hellmann, K. W.; Gade, L. H.; Steiner, A.; Stalke, D.; Möller, F. *Angew. Chem. Int. Ed. Engl.* **1997**, *36*, 160–163.
114. Veith, M.; Spaniol, A.; Pöhlmann, J.; Gross, F.; Huch, V. *Chem. Ber.* **1993**, *126*, 2625.
115. Hellmann, K. W.; Gade, L. H.; Scown, I. J.; McPartlin, M. *Chem. Commun.* **1996**, 2515.
116. Hellmann, K. W.; Gade, L. H.; Fleischer, R.; Kottke, T. *Chem. Eur. J.* **1997**, *3*, 1801.
117. Galka, C. H.; Gade, L. H. *Inorg. Chem.* **1999**, *38*, 1038.
118. Hellmann, K. W.; Gade, L. H.; Fleischer, R.; Stalke, D. *Chem. Commun.* **1997**, 527.
119. Hellmann, K. W.; Bergner, A.; Gade, L. H.; Scown, I. J.; McPartlin, M. J. *Organomet. Chem.* **1999**, *573*, 156–164.
120. Dias, H. V. R. In Abel, E. W.; Stone, F. G. A., Wilkinson, G., Eds.; *Comprehensive Coordination Chemistry II*; Pergamon Press: Oxford, 1995; Vol. 2, p 383.
121. Gade, L. H. *Dalton Trans.* **2003**, 267.
122. Reedijk, J.; Roelofsen, G.; Siedle, A. R.; Spek, A. L. *Inorg. Chem.* **1979**, *18*, 1947.
123. Beck, J.; Strähle, J. Z. *Naturforsch. B: Anorg. Chem. Org. Chem.* **1986**, *41B*, 1381.
124. Lee, H. S.; Hauber, S.-O.; Vindus, D.; Niemeyer, M. *Inorg. Chem.* **2008**, *47*, 4401.
125. Dias, H. V. R.; Singh, S.; Cundari, T. R. *Angew. Chem. Int. Ed.* **2005**, *44*, 4907.
126. Johnson, M. T.; Campana, C. F.; Foxman, B. M.; Desmarais, W.; Vela, M. J.; Miller, J. S. *Chem. Eur. J.* **2000**, *6*, 1805.
127. Manke, D. R.; Nocera, D. G. *Polyhedron* **2006**, *25*, 493.
128. Wiberg, N.; Blank, T.; Amelunxen, K.; Nöth, H.; Knizek, J.; Habereeder, T.; Kaim, W.; Wanner, M. *Eur. J. Inorg. Chem.* **2001**, 1719–1727.
129. Wright, R. J.; Brynda, M.; Fetting, J. C.; Betzer, A. R.; Power, P. P. *J. Am. Chem. Soc.* **2006**, *128*, 12498–12509.
130. Cui, C.; Li, X.; Wang, C.; Zhang, J.; Cheng, J.; Zhu, X. *Angew. Chem. Int. Ed.* **2006**, *45*, 2245–2247.
131. Wright, R. J.; Phillips, A. D.; Power, P. P. *J. Am. Chem. Soc.* **2003**, *125*, 10784–10785.
132. Armstrong, D. R.; Barr, D.; Clegg, W.; Hodgson, S. M.; Mulvey, R. E.; Reed, D.; Snaith, R.; Wright, D. S. *J. Am. Chem. Soc.* **1989**, *111*, 4719–4727.
133. Hardman, N. J.; Wright, R. J.; Phillips, A. D.; Power, P. P. *Angew. Chem.* **2002**, *114*, 2966–2968.
134. Hardman, N. J.; Wright, R. J.; Phillips, A. D.; Power, P. P. *J. Am. Chem. Soc.* **2003**, *125*, 2667–2679.
135. Uhl, W.; Hiller, W.; Layh, M.; Schwarz, W. *Angew. Chem. Int. Ed. Engl.* **1992**, *31*, 1364–1366.
136. Uhl, W.; Jantschak, A. J. *Organomet. Chem.* **1998**, *555*, 263.
137. Schultz, S., In *Comprehensive Organometallics Chemistry III*, Mingos, D. M. P., Crabtree, R. H., Eds.; Elsevier: Oxford, UK, **2007**, Vol. 3, pp. 287–342.
138. Niemeyer, M.; Power, P. P. *Angew. Chem.* **1998**, *110*, 1291.
139. Wright, R. J.; Phillips, A. D.; Hino, S.; Power, P. P. *J. Am. Chem. Soc.* **2005**, *127*, 4794.
140. Wright, R. J.; Brynda, M.; Power, P. P. *Angew. Chem. Int. Ed.* **2006**, *45*, 5953–5956.
141. Su, J.; Li, X.-W.; Crittendon, R. C.; Robinson, G. H. *J. Am. Chem. Soc.* **1997**, *119*, 5471–5472.
142. Wang, Y.; Robinson, G. H. *Organometallics* **2007**, *26*, 2–11.
143. Uhl, W.; Vester, A.; Hiller, W. *J. Organomet. Chem.* **1993**, *443*, 9–17.
144. Pluta, C.; Pörschke, K.-R.; Krüger, C.; Hildenbrand, K. *Angew. Chem. Int. Ed. Engl.* **1993**, *32*, 388.
145. Uhl, W.; Vester, A.; Fenske, D.; Baum, G. *J. Organomet. Chem.* **1994**, *464*, 23.
146. Uhl, W.; Gerding, R.; Vester, A. *J. Organomet. Chem.* **1996**, *513*, 163.
147. Uhl, W.; Graupner, R.; Layh, M.; Schütz, U. *J. Organomet. Chem.* **1995**, 493.
148. Linti, G.; Köstler, W.; Rodig, A. Z. *Anorg. Allg. Chem.* **2002**, *628*, 1319–1326.
149. Henke, P.; Pankewitz, T.; Klopfer, W.; Breher, F.; Schnöckel, H. *Angew. Chem.* **2009**, *121*, 8285–8290.
150. Uhl, W.; Vester, A. *Chem. Ber.* **1993**, *126*, 941–945.
151. Uhl, W.; Schütz, U.; Pohl, S.; Saak, W. Z. *Naturforsch.* **1994**, *49b*, 637.
152. Uhl, W.; Schütz, U.; Vester, A.; Karsch, H. H. *Chem. Ber.* **1993**, *126*, 2637–2641.
153. Uhl, W.; Spies, T. Z. *Anorg. Allg. Chem.* **2000**, *626*, 1059–1064.
154. Linti, G.; Rodig, A.; Köstler, W. Z. *Anorg. Allg. Chem.* **2001**, *627(7)*, 1465–1476.
155. Veith, M.; Goffing, F.; Becker, S.; Huch, V. *J. Org. Chem.* **1991**, *406*, 105–118.
156. Grocholl, L.; Schranz, I.; Stahl, L.; Staples, R. J. *Inorg. Chem.* **1998**, *37*, 2496–2499.
157. Chen, Y.; Araki, Y.; Hanack, M.; Fujitsuka, M.; Ito, O. *Eur. J. Inorg. Chem.* **2005**, *2005*, 4655–4658.
158. Bertagnolli, H.; Blau, W. J.; Chen, Y.; Dini, D.; Feth, M. P.; O'Flaherty, S. M.; Hanack, M.; Krishnan, V. J. *Mater. Chem.* **2005**, *15*, 683–689.
159. Chen, Y.; Barthel, M.; Seiler, M.; Subramanian, L. R.; Bertagnolli, H.; Hanack, M. *Angew. Chem. Int. Ed.* **2002**, *41*, 3239–3242.
160. García-Castro, M.; Martín, A.; Mena, M.; Yélamos, C. *Chem. Eur. J.* **2009**, *15*, 7180–7191.
161. Valean, A.-M.; Gomez-Ruiz, S.; Lonneck, P.; Silaghi-Dumitrescu, I.; Silaghi-Dumitrescu, L.; Hey-Hawkins, E. *New J. Chem.* **2009**, *33*, 1771–1779.
162. Hoberg, H.; Krause, S. *Angew. Chem. Int. Ed. Engl.* **1978**, *17*, 949–950.
163. Schnepf, A.; Weckert, E.; Linti, G.; Schnöckel, H. *Angew. Chem.* **1999**, *111*, 3578–3581.
164. Wiberg, N.; Blank, T.; Westerhausen, M.; Schneiderbauer, S.; Schnöckel, H.; Krossing, I.; Schnepf, A. *Eur. J. Inorg. Chem.* **2002**, *2002*, 351–356.
165. Uhl, W.; Melle, S. *Chem. Eur. J.* **2001**, *7*, 4216–4221.
166. Uhl, W.; Voss, M.; Luftmann, H. *Chem. Commun.* **2009**, 6854–6856.
167. Uhl, W.; El-Hamdan, A.; Geiseler, G.; Harms, K. Z. *Anorg. Allg. Chem.* **2004**, *630*, 821–828.
168. Uhl, W.; El-Hamdan, A.; Prött, M.; Spühler, P.; Frenking, G. *J. Chem. Soc. Dalton Trans.* **2003**, 1360–1364.
169. Cowley, A. H.; Decken, A.; Olazábal, C. A. *J. Org. Chem.* **1996**, *524*, 271–273.
170. Klimek, K. S.; Cui, C.; Roesky, H. W.; Noltemeyer, M.; Schmidt, H.-G. *Organometallics* **2000**, *19*, 3085–3090.
171. Beachley, O. T.; Gardinier, J. R.; Churchill, M. R. *Organometallics* **2000**, *19*, 4544–4549.
172. Jones, C.; Junk, P. C.; Kloth, M.; Proctor, K. M.; Stasch, A. *Polyhedron* **2006**, *25*, 1592–1600.
173. Linti, G.; Zessin, T. *Dalton Trans.* **2011**, *40*, 5591–5598.
174. Rudolf, D.; Kaifer, E.; Himmel, H.-J. *Eur. J. Inorg. Chem.* **2010**, *2010*, 4952–4961.
175. Lomell, V.; McBurnett, B. G.; Cowley, A. H. *J. Org. Chem.* **1998**, *562*, 123–125.
176. Schmidt, E. S.; Schier, A.; Mitzel, N. W.; Schmidbauer, H. Z. *Naturforsch.* **2001**, *56b*, 458.
177. Cheng, Y.; Doyle, D. J.; Hitchcock, P. B.; Lappert, M. F. *Dalton Trans.* **2006**, 4449–4460.
178. Stender, M.; Power, P. P. *Polyhedron* **2002**, *21*, 525–529.
179. Baker, R. J.; Farley, R. D.; Jones, C.; Kloth, M.; Murphy, D. M. *Chem. Commun.* **2002**, 1196–1197.
180. Baker, R. J.; Farley, R. D.; Jones, C.; Mills, D. P.; Kloth, M.; Murphy, D. M. *Chem. Eur. J.* **2005**, *11*, 2972–2982.
181. Jones, C.; Baker, R. J.; Farley, R. D.; Kloth, M.; Murphy, D. M. *Dalton Trans.* **2002**, 3844–3850.

182. Linti, G.; Köstler, W. *Chem. Eur. J.* **1998**, *4*, 942–949.
183. Fischer, R. A.; Weiß, J. *Angew. Chem.* **1999**, *113*, 589–591.
184. Gemel, C.; Steinke, T.; Cokoja, M.; Kamptner, A.; Fischer, R. A. *Eur. J. Inorg. Chem.* **2004**, 4161–4176.
185. Vidovic, D.; Aldridge, S. *Chem. Sci.* **2011**, *2*, 601.
186. Whitmire, K. H. In *Comprehensive Organometallic Chemistry III*; Mingos, D. M. P., Crabtree, R. H., Eds.; Elsevier: Oxford, **2007**; Vol. 3, pp 343–407.
187. Uhl, W. *Chem. Soc. Rev.* **2000**, *29*, 259–265.
188. Uhl, W.; Graupner, R.; Pohl, S.; Saak, W.; Hiller, W.; Neumayer, M. Z. *Anorg. Allg. Chem.* **1997**, *623*, 883–891.
189. Uhl, W.; El-Hamdan, A. *Eur. J. Inorg. Chem.* **2004**, 2004, 969–972.
190. Uhl, W.; Lawrenz, A.; Zemke, S. Z. *Anorg. Allg. Chem.* **2007**, *633*, 979–985.
191. Uhl, W.; El-Hamdan, A.; Schindler, K. P. *Eur. J. Inorg. Chem.* **2006**, 1817–1823.
192. Uhl, W.; Spies, T.; Saak, W. *Eur. J. Inorg. Chem.* **1998**, 1661–1665.
193. Uhl, W.; Spies, T.; Haase, D.; Winter, R.; Kaim, W. *Organometallics* **2000**, *19*, 1128–1131.
194. Uhl, W.; Fick, A.-C.; Spies, T.; Geiseler, G.; Harms, K. *Organometallics* **2003**, *23*, 72–75.
195. Uhl, W.; Cuyper, L.; Prott, M.; Harms, K. *Polyhedron* **2002**, *21*, 511–518.
196. Uhl, W.; Voß, M.; Layh, M.; Rogel, F. *Dalton Trans.* **2010**, *39*, 3160–3162.
197. Uhl, W.; Prött, M.; Geiseler, G.; Harms, K. Z. *Naturforsch.* **2002**, *57b*, 141–144.
198. Uhl, W.; Spies, T.; Koch, R. J. *Chem. Soc. Dalton Trans.* **1999**, 2385–2391.
199. Uhl, W.; Spies, T.; Saak, W. Z. *Anorg. Allg. Chem.* **1999**, *625*, 2095–2102.
200. Uhl, W.; Graupner, R.; Hahn, I.; Spies, T.; Frank, W. *Eur. J. Inorg. Chem.* **1998**, 355–360.
201. Uhl, W.; Cuyper, L.; Schuler, K.; Spies, T.; Strohmman, C.; Lehmen, K. Z. *Anorg. Allg. Chem.* **2000**, *626*, 1526–1534.
202. Uhl, W.; El-Hamdan, A.; Lawrenz, A. *Eur. J. Inorg. Chem.* **2005**, 1056–1062.
203. Üffing, C.; Baum, E.; Köppe, R.; Schnöckel, H. *Angew. Chem. Int. Ed.* **1998**, *37*, 2397–2400.
204. Hardman, N. J.; Eichler, B. E.; Power, P. P. *J. Chem. Soc., Chem. Commun.* **2000**, 1991–1992.
205. Baker, R. J.; Jones, C.; Kloth, M.; Platts, J. A. *Angew. Chem. Int. Ed.* **2003**, *42*, 2660–2663.
206. Kamptner, A.; Gemel, C.; Fischer, R. A. *Inorg. Chem.* **2008**, *47*, 7279–7285.
207. Yurkerwicz, K.; Buccella, D.; Melnick, J. G.; Parkin, G. *Chem. Sci.* **2010**, *1*, 210–214.
208. Sandholzer, N. Diplomarbeit, Universität Karlsruhe.
209. Linti, H. S., Unpublished results.
210. Henke, P.; Huber, M.; Steiner, J.; Bowen, K.; Eichhorn, B.; Schnöckel, H. J. *Am. Chem. Soc.* **2009**, *131*, 5698–5704.
211. Li, X.-W.; Wei, P.; Beck, B. C.; Xie, Y.; Schaefer, Iii, H. F.; Su, J.; Robinson, G. H. *Chem. Commun.* **2000**, 453–454.
212. Uhl, W.; Melle, S.; Geiseler, G.; Harms, K. *Organometallics* **2001**, *20*, 3355–3357.
213. Uhl, W.; Schmock, F.; Geiseler, G. Z. *Anorg. Allg. Chem.* **2002**, *628*, 1963–1966.
214. Linti, G.; Köstler, W.; Rodig, A. *Eur. J. Inorg. Chem.* **1998**, 745–749.
215. Linti, G.; Köstler, W.; Piotrowski, H.; Rodig, A. *Angew. Chem.* **1998**, *110*, 2331–2333.
216. Li, X.-W.; Xie, Y.; Schreiner, P. R.; Gripper, K. D.; Crittendon, R. C.; Campana, C. F.; Schaefer, H. F.; Robinson, G. H. *Organometallics* **1996**, *15*, 3798.
217. Hill, M. S.; Pongtavornpinyo, R.; Hitchcock, P. B. *Chem. Commun.* **2006**, 3720–3722.
218. Wiberg, N.; Blank, T.; Lerner, H.-W.; Fenske, D.; Linti, G. *Angew. Chem.* **2001**, *113*, 1275–1278.
219. Hill, M. S.; Hitchcock, P. B.; Pongtavornpinyo, R. *Dalton Trans.* **2005**, 273.
220. Holland, P. L.; Cundari, T. R.; Perez, L. L.; Eckert, N. A.; Lachicotte, R. J. *J. Am. Chem. Soc.* **2002**, *124*, 14416.
221. Cheng, Y.; Hitchcock, P. B.; Lappert, M. F.; Zhou, M. *Chem. Commun.* **2005**, 752.
222. Mocker, M.; Robl, C.; Schnöckel, H. *Angew. Chem. Int. Ed. Engl.* **1994**, *33*, 1754–1755.
223. Ecker, A.; Schnöckel, H. Z. *Anorg. Allg. Chem.* **1996**, *622*, 149–152.
224. Ecker, A.; Schnöckel, H. Z. *Anorg. Allg. Chem.* **1998**, *624*, 813–816.
225. Ecker, A.; Köppe, R.; Üffing, C.; Schnöckel, H. Z. *Anorg. Allg. Chem.* **1998**, *624*, 817–822.
226. Klemp, C.; Köppe, R.; Weckert, E.; Schnöckel, H. *Angew. Chem. Int. Ed.* **1999**, *38*, 1740.
227. Klemp, C.; Bruns, M.; Gauss, J.; Häussermann, U.; Stösser, G.; van Wüllen, L.; Jansen, M.; Schnöckel, H. J. *Am. Chem. Soc.* **2001**, *123*, 9099–9106.
228. Duan, T.; Stöber, G.; Schnöckel, H. *Angew. Chem. Int. Ed.* **2005**, *44*, 2973–2975.
229. Duan, T.; Henke, P.; Stöber, G.; Zhang, Q.-F.; Schnöckel, H. J. *Am. Chem. Soc.* **2010**, *132*, 1323–1327.
230. Duan, T.; Stöber, G.; Schnöckel, H. Z. *Anorg. Allg. Chem.* **2005**, *631*, 1129–1133.
231. Loos, D.; Schnöckel, H.; Fenske, D. *Angew. Chem. Int. Ed. Engl.* **1993**, *32*, 1059.
232. Hardman, N. J.; Power, P. P.; Gorden, J. D.; Macdonald, C. L. B.; Cowley, A. H. *Chem. Commun.* **2001**, 1866–1867.
233. Hartig, J.; Steiner, J.; Stöber, A.; Schnöckel, H. *Chem. Eur. J.* **2007**, *13*, 4475–4482.
234. Cole, M. L.; Jones, C.; Kloth, M. *Inorg. Chem.* **2005**, *44*, 4909–4911.
235. Zessin, T. Dissertation, Ruprecht-Karls-Universität Heidelberg, 2011.
236. Seifert, A.; Linti, G. *Eur. J. Inorg. Chem.* **2007**, 5080–5086.
237. Wehmschulte, R. J.; Power, P. P. *Angew. Chem.* **1998**, *110*, 3344.
238. Linti, G.; Köstler, W. *Angew. Chem.* **1997**, *109*, 2758–2760.
239. Twamley, B.; Power, P. P. *Angew. Chem. Int. Ed.* **2000**, *39*, 3500–3503.
240. Donchev, A.; Schnepf, A.; Baum, E.; Stöber, G.; Schnöckel, H. Z. *Anorg. Allg. Chem.* **2002**, *628*, 157–161.
241. Hill, M. S.; Hitchcock, P. B.; Pongtavornpinyo, R. *Science* **2006**, *311*, 1904–1907.
242. Hill, M. S.; Hitchcock, P. B.; Pongtavornpinyo, R. *Dalton Trans.* **2007**, 731–733.
243. Dohmeier, C.; Loos, D.; Schnöckel, H. *Angew. Chem. Int. Ed. Engl.* **1996**, *35*, 129–149.
244. Steiner, J.; Stöber, G.; Schnöckel, H. Z. *Anorg. Allg. Chem.* **2004**, *630*, 1879–1882.
245. Steiner, J.; Schnöckel, H. *Chem. Eur. J.* **2006**, *12*, 5429–5433.
246. von Hänisch, C.; Fenske, D.; Kattanek, M.; Ahlrichs, R. *Angew. Chem. Int. Ed.* **1999**, *38*, 2736–2738.
247. Dohmeier, C.; Robl, C.; Tacke, M.; Schnöckel, H. *Angew. Chem. Int. Ed. Engl.* **1991**, *30*, 564–565.
248. Loos, D.; Baum, E.; Ecker, A.; Schnöckel, H.; Downs, A. J. *Angew. Chem.* **1997**, *109*, 894.
249. Schmidt, E. S.; Jokisch, A.; Schmidbaur, H. J. *Am. Chem. Soc.* **1999**, *121*, 9758.
250. Schmidbaur, H.; Schmidt, E. S.; Schier, A. *Dalton Trans.* **2001**, 505–507.
251. Kuchta, M. C.; Bonanno, J. B.; Parkin, G. J. *Am. Chem. Soc.* **1996**, *118*, 10914–10915.
252. Cowley, A. H. *Chem. Commun.* **2004**, 2369–2375.
253. Dias, H. V. R.; Jin, W. *Inorg. Chem.* **2000**, *39*, 815–819.
254. Frazer, A.; Hodge, P.; Piggott, B. *Chem. Commun.* **1996**, 1727–1728.
255. Green, J. C.; Suter, J. L. J. *Chem. Soc. Dalton Trans.* **1999**, 4087–4092.
256. Reger, D. L. *Coord. Chem. Rev.* **1996**, *147*, 571–595.
257. Andrews, C. G.; Macdonald, C. L. B. *Angew. Chem.* **2005**, *117*, 7619–7622.
258. Cooper, B. F. T.; Macdonald, C. L. B. In *The Group 13 Metals Aluminium, Gallium, Indium and Thallium – Chemical Patterns and Peculiarities*; Aldridge, S., Downs, A. J., Eds.; Wiley: New York, 2011; pp 342–401.
259. Macdonald, C. B.; Cowley, A. H. J. *Am. Chem. Soc.* **1999**, *121*, 12113–12126.
260. Jutzi, P.; Neumann, B.; Reumann, G.; Schebaum, L. O.; Stammli, H.-G. *Organometallics* **1999**, *18*, 2550–2552.
261. Jutzi, P.; Neumann, B.; Reumann, G.; Stammli, H.-G. *Organometallics* **1998**, *17*, 1305–1314.
262. Weiß, J.; Stetzkamp, D.; Nuber, B.; Fischer, R. A.; Boehme, C.; Frenking, G. *Angew. Chem.* **1997**, *109*, 95–97.
263. Yu, Q.; Purath, A.; Donchev, A.; Schnöckel, H. J. *Organomet. Chem.* **1999**, *584*, 94–97.
264. Weiss, D.; Steinke, T.; Winter, M.; Fischer, R. A.; Fröhlich, N.; Uddin, J.; Frenking, G. *Organometallics* **2000**, *19*, 4583–4588.
265. Gorden, J. D.; Voigt, A.; Macdonald, C. L. B.; Silverman, J. S.; Cowley, A. H. *J. Am. Chem. Soc.* **2000**, *122*, 950–951.
266. Yang, Z.; Ma, X.; Oswald, R. B.; Roesky, H. W.; Zhu, H.; Schulzke, C.; Starke, K.; Baldus, M.; Schmidt, H.-G.; Noltemeyer, M. *Angew. Chem.* **2005**, *117*, 7234–7236.
267. Gorden, J. D.; Macdonald, C. L. B.; Cowley, A. H. *Chem. Commun.* **2001**, 75–76.
268. Schulz, S.; Kuczkowski, A.; Schuchmann, D.; Flörke, U.; Nieger, M. *Organometallics* **2006**, *25*, 5487–5491.
269. Jutzi, P.; Neumann, B.; Reumann, G.; Schebaum, L. O.; Stammli, H. G. *Organometallics* **2001**, *20*, 2854–2858.
270. Linti, G.; Monakhov, K.; Bühler, M.; Zessin, T. *Dalton Trans.* **2009**, *38*, 8071–8078.
271. Wade, K. *Chem. Commun.* **1971**, 792–793.
272. Uhl, W. *Naturwissenschaften* **2004**, *91*, 305–319.
273. Uhl, W. *Adv. Organomet. Chem.* **2004**, *51*, 53–108.
274. Baker, R. J.; Jones, C. J. *Chem. Soc. Dalton Trans.* **2005**, 1341–1348.
275. Linti, G.; Schnöckel, H.; Uhl, W.; Wiberg, N. In *Molecular Clusters of the Main Group Elements*; Driess, M., Nöth, H., Eds.; Wiley-VCH: Weinheim, 2004; pp 126–168.

276. Uhl, W. *Phosphorus, Sulfur Silicon Relat. Elem.* **2004**, *179*, 743–748.
277. Rivard, E.; Power, P. P. *Inorg. Chem.* **2007**, *46*, 10047–10064.
278. Uhl, W. *Rev. Inorg. Chem.* **1998**, *18*, 239–282.
279. Power, P. J. *Chem. Soc. Dalton Trans.* **1998**, 2939–2951.
280. Power, P. P. *Chem. Rev.* **1999**, *99*, 3463–3504.
281. Power, P. In *Group 13 Chemistry I*; Roesky, H., Atwood, D., Eds.; Springer: Berlin, **2002**; Vol. 103, pp 57–84.
282. Maier, C.-F.; Pritzkow, H.; Siebert, W. *Angew. Chem.* **1999**, *111*, 1772.
283. Huber, M.; Schnöckel, H. *Inorg. Chim. Acta* **2008**, *361*, 457–461.
284. Schnitter, C.; Roesky, H. W.; Röpken, C.; Herbst-Irmer, R.; Schmidt, H.-G.; Noltemeyer, M. *Angew. Chem. Int. Ed.* **1998**, *37*, 1952–1955.
285. Purath, A.; Dohmeier, C.; Ecker, A.; Schnöckel, H.; Amelunxen, K.; Passler, T.; Wiberg, N. *Organometallics* **1998**, *17*, 1894–1896.
286. Purath, A.; Schnöckel, H. *J. Org. Chem.* **1999**, *579*, 373–375.
287. Schiefer, M.; Reddy, N. D.; Roesky, H. W.; Vidovic, D. *Organometallics* **2003**, *22*, 3637–3638.
288. Sitzmann, H.; Lappert, M. F.; Dohmeier, C.; Üffing, C.; Schnöckel, H. *J. Org. Chem.* **1998**, *561*, 203–208.
289. Schram, E. P.; Sudha, N. *Inorg. Chim. Acta* **1991**, *183*, 213–216.
290. Gauss, J.; Schneider, U.; Ahlrichs, R.; Dohmeier, C.; Schnöckel, H. *J. Am. Chem. Soc.* **1993**, *115*, 2402–2408.
291. Green, M. L. H.; Mountford, P.; Smout, G. J.; Speel, S. R. *Polyhedron* **1990**, *9*, 2763–2765.
292. Wright, R. J.; Bynda, M.; Fettingner, J. C.; Betzer, A. R.; Power, P. P. *J. Am. Chem. Soc.* **2006**, *128*, 12498–12509.
293. Linti, G. *J. Organomet. Chem.* **1996**, *520*, 107–113.
294. Linti, G.; Rodig, A. *J. Chem. Soc., Chem. Commun.* **2000**, 127–128.
295. Wiberg, N.; Amelunxen, K.; Lerner, H. W.; Nöth, H.; Ponikvar, W.; Schwenk, H. *J. Organomet. Chem.* **1999**, *574*, 246.
296. Schlüter, R. D.; Cowley, A. H.; Atwood, D. A.; Jones, R. A. *J. Coord. Chem.* **1993**, *30*, 25–28.
297. Uhl, W.; Jantschak, A.; Saak, W.; Kaupp, M.; Wartchow, R. *Organometallics* **1998**, *17*, 5009–5017.
298. Bühler, M.; Linti, G. *Z. Anorg. Allg. Chem.* **2006**, 2453–2460.
299. Uhl, W.; Keimling, S. U.; Klinkhammer, K. W.; Schwarz, W. *Angew. Chem. Int. Ed. Engl.* **1997**, *36*, 64–65.
300. Loos, D.; Schnöckel, H. *J. Organomet. Chem.* **1993**, *463*, 37–40.
301. Buchin, B.; Gemel, C.; Cadenbach, T.; Fischer, R. A. *Inorg. Chem.* **2006**, *45*, 1789–1794.
302. Francis, M. D.; Hitchcock, P. B.; Nixon, J. F.; Schnöckel, H.; Steiner, J. *J. Org. Chem.* **2002**, *646*, 191–195.
303. Chojnacki, J.; Baum, E.; Krossing, I.; Carmichael, D.; Mathey, F.; Schnöckel, H. *Z. Anorg. Allg. Chem.* **2001**, *627*, 1209–1212.
304. Jutz, P.; Schebaum, L. O. *J. Organomet. Chem.* **2002**, *654*, 176–179.
305. Haaland, A.; Martinsen, K.-G.; Volden, H. V.; Loos, D.; Schnöckel, H. *Acta Chem. Scand.* **1994**, *48*, 172–174.
306. Beachley, O. T., Jr.; Churchill, M. R.; Fettingner, J. C.; Pazik, J. C.; Victoriano, L. *J. Am. Chem. Soc.* **1986**, *108*, 4666–4668.
307. Beachley, O. T., Jr.; Blom, R.; Churchill, M. R.; Faegri, J. K.; Fettingner, J. C.; Pazik, J. C.; Victoriano, L. *Organometallics* **1989**, *8*, 346–356.
308. Haaland, A.; Martinsen, K.-G.; Volden, H. V.; Kaim, W.; Waldhoer, E.; Uhl, W.; Schuetz, U. *Organometallics* **1996**, *15*, 1146–1150.
309. Ahlrichs, R.; Ehrig, M.; Horn, H. *Chem. Phys. Lett.* **1991**, *183*, 227.
310. Schneider, U.; Ahlrichs, R.; Horn, H.; Schäfer, A. *Angew. Chem. Int. Ed. Engl.* **1992**, *31*, 353.
311. Linti, G. Unpublished results.
312. Schulz, S.; Roesky, H. W.; Koch, H. J.; Sheldrick, G. M.; Stalke, D.; Kuhn, A. *Angew. Chem. Int. Ed. Engl.* **1993**, *32*, 1107.
313. Linti, G.; Köstler, W.; Kehrwald, M.; Rodig, A.; Blank, T.; Wiberg, N. *Organometallics* **2001**, *20*, 860–867.
314. Uhl, W.; Benter, M.; Saak, W.; Jones, P. G. *Z. Anorg. Allg. Chem.* **1998**, *624*, 1622–1628.
315. Linti, G.; Bühler, M.; Urban, H. *Z. Anorg. Allg. Chem.* **1998**, *624*, 517–520.
316. Uhl, W.; Graupner, R.; Pohlmann, M.; Pohl, S.; Saak, W. *Chem. Ber.* **1996**, *129*, 143.
317. Uhl, W.; Pohlmann, M. *Chem. Commun.* **1998**, 451.
318. Seifert, A. Dissertation, Heidelberg, 2008.
319. Mason, M. R.; Smith, J. M.; Bott, S. G.; Barron, A. B. *J. Am. Chem. Soc.* **1993**, *115*, 4971–4984.
320. Storre, J.; Klemp, A.; Roesky, H. W.; Fleischer, R.; Stalke, D. *Organometallics* **1997**, *16*, 3074–3076.
321. Harlan, C. J.; Bott, S. G.; Barron, A. R. *J. Am. Chem. Soc.* **1995**, *117*, 6465–6474.
322. Uhl, W.; Graupner, R.; Hiller, W.; Neumayer, M. *Angew. Chem.* **1997**, *109*, 62–64.
323. Vollet, J.; Stösser, G.; Schnöckel, H. *Inorg. Chim. Acta* **2007**, *360*, 1298–1304.
324. Dohmeier, C.; Mocker, M.; Schnöckel, H.; Löt, A.; Schneider, U.; Ahlrichs, R. *Angew. Chem. Int. Ed. Engl.* **1993**, *32*, 1428–1430.
325. Hiller, W.; Klinkhammer, K.-W.; Uhl, W.; Wagner, J. *Angew. Chem.* **1991**, *103*, 103.
326. Linti, G.; Çoban, S.; Dutta, D. *Z. Anorg. Allg. Chem.* **2004**, *630*, 319–323.
327. McKee, M. L.; Wang, Z.-X.; Schleyer, P. v. R. *J. Am. Chem. Soc.* **2000**, *122*, 4781–4793.
328. Quillian, B.; Wei, P.; Wannere, C. S.; Schleyer, P. v. R.; Robinson, G. H. *J. Am. Chem. Soc.* **2009**, *131*, 3168–3169.
329. Wolf, R.; Uhl, W. *Angew. Chem.* **2009**, *121*, 6905–6907.
330. Wolf, R.; Uhl, W. *Angew. Chem. Int. Ed.* **2009**, *48*, 6774–6776.
331. Wang, Y.; Xie, Y.; Wei, P.; King, R. B.; Schaefer, H. F.; Schleyer, P. v. R.; Robinson, G. H. *Science* **2008**, *321*, 1069–1071.
332. Wang, Y.; Xie, Y.; Wei, P.; King, R. B.; Schaefer, H. F., III; Schleyer, P. v. R.; Robinson, G. H. *J. Am. Chem. Soc.* **2008**, *130*, 14970–14971.
333. Wang, Y.; Quillian, B.; Wei, P.; Xie, Y.; Wannere, C. S.; King, R. B.; Schaefer, H. F.; Robinson, P. v. R.; Robinson, G. H. *J. Am. Chem. Soc.* **2008**, *130*, 3298–3299.
334. David, S. *Angew. Chem.* **2008**, *120*, 2021–2023.
335. Schneepf, A.; Stöber, G.; Schnöckel, H. *Z. Anorg. Allg. Chem.* **2000**, *626*, 1676.
336. Guggenberger, L. *J. Inorg. Chem.* **1969**, *8*, 2771.
337. Jacobson, R. A.; Lipscomb, W. N. *J. Chem. Phys.* **1959**, *31*, 605.
338. Pawley, G. S. *Acta Cryst.* **1966**, *20*, 631.
339. Johnson, N. W. *Canad. J. Math.* **1966**, *18*, 169–200.
340. Uhl, W. *Rev. Inorg. Chem.* **1998**, *18*, 239.
341. Schneepf, A.; Stöber, G.; Köppe, R.; Schnöckel, H. *Angew. Chem. Int. Ed. Engl.* **2000**, *39*, 1637.
342. Mingos, D. M. P. *Acc. Chem. Res.* **1984**, *17*, 311–319.
343. Baslarkrishnarajan, M. M.; Jemmis, E. D. *J. Am. Chem. Soc.* **2000**, *122*, 4516.
344. Jemmis, E. D.; Baslarkrishnarajan, M. M.; Pancharatna, P. D. *J. Am. Chem. Soc.* **2001**, *123*, 4313–4323.
345. Chen, Z.; Wannere, C. S.; Corminboeuf, C.; Puchta, R.; Schleyer, P. v. R. *Chem. Rev.* **2005**, *105*, 3842–3888.
346. Neuss, J. *Aromatizität, Geschichte und mathematische Analyse eines fundamentalen chemischen Begriffs*. Hyle Publications: Karlsruhe, 2002.
347. Aihara, J. *J. Am. Chem. Soc.* **1978**, *100*, 3339.
348. Schleyer, P. v. R.; Maerker, C.; Dransfeld, A.; Jiao, H.; Hommes, N. J. R. v. E. *J. Am. Chem. Soc.* **1996**, *118*, 6317–6318.
349. Saunders, M.; Jimenez-Vazquez, H. A.; Cross, R. J.; Mroczkowski, S.; Freedberg, D. I.; Anet, F. A. L. *Nature* **1994**, *367*, 256.
350. McKee, M. *J. Inorg. Chem.* **2002**, *41*, 1299.
351. Hönle, W.; Grin, Y.; Burckhardt, A.; Wedig, U.; von Schnerig, H. G.; Kallner, R.; Binder, H. *J. Solid State Chem.* **1997**, *173*, 59.
352. King, R. B.; Schleyer, P. v. R. In *Molecular Clusters of the Main Group Elements*; Driess, M., Nöth, H., Eds.; Wiley-VCH: Weinheim, 2004; pp 1–33.
353. Schleyer, P. v. R.; Subramanian, G.; Jiao, J.; Najafian, K.; Hofmann, M. In *Advances in Boron Chemistry*, Siebert, W., Ed.; Royal Society of Chemistry: Cambridge, 1997; pp 3–14.
354. Schleyer, P. v. R.; Subramanian, G.; Najafian, K. In *The Borane, Carborane and Carbocation Continuum*; Casanova, J., Ed.; Wiley: New York, 1998; pp 169–190.
355. Schleyer, P. v. R.; Subramanian, G. *Inorg. Chem.* **1998**, *37*, 3455–3470.
356. Chi, X.; Xu, X.; Chen, X.; Yuan, Z. *Huaxue Wuli Xuebao* **2005**, *18*, 941–946.
357. Chi, X. X.; Chen, X. J.; Yuan, Z. S. *J. Mol. Struct. (THEOCHEM)* **2005**, *732*, 149–153.
358. Chi, X. X.; Li, X. H.; Chen, X. J.; Yuang, Z. S. *J. Mol. Struct. (THEOCHEM)* **2004**, *677*, 21–27.
359. Feixas, F.; Jimenez-Halla, J. O. C.; Matito, E.; Poater, J.; Sola, M. *J. Chem. Theory Comput.* **2010**, *6*, 1118–1130.
360. Gorlov, M.; Kloo, L. *Coord. Chem. Rev.* **2008**, *252*, 1564–1576.
361. Juselius, J.; Straka, M.; Sundholm, D. *J. Phys. Chem. A* **2001**, *105*, 9939–9944.
362. Kuznetsov, A. E.; Boldyrev, A. I. *Struct. Chem.* **2002**, *13*, 141–148.
363. Kuznetsov, A. E.; Boldyrev, A. I.; Li, X.; Wang, L.-S. *J. Am. Chem. Soc.* **2001**, *123*, 8825–8831.
364. Melko, J. J.; Ong, S. V.; Gupta, U.; Reveles, J. U.; D'Emidio, J.; Khanna, S. N.; Castleman, A. W., Jr. *Chem. Phys. Lett.* **2010**, *500*, 196–201.
365. Nigam, S.; Majumder, C.; Kulshreshtha, S. K. *J. Mol. Struct. (THEOCHEM)* **2005**, *755*, 187–194.
366. Nigam, S.; Majumder, C.; Kulshreshtha, S. K. *J. Chem. Sci. (Bangalore, India)* **2006**, *118*, 575–578.
367. Seal, P. *J. Mol. Struct. (THEOCHEM)* **2009**, *893*, 31–36.
368. Zhai, H.-J.; Kiran, B.; Li, J.; Wang, L.-S. *Nat. Mater.* **2003**, *2*, 827–833.

369. Li, X.-W.; Pennington, W. T.; Robinson, G. H. *J. Am. Chem. Soc.* **1995**, *117*, 7578.
370. Bühler, M., Dissertation, Heidelberg, 2007.
371. Linti, G.; Bühler, M.; Monakhov, K.; Zessin, T. In *Molecular Modeling*; Comba, P., Ed.; Wiley-VCH: Weinheim, 2011.
372. King, R. B. *Inorg. Chim. Acta* **1981**, *49*, 237.
373. von Hänisch, C. K. F.; Üffing, C.; Junker, M. A.; Ecker, A.; Kneisel, B. O.; Schnöckel, H. *Angew. Chem.* **1996**, *108*, 3003–3005.
374. Antipin, M.; Boese, R.; Bläser, D.; Maulitz, A. *J. Am. Chem. Soc.* **1997**, *119*, 326–333.
375. Brack, M. *Rev. Mod. Phys.* **1993**, *65*, 677.
376. Martin, T. *Phys. Report* **1996**, *273*, 199.
377. Heer, W. A. d. *Rev. Mod. Phys.* **1993**, *65*, 611.
378. Huber, M.; Henke, P.; Schnöckel, H. *Chem. Eur. J.* **2009**, *15*, 12180–12183.
379. Schnöckel, H.; Schnepf, A. In *The Group 13 Metals Aluminium, Gallium, Indium and Thallium – Chemical Patterns and Peculiarities*; Aldridge, S., Downs, A. J., Eds.; Wiley: New York, 2011; pp 402–487.
380. Coban, S., Diploma Thesis, Universität Karlsruhe, 1999.
381. Linti, G.; Seifert, A. *Z. Anorg. Allg. Chem.* **2008**, *634*, 1312–1320.
382. Purath, A.; Köppe, R.; Schnöckel, H. *J. Chem. Soc., Chem. Commun.* **1999**, 1933.
383. Wiberg, N.; Blank, T.; Nöth, H.; Ponikvar, W. *Angew. Chem.* **1999**, *111*, 887.
384. Maxwell, W. M.; Weiss, R.; Sinn, E.; Grimes, R. N. *J. Am. Chem. Soc.* **1977**, *99*, 4016–4029.
385. Sevov, S. C.; Corbett, J. D. *Inorg. Chem.* **1991**, *30*, 4875–4877.
386. Linti, G.; Seifert, A. *Dalton Trans.* **2008**, 3688–3693.
387. Ecker, A.; Weckert, E.; Schnöckel, H. *Nature* **1997**, *387*, 379.
388. Köhnlein, H.; Purath, A.; Klemp, C.; Baum, E.; Krossing, I.; Stösser, G.; Schnöckel, H. *Inorg. Chem.* **2001**, *40*, 4830–4838.
389. Bazhin, I.; Leshcheva, O.; Nikiforov, I. *Phys. Solid State* **2006**, *48*, 774–779.
390. Schmid, G.; Alexander, B. D.; Barthelme, J.; Mueting, A. M.; Pignolet, L. H. In *Inorganic Synthesis*; Wiley: New York, 2007; pp 214–218.
391. Tran, N. T.; Powell, D. R.; Dahl, L. F. *Angew. Chem.* **2000**, *112*, 4287–4291.
392. Jadzinsky, P. D.; Calero, G.; Ackerson, C. J.; Bushnell, D. A.; Kornberg, R. D. *Science* **2007**, *318*, 430–433.
393. Jarrod, M. F.; Bower, J. E.; Kraus, J. S. *J. Chem. Phys.* **1987**, *86*, 3876.
394. Jarrod, M. F.; Bower, J. E. *J. Am. Chem. Soc.* **1988**, *110*, 6706.
395. Leuchtner, R. E.; Harms, A. C.; Castleman, A. W. *J. Chem. Phys.* **1991**, *94*, 1093.
396. Kaya, K.; Fuke, K.; Nonose, S.; Kikuchi, N. *Z. Phys. D: At. Mol. Clusters* **1989**, *12*, 571.
397. Bergeron, D. E.; Roach, P. J.; Castleman, A. W.; Jones, N.; Khanna, S. N. *Science* **2005**, *307*, 231.
398. Vollet, J.; Hartig, J. R.; Schnöckel, H. *Angew. Chem.* **2004**, *116*, 3248–3252.
399. Purath, A.; Dohmeier, C.; Ecker, A.; Köppe, R.; Krautscheid, H.; Schnöckel, H.; Ahlrichs, R.; Stoermer, C.; Friedrich, J.; Jutzi, P. *J. Am. Chem. Soc.* **2000**, *122*, 6955–6959.
400. Huber, M.; Hartig, J.; Koch, K.; Schnöckel, H. *Z. Anorg. Allg. Chem.* **2009**, *635*, 423.
401. Huber, M.; Schnepf, A.; Anson, C. E.; Schnöckel, H. *Angew. Chem. Int. Ed.* **2008**, *47*, 8201.
402. Schnepf, A.; Köppe, R.; Schnöckel, H. *Angew. Chem.* **2001**, *113*, 1287.
403. Wiberg, N.; Blank, T.; Nöth, H.; Suter, M.; Warchold, M. *Eur. J. Inorg. Chem.* **2002**, *4*, 929.
404. Wiberg, N.; Blank, T.; Purath, A.; Stoesser, G.; Schnöckel, H. *Angew. Chem.* **1999**, *111*, 2745.
405. Jemmis, E. D.; Baslarkrishnarajan, M. M.; Pancharatna, P. D. *J. Am. Chem. Soc.* **2000**, *123*, 4313.
406. King, R. B. *J. Organomet. Chem.* **2002**, *646*, 146–152.
407. King, R. B. *Inorg. Chim. Acta* **1996**, *252*, 115–121.
408. Wang, Z. X.; Schleyer, P. v. R. *Angew. Chem.* **2002**, *114*, 4256–4259.
409. Steiner, J. E. B.; Linti, G.; Schnöckel, H. Unpublished results, structural data: CCDC180407.
410. Stöber, A. H. S.; Steiner, J.; Anson, C. Unpublished results.
411. Steiner, J.; Stöber, G.; Schnöckel, H. *Angew. Chem. Int. Ed.* **2003**, *42*, 1971–1974.
412. Donchev, A.; Schnepf, A.; Stöber, G.; Baum, E.; Schnöckel, H.; Blank, T.; Wiberg, N. *Chem. Eur. J.* **2001**, *7*, 3348–3353.
413. Schnöckel, H.; Schnepf, A. In *Group 13 Chemistry*; Shapiro, P. J., Atwood, D. A., Eds.; ACS Symp. Ser.; American Chemical Society: Washington, DC, 2002; Vol. 822, p 154.
414. Deglyareva, O.; McMahon, M. I.; Allan, D. R.; Nelmes, R. J. *Phys. Rev. Lett.* **2004**, *93*, 205502.
415. Weiß, K.; Schnöckel, H. *Z. Anorg. Allg. Chem.* **2003**, *629*, 1175–1183.
416. Weiß, K.; Schnöckel, H. *Anal. Bioanal. Chem.* **2003**, *377*, 1098–1101.
417. Corbett, J. D. *Struct. Bonding* **1997**, *87*, 157.
418. Corbett, J. D. *Angew. Chem. Int. Ed.* **2000**, *39*, 670.
419. Corbett, J. D. *Inorg. Chem.* **2000**, *39*, 5178.
420. Ponou, S.; Fässler, T. F.; Tobias, G.; Canadell, E.; Cho, A.; Sevov, S. C. *Chem. Eur. J.* **2004**, *10*, 3615–3621.
421. Schnepf, A.; Stöber, G.; Schnöckel, H. *Angew. Chem.* **2002**, *114*, 1959–1962.
422. Schnepf, A.; Köppe, R.; Weckert, W.; Schnöckel, H. *Chem. Eur. J.* **2004**, *10*, 1977–1981.
423. Steiner, J.; Stöber, G.; Schnöckel, H. *Angew. Chem.* **2004**, *116*, 6712–6715.
424. Hartig, J.; Stöber, A.; Hauser, P.; Schnöckel, H. *Angew. Chem.* **2007**, *119*, 1689–1691.
425. Duan, T.; Baum, E.; Burgert, R.; Schnöckel, H. *Angew. Chem.* **2004**, *116*, 3252–3255.
426. Hartig, J.; Klöwer, F.; Rinck, J.; Unterreiner, A.-N.; Schnöckel, H. *Angew. Chem.* **2007**, *119*, 6669–6672.
427. Linti, G.; Rodig, A. *Angew. Chem.* **2000**, *112*, 3076.
428. Steiner, J.; Stöber, G.; Schnöckel, H. *Angew. Chem.* **2004**, *116*, 306–309.
429. Wang, Z.-X.; Schleyer, P. V. R. *J. Am. Chem. Soc.* **2003**, *125*, 10484.
430. Fehner, T.; Halet, J.-F.; Saillard, J.-Y. *Molecular Clusters*. Cambridge University Press: Cambridge, 2007.
431. Hartig, J.; Schnepf, A.; Jongh, L. H. d.; Bono, D.; Schnöckel, H. *Z. Anorg. Allg. Chem.* **2007**, *633*, 63–76.
432. Bakharev, O. N.; Bono, D.; Brom, H. B.; Schnepf, A.; Schnöckel, H.; Jongh, L. J. d. *Phys. Rev. Lett.* **2006**, *96*, 117002-1.
433. Bono, D.; Bakharev, O. N.; Schnepf, A.; Hartig, J.; Schnöckel, H.; Jongh, L. J. d. *Z. Anorg. Allg. Chem.* **2007**, *633*, 2173–2177.
434. Bono, D.; Schnepf, A.; Hartig, J.; Schnöckel, H.; Nieuwenhuys, G. J.; Amato, A.; Jongh, L. J. d. *Phys. Rev. Lett.* **2006**, *97*, 077601–077605.
435. Eichler, B. E.; Hardman, N. J.; Power, P. P. *Angew. Chem.* **2000**, *112*, 391.



This page intentionally left blank

## 1.02 Catenated Silicon Compounds

J Baumgartner and C Grogger, Technische Universität Graz, Graz, Austria

© 2013 Elsevier Ltd. All rights reserved.

<b>1.02.1</b>	<b>Introduction</b>	51
<b>1.02.2</b>	<b>Hydrosilanes</b>	52
1.02.2.1	Synthesis	53
1.02.2.2	Properties and Reactivity	54
1.02.2.3	Applications	54
<b>1.02.3</b>	<b>Halohydrosilanes</b>	54
1.02.3.1	Acyclic Chlorohydrosilanes	55
1.02.3.2	Acyclic Bromohydrosilanes	57
1.02.3.3	Acyclic Iodohydrosilanes	57
1.02.3.4	Acyclic Fluorohydrosilanes	58
1.02.3.5	Mixed Acyclic Halohydrosilanes	59
1.02.3.6	Cyclic Halohydrosilanes	59
<b>1.02.4</b>	<b>Halosilanes</b>	59
1.02.4.1	Acyclic Perchlorosilanes	60
1.02.4.2	Acyclic Perbromosilanes	61
1.02.4.3	Acyclic Periodosilanes	61
1.02.4.4	Acyclic Perfluorosilanes	61
1.02.4.5	Mixed Acyclic Perhalosilanes	61
1.02.4.6	Cyclic Perhalosilanes	62
<b>1.02.5</b>	<b>Chalcogenosilanes</b>	62
1.02.5.1	Si–O Compounds	62
1.02.5.2	Acyclic Si–O Compounds	62
1.02.5.3	Siloxenes	63
1.02.5.4	Si–S Compounds	63
1.02.5.5	Si–Se, Si–Te, and Si–Po Compounds	64
<b>1.02.6</b>	<b>Silanes with Group-15 Substituents</b>	64
1.02.6.1	Si–N Compounds	64
1.02.6.2	Acyclic Si–N Compounds	65
1.02.6.3	Cyclic Si–N Compounds	66
1.02.6.4	<i>N</i> -Heterocyclic Silylenes as Starting Material for Acyclic and Cyclic Silanes	67
1.02.6.5	N-Substituted Pentacoordinated Si Compounds	69
1.02.6.6	Si–P Compounds	71
1.02.6.7	Si–As, Si–Sb, and Si–Bi Compounds	72
<b>1.02.7</b>	<b>Silanes with Other Group-14 Substituents Except Organic Groups</b>	72
<b>1.02.8</b>	<b>Silanes with Other Group-13 Substituents</b>	73
<b>1.02.9</b>	<b>Silanes and Group-1 and -2 Metals</b>	73
<b>1.02.10</b>	<b>Silanes and Transition Metals</b>	73
<b>1.02.11</b>	<b>Silanes and Lanthanoids and Actinoids</b>	78
<b>1.02.12</b>	<b>Conclusion</b>	79
<b>References</b>		79

### 1.02.1 Introduction

In 1973, the first edition of Comprehensive Inorganic Chemistry was published with the chapter about silicon written by E.G. Rochow. At this time compounds possessing silicon–silicon bonds were comparably rare. Rochow mentioned around 14000 known organosilicon compounds by 1965, but this number tells nothing about the percentage of disilanes or even higher silanes. With the kind support of the CAS Customer Service, we were able to figure out that by this time (1965) 392 substances with 728 references were available in

published literature containing one or more silicon–silicon bonds. Today (2011), a search in SciFinder gives a number of 22688 substances bearing at least one Si–Si single bond, covered by a total of 14895 references. Since the year 2000, 5745 of these references were published and 728 before 1965, which leaves 8433 references for the 35 years in between. This numeric example shows that the rate of publications concerning oligo- and polysilanes increases rapidly and without a restriction of any kind, a review of this subject will get out of hand. Forced to make a decision, we resolved to take the title Comprehensive Inorganic Chemistry literally and to omit

all organosilicon compounds, thus restraining ourselves to no silicon-carbon bonds at all! Besides the overwhelming numbers of compounds, another critical factor convinced us: there is no such compilation available in the literature so far. Especially, halo-, hydro-, and halohydrosilanes, on the one hand, are simply neglected but, on the other hand, have gained increasing interest over the last years for new and exciting applications. This neglect may have 'good reasons' or is comprehensible, although silanes with hydrogen substituents are frequently used in calculations or more generally in all kinds of theoretical studies; working with real hydrosilanes is an entirely different story. Excellent skills in inert gas technique are essential to succeed in this area.

### 1.02.2 Hydrosilanes

Polysilanes are the silicon congeners of alkanes. In analogy to hydrocarbons, linear and branched silanes  $\text{Si}_n\text{H}_{2n+2}$ , cyclosilanes  $\text{Si}_n\text{H}_{2n}$ , and even a polycyclic system are known. However, in contrast to hydrocarbons, which are chemically inert to a great extent, silanes are highly reactive. One reason for the different chemical behavior is the reverse polarity of the Si-H bond ( $\text{Si}^{\delta+}-\text{H}^{\delta-}$ ) in comparison with the C-H bond due to the different electronegativities of silicon (1.74) and carbon (2.50). As a consequence,  $\text{H}^-$  serves as a leaving group that enhances nucleophilic substitution of Si-H bonds, which is not the case for C-H bonds. Furthermore, Si-Si bonds are weaker than C-C bonds, but bonds to electronegative elements such as halogens, nitrogen, or oxygen are stronger for silicon than for carbon.

Therefore, Si-halogen or Si-O bonds are formed whenever possible at the cost of the weaker Si-Si, Si-C, Si-N, or Si-H bonds. Regarding those facts, which express themselves in the everyday laboratory routine as extreme sensitivity toward oxygen and moisture and the pyrophoric behavior of the lower silanes, it is not astonishing that only few research groups dedicated their efforts to the field of hypopolysilanes (as they shall be called from here on, to distinguish them from organopolysilanes).

Two review articles cover the state of the art on synthesis and properties of hydrosilanes up to 1983.<sup>1,2</sup> Figure 1 gives a survey on all hydrosilanes isolated and characterized up to now and at first sight, it might be surprising that no new hydrosilanes have been isolated since the mid-1980s (compare Ref. [1]) although the literature on this topic is numerous. However besides theoretical studies, a substantial quantity of the literature consists of patents and articles related to the deposition of elemental silicon from hydrosilanes. Based on the pool of already known compounds 1-11 (and in particular 1 and 2 above all others) and their syntheses, the main goal was the optimization of processes, thus reducing the costs for technological applications. The isolation and characterization of new compounds were thus of minor relevance in this context. Only very recently, with the entry of solution-processing methods (which have been used for organic materials before) the interest in higher silanes experienced an abrupt increase.<sup>3</sup> In comparison to conventional surface-generation methods such as sputtering or chemical vapor deposition (CVD), the costs for deposition from the liquid phase should be much lower due to higher efficiency in material utilization, lower energy consumption, and simplification of the production process. Therefore, during the last 5 years new

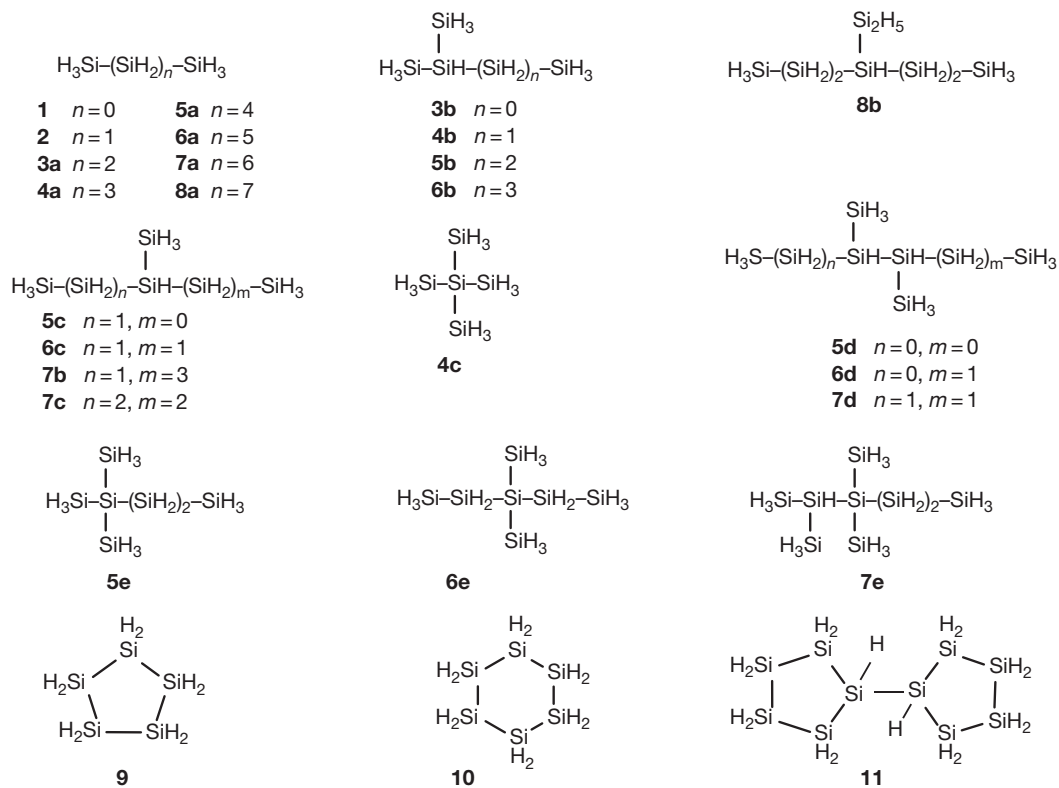
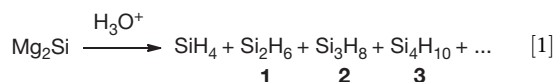


Figure 1 Linear, branched and cyclic hydrosilanes.

methods have been sought for the cost-efficient formation and processing of silanes  $\text{Si}_n\text{H}_{2n+2}$  and cyclosilanes  $\text{Si}_n\text{H}_{2n}$  with  $n > 3$  as those compounds are liquid at room temperature. Even more useful are compounds with  $n > 10$  as the boiling points of those compounds are above the temperature of Si deposition, thus facilitating the handling during processing.<sup>3</sup>

### 1.02.2.1 Synthesis

The acidic hydrolysis of silicides is the oldest and best-studied method for the synthesis of monosilane as well as of higher silanes.<sup>1</sup> Originally,  $\text{MgSi}_2$  was hydrolyzed with aqueous HCl (eqn [1]) but the silicides of Ca, Al, Na, and Li or of the rare earth metals La, Ce, and Nd also react with proton sources such as  $\text{NH}_4\text{Br}$ ,  $\text{H}_2\text{SO}_4$ , or  $\text{H}_3\text{PO}_4$ . In all cases, mixtures of silanes are obtained. Yield and product distribution vary to a great extent, depending on the purity of the starting silicide, on the choice of solvent and acid, and on the reaction conditions. The linear silanes 1 and 2–6a as well as the branched silanes 3b–5b (Figure 1) have been isolated and characterized following this method.<sup>1,2</sup>



The acidic hydrolysis process has been employed in a pilot plant scale,<sup>4,5</sup> but due to the impurities of the used technical grade  $\text{Mg}_2\text{Si}$  the raw silane's purity was poor compared to material obtained by other methods.<sup>6</sup>

A Japanese patent describes that hydrolysis of  $\text{Mg}_2\text{Si}$  with aqueous HCl in the presence of organic solvents such as diethyl ether increases the overall yield but decreases the portion of higher silanes.<sup>7</sup> Several other patents deal with the optimization of yield and conversion rate.<sup>8–13</sup>

A relatively new variation of the hydrolysis method is based on the reaction of  $\text{Mg}_2\text{Si}$  with fluorosilicic acid. The process has been optimized toward maximum yields of  $\text{SiH}_4$  and  $\text{Si}_2\text{H}_6$  (1), with higher silanes only as side products.<sup>14,15</sup>

If energy in different forms (via pyrolysis, photolysis, or electrical discharge) acts on  $\text{SiH}_4$  or  $\text{Si}_2\text{H}_6$  (1), higher silanes are formed.<sup>1</sup> The main advantage of this method is the high purity of the obtained products,<sup>6</sup> but usually the formation of silicon subhydrides or amorphous silicon has to be taken into consideration.

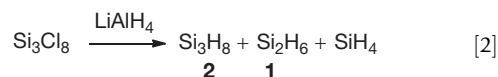
Based on the original publication from 1962,<sup>16</sup> a series of patents describes reactors for the treatment of  $\text{SiH}_4$  with a silent electrical discharge.  $\text{SiH}_4$  can be used either in pure form at

reduced pressure<sup>17,18</sup> or diluted with inert gases such as He, Ar, or  $\text{N}_2$ .<sup>19</sup> Compounds 1 and 2 can also be obtained by passing  $\text{SiH}_4$  and  $\text{H}_2$  through a plasma-discharge zone.<sup>20</sup>

It is known that the photochemical disproportionation of 3a, 4a, 4b, and 5a leads to higher, more branched silanes.<sup>1</sup> More recently, photolysis has been investigated in order to oligomerize  $\text{SiH}_4$ . The observed products are 1, 2, 3, and 4 besides solid  $(\text{SiH}_x)_n$ .<sup>21</sup> Compound 1 is the main reaction product of the irradiation of  $\text{SiH}_4$  with pulsed laser light.<sup>22</sup>

The thermal decomposition of  $\text{SiH}_4$  yields higher silanes in a first step, but longer reaction times result in the exclusive formation of polymeric silicon subhydrides. If the reaction time is sufficiently short, the accumulation of solid side products can be minimized.<sup>23,24</sup>

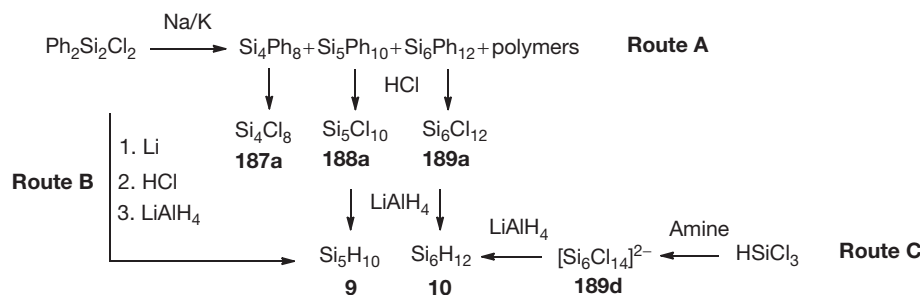
The hydrogenation of chlorosilanes certainly is the most common method for the synthesis of hydrosilanes on the laboratory scale.  $\text{LiAlH}_4$  or other mild hydrogenation reagents (e.g.,  $\text{NaBH}_4$ ) can be used.<sup>1,2</sup> The limiting factors are the availability of perchlorinated precursors on the one hand and the occurrence of Si–Si bond scission reactions during the hydrogenation process on the other. The optimized yield for the formation of trisilane 2 from  $\text{Si}_3\text{Cl}_8$  (154) for example is 60% with  $\text{SiH}_4$  (14%) and 1 (10%) always obtained as side products (eqn. [2]).<sup>25</sup>



A crucial improvement in this context is the use of diisobutylaluminumhydride  $i\text{Bu}_2\text{AlH}$  instead of  $\text{LiAlH}_4$ . As shown for the formation of neopentasilane 4c, formed starting from  $(\text{Cl}_3\text{Si})_4\text{Si}$  (158), it effects the hydrogenation without noteworthy side products.<sup>26</sup> However with  $\text{LiAlH}_4$  a 1:2 mixture of 3b and 4c is formed, together with considerable amounts of  $\text{SiH}_4$  and polymers.<sup>27</sup>

For technical applications, it turned out to be useful to hydrogenate mixtures of chlorosilanes, for example, largely chlorinated oligosilane mixtures obtained from plasma chemical methods<sup>28,29</sup> or from the reaction of simple chlorosilanes (e.g.,  $\text{H}_3\text{SiCl}$ ,  $\text{H}_2\text{SiCl}_2$ , and  $\text{HSiCl}_3$ ) with elemental silicon in the presence of Cu/CuO catalysts.<sup>30</sup>

Bond scission during hydrogenation does not occur if cyclic chlorosilanes are used as starting materials.  $\text{Si}_5\text{H}_{10}$  (9)<sup>31,32</sup> and  $\text{Si}_6\text{H}_{12}$  (10)<sup>33</sup> are formed quantitatively from the corresponding perchlorinated derivatives  $\text{Si}_5\text{Cl}_{10}$  (188a) and  $\text{Si}_6\text{Cl}_{12}$  (189a). However, the formation of  $\text{Si}_n\text{Ph}_{2n}$  from  $\text{Ph}_2\text{SiCl}_2$  followed by chlorodephenylation and isolation of  $\text{Si}_n\text{Cl}_{2n}$



**Scheme 1** Different routes to cyclopentasilane (9) and cyclohexasilane (10).



systematically by Hassler and coworkers in the 1990s in order to study their spectroscopic properties (Tables 2 and 3). However, chlorinated and fluorinated hydrodisilanes are relevant for the semiconductor industry in the same way as hydrosilanes: as precursor materials for the formation of semiconductor devices (e.g., see Pope et al.,<sup>69</sup> Bauer and Thomas,<sup>70</sup> Tomasini and Cody,<sup>71</sup> Tomasini et al.<sup>72</sup>).

### 1.02.3.1 Acyclic Chlorohydrosilanes

Table 1 summarizes the synthetic methods with the respective references for all isolated and characterized linear and branched chlorohydrosilanes.

Starting in the 1960s, attempts for the synthesis of chlorohydrosilanes focused on the reaction of hydrosilanes 1–3 with various chlorinating agents (Scheme 3, methods 1A, 1B, 1C, 1D, and 1E) such as BCl<sub>3</sub> (method 1A),<sup>73–76</sup> HCl (method

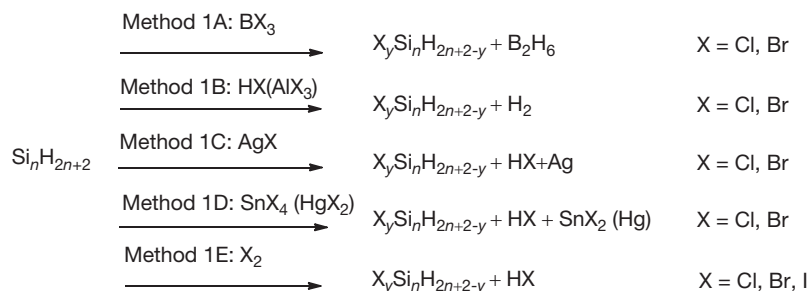
1B),<sup>77,78</sup> AgCl (method 1C),<sup>79,80</sup> SnCl<sub>4</sub> (method 1D),<sup>81,82</sup> or Cl<sub>2</sub> (method 1E).<sup>83</sup> With these methods, product mixtures were obtained that are difficult or even impossible to separate and also yields are average. An additional problem arises from the tendency of higher silanes to isomerize.<sup>81</sup> In addition, the hazardous nature of the starting materials has to be taken into account. Nonetheless, these methods comprise the only reported synthetic access to several chlorohydrosilanes (e.g., 21, 22, or 38–41; in Table 1).

In contrast to hydrosilanes, arylated silanes Ar<sub>y</sub>Si<sub>n</sub>H<sub>2n+2–y</sub> are very suitable precursors for the selective preparation of chlorohydrosilanes Cl<sub>y</sub>Si<sub>n</sub>H<sub>2n+2–y</sub> (*n* = 2–7) as aryl groups are easily replaced by halogen atoms upon reaction with either liquefied hydrogen chloride or solutions of HCl<sup>84</sup> in benzene<sup>85</sup> (Scheme 4, method 2 in Table 1). The latter alternative has the disadvantage that small amounts of AlCl<sub>3</sub> are required as catalysts which are difficult to be removed completely.

**Table 1** Isolated linear and branched chlorohydrosilanes

Chlorohydrosilane	Synthetic method <sup>a</sup>	Chlorohydrosilane	Synthetic method <sup>a</sup>
ClH <sub>2</sub> Si–SiH <sub>3</sub> ( <b>12</b> )	1A, <sup>75</sup> 1B, <sup>78</sup> 1C, <sup>79</sup> 1D, <sup>81</sup> 1E, <sup>83</sup> 4 <sup>91</sup>	ClSi–(SiH <sub>3</sub> ) <sub>3</sub> ( <b>38</b> )	1D <sup>82</sup>
ClH <sub>2</sub> Si–SiH <sub>2</sub> Cl ( <b>13</b> )	1A, <sup>74</sup> 1C, <sup>80</sup> 1D, <sup>81</sup> 1E, <sup>83</sup> 2, <sup>84</sup> 4 <sup>91</sup>	Cl <sub>2</sub> HSi–SiH–(SiH <sub>3</sub> ) <sub>2</sub> ( <b>39</b> )	1D <sup>82</sup>
Cl <sub>2</sub> HSi–SiH <sub>3</sub> ( <b>14</b> )	1A, <sup>74,85</sup> 1B, <sup>77</sup> 1C, <sup>80</sup> 1E, <sup>83</sup> 3 <sup>90</sup>	ClH <sub>2</sub> Si–SiCl(SiH <sub>3</sub> ) <sub>2</sub> ( <b>40</b> )	1D <sup>82</sup>
Cl <sub>3</sub> Si–SiH <sub>3</sub> ( <b>15</b> )	2, <sup>85</sup> 3, <sup>90</sup> 4 <sup>91</sup>	(ClH <sub>2</sub> Si) <sub>2</sub> –SiH–SiH <sub>3</sub> ( <b>41</b> )	1D <sup>82</sup>
Cl <sub>2</sub> HSi–SiH <sub>2</sub> Cl ( <b>16</b> )	1A, <sup>74</sup> 1B, <sup>77</sup> 1C, <sup>80</sup> 2 <sup>84</sup>	H <sub>3</sub> Si–(SiCl <sub>2</sub> ) <sub>2</sub> –SiH <sub>3</sub> ( <b>42</b> )	1D <sup>82</sup>
Cl <sub>2</sub> HSi–SiHCl <sub>2</sub> ( <b>17</b> )	1A, <sup>74</sup> 1B, <sup>77</sup> 1A <sup>87</sup>	Cl <sub>2</sub> HSi–(SiCl <sub>2</sub> ) <sub>2</sub> –SiH <sub>2</sub> Cl ( <b>43</b> )	2 <sup>88</sup>
Cl <sub>3</sub> Si–SiH <sub>2</sub> Cl ( <b>18</b> )	2 <sup>86</sup>	Cl <sub>3</sub> Si–(SiHCl) <sub>2</sub> –SiCl <sub>3</sub> ( <b>44</b> )	2 <sup>95</sup>
Cl <sub>3</sub> Si–SiHCl <sub>2</sub> ( <b>19</b> )	1E, <sup>83</sup> 2 <sup>86</sup>	Cl <sub>2</sub> HSi–(SiCl <sub>2</sub> ) <sub>2</sub> –SiHCl <sub>2</sub> ( <b>45</b> )	2 <sup>96</sup>
ClH <sub>2</sub> Si–Si <sub>2</sub> H <sub>5</sub> ( <b>20</b> )	1C, <sup>80</sup> 1D, <sup>82</sup> 1E, <sup>83</sup> 4 <sup>92</sup>	Cl <sub>3</sub> Si–(SiCl <sub>2</sub> ) <sub>2</sub> –SiHCl <sub>2</sub> ( <b>46</b> )	2 <sup>96</sup>
H <sub>3</sub> Si–SiHCl–SiH <sub>3</sub> ( <b>21</b> )	1A, <sup>76</sup> 1C, <sup>80</sup> 1D, <sup>82</sup> 1E <sup>83</sup>	Cl <sub>3</sub> Si–SiCl <sub>2</sub> –SiHCl–SiCl <sub>3</sub> ( <b>47</b> )	2 <sup>97</sup>
ClH <sub>2</sub> Si–SiHCl–SiH <sub>3</sub> ( <b>22</b> )	1C, <sup>80</sup> 1D <sup>82</sup>	HSi–(SiCl <sub>3</sub> ) <sub>3</sub> ( <b>48</b> )	5 <sup>93</sup>
ClH <sub>2</sub> Si–SiH <sub>2</sub> –SiH <sub>2</sub> Cl ( <b>23</b> )	1A, <sup>76</sup> 1D, <sup>82</sup> 4 <sup>92</sup>	ClSi <sub>5</sub> H <sub>11</sub> ( <b>49</b> )	1D <sup>82</sup>
Cl <sub>3</sub> Si–SiH <sub>2</sub> –SiH <sub>3</sub> ( <b>24</b> )	1A <sup>76</sup>	H <sub>3</sub> Si–SiHCl–(SiH <sub>2</sub> ) <sub>2</sub> –SiH <sub>3</sub> ( <b>50</b> )	1D <sup>82</sup>
Cl <sub>2</sub> HSi–SiCl <sub>2</sub> –SiH <sub>3</sub> ( <b>25</b> )	1A <sup>76</sup>	H <sub>5</sub> Si <sub>2</sub> –SiHCl–Si <sub>2</sub> H <sub>5</sub> ( <b>51</b> )	1D <sup>82</sup>
Cl <sub>2</sub> HSi–SiHCl–SiHCl <sub>2</sub> ( <b>26</b> )	2 <sup>88</sup>	H <sub>2</sub> ClSi–SiHCl–Si <sub>3</sub> H <sub>7</sub> ( <b>52</b> )	1D <sup>82</sup>
Cl <sub>3</sub> Si–SiCl <sub>2</sub> –SiH <sub>2</sub> Cl ( <b>27</b> )	2 <sup>88</sup>	H <sub>2</sub> ClSi–SiH <sub>2</sub> –SiHCl–Si <sub>2</sub> H <sub>5</sub> ( <b>53</b> )	1D <sup>82</sup>
Cl <sub>2</sub> HSi–SiCl <sub>2</sub> –SiHCl <sub>2</sub> ( <b>28</b> )	2 <sup>96</sup>	H <sub>3</sub> Si–(SiHCl) <sub>2</sub> –SiH <sub>2</sub> –SiH <sub>3</sub> ( <b>54</b> )	1D <sup>82</sup>
H <sub>2</sub> Si–(SiH <sub>3</sub> ) <sub>2</sub> ( <b>29</b> )	5 <sup>93</sup>	H <sub>3</sub> Si–SiHCl–SiH <sub>2</sub> –SiHCl–SiH <sub>3</sub> ( <b>55</b> )	1D <sup>82</sup>
Cl <sub>3</sub> Si–SiCl <sub>2</sub> –SiHCl <sub>2</sub> ( <b>30</b> )	2 <sup>88</sup>	ClH <sub>2</sub> Si–(SiH <sub>2</sub> ) <sub>3</sub> –SiH <sub>2</sub> Cl ( <b>56</b> )	1D, <sup>82</sup> 4 <sup>92</sup>
Cl <sub>3</sub> Si–SiHCl–SiCl <sub>3</sub> ( <b>31</b> )	2 <sup>98</sup>	Cl <sub>2</sub> HSi–(SiCl <sub>2</sub> ) <sub>3</sub> –SiH <sub>2</sub> Cl ( <b>57</b> )	2 <sup>96</sup>
ClSi <sub>4</sub> H <sub>9</sub> ( <b>32</b> )	1D, <sup>82</sup> 4 <sup>92</sup>	Cl <sub>5</sub> Si <sub>2</sub> –SiHCl–Si <sub>2</sub> Cl <sub>5</sub> ( <b>58</b> )	2 <sup>97</sup>
H <sub>3</sub> Si–SiHCl–SiH <sub>2</sub> –SiH <sub>3</sub> ( <b>33</b> )	1D <sup>82</sup>	Cl <sub>2</sub> HSi–(SiCl <sub>2</sub> ) <sub>4</sub> –SiH <sub>2</sub> Cl ( <b>59</b> )	2 <sup>96</sup>
ClH <sub>2</sub> Si–SiHCl–SiH <sub>2</sub> –SiH <sub>3</sub> ( <b>34</b> )	1D <sup>82</sup>	(ClH <sub>2</sub> Si) <sub>2</sub> Hsi–SiH(SiH <sub>2</sub> Cl) <sub>2</sub> ( <b>60</b> )	2 <sup>98</sup>
ClH <sub>2</sub> Si–(SiH <sub>2</sub> ) <sub>2</sub> –SiH <sub>2</sub> Cl ( <b>35</b> )	4 <sup>92</sup>	Cl <sub>2</sub> HSi–(SiCl <sub>2</sub> ) <sub>5</sub> –SiH <sub>2</sub> Cl ( <b>61</b> )	2 <sup>96</sup>
H <sub>3</sub> Si–(SiHCl) <sub>2</sub> –SiH <sub>3</sub> ( <b>36</b> )	1D, <sup>82</sup> 2 <sup>99</sup>		
ClSiH <sub>2</sub> –SiH–(SiH <sub>3</sub> ) <sub>2</sub> ( <b>37</b> )	1D <sup>82</sup>		

<sup>a</sup>For methods 1A, 1B, 1C, 1D, and 1E, see Scheme 3; method 2, see Scheme 4; method 3, see Scheme 5; method 4, see Scheme 6; and for method 5, see Scheme 7.



**Scheme 3** Methods for the formation of acyclic chlorohydrosilanes from hydrosilanes.



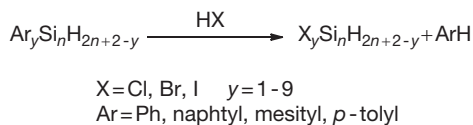
In addition, also halogen/hydrogen exchange reactions and Si-Si bond cleavage are catalyzed by traces of  $\text{AlCl}_3$ , thus leading to rapid decomposition and/or redistribution of higher chlorosilanes.<sup>80,86</sup>

Frequently, phenylated silanes were used as precursors for the dearylation reactions, as those compounds are easily available. However, if the boiling points of the obtained chlorohydrosilanes and the formed benzene (Scheme 4) are too close, isolation of the pure products is not possible. In several cases, azeotropic mixtures of the chlorosilanes and the formed benzene occurred, thus impeding the isolation of the pure products.<sup>86</sup> This problem can be solved by replacing phenyl substituents with larger aryl groups such as naphthyl,<sup>84</sup> mesityl,<sup>87</sup> or *p*-tolyl.<sup>88</sup>

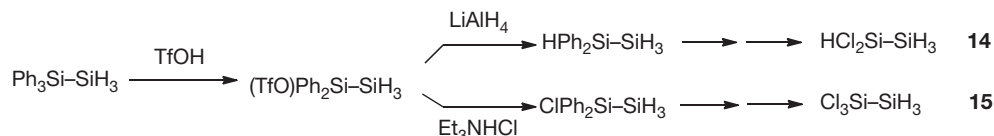
When the dichlorotetrasilane 36 was synthesized from the corresponding arylated hydrosilanes,<sup>89</sup> the  $^{29}\text{Si}$  NMR spectrum indicated the formation of all possible diastereomers (+, -, and *meso* form). Separation of the diastereomers was not reported.<sup>89</sup>

To avoid equilibration reactions of the chlorinated products,<sup>86</sup> W. Uhlig suggested a stepwise dephenylation procedure with triflic acid followed by subsequent hydrogenation with  $\text{LiAlH}_4$  or chlorination with  $\text{Et}_3\text{NHCl}$  (Scheme 5, method 3 in Table 1).<sup>90</sup> Starting from  $\text{H}_3\text{Si-SiPh}_3$ , the selective formation of 14 or 15, respectively, was thus possible.<sup>90</sup>

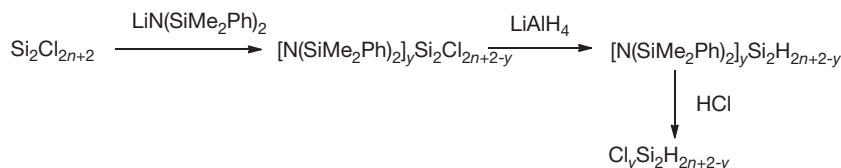
If perchlorosilanes are treated with hydrogenating agents such as  $\text{LiAlH}_4$ , all Si-Cl bonds are reduced. Nevertheless, a



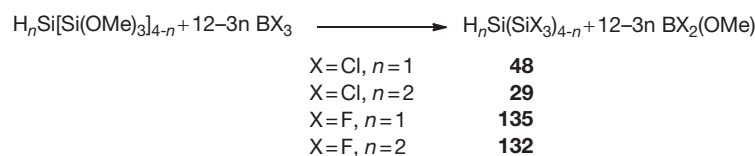
**Scheme 4** Formation of halohydrosilanes by halogenation of arylated silanes.



**Scheme 5** Formation of chlorohydrodisilanes 14 and 15 by stepwise dephenylation with triflic acid.



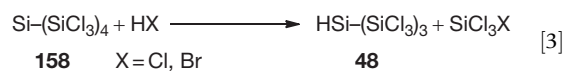
**Scheme 6** Formation of chlorohydrodisilanes from perchlorosilanes via aminosilanes.



**Scheme 7** Formation of branched halohydrosilanes by the reaction of methoxysilanes with  $\text{BX}_3$ .

selective synthesis of chlorodisilanes starting from  $\text{Si}_2\text{Cl}_6$  (153) was reported by Stüger et al. (Scheme 6, method 4 in Table 1).<sup>91</sup> To avoid complete hydrogenation of the chlorosilane,  $\text{N}(\text{SiMe}_2\text{Ph})_2$  or  $\text{N}(\text{SiMe}_3)_2$  substituents were introduced into the molecule. After hydrogenation, the protective groups were easily cleaved off by treatment with HCl. Compounds 12, 13, and 15 were isolated this way in good yields.<sup>91</sup> It was further shown that even in reactive molecules such as  $\text{XH}_2\text{Si}(\text{SiH}_2)_2\text{SiH}_2\text{X}$  or  $\text{H}_3\text{Si}(\text{SiHX})_2\text{SiH}_3$  (X = Cl: 35 and 36; X = Br: 86 and 87), the  $\text{NR}_2$  groups can be introduced. Thus, the linear and cyclic oligosilanes 20, 23, 32, 35, and 56 have been prepared.<sup>92</sup> However, the crude products contained also variable amounts of lower chlorosilanes due to Si-Si bond rupture.<sup>92</sup>

$\text{HSi}(\text{SiCl}_3)_3$  (48) was found to be the reaction product of the cleavage of  $\text{Si}(\text{SiCl}_3)_4$  (158) with HCl in a  $\text{SiCl}_4$  solution (eq. [3]).<sup>93</sup>



The reaction of methoxyhydrosilanes with  $\text{BX}_3$  (X = Cl<sub>2</sub> and F<sub>2</sub>) was used for the formation of branched halohydrosilanes (Scheme 7). Compounds 29 and 48 were prepared by reaction of the methoxy compounds  $\text{HSi}[\text{Si}(\text{OMe})_3]_3$  (194) and  $\text{H}_2\text{Si}[\text{Si}(\text{OMe})_3]_2$  (192) with  $\text{BCl}_3$  (method 5 in Table 1).<sup>93</sup>

In 1962, the ozonizer-type silent-electric discharge was introduced as a method to convert monosilanes into higher silanes.<sup>16</sup> Ten years later, Drake and Westwood reported that the action of such electrical discharges on halomonosilanes (X = F, Cl, and Br) led to the formation of product mixtures containing halogenated di- and trisilanes (method 6). The condensed products could be partly separated by trap-to-trap distillations, but yields of the individual compounds were rather low (if even reported).<sup>94</sup>

### 1.02.3.2 Acyclic Bromohydrosilanes

$\text{BBr}_3$ ,<sup>76</sup>  $\text{HBr}$ ,<sup>78</sup>  $\text{SnBr}_4$ ,<sup>99</sup> and  $\text{Br}_2$ <sup>83,100</sup> have all been used for the bromination of di-, tri-, and tetrasilane **1**, **2**, and **3a** (methods 1A, 1B, 1D, and 1E in **Scheme 3**). Passage of  $\text{Si}_2\text{H}_5\text{I}$  (**92**) over  $\text{AgBr}$  gave  $\text{Si}_2\text{H}_5\text{Br}$  (**62**).<sup>101</sup>

More recent attempts exploited the possibility of electrophilic cleavage of silicon-aryl bonds with  $\text{HBr}$  (method 2, **Scheme 4**). Hassler and coworkers optimized this method and synthesized, among others, bromohydrotrisilanes **73–81**.<sup>88</sup> If the boiling points of the products differ considerably from that of formed benzene, hydridophenyldi- and trisilanes can be used as starting materials as they are comparably easily accessible. In all other cases, larger aryl groups such as mesityl or naphthyl have to be used. The challenge of this method is the preparation of the starting materials. Most of the formed compounds have been studied by <sup>29</sup>Si NMR, IR, and Raman spectroscopy.<sup>102</sup> The obtained spectral data were evaluated and interpreted on the basis of normal coordinate analyses.<sup>88,103</sup>

Just like the chloro congener  $\text{H}_3\text{Si}-(\text{SiHCl})_2-\text{SiH}_3$  (**36**), the dibromotetrasilane  $\text{BrH}_2\text{Si}-(\text{SiH}_2)_2-\text{SiH}_2\text{Br}$  (**86**) has two asymmetric centers, and the signals of all diastereomers (+, −, and *meso* form) appear in the NMR spectra. Separation of the diastereomers was not reported.<sup>89</sup> All isolated linear and branched bromosilanes are summarized in **Table 2**.

### 1.02.3.3 Acyclic Iodohydrosilanes

When Feher et al. studied the reactions of hydrosilanes with halogens in the 1970s, they found that di-, tri-, or tetrasilane (**1**, **2**, or **3a**) reacted with  $\text{I}_2$  in pentane<sup>108</sup> or in the absence of any solvent in vacuum.<sup>109</sup> In any case, they obtained mixtures of monoiodo- and diiodosilanes (method 1E, **Scheme 3**). Isolation of the pure isomers of iododisilanes **92–94**, iodotrisilanes **100–105**, and iodotetrasilanes **120** and **121** was possible by preparative gas chromatography (**Table 3**).<sup>108,109</sup>

It took almost 20 years before next relevant advances in the synthesis of iodosilanes were reported by Hassler et al.<sup>104</sup>

**Table 2** Isolated linear and branched bromohydrosilanes

Bromohydrosilanes	Synthetic method <sup>a</sup>	Bromohydrosilanes	Synthetic method <sup>a</sup>
$\text{BrSi}_2\text{H}_5$ ( <b>62</b> )	1A, <sup>74</sup> 1B, <sup>78</sup> 1C, <sup>101</sup> 1D, <sup>99</sup> 1E, <sup>83,100</sup> 2 <sup>103</sup>	$\text{Br}_2\text{HSi}-\text{SiHBr}-\text{SiHBr}_2$ ( <b>77</b> )	2 <sup>88</sup>
$\text{BrH}_2\text{Si}-\text{SiH}_2\text{Br}$ ( <b>63</b> )	1A, <sup>74</sup> 1D, <sup>99</sup> 1E, <sup>83</sup> 2 <sup>104</sup>	$\text{Br}_3\text{Si}-\text{SiBr}_2-\text{SiH}_2\text{Br}$ ( <b>78</b> )	2 <sup>88</sup>
$\text{Br}_2\text{HSi}-\text{SiH}_3$ ( <b>64</b> )	1A, <sup>74</sup> 2 <sup>102</sup>	$\text{Br}_2\text{HSi}-\text{SiBr}_2-\text{SiHBr}_2$ ( <b>79</b> )	2 <sup>88</sup>
$\text{Br}_3\text{Si}-\text{SiH}_3$ ( <b>65</b> )	2 <sup>104</sup>	$\text{Br}_3\text{Si}-\text{SiH}_2-\text{SiBr}_2$ ( <b>80</b> )	2 <sup>105</sup>
$\text{Br}_2\text{HSi}-\text{SiH}_2\text{Br}$ ( <b>66</b> )	1A, <sup>74</sup> 1E, <sup>83</sup> 2 <sup>102</sup>	$\text{Br}_3\text{Si}-\text{SiBr}_2-\text{SiHBr}_2$ ( <b>81</b> )	2 <sup>88</sup>
$\text{Br}_3\text{Si}-\text{SiH}_2\text{Br}$ ( <b>67</b> )	2 <sup>102</sup>	$\text{Br}_2\text{HSi}-\text{SiBr}_2-\text{SiH}_2\text{Br}$ ( <b>82</b> )	2 <sup>88</sup>
$\text{Br}_2\text{HSi}-\text{SiHBr}_2$ ( <b>68</b> )	1A, <sup>74</sup> 2 <sup>104</sup>	$\text{BrSi}_4\text{H}_9$ ( <b>83</b> )	1E <sup>83</sup>
$\text{Br}_3\text{Si}-\text{SiHBr}_2$ ( <b>69</b> )	2 <sup>102</sup>	$\text{H}_3\text{Si}-\text{SiHBr}-\text{Si}_2\text{H}_5$ ( <b>84</b> )	1E <sup>83</sup>
$\text{BrSi}_3\text{H}_7$ ( <b>70</b> )	1A, <sup>76</sup> 1E <sup>83,100</sup>	$\text{BrH}_2\text{Si}-\text{SiH}(\text{SiH}_3)_2$ ( <b>85</b> )	2 <sup>106</sup>
$\text{H}_3\text{Si}-\text{SiHBr}-\text{SiH}_3$ ( <b>71</b> )	1A, <sup>76</sup> 1E <sup>83,100</sup>	$\text{BrH}_2\text{Si}-(\text{SiH}_2)_2-\text{SiH}_2\text{Br}$ ( <b>86</b> )	2 <sup>107</sup>
$\text{BrH}_2\text{Si}-\text{SiHBr}-\text{SiH}_3$ ( <b>72</b> )	1E <sup>83</sup>	$\text{H}_3\text{Si}-(\text{SiHBr})_2-\text{SiH}_3$ ( <b>87</b> )	2 <sup>89</sup>
$\text{BrH}_2\text{Si}-\text{SiH}_2-\text{SiH}_2\text{Br}$ ( <b>73</b> )	2 <sup>88</sup>	$\text{Br}_3\text{Si}-\text{SiHBr}-\text{SiBr}_2-\text{SiH}_2\text{Br}$ ( <b>88</b> )	2 <sup>88</sup>
$\text{BrH}_2\text{Si}-\text{SiHBr}-\text{SiH}_2\text{Br}$ ( <b>74</b> )	2 <sup>88</sup>	$\text{BrH}_2\text{Si}-\text{Si}(\text{SiH}_3)_3$ ( <b>89</b> )	2 <sup>106</sup>
$\text{Br}_3\text{Si}-\text{SiBr}_2-\text{SiH}_3$ ( <b>75</b> )	2 <sup>88</sup>	$\text{BrH}_2\text{Si}-\text{Si}(\text{SiH}_3)_2-\text{Si}_2\text{H}_5$ ( <b>90</b> )	2 <sup>106</sup>
$\text{Br}_2\text{HSi}-\text{SiBr}_2-\text{SiH}_2\text{Br}$ ( <b>76</b> )	2 <sup>88</sup>	$(\text{BrH}_2\text{Si})_2\text{HSi}-\text{SiH}(\text{SiH}_2\text{Br})_2$ ( <b>91</b> )	2 <sup>98</sup>

<sup>a</sup>For methods 1A, 1B, 1C, 1D, and 1E see **Scheme 3**, and method 2 see **Scheme 4**.

**Table 3** Isolated iodohydrosilanes

Iodohydrosilane	Synthetic method <sup>a</sup>	Iodohydrosilane	Synthetic method <sup>a</sup>
$\text{I}_2\text{Si}_2\text{H}_5$ ( <b>92</b> )	1E, <sup>108</sup> 2 <sup>102</sup>	$\text{I}_2\text{HSi}-\text{SiH}_2-\text{SiHl}_2$ ( <b>108</b> )	2 <sup>88</sup>
$\text{I}_2\text{HSi}-\text{SiH}_3$ ( <b>93</b> )	1E, <sup>108</sup> 2 <sup>110</sup>	$\text{I}_2\text{HSi}-\text{SiHl}-\text{SiH}_2\text{I}$ ( <b>109</b> )	2 <sup>88</sup>
$\text{IH}_2\text{Si}-\text{SiH}_2\text{I}$ ( <b>94</b> )	1E, <sup>108</sup> 2 <sup>104</sup>	$\text{Br}_2\text{HSi}-\text{SiH}_2-\text{SiHBr}_2$ ( <b>110</b> )	2 <sup>88</sup>
$\text{I}_3\text{Si}-\text{SiH}_3$ ( <b>95</b> )	2 <sup>104</sup>	$\text{I}_3\text{Si}-\text{SiI}_2-\text{SiH}_3$ ( <b>111</b> )	2 <sup>111</sup>
$\text{I}_2\text{HSi}-\text{SiH}_2\text{I}$ ( <b>96</b> )	2 <sup>102</sup>	$\text{I}_2\text{HSi}-\text{SiI}_2-\text{SiH}_2\text{I}$ ( <b>112</b> )	2 <sup>88</sup>
$\text{I}_3\text{Si}-\text{SiH}_2\text{I}$ ( <b>97</b> )	2 <sup>102</sup>	$\text{I}_2\text{HSi}-\text{SiHl}-\text{SiHl}_2$ ( <b>113</b> )	2 <sup>88</sup>
$\text{I}_2\text{HSi}-\text{SiHl}_2$ ( <b>98</b> )	2 <sup>104</sup>	$\text{IH}_2\text{Si}-\text{Si}_2\text{I}_5$ ( <b>114</b> )	2 <sup>88</sup>
$\text{I}_3\text{Si}-\text{SiHl}_2$ ( <b>99</b> )	2 <sup>102</sup>	$\text{I}_3\text{Si}-\text{SiH}_2-\text{SiI}_3$ ( <b>115</b> )	2 <sup>111</sup>
$\text{ISi}_3\text{H}_7$ ( <b>100</b> )	1E <sup>108</sup>	$\text{I}_2\text{HSi}-\text{SiHl}-\text{SiI}_3$ ( <b>116</b> )	2 <sup>88</sup>
$\text{H}_3\text{Si}-\text{SiHl}-\text{SiH}_3$ ( <b>101</b> )	1E <sup>108</sup>	$\text{I}_2\text{HSi}-\text{SiI}_2-\text{SiHl}_2$ ( <b>117</b> )	2 <sup>88</sup>
$\text{I}_2\text{HSi}-\text{Si}_2\text{H}_5$ ( <b>102</b> )	1E <sup>109</sup>	$\text{Si}_3\text{I}_7\text{H}$ ( <b>118</b> )	2 <sup>88</sup>
$\text{IH}_2\text{Si}-\text{SiHl}-\text{SiH}_3$ ( <b>103</b> )	1E <sup>108</sup>	$\text{I}_3\text{Si}-\text{SiHl}-\text{SiI}_3$ ( <b>119</b> )	2 <sup>88</sup>
$\text{IH}_2\text{Si}-\text{SiH}_2-\text{SiH}_2\text{I}$ ( <b>104</b> )	1E, <sup>109</sup> 2 <sup>111</sup>	$\text{ISi}_4\text{H}_9$ ( <b>120</b> )	1E <sup>108</sup>
$\text{H}_3\text{Si}-\text{SiI}_2-\text{SiH}_3$ ( <b>105</b> )	1E <sup>109</sup>	$\text{H}_3\text{Si}-\text{SiHl}-\text{Si}_2\text{H}_5$ ( <b>121</b> )	1E <sup>108</sup>
$\text{I}_2\text{HSi}-\text{SiH}_2-\text{SiH}_2\text{I}$ ( <b>106</b> )	2 <sup>88</sup>	$\text{I}_2\text{HSi}-(\text{SiH}_2)_2-\text{SiH}_2\text{I}$ ( <b>122</b> )	2 <sup>88</sup>
$\text{IH}_2\text{Si}-\text{SiHl}-\text{SiH}_2\text{I}$ ( <b>107</b> )	2 <sup>111</sup>		

<sup>a</sup>For method 1E see **Scheme 3**, and method 2 see **Scheme 4**.



As outlined already for the syntheses of chloro- and bromohydrosilanes, the selective introduction of halogen substituents into a silane is possible by the electrophilic cleavage of silicon-aryl bonds with HX (method 2, **Scheme 4**). Thus, Hassler et al. were able to synthesize most of the up-to-now known iodohydrosilanes in excellent yields (in general, more than 90% crude yield).<sup>88,102,104,110,111</sup> While the reaction of arylated silanes with a solution of gaseous HI in benzene is a convenient procedure, the enhanced sensitivities of iodohydrosilanes toward thermal decomposition as well as toward Si-H bond cleavage makes the elaborate use of liquefied HI in sealed tubes sometimes unavoidable.<sup>88</sup> It is noteworthy that due to the bulk of iodine, the substitution of three phenyl groups at one silicon atom is sterically hindered and Si-Si bond rupture occurs when  $\text{Ph}_3\text{Si-SiH}_3$  is used as starting material for the formation of  $\text{I}_3\text{Si-SiH}_3$  (**95**).<sup>104</sup> In this case, the enhanced reactivity of *p*-tolyl substituents can be turned to account. Thus, **95** can be synthesized easily from *p*-Tol<sub>3</sub>Si-SiH<sub>3</sub>.<sup>104</sup>

<sup>29</sup>Si NMR spectroscopic data are available for all compounds synthesized by Hassler and coworkers.<sup>88</sup> Iodohydrosilanes **92**–**99** have been studied by IR and Raman spectroscopy as well as *ab initio* molecular orbital- and density functional calculations.<sup>88</sup> Furthermore, the molecular structures of **94**,<sup>112</sup> **96**,<sup>113</sup> and **98**<sup>112</sup> were determined by gas-phase electron diffraction (GED). No branched iodohydrosilanes are known in the literature so far. All isolated linear iodohydrosilanes are summarized in **Table 3**.

### 1.02.3.4 Acyclic Fluorohydrosilanes

Just as for the other halohydrosilanes, research on syntheses, properties, and reactivity of fluorohydrosilanes started

sometime at the beginning of the 1970s. Disilane derivatives have been studied more extensively due to their possible applications in the semiconductor industry, while the literature on the synthesis of higher fluorosilanes is relatively scarce. All isolated linear and branched fluorosilanes **123**–**135** are summarized in **Table 4**.

A unique possibility for the synthesis of fluorosilanes comes from the fact that the metastable molecule SiF<sub>2</sub> is formed when SiF<sub>4</sub> is passed over silicon at high temperatures.<sup>114</sup> The thus obtained highly reactive gas can be used as a precursor for the formation of several fluorosilanes (method 7, **Scheme 8**).<sup>114</sup>

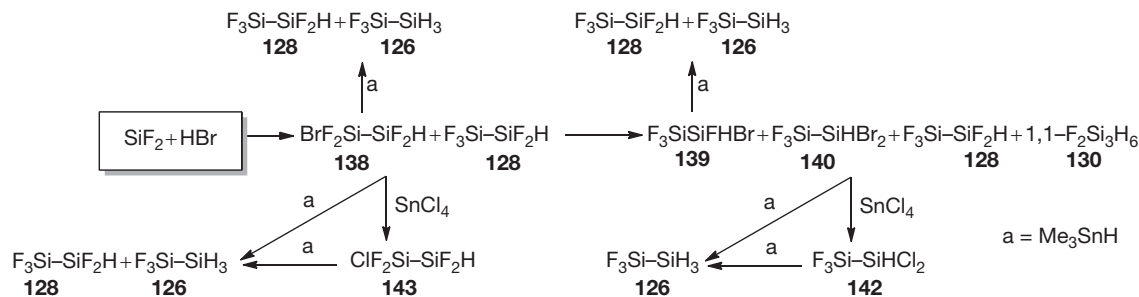
Co-condensation of SiF<sub>2</sub> with B<sub>2</sub>H<sub>6</sub> at a cool copper surface led to the formation of a mixture of fluorosilanes from which F<sub>3</sub>Si-SiH<sub>3</sub> (**126**), F<sub>3</sub>Si-SiF<sub>2</sub>H (**128**), and H<sub>2</sub>Si-(SiF<sub>3</sub>)<sub>2</sub> (**132**) were isolated by high-vacuum, low-temperature fractional condensation.<sup>114</sup> Compound **128** also was prepared by the co-condensation of SiF<sub>2</sub> with PH<sub>3</sub>.<sup>115</sup> When SiF<sub>2</sub> is reacted with HBr, the primarily formed 1-bromo-1,1,2,2-tetrafluorodisilane (**138**) decomposed rapidly. Treatment of the formed product mixture with excess SbF<sub>3</sub> gave **128** in high yields (**Scheme 8**).<sup>116</sup> In the reaction of SiF<sub>2</sub> with H<sub>2</sub>S, the primarily formed silanethiol F<sub>2</sub>HSi-SiF<sub>2</sub>SH decomposed after a few minutes and F<sub>3</sub>Si-SiF<sub>2</sub>H (**128**) was isolated as the main reaction product.<sup>117</sup>

The fluorination of hydrosilanes according to the methods in **Scheme 3** was not reported in the literature nor was the dearyllating fluorination of arylsilanes with HF (method 2, **Scheme 4**). The hydrogenation of halosilanes (method 3, **Scheme 5**) can be used indirectly: In mixed halosilanes X<sub>γ</sub>Si<sub>n</sub>H<sub>2n+2-γ</sub> (X=F and Cl, or F and Br), the chloro or bromo functionalities can be reduced selectively with Me<sub>3</sub>SnH without Si-F bond cleavage (**Scheme 8**). Thus, F<sub>3</sub>Si-SiH<sub>3</sub> (**126**) can be prepared by the reduction of F<sub>3</sub>Si-SiHX<sub>2</sub>

**Table 4** Isolated fluorohydrosilanes

Fluorohydrosilane	Synthetic method <sup>a</sup>	Fluorohydrosilane	Synthetic method <sup>a</sup>
FH <sub>2</sub> Si-SiH <sub>3</sub> ( <b>123</b> )	8, <sup>120</sup> 9 <sup>121</sup>	F <sub>2</sub> HSi-Si <sub>2</sub> H <sub>5</sub> ( <b>130</b> )	6, <sup>94</sup> 8 <sup>76</sup>
F <sub>2</sub> HSi-SiH <sub>3</sub> ( <b>124</b> )	6, <sup>76</sup> 8 <sup>74,120</sup>	F <sub>3</sub> Si-Si <sub>2</sub> H <sub>5</sub> ( <b>131</b> )	6 <sup>94</sup>
FH <sub>2</sub> Si-SiH <sub>2</sub> F ( <b>125</b> )	6 <sup>76</sup>	H <sub>2</sub> Si-(SiF <sub>3</sub> ) <sub>2</sub> ( <b>132</b> )	5, <sup>119</sup> 7 <sup>114</sup>
F <sub>3</sub> Si-SiH <sub>3</sub> ( <b>126</b> )	6	F <sub>3</sub> Si-SiF <sub>2</sub> -SiHF <sub>2</sub> ( <b>133</b> )	7 <sup>114</sup>
F <sub>2</sub> HSi-SiHF <sub>2</sub> ( <b>127</b> )	3, <sup>118</sup> 6, <sup>76</sup> 8 <sup>87</sup>	FH <sub>2</sub> Si-(SiH <sub>2</sub> ) <sub>2</sub> -SiH <sub>2</sub> F ( <b>134</b> )	8 <sup>107</sup>
F <sub>3</sub> Si-SiF <sub>2</sub> H ( <b>128</b> )	3, <sup>118</sup> 7 <sup>114,115</sup>	HSi-(SiF <sub>3</sub> ) <sub>3</sub> ( <b>135</b> )	5 <sup>119</sup>
FH <sub>2</sub> Si-Si <sub>2</sub> H <sub>5</sub> ( <b>129</b> )	8 <sup>76</sup>		

<sup>a</sup>For method 3 see **Scheme 5**, method 5 see **Scheme 7**, method 6 = electrical discharge method 7 see **Scheme 8**, method 8 = fluorination of chloro- or bromosilanes, method 9 see eqn [4].



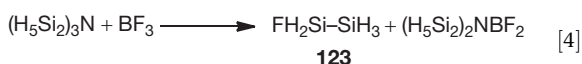
**Scheme 8** Possible routes to fluorohydrodisilanes, bromofluorodisilanes and chlorofluorodisilanes.

[X=Br (140), Cl (142)] with  $\text{Me}_3\text{SnH}$  in 90% yield.<sup>118</sup> In contrast to this,  $\text{BrF}_2\text{Si-SiF}_2\text{H}$  (138) and  $\text{F}_3\text{Si-SiFBrH}$  (139) cannot be hydrogenated to the corresponding fluorodisilanes.<sup>118</sup> F/Br redistribution precedes the reduction reaction, resulting in both cases in mixtures of  $\text{F}_3\text{Si-SiF}_2\text{H}$  (128) and  $\text{F}_3\text{Si-SiH}_3$  (126) (Scheme 8). Reduction of  $\text{F}_3\text{SiSiHX}_2$  [X=Br (140), Cl (142)] with reducing agents such as  $\text{LiAlH}_4$ ,  $\text{NaAlH}_2(\text{OCH}_2\text{CH}_2\text{OCH}_3)_2$ , and  $i\text{Bu}_2\text{AlH}$  resulted in cleavage of the Si-Si bond and reduction of some Si-F bonds.<sup>118</sup>

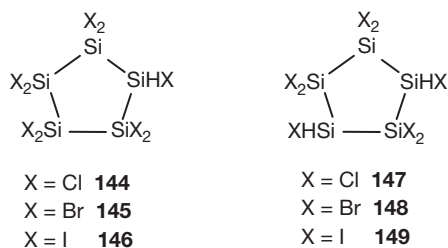
The fluorination reaction of  $\text{HSi}[\text{Si}(\text{OMe})_3]_3$  (194) and  $\text{H}_2\text{Si}[\text{Si}(\text{OMe})_3]_2$  (192) with  $\text{BF}_3$  (method 5, Scheme 7) was used for the formation of  $\text{H}_2\text{Si}-(\text{SiF}_3)_2$  (132) and  $\text{HSi}-(\text{SiF}_3)_3$  (135).<sup>119</sup>

Another possibility for the formation of fluorohydrosilanes is the fluorination of chloro- or bromohydrosilanes (method 8). Compound  $\text{FH}_2\text{Si-SiH}_3$  (123) was prepared by chlorination of  $\text{Si}_2\text{H}_6$  (1) with  $\text{HCl}$ , followed by fluorination of the formed  $\text{ClH}_2\text{Si-SiH}_3$  (12) with  $\text{SbF}_3$ .<sup>120</sup> It appears that the conversion of chloro- to fluorosilanes is mainly an exchange reaction, because  $\text{SbF}_3$  does not fluorinate 1 directly.<sup>74</sup>  $\text{F}_2\text{HSi-SiH}_3$  (124), with traces of  $\text{F}_3\text{Si-SiH}_3$  (126), was generated by the reaction of  $\text{Cl}_2\text{HSi-SiH}_3$  (14) with  $\text{SbF}_3$ .<sup>74,120</sup> Also,  $\text{FH}_2\text{Si-Si}_2\text{H}_5$  (129) was prepared by fluorination of 1- $\text{ClSi}_3\text{H}_7$  (20) with  $\text{SbF}_3$ .<sup>76</sup> Another well-established fluorinating agent is  $\text{ZnF}_2$ , which was used for the formation of  $\text{F}_2\text{HSi-SiHF}_2$  (127)<sup>87</sup> and  $\text{FH}_2\text{Si}-(\text{SiH}_2)_2-\text{SiH}_2\text{F}$  (134) from the respective chlorides.<sup>107</sup>

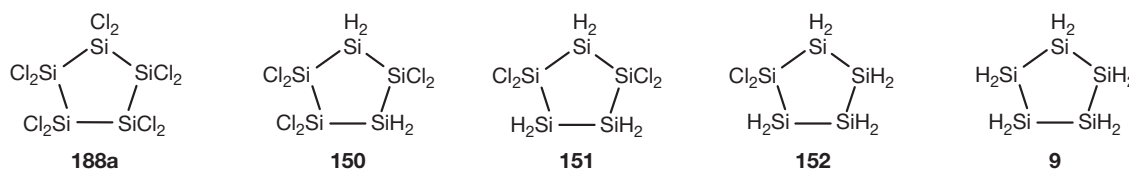
The cleavage of Si-N bonds in  $(\text{Si}_2\text{H}_5)_3\text{N}$  by  $\text{BF}_3$  can also be used for the formation of 123 (method 9, eqn [4]).<sup>121</sup>



Using the electrical discharge method, silanes 124, 125, 127, and 128 as well as  $\text{F}_2\text{HSi-Si}_2\text{H}_5$  (130) and  $\text{F}_3\text{Si-Si}_2\text{H}_5$  (131) were generated from various monofluorosilanes, although separation of the product mixtures was difficult to impossible (method 6, Table 4).<sup>76,94</sup>



**Figure 2** Cyclic halohydrosilanes.



**Figure 3** Cyclopentasilane 9 and its chlorinated derivatives.

### 1.02.3.5 Mixed Acyclic Halohydrosilanes

The possibility to brominate Si-H bonds with  $\text{BBr}_3$  (according to synthesis method 1A) was utilized to form chlorobromohydrosilanes  $\text{HBrClSi-SiH}_3$  (136) and  $\text{BrCl}_2\text{Si-SiH}_3$  (137) from  $\text{ClH}_2\text{Si-SiH}_3$  (12) and  $\text{Cl}_2\text{HSi-SiH}_3$  (14), respectively.<sup>74</sup> These products were detected by GC but isolation was not reported.<sup>74</sup>

Mixed halohydrodisilanes of the general formula  $\text{Si}_2\text{X}_m\text{Y}_n\text{H}_{6-m-n}$  with  $\text{X} = \text{F}$  and  $\text{Y} = \text{Br}$  are formed when  $\text{SiF}_2$  is co-condensated with  $\text{HBr}$ . During warming up to room temperature, the composition of the reaction mixture changes, but halohydrosilanes 138–140 (Scheme 8) could be isolated.  $\text{HBrFSi-SiF}_2\text{Br}$  (141a) and  $\text{HBr}_2\text{Si-SiF}_2\text{Br}$  (141b) were detected in the final reaction mixture by  $^{19}\text{F}$  NMR, but were not isolated. Chlorination of 138 and 140 using  $\text{SnCl}_4$  led to the formation of  $\text{F}_3\text{Si-SiHCl}_2$  (142) and  $\text{ClF}_2\text{Si-SiHF}_2$  (143) (Scheme 8).<sup>118</sup>

### 1.02.3.6 Cyclic Halohydrosilanes

The synthesis and properties of monocyclic tetra-, penta-, and hexasilanes as well as of polycyclic silanes and cages have been summarized in a review by Stüger and Hengge.<sup>122</sup> The nonahalocyclopentasilanes  $\text{HSi}_5\text{X}_9$  (144–146) and the octahalocyclopentasilanes 1,3- $\text{H}_2\text{Si}_5\text{X}_8$  ( $\text{X} = \text{Cl}, \text{Br}, \text{I}$ , 147–149) are accessible by dephenylation of  $\text{HSi}_5\text{Ph}_9$  and  $\text{H}_2\text{Si}_5\text{Ph}_8$ , respectively (Figure 2).<sup>123</sup>

Partially chlorinated cyclopentasilanes 150–152 (Figure 3) were obtained by Roewer et al. upon the hydrogenation of  $\text{Si}_5\text{Cl}_{10}$  188a with  $\text{Me}_3\text{SnH}$ .<sup>124</sup> The reaction proceeds stepwise without formation of any  $\text{SiHCl}$  units. The dominating product is 1,1,1,3,3-tetrachlorocyclopentasilane (151), whereas 1,1-dihydrooctachlorocyclopentasilane could not be detected. These products were identified only by  $^{29}\text{Si}$  NMR spectroscopy but not isolated.<sup>124</sup>

Partially halogenated cyclohexasilanes  $\text{Si}_6\text{H}_{11}\text{X}$  ( $\text{X} = \text{F}, \text{Cl}, \text{Br}, \text{I}$ ) have been studied by Hassler et al. by DFT calculations.<sup>125</sup>

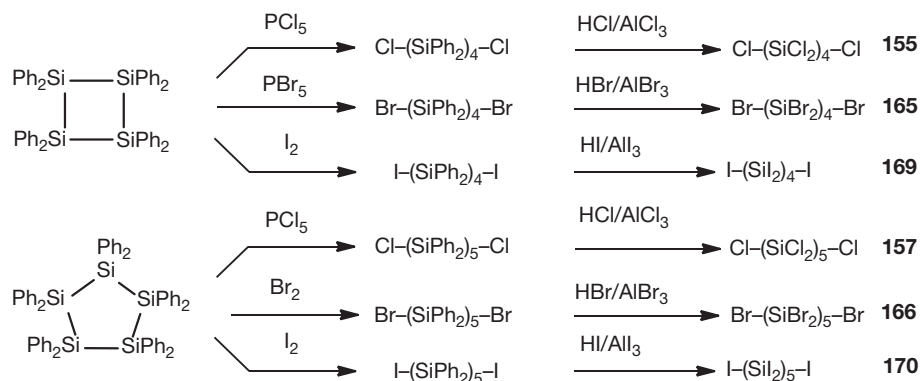
## 1.02.4 Halosilanes

Surveying the literature for the chemistry of perhalosilanes, basically the same pattern unfolds as for the hydrosilanes: the derivatives of  $\text{Si}_n\text{X}_{2n+2}$  with  $\text{X} = \text{Cl}$  and  $\text{F}$ , and  $n = 1, 2$  are relatively well studied due to their possibilities of application in the semiconductor industry,<sup>126</sup> whereas synthetic methodology for all other congeners is less developed (Table 5). Perbrominated and periodated silanes have been studied only in the context of fundamental research, and publications in this field stem mainly from Hengge, Hoeffler and coworkers.<sup>111,127</sup> A list of all perhalosilanes is given in Table 5.

**Table 5** Perhalogenated silanes

Silane	Synthesis (S) and analytical data	Silane	Synthesis (S) and analytical data
Si <sub>2</sub> Cl <sub>6</sub> ( <b>153</b> )	S, <sup>128–130</sup> NMR <sup>152</sup>	Si <sub>4</sub> Br <sub>10</sub> ( <b>165</b> )	S, <sup>127</sup> IR/R, <sup>127</sup> NMR <sup>127</sup>
Si <sub>3</sub> Cl <sub>8</sub> ( <b>154</b> )	S, <sup>128–130</sup> NMR <sup>152</sup>	Si <sub>5</sub> Br <sub>12</sub> ( <b>166</b> )	S, <sup>127</sup> IR/R, <sup>127</sup> NMR <sup>127</sup>
Si <sub>4</sub> Cl <sub>10</sub> ( <b>155</b> )	S, <sup>92,98,128,130</sup> IR/R, <sup>153</sup> NMR <sup>152</sup>	Si <sub>2</sub> I <sub>6</sub> ( <b>167</b> )	S, <sup>144</sup> X-ray <sup>145</sup>
ClSi–(SiCl <sub>3</sub> ) <sub>3</sub> ( <b>156</b> )	S, <sup>139</sup> NMR, <sup>139,152</sup> MS, <sup>139</sup> IR/R <sup>153</sup>	Si <sub>3</sub> I <sub>8</sub> ( <b>168</b> )	S, <sup>111</sup> NMR <sup>111</sup>
Si <sub>5</sub> Cl <sub>12</sub> ( <b>157</b> )	S, <sup>128,129</sup> IR/R, <sup>153</sup> NMR <sup>152</sup>	Si <sub>4</sub> I <sub>10</sub> ( <b>169</b> )	S, <sup>127</sup> IR/R <sup>127</sup>
Si–(SiCl <sub>3</sub> ) <sub>4</sub> ( <b>158</b> )	S, <sup>64,65,139</sup> IR/R <sup>153</sup>	Si <sub>5</sub> I <sub>12</sub> ( <b>170</b> )	S, <sup>127</sup> IR/R <sup>127</sup>
Si <sub>6</sub> Cl <sub>14</sub> ( <b>159</b> )	S <sup>140</sup>	Si <sub>2</sub> F <sub>6</sub> ( <b>171</b> )	S, <sup>130,147–150,154</sup> NMR <sup>149</sup>
1,1-(SiCl <sub>3</sub> ) <sub>2</sub> Si <sub>4</sub> Cl <sub>8</sub> ( <b>160</b> )	S, <sup>155</sup> NMR <sup>152</sup>	Si <sub>3</sub> F <sub>8</sub> ( <b>172</b> )	S, <sup>146,148,151</sup> NMR <sup>149</sup>
1,2-(SiCl <sub>3</sub> ) <sub>2</sub> Si <sub>4</sub> Cl <sub>8</sub> ( <b>161</b> )	S, <sup>98</sup> NMR, <sup>98</sup> IR, <sup>98</sup> MS <sup>98</sup>	Si <sub>4</sub> F <sub>10</sub> ( <b>173</b> )	S, <sup>146</sup> IR, <sup>146</sup> NMR, <sup>146</sup> MS <sup>146</sup>
(Cl <sub>3</sub> Si) <sub>3</sub> Si–Si(SiCl <sub>3</sub> ) <sub>3</sub> ( <b>162</b> )	S, <sup>138</sup> IR/R <sup>153</sup>	FSi–(SiF <sub>3</sub> ) <sub>3</sub> ( <b>174</b> )	S, <sup>114</sup> IR, <sup>114</sup> MS <sup>114</sup>
Si <sub>2</sub> Br <sub>6</sub> ( <b>163</b> )	S <sup>141</sup>	Si–(SiF <sub>3</sub> ) <sub>4</sub> ( <b>175</b> )	S, <sup>114</sup> IR, <sup>114</sup> MS <sup>114</sup>
Si <sub>3</sub> Br <sub>8</sub> ( <b>164</b> )	S, <sup>142</sup> IR/R <sup>143</sup>		

IR/R, IR and Raman spectroscopy.

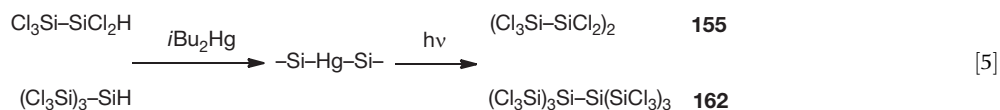
**Scheme 9** Formation of acyclic perhalogenated tetra- and pentasilanes.

### 1.02.4.1 Acyclic Perchlorosilanes

Several methods have been reported for the formation of mixtures of perchlorosilanes Si<sub>n</sub>Cl<sub>2n+2</sub>. The reaction of silicon with HCl (direct process) for the formation of trichlorosilanes gives actually a variety of chlorinated silanes. The high boiling fraction of the reaction has been identified as a mixture consisting of Si<sub>2</sub>Cl<sub>6</sub> (**153**), Si<sub>3</sub>Cl<sub>8</sub> (**154**), Si<sub>4</sub>Cl<sub>10</sub> (**155**), and Si<sub>5</sub>Cl<sub>12</sub> (**157**).<sup>128</sup> The same product mixture **153–155** and **157** was obtained in a process where SiCl<sub>4</sub> was reacted with silicon to give (SiCl<sub>2</sub>)<sub>x</sub>, which was subsequently treated with Cl<sub>2</sub>.<sup>129</sup>

When an electrical discharge acts on halomonosilanes, redistribution reactions occur and, depending on the starting materials and the sort of discharge, various product mixtures are obtained.<sup>130</sup> Passing HSiCl<sub>3</sub> through a glow discharge produced Si<sub>2</sub>Cl<sub>6</sub> (**153**), HCl, SiCl<sub>4</sub>, and solid residue. In an ozonizer discharge, HSiCl<sub>3</sub> gave **153–155**. In both discharge methods, reactions of initially formed SiHCl moieties are postulated.<sup>130</sup> If SiCl<sub>4</sub> was subjected to a nonthermal plasma, Si<sub>3</sub>Cl<sub>8</sub> (**154**) could be isolated as a reaction product.<sup>131</sup>

Disilane **153** and trisilane **154** are both formed in reaction mixtures by oxidative cleavage of a chlorinated polysilane



Si<sub>n</sub>Cl<sub>2n+2</sub> (*n* > 4),<sup>132</sup> SiCl<sub>x</sub> (*x* = 0.2–0.8),<sup>133</sup> or Si particles<sup>134,135</sup> with Cl<sub>2</sub> in the presence of Cu containing catalysts.

The selective synthesis of **153–155** or **157** is also possible by the chlorodephenylation method from Si<sub>2</sub>Ph<sub>6</sub>,<sup>136</sup> Si<sub>3</sub>Ph<sub>8</sub>,<sup>92</sup> Si<sub>4</sub>Ph<sub>8</sub>,<sup>92</sup> or Si<sub>5</sub>Ph<sub>10</sub>.<sup>92</sup> in good yields (**Scheme 9**).

Another method for the selective synthesis of the tetrasilane **155**<sup>137</sup> and also for the branched octasilane (SiCl<sub>3</sub>)<sub>3</sub>Si–Si(SiCl<sub>3</sub>)<sub>3</sub> (**162**)<sup>98,138</sup> starts with the coupling of the respective hydrosilanes with *t*Bu<sub>2</sub>Hg, followed by photolysis of the formed Si–Hg–Si compounds (eqn [5]).

The perchlorinated isotetrasilane (**158**) can be isolated from the reaction of ClSi[Si(OMe)<sub>3</sub>]<sub>3</sub> with BCl<sub>3</sub> (**Scheme 7**).<sup>139</sup>

Due to the need for higher hydrosilanes in the semiconductor industry, methods for the formation of higher perchlorosilanes as their precursors attracted some attention in the last few years.<sup>64</sup> Therefore, well-known reactions have been re-studied, such as the amine-promoted redistribution reaction of Si<sub>2</sub>Cl<sub>6</sub> (**153**), which was known in the literature for about 40 years. Urray et al. discovered that **153** disproportionates quantitatively to Si<sub>6</sub>Cl<sub>14</sub> (**159**) in the presence of NMe<sub>3</sub>.<sup>140</sup> In 2010, researchers from Wacker Chemie claimed that perchlorosilanes

are redistributed in the presence of ethers.<sup>64</sup> Refluxing 153 in the presence of tetrahydrofuran (THF) was reported to lead to the formation of  $\text{Si}(\text{SiCl}_3)_4$  (158).<sup>64</sup> Shortly afterward, the formation of 158 (and other higher hydrosilanes) in the redistribution of perhalosilanes with tertiary amines was patented by Evonik Degussa.<sup>65</sup> Together with the discovery that the use of  $i\text{Bu}_2\text{AlH}$  allows the hydrogenation of Si–Cl bonds without Si–Si bond scission,<sup>26</sup> new routes to higher hydrosilanes in large scale finally seem to become feasible.

#### 1.02.4.2 Acyclic Perbromosilanes

The standard procedure for the formation of  $\text{Si}_2\text{Br}_6$  (163) consists in the passage of a gas stream of an  $\text{O}_2/\text{Br}_2$  mixture over  $\text{CaSi}$  that has been heated to 200 °C. By condensation of the volatile reaction products, pure 163 is obtained.<sup>141</sup> The only reliable citation of a preparation method for  $\text{Si}_3\text{Br}_8$  (164) stems from 1911.<sup>142</sup> In this chapter, the formation of 164, together with  $\text{SiBr}_4$ ,  $\text{Si}_2\text{Br}_6$  (163), and  $\text{Si}_4\text{Br}_{10}$  (165), is reported to take place upon action of an electrical discharge on  $\text{SiHBr}_3$ .<sup>142</sup> Although cited later on, it is not clear from the original article, whether or not Höfler used this method for the isolation of 164 in order to investigate its vibrational properties.<sup>143</sup>

The cleavage of cyclotetrasilane  $\text{Si}_4\text{Ph}_8$  with  $\text{PBr}_5$  leads to the formation of 1,4- $\text{Br}_2\text{Si}_4\text{Ph}_8$ , which subsequently can undergo complete dearylation with  $\text{HBr}/\text{AlBr}_3$  to form  $\text{Si}_4\text{Br}_{10}$  (165).<sup>127</sup> Using the analogous strategy,  $\text{Si}_5\text{Br}_{12}$  (166) was formed starting from  $\text{Si}_5\text{Ph}_{10}$  and  $\text{Br}_2$  (Scheme 9).<sup>127</sup>

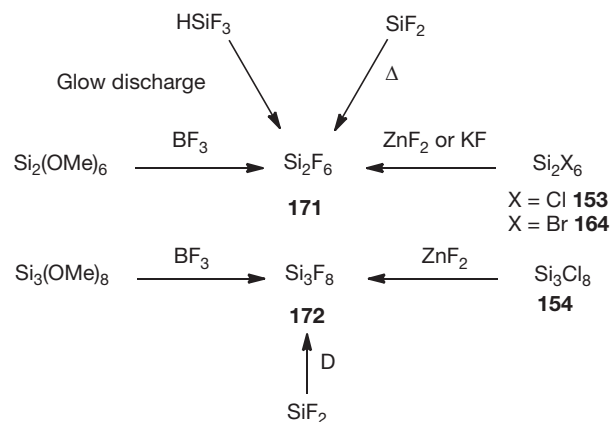
#### 1.02.4.3 Acyclic Periodosilanes

When  $\text{SiI}_4$  is reacted with finely divided metallic silver in an evacuated glass tube,  $\text{Si}_2\text{I}_6$  (167) can be obtained.<sup>144</sup> Utilizing this method, 50 years later Jansen and Friede were able to determine the x-ray crystal structure of 167.<sup>145</sup> The molecules are arranged in a staggered conformation, with Si–I bond lengths (2.42 Å) in good agreement with the bond length reported for  $\text{SiI}_4$  and the Si–Si bond length (2.32 Å) in the same range as those of the analogous disilanes  $\text{Si}_2\text{H}_6$  (1) and  $\text{Si}_2\text{F}_6$  (171).<sup>145</sup>

Periodotrisilane  $\text{Si}_3\text{I}_8$  (168) can be obtained in 65% yield by dearylation of  $\text{Si}_3\text{Ph}_8$  with  $\text{HI}$  and  $\text{AlI}_3$  as a catalyst.<sup>111</sup> The iodine derivatives  $\text{Si}_4\text{I}_{10}$  (169) and  $\text{Si}_5\text{I}_{12}$  (167) were obtained by treatment of  $\text{Si}_4\text{Ph}_8$  or  $\text{Si}_5\text{Ph}_{10}$  with  $\text{I}_2$  in the first step and with  $\text{HI}/\text{AlI}_3$  in the second one (Scheme 9).<sup>127</sup> The obtained IR and Raman spectra were discussed with the aid of a normal coordinate analysis.<sup>127</sup>

#### 1.02.4.4 Acyclic Perfluorosilanes

When the polymer  $(\text{SiF}_2)_x$ , prepared by condensation and warming of the gas mixture emerging from the reaction of  $\text{SiF}_4$  and silicon at high temperatures (around 1100 °C) and reduced pressure, is heated under vacuum to 250–300 °C, it melts and decomposes to give perfluorosilanes  $\text{Si}_n\text{F}_{2n+2}$  and a solid, silicon-rich polymer.<sup>146</sup> In the mixture, silanes with  $n = 1$  up to 14 were detected by mass spectroscopy, but only the perfluorinated di-, tri-, and tetrasilanes  $\text{Si}_2\text{F}_6$  (171),  $\text{Si}_3\text{F}_8$  (172), and  $\text{Si}_4\text{F}_{10}$  (173) were isolated.<sup>146</sup>  $\text{FSi}(\text{SiF}_3)_3$  (174) and  $\text{Si}(\text{SiF}_3)_4$  (175) were generated in small quantities by the



**Scheme 10** Various pathways to hexafluorodisilane 171 and octafluorotrisilane 172.

co-condensation reaction of gaseous  $\text{SiF}_2$  with  $\text{B}_2\text{H}_6$ , but isolation was not possible.<sup>114</sup>

Alternative methods for the formation of 171 consist of the fluorination of  $\text{Si}_2\text{Cl}_6$  (153) with  $\text{SbF}_3$ ,<sup>147</sup>  $\text{ZnF}_2$ ,<sup>148</sup> or  $\text{KF}$ ,<sup>149</sup> of  $\text{Si}_2\text{Br}_6$  (164) with  $\text{ZnF}_2$ ,<sup>150</sup> or of  $\text{Si}_2(\text{OMe})_6$  with  $\text{BF}_3$ . Furthermore, formation of 171 was reported to occur in the redistribution reaction of  $\text{HSiF}_3$  in a glow discharge.<sup>130</sup> Trisilane 172 can be prepared by fluorination of  $\text{Si}_3\text{Cl}_8$  (154) with  $\text{ZnF}_2$ <sup>148</sup> and of  $\text{Si}_3(\text{OMe})_8$  with  $\text{BF}_3$ .<sup>151</sup> In all cases, moderate yields around 65% were observed (Scheme 10).

#### 1.02.4.5 Mixed Acyclic Perhalosilanes

Only few studies on mixed perhalosilanes have been reported, a fact probably caused by the lack of suitable synthetic methods (Figure 4).

Distribution reactions between  $\text{Si}_2\text{Cl}_6$  (153) and  $\text{Si}_2\text{Br}_6$  (164) yielded all possible mixed chlorobromosilanes,  $\text{Si}_2\text{Cl}_x\text{Br}_{6-x}$  176a–183a.<sup>156</sup> The products in the reaction mixture were assigned by <sup>29</sup>Si NMR and Raman studies.<sup>156</sup> Pure  $\text{Cl}_3\text{SiSiBr}_3$  (178a) could be obtained by bromination of  $\text{Ph}_3\text{SiSiCl}_3$  with  $\text{HBr}/\text{AlBr}_3$ .<sup>156</sup>

In order to isolate mixed halosilanes, the reaction of  $\text{SiF}_2$  with halogens  $\text{X}_2$  ( $\text{X} = \text{Cl}_2$ ,  $\text{Br}_2$ , and  $\text{I}_2$ ) was studied. In the co-condensation with  $\text{Cl}_2$ , the three disilane derivatives  $\text{Cl}_2\text{FSi-SiCl}_3$  (176b),  $\text{Cl}_3\text{Si-SiF}_3$  (178b), and  $\text{ClF}_2\text{Si-SiF}_2\text{Cl}$  (182b) were postulated to be the major reaction products in the formed mixture. Reaction of  $\text{SiF}_2$  with  $\text{Br}_2$  also yielded mixtures in which  $\text{Si}_2\text{F}_5\text{Br}$  (176d),  $\text{F}_3\text{Si-SiBr}_2\text{-SiF}_3$  (184b),  $\text{F}_3\text{Si-Si}_2\text{Br}_5$  (185a), and  $\text{F}_5\text{Si}_2\text{-SiBr}_3$  (185b) were identified.<sup>157</sup> In contrast to this, the reaction of  $\text{SiF}_2$  with  $\text{I}_2$  unexpectedly led to the formation of only monosilanes.<sup>158</sup> The formation of higher fluoroiodosilanes finally was successful when  $\text{SiF}_2$  was cocondensed with  $\text{CF}_3\text{I}$ :  $\text{F}_3\text{Si-SiF}_2\text{I}$  (176c) was definitely identified in the product mixture and MS and NMR data suggested the presence of  $\text{IF}_2\text{Si-SiF}_2\text{I}$  (180c) and some trisilanes.<sup>159</sup> The only examples for branched mixed halosilanes are the different homologs of the isotetrasilane  $\text{XSi}(\text{SiY})_3$ . Synthesis of  $\text{ClSi}(\text{SiF}_3)_3$  (186b) was accomplished by the reaction of  $\text{ClSi}(\text{Si}(\text{OMe})_3)_3$  with  $\text{BF}_3$ ,<sup>139</sup> whereas  $\text{BrSi}(\text{SiCl}_3)_3$  (186a) and  $\text{ISi}(\text{SiCl}_3)_3$  (186c) were prepared by the reaction of  $\text{HSi}(\text{SiCl}_3)_3$  (48) with  $\text{CHBr}_3$  and  $\text{CHI}_3$ , respectively.<sup>155</sup>

### 1.02.4.6 Cyclic Perhalosilanes

Utilizing synthetic method 2 (Scheme 4), perphenylcyclopolysilanes  $\text{Si}_n\text{Ph}_{2n}$  are easily dephenylated with  $\text{HX}/\text{AlX}_3$  and all phenyl groups can be replaced by halogen. Thus, the perhalocyclopolysilanes  $(\text{X}_2\text{Si})_n$  with  $\text{X} = \text{Cl}$ ,<sup>160</sup>  $\text{Br}$ ,<sup>160</sup> and  $\text{I}$ <sup>161</sup> and  $n = 4, 5,$  and  $6$  can be obtained (Figure 5). Generally, the reaction follows an electrophilic substitution mechanism of the aromatic ring. Acetyl chloride can also be used as a halogenating agent for the formation of  $\text{Si}_5\text{Cl}_{10}$  (188a).<sup>124</sup>

The amine-promoted redistribution and disproportionation of chlorosilanes was already mentioned as a possible route to perhalogenated silanes.<sup>140</sup> Boudjouk et al. reported that the reaction of  $\text{HSiCl}_3$  with pentaethyldiethylene triamine (=pedeta) in  $\text{CH}_2\text{Cl}_2$  leads to the formation of the complex  $[\text{pedetaH}_2\text{SiCl}^+]_2[\text{Si}_6\text{Cl}_{14}]^{2-}$ .<sup>36</sup> X-ray crystal diffraction analysis of the product showed that the dianion  $[\text{Si}_6\text{Cl}_{14}]^{2-}$  (189d) comprised a planar dodecachlorocyclohexasilane ring with a chloride ion above and below the ring plane. This structural type is unique in group-14 chemistry. Reduction of 189d afforded  $\text{Si}_6\text{H}_{12}$  (10) in excellent yields (Scheme 1).<sup>35,36</sup>

The bi(cyclopentasilanyl) compounds  $(\text{SiX}_2)_5-(\text{SiX}_2)_5$  (190, with  $\text{X} = \text{Cl}, \text{Br}$ ) can be prepared by treatment of nonachlorocyclopentasilanes  $\text{HSi}_5\text{Cl}_9$  (144) with  $(t\text{Bu})_2\text{Hg}$ .<sup>37</sup> Alternatively, the phenyl derivative bi(nonaphenylcyclopentasilanyl), prepared from  $\text{BrSi}_5\text{Ph}_9$  with naphthyllithium, was treated with  $\text{HX}/\text{AlX}_3$  ( $\text{X} = \text{Cl}, \text{Br}$ ) to afford 190a and 190b (Figure 5).<sup>37</sup>

## 1.02.5 Chalcogenosilanes

### 1.02.5.1 Si–O Compounds

Silicon dioxide and silica rank among the best-studied substances with a wide variety of appearance in nature and

technical applications. Silanediols, disiloxanes, metallasiloxanes, and similar compounds also attracted much interest, but by contrast compounds bearing Si–Si–O units without any carbon substituents to silicon are comparatively rare.<sup>162</sup>

### 1.02.5.2 Acyclic Si–O Compounds

Investigations into bis-disilanyl- $[(\text{H}_3\text{SiH}_2\text{Si})_2\text{O}$  191] and higher symmetric as well as asymmetric ethers started in the 1960s.<sup>163,164</sup> These silylethers are spontaneously inflammable in air. The silicon–oxygen bond in 191 can be cleaved with boron trichloride<sup>164,165</sup> or phosphorus pentafluoride.<sup>166</sup> Alkoxy-substituted silanes such as bis-, tris-, or tetrakis(trimethoxysilyl)silane were obtained by the reaction of tetrakis(trichlorosilyl)silane with methanol and triethylamine, depending on the reaction conditions.<sup>167</sup>

Mercury-sensitized photolysis of siloxane 192 (Scheme 11) gave besides polymeric polysilanes also 193 in 60% yield and starting from 194, disilane 195 in 37% yield.<sup>168</sup> Unfortunately, no further chemistry was reported with 193, which combines the interesting functionalities of disilane, silicon hydride, and siloxane. Hexamethoxydisilane and hexaisopropoxydisilane afford under pyrolytic conditions dimethoxysilylene and diisopropoxydisilylene, respectively, and both can be used in addition reactions with acetylenes or butadienes.<sup>169</sup>

A compound that has gained some interest is 1,2-bis(trifluoromethylsulfonyloxy)disilane (196) obtained by treatment of 1,2-bis(*p*-tolyl)disilane with trifluoromethylsulfonic acid.<sup>170,171</sup> Even though 196 has the tendency to decompose explosively, it was possible to confirm its structure by means of x-ray single-crystal diffraction analysis.<sup>172</sup> Despite its difficulties in handling, 196 represents a relatively simple available material that offers the possibility of nucleophilic substitution

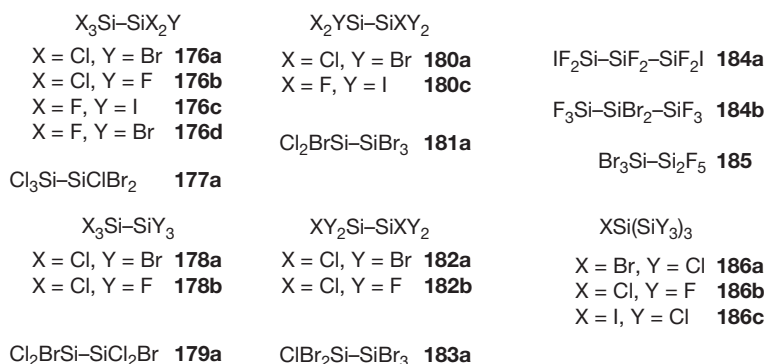


Figure 4 Mixed acyclic perhalosilanes.

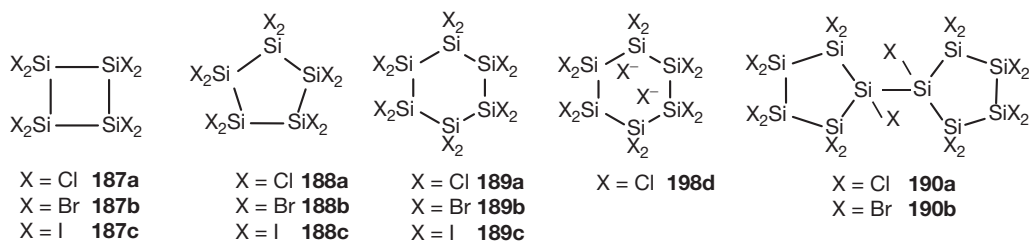
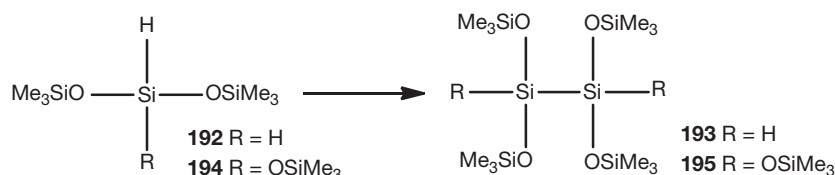
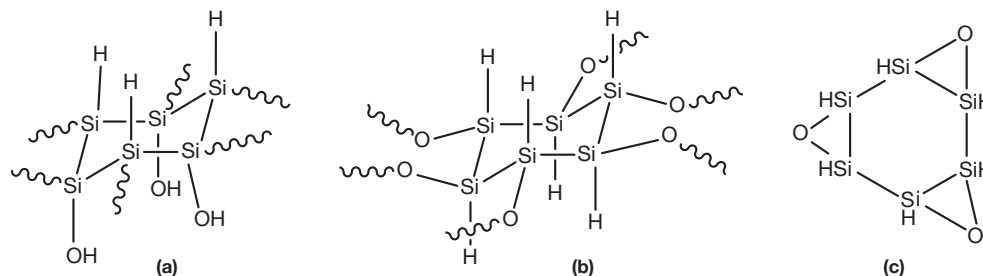


Figure 5 Cyclic perhalosilanes.





**Scheme 11** Synthesis of acyclic Si-O compounds **193** and **195**.



**Scheme 12** Different siloxenes.

on a disilane in the 1,2-position. At low temperature, **196** reacts rapidly and completely with organolithium and organomagnesium compounds.<sup>173</sup> The compound was used in investigations toward the UV behavior of silanes, as starting material in the field of ceramics and conducting materials, polymers, or simply as a building block for higher silanes.<sup>90,173–176</sup>

### 1.02.5.3 Siloxenes

Two-dimensional layered polymers with the empirical formula  $\text{Si}_6\text{H}_{6-n}\text{O}_n$  are referred to as siloxene. They turn white when exposed to sunlight and burst into flame by heating on air.<sup>177</sup> Upon treatment with strong oxidants, siloxenes are known to chemiluminesce and to evolve  $\text{H}_2$ .<sup>178</sup> Siloxenes are not affected by concentrated  $\text{H}_2\text{SO}_4$ , but show incandescence by treatment with fuming  $\text{HNO}_3$ .<sup>177</sup> What is often called in the literature ‘porous silicon’ consists of small siloxene layers.<sup>179</sup>

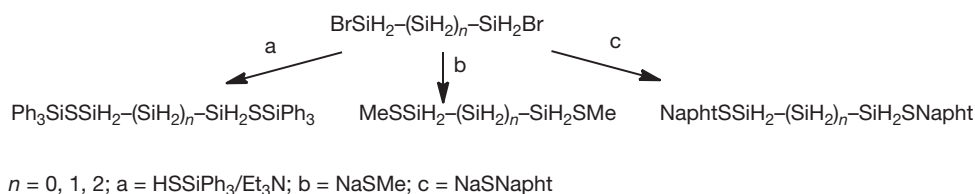
Woehler in 1863<sup>180</sup> as well as Kautsky in 1924<sup>181</sup> treated  $\text{CaSi}_2$  with  $\text{HCl}$  following somewhat different procedures and obtained what became known as Woehler-siloxene and Kautsky-siloxene. The name ‘siloxene’ traces back to Kautsky’s original publication.<sup>181</sup> He suggested a structure, which he named in accordance with the then valid rules of nomenclature cyclohexasilatrioxene (**Scheme 12, C**). This was then simplified for reasons of convenience to siloxene. Woehler-siloxene is a yellow crystalline polymer, which predominately consists of the planar modification (**Scheme 12, A**), as was first shown by Weiss et al.<sup>182</sup> These sheet polymers do not necessarily have to exist in planar forms but can also form nanotubes.<sup>183,184</sup> The ongoing research on the properties of nanosheets might be of interest to nanotechnology.<sup>184</sup> The Kautsky-siloxene is a gray-green amorphous material, which can be easily modified by various substitution reactions, thus shifting the luminescence wavelength. Due to being amorphous and generally insoluble in organic solvents, Kautsky-siloxene is more difficult to analyze structurally and has an inhomogeneous composition. X-ray emission and infrared spectra confirm the existence of several modifications with a predominant contribution of

$\text{Si}_6$  rings, which are linked by oxygen bridges to form planes (**Scheme 12, B**).

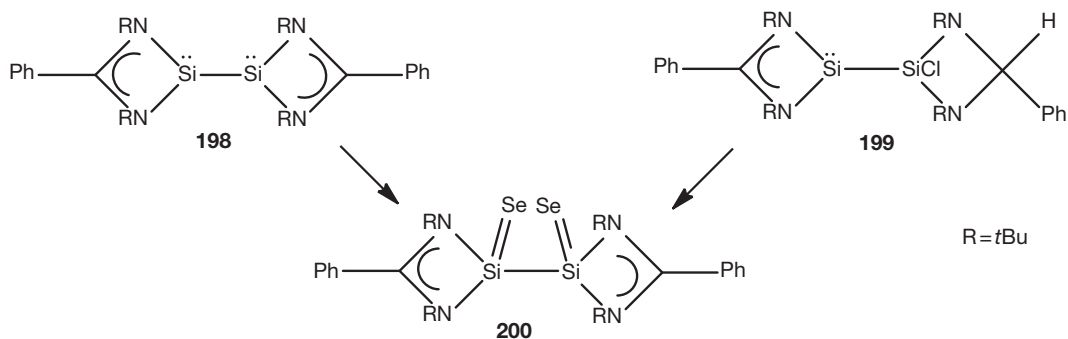
In general, siloxenes show strong photoluminescence even at room temperature and are responsible for the visible luminescence in porous silicon, a fact that makes these materials potentially useful for optoelectronic applications.<sup>182</sup> The interest siloxenes gained over the years stems partly from these fundamental optical properties<sup>185</sup> and led to efforts to synthesize functionalized six-membered Si-rings as well as oligosilanes with similar characteristics.<sup>177,186</sup> These efforts led to the finding that also siloxy-substituted monomeric cyclohexasilanes show photoluminescence with remarkable fluorescence intensities and further supported the assumption that the luminescence of siloxene is a molecular rather than a solid-state property.<sup>178</sup> Further, calculations support this assumption by indicating interaction of the oxygen lone pair with the Si–Si backbone.<sup>178</sup>

### 1.02.5.4 Si–S Compounds

Like bis-disilanyl-ether  $[(\text{H}_3\text{SiH}_2\text{Si})_2\text{O}]$  **191** also the first bis-disilanyl-sulfide  $[(\text{H}_3\text{SiH}_2\text{Si})_2\text{S}]$  **197** was prepared in the 1960s reacting  $\text{H}_3\text{SiH}_2\text{SiI}$  (**92**) with  $\text{HgS}$ .<sup>187</sup> Treating silyl halides ( $\text{H}_3\text{SiH}_2\text{SiX}$ ) with lithium tetra(methylthio)aluminate affords silyl thioethers such as  $\text{H}_3\text{SiH}_2\text{Si-SMe}$  in good yields,<sup>188</sup> whereas  $\alpha,\omega$ -dihalooligosilanes react with alkali metal thiophenolates to the corresponding di(phenylthio)silanes such as  $\text{PhS-SiH}_2\text{SiH}_2\text{-SPh}$  and  $\text{PhS-SiH}_2\text{SiH}_2\text{SiH}_2\text{-SPh}$ .<sup>189</sup> A systematic access to S-functional derivatives of higher silicon hydrides by nucleophilic displacement of halo-substituents by sulfur nucleophiles was established by Stueger et al. (**Scheme 13**).<sup>190</sup> Only in the case of  $\text{HSSiPh}_3$  the use of  $\text{Et}_3\text{N}$  as auxiliary base was necessary. Stronger nucleophilic systems such as  $\text{HSPH}/\text{Et}_3\text{N}$  cause Si–Si and Si–H scission reactions so that alkali metal thiolates are here the reagents of choice.<sup>30</sup> These thus-obtained methyl derivatives are thermally stable and can be distilled without decomposition whereas the phenyl compounds show thermal and hydrolytic lability.<sup>190</sup>



**Scheme 13** Systematic access to S-functional derivatives of higher silicon hydrides.



**Scheme 14** Possible routes to di(silaneselone) **200**.

One cyclic compound containing a  $\text{-SiH}_2\text{SiH}_2\text{-S-}$  unit is known, namely 1,4-dithiacyclohexasilane obtained from the reaction of 1,2-dichlorodisilane (**13**) and  $(\text{H}_3\text{Si})_2\text{S}$ .<sup>191</sup> This compound shows thermal instability and can be converted within 1 h at 90 °C to **197**.

### 1.02.5.5 Si–Se, Si–Te, and Si–Po Compounds

Nearly 30 years after the first sulfur-containing compounds, the first selenium analogs were reported in the literature namely disilanyl silyl selenane ( $\text{H}_3\text{SiH}_2\text{Si-Se-SiH}_3$ ), bis(disilanyl)selenane [ $(\text{H}_3\text{SiH}_2\text{Si})_2\text{Se}$ ], and 1,4-diselenacyclohexasilane.<sup>191</sup> All three compounds were prepared the same way as their sulfur congeners and they also show very similar properties. No further attention was given to Si–Si–Se compounds except for some theoretical investigations in comparison with <sup>77</sup>Se NMR and stabilization of silicon–selenium double bonds.<sup>192–195</sup> Recently, reaction of the stable silylenes **198** or **199** (see **Chapter 6.12**) with one or two equivalents of elemental selenium in THF afforded the di(silaneselone) **200** in 24% and 10% yield (**Scheme 14**).<sup>196</sup> X-ray crystallography of **200** proved the assigned structure unambiguously. Thus, **200** is the first example of a pentavalent silicon with a Si–Se double bond. It was found to be a highly air- and moisture-sensitive colorless solid, which is stable at room temperature under inert atmosphere.<sup>197</sup>

No compounds containing silyl–polonium bond lacking silyl–carbon bonds are known in the literature. Maybe worth to note in this context are polyatomic anions with coordinating cationic species consisting of pairs of bonded atoms such as  $[\text{Si}_2\text{Te}_6]^{6-}$  and  $[\text{Si}_2\text{Se}_6]^{6-}$ . These  $[\text{Si}_2\text{Te}_6]^{6-}$  anions are the only compounds bearing a silyl–tellurium bond. Only few examples of these silicates containing an ethane-like Si–Si bond are known:  $\text{K}_6\text{Si}_2\text{Te}_6$  (**201**),<sup>198</sup>  $\text{Mn}_3\text{Si}_2\text{Te}_6$  (**202**),<sup>198,199</sup>  $\text{Cr}_2\text{Si}_2\text{Te}_6$  (**203**),<sup>198,200,201</sup>  $\text{Na}_6\text{Si}_2\text{S}_6$  (**204**),<sup>202</sup>  $\text{Na}_6\text{Si}_2\text{Se}_6$  (**205**),<sup>202</sup>

$\text{Ba}_4\text{Ag}_4\text{Si}_2\text{Te}_9$  (**206**),<sup>203</sup> and  $\text{Ba}_4\text{Cu}_4\text{Si}_2\text{Te}_9$  (**207**).<sup>203</sup> The reported Si–Si bond length in these compounds correspond to 2.40 Å for **201**, 2.33 Å for **206**, 2.32 Å for **202**, 2.31 Å for **207**, and 2.27 Å for **203** to simple  $\sigma$  bonds. Ethane-like Si–Si bonds appear also in quaternary silicates resulting from the combination of alkali metals, transition or rare earth metals, main group elements (in this context silicon), and heavy chalcogens:  $\text{Na}_8\text{Eu}_2(\text{Si}_2\text{Se}_6)_2$ ,<sup>204</sup>  $\text{Na}_8\text{Pb}_2(\text{Si}_2\text{Se}_6)_2$ ,<sup>205</sup>  $\text{Na}_8\text{Eu}_2(\text{Si}_2\text{Te}_6)_2$ ,<sup>206</sup> and  $\text{Na}_9\text{Sm}(\text{Si}_2\text{Se}_6)_2$ .<sup>206</sup>

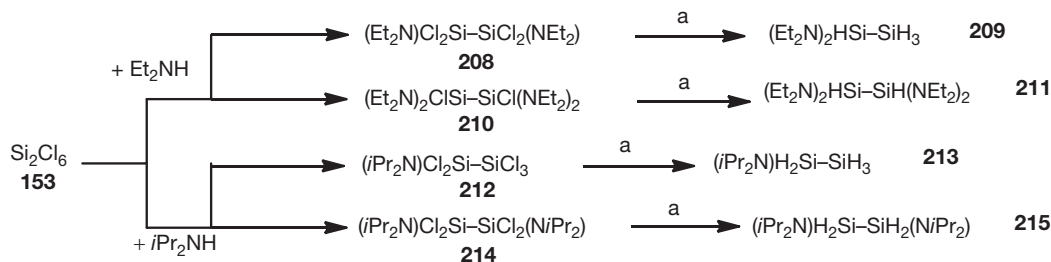
## 1.02.6 Silanes with Group-15 Substituents

### 1.02.6.1 Si–N Compounds

The planar structure of trisilylamine ( $\text{SiH}_3$ )<sub>3</sub>N and its lack of basicity as compared to the pyramidal structure of trimethylamine  $(\text{CH}_3)_3\text{N}$  are discussed textbook cases, which reflect the fundamental variations in ground-state geometries. In general, more the silicon atoms attached to a given nitrogen atom, less basic is the behavior of the nitrogen.  $(\text{H}_3\text{Si})_3\text{N}$  shows all the common behaviors of Si–N compounds: thermal and moderate hydrolytic stability and reduced basicity. Silylated amines can be metalated with alkali metals or lithium alkyls and can be treated with  $\text{LiAlH}_4$  without Si–N bond scission. Si–N bond cleavage occurs upon treatment with acids and various organic or inorganic electrophiles. When fewer than three Si atoms are attached to a nitrogen atom, the kinetic stability of the Si–N linkage can be enhanced by the presence of bulky substituents. The stability of the Si–N bond against nucleophiles allows carrying out reactions at the Si center without affecting the Si–N moiety. A feature of the Si–Si–N linkage is an intense UV absorption leading sometimes to photoluminescence.<sup>207,208</sup>

Silicon nitride ( $\text{Si}_2\text{N}_4$ ) is used in high-temperature applications, in electronics, and for all kinds of bearings.





**Scheme 15** Synthesis of acyclic Si-N compounds starting from  $\text{Si}_2\text{Cl}_6$  (153).

Silicon–nitrogen compounds with silicon–silicon bonds have been investigated as precursors for silicon–nitride ceramics,<sup>209</sup> as single-source precursors for CVD,<sup>210</sup> as components for sol-gel preparations of silazane frameworks,<sup>210</sup> and photophysical applications.<sup>210</sup> Despite these interesting application possibilities, aminodi- and -polysilanes are still a poorly investigated class of compounds.

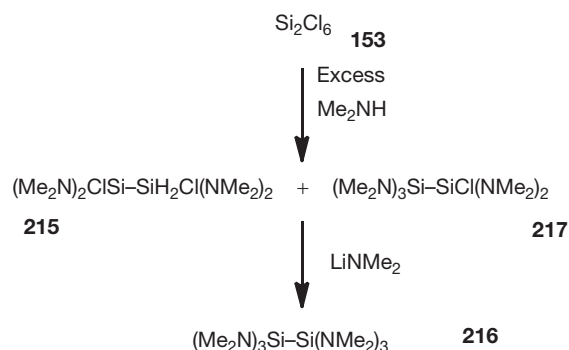
### 1.02.6.2 Acyclic Si–N Compounds

Amino groups can easily be attached to silicon by employing reactions of halosilanes with ammonia, amines, or alkali-metal amides.

The first syntheses of symmetric 1,2-di- and 1,1,2,2-tetra- as well as of some 1,1-di-substituted aminodisilanes were reported by Schmidbaur and coworkers.<sup>211</sup> The reaction of halodisilanes with tertiary amines led only to an amine-catalyzed dismutation to afford only perchloro-polysilanes and tetrachlorosilane.<sup>211</sup> Using a secondary amine namely dimethylamine showed the same result,<sup>211</sup> but by changing the alkyl substituent to ethyl a series of compounds containing the Si–Si– $\text{NEt}_2$  structural unit became available. Depending on the reaction conditions in the case of  $\text{Et}_2\text{NH}$  either di- (208) or tetra- (210) substitution occurred, whereas the use of  $i\text{Pr}_2\text{NH}$  only led to mono- or di-substitution yielding either asymmetric 212 or symmetric 214 (Scheme 15). Alternatively, 1,2-diaminotetrahalodisilanes similar to 208 can be obtained by treating hexachlorodisilane (153) with the lithium or potassium amides of the N-ligand.<sup>212</sup>

All these compounds can be hydrogenated with an excess of  $\text{LiAlH}_4$  (211, 213, and 215). The only difficulties were reported for the hydrogenation of 208 as it gave not the expected 1,2-bis(diethylamino)disilane but the isomer 209 in only 25% yield.<sup>211</sup> Another route to 215 utilized 1,2-bis(trifluoromethylsulfonyloxy)disilane (196) as starting material.<sup>213</sup> Roesky et al. showed that replacement of the halides of 1,2-diamino-tetrahalodisilanes, such as 208, with  $\text{NH}_2$  groups can be achieved by sodium in liquid ammonia. The transformation gives even higher yields using just ammonia without sodium, or was carried out in cases of sterically demanding nitrogen substituents with ammonia at 80 °C in an autoclave.<sup>212</sup>

The reductive homo-coupling of a diaminochlorohydrodisilane with lithium constitutes an alternative route to 1,1,2,2-tetra-substituted aminodisilanes similar to 211 as was demonstrated by Heinicke and coworkers.<sup>214</sup> This way it was possible to achieve also tetra-substitution with diisopropylamine substituents affording  $(i\text{Pr}_2\text{N})_2\text{HSiSiH}(\text{NiPr}_2)_2$ .<sup>214</sup>



**Scheme 16** Synthesis of hexa-N-substituted disilane 216.

Polychlorodisilanes with  $(\text{R}_3\text{Si})_2\text{N}$  groups and their facile conversion to multifunctionalized disilanes by various selective substituent-exchange reactions were studied by Stueger and coworkers.<sup>91</sup> Synthesis of  $[(\text{Me}_3\text{Si})_2\text{N}]\text{SiCl}_2\text{SiCl}_2[\text{N}(\text{SiMe}_3)_2]$  was achieved by the reaction of  $\text{Si}_2\text{Cl}_6$  (153) with the respective lithium amide and stoichiometric amounts of TMEDA (*N,N,N',N'*-tetramethylethane-1,2-diamine). The use of the bulky  $\text{N}(\text{SiMe}_3)_2$  substituent led to a change of behavior of the generally very moisture-sensitive chlorosilanes. While compounds bearing just one  $\text{N}(\text{SiMe}_3)_2$  group decompose readily by atmospheric moisture, compounds with two  $\text{N}(\text{SiMe}_3)_2$  groups could be handled in air for a limited period of time.

The formation of the hexa-N-substituted disilane  $(\text{Me}_2\text{N})_3\text{Si-Si}(\text{NMe}_2)_3$  (216) was first reported in 1965,<sup>215</sup> but later problems repeating the procedure became known.<sup>216</sup> Verkade et al.<sup>216</sup> demonstrated the synthesis of 216 in two steps and good yield (Scheme 16). With the use of  $\text{LiNEt}_2$ , they could also establish the formation of hexakis(diethylamino)disilane<sup>216</sup> and, furthermore, by treatment of 217 with  $\text{NaOMe}$  the methoxy derivative  $(\text{Me}_2\text{N})_3\text{Si-Si}(\text{NMe}_2)_2\text{OMe}$  (218) was obtained.<sup>216</sup> Hexa(amino)disilanes similar to 216 with cyclic amino substituents such as aziridino, azetidino, pyrrolidino, and piperidino were prepared starting from  $\text{Si}_2\text{Cl}_6$  (153) and excess of the cyclic amines without the use of additional lithium amide.<sup>217</sup>

Structural characterization of amino-substituted silanes was achieved for the acyclic compounds 211 ( $\text{R} = i\text{Pr}$ ),<sup>214</sup> 214,<sup>211</sup> and 216.<sup>216</sup> The length of the Si–N bond is for 211 with 1.73 Å and for 214 with 1.72 Å in the normal value range, but 216 exhibits an extremely short Si–N bond of 1.67 Å. All three structures show the expected, almost planar configuration of the nitrogen atom.

Examples of higher N-substituted silanes are scarce. Nevertheless, their preparation can be achieved starting from the respective perchlorinated oligosilanes upon reaction with different amines or alkali-metal amides. The outcome of these reactions depends, on the one hand, on the nucleophilicity of the used amines and, on the other hand, on the constitution of the starting material. Stueger et al.<sup>218,92</sup> could show that by increasing the nucleophilicity of the amine not only Si-Si bonds but also Si-H and Si-halogen bonds were cleaved. Remarkable in the synthetic approach using bromo-, hydro-, or chlorosilanes as starting materials are the obtained yields and the purity of the rather reactive products. (Figure 6, 219–226). The bulkiness of the (Me<sub>3</sub>Si)<sub>2</sub>N group led to substitution only at the terminal SiCl<sub>3</sub> groups; therefore, mono- or disubstitution can be achieved but the introduction of a third (Me<sub>3</sub>Si)<sub>2</sub>N group to a trisilane failed even under very harsh conditions. However, this effect was observed only for trisilanes, but not for higher silanes. Stueger and coworkers also reported mild conditions under which amino groups could be

replaced by chlorine, for example, by treatment of 226 with dry HCl gas at 0 °C without affecting Si-Si and Si-H bonds.<sup>219</sup>

### 1.02.6.3 Cyclic Si-N Compounds

Just two examples (227 and 228)<sup>92,220</sup> of inorganic ring systems consisting only of silicon atoms with attached nitrogen substituents can be found in the literature; all others are heterocyclic compounds containing one or two disilanylene units (229–234, Figure 7).

Decachlorocyclopentasilane (Si<sub>5</sub>Cl<sub>10</sub> 188a) was found to react with lithium amides to mono- (227) or di- (228) substituted cyclopentasilanes depending on the reaction conditions.<sup>92,220</sup> The hydrogenation of 227 and 228 with LiAlH<sub>4</sub> did not proceed in the same clean way as mentioned above for the acyclic compounds. It afforded besides the expected hydrogenated cyclic aminosilanes also considerable amounts of linear silanes, arising from ring-cleavage reactions. A separation of the obtained mixtures could be achieved neither by distillation

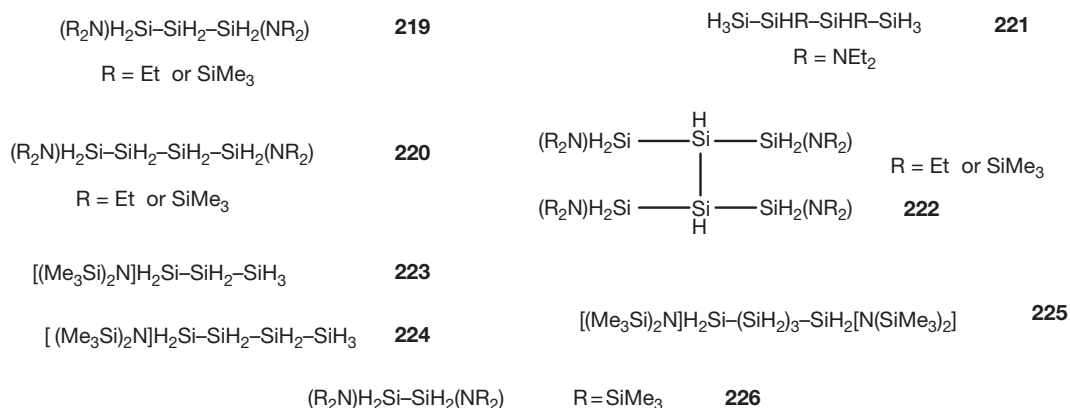


Figure 6 Acyclic Si-N compounds.

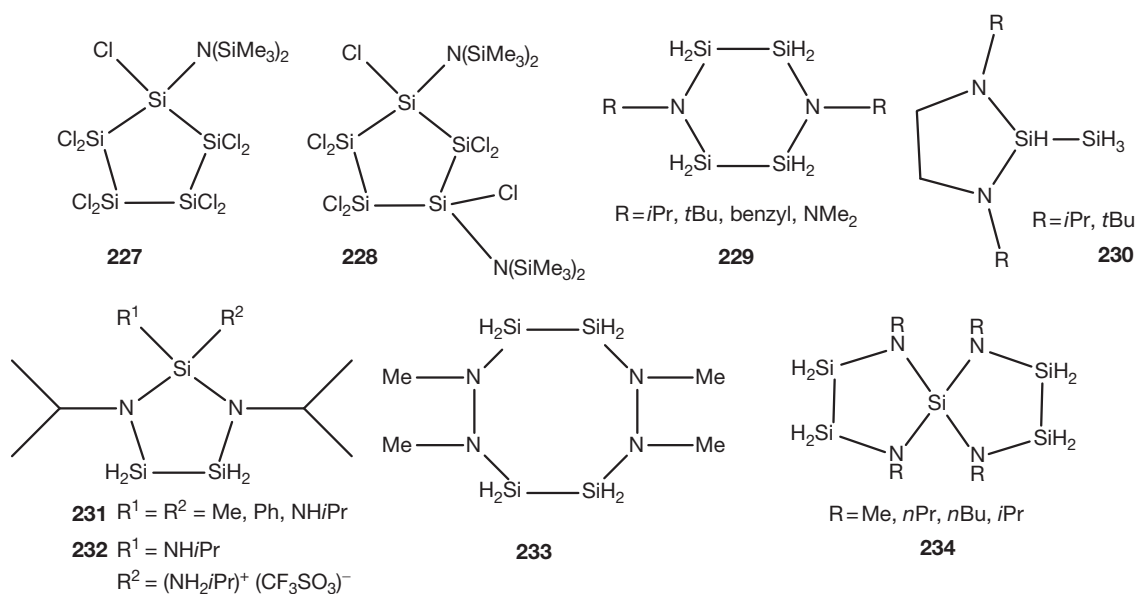


Figure 7 Cyclic Si-N compounds.

nor by fractional condensation due to the limited thermal stability of these cyclosilanes.<sup>92,220</sup>

1,2-Bis(trifluoromethylsulfonyloxy)disilane (196) and primary amines were used as starting materials for 229 (R = *i*Pr, *t*Bu, benzyl), 230, and 231 (Figure 7).<sup>213</sup> Under the chosen reaction conditions, ring formation of 229 is kinetically preferred over the competitive polymerization reaction. Using bis(isopropylamino)dimethyl- or -diphenylsilane for this reaction, the five-membered rings (231; R = Me or Ph) could be obtained.<sup>213</sup> All attempts to obtain six-membered rings with one disilanylene and one ethylene unit using *N,N'*-diisopropyl- or di-*tert*-butylethylenediamine were not successful.<sup>213</sup> In both cases, a five-membered ring (230) with an exocyclic SiH<sub>3</sub> unit was obtained. Compounds 229 and 231 were described as volatile and not spontaneously inflammable.<sup>213</sup>

Reactions of different hydrazine derivatives with 1,2-bis(trifluoromethylsulfonyloxy)disilane (196) led to 229 (R = NMe<sub>2</sub>) and 233 (Figure 7).<sup>210</sup> Using two equivalents of 196, all reactions were carried out by addition of also two equivalents of triethylamine as auxiliary base to trap the produced triflic acid. Monocyclization of tetra(isopropylamino)silane was achieved by using just one equivalent of 1,2-bis(trifluoromethylsulfonyloxy)disilane (196) yielding 231 (R = NHiPr) in high yield. The same reaction with two equivalents of 196 yielded a mixture of spirocyclic 234 (R = *i*Pr), 231 (R = NHiPr), and a monocyclic silylammonium triflate 232 (Figure 7).<sup>221</sup>

In the cases of the five-membered rings, structural information for 231 (R = Ph)<sup>213</sup> and 232<sup>221</sup> is available and for the six-membered rings information is available for 229 (R = *t*Bu)<sup>213</sup> and 229 (R = NMe<sub>2</sub>) (Figure 7).<sup>210</sup> A length of 2.33 Å for the H<sub>2</sub>Si–SiH<sub>2</sub> unit turned out to be a good reference value for the Si–Si bond length in ring systems where the Si atoms have no substituents other than hydrogen. The five-membered ring in 231 has a twisted conformation whereas in 232 it is planar. In the spirocyclic compound 234, two almost planar rings were found (Figure 7).<sup>221</sup>

The ammonium nature of the *i*PrNH<sub>2</sub>Si in 232 is clearly evident from the lengthening of the Si–N bond (1.83 Å). The six-membered ring in 229 (R = *t*Bu)<sup>213</sup> shows a rare example of a twist conformation and in 229 (R = NMe<sub>2</sub>)<sup>210</sup> a nearly planar conformation was found, with two ring nitrogen atoms only slightly above and below the plane of the silicon atoms, indicating at best a very flat chair. The two endocyclic nitrogen atoms have both the expected planar configuration in contrast to the exocyclic NMe<sub>2</sub> groups, which are pyramidal.

Different sulfur diimides (R<sup>1</sup>NSNR<sup>2</sup>, R<sup>1</sup>, R<sup>2</sup> = *t*Bu and/or SiMe<sub>3</sub>) were reacted with octachlorotrisilane (154) to give diaminosulfanes 235 (Figure 8).<sup>222</sup> Upon heating 235 in toluene, the five-membered heterocycles 236 (Figure 8) and SiCl<sub>4</sub> were formed.

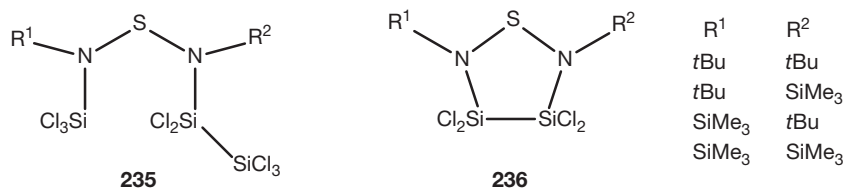


Figure 8 Sulfur diimides 235 and 236.

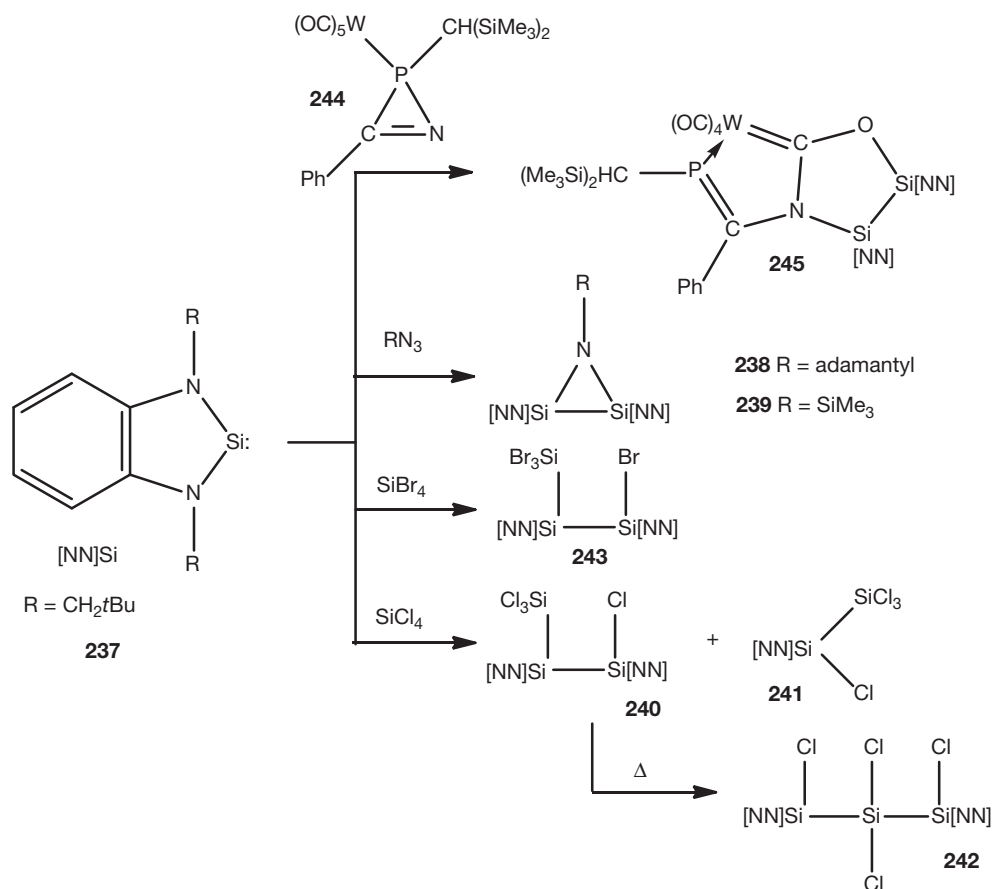
#### 1.02.6.4 *N*-Heterocyclic Silylenes as Starting Material for Acyclic and Cyclic Silanes

*N*-Heterocyclic silylenes (NHS), particularly five-membered ones, are the largest group of known silylenes and have been reviewed several times (Chapter 1.18 in this volume is also devoted to low oxidation states of silicon).<sup>223</sup> The first stable silylene was reported by Denk et al. in 1994<sup>224</sup> and since then, a number of isolable silylenes have been reported. Compounds derived from NHS with Si–Si bonds lacking carbon substituents were obtained starting from a benzo-fused silylene {[NN]Si 237} via nucleophilic addition of adamantyl azide (Scheme 17).<sup>225</sup> A reaction mechanism was postulated including the formation of an intermediate silimine, which reacts further with an additional silylene 237 to give the three-membered heterocycle 238. Using azidotrimethylsilane in the reaction with 237, the 1,3-disila-1-azacyclopropane derivative 239 was obtained which could be fully characterized, although thermal degradation was observed.<sup>226</sup> Insertion of 237 into Si–Cl or Si–Br bonds was examined by Gehrhus et al.<sup>227</sup> The reaction of silylene 237 with SiCl<sub>4</sub> proceeded under mild conditions to trisilane 240 as the main product and traces of [NN]Si(Cl)SiCl<sub>3</sub> (241), irrespective of the relative molar ratio of the reactants. Trisilane 240 was found to be thermally labile, being converted into 242 upon heating. The pathway to trisilane 242 was indicated to proceed via an  $\alpha$ -elimination and coincidental insertion of [NN]Si into the Si–Cl bond of the intermediate [NN]Si(Cl)–SiCl<sub>3</sub> (241). Evidence for this assumption could be found in the literature.<sup>228</sup> Contrary to the use of SiCl<sub>4</sub>, reaction with SiBr<sub>4</sub> was found to be very dependent on the molar ratio: using an excess afforded a product mixture of several tri-, di-, and monosilanes whereas using half an equivalent of SiBr<sub>4</sub> led cleanly to trisilane 243.

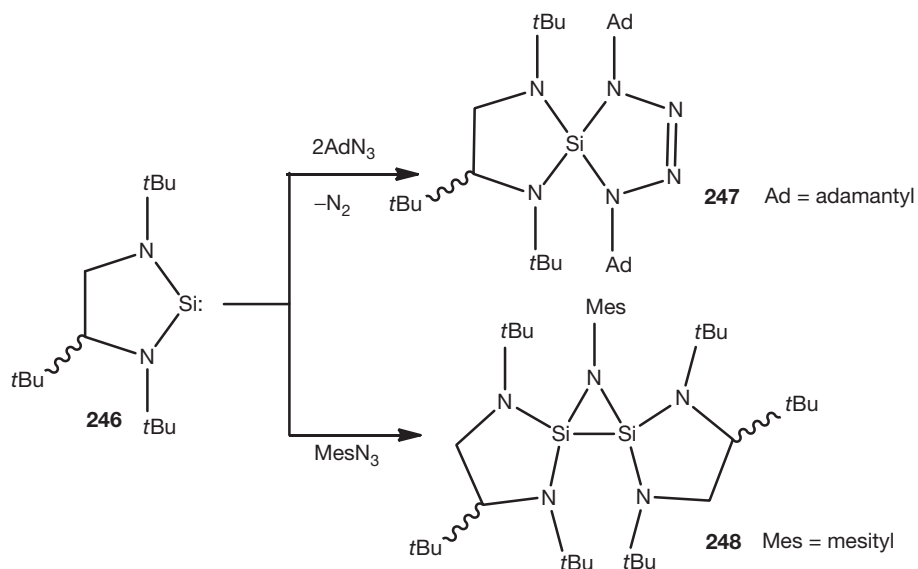
Complex 245, which has an interesting structural motif, was obtained in 62% yield by reaction of silylene 237 with the 2H-azaphosphirene complex, 244 (Scheme 17).<sup>229</sup> Its formation was independent of the stoichiometry of 237 and 244. No further insight into the reaction course was obtained, but a plausible explanation for the formation of 245 was given.

Nucleophilic addition of two equivalents of adamantyl azide to the racemic silylene 246 exhibited evolution of N<sub>2</sub> and yielded a white solid product 247 (Scheme 18).<sup>230</sup> The structure of 247 could be unambiguously verified by single-crystal x-ray diffraction, whereas no structural data are available for the adamantyl derivative, 238. Treatment of silylene 246 with just one equivalent of mesityl azide gave the azadisilacyclopropane, 248, which has great structural similarity to 238 and 239.<sup>230</sup>

The tris(silyl)chlorostannane 249 was obtained by reaction of tin(II)chloride with the respective silylene (250). Photolytic



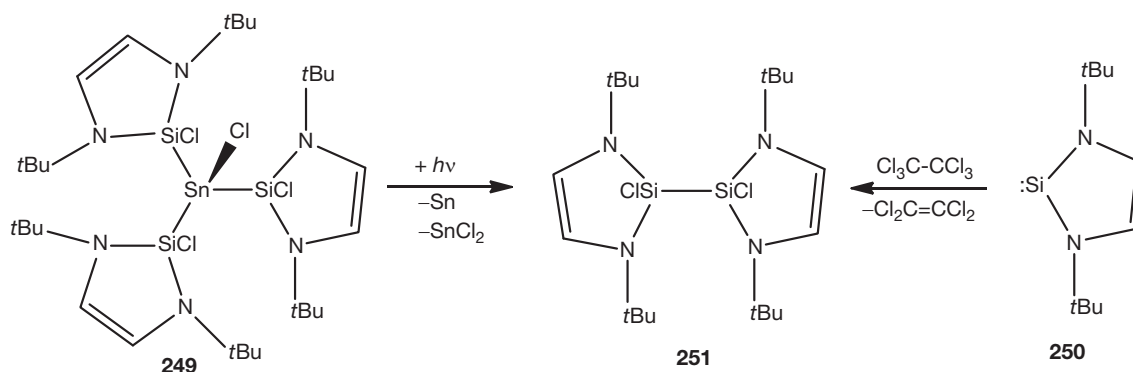
**Scheme 17** Reactivity of silylene **237**.



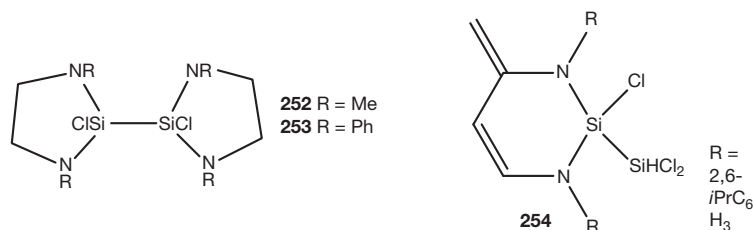
**Scheme 18** Possible reactions of silylene **246** with azides.

conditions led to a fragmentation of **249** and to the formation of disilane **251** together with elemental tin and tin(II)chloride (**Scheme 19**), whereas a thermolytic decomposition of **249** follows a different pathway yielding a complex mixture of

**251** together with silylene **250**, the dichlorinated precursor of **250**, and tin.<sup>231</sup> Recently, West et al. investigated the formation of disilane **251** by reaction of silylene **250** with hexachloroethane.<sup>232</sup> Their results are explicable in terms of a free-radical



**Scheme 19** Different routes to disilane 251.



**Figure 9** Disilane compounds 252–254.

chain mechanism where the radical  $\text{Cl}_3\text{C}-\text{CCl}_2$  loses a chlorine atom, with formation of a  $\text{C}=\text{C}$  double bond.

Two disilanes structurally comparable to 251 were published by Knopf et al.<sup>209</sup> Instead of a silylene, hexachlorodisilane (153) was used as starting material and reacted with *N,N'*-dimethyl- or *N,N'*-diphenylethylenediamine in the presence of triethylamine. The *N,N'*-dimethyl-substituted material 252 (Figure 9) could only be observed in a mixture with two other products and no yield for the disilane was reported. The respective *N,N'*-diphenyldisilane 253 (Figure 9) was also part of a mixture but could be isolated after a recrystallisation step in 21%.

A silylene with a modified  $\beta$ -diketiminate backbone (L) was the starting material for disilane 254 (Figure 9), which was obtained in excellent yield (80%) along with some 20% of the monomeric compound  $\text{LSiHCl}$ .<sup>233,234</sup> This  $\beta$ -diketiminate silylene is unique because of its ylide-like character and, in contrast to other silylenes, exhibits a different reactivity toward halosilanes and haloalkanes. The exclusive formation of 1,1-insertion products was observed to involve as the initial step a dipolar 1,4-addition and subsequent rearrangement of the latter kinetic product to the 1,1-adduct.<sup>233,234</sup>

An unusual route (Scheme 20) was reported to the trisilane 255: reaction of the stable silylene 250 with *tert*-butoxy radical (obtained from di-*tert*-butyl peroxide) resulted in formation of 255 and 256 (15%) and separation could be accomplished by vacuum distillation.<sup>235</sup>

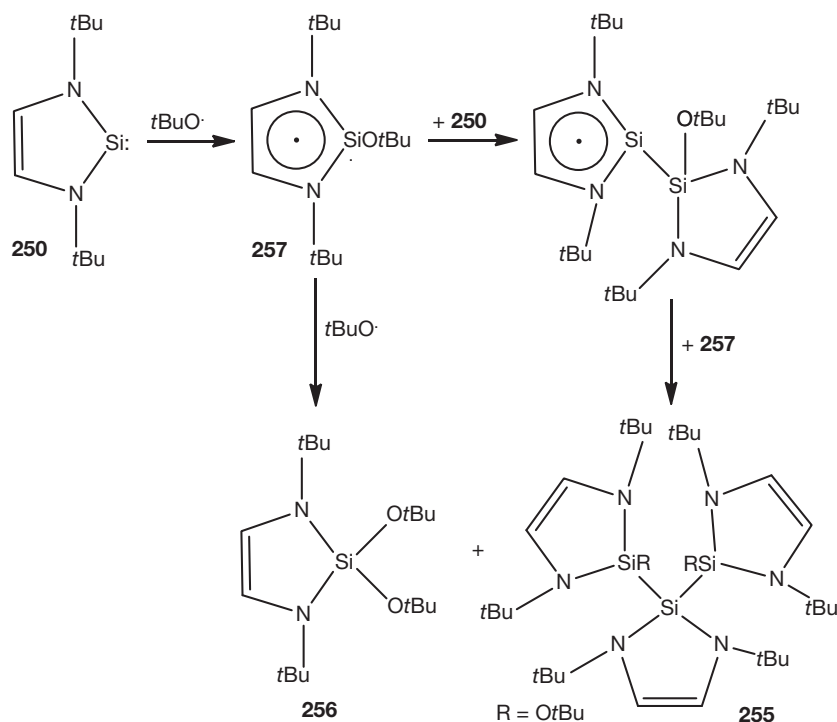
Single-crystal x-ray structure determination could be accomplished only for 240,<sup>227</sup> 248,<sup>230</sup> 255,<sup>235</sup> and 256.<sup>235</sup> The Si–N bond length for all three structures is within the normal range. For the azadisilacyclopropane 248<sup>230</sup> the Si–Si bond length was assigned to be with 2.23 Å conspicuously shortened. In 240<sup>227</sup> the [NN]Si–Si[NN] bond is with 2.40 Å

slightly longer than the  $\text{Cl}_3\text{Si}-\text{Si}$  (2.38 Å) bond, whereas in 255<sup>235</sup> Si–Si bonds are extremely elongated to 2.51 Å.

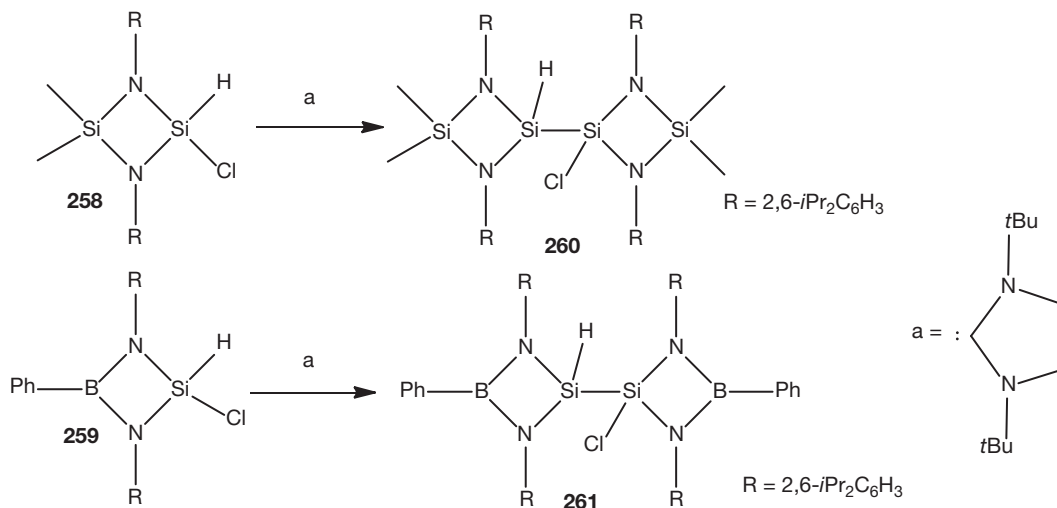
All common synthetic routes toward stable silylenes require either harsh conditions or highly reactive metallic reagents. In the quest to alternative methods utilizing milder conditions, the *N*-heterocyclic carbene 1,3-bis(*t*butyl)imidazol-2-ylidene was introduced to form cyclic silylenes via dehydrochlorination of cyclic diaminohydrochlorosilanes (258, 259) in the absence of any metallic reagents (Scheme 21).<sup>236</sup> Using this approach, disilanes 260 and 261 could be prepared in satisfying yields of 62 and 78%, respectively (Scheme 21). Their formation was explained by an initial generation of transient four-membered heterocyclic silylenes, which reduce the hydrochlorosilanes 258 and 259. The reaction was found to be too fast to allow monitoring of possible intermediates by means of NMR spectroscopy.

### 1.02.6.5 *N*-Substituted Pentacoordinated Si Compounds

In 2008<sup>237</sup> and 2009,<sup>238</sup> the first compounds containing a Si–Si single bond and one-electron lone pair on each silicon atom were reported. In 198 (Scheme 22), the Si–Si single bond is stabilized by a  $\sigma$ -donor ligand, an amidinate ligand with *t*Bu substituents on the nitrogen atoms, thus preventing the lone pair of electrons from taking part in any bonding. The air-sensitive, orange–red crystalline 198 with the formal oxidation state of the silicon atoms being +1, could be fully characterized by elemental analysis, spectroscopic methods, and x-ray structural analysis. Theoretical studies (NAO and NBO) were involved to understand the unprecedented electronic structure of 198.<sup>239</sup> These analyses showed a Wiberg bond order of 0.9768 with high *p*-character for the Si–Si bond.



Scheme 20 Synthesis of trisilane 255.



Scheme 21 Alternative method to silylenes under mild conditions in the absence of any metallic reagents.

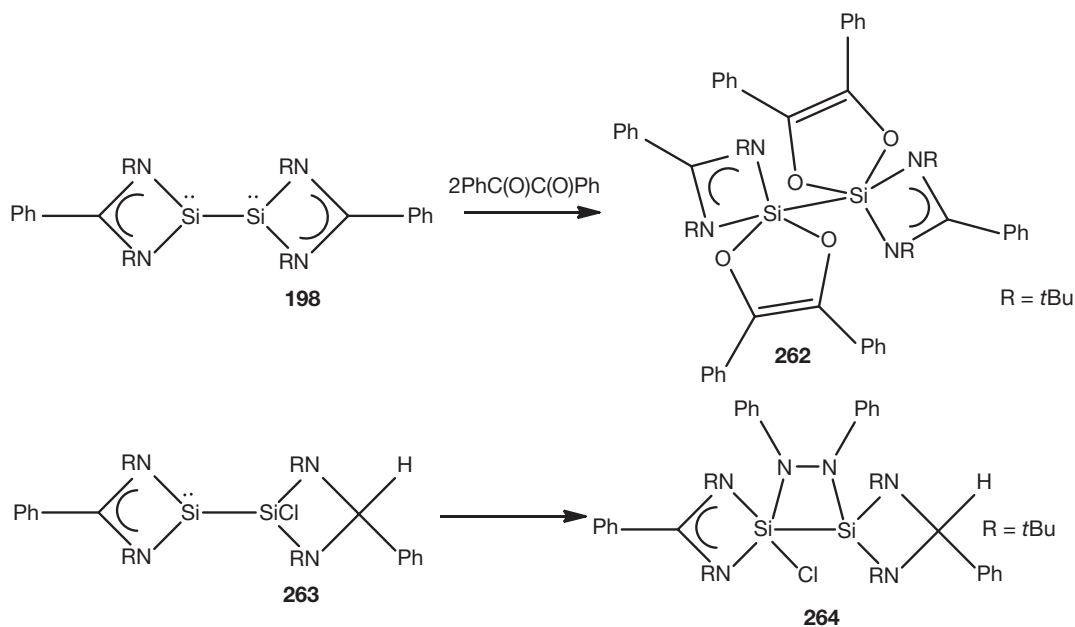
Reaction of 198 with two equivalents of benzyl yielded colorless crystalline 262<sup>240</sup> by two [1+4]-cycloaddition reactions, a compound where the Si–Si bond remains intact involving dioxolane rings on each silicon atom (Scheme 22). The formal oxidation state of silicon in 262 is +3 and the siladioxolanes are electronically stabilized by the  $\sigma$ -donor ligands. The surprising feature in this reaction was the preservation of the Si–Si bond, because it was known that treatment of 198 with Br<sub>2</sub><sup>239</sup> or N<sub>2</sub>O<sup>241</sup> led to cleavage of the Si–Si bond.

Silylsilylene 263 (Scheme 22) was formed by treatment of [PhC(NtBu)<sub>2</sub>SiHCl<sub>2</sub>] with two equivalents of potassium

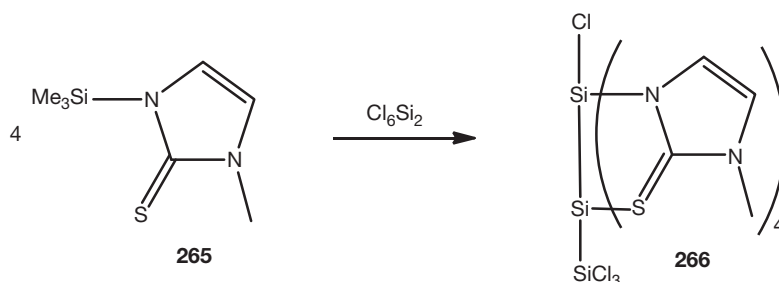
graphite and does not dimerize further to form the corresponding disilene.<sup>197</sup> Here again calculations showed a Wiberg bond index of 0.87, which indicates clearly a Si–Si single bond. Reaction of 263 with azobenzene afforded 264, which is the first example of a 1,2-diaza-3,4-disilacyclobutane containing a pentacoordinated silicon center (Scheme 22).<sup>196</sup> Compound 264 was described as a highly air- and moisture-sensitive colorless crystalline solid stable both in solution and in the solid state at room temperature under an inert atmosphere.

The structure of 262<sup>240</sup> shows a shortening of the Si–Si bond length from 2.41 Å in the starting material 198<sup>238</sup> to





**Scheme 22** Synthesis of hypercoordinated silanes starting from silylenes.



**Scheme 23** Possible route to hypercoordinated oligosilanes used by Wagler et al.

2.36 Å, a fact, which was explained by the authors by the nonexistence of a lone pair–lone pair repulsion in **262**. Remarkable are the differences within the Si–N bond length in **262**, which are between 2.01 and 1.82 Å in comparison again to the starting material **198**, where the Si–N bond length was determined to be 1.87 Å.

A completely different route to hypercoordinated oligosilanes was pursued by Wagler et al.<sup>242</sup> using a methimazolyl-substituted silane (**265**) and hexachlorodisilane (**153**), leading to stabilized bis(silyl)silylene **266** (Scheme 23). This compound is, on the one hand, the first example of a structurally characterized oligosilane bearing two neighboring hexacoordinated Si atoms and, on the other hand, the first compound comprising more than two chalcogen atoms heavier than oxygen in the Si coordination sphere.

### 1.02.6.6 Si–P Compounds

The interest in the preparation of silylphosphanes ( $\text{Si}_n\text{-P}$ ) bearing no organic substituents on silicon was never high and faded completely in the last 10 years; thus, only a handful of such compounds are known in the literature.

Silylphosphanes bearing only hydrogen as substituent are however popular compounds in theoretical studies.<sup>243–246</sup>

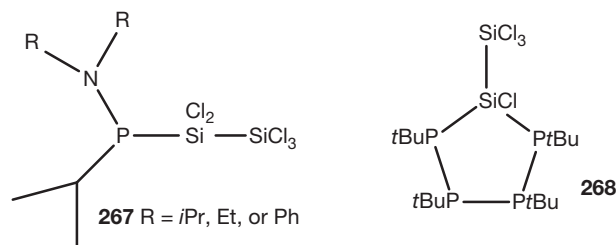
Salt elimination between polar Si- and P-compounds turned out to be useful for the formation of silylphosphanes even with some functional groups. Fritz and Scheer described in their review the importance of silylphosphanes for the preparation of new metal complexes, metal cluster compounds, nanostructures, and semiconductors.<sup>247</sup> Contrary to trisilylamines which have planar three-coordinated nitrogen atoms in their ground state, trisilylphosphanes display pyramidal configurations. However, upon increasing the steric demand of silyl groups in trisilylphosphanes, an almost planar configuration can be achieved.<sup>248</sup>

Disilanylphosphane ( $\text{H}_3\text{Si-SiH}_2\text{PH}_2$ ), which was the first synthesized disilanylphosphane, formed when a mixture of silane and phosphane was passed through an ozonizer-type silent discharge tube.<sup>249,250</sup> In a more general way, the compound was also obtained by phosphination of halosilanes using lithium tetrakis(dihydrogenphosphido)aluminate  $\text{LiAl}(\text{PH}_2)_4$  and  $\text{H}_3\text{Si-SiH}_2\text{Br}$  (**62**).<sup>251</sup> The disilanyltriphosphane [ $\text{H}_3\text{Si-Si}(\text{PET}_2)_3$ ] was formed in the reaction of  $\text{LiSi}(\text{PET}_2)_3$  with bromosilane.<sup>252</sup> The use of aluminates has the advantage

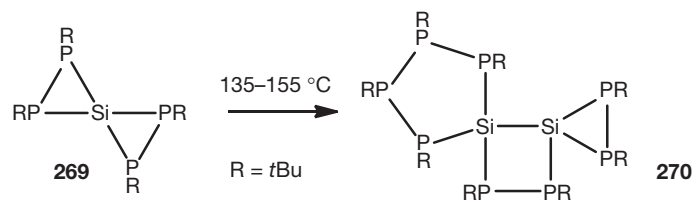
of avoiding transmetalation reactions.<sup>253</sup> 1,2-Di[bis(trimethylsilyl)]phosphinodisilane  $\{[(\text{Me}_3\text{Si})_2\text{P}]\text{H}_2\text{Si}-\text{SiH}_2[\text{P}(\text{SiMe}_3)_2]\}$  could be isolated by reacting  $\text{LiP}(\text{SiMe}_3)_2$  with  $\text{H}_2\text{ISI}-\text{SiH}_2$  (**94**). Crucial for this synthesis was the use of strictly ether-free  $\text{LiP}(\text{SiMe}_3)_2$  because otherwise the only observed reaction is cleavage of the Si-Si bond leading to the exclusive formation of  $\text{H}_3\text{SiP}(\text{SiMe}_3)_2$ .<sup>254</sup>

The synthesis of trichlorosilylphosphanes **267** (**Figure 10**) was achieved starting with chlorodialkyl- or chlorodiarylaminoisopropylphosphane and hexachlorodisilane (**153**), yielding inseparable mixtures containing some **267**.<sup>255,256</sup> The reaction of a diphosphide  $\text{K}_2(\text{tBuP})_4$  with **153** led via a [4+1]-cyclocondensation reaction to silatetraphospholane **268** (**Figure 10**).<sup>257</sup>

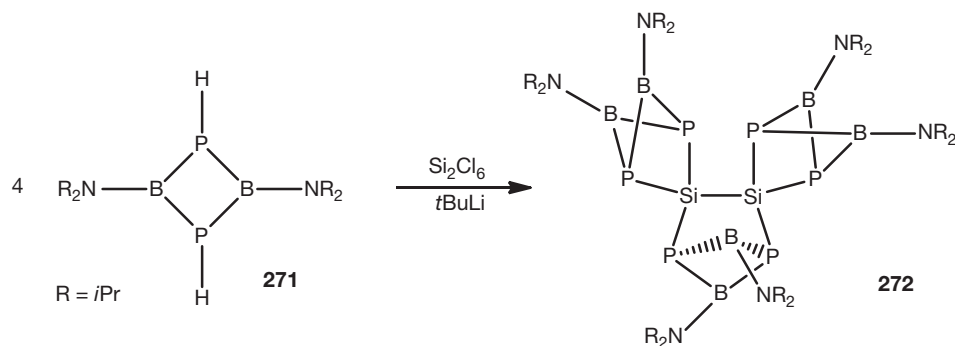
Another cyclic compound is the comparatively complex spiro-cyclic compound **270**, which consists of a four-membered ring which is linked via the two silicon atoms spiro-cyclic with a  $\text{P}_2\text{Si}$ -three and a  $\text{P}_4\text{Si}$ -five-membered ring (**Scheme 24**).<sup>258</sup> The structure of **270** could be undoubtedly proved by x-ray structure analysis,<sup>259</sup> but any mechanistic details for this interesting thermal rearrangement or even explanations are missing. Cyclocondensation of diphosphide  $\text{K}_2(\text{tBuP})_4$  with  $\text{SiCl}_4$  led to the starting material **269**.<sup>258</sup>



**Figure 10** Compounds bearing a silicon-phosphorus bond.



**Scheme 24** Synthesis of the complex spiro-cyclic compound **270**.



**Scheme 25** Interesting ring systems containing silicon, boron, and phosphorus atoms.

The last examples in this section are from Nöth and co-workers investigating ring systems containing boron and phosphorus atoms (**Scheme 25**).<sup>260</sup> The complex cage structure **272** was obtained by reacting the cyclic phosphaborane **271** with  $\text{Si}_2\text{Cl}_6$  (**153**) and  $\text{tBuLi}$ . The reaction pathway was explained and the molecular structure of triple cage molecule **272** was elucidated by single-crystal x-ray-diffraction analysis. The compound is stable in dry air and is slowly hydrolyzed by water or wet solvents.

### 1.02.6.7 Si-As, Si-Sb, and Si-Bi Compounds

The number of silylarsines as well as silylstibines listed in Chemical Abstracts is small: a search for Si-Si-As and Si-Si-Sb led to a total number of 29 structures each and for Si-Si-Bi only to 11. None of the disilanes bearing antimony or bismuth fit into the context of this review and for arsenic, the only fitting compound is  $\text{H}_3\text{Si}-\text{SiH}_2\text{AsH}_2$ . Its synthesis was accomplished analogous to  $\text{H}_3\text{Si}-\text{SiH}_2\text{PH}_2$ .<sup>261,262</sup>

### 1.02.7 Silanes with Other Group-14 Substituents Except Organic Groups

In Volume I of this series, Rochow described the chemistry of silicon and group-IV elements in exactly three lines. At that time, lead-silicon compounds were not known at all. Meanwhile, some silicon-lead compounds were synthesized but none fitting into this context. Just one matching silicon-tin compound:  $(\text{Me}_3\text{Sn})_2\text{Si}(\text{SiCl}_3)_2$  (**273**) was described.

First attempts to produce germanium-silicon fluoride compounds from silicon difluoride and germanium tetrafluoride led to the explosive formation of polymers rather than to the desired fluorinated products.<sup>263</sup> Synthetic access to pure compounds even to the simple disilylgermanium hydride

$\text{H}_3\text{SiSiH}_2\text{-GeH}_3$  was never established; they were only observed in mixtures.<sup>264</sup> Recently, halosilylgermanes<sup>265,266</sup> and silylgermanium hydrides<sup>175,267</sup> found increasing interest exclusively in patent literature due to their applications in optoelectronics, silicon-germanium alloys,<sup>268</sup> and semiconductor structures and devices.<sup>269</sup> Their controlled deposition to produce stoichiometric films ( $\text{Si}_x\text{Ge}_{1-x}$ ) with a perfect crystalline microstructure is an ideal property for semiconductor application.<sup>265</sup> Because of these applications, silylgermanium compounds were the subject of theoretical investigations.<sup>269</sup> Synthesis of  $\text{H}_3\text{Ge-SiH}_2\text{SiH}_2\text{-GeH}_3$  (274), a colorless pyrophoric liquid, was accomplished via reaction of  $\text{H}_3\text{GeK}$  with 1,2-bis(trifluoromethylsulfonyloxy)disilane (196) in 26% yield.<sup>267</sup> Depending on the reaction conditions,  $(\text{H}_3\text{Ge})_2\text{SiHSiH}_3$  (275) and  $\text{H}_3\text{GeSiH}_2\text{GeH}_2\text{GeH}_3$  are the main byproducts, which were also fully characterized.<sup>270</sup> Halosilylgermanes are prepared by treatment of the corresponding silylgermanium hydrides with  $\text{BCl}_3$  and the degree of halogenation can be controlled by the amount of used  $\text{BCl}_3$ .<sup>265,271</sup> When 274 reacts with  $\text{BCl}_3$  in a 1:1 ratio halogenation occurs only at the silicon atoms, but the reaction ends up with a mixture of  $\text{H}_3\text{Ge-SiHClSiHCl-GeH}_3$  and  $\text{H}_3\text{Ge-SiCl}_2\text{-SiH}_2\text{-GeH}_3$ .<sup>265</sup>

The synthesis of the moisture-sensitive but thermally quite stable  $(\text{Me}_3\text{Ge})_2\text{Si}(\text{SiCl}_3)_2$  (276) was reported by reacting chlorotrimethylgermane with trichlorosilane/triethylamine over several days in about 40% yield.<sup>272</sup>  $(\text{Me}_3\text{Sn})_2\text{Si}(\text{SiCl}_3)_2$  (273) can be obtained via the same route using chlorotrimethylstannane but the reaction time requires 14 days.<sup>272</sup> Structural proof for 276 and 273 was provided by x-ray structure determination.<sup>272</sup>

### 1.02.8 Silanes with Other Group-13 Substituents

Silicon-boron fluorides with the formula  $\text{F}_{2n+2}\text{Si}_n\text{B}$  with  $n$  ranging from 2 to 13 were prepared by a low-temperature acid-base reaction between  $\text{SiF}_2$  and  $\text{BF}_3$ .<sup>273</sup> They are thermally stable up to at least 200 °C as vapors and ignite spontaneously in air.<sup>273</sup> These compounds could be identified as a homologous series of  $\text{F}_3\text{Si}-(\text{SiF}_2)_n\text{-BF}_2$ , and the molecular structure of the simplest one,  $\text{F}_3\text{Si-SiF}_2\text{-BF}_2$ , was determined by electron diffraction.<sup>274</sup>

These are the only existing examples of compounds fitting to the used pattern for the whole group-13 elements. Theoretical investigations were done for all elements (Al,<sup>275-280</sup> Ga,<sup>275,276</sup> In,<sup>275,276,281</sup> and Tl<sup>275</sup>), but extensively for boron<sup>275,282,283</sup> and to be more precise for nido-boranes.<sup>284-286</sup>

### 1.02.9 Silanes and Group-1 and -2 Metals

The best-studied class of silyl anions is the one of alkali metals because of their interesting molecular structures and due to their synthetic abilities. Applications of alkali silanides can be found in several areas such as optoelectronics<sup>287</sup> or semiconductors.<sup>288</sup> Silanides of group-1 and -2 metals were reviewed by Lickiss and Smith<sup>289</sup> and Tamao and Kawachi<sup>290</sup> both in 1995, Belzner and Dehnert<sup>291</sup> in 1998, and more recently by Lerner in 2005.<sup>292</sup> Four main reaction pathways for alkali-

silanide preparations are available: (i) cleavage of Si-Si bonds (using lithium alkyls, alkali metals, potassium, sodium, or cesium alkoxides, or alkali-metal hydrides), (ii) cleavage of a Si-H bond (using alkali metals or alkali-metal hydrides), (iii) metathesis reactions, or (iv) transmetallation reactions. Routes to alkaline-earth metal silanides are similar to the synthesis of alkali-metal silanides but here the most preferable method is the transmetallation reaction of alkali-metal silanides with  $\text{MX}_2$  ( $\text{M} = \text{Be, Mg, Ba}$ ;  $\text{X} = \text{halogen}$ ).

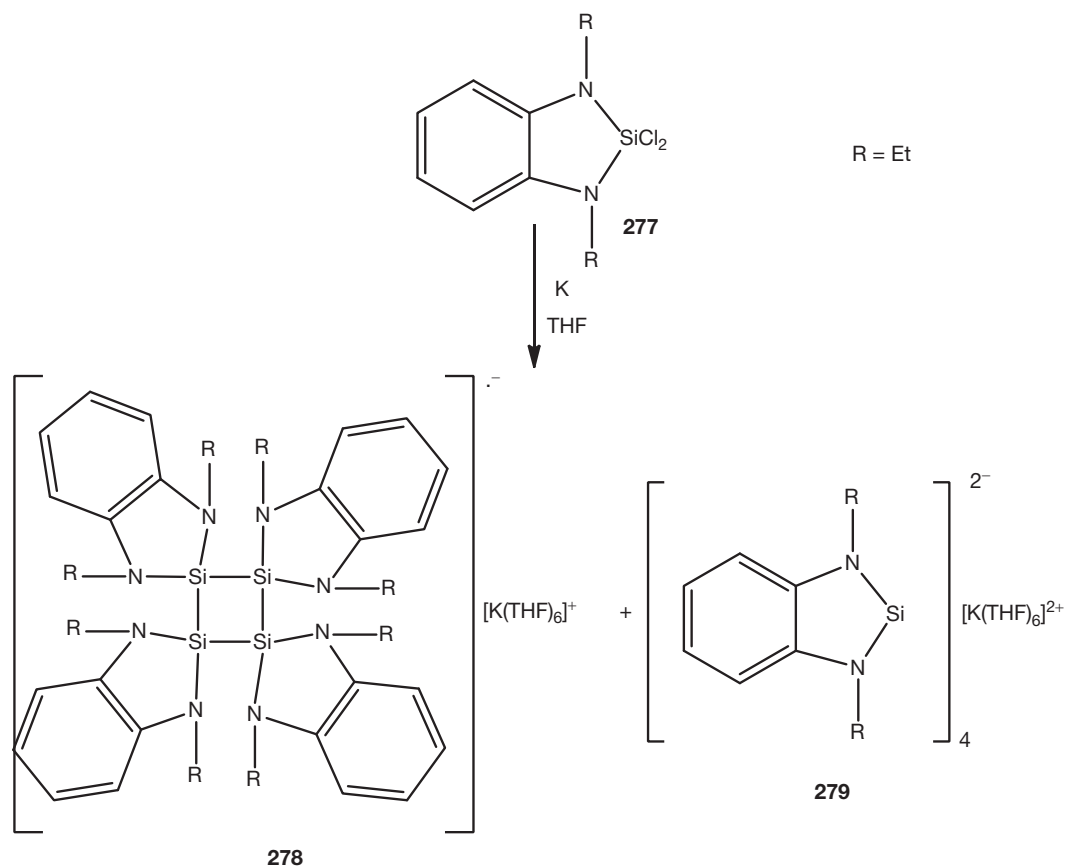
The compounds  $\text{LiSiH}_2\text{SiH}_3$ ,<sup>292</sup>  $\text{LiSiH}(\text{SiH}_3)_2$ ,<sup>292</sup>  $\text{NaSi}(\text{SiH}_3)_3$ ,<sup>291-293</sup>  $\text{NaSiH}(\text{SiH}_3)_2$ ,<sup>292</sup>  $\text{NaSiH}_2\text{SiH}_3$ ,<sup>292</sup>  $\text{KSi}_2\text{H}_5$ ,<sup>290,291</sup>  $\text{KSiH}(\text{SiH}_3)_2$ ,<sup>290,291</sup> and  $\text{KSi}(\text{SiH}_3)_3$ <sup>290,291,294</sup> are discussed in detail in the above-mentioned reviews. Unfortunately, no alkaline-earth silyl compounds fitting into the context of this review are known so far.

Alkali metals have been used over the last decades for the synthesis and further reactions of silylenes, disilyenes, and other compounds with low-coordinated Si atoms. Gehrhus et al.<sup>295</sup> were able to prepare the first thermally robust and crystalline radical anion (278, Scheme 26). The dichloride 277 was treated with potassium in a 1:2 ratio and afforded a mixture of two cyclo-tetrasilanes – anion radical 278 and dianion 279 – which could be crystallized by treatment with DME (1,2-dimethoxyethane). The crystal structure of 278 shows the potassium ion to be solvent separated from the radical anion, whereas in 279 the solvated potassium ions display an  $\eta^2$ -coordination to carbon atoms of the phenylene ring. In both compounds, the four-membered silicon rings are square planar with a Si-Si bond length of 2.34 Å for 278 and 2.28 Å for 279, a value which is in close range to Si-Si double bonds. The use of more potassium or  $\text{C}_8\text{K}$  shifts the outcome of the reaction to the dianion 279.<sup>296</sup>

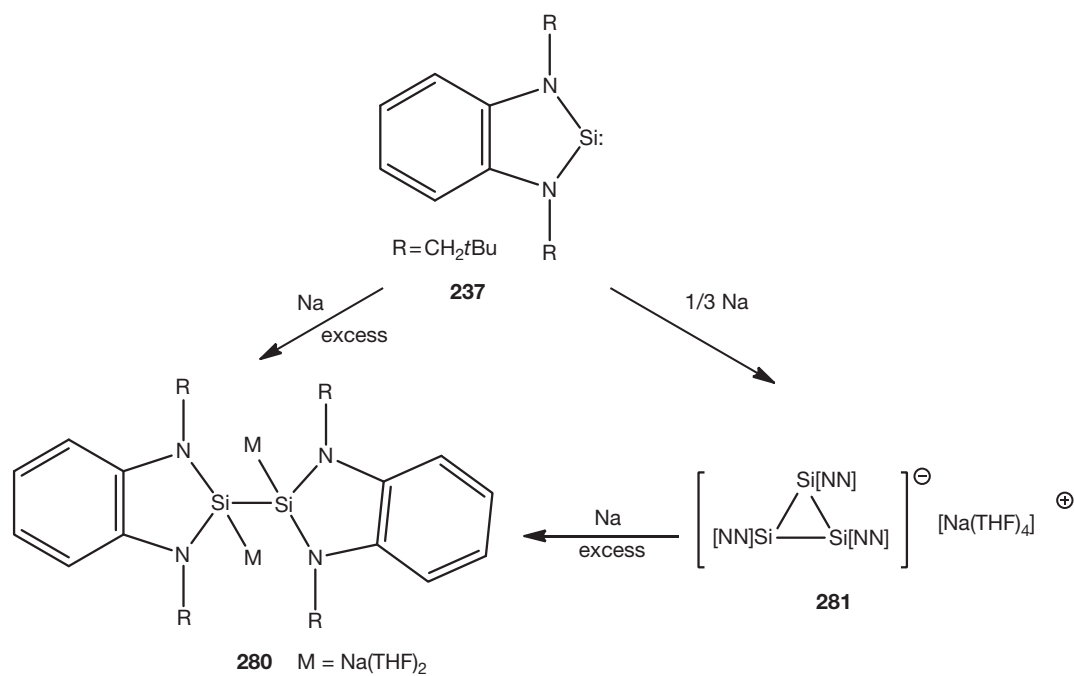
Treatment of the benzo-fused silylene ( $[\text{NN}]\text{Si}$  237) with an excess of sodium led to the crystalline disodium disilyl compound 280 (Scheme 27).<sup>297</sup> The crystalline radical cyclotrisilyl anion 281 was prepared from three equivalents of ( $[\text{NN}]\text{Si}$  237) reacting with one equivalent of sodium. Further reaction of 281 with sodium yielded compound 280. The length of the Si-Si bond is, in 280, 2.48 Å and, in 281, 2.34 Å.<sup>296</sup> Running the reaction with potassium instead of sodium led to the dipotassium disilyl compound analogous to 280 but no cyclotrisilyl anion could be detected.<sup>296</sup>

### 1.02.10 Silanes and Transition Metals

Silylmetal complexes are known for all transition metals, and a variety of ligands on both the metal center and the silicon have been utilized. A number of reviews are available on this subject<sup>298</sup> and those by Corey in 2011<sup>299</sup>, and Corey and Braddock-Wilking in 1999<sup>300</sup> are especially recommended. A variety of synthetic methods for the formation of a metal-silicon bond are available, whereupon the most common and versatile one involves the oxidative addition of a Si-H bond of a hydrosilane to a transition-metal center. Complexes containing  $\text{SiH}_3$  substituents are scarce and the reasons therefore might be associated with difficulties arising from the handling of  $\text{SiH}_4$ , but also with consecutive reactions that can occur at Si-H bonds of the initially formed TM-SiH<sub>3</sub> complex in the coordination sphere of the metal. As a consequence, complexes bearing higher hydrosilanyls are certainly even scarcer.



**Scheme 26** Synthesis of the first thermally robust and crystalline radical anion **278**.

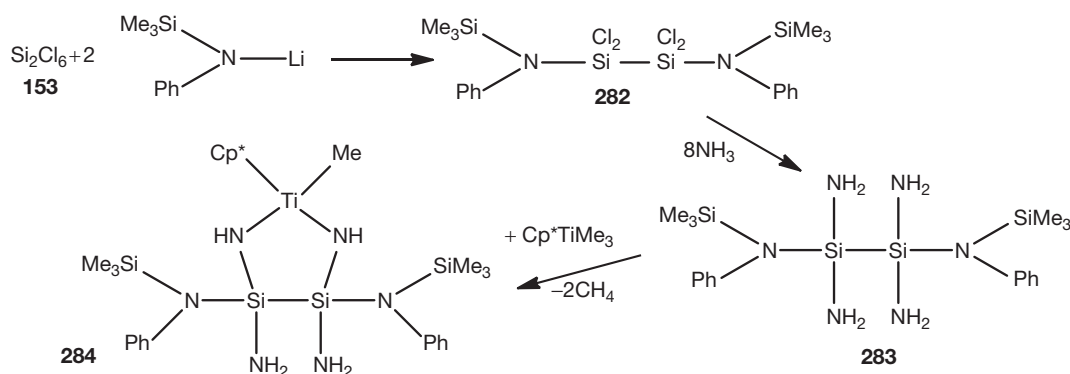


**Scheme 27** Treatment of benzo-fused silylene **237** with different amounts of sodium.

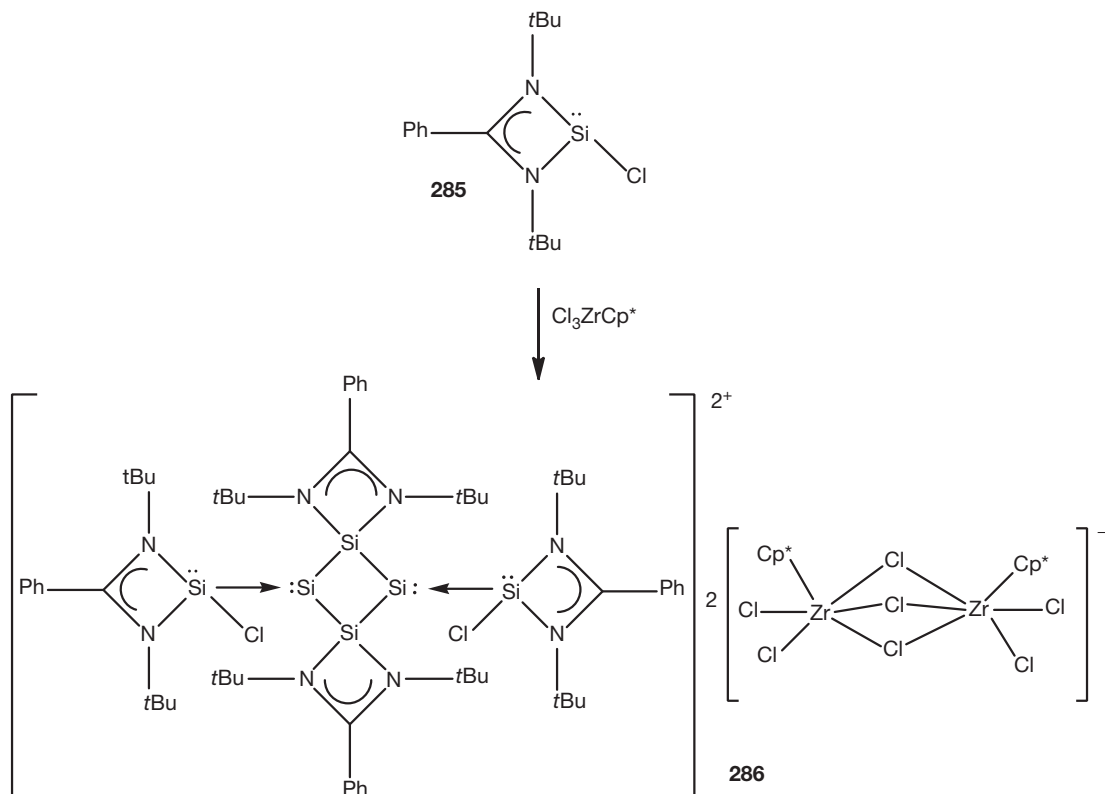
Silylscandocenes such as  $\text{Cp}_2\text{ScSi}(\text{SiMe}_3)_3\cdot\text{THF}$  or  $\text{Cp}_2\text{ScSi}(\text{SiMe}_3)_2\text{Ph}$  are extremely reactive toward small molecules ( $\text{CO}$  and  $\text{CO}_2$ ) and are active as ethylene polymerization catalysts, but no compounds containing Si–Si–H or Si–Si–halogen units are yet known.<sup>301</sup> Unlike scandium, yttrium, and hafnium, the more common titanium and zirconium attracted some attention in Si–N chemistry. In the given examples, no transition-metal–silicon bond was formed but nevertheless they might be of some interest. Aminosilanes can be used for the preparation of titanium-containing heterocycles, which were expected to gain relevance in the development of homogeneous and heterogeneous catalysis or ceramic materials.<sup>302</sup> *N,N*-Tetrachlorodisilane **282** afforded under the treatment with liquid ammonia the *N,N*-tetraaminodisilane **283** (Scheme 28)

and further reaction with an excess of  $\text{Cp}^*\text{TiMe}_3$  led to titanadisilazane **284**.<sup>303,304</sup> The latter is stable at room temperature under an inert atmosphere and soluble in common organic solvents. Its molecular structure was fully elucidated by an x-ray crystal structure analysis.<sup>304</sup> The five-membered TiNSiN ring shows an envelope conformation with one nitrogen on the flap and the Si–Si bond length was found to be 2.36 Å.

Recently, a Lewis acid-assisted reaction of the *N*-heterocyclic chlorosilylene **285** (Scheme 29) with  $\text{Cp}^*\text{ZrCl}_3$  in a molar ratio of 3:2 led to **286**, a four-membered donor-stabilized silyl dication species comparable to a tetrasilacyclobutadiene, which could be isolated as yellow crystals in 29% yield.<sup>305</sup> The four-membered ring in **286** consists of two silylene moieties and two *N*-donor-stabilized silylium subunits. X-ray



**Scheme 28** Use of an aminosilane for the preparation of a titanium-containing heterocycle.



**Scheme 29** Reaction of the *N*-heterocyclic chlorosilylene **285** with  $\text{Cp}^*\text{ZrCl}_3$ .

diffraction analysis shows interesting Si–Si bond lengths: the distances in the four-membered ring are with 2.30 and 2.32 Å comparable to the central aromatic four-membered ring subunit of hexasilabenzene.<sup>305</sup> The exocyclic Si–Si distance is with 2.33 Å a typical Si–Si single bond, which suggests a strong donor–acceptor interaction between Si lone pair of the ligand and the silylene-like Si ring atom.

In addition to these two examples, there were some calculations done toward reaction of titanyporphyrin with silyl radicals,<sup>306</sup> silylidene complexes of transition metals of group 4, 5, and 6,<sup>307,308</sup> and silane derivatives of a chromium aminoborylene complex.<sup>309</sup>

For group 5, the situation is similar to group 3. No compounds fitting into the scope of this review containing vanadium, niobium, or tantalum are known. For group 6, the same is true for chromium but some examples with molybdenum and tungsten are known. Here for the first time in this chapter, silicon–transition metal bond formation was observed. The salt-elimination reaction of lithium metallates of tungsten and molybdenum (287–290) with Si<sub>2</sub>Cl<sub>6</sub> (153) under exclusion of light led to the formation of pentachloro(metallo)disilanes (291–294), which upon treatment with LiAlH<sub>4</sub> were transformed into the metallodisilanes (295–298) (Scheme 30).<sup>310</sup> The use of either Cp or Cp\* had no influence on the reaction time. The pentachloro(metallo)disilanes (291–294) are storable at –20 °C for an indefinite period and differ with this behavior from tricarbonyl complexes Cp(OC)<sub>3</sub>M–SiCl<sub>2</sub>–SiCl<sub>3</sub> (M=Mo, W), which expel even at this temperature ‘SiCl<sub>2</sub>’ to give Cp(OC)<sub>3</sub>M–SiCl<sub>3</sub>.<sup>310</sup> The enhanced stability was explained with the increased nucleophilicity of the metal center accomplished by the replacement of one carbonyl ligand by phosphane. The metallodisilanes (295–298) were obtained in good yields (68–83%) and are all stable in air for short times. The structure of 294 was confirmed by x-ray analysis with a Si–Si bond length of 2.35 Å.<sup>310</sup>

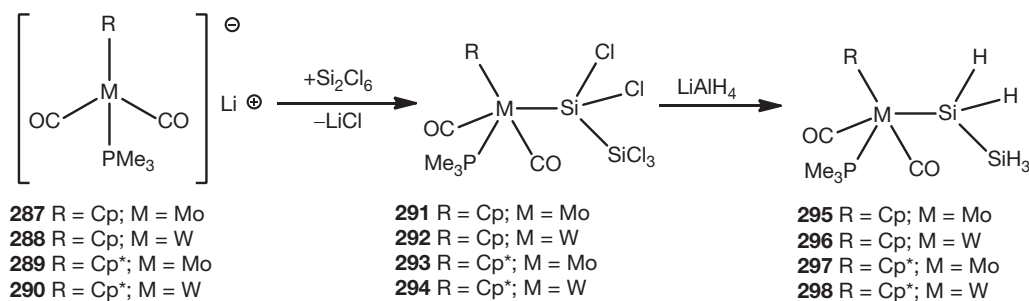
The mentioned instability of Mo tricarbonyl complexes was also observed by Hengge et al. (Scheme 31).<sup>311</sup> They were able

to synthesize and characterize the dimolybdenum disilanyl compound 299, which decomposes even at –30 °C within a few hours. The reaction carried out in DME and NMR data provided evidence that in compound 299, DME serves as an additional stabilizing ligand for the Mo–Si bond.<sup>311</sup>

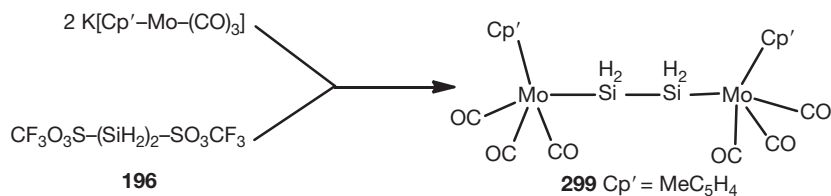
Zechmann and Hengge explored tungsten tricarbonyl complexes (300, 301; Scheme 32) and observed an enhanced stability compared to the molybdenum complex 299 but also, maybe more surprising, to analogous methylated complexes [(OC)<sub>3</sub>W–(SiMe<sub>2</sub>)<sub>n</sub>–W(CO)<sub>3</sub>, n = 3, 4].<sup>312</sup>

For the next two groups, a retaining pattern can be seen: no manganese, technetium, or rhenium compounds with inorganic oligosilyl groups are known. For group 8 also, none of these compounds are known for osmium but some examples of iron and ruthenium were synthesized. Again analogous to the Mo complex 300 (Scheme 32), the salt-elimination reaction of NaFe(CO)<sub>2</sub>Cp and Si<sub>2</sub>Cl<sub>6</sub> (153) in THF and subsequent reduction with LiAlH<sub>4</sub> led to the main product 303 and the byproduct 302 (Figure 11).<sup>311</sup> The reduction step was done at –70 °C as at higher temperature Si–Si bond cleavage was observed. Compounds 304 and 305 were obtained starting from the 1,4-dibromotetrasilane (86) and 1,3-dibromotrisilane (79), respectively (Figure 11).<sup>311</sup> An example for the stability of the Si–N bond toward nucleophilic attack is the clean reaction of Cl<sub>3</sub>Si–SiCl<sub>2</sub>–N(SiMe<sub>3</sub>)<sub>2</sub> with the transition metal anion NaFe(CO)<sub>2</sub>Cp to 306 (Figure 11).<sup>91,219</sup> Here, the hydrogenation of the Si–Cl bonds (307, Figure 11) with LiAlH<sub>4</sub> could be carried out at 0 °C in excellent yields without any observed Si–Si bond cleavage.<sup>91,219</sup>

Salt elimination of NaM(CO)<sub>2</sub>R (M=Fe or Ru; R=Cp or Cp\*) and Si<sub>2</sub>Cl<sub>6</sub> (153) in a molar ratio of 1:1 in cyclohexane and under exclusion of light gave R(CO)<sub>2</sub>M–SiCl<sub>2</sub>SiCl<sub>3</sub> (R=Cp or Cp\*, M=Fe or Ru 308–311) as the main products (Scheme 33).<sup>313</sup> All four compounds are stable and can be stored under nitrogen as solids for months. Again, full hydrogenation was achieved by using LiAlH<sub>4</sub> (302, 312, and 313).<sup>313</sup> X-ray crystallographic studies of 308 and 312 verified the

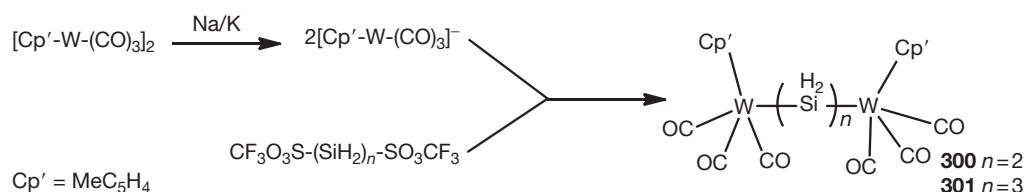
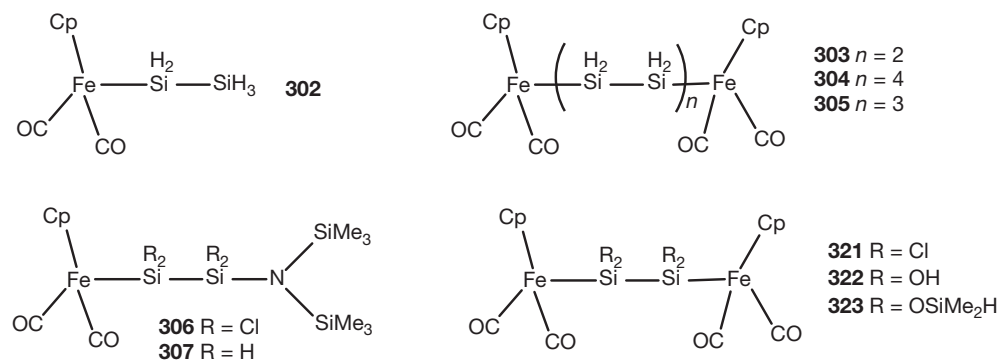
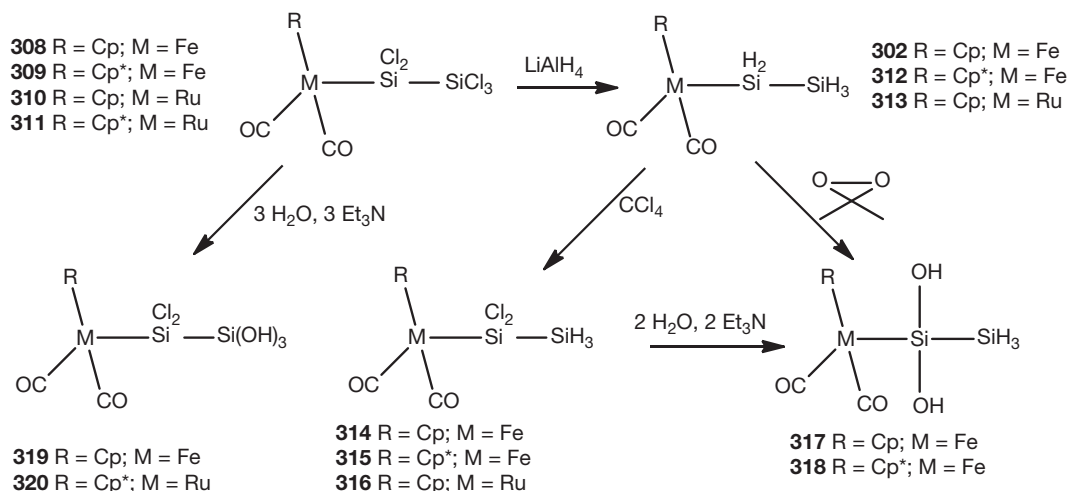


**Scheme 30** Metallodisilanes (295–298) were obtained by salt-elimination reaction followed by a hydrogenation step.



**Scheme 31** Synthetic access to dimolybdenum disilanyl compound 299.



**Scheme 32** Synthesis of tungsten tricarbonyl complexes **300** and **301**.**Figure 11** Iron and diiron silicon complexes.**Scheme 33** Reactivity of **302** and **308–312** with  $\text{CCl}_4$ ,  $\text{H}_2\text{O}/\text{Et}_3\text{N}$ , and dimethyldioxirane.

proposed structures. The bond lengths of the Si–Si bonds with 2.33 Å (**308**) and 2.34 Å (**312**) are close to those of other disilanes.<sup>313</sup> The higher hydridic character of the hydrogens at the  $\alpha$ -silicon compared to the ones at the  $\beta$ -silicon was proved by treatment with  $\text{CCl}_4$  or under harsher conditions with chloroform. The hydrogens next to the metal center could be selectively substituted by chlorine (**314–316**).<sup>313</sup> Attempted hydrolysis of **314** and **315** with  $\text{H}_2\text{O}/\text{Et}_3\text{N}$  took place only in the case of **314** and led to **317**.<sup>314</sup> This result illustrates that the  $\text{Cp}^*$  ligand reduces the electrophilicity of the  $\alpha$ -silicon atom and consequently allows the regio-specific hydroxylation in the  $\beta$ -position of **308** and **311** by base-assisted hydrolysis.<sup>314</sup> These two metallodisilanetrioles (**319** and **320**) show remarkable stability without any self-condensation. Treatment of **302** and **312** with dimethyldioxirane resulted in the formation of dihydroxydisilanes **317** and **318**.<sup>314,315</sup> Attempts to replace

all hydrogens by using an excess of reagent failed and led only to decomposition of the starting material. Diiron complex **321** underwent successful tetrahydroxylation to **322** again with  $\text{H}_2\text{O}/\text{Et}_3\text{N}$  (**Figure 11**).<sup>316</sup> Base-assisted condensation of **322** with chlorodimethylsilane gives metallodisiloxane **323** (**Figure 11**).<sup>316</sup>

For group 9, no compounds of cobalt meeting the requirements of this review are present in the literature and for rhodium only one theoretical proposal concerning the coordination of rhodium to a  $\text{Si}_2\text{H}_2$  unit is available.<sup>317</sup> For iridium, calculations on the system  $[\text{Cp}(\text{PH}_3)\text{Ir}(\text{SiH}(\text{SiH}_3)_2)]^+$  were carried out and the structures of complexes  $[(\text{CO})\text{H}(\text{Cl})(\text{PEt}_3)_2\text{IrSiH}_2\text{SiH}_3]$ <sup>318</sup> and  $[(\text{CO})\text{H}_2(\text{PPh}_3)_2\text{IrSiH}_2\text{SiH}_3]$ <sup>319</sup> were determined by  $^1\text{H}$  and  $^{31}\text{P}$  NMR spectroscopy.

For the group 10, only few examples are known for platinum. One unique complex containing a hydride ligand located

*trans* to a silicon was reported by Ebsworth et al. as *trans*-[Pt(Si<sub>2</sub>SiH<sub>3</sub>)(H)(PCy<sub>3</sub>)<sub>2</sub>] (Cy=cyclohexyl).<sup>320</sup> The first isolated example of a platinum complex containing terminal Si<sub>2</sub>H<sub>5</sub> groups and an unusual Pt<sub>2</sub>Si<sub>4</sub> ring system containing a bridging disilane unit was reported by Michalczyk, Fink, and coworkers (Scheme 34).<sup>321</sup> Addition of Si<sub>2</sub>H<sub>6</sub> (1) to the Pt complex 324 produced 325 and a small amount of 326, but upon adding an excess of the starting Pt complex 324 the Pt<sub>2</sub>Si<sub>4</sub> ring compound 326 could be obtained in quantitative yield. The cyclic compound 326 shows an unusual stability to air both as a solid and in solution, whereas the bis(silyl) complex 325 is, as expected, air sensitive. The molecular structure of 326 was determined by x-ray crystal-structure analysis. Its six-membered ring adopts a chair conformation with a Si-Si bond length of 2.36 Å.

Cuprates with organic ligands are a well-established class of compounds, especially lithium-alkyl cuprates are important and versatile reagents in organic synthesis. However, only few compounds with a Si-Si-Cu bond are known and none without organic substituents. The same is true for silver and gold and even more disappointing for the whole group 12.

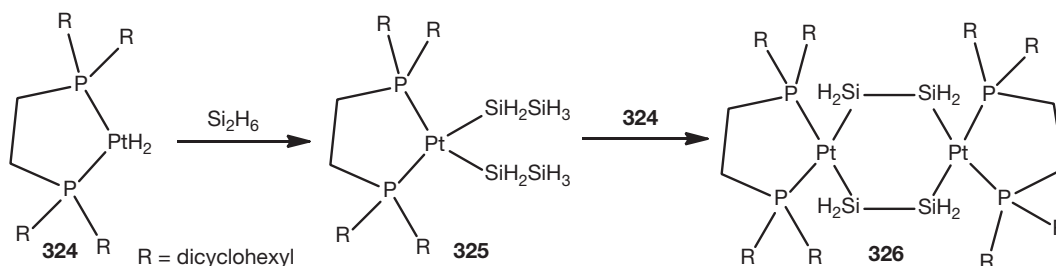
### 1.02.11 Silanes and Lanthanoids and Actinoids

Transformations such as hydrogenation, hydrosilylation, polymerization of olefins, and dehydrogenative coupling of hydrosilanes can be effected by organolanthanide alkyl and silyl

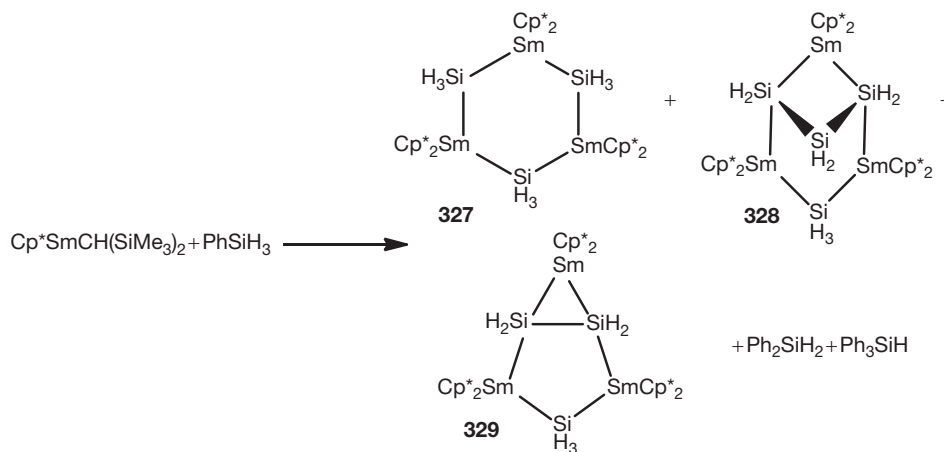
complexes.<sup>301,322-324</sup> Despite this wide and promising application range, the numbers of silyl-lanthanides or also silyl-actinides are very small.<sup>299,325,326</sup> The first f-element compound with a SiH<sub>3</sub> ligand was synthesized by Tilley et al. in 2000<sup>327</sup> and was the result of a detailed investigation into the formation of a samarium-silicon cluster achieved by samarium-mediated redistribution of phenylsilane (PhSiH<sub>3</sub>) some years before.<sup>328</sup> The samarium clusters 327-329 were produced besides a number of soluble silane products in a ratio of 5:4:1 and all three of them have been structurally characterized (Scheme 35). Recently, theoretical mechanistic investigations were carried out on the bond activation of PhSiH<sub>3</sub> by Cp<sub>2</sub>SmH.<sup>329</sup>

The silicate compounds containing ethane-like Si-Si bonds as in Na<sub>8</sub>Eu<sub>2</sub>(Si<sub>2</sub>Se<sub>6</sub>)<sub>2</sub>,<sup>204</sup> Na<sub>9</sub>Sm(Si<sub>2</sub>Se<sub>6</sub>)<sub>2</sub>,<sup>206</sup> and Na<sub>8</sub>Eu<sub>2</sub>(Si<sub>2</sub>Te<sub>6</sub>)<sub>2</sub><sup>206</sup> have been already mentioned earlier in this chapter.

Only a single silyl-uranium compound namely [(tBu)ArN]<sub>3</sub>USi(SiMe<sub>3</sub>)<sub>3</sub> was reported and fully characterized over the last 10 years<sup>330</sup> and for Cp<sub>3</sub>USi(SiMe<sub>3</sub>)<sub>3</sub> theoretical investigations are available.<sup>331</sup> The formation of actinide-silicon bonds was investigated by Tilley and coworkers. They mentioned the difficulties in isolation due to the rapid decomposition of a thorium silyl complex Cp\*<sub>2</sub>Th[Si(SiMe<sub>3</sub>)<sub>3</sub>]Cl, which could be identified only by means of NMR spectroscopy, but was trapped by reaction with 2 mol CO, thus yielding an isolable silylthoroxylketene compound.<sup>332,333</sup>



**Scheme 34** First example of a platinum complex containing terminal Si<sub>2</sub>H<sub>5</sub> groups and an unusual Pt<sub>2</sub>Si<sub>4</sub> ring system.



**Scheme 35** Synthesis of samarium-silicon clusters 327-329.

## 1.02.12 Conclusion

This chapter deals with compounds bearing at least one silicon-silicon single bond, with the restriction of no carbon substituents on the silicon atoms, and covers mainly the literature starting from 2000. Emphasis is given to halo-, hydro-, and halohydrosilanes a neglected class of compounds for which intensive investigations already started in the 1960s and which have again gained increasing interest over the last years for new and exciting applications. Nevertheless, no review can be found in literature which is devoted to them.

## References

1. *Gmelin Handbook of Inorganic Chemistry* **1982**, Vol.5 (Suppl B1) B1 8th ed.; Springer-Verlag.
2. Lorenz, J. H. *Survey of the Preparation, Purity, and Availability of Silanes*; SERI/STR-211-2092, DE84000090; Sol. Energy Res. Inst., CO, 1983.
3. Furusawa, M.; Tanaka, H. *Liquid Silicon Materials*. In *Solution Processing of Inorganic Materials*; Miltz, D. B., Ed.; Wiley: Hoboken, 2009; pp 131–155.
4. Feher, F.; Baier, H.; Enders, B.; Krancher, M.; Laakmann, J.; Ocklenburg, F. J.; Skrodski, D. Z. *Anorg. Allg. Chem.* **1985**, *530*, 191–195.
5. Belot, D.; Rade, J. Y.; Piffard, J. F.; Larquet, C.; Cornut, P. *Apparatus and Method for Silicon Hydrides and Their Use*. EP146456A2, June 26, 1985.
6. Akhtar, M. *Synth. React. Inorg. Met.-Org. Chem.* **1986**, *16*, 729–748.
7. Miyagawa, H.; Itoh, M.; Abe, T.; Iwata, K.; Koizumi, K. *Silicon Hydrides*. EP149363A2, July 24, 1985.
8. Ito, M.; Miyagawa, H.; Abe, T.; Inoue, K.; Iwata, K.; Murakami, M. *Manufacture of Silanes*. JP61155213A, July 14, 1986.
9. Ito, M.; Miyagawa, H.; Abe, T.; Koizumi, K. *Manufacture of Silanes*. JP61122112A, June 10, 1986.
10. Miyagawa, H.; Myagawa, H.; Abe, T.; Iwata, K.; Koizumi, K. *Manufacture of Silicon Hydride*. JP60166215A, August 29, 1985.
11. Miyagawa, H.; Tsukahara, T.; Abe, T.; Amita, H.; Tsukahara, T. *Manufacture of Silicon Hydride*. JP60166214A, August 29, 1985.
12. Miyagawa, H.; Tsukahara, T.; Abe, T.; Iwata, K.; Tsukahara, T. *Manufacture of Silicon Hydride*. JP60166216A, August 29, 1985.
13. Ito, M.; Miyagawa, H.; Abe, T.; Inoue, K.; Amita, H.; Yanagawa, N. *Manufacture of Silicon Hydrides*. JP61091011A, May 9, 1986.
14. Kvaratskheli, Y. K.; Zhirkov, M. S.; Fadeev, L. L.; Filinov, V. T. *Method of Production of Monosilane and Disilane*. RU2160706C1, December 20, 2000.
15. Kvaratskheli, Y. K.; Zhirkov, M. S.; Lobachev, Y. A.; Fadeev, L. L. *Khim. Tekhnol.* **2005**, *3*, 2–6.
16. Spanier, E. J.; MacDiarmid, A. G. *Inorg. Chem.* **1962**, *1*, 432–433.
17. Izeki, N.; Nagasawa, M.; Kazama, T. *Manufacture of Silanes*. JP62132720A, June 16, 1987.
18. Izeki, N.; Nagasawa, M.; Kazama, T. *Manufacture of Silanes*. JP62132721A, June 16, 1987.
19. Villermet, A.; Didier, P. *High-Frequency Electric Discharge Process for Manufacturing Trisilane from Monosilane*. WO9606802A1, March 7, 1996.
20. Sundermeyer, W.; Mueller, M.; Klockner, H. J. *Method for the Manufacture of Disilane from Monosilane by Plasma Discharge*. DE3639202A1, May 19, 1988.
21. Longeway, P. A.; Lampe, F. W. *J. Am. Chem. Soc.* **1981**, *103*, 6813–6818.
22. Zavelovich, J.; Hacker, D. S. *Photochemical Preparation of Disilane*. US4604274A, August 5, 1986.
23. Kitsuno, Y.; Yano, K.; Tazawa, S. *High-Order Silane Manufacture from Silane*. JP03183614A, August 9, 1991.
24. Kitsuno, H.; Yano, K.; Tazawa, S.; Matsuhira, S.; Nakajo, T. *Manufacture of Higher Silanes as Raw Materials of Silicon, Semiconductors*. JP11260729A, September 24, 1999.
25. Gaspar, P. P.; Levy, C. A.; Adair, G. M. *Inorg. Chem.* **1970**, *9*, 1272–1273.
26. Cannady, J. P.; Zhou, X. *Composition Comprising Neopentasilane and Method of Preparing Same*. WO2008051328, May 2, 2008.
27. Hoefler, F.; Jannach, R. *Inorg. Nucl. Chem. Lett.* **1973**, *9*, 723–725.
28. Auner, G. A.; Bauch, C.; Lippold, G.; Deltshew, R. *Processing and Use of Halogenated Polysilanes*. WO2008009473A1, January 24, 2008.
29. Auner, N. *Production of Silicon from Silyl Halides*. WO2006125425A1, November 30, 2006.
30. Plichta, P. *Procedure for the Production of Higher Silanes as Fuels*. DE10059625A1, May 16, 2002.
31. Hengge, E.; Bauer, G. *Angew. Chem.* **1973**, *85*, 304–305.
32. Lee, D. W.; Park, Y. W.; Han, J. S.; Yoo, B. R. *Bull. Korean Chem. Soc.* **2009**, *30*, 2443–2445.
33. Hengge, E.; Kovar, D. *Angew. Chem.* **1977**, *89*, 417–418.
34. Shihō, H.; Kato, H. *Method for Forming a Silicon Film for Use in Solar Cells and Electronic Devices*. EP1284306A2, February 19, 2003.
35. Boudjouk, P. R.; Kim, B.-K.; Remington, M. P.; Chauhan, B. *Compounds Containing Tetradechlorocyclohexasilane Dianion*. EP902030A2, March 17, 1999.
36. Choi, S.-B.; Kim, B.-K.; Boudjouk, P.; Grier, D. G. *J. Am. Chem. Soc.* **2001**, *123*, 8117–8118.
37. Stueger, H.; Lassacher, P.; Hengge, E. *Z. Anorg. Allg. Chem.* **1995**, *621*, 1517–1522.
38. Corey, J. Y. *Adv. Organomet. Chem.* **2004**, *51*, 1–52.
39. Harrod, J. F. *NATO ASI Ser., Ser. E., Applied Sciences* **1988**, *141*, 103–115.
40. Okumura, Y.; Takatsuna, K.; Yagihashi, J. *Disilane and Trisilane Preparation from Monosilane*. JP02184513A, July 19, 1990.
41. Brausch, N.; Ebbes, A.; Stochniol, G.; Trocha, M.; Oenal, Y.; Sauer, J.; Stuetzel, B.; Wolf, D.; Stueger, H. *Process for Preparing Higher Hydridosilanes*. WO2010003729A1, January 14, 2010.
42. Horn, H. G. *Chem.-Ztg.* **1986**, *110*, 131–150.
43. Albinsson, B.; Teramae, H.; Plitt, H. S.; Goss, L. M.; Schmidbaur, H.; Michl, J. *J. Phys. Chem.* **1996**, *100*, 8681–8691.
44. Stueger, H.; Hengge, E.; Janoschek, R. *Phosphorus, Sulfur Silicon Relat. Elem.* **1990**, *48*, 189–201.
45. Haaland, A.; Rypdal, K.; Stuger, H.; Volden, H. V. *Acta Chem. Scand.* **1994**, *48*, 46–51.
46. Løbreyer, T.; Sundermeyer, W.; Oberhammer, H. *Chem. Ber.* **1994**, *127*, 2111–2115.
47. Smith, Z.; Almenningen, A.; Hengge, E.; Kovar, D. *J. Am. Chem. Soc.* **1982**, *104*, 4362–4366.
48. Ortiz, J. V.; Mintmire, J. W. *J. Am. Chem. Soc.* **1988**, *110*, 4522–4527.
49. Corminboeuf, C.; Heine, T.; Weber, J. *Chem. Phys. Lett.* **2002**, *357*, 1–7.
50. Milbradt, M.; Marsmann, H.; Heine, T.; Seifert, G.; Frauenheim, T. *Calculation of <sup>29</sup>Si Chemical Shifts Using a Density-Functional Based Tight-Binding Scheme*. In *Organosilicon Chemistry V: From Molecules to Materials*; Auner, N., Weis, J., Eds.; Wiley: Weinheim, 2003; pp 324–328.
51. Chen, K.; Allinger, N. L. *J. Phys. Org. Chem.* **1997**, *10*, 697–715.
52. Adamczyk, A. J.; Reyniers, M.-F.; Marin, G. B.; Broadbelt, L. J. *ChemPhysChem* **2010**, *11*, 1978–1994.
53. Swihart, M. T.; Girshick, S. L. *J. Phys. Chem. B.* **1999**, *103*, 64–76.
54. Adamczyk, A. J.; Reyniers, M.-F.; Marin, G. B.; Broadbelt, L. J. *Phys. Chem. Chem. Phys.* **2010**, *12*, 12676–12696.
55. Tonokura, K.; Murasaki, T.; Koshi, M. *J. Phys. Chem. B.* **2002**, *106*, 555–563.
56. Eger, W.; Genest, A. *Roesch Books of Abstracts, 1st Munich Forum on Functional Material*. *Frontiers in Silicon Chemistry: Germany, Munich, 2011*; April 14–15.
57. Paggi, R. E.; Redemer, M. D.; Root, B. *Hydrogen Generation Processes Using Silicon Compounds*. WO2008094840A2, August 7, 2008.
58. Hidding, B.; Pflitzner, M. *J. Propul. Power.* **2006**, *22*, 786–789.
59. Gao, Y.; Zhou, Y. S.; Qian, M.; Xie, Z. Q.; Xiong, W.; Luo, H. F.; Jiang, L.; Lu, Y. F. *Nanotechnology* **2011**, *22*, 1 235602/1-235602/5.
60. Myronov, M.; Shah, V. A.; Dobbie, A.; Liu, X.-C.; Nguyen, V.; Leadley, D. R.; Parker, E. H. C. *Phys. Status Solidi C.* **2011**, *8*, 952–955.
61. Katayama, D.; Honda, M.; Kohno, M.; Nakanishi, T. *Plasma CVD Process and Apparatus for the Deposition of Crystalline Silicon Films for the Manufacture of a Crosspoint Nonvolatile Semiconductor Memory Device*. WO2011040394A1, April 7, 2011.
62. Shimoda, T.; Matsuki, Y.; Furusawa, M.; Aoki, T.; Yudasaka, I.; Tanaka, H.; Iwasawa, H.; Wang, D.; Miyasaka, M.; Takeuchi, Y. *Nature* **2006**, *440*, 783–786.
63. Brausch, N.; Stochniol, G.; Quandt, T. *Method for Producing Higher Hydridosilanes Through Catalyzed Dehydropolymerization of Lower Hydridosilanes Using Supported Transition Metal Catalyst*. DE102009048087A1, April 7, 2011.
64. Knies, W.; Eiblmeier, H. *Method for Producing Neopentasilanes*. WO2010043551A1, April 22, 2010.
65. Wieber, S.; Patz, M.; Trocha, M.; Rauleder, H.; Mueh, E.; Stueger, H.; Walkner, C. *Production of Linear Silanes by Hydride Reaction of Halosilanes*. WO2011061088A1, May 26, 2011.
66. Elangovan, A.; Anderson, K.; Boudjouk, P. R.; Schulz, D. L. *Method of Producing Cyclohexasilane Compounds*. WO2011094191A1, August 4, 2011.
67. Schulz, D. L.; Hoey, J.; Smith, J.; Elangovan, A.; Wu, X.-F.; Akhatov, I.; Payne, S.; Moore, J.; Boudjouk, P.; Pederson, L.; Xiao, J.; Zhang, J.-G. *Electrochem. Solid-State Lett.* **2010**, *13*, A143–A145.

68. Han, S.; Dai, X.; Loy, P.; Lovaaen, J.; Huether, J.; Hoey, J. M.; Wagner, A.; Sandstrom, J.; Bunzow, D.; Swenson, O. F.; Akhatov, I. S.; Schulz, D. L. *J. Non-Cryst. Solids*. **2008**, *354*, 2623–2626.
69. Pope, E. J. A.; Hill, C. L.; Brabham, C. N.; King, J. M.; Morkunas, B. T. *Stoichiometric Silicon Carbide Fibers from Thermo-Chemically Cured Polysilazanes*. US20110212329A1, September 1, 2011.
70. Bauer, M.; Thomas, S. G. *Cyclical Epitaxial Deposition and Etch*. US20110117732A1, May 19, 2011.
71. Tomasini, P.; Cody, N. *Methods of Selectively Depositing Silicon-Containing Films*. US20090117717A1, May 7, 2009.
72. Tomasini, P.; Wen, J.; Bertram, R.; Arena, C.; Bauer, M.; Cody, N. *Methods and Systems for Selectively Depositing Silicon-Containing Films Using Chloropolysilanes*. WO2007140375A2, December 6, 2007.
73. Van, D.; MacDiarmid, A. G. *J. Inorg. Nucl. Chem.* **1963**, *25*, 1503–1506.
74. Drake, J. E.; Goddard, N. *J. Chem. Soc. A*. **1970**, 2587–2590.
75. Drake, J. E.; Goddard, N. *Inorg. Nucl. Chem. Lett.* **1968**, *4*, 385–388.
76. Drake, J. E.; Goddard, N.; Westwood, N. P. C. *J. Chem. Soc. A*. **1971**, 3305–3308.
77. Hollandsworth, R. P.; Ring, M. A. *Inorg. Chem.* **1968**, *7*, 1635–1637.
78. Abedini, M.; Dyke, C. H. V.; Diarmid, A. G. M. *J. Inorg. Nucl. Chem.* **1963**, *25*, 307–309.
79. Hollandsworth, R. P.; Ingle, W. M.; Ring, M. A. *Inorg. Chem.* **1967**, *6*, 844–845.
80. Vanderwielen, A. J.; Ring, M. A. *Inorg. Chem.* **1972**, *11*, 246–250.
81. Benthham, J. E.; Craddock, S.; Ebsworth, E. A. V. *Inorg. Nucl. Chem. Lett.* **1971**, *7*, 1077–1079.
82. Feher, F.; Ocklenburg, F. *Z. Anorg. Allg. Chem.* **1984**, *515*, 36–40.
83. Feher, F.; Plichta, P.; Guillery, R. *Inorg. Chem.* **1971**, *10*, 606–608.
84. Gupper, A.; Hassler, K. *Eur. J. Inorg. Chem.* **2001**, 2007–2011.
85. Haas, A.; Suellentrop, R.; Krueger, C. Z. *Anorg. Allg. Chem.* **1993**, *619*, 819–826.
86. Soellradl, H.; Hengge, E. *J. Organomet. Chem.* **1983**, *243*, 257–269.
87. Hassler, K.; Koell, W. *J. Organomet. Chem.* **1995**, *487*, 223–226.
88. Hassler, K.; Koell, W. *J. Organomet. Chem.* **1997**, *540*, 113–118.
89. Stueger, H. *J. Organomet. Chem.* **1993**, *458*, 1–7.
90. Uhlig, W. Z. *Anorg. Allg. Chem.* **1993**, *619*, 1479–1482.
91. Stueger, H.; Lassacher, P.; Hengge, E. *J. Organomet. Chem.* **1997**, *547*, 227–233.
92. Gollner, W.; Renger, K.; Stueger, H. *Inorg. Chem.* **2003**, *42*, 4579–4584.
93. Hoefler, F.; Jannach, R.; Raml, W. *Z. Anorg. Allg. Chem.* **1977**, *428*, 75–82.
94. Drake, J. E.; Westwood, N. P. C. *J. Chem. Soc. A*. **1971**, 3300–3305.
95. Hengge, E.; Mitter, F. K. *Monatsh. Chem.* **1986**, *117*, 721–728.
96. Hengge, E.; Miklau, G. *Inorg. Allg. Chem.* **1984**, *508*, 33–42.
97. Hengge, E.; Mitter, F. K. *Z. Anorg. Allg. Chem.* **1985**, *529*, 22–28.
98. Stueger, H.; Lassacher, P. *J. Organomet. Chem.* **1993**, *450*, 79–84.
99. Hosmane, N. S. *Inorg. Nucl. Chem. Lett.* **1974**, *10*, 1077–1079.
100. Geisler, T. C.; Cooper, C. G.; Norman, A. D. *Inorg. Chem.* **1972**, *11*, 1710–1713.
101. Ward, L. G. L.; MacDiarmid, A. G. *J. Inorg. Nucl. Chem.* **1961**, *20*, 345–347.
102. Hassler, K.; Koell, W.; Schenzel, K. *J. Mol. Struct.* **1995**, *348*, 353–356.
102. Schenzel, K.; Hassler, K. *Spectrochim. Acta, Part A*. **1994**, *50A*, 139–144.
104. Hassler, K.; Poeschl, M. *J. Organomet. Chem.* **1990**, *398*, 225–227.
105. Johansen, T. H.; Hagen, K.; Stolevik, R.; Ernst, M.; Hassler, K. *J. Mol. Struct.* **1995**, *372*, 161–172.
106. Feher, F.; Freund, R. *Inorg. Nucl. Chem. Lett.* **1973**, *9*, 937–940.
107. Stueger, H. *J. Organomet. Chem.* **1992**, *433*, 11–19.
108. Feher, F.; Plichta, P.; Guillery, R. *Chem. Ber.* **1970**, *103*, 3028–3033.
109. Feher, F.; Mostert, B.; Wronka, A. G.; Betzen, G. *Monatsh. Chem.* **1972**, *103*, 959–964.
110. Hassler, K.; Koell, W.; Ernst, M. *Spectrochim. Acta, Part A*. **1997**, *53A*, 213–224.
111. Hassler, K.; Kaizenbeisser, U. *J. Organomet. Chem.* **1994**, *480*, 173–175.
112. Johansen, T. H.; Hassler, K.; Tekautz, G.; Hagen, K. *J. Mol. Struct.* **2001**, *598*, 171–195.
113. Johansen, T. H.; Hagen, K.; Hassler, K.; Tekautz, G.; Stolevik, R. *J. Mol. Struct.* **1999**, *509*, 237–254.
114. Solan, D.; Burg, A. B. *Inorg. Chem.* **1972**, *11*, 1253–1258.
115. Langford, G. R.; Moody, D. C.; Odom, J. D. *Inorg. Chem.* **1975**, *14*, 134–136.
116. Bald, J. F.; Sharp, K. G.; MacDiarmid, A. G. *J. Fluorine Chem.* **1973**, *3*, 433–435.
117. Sharp, K. G.; Margrave, J. L. *Inorg. Chem.* **1969**, *8*, 2655–2658.
118. D'Errico, J. J.; Sharp, K. G. *Inorg. Chem.* **1989**, *28*, 2886–2888.
119. Hoefler, F.; Jannach, R. *Inorg. Nucl. Chem. Lett.* **1974**, *10*, 711–714.
120. Jenkins, R. L.; Vandersielen, A. J.; Ruis, S. P.; Gird, S. R.; Ring, M. A. *Inorg. Chem.* **1973**, *12*, 2968–2972.
121. Abedini, M.; MacDiarmid, A. G. *Inorg. Chem.* **1963**, *2*, 608–613.
122. Hengge, E.; Stueger, H. *Recent Advances in the Chemistry of Cyclopolysilanes*. In Rappoport, Z., Apeloig, Y., Eds.; Chemistry of Organic Silicon Compounds; Wiley: Chichester, 1998; Vol. 2, p 2177.
123. Poeschl, U.; Hassler, K. *Organometallics* **1996**, *15*, 3238–3240.
124. Herzog, U.; Roewer, G. *J. Organomet. Chem.* **1997**, *544*, 217–223.
125. Hoelbling, M.; Flock, M.; Hassler, K. *ChemPhysChem*. **2007**, *8*, 735–744.
126. Sevast'yanov, V. G.; Ezhov, Y. S.; Pavelko, R. G.; Kuznetsov, N. T. *Inorg. Mater.* **2007**, *43*, 369–372.
127. Hassler, K.; Kovar, D.; Soellradl, H.; Hengge, E. *Z. Anorg. Allg. Chem.* **1982**, *488*, 27–37.
128. Cerny, M.; Joklik, J.; Trka, A.; Dolejs, L. *Chem. Prum.* **1975**, *25*, 191–193.
129. Parissakis, G.; Vrandi-Piskou, D.; Carambelas, A. *Formation of the First Members of the Homologous Series Silicon Chloride 2n+2 and Their Gas Chromatographic Identification*. *Chromatogr. Methods Immed. Sep., Proc.* **1966**; *Meet.* **1965**, *1*, 329–335.
130. Kirpichnikova, A. A.; Noskov, V. G.; Englin, M. A.; Chumakov, A. A.; Medvedev, A. N. *Zh. Vses. Khim. Ova*. **1977**, *22*, 465–466.
131. Niemann, U.; Marsmann, H. C. Z. *Naturforsch., B: Anorg. Chem., Org. Chem.* **1975**, *30B*, 202–206.
132. Ogi, K.; Kurashige, T.; Kimura, E. *Hexachlorodisilane and Octachlorotrisilane Preparation*. JP01278411A, November 8, 1989.
133. Auner, N.; Bauch, C.; Holl, S.; Deltshew, R.; Mohsseni, J.; Lippold, G.; Gebel, T. *Process for Production of Hexachlorodisilane by Oxidative Cleavage of a Chlorinated Polysilane with Chlorine Gas*. DE102009056438A1, June 9, 2011.
134. Ogi, K.; Kurashige, T.; Kimura, E. *Manufacture of Chloropolysilanes by Direct Chlorination of Silicon*. JP01219012A, September 1, 1989.
135. Ikeda, H.; Tsunashima, M.; Mieda, A. *Chlorination Catalysts for Preparation of Hexachlorodisilane and Octachlorotrisilane*. EP283905A2, September 28, 1988.
136. Hengge, E.; Kovar, D. *J. Organomet. Chem.* **1977**, *125*, C29–C32.
137. Raml, W.; Hengge, E. *Z. Naturforsch., B: Anorg. Chem., Org. Chem.* **1979**, *34B*, 1457–1458.
138. Raml, W.; Hengge, E. *Monatsh. Chem.* **1979**, *110*, 1257–1261.
139. Hoefler, F.; Jannach, R. *Inorg. Nucl. Chem. Lett.* **1975**, *11*, 743–747.
140. Kaczmarczyk, A.; Nuss, J. W.; Urry, G. J. *Inorg. Nucl. Chem.* **1964**, *26*, 427–433.
141. Schumb, W. C. *Inorg. Syntheses II* **1946**, 98–102.
142. Besson, A.; Fournier, L. *Compt. rend.* **1911**, *151*, 1055–1057.
143. Hoefler, F. *Ber. Bunsenges. Phys. Chem.* **1974**, *78*, 1246–1248.
144. Schwarz, R.; Pflugmacher, A. *Ber. Dtsch. Chem. Ges. B*. **1942**, *75B*, 1062–1071.
145. Jansen, M.; Friede, B. *Acta Crystallogr., Sect. C: Cryst. Struct. Commun.* **1996**, *C52*, 1333–1334.
146. Timms, P. L.; Kent, R. A.; Ehlert, T. C.; Margrave, J. L. *J. Am. Chem. Soc.* **1965**, *87*, 2824–2828.
147. Isomura, S.; Takeuchi, K. *J. Fluorine Chem.* **1997**, *83*, 89–91.
148. Kitsugi, N.; Aono, K.; Yamamoto, T. *Manufacture of Perfluorosilane by Transhalogenation*. JP62187106A, August 15, 1987.
149. Suresh, B. S.; Padma, D. K. *Bull. Chem. Soc. Jpn.* **1985**, *58*, 1867–1868.
150. Schmeisser, M.; Ehlers, K. P. *Angew. Chem.* **1964**, *76*, 781–782.
151. Hoefler, F.; Jannach, R. *Monatsh. Chem.* **1976**, *107*, 731–735.
152. Marsmann, H. C.; Raml, W.; Hengge, E. *Z. Naturforsch., B: Anorg. Chem., Org. Chem.* **1980**, *35b*, 35–37.
153. Hassler, K.; Hengge, E.; Raml, W. *Monatsh. Chem.* **1980**, *111*, 581–590.
154. Hengge, E.; Waldhoer, S. *Z. Naturforsch., Teil B*. **1974**, *29*, 437.
155. Marsmann, H. C.; Raml, W.; Hengge, E. *Z. Naturforsch., B: Anorg. Chem., Org. Chem.* **1980**, *35B*, 1541–1547.
156. Schmoelzer, H.; Hengge, E. *J. Organomet. Chem.* **1982**, *225*, 171–176.
157. Suresh, B. S.; Thompson, J. C. *J. Chem. Soc. Dalton Trans.* **1987**, 1123–1126.
158. Margrave, J. L.; Sharp, K. G.; Wilson, P. W. *J. Inorg. Nucl. Chem.* **1970**, *32*, 1813–1816.
159. Margrave, J. L.; Sharp, K. G.; Wilson, P. W. *J. Inorg. Nucl. Chem.* **1970**, *32*, 1817–1825.
160. Hengge, E.; Kovar, D. *Z. Anorg. Allg. Chem.* **1979**, *458*, 163–167.
161. Hengge, E.; Kovar, D. *Angew. Chem.* **1981**, *93*, 698–701.
162. Murugavel, R.; Voigt, A.; Walawalkar, M. G.; Roesky, H. *W. Chem. Rev.* **1996**, *96*, 2205–2236.
163. Ward, L. G. L.; MacDiarmid, A. G. *J. Am. Chem. Soc.* **1960**, *82*, 2151–2153.
164. Van Dyke, C. H.; MacDiarmid, A. G. *Inorg. Chem.* **1964**, *3*, 747–752.
165. Höfler, F.; Jannach, R.; Raml, W. *Z. Anorg. Allg. Chem.* **1977**, *428*, 75–82.
166. Kifer, E. W.; Van Dyke, C. H. *Inorg. Chem.* **1972**, *11*, 404–408.
167. Höfler, F.; Jannach, R. *Z. Anorg. Allg. Chem.* **1975**, *413*, 285–292.
168. Seyferth, D.; Prudhomme, C. C.; Wang, W.-L. *J. Organomet. Chem.* **1984**, *277*, 203–209.
169. Maier, G.; Reisenauer, H. P.; Schoettler, K.; Wessolek-Kraus, U. *J. Organomet. Chem.* **1989**, *366*, 25–38.
170. Hassler, K.; Hengge, E.; Schrank, F.; Weidenbruch, M. *Spectrochim. Acta A*. **1991**, *47*, 57–62.



171. Söldner, M.; Schier, A.; Schmidbaur, H. *J. Organomet. Chem.* **1996**, *521*, 295–299.
172. Jaeschke, B.; Jansen, M. Z. *Kristallogr. New Cryst. Str.* **2004**, *219*, 355–366.
173. Uhlig, W. *J. Organomet. Chem.* **2003**, *685*, 70–78.
174. Söldner, M.; Sandor, M.; Schier, A.; Schmidbaur, H. *Chem. Ber.* **1997**, *130*, 1671–1676.
175. Kouvetakis, J.; Ritter, C. J. I.; Changwu, H.; S.T., T. I.; Chizmeshya, A. *Novel Silicon-Germanium Hydrides and Methods for Making and Using Same*. WO 2007062056(A2), May 31, 2007.
176. Uhlig, W. *Silicon Chem.* **2002**, *1*, 129–137.
177. Stueger, H. *Kautsky-Siloxene Analogous Monomers and Oligomers*. In *Silicon Chemistry: From the Atom to Extended Systems*; Jutzi, P., Schubert, U., Eds.; Wiley: Weinheim, 2003; pp 214–225.
178. Stueger, H.; Albering, J.; Flock, M.; Fuerpass, G.; Mitterfellner, T. *Organometallics* **2011**, *30*, 2531–2538.
179. McCord, P.; Yau, S.-L.; Bard, A. J. *Science* **1992**, *257*, 68–69.
180. Wöhler, F. *Justus Liebigs Ann. Chem.* **1863**, *127*, 257–274.
181. Kautsky, H.; Herzberg, G. Z. *Anorg. Allg. Chem.* **1924**, *139*, 135–160.
182. Stutzmann, M.; Brandt, M. S.; Rosenbauer, M.; Fuchs, H. D.; Finkbeiner, S.; Weber, J.; Deak, P. *J. Lumin.* **1993**, *57*, 321–330.
183. Brandt, M. S.; Vogt, G.; Stutzmann, M. *Silicon- and Germanium-Based Sheet Polymers and Zintl Phases*. In *Silicon Chemistry: From the Atom to Extended Systems*; Jutzi, P., Schubert, U., Eds.; Wiley: Weinheim, 2003; p pp 194.
184. Nakano, H.; Ishii, M.; Nakamura, H. *Chem. Commun.* **2005**, 2945–2947.
185. Vogt, G.; Zamanzadeh-Hanebuth, N.; Brandt, M. S.; Stutzmann, M.; Albrecht, M. *Monatsh. Chem.* **1999**, *130*, 79–87.
186. Kleewein, A.; Stüger, H. *Monatsh. Chem.* **1999**, *130*, 69–77.
187. Ward, L. G. L.; MacDiarmid, A. G. *J. Inorg. Nucl. Chem.* **1961**, *21*, 287–293.
188. Anderson, J. W.; Drake, J. E. *Inorg. Nucl. Chem. Lett.* **1971**, *7*, 1007–1010.
189. Uhlig, F.; Stadelmann, B.; Zechmann, A.; Lassacher, P.; Stüger, H.; Hengge, E. *Phosphorus, Sulfur Silicon Relat. Elem.* **1994**, *90*, 29–39.
190. Stueger, H.; Lassacher, P. *Oligosilanylulfanes: New Functional Derivatives of Higher Silicon Hydrides*. In *Organosilicon Chem. II, 2nd ed.*; Auner, N., Weis, J., Eds.; VCH: Weinheim, 1996; pp 121–125.
191. Haas, A.; Stüllentrup, R.; Krüger, C. Z. *Anorg. Allg. Chem.* **1993**, *619*, 819–826.
192. Maaninen, T.; Tuononen, H. M.; Kosunen, K.; Oilunkaniemi, R.; Hiitola, J.; Laitinen, R.; Chivers, T. Z. *Anorg. Allg. Chem.* **2004**, *630*, 1947–1954.
193. Liao, H.-Y.; Su, M.-D.; Chu, S.-Y. *Int. J. Quantum Chem.* **2002**, *90*, 663–668.
194. Timberlake, J. M.; Green, J.; Christou, V.; Arnold, J. J. *Chem. Soc., Dalton Trans.* **1998**, 4029–4034.
195. Yoshida, H.; Takahara, Y.; Erata, T.; Ando, W. *J. Am. Chem. Soc.* **1992**, *114*, 1098–1100.
196. Zhang, S.-H.; Yeong, H.-X.; So, C.-W. *Chem. Eur. J.* **2011**, *17*, 3490–3499.
197. Zhang, S.-H.; Yeong, H.-X.; Xi, H.-W.; Lim, K. H.; So, C.-W. *Chem. Eur. J.* **2010**, *16*, 10250–10254.
198. Ouvrard, G.; Sandre, E.; Brec, R. *J. Solid State Chem.* **1988**, *73*, 27–32.
199. Vincent, H.; Leroux, D.; Bijaoui, D.; Rimet, R.; Schlenker, C. *J. Solid State Chem.* **1986**, *63*, 349–352.
200. Marsh, R. E. J. *Solid State Chem.* **1988**, *77*, 190–191.
201. Carteaux, V.; Moussa, F.; Spiesser, M. *Europhys. Lett.* **1995**, *29*, 251–256.
202. Feltz, A.; Pfaff, G. Z. *Anorg. Allg. Chem.* **1983**, *504*, 173–178.
203. Cui, Y.; Mayasree, O.; Assoud, A.; Kleinke, H. J. *Alloys Compd.* **2010**, *493*, 70–76.
204. Martin, B. R.; Polyakova, L. A.; Dorhout, P. K. J. *Alloys Compd.* **2006**, *408–412*, 490–495.
205. Marking, G. A.; Kanatzidis, M. G. *J. Alloys Compd.* **1997**, *259*, 122–128.
206. Knaust, J. M.; Polyakova, L. A.; Dorhout, P. K. Z. *Kristallogr. New Cryst. Str.* **2005**, *220*, 295–297.
207. Miller, R. D.; Michl, J. *Chem. Rev.* **1989**, *89*, 1359–1410.
208. Itoh, U. *J. Chem. Phys.* **1986**, *85*, 4867.
209. Knopf, C.; Wagler, J.; Brendler, E.; Borrmann, H.; Roewer, G. Z. *Naturforsch., B: Chem Sci.* **2004**, *59b*, 1337–1347.
210. Söldner, M.; Riede, J.; Schier, A.; Schmidbaur, H. *Inorg. Chem.* **1998**, *37*, 601–603.
211. Schuh, H.; Schlosser, T.; Bissinger, P.; Schmidbaur, H. Z. *Anorg. Allg. Chem.* **1993**, *619*, 1347–1352.
212. Ackerhans, C.; Böttcher, P.; Müller, P.; Roesky, H. W.; Usón, I.; Schmidt, H.-G.; Noltemeyer, M. *Inorg. Chem.* **2001**, *40*, 3766–3773.
213. Söldner, M.; Schier, A.; Schmidbaur, H. *Inorg. Chem.* **1997**, *36*, 1758–1763.
214. Heinicke, J.; Mantey, S.; Oprea, A.; Kindermann, M. K.; Jones, P. G. *Heteroatom Chem.* **1999**, *10*, 605–614.
215. Wiberg, E.; Stecher, O.; Neumaier, A. *Inorg. Nucl. Chem. Lett.* **1965**, *1*, 33–34.
216. Wan, Y.; Verkade, J. G. *Inorg. Chem.* **1993**, *32*, 341–344.
217. Huber, G.; Schmidbaur, H. *Monatsh. Chem.* **1999**, *130*, 133–138.
218. Stueger, H.; Lassacher, P. *Monatsh. Chem.* **1994**, *125*, 615–622.
219. Lassacher, P.; Stueger, H.; Hengge, E. *Multifunctional Disilane Derivatives*. In *From Organosilicon Chemistry III: From Molecules to Materials*; Auner, N., Weis, J., Eds.; Wiley: Weinheim, 1999; pp 257–261.
220. Gollner, W.; Kleewein, A.; Renger, K.; Stueger, H. *Synthesis of Linear and Cyclic bis(trimethylsilyl)aminoaligosilanes*. In *Organosilicon Chemistry IV*; Auner, N., Weis, J., Eds.; Wiley: Weinheim, 1998; pp 346–351.
221. Söldner, M.; Schier, A.; Schmidbaur, H. *Inorg. Chem.* **1998**, *37*, 510–515.
222. Wrackmeyer, B.; Frank, S. M.; Herberhold, M.; Simon, A.; Borrmann, H. J. *Chem. Soc., Dalton Trans.* **1991**, 2607–2613.
223. Asay, M.; Jones, C.; Driess, M. *Chem. Rev.* **2011**, *111*, 354–396.
224. Denk, M.; Lennon, R.; Hayashi, R.; West, R.; Belyakov, A. V.; Verne, H. P.; Haaland, A.; Wagner, M.; Metzler, N. J. *Am. Chem. Soc.* **1994**, *116*, 2691–2692.
225. Gehrhus, B.; Lappert, M. F. *Polyhedron.* **1998**, *17*, 999–1000.
226. Gehrhus, B.; Hitchcock, P. B.; Lappert, M. F. Z. *Anorg. Allg. Chem.* **2001**, *627*, 1048–1054.
227. Gehrhus, B.; Hitchcock, P. B.; Jansen, H. J. *Organomet. Chem.* **2006**, *691*, 811–816.
228. Delawar, M.; Gehrhus, B.; Hitchcock, P. B. *Dalton Trans.* **2005**, 2945–2953.
229. Ionescu, E.; Gehrhus, B.; Hitchcock, P. B.; Nieger, M.; Streubel, R. *Chem. Commun.* **2005**, 4842–4844.
230. Tomasiak, A. C.; Mitra, A.; West, R. *Organometallics* **2009**, *28*, 378–381.
231. Denk, M. K.; Hatano, K.; Lough, A. J. *Eur. J. Inorg. Chem.* **1998**, 1067–1070.
232. Moser, D. F.; Naka, A.; Guzei, I. A.; Müller, T.; West, R. *J. Am. Chem. Soc.* **2005**, *127*, 14730–14738.
233. Meltzer, A.; Inoue, S.; Praesang, C.; Driess, M. *J. Am. Chem. Soc.* **2010**, *132*, 3038–3046.
234. Xiong, Y.; Yao, S.; Driess, M. *Organometallics* **2009**, *28*, 1927–1933.
235. Naka, A.; Hill, N. J.; West, R. *Organometallics* **2004**, *23*, 6330–6332.
236. Cui, H.; Shao, Y.; Li, X.; Kong, L.; Cui, C. *Organometallics* **2009**, *28*, 5191–5195.
237. Wang, Y.; Xie, Y.; Wei, P.; King, R. B.; Schaefer, H. F.; von R. Schleyer, P.; Robinson, G. H. *Science* **2008**, *321*, 1069–1071.
238. Sen, S. S.; Jana, A.; Roesky, H. W.; Schulzke, C. *Angew. Chem. Int. Ed.* **2009**, *48*, 8536–8538.
239. Yeong, H.-X.; Lau, K.-C.; Xi, H.-W.; Hwa Lim, K.; So, C.-W. *Inorg. Chem.* **2010**, *49*, 371–373.
240. Tavcar, G.; Sen, S. S.; Roesky, H. W.; Hey, J.; Kratzert, D.; Stalke, D. *Organometallics* **2010**, *29*, 3930–3935.
241. Sen, S. S.; Tavcar, G.; Roesky, H. W.; Kratzert, D.; Hey, J.; Stalke, D. *Organometallics* **2010**, *29*, 2343–2347.
242. Wagler, J.; Brendler, E.; Langer, T.; Pöttgen, R.; Heine, T.; Zhechkov, L. *Chem. Eur. J.* **2010**, *16*, 13429–13434.
243. Cappello, V.; Baumgartner, J.; Dransfeld, A.; Flock, M.; Hassler, K. *Eur. J. Inorg. Chem.* **2006**, 2393–2405.
244. Cappello, V.; Baumgartner, J.; Dransfeld, A.; Hassler, K. *Eur. J. Inorg. Chem.* **2006**, 4589–4599.
245. Tekautz, G.; Baumgartner, J.; Dransfeld, A.; Hassler, K. *Eur. J. Inorg. Chem.* **2007**, 4071–4077.
246. Wittbrodt, J. M.; Schlegel, H. B. *J. Phys. Chem. A.* **1999**, *103*, 8547–8558.
247. Fritz, G.; Scheer, P. *Chem. Rev.* **2000**, *100*, 3341–3402.
248. Driess, M.; Merz, K.; Monsé, C. Z. *Anorg. Allg. Chem.* **2000**, *626*, 2264–2268.
249. Gokhale, S. D.; Jolly, W. L. *Inorg. Chem.* **1964**, *3*, 1141–1143.
250. Gokhale, S. D.; Jolly, W. L. *Inorg. Chem.* **1965**, *4*, 596–597.
251. Norman, A. D. *Chem. Commun.* **1968**, 812–813.
252. Fritz, G.; Becker, G. Z. *Anorg. Allg. Chem.* **1970**, *372*, 180–195.
253. Norman, A. D.; Wingleth, D. C. *Inorg. Chem.* **1970**, *9*, 98–103.
254. Hassler, K.; Katzenbeisser, U. *J. Organomet. Chem.* **1990**, *399*, C18–C20.
255. Müller, L.-P.; Mont, W.-W. D.; Jeske, J.; Jones, P. G. *Chem. Ber.* **1995**, *128*, 615–619.
256. Müller, L.-P.; Zanin, A.; Du Mont, W.-W.; Jeske, J.; Martens, R.; Jones, P. G. *Chem. Ber.* **1997**, *130*, 377–384.
257. Riegel, B.; Pfitzner, A.; Heckmann, G.; Binder, H.; Fluck, E. Z. *Anorg. Allg. Chem.* **1995**, *621*, 1989–1994.
258. Baudler, M.; Pontzen, T.; Schings, U.; Tebbe, K.-F.; Fehér, M. *Angew. Chem.* **1983**, *95*, 803–804.
259. Tebbe, K.-F.; Fehér, M. *Acta Cryst. C.* **1984**, *40*, 1879–1882.
260. Chen, T.; Duesler, E. N.; Paine, R. T.; Nöth, H. *Inorg. Chem.* **1997**, *36*, 1534–1535.
261. Anderson, J. W.; Drake, J. E. *J. Chem. Soc., A.* **1970**, 3131–3134.
262. Drake, J. E.; Goddard, N.; Simpson, J. *Inorg. Nucl. Chem. Lett.* **1968**, *4*, 361–363.

263. Solan, D.; Timms, P. L. *Inorg. Chem.* **1968**, *7*, 2157–2160.
264. Mackay, K. M.; Hosfield, S. T.; Stobart, S. R. *J. Chem. Soc. A.* **1969**, 2937–2942.
265. Kouvetakis, J.; Tice, J.; Fang, Y.-Y. *Novel Methods for Making and Using Halosilylgermanes*. WO2009005862A2, January 8, 2009.
266. Singh, K. K.; Comita, P. B.; Scudder, L. A.; Carlson, D. K. *Silicon-Containing Layer Deposition with Silicon Compounds*. WO2004036631A2, April 29, 2004.
267. Kouvetakis, J.; Ritter, C. J. *Novel Silicon-Germanium Hydrides Which Give Ge-Si Films with Low Dislocation Densities and Surface Roughness and Methods for Synthesis and Use in Deposition, Methods*. WO2007062096A2, May 31, 2007.
268. Hu, C.-W.; Menendez, J.; Tsong, I. S. T.; Tolle, J.; Chizmeshya, A. V. G.; Ritter, C.; Kouvetakis, J. *Appl. Phys. Lett.* **2005**, *87*, 181903.
269. Weng, C.; Kouvetakis, J.; Chizmeshya, A. V. G. *J. Comput. Chem.* **2011**, *32*, 835–853.
270. Chizmeshya, A. V. G.; Ritter, C. J.; Hu, C.; Tice, J. B.; Tolle, J.; Nieman, R. A.; Tsong, I. S. T.; Kouvetakis, J. *J. Am. Chem. Soc.* **2006**, *128*, 6919–6930.
271. Tice, J. B.; Fang, Y.-Y.; Tolle, J.; Chizmeshya, A.; Kouvetakis, J. *Chem. Mater.* **2008**, *20*, 4374–4385.
272. Müller, L.; du Mont, W.-W.; Ruthe, F.; Jones, P. G.; Marsmann, H. C. *J. Organomet. Chem.* **1999**, *579*, 156–163.
273. Timms, P. L.; Ehlert, T. C.; Margrave, J. L.; Brinckman, F. E.; Farrar, T. C.; Coyle, T. D. *J. Am. Chem. Soc.* **1965**, *87*, 3819–3823.
274. Chang, C.-H.; Porter, R. F.; Bauer, S. H. *J. Phys. Chem.* **1970**, *74*, 1363–1367.
275. Hsiao, J.; Su, M.-D. *Organometallics* **2007**, *26*, 4432–4438.
276. Majumder, C.; Kulshreshtha, S. *Phys. Rev. B.* **2004**, *70*, 125416.
277. Sun, Q.; Wang, Q.; Jena, P.; Rao, B.; Kawazoe, Y. *Phys. Rev. Lett.* **2003**, *90*, 245426.
278. Majumder, C.; Kulshreshtha, S. *Phys. Rev. B.* **2004**, *70*, 245426.
279. Majumder, C.; Kulshreshtha, S. *Phys. Rev. B.* **2004**, *69*, 115432.
280. Majumder, C.; Kulshreshtha, S. *Phys. Rev. B.* **2004**, *69*, 75419.
281. Saranin, A.; Zotov, A.; Kuyanov, I.; Kishida, M.; Murata, Y.; Honda, S.; Katayama, M.; Oura, K.; Wei, C.; Wang, Y. *Phys. Rev. B.* **2006**, *74*, 115432.
282. Giju, K. T.; Phukan, A. K.; Jemmis, E. D. *Angew. Chem. Int. Ed.* **2003**, *42*, 539–542.
283. Jemmis, E. D.; Kiran, B. *J. Am. Chem. Soc.* **1997**, *119*, 4076–4077.
284. Oliva, J. M.; Schleyer, P. von R.; Aullon, G.; Burgos, J. I.; Fernandez-Barbero, A.; Alkorta, I. *Phys. Chem. Chem. Phys.* **2010**, *12*, 5101–5108.
285. Kiani, F. A.; Hofmann, M. *J. Mol. Model.* **2005**, *12*, 597–609.
286. Kiran, B.; Anoop, A.; Jemmis, E. D. *J. Am. Chem. Soc.* **2002**, *124*, 4402–4407.
287. Lobreyer, T.; Oeler, J.; Sundermeyer, W.; Oberhammer, H. *Chem. Ber.* **1993**, *126*, 665–668.
288. Lobreyer, T.; Sundermeyer, W.; Oberhammer, H. *Chem. Ber.* **1994**, *127*, 2111–2115.
289. Lickiss, P. D.; Smith, C. M. *Coord. Chem. Rev.* **1995**, *145*, 75–124.
290. Tamao, K.; Kawachi, A. *Silyl Anions*. In Stone, F. G. A., West, R., Hill, A. F., Eds.; *Advances in Organometallic Chemistry*; Academic Press, 1995; Vol. 38, pp 1–58.
291. Belzner, J.; Dehnert, U. *Alkali and Alkaline Earth Silyl Compounds-Preparation and Structure*. In Rappoport, Z. Z., Apeloig, Y., Eds.; Wiley: Chichester, 1998; Vol. 2, pp 779–825.
292. Lerner, H.-W. *Coord. Chem. Rev.* **2005**, *249*, 781–798.
293. Fehér, F.; Krancher, M.; Fehér, M. *Z. Anorg. Allg. Chem.* **1991**, *606*, 7–16.
294. Wieber, S.; Stueger, H.; Walkner, C. *Verfahren Zur Herstellung Metallierter Hydridosilanverbindungen*. DP Appl. Nr. 102010028170.0-44.
295. Gehrhus, B.; Hitchcock, P. B.; Zhang, L. *Angew. Chem., Int. Ed.* **2004**, *43*, 1124–1126.
296. Gehrhus, B.; Hitchcock, P. B.; Pongtavornpinyo, R.; Zhang, L. *Dalton Trans.* **2006**, 1847–1857.
297. Antolini, F.; Gehrhus, B.; Hitchcock, P. B.; Lappert, M. F. *Chem. Commun.* **2005**, 5112–5114.
298. Kornev, A. N. *Russ. Chem. Rev.* **2004**, *73*, 1065–1089.
299. Corey, J. Y. *Chem. Rev.* **2011**, *111*, 863–1071.
300. Corey, J. Y.; Braddock-Wilking, J. *Chem. Rev.* **1999**, *99*, 175–292.
301. Nief, F. *Coord. Chem. Rev.* **1998**, *178–180*, 13–81.
302. Murugavel, R.; Bhattacharjee, M.; Roesky, H. W. *Appl. Organometal. Chem.* **1999**, *13*, 227–243.
303. Boettcher, P.; Roesky, H. W. *Synthesis and Structures of Stable Aminosilanes and Their Metal Derivatives: Building Blocks for Metal-Containing Nitridosilicates*. In *Organosilicon Chemistry IV*; Auner, N., Weis, J., Eds.; Wiley: Weinheim, 2000; pp 317–322.
304. Böttcher, P.; Wraage, K.; Roesky, H. W.; Lanfranchi, M.; Tiripicchio, A. *Chem. Ber.* **1997**, *130*, 1787–1790.
305. Inoue, S.; Epping, J. D.; Irran, E.; Driess, M. *J. Am. Chem. Soc.* **2011**, *133*, 8514–8517.
306. Sakurai, Y.; Shiozaki, H.; Yokoyama, M. *J. Mol. Struct.* **2006**, *766*, 41–47.
307. Cundari, T. R.; Gordon, M. S. *Organometallics* **1992**, *11*, 3122–3129.
308. Takahashi, K.; Lee, V. Y.; Yokoyama, T.; Sekiguchi, A. *J. Am. Chem. Soc.* **2009**, *131*, 916–917.
309. Braunschweig, H.; Colling, M.; Kollann, C.; Merz, K.; Radacki, K. *Angew. Chem. Int. Ed.* **2001**, *40*, 4198–4200.
310. Malisch, W.; Lankat, R.; Seelbach, W.; Reising, J.; Noltemeyer, M.; Piki, R.; Posset, U.; Kiefer, W. *Chem. Ber.* **1995**, *128*, 1109–1115.
311. Stadelmann, B.; Lassacher, P.; Stueger, H.; Hengge, E. *J. Organomet. Chem.* **1994**, *482*, 201–206.
312. Zechmann, A.; Hengge, E. *J. Organomet. Chem.* **1996**, *508*, 227–230.
313. Malisch, W.; Jehle, H.; Moller, S.; Thum, G.; Reising, J.; Gbureck, A.; Nagel, V.; Fickert, C.; Kiefer, W.; Nieger, M. *Eur. J. Inorg. Chem.* **1999**, 1597–1605.
314. Malisch, W.; Jehle, H.; Möller, S.; Saha-Möller, C.; Adam, W. *Eur. J. Inorg. Chem.* **1998**, 1585–1587.
315. Moeller, S.; Jehle, H.; Malisch, W.; Seelbach, W. *Synthesis and Reactivity of Silicon Transition Metal Complexes. 42. Metallo-Silanol and Metallo-Siloxanes. 16. Regiospecific Chlorination and Oxygenation of Pentahydridodisilyl Complexes of Iron and Ruthenium*. In *Organosilicon Chemistry III*; Auner, N., Weis, J., Eds.; Wiley: Weinheim, 1998; pp 267–270.
316. Malisch, W.; Jehle, H.; Lager, M. *Metal-Fragment Substituted Disilanol*. In *Organosilicon Chemistry IV*; Auner, N., Weis, J., Eds.; Wiley-VCH, 2000; pp 437–441.
317. Kuramoto, Y.; Sawai, N.; Fujiwara, Y.; Sumimoto, M.; Nakao, Y.; Sato, H.; Sakaki, S. *Organometallics* **2005**, *24*, 3655–3663.
318. Ebsworth, E. A. V.; Fraser, T. E. *J. Chem. Soc., Dalton Trans.* **1979**, 1960–1964.
319. Ebsworth, E. A. V.; Fraser, T. E.; Henderson, S. G.; Leitch, D. M.; Rankin, D. W. H. *J. Chem. Soc., Dalton Trans.* **1981**, 1010–1018.
320. Ebsworth, E. A. V.; Marganian, V. M.; Reed, F. J. S.; Gould, R. O. *J. Chem. Soc., Dalton Trans.* **1978**, 1167–1170.
321. Michalczyk, M. J.; Calabrese, J. C.; Recatto, C. A.; Fink, M. J. *J. Am. Chem. Soc.* **1992**, *114*, 7955–7957.
322. Hou, Z.; Zhang, Y.; Nishiura, M.; Wakatsuki, Y. *Organometallics* **2003**, *22*, 129–135.
323. Castillo, I.; Tilley, T. D. *J. Am. Chem. Soc.* **2001**, *123*, 10526–10534.
324. Castillo, I.; Tilley, T. D. *Organometallics* **2001**, *20*, 5598–5605.
325. Gossage, R. A. *J. Organomet. Chem.* **2000**, *608*, 164–171.
326. Zakharov, L. N.; Struchkov, Y. T. *J. Organomet. Chem.* **1997**, *536–537*, 65–71.
327. Castillo, I.; Tilley, T. D. *Organometallics* **2000**, *19*, 4733–4739.
328. Radu, N. S.; Hollander, F. J.; Tilley, T. D.; Rheingold, A. L. *Chem. Commun.* **1996**, 2459–2460.
329. Perrin, L.; Maron, L.; Eisenstein, O.; Tilley, T. D. *Organometallics* **2009**, *28*, 3767–3775.
330. Diaconescu, P. L.; Odum, A. L.; Agapie, T.; Cummins, C. C. *Organometallics* **2001**, *20*, 4993–4995.
331. King, W. A.; Marks, T. J. *Inorg. Chim. Acta.* **1995**, *229*, 343–354.
332. Radu, N. S.; Engeler, M. P.; Gerlach, C. P.; Tilley, T. D.; Rheingold, A. L. *J. Am. Chem. Soc.* **1995**, *117*, 3621–3622.
333. Barnea, E.; Eisen, M. S. *Coord. Chem. Rev.* **2006**, *250*, 855–899.



## 1.03 Catenated Compounds – Group 14 (Ge, Sn, Pb)

C Marschner and J Hlina, Technische Universität Graz, Graz, Austria

© 2013 Elsevier Ltd. All rights reserved.

<b>1.03.1</b>	<b>Germanium</b>	84
1.03.1.1	Introduction	84
1.03.1.2	Synthetic Methods	84
1.03.1.3	Reactivity of the Ge–Ge Bond	84
1.03.1.4	Structural Features of the Ge–Ge Bond	84
1.03.1.5	Digermanes	84
1.03.1.5.1	Synthesis by coupling	84
1.03.1.5.2	Synthesis by addition	85
1.03.1.5.3	Functionalized digermanes	87
1.03.1.6	Linear and Branched Oligogermanes	87
1.03.1.6.1	Trigermanes	87
1.03.1.6.2	Tetragermanes	88
1.03.1.6.3	Penta-, hexa-, and higher oligogermanes	88
1.03.1.7	Cyclogermanes	88
1.03.1.7.1	Cyclotrigermanes	88
1.03.1.7.2	Cyclotetragermanes	89
1.03.1.7.3	Cyclopenta- and -hexagermanes	90
1.03.1.7.4	Heterocyclogermanes	90
1.03.1.8	Germanium Cages	91
1.03.1.9	Germanium Clusters	92
1.03.1.10	Polygermanes	95
<b>1.03.2</b>	<b>Tin</b>	96
1.03.2.1	Introduction	96
1.03.2.2	Synthetic Methods	96
1.03.2.3	Reactivity of the Sn–Sn Bond	97
1.03.2.4	Structural Features of the Sn–Sn Bond	97
1.03.2.5	Di- and Oligostannanes	97
1.03.2.5.1	Condensation reactions	97
1.03.2.5.2	Wurtz-type coupling reactions and comparable methods	98
1.03.2.5.3	Derivatives of unsaturated organotin compounds	100
1.03.2.5.4	Di- and oligostannanes as part of transition-metal complexes	101
1.03.2.5.5	Derivatization of di- and oligostannanes	103
1.03.2.5.6	Formation of Sn–Sn bonds via dehydrogenative coupling	103
1.03.2.5.7	Dehydrogenative coupling catalyzed by transition-metal and f-block element complexes	104
1.03.2.6	Polystannanes	104
1.03.2.7	Tin Cages and Clusters	106
<b>1.03.3</b>	<b>Lead</b>	108
1.03.3.1	Introduction	108
1.03.3.2	Synthetic Methods	108
1.03.3.3	Reactivity of the Pb–Pb Bond	108
1.03.3.4	Structural Features of the Pb–Pb Bond	109
1.03.3.5	Diplumbanes	109
1.03.3.5.1	Synthesis	109
1.03.3.6	Oligoplumbanes	110
1.03.3.7	Lead Clusters	111
<b>1.03.4</b>	<b>Conclusion</b>	111
<b>References</b>		112

### 1.03.1 Germanium

#### 1.03.1.1 Introduction

Of all of the group-14 elements, germanium is probably the least well-known. It may be telling that the element was the last of this group to be discovered. Only when the periodic table had been outlined did it become evident that there was something missing between silicon and tin. Even when Winkler finally discovered germanium in 1886,<sup>1,2</sup> little more was done than to establish its existence. Therefore, it may not be surprising that after Winkler's synthesis of the first organogermane, Et<sub>4</sub>Ge, in 1887,<sup>3</sup> 38 years passed before someone else prepared another organogermane. The first compound containing a Ge–Ge bond, Ph<sub>3</sub>GeGePh<sub>3</sub>, was reported in 1925.<sup>4</sup> Voronkov and Abzaeva offer an insightful discussion of organogermanium chemistry up to 1967.<sup>5</sup> More recent reviews of the topic are offered by Baines and Stibbs<sup>6</sup> and especially Amadoruge and Weinert,<sup>7,8</sup> who cover essentially all compounds with Ge–Ge bonds of catenated germanes up to 2007.

#### 1.03.1.2 Synthetic Methods

The number of synthetic methods for the preparation of compounds containing Ge–Ge single bonds is not very high. There are condensation-type reactions such as the Wurtz-type coupling of germyl halides with alkali or alkaline earth metals, the dehydrocoupling of hydrogermanes, or the recently popularized hydrogermylolytic reaction. Because of the relatively high stability of germynes, insertion reactions of germynes into Ge–X bonds constitute another synthetic route. Most recently, the strong interest in the chemistry of unsaturated compounds such as germynes, digermanes, and digermynes has introduced addition reactions to these compounds as yet another method for the preparation of di- and oligogermanes.

Because this chapter is organized by compound types, information concerning synthetic details can be found in the respective sections, though a general overview of preparation methods can be found in [Section 1.03.1.5](#).

#### 1.03.1.3 Reactivity of the Ge–Ge Bond

Compared with C–C and C–H bonds, the Ge–Ge single bond is relatively weak (Ge–Ge 190–210 kJ mol<sup>-1</sup>; Ge–C ca. 255 kJ mol<sup>-1</sup>).<sup>9</sup> As with Si–Si, Sn–Sn, and Pb–Pb bonds, low energy  $\sigma$ – $\sigma^*$  transitions are known for the Ge–Ge bond. In accordance with this, the possible photochemical processes have been reviewed.<sup>10</sup> Several reactions are known to cleave the Ge–Ge bond. Reactions of digermanes with chlorine, bromine, or iodine lead to the formation of triorganylgermanium halides. Reductive cleavage with alkali metals provides a convenient source of germanides. Transition metals (especially Pd) are known to add to Ge–Ge bonds by oxidation, permitting metal-catalyzed additions across unsaturated organic substrates such as alkenes or alkynes. Examples for these and other reactions can be found in the discussion of specific oligo- and polygermanes.

#### 1.03.1.4 Structural Features of the Ge–Ge Bond

A search for Ge–Ge single bonds in the Cambridge Crystallographic Database (Conquest 1.12) yielded 275 hits. Excluding Zintl-type clusters and bonds of divalent Ge atoms to each other left 186 compounds with 399 single Ge–Ge bonds. Bond distances range from 2.320 Å for 2,2,3,3-tetramesitylthiadigermirane (1)<sup>11</sup> to 2.710 Å for hexa-*tert*-butyldigermene (2),<sup>12</sup> with the mean value being 2.482 Å. The latter digermene also features the longest known Ge–C bonds (2.076 Å). The lengths of acyclic Ge–Ge bonds typically lie between 2.40 and 2.50 Å. The review by Amadoruge and Weinert<sup>7</sup> offers a good compilation of structural properties of digermanes.

Whereas all other group-14 elements have stable isotopes with a nuclear spin of 1/2, the nuclear magnetic resonance (NMR)-active germanium nucleus is <sup>73</sup>Ge with a nuclear spin of 9/2 and a natural abundance of 7.73%. In addition, the relative sensitivity ( $1.4 \times 10^{-3}$  compared to 1 for <sup>1</sup>H) and the resonance frequency (17.44 MHz relative to <sup>1</sup>H = 500 MHz) are very low. These facts have limited the popularity of Ge-NMR spectroscopy as a tool for the characterization and study of germanium compounds.<sup>13</sup> To date, most <sup>73</sup>Ge-NMR studies have relied on compounds with high molecular symmetry,<sup>14,15</sup> but the advent of high-field instruments and advanced pulse techniques has allowed for the study of compounds with lower symmetry, as well.<sup>16,17</sup> The principal chemical shift behavior of <sup>73</sup>Ge was found to be similar to that of <sup>29</sup>Si and <sup>117/119</sup>Sn.<sup>16</sup>

As with Si–Si and Sn–Sn bonds,  $\sigma$ -bond electron delocalization is a known phenomenon in Ge–Ge bonds. Similar to the related delocalization of  $\pi$ -electrons in polyenes, catenated chains of the higher group-14 elements display delocalization of binding electrons along segments of the chain, which require the adoption of a distinct (all-*transoid*) spatial orientation. Elongation of the chain thus leads to a higher degree of  $\sigma$ -bond electron delocalization and is correlated with  $\sigma$ – $\sigma^*$  transitions of lower energy (bathochromic shift).<sup>18</sup> Conformational changes caused, for example, by different temperatures (thermochromic behavior) are also factors influencing the degree of electron delocalization. For this reason, UV/vis spectroscopy is an important method for the characterization of compounds containing Ge–Ge bonds.<sup>19–23</sup> Absorption properties of digermanes up to hexagermanes are compiled in the review by Amadoruge and Weinert<sup>7</sup> and are similar to what was found for the analogous oligosilanes.<sup>24</sup> Comparison of the absorption properties of polygermanes<sup>25</sup> with those of polysilanes<sup>26</sup> is somewhat difficult because of different molecular weights. In general, there seems to be a tendency for a slight bathochromic shift in polygermanes when compared with polysilanes with the same substitution pattern.

#### 1.03.1.5 Digermanes

Although digermanes originally were obtained mainly by coupling reactions of monogermanes, several compounds were reported more recently to form in the course of addition reactions to germynes, digermanes, or digermynes.

##### 1.03.1.5.1 Synthesis by coupling

A simple way to obtain digermanes is the reaction of GeX<sub>4</sub> (X = Cl, Br) with Grignard reagents in tetrahydrofuran (THF). While the reaction using a large excess of RMgX in Et<sub>2</sub>O leads to

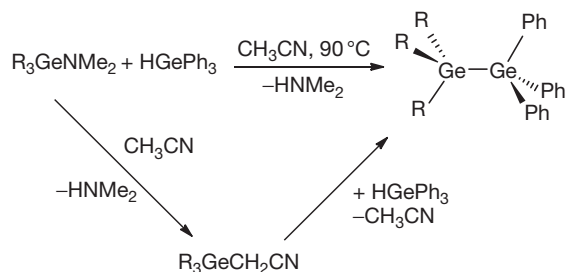
formation of  $R_4Ge$ , the use of THF and excess Mg allows the isolation of substantial amounts of digermanes.<sup>27</sup>

Another popular method for Ge–Ge bond formation is the Wurtz-type coupling. In the presence of a reducing agent, such as an alkali metal, two germylhalides  $R_3GeX$  can be coupled to a symmetrical digermane  $R_3GeGeR_3$ .<sup>28–30</sup> Because of the rather drastic reaction conditions of the Wurtz reaction, the nature of the substituents is mainly restricted to alkyl and aryl groups. However, reaction of  $Ph_2GeBr_2$  (3) with Li amalgam was reported to give digermane  $BrPh_2GeGePh_2Br$  (4) in 60% yield.<sup>31</sup> The Wurtz protocol is, of course, also well suited for intramolecular Ge–Ge bond formation steps leading to cyclic compounds.<sup>32–35</sup> Recently, Wurtz-type coupling with  $SmI_2$  or  $NdI_2$  has emerged as an attractive alternative to the use of alkali metals. The reaction can be conducted under homogeneous conditions and with diminished reduction potential ( $E^\circ Sm(II)/Sm(III) -1.55 V$ ;  $E^\circ Nd(II)/Nd(III) -2.66 V$ ;  $E^\circ M/M(I) -2.9$  to  $-3.0 V$  ( $M = \text{alkali metals}$ )). Using this method, good to excellent yields of digermanes were obtained from the coupling of triorganogermanium chlorides and bromides in THF. Even asymmetric digermanes such as 1,1,1-triethyl-2,2,2-triphenyldigermane (5) or 1,1,1-tributyl-2,2,2-trimethyldigermane (6) could be prepared from the respective chloro- and bromogermanes in good to excellent yields. The method also is suitable for use in the preparation of trigermanes such as  $(Me_3Ge)_2GePh_2$  (7) or even polygermanes.<sup>36</sup> One interesting modification is a protocol that requires only a catalytic amount of  $SmI_2$  and samarium or magnesium metal as reducing agent.<sup>37</sup> Reaction of the Sm adduct of stilbene  $[(PhCHCHPh)Sm(DME)_2]$  with  $Ph_3GeH$  (8) was found to yield  $Ph_3GeGePh_3$  (9).<sup>38</sup> Compared with the use of  $SmI_2$ , the stronger reducing agent  $NdI_2$  was found to be less selective in the formation of digermanes.<sup>39</sup>

As a more finely tuned alternative to the Wurtz-type coupling that also allows access to asymmetric digermanes,<sup>40–44</sup> the use of germyl anions<sup>45</sup> is an option. Several methods are known to obtain anionic germanes, including digermane cleavage,<sup>46–50</sup> deprotonation of hydrogermanes,<sup>41,44,51,52</sup> metal–halogen exchange,<sup>53–56</sup> and transmetalation.<sup>57–59</sup>

Currently, the most versatile reaction for the formation of Ge–Ge bonds is arguably the hydrogermylation reaction, a cross-coupling process of aminogermanes with hydrogermanes (Scheme 1).<sup>60,61</sup>

Weinert<sup>8</sup> recently has studied this reaction in particular depth and demonstrated its high utility. Its inherent asymmetry, combined with a deliberate protection group strategy, makes it a powerful method for the synthesis not only of



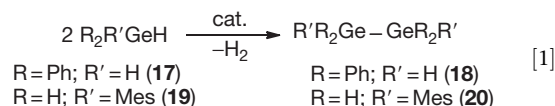
**Scheme 1** Digermane formation via hydrogermylation reaction.

digermanes but also of linear and branched oligogermanes.<sup>8</sup> Mechanistic studies have shown that the aminogermanes first undergo reaction with acetonitrile, leading to  $\alpha$ -germylnitriles as reactive intermediates (Scheme 1).<sup>62,63</sup>

Silylated digermanes were obtained by reaction of the bulky silyl anion  $(Me_3Si)_3SiLi$  with  $R_2GeCl_2$ , leading to the formation of  $(Me_3Si)_3SiGeR_2GeR_2Si(SiMe_3)_3$  with  $R = Cl$  (10),  $Me$  (11), and  $Ph$  (12). The tetrachloro derivative was characterized by single-crystal-structure analysis.<sup>64</sup> The persilylated digermane  $(Me_3Si)_3GeGe(SiMe_3)_3$  (13) was prepared by oxidative coupling of  $(Me_3Si)_3GeM$  ( $M = Li$  (14),  $K$  (15)) with 1,2-dibromoethane<sup>65–67</sup> or  $PbCl_2$ .<sup>68,69</sup>

Reductive coupling of  $GeI_2$  was reported by reaction with  $[M_2(CO)_{10}]^{2-}$  ( $M = Cr, W$ ) to produce  $Na_2\{[(OC)_5M]_2Ge-GeI_2\{M(CO)_5\}}$  (16). The  $[Ph_4P]^+$  salts of these anions, obtained by halide metathesis with  $[Ph_4P]Cl$ , were characterized by x-ray structure analysis.<sup>70</sup>

Dehydrocoupling of hydrogermanes is another attractive alternative to the Wurtz-type coupling because no alkali metals are required and the byproduct is hydrogen instead of alkali-metal halides. Compared to the well-studied area of hydrosilane dehydrocoupling, not much is known about the analogous reaction of hydrogermanes (eqn [1]). An example of an early transition-metal catalyst that refers explicitly to oligomerization is Harrod's reaction of  $Ph_2GeH_2$  (17) with dimethyltitanocene, which was reported to give 1,1,2,2-tetraphenyldigermane (18) in a 90% yield.<sup>71</sup> Employing Wilkinson's catalyst, it was possible to dimerize mesitylgermane (19) in 15% yield to 1,2-dimesityldigermane (20).<sup>72</sup>



### 1.03.1.5.2 Synthesis by addition

Addition reactions to tetramesityldigermene (21), prepared by the photolysis of hexamesitylcyclotrigermane (22) with several reagents and under a variety of conditions, were studied extensively by Baines and coworkers (Scheme 2). Reaction with oxygen cleanly afforded 3,3,4,4-tetramesityl-3,4-digermadi-oxetane (23),<sup>73</sup> whereas the addition of chloroform and acetic acid gave 1,1,2,2-tetramesityl-1-chloro-2-(dichloromethyl) digermane (24)<sup>74</sup> and  $Mes_2HGeGe(OAc)Mes_2$  (25),<sup>75</sup> respectively. Clean addition of  $MeMgBr$  was observed to give 2-methyltetramesityl-digermanylmagnesium bromide (26).<sup>76,77</sup> The latter was found to undergo facile elimination of  $MesMgBr$  to a germylgermylene, to which excess  $MeMgBr$  adds, resulting in the formal exchange of mesityl and methyl groups (27). Addition of  $MeLi$  occurred in a similar way,<sup>76</sup> whereas reaction with an aldehyde led to a 3,4-digermadi-oxetane (28) (Scheme 2).<sup>78</sup>

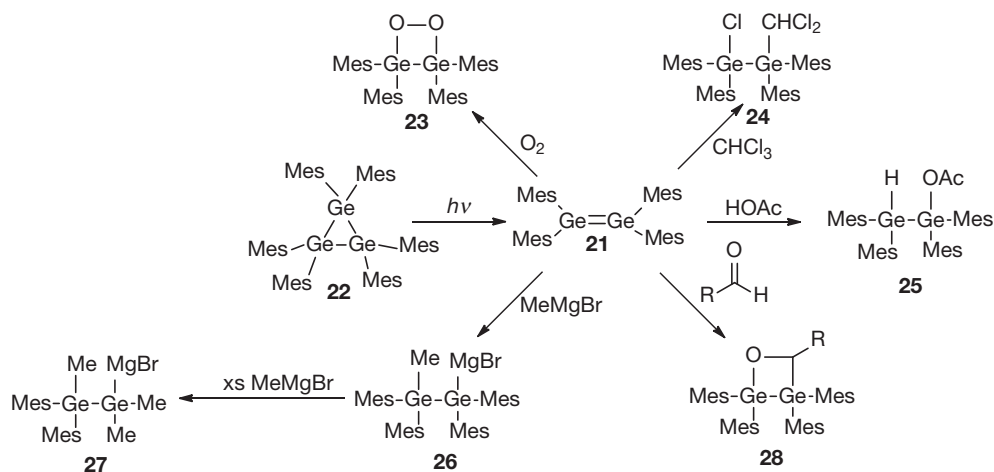
The addition of water or oxygen to Weidenbruch's related digermene,  $Ar_2GeGeAr_2$  [ $Ar = 2,5-(tBu)_2C_6H_3$ ] (29), gave  $Ar_2HGeGe(OH)Ar_2$  (30) or a trigermane-1,3-dioxolane (31), which likely formed by insertion of a germylene into the peroxy bond of the initially formed digermadi-oxetane.<sup>79</sup>

Mochida et al.<sup>80</sup> studied the reactivity of tetraalkyldigermenes (32) obtained by photolysis of 7,8-digermabicyclo[2.2.2]octadienes (33). Reactions with butadienes, carbon tetrachloride, and methanol gave the corresponding digermene-trapping

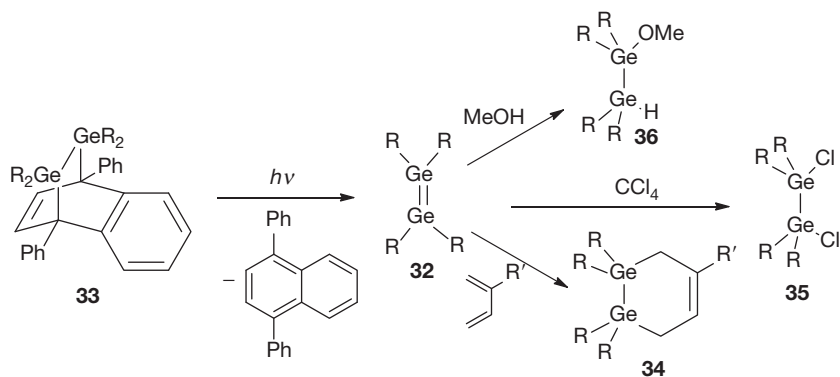
products, 1,2-digermacyclohex-4-enes (34), 1,2-dichlorodigermanes (35), and methoxydigermanes (36), respectively, in good yields (Scheme 3).

Reactions of digermynes have been studied by Power and coworkers.<sup>81</sup> The addition of different amounts of hydrogen to

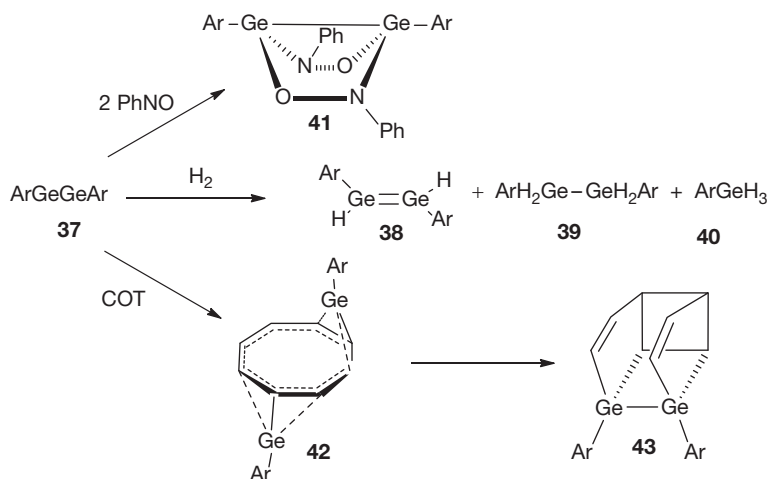
ArGeGeAr (Ar = C<sub>6</sub>H<sub>3</sub>-2,6-(C<sub>6</sub>H<sub>3</sub>-2,6-<sup>i</sup>Pr<sub>2</sub>)<sub>2</sub>) (37) led to mixtures of the respectively hydrogenated digermene (38), digermene (39), and primary germane (40) (Scheme 4). The addition of two equivalents of nitrosobenzene afforded a strained digermene containing a bicyclo[2.2.0]hexane (41) system (Scheme 4).<sup>82</sup>



**Scheme 2** Digermene formation by addition to tetramesityldigermene.



**Scheme 3** Addition reactions of photolytically generated digermenes.



**Scheme 4** Addition reactions to digermynes.

The addition of cyclooctatetraene (COT) gave a Ge(II) inverse sandwich compound (42), which isomerized in solution to a tetracyclic dimerdigermane (43) (Scheme 4).<sup>83</sup>

Reaction of the digermine BbtGeGeBbt (Bbt=2,6-bis[tris(trimethylsilyl)methyl]-4-[tris(trimethylsilyl)methyl]phenyl) (44) with water gave Bbt(HO)<sub>2</sub>GeGeH<sub>2</sub>Bbt (45).<sup>84</sup>

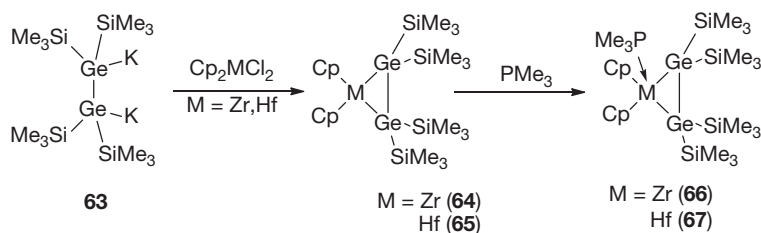
### 1.03.1.5.3 Functionalized digermanes

Digermanes carrying functional groups can be obtained either by dimerization of functionalized monogermanes, by addition reactions of digermenes, or – perhaps most conveniently – by functionalization of alkylated or arylated digermanes.

As is known for the chemistry of the analogous phenylsilanes, phenyl groups of organogermanes can be removed by reaction with strong acids. Ph<sub>3</sub>GeGePh<sub>3</sub> (7) can thus conveniently be reacted with HX (X=Cl, Br)<sup>85,86</sup> or even with Cl<sub>3</sub>CCOOH<sup>87,88</sup> to obtain compounds such as ClPh<sub>2</sub>GeGePh<sub>2</sub>Cl (46),<sup>86</sup> X<sub>2</sub>PhGeGePhX<sub>2</sub> [X=Cl (47), Br (48)],<sup>85</sup> or RPh<sub>2</sub>GeGePh<sub>2</sub>R (R=Cl<sub>3</sub>CCOO) (49),<sup>87,88</sup> which can be converted to ClPh<sub>2</sub>GeGePh<sub>2</sub>Cl (46) by reaction with concentrated HCl.<sup>88</sup> The reaction of Me<sub>3</sub>GeGeMe<sub>3</sub> (50) with one or two equivalents of H<sub>2</sub>SO<sub>4</sub>, followed by treatment with NH<sub>4</sub>Cl, gave Me<sub>3</sub>GeGeMe<sub>2</sub>Cl (51) (76%) or ClMe<sub>2</sub>GeGeMe<sub>2</sub>Cl (52) (95%).<sup>89</sup> The analogous ethyl derivatives Et<sub>3</sub>GeGeEt<sub>2</sub>Cl (53) and ClEt<sub>2</sub>GeGeEt<sub>2</sub>Cl (54) were obtained by reaction of Et<sub>3</sub>GeGeEt<sub>3</sub> (55) with optimized amounts of ECl<sub>4</sub> (E=Ge, Sn).<sup>90</sup>

The stability of the oxidation state (II) for group-14 elements is known to increase with increased atomic weight. GeX<sub>2</sub> is thus fairly stable and, consequently, perhalogenated cyclogermanes of the general formula (GeX<sub>2</sub>)<sub>n</sub> are not known. Even the hexahalo-digermanes Ge<sub>2</sub>Cl<sub>6</sub> (56) and Ge<sub>2</sub>Br<sub>6</sub> (57) are somewhat difficult to prepare and not stable at ambient temperature, disproportionating to GeX<sub>2</sub> and GeX<sub>4</sub>.<sup>85,91,92</sup> While hexabromodigermane (57) is formed in a comparably easy setup of the reaction of GeBr<sub>2</sub> with GeBr<sub>4</sub> in refluxing toluene,<sup>85,91</sup> procedures to prepare hexachlorodigermane (56) require high temperatures, germanium vapor, or microwave discharge conditions.<sup>93,94</sup>

The fact that germanium is slightly more electronegative than silicon, combined with a weaker bond strength, allows facile deprotonation of molecules containing Ge–H bonds with strong bases. Reaction of Me<sub>3</sub>GeGeR<sub>2</sub>H [R=Me (58), Ph (59)] with <sup>t</sup>BuLi/THF gave quantitative yields of the respective lithium digermanyls (60, 61).<sup>95</sup> Two equivalents of Me<sub>3</sub>GeGePh<sub>2</sub>Li (61) reacted with *cis*-PtCl<sub>2</sub>(PMe<sub>2</sub>Ph)<sub>2</sub> in benzene to *trans*-Pt(GePh<sub>2</sub>GeMe<sub>3</sub>)<sub>2</sub>(PMe<sub>2</sub>Ph)<sub>2</sub> (62).<sup>95</sup> Reaction of the dianionic (Me<sub>3</sub>Si)<sub>2</sub>KGeGeK(SiMe<sub>3</sub>)<sub>2</sub> (63) with CpMCl<sub>2</sub> (M=Zr, Hf) gave metallacyclotrigermanes Cp<sub>2</sub>M[(Me<sub>3</sub>Si)<sub>2</sub>GeGe(SiMe<sub>3</sub>)<sub>2</sub>] (64, 65) and Cp<sub>2</sub>M[(Me<sub>3</sub>Si)<sub>2</sub>GeGe(SiMe<sub>3</sub>)<sub>2</sub>]·PMe<sub>3</sub> (66, 67) (Scheme 5).<sup>96</sup>

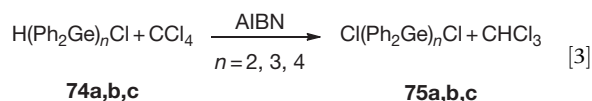
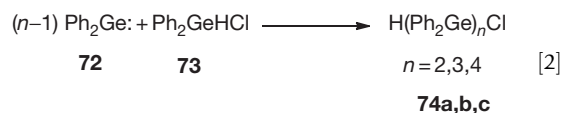


Scheme 5 Metallacyclotrigermane formation.

### 1.03.1.6 Linear and Branched Oligogermanes

While the reaction of PhMgBr with GeCl<sub>4</sub> in THF or ether/toluene is the standard procedure for the preparation of GePh<sub>4</sub> and Ge<sub>2</sub>Ph<sub>6</sub> (7)<sup>27</sup>, it was also found to produce Ge<sub>3</sub>Ph<sub>8</sub> (68) (up to 11%) and Ge<sub>4</sub>Ph<sub>10</sub> (69) (up to 18%) as byproducts when an excess of magnesium was used.<sup>97</sup> Crystal structures of Ge<sub>3</sub>Ph<sub>8</sub> (68) and Ge<sub>4</sub>Ph<sub>10</sub> (69) were determined.<sup>97</sup> The actual Ge–Ge bond-formation steps in these reactions were explained by the transient formation of germyl magnesium compounds such as Ph<sub>3</sub>GeMgCl (70) and Ph<sub>3</sub>GeGePh<sub>2</sub>MgCl (71). Similar behavior was observed in the reaction of GeCl<sub>4</sub> with vinylmagnesium chloride.<sup>98</sup>

Another reaction that leads to the formation of small polygermane chains is the insertion of diphenyl germylene (72) into molecules of the type Cl(Ph<sub>2</sub>Ge)<sub>n</sub>H (74a,b,c). Germylene formation can be achieved from ClPh<sub>2</sub>GeH (73) in the presence of Et<sub>3</sub>N as a base. Optimized conditions led to a mixture of digermane, trigermane, and tetragermane in a ratio of 23/21/36, respectively (eqn [2]). Treatment of the oligomers thus obtained with CCl<sub>4</sub>/2'-azobisisobutyronitrile (AIBN) led to the formation of α,ω-dichlorinated compounds (75a,b,c) (eqn [3]).<sup>99</sup>

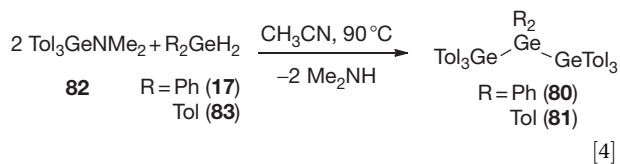


#### 1.03.1.6.1 Trigermanes

Trigermanes Ge<sub>3</sub>Ph<sub>8</sub> (68) and Ge<sub>3</sub>Me<sub>2</sub>Ph<sub>6</sub> (76) were prepared in a selective way by reaction of R<sub>2</sub>GeCl<sub>2</sub> [R=Ph (77), Me (78)] with 2 Ph<sub>3</sub>GeM (M=Li (79a), K (79b)) in yields of 34% and 44%, respectively.<sup>100</sup> Synthesis of the *p*-tolyl (Tol) substituted trigermanes Tol<sub>3</sub>GeGePh<sub>2</sub>GeTol<sub>3</sub> (80) and Tol<sub>3</sub>GeGeTol<sub>2</sub>GeTol<sub>3</sub> (81) was achieved by hydrogermylation reaction of Tol<sub>3</sub>GeNMe<sub>2</sub> (82) with R<sub>2</sub>GeH<sub>2</sub> (R=Ph (17), Tol (83)) (eqn [4]).<sup>87</sup>

The incorporation of the EtOCH<sub>2</sub>CH<sub>2</sub>-substituent into oligogermanes allows the subsequent transformation into hydrogermanes by reaction with DIBAL-H (*vide infra*). With this in mind, the trigermanes (EtOCH<sub>2</sub>CH<sub>2</sub>)<sub>2</sub>R<sub>2</sub>GeGePh<sub>2</sub>GeR<sub>2</sub>(CH<sub>2</sub>CH<sub>2</sub>OEt) [R=Et (84), <sup>n</sup>Bu (85), Ph (86)] and Ph<sub>3</sub>GeGe<sup>n</sup>Bu<sub>2</sub>GePh<sub>2</sub>(CH<sub>2</sub>CH<sub>2</sub>OEt) (77) were prepared utilizing the hydrogermylation reaction.<sup>101</sup>





### 1.03.1.6.2 Tetragermanes

#### 1.03.1.6.2.1 Linear

Tetragermanes  $\text{ToI}_3\text{Ge}(\text{GePh}_2)_2\text{GeTol}_3$  (**88**)<sup>87</sup> and  $\text{Ph}_3\text{GeGe}^n\text{Bu}_2(\text{GeR}_2)_2(\text{CH}_2\text{CH}_2\text{OEt})$  ( $\text{R} = \text{Et}$  (**89**),  $^n\text{Bu}$  (**90**)) have been prepared using a hydrogermylation reaction.<sup>101</sup> The stepwise introduction of  $\text{R}_2\text{Ge}$  units allows the synthesis of linear oligogermanes with a complicated substitution pattern. The way this is accomplished is depicted in Scheme 6. Hydrogenation of the ethoxyethyl-substituted trigermanes (**84**, **85**) with DIBAL-H to the respective hydrogermanes (**91**, **92**) is followed by coupling to the tetragermanes (**89**, **90**).

An  $\alpha,\omega$ -diiodooctaphenyltetragermane (**93**) was obtained from the ring cleavage of octaphenylcyclotetragermane (**94**) with  $\text{I}_2$ .<sup>102,103</sup> Its crystal structure revealed an all-*trans* conformation with Ge–Ge distances of 2.451(1) and 2.459(2) Å.<sup>102</sup>

#### 1.03.1.6.2.2 Branched

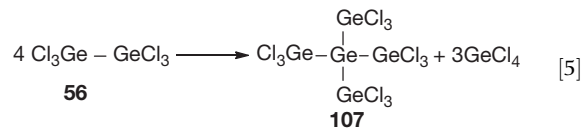
The first branched isotetragermane  $(\text{Ph}_3\text{Ge})_3\text{GeH}$  (**95**) was obtained by reaction of  $\text{Ph}_3\text{GeLi}$  (**79a**) with  $\text{GeI}_2$ . Subsequent deprotonation with  $^n\text{BuLi}$  gave  $(\text{Ph}_3\text{Ge})_3\text{GeLi}$  (**96**), which reacted with methyl iodide to give  $(\text{Ph}_3\text{Ge})_3\text{GeMe}$  (**97**).<sup>104</sup>  $(\text{Ph}_3\text{Ge})_3\text{GePh}$  (**98**) was prepared by hydrogermylation of  $\text{PhGeH}_3$  (**8**) with three equivalents of  $\text{Ph}_3\text{GeCH}_2\text{CN}$  (**99**). A similar process was used to produce  $[(\text{EtOCH}_2\text{CH}_2)^n\text{Bu}_2\text{Ge}]_3\text{GePh}$  (**100**), which was converted to  $(\text{H}^n\text{Bu}_2\text{Ge})_3\text{GePh}$  (**101**) by reduction with DIBAL-H.<sup>105</sup>  $(^n\text{Bu}_3\text{Ge})_3\text{GePh}$  (**102**)<sup>16</sup> and  $(\text{Ph}_3\text{Ge})_3\text{GeH}$  (**95**)<sup>106</sup> were prepared employing hydrogermylation reactions with  $\text{GeH}_4$  and  $\text{PhGeH}_3$ , respectively. In an attempt to obtain the respective germylium ion, compound **95** was converted to the respective halides  $(\text{Ph}_3\text{Ge})_3\text{GeX}$  ( $\text{X} = \text{Cl}$  (**103a**),  $\text{Br}$  (**103b**),  $\text{I}$  (**103c**)) by reaction with  $[\text{Ph}_3\text{C}][\text{PF}_6]$  in  $\text{CH}_2\text{X}_2$  as solvent.<sup>106</sup>

#### 1.03.1.6.3 Penta-, hexa-, and higher oligogermanes

Reaction of  $\text{Ph}_3\text{GeGePh}_2\text{Li}$  (**104**), obtained by deprotonation of  $\text{Ph}_3\text{GeGePh}_2\text{H}$  (**105**) with  $^n\text{BuLi}$ , with  $\text{Ph}_2\text{GeCl}_2$  at  $-65^\circ\text{C}$  in ether yielded  $n\text{-Ge}_5\text{Ph}_{12}$  (**106**) as the main product, in addition to shorter chains.<sup>107</sup>

The only known perhalogenated oligogermane is dodecachloroneopentagermane  $(\text{Cl}_3\text{Ge})_4\text{Ge}$  (**107**), which was reported to crystallize at room temperature from a sample of  $\text{Ge}_2\text{Cl}_6$  (**56**) with one molecule of  $\text{GeCl}_4$  (eqn [5]).<sup>92</sup> This compound can be interpreted as the product of fourfold

insertion of  $\text{GeCl}_2$  into the Ge–Cl bonds of  $\text{GeCl}_4$ . A similar reaction is known for the formation of  $\text{Si}(\text{SiCl}_3)_4$  from  $\text{Si}_2\text{Cl}_6$ .<sup>108</sup>



Not many other examples of neopentagermanes are known. Evidence for the formation of  $(\text{Me}_3\text{Ge})_4\text{Ge}$  (**108**) was first reported by reaction of trimethylgermyllithium (**109**) with  $\text{GeCl}_4$ .<sup>109,110</sup> More recently, preparation of this compound was reported by reaction of trimethylchlorogermane and  $\text{GeBr}_4$  with lithium at low temperature.<sup>111</sup> Reaction of  $(\text{Me}_3\text{Ge})_4\text{Ge}$  (**108**) with  $^t\text{BuOK}$  in the presence of 18-crown-6 gave  $(\text{Me}_3\text{Ge})_3\text{GeK}\cdot 18\text{-crown-6}$  (**110**), which was further converted to a number of oligogermanes such as  $(\text{Me}_3\text{Ge})_3\text{GeH}$  (**111**),  $[(\text{Me}_3\text{Ge})_3\text{Ge}]_2$  (**112**),  $[(\text{Me}_3\text{Ge})_3\text{Ge}]_2\text{GeMe}_2$  (**113**),  $(\text{Me}_3\text{Ge})_3\text{GeSiMe}_3$  (**114**), and  $(\text{Me}_3\text{Ge})_3\text{GeSi}^i\text{Pr}_3$  (**115**) (Scheme 7).<sup>111</sup>

The synthesis of the related isotetragermanyl anion bearing phenylethynyl substituents,  $[(\text{PhCC})_3\text{Ge}]_3\text{GeLi}$  (**116**), was reported by the reaction of a donor-stabilized germylene chloride with three equivalents of  $(\text{PhCC})_3\text{GeLi}$  (**117**).<sup>112</sup>

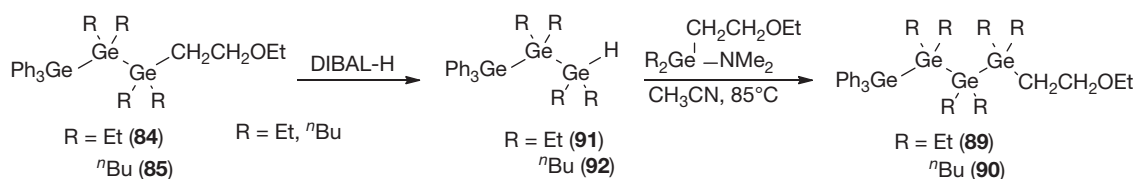
Recently, a stepwise procedure for the construction of oligogermanes was reported to utilize a Lewis acid-catalyzed rearrangement.<sup>113</sup> Starting out from an oligosilane with trimethylgermyl groups (**118**), an  $\text{AlCl}_3/\text{FeCl}_3$ -catalyzed reaction allowed the Ge atoms to migrate to the less-alkylated positions of the molecule (**119**). Successive introduction of additional trimethylgermyl groups via dianion formation and treatment with trimethylchlorogermane (**120**), followed by  $\text{AlCl}_3/\text{FeCl}_3$ -catalyzed rearrangement, led eventually to a molecule with a linear hexagermane segment (**121**) (Scheme 8).<sup>113</sup>

Reaction of  $(\text{H}^n\text{Bu}_2\text{Ge})_3\text{GePh}$  (**101**) (*vide supra*) with  $\text{R}_2(\text{EtOCH}_2\text{CH}_2)\text{GeNMe}_2$  ( $\text{R} = ^n\text{Bu}$  (**122**),  $\text{Et}$  (**123**),  $\text{Ph}$  (**124**)) in acetonitrile led to the respective isoheptagermanes  $[(\text{EtOCH}_2\text{CH}_2)\text{R}_2\text{Ge}^n\text{Bu}_2\text{Ge}]_3\text{GePh}$  ( $\text{R} = ^n\text{Bu}$  (**125**),  $\text{Et}$  (**126**),  $\text{Ph}$  (**127**)).<sup>105</sup> The mobilities of charge carriers of the two dendritic oligogermanes  $[(\text{Me}_3\text{Ge})_2\text{GeMeGeMe}_2]_3\text{GeMe}$  (**128**) and  $[(\text{PhMe}_2\text{Ge})_2\text{GeMeGeMe}_2]_3\text{GeMe}$  (**129**), each containing 13 germanium atoms, were studied.<sup>114</sup>

### 1.03.1.7 Cyclogermanes

#### 1.03.1.7.1 Cyclotrigermanes

The first cyclotrigermane was reported by Masamune in 1982 via the reaction of bis(2,6-dimethylphenyl)germanium dichloride (**130**) with lithium naphthalenide, which gave



Scheme 6 Stepwise elongation of oligogermane chains.



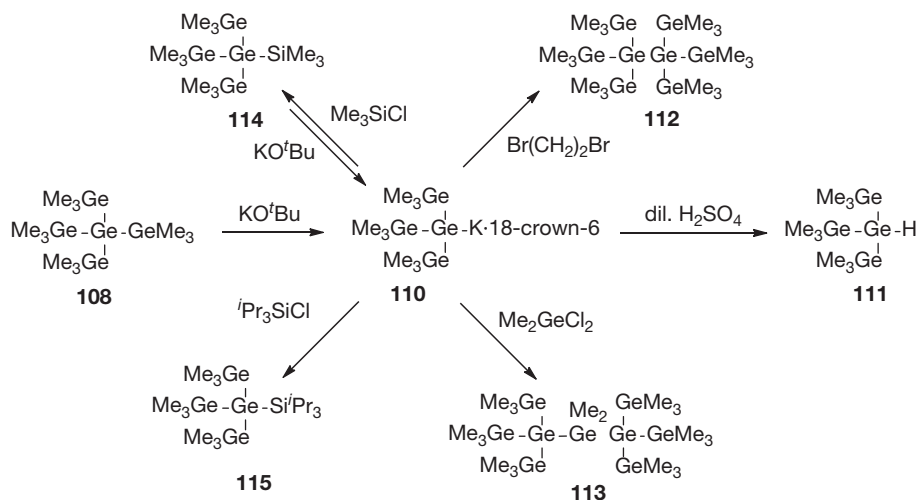
17% of hexakis(2,6-dimethylphenyl)cyclotrigermane (131).<sup>115</sup> The use of Mg/MgBr<sub>2</sub> as a reducing agent allowed the preparation of several cyclo-trigermanes and -tetragermanes from the respective dichlorides in yields from 10% to 62%.<sup>116,117</sup> The first hexaalkylated cyclotrigermane with six bulky *tert*-butyl groups (132) was obtained in 15% yield by reaction of the respective dichloride <sup>t</sup>Bu<sub>2</sub>GeCl<sub>2</sub> (133) with lithium naphthalenide.<sup>118,119</sup> Reaction of (Me<sub>3</sub>Si)<sub>3</sub>GeLi (14) with GeCl<sub>2</sub>-dioxane provided hexakis(trimethylsilyl)cyclotrigermane (134) along with the cyclotetragermane [(Me<sub>3</sub>Si)<sub>3</sub>Ge(Cl)Ge]<sub>4</sub> (135).<sup>120</sup> [(Me<sub>3</sub>Si)<sub>2</sub>Ge]<sub>3</sub> (134) was also prepared by reaction of tris(trimethylsilyl)germanides (14, 15) with bis[bis(trimethylsilyl)amino]germylene (136).<sup>121</sup>

A halide-substituted cyclotrigermane [<sup>t</sup>Bu<sub>3</sub>Si(Cl)Ge]<sub>3</sub> (137)<sup>122,123</sup> was found to be an intermediate in the reaction of GeCl<sub>2</sub>-dioxane with <sup>t</sup>Bu<sub>3</sub>SiNa to yield the first cyclotrigermane (138) (Scheme 9).<sup>124</sup>

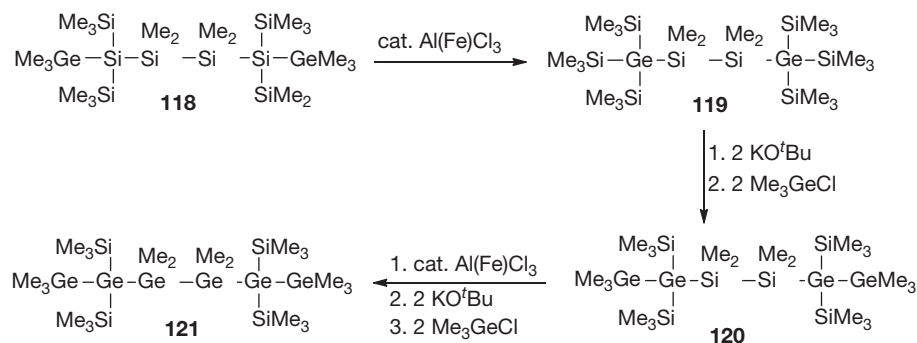
Due to steric overcrowding, 138 could not undergo cyclo-addition reactions; however, replacement of one <sup>t</sup>Bu<sub>3</sub>Si group for mesityl (139) allowed the formation of fused bicyclic cyclotrigermanes 140 and 141 (Scheme 10).<sup>125</sup>

### 1.03.1.7.2 Cyclotetragermanes

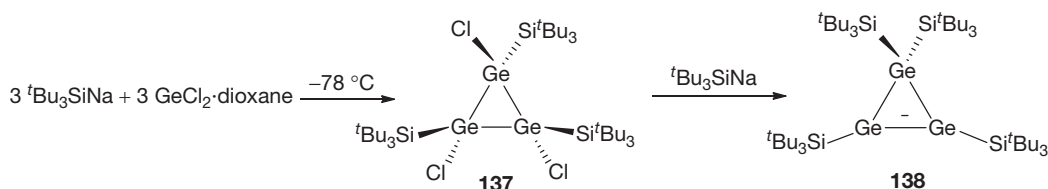
The first example of a four-membered germanium ring, namely octaphenylcyclotetragermane (94), was obtained by reaction of diphenylgermane (17) with stoichiometric amounts of



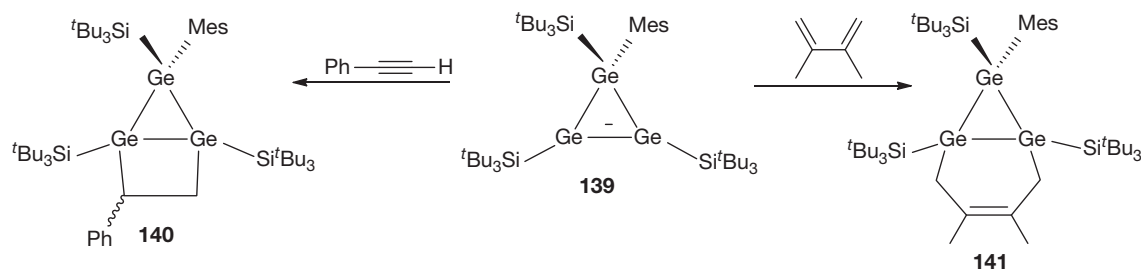
**Scheme 7** Isotetragermanide formation and subsequent derivatization reactions.



**Scheme 8** Stepwise construction of a linear hexagermane chain.



**Scheme 9** Cyclotrigermane formation via an intermediate 1,2,3-trichlorocyclotrigermane.



**Scheme 10** Addition reactions to a cyclotrigermene.

diethylmercury in 35% yield along with some 65% of a polymeric diphenylgermylene.<sup>103,126</sup> Crystal-structure analysis showed an almost planar arrangement of the cyclotetragermane with an average Ge–Ge distance of 2.465 Å.<sup>127</sup>

The formation of octakis(isopropyl)cyclotetragermane (142) was reported as a byproduct in the reaction of GeCl<sub>4</sub> with isopropylmagnesium chloride and lithium aluminum hydride.<sup>128</sup>

The photolysis of decamethylcyclopentagermane (168) proceeded with the generation of dimethylgermylene to give octamethylcyclotetragermane (143).<sup>129,130</sup>

Dehydrochlorination of R<sub>2</sub>ClGeH (R = Et (144), Ph (73)) with DBU (1,8-diazabicyclo[5.4.0]undec-7-ene) led to the formation of the respective germynes, which further reacted to give cyclic compounds (R<sub>2</sub>Ge)<sub>n</sub> (n = 4 (145), 5 (146), 6 (147) for R = Et; n = 4 for Ph (94)) and polymeric material.<sup>131</sup>

Condensations of R(Ph)GeCl<sub>2</sub> (R = <sup>t</sup>Bu (148), CEt<sub>2</sub>Me (149)) with Mg/MgBr<sub>2</sub> in THF produced cyclotetragermanes [R(Ph)Ge]<sub>4</sub> (R = <sup>t</sup>Bu (150), CEt<sub>2</sub>Me (151)), which were converted to [R(Cl)Ge]<sub>4</sub> (R = <sup>t</sup>Bu (152), CEt<sub>2</sub>Me (153)) by treatment with HCl/AlCl<sub>3</sub> or with CF<sub>3</sub>SO<sub>3</sub>H followed by CH<sub>3</sub>COCl.<sup>132</sup>

Reaction of the dianionic Ph<sub>2</sub>LiGeGeLiPh<sub>2</sub> (154) with Et<sub>2</sub>(MeO)GeGe(OMe)Et<sub>2</sub> (155) gave 1,1,2,2-tetraphenyl-3,3,4,4-tetraethylcyclotetragermane (156).<sup>133</sup>

Hepta-*tert*-butylcyclotetragermane (157) was synthesized from 1,2-dichlorotetra-*tert*-butyldigermane (158) by reaction with lithium. Chlorination with CCl<sub>4</sub> gave the corresponding hepta-*tert*-butylchlorocyclotetragermane (159).<sup>134</sup>

Octatolylcyclotetragermane (160) was obtained by the reaction of an *N*-heterocyclic carbene (NHC) adduct of GeCl<sub>2</sub> (161) with TolMgBr.<sup>135</sup>

Octakis(trimethylsilyl)cyclotetragermane (162) was formed by [2+2] cycloaddition of tetrakis(trimethylsilyl)digermene (163).<sup>65,96</sup>

[(Me<sub>3</sub>Si)<sub>3</sub>Si(Cl)Ge]<sub>4</sub> (164) was formed in the reaction of (Me<sub>3</sub>Si)<sub>3</sub>SiLi with GeCl<sub>4</sub>,<sup>68</sup> likely in a manner similar to the formation of [(Me<sub>3</sub>Si)<sub>3</sub>Ge(Cl)Ge]<sub>4</sub> (135)<sup>120</sup> from (Me<sub>3</sub>Si)<sub>3</sub>GeLi (14) and GeCl<sub>2</sub>-dioxane.

In the reaction of the metastable GeBr<sup>136</sup> with NaMn(CO)<sub>5</sub>, the cyclotetragermane Ge<sub>4</sub>Br<sub>4</sub>[Mn(CO)<sub>5</sub>]<sub>4</sub> (165)<sup>137</sup> was obtained as the first example of a cyclogermane with Mn(CO)<sub>5</sub> substituents.

### 1.03.1.7.3 Cyclopenta- and -hexagermanes

With respect to Wurtz-type coupling reactions, the situation for cyclogermanes is similar to that for cyclosilanes. In the reaction of dichlorodiorganogermanes with alkali metals, the steric

demand of the substituent determines the ring size. In the case of small alkyl (methyl, ethyl) or aryl groups, preferentially five- and six-membered rings are formed. Addition of diphenyldichlorogermane to naphthalene/sodium in dimethoxyethane (DME) gave decaphenylcyclopentagermane (166) and dodecaphenylcyclohexagermane (167) in 37% and 17% yield, respectively.<sup>103,126</sup> Wurtz-type coupling of dimethyldichlorogermane with lithium gave a fraction of cyclic germanes consisting of five- (168), six- (169), and seven-membered (170) rings in a ratio of 1/18/1, respectively. Alternatively, the same cyclogermanes can be obtained by redistribution of polymeric dimethylgermylene (171) with naphthalene radical anion in a ratio of 2/20/1, respectively.<sup>138</sup> Crystal structures of decaphenylcyclopentagermane (166)<sup>139</sup> and dodecaphenylcyclohexagermane (167)<sup>140</sup> were determined and exhibited Ge–Ge distances of 2.438–2.473 Å for the five-membered ring and 2.457(1) Å for the six-membered ring.

Analogous reactions of Tol<sub>2</sub>GeCl<sub>2</sub> with lithium, sodium, or sodium/naphthalene led to mixtures of (Tol<sub>2</sub>Ge)<sub>4</sub> (160) and (Tol<sub>2</sub>Ge)<sub>5</sub> (172) in different ratios with the cyclohexagermane (Tol<sub>2</sub>Ge)<sub>6</sub> (173) as a minor byproduct in all cases.<sup>141</sup>

### 1.03.1.7.4 Heterocyclogermanes

A fair number of heterocyclogermanes containing Ge–Ge bonds are known. Several were already mentioned in Section 1.03.1.5.2.

The 1,4-chalcogenacyclohexagermanes Ph<sub>8</sub>Ge<sub>4</sub>O<sub>2</sub> (174) and Ph<sub>8</sub>Ge<sub>4</sub>S<sub>2</sub> (175) were obtained from the reaction of [(Cl<sub>3</sub>CCOO)Ph<sub>2</sub>Ge]<sub>2</sub> (49) with wet acetone and with dry H<sub>2</sub>S, respectively. Conversion of Ph<sub>4</sub>Ge<sub>2</sub>Cl<sub>2</sub> (46) with Na<sub>2</sub>S or NaHSe yielded Ph<sub>8</sub>Ge<sub>4</sub>S<sub>2</sub> (175) and Ph<sub>8</sub>Ge<sub>4</sub>Se<sub>2</sub> (176), while only Ph<sub>6</sub>Ge<sub>3</sub>S<sub>2</sub> (177) or Ph<sub>6</sub>Ge<sub>3</sub>Se<sub>2</sub> (178) but no Ph<sub>6</sub>Ge<sub>3</sub>O<sub>2</sub> could be obtained from analogous reactions with a mixture of Ph<sub>4</sub>Ge<sub>2</sub>Cl<sub>2</sub> (46) and Ph<sub>2</sub>GeCl<sub>2</sub>.<sup>142</sup>

Reactions of 1,4-diiodooctaphenyltetragermane (93) with wet pyridine, Na<sub>2</sub>S, H<sub>2</sub>Se, or NaHTe proceeded to the respective octaphenylchalcogenacyclopentagermanes (X = O (179), S (180), Se (181), and Te (182)) in good yields.<sup>143</sup> Structural characterization of the sulfur compound (180) revealed an envelope conformation with one GePh<sub>2</sub> unit being 0.966 Å above the plane.

Most recently, the groups of Osakada and Braddock-Wilking reported the formation of pallada- (183) and platina- (184) cyclogermanes in the reaction of [(dmpe)PtMe<sub>2</sub>] with Ph<sub>2</sub>GeH<sub>2</sub> (17) via dehydrocoupling chemistry (Scheme 11).<sup>144–146</sup>

### 1.03.1.8 Germanium Cages

Polyhedral compounds of the type  $(RE)_n$  ( $E = \text{Si, Ge, Sn}$ ) have been the subject of interest for some time.<sup>147,148</sup> The simplest examples of this general formula with  $n=2$  are the heavy-element isomers of alkynes. Stable compounds of this type have only recently been prepared for the heavier elements (Si,<sup>149</sup> Ge,<sup>150,151</sup> and Sn<sup>152</sup>). Polyhedral compounds of the formulas  $(RE)_4$ ,  $(RE)_6$ , and  $(RE)_8$  can therefore be considered as the cycloaddition products of alkyne analogs with insufficient steric protection to prohibit the oligomerization process. Precursor molecules of alkyne analogs and polyhedral cages are therefore frequently of the same type:  $\text{REX}_2\text{EX}_2\text{R}$ .

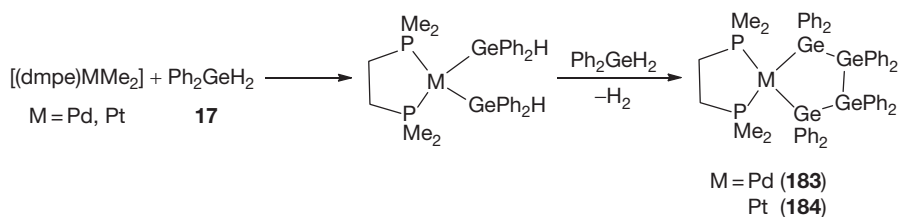
The only known example of a germatetrahedrane (**185**) was synthesized by Wiberg in a way analogous to that previously reported for  $(\text{tBu}_3\text{SiSi})_4$ .<sup>153</sup> Reaction of  $\text{tBu}_3\text{SiGeCl}_2\text{GeCl}_2\text{Si-tBu}_3$  (**186**), obtained from  $\text{GeCl}_4$  and  $\text{tBu}_3\text{SiNa}$ , with  $\text{tBu}_3\text{SiNa}$  in THF yielded tetragermatetrahedrane:  $(\text{tBu}_3\text{SiGe})_4$  (**185**) in 11% yield (Scheme 12).<sup>154</sup> Later, Sekiguchi and coworkers reported that  $(\text{tBu}_3\text{SiGe})_4$  (**185**) can also be prepared by the reaction of  $\text{GeCl}_2$ -dioxane with  $\text{tBu}_3\text{SiNa}$  in THF at room temperature (Scheme 12). The authors noted that the same reaction

stoichiometry leads to tetrakis(tri-*tert*-butylsilyl)cyclotrigermene (**137**) at low temperature.<sup>124</sup>  $(\text{tBu}_3\text{SiGe})_4$  (**185**) was slowly hydrolyzed by water and rapidly oxidized by air.<sup>147</sup>

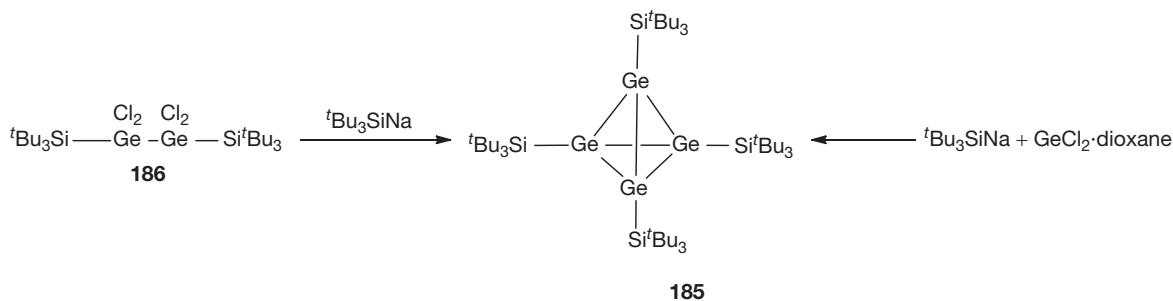
The first hexagermaprismane, hexakis[bis(trimethylsilyl)methyl]tetracyclo[2.2.0.0<sup>2,6</sup>.0<sup>3,5</sup>]hexa-germane (**187**), was reported by Sekiguchi and coworkers to form in the reaction of bis(trimethylsilyl)methyltrichlorogermane (**188**) with Li in THF at  $-78^\circ\text{C}$  (or Mg in THF at  $0^\circ\text{C}$ ) as yellow-orange crystals in 12% (Li) or 24% (Mg) yield (Scheme 13).<sup>147,155</sup> The same group reported another hexagermaprismane, hexakis(2,6-diisopropylphenyl)tetracyclo[2.2.0.0<sup>2,6</sup>.0<sup>3,5</sup>]hexagermane (**189**), again by reductive coupling of the respective trichlorogermane **190** with Mg in THF (Scheme 13).<sup>156,157</sup>

Irradiation of **189** with 360–380 nm light at low temperature produced the hexagerma-Dewar benzene **191**. Excitation of **191** with longer than 460 nm wavelength light or raising the temperature above  $-160^\circ\text{C}$  regenerated **189** (eqn [6]).<sup>147</sup>

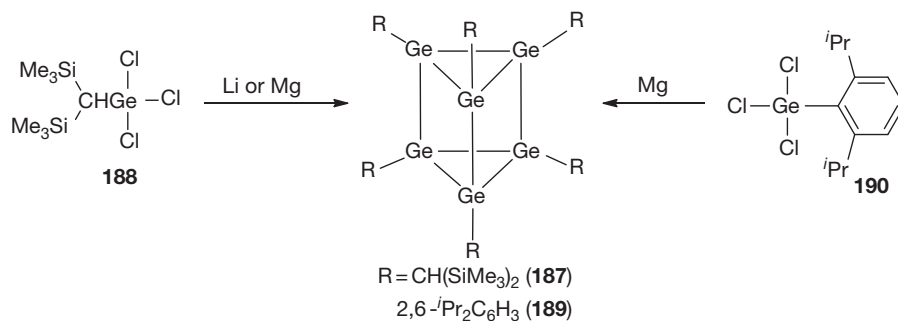
The first octagermacubanes were also prepared by Sekiguchi and coworkers. Reaction of (1-ethyl-1-methylpropyl)trichlorogermane (**192**) with Mg/MgBr<sub>2</sub> in THF provided 3% of octakis



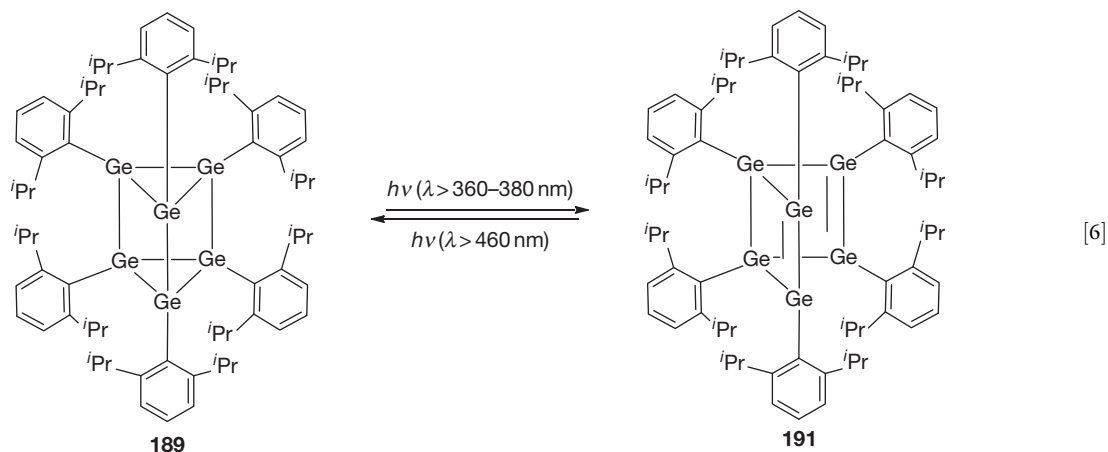
**Scheme 11** Formation of metallacyclopentagermanes by dehydrocoupling of  $\text{Ph}_2\text{GeH}_2$ .



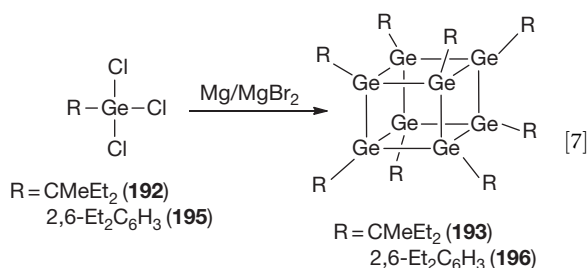
**Scheme 12** Synthetic pathways to tetragermatetrahedrane.



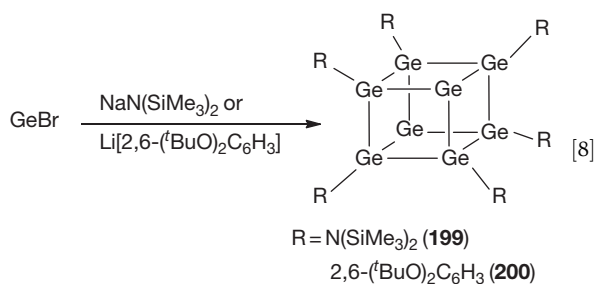
**Scheme 13** Hexagermaprismane formation from different precursors.



(1-ethyl-1-methylpropyl)pentacyclo[4.2.0.0<sup>2,5</sup>.0<sup>3,8</sup>.0<sup>4,7</sup>]octagermane (193) (eqn [7]). This compound was also obtained in a stepwise procedure utilizing 1,2,3,4-tetrachloro-1,2,3,4-tetrakis(1-ethyl-1-methylpropyl)cyclotetragermane (194) as an intermediate.<sup>158</sup> In a similar reaction, (2,6-diethylphenyl)trichlorogermane (195) was coupled with Mg/MgBr<sub>2</sub> to octakis(2,6-diethylphenyl)pentacyclo[4.2.0.0<sup>2,5</sup>.0<sup>3,8</sup>.0<sup>4,7</sup>]octagermane (196) in 1% yield (eqn [7]).<sup>156,158</sup> Matsumoto and coworkers utilized the same protocol to obtain octakis(1,1,2-trimethylpropyl)pentacyclo[4.2.0.0<sup>2,5</sup>.0<sup>3,8</sup>.0<sup>4,7</sup>]octagermane (197) from the coupling of (1,1,2-trimethylpropyl)trichlorogermane (198) with Mg/MgBr<sub>2</sub> in THF in 3% yield.<sup>159</sup>



A completely different route to germacubanes was taken by Schnepf and coworkers. The reaction of GeBr<sub>4</sub> obtained as a metastable compound, with NaN(SiMe<sub>3</sub>)<sub>2</sub>, gave Ge<sub>8</sub>[N(SiMe<sub>3</sub>)<sub>2</sub>]<sub>6</sub> (199) (eqn [8]), a ligand-stabilized germanium cluster with two formally zero-valent Ge atoms.<sup>160</sup> In a similar way, treatment of GeBr<sub>4</sub> with Li[2,6-(<sup>t</sup>BuO)<sub>2</sub>C<sub>6</sub>H<sub>3</sub>] gave a small amount of Ge<sub>8</sub>[2,6-(<sup>t</sup>BuO)<sub>2</sub>C<sub>6</sub>H<sub>3</sub>]<sub>6</sub> (200) in addition to 10% of Ge(Br)[2,6-(<sup>t</sup>BuO)<sub>2</sub>C<sub>6</sub>H<sub>3</sub>]<sub>3</sub> (201) (eqn [8]).<sup>161</sup>



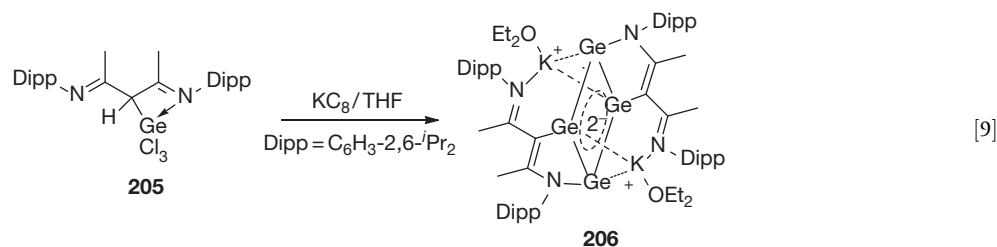
The incompletely substituted octagermanes raise an important question about the oxidation state of germanium atoms in polyhedral compounds. These can be divided into two broad categories: Zintl anions, which have oxidation states below 0, and the ligand-stabilized cage compounds with the general formula Ge<sub>n</sub>R<sub>n</sub> (*n* = 4, 6, 8) just discussed, which have an oxidation state of +1. Schnepf's cubanes and some other clusters, which will be discussed below, feature germanium atoms in a regime between the ligand-stabilized cages (+1) and the elemental state (0).<sup>160</sup>

### 1.03.1.9 Germanium Clusters

Numerous germanium clusters are known. Most of them are Zintl-type ions. Given that a separate chapter of this volume is devoted to Zintl type ions (see **Chapter 1.08**), this section focuses only on germanium clusters that have not been prepared or formed using Zintl anions.

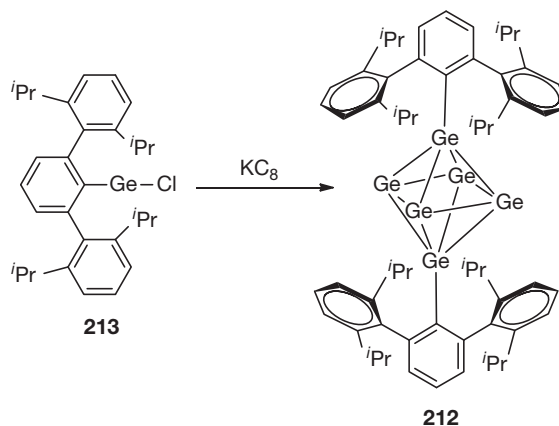
[1.1.1]Propellanes of the heavier group-14 elements [E<sub>5</sub>R<sub>6</sub>] (E = Si, Ge, Sn) have been suggested to possess substantial singlet biradical character.<sup>162</sup> Synthesis of the first pentagerma[1.1.1]propellane (202) was accomplished by Breher and coworkers utilizing either the reaction of hexamesitylcyclotrigermane (22) with lithium and GeCl<sub>2</sub>-dioxane or the reaction of dimesityldichlorogermane (203) with lithium naphthalenide and GeCl<sub>2</sub>-dioxane (**Scheme 14**).<sup>163</sup> While the separation between the two bridgehead atoms of 2.869(2) Å is ~0.45 Å longer than a typical Ge–Ge single bond, the compound was found to be electron paramagnetic resonance (EPR)-silent at ambient temperature and 100 K. However, addition of Me<sub>3</sub>SnH occurred smoothly to give the respective bridgehead stannylated bicyclo[1.1.1]pentagermane (204), indicating at least some biradicaloid character of 202.<sup>163</sup>

In the course of studying the reduction of a β-diketiminato germanium trichloride (205) with KC<sub>8</sub>, Driess and coworkers obtained the dipotassium salt of the first heavy cyclobutadiene-like dianion (206) (eqn [9]) consisting of a Ge<sub>4</sub> core as a side product with a cyclogermylidene (207) and a β-diketiminato Ge(II) amide (208) being the major components.<sup>164</sup> Crystal-structure analysis of 206 indicated that the planar Ge<sub>4</sub> core consists of a parallelogram with Ge–Ge distances of 2.512(1) and 2.553(1) Å and a transannular Ge–Ge distance of 2.747(1) Å.

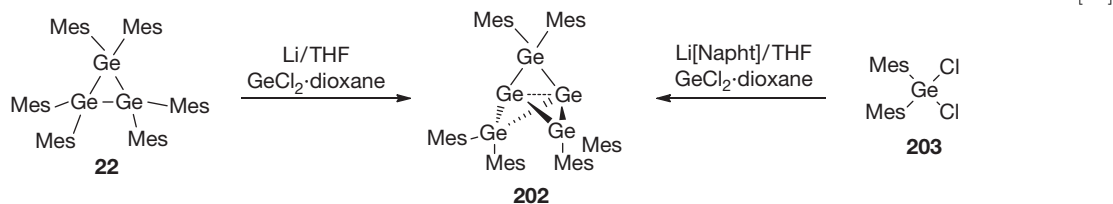


A cationic germanium cluster was reported by Sekiguchi and coworkers. Reaction of tris(tri-*tert*-butylsilyl)cyclotrimergermylium- $\text{TTFPB}^-$  ( $\text{TTFPB}^- = \text{tetrakis}(2,3,5,6\text{-tetrafluorophenyl})\text{borate}$ ) (**209**) with excess potassium iodide in ether was found to give 3-iodo-1,2,3-tris(tri-*tert*-butylsilyl)cyclotrimergermane (**210**), which eventually, converted to 5-iodo-2,4,6,8,9,10-hexakis(tri-*tert*-butylsilyl)heptacyclo[4.4.0.0<sup>1,3</sup>.0<sup>2,5</sup>.0<sup>3,9</sup>.0<sup>4,7</sup>.0<sup>8,10</sup>]decagerman-7-ylum tetrakis(2,3,5,6-tetrafluorophenyl)borate (**211**) (Scheme 15) as air- and moisture-sensitive brown crystals in 37% yield.<sup>165</sup> This  $\text{Ge}_{10}$  cluster is composed of six Ge atoms with  $^t\text{Bu}_3\text{Si}$  groups, one with an iodine substituent and three remaining naked atoms. The distances between these are in a range from 3.2542(15) to 3.2642(15) Å, which is considerably longer than a typical Ge–Ge single bond but is close to the metallic Ge–Ge bond lengths found in Zintl anions such as  $\text{Ge}_9^{3-}$ .<sup>166</sup>

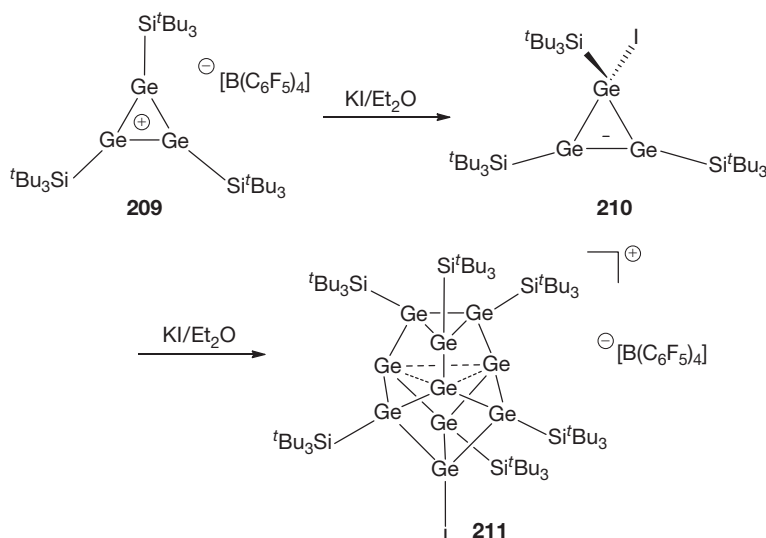
crystallography of **212** showed a structure with a distorted octahedron in which two of the six vertices carry bulky aryl groups. The unsubstituted  $\text{Ge}_4$  atoms comprise an almost perfectly square array that features Ge–Ge distances averaging 2.86(1) Å. The  $\text{Ar}'\text{Ge}$ –Ge distances range from 2.498(2) to 2.546(1) Å.<sup>167</sup>



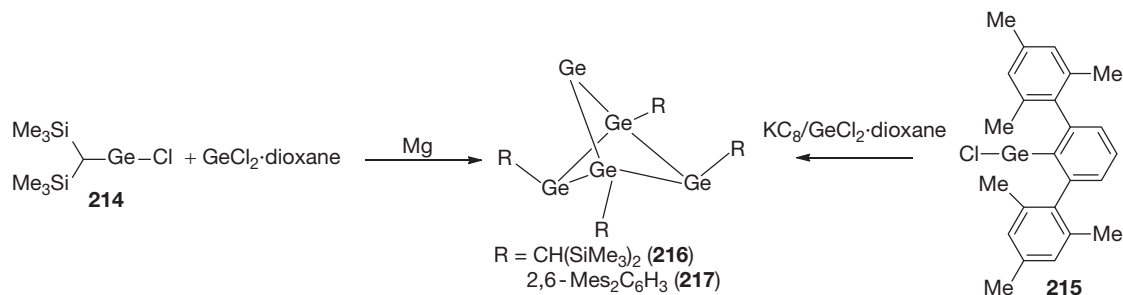
Power and coworkers obtained clusters of the type  $\text{Ge}_6\text{Ar}_2$  with  $\text{Ar} = \text{C}_6\text{H}_3\text{-2,6-Dipp}_2$  ( $\text{Dipp} = \text{C}_6\text{H}_3\text{-2,6-}^i\text{Pr}_2$ ) (**212**) via the reduction of  $\text{Ge}(\text{Cl})\text{Ar}$  (**213**) and  $\text{GeCl}_2$ -dioxane with  $\text{KC}_8$  in THF at room temperature in 40% yield (eqn [10]). X-ray



**Scheme 14** Pentagerma[1.1.1]propellane formation.



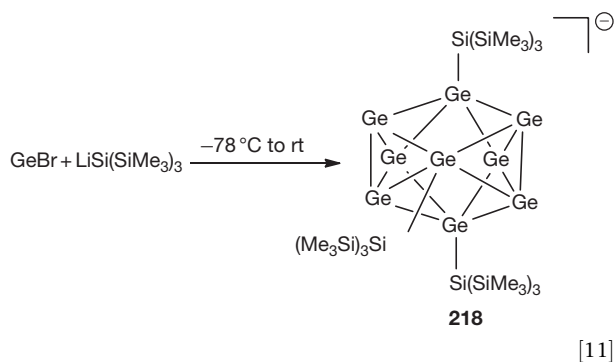
**Scheme 15** Formation of a cationic  $\text{Ge}_{10}$  cluster from a cyclotrimergermylium ion.



**Scheme 16** Formation of bicyclo[1.1.1]tetragermanes containing subvalent Ge atoms.

In a related study, reduction of the slightly less bulky organogermanium(II) halides  $\text{Ge}(\text{Cl})\text{CH}(\text{SiMe}_3)_2$  (**214**) and  $\text{Ge}(\text{Cl})\text{C}_6\text{H}_3\text{-2,6-Mes}_2$  (**215**) in the presence of  $\text{GeCl}_2 \cdot \text{dioxane}$  with Mg and  $\text{KC}_8$ , respectively, afforded the clusters  $\text{Ge}_5\text{R}_4$  [ $\text{R} = \text{CH}(\text{SiMe}_3)_2$  (**216**) and  $\text{C}_6\text{H}_3\text{-2,6-Mes}_2$  (**217**)] (Scheme 16), where an unsubstituted germanium atom caps a butterfly  $\text{Ge}_4\text{R}_4$  array. The bonding in these clusters involves six two-center-two-electron Ge–Ge bonds and a lone pair at the unsubstituted germanium as well as nonbonding electron density at two of the substituted germaniums indicating possible biradical character.<sup>168</sup>

A comprehensive approach toward the preparation of clusters with some degree of partial unsaturation was undertaken by Schnepf and coworkers. As already outlined above in the context of germacubanes, their synthetic strategy involves the use of metastable  $\text{GeBr}$ .<sup>136</sup> Treatment with  $\text{LiSi}(\text{SiMe}_3)_3$  at  $-78^\circ\text{C}$  followed by warming to room temperature gave the Ge cluster anion  $\text{Li}[\text{Ge}_9\{\text{Si}(\text{SiMe}_3)_3\}_3]$  (**218**) (eqn [11]).<sup>169</sup> Single-crystal x-ray diffraction analysis showed the cluster to be a tricapped trigonal prism with only three of the nine Ge atoms bound to a ligand. The Ge–Ge bonds between naked Ge atoms



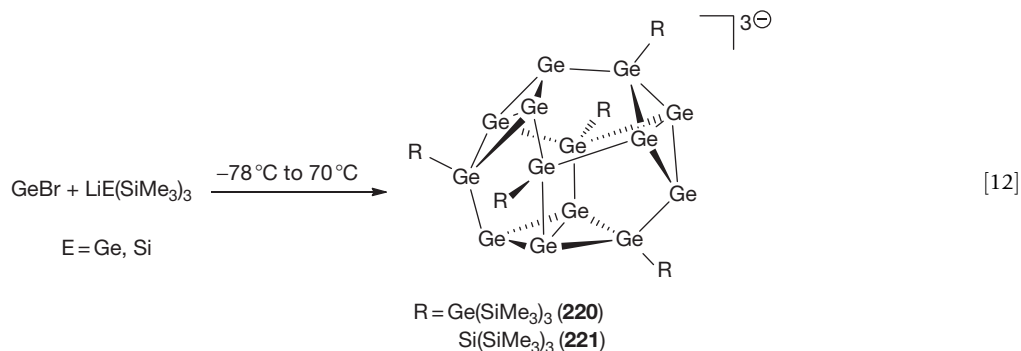
are, at  $2.67 \text{ \AA}$ , longer than the bonds between the naked and the ligand-bound Ge atoms ( $2.53 \text{ \AA}$ ). This behavior is different from Zintl anions, where the Ge atoms with higher coordination numbers form longer Ge–Ge bonds.<sup>169</sup>

An investigation concerning the behavior of **218** in the gas phase after electrospray ionization allowed the observation of the anions  $[\text{Ge}_9]^-$  and  $[\text{Ge}_9\text{Si}]^-$ . Considering that the formation of  $[\text{Ge}_9]^-$  from **218** can be interpreted as a formal reduction process and that  $[\text{Ge}_9]^-$  can also be generated from Zintl anions  $[\text{Ge}_9]^{n-}$  via a formal oxidation process, these experiments link the solid-state chemistry of Zintl anions to the molecular chemistry of metalloids clusters.<sup>170</sup>

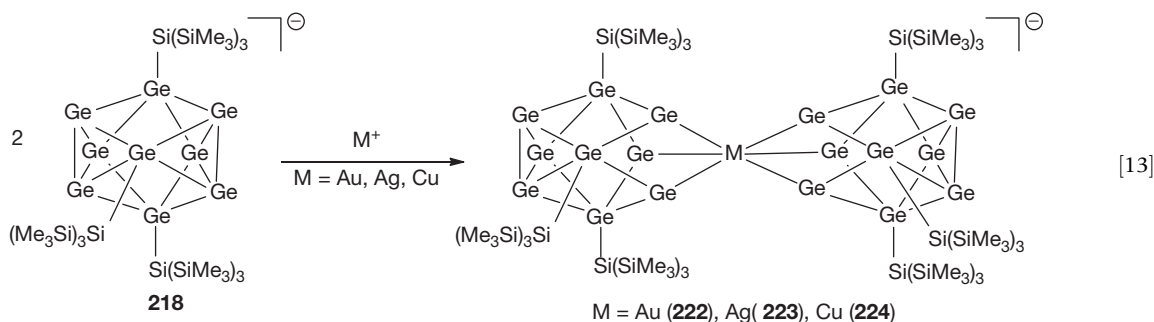
Compound **218** was also found in the reaction of the metastable  $\text{GeCl}$  with  $\text{LiSi}(\text{SiMe}_3)_3$ . In addition,  $\{\text{Ge}_{10}\text{Si}[\text{Si}(\text{SiMe}_3)_3]_4[\text{Si}(\text{SiMe}_3)_2\text{Me}]^-\}$  (**219**) was also found, in which 10 germanium atoms and one silicon atom constitute the cluster core. Although an anionic cluster, the structure of **219** is remarkably similar to Sekiguchi's cationic cluster **211**.<sup>165</sup> Both structures can be described as a distorted part of the solid-state structure of  $\alpha$ -germanium.<sup>171</sup>

Even larger clusters were found by reaction of  $\text{GeBr}$  with  $\text{LiGe}(\text{SiMe}_3)_3$  (**14**) and subsequent heating to  $70^\circ\text{C}$  giving  $\text{Ge}_{14}[\text{Ge}(\text{SiMe}_3)_3]_5[\text{Li}(\text{THF})_2]_3$  (**220**), in which 14 germanium atoms form a hollow sphere (eqn [12]).<sup>172</sup> The isostructural  $\text{Ge}_{14}[\text{Si}(\text{SiMe}_3)_3]_5[\text{Li}(\text{THF})_2]_3$  (**221**) was formed with  $\text{LiSi}(\text{SiMe}_3)_3$ .<sup>173</sup> Both clusters are remarkable in the sense that they open up possibilities for the formation of fullerene-like structures composed of germanium.

$\text{Li}[\text{Ge}_9\{\text{Si}(\text{SiMe}_3)_3\}_3]$  (**218**)<sup>169</sup> was found to react with  $[\text{ClAu}(\text{PPh}_3)]$  to  $[\text{Li}(\text{THF})_6][\{\text{Me}_3\text{Si}\}_3\text{Ge}_{18}\text{Au}]$  (**222**) (eqn [13]).<sup>174</sup> In the anionic structure, the gold atom bridges two  $[\text{Ge}_9\{\text{Si}(\text{SiMe}_3)_3\}_3]^-$  units, coordinating to six germanium atoms. This bonding leads to a significant distortion of the cluster arrangement compared to **218**. The bond lengths between gold-bound







germanium atoms in **222** are elongated by 0.28 Å from 2.68 Å in **218** to 2.96 Å. The other Ge–Ge bond lengths in the Ge<sub>9</sub> clusters are essentially undistorted.<sup>174</sup> Further reactions of **218** with Ag<sup>+</sup> and Cu<sup>+</sup> salts of weakly coordinating anions led to the isostructural compounds [Li(THF)<sub>6</sub>][{(Me<sub>3</sub>Si)<sub>3</sub>Ge<sub>18</sub>Ag}] (**223**) and [Li(THF)<sub>6</sub>][{(Me<sub>3</sub>Si)<sub>3</sub>Ge<sub>18</sub>Cu}] (**224**).<sup>175</sup>

In order to obtain neutral clusters of this type, **218** was treated with ZnCl<sub>2</sub>, CdCl<sub>2</sub>, and HgCl<sub>2</sub> and the isostructural clusters [Si(SiMe<sub>3</sub>)<sub>3</sub>Ge<sub>18</sub>M] (M = Zn (**225**), Cd (**226**), Hg (**227**)) were obtained.<sup>176</sup>

Reaction of **218** with Cr(CO)<sub>5</sub>(COE) (COE = cyclooctene) gave [Ge<sub>9</sub>{Si(SiMe<sub>3</sub>)<sub>3</sub>Cr(CO)<sub>5</sub>}<sup>−</sup> (**228**), in which the tri-capped trigonal prismatic arrangement of **218** is changed to a mono-capped square antiprism. The capping germanium atom and two opposite germanium atoms of the open square carry the Si(SiMe<sub>3</sub>)<sub>3</sub> ligand with a third Ge atom of the open square coordinating to the Cr(CO)<sub>5</sub> fragment.<sup>177</sup> If, instead of Cr(CO)<sub>5</sub>(COE), Cr(CO)<sub>3</sub>(CH<sub>3</sub>CN)<sub>3</sub> was reacted with **218**, another cluster compound Ge<sub>9</sub>[Si(SiMe<sub>3</sub>)<sub>3</sub>Cr(CO)<sub>3</sub>] (**229**) was isolated, in which the Cr atom was incorporated into the cluster core that can be described as a bicapped square antiprism, where three germanium atoms are bound to Si(SiMe<sub>3</sub>)<sub>3</sub> ligands and the chromium atom still carries the three CO ligands.<sup>177</sup>

The preparation of another transition-metal-substituted germanium cluster was accomplished in a manner related to the synthesis of Ge<sub>4</sub>Br<sub>4</sub>[Mn(CO)<sub>5</sub>]<sub>4</sub> (**165**)<sup>137</sup> as outlined above. Instead of NaMn(CO)<sub>5</sub>, Collman's reagent Na<sub>2</sub>[Fe(CO)<sub>4</sub>] was reacted with GeBr<sub>3</sub><sup>136</sup> to obtain a cluster compound (**230**) consisting of a Ge<sub>10</sub> framework in which eight of the ten Ge atoms are bound to Fe(CO)<sub>4</sub> ligands (Ge–Fe: 2.43 Å). The Fe(CO)<sub>4</sub> ligands are further bound to six Na cations, each of which is coordinated to three THF molecules. The cluster core thus consists of a distorted cube of eight GeFe(CO)<sub>4</sub> units with two of the six faces capped by naked germanium atoms, which are directly bound to each other.<sup>178</sup>

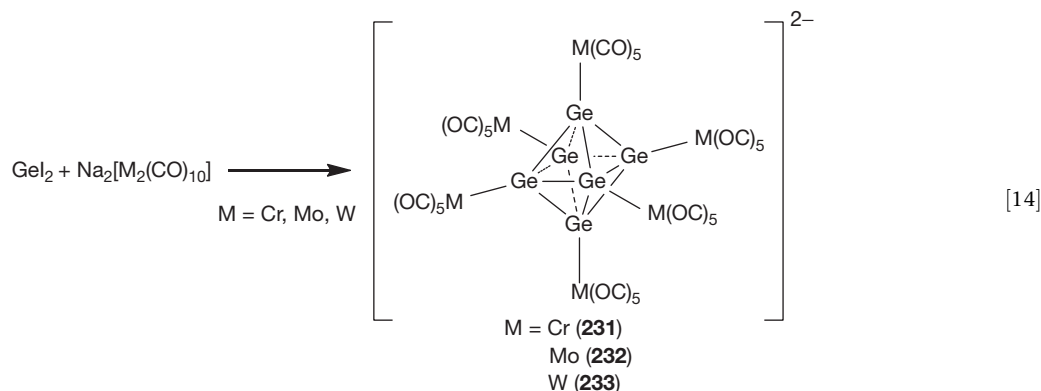
Octahedral Ge clusters with six attached M(CO)<sub>5</sub> (M = Cr, Mo, W) fragments of the type [(OC)<sub>5</sub>M]<sub>6</sub>Ge<sub>6</sub>]<sup>2−</sup> (M = Cr (**231**), Mo (**232**), W (**233**)) were isolated as crystalline [Ph<sub>4</sub>P]<sup>+</sup> salts by the reaction of Na<sub>2</sub>[M<sub>2</sub>(CO)<sub>10</sub>] with GeI<sub>2</sub> in the presence of bipyridine (eqn [14]).<sup>179,180</sup>

### 1.03.1.10 Polygermanes

While the methods for the synthesis of polymers with catenated germanium atoms in the main chain are quite similar to those of the related polysilanes, the interest in polygermanes was always significantly lower.<sup>25</sup> This may be explained by the high cost of germanium when compared to silicon, the difficulties involved in obtaining reliable structural insight into the electronic situation of the main chain, and the prevalent assumption that germanium behaves very much like silicon anyway.

In this sense, it is not surprising to find the Wurtz-type coupling of diorganogermanium dihalides with alkali metals to be the preferred method for the synthesis of polygermanes.<sup>19,181,182</sup> A modification using Sml<sub>2</sub> as a reducing agent gave polymers of relatively low molecular weight (M<sub>w</sub> = 2380–4890) in modest yields.<sup>36</sup>

Reports about dehydrogenative polymerization of phenylgermane are somewhat contradictory. Phenylgermane (**8**) and diphenylgermane (**17**) are both said to show greater activity toward dehydrocoupling with dimethyltitanocene than their silicon analogs. However, while PhGeH<sub>3</sub> (**8**) was reported to polymerize to a three-dimensional gel with dimethyltitanocene and to undergo stepwise oligomerization with vanadocene, Ph<sub>2</sub>GeH<sub>2</sub> (**17**) only dimerized with dimethyltitanocene. Further reaction of **17** with dimethyltitanocene eventually led to a purple product, which is a more powerful catalyst to oligomerize Ph<sub>2</sub>GeH<sub>2</sub> (**17**), with octaphenyltetragermane (**234**) being the main product.<sup>71</sup> Reactions of PhGeH<sub>3</sub> (**8**) utilizing the catalyst systems Cp<sub>2</sub>ZrCl<sub>2</sub>/2<sup>n</sup>BuLi and CpCp\*ZrCl<sub>2</sub>/2





source concerning the major synthetic methods to form Sn–Sn bonds and the characteristics of these catenates.<sup>198</sup> The early chemistry of organotin compounds (up to the late 1960s) is covered by the outstanding work of Voronkov and Abzaeva.<sup>5</sup>

The chemistry of catenated compounds of tin is dominated by organo-substituted systems. Recent developments dealing with catenates without C–Sn-bonds are comparatively rare and limited to distannanes. There is a broad variety of synthetic methods concerning the formation of Sn–Sn bonds. The most important starting materials are tin halides and hydrides. Basic synthetic pathways include Wurtz-type coupling reactions of halostannanes as well as their conversions with metalated stannanes. Various condensation reactions are known for tin hydrides with tin halides, -amides, -oxides, and -alkoxides. The major advantage of organotin hydrides is that the Sn–H bond can undergo facile homolytic and heterolytic cleavage. Catalytic methods also profit from this advantage, allowing dehydrogenative coupling of tin hydrides to form catenates ranging from di- to polystannanes. A review by Davies covers recent developments in the chemistry of organotin hydrides.<sup>197</sup> Another way to form Sn–Sn bonds is the insertion of Sn(II) reagents into tin-element bonds.<sup>206–209</sup> While many reactions are considered to involve transient organostannylenes (*vide infra*), cases of explicit employment of this reagent type toward synthesis of oligostannanes are rare.<sup>209</sup> Catenates derived from systems with Sn–Sn multiple bonds are mostly limited to short chains, particularly distannanes, and represent results of investigations on the reactivity of distannenes and distannynes (*vide infra*).

### 1.03.2.3 Reactivity of the Sn–Sn Bond

The Sn–Sn bond is comparably weak (Sn–Sn ca. 105–145 kJ mol<sup>-1</sup>; Sn–C ca. 193 kJ mol<sup>-1</sup>),<sup>9</sup> allowing a large spectrum of cleavage reactions. Hexaalkyldistannanes can be reductively cleaved with alkali metals (Li,<sup>210–212</sup> Na,<sup>213–217</sup> K,<sup>210,218,219</sup> and Cs<sup>220</sup>), as well as with some alkaline earth metals (Ca,<sup>221,222</sup> Sr,<sup>221</sup> and Ba<sup>221</sup>). Further cleavage of Sn–Sn bonds via insertion of oxygen<sup>223–227</sup> and its heavier congeners (S,<sup>223,224,226,228–232</sup> Se,<sup>223,224,226,228,229,233</sup> and Te,<sup>223,224,226,228,234</sup>), usually at elevated temperatures or with photo-induction, is also known. Reaction with bromine<sup>235–237</sup> and iodine<sup>225,226,235,236,238–243</sup> can also break Sn–Sn bonds.

Distannanes can also undergo oxidative addition with transition-metal complexes, representing a key step in catalytic cycles of some transition-metal-catalyzed stannylation reactions.<sup>244–252</sup> The low Sn–Sn bond energy is a major advantage in organic synthesis in that it allows the introduction of stannyl groups under mild conditions, but represents a significant drawback with respect to the stability of larger catenates, that is, polystannanes.

### 1.03.2.4 Structural Features of the Sn–Sn Bond

A search for Sn–Sn single bonds in the Cambridge Crystallographic database (Conquest 1.12) yielded 224 hits. Excluding Zintl-type clusters and bonds to divalent Sn atoms left 148 compounds with 398 single Sn–Sn bonds. Bond distances range from 2.588 Å for the tris(triphenylstannyl)stannyl cation<sup>253</sup> to 3.423 Å for a pentastanna[1.1.1]propellane,<sup>254</sup>

with the mean value being 2.88 Å. Typically, the length of acyclic Sn–Sn bonds of neutral compounds lies between 2.74 and 3.03 Å.

The NMR spectroscopy of Sn was recently reviewed by Wrackmeyer<sup>255</sup> and Davies.<sup>199</sup> In contrast to Ge, discussed in Section 1.03.1.4, there are three Sn nuclei with spin of 1/2 that are potentially suitable for NMR spectroscopy: <sup>115</sup>Sn, <sup>117</sup>Sn, and <sup>119</sup>Sn. For several reasons, the <sup>119</sup>Sn nucleus is preferably observed in both the liquid and the solid state; nevertheless, the <sup>117</sup>Sn isotope also shows suitable properties. Chemical shifts of <sup>119</sup>Sn cover a range from ca. +4000 to –2500 ppm, referenced against the <sup>119</sup>Sn chemical shift of tetramethylstannane (<sup>119</sup>Sn(Me<sub>4</sub>Sn) = 0 ppm).

As solid-state Sn NMR spectroscopy became more easily available and structure determination via x-ray diffraction became more common, the use of <sup>119</sup>Sn Mössbauer spectroscopy decreased extensively.<sup>199</sup> Mössbauer parameters (isomeric shift (IS), quadruple coupling (QC), and magnetic hyperfine splitting) provide interesting information when discussing certain structural situations such as Sn-clusters. Extensive use in the past led to a vast amount of data for comparison.<sup>256,257</sup>

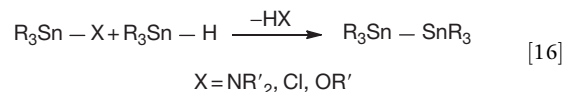
Especially for larger Sn-catenates, that is, polystannanes, UV/vis spectroscopy is of significant importance.<sup>209</sup> The UV/vis absorption bands mainly depend on the orientation and length of the catenates as well as the substituents and range from 210 nm<sup>258</sup> to more than 500 nm.<sup>259</sup>

### 1.03.2.5 Di- and Oligostannanes

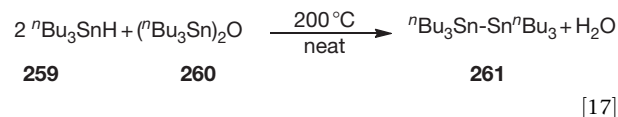
The chemistry of catenated tin compounds is dominated by distannanes, R<sub>3</sub>SnSnR<sub>3</sub>. Their extensive use in organic chemistry, especially of hexa-*n*-butyldistannane, and interest in organotin building blocks led to the development of several synthetic approaches to distannanes. Most of these methods are not limited to distannanes and can also be employed to form larger catenates.

#### 1.03.2.5.1 Condensation reactions

Sn–Sn bonds can be formed by condensation reactions of organotin hydrides with organotin-electrophiles (amides, halides, oxides, and alkoxides) (eqn [16]).<sup>200,226,238,260–264</sup>

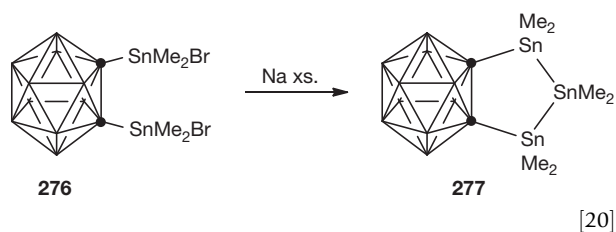


A recent reinvestigation of the reaction of tri-*n*-butyltinhydride (259) with bis(tri-*n*-butyltin)oxide (260) in neat mixtures at elevated temperatures yielded hexa-*n*-butyldistannane (261) quantitatively (eqn [17]).<sup>265–267</sup>

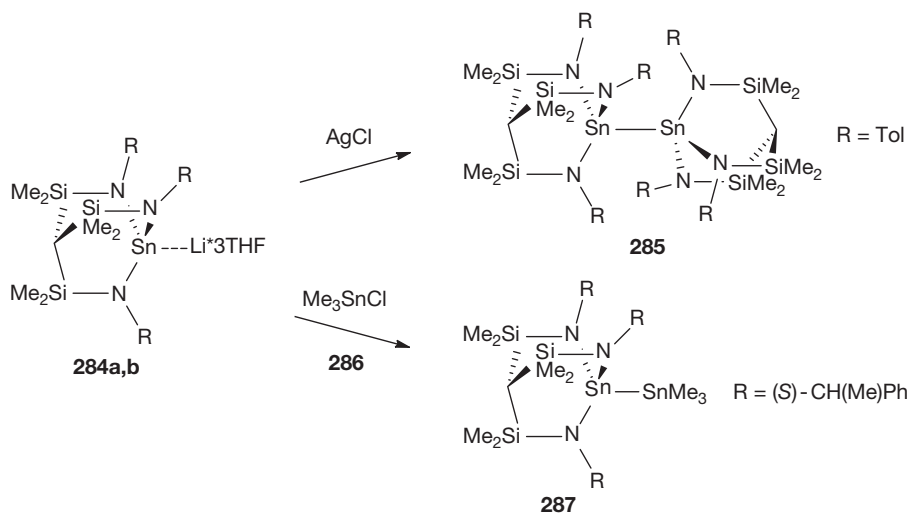


Sita and coworkers presented a synthetic protocol allowing a controlled stepwise build-up of linear oligostannanes using tin amides.<sup>260</sup> The method involves Sn–Sn bond formation via reaction of an organotin hydride (259) with Me<sub>2</sub>N<sup>n</sup>Sn<sup>n</sup>Bu<sub>2</sub>(CH<sub>2</sub>)<sub>2</sub>OEt (262) to give 65% of the

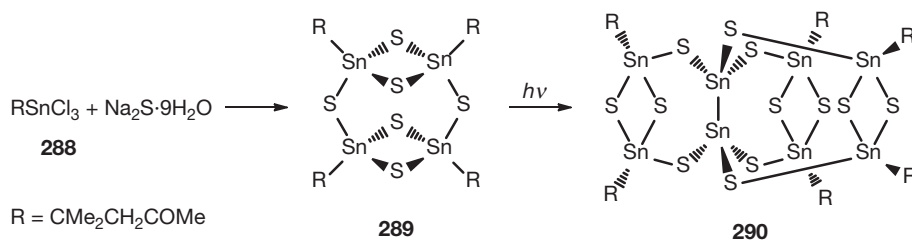




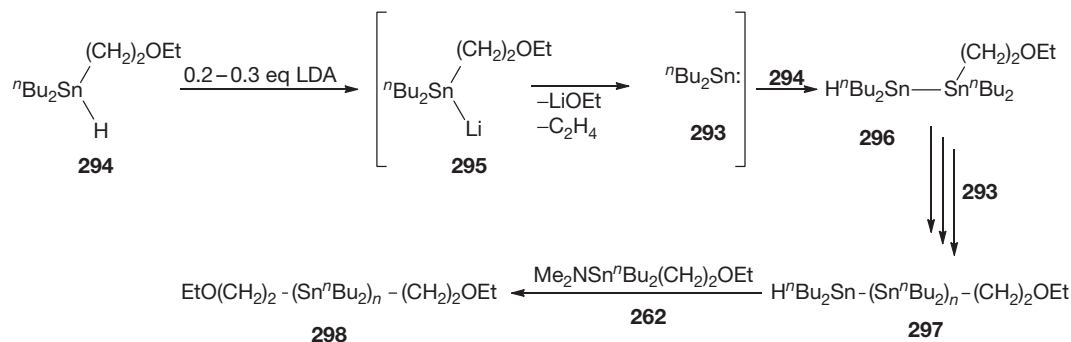
The reaction of *n*-butyldichloro-[2-(*N,N*-dimethylamino)phenyl]stannane (278), bearing a penta-coordinated tin atom, with potassium formed a distannane (279) in 65% yield,<sup>224,230</sup> while treatment of diorganotin dichlorides with alkali metals generally results in formation of oligomers and polymers.



**Scheme 18** Coupling reactions of a triaminostannide to distannanes.



**Scheme 19** Thiostannate embedded distannane cluster.



**Scheme 20** Oligostannane formation by stannylene insertion into Sn–H bond.

A metalated derivative of a cyclotetrastannane (<sup>t</sup>Bu<sub>2</sub>Sn)<sub>3</sub>Sn (<sup>t</sup>Bu)MgCl (280) was found to be accessible via treatment of Cl-(<sup>t</sup>Bu<sub>2</sub>Sn)<sub>n</sub>-Cl (*n*=1 (269), 4 (281)) with excess of magnesium.<sup>278</sup> Alternatively, reaction of (<sup>t</sup>Bu<sub>2</sub>Sn)<sub>4</sub> (282) with <sup>t</sup>BuCl and magnesium also led to this compound. Investigations into the reactivity of the metalated species toward some electrophiles (Me<sub>2</sub>SO<sub>4</sub>, EtBr, <sup>n</sup>PrCl, Cl-(CH<sub>2</sub>)<sub>3</sub>-Cl, and CHCl<sub>3</sub>) resulted in alkylated and chlorinated derivatives, respectively.

Examples of oxidation reactions of tin–metal bonds toward formation of new symmetric catenates are comparably rare. In systems with organic substituents, reductive reaction mechanisms are preferred due to easier accessibility of tin halides, compared to metalates. In the reaction of HC [SiMe<sub>2</sub>N(R)Li]<sub>3</sub> with SnCl<sub>2</sub> (283), the formation of HC



**Table 2** Comparison of lowest-energy transitions of EtO(CH<sub>2</sub>)<sub>2</sub>(Sn<sup>n</sup>Bu)<sub>n</sub>(CH<sub>2</sub>)<sub>2</sub>OEt (**298**) with different chain lengths<sup>209</sup>

Number of Sn atoms n	$\lambda_{max}$ (nm)
3	254
4	273
5	296
6	312
7	323
8	332
10	346
15	362

[SiMe<sub>2</sub>N(R)]<sub>3</sub>SnLi [R=(S)-CH(Me)Ph (**284a**), Tol (**284b**)] was reported. This structure can be interpreted as a stannyl anion but also as an intramolecular R'RNLi adduct of stannylene (R'RN)<sub>2</sub>Sn. Oxidative homocoupling of **284** with an excess of silver chloride gave the corresponding hexaaminodistannane (**285**) in 68% yield (Scheme 18).<sup>279–281</sup> Reactions of **284** with electrophiles such as Me<sub>3</sub>SnCl (**286**) led to the related asymmetric distannanes (**287**).

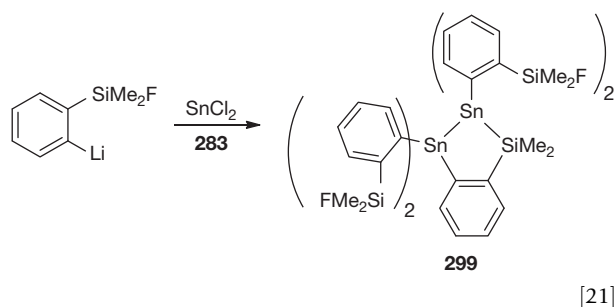
Another example of a distannane lacking organic substituents is a structure embedded in a thiostannate. Reaction of RSnCl<sub>3</sub> (R=CMe<sub>2</sub>CH<sub>2</sub>COMe) (**288**) with Na<sub>2</sub>S·9H<sub>2</sub>O gave (RSn<sup>IV</sup>)<sub>4</sub>S<sub>6</sub> (**289**). Subsequent UV irradiation-induced rearrangement and elimination reactions led to [(RSn<sup>IV</sup>)<sub>2</sub>(μ-S)]<sub>3</sub>Sn<sup>III</sup><sub>2</sub>S<sub>6</sub> (**290**) (Scheme 19).<sup>282</sup> A persilylated distannane derivative [(Me<sub>3</sub>Si)<sub>3</sub>Sn]<sub>2</sub> (**291**) was formed via oxidation of (Me<sub>3</sub>Si)<sub>3</sub>SnK (**292**) with 1,2-dibromoethane at –78 °C.<sup>69,96</sup>

### 1.03.2.5.3 Derivatives of unsaturated organotin compounds

An interesting example of utilizing stannylene-insertion reactions to build up oligostannanes was reported by Sita and coworkers (Scheme 20).<sup>209</sup> Generation of the <sup>n</sup>Bu<sub>2</sub>Sn: (**293**) species was achieved via treatment of EtO(CH<sub>2</sub>)<sub>2</sub>Sn<sup>n</sup>Bu<sub>2</sub>H (**294**) with small amounts of lithiumdiisopropyl amide (LDA). The initial deprotonation was followed by an elimination releasing the stannylene. Subsequent reaction of the stannylene with unreacted tin hydride resulted in formation of a variety of oligostannanes, predominating penta- to heptastannanes, with chain lengths of up to 15 Sn atoms.

UV/vis spectroscopic measurements of oligostannanes showed, as noted previously, a bathochromic shift of the lowest-energy transition with growing number of Sn atoms in the catenate (Table 2).

There are some more recent reports of reactions of Sn(II) compounds leading to distannane formation.<sup>283–288</sup> For instance, the reaction of 2-(fluorodimethylsilyl)phenyl lithium with SnCl<sub>2</sub> (**283**) gave the siladistannaindane derivative **299** in 18% yield (eqn [21]).<sup>286</sup>



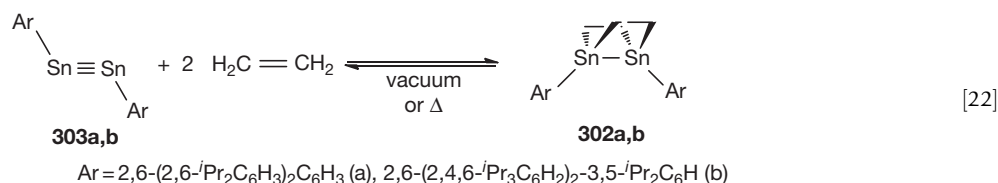
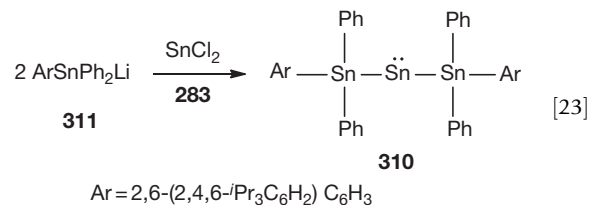
Efforts to synthesize cluster compounds (*vide infra*) led to a cyclotristannene byproduct [(Me<sub>3</sub>Si)<sub>3</sub>Si]<sub>4</sub>Sn<sub>3</sub> (**300**).<sup>289</sup> The compound seemed to be formed via reaction of (Me<sub>3</sub>Si)<sub>3</sub>SiLi with *in situ* generated SnBr<sub>2</sub> (**301**). Sn–Sn bond lengths were found to be about 2.84 Å for the two single bonds and 2.56 Å for the double bond.

Distannenes and distannynes, usually kinetically stabilized with bulky substituents to prevent homocycloaddition, can also be converted to distannanes. Most results derived from investigations into the reactivity of such unsaturated systems.<sup>290</sup> The formation of bicyclic distannanes (**302a,b**) via addition of two equivalents of ethylene to a terphenyl-substituted distannylene (**303a,b**) was found to be reversible (eqn [22]).<sup>291</sup>

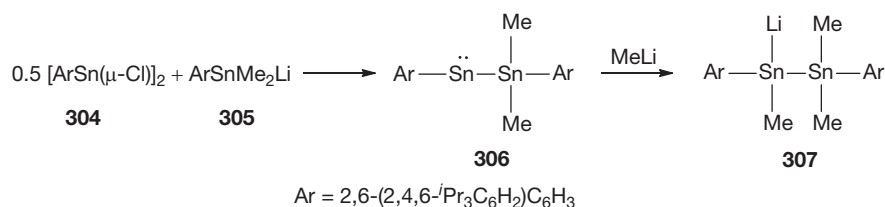
Some reactions of Sn(II) compounds and other unsaturated ditin compounds lead to compounds bearing the structural motif of a stannylstannylene, a saturated Sn atom bound to a low valent Sn atom. This behavior seems to be facilitated when very sterically demanding substituents are present.

Direct synthesis of such compounds was achieved via reaction of [ArSn(μ-Cl)]<sub>2</sub> (**304**) with ArSnMe<sub>2</sub>Li (Ar=2,6-(2,4,6-*i*-Pr<sub>3</sub>C<sub>6</sub>H<sub>2</sub>)C<sub>6</sub>H<sub>3</sub>) (**305**), leading to ArSnSnMe<sub>2</sub>Ar (**306**) in 85% yield. Further addition of MeLi gave ArSn(Me)(Li)SnMe<sub>2</sub>Ar (**307**) (Scheme 21).<sup>292</sup>

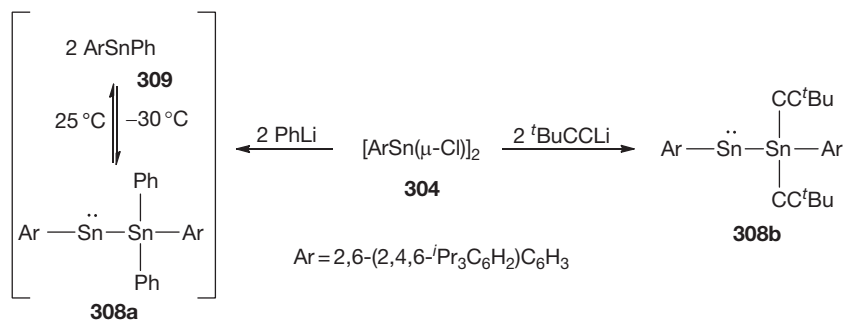
Treatment of [ArSn(μ-Cl)]<sub>2</sub> (**304**) with other organic nucleophiles (PhLi, <sup>t</sup>BuCCl) allowed formation of ArSnSnR<sub>2</sub>Ar (R=Ph (**308a**), CC<sup>t</sup>Bu (**308b**)) (Scheme 22).<sup>293,294</sup> At low temperature, in the case of R=Ph, **308a** was found to be dominant in solution, but when warmed to ambient temperature, ArSnPh (**309**), the product of a reversible dissociation, could be isolated. As part of these investigations, a distannylstannylene, (ArPh<sub>2</sub>Sn)<sub>2</sub>Sn (**310**), was obtained in 24% yield via reaction of ArPh<sub>2</sub>SnLi (**311**) with SnCl<sub>2</sub> (**283**) (eqn [23]).<sup>295</sup>



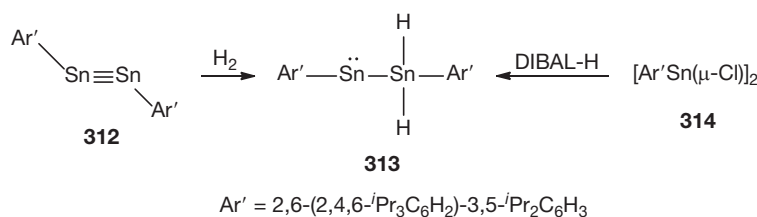




**Scheme 21** Stannylstannylene formation by addition of a stannide to a chlorostannylene.



**Scheme 22** Stannylene-stannylstannylene equilibrium.



**Scheme 23** Stannylstannylene formation by hydrogenation of a distannylene.

1,1-Dihydro derivatives of the stannylstannylene structural motif were accessible via direct addition of H<sub>2</sub> to Ar'SnSnAr' (Ar' = 2,6-(2,4,6-*i*Pr<sub>3</sub>C<sub>6</sub>H<sub>2</sub>)-3,5-*i*Pr<sub>2</sub>C<sub>6</sub>H<sub>3</sub>) (312), giving Ar'SnSnH<sub>2</sub>Ar' (313) or by reaction of [Ar'Sn(μ-Cl)]<sub>2</sub> (314) with <sup>t</sup>Bu<sub>2</sub>AlH (DIBAL-H) (Scheme 23).<sup>296,297</sup> Slight changes in the substitution pattern of the aryl group combined with different reactants (reaction of [Ar'Sn(μ-Cl)]<sub>2</sub> (315a-d) [Ar\* = 4-X-2,6-(2,6-*i*Pr<sub>2</sub>C<sub>6</sub>H<sub>3</sub>)C<sub>6</sub>H<sub>2</sub>; X = H (a), MeO (b), <sup>t</sup>Bu (c), Me<sub>3</sub>Si (d)] with LiBH<sub>4</sub> or of Ar\*SnNMe<sub>2</sub> (316a-d) with BH<sub>3</sub>·THF) resulted in formation of hydrogen-bridged dimers, [Ar\*Sn(μ-H)]<sub>2</sub> (317a-d), rather than Sn-Sn bonded compounds.

Stannylstannylenes are structural isomers of distannenes, and there has been an example reported that bridges the two isomers, with a bromine atom coordinated to both tin atoms.<sup>298</sup>

In contrast to the synthetic routes mentioned, Kira et al. reported a fairly complex example of a stannylstannylene where an aryldiazomethylstannylene, ArSnC(N<sub>2</sub>)SiMe<sub>3</sub> (318) (Ar = 2,6-(2,4,6-*i*Pr<sub>3</sub>C<sub>6</sub>H<sub>2</sub>)C<sub>6</sub>H<sub>3</sub>), was used as substrate. Photo-induced elimination of N<sub>2</sub>, which released a carbene, triggered a reaction cascade including dimerization and a transient stannaacetylene, which led to a macrocyclic compound containing a Sn(III)-Sn(I) bond.<sup>299</sup>

Stannyl-stannylene bonds were found to be slightly longer than those of saturated distannanes (bond distance in Ph<sub>6</sub>Sn<sub>2</sub> (267) is 2.77 Å). Sn-Sn bonds of the terphenyl-substituted

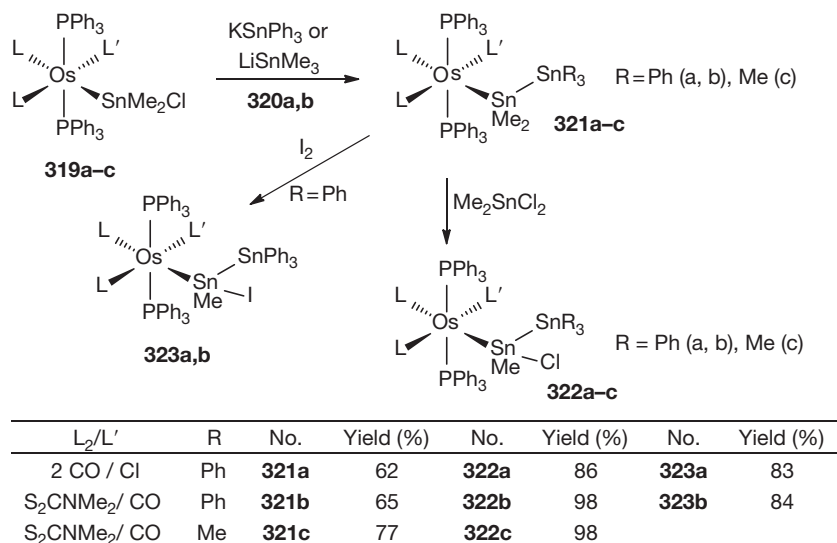
systems mentioned above range from 2.89 Å in ArSnSnMe<sub>2</sub>Ar (306) to 2.97 Å in ArSnSnPh<sub>2</sub>Ar (308a). In the case of the distannylstannylene (311), Sn-Sn bond distances are 2.9644 (3) and 2.9630(3) Å.

#### 1.03.2.5.4 Di- and oligostannanes as part of transition-metal complexes

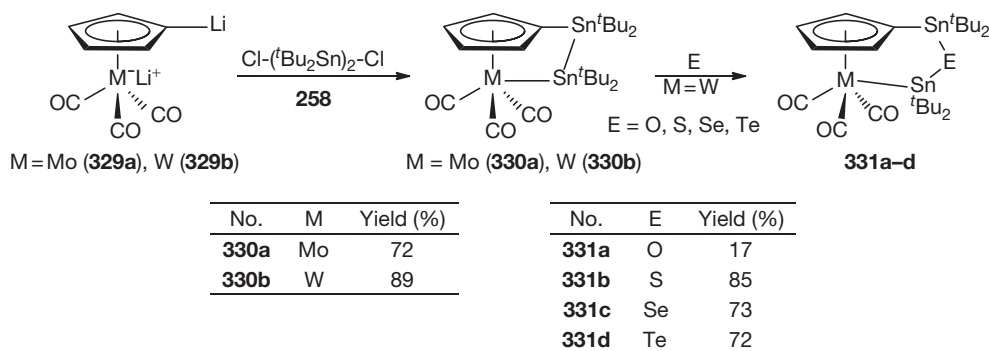
Stannylated transition-metal complexes were first reported in the 1960s.<sup>300-302</sup> Recent investigations into transition-metal complexes containing Sn-Sn units in the ligand system focused on modification of the tin ligands and the use of different types of *ansa* complexes.

Investigations of osmium complexes showed Sn-Sn bond formation and further functionalization of metal-bound organodistannanes. Reaction of L<sub>2</sub>L'(PPh<sub>3</sub>)<sub>2</sub>OsSnMe<sub>2</sub>Cl (319a,b) (L<sub>2</sub> = Me<sub>2</sub>NCS<sub>2</sub>, 2CO/L' = CO, Cl) with KSnPh<sub>3</sub> (320a) or LiSnMe<sub>3</sub> (320b) gave L<sub>2</sub>L'(PPh<sub>3</sub>)<sub>2</sub>OsSnMe<sub>2</sub>SnR<sub>3</sub> (321a-c) [R = Ph (a, b), Me (c)]. Treatment of osmium-pentaorganodistannanes with Me<sub>2</sub>SnCl<sub>2</sub> or iodine led to halogenation of the metal-bound tin atoms (Scheme 24).<sup>239</sup>

General interest in the synthesis of *ansa* complexes bearing group-14 bridges led to the preparation of stanna[n]ferrocenophanes (*n* = 2, 3).<sup>303</sup> Compounds of this type are potential precursors for metal-containing polymers, accessible via ring-opening polymerization. The first methods used for synthesis of 1,2-distanna derivatives were based on reductive coupling of



**Scheme 24** Formation and conversion of osmium distannanyl complexes.

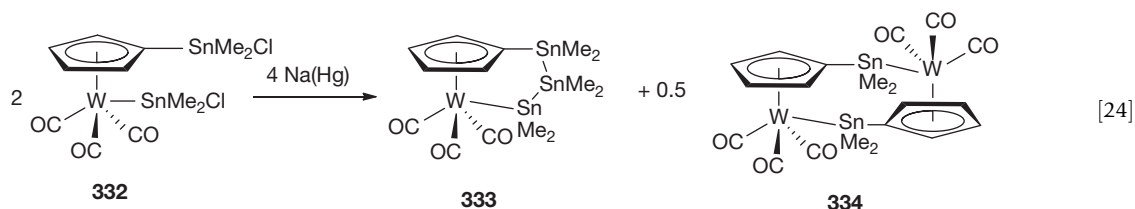


**Scheme 25** Formation of distanna *ansa* half-sandwich Mo and W complexes.

( $\eta^5\text{-C}_5\text{H}_4\text{SnMe}_2\text{Cl}$ )<sub>2</sub>Fe (**324**) with (Me<sub>3</sub>Si)<sub>2</sub>Hg and of ( $\eta^5\text{-C}_5\text{H}_4\text{SnMe}_2\text{H}$ )<sub>2</sub>Fe (**325**) with (Et<sub>2</sub>N)<sub>2</sub>SnR<sub>2</sub> [R = NEt<sub>2</sub> (**326a**), Et (**326b**), <sup>*t*</sup>Bu (**326c**)], forming distannanylene bridges. It should be mentioned that, in the case of using (Et<sub>2</sub>N)<sub>2</sub>SnMe<sub>2</sub> (**326d**), a tristanna[3]ferrocenophane was formed. Alternatively, reaction of ( $\eta^5\text{-C}_5\text{H}_4\text{Li}$ )<sub>2</sub>Fe with Cl-(<sup>*t*</sup>Bu<sub>2</sub>Sn)<sub>2</sub>-Cl (**275**) led to 1,1,2,2-tetra-*tert*-butyl-1,2-distanna[2]ferrocenophane (**327a**).<sup>304</sup> The method of employing a dilithiated metal fragment was also used to synthesize a distanna[2]troticenophane derivative, [Ti( $\eta^5\text{-C}_5\text{H}_4$ )( $\eta^7\text{-C}_7\text{H}_6$ )Sn<sub>2</sub><sup>*t*</sup>Bu<sub>4</sub>] (**327b**), by reaction of [Ti( $\eta^5\text{-C}_5\text{H}_4\text{Li}$ )( $\eta^7\text{-C}_7\text{H}_6\text{Li}$ )]•pmdta (pmdta = N,N',N'',N'',N''-pentamethyldiethylenetriamine) with Cl-(<sup>*t*</sup>Bu<sub>2</sub>Sn)<sub>2</sub>-Cl (**275**).<sup>305</sup> As the conversion of Cp(CO)<sub>3</sub>MoLi with Cl-(<sup>*t*</sup>Bu<sub>2</sub>Sn)<sub>2</sub>-Cl (**275**) gave Cp(CO)<sub>3</sub>Mo(<sup>*t*</sup>Bu<sub>2</sub>Sn)<sub>2</sub>-Cl (**328**),<sup>306</sup> a combination of these synthetic approaches allowed formation of *ansa* complexes where M–Sn and C–Sn bonds were formed in

the same synthetic step (**Scheme 25**).<sup>223</sup> Investigations into the reactivity of the tungsten derivative (**330b**) toward chalcogens resulted not in the expected cleavage of the M–Sn bond, but the cleavage of the Sn–Sn bond and formation of the respective tin chalcogenides (**Scheme 25**).

In this context, the reaction of [ClMe<sub>2</sub>Sn( $\eta^5\text{-C}_5\text{H}_4$ )](CO)<sub>3</sub>-WSnMe<sub>2</sub>Cl (**332**) with sodium amalgam is interesting. The reaction led to 44% of a tristannanylene-bridged *ansa*- (**333**) and 23% of a cyclic dinuclear tungsten complex (**334**), rather than the expected distannanylene-bridged derivative (eqn [24]).<sup>307</sup> The formation of the tristannanylene bridge is attributed to the insertion of dimethylstannylene into a strained distannanylene intermediate. The second product is proposed to be the result of dimerization of a metalated tungsten species formed via reductive elimination of [ClMe<sub>2</sub>Sn( $\eta^5\text{-C}_5\text{H}_4$ )](CO)<sub>3</sub>WSnMe<sub>2</sub>Na acting as a stannylene source.<sup>307</sup>



### 1.03.2.5.5 Derivatization of di- and oligostannanes

Treatment of hexaphenyldistannane (267) with two equivalents of perfluoroalkylsulfonic acids resulted in the cleavage of two Sn–Ph bonds.<sup>308</sup> By this method, aryl groups can be utilized to generate Sn-electrophiles, allowing further derivatization. A symmetric step-by-step exchange of phenyl against ethyl groups was reported using tetraorganodistanna-1,2-diperfluoroalkylsulfonates as electrophilic intermediates.

In order to prepare a 1,2-ditin nucleophile,  $[(\text{Me}_3\text{Si})_3\text{Sn}]_2$  (291) was treated with two equivalents of  ${}^t\text{BuOK}/18\text{-crown-6}$  to form the corresponding 1,2-dianion, 18-crown-6 $\cdot\text{K}[\text{Sn}(\text{SiMe}_3)_2]_2\text{K}\cdot 18\text{-crown-6}$  (335) (Scheme 26).<sup>96</sup> The driving force for this reaction is the formation of strong Si–O bonds ( $\text{Me}_3\text{SiO}{}^t\text{Bu}$ ), resulting in fast conversion. Investigations into the reactivity of this nucleophile with group 4 metallocene dichlorides led to metallacyclotetrastannanes (336a,b) that were likely formed via insertion of stannylene ( $\text{Me}_3\text{Si})_2\text{Sn}$  into a strained metallacyclotristannane intermediate.

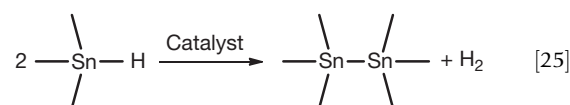
Metalation of  $\text{H}-({}^t\text{Bu}_2\text{Sn})_2\text{-H}$  (337), synthesized via reaction of  $\text{LiAlH}_4$  with  $\text{Cl}-({}^t\text{Bu}_2\text{Sn})_2\text{-Cl}$  (275), was achieved via conversion with  $\text{KH}$  or  ${}^i\text{Pr}_2\text{NLi}$  (LDA).<sup>309</sup> The use of  $\text{KH}$  allowed stepwise formation of both the mono- and dipotassium derivatives, while in the case of LDA only one proton per molecule could be abstracted. Formation of  $\text{Li}-({}^t\text{Bu}_2\text{Sn})_2\text{-H}$  (338) was also observed in the synthesis of  ${}^t\text{Bu}_2\text{SnHLi}$  (339) via treatment of  ${}^t\text{Bu}_2\text{SnH}_2$  (340) with  ${}^t\text{BuLi}$  or LDA after 12–48 h via elimination of  $\text{LiH}$ , with complete conversion reached after 5–7 days.<sup>310</sup>

Reaction with LDA was also found to lead to cyclic compounds in the case of linked organotin hydrides.<sup>261,311</sup> Treatment of  $\text{MeSi}[\text{SiMe}_2\text{Sn}(\text{H}){}^t\text{Bu}_2]_3$  (341) with three equivalents of LDA resulted in the formation of 35% of a 1,2-distannacyclopentasilane (342) (Scheme 27). When 341 was

reacted with  $\text{Et}_3\text{N}$  or  $(\text{Et}_2\text{N})_3\text{SnPh}$  (343) instead, a six-membered ring (344) containing a tristannanylene unit was formed in 75% yield.

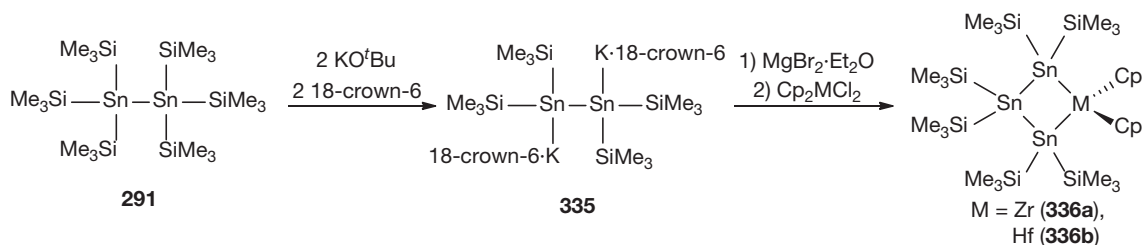
### 1.03.2.5.6 Formation of Sn–Sn bonds via dehydrogenative coupling

Another major pathway toward distannane formation is the dehydrogenative coupling of organotin hydrides (eqn [25]). The steady decrease of E–H bond energy when going down group 14 reaches a value of ca.  $252\text{ kJ mol}^{-1}$  for the Sn–H bond.<sup>9</sup> A small difference in the electronegativities of tin and hydrogen leads to a low polarity of Sn–H bonds. In combination, these circumstances allow reaction mechanisms in which hydrogen is abstracted as a proton, as a hydride, or even as a radical. Reviews by Davies<sup>197</sup> and Braunstein<sup>198</sup> provide insight into recent developments as well as basic knowledge concerning the field of organotin hydrides in general and dehydrogenative Sn–Sn bond formation in particular.

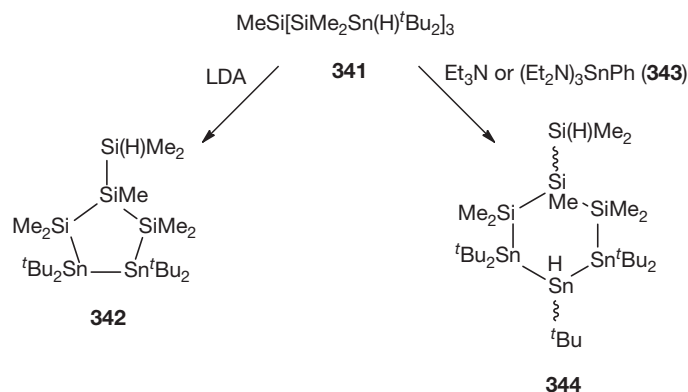


An example for this type of reaction is the synthesis of hexa-*n*-butyldistannane (261) by reduction of bis(tri-*n*-butyltin) oxide (260) with sodium borohydride in ethanol.<sup>312</sup> The immediate formation of tri-*n*-butyltin hydride (259) was followed by its dehydrogenative decomposition under basic conditions, giving hexa-*n*-butyldistannane (261) in high yield.

Early investigations of dehydrogenation reactions were reported by Neumann and coworkers in the 1960s for  $\text{Ar}_2\text{SnH}_2$  which was treated with amines, such as  $\text{Et}_2\text{NH}$  or pyridine, or dissolved in DMF or MeOH at ambient



**Scheme 26** Formation of 1,2-dipotassium tetrakis(trimethylsilyl)distannane and subsequent reaction with group 4 metallocene dichlorides.



**Scheme 27** Base promoted silacyclopentastannane formation.

temperature.<sup>313</sup> Impurities remaining from the previous hydrogenation step as well as the addition of catalytic amounts of the corresponding aryltin chloride to solutions of the aryltin hydride were found to have a promoting effect on the reaction.<sup>314,315</sup> This approach was used by Davies and Osei-Kissi to prepare functionalized distannanes of the type  $X(^n\text{Bu}_2\text{Sn})_2X$  (**345a,b**) ( $X = \text{Cl}, \text{OAc}$ ).<sup>316</sup>  $^n\text{Bu}_2\text{SnH}_2$  (**346**) and  $^n\text{Bu}_2\text{SnX}_2$  (**347a,b**) were mixed and the resulting disproportionation product,  $\text{Bu}_2\text{SnHX}$  (**348a,b**), was dehydrogenated in the presence of pyridine (Scheme 28). The dehydrogenative coupling reaction was also used to synthesize hexaaryldistannanes by heating the corresponding triaryltin hydride in the presence of a radical initiator (AIBN).<sup>317</sup>

### 1.03.2.5.7 Dehydrogenative coupling catalyzed by transition-metal and f-block element complexes

Over the years, several different transition-metal catalyst systems for dehydrogenative coupling of hydrostannanes have been developed. A comparative overview on this issue was published by Davies in 2006.<sup>197</sup> The formation of Sn–Sn bonds via dehydrogenation of organotin hydrides is usually not observed at ambient temperature but can be promoted by various catalysts and conditions as mentioned in the previous section.

Synthesis of a bifunctional organotin compound,  $\text{H}(^n\text{Bu}_2\text{Sn})_2\text{H}$  (**337**), from the corresponding monostannane,  $^n\text{Bu}_2\text{SnH}_2$  (**340**), was achieved with iron ( $\text{Cp}(\text{CO})_2\text{FeMe}$ ,  $\text{Cp}(\text{CO})\text{FePPh}_3\text{Me}$ ) and molybdenum catalysts ( $\text{Cp}(\text{CO})_3\text{MoMe}$ ,  $\text{Cp}(\text{CO})_2\text{MoPPh}_3\text{Me}$ ) in combination with UV irradiation or elevated temperature.<sup>318</sup> Photo-initiation was used for  $\text{Cp}(\text{CO})_n\text{MMe}$  ( $n=2$  for  $\text{M}=\text{Fe}$ ;  $n=3$  for  $\text{M}=\text{Mo}$ ) and thermal induction for  $\text{Cp}(\text{CO})_n\text{MPPh}_3\text{Me}$  ( $n=1$  for  $\text{M}=\text{Fe}$ ;  $n=2$  for  $\text{M}=\text{Mo}$ ). Use of 3–5 mol% catalyst resulted in isolated yields of 80–90%, representing a valuable synthetic alternative to low-yielding stoichiometric methods.<sup>309</sup>

Another study showed that redistributions can take place when using  $\text{Cp}_2\text{MCl}_2/\text{Red-Al}$  ( $\text{M}=\text{Ti}, \text{Zr}, \text{Hf}$ ;  $\text{Red-Al}=\text{NaAlH}_2(\text{OC}_2\text{H}_4\text{OMe})_2$ ) for conversion of  $^n\text{Bu}_3\text{SnH}$  (**259**), leading to mixtures of  $^n\text{Bu}_6\text{Sn}_2$  (**261**) (69–90%) and poly(*di-n*-butylstannane),  $(^n\text{Bu}_2\text{Sn})_n$  (7–23%).<sup>319</sup>

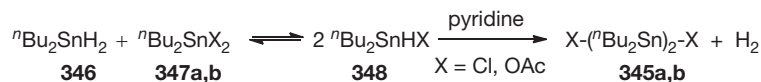
Another example of a metallacycloodigostannane (**349**) was formed in 89% yield via dehydrogenative coupling of  $\text{Ph}_2\text{SnH}_2$  (**350**) with  $[\text{Pd}(\text{dmpe})_2]_n$  ( $n=1, 2$ ;  $\text{dmpe}=\text{Me}_2\text{PCH}_2\text{CH}_2\text{PMe}_2$ ) (Scheme 29).<sup>320</sup> Alternatively, the palladacyclopentastannane was also formed when the disilylated precursor  $[\text{dmpePd}(\text{SiPh}_2\text{H})_2]$  was employed (64%). Heating a toluene solution of **349** led to degradation of the cyclostannane and gave 87% of  $[\text{dmpePd}(\text{SnPh}_3)_2]$  (**351**).

Further, complexes of f-block elements were investigated with respect to their ability to dehydrogenate heavier organotetrel hydrides forming new element–element bonds.<sup>321,322</sup> For instance, formation of  $^n\text{Bu}_6\text{Sn}_2$  (**261**) from  $^n\text{Bu}_3\text{SnH}$  (**259**) was catalyzed by  $[(^n\text{BuC}_5\text{H}_4)_2\text{Y}(\mu\text{-Me})_2]$  (1 mol%) at 70 °C in 91% yield after 0.5 h.

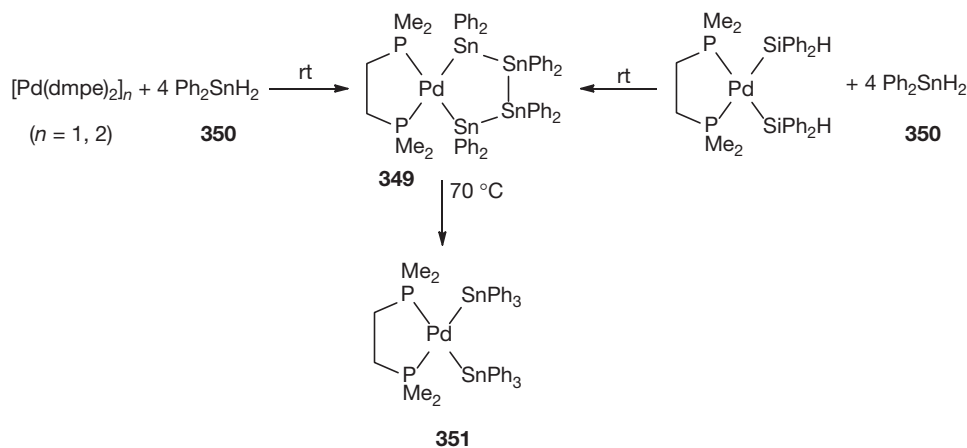
A series of organodiamidolanthanides  $(\text{CH}_2)_3\text{-1,3-}[\text{N}(\text{Dipp})]_2\text{LnMe}$  ( $\text{Ln}=\text{La}, \text{Ce}, \text{Nd}, \text{Dy}$ ;  $\text{Dipp}=2,6\text{-}^i\text{Pr}_2\text{C}_6\text{H}_3$ ) were found to catalyze the synthesis of sterically demanding tetraorganodihydrodistannanes,  $\text{H}(\text{R}_2\text{Sn})_2\text{H}$  ( $\text{R}=\text{tBu}$  (**337**),  $\text{Mes}$  (**352**)).<sup>323</sup> These reactions of  $\text{R}_2\text{SnH}_2$  were carried out at ambient temperature with 2–5 mol% catalysts. In contrast to the tin hydrides with bulky substituents, the analogous conversion of  $\text{Ph}_2\text{SnH}_2$  (**350**) yielded a polymer  $(\text{Ph}_2\text{Sn})_n$ . All reactions were carried out under exclusion of light to avoid photo-induced degradation processes.

### 1.03.2.6 Polystannanes

Polystannanes have attracted significant interest and have thus been discussed in the literature.<sup>18,197,198,201,202,324–327</sup> In particular, Braunstein and Morise<sup>198</sup> and, more recently, Sharma



**Scheme 28** Disproportionation of tin hydrides and halides followed by base promoted dehydrogenative coupling.



**Scheme 29** Palladacycloodigostannane formation by dehydrogenative coupling of  $\text{Ph}_2\text{SnH}_2$ .

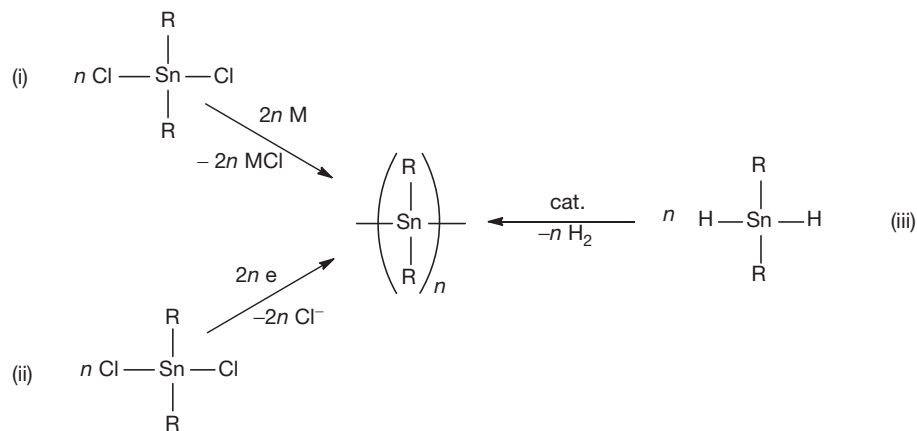
and Pannell<sup>324</sup> have reviewed this topic in depth. The interest in Sn polymers can be attributed to their optical and electronic properties, suggesting a broad variety of possible applications including nonlinear optical materials, semiconducting materials, and microlithography. These macromolecular properties originate from  $\sigma$ -bond electron delocalization along the Sn–Sn bonded systems.<sup>209</sup> While this feature is also known from lighter group-14 elements,<sup>19–23,328,329</sup> tin catenates show the lowest excitation energies for  $\sigma$ – $\sigma^*$  transitions. The magnitude of this effect mainly depends on the substituents and the conformation of the catenate. The strongest conjugation and thus the lowest excitation bandgap is reached when the backbone is completely all-*trans* orientated. Due to substituent interactions, a slight deviation from a strict all-*trans* alignment is common. At short chain lengths, every additional atom strongly contributes to the lowering of the  $\sigma$ – $\sigma^*$ -transition energy, but with increasing chain length the bathochromic shift gained by additional stannylene units converges to zero (cf. Table 2). The lowest-energy UV/vis absorptions for polystannanes are in range from 367 nm for  $(\text{Et}_2\text{Sn})_n$ <sup>271</sup> to 506 nm for  $[(o\text{-Et-}p\text{-}^t\text{BuO-C}_6\text{H}_3)\text{Sn}]_n$ .<sup>259</sup> In the case of polystannanes with comparable composition, a higher degree of branching results in a slightly more pronounced bathochromic shift of the lowest-energy transition (branched  $(^n\text{Bu}_2\text{Sn})_n$ :  $\lambda_{\text{max}}=394$  nm) when compared to a completely linear polymer (linear  $(^n\text{Bu}_2\text{Sn})_n$ :  $\lambda_{\text{max}}=378$  nm).<sup>330</sup> Despite diverse application possibilities, the degradation of polystannanes under ambient conditions, especially daylight, still limits their use.

The major synthetic methods to generate organopolystannanes are (i) reduction of diorganotin dihalides with alkali or alkaline earth metals, (ii) reduction via electrochemical methods, and (iii) catalytic dehydrogenative coupling of diorganotin dihydrides (Scheme 30).

Polymerizations utilizing Wurtz-type coupling reactions are generally performed by reduction of diorganotin dihalides with alkali or alkaline earth metals in polar solvents.<sup>18,198,201,202,324</sup> In general, these reactions suffer from several drawbacks such as difficult reproducibility, laborious work-up processes, and polymers of comparably low molecular weight. The last was attributed to harsh reaction conditions leading to fission of Sn–Sn bonds, further promoted by reaction conditions such as long reaction times and

elevated temperatures. Over the years modifications of this method were developed, for instance the use of crown ethers in nonpolar solvents<sup>331,332</sup> or the use of electric current as a reducing agent.<sup>268,333,334</sup> Polymerization of  $^n\text{Bu}_2\text{SnCl}_2$  (347a) with sodium in the presence of 15-crown-5 resulted in polydi-*n*-butylstannanes of average molecular weights ( $M_w$ ) of  $2.4 \times 10^3$  and  $1.4 \times 10^4$  when heated in toluene for 14 h. Reduction of the reaction time to 4 h led to a polymer of much higher molecular weight ( $M_w=1.09 \times 10^6$ ). Another approach to avoid side reactions is the use of milder reducing agents. Polymerization under homogeneous conditions can be achieved using  $\text{SmI}_2$  in stoichiometric or even in catalytic amounts in combination with alkaline earth metals.<sup>36,271,272</sup>

Dehydrogenative coupling of diorganotin dihydrides as a way to form polymeric compounds received significant attention, especially involving systems using catalysts based on d- or f-block metals. Dehydropolymerization reactions frequently produce polymers with much higher molecular weight compared to Wurtz-type polymerization methods. Early investigations into dehydropolymerization of hydrostannanes catalyzed by early transition metals suffered from low polymer weights and significant amounts of byproducts.<sup>335</sup> Recent progress led to synthetic protocols that allowed formation of polystannanes of high molecular weights with narrow polydispersities and very low amounts of side products.<sup>324</sup> An example that employed Wilkinson's catalyst,  $(\text{PPh}_3)_3\text{RhCl}$ , resulted in formation of  $(^n\text{Bu}_2\text{Sn})_n$  with  $M_w=2.0 \times 10^4$  in high yield without cyclic byproducts.<sup>336</sup> The major side products in all methods for polystannane formation are small cyclic compounds, predominantly cyclopenta- and cyclohexastannanes. These were also reported to form via photo-induced degradation of isolated polymers under inert conditions. Such degradation processes were found to be retarded by the presence of chlorinated solvents and styrene as well as dyes and radical scavengers.<sup>337</sup> Recent efforts to form oligomeric and polymeric organostannanes bearing chiral information led to the synthesis of cyclopentastannanes and polystannanes with *cis*- and *trans*-myrtanyl substituents, respectively.<sup>338</sup> The cyclopentastannanes,  $(\text{R}_2\text{Sn})_5$  ( $\text{R}=\textit{cis}$ -Myr (353a), *trans*-Myr (353b)), were formed via Wurtz-type coupling of  $\text{R}_2\text{SnCl}_2$  (354a,b) with magnesium. Polymerization was achieved by catalytic dehydrogenative coupling of the respective dihydrostannane,  $\text{R}_2\text{SnH}_2$  (355a,b), with Wilkinson's catalyst.<sup>338</sup>



**Scheme 30** Polymerization methods for polystannanes.



## 1.03.2.7 Tin Cages and Clusters

Tin cages,  $(\text{RSn})_n$ , represent a class of polycyclic saturated catenates exhibiting a clearly defined bonding situation with tin atoms linked to three other tin atoms and a fourth substituent (R) saturating its remaining valence. By contrast, the bonding situation in clusters cannot be described simply in terms of 2c–2e bonds, but needs involvement of the Wade–Mingos rules<sup>339–343</sup> to describe the electronic situation. Recent progress in the chemistry of tin cages and clusters was reviewed by Wiberg and Power.<sup>148</sup>

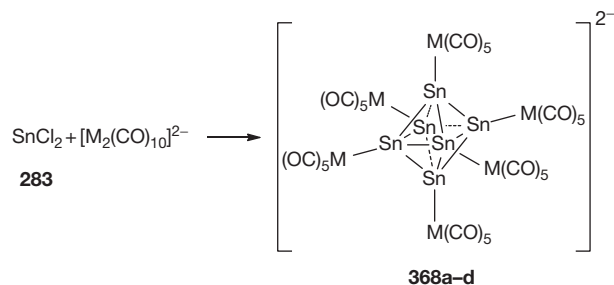
The situation with respect to tin cages,  $[\text{RSn}]_n$ , is quite similar to what was found for analogous germanium compounds (*vide supra*). Examples of tetrahedral ( $n=4$ ,  $\text{R}=\text{Si}^t\text{Bu}_3$  (356)),<sup>344</sup> trigonal-prismatic ( $n=6$ ,  $\text{R}=\text{Si}^t\text{Bu}_3$  (357)),<sup>345</sup> cubic ( $n=8$ ,  $\text{R}=2,6\text{-Et}_2\text{C}_6\text{H}_3$  (358)),<sup>346</sup> and pentagonal-prismatic ( $n=10$ ,  $\text{R}=2,6\text{-Et}_2\text{C}_6\text{H}_3$  (359))<sup>347</sup> polyhedra were reported. Furthermore, a dianionic stannacubane derivative,  $(\text{Bu}_3\text{Si})_6\text{Sn}_8[\text{Na}(\text{THF})_2]_2$  (360), was prepared.<sup>348</sup> Recent efforts to synthesize persistent radicals of heavier group-14 elements resulted in the formation of small amounts of the silylated stannahexaprismane,  $[\{(\text{Me}_3\text{Si})_2\text{MeSi}\}\text{Sn}]_6$  (361).<sup>349</sup>

Stepwise incorporation of tin atoms into a *nido*-borane ( $\text{B}_{10}\text{H}_{14}$ ) led to 67% yield of a borane-embedded tetrastannane (362) (Scheme 31).<sup>350</sup> The preparation of the starting material, stanna-*nido*-undecaborate  $[\text{C}_{14}\text{H}_{19}\text{N}_2][\text{ClSnB}_{10}\text{H}_{12}]$  (363), was achieved via reaction of tin(II) chloride (283) with  $\text{B}_{10}\text{H}_{14}$  in the presence of a strong base, 1,8-bis(dimethylamino)naphthalene. Further addition of  $\text{SnCl}_2$  (283) to 363 did not lead directly to a distanna derivative. Only when triethylamine was used as a base the second tin atom was integrated and the dianionic dimer (362) formed. While a monomeric distanna-*closo*-dodecaborate was not observed during that reaction, further treatment of 362 with  $\text{KBHET}_3$  led to cleavage of the linking Sn–Sn bond affording the dianionic *closo*-heteroborate (364).

Compounds where Sn–Sn subunits were incorporated into group-15 (P, As) element clusters saturated with silyl

substituents were reported recently.<sup>351,352</sup> Work on stanna [1.1.1]propellane clusters,  $\text{R}_6\text{Sn}_5$  (366),<sup>254,346,347,353–356</sup> led to transition-metal-substituted derivatives,  $[\text{MCp}(\text{CO})_2]_2[\mu\text{-Sn}_5\text{Dep}_6]$  (365a,b) ( $\text{M}=\text{Fe}, \text{Ru}$ ;  $\text{Dep}=2,6\text{-Et}_2\text{C}_6\text{H}_3$ ), displaying a complex electrochemistry (Scheme 32).<sup>163</sup>

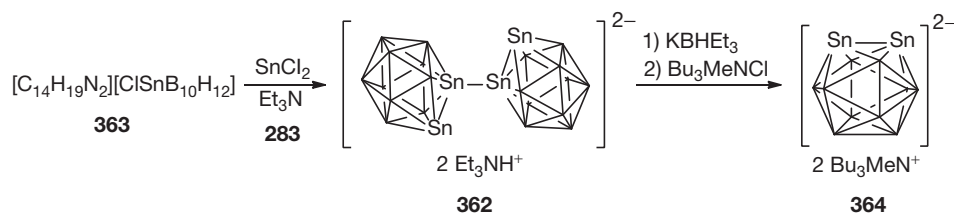
Compounds of the type  $\{\text{Sn}[\text{M}(\text{CO})_5]\}_6^{2-}$  are rare examples of transition-metal-substituted tetrel clusters or, from another perspective, transition-metal complexes sharing a tin cluster as ligand.<sup>180,357</sup> Formation of these clusters was achieved by reaction of tin(II) chloride (283) with  $\text{M}'_2[\text{M}_2(\text{CO})_{10}]$  ( $\text{M}'=\text{Na}, \text{K}$ ;  $\text{M}=\text{Cr}, \text{Mo}, \text{W}$ ) (eqn [26]). Sn–Sn bond distances in these clusters range from 2.89 to 2.93 Å.



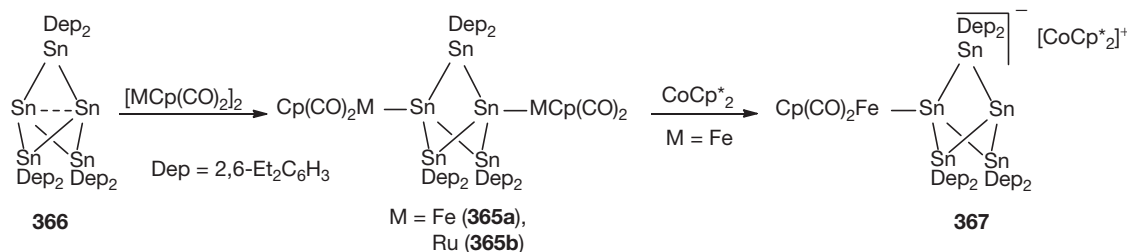
No.	Metal	Cation	Yields (%)
368a	Cr	crypt[2.2.2]-K <sup>+</sup>	7
368b	Cr	Ph <sub>4</sub> P <sup>+</sup>	11
368c	Mo	Ph <sub>4</sub> P <sup>+</sup>	36
368d	W	Ph <sub>4</sub> P <sup>+</sup>	9

[26]

A related octahedral cluster was obtained in a yield of 17% via reduction of an asymmetric Ge(II) compound,  $\text{ArGeCl}$  ( $\text{Ar}=2,6\text{-}(2,6\text{-}^i\text{Pr}_2\text{C}_6\text{H}_3)\text{C}_6\text{H}_3$ ) (213), with  $\text{KC}_8$  in the presence of  $\text{SnCl}_2$  (283) (eqn [27]).<sup>358</sup> The resulting heteronuclear Ge/Sn cluster (369) consists of four unsubstituted tin atoms in equatorial position and two apical germanium atoms still attached to the aryl substituents. The Sn ring within the cluster



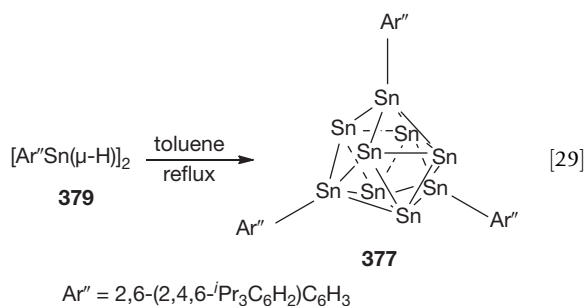
Scheme 31 Preparation of a borane cluster embedded tetrastannane.



Scheme 32 Conversion of pentastanna[1.1.1]propellane to transition-metal derivatives.







In contrast to most synthetic routes utilizing divalent tin compounds, SnBr (380), a tin(I) halide, was also employed as a substrate. This highly reactive species was prepared by a co-condensation technique.<sup>364,365</sup> Treatment of SnBr (380) with  $(\text{Me}_3\text{Si})_3\text{SiLi}$  gave  $[\text{Sn}_{10}\{\text{Si}(\text{SiMe}_3)_3\}_6]$  (381) and a small amount of a tetrasilylated cyclotristannene,  $[(\text{Me}_3\text{Si})_3\text{Si}]_4\text{Sn}_3$  (300), as a byproduct (eqn [30]).<sup>289,366</sup> Bond distances in the  $\text{Sn}_{10}$ -cluster range from 2.85 to 3.07 Å.

Metal clusters constructed of enough atoms to have embedded atoms that only interact with other cluster atoms are called 'metalloid clusters' as they mark the transition between molecules and bulk metal.<sup>367–370</sup> Examples of such clusters containing tin are  $\{[(\text{ddp})\text{ClGa}]_4\text{Sn}_{17}\}$ <sup>360</sup> (373) (*vide supra*) and  $[\text{Sn}_{15}\{\text{N}(2,6\text{-}i\text{-Pr}_2\text{C}_6\text{H}_3)(\text{SiMe}_2\text{R})\}]$ <sup>371</sup> (R=Me (382a), Ph (382b)) (Scheme 35). The latter clusters were synthesized via reduction of an asymmetric Sn(II) compound,  $\{\text{Sn}[\text{N}(2,6\text{-}i\text{-Pr}_2\text{C}_6\text{H}_3)(\text{SiMe}_3)](\mu\text{-Cl})\}_2$  (383), with  $\text{KC}_8$ , as well as by treatment of a mixture of  $\text{Sn}[\text{N}(2,6\text{-}i\text{-Pr}_2\text{C}_6\text{H}_3)(\text{SiMe}_2\text{R})]_2$  (R=Me (384a), Ph (384b)) and  $\text{SnCl}_2$  (283) with Li ( $\text{BH}^t\text{Bu}_3$ ).<sup>148</sup> The <sup>119</sup>Sn Mössbauer spectrum showed two different quadrupole-splitting sites that were assigned to the six ligand-bound outer Sn atoms and the  $\text{Sn}_9$  cluster core. The bond lengths of the central Sn atom to the unsubstituted Sn atoms range from 3.15 to 3.18 Å, while the distances between unsubstituted and ligand-bound cluster atoms are in the range from 2.99 to 3.02 Å. In the case of the anionic  $[\text{Sn}_{17}]^{4-}$  cluster the bond distances between unsubstituted cluster atoms range from 2.896 to 3.286 Å, with the bonds to the central Sn atom at 3.073 to 3.124 Å. For comparison, the bond distances in the β-Sn modification were found to be 3.016 and 3.175 Å.<sup>195</sup>

### 1.03.3 Lead

#### 1.03.3.1 Introduction

With the decrease in bond energies when going down group 14, molecules with E–E bonds become less stable. While nowadays a fairly large number of polysilanes are known, ranging

from examples with rather high structural complexity to polymers with several hundred catenated silicon atoms, the situation for germanium and tin is much more manageable. With respect to polyplumbanes, containing Pb–Pb bonds, a fair number of diplumbanes are known, while there are only very few compounds containing more than one Pb–Pb bond. While true polymers of catenated silicon, germanium, and even tin atoms are well-established classes of compounds, with polystannanes being fairly light sensitive, no examples of polyplumbanes have been reported so far.

The chemistry of organolead compounds experienced its climax during the times when tetraethyllead was used as an anti-knock additive in gasoline. It has been covered in several reviews,<sup>372–375</sup> with the one by Weidenbruch<sup>373</sup> being the most recent. A marvelous description of 'the rise and fall of tetraethyllead,' which also covers some diplumbane chemistry, was given recently by Seyferth.<sup>376,377</sup> A most comprehensive treatment of the early chemistry of organolead compounds up to the late 1960s is given by Voronkov and Abzaeva.<sup>5</sup>

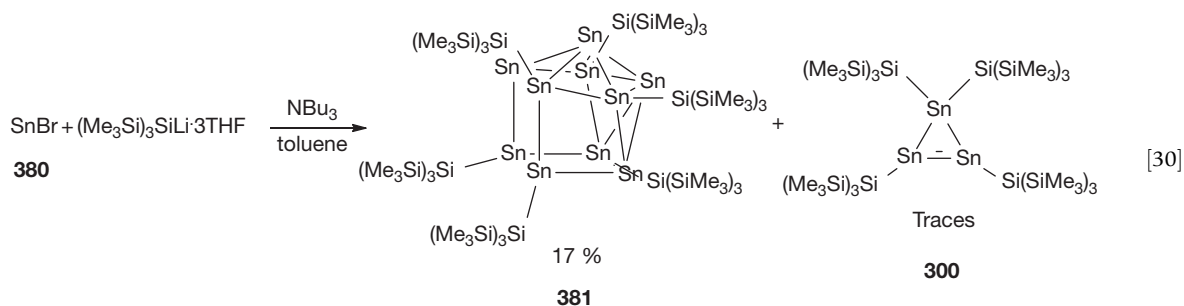
#### 1.03.3.2 Synthetic Methods

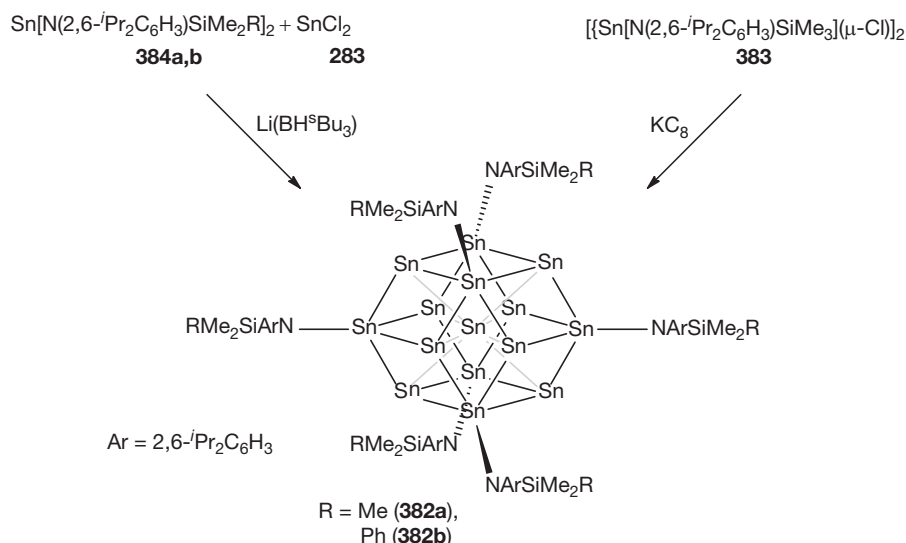
As there are comparatively few examples of diplumbanes and even fewer examples of oligoplumbanes, the synthetic methods utilized for their preparation are outlined below in the respective sections.

#### 1.03.3.3 Reactivity of the Pb–Pb Bond

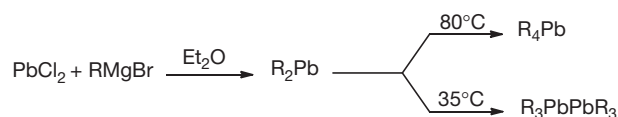
The cleavage of or insertion into the weak Pb–Pb bond (Pb–Pb ca. 100 kJ mol<sup>−1</sup>, Pb–C ca. 130 kJ mol<sup>−1</sup>)<sup>378</sup> has been studied to some extent. A number of nucleophilic and weakly electrophilic reagents (organolithium and organomagnesium compounds,<sup>379</sup> alkali metals,<sup>46,380–382</sup> potassium permanganate,<sup>383</sup> alkali-metal alkoxides,<sup>47,379</sup> diaryl disulfides,<sup>379</sup> sulfur,<sup>384</sup> ozone,<sup>379</sup> hypochlorous acid,<sup>379</sup> and iodine/iodide<sup>379</sup>) selectively cleave the Pb–Pb bond of hexaphenyldiplumbane (385).<sup>379</sup> The phenyl-lead bond is preserved under these conditions. Cleavage of the Pb–Pb bonds of hexaalkyldiplumbanes with halogens proceeds cleanly to the triorganylplumbyl halides. In the case of arylated diplumbanes, Pb–C bonds are also split to a considerable degree under these conditions.<sup>385</sup>

Promoted by daylight, the insertion of chalcogens into the Pb–Pb bond of  $\text{Ph}_3\text{PbPbPh}_3$  (385) can be accomplished with organic dichalcogenides  $\text{R}'\text{EER}'$  (E=S, Se, Te,  $\text{R}'=^n\text{Bu}$ , Ph) to produce the corresponding organolead chalcogenides  $\text{Ph}_3\text{PbER}'$  [ $\text{R}'=\text{Bu}$  (386), Ph (387)].<sup>386</sup> Catalyzed by  $^t\text{Bu}_3\text{P}$ , elemental tellurium efficiently inserted into the Pb–Pb bond of  $\text{Ph}_3\text{PbPbPh}_3$  (385) as well, giving  $\text{Ph}_3\text{PbTePbPh}_3$  (388).<sup>234</sup> Photolysis of hexaphenyldiplumbane (385) in benzene in the





**Scheme 35** Formation of metalloid clusters by reduction of organostannylene chlorides.



**Scheme 36** Temperature dependence of diplumbane versus monplumbane formation.

presence of *tert*-butylperoxide yielded the triphenylplumbyl radical (389).<sup>12</sup> Electron spin resonance spectroscopy was used to study spin adducts from the reaction of plumbyl radicals with quinones on several occasions.<sup>387–390</sup>

Not much is known about reactions of diplumbanes with transition metals. Work by Eaborn, Pidcock, and others showed that the initial product of the reaction of Ph<sub>6</sub>Pb<sub>2</sub> (385) with [Pt(C<sub>2</sub>H<sub>4</sub>)(PPh<sub>3</sub>)<sub>2</sub>] is *cis*-[PtPh(Pb<sub>2</sub>Ph<sub>5</sub>)(PPh<sub>3</sub>)<sub>2</sub>] (390) which, after some time, decomposes to *cis*-[PtPh(PbPh<sub>3</sub>)(PPh<sub>3</sub>)<sub>2</sub>] (391).<sup>391–393</sup> This facile oxidative addition of the Pb–Ph bond allowed similar reactions with compounds such as PhPbMe<sub>3</sub> (392).<sup>393</sup>

### 1.03.3.4 Structural Features of the Pb–Pb Bond

A search for Pb–Pb single bond in the Cambridge Crystallographic database (Conquest 1.12) yielded 44 hits. Excluding Zintl-type clusters and bonds of divalent Pb atoms to each other left 16 compounds with 25 Pb–Pb bonds. The bond distances ranged from 2.839 Å for hexaphenyl- (385) and 1,1,2-triphenyl-1,2,2-tri(4-tolyl)diplumbane (393)<sup>394,395</sup> to 3.201 Å for hexakis(2,4,6-triethylphenyl)cyclotriplumbane (394),<sup>396</sup> with the mean value being 2.946 Å. For diplumbanes, which constitute with 12 examples the majority of the structurally characterized compounds, the Pb–Pb bonding distance falls within the range of the above-mentioned 2.839 and 2.970 Å for 1,2-bis(trimethylsilyl)methyltetramethyldiplumbane (395).<sup>397</sup> Like <sup>13</sup>C, <sup>29</sup>Si, and <sup>117/119</sup>Sn, lead also possesses an NMR-active isotope with nuclear spin 1/2. <sup>207</sup>Pb has a natural abundance of 22.1%, relative sensitivity of 9.2 × 10<sup>−3</sup> compared to 1 for <sup>1</sup>H and a resonance frequency of 104.60 MHz relative to 500 MHz for <sup>1</sup>H. NMR techniques and the chemical-shift

behavior of organolead compounds has been the subject of several reviews.<sup>13,398,399</sup> Comparison of UV-absorption data of some oligoplumbanes with structurally related oligomers of other heavy group-14 elements revealed the expected bathochromic shift for the plumbanes, consistent with low energy σ–σ\* transitions.<sup>400</sup>

### 1.03.3.5 Diplumbanes

#### 1.03.3.5.1 Synthesis

Reexamining the papers published by Löwig<sup>401</sup> in 1853 on the synthesis of tetraethyllead (396), it now seems evident<sup>376</sup> that hexaethyldiplumbane (397), the first diplumbane, was also formed as a byproduct. Unfortunately, this was not recognized by Löwig. With rather unclear perceptions on the valence properties of lead, it was not until 1923 that Calingaert and coworkers<sup>402</sup> unequivocally proved the existence of hexaethyl-diplumbane formed by electrolysis of Et<sub>3</sub>PbOH (398). While Löwig's synthesis engaged the reaction of ethyl iodide with a Pb–Na alloy, the preparative methods currently utilized involve the reaction of appropriate Grignard reagents with PbX<sub>2</sub> or Pb(OAc)<sub>4</sub>.<sup>385</sup> The use of PbCl<sub>4</sub> or K<sub>2</sub>PbCl<sub>6</sub> is discouraged because of the strong oxidizing character of these reagents.

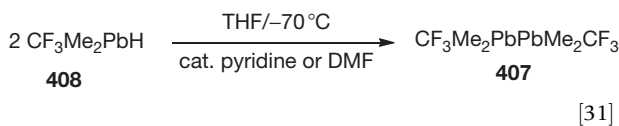
Depending on the conditions, reactions with Grignard reagents lead either to mono- or diplumbanes. While the primary products formed in these reactions are the unstable plumbylenes R<sub>2</sub>Pb, temperature is a decisive parameter for the formation of either mono- or diplumbanes. If the reaction is heated at about 80 °C, mainly R<sub>4</sub>Pb and elemental lead are formed. Alternatively, temperatures below 40 °C (refluxing Et<sub>2</sub>O) lead to the almost exclusive formation of diplumbanes (hexaalkyl or -aryl) and lead (Scheme 36). The series of arylated diplumbanes of the type R<sub>3</sub>PbPbR<sub>3</sub> prepared this way includes R = phenyl (385), *o*-Tol (399), *m*-Tol (400), *p*-Tol (401), *p*-anisyl (402), 1-naphthyl (403), and 2-naphthyl (404).<sup>403</sup>

An unusually bulky diplumbane (405) was formed in the reaction of 2,4,6-tris(*tert*-butyl)phenyllithium with PbCl<sub>2</sub>.

Instead of the expected plumbylene  $\text{Ar}_2\text{Pb}$ , a diplumbane was formed with rearranged arylalkyl substituents (Scheme 37).<sup>404</sup>

An inherent limitation of this method for the preparation of diplumbanes is that it yields only symmetrically substituted compounds. Reactions of  $\text{Ar}_3\text{PbLi}$  with  $\text{Ar}'_3\text{PbCl}$  ( $\text{Ar}=\text{Ar}'=\text{Ph}$ , *o*-Tol, *p*-Tol) gave inseparable mixtures of  $\text{Pb}_2\text{Ar}_{6-n}\text{Ar}'_n$  ( $n=0-6$ ) instead of the expected asymmetric diplumbanes  $\text{Ar}_3\text{PbPbAr}'_3$  (406).<sup>394</sup> Changing to the more soluble  $\text{Ar}'_3\text{PbI}$  improved the situation but still could not fully suppress the formation of the symmetric compounds  $\text{Pb}_2\text{Ar}_6$  and  $\text{Pb}_2\text{Ar}'_6$  ( $\text{Ar}=\textit{o}$ -Tol, *m*-Tol, *p*-Tol, 2,5-Xyl, 2,4-Xyl, *p*-Anis, 2-Napht;  $\text{Ar}'=\textit{o}$ -Tol, *m*-Tol, *p*-Tol, 2,5-Xyl, 2,4-Xyl).<sup>405</sup>

Formation of  $(\text{CF}_3\text{Me}_2\text{Pb})_2$  (407) was possible by base-catalyzed dehydrogenation of  $\text{CF}_3\text{Me}_2\text{PbH}$  (408) (eqn [31]).<sup>406,407</sup>



A few diplumbanes with silyl and germyl substituents are known. Reacting  $\text{Ph}_2\text{PbCl}_2$  (409) with  $(\text{Me}_3\text{Si})_3\text{SiLi}$  gave, in addition to the expected  $[(\text{Me}_3\text{Si})_3\text{Si}]_2\text{PbPh}_2$  (410),  $[(\text{Me}_3\text{Si})_3\text{Si}]_2\text{PbPhPbPh}_2[\text{Si}(\text{SiMe}_3)_3]$  (411) as the major product.<sup>408</sup> Repeating the reaction with  $(\text{Me}_3\text{Si})_3\text{GeLi}$  (14) led to an almost identical situation, with  $[(\text{Me}_3\text{Si})_3\text{Ge}]_2\text{PbPh}_2$  (412) being the major product (37%), accompanied by  $[(\text{Me}_3\text{Si})_3\text{Ge}]_2\text{PbPh}_2$  (413) (26%).<sup>409</sup> The UV/vis spectra of  $[(\text{Me}_3\text{Si})_3\text{Si}]_2\text{PbPhPbPh}_2[\text{Si}(\text{SiMe}_3)_3]$  (411) and  $[(\text{Me}_3\text{Si})_3\text{Ge}]_2\text{PbPhPbPh}_2[\text{Ge}(\text{SiMe}_3)_3]$  (412) showed strong absorptions at 369 and 375 nm, respectively, consistent with  $\sigma$ -electron delocalization. Formation of both diplumbanes

was postulated to occur via transient formation of the radical  $[(\text{Me}_3\text{Si})_3\text{E}]\text{PbPh}_2$  ( $\text{E}=\text{Si}$  (410),  $\text{Ge}$  (413)).

While a related reaction of  $\text{Ph}_2\text{PbCl}_2$  with  $(\text{Me}_3\text{Si})_3\text{CLi}$  gave  $[(\text{Me}_3\text{Si})_3\text{C}]\text{Ph}_2\text{PbPbPh}_3$  (414) instead of the expected  $[(\text{Me}_3\text{Si})_3\text{C}]\text{Ph}_2\text{PbPbPh}_2[\text{C}(\text{SiMe}_3)_3]$  (415),<sup>410</sup> the analogous methylated derivative  $[(\text{Me}_3\text{Si})_3\text{C}]\text{Me}_2\text{PbPbMe}_2[\text{C}(\text{SiMe}_3)_3]$  (416) formed smoothly by reaction of  $[(\text{Me}_3\text{Si})_3\text{C}]\text{Me}_2\text{PbBr}$  (417) with either  $\text{Ph}_3\text{SnLi}$  or  $\text{Mg}$ .<sup>397</sup>

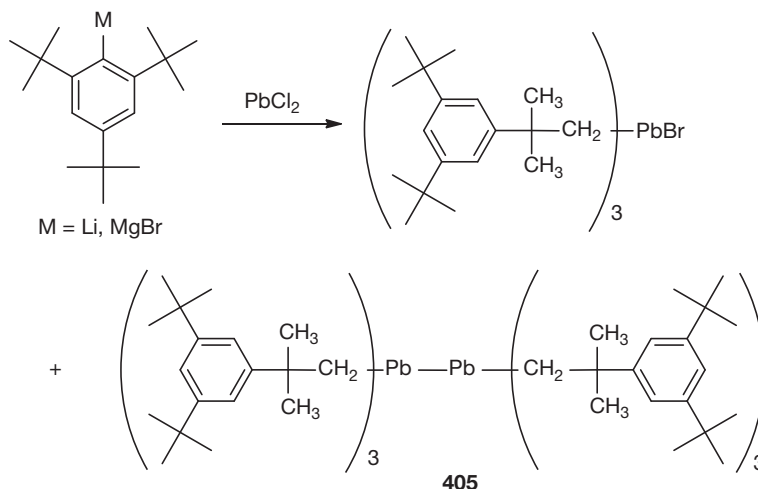
The reaction of (tri-*tert*-butylplumbyl)lithium (418) with diphenyl- and amino(phenyl)phosphorus chlorides led to the formation of hexa-*tert*-butyldiplumbane (419) and the respective diphosphanes.<sup>411</sup>

The availability of plumbates facilitates the synthesis of asymmetric diplumbanes by the reaction of  $\text{R}_3\text{PbM}$  with  $\text{R}^1_3\text{PbX}$ .<sup>405</sup>

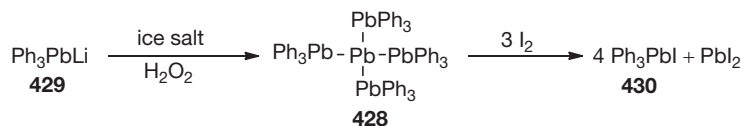
The reaction of trialkylplumbyl methoxides ( $\text{R}=\text{Et}$  (420),  $^n\text{Pr}$  (421),  $^n\text{Bu}$  (422)) with diborane led to formation of trialkylplumbyl boranates  $\text{R}_3\text{PbBH}_4$  ( $\text{R}=\text{Et}$  (423),  $^n\text{Pr}$  (424),  $^n\text{Bu}$  (425)) which at temperatures above  $-20^\circ\text{C}$  slowly decompose to diplumbanes  $\text{R}_3\text{PbPbR}_3$  ( $\text{R}=\text{Et}$  (382),  $^n\text{Pr}$  (426),  $^n\text{Bu}$  (427)), diborane, and hydrogen.<sup>412</sup>

### 1.03.3.6 Oligoplumbanes

It is interesting to note that the number of compounds with more than one Pb–Pb bond is extremely small. As early as 1964, Willemsens and van der Kerk reported the synthesis of the bright red  $(\text{Ph}_3\text{Pb})_4\text{Pb}$  (428).<sup>413,414</sup> Reinvestigating an older report by Krause<sup>415</sup> on the formation of diphenyllead,  $(\text{Ph}_3\text{Pb})_4\text{Pb}$  (428) was obtained by simultaneous hydrolysis and oxidation of  $\text{Ph}_3\text{PbLi}$  (429) (Scheme 38). Although the identity of 428 was strongly suggested by elemental analysis



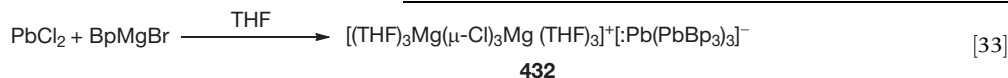
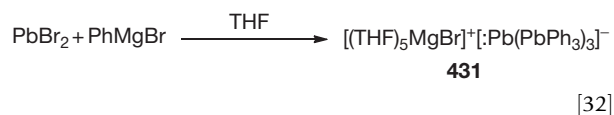
**Scheme 37** Formation of a bulky diplumbane by rearrangement of a diarylplumbylene.



**Scheme 38** Formation of a neopentaplumbane by simultaneous hydrolysis and oxidation of  $\text{Ph}_3\text{PbLi}$ .

and reaction with iodine, which gave four equivalents of  $\text{Ph}_3\text{PbI}$  (430) and  $\text{PbI}_2$ , crystallographic and NMR spectroscopic characterization are still missing. UV/vis spectroscopy of this and related compounds with other group-IV elements revealed that only compounds containing at least one Pb atom are colored.<sup>400</sup> In addition to an absorption band at 358 nm, which would be consistent with a triplumbane,  $(\text{Ph}_3\text{Pb})_4\text{Pb}$  was found to exhibit another strong absorption band at 444 nm.<sup>400</sup>

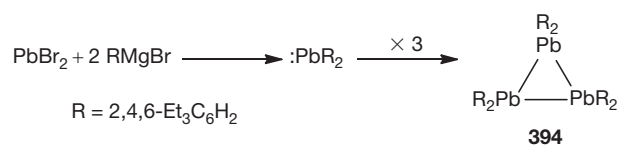
Almost 40 years after Willemsens' work, Weidenbruch<sup>416</sup> reported the formation of the structurally related  $(\text{Ph}_3\text{Pb})_3\text{PbMgBr}$  (431) (eqn [32]) followed by a similar study by Robinson<sup>417</sup> about  $(\text{Bp}_3\text{Pb})_3\text{PbMgCl}$  (432) ( $\text{Bp} = 4$ -biphenyl) (eqn [33]). Single-crystal-diffraction studies of both plumbates reveal elongated Pb–Pb bonds of around 2.97 Å compared to a mean value of 2.857 Å for  $\text{Ar}_3\text{PbPbAr}_3$ .<sup>394,395,417–420</sup> Neither NMR spectroscopic properties ( $(\text{Ph}_3\text{Pb})_3\text{PbMgBr}$  was described as very insoluble at low temperature and not stable at higher temperature)<sup>416</sup> nor basic reactivity of the plumbates were reported.



The only known cyclic molecule with several Pb–Pb bonds is hexakis(2,4,6-triethylphenyl)cyclotriplumbane (394), also reported by Weidenbruch.<sup>396</sup> By delicate tuning of the steric properties of the aryl group, the cyclotriplumbane can be considered as an alternative arrangement to the monomeric (plumbylene, e.g.,  $\text{Ar} = 2$ -*t*-Bu-4,5,6-Me<sub>3</sub>C<sub>6</sub>H) and dimeric forms (diplumbene, less bulky substituent, f.i.  $\text{Ar} = 2,4,6$ -*i*-Pr<sub>3</sub>C<sub>6</sub>H<sub>2</sub>) of  $\text{Ar}_2\text{Pb}$  (Scheme 39). This assignment is further supported by the unusually long Pb–Pb bonds (3.184 Å) and the orientation of the substituents at Pb, which are twisted by some 37° out of the ideal positions.<sup>396</sup>

### 1.03.3.7 Lead Clusters

The chemistry of Zintl-type cluster ions such as  $\text{Pb}_5^{2-}$ ,  $\text{Pb}_9^{3-}$ , and  $\text{Pb}_9^{4-}$  and related structures of Si, Ge, and Sn has become the subject of intense research over the last some 20 years. It will therefore be treated in Chapter 1.08. Through the use of coordinating agents, many of these ions have been brought into solution and could even be derivatized. For lead clusters, alkyl- or aryl-substituted examples are not known, but Klinckhammer and coworkers were able to obtain tris(trimethylsilyl)



**Scheme 39** Cyclotriplumbane as trimeric form of a plumbylene.

silylated lead clusters.<sup>421</sup> During investigations concerning the reaction of  $[(\text{Me}_3\text{Si})_3\text{Si}]_2\text{Pb}$  (433)<sup>422</sup> with  $\text{PH}_3$ , which leads mainly to the heterocubane  $[(\text{HypPPb})_4]$  (434) [ $\text{Hyp} = \text{Si}(\text{SiMe}_3)_3$ ], a molecular lead cluster  $[\text{Pb}_{12}\text{Hyp}_6]$  (435) was obtained in minute amounts. Crystal-structure analysis showed the Pb atoms to constitute a distorted icosahedron. In the course of verification of the assumed intermediate  $\text{HypPbH}$  (436), the reaction of  $\text{Hyp}_2\text{Pb}$  (433) with a copper hydride gave another molecular lead cluster  $[\text{Pb}_{10}\text{Hyp}_6]$  (437) in a yield of 47%. The observed  $\text{Pb}_{10}$  core with approximately  $\text{C}_{3v}$  symmetry can be envisioned to be constructed from a  $\text{Pb}_{12}$  icosahedron by replacing one trigonal face by a single Pb atom.<sup>421</sup>

### 1.03.4 Conclusion

Compared to the chemistry of catenated silicon compounds, the related areas of the analogous chemistry of germanium, tin, and lead are much less developed. The research efforts in these fields are quite different. In particular, the chemistry of catenated lead compounds has been developed very little. One reason for this is certainly the weak Pb–Pb bond, but the chemistry of polyplumbanes suffers from more than problems associated with weak bonds. The decline of the use of organo-

lead compounds as additives for gasoline was strongly connected to a growing awareness of the toxicological properties of these substances. The stigma of being a notorious class of compounds has also become attached to oligoplumbanes and, consequently, not much research in this field has been published over the last decade.

The situation for catenated germanium compounds is hampered by some other problems. Probably the most serious problem of germanium chemistry in comparison to silicon and tin is the high commodity price of germanium. With germanium compounds being  $10^2$ – $10^3$  times more expensive than the analogous silicon compounds, research on germanium chemistry needs to establish germanium as an element with unique properties and a unique chemistry in order to justify any application of germanium in synthesis or in industry. Together with some analytical problems associated with germanium, namely the difficulties in applying NMR spectroscopy, the cost problem has likely impeded systematic advances in the chemistry of oligo- and polygermanes for a long time. Only very recently have several research groups begun investigations into the development of methods for the formation of Ge–Ge bonds. The results of these studies have already indicated a surprisingly unique behavior of germanium compared to silicon and tin. Therefore, it seems likely that further research can be expected in this area.

While tin is not expensive and can easily be studied by NMR spectroscopy, the toxicity of tin compounds has become an increasing concern in recent years. Nevertheless, the chemistry of oligo- and polystannanes is well established. Tin-containing chemicals have already proven useful for a wide



spectrum of applications ranging from polymer stabilizers, wood preservatives, disinfectants, fungicides, material science, synthetic chemistry, and so on.<sup>199,202</sup> Among the compounds used, the number of those having Sn–Sn bonds is quite small and mostly limited to distannanes. Applications of these compounds usually employ the Sn–Sn bond as a source of functionality rather than making use of the physical properties. Distannanes are thus mainly used in organic synthesis to introduce stannyl substituents via catalytic cleavage of the Sn–Sn bond.<sup>423</sup> Frequently, the obtained stannylated compounds are then used as synthetic intermediates for cross-coupling reactions such as the Stille reaction.<sup>196</sup> The comparably high stability of stannyl radicals has further led to their use as initiators for polymerization as well as various cyclization reactions. Usually, these reactions involve organotin hydrides in combination with AIBN or hexaorganodistannanes, which are irradiated with UV light to generate radicals. Alternatively, a system based on a polymer-bound distannane was reported.<sup>424</sup> The removal of residues of organotin compounds, a sometimes difficult task that is of high importance in the synthesis of pharmaceuticals, is thus facilitated.

Polystannanes are a very interesting class of compounds with respect to their physical properties. The phenomenon of  $\sigma$ -bond electron delocalization would suggest applications as molecular semi-conductors, resists for microlithography, or optoelectronic materials. Good synthetic methods for the preparation of polystannanes have already been worked out. However, a major problem impeding immediate application is associated with their limited stability, especially toward light. Clearly, this has to be addressed and solved before technological applications of this interesting class of compounds can be expected to emerge.

In contrast to the chemistry of oligo- and polymers of germanium, tin, and lead, which cannot be considered as fields of very active research, the cluster chemistry of these elements currently emerges as a very interesting area at the interface of molecular and solid-state chemistry of group-14 elements. This development includes both the chemistry of Zintl anions and the field of compounds in which the oxidation state of the cluster atoms is close to that of the elemental state. With many applications of nano-sized materials under intense investigation, there will be a huge demand for materials with defined molecular structure and the possibility of selective chemical manipulation. It is quite likely that nano-clusters of germanium, tin, and lead will play an important role in this field. While currently mainly germanium and tin are used as the elements of choice in this chemistry, there are some examples of related lead clusters and it can be expected that organolead chemistry may experience something of a renaissance in this area.

## References

- Winkler, C. *Ber. Dtsch. Chem. Ges.* **1886**, *19*, 210–211.
- Winkler, C. *J. Prakt. Chem.* **1886**, *34*, 177–229.
- Winkler, C. *J. Prakt. Chem.* **1887**, *36*, 177–209.
- Morgan, G. T.; Drew, H. D. K. *J. Chem. Soc. Trans.* **1925**, *127*, 1760–1768.
- Voronkov, M. G.; Abzaeva, K. A. *In The Chemistry of Organic Germanium, Tin and Lead Compounds*; Rappoport, Z., Ed.; Wiley: Chichester (England), New York, 2002; Vol. 2, pp 1–130.
- Baines, K. M.; Stibbs, W. G. *Coord. Chem. Rev.* **1995**, *145*, 157–200.
- Amadoruge, M. L.; Weinert, C. S. *Chem. Rev.* **2008**, *108*, 4253–4294.
- Weinert, C. S. *Dalton Trans.* **2009**, 1691–1699.
- Cotton, A. F.; Wilkinson, G.; Murillo, C. A.; Bochmann, M. *Advanced Inorganic Chemistry*, 6th ed.; Wiley: New York, 1999.
- Long, C.; Pryce, M. T. *In The Chemistry of Organic Germanium, Tin and Lead Compounds*; Rappoport, Z., Ed.; Wiley: Chichester (England), New York, 2002; Vol. 2, pp 1521–1542.
- Tsumuraya, T.; Sato, S.; Ando, W. *Organometallics* **1988**, *7*, 2015–2019.
- Weidenbruch, M. *J. Organomet. Chem.* **1988**, *341*, 335–343.
- Marsmann, H. C.; Uhlig, F. *In The Chemistry of Organic Germanium, Tin and Lead Compounds*; Rappoport, Z., Ed.; Wiley: Chichester (England), New York, 2002; Vol. 2, pp 399–460.
- Aoyagi, S.; Tanaka, K.; Zicmane, I.; Takeuchi, Y. *J. Chem. Soc., Perkin Trans.* **1992**, *2*, 2217–2220.
- Wrackmeyer, B.; Bernatowicz, P. *J. Organomet. Chem.* **1999**, *579*, 133–138.
- Amadoruge, M. L.; Yoder, C. H.; Hope, C.; Heroux, K.; Rheingold, A. L.; Weinert, C. S. *Organometallics* **2009**, *28*, 3067–3073.
- Yoder, C. H.; Agee, T. M.; Schaeffer, C. D.; Carroll, M. J.; Fleisher, A. J.; DeToma, A. S. *Inorg. Chem.* **2008**, *47*, 10765–10770.
- Hill, M. *In Metal–Metal Bonding*. Parkin, G., Ed.; Springer: Berlin/Heidelberg, 2010; Vol. 136, pp 189–216.
- Mochida, K.; Chiba, H. *J. Organomet. Chem.* **1994**, *473*, 45–54.
- Kodaira, T.; Watanabe, A.; Ito, O.; Matsuda, M.; Tokura, S.; Kira, M.; Nagano, S. S.; Mochida, K. *Adv. Mater.* **1995**, *7*, 917–919.
- Seki, K.; Yuyama, A.; Narioka, S.; Ishii, H.; Hasegawa, S.; Isaka, H.; Fujino, M.; Fujiki, M.; Matsumoto, N. *ACS Symp. Ser.* **1994**, *579*, 398–407.
- Ishii, H.; Yuyama, A.; Narioka, S.; Seki, K.; Hasegawa, S.; Fujino, M.; Isaka, H.; Fujiki, M.; Matsumoto, N. *Synth. Met.* **1995**, *69*, 595–596.
- Watanabe, A.; Sato, T.; Matsuda, M. *Jpn. J. Appl. Phys.* **2001**, *Part 1* *40*, 6457–6463.
- Kumada, M.; Tamao, K. *Adv. Organomet. Chem.* **1968**, *6*, 19–117.
- Jurkschat, K.; Mehring, M. *In The Chemistry of Organic Germanium, Tin and Lead Compounds*; Rappoport, Z., Ed.; Wiley: Chichester (England), New York, 2002; Vol. 2, pp 1543–1652.
- Miller, R. D.; Michl, J. *Chem. Rev.* **1989**, *89*, 1359–1410.
- Glockling, F.; Hooton, K. A.; Kotz, J. C.; Laubengayer, A. W. *Inorg. Synth.* **1966**, *8*, 31–34.
- Kraus, C. A.; Flood, E. A. *J. Am. Chem. Soc.* **1932**, *54*, 1635–1644.
- Brown, M. P.; Fowles, G. W. A. *J. Chem. Soc.* **1958**, 2811–2814.
- Triplett, K.; Curtis, M. D. *J. Organomet. Chem.* **1976**, *107*, 23–32.
- Metlesics, W.; Zeiss, H. *J. Am. Chem. Soc.* **1960**, *82*, 3321–3323.
- Lalov, A. V.; Nosov, K. S.; Egorov, M. P.; Nefedov, O. M. *Russ. Chem. Bull.* **2004**, *53*, 2334–2335.
- Lee, C.; Lee, J.; Lee, S. W.; Kang, S. O.; Ko, J. *Inorg. Chem.* **2002**, *41*, 3084–3090.
- Mochida, K.; Karube, H.; Nanjo, M.; Nakadaira, Y. *J. Organomet. Chem.* **2005**, *690*, 2967–2974.
- Takeuchi, Y.; Suzuki, Y.; Ono, F.; Manabe, K. *J. Organomet. Chem.* **2003**, *678*, 61–67.
- Azemi, T.; Yokoyama, Y.; Mochida, K. *J. Organomet. Chem.* **2005**, *690*, 1588–1593.
- Kamiya, I.; Iida, K.; Harato, N.; Li, Z.-f.; Tomisaka, Y.; Ogawa, A. *J. Alloys Compd.* **2006**, *408–412*, 437–440.
- Trifonov, A. A.; Fedorova, E. A.; Kirillov, E. N.; Bochkarev, M. N.; Girgsdies, F.; Schumann, H. *Russ. Chem. Bull.* **2000**, *49*, 1436–1439.
- Balashova, T. V.; Kusyayev, D. M.; Kulikova, T. I.; Kuznetsova, O. N.; Edelmann, F. T.; Giessmann, S.; Blaurock, S.; Bochkarev, M. N. *Z. Anorg. Allg. Chem.* **2007**, *633*, 256–260.
- Bulten, E. J.; Noltes, J. G. *Tetrahedron Lett.* **1966**, *7*, 4389–4392.
- Castel, A.; Riviere, P.; Satge, J.; Ko, Y. H. *J. Organomet. Chem.* **1988**, *342*, C1–C4.
- Inoue, S.; Sato, Y. *Organometallics* **1989**, *8*, 1237–1241.
- Pigarev, S.; Bravozhivotovskii, D.; Kalikhman, I.; Vyazankin, N.; Voronkov, M. *J. Organomet. Chem.* **1989**, *369*, 29–41.
- Castel, A.; Riviere, P.; Satge, J.; Ko, Y. H.; Desor, D. *J. Organomet. Chem.* **1990**, *397*, 7–15.
- Takeda, N.; Tokitoh, N.; Okazaki, R. *Sci. Synth.* **2003**, *5*, 33–37.
- Tamborski, C.; Ford, F. E.; Lehn, W. L.; Moore, G. J.; Soloski, E. J. *J. Org. Chem.* **1962**, *27*, 619–621.
- Buncel, E.; Venkatachalam, T. K. *Heteroat. Chem.* **1994**, *5*, 201–204.
- Buncel, E.; Venkatachalam, T. K.; Edlund, U.; Eliasson, B. *J. Chem. Soc. Chem. Commun.* **1984**, 1476–1477.
- Bulten, E. J.; Noltes, J. G. *J. Organomet. Chem.* **1971**, *29*, 397–407.



50. Baines, K. M.; Mueller, K. A.; Sham, T. K. *Can. J. Chem.* **1992**, *70*, 2884–2886.
51. Nanjo, M.; Maehara, M.; Ushida, Y.; Awamura, Y.; Mochida, K. *Tetrahedron Lett.* **2005**, *46*, 8945–8947.
52. Piers, E.; Lemieux, R. *Organometallics* **1995**, *14*, 5011–5012.
53. Hashimoto, H.; Yagihashi, Y.; Ignatovich, L.; Kira, M. *Heteroat. Chem.* **2001**, *12*, 398–405.
54. Kusakawa, T.; Ando, W. *J. Organomet. Chem.* **1998**, *561*, 109–120.
55. Chisholm, M. H.; Gama, G. J.; Parkin, I. P. *Polyhedron* **1993**, *12*, 961–965.
56. Wickham, G.; Young, D.; Kitching, W. *J. Org. Chem.* **1982**, *47*, 4884–4895.
57. Vyazankin, N. S.; Razuvaev, G. A.; Gladyshev, E. N.; Korneva, S. P. *J. Organomet. Chem.* **1967**, *7*, 353–357.
58. Gladyshev, E. N.; Vyazankin, N. S.; Fedorova, E. A.; Yuntala, L. O.; Razuvaev, G. A. *J. Organomet. Chem.* **1974**, *64*, 307–314.
59. Nanjo, M.; Matsudo, K.; Mochida, K. *Inorg. Chem. Commun.* **2003**, *6*, 1065–1067.
60. Riviere, P.; Satgé, J. *Bull. Soc. Chim. Fr.* **1971**, 3221–3231.
61. Bochkarev, M. *J. Organomet. Chem.* **1976**, *110*, 149–157.
62. Subashi, E.; Rheingold, A. L.; Weinert, C. S. *Organometallics* **2006**, *25*, 3211–3219.
63. Amadoruge, M. L.; DiPasquale, A. G.; Rheingold, A. L.; Weinert, C. S. *J. Organomet. Chem.* **2008**, *693*, 1771–1778.
64. Mallela, S. P.; Geanangel, R. A. *Inorg. Chem.* **1991**, *30*, 1480–1482.
65. Fischer, J.; Baumgartner, J.; Marschner, C. *Organometallics* **2005**, *24*, 1263–1268.
66. Baumgartner, J.; Fischer, R.; Fischer, J.; Wallner, A.; Marschner, C.; Floerke, U. *Organometallics* **2005**, *24*, 6450–6457.
67. Brook, A. G.; Abdesaken, F.; Söllradl, H. *J. Organomet. Chem.* **1986**, *299*, 9–13.
68. Mallela, S. P.; Geanangel, R. A. *Inorg. Chem.* **1994**, *33*, 1115–1120.
69. Mallela, S. P.; Geanangel, R. A. *Inorg. Chem.* **1993**, *32*, 5623–5625.
70. Renner, G.; Kircher, P.; Huttner, G.; Rutsch, P.; Heinze, K. *Eur. J. Inorg. Chem.* **2000**, 879–887.
71. Aitken, C.; Harrod, J. F.; Malek, A.; Samuel, E. *J. Organomet. Chem.* **1988**, *349*, 285–291.
72. Castel, A.; Riviere, P.; Satgé, J.; Ahbala, M.; Abdenadher, C.; Desor, D. *Main Group Met. Chem.* **1993**, *16*, 291–303.
73. Samuel, M. S.; Jennings, M. C.; Baines, K. M. *J. Organomet. Chem.* **2001**, *636*, 130–137.
74. Samuel, M. S.; Jennings, M. C.; Baines, K. M. *Organometallics* **2001**, *20*, 590–592.
75. Huck, L. A.; Leigh, W. J. *Organometallics* **2007**, *26*, 1339–1348.
76. Fujidala, K. L.; Gracey, D. W. K.; Wong, E. F.; Baines, K. M. *Can. J. Chem.* **2002**, *80*, 1387–1392.
77. Dixon, C. E.; Netherton, M. R.; Baines, K. M. *J. Am. Chem. Soc.* **1998**, *120*, 10365–10371.
78. Samuel, M. S.; Baines, K. M. *J. Am. Chem. Soc.* **2003**, *125*, 12702–12703.
79. Pampuch, B.; Saak, W.; Weidenbruch, M. *J. Organomet. Chem.* **2006**, *691*, 3540–3544.
80. Mochida, K.; Kayamori, T.; Wakasa, M.; Hayashi, H.; Egorov, M. P. *Organometallics* **2000**, *19*, 3379–3386.
81. Spikes, G. H.; Fettingner, J. C.; Power, P. P. *J. Am. Chem. Soc.* **2005**, *127*, 12232–12233.
82. Wang, X.; Peng, Y.; Zhu, Z.; Fettingner, J. C.; Power, P. P.; Guo, J.; Nagase, S. *Angew. Chem. Int. Ed.* **2010**, *49*, 4593–4597.
83. Summerscales, O. T.; Jimenez-Halla, J. O. C.; Merino, G.; Power, P. P. *J. Am. Chem. Soc.* **2011**, *133*, 180–183.
84. Sugiyama, Y.; Sasamori, T.; Hosoi, Y.; Furukawa, Y.; Takagi, N.; Nagase, S.; Tokitoh, N. *J. Am. Chem. Soc.* **2006**, *128*, 1023–1031.
85. Höfler, F.; Brandstätter, E. *Monatsh. Chem.* **1975**, *106*, 893–904.
86. Häberle, K.; Dräger, M. *Z. Naturforsch. B* **1987**, *42*, 323–329.
87. Amadoruge, M. L.; Short, E. K.; Moore, C.; Rheingold, A. L.; Weinert, C. S. *J. Organomet. Chem.* **2010**, *695*, 1813–1823.
88. Simon, D.; Häberle, K.; Dräger, M. *J. Organomet. Chem.* **1984**, *267*, 133–142.
89. Barrau, J.; Rima, G.; El, A.; Satgé, J. *Synth. React. Inorg. Met. Org. Chem.* **1988**, *18*, 21–28.
90. Bulten, E. J.; Noltes, J. G. *Tetrahedron Lett.* **1966**, *7*, 3471–3476.
91. Curtis, M. D.; Wolber, P. *Inorg. Chem.* **1972**, *11*, 431–433.
92. Beattie, I. R.; Jones, P. J.; Reid, G.; Webster, M. *Inorg. Chem.* **1998**, *37*, 6032–6034.
93. Shriver, D.; Jolly, W. L. *J. Am. Chem. Soc.* **1958**, *80*, 6692–6693.
94. Jolly, W. L.; Lindahl, C. B.; Kopp, R. W. *Inorg. Chem.* **1962**, *1*, 958–960.
95. Mochida, K.; Ogawa, S.; Naito, N.; Gaber, A. E.-A.; Usui, Y.; Nanjo, M. *Chem. Lett.* **2007**, *36*, 414–415.
96. Zirngast, M.; Flock, M.; Baumgartner, J.; Marschner, C. *J. Am. Chem. Soc.* **2009**, *131*, 15952–15962.
97. Roller, S.; Simon, D.; Dräger, M. *J. Organomet. Chem.* **1986**, *301*, 27–40.
98. Zhun, V. I.; Sbitneva, I. V.; Kisin, A. V.; Chernyshev, E. A. *Russ. J. Gen. Chem.* **2004**, *74*, 1130–1131.
99. Häberle, K.; Dräger, M. *J. Organomet. Chem.* **1986**, *312*, 155–165.
100. Dräger, M.; Simon, D. *J. Organomet. Chem.* **1986**, *306*, 183–192.
101. Amadoruge, M. L.; Gardinier, J. R.; Weinert, C. S. *Organometallics* **2008**, *27*, 3753–3760.
102. Dräger, M.; Simon, D. *Z. Anorg. Allg. Chem.* **1981**, *472*, 120–128.
103. Neumann, W. P.; Kühlein, K. *Justus Liebigs Ann. Chem.* **1965**, *683*, 1–11.
104. Glockling, F.; Hooton, K. A. *J. Chem. Soc.* **1963**, 1849–1854.
105. Amadoruge, M. L.; Golen, J. A.; Rheingold, A. L.; Weinert, C. S. *Organometallics* **2008**, *27*, 1979–1984.
106. Samanamu, C. R.; Amadoruge, M. L.; Yoder, C. H.; Golen, J. A.; Moore, C. E.; Rheingold, A. L.; Materer, N. F.; Weinert, C. S. *Organometallics* **2011**, 1046–1058.
107. Roller, S.; Dräger, M. *J. Organomet. Chem.* **1986**, *316*, 57–65.
108. Meyer-Wegner, F.; Nadj, A.; Bolte, M.; Auner, N.; Wagner, M.; Holthausen, M. C.; Lerner, H.-W. *Chem. Eur. J.* **2011**, *17*, 4715–4719.
109. Glockling, F.; Light, J. R. C.; Strafford, R. G. *J. Chem. Soc. A* **1970**, 426–432.
110. Glockling, F.; Light, J. R. C.; Walker, J. *Chem. Commun. (London)* **1968**, 1052–1053.
111. Hlina, J.; Baumgartner, J.; Marschner, C. *Organometallics* **2010**, *29*, 5289–5295.
112. Leung, W.-P.; So, C.-W.; Chong, K.-H.; Kan, K.-W.; Chan, H.-S.; Mak, T. C. W. *Organometallics* **2006**, *25*, 2851–2858.
113. Wagner, H.; Baumgartner, J.; Müller, T.; Marschner, C. *J. Am. Chem. Soc.* **2009**, *131*, 5022–5023.
114. Seki, S.; Acharya, A.; Koizumi, Y.; Saeki, A.; Tagawa, S.; Mochida, K. *Chem. Lett.* **2005**, *34*, 1690–1691.
115. Masamune, S.; Hanzawa, Y.; Williams, D. J. *J. Am. Chem. Soc.* **1982**, *104*, 6136–6137.
116. Ando, W.; Tsumuraya, T. *J. Chem. Soc., Chem. Commun.* **1987**, 1514–1515.
117. Tsumuraya, T.; Kabe, Y.; Ando, W. *J. Organomet. Chem.* **1994**, *482*, 131–138.
118. Weidenbruch, M.; Grimm, F. T.; Herrndorf, M.; Schaefer, A.; Peters, K.; von Schnering, H. G. *J. Organomet. Chem.* **1988**, *341*, 335–343.
119. Weidenbruch, M.; Ritschl, A.; Peters, K.; von Schnering, H. G. *J. Organomet. Chem.* **1992**, *438*, 39–44.
120. Mallela, S. P.; Hill, S.; Geanangel, R. A. *Inorg. Chem.* **1997**, *36*, 6247–6250.
121. Klinkhammer, K. W. In *Organosilicon Chem. III [Muench. Silicontage]*, 3rd ed.; Wiley-VCH Verlag GmbH: Weinheim, 1998; pp 82–85.
122. Ichinohe, M.; Sekiyama, H.; Fukaya, N.; Sekiguchi, A. *J. Am. Chem. Soc.* **2000**, *122*, 6781–6782.
123. Lerner, H.-W.; Schoedel, F.; Sanger, I.; Wagner, M.; Bolte, M. *Z. Naturforsch. B: Chem. Sci.* **2004**, *59*, 277–280.
124. Sekiguchi, A.; Yamazaki, H.; Kabuto, C.; Sakurai, H.; Nagase, S. *J. Am. Chem. Soc.* **1995**, *117*, 8025–8026.
125. Fukaya, N.; Ichinohe, M.; Sekiguchi, A. *Angew. Chem. Int. Ed.* **2000**, *39*, 3881–3884.
126. Neumann, W. P.; Kuhlein, K. *Tetrahedron Lett.* **1963**, 1541–1545.
127. Ross, L.; Dräger, M. *J. Organomet. Chem.* **1980**, *199*, 195–204.
128. Carrick, A.; Glockling, F. *J. Chem. Soc. A* **1966**, 623–629.
129. Mochida, K.; Tokura, S. *Bull. Chem. Soc. Jpn.* **1992**, *65*, 1642–1647.
130. Mochida, K.; Kanno, N.; Kato, R.; Kotani, M.; Yamauchi, S.; Wakasa, M.; Hayashi, H. *J. Organomet. Chem.* **1991**, *415*, 191–201.
131. Riviere, P.; Castel, A.; Guyot, D.; Satgé, J. *J. Organomet. Chem.* **1985**, *290*, C15–C18.
132. Sekiguchi, A.; Yatabe, T.; Naito, H.; Kabuto, C.; Sakurai, H. *Chem. Lett.* **1992**, 1697–1700.
133. Castel, A.; Riviere, P.; Satgé, J.; Desor, D.; Ahbala, M.; Abdenadher, C. *Inorg. Chim. Acta* **1993**, *212*, 51–55.
134. Unno, M.; Tanaka, R.; Kyushin, S.; Matsumoto, H. *Phosphorus Sulfur Silicon Relat. Elem.* **1999**, *150–151*, 167–176.
135. Rugar, P. A.; Jennings, M. C.; Baines, K. M. *Organometallics* **2008**, *27*, 5043–5051.
136. Schnepf, A.; Köppe, R. *Z. Anorg. Allg. Chem.* **2002**, *628*, 2914–2918.
137. Schenk, C.; Schnepf, A. *Dalton Trans.* **2007**, 5400–5404.
138. Carberry, E.; Dombek, B. D.; Cohen, S. C. *J. Organomet. Chem.* **1972**, *36*, 61–70.
139. Ross, L.; Dräger, M. *Z. Anorg. Allg. Chem.* **1984**, *519*, 225–232.
140. Dräger, M.; Ross, L.; Simon, D. *Z. Anorg. Allg. Chem.* **1980**, *466*, 145–156.
141. Richter, M.; Neumann, W. P. *J. Organomet. Chem.* **1969**, *20*, 81–90.
142. Dräger, M.; Häberle, K. *J. Organomet. Chem.* **1985**, *280*, 183–196.

143. Ross, L.; Dräger, M. *J. Organomet. Chem.* **1980**, *194*, 23–32.
144. Braddock-Wilking, J.; Bandrowsky, T.; Praingam, N.; Rath, N. P. *Organometallics* **2009**, *28*, 4098–4105.
145. Tanabe, M.; Hanzawa, M.; Ishikawa, N.; Osakada, K. *Organometallics* **2009**, *28*, 6014–6019.
146. Tanabe, M.; Ishikawa, N.; Hanzawa, M.; Osakada, K. *Organometallics* **2008**, *27*, 5152–5158.
147. Sekiguchi, A.; Lee, V. Y. In *The Chemistry of Organic Germanium, Tin and Lead Compounds*; Rappoport, Z., Ed.; Wiley: Chichester (England), New York, 2002; Vol. 2, pp 935–962.
148. Wiberg, N.; Power, P. P. In *Molecular Clusters of the Main Group Elements*; Driess, M., Nöth, H., Eds.; Wiley-VCH: Weinheim, 2004.
149. Sekiguchi, A.; Kinjo, R.; Ichinoe, M. *Science* **2004**, *305*, 1755–1757.
150. Stender, M.; Phillips, A. D.; Wright, R. J.; Power, P. P. *Angew. Chem. Int. Ed.* **2002**, *41*, 1785–1787.
151. Pu, L.; Phillips, A. D.; Richards, A. F.; Stender, M.; Simons, R. S.; Olmstead, M. M.; Power, P. P. *J. Am. Chem. Soc.* **2003**, *125*, 11626–11636.
152. Pu, L.; Twamley, B.; Power, P. P. *J. Am. Chem. Soc.* **2000**, *122*, 3524–3525.
153. Wiberg, N.; Finger, C. M. M.; Polborn, K. *Angew. Chem. Int. Ed. Engl.* **1993**, *32*, 1054–1056.
154. Wiberg, N.; Hochmuth, W.; Noeth, H.; Appel, A.; Schmidt-Amelunxen, M. *Angew. Chem. Int. Ed. Engl.* **1996**, *35*, 1333–1334.
155. Sekiguchi, A.; Kabuto, C.; Sakurai, H. *Angew. Chem. Int. Ed. Engl.* **1989**, *28*, 55–56.
156. Sekiguchi, A.; Yatabe, T.; Doi, S.; Sakurai, H. *Phosphorus Sulfur Silicon Relat. Elem.* **1994**, *93–94*, 193–196.
157. Sekiguchi, A.; Yatabe, T.; Kabuto, C.; Sakurai, H. *J. Am. Chem. Soc.* **1993**, *115*, 5853–5854.
158. Sekiguchi, A.; Yatabe, T.; Kamatani, H.; Kabuto, C.; Sakurai, H. *J. Am. Chem. Soc.* **1992**, *114*, 6260–6262.
159. Unno, M.; Higuchi, K.; Furuya, K.; Shioyama, H.; Kyushin, S.; Goto, M.; Matsumoto, H. *Bull. Chem. Soc. Jpn.* **2000**, *73*, 2093–2097.
160. Schnepf, A.; Koppe, R. *Angew. Chem. Int. Ed.* **2003**, *42*, 911–913.
161. Schnepf, A.; Drost, C. *Dalton Trans.* **2005**, 3277–3280.
162. Schleyer, P. v. R.; Janoschek, R. *Angew. Chem. Int. Ed. Engl.* **1987**, *26*, 1267–1268.
163. Nied, D.; Klopfer, W.; Breher, F. *Angew. Chem. Int. Ed.* **2009**, *48*, 1411–1416.
164. Wang, W.; Yao, S.; Van, W.; Driess, M. *J. Am. Chem. Soc.* **2008**, *130*, 9640–9641.
165. Sekiguchi, A.; Ishida, Y.; Kabe, Y.; Ichinoe, M. *J. Am. Chem. Soc.* **2002**, *124*, 8776–8777.
166. Fässler, T. F.; Hunziker, M. *Inorg. Chem.* **1994**, *33*, 5380–5381.
167. Richards, A. F.; Hope, H.; Power, P. P. *Angew. Chem. Int. Ed.* **2003**, *42*, 4071–4074.
168. Richards, A. F.; Brynda, M.; Olmstead, M. M.; Power, P. P. *Organometallics* **2004**, *23*, 2841–2844.
169. Schnepf, A. *Angew. Chem. Int. Ed.* **2003**, *42*, 2624–2625.
170. Koch, K.; Schnepf, A.; Schnöckel, H. Z. *Anorg. Allg. Chem.* **2006**, *632*, 1710–1716.
171. Schnepf, A. *Chem. Commun.* **2007**, 192–194.
172. Schenk, C.; Schnepf, A. *Chem. Commun.* **2008**, 4643–4645.
173. Schenk, C.; Kracke, A.; Fink, K.; Kubas, A.; Klopfer, W.; Neumaier, M.; Schnöckel, H.; Schnepf, A. *J. Am. Chem. Soc.* **2011**, *133*, 2518–2524.
174. Schenk, C.; Schnepf, A. *Angew. Chem. Int. Ed.* **2007**, *46*, 5314–5316.
175. Schenk, C.; Henke, F.; Santiso-Quinones, G.; Krossing, I.; Schnepf, A. *Dalton Trans.* **2008**, 4436–4441.
176. Henke, F.; Schenk, C.; Schnepf, A. *Dalton Trans.* **2009**, 9141–9145.
177. Schenk, C.; Schnepf, A. *Chem. Commun.* **2009**, 3208–3210.
178. Schnepf, A.; Schenk, C. *Angew. Chem. Int. Ed.* **2006**, *45*, 5373–5376.
179. Kircher, P.; Huttner, G.; Heinze, K.; Renner, G. *Angew. Chem. Int. Ed.* **1998**, *37*, 1664–1666.
180. Renner, G.; Kircher, P.; Huttner, G.; Rutsch, P.; Heinze, K. *Eur. J. Inorg. Chem.* **2001**, 973–980.
181. Hayashi, T.; Uchimarui, Y.; Reddy, N. P.; Tanaka, M. *Chem. Lett.* **1992**, 647–650.
182. Miller, R. D.; Sooriyakumaran, R. *J. Polym. Sci. A: Polym. Chem.* **1987**, *25*, 111–125.
183. Choi, N.; Tanaka, M. *J. Organomet. Chem.* **1998**, *564*, 81–84.
184. Szymanski, W. J.; Visscher, G. T.; Bianconi, P. A. *Macromolecules* **1993**, *26*, 869–871.
185. Reichl, J. A.; Popoff, C. M.; Gallagher, L. A.; Remsen, E. E.; Berry, D. H. *J. Am. Chem. Soc.* **1996**, *118*, 9430–9431.
186. Katz, S. M.; Reichl, J. A.; Berry, D. H. *J. Am. Chem. Soc.* **1998**, *120*, 9844–9849.
187. Motonaga, M.; Nakashima, H.; Katz, S.; Berry, D. H.; Imase, T.; Kawauchi, S.; Watanabe, J.; Fujiki, M.; Koe, J. R. *J. Organomet. Chem.* **2003**, *685*, 44–50.
188. Aeiyaich, S.; Lacaze, P.-C.; Satge, J.; Rima, G. *Synth. Met.* **1993**, *58*, 267–270.
189. Kashimura, S.; Ishifune, M.; Yamashita, N.; Bu, H.-B.; Takebayashi, M.; Kitajima, S.; Yoshiwara, D.; Kataoka, Y.; Nishida, R.; Kawasaki, S.-i.; Murase, H.; Shono, T. *J. Org. Chem.* **1999**, *64*, 6615–6621.
190. Okano, M.; Takeda, K.-I.; Toriumi, T.; Hamano, H. *Electrochim. Acta* **1998**, *44*, 659–666.
191. Okano, M.; Fukai, H.; Arakawa, M.; Hamano, H. *Electrochem. Commun.* **1999**, *1*, 223–226.
192. Barrau, J.; Rima, G.; Akkari, A.; Satge, J. *Inorg. Chim. Acta* **1997**, *260*, 11–15.
193. Kong, E. S. W.; Wunderlich, B. *Macromol. Chem. Phys.* **1981**, *182*, 81–87.
194. Fagan, P. J. *Polym. Prepr.* **1991**, *32*, 443–444.
195. Hollemann, A. F.; Wiberg, E. *Lehrbuch der anorganischen Chemie*, 101st ed.; Walter de Gruyter: Berlin, 1995.
196. Duncton, M. A. J.; Pattenden, G. *J. Chem. Soc., Perkin. Trans.* **1999**, *1*, 1235–1246.
197. Davies, A. G. *J. Chem. Res.* **2006**, 141–148.
198. Braunstein, P.; Morise, X. *Chem. Rev.* **2000**, *100*, 3541–3552.
199. Davies, A. *Organotin Chemistry (CD-ROM included)*, 2nd ed.; Wiley-VCH: Weinheim, 2004.
200. Sawyer, A. K. *Organotin Compounds 3*. Dekker, 1972; Vol. 3, pp 823–879.
201. Davies, A. G. *Comprehensive Organometallic Chemistry III*. Elsevier: Oxford, 2007; pp 809–883.
202. Davies, A.; Pannell, K.; Tiekink, E.; Gielen, M. *Tin Chemistry: Fundamentals, Frontiers, and Applications*. Wiley: Chichester, UK, 2008.
203. Patai, S. *The Chemistry of Organic Germanium, Tin and Lead Compounds*. Wiley: Chichester, 1995.
204. Rappoport, Z. *The Chemistry of Organic Compounds of Ge, Sn, Pb*. Wiley: Chichester, 2001.
205. Davies, A. *Organotin Chemistry*. VCH: Weinheim, Basel, 1997.
206. Neumann, W. P.; Schwarz, A. *Angew. Chem. Int. Ed. Engl.* **1975**, *14*, 812.
207. Arnold, D. *J. Organomet. Chem.* **1980**, *184*, 39–47.
208. Cuthbertson, M. *J. Organomet. Chem.* **1981**, *216*, 331–348.
209. Sita, L. R.; Terry, K. W.; Shibata, K. *J. Am. Chem. Soc.* **1995**, *117*, 8049–8050.
210. Weibel, T. A.; Oliver, J. P. *J. Organomet. Chem.* **1974**, *82*, 281–290.
211. Still, W. C. *J. Am. Chem. Soc.* **1977**, *99*, 4836–4838.
212. Wells, W. L.; Brown, T. L. *J. Organomet. Chem.* **1968**, *11*, 271–280.
213. Breiting, D. K.; Stangl, C. In *Organometallic Syntheses*; King, R., Eisch, J. J., Eds.; Elsevier: Amsterdam, Oxford, New York, 1988; Vol. 4, p 555.
214. Wursthorn, K. R.; Kuivila, H. G.; Smith, G. F. *J. Am. Chem. Soc.* **1978**, *100*, 2779–2789.
215. Wursthorn, K. *J. Organomet. Chem.* **1977**, *140*, 29–39.
216. Rot, N.; De Kanter, F.; Bickelhaupt, F.; Smeets, W.; Spek, A. *J. Organomet. Chem.* **2000**, *593–594*, 369–379.
217. Blake, D.; Coates, G. E.; Tate, J. M. *J. Chem. Soc.* **1961**, 618–622.
218. Kugita, T.; Wakasa, M. *Phosphorus Sulfur Silicon Relat. Elem.* **1999**, *150*, 271–276.
219. Wakasa, M.; Kugita, T. *Organometallics* **1999**, *18*, 2941–2943.
220. Artamkina, G. A.; Egorov, M. P.; Beletskaya, I. P.; Reutov, O. A. *Zh. Org. Khim.* **1984**, *20*, 1809–1820.
221. Englich, U.; Ruhlandt-Senge, K.; Uhlrig, F. *J. Organomet. Chem.* **2000**, *613*, 139–147.
222. Westerhausen, M. *Angew. Chem.* **1994**, *106*, 1585–1587.
223. Bera, H.; Braunschweig, H.; Doerfler, R.; Hammond, K.; Oechsner, A.; Radacki, K.; Uttinger, K. *Chem. Eur. J.* **2009**, *15*, 12092–12098.
224. Turek, J.; Padelkova, Z.; Nechaev, M. S.; Ruzicka, A. *J. Organomet. Chem.* **2010**, *695*, 1843–1847.
225. Sita, L. R.; Kinoshita, I.; Lee, S. P. *Organometallics* **1990**, *9*, 1644–1650.
226. Herberhold, M.; Steffl, U.; Milius, W.; Wrackmeyer, B. *Z. Anorg. Allg. Chem.* **1998**, *624*, 386–392.
227. Cardin, C. J.; Cardin, D. J.; Convery, M. A.; Devreux, M. M. *J. Organomet. Chem.* **1991**, *411*, C3–C6.
228. Puff, H.; Breuer, B.; Schuh, W.; Sievers, R.; Zimmer, R. *J. Organomet. Chem.* **1987**, *332*, 279–288.
229. Schaefer, A.; Weidenbruch, M.; Saak, W.; Pohl, S.; Marsmann, H. *Angew. Chem.* **1991**, *103*, 978–979.
230. Turek, J.; Padelkova, Z.; Cernosek, Z.; Erben, M.; Lycka, A.; Nechaev, M. S.; Cisarova, I.; Ruzicka, A. *J. Organomet. Chem.* **2009**, *694*, 3000–3007.
231. Kuivila, H. G.; Jakusik, E. R. *J. Org. Chem.* **1961**, *26*, 1430–1433.
232. Vyazankin, N. S.; Bochkarev, M. N.; Sanina, L. P. *J. Gen. Chem. USSR* **1966**, *36*, 1954.
233. Arad-Yellin, R.; Wudl, F. *J. Organomet. Chem.* **1985**, *280*, 197–201.
234. Han, L.-B.; Mirzaei, F.; Tanaka, M. *Organometallics* **2000**, *19*, 722–724.

235. Girbasova, N. V.; Bogoradovskii, E. T.; Zavgorodnii, V. S.; Petrov, A. A. *Zh. Obshch. Khim.* **1986**, *56*, 2753–2760.
236. Pruchnik, F. P.; Pruchnik, H.; Ostropolska, L.; Ciunik, L. Z. *Polyhedron* **2008**, *27*, 1093–1101.
237. Puff, H.; Breuer, B.; Gehrke-Brinkmann, G.; Kind, P.; Reuter, H.; Schuh, W.; Wald, W.; Weidenbrueck, G. *J. Organomet. Chem.* **1989**, *363*, 265–280.
238. Watta, B.; Neumann, W. P.; Sauer, J. *Organometallics* **1985**, *4*, 1954–1957.
239. Moehlen, M. M.; Rickard, C. E. F.; Roper, W. R.; Whittell, G. R.; Wright, L. J. *J. Organomet. Chem.* **2006**, *691*, 4065–4075.
240. Adams, S.; Draeger, M. *J. Organomet. Chem.* **1985**, *288*, 295–304.
241. Fu, J.; Neumann, W. P. *J. Organomet. Chem.* **1984**, *272*, C5–C9.
242. Muegge, C.; Pepermans, H.; Gielen, M.; Willem, R.; Tzschach, A.; Jurkschat, K. *Z. Anorg. Allg. Chem.* **1988**, *567*, 122–130.
243. Rupnicki, L.; Urbanczyk-Lipkowska, Z.; Stepien, A.; Cmoch, P.; Pianowski, Z.; Stalinski, K. *J. Organomet. Chem.* **2005**, *690*, 3690–3696.
244. Lee, C.; Lee, J.; Lee, S. W.; Kang, S. O.; Ko, J. *Inorg. Chem.* **2002**, *41*, 3084–3090.
245. Singer, R. D.; Hutzinger, M. W.; Oehlschlager, A. C. *J. Org. Chem.* **1991**, *56*, 4933–4938.
246. Al-Allaf, T. A. K. *J. Organomet. Chem.* **2002**, *654*, 21–28.
247. Yoshida, H.; Tanino, K.; Ohshita, J.; Kunai, A. *Angew. Chem. Int. Ed.* **2004**, *43*, 5052–5055.
248. Sagawa, T.; Ohtsuki, K.; Ishiyama, T.; Ozawa, F. *Organometallics* **2005**, *24*, 1670–1677.
249. Echavarran, A. M.; Stille, J. K. *J. Am. Chem. Soc.* **1987**, *109*, 5478–5486.
250. Sessler, J. L.; Wang, B.; Harriman, A. *J. Am. Chem. Soc.* **1995**, *117*, 704–714.
251. Holtrup, F. O.; Müller, G. R. J.; Uebe, J.; Müllen, K. *Tetrahedron* **1997**, *53*, 6847–6860.
252. Lautens, M.; Rovis, T. *Tetrahedron* **1999**, *55*, 8967–8976.
253. Nardelli, M.; Pelizzi, C.; Pelizzi, G.; Tarasconi, P. *Z. Anorg. Allg. Chem.* **1977**, *431*, 250–260.
254. Drost, C.; Hildebrand, M.; Lonneck, P. *Main Group Met. Chem.* **2002**, *25*, 93–98.
255. Wrackmeyer, B. In *Tin Chemistry: Fundamentals, Frontiers, and Applications*; Davies, A., Pannell, K., Tiekink, E., Gielen, M., Eds.; Wiley: Chichester, UK, 2008; pp 17–52.
256. Stevens, J. G.; Stevens, V. E. *Mössbauer Effect Data Index*. A. Hilger and IFI-Plenum: London and New York, 1978.
257. Stevens, J. G.; Stevens, V. E. *Mössbauer Effect References and Data Journal*. A. Hilger and IFI-Plenum: London and New York, 1995.
258. Pitt, C. G.; Bursley, M. M.; Rogerson, P. F. *J. Am. Chem. Soc.* **1970**, *92*, 519–522.
259. Lu, V. Y.; Tilley, T. D. *Macromolecules* **2000**, *33*, 2403–2412.
260. Sita, L. R. *Organometallics* **1992**, *11*, 1442–1444.
261. Costisella, B.; English, U.; Prass, I.; Schuermann, M.; Ruhlandt-Senge, K.; Uhlig, F. *Organometallics* **2000**, *19*, 2546–2550.
262. Reimann, W.; Kuivila, H. G.; Farah, D.; Apoussidis, T. *Organometallics* **1987**, *6*, 557–565.
263. Ascher, K. R. S.; Eliyahu, M.; Bultent, E. J.; Meinema, H. A. *Appl. Organomet. Chem.* **1987**, *1*, 303–309.
264. Podlech, J. In *Science of Synthesis: Houben-Weyl Methods of Molecular Transformations*; Moloney, M., Ed.; Thieme: Stuttgart, 2003; pp 273–284.
265. Darwish, A.; Chong, J. M. *Synth. Commun.* **2004**, *34*, 1885–1890.
266. Sawyer, A. K. *J. Am. Chem. Soc.* **1965**, *87*, 537–539.
267. Neumann, W. P.; Schneider, B. *Angew. Chem. Int. Ed. Engl.* **1964**, *3*, 751–752.
268. Okano, M.; Matsumoto, N.; Arakawa, M.; Tsuruta, T.; Hamano, H. *Chem. Commun.* **1998**, 1799–1800.
269. von Gyldenfeldt, F.; Marton, D.; Tagliavini, G. *Organometallics* **1994**, *13*, 906–913.
270. Marton, D.; Tari, M. *J. Organomet. Chem.* **2000**, *612*, 78–84.
271. Yokoyama, Y.; Hayakawa, M.; Azemi, T.; Mochida, K. *J. Chem. Soc., Chem. Commun.* **1995**, 2275.
272. Mochida, K.; Hayakawa, M.; Tsuchikawa, T.; Yokoyama, Y.; Wakasa, M.; Hayashi, H. *Chem. Lett.* **1998**, 91–92.
273. Baumgartner, J.; Schollmeier, T.; Schuermann, M.; Uhlig, F. *Phosphorus Sulfur Silicon Relat. Elem.* **2004**, *179*, 771–774.
274. Schuermann, M.; Uhlig, F. *Organometallics* **2002**, *21*, 986–988.
275. Zarl, E.; Albering, J. H.; Fischer, R. C.; Flock, M.; Genser, D.; Seibt, B.; Uhlig, F. *Z. Naturforsch. B: J. Chem. Sci.* **2009**, *64*, 1591–1597.
276. Lee, J.-D.; Kim, S.-J.; Yoo, D.; Ko, J.; Cho, S.; Kang, S. O. *Organometallics* **2000**, *19*, 1695–1703.
277. Lee, T.; Lee, S. W.; Jang, H. G.; Kang, S. O.; Ko, J. *Organometallics* **2001**, *20*, 741–748.
278. Lechner, M.-L.; Fuerpass, K.; Sykora, J.; Fischer, R. C.; Albering, J.; Uhlig, F. *J. Organomet. Chem.* **2009**, *694*, 4209–4215.
279. Memmler, H.; Kauper, U.; Gade, L. H.; Stalke, D.; Lauher, J. W. *Organometallics* **1996**, *15*, 3637–3639.
280. Galka, C. H.; Memmler, H.; Gade, L. H.; McPartlin, M. Z. *Anorg. Allg. Chem.* **2001**, *627*, 1417–1419.
281. Lutz, M.; Haukka, M.; Pakkanen, T. A.; Gade, L. H. *Z. Anorg. Allg. Chem.* **2003**, *629*, 182–184.
282. Fard, Z. H.; Mueller, C.; Harmening, T.; Poettgen, R.; Dehnen, S. *Angew. Chem. Int. Ed.* **2009**, *48*, 4441–4444.
283. Stewart, C. A.; Dickie, D. A.; Parkes, M. V.; Saria, J. A.; Kemp, R. A. *Inorg. Chem.* **2009**, *49*, 11133–11141.
284. Padelkova, Z.; Nechaev, M. S.; Lycka, A.; Holubova, J.; Zevaco, T. A.; Ruzicka, A. *Eur. J. Inorg. Chem.* **2009**, 2058–2061.
285. Bares, J.; Padelkova, Z.; Meunier, P.; Pirio, N.; Ruzicka, A. *J. Organomet. Chem.* **2009**, *694*, 1263–1265.
286. Kawachi, A.; Machida, K.; Yamamoto, Y. *Organometallics* **2009**, *28*, 6347–6351.
287. Veith, M.; Gasthauer, M.; Zimmer, M.; Huch, V. *Z. Anorg. Allg. Chem.* **2007**, *633*, 2274–2277.
288. Baiget, L.; Ranaivonjatovo, H.; Escudie, J.; Gornitzka, H. *J. Am. Chem. Soc.* **2004**, *126*, 11792–11793.
289. Schrenk, C.; Schnepf, A. *Chem. Commun.* **2010**, *46*, 6756–6758.
290. Lee, V. Y.; Fukawa, T.; Nakamoto, M.; Sekiguchi, A.; Tumanski, B. L.; Karni, M.; Apeloig, Y. *J. Am. Chem. Soc.* **2006**, *128*, 11643–11651.
291. Peng, Y.; Ellis, B. D.; Wang, X.; Fettinger, J. C.; Power, P. P. *Science* **2009**, *325*, 1668–1670.
292. Eichler, B. E.; Power, P. P. *Inorg. Chem.* **2000**, *39*, 5444–5449.
293. Phillips, A. D.; Hino, S.; Power, P. P. *J. Am. Chem. Soc.* **2003**, *125*, 7520–7521.
294. Lei, H.; Fettinger, J. C.; Power, P. P. *Organometallics* **2010**, *29*, 5585–5590.
295. Eichler, B. E.; Phillips, A. D.; Power, P. P. *Organometallics* **2003**, *22*, 5423–5426.
296. Peng, Y.; Brynda, M.; Ellis, B. D.; Fettinger, J. C.; Rivard, E.; Power, P. P.; Peng, Y.; Brynda, M.; Ellis, B. D.; Fettinger, J. C.; Rivard, E.; Power, P. P. *Chem. Commun.* **2008**, 6042–6044.
297. Rivard, E.; Fischer, R. C.; Wolf, R.; Peng, Y.; Merrill, W. A.; Schley, N. D.; Zhu, Z.; Pu, L.; Fettinger, J. C.; Teat, S. J.; Nowik, I.; Herber, R. H.; Takagi, N.; Nagase, S.; Power, P. P. *J. Am. Chem. Soc.* **2007**, *129*, 16197–16208.
298. Stanciu, C.; Richards, A. F.; Power, P. P. *J. Am. Chem. Soc.* **2004**, *126*, 4106–4107.
299. Setaka, W.; Hirai, K.; Tomioka, H.; Sakamoto, K.; Kira, M. *Chem. Commun.* **2008**, 6558–6560.
300. Cardin, D.; Keppie, S. A.; Lappert, M. F. *Inorg. Nucl. Chem. Lett.* **1968**, *4*, 365–369.
301. Kingston, B.; Lappert, M. F. *Inorg. Nucl. Chem. Lett.* **1968**, *4*, 371–373.
302. Bonati, F.; Wilkinson, G. *J. Chem. Soc.* **1964**, 179–181.
303. Herberhold, M.; Steffl, U.; Milius, W.; Wrackmeyer, B. *Angew. Chem. Int. Ed. Engl.* **1996**, *35*, 1803–1804.
304. Bera, H.; Braunschweig, H.; Oechsner, A.; Seeler, F.; Sigritz, R. *J. Organomet. Chem.* **2010**, *695*, 2609–2613.
305. Braunschweig, H.; FuB, M.; Mohapatra, S. K.; Kraft, K.; Kupfer, T.; Lang, M.; Radacki, K.; Daniliuc, C. G.; Jones, P. G.; Tamm, M. *Chem. Eur. J.* **2010**, *16*, 11732–11743.
306. Braunschweig, H.; Doerfler, R.; Mager, J.; Radacki, K.; Seeler, F. *J. Organomet. Chem.* **2009**, *694*, 1134–1137.
307. Bera, H.; Braunschweig, H.; Doerfler, R.; Kupfer, T.; Radacki, K.; Seeler, F. *Organometallics* **2010**, *29*, 5111–5120.
308. Zarl, E.; Baumgartner, J.; Decker, K.; Fischer, R.; Seibt, B.; Uhlig, F. *Phosphorus Sulfur Silicon Relat. Elem.* **2008**, *183*, 1923–1934.
309. English, U.; Hermann, U.; Prass, I.; Schollmeier, T.; Ruhlandt-Senge, K.; Uhlig, F. *J. Organomet. Chem.* **2002**, *646*, 271–276.
310. Schollmeier, T.; English, U.; Fischer, R.; Prass, I.; Ruhlandt, K.; Schuermann, M.; Uhlig, F. *Z. Naturforsch. B: Chem. Sci.* **2004**, *59*, 1462–1470.
311. Hermann, U.; Prass, I.; Uhlig, F. *Phosphorus Sulfur Silicon Relat. Elem.* **2001**, *168–169*, 145–150.
312. McAlonan, H.; Stevenson, P. *J. Organometallics* **1995**, *14*, 4021–4022.
313. Neumann, W. P.; König, K. *Angew. Chem. Int. Ed. Engl.* **1962**, *1*, 212–213.
314. Neumann, W. P.; König, K. *Justus Liebigs Ann. Chem.* **1964**, *677*, 1–11.
315. Neumann, W. P.; König, K. *Justus Liebigs Ann. Chem.* **1964**, *677*, 12–18.
316. Davies, A. G.; Osei-Kissi, D. K. *J. Organomet. Chem.* **1994**, *474*, C8–C10.
317. Buschhaus, H. U.; Neumann, W. P. *Angew. Chem. Int. Ed. Engl.* **1978**, *17*, 59.
318. Sharma, H. K.; Arias-Ugarte, R.; Metta-Magana, A. J.; Pannell, K. H. *Angew. Chem. Int. Ed.* **2009**, *48*, 6309–6312, S6309/1–S6309/7.

319. Woo, H.-G.; Kim, S.-Y.; Hwang, Y.-M.; Cho, M.-S.; Pyo, B.-S.; Kim, B.-H. *Polym. Prepr. (Am. Chem. Soc., Div. Polym. Chem.)* **2007**, *48*, 495–496.
320. Tanabe, M.; Hanzawa, M.; Osakada, K. *Organometallics* **2010**, *29*, 3535–3540.
321. Voskoboinikov, A. Z.; Parshina, I. N.; Shestakova, A. K.; Butin, K. P.; Beletskaya, I. P.; Kuz'mina, L. G.; Howard, J. A. K. *Organometallics* **1997**, *16*, 4041–4055.
322. Raynaud, C.; Perrin, L.; Maron, L. *Organometallics* **2006**, *25*, 3143–3151.
323. Schittelkopf, K.; Fischer, R. C.; Meyer, S.; Wilfling, P.; Uhlig, F. *Appl. Organomet. Chem.* **2010**, *24*, 897–901.
324. Pannell, K. H.; Sharma, H. K. In *Tin Chemistry: Fundamentals, Frontiers, and Applications*; Davies, A., Pannell, K., Tiekink, E., Gielen, M., Eds.; Wiley: Chichester, UK, 2008; pp 376–391.
325. Choffat, F.; Smith, P.; Caseri, W. *Adv. Mater.* **2008**, *20*, 2225–2229.
326. Manners, I. *Angew. Chem. Int. Ed. Engl.* **1996**, *35*, 1603–1621.
327. Sita, L. R. *Adv. Organomet. Chem.* **1995**, *38*, 189–243.
328. Klingensmith, K. A.; Downing, J. W.; Miller, R. D.; Michl, J. *J. Am. Chem. Soc.* **1986**, *108*, 7438–7439.
329. Plitt, H. S.; Downing, J. W.; Raymond, M. K.; Balaji, V.; Michl, J. *Faraday Trans.* **1994**, *90*, 1653–1662.
330. Babcock, J. R.; Sita, L. R. *J. Am. Chem. Soc.* **1996**, *118*, 12481–12482.
331. Imori, T.; Lu, V.; Cai, H.; Tilley, T. D. *J. Am. Chem. Soc.* **1995**, *117*, 9931–9940.
332. Devylder, N.; Hill, M.; Molloy, K. C.; Price, G. J. *Chem. Commun.* **1996**, 711–712.
333. Elangovan, M.; Muthukumar, A.; Anbukulandainathan, M. *Mater. Lett.* **2006**, *60*, 1099–1105.
334. Okano, M.; Watanabe, K.; Totsuka, S. *Electrochemistry (Tokyo, Japan)* **2003**, *71*, 257–259.
335. Ding, Y.; Corey, J. Y. *Polym. Prepr. (Am. Chem. Soc., Div. Polym. Chem.)* **1995**, *36*, 192–193.
336. Choffat, F.; Smith, P.; Caseri, W. *J. Mater. Chem.* **2005**, *15*, 1789–1792.
337. Choffat, F.; Wolfer, P.; Smith, P.; Caseri, W. *Macromol. Mater. Eng.* **2010**, *295*, 210–221.
338. Beckmann, J.; Duthie, A.; Grassmann, M.; Semisch, A. *Organometallics* **2008**, *27*, 1495–1500.
339. Mingos, D. M. P. *Nat. (London) Phys. Sci.* **1972**, *236*, 99–102.
340. Wade, K. *Advances in Inorganic Chemistry*; Elsevier: Amsterdam, 1976; Vol. 18, pp 1–66.
341. Williams, R. E. *Advances in Inorganic Chemistry*; Elsevier: Amsterdam, 1976; Vol. 18, pp 67–142.
342. Rudolph, R. W. *Acc. Chem. Res.* **1976**, *9*, 446–452.
343. Mingos, D. M. P. *Acc. Chem. Res.* **1984**, *17*, 311–319.
344. Weidenbruch, M.; Stülter, A.; Marsmann, H.; Peters, K.; von Schnering, H. G. *Eur. J. Inorg. Chem.* **1998**, *1998*, 1333–1336.
345. Wiberg, N.; Lerner, H.-W.; Noth, H.; Ponikvar, W. *Angew. Chem. Int. Ed.* **1999**, *38*, 1103–1105.
346. Sita, L. R.; Kinoshita, I. *Organometallics* **1990**, *9*, 2865–2867.
347. Sita, L. R.; Kinoshita, I. *J. Am. Chem. Soc.* **1991**, *113*, 1856–1857.
348. Wiberg, N.; Lerner, H.-W.; Wagner, S.; Noth, H.; Seifert, T. Z. *Naturforsch. B: Chem. Sci.* **1999**, *54*, 877–880.
349. Becker, M.; Foerster, C.; Franzen, C.; Hartrath, J.; Kirsten, E.; Knuth, J.; Klinkhammer, K. W.; Sharma, A.; Hinderberger, D. *Inorg. Chem.* **2008**, *47*, 9965–9978.
350. Joosten, D.; Pantenburg, I.; Wesemann, L. *Angew. Chem. Int. Ed.* **2006**, *45*, 1085–1087.
351. von Hänisch, C.; Rubner, O. *Eur. J. Inorg. Chem.* **2006**, 1657–1661.
352. Nikolova, D.; von Hänisch, C.; Adolf, A. *Eur. J. Inorg. Chem.* **2004**, 2321–2325.
353. Sita, L. R.; Bickerstaff, R. D. *J. Am. Chem. Soc.* **1989**, *111*, 6454–6456.
354. Sita, L. R.; Kinoshita, I. *J. Am. Chem. Soc.* **1990**, *112*, 8839–8843.
355. Sita, L. R.; Kinoshita, I. *J. Am. Chem. Soc.* **1991**, *113*, 5070–5072.
356. Sita, L. R.; Kinoshita, I. *J. Am. Chem. Soc.* **1992**, *114*, 7024–7029.
357. Schiemenz, B.; Huttner, G. *Angew. Chem.* **1993**, *105*, 295–296.
358. Richards, A. F.; Hope, H.; Power, P. P. *Angew. Chem. Int. Ed.* **2003**, *42*, 4071–4074.
359. Rivard, E.; Steiner, J.; Fettingner, J. C.; Giuliani, J. R.; Augustine, M. P.; Power, P. P. *Chem. Commun.* **2007**, 4919–4921.
360. Prabusankar, G.; Kempter, A.; Gemel, C.; Schroeter, M.-K.; Fischer, R. A. *Angew. Chem. Int. Ed.* **2008**, *47*, 7234–7237.
361. Esenturk, E. N.; Fettingner, J. C.; Eichhorn, B. W. *J. Am. Chem. Soc.* **2006**, *128*, 12–13.
362. Eichler, B. E.; Power, P. P. *Angew. Chem. Int. Ed.* **2001**, *40*, 796–797.
363. Richards, A. F.; Eichler, B. E.; Brynda, M.; Olmstead, M. M.; Power, P. P. *Angew. Chem. Int. Ed.* **2005**, *44*, 2546–2549.
364. Schrenk, C.; Köppe, R.; Schellenberg, I.; Pöttgen, R.; Schnepf, A. *Z. Anorg. Allg. Chem.* **2009**, *635*, 1541–1548.
365. Pacher, A.; Schrenk, C.; Schnepf, A. *J. Organomet. Chem.* **2010**, *695*, 941–944.
366. Schrenk, C.; Schellenberg, I.; Poettgen, R.; Schnepf, A. *Dalton Trans.* **2010**, *39*, 1872–1876.
367. Purath, A.; Köppe, R.; Schnöckel, H. *Angew. Chem. Int. Ed.* **1999**, *38*, 2926–2928.
368. Schnepf, A.; Schnöckel, H. *Angew. Chem. Int. Ed.* **2002**, *41*, 3532–3554.
369. Lintii, G.; Schnöckel, H.; Uhl, W.; Wiberg, N. In *Molecular Clusters of the Main Group Elements*; Driess, M., Nöth, H., Eds.; Wiley-VCH: Weinheim, 2004; pp 126–168.
370. Schnöckel, H. *Dalton Trans.* **2005**, 3131–3136.
371. Brynda, M.; Herber, R.; Hitchcock, P. B.; Lappert, M. F.; Nowik, I.; Power, P. P.; Protchenko, A. V.; Ruzicka, A.; Steiner, J. *Angew. Chem. Int. Ed.* **2006**, *45*, 4333–4337.
372. Harrison, P. G. In *Comprehensive Organometallic Chemistry*; Wilkinson, G., Stone, F. G. A., Abel, E. W., Eds.; Elsevier: Amsterdam, 1982; Vol. 2, pp 629–680.
373. Weidenbruch, M. In *Comprehensive Organometallic Chemistry III*; Housecroft, C., Ed.; Elsevier: Amsterdam, 2007; Vol. 3, pp 885–903.
374. Harrison, P. G. *Silicon Group, Arsenic, Antimony, and Bismuth; Comprehensive Organometallic Chemistry II*; Elsevier: Amsterdam, 1995; Vol. 2, pp 305–319.
375. Pinhey, J. T.; Pinhey, J. T. *Main-group Metal Organometallics in Organic Synthesis; Comprehensive Organometallic Chemistry II*; Elsevier: Amsterdam, 1995; Vol. 11, pp 461–485.
376. Seyferth, D. *Organometallics* **2003**, *22*, 2346–2357.
377. Seyferth, D. *Organometallics* **2003**, *22*, 5154–5178.
378. Elschenbroich, C. *Organometallics*, 5th ed.; Teubner: Wiesbaden, 2005.
379. Willemsens, L. C.; van der Kerk, G. J. M. *J. Organomet. Chem.* **1968**, *15*, 117–124.
380. Gilman, H.; Bindschadler, E. J. *Org. Chem.* **1953**, *18*, 1675–1678.
381. Edlund, U.; Lejon, T.; Pyykko, P.; Venkatachalam, T. K.; Buncel, E. *J. Am. Chem. Soc.* **1987**, *109*, 5982–5985.
382. Herberhold, M.; Trobs, V.; Wrackmeyer, B. *J. Organomet. Chem.* **1997**, *541*, 391–400.
383. Bähr, G. *Z. Anorg. Chem.* **1947**, *253*, 330–336.
384. Krebs, A. W.; Henry, M. C. *J. Org. Chem.* **1963**, *28*, 1911–1912.
385. van der Kerk, G. J. M. *Ind. Eng. Chem.* **1966**, *58*, 29–35.
386. Mirzaei, F.; Han, L.-B.; Tanaka, M. *Chem. Commun.* **2000**, 657–658.
387. Alberti, A.; Pedulli, G. F. *J. Organomet. Chem.* **1983**, *248*, 261–267.
388. Ahmed, I. M.; Hudson, A.; Alberti, A. *J. Organomet. Chem.* **1987**, *333*, 9–16.
389. Stegmann, H. B.; Schenkl, M.; Scheffler, K. *J. Organomet. Chem.* **1991**, *414*, 145–153.
390. Chen, K. S.; Foster, T.; Wan, J. K. S. *J. Chem. Soc., Perkin Trans.* **1979**, *2*, 1288–1292.
391. Al-Allaf, T. A. K.; Butler, G.; Eaborn, C.; Pidcock, A. *J. Organomet. Chem.* **1980**, *188*, 335–343.
392. Butler, G.; Eaborn, C.; Pidcock, A. *J. Organomet. Chem.* **1978**, *144*, C23–C25.
393. Carr, S.; Colton, R.; Dakternieks, D. *J. Organomet. Chem.* **1982**, *240*, 143–151.
394. Kleiner, N.; Dräger, M. *J. Organomet. Chem.* **1985**, *293*, 323–341.
395. Preut, H.; Huber, F. *Z. Anorg. Allg. Chem.* **1976**, *419*, 92–96.
396. Stabenow, F.; Saak, W.; Marsmann, H.; Weidenbruch, M. *J. Am. Chem. Soc.* **2003**, *125*, 10172–10173.
397. Whittaker, S. M.; Cervantes-Lee, F.; Pannell, K. H. *Inorg. Chem.* **1994**, *33*, 6406–6408.
398. Wrackmeyer, B. *Annual Reports on NMR Spectroscopy*. Academic Press, 2002; Vol. 47, pp 1–37.
399. Wrackmeyer, B.; Horchler, K. *Annual Reports on NMR Spectroscopy*. Academic Press, 1990; Vol. 22, pp 249–306.
400. Drenth, W.; Janssen, M. J.; van der Kerk, G. J. M.; Vliegthart, T. A. *J. Organomet. Chem.* **1964**, *2*, 265–270.
401. Löwig, C. J. *J. Prakt. Chem.* **1853**, *60*, 304–310.
402. Midgley, T.; Hochwalt, C. A.; Calingaert, G. *J. Am. Chem. Soc.* **1923**, *45*, 1821–1823.
403. Willemsens, L. C.; van der Kerk, G. J. M. *J. Organomet. Chem.* **1970**, *21*, 123–130.
404. Okazaki, R.; Shibata, K.; Tokitoh, N. *Tetrahedron Lett.* **1991**, *32*, 6601–6604.
405. Koglin, H.-J.; Behrends, K.; Draeger, M. *Organometallics* **1994**, *13*, 2733–2742.
406. Eujen, R.; Patorra, A. *J. Organomet. Chem.* **1992**, *438*, 57–75.
407. Eujen, R.; Patorra, A. *J. Organomet. Chem.* **1994**, *481*, 75–82.
408. Mallela, S. P.; Geanangel, R. A. *Inorg. Chem.* **1993**, *32*, 602–605.
409. Mallela, S. P.; Geanangel, R. A. *Inorg. Chem.* **1994**, *33*, 6357–6360.
410. Mallela, S. P.; Myrczek, J.; Bernal, I.; Geanangel, R. A. *J. Chem. Soc. Dalton Trans.* **1993**, 2891–2894.



411. Herberhold, M.; Kohler, C.; Trobs, V.; Wrackmeyer, B. *Z. Naturforsch. B: Chem. Sci.* **2000**, *55*, 939–945.
412. Amberger, E.; Hönigschmid-Grossich, R. *Chem. Ber.* **1966**, *99*, 1673–1677.
413. Willemsens, L. C.; van der Kerk, G. J. M. *J. Organomet. Chem.* **1964**, *2*, 260–264.
414. Willemsens, L. C.; van der Kerk, G. J. M. *J. Organomet. Chem.* **1964**, *2*, 271–276.
415. Krause, E.; Reißaus, G. G. *Ber. Dtsch. Chem. Ges. A/B* **1922**, *55*, 888–902.
416. Stabenow, F.; Saak, W.; Weidenbruch, M. *Chem. Commun.* **2003**, 2342–2343.
417. Wang, Y.; Quillian, B.; Wei, P.; Yang, X.-J.; Robinson, G. H. *Chem. Commun.* **2004**, 2224–2225.
418. Schneider-Koglin, C.; Behrends, K.; Dräger, M. *J. Organomet. Chem.* **1993**, *448*, 29–38.
419. Schneider, C.; Dräger, M. *J. Organomet. Chem.* **1991**, *415*, 349–362.
420. Kleiner, N.; Dräger, M. *J. Organomet. Chem.* **1984**, *270*, 151–170.
421. Klinkhammer, K. W.; Xiong, Y.; Yao, S. *Angew. Chem. Int. Ed.* **2004**, *43*, 6202–6204.
422. Klinkhammer, K. W.; Schwarz, W. *Angew. Chem. Int. Ed. Engl.* **1995**, *34*, 1334–1336.
423. Ross Kelly, T.; Li, Q.; Bhushan, V. *Tetrahedron Lett.* **1990**, *31*, 161–164.
424. Junggebauer, J.; Neumann, W. P. *Tetrahedron* **1997**, *53*, 1301–1310.

This page intentionally left blank



## 1.04 Catenated Phosphorus Compounds

JJ Weigand, TU Dresden, Dresden, Germany

N Burford, University of Victoria, Victoria, BC, Canada

© 2013 Elsevier Ltd. All rights reserved.

1.04.1	Introduction	119
1.04.2	Nomenclature	119
1.04.3	Neutral Compounds	127
1.04.4	Anionic Compounds	135
1.04.5	Cationic Compounds	142
1.04.6	Conclusion	146
References		146

### 1.04.1 Introduction

Society has developed synthetic strategies to access essentially any C—C-bonded molecular framework including carbon-based materials that exhibit a wide range of properties and are sometimes superior to those properties observed for natural compounds. Many analogies have been described between carbon and phosphorus that are often justified by the diagonal relationship between the elements in the periodic table, and the similarities in electronegativity.<sup>1</sup> Nevertheless, the extent of established and documented phosphorus chemistry is limited compared to the vast chemistry that is understood for carbon. Moreover, compounds containing P—P-bonded frameworks are rare compared to C—C-bonded compounds.<sup>2</sup> Although the P—P bond energy (200 kJ mol<sup>-1</sup>) is relatively weak compared to the C—C bond (350 kJ mol<sup>-1</sup>),<sup>3</sup> examples of polyphosphanes,<sup>4</sup> polyphosphide anions,<sup>5,6</sup> and polyphosphorus cations<sup>7</sup> have been isolated and characterized to show that P—P-bonded frameworks are viable. It is expected that compounds and materials involving P—P-bonded frameworks will exhibit a catalog of properties, some of which are not offered by C—C-bonded frameworks. This chapter provides an overview of the types of P—P-bonded compounds that have been prepared and characterized, a listing of synthetic methods, and a discussion of some of the structural and spectroscopic features. The discussion is limited to compounds containing main-group elements, as the synthesis, structure, and reactivity of compounds containing *catena*-phosphorus units bound to transition metals have recently been reviewed.<sup>8</sup>

### 1.04.2 Nomenclature

The *catena*-phosphorus compounds described and discussed in this chapter are named using the guidelines recommended by the International Union of Pure and Applied Chemistry (IUPAC),<sup>9</sup> and in some cases the Chemical Substance Index edited by the American Chemical Society's Chemical Abstracts Service (CA). The three basic nomenclature systems (compositional, substitutive, and additive) can provide

different unambiguous names for a given compound. The choice of system depends on the class of inorganic compound under consideration and the degree of details one wishes to provide. An emphasis is given to the substitutive nomenclature derived from parent hydride names, inorganic chains, and ring compounds.<sup>10,11</sup> The name construction follows the general procedure and choice of the senior compound class of general organic and inorganic chemistry according to CA's 'Index Guide' or IUPAC's 'Blue and Red Book' and complementary recommendations.<sup>12</sup>

The 'substitutive nomenclature' is based on a parent phosphane with a standard population of hydrogen atoms attached to the skeletal structure. (IUPAC recommends neutral phosphorus hydrides are called 'phosphanes' which is used throughout this chapter instead of 'phosphanes' according to the CA index name. The name 'phosphane' is no longer acceptable.) The name of the 'derivative' results from the unsubstituted parent phosphorus hydride by replacing a hydrogen atom and citing appropriate prefixes (name of a substituent that is not the principal group (substituent derived from a functional parent), e.g., 'methyl-' (Me-) in 'methylphosphane' (MePH<sub>2</sub>)) or suffixes (name of the principal group in a substitutive name consisting of prefix(es), molecular-skeleton parent name, and ending (i.e., suffix), e.g., '-phosphonic acid' (—P(=O)(OH)<sub>2</sub>) in 'methylphosphonic acid' (MeP(=O)(OH)<sub>2</sub>)) of the 'substitute groups' (substituents) in conjunction with locants when required. Additive nomenclature also known as coordination nomenclature is typically used for coordination and organometallic compounds or inorganic acids in which a compound or species is treated as a combination of a central atom or atoms with associated ligands. For cases where the bonding number of a phosphorus atom in a compound deviates from the valence number III, IUPAC uses the  $\lambda$  convention to designate formally charge-neutral structures that contain heteroatoms with nonstandard valence.<sup>13</sup>

**Table 1** lists parent phosphanes and polyphosphanes to summarize the recommendations of IUPAC as applied to PH compounds. The 'bonding number'  $n$  refers to valence bonds to a phosphorus atom and is indicated in the compound name by the symbol  $\lambda^n$ . The standard valence of phosphorus (P<sup>III</sup>) is not expressed in the compound name. Naming a *catena*-phosphorus compound according to substitutive nomenclature

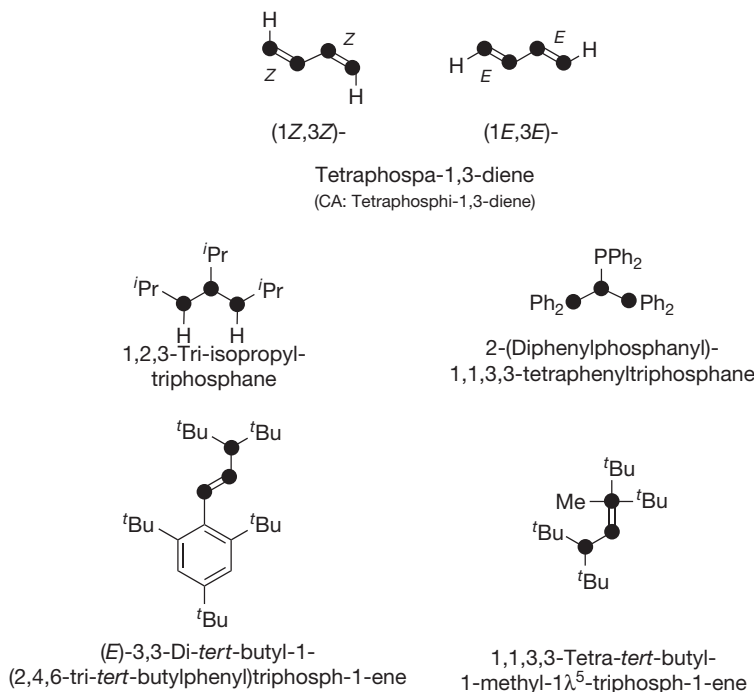
**Table 1** IUPAC nomenclature for parent phosphanes (CA refers to chemical abstracts)

				<i>As prefix:</i>		
PH <sub>3</sub>		'Phosphane'			'Phosphan-1-yl-'	H <sub>2</sub> P—
PH <sub>5</sub>	CA:	'Phosphane'			'Phosphino-'	
	CA:	'λ <sup>5</sup> -Phosphane'			'λ <sup>5</sup> -Phosphan-1-yl-'	H <sub>4</sub> P—
H <sub>2</sub> PPH <sub>2</sub>		'Phosphorane' ('-orane' indicates in CA nomenclature the degree of saturation of P <sup>V</sup> .)			'Phosphoranyl-'	
	CA:	'Diphosphane'			'Diphosphan-1-yl-'	H <sub>2</sub> PPH—
H <sub>2</sub> PPHPH <sub>2</sub>		'Diphosphane'			'Diphosphinyl-'	
	CA:	'Triphosphane'			'Triphosphan-1-yl-'	H <sub>2</sub> PPHPH—
H <sub>2</sub> PPHPHPH <sub>2</sub>		'Triphosphane'			'Triphosphinyl-'	
	CA:	'Tetraphosphane'			'Tetraphosphan-1-yl-'	H <sub>2</sub> PPHPHPH—
H <sub>4</sub> PPH <sub>3</sub> PH <sub>4</sub>		'Tetraphosphane'			'Tetraphosphinyl-'	
	CA:	'Tri-λ <sup>5</sup> -phosphane'			'Tri-λ <sup>5</sup> -phosphan-1-yl-'	H <sub>4</sub> PPH <sub>3</sub> PH <sub>3</sub> —
H <sub>4</sub> PPHPH <sub>4</sub>		'Triphosphorane'			'Triphosphoranyl-'	
	CA:	'1λ <sup>5</sup> ,3λ <sup>5</sup> -Triphosphane'			'1λ <sup>5</sup> ,3λ <sup>5</sup> -Triphosphan-1-yl-'	H <sub>4</sub> PPHPH <sub>3</sub> —
H <sub>2</sub> PPH <sub>2</sub>		'1λ <sup>5</sup> -Triphosphane'			'1λ <sup>5</sup> -Triphosphan-1-yl-'	H <sub>2</sub> PPHPH <sub>3</sub> —
		or			'1λ <sup>5</sup> -Triphosphan-3-yl-'	H <sub>4</sub> PPHPH—
H <sub>4</sub> PPH <sub>4</sub>		vs.	HP=PH	'Diphosphene'	'Diphosphenyl-'	HP=P—
		vs.	H <sub>2</sub> P≡P	'λ <sup>5</sup> -Diphosphyne'	'1λ <sup>5</sup> -Diphosphynyl-'	P≡PH—
H <sub>4</sub> PPH <sub>4</sub>		'1λ <sup>5</sup> ,2λ <sup>5</sup> -Diphosphane'				
	CA:	(CA: 'Diphosphorane')	H <sub>3</sub> P=PH <sub>3</sub>	'1λ <sup>5</sup> ,2λ <sup>5</sup> -Diphosphene'	'1λ <sup>5</sup> ,2λ <sup>5</sup> -Diphosphenyl-'	H <sub>3</sub> P=PH <sub>2</sub> —
		vs.		'Diphosphorene'	'Diphosphorenyl-('(-orene', '-oradiene', '-oryne', etc., indicates in CA nomenclature the degree of unsaturation of P <sup>V</sup> .)	
H <sub>2</sub> PPHPH <sub>2</sub>		vs.	H <sub>2</sub> PP=PH	'Triphosph-1-ene'	'Triphosph-1-enyl-'	H <sub>2</sub> PP=P—
		vs.	H <sub>3</sub> P=PH=PH <sub>3</sub>	or '1λ <sup>5</sup> ,2λ <sup>5</sup> ,3λ <sup>5</sup> -Triphospha-1,2-diene'	'Triphosph-3-enyl-'	HP=PPH—
	CA:			'Triphosphora-1,2-diene'		
		vs.			'1λ <sup>5</sup> ,2λ <sup>5</sup> ,3λ <sup>5</sup> -Triphospha-1,2-dienyl'	H <sub>3</sub> P=PH=PH <sub>2</sub> —
	CA:		HP=P≡P	'2λ <sup>5</sup> -Triphosphenyne'	'2λ <sup>5</sup> -Triphosphenynyl-'	P≡P=P—
				'Phosphinidene phosphinidynephosphorane'		

generally involves the replacement of hydrogen atoms in a phosphane with other atoms or atom groups. Homopolynuclear (*catena*) phosphorus hydrides are constructed by prefixing the '-ane' name of  $\text{PH}_3$  with the appropriate multiplicative prefix ('di', 'tri', 'tetra', etc.) corresponding to the number of consecutive phosphorus atoms. In cases where the bonding number of a phosphorus atom of the chain bonded in a series is different from  $n=3$ , the name of the *catena*-phosphane is formed as if all the phosphorus atoms adopt standard bonding numbers, but is preceded by locants and using the  $\lambda$  convention.

Unsaturated acyclic phosphorus hydrides are not classified as parent hydrides. The names of phosphorus chains containing unsaturation are derived in substitutive nomenclature by following the rules as used for the corresponding hydrocarbon chain with the final syllable '-ene' (alkene) or '-yne' (alkyne). (The final degree of unsaturation is expressed by a numerical term; '-ene' (1 bond) etc.; '-enyne' (1 double + 1 triple bonds), '-dienyne' (2 double + 1 triple bonds), '-enediyne' (1 double + 2 triple bonds), etc.; The numbering of the double bond follows the *hierarchical rules of the substitutive nomenclature* and will be derived after various groups and modifications have been numbered.) For double-bonded isomers (configurational isomers) the relative stereodescriptors '(E)' or '(Z)' are used for the assignment, as illustrated in **Figure 1**. (A reference plane is vertical to each double-bond plane which contains the atoms directly connected to the double bond. Taking into account the priority order of the substituents attached to the phosphorus atoms, the configuration is assigned '(Z)' where the higher priority substituents are on the same side of the reference plane and '(E)' where the higher priority substituents are on the opposite side of the reference plane. IUPAC still accepts the relative stereodescriptors '(cis)''(trans)' instead of '(Z)''(E)'.)

For *catena*-phosphorus derivatives containing special substituents, the name of the heterochain is derived as previously described. The special substituent is designated either as a prefix or by an additive name. (The recommendations for *monovalent-acyl prefixes* in CA or IUPAC nomenclature are derived from *P-oxoacids* with or without acid function. For compounds where the acid function is lost by replacement of OH groups, compounds of lower priority are generated, e.g., acid *vs.* acid halide or an amide.) The recommendations for monovalent-acyl prefixes for acidic- and nonacidic-acyl prefixes are summarized in **Table 2** including pseudoesters  $-\text{P}-\text{X-acyl}$ , pseudoacids  $-\text{P}(=\text{X})(\text{Y})$ , pseudoketones  $-\text{P}(=\text{X})$  or  $-\text{P}(=\text{X})-$ , pseudoalcohols  $-\text{P}-\text{XH}$  or  $-\text{P}^{\text{V}}-\text{XH}$ , and P-acyl-substituted homogeneous heterochains  $-\text{P}-\text{acyl}$  or  $\text{P}^{\text{V}}-\text{acyl}$  ( $\text{X}=\text{O}, \text{S}, \text{Se}, \text{Te}; \text{Y}=\text{OH}, \text{OR}, \text{Hal}$ ; **Figure 2**). (def. acyl: a group that can be mono- or polyvalent and is formed by a subsequent removal of OH groups and/or chalcogen analogs from an acid. E.g.  $\text{P}(=\text{O})(\text{OH})_2^-$ ,  $\text{MeP}(=\text{O})(\text{OH})_2^-$ ,  $\text{PH}(=\text{O})(\text{OH})-$ ,  $\text{PH}(=\text{O})-$ . In additive nomenclature prefixes are derived for formic acids, carbonic acids and analogs as well as for alcohols, aldehydes and carboxylic acids according to organic nomenclature. E.g.  $\text{RO}-$  'alkoxy-';  $\text{H}(\text{C}=\text{X})-$  'formyl-' ( $\text{X}=\text{O}$ ), '(thioxomethyl)-' ( $\text{X}=\text{S}$ ), '(selenoxomethyl)-' ( $\text{X}=\text{Se}$ ), '(telluroxomethyl)-' ( $\text{X}=\text{Te}$ );  $\text{MeC}(=\text{O})-$  'acetyl-';  $\text{PhC}(=\text{O})-$  'benzoyl-';  $\text{PhC}(=\text{O})\text{O}$  'benzoyloxy-'. In certain cases the *special substituent* is designated by an *additive name*. A heteroatom ( $\text{O}^{\text{II}}, \text{S}^{\text{II}}, \text{Se}^{\text{II}}, \text{Te}^{\text{II}}$ ) added to a phosphorus atom with its standard valence ( $\lambda$  convention is considered for the other phosphorus atoms) is denoted by means of a modification after the parent name, parent name+suffix, or after the functional-parent name. Modification: 'oxide' ( $\text{O}=\text{}$ ), 'sulfide' ( $\text{S}=\text{}$ ), 'selenide' ( $\text{Se}=\text{}$ ), 'telluride' ( $\text{Te}=\text{}$ ). A heteroatom ( $\text{O}^{\text{II}}, \text{S}^{\text{II}}, \text{Se}^{\text{II}}, \text{Te}^{\text{II}}$ ) added to a phosphorus atom of a substituent that



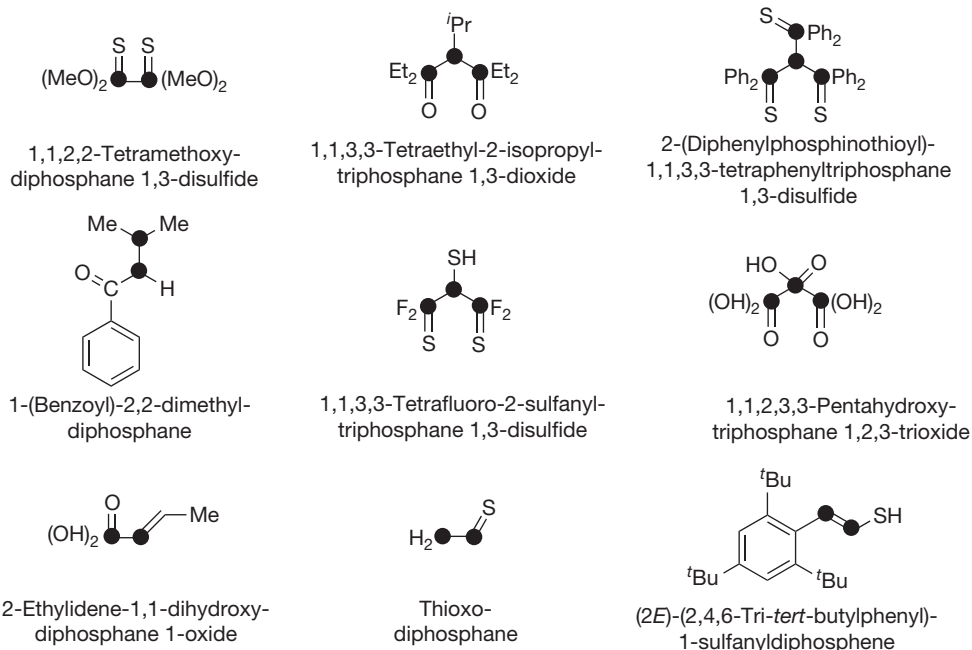
**Figure 1** Examples of polyphosphanes to illustrate IUPAC nomenclature.

**Table 2** Mono- and multivalent-acyl prefixes. (This table contains only the IUPAC recommendations for acyl names and acyl replacement-analog names for mono- and multivalent-acyl prefixes.)

$P(=O)(OH)_2-$	'Phosphono-'
$P(OH)_2-$	'Dihydroxyphosphanyl-'
$PH(=O)(OH)-$	'Hydrohydroxyphosphoryl-'
$PH_2(=O)-$	'Phosphinoyl-'
$PH(OH)-$	'(Hydroxyphosphanyl)-'
$PH_2-$	'Phosphanyl-'
$P(=X)_2-$	'Dioxo- $\lambda^5$ -phosphanyl-' (X=O), 'dithioxo- $\lambda^5$ -phosphanyl-' (X=S), 'diselenoxo- $\lambda^5$ -phosphanyl-' (X=Se), 'ditelluroxo- $\lambda^5$ -phosphanyl-' (X=Te)
$P(=X)-$	'Oxophosphanyl-' (X=O), 'thioxophosphanyl-' (X=S), 'selenoxophosphanyl-' (X=Se), 'telluroxophosphanyl-' (X=Te)
$PH_2(=X)-$	'Phosphinoyl-' (X=O), 'phosphinothiyl-' (X=S), 'phosphinoselenoyl-' (X=Se), 'phosphinotelluroyl-' (X=Te)
$PH_2(=NH)-$	'Phosphonamidoyl-'
$PH(=X)(NH_2)-$	'Phosphonamidoyl-' (X=O), 'phosphonamidothiyl-' (X=S), 'phosphonamidoselenoyl-' (X=Se), 'phosphonamidotelluroyl-' (X=Te)
$PH(=NH)(NH_2)-$	'Phosphonamidimidoyl-' (X=O)
$PH(=N)-$	'Phosphonitridoyl-'
$P(=O)OH-$	'Phosphinico-'
$PH(=X)-$	'Phosphonyl-' (X=O), 'phosphonothiol-' (X=S), 'phosphonoselenoyl-' (X=Se), 'phosphonotelluroyl-' (X=Te)
$-P(=X)-$	'Phosphoryl-' (X=O), 'phosphorothiol-' (X=S), 'phosphoroselenoyl-' (X=Se), 'phosphorotelluroyl-' (X=Te)
$PH-$	'Phosphanediyl-'
$-P-$	'Phosphantriyl-'
$PH(=NH)-$	'Phosphonimidoyl-'
$P(=N)-$	'Phosphonitridoyl-'

cannot be expressed by a parent name is named in the substituent by a pseudoprefix and a corresponding locant; pseudoprefix: 'oxido-' (O=), 'sulfido-' (S=), 'selenido-' (Se=), 'tellurido-' (Te=). Pseudoprefixes are treated like prefixes although no H atoms of the parent compound are substituted. Exceptions are made when names are derived from a mononuclear formal phosphane or  $\lambda^5$ -phosphane. Derivatives with =X and -YH or =X and -Hal, e.g.,  $P(=X)YH$ ,  $P(=X)Hal$  or  $P^V(=X)YH$ ,  $P^V(=X)Hal$  (X=O, S, Se, Te, NH; Y=O, S, Se, Te, OO, OS, etc.; -Hal=-F, -Cl, -Br, -I, -N<sub>3</sub>, -NCO, etc., -NC, -CN, -OR, -NH<sub>2</sub>, -NHNH<sub>2</sub>, -OCN, etc., ( $\equiv N$ )) are denoted as *oxoacids* or their derivatives. It is important to note that *oxoacids* and derivatives thereof are higher priority. For a detailed description see IUPAC's 'Blue Book.'

CA and IUPAC recommend the Hantzsch-Widmann names for unsaturated and partly saturated heteromonocycles containing ten or fewer ring members ( $\leq 10$  ring members). (Unsaturation is understood in terms of the maximum number of noncumulative double bonds with heteroatoms in their standard valence. The presence of at least one double bond in the ring is required. The prefix 'hydro-' (if necessary) with a corresponding multiplying affix is employed without a corresponding locant for heteromonocycles with 6-10 ring members (however, *not* for 'perhydro-'). For homogeneous heteromonocycles with ring members  $>10$ , replacement names are employed, however, cyclophosphanes with more than 10 phosphorus atoms are not considered here. In CA nomenclature the nonstandard valence of a heteroatom in heterocycles is addressed by the prefix 'hydro-' when the usual rules for substitutive nomenclature (see Blue Book) cannot be applied. In such cases IUPAC recommends the  $\lambda$  convention. For cyclic structures with cumulative double bonds, except for chain and ring structures whose names are based on saturated structures, the  $\delta$  convention is used;  $\delta^n$ ,  $n$  = number of double bonds terminating in a molecular-skeleton atom.)

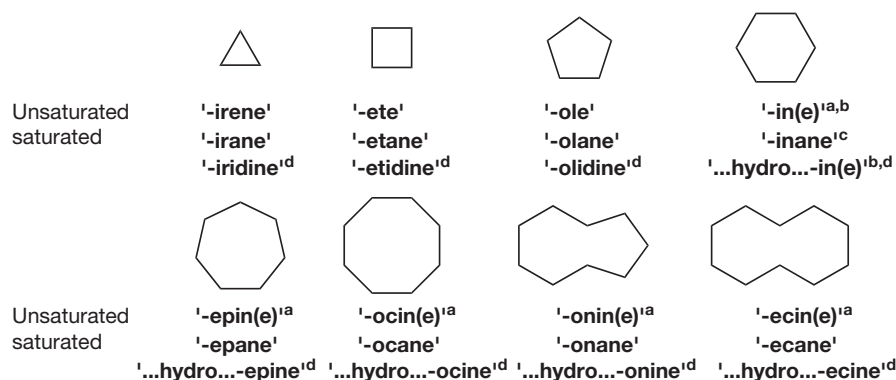
**Figure 2** Selected examples for the nomenclature of substituted *catena*-phosphorus derivatives.

Homopolynuclear saturated phosphorus monocycles can also be constructed by prefixing the '-ane' name of the mononuclear phosphorus(III) hydride  $\text{PH}_3$  with the appropriate multiplicative prefix ('di', 'tri', 'tetra', etc.) corresponding to the number of consecutive phosphorus atoms in conjunction with the prefix cyclo (Figure 3; The constitution of polyphosphanes ( $\text{R}_x\text{P}_x$ ) with more than six phosphorus atoms normally involves side-chain substituted arrangements rather than the formation of a  $x$ -membered ring. The same normally accounts for polycyclic phosphanes in which the constitution of the system is the result of the maximum number of fused cyclopentaphosphane and cyclotetraphosphane rings.)

Radicals, ions, and related species containing phosphorus can be formally considered as derived from parent hydrides or characteristic groups by the loss of hydrogen atoms, or by the addition or loss of hydrogen ions. (The term 'free' for radicals is no longer accepted, since radicals are distinct chemical species. However, in subsequent recommendations on organic nomenclature, the term 'group' is used rather than 'radical' to

designate a substituting group. Although prefixes are used to designate a mononuclear species, the free valency does not necessarily reside on the radical or ionic center.) Depending on the operation, the number of hydrogen atoms that can be substituted are altered at the radical or ionic centers and are described mainly by the operational suffixes or prefixes. (Operational suffixes are used to indicate that the number of hydrogen atoms to be substituted is different from that implied by the parent name or suffix name, e.g. '-ium', '-ylum', '-ide', and the traditional subtractive suffixes such as '-yl', '-ene', and '-yne' are introduced to express the final degree of unsaturation of a parent hydride (*vide supra*).

Table 3 lists examples of cationic compounds that can be considered as formally derived by the addition of hydrons to a phosphorus hydride in its standard bonding state by adding the suffix '-ium' to the root of the compound name. ('Hydrons' stands for the naturally occurring mixture of protons, deuterons, and tritons. In the following only the name proton,  $^1\text{H}^+$ , will be used for simplicity. In the case of the mononuclear



a) Deviating from *IUPAC*, *CA* uses for saturated phosphorus monocycles, exclusively the Hantzsch–Widmann names. For unsaturated N-containing 6- to 10-membered rings, *CA* employs '-ine', '-epine', '-ocine', '-onine', and '-ecine'; for non-N-containing unsaturated rings the names are derived without a final 'e' ('-in', '-epin', '-ocin', '-onin', and '-ecin'); b) *IUPAC* recommends for unsaturated P-containing 6-membered rings: '-in(e)', *CA* 'phosphor-' directly before '-in(e)'; c) *CA*: '-ane'; *IUPAC*: '-inane'; d) *CA* nomenclature, when N-containing; *IUPAC* recommends '-epane', '-ocane', '-onane', and '-ecane', for all saturated 7- to 10-membered rings.

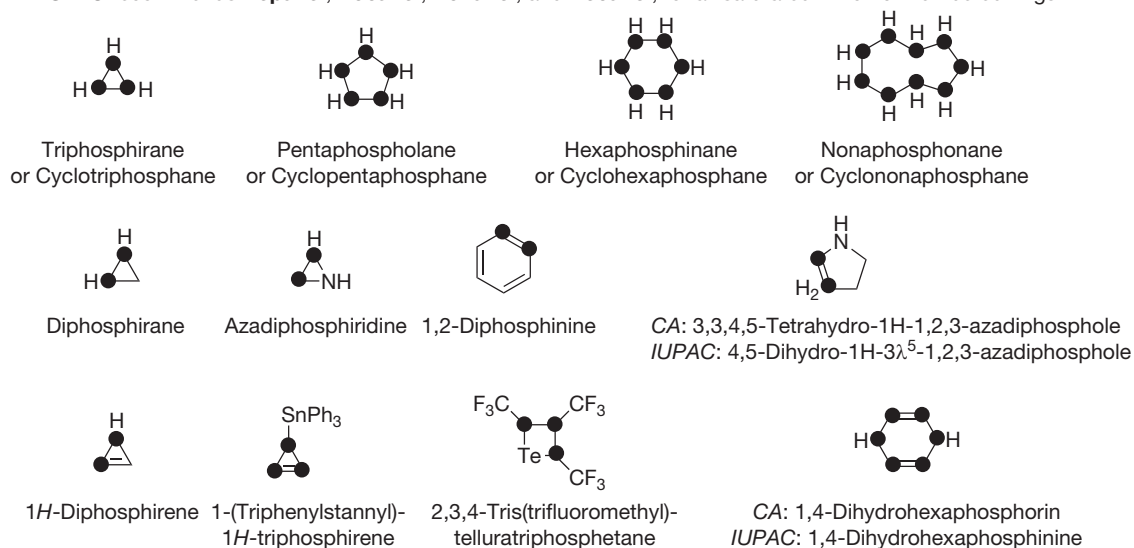
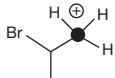

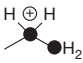
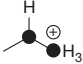
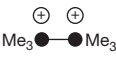
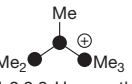
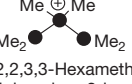
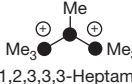
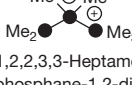
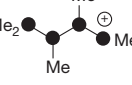



Figure 3 Hantzsch–Widmann names and selected examples.

**Table 3** Suffix endings and prefixes to describe phosphorus-centered cations resulting from addition of H<sup>+</sup> to a phosphorus hydride

Operation		Suffix		Cation substituent (prefix)	Examples <sup>a</sup>
PH <sub>3</sub> Phosphane	+H <sup>+</sup>	H <sub>4</sub> P <sup>+</sup> -phosphonium	-H•	-PH <sub>3</sub> <sup>+</sup> Phosphoniumyl-	 (1-Bromoethyl) phosphonium
P <sub>2</sub> H <sub>2</sub> Diphosphene	+H <sup>+</sup>	HP=PH <sub>2</sub> <sup>+</sup> -diphosphen-1-ium	-H•	-P=PH <sub>2</sub> <sup>+</sup> Diphosphen-1-ium-2-yl- -HP <sup>+</sup> =PH Diphosphen-2-ium-2-yl-	 (E)-1,2-Bis(2,4,6-tri- <i>tert</i> -butylphenyl)- 1-methyldiphosphen-1-ium <sup>a</sup>
P <sub>2</sub> H <sub>4</sub>	+H <sup>+</sup>	H <sub>2</sub> PPH <sub>3</sub> <sup>+</sup> -phosphanylphosphonium -diphosphan-1-ium	-H•	-PPH <sub>3</sub> <sup>+</sup> Diphosphan-1-ium-2-yl- - <sup>+</sup> PH <sub>2</sub> PH <sub>2</sub> Diphosphan-2-ium-2-yl-	 1-Methyl- diphosphan-1-ium  2-Methyl- diphosphan-1-ium
	+2H <sup>+</sup>	H <sub>3</sub> PPH <sub>3</sub> <sup>2+</sup> -diphosphane-1,2-dium	-H•	-PH <sub>2</sub> <sup>+</sup> PH <sub>3</sub> <sup>+</sup> Diphosphane-1,2-dium-2-yl-	 1,1,1,2,2,2-Hexamethyl- diphosphane-1,2-dium
P <sub>3</sub> H <sub>5</sub> Triphosphane	+H <sup>+</sup>	H <sub>2</sub> PPHPH <sub>3</sub> <sup>+</sup> -triphosphan-1-ium H <sub>2</sub> PPH <sub>2</sub> <sup>+</sup> PH <sub>2</sub> -triphosphan-2-ium	-H•	-PPHPH <sub>3</sub> <sup>+</sup> Triphosphan-1-ium-3-yl- -PPH <sub>2</sub> <sup>+</sup> PH <sub>2</sub> Triphosphan-2-ium-3-yl- -PH <sub>2</sub> <sup>+</sup> PPH <sub>2</sub> Triphosphan-3-ium-3-yl-	 1,1,1,2,3,3-Hexamethyl- triphosphan-1-ium  1,1,2,2,3,3-Hexamethyl- triphosphan-2-ium
	+2H <sup>+</sup>	H <sub>2</sub> PPH <sub>2</sub> <sup>+</sup> PH <sub>3</sub> <sup>+</sup> -triphosphane-1,2-dium H <sub>3</sub> P <sup>+</sup> PPHPH <sub>3</sub> <sup>+</sup> -triphosphane-1,3-dium	-H•	-PPHPH <sub>2</sub> <sup>+</sup> PH <sub>3</sub> <sup>+</sup> Triphosphane-1,2-dium-3-yl- -PH <sub>2</sub> <sup>+</sup> PPHPH <sub>3</sub> <sup>+</sup> Triphosphane-1,3-dium-3-yl- -PH <sub>2</sub> <sup>+</sup> PH <sub>2</sub> <sup>+</sup> PH <sub>2</sub> Triphosphane-2,3-dium-3-yl-	 1,1,1,2,3,3,3-Heptomethyl triphosphane-1,3-dium  1,1,1,2,2,3,3-Heptomethyl- triphosphane-1,2-dium
P <sub>4</sub> H <sub>6</sub> Tetraphosphane	+1H <sup>+</sup>	H <sub>2</sub> PPHPHPH <sub>3</sub> <sup>+</sup> -tetraphosphan-1-ium ...	-H•	-HPPHPHPH <sub>3</sub> <sup>+</sup> Tetraphosphan-1-ium-4-yl- ...	 1,1,1,2,3,4,4-Heptomethyl- tetraphosphan-1-ium
	+2H <sup>+</sup>	H <sub>3</sub> P <sup>+</sup> PPHPHPH <sub>3</sub> <sup>+</sup> -tetraphosphane-1,4-dium ...	-H•	-H <sub>2</sub> P <sup>+</sup> PPHPHPH <sub>3</sub> <sup>+</sup> Tetraphosphane-1,4-dium-4-yl- ...	 1,1,1,2,3,4,4,4-Octamethyl- tetraphosphane-1,4-ium

<sup>a</sup>Mes\* = 2,4,6-tri-*tert*-butylphenyl. <sup>118c</sup>



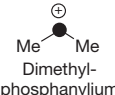
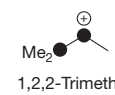
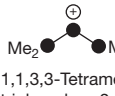
parent phosphorus hydride  $\text{PH}_3$  the suffix '-onium' is used (Table 3). E.g. Chlorotrimethylphosphonium ( $\text{ClMe}_3\text{P}^+$ ). In cations with two or more cationic centers in the same parent molecular skeleton, the suffixes '-dium', '-trium', etc. are added to the polyphosphane name without the deletion of the final 'e'. In all cases, appropriate locants of the cationic center(s) are added as needed. According to substitutive nomenclature, the suffixes are added individually or in combination to the name of the phosphane or traditional suffixes are used to express principal characteristic groups. Locants for the cationic centers are sometimes omitted, when a cationic center is fully substituted and locants are cited for the substituents. The operational suffix '-ium', when added to the name of the phosphane, indicates only that the number of substitutable hydrogen atoms at the position given by the appropriate locant has been increased by the addition of a hydron. Accordingly, there is no change in the bonding pattern at that position from that of the neutral phosphane.

A cationic center derived formally from the removal of one or more hydrogen atom as a hydride ion from any position of a neutral phosphane is named by replacing the final 'e' by adding the operational suffixes such as '-bis(ylium)', or without removing 'e' the operational suffixes such as '-bis(ylium)', '-tris(ylium)', etc., to the name of the phosphane. Locants are used to describe the position of the cationic center(s) and are placed in front of the name (Table 4). The systematic name for  $\text{PH}_3$  (phosphane) must be used for naming cationic (radical) derivatives, because the traditional name phosphane would lead to the name 'phosphinylium' ('phosphinyl') which is the same name that would be generated from the well-established name

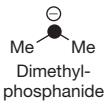
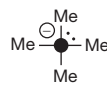
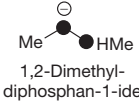
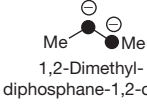
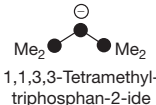
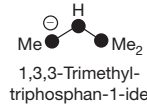
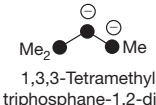
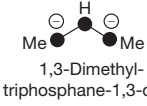
'phosphinyl', the name for the acyl groups  $\text{H}_2\text{P}(\text{O})-$  derived from phosphonic acid. However, the latter should be named according to IUPAC recommendation 'phosphinoyl'. Suffixes based on '-ylene', '-ylidene' and '-ylidene', such as '-ylenium' or '-ylidenium', are not used for describing cationic centers. Systematically derived prefixes for expressing cationic structural units as substituents are formed by adding the operational suffixes '-yl', '-ylidene', '-diyl', etc., with appropriate locants to the name of the parent cation (Tables 3 and 4). The operational suffix '-ylidene' is to be used only to describe the presence of a double bond between the substituting group and a parent hydride or parent substituent. Cationic phosphorus substituents with the free valence at a cationic phosphorus centre may also be derived by changing the '-ium' ending in the parent cation to '-io'. Thus  $-\text{PH}_3^+$  may also be named as 'phosphonio-'. This is especially important in polycations in which all cationic centers cannot be included in a cationic parent hydride or parent compound. The part of the structure which contains most of the cationic centers represents the cationic parent hydride or parent compound. Locants for added protons take precedence over locants for unsaturation.

Analogous to the formation of cations, anions are formed by the removal of one or more protons (Table 5), by the addition of one or more hydride ions (Table 6), or by a combination of both from a parent phosphane. The atom on which the negative charge resides is considered the anionic center. An anion formally obtained by removal of protons from the phosphane is named by adding '-ide', '-diide', etc. to the phosphane, with deletion of a terminal 'e' before '-ide' but

**Table 4** Suffix endings and prefixes for phosphorus-centered cations resulting from loss of hydride ions

Operation	Suffix	Cation substituent (prefix)	Examples
$\text{PH}_3$ Phosphane	$-\text{H}^-$ $\text{H}_2\text{P}^+$ -phosphenium -phosphanylium	$-\text{H}\bullet$ $-\text{PH}^+$ Phospheniumyl- Phosphanyliumyl- $-\text{P}^{2+}$	 Dimethyl- phosphanylium
$\text{PH}_5$ $\lambda^5$ -Phosphane	$-\text{H}^-$ $\text{H}_4\text{P}^+$ -phosphabis(ylium) $-\lambda^5$ -phosphanylium (This cation can also be named by adding the suffix '-ium' to the name of $\text{PH}_3$ where phosphorus is in the standard valency (phosphonium) by formally adding a hydron (Table 2), the use of '-ylium' in combination with the $\lambda$ -convention is much preferred.)	$-\text{H}\bullet$ $-\text{PH}_3^+$ $-\lambda^5$ -Phosphanyliumyl-	
$\text{P}_2\text{H}_4$	$-\text{H}^-$ $\text{H}_2\text{PPH}^+$ -phosphanylphosphenium -phosphanylphosphanylium -diphosphan-1-ylium	$-\text{H}\bullet$ $-\text{P}^+\text{PH}_2$ Phosphanylphospheniumyl- Phosphanylphosphanyliumyl- Diphosphan-2-ylium-2-yl- $-\text{PPH}^+$	 1,2-Trimethyl- diphosphan-1-ylium
$\text{P}_2\text{H}_4$	$-\text{H}^-$ $\text{H}_2\text{PP}^{2+}$ -diphosphan-1-bis(ylium) $\text{HP}^+\text{PH}^+$ -diphosphan-1,2-bis(ylium)	$-\text{H}\bullet$ $-\text{PPH}^{+2}$ Diphospha-1-bis(ylium)-2-yl- $-\text{PH}^+\text{PH}^+$	
$\text{P}_3\text{H}_5$ Triphosphane	$-\text{H}^-$ $\text{H}_2\text{PP}^+\text{PH}_2$ -triphosphan-2-ylium -bis(phosphanyl)phosphenylium $\text{HP}^+\text{PPH}_2$ -triphosphan-1-ylium	$-\text{H}\bullet$ $-\text{PPH}^+\text{PH}_2$ Triphosphan-2-ylium-3-yl- $-\text{P}^+\text{PPH}_2$ Triphosphan-3-ylium-3-yl-	 1,1,3,3-Tetramethyl- triphosphan-2-ylium

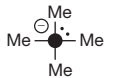
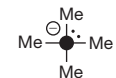
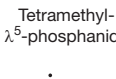
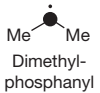
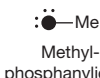
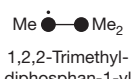
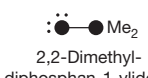
**Table 5** Suffix endings and prefixes for describing phosphorus-centered anions resulting from removal of protons

Operation		Suffix		Anionic substituent (prefix)	Examples
PH <sub>3</sub> Phosphane	-H <sup>+</sup>	H <sub>2</sub> PH <sub>2</sub> <sup>-</sup> -phosphanide	-H•	-HP <sup>-</sup> Phosphanidyl-	 Dimethylphosphanide
	-2H <sup>+</sup>	HP <sup>2-</sup> -phosphanediide	-H•	-P <sup>2-</sup> Phosphanediidyl-	
	-3H <sup>+</sup>	P <sup>3-</sup> Phosphide			
PH <sub>5</sub>	-H <sup>+</sup>	H <sub>4</sub> P <sup>-</sup> -λ <sup>5</sup> -phosphanide	-H•	-PH <sub>3</sub> <sup>-</sup> λ <sup>5</sup> -Phosphanidyl-	 Tetramethyl-λ <sup>5</sup> -phosphanide
P <sub>2</sub> H <sub>4</sub> Diphosphane	-H <sup>+</sup>	H <sub>2</sub> PPH <sup>-</sup> -diphosphan-1-ide	-H•	-PPH <sup>-</sup> Diphosphan-1-id-2-yl- -P <sup>-</sup> PH <sub>2</sub> Diphosphan-2-id-2-yl-	 1,2-Dimethyl-diphosphan-1-ide
	-2H <sup>+</sup>	HP <sup>-</sup> PH <sup>-</sup> -diphosphane-1,2-diide HPP <sup>2-</sup> -diphosphane-1-diide	-H•	-P <sup>-</sup> PH <sup>-</sup> Diphosphane-1,2-diid-2-yl- -PH <sup>-</sup> PH <sup>-</sup> Diphospha-1-diid-2-yl-	 1,2-Dimethyl-diphosphane-1,2-diide
P <sub>3</sub> H <sub>5</sub> Triphosphane	-H <sup>+</sup>	H <sub>2</sub> PP <sup>-</sup> PH <sub>2</sub> -Triphosphan-2-ide H <sub>2</sub> PPHPH <sup>-</sup> -Triphosphan-1-ide	-H•	-PHP <sup>-</sup> PH <sub>2</sub> Triphosphan-1-id-2-yl- -PPHPH <sup>-</sup> Triphosphan-1-id-3-yl-	 1,1,3,3-Tetramethyl-triphosphan-2-ide
					 1,3,3-Trimethyl-triphosphan-1-ide
	-2H <sup>+</sup>	H <sub>2</sub> PP <sup>-</sup> PH <sup>-</sup> -Triphosphane-1,2-diide HP <sup>-</sup> PPHPH <sup>-</sup> -Triphosphane-1,3-diide	-H•	-PHP <sup>-</sup> PH <sup>-</sup> Triphosphane-1,2-diid-3-yl- -P <sup>-</sup> PPHPH <sup>-</sup> Triphosphane-1,3-diid-3-yl-	 1,3,3-Tetramethyl-triphosphane-1,2-diide
				 1,3-Dimethyl-triphosphane-1,3-diide	

not in any other cases. Also in this case the locants for removed protons take precedence over locants for unsaturation. Analogous to the naming of cations, systematically derived prefixes for expressing anionic structural units as substituent (cation substituent as prefixes) are formed by adding the operational suffixes '-yl', '-ylidene', '-diyl', etc., with appropriate locants to the name of the parent phosphane. This also applies for corresponding phosphorus radicals (*vide infra*). If an anion results from the addition of a hydride ion, the operational suffix '-uide' or '-diuide', etc. replaces the 'e' of the phosphane. The operational suffix '-ide', '-diide', etc. can also be used in combination with the λ convention when the anionic center is derived from any position of the neutral phosphane that has at least two or more hydrogen atoms than are normally

present in the neutral polyphosphane. The original nomenclature systems do not provide an operational suffix for indicating addition of a hydride ion to a parent compound comparable to the '-ium' suffix for naming cations, however, some recommendations have been provided by using the operation suffix '-uide' or '-ide' in combination with λ convention. A radical derived by the formal removal of one hydrogen atom from any position of a phosphane is named by adding the operational suffix '-yl' to the name, replacing the final 'e' of the name of the phosphane. The formal removal of more than one hydrogen atom of a phosphane leads to monovalent radicals of a parent phosphane. By definition the free (nonbonding) electrons of a radical must be unpaired and, therefore, a mono- or divalent radical center with paired electrons (singlet state) is not

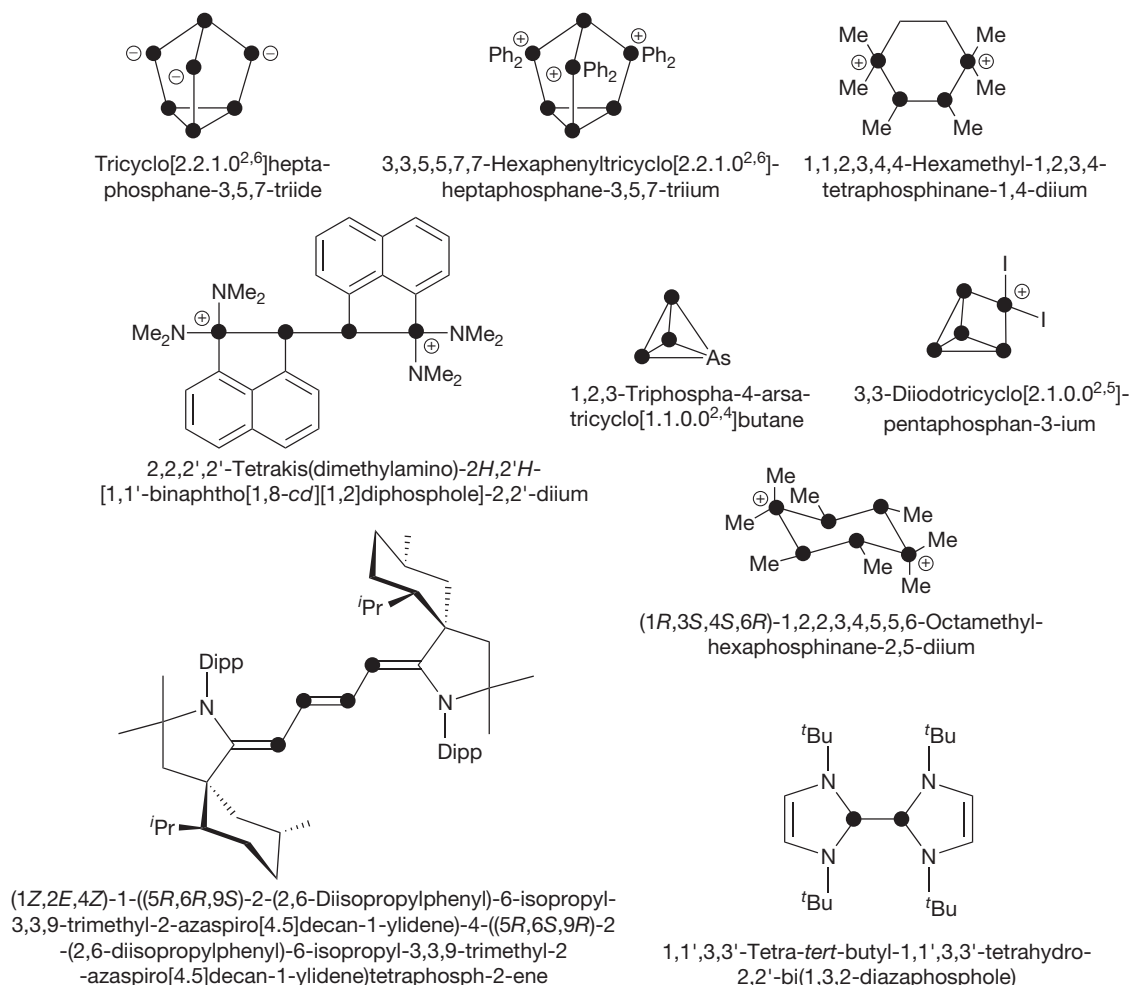
**Table 6** Suffix endings and prefixes for describing phosphorus-centered anions and radicals resulting from addition of hydride ions or removal of hydrogen radicals

Operation		Suffix		Substituent (prefix)	Examples
PH <sub>3</sub> Phosphane	+H <sup>-</sup>	H <sub>4</sub> P <sup>-</sup> -phosphanuide	-H•	-PH <sub>3</sub> <sup>-</sup> Phosphanuidyl-	 Tetramethylphosphanuide
P <sub>2</sub> H <sub>4</sub> Diphosphane	+H <sup>-</sup>	H <sub>2</sub> PPH <sub>3</sub> <sup>-</sup> -diphosphan-1-nuide -λ <sup>5</sup> -phosphanide	-H•	-PHPH <sub>3</sub> <sup>-</sup> Diphosphan-1-nuid-2-yl- -PH <sub>2</sub> <sup>-</sup> PH <sub>2</sub> Diphosphan-1-nuid-1-yl-	 Tetramethylphosphanuide  Tetramethyl-λ <sup>5</sup> -phosphanide
PH <sub>3</sub>	-H•	H <sub>2</sub> P• -phosphanyl	-H•	-PH• Ylophosphanyl-	 Dimethylphosphanyl
	-2H•	HP: -phosphanylidene	-H•	-P: Ylophosphanylidene-	 Methylphosphanylidene
PH <sub>5</sub> λ <sup>5</sup> -Phosphane	-H•	PH <sub>4</sub> • -λ <sup>5</sup> -phosphanyl	-H•	-PH <sub>3</sub> • Ylo-λ <sup>5</sup> -phosphanyl-	
P <sub>2</sub> H <sub>4</sub> Diphosphane	-H•	H <sub>2</sub> PPH• -diphosphanyl	-H•	-PHPH• 2-Ylodiphosphan-1-yl-	 1,2,2-Trimethyldiphosphan-1-yl
	-2H•	H <sub>2</sub> PP: -diphosphanylidene	-H•	-PHP: 2-Ylodiphosphan-1-ylidene-	 2,2-Dimethyldiphosphan-1-ylidene

considered to be a radical. Regardless of the electronic state of the nonbonding, free electrons, the 'radical suffixes' such as '-diyl' and '-ylidene' are used to describe monovalent radical phosphorus centers. The distinction with respect to the electronic state should be made by adding the separate word 'singlet' or 'triplet' to describe the radical center. For anions and radicals, locants are also used to describe the position of the anionic or radical center(s) and are placed in front of the name. There are derivatives in which more than one ionic or radical centers are present. Very often, such compounds can be named by following the rules described here. However, there are many compounds where the rules cannot be extended to multi-ionic or radical centers as well as a combination of such (radical cations, radical anions, and zwitterions) and in those cases refer to the appropriate literature.<sup>10–13</sup> The nomenclature of fused polyphosphanes and cage compounds follows similar rules as introduced by IUPAC recommendation of carbo- and heterocycles. Also, the stereodescriptions for the denotation of the absolute and relative configuration in names of polyphosphorus compounds follow the rules of organic chemistry.<sup>9–12,15</sup> Figure 4 provides a selection of recently published compounds and recommended naming according to IUPAC.

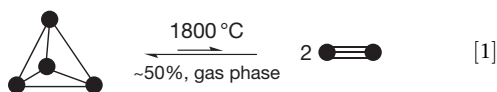
### 1.04.3 Neutral Compounds

Examples of polyphosphorus compounds have been reported to exhibit superconductivity, interesting thermochemistry, and magnetic behavior,<sup>6</sup> and some compounds have importance in homogeneous and heterogeneous catalysis (e.g., hydrodesulfurization and hydrodenitrogenation of petroleum fuels),<sup>24,25</sup> new inorganic polymers,<sup>26</sup> energy storage systems,<sup>27</sup> functional molecules (sensors, oxygen barriers in capacitors, molecular magnets, organic light-emitting diodes (OLEDs)),<sup>28</sup> optical applicatons,<sup>29,30</sup> and corrosion resistance.<sup>31</sup> The chemistry of many polyphosphorus compounds has been developed from the large number of modifications of phosphorus, some of which have been known for more than a century. The most important allotropes are orthorhombic black phosphorus,<sup>32</sup> the violet<sup>33</sup> and fibrous phosphorus,<sup>34</sup> amorphous red phosphorus (two allotropes, various degrees of disorder), and the cubic white phosphorus.<sup>35</sup> The relative thermodynamic stability increases from P<sub>4</sub> → P<sub>red</sub> → P<sub>violet</sub> → P<sub>black</sub>. Black phosphorus represents the only thermodynamically stable modification under standard conditions; however, the conversion rates of the other metastable allotropes are very slow and they can be stored.



**Figure 4** Examples of polyphosphorus derivatives and naming recommended by IUPAC.<sup>16–23</sup>

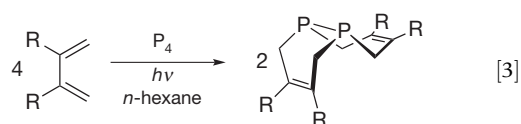
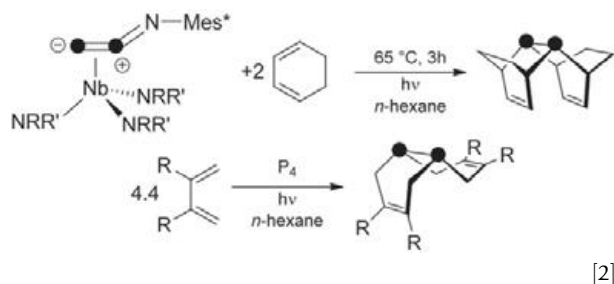
Physical properties and structures for most of the modifications have been extensively studied and reviewed in detail but new modifications are regularly discovered.<sup>36</sup>



The diatomic allotrope P<sub>2</sub> has been considered for a long time as a laboratory curiosity since an equilibrium with an equimolar ratio of P<sub>2</sub> and P<sub>4</sub> exists at 1800 °C under low pressure, as illustrated in eqn [1]. Thus, the application of such chemistry was in astronomy, in plasma media, and under matrix isolation conditions.<sup>37</sup> The P<sub>2</sub> molecule is 49 kcal mol<sup>-1</sup> higher in energy than P<sub>4</sub> and has not been observed at room temperature.<sup>38</sup> However, Raman spectroscopic studies on matrix-isolated P<sub>2</sub> in a combination of Kr and adamantane at 77 K provide new insights into P<sub>2</sub> isolation.<sup>39</sup> The most common method for the stabilization of P<sub>2</sub> is the coordination to transition metals,<sup>40</sup> but the extrusion and capture of P<sub>2</sub> fragments has yielded access to novel P<sub>2</sub> chemistry. For example, the niobium complex in eqn [2], containing an η<sup>2</sup>-P<sub>2</sub>NRR'-moiety (R = neopentyl, R' = 3,5-C<sub>6</sub>H<sub>3</sub>Me<sub>2</sub>; Mes\* = 2,4,6-C<sub>6</sub>H<sub>2</sub>(<sup>t</sup>Bu)<sub>3</sub>) and sterically

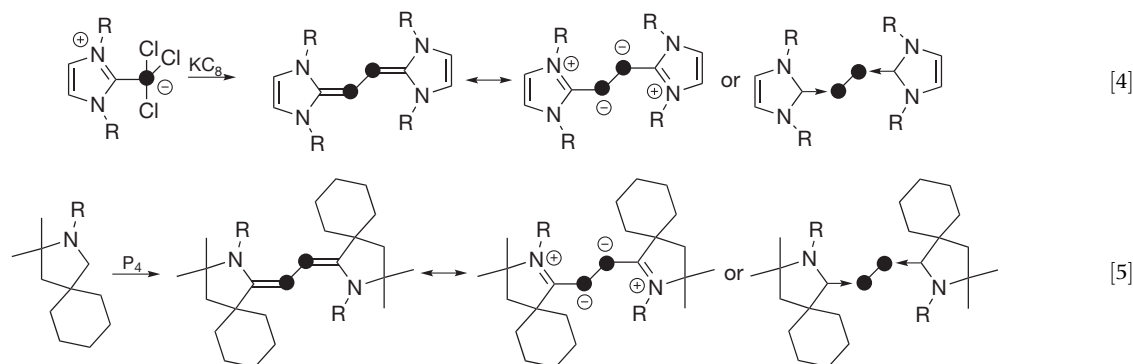
encumbered amido groups, releases P<sub>2</sub> under mild conditions (~65 °C), which can be captured in a double Diels–Alder reaction with cyclohexadiene to give a diphosphane.<sup>41</sup> A more convenient but low yield route to P<sub>2</sub> chemistry is the photochemical reaction of P<sub>4</sub> in the presence of an excess of diene to form diphosphanes, as illustrated in eqn [3].

Other approaches to dinuclear compounds have been recently reported to give compounds containing low-coordinate



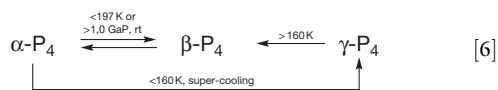
phosphorus centers in the P–P units.<sup>42</sup> The reduction of a *N*-heterocyclic carbene adduct (NHC → PCl<sub>3</sub>)<sup>43</sup> with potassium graphite in eqn [4] results in the formation of an electron-rich P<sub>2</sub>-species. A comparable P<sub>2</sub>-species is obtained from the reaction of a cyclic-aminoalkyl carbene (CAAC)<sup>44</sup> in eqn [5], which is less electron rich according to electrochemical studies. Thus, the NHC-ligated species can be oxidized stepwise to the dication *via* the radical cation, whereas the CAAC-ligated derivative may only be singly oxidized.<sup>14</sup> Experimental data and computational investigations favored a bisphosphinidene-like arrangement for both compounds, in which the two P centers are singly bonded

polymorphism in disordered states where the phase separation in the disordered state is density driven.<sup>46</sup> *In situ* x-ray radiography clearly demonstrates allotropic phase separation in the molten state of phosphorus at high temperatures and pressures. Two bulk liquid phases of phosphorus (liquid I and II), having distinct molecular structures and different mass densities, coexist in thermodynamic equilibrium along a line in the temperature–pressure phase diagram. The transition between the two liquid forms is as abrupt as it is for the melting transition and the various solid–solid phase transformations observed for phosphorus.<sup>47</sup> The reactivity of the P<sub>4</sub> molecule



to each other, each possessing two lone pairs of electrons.

Besides P<sub>2</sub>, the most reactive modification of phosphorus is P<sub>4</sub> of which three allotropes ( $\alpha$ ,  $\beta$ ,  $\gamma$ -P<sub>4</sub>) are known, and phase relationships among these at ambient pressure were established by differential thermal analysis (DTA) and x-ray powder diffraction experiments. The P<sub>4</sub> molecules rotate dynamically around their centers of gravity in the room-temperature plastic  $\alpha$ -P<sub>4</sub> modification. As shown in eqn [6], one of two low-temperature modifications,  $\beta$ -P<sub>4</sub>, is stable only at temperatures below 197 K at ambient pressures or higher than 1.0 GPa at ambient temperature. In the crystal structure of  $\beta$ -P<sub>4</sub>, the P<sub>4</sub> molecules have fixed orientations. The new  $\gamma$ -modification exists as a stable lower-temperature modification up to approximately 160 K and is obtained by super-cooling of  $\alpha$ -P<sub>4</sub> by rapid quenching from room to liquid nitrogen temperature and slow warming transforms *via*  $\beta$ -P<sub>4</sub> back to  $\alpha$ -P<sub>4</sub> at about 193 K; however, a  $\beta$  to  $\gamma$  transformation has not been reported.<sup>35</sup>



The occurrence of different liquid forms of the same chemical composition, with different atomic or molecular arrangements, is less common. White phosphorus is an interesting candidate for the investigation of structural transformations between different liquid phases due to its abrupt structural change between two stable disordered states above the melting temperature when the pressure is changed at about 1 GPa and 1000 °C.<sup>45</sup> Only very few examples are known for

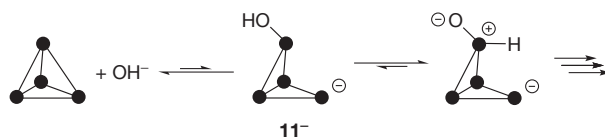
has been controlled in inclusion and intercalation complexes with supramolecular assemblies.<sup>48</sup> The 2:1 inclusion complex [(P<sub>4</sub>)<sub>2</sub>C<sub>60</sub>] is formed in a 90% yield when a solution of white phosphorus in CS<sub>2</sub> is added to a solution of C<sub>60</sub> in toluene. The observed upfield chemical shift in the <sup>31</sup>P-nuclear magnetic resonance (NMR) of the complex indicates that C<sub>60</sub> has some electronic effects; however, no electron transfer had occurred between the carbon C<sub>60</sub> allotrop and P<sub>4</sub> units.<sup>49a</sup> White phosphorus has been recently also encapsulated in a self-assembly mechanism with an iron(II)-based capsule.<sup>49b</sup>

There has been a recent revival in the developing chemistry of P<sub>4</sub> since this allotrope represents the entry point for the preparation of most P(III) and P(V) compounds. Chlorination or oxychlorination of P<sub>4</sub> provides the very important phosphorus bulk chemicals PCl<sub>3</sub>, PCl<sub>5</sub>, and POCl<sub>3</sub>. These compounds are used in subsequent reactions for the generation of organophosphorus compounds (OPCs) of tri- and pentavalent phosphorus as well as phosphoric and phosphonic acids and esters. Increasingly stringent environmental and transportation regulations with respect to P<sub>4</sub> handling, together with the drawbacks of chlorine-based and heavy salt-waste syntheses, require new ways of P<sub>4</sub> functionalization to useful molecules. A number of reviews deal with the functionalization of P<sub>4</sub> with compounds of the p-block<sup>50</sup> and coordination chemistry<sup>51,52</sup> as well as electrochemical/electrocatalytic formation<sup>53</sup> of OPCs from P<sub>4</sub>. Chapter 1.35 discusses the P<sub>4</sub> chemistry in detail; therefore, only functionalization and degradation pathways of P<sub>4</sub> to interesting *catena*-phosphorus compounds are discussed here. Four types of molecules have been employed to activate white

phosphorus – p-block nucleophiles, electrophiles, molecules containing ambiphilic centers,<sup>54</sup> and radicals.

The first and most commonly investigated functionalization of  $P_4$  involves the nucleophilic attack by group 14 anions (e.g., organoalkali and organoalkali earth metal compounds and bulky silanides), group 15 anions (alkali metal phosphides and phosphinites) or group 16 anions (hydroxide, alkoxides, thiolates, polysulfides, and dichalcogen dianions  $Q_2^{2-}$  ( $Q=S, Se, Te$ )).<sup>50a</sup> The nucleophilic  $R^-$  likely engages an empty p-orbital of one of the phosphorus atoms of  $P_4$  (step 1, **Scheme 1**) to access a monosubstituted bicyclo[1.1.0]tetraphosphanide anion  $[RP_4]^-$ . Subsequent attacks of nucleophiles followed by rearrangement processes explain the formation of a series of phosphorus anions which can be isolated in many cases or sequestered into stable products by electrophiles. However, if the reactions occur in the absence of electrophilic reagents, the reformation of starting compounds are observed for almost all types of nucleophiles, except for the very strong nucleophiles such as carbanions. In protic solvents, the formation

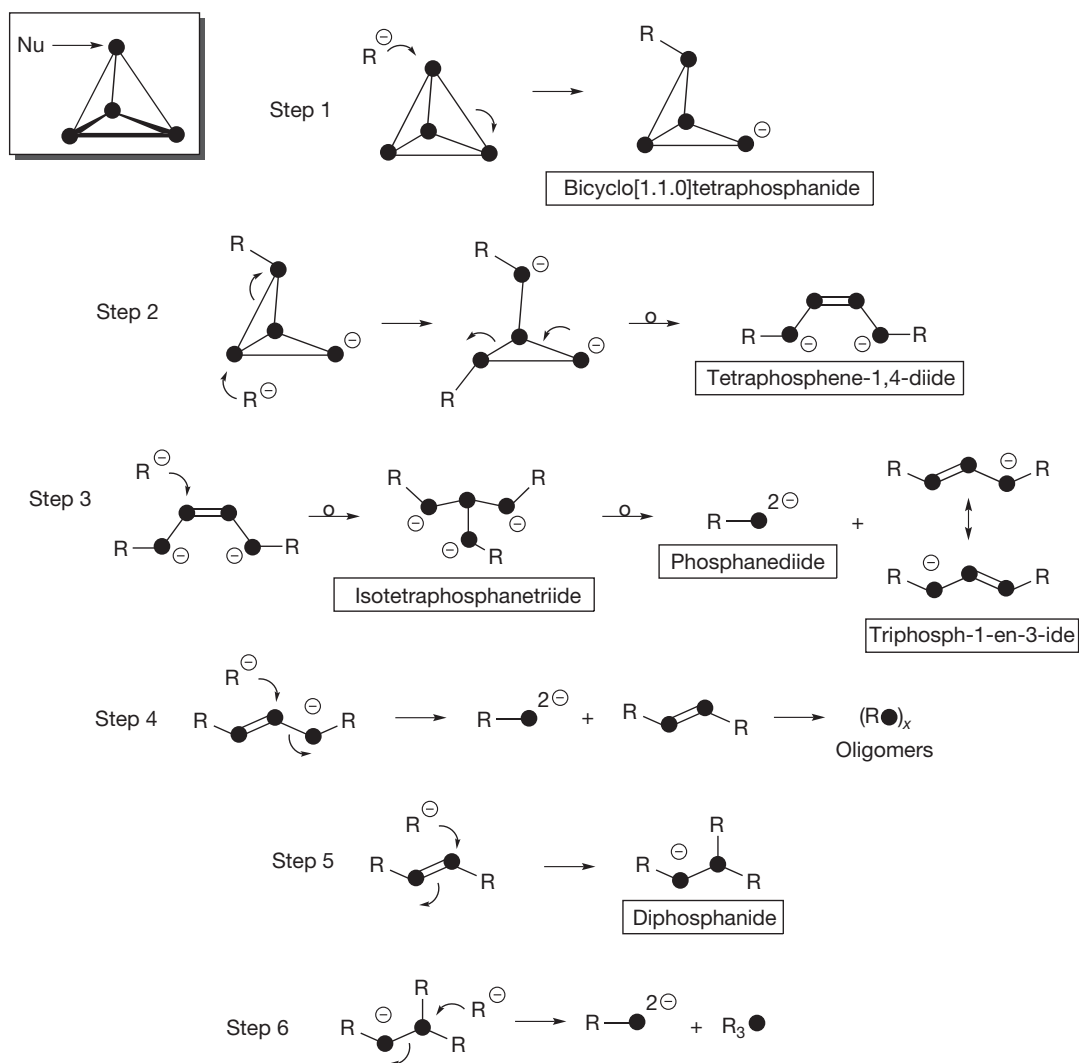
of unstable intermediates results from the very basic properties of the initially formed polyphosphide anion in step 1, giving rise to the formation of unstable intermediates such as a bicyclo[1.1.0]tetraphosphanide anion ( $R=OH^-$ ) and decomposition products (eqn [7]). In the case of group 16 anions (e.g., hydroxide and alkoxide anion), disproportionation reactions such as shown in eqn [8] are often involved allowing the ultimate formation of phosphane ( $PH_3$ ), along with salts of  $H_3PO_2$  via a stepwise degradation mechanism.



[7]



[8]



**Scheme 1** Proposed mechanism for the stepwise nucleophilic degradation of  $P_4$ .



Thus, in an uncontrolled way, the resulting intermediates spontaneously decompose with evolution of hydrogen, phosphane, hypophosphite anions, and phosphite anions, but when controlled, the fundamental phosphane molecule  $\text{PH}_3$  provides entry to the preparation of organophosphorus compounds.<sup>55</sup> The addition of further nucleophiles in step 2 leads to the attack at one of the bridgehead phosphorus atoms followed by a rearrangement to yield 1,4-disubstituted tetraphosphen-1,4-diide anions  $[\text{R}_2\text{P}_4]^{2-}$ . These species can either dimerize by a [2+2] cycloaddition reaction *via* the P–P double bond or undergo a subsequent nucleophilic attack of the central phosphorus atom as indicated in step 3.

Another rearrangement step provides the structural motif of an isotetraphosphanetriide anion  $[\text{P}(\text{PR})_3]^{3-}$  that can fragment by loss of phosphanediide  $\text{RP}^{2-}$  and triphosphenide anions  $[\text{R}_2\text{P}_3]^-$ . The latter reacts with further nucleophiles in step 4 to form the phosphanediide  $\text{RP}^{2-}$  anion and a diphosphene which either oligomerizes to cyclophosphanes  $(\text{RP})_n$  ( $n=2,4,6$ ) or yields diphosphenide  $[\text{R}_3\text{P}_2]^-$  by a fast subsequent nucleophilic attack as indicated in step 5. Diphosphenides  $[\text{R}_3\text{P}_2]^-$  decompose to a tertiary phosphane and an  $\text{RP}^{2-}$  anion on reaction with a nucleophile (step 6). The rupture of the P–P bonds in  $\text{P}_4$  can also proceed by a pattern much more complicated than the successive addition of nucleophilic reagents as indicated in Scheme 1. Thus, the formation of oligomeric phosphides is also observed as the negative charge on the phosphorus atom in the ‘butterfly’-type intermediate of step 1 can be stabilized by interaction with a second  $\text{P}_4$  molecule. Many transformations have been studied, taking reactions of  $\text{P}_4$  with a series of different anions and other nucleophiles, in order to elucidate the factors that would suppress disproportionation. The selection of the optimal conditions ensures in some cases the selective formation of the target products from the intermediate phosphorus oligomers; however, predicting certain structural outcomes is often still not possible and requires further investigations.

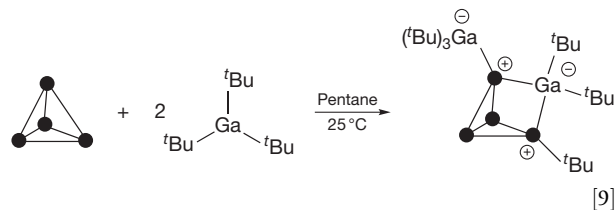
Studies of the reactivity of white phosphorus with p-block electrophiles are limited and many are based on reactions in combination with nucleophiles such as the hydroxide anion. In those cases, the simple procedures, mild conditions, ready availability of the initial reactants, and the easy isolation and identification of products are the reasons for the fast progress in this field. The reaction of elemental phosphorus with electrophilic agents in the presence of strong alkalis (so-called superbasic media) is a convenient preparation of OPCs and a comprehensive overview has recently been published.<sup>55</sup> The reactivity of white phosphorus with Lewis acids is difficult, most likely due to the low nucleophilicity of the  $\text{P}_4$  molecule.<sup>56</sup> However, examples are known from the reaction of sterically encumbered group 13 molecules, such as  ${}^t\text{Bu}_3\text{Ga}$ , which reacts with half an equivalent of white phosphorus at room

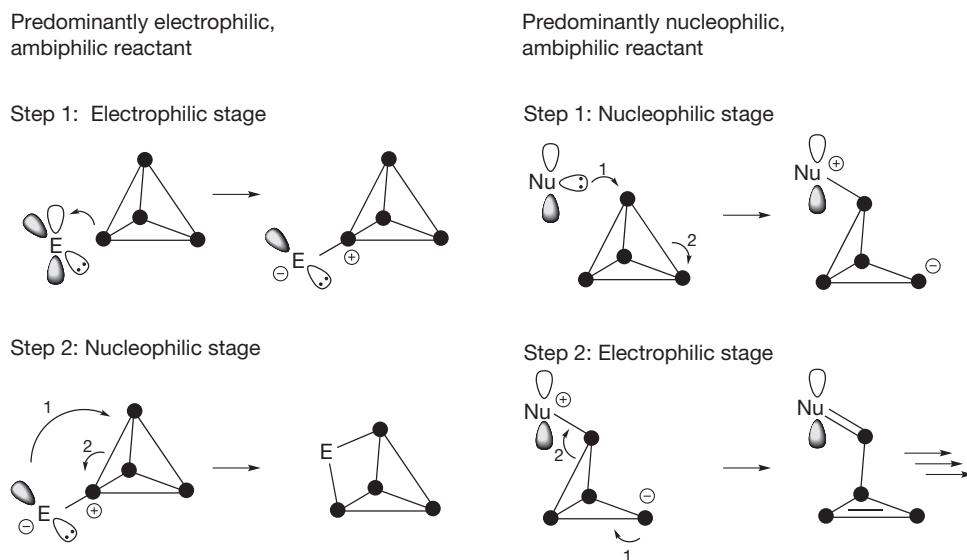
temperature to give the chelated gallium complex shown in eqn [9].<sup>57</sup>

The amphiphilic character of main-group molecules represents a new tool for the activation of elemental phosphorus and stems from the potential of such molecules to act as Lewis acids and Lewis bases at the same time. Different reaction pathways are possible for the functionalization of  $\text{P}_4$  depending on the dual nature and the electronic structure of the reactants in question.<sup>54</sup> The full description of the frontier orbitals of  $\text{P}_4$  is beyond the scope of this chapter; however, the sets of local orbitals for  $\text{P}_4$ , which are in  $T_d$  symmetry, can be constructed from the local orbitals of  $\text{PH}_3$  units since each corner of the  $\text{P}_4$  tetrahedron can be represented by a pseudo- $\text{PH}_3$  molecular orbital system.<sup>58</sup> Important to note is that in  $\text{P}_4$ , the  $4 \times a_1$  local orbital sets of  $\text{PH}_3$  (highest occupied molecular orbital (HOMO)) transform as  $a_1 + t_2$ , whereas the  $4 \times e$  local orbital sets of  $\text{PH}_3$  (lowest unoccupied molecular orbital (LUMO)) transform as  $e + t_1 + t_2$ . The corresponding Kohn–Sham orbitals correspond to HOMO – 1  $6t_2$  (–7.5 eV), HOMO  $2e$  (–6.7 eV), LUMO  $2t_1$  (–1.8 eV), and LUMO + 1  $7t_2$  (–1.5 eV) according to calculations (RI-BP86/TZVP). The HOMO – 1 ( $t_2$ ) represents a combination of lone-pair orbitals at P and the HOMO ( $e$ ) a combination of PP-bonding orbitals. The LUMO provides (antibonding) p-orbitals that are perpendicular to the directions of the lone pairs. Based on symmetry considerations of the frontier orbitals of  $\text{P}_4$ , the attack of the reactants depends on their philicity.

Electrophiles (E) or nucleophiles (Nu) may attack the  $\text{P}_4$  tetrahedron at various positions, as illustrated in Scheme 2. Edge attack is less likely since white phosphorus possesses almost no strain<sup>59,60</sup> and the P–P bonds possess little, if any,  $\pi$ -character since the resulting bonds are only slightly bent.<sup>54,61</sup> The amphiphilic functionalization of  $\text{P}_4$  can be divided into two categories assuming a nonsynchronous processes with two consecutive steps. In step 1 of the reaction of a predominantly electrophilic, amphiphilic molecule, electron density is transferred from one of the phosphorus atoms into the unoccupied p-orbital at the acceptor molecule ( $\sigma \rightarrow p$ , step 1: electrophilic stage, Scheme 2, left). Alternatively, a simultaneous combination of an electrophilic and a nucleophilic approach can be considered, however, experimental evidence of a bimolecular mechanism involving e.g. two  $\text{P}_4$  molecules has yet to be reported. The resulting zwitterionic adduct can then undergo an electronic rearrangement to a bicyclo [1.1.0]tetraphosphane derivative (step 2: nucleophilic stage). Examples of amphiphilic systems that are predominantly electrophilic in nature include, for example, group 13 (aluminum(I) and gallium(I) species), group 14 (disilylenes and silylenes), and group 15 (phosphenium cations) compounds. The low-valent atoms in these heavier element systems typically have a lower energy lone pair (i.e., not the HOMO) and thus tend to initially react *via* the low-lying empty orbital, as demonstrated for main-group carbene analogs.<sup>54</sup> The dominant electrophilic, amphiphilic reaction mechanism typically results in complex fragmentation and/or derivatization of  $\text{P}_4$  and may subsequently lead to phosphorus-rich ring and cluster systems.<sup>50</sup>

For a molecule with predominantly nucleophilic, amphiphilic properties the donor molecule transfers electron density from a  $\sigma$ -orbital into to the  $\pi^*$  orbital of  $\text{P}_4$  ( $\sigma \rightarrow \pi^*$ , step 1



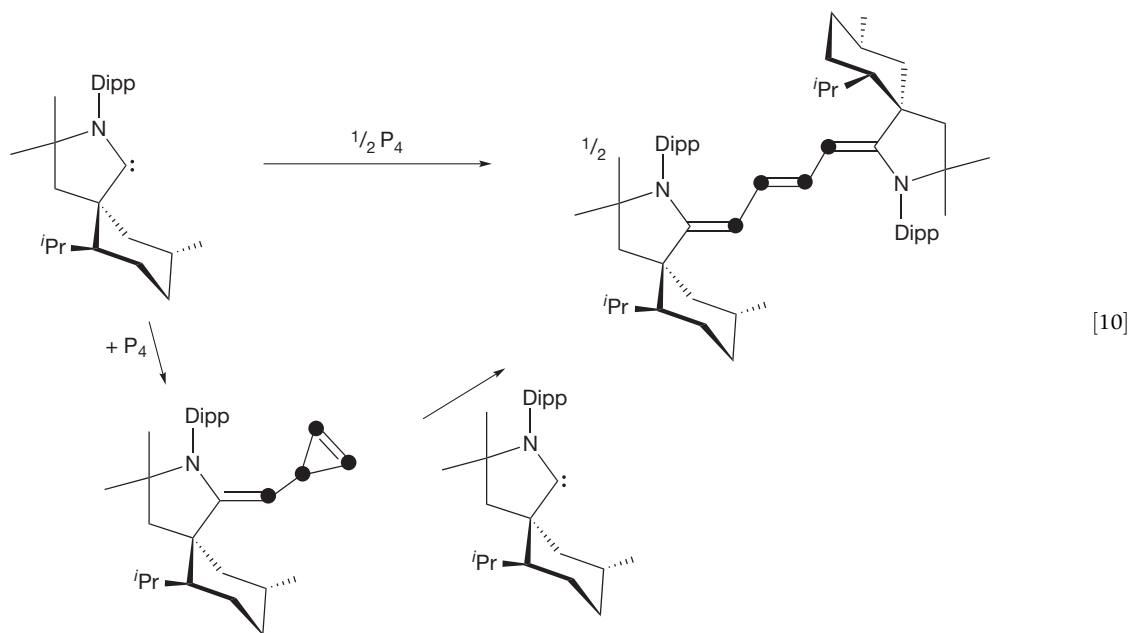


**Scheme 2** Proposed mechanism for the functionalization of  $P_4$  by ambiphilic molecules.

nucleophilic stage, **Scheme 2**, right). Since carbenes exhibit a dual reactivity, this reaction pathway is best exemplified by singlet carbenes. These systems are known for being strong  $\sigma$ -donors through the lone pair of electrons as well as having electrophilic character at the carbene center.<sup>62</sup> Those reactions initiated by nucleophilic attack on a vacant orbital of  $P_4$  to yield a triphosphirene intermediate, as shown in eqn [10], are followed by an electrophilic stage with a second carbene.<sup>23</sup> To date, this type of reactivity has been limited to singlet carbenes<sup>23</sup>:

energy barriers and, therefore, lower efficiency in nucleophilic insertion reactions of silylenes.<sup>50b,63</sup>

Although reactivity studies of white phosphorus with p-block radicals are limited to a few examples, the attack of  $P_4$  with a radical typically results in a homolytic cleavage of a P–P bond to yield a bicyclo[1.1.0]tetraphosphanyl as an intermediate (**Scheme 3**, step 1) that can undergo a recombination reaction with a second radical to form bicyclo[1.1.0]tetraphosphane derivative (**Scheme 3**, step 2). Cleavage of the P–P



The reluctance of silicon to hybridize dictates the electrophilic behavior of silylenes compared to carbenes and explains their different reactivity. In addition, the  $\pi$ -interaction of electrons from the amino substituents to the vacant p-orbital at carbon is more efficient than the analogous interaction with the silylene center, which manifests itself as high activation

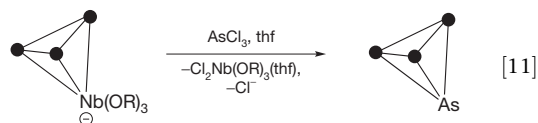
bridge and formation of the four-membered cyclotetraphosphanyl radical results from the attack of a third radical (**Scheme 3**, step 3). This species can then either react with another radical to form a cyclotetraphosphane (**Scheme 3**, step 4) or eject a phosphorus atom and ring close to yield a cyclotriphosphane and  $P_4$  (**Scheme 3**, step 4'). Further reaction

with radicals would result in degradation of the  $(RP)_n$  rings and formation of diphosphanes (Scheme 3, step 5) and finally ends in the formation of tertiary phosphanes (Scheme 3, step 6). Bicyclo[1.1.0]tetraphosphanes are the main isolated products in most of the reported reactions of  $P_4$  with radicals. However, in some cases, a concerted reaction mechanism cannot be excluded where a P–P bond of white phosphorus adds across an element–element bond *via* a four-centered transition state. The observed species are dependent on the electronic and the steric requirements of the radical species.<sup>50b</sup> The most prominent radical reaction with  $P_4$  involves the molecular ‘jack in the box’ diphosphane,  $[P\{N-^iPr_2\}(N\{SiMe_3\}_2)]_2$ , illustrated in Scheme 4.<sup>64</sup>

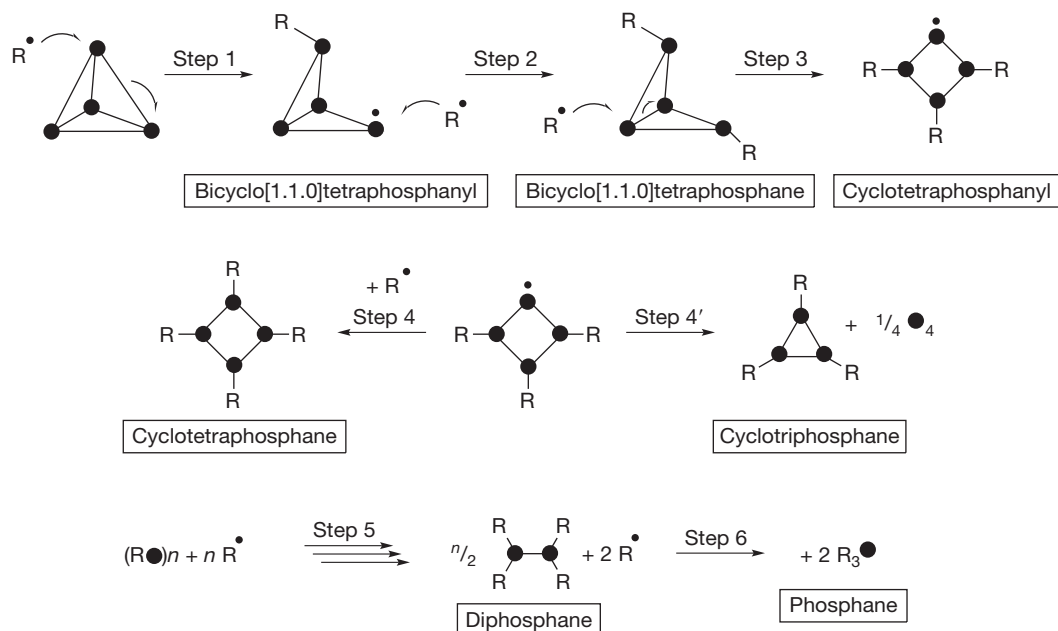
Homolytic P–P bond cleavage of the diphosphane gives the phosphanyl radical, which reacts with white phosphorus in refluxing toluene to give the bisphosphane-substituted bicyclo[1.1.0]tetraphosphane according to steps 1 and 2 in Scheme 3.<sup>65</sup> More recently, a number of phosphanes and polyphosphanes were prepared *via* a radical route through the use of  $Ti(N[^iBuAr]_3)$  ( $Ar = 3,5-Me_2C_6H_3$ ), and various R–X species ( $R-X = PhBr, CyBr, Me_3SiI, Ph_3SnCl$ ). The titanium complex is used in these reactions to generate group 14 radicals ( $R\bullet$ ), which then react

with  $P_4$  to yield tetraphosphanes and tertiary phosphanes, according to steps 5 and 6 in Scheme 3.<sup>66</sup>

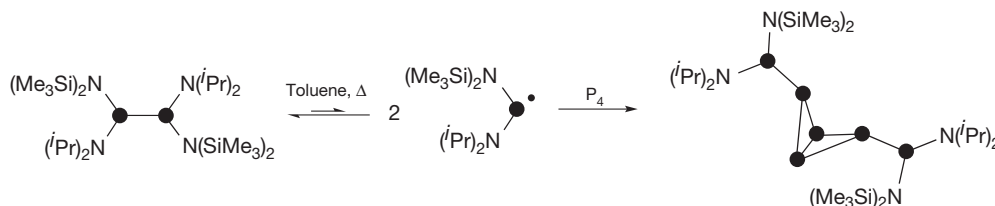
Binary interpnictogen compounds of the type  $As_nP_{4-n}$  ( $n = 1-3$ ), which are structurally related to  $P_4$  were, until recently, only observed in gas-phase studies wherein hot ( $660^\circ C$ ) vapors of phosphorus and arsenic mixtures under equilibrium reaction conditions were subjected to Raman spectroscopic analysis.<sup>67</sup> A directed metal–organic synthetic pathway for the synthesis of the binary interpnictogen compound  $AsP_3$  has been developed by reacting  $AsCl_3$  with the *in situ* formed  $[P_3Nb(OR)_3]^-$  anion ( $R = 2,6$ -diisopropylphenyl) as shown in eqn [11].<sup>19</sup>



Interestingly, the synthetic strategy developed for the  $P_3^-$  transfer with formation of an  $EP_3$  tetrahedron is not limited to  $E = As$ . When using  $SbCl_3$  in place of  $AsCl_3$  in the synthesis, the



**Scheme 3** Proposed mechanism for the stepwise degradation of  $P_4$  by radicals.



**Scheme 4** Radical formation from the ‘Jack in the box’ diphosphane and subsequent reaction with  $P_4$ .

generation of the exotic  $\text{SbP}_3$  molecule could also be justified by  $^{31}\text{P}$  NMR spectroscopic investigations.<sup>19</sup> Detailed investigations also confirmed that  $\text{AsP}_3$  can be thought of as a strongly spherical aromatic system similar to  $\text{P}_4$ . The nucleus-independent chemical shift (NICS) value<sup>68</sup> calculated for  $\text{P}_3\text{As}$  ( $-58.230$ ) compares to  $\text{P}_4$  ( $-59.444$ ). This indicates that despite the lower molecular symmetry of  $\text{P}_3\text{As}$ , a significant spherical aromaticity is retained. This is due to the fact, that  $\text{P}_3\text{As}$ , like  $\text{P}_4$ , maintains closed-shell  $\sigma$  and  $\pi$  subsystems, resulting in symmetrically distributed angular momentum. The new data provide a more complete understanding of the fundamental physical properties of these tetrahedral, elemental entities and beckon further development of the molecular chemistry of group 15 elements.<sup>69</sup>

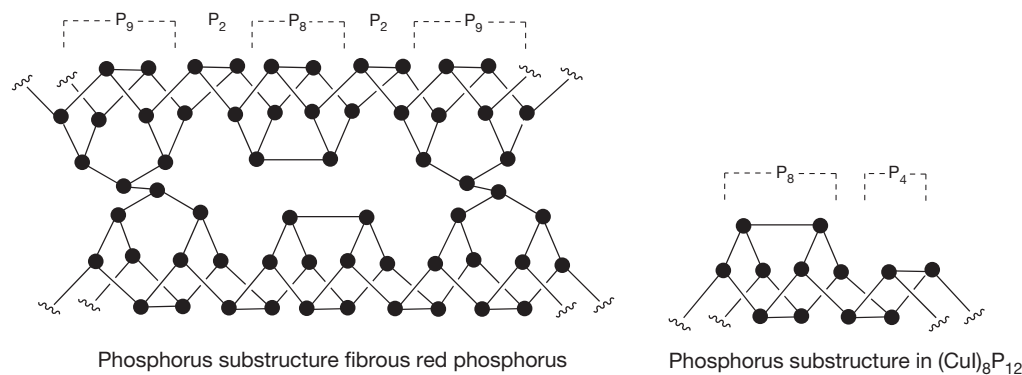
The densest and least reactive allotrope of phosphorus, black phosphorus, has both pressure-induced and temperature-dependent phase transitions to rhombohedral semimetallic as well as cubic metallic phases.<sup>70</sup> Crystalline black phosphorus was first isolated using a growth medium of liquid bismuth. Black phosphorus is orthorhombic under standard conditions and consists of puckered layers oriented parallel to the *ac* plane.<sup>71</sup> Three classical routes are known for the preparation of this allotrope.<sup>72</sup> Recently, the preparation of black phosphorus under low-pressure conditions at 873 K was reported from red phosphorus *via* the addition of small quantities of gold, tin, and tin(IV) iodides. This new preparative method of black phosphorus represents an easy and effective way to avoid complicated preparative setups, toxic catalysts, or 'dirty' flux methods and is of general interest in elemental chemistry to access this important semiconducting material. Furthermore, the crystal structure of black phosphorus was redetermined from single crystals and a possible mechanism for its formation has been suggested. Calculations of thermodynamic values showed that the only relevant gas-phase species is  $\text{P}_4$ , and the transport reactions are not suitable for the preparation of orthorhombic black phosphorus at temperatures above 773 K. A kinetically controlled mechanism is favored over a thermodynamically controlled formation.<sup>73</sup> Very recently, black phosphorus was drawn back into the focus of material scientists as an anode material for lithium ion batteries.<sup>74</sup>

In comparison to the white and black allotropes, the definition of red phosphorus is less complete and very complicated. The red allotrope has been proposed to exist in five unambiguous forms denoted as types I–V.<sup>75</sup> Type I represents the commercially available amorphous red phosphorus

through which types II–V are generated *via* high-temperature annealing processes. Several suggestions are proposed for the structural arrangement in the different types of red phosphorus. Type I is proposed to be a combination of fibrous red and Hittorf's phosphorus, whereas types IV/V were shown to consist of  $\text{P}_{12}$  helical structures by characterization in CuI matrices and x-ray crystallography.<sup>75</sup> Characterized as fibrous red phosphorus (type IV), the most recent addition to the phosphorus family exists as a polymeric structure of linked pentagonal rings, illustrated in Figure 5. Type V is the branched violet form known as Hittorf's phosphorus. Fibrous red and Hittorf's phosphorus are proposed to be energetically equivalent and the most stable conformation to date. Both show structural similarities including a repeating unit of 21 single phosphorus atoms. On the basis of x-ray crystallographic data, the fibrous red allotrope is proposed to adopt a similar arrangement of the phosphorus atoms to that in Hittorf's phosphorus with the exception of the branches, which are instead oriented in a parallel manner.<sup>76</sup>

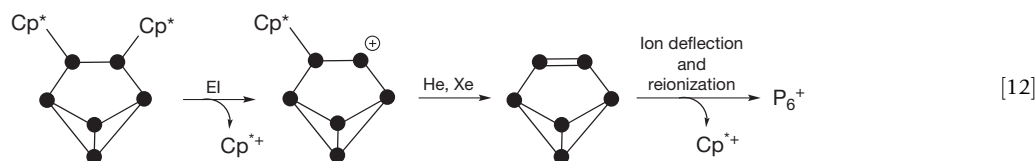
More recently, theoretical studies indicate that energetically related polymeric forms of red phosphorus have similar stabilities. Energetically analogous polymeric units have been supported experimentally by the repeating phosphorus units found in CuI based matrices.<sup>77</sup>  $(\text{CuI})_3\text{P}_{12}$ ,  $(\text{CuI})_8\text{P}_{12}$  (Figure 5), and  $(\text{CuI})_2\text{P}_{14}$  structures have been observed to date, through which nanorod-like materials may be formed through removal of CuI by a KCN solution.<sup>75d</sup> Nanocomposite  $\text{P}_n$  materials are also formed from the  $^{60}\text{Co}$  radiation of  $\text{P}_4$  in benzene solution<sup>78</sup> and from polymerization of  $\text{P}_4$  with bismuth nanoparticles for which the latter was proposed as a red phosphorus structure.<sup>79</sup> A chemical heuristic for the deduction and classification of covalent partial structures of phosphorus in polycyclic phosphanes, phosphorus-rich polycyclic phosphides, and allotropes of phosphorus has been deduced from work of Baudler. This approach can be used to direct *ab initio* techniques in the quest of for as yet unknown forms of molecular or macromolecular phosphorus.

Based on calculated stabilities of systematically generated structural alternatives, it was rationalized from the stabilities of Hittorf's phosphorus and of molecular  $\text{P}_4$  that other crystalline allotropic forms of phosphorus must exist.<sup>80</sup> Small-molecule allotropes of phosphorus in which the phosphorus atom is three-coordinate (either three  $\sigma$ -bonds or one  $\sigma$ -bond and one  $\pi$ -bond) would always contain an even number of



**Figure 5** Phosphorus substructure in red phosphorus and in  $(\text{CuI})_8\text{P}_{12}$ .

phosphorus atoms  $P_n$  ( $n=2, 4, 6, 8$  etc.). Several structural alternatives are possible. For example, of the isomers of  $P_6$  listed in Figure 6, *ab initio* calculations indicate that the isomers benzvalene (a) and prismane (b) structures have the lowest energy and the planar hexagon (e) has the highest energy. As a general rule, small  $P_n$ -molecules prefer cage-like structures with as many annulated  $P_5$ -rings as possible and as few as possible  $P_4$ -rings (ring stability for phosphorus:  $P_5 > P_3$ ,  $P_6 \gg P_4$ ). Structures with single bonds are always energetically favored over structures with double bonds. Therefore, structures c and d lie energetically between b and e. For the lowest energy  $P_6$  structure, benzvalene- $P_6$ , the energy of  $2P_6$  is only 30–35 kcal mol<sup>-1</sup> above  $3P_4$  and 60–100 kcal mol<sup>-1</sup> below  $6P_2$ .<sup>81</sup> Due to the presence of the double bond in a, this molecule appears to be rather labile toward dimerization. However, the existence of the species a was detected as a short-lived species in the gas phase using the polyphosphane derivative  $Cp^*_2P_6$ <sup>82</sup> by means of EI and neutralization-reionization (NR)<sup>83</sup> mass spectrometry.



As shown in eqn [12], electron ionization (EI) of  $Cp^*_2P_6$  ( $Cp^*$  = pentamethylcyclopentadienyl) affords a molecular ion  $Cp^*P_6^+$  and  $Cp^{*+}$ . The NR spectra of  $Cp^*P_6^+$  (He, Xe) are dominated by  $P_n^+$  fragments ( $n=1-6$ ). Hydrocarbon fragments due to the  $Cp^*$  ligand are almost absent which implies that only minor amounts of neutral  $C_mH_n$  fragments are formed in the experiment. Collision-induced dissociation experiments with two different gases (He, Xe) provided firm evidence for the existence of neutral  $P_6$  in the gas phase with minimal lifetime on the order of microseconds. The *ab initio* calculations indicate that the benzvalene structure is retained in the cation  $Cp^*P_6^+$ ,<sup>84</sup> suggesting that the neutral  $P_6$  species adopts a similar structure.<sup>85</sup> Calculated structures for even  $P_n$ -cage compounds

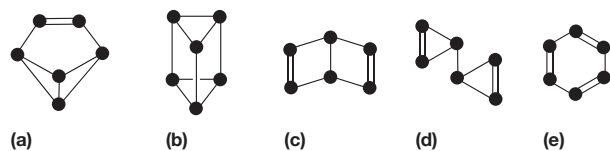


Figure 6 Structural isomers of  $P_6$ .

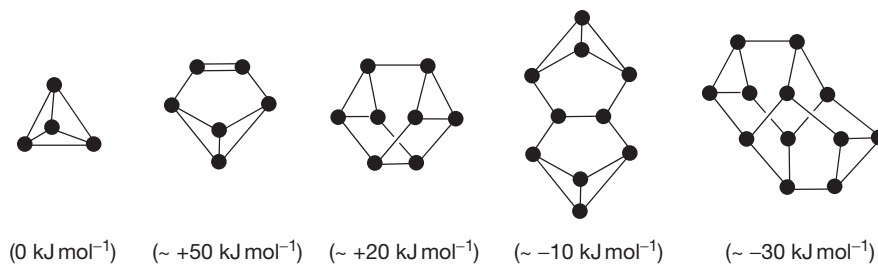


Figure 7 Calculated structures and energies for  $P_n$ -cage compounds ( $n$  = even).

shown in Figure 7 ( $n=2, 4, 6, 8, 10, 12$ ) indicate that the  $P_8$ -cuneane allotrope maybe an accessible synthetic target.<sup>86</sup>

#### 1.04.4 Anionic Compounds

Almost every element of the periodic table can be directly reacted with elemental phosphorus under solid-state conditions to gain a plethora of phosphides and the extraordinary structural and chemical variability of phosphorus defines the huge field of phosphide and polyphosphide solid-state chemistry.<sup>6</sup> Some phosphides adopt the structural arrangements of phosphorus modifications (e.g.,  $(CuI)_3P_{12}$ ,  $(CuI)_8P_{12}$ , and  $(CuI)_2P_{14}$ ) due to the fact that the three-coordinate neutral phosphorus atom acts like a fragment of surface structures. Discussion of the solid-state chemistry of polymeric and extended polycyclic structures of phosphides as well as heteroatomic intermetalloid phosphorus clusters<sup>87</sup> is beyond the scope of this chapter since the primary structural feature of phosphides are homoatomic-bonded P atoms that offer a range of complexity.<sup>6</sup> In contrast

to homoatomic cages composed of group 14 elements, phosphorus cages are limited to molecular  $P_4$ , polyphosphides, and very few cationic species.<sup>56,87</sup>

The term 'phosphide' is used here when the phosphorus atoms are considered to be the most electronegative atoms in a compound  $MP_x$ , representing the anionic part with the mean oxidation state  $q(P_x) = -q(M)$ . In a more general sense, phosphides are ordered from normal phosphides with only heteroatomic bonds ( $3x = q(M)$ ), polyphosphides ( $3x > q(M)$ ), from metal-rich ( $3x < q(M)$ ) to phosphorus-rich as well as from main-group binary compounds to binary and ternary polyphosphides. The value for  $q(P_x)$  is derived either from  $q(M)$  or from structural details. Independent from the real effective charges, the formal oxidation states ( $P(-III)$ ,  $P(-II)$ ,  $P(-I)$ ,  $P(0)$ ,  $P(+1)$ , etc.) are assigned from the homoatomic P–P bond numbers and can be directly derived from the Zintl–Klemm<sup>88</sup> concept and the Mooser–Pearson<sup>89</sup> extended (8- $N$ ) rule. (Count the number of P–P bonds,  $\Sigma_b$ , to calculate  $q(P_x) = -x(3 - 2\Sigma_b/N)$  or, calculate  $\Sigma_b$  from  $q(M)$  according to  $\Sigma_b = N/2(3 - q(M)/x)$ .) The latter applies in contrast to the classical 2c–2e bonds according to the Zintl–Klemm concept to

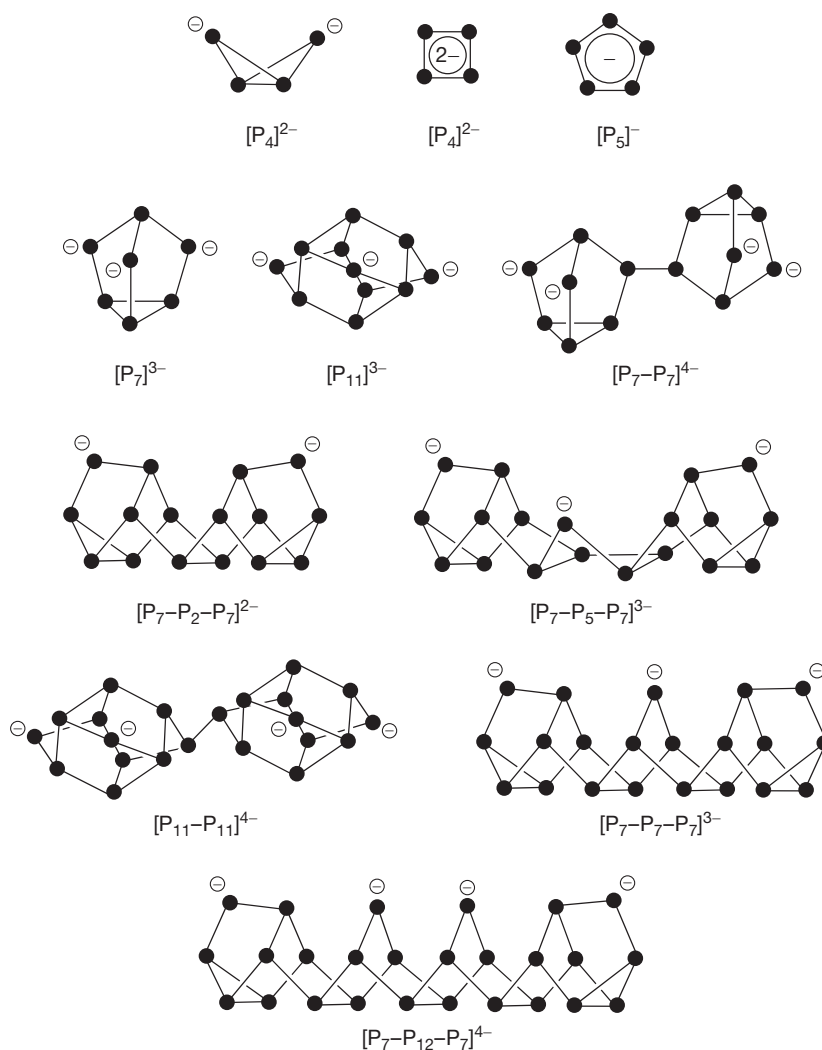
all varieties of bonds (multiple bonds, partial bonds, multi-center systems, radicals, and free electrons). Thus, for compounds of the type  $A_mB_n$ , the electron transfer  $A \rightarrow A^{p+}$ ,  $B \rightarrow B^{q-}$  ( $|mp| = |nq|$ ) to the more electronegative element B results in the formation of pseudoelements  $A^*$ ,  $B$  that show the structural principles of the corresponding isoelectronic elements with the whole spread of homoatomic bond types.<sup>6</sup>

There are many possibilities for the variation of polyanionic structures; however, these remarkable stoichiometric variations can be rationalized by only a few simple structural subunits that are mostly parts of the known modifications of phosphorus.<sup>90</sup> Many of the structures can be considered to be assembled from four- to six-membered rings as well as the well-known building units of the  $P_8$  realgar or the norbornane analogs. Figure 8 summarizes the established polyphosphide anions for which examples retain the same structural features in the solid state and in solution such as liquid ammonia or amines.

Solutions of alkali metals in  $NH_3$  (l) are strong reducing media and have been extensively used for the preparation of a variety of metal-supported phosphides and polyphosphide

anions.<sup>4-6</sup> Solvated alkali and alkaline-earth metal polyphosphides are typically obtained from reactions in  $NH_3$  or ethylenediamine (en) using either compounds containing polyanions or  $P_4$  in combination with compounds having isolated phosphorus anions. Extended frameworks such as  $[P_{19}]^{3-}$  ( $= [P_7-P_5-P_7]^{3-}$ ),  $[P_{21}]^{3-}$  ( $= [P_7-P_7-P_7]^{3-}$ ),  $[P_{22}]^{4-}$  ( $[P_{11}-P_{11}]$ ), or  $[P_{26}]^{4-}$  ( $[P_7-P_{12}-P_7]^{4-}$ ) are formed in solution using metal-organic reactions.<sup>6,91</sup> Structural differences are often imposed by the presence of solvent molecules in the solid state, as evident for solvent-free  $Li_3P_7$  and solvated  $(Li(\text{tmeda}))_3P_7$  (tmeda =  $N,N,N',N'$ -tetra-methylethylenediamine).<sup>92,93</sup>

Polyphosphides have very good donor qualities which results very often in the formation of insoluble derivatives. However, with the help of crown ether, cryptands, or large cations, a comparison of the crystal structures of solvent-free and solvated compounds can be achieved *via* the separation of cation and polyanions. Unfortunately, systematic studies of the reactivity of those polyphosphides are limited; nevertheless, it has been shown that certain polyphosphides can be transformed to molecules and other derivatives as a result of chemical reactions. For example, derivatives of  $M_3P_7$  react under

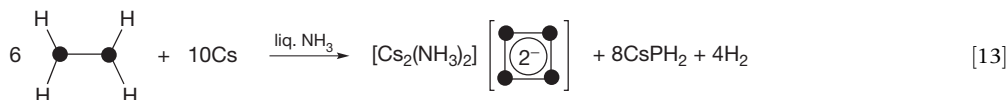


**Figure 8** Examples of polyphosphide anions which retain the same structural features in the solid state as in solution.

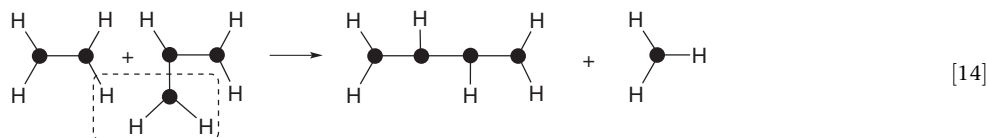


heterogeneous as well as homogeneous conditions. Metathesis reactions give access to a series of new compounds such as  $P_7(MR_3)$  ( $R = \text{alkyl, aryl; } M = \text{Si, Ge, Sn, Pb}$ ).<sup>94</sup> Polyanions are also converted into alkylated polyphosphanes, e.g.,  $[P_7]^{3-}$  into  $R_3P_7$  ( $R = \text{alkyl, SiMe}_3$ ) of which the  $\text{Me}_3\text{Si}$ -derivative can also be prepared from Na/K alloy and white phosphorus in monoglyme with  $\text{Me}_3\text{SiCl}$ .<sup>4,5</sup>

The reaction of white or red phosphorus with alkali metals or alkali or alkaline-earth metal phosphides in liquid ammonia has been extensively studied and examples of isolated compounds are presented in Table 7. The ammonia solvated alkali metal phosphides  $\text{Cs}_2\text{P}_4(\text{NH}_3)_2$ <sup>111</sup> and  $\text{Cs}_3\text{P}_{11}(\text{NH}_3)_3$ <sup>112</sup> are obtained in the reaction of diphosphane and cesium in liquid ammonia, as shown in eqn [13]. The solvated compound  $\text{Cs}_2\text{P}_4(\text{NH}_3)_4$  contains the square-planar, four-membered ring ( $[P_4]^{2-}$ ) which was confirmed by x-ray diffraction ( $d(\text{P}-\text{P}) = 214.7 \text{ pm}$ ) and  $^{31}\text{P}$  NMR spectroscopy. Computational studies indicate an aromatic  $6\pi$   $[P_4]^{2-}$  anion.<sup>105</sup>



Reduction of red phosphorus with Ba in liquid ammonia yields  $\text{Ba}_3\text{P}_{14} \cdot 18\text{NH}_3$  where  $[P_7]^{3-}$  units are joined *via* P–Ba contacts to  ${}^\infty [\text{Ba}(\text{P}_7)_2]^{2-}$  that are separated by the  $[\text{Ba}(\text{NH}_3)_8]^{2+}$  solvate.<sup>102</sup> A series of solvated  $[P_7]^-$  ions were isolated and structurally characterized as  $\text{Rb}_3\text{P}_7(\text{NH}_3)_7$ ,  $[\text{K}(\text{[18]crown-6})]_3\text{K}_3[\text{P}_7]_2(\text{NH}_3)_{10}$ , and  $[\text{Rb}(\text{[18]crown-6})]_3[\text{P}_7](\text{NH}_3)_6$ .<sup>97</sup> Ion exchange was achieved using a resin loaded with an appropriate cation, through which complete ion exchange was observed for  $\text{Cs}_3\text{P}_{11}$  to from  $[\text{Li}(\text{NH}_3)_4]_3\text{P}_{11}(\text{NH}_3)_5$ .<sup>106</sup> This approach is nicely adjusted to exchange some of the alkali metal ions by much larger substituted ammonia cations as shown by the recently reported examples of  $(\text{NEtMe}_3)\text{Cs}_2\text{P}_7(\text{NH}_3)_2$ ,  $(\text{NEt}_3\text{Me})\text{Cs}_2\text{P}_7 \cdot \text{NH}_3$ ,  $(\text{NEt}_4)\text{Cs}_2\text{P}_7 \cdot (\text{NH}_3)_4$ ,<sup>101</sup>  $(\text{NMe}_4)_2\text{RbP}_7(\text{NH}_3)_3$ ,<sup>99</sup>  $(\text{NEt}_4)\text{Cs}_2\text{P}_{11}$ ,<sup>99</sup> or  $[\text{NMeEt}_3]_3\text{CsP}_{11} \cdot (\text{NH}_3)_5$ .<sup>107</sup>



Hydrogen polyphosphides are rarely described in the literature and can be considered as intermediates in protonation/deprotonation reactions of polyphosphides or polyphosphanes. The first contributions to this field were obtained from the reaction of diphosphane ( $\text{P}_2\text{H}_4$ ) in liquid ammonia and amines as a new route to polyphosphides. Diphosphane reacts with liquid ammonia in the temperature range  $-76$  to  $-40$  °C to yield a mixture of the ammonium polyphosphides  $[\text{NH}_4]_2[\text{H}_2\text{P}_{14}]$ ,  $[\text{NH}_4]_2[\text{P}_{16}]$ ,  $[\text{NH}_4]_3[\text{P}_{19}]$ , and  $[\text{NH}_4]_3[\text{H}_2\text{P}_{21}]$  and  $\text{PH}_3$ . The formation of these hydrogen polyphosphides can be rationalized in terms of thermodynamic aspects. In contrast to  $\text{PH}_3$ , all polyphosphanes are endothermic compounds in which the decomposition toward the elements is kinetically inhibited. Therefore,

**Table 7** Selected examples of compounds with anionic phosphorus polyhedra

$[P_4]^{2-}$	$\text{Cs}_2\text{P}_4(\text{NH}_3)_2$ , <sup>111</sup> $[\text{K}(\text{[18]crown-6})]_2\text{P}_4(\text{NH}_3)_2$ <sup>105</sup>
$[P_7]^{3-}$	$\text{Rb}_3\text{P}_7(\text{NH}_3)_7$ , <sup>97</sup> $\text{Cs}_3\text{P}_7(\text{NH}_3)_3$ , <sup>98</sup> $[\text{K}(\text{[18]crown-6})]_3\text{K}_3[\text{P}_7]_2(\text{NH}_3)_{10}$ , <sup>97</sup> $[\text{Rb}(\text{[18]crown-6})]_3[\text{P}_7](\text{NH}_3)_6$ , <sup>97</sup> $[\text{NMe}_4]_2\text{RbP}_7(\text{NH}_3)_3$ , <sup>99</sup> $[\text{NMe}_3\text{Et}]\text{Cs}_2\text{P}_7(\text{NH}_3)_2$ , <sup>100</sup> $[\text{NMeEt}_3]\text{Cs}_2\text{P}_7(\text{NH}_3)_2$ , <sup>101</sup> $[\text{NEt}_4]\text{Cs}_2\text{P}_7(\text{NH}_3)_4$ , <sup>101</sup> $\text{Ba}_3(\text{P}_7)_2(\text{NH}_3)_{18}$ <sup>102</sup>
$[P_{11}]^{3-}$	$\text{Cs}_3\text{P}_{11}(\text{NH}_3)_3$ , <sup>112</sup> $\text{BaCsP}_{11}(\text{NH}_3)_{11}$ , <sup>104</sup> $[\text{Li}(\text{NH}_3)_4]_3\text{P}_{11}(\text{NH}_3)_5$ , <sup>106</sup> $[\text{NMeEt}_3]_3\text{CsP}_{11}(\text{NH}_3)_5$ , <sup>107</sup> $[\text{NEt}_4]\text{Cs}_2\text{P}_{11}$ , <sup>99</sup> $[\text{NEtMe}_3]_3\text{P}_{11}$ , <sup>107</sup> $[\text{K}(\text{[18]crown-6})]_3\text{P}_{11}(\text{en})_2$ <sup>108</sup>
$[P_{14}]^{4-}$	$[\text{Li}(\text{NH}_3)_4]_4\text{P}_{14}(\text{NH}_3)_3$ , <sup>109</sup> $\text{Na}_4\text{P}_{14}(\text{dme})_{7.5}$ , <sup>110</sup> $\text{Na}_4\text{P}_{14}(\text{en})_6$ <sup>110</sup>
$[P_{19}]^{3-}$	$\text{M}_3\text{P}_{19}(\text{solvent})_x$ ( $M = \text{Li, Na, K}$ ) (Anion $[P_{19}]^{3-}$ has been characterized by $^{31}\text{P}$ NMR spectroscopy in solution, <sup>5</sup> and a binary system has yet to be observed.)
$[P_{21}]^{3-}$	$[\text{Li}(\text{[12]crown-4})]_3\text{P}_{21}(\text{thf})_2$ <sup>95</sup>
$[P_{22}]^{4-}$	$[\text{NEtMe}_3]_4\text{P}_{22}(\text{NH}_3)_2$ <sup>103</sup>
$[P_{26}]^{4-}$	$\text{Li}_4\text{P}_{26}(\text{thf})_{16}$ <sup>96</sup>

disproportionation reactions of polyphosphanes, e.g.,  $\text{P}_n\text{H}_{n+2}$  and  $\text{P}_m\text{H}_{m+2}$  (saturated acyclic phosphanes) to  $\text{PH}_3$  and the condensation product  $\text{P}_{n+m-1}\text{H}_{n+m+1}$  is the main decomposition pathway for this class of compounds. The elimination of  $\text{PH}_3$  results in the formation of  $\sigma$ -bonds. In contrast the corresponding nitrogen hydrides,  $\text{N}_n\text{H}_{n+2}$  release ammonia to form acyclic structures with double bonds, whereas polyphosphanes and the corresponding derivatives prefer cyclic structures without double bonds.<sup>4,5,86</sup> Thus,  $\text{P}_2\text{H}_4$  can be used for the formation of phosphorus-rich and hydrogen-depleted acyclic and cyclic polyphosphanes that are formed *via* consecutive intramolecular and intermolecular condensation reactions, as demonstrated in eqn [14].

A series of monocyclic ( $\text{P}_x\text{H}_x$ ), bicyclic ( $\text{P}_x\text{H}_{x-2}$ ), and tricyclic ( $\text{P}_x\text{H}_{x-4}$ ) polyphosphanes as well as isolated and branched polyphosphorus cages ( $\text{P}_x\text{H}_{x+y}$ ;  $y = -6, -8, -10, \dots$ ) are accessible in a similar fashion. Ultimately, this reaction sequence leads to the formation of monophosphane  $\text{PH}_3$  and phosphorus  $\text{P}_x$ . However, intercepting these species by the addition of a base such as ammonia offers synthetic access to polyphosphides and hydrogen polyphosphides (Figure 9). Important to note is that the stability of cyclophosphanes  $\text{P}_x\text{H}_x$  follows the trend cyclopentaphosphane ( $x=5$ ) > cyclotriphosphane ( $x=3$ ) > cyclohexaphosphane ( $x=6$ )  $\gg$  cyclotetraphosphane ( $x=4$ ) > cyclophosphanes ( $x > 7$ ). Therefore, the constitution of polyphosphanes with more than six phosphorus atoms involves side-chain-substituted arrangements rather than the formation

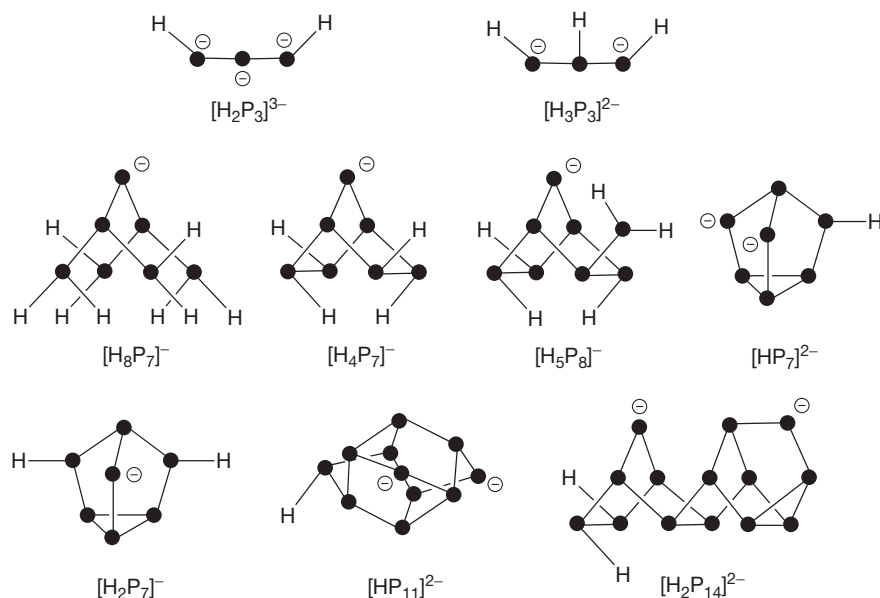


Figure 9 Examples of hydrogen polyphosphide anions.

of  $x$ -membered rings. The same accounts for polycyclic phosphanes in which the constitution of the system is the result of the maximum number of cyclopentaphosphane rings. In addition, cyclotri- and cyclohexaphosphane rings are observed in the constitutional framework but not cyclotetra- and cycloheptaphosphane rings. In agreement with this  $^{31}\text{P}$  NMR spectroscopic investigations detected the bicyclo  $[\text{H}_4\text{P}_7]^-$  anion as the first, very reactive intermediate in the reaction of  $\text{P}_2\text{H}_4$  in ammonia. This anion reacts further with additional  $\text{P}_2\text{H}_4$  to form the more phosphorus-rich polycyclic phosphides.

Interestingly, the reaction of  $\text{P}_2\text{H}_4$  in ammonia in the presence of tetrahydrofuran gives the hydrogen phosphides  $[\text{NH}_4][\text{H}_4\text{P}_7]$  and  $[\text{NH}_4][\text{H}_5\text{P}_8]$  and  $\text{PH}_3$ , and the open-chain heptaphosphide  $[\text{NH}_4][\text{H}_8\text{P}_7]$  has been identified as their precursor.<sup>113</sup> The isolation and characterization of such species are often hampered by their instability toward temperature and pH changes. Several hydrogen polyphosphides were identified by solution NMR methods; however, direct synthetic routes to stable, crystalline hydrogen polyphosphides were implemented only very recently. Nowadays, hydrogen polyphosphides can be obtained from dissolution of corresponding alkali metal polyphosphides in liquid ammonia *via* controlled protonation in the presence of very bulky cations. The same approach was used for the preparation of the protonated species  $[\text{H}_2\text{P}_7]^-$ ,<sup>114</sup>  $[\text{HP}_7]^{2-}$ ,<sup>115,116</sup>  $[\text{H}_2\text{P}_7]^-$ ,<sup>114</sup>  $[\text{HP}_{11}]^{2-}$ ,<sup>103,106,107,117</sup> or  $[\text{Na}(\text{NH}_3)_3(\text{P}_3\text{H}_3)]^-$ <sup>118</sup> as ammoniates. Polyphosphides and polyphosphanes normally dissolve incongruently in liquid ammonia,<sup>95,97,119</sup> reactions; however, they were found to yield good results only when the starting materials dissolve congruently in liquid ammonia. Therefore, a new family of hydrogen phosphides such as  $[\text{H}_3\text{P}_3]^{2-}$  and  $[\text{H}_2\text{P}_3]^{3-}$  were used as starting materials in synthesis.

Derivatives of the  $[\text{H}_3\text{P}_3]^{2-}$  anion have been observed in compounds  $[\text{Rb}(18\text{-crown-6})]_2[\text{H}_3\text{P}_3] \cdot 7\frac{1}{2}\text{NH}_3$  and  $[\text{Cs}(18\text{-crown-6})]_2[\text{H}_3\text{P}_3] \cdot 7\text{NH}_3$  which were synthesized by incongruous solvation of diphosphane, or cyclohexaphosphide

$[\text{P}_6]^{4-}$ .<sup>180</sup> Derivatives of the  $[\text{H}_2\text{P}_3]^{3-}$  anion were obtained as  $\text{K}_3[\text{H}_2\text{P}_3] \cdot 2.3\text{NH}_3$  and  $\text{Rb}_3[\text{H}_2\text{P}_3] \cdot \text{NH}_3$  and are the result of the direct reaction of white phosphorus and incongruous solvation of a cyclohexaphosphide  $[\text{P}_6]^{4-}$  in liquid ammonia.<sup>118</sup> Organo-substituted derivatives of this novel class of compounds have already been introduced; however, only a few examples have been described and all of them have shown that the cyclic and catenated oligophosphanide and oligophosphenide anions can exhibit a rich coordination chemistry due to the presence of free electron pairs.<sup>8</sup> This might be best explained by the fact that selective and facile synthetic methods were mostly unknown for the corresponding oligophosphanide anions.

Interest in the solution chemistry of anionic polyphosphorus ligands stems from their potential use as precursors for the development of rational syntheses of binary metal phosphides  $[\text{M}_x\text{P}_y]$ , which are compounds with rare structures and interesting properties for material science (*vide supra*). The number of accessible complexes with acyclic and cyclic polyphosphanides and unsaturated polyphosphenide anions are rare. Unsaturated phosphenides such as  $[\text{R}_2\text{P}_3]^-$  and  $[\text{R}_2\text{P}_4]^{2-}$  with sterically overloaded substituents R are readily formed either from the nucleophilic degradation of  $\text{P}_4$  with appropriate substrates (*vide supra*) or *via* deprotonation of a corresponding polyphosphane since in some cases the negatively charged polyphosphides obtained may be better stabilized by a  $\pi$  system in a phosphorus chain. Thus, compounds such as  $\text{Mes}^* \cdot 2\text{P}_3\text{Li}$  ( $\text{Mes}^* = 2,4,6\text{-tri-}t\text{-butylphenyl}$ ) are accessible,<sup>122</sup> and derivatives with the 1,3-bis(bis(trimethylsilyl)-methylene) triphosphene-2-ide  $[(\text{Me}_3\text{Si})_2\text{C}=\text{PPP}=\text{C}(\text{SiMe}_3)_2]^-$ <sup>123</sup> and 1,3-di-*tert*-butyltriphosph-2-en-1-ide  $[\text{tBuPPP}^t\text{Bu}]^-$ <sup>124</sup> anions also contain a  $\text{P}_3$  skeleton (Figure 10). A Tl(I) coordination complex containing a tetraphosphene dianion  $[(\text{Ar}^{\text{Dipp}})_2\text{P}_4]^{2-}$  ( $\text{Ar}^{\text{Dipp}} = \text{C}_6\text{H}_3\text{-2,6-(Dipp)}_2$ ) was recently prepared.<sup>125</sup> The sterically overloaded supersilyl group was successfully used for the isolation of a series of polyphosphane and polyphosphanide clusters.<sup>126</sup> The hypersilyl group ( $\text{R} = \text{Si}(\text{SiMe}_3)_3$ ) behaves as a

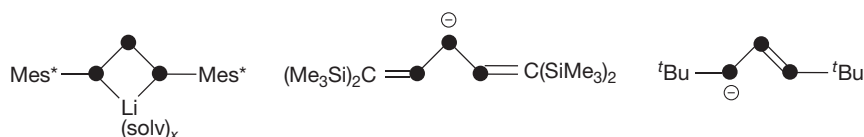
very bulky, electron-releasing substituent and can be used for the stabilization of main-group elements in low oxidation states to realize unusual structural arrangements.

Base-free alkali metal hypersilanides ( $(\text{Me}_3\text{Si})_3\text{SiM}$ ,  $M = \text{Li}$ ,  $\text{Na}$ ,  $\text{K}$ ) react readily with white phosphorus to form alkali metal salts of the bis(hypersilyl)tetraphosph-2-ene-1,4-diide dianion, which are the alkali metal salts of the tetraphosphene  $(\text{Me}_3\text{Si})_3\text{SiPHP}=\text{PPHSi}(\text{SiMe}_3)_3$  (**Scheme 5(a)**). Depending on the reaction conditions, the bis(supersilyl)tetraphosphane ( $^t\text{Bu}_3\text{Si})_2\text{P}_4$ , tris(supersilyl)heptaphosphane ( $^t\text{Bu}_3\text{Si})_3\text{P}_7$ , and tris(supersilyl)nanophosphane  $[(\text{Me}_3\text{C})_3\text{Si}]_3\text{P}_9$  can be isolated. Also unsaturated  $\text{P}=\text{P}$  containing phosphenides  $[(\text{Me}_3\text{C})_3\text{Si}]_2\text{P}_3\text{M}$  and  $[(\text{Me}_3\text{C})_3\text{Si}]_2\text{P}_4\text{M}_2$  as well as polyphosphanides  $[(\text{Me}_3\text{C})_3\text{Si}]_4\text{P}_8\text{M}_4$  and  $[(\text{Me}_3\text{C})_3\text{Si}]_3\text{P}_5\text{M}_2$  were prepared as ether adducts ( $M = \text{Na}$ ,<sup>127</sup>  $\text{K}$ <sup>128</sup>). However, the observation of these species strongly depends on the solvent; thus, in toluene or benzene an equilibrium exists between  $[(\text{Me}_3\text{C})_3\text{Si}]_2\text{P}_4\text{M}_2$  and the dimer  $[(\text{Me}_3\text{C})_3\text{Si}]_4\text{P}_8\text{M}_4$  ( $M = \text{K}$ ). Both compounds can be obtained as solids from benzene solution by fractional crystallization.

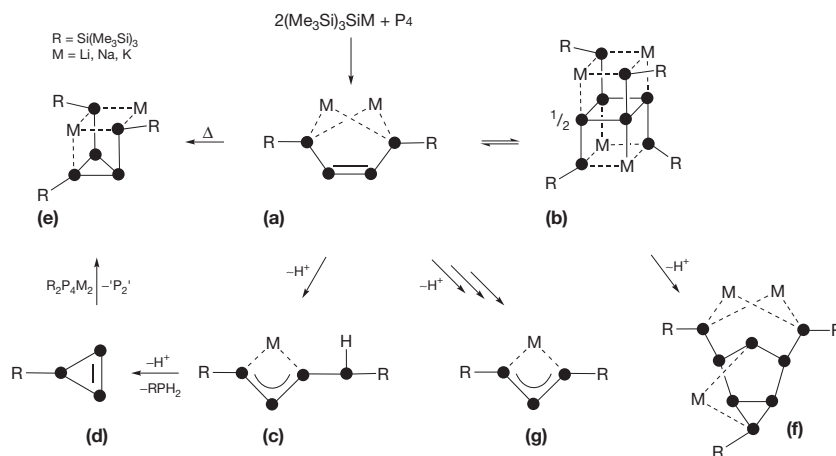
The formation of the octaphosphanide  $[(\text{Me}_3\text{C})_3\text{Si}]_4\text{P}_8\text{M}_4$  ( $M = \text{Na}$ ,  $\text{K}$ ) (**Scheme 5(b)**) might be understood in terms of a  $[2+2]$  cycloadduct of  $[(\text{Me}_3\text{C})_3\text{Si}]_2\text{P}_4\text{M}_2$ . The formation of a four-membered ring of phosphorus atoms is normally not preferred compared to the thermodynamically more favored six-, three-, and five-membered rings and might be rationalized by the influence of the coordinated solvated alkali metal cations. Tetraphosph-2-ene-1,4-diide dianions such as depicted in **Scheme 5(a)** are not stable in solution and slowly decompose *via* the formation of an intermediate (**Scheme 5(c)**) by subsequent protonation and elimination of  $\text{RPH}_2$  to a triphosphirene intermediate (**Scheme 5(d)**) which reacts

with  $[(\text{Me}_3\text{C})_3\text{Si}]_2\text{P}_4\text{M}_2$  (**Scheme 5(a)**) and eliminates  $\text{P}_2'$  to yield the pentaphosphanides  $[(\text{Me}_3\text{C})_3\text{Si}]_3\text{P}_5\text{M}_2$  (**Scheme 5(e)**,  $M = \text{Na}$ ,  $\text{K}$ ). The formation of octaphosphanides such as  $[(\text{Me}_3\text{C})_3\text{Si}]_3\text{P}_8\text{M}_3$  (**Scheme 5(f)**) results very likely from the partial protolysis of the dimer  $[(\text{Me}_3\text{C})_3\text{Si}]_4\text{P}_8\text{M}_4$  (**Scheme 5(b)**).<sup>127,128</sup> The *in situ* formed tetraphosph-2-ene-1,4-diide dianions from the reaction of  $\text{P}_4$  and the hypersilanide anion ( $M = \text{Na}$ ,  $\text{K}$ ) is not the main product, when coordinating solvents such as  $\text{Et}_2\text{O}$  or  $\text{thf}$  are used. From such reactions the blue triphosphenide  $[(\text{Me}_3\text{C})_3\text{Si}]_2\text{P}_3\text{M}$  (**Scheme 5(g)**), which comprises a triphosphallyl anion with a partial  $\text{P}-\text{P}$  double bond, can be isolated. The tetraphosph-2-ene-1,4-diide dianion (**Scheme 5(a)**) can also be conveniently transformed into triphosphenide anion (**Scheme 5(g)**) by the protonation with equimolar amounts of a strong acids ( $\text{CF}_3\text{CO}_2\text{H}$  or  $\text{CF}_3\text{SO}_3\text{H}$ ) in  $\text{thf}$  at  $-78^\circ\text{C}$ . By warming up of the reaction mixtures, a disproportionation reaction takes place to form the monoanion and  $\text{RPH}_2$ .

Reaction of lithium hypersilanide with  $\text{P}_4$  in toluene gives dramatically different products. Several polyphosphanes such as  $[(\text{Me}_3\text{Si})_3\text{Si}]_2\text{P}_4$  are observed and the  $[(\text{Me}_3\text{Si})_3\text{Si}]_2\text{P}_4\text{Li}_2$  represents only a minor product. The presence of hexahydro-1,3,5-trimethyl-*s*-triazine triggers the reaction of lithium hypersilanide with  $\text{P}_4$  to yield  $[(\text{Me}_3\text{Si})_3\text{Si}]_2\text{P}_3\text{Li}$  (**Scheme 5(g)**,  $R = \text{Li}$ ) along with considerable amounts of  $(\text{Me}_3\text{Si})_4\text{Si}$ , suggesting that cleavage of  $\text{Si}-\text{Si}$  bonds took place during the reaction process.<sup>128</sup> In those investigations, supersilyl groups were not only introduced by the reaction of supersilyl anions with white phosphorus but also *via* supersilyl radicals with white phosphorus (*vide supra*), and by the reaction of supersilyl anions with phosphorus trichloride.<sup>127d</sup>



**Figure 10** Examples of triphosphene anions.



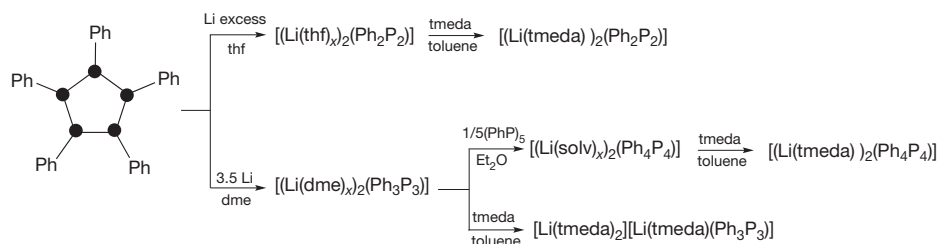
**Scheme 5** Transformations between examples of polyphosphorus anions.

Another class of tetraphosphanides displaying a very interesting coordination chemistry was introduced with the alkali metal salts  $[(\text{Me}_3\text{C})_3\text{Si}]_3\text{P}_4\text{M}_3$  ( $\text{M}=\text{Li}, \text{Na}$ ) and  $[(\text{Me}_3\text{C})_2\text{PhSi}]_3\text{P}_4\text{Na}_3$ .<sup>129</sup>

The syntheses and preparation of main-group element complexes of organosubstituted oligophosphanide ligands are challenging and in many cases the complexes are obtained serendipitously. Very often, the reactions yield inseparable mixtures and only very few protocols have proven successfully for the preparation of main-group element complexes with  $\text{P}_n\text{R}_n$  units ( $\text{R}=\text{alkyl}, \text{aryl}; n=3-6$ ). The formation of Lewis acid–base adducts from cyclophosphanes such as  $\text{Ph}_5\text{P}_5$  and  $\text{BH}_3$  yields compounds such as  $\text{cyclo-1,2-(BH}_3)_2(\text{Ph}_5\text{P}_5)$ .<sup>130</sup> The reaction of cyclophosphanes with complexes of valence electron-rich metals initiate P–P bond cleavage and insertion of the corresponding metal center. Thus, the triphosphane-diide complexes  $\text{cyclo-}[\text{ER}'(\text{tBuP})_3]$  ( $\text{E}=\text{Ga}, \text{R}'=\text{C}(\text{SiMe}_3)_3$ ;  $\text{E}=\text{Al}, \text{R}'=\text{Cp}^*$ ) are obtained from the reaction of  $\text{cyclo-}(\text{tBuP})_3$  and alkyl gallium(I) or cyclopentadienyl aluminum (I) compounds, respectively.<sup>131,132</sup> Another method is the oligomerization of phosphanes or phosphanides mediated by main-group elements to form complexes with oligophosphane-diide ligands. This approach was successfully applied for the syntheses of  $\{[\text{Na}(\text{tmeda})(\text{NHMe}_2)]\{\text{cyclo-Sb}(\text{CyP})_4\}\}_2$  ( $\text{Cy}=\text{cyclohexane}, \text{tmeda}=\text{N,N,N',N'-tetra-methylethylenediamine}$ ) by the 1:1:1 reaction of  $\text{Sb}(\text{NMe}_2)_3$ ,  $\text{CyPH}_2$ , and  $\text{NaPHCy}$  and also for the lithium salt  $[\text{Li}(\text{tmeda})(\text{thf})\{\text{cyclo-As}(\text{tBuP})_3\}]$  by the 1:3 reaction of  $\text{As}(\text{NMe}_2)_3$  and  $\text{Li}[\text{tBuPH}]$ .<sup>133</sup>

The reduction of cyclooligophosphanes with alkali metals is a very efficient route to oligophosphanides anions and allows the preparation of a plethora of metal complexes.<sup>8</sup> The advantage of these entry points is that the chain length of the  $\text{P}_n$  ligands is often retained. Although the formation of compounds of the type  $\text{M}_2(\text{P}_n\text{R}_n)$  ( $n=2-4$ ;  $\text{M}=\text{Li}, \text{K}, \text{Na}$ )<sup>134</sup> was introduced 40 years ago and other compounds such as  $\text{K}[\text{cyclo-}(\text{tBu}_2\text{P}_3)]$ ,<sup>135</sup>  $\text{K}[\text{cyclo-}(\text{Ph}_4\text{P}_5)]$ ,<sup>136</sup> and  $\text{Li}[\text{cyclo-}(\text{tBu}_{n-1}\text{P}_n)]$  ( $n=3-5$ )<sup>137</sup> were also reported, their use as suitable synthetic reagents was hampered since they are only obtained as inseparable mixtures. However, with the help of ethers (thf) or basic, flexible polydentate ligands [e.g., bidentate:  $\text{tmeda}$  ( $\text{N,N,N',N'-tetramethylethylenediamine}$ ); tridentate:  $\text{pmdeta}$  ( $\text{N,N,N,N',N',N'-pentamethyldiethylenetriamine}$ )] a wider variety of alkali metal oligophosphane-diides are accessible. For example, as shown in Scheme 6, lithium oligophosphane-diides  $[\text{Li}(\text{tmeda})_x(\text{Ph}_n\text{P}_n)]$  ( $n=2-4$ ) result from different stoichiometric combinations of the cyclopentaphosphane ( $\text{PhP}_5$ ), lithium sand, and  $\text{tmeda}$  in the appropriate solvent.<sup>138</sup>

Open-chain dianions  $[\text{R}_3\text{P}_3]^{2-}$  and  $[\text{R}_4\text{P}_4]^{2-}$  are known in derivatives such as  $[(\text{Na}(\text{tmeda}))(\text{Na}(\text{tmeda})_2)(\text{Ph}_3\text{P}_3)]$ ,



**Scheme 6** Oligophosphane-diides from  $(\text{PhP})_5$ .

$[(\text{Na}(\text{tmeda}))_2(\text{Ph}_4\text{P}_4)]^{139}$ ,  $[(\text{Na}_2(\text{thf})_5)(\text{Ph}_4\text{P}_4)]$ ,  $[(\text{Na}(\text{thf})_2)_2(\text{Mes}_4\text{P}_4)]$ ,  $[(\text{Na}(\text{thf})_2)_2(\text{tBu}_4\text{P}_4)]$ ,  $[(\text{K}(\text{thf})_3)_2(\text{Mes}_4\text{P}_4)]$  ( $\text{Mes}=2,4,6\text{-Me}_3\text{C}_6\text{H}_2$ ),<sup>140</sup>  $[(\text{K}(\text{pmdeta}))_2(\text{Ph}_4\text{P}_4)]$ , and  $[(\text{K}_2(\text{pmdeta}))(\text{tBu}_4\text{P}_4)]_2$ .<sup>141</sup> As shown in Scheme 7, the salts are synthesized by the appropriate stoichiometric reaction of the corresponding  $\text{R}_2\text{P}_2$  and alkali metals [3:8 for triphosphane-1,4-diide anions and 4:10 for tetraphosphane-diide anions;  $\text{R}=\text{tBu}, \text{Ph}, \text{Mes}$ ;  $\text{M}=\text{Na}, \text{K}$ ]. In the solid state the *catena*-tetraphosphane-1,4-diides  $[\text{R}_4\text{P}_4]^{2-}$  form isolated ion-contact complexes, in which the  $\text{P}_4$  chain has typically a *sym* arrangement and the coordination sphere of the two alkali metal cations is completed by solvent molecules and/or polydentate ligands.<sup>139a,140,141</sup>

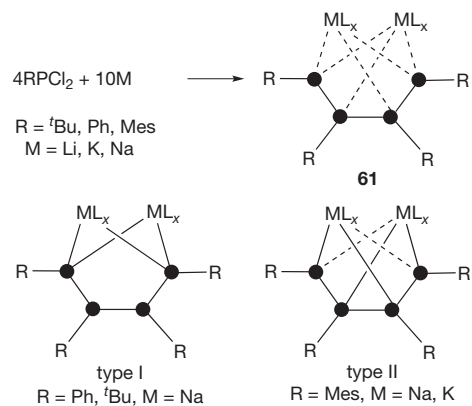
Two coordination types (I and II, Scheme 7) are typically found in these complexes. Alkali metals can coordinate with the phosphorus atoms in 1- and 4-position to form five-membered  $\text{MP}_4$  chelate rings (type I) or in 1- and 3-position to form  $\text{MP}_3$  chelate rings (type II). The phosphorus–sodium distances are in the typical range for related sodium and potassium phosphanides. In the case of  $\text{M}=\text{Na}$  and  $\text{R}=\text{tBu}, \text{Ph}$ , coordination mode type I is exclusively found, whereas for  $\text{M}=\text{K}$  and  $\text{R}=\text{Mes}$ , type II is preferred. The *catena*-tetraphosphane-diides  $[\text{R}_4\text{P}_4]^{2-}$  dianion can be nicely identified with their characteristic AA'BB' spin system in the  $^{31}\text{P}$  NMR spectra. Monoprotonation of tetraphosphane-diide anions with 1 equiv. of  $\text{HCl}$  (dissolved in  $\text{Et}_2\text{O}$ ) yields the tetraphosphane-diide anion  $[\text{R}_4\text{P}_4\text{H}]^-$ .  $^{31}\text{P}$  NMR spectroscopic studies indicate a fluxional behavior of the P–H hydrogen atom allowing for different alternative structures of anion  $[\text{R}_4\text{P}_4\text{H}]^-$  in solution.<sup>142</sup>

The highly reducing nature of the  $[\text{R}_4\text{P}_4]^{2-}$  dianions limits their use as *trans*-metallation reagents with p-block main-group metals such as  $\text{SnCl}_2$ ,  $\text{AlEt}_2\text{Cl}$ ,  $\text{AlCyCl}_2$ ,  $\text{Ga}(\text{dab})_2$ ,  $\text{GaI}$ ,  $\text{InCyBr}_2$ , or  $\text{GaCl}_3$  ( $\text{Cy}=\text{cyclohexyl}, \text{dab}=\text{N,N'-bis}(2,6\text{-diisopropyl})\text{phenyldiazabutadiene}$ ). In most cases, only elemental metal, cyclophosphanes, or unidentified products are obtained.<sup>143</sup> However, the group 13 metal complex  $[\text{K}(\text{tmeda})\{\text{Ga}(\text{Ph}_4\text{P}_4)(\text{dab})\}]$  was obtained from the reaction of  $\text{cyclo-}(\text{PhP})_5$  with  $[\text{K}(\text{tmeda})\{\text{Ga}(\text{dab})\}]$ .<sup>144</sup> Variation in the stoichiometry of combinations of dichlorophosphanes, phosphorus trichloride, and alkali metal salts together with the appropriate ligand leads to the formation of metal cyclooligophosphanides and small amounts of cyclooligophosphanes. A product mixture comprising  $\text{M}[\text{cyclo-}(\text{R}_2\text{P}_3)]$ ,  $\text{M}[\text{cyclo-}(\text{R}_3\text{P}_4)]$ ,  $\text{cyclo-}(\text{R}_4\text{P}_4)$ , and  $\text{M}[\text{cyclo-}(\text{R}_4\text{P}_5)]$  is normally obtained.

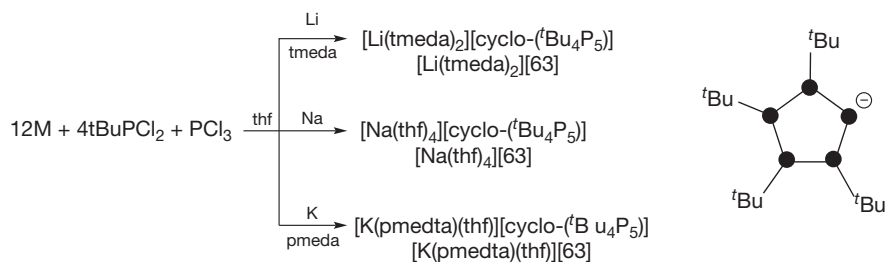
Salts of  $\text{M}[\text{cyclo-}(\text{R}_4\text{P}_5)]$  ( $\text{M}=\text{Li}, \text{Na}, \text{K}$ ;  $\text{R}=\text{tPr}, \text{tBu}, \text{Ph}$ ) are soluble in *n*-pentane to be separated from the other salts, and  $\text{cyclo-}(\text{R}_4\text{P}_4)$  derivatives are readily removed from  $\text{M}[\text{cyclo-}(\text{R}_4\text{P}_5)]$  by sublimation. Further purification of  $\text{M}[\text{cyclo-}(\text{R}_4\text{P}_5)]$

is achieved by crystallization, and a series of alkali metal salts ( $[\text{Li}(\text{tmeda})_2][\text{tBu}_4\text{P}_5]^-$ ,<sup>145</sup>  $[\text{Na}(\text{thf})_4][\text{tBu}_4\text{P}_5]^-$ ,<sup>146</sup> and  $[\text{K}(\text{pmedta})(\text{thf})][\text{tBu}_4\text{P}_5]^-$ <sup>141</sup> have been crystallographically characterized. All are formed from  $\text{tBuPCl}_2$ , as shown in Scheme 8. The anion in the isolated salts typically adopts an envelope conformation in which the *tert*-butyl groups of the  $\text{P}_5$  ring are all-*trans* arranged, the tricoordinate phosphorus atoms are almost coplanar, and the anionic phosphorus atom lies above the plane. The molecular structure of this chiral anion is retained in solution, as shown in the  $^{31}\text{P}\{^1\text{H}\}$  NMR spectrum, which displays the expected ABB'CC' spin system. The derived coupling constant indicates that the inversion barrier for the phosphorus atom in these compounds is high.

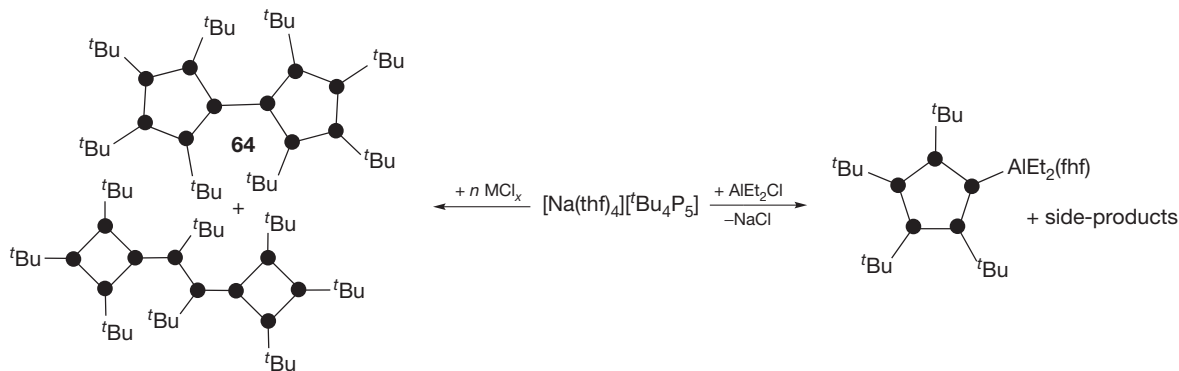
A series of linear and cyclic phosphorus-rich anions are now available and have been studied in reactions with appropriate



Scheme 7 Formation of  $[\text{R}_4\text{P}_4]^{2-}$  salts and coordination types.



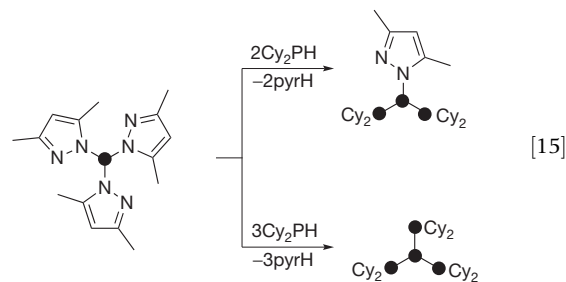
Scheme 8 Formation of  $[\text{tBu}_4\text{P}_5]^-$ .



Scheme 9 Reactions of  $[\text{tBu}_4\text{P}_5]^-$ .

main-group and transition-metal precursors.<sup>8</sup> The highly reductive nature of polyphosphanides complicates their use in *trans*-metallation chemistry using metals in high oxidation states. However, as shown in Scheme 9,  $[\text{tBu}_4\text{P}_5]^-$  reacts with  $\text{SnCl}_2$  (2:1),  $\text{PbCl}_2$  (2:1), or  $\text{BiCl}_3$  (1:1) to give the tethered bicyclic oligophosphanes and with  $\text{AlEt}_2\text{Cl}$  yields an alane derivative together with a mixture of products.<sup>147</sup>

Access to catenated and branched tri- and isotetraphosphane ligands (eqn [15]) results from the reaction of tri(3,5-dimethyl-1-pyrazolyl)phosphane with various amounts of a secondary phosphane.<sup>148</sup> This method is highly efficient and typically gives very high yields. This simple protocol opens the access to other polyphosphanes and allows for the systematic development of a plethora of other tri- and isotetraphosphanes with a highly diverse substitution pattern. This approach of P-P bond formation using pyrazolyl-substituted phosphanes as easily accessible  $\text{P}_1$  units in combination with a series of primary and secondary phosphanes is related to the known phosphanylation reaction of primary and secondary phosphanes utilizing alkylaminophosphanes along with the elimination of a corresponding sec-amine.<sup>149</sup>





## 1.04.5 Cationic Compounds

While the phosphonium cation represents one of the prototypical bonding environments for phosphorus, a variety of cationic environments can be envisaged, but few have been realized. Figure 11 classifies cations (A–M) according to the coordination number (CN)<sup>150</sup> and illustrates the Lewis acceptor potential for phosphorus. Also summarized are generic examples of donor–acceptor complexes that have been structurally characterized for monocations of each type.<sup>7,151–156</sup> Although salts of the tricoordinate phosphonium E are well known,<sup>120</sup> the first complexes were only recently reported.<sup>157,158</sup> Complexes of multiply charged phosphorus cations such as polyonio-substituted ‘Weiss-type’ compounds have been proposed on the basis of spectroscopic and chemical analysis data.<sup>159</sup> An example of bonding environment I (L = tris(1,3-dimethylpyrazolyl)phosphane) was recently reported.<sup>160</sup> Solid-state structures have been confirmed for only two complexes of bonding environment G [R = Cy<sub>2</sub>N, L = DBN] (1,5-diazabicyclo [4.3.0]-non-5-ene)<sup>154a,b</sup>; R = H, L = Ph<sub>3</sub>P.<sup>161e</sup> There are no structural reports of J, K, L, or M and, only one example of bonding environment H (L = DMAP)<sup>162</sup>

The phosphonium center is analogous to an ammonium center and is conventionally defined as a tetracoordinate phosphorus center bearing a formal positive charge. Examples of compounds containing P–P-bonded phosphonium centers were first identified spectroscopically<sup>163</sup> and have been recently

structurally characterized,<sup>164</sup> representing the prototypical phosphanylphosphonium cation, illustrated in Figure 12(a). Derivatives of phosphanylphosphonium cations are most effectively prepared by the reaction of a chlorophosphane with a halide abstracting agent (eqn [16]), by the reaction of a chlorophosphane, a phosphane, and a halide abstracting agent (eqn [17]) or by reaction of a diphosphane with a proton or a methyl cation (eqn [18]). Crystallographic data for a variety of derivatives<sup>165</sup> show a consistent P–P distance of close to 2.2 Å, which is similar to the P–P bond in diphosphanes. A comprehensive series of acyclic and cyclic catena-polyphosphanylphosphonium cations has been recently reported and offers new synthetic approaches to P–P bond formation.

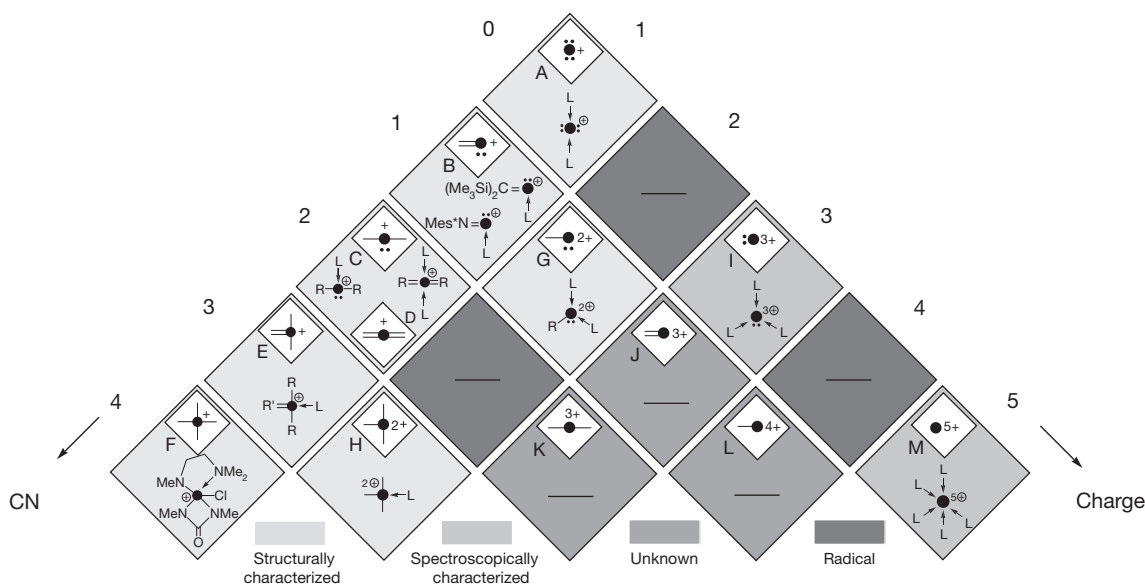
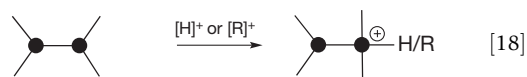
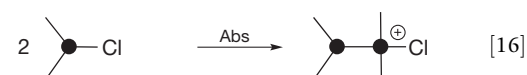


Figure 11 Bonding environments for phosphorus.

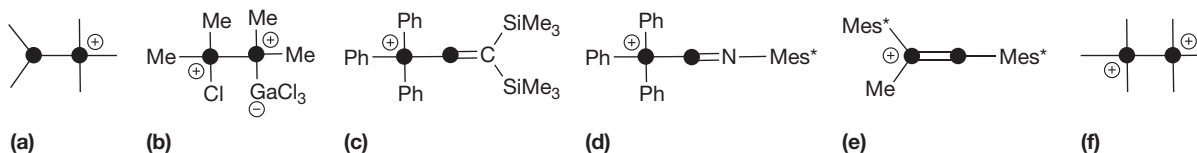


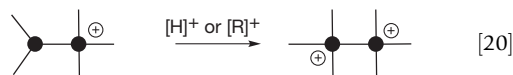
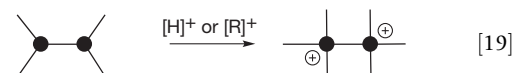
Figure 12 Diphosphorus cations.



All derivatives of phosphanylphosphonium cations (Figure 12(a)) exhibit two well-separated doublets in  $^{31}\text{P}$  NMR spectra with the high-field shift typically corresponding to the tricoordinate phosphorus atom and the low-field shift to the tetracoordinate phosphorus atom, with a  $^1J_{\text{PP}}$  in the range 300–360 Hz. In the solid state phosphanylphosphonium cations contain a slightly distorted tetrahedral environment for the tetracoordinate phosphorus atom and a pyramidal geometry for the tricoordinate phosphorus atom that is typical of a phosphane.

In the presence of excess gallium chloride,  $\text{Me}_2\text{PCL}$  undergoes chloride abstraction with consequential P–P bond formation as well as secondary coordination of the resulting tricoordinate phosphorus atom with the Lewis acid to give Figure 12(b) as a tetrachlorogallate salt.<sup>164a,166</sup> The unusual P–P–Ga bonding framework is described as an ‘in-series’ coordination complex indicating that the phosphane donates to the acceptor phosphonium moiety, which in turn donates to the gallium center. Nevertheless, the framework imposes two neighboring tetracoordinate phosphonium atoms that carry a formal positive charge, but this has minimal impact on the P–P distance, the chemical shifts of the phosphorus atoms or the  $^1J_{\text{PP}}$  coupling constant, relative to the phosphanylphosphonium cations (Figure 12(a)) indicating fast exchange in solution. Salts of a formal coordination complex of a phosphane on a methylenephosphorus cation of bonding type B are formed in the reaction of  $\text{ClP}=\text{C}(\text{SiMe}_3)_2$  with  $\text{PPh}_3$  in the presence of a halide abstracting agent, as shown in Figure 12(c),<sup>152</sup> and the cation retains the phosphalkene motif, while the P–P distance is very similar to those in the phosphanylphosphonium cations. The imine derivative (Figure 12(d)), is formed in an analogous reaction, and the acceptor capabilities of the iminophosphonium cation have been demonstrated by the development of a series of complexes accommodating a variety of ligands.<sup>153</sup>

The second period p-block elements ( $n=2$ ) are distinct from the heavier elements in that homoatomic  $\pi$ -bonds are thermodynamically more stable than homoatomic  $\sigma$ -bonds. Nevertheless, compounds containing double or triple bonds between p-block elements with  $n>2$  can be prepared and isolated if they contain sterically bulky substituents or other special features.<sup>167</sup> Compounds containing  $\text{P}=\text{P}$  double bonds, diphosphenes, were first isolated in 1981<sup>168</sup> and many derivatives have since been prepared by a variety of methods. The prototypical diphosphene,  $\text{Mes}^*\text{P}=\text{PMes}^*$ <sup>168</sup> is methylated in the environment of a 35-fold excess of  $\text{MeOTf}$  to give the unusual diphosphen-1-ium cation (Figure 12(e)) as a triflate salt.<sup>169</sup> The two phosphorus atoms in the diphosphen-1-ium cation are predictably distinct and show in solution two doublets (237 ppm, 332 ppm) in the  $^{31}\text{P}$  NMR spectrum with a  $^1J_{\text{PP}}$  coupling constant (633 Hz) that is very large relative to those observed for phosphanylphosphonium cations (300–360 Hz). Moreover, the solid-state structure reveals a relatively short P–P distance [2.024(2) Å] and a distorted trigonal planar environment [C–P–C: 111.7(3)°, C–P–P: 123.1(2)°, 125.2(2)°] for the tricoordinate phosphorus center consistent with the ion being a representative of a phosphorus analog of an alkene. Computational studies indicate that the  $\text{P}=\text{P}$  bond is strengthened as a result of protonation, and vibrational spectroscopic studies show a  $\text{P}=\text{P}$  stretch at  $636\text{ cm}^{-1}$ , which compares with  $610\text{ cm}^{-1}$  in  $\text{Mes}^*\text{P}=\text{PMes}^*$ .



Compounds containing a dicationic charge borne by two P–P bonded phosphonium atoms, represented by Figure 12(f), are phosphorus analogs of the C–C bond in ethane. Examples were first extensively studied by  $^{31}\text{P}$  NMR spectroscopy,<sup>170</sup> and the structural motif of adjacent tetracoordinate phosphorus atoms has been confirmed for a number of derivatives by x-ray crystallography. Most derivatives have been prepared by alkylation of diphosphanes (eqn [19]) or phosphanylphosphonium cations (eqn [20]),<sup>171</sup> and the diethylamino-derivative was prepared by the electrochemical oxidation of  $(\text{Et}_2\text{N})_3\text{P}$ .<sup>172</sup> Despite the double cationic charge in these diphosphane-1,2-dium cations, the P–P distance ranges from 2.16 Å in  $[\text{P}_2\{(\text{CH}_2)_4\}_3][\text{SO}_3\text{CF}_3]_2$  to 2.36 Å in  $[(\text{Et}_2\text{N})_3\text{PP}(\text{NEt}_2)_3][\text{ClO}_4]_2$ , which is surprisingly similar to the P–P bonds in the monocationic phosphanylphosphonium salts. Nevertheless, in general, the  $^1J_{\text{PP}}$  coupling constants in these compounds are substantially smaller than those in phosphanylphosphonium cations.

Monocationic molecules containing three catenated phosphorus centers have been confirmed with a variety of topologies. Triphosphan-2-ium cations (Figure 13(a)) are generally formed in reactions of a phosphonium cation  $[\text{R}_2\text{P}]^+$  with a diphosphane.<sup>173,174</sup> The phosphonium cation is formed *in situ* via halide abstraction from a halophosphane or by dissociation of a phosphanylphosphonium cation. The iodo-derivative,  $\text{P}_3\text{I}_6^+$ , is also observed as a product of the reaction of  $\text{P}_4$ ,  $\text{I}_2$ , and  $\text{Ag}[\text{Al}(\text{OCCF}_3)_4]$ .<sup>173</sup> Interestingly, the  $^{31}\text{P}$  NMR spectra of  $\text{P}_3\text{I}_6^+$  exhibits an  $\text{A}_2\text{B}$  spin system while derivatives of  $\text{P}_3\text{R}_6^+$  and  $\text{P}_3\text{R}_4\text{R}'_2^+$  exhibit  $\text{AB}_2$  spin systems with the observation of the resonance of the tetracoordinate phosphonium atom at lower field. The  $^1J_{\text{PP}}$  values are consistent with those observed for phosphanylphosphonium cations. The unusual square-pyramidal cluster structure of Figure 13(b) was formed in the reaction of  $\text{Cp}^*\text{Zr}(\text{C}^t\text{Bu})_2\text{P}_2$ ,<sup>175</sup> and the heterocyclic derivative Figure 13(c) was obtained from the reaction of the secondary 1,2-bis(phosphanyl)benzene  $\text{C}_6\text{H}_4\text{P}_2(\text{tBu})_2\text{H}_2$  with a phosphonium cation  $[\text{R}_2\text{P}]^+$ , involving the formal removal of dihydrogen.<sup>164c</sup> The symmetric frameworks of Figure 13(a)–13(c) exhibit P–P distances consistent with those of phosphanylphosphonium cations. The unusual triphosph-1-en-3-ium framework in Figure 13(d) is formed by the deamination reaction of an aminodiphosphene by triflic acid in the presence of  $\text{PPh}_3$ .<sup>176</sup> The structural features are consistent with the drawing in Figure 13(d), in that the designated  $\text{P}=\text{P}$  double bond is 2.025(1) Å and the P–P single bond [2.206(1) Å] is very similar to those in derivatives of cations phosphanylphosphonium. The only three-membered cyclic catena-phosphorus cation in Figure 13(e)<sup>177</sup> is obtained by the methylation of  $^t\text{Bu}_3\text{P}_3$ .<sup>178</sup> While the neutral cyclotriphosphane framework exhibits difference in the three P–P bonds, the differences are exaggerated in the cation with the P–P bonds involving the tetracoordinate phosphorus center significantly shorter than those involving tricoordinate phosphorus centers. Interestingly,

the three  $^{31}\text{P}$  chemical shifts are quite distinct and a  $^{31}\text{P}$  NMR AMX spin system is observed in solution.

The reduction of  $\text{PCl}_3$  with  $\text{SnCl}_2$  in the presence of  $\text{PR}_3$  results in the triphosphorus cation (Figure 13(f)),<sup>151a,b,179</sup> which is an isomer of Figure 13(a) with all substituents at the terminal sites. Structural data for the phenylated derivative of Figure 13(f) reveals an angle of approximately  $102^\circ$  at the central dicoordinate phosphorus atom, implicating a bonding model involving a phosphide interacting with two cationic tetracoordinate phosphorus atoms. Framework Figure 13(f) may also be interpreted as a phosphorus cation [ $\text{P}^+$  or  $\text{P}(\text{I})$ ] complexed by two phosphane ligands. In this context, a variety of cyclic derivatives of the type Figure 13(g) have been obtained in analogous reactions,<sup>151c,d,180</sup> and structurally characterized to show a narrow range of P–P bond distances (approximately 2.1–2.2 Å), in which diphosphane-chelate ligands support the  $\text{P}(\text{I})$  center. Cations f and g have been referred to as triphosph-2-en-1-ium cations, and many more derivatives have been identified by  $^{31}\text{P}$  NMR spectroscopy showing the chemical shifts of the dicoordinate phosphorus atoms to be distinct from the tetracoordinate phosphorus centers by almost 300 ppm, and  $^1J_{\text{PP}}$  values are consistently larger than 400 Hz.

Triphosphane-1,3-diiium ions in Figure 13(h) and 13(i) are formed in reactions of  $\text{R}_3\text{P}$  or diphosphanes with  $\text{RPCl}_2$  and  $\text{AlCl}_3$ , or by alkylation of a triphosph-2-en-1-ium cation, and cyclic derivatives have been extensively studied.<sup>181</sup> Introduction of the increased charge and alkylation at the unique (central) phosphorus atom of the triphosph-2-en-1-ium cations in Figure 13(f) and 13(g) has minimal influence on the

structural features of the PPP moiety, showing only a slight extension of the P–P bond and no significant adjustment in PPP angle. Nevertheless, the  $^{31}\text{P}$  NMR signal assigned to the alkylated central phosphorus atoms exhibits a substantial downfield shift relative to triphosph-2-en-1-ium cations and the  $^1J_{\text{PP}}$  is substantially reduced. The cation in Figure 13(j) is a unique analog of derivatives of Figure 13(i).<sup>182</sup> It is formed by reaction of the corresponding diphosphane with the iminophosphonium cation, and represents an unusual bonding environment for the central phosphorus atom, which can be described as a tricoordinate pyramid with one of the bonds being a multiple bond to nitrogen and the others are to tetracoordinate phosphorus atoms. The compound also represents an example of a diphosphane-chelate complex of the iminophosphonium cation.

A variety of salts containing cations composed of four catenated phosphorus atoms have been reported recently, as illustrated in Figure 14. A number of derivatives of the acyclic tetraphosphorus dicationic framework (a) are formed by reductive coupling of chlorophosphanylphosphonium cations (chlorine substitution at the tricoordinate phosphane atom), and further derivatives are accessible by exchange of the terminal phosphorus centers by more basic phosphanes.<sup>183</sup> Organo-cyclic derivatives (b) are prepared by a similar method.<sup>184</sup> Unique cyclic organo-derivatives (c)<sup>185</sup> and (d)<sup>186</sup> have been formed by alternative methods.

Examples of the framework in Figure 14(a) are demonstrated to have two tricoordinate phosphane atoms between two terminal tetracoordinate phosphorus atoms. In the context of coordination chemistry models described for other

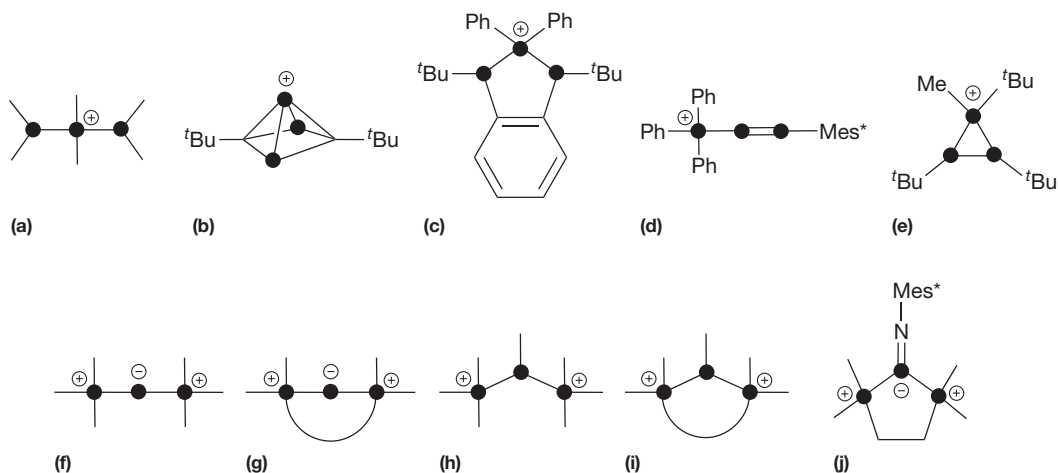


Figure 13 Triphosphorus cations.

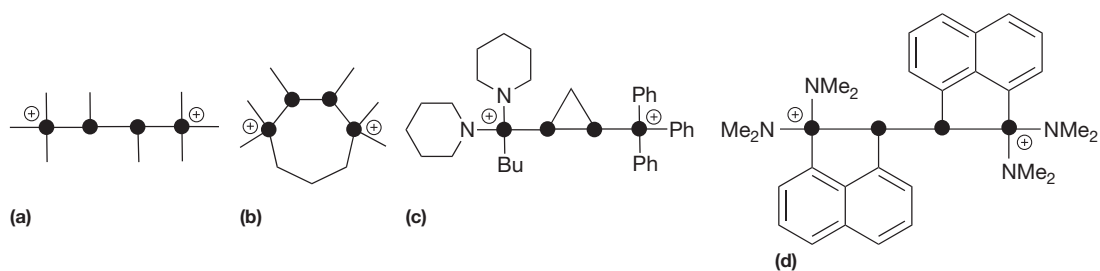


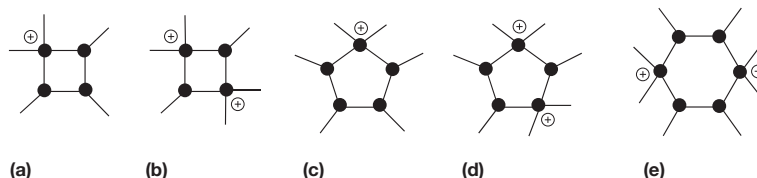
Figure 14 Tetraphosphorus cations.

phosphanylphosphonium cations (*vide supra*), derivatives of (a) represent diphosphane-1,2-dium dications stabilized by two phosphane ligands or a chelating diphosphane.<sup>18</sup> The facile derivatization of (a) by ligand exchange reactions validates this coordination model.

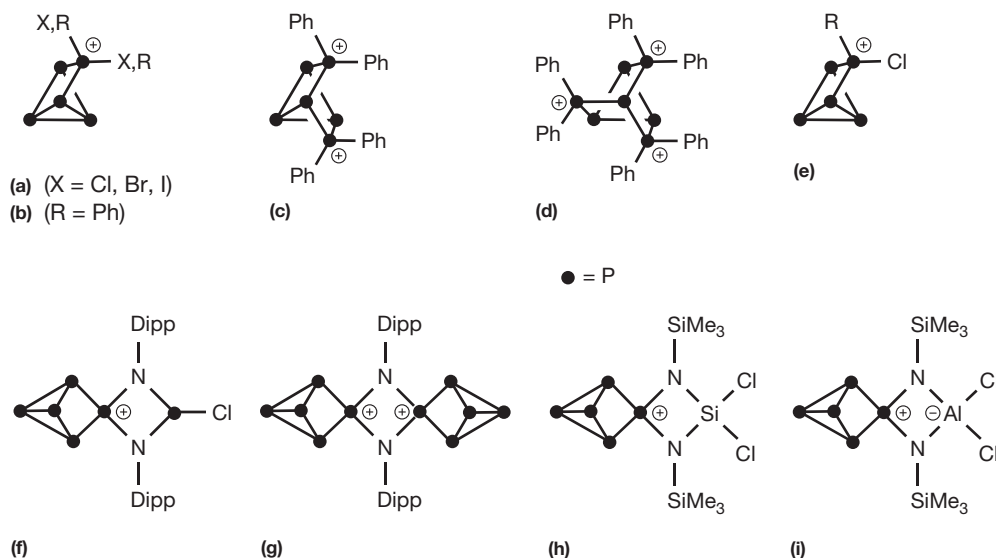
Cyclotetraphosphetan-2-ium cations of type **Figure 15(a)** are formed by methylation<sup>187</sup> and halonium<sup>188</sup> addition to cyclotetraphosphanes, and alkylated derivatives have also been formed by the insertion of a phosphonium cation  $[R_2P]^+$  into the cyclotriphosphane.<sup>177</sup> Derivatives of the tetraphosphetane-2,4-dium dication in **Figure 15(a)** are obtained by the reaction of the corresponding cyclotetraphosphane with an excess of MeOTf<sup>150</sup> or by introducing a source of excess halonium reagent.<sup>188</sup> The first example of **Figure 15(b)** was isolated, however, in very low yield from a metathesis reaction.<sup>161</sup> Pentaphospholan-2-ium cations of type **Figure 15(c)** are likewise formed by methylation or protonation of cyclopentaphosphane, and by phosphonium ion insertion  $[R_2P]^+$  into a cyclotetraphosphane.<sup>174,189</sup> In addition, a complicated redistribution reaction is implied from the reaction of cyclo-(Ph<sub>5</sub>P<sub>5</sub>) with phosphonium cations  $[R_2P]^+$ , which also provides derivatives of **Figure 15(c)**. Pentaphospholane-2,5-dium dications in **Figure 15(d)** are obtained by reaction of derivatives of **Figure 15(c)** with neat MeOTf.<sup>150</sup> Hexaphosphinane-1,4-dium dications such as depicted in **Figure 15(e)** are obtained from stoichiometric combinations of cyclo-(Ph<sub>5</sub>P<sub>5</sub>),

a chlorophosphane and a halide abstracting agent in a melt reaction.<sup>190</sup> Derivatives of **Figure 1(a)** and **15(b)** exhibit first-order <sup>31</sup>P{<sup>1</sup>H} NMR spectra, but the larger frames of **Figure 15(c)–15(e)** involve magnetic nonequivalence that give rise to complex second-order spectra. Interpretation of the experimental spectra for derivatives of **Figure 15(e)** have been simulated as AA'BB'X or ABCDX spin systems implicating a low-energy conformational pseudo-rotation process. Derivatives of **Figure 15(d)** are simulated as ABGMX spin systems and derivatives of **Figure 15(e)** are examples of rare AA'A''A'''XX' spin systems.<sup>174,190</sup>

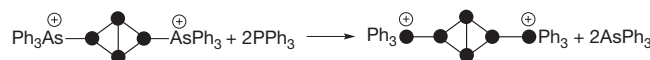
Cationic  $[P_5X_2]^+$ -cages shown in **Figure 16** were reported only recently. Cations of type (a) resulted from the reaction of the silver salt  $Ag[Al\{OC(CF_3)_3\}_4]$  with  $PX_3$  ( $X = Cl, Br, I$ ) in the presence of  $P_4$ .<sup>20,191</sup> Applying a stoichiometric melt approach at elevated temperatures (60–100 °C),<sup>192</sup> it is possible to extend this chemistry by intercepting the more stable diorganophosphonium cation  $[Ph_2P]^+$  with  $P_4$ . This approach resulted in the formation of the cationic cages  $[Ph_2P_5]^+$  (b),  $[Ph_4P_6]^{2+}$  (c), and  $[Ph_6P_7]^{3+}$  (d) *via* the consecutive insertion of up to three  $[Ph_2P]^+$  units into the P–P bonds of the  $P_4$  tetrahedron.<sup>16</sup> Fluorobenzene solutions of  $RP_2Cl_2$  and a Lewis acid such as  $ECl_3$  ( $E = Al, Ga$ ) in a 1:1 ratio can be used as reactive sources of chlorophosphonium cations  $[RP_2Cl]^+$ , which formally insert into P–P bonds of dissolved  $P_4$ . This represents a general, powerful protocol for the synthesis of cationic



**Figure 15** Cyclic polyphosphorus cations.



**Figure 16** Polyphosphorus cationic cages.



[21]

chloro-substituted organophosphorus  $[RP_5Cl]^+$ -cages as illustrated by the isolation of several monocations of type (e). According to quantum calculations, it is most likely that the formation of the cationic  $P_5$  cage compounds proceeds via a two-step reaction mechanism which may be best described as an adduct formation, addition, and subsequent rearrangement.<sup>193</sup> Similarly, the reaction of  $P_4$  with the cyclodiphosphadiazane  $[DippNPCl_2]$  (Dipp = 2,6-disopropyl-phenyl) and  $GaCl_3$  in fluorobenzene yielded cation (f) as tetrachlorogallate salt. The addition of an excess  $GaCl_3$  and a second equivalent  $P_4$  to a solution of (f) afforded the dicationic species (g) and was isolated as a  $[Ga_2Cl_7]^-$  salt.<sup>194</sup> This approach has been extended to the highly functionalized cation (h) and the zwitterionic  $P_5$ -cage (i), which are formed by the insertion of the corresponding phosphonium cations that are derived from four-membered phosphorus–nitrogen–metal heterocycles.<sup>195</sup>

The bistrphenylarsane complex  $[P_4(Ph_3As)_2]^{2+}$  is formed in a high-yielding one-pot synthesis from  $PCl_3$ ,  $AsPh_3$  and  $AlCl_3$ . The structure of this unusual dication reveals a 'butterfly' structure of the bicyclo[1.1.0]-tetraphosphane-1,4-dium core with two triphenylarsane ligands in an *exo,exo* configuration. Theoretical calculations describe a dative As–P bonding interactions and consistent with this model, the reaction of  $[P_4(Ph_3As)_2]^{2+}$  with 2 equiv.  $Ph_3P$  results in quantitative formation of  $[P_4(Ph_3P)_2]^{2+}$  and 2 equiv.  $Ph_3As$  (eqn [21]). The new frameworks provide a versatile source of low-valent polyphosphorus cations, which may have high potential as very valuable synthons in *catena*-phosphorus chemistry.<sup>196</sup>

### 1.04.6 Conclusion

The variety of P–P-bonded frameworks that have been characterized illustrate a diverse chemistry that competes with the established knowledge of C–C-bonded frameworks. Moreover, the systematic development of synthetic methods for P–P bond formation provides opportunities for the discovery of new compounds and ultimately materials exhibiting new properties.

### References

- Dillon, K. B.; Mathey, F.; Nixon, J. F. *Phosphorus: The Carbon Copy: From Organophosphorus to Phospha-organic Chemistry*. Wiley: Chichester, 1998.
- Schnering, H. G. *Angew. Chem. Int. Ed. Engl.* **1981**, *20*, 33–53.
- (a) Greenwood, N. N.; Earnshaw, A. *Chemistry of the Elements*, 2nd ed.; Butterworth Heinemann: Oxford, 1997; (b) Luo, Y. R. *Comprehensive Handbook of Chemical Bond Energies*. CRC Press: Boca Raton, 2007.
- (a) Baudler, M. *Angew. Chem. Int. Ed.* **1982**, *21*, 492–512; (b) Baudler, M. *Angew. Chem. Int. Ed.* **1987**, *26*, 419–441; (c) Baudler, M.; Glinka, K. *Chem. Rev.* **1993**, *93*, 1623–1667; (d) Baudler, M.; Glinka, K. *Chem. Rev.* **1994**, *94*, 1273–1297.
- Baudler, M.; Glinka, K. *Chem. Rev.* **1993**, *93*, 1623–1667.
- (a) Hönle, W.; von Schnering, H. G. *Z. Kristallogr.* **1980**, *153*, 339–350; (b) von Schnering, H. G.; Hönle, W. In King, R. B. *Encyclopedia of Inorganic Chemistry*, King, R. B., Ed.; Wiley: Chichester, 1994 pp 3106–3140; (c) Pöttgen, R.; Hönle, W.; von Schnering, H. G. In King, R. B., Ed.; *Encyclopedia of Inorganic Chemistry*, 2nd ed. Wiley: Chichester, 2005; vol. VIII, pp 4255–4308 and reference therein.
- Dyker, C. A.; Burford, N. *Chem. Asian J.* **2008**, *3*, 28–36.
- Gomez-Ruiz, S.; Hey-Hawkins, E. *Coord. Chem. Rev.* **2011**, *255*, 1360–1386.

- Connelly, N. G.; Damhus, T.; Hartshorn, R. M.; Hutton, A. T., Eds.; In *International Union of Pure and Applied Chemistry, Nomenclature of Inorganic Chemistry, IUPAC Recommendations 2005*; RSC Publishing: Cambridge, 2005.
- Bünzli-Trepp, U., Ed.; In *Fundamental Science, Systematic Nomenclature of Organic, Organometallic and Coordination Chemistry*; EPFL Press: Lausanne, CH, 2007.
- Fluck, E. O.; Laitinen, R. S. *Pure Appl. Chem.* **1997**, *69*, 1659–1692.
- (a) The procedure recommended by the IUPAC does not always coincide with the index names of organic, organometallic, or coordination compounds used by CA. For a detailed guide to name construction and name interpretation refer to Bünzli-Trepp<sup>10</sup> (2007); (b) IUPAC, Revised Nomenclature for Radicals, Ions, Radical Ions and Related Species Treatment of ; (c) *Pure Appl. Chem.* **1993**, *65*, 1357–1455.
- IUPAC, *Pure Appl. Chem.* **1984**, *56*, 769. <http://www.chem.qmul.ac.uk/iupac>.
- Back, O.; Donnadiou, B.; Parameswaran, P.; Frenking, G.; Bertrand, G. *Nat. Chem.* **2010**, *2*, 369–373.
- Moss, G. P. *Pure Appl. Chem.* **1998**, *70*, 143–216.
- Weigand, J. J.; Holthausen, M.; Fröhlich, R. *Angew. Chem. Int. Ed.* **2009**, *48*, 295–298.
- (a) Boyall, A. J.; Dillon, K. B.; Howard, J. A. K.; Monks, P. K.; Thompson, A. L. *Dalton Trans.* **2007**, *14*, 1374–1376; (b) Weigand, J. J.; Burford, N.; Davidson, R. J.; Cameron, T. S.; Seelheim, P. *J. Am. Chem. Soc.* **2009**, *131*, 17943–17953.
- Kilian, P.; Slawin, A. M. Z.; Woollins, J. D. *Dalton Trans.* **2006**, *18*, 2175–2183.
- (a) Cossairt, B. M.; Diawara, M. C.; Cummins, C. C. *Science* **2009**, *323*, 602; (b) Cossairt, B. M.; Cummins, C. C. *J. Am. Chem. Soc.* **2009**, *131*, 15501–15511.
- (a) Krossing, I.; Raabe, I. *Angew. Chem. Int. Ed.* **2001**, *40*, 4406–4409; Krossing, I. *J. Chem. Soc. Dalton Trans.* **2002**, *4*, 500–512.
- Weigand, J. J.; Burford, N.; Lumsden, M. D.; Decken, A. *Angew. Chem. Int. Ed.* **2006**, *45*, 6733–6736.
- Edge, R.; Less, R. J.; McInnes, E. J. L.; Mütter, K.; Naseri, V.; Rawson, J. M.; Wright, D. S. *Chem. Commun.* **2009**, *13*, 1691–1693.
- Masuda, J. D.; Schoeller, W. W.; Donnadiou, B.; Bertrand, G. *Angew. Chem. Int. Ed.* **2007**, *46*, 7052–7055.
- (a) Brock, S. L.; Perera, S. C.; Stamm, K. L. *Chem. Eur. J.* **2004**, *10*, 3364–3371; (b) Weiping, S.; McLeod, D.; Verkade, J. G. *J. Org. Chem.* **2003**, *68*, 9499–9501; (c) Ertl, G.; Knözinger, H.; Schüth, F.; Weitkamp, J. *Handbook of Heterogeneous Catalysis*, 2nd ed. Wiley-VCH: Weinheim, 2008; vol. VI.
- (a) Rodriguez, J. A.; Kim, J.-Y.; Hanson, J. C.; Sawhill, S. J.; Bussell, M. E. *J. Phys. Chem. B* **2003**, *107*, 6276–6285; (b) Zuzaniuk, V.; Prins, R. *J. Catal.* **2003**, *219*, 85–96; (c) Shu, Y.; Oyama, S. T. *Carbon* **2005**, *43*, 1517–1532; (d) Prins, R.; Pirngruber, G.; Weber, T. *Chimia* **2001**, *55*, 791–795; (e) Senevirathne, K.; Burns, A. W.; Bussell, M. E.; Brock, S. L. *Adv. Funct. Mater.* **2007**, *17*, 3933–3939; (f) Abu, I. I.; Smith, K. J. *Appl. Catal. A: Gen.* **2007**, *328*, 58–67.
- (a) Manners, I. *Angew. Chem. Int. Ed.* **1996**, *35*, 1602–1621; (b) Chandrasekhar, V.; Krishnan, V.; Athimoolam, A.; Senthil Andavan, G. T. *Can. J. Chem.* **2002**, *80*, 1415–1420; (c) Chivers, T.; Manners, I. *Inorganic Rings and Polymers of the p-Block Elements*. RSC Publishing: Cambridge, 2009;.
- Liu, C.; Li, F.; Ma, L. P.; Cheng, H. M. *Adv. Mater.* **2010**, *22*, E28–E62.
- (a) Stinner, C.; Prins, R.; Weber, T. *J. Catal.* **2001**, *202*, 187–194; (b) Chiriac, H.; Moga, A.-E.; Urse, M.; Paduraru, I.; Lupu, N. *J. Magn. Magn. Mater.* **2004**, *272–276*, 1678–1680; (c) Park, J.; Koo, B.; Yoon, K. Y.; Hwang, Y.; Kang, M.; Park, J. G.; Hyeon, T. *J. Am. Chem. Soc.* **2005**, *127*, 8433–8440; (d) Gu, Z.; Parans Paranthaman, M.; Pan, Z. *Cryst. Growth Des.* **2009**, *9*, 525–527; (e) Boyanov, S.; Bernardi, J.; Gillot, F.; Dupont, L.; Womes, M.; Tarascon, J. M.; Monconduit, L.; Doublet, M. L. *Chem. Mater.* **2006**, *18*, 3531–3538.
- Prescott, W. V.; Schwartz, A. I. *Nanorods, Nanotubes and Nanomaterials Research Progress*. NOVA Science Publisher: New York, 2008.
- Gärtner, S.; Korber, N. *Struct. Bond.* **2011**, *140*, 25–57.
- Liu, L.; Chen, X.; Shao, M.; An, C.; Yu, W.; Qian, Y. *J. Cryst. Growth* **2003**, *252*, 297–301.
- Hultgren, R.; Gingrich, N. S.; Warren, B. E. *J. Chem. Phys.* **1935**, *3*, 351–355.
- (a) Hittorf, W. *Ann. Phys. Chem.* **1865**, *126*, 193–215; (b) Thurn, H.; Krebs, H. *Acta Crystallogr. Sect. B* **1969**, *25*, 125–135.
- Ruck, M.; Hoppe, D.; Wahl, B.; Simon, P.; Wang, Y.; Seifert, G. *Angew. Chem.* **2005**, *117*, 7788–7792 *Angew. Chem., Int. Ed.* **2005**, *44*, 7616–7619.
- Simon, A.; Borrmann, H.; Horakh, J. *Chem. Ber.* **1997**, *130*, 1235–1240.
- (a) Schlesinger, M. E. *Chem. Rev.* **2002**, *102*, 4267–4302; (b) Pflitzner, A. *Angew. Chem. Int. Ed.* **2006**, *45*, 699–700; (c) Clark, S. M.; Zang, J. M. *Phys. Rev.* **2010**, *B82*, 134111–134117.
- Russell, C. A. *Angew. Chem. Int. Ed.* **2010**, *49*, 9572–9573.



38. Douglas, A. E.; Rao, K. S. *Can. J. Phys.* **1958**, *36*, 565–571.
39. Kaufmann, A. *Homonukleare Cluster in Wirtsgittern*, Ph.D. Thesis, LMU Munich, 2009.
40. Caporali, M.; Gonsalvi, L.; Rossin, A.; Peruzzini, M. *Chem. Rev.* **2010**, *110*, 4178–4235.
41. Piro, N. A.; Figueroa, J. S.; McKellar, J. T.; Cummins, C. C. *Science* **2006**, *313*, 1276–1278.
42. Wolf, R.; Uhl, W. *Angew. Chem. Int. Ed.* **2009**, *48*, 6774–6776.
43. Wang, Y.; Xie, Y.; Wei, P.; King, R. B.; Schaefer, H. F., III; Schleyer, P. v. R.; Robinson, G. H. *J. Am. Chem. Soc.* **2008**, *130*, 14970–14971.
44. Back, O.; Kuchenbeiser, G.; Donnadiue, B.; Bertrand, G. *Angew. Chem. Int. Ed.* **2009**, *48*, 5530–5533.
45. (a) Katayama, Y.; Mizutani, T.; Utsumi, W.; Shimomura, O.; Yamakata, M.; Funakoshi, K.-I. *Nature* **2000**, *403*, 170–172; (b) Katayama, Y. *J. Non-Cryst. Solids* **2002**, *312–314*, 8–14.
46. Katayama, Y.; Inamuri, Y.; Mizutani, T.; Yamakata, M.; Utsumi, W.; Shimomura, O. *Science* **2004**, *306*, 848–851.
47. Yarger, J. L.; Wolf, G. H. *Science* **2004**, *306*, 820–821.
48. Andrews, P. C.; Hardie, M. J.; Raston, C. L. *Coord. Chem. Rev.* **1999**, *189*, 169–198.
49. (a) Douthwaite, R. E.; Green, M. L. H.; Heyes, S. J.; Rosseinsky, M. J.; Turner, J. F. C. *J. Chem. Soc. Chem. Commun.* **1994**, 1367–1368; (b) Mal, P.; Breiner, B.; Rissanen, K.; Nitschke, J. R. *Science* **2009**, *324*, 1697–1699.
50. (a) Scheer, M.; Balazs, G.; Seitz, A. *Chem. Rev.* **2010**, *110*, 4236–4256; (b) Giffin, N. A.; Masuda, J. D. *Coord. Chem. Rev.* **2011**, *255*, 1342–1359.
51. (a) Scherer, O. J. *Acc. Chem. Res.* **1999**, *32*, 751–762; (b) Scherer, O. J. *Chem. unserer Zeit* **2000**, *34*, 374–381.
52. (a) Ehses, M.; Romerosa, A.; Peruzzini, M. *Top. Curr. Chem.* **2002**, *220*, 107–140; (b) Peruzzini, M.; Gonsalvi, L.; Romerosa, A. *Chem. Soc. Rev.* **2005**, *34*, 1038–1047.
53. (a) Budnikova, Y. H.; Yakhvarov, D. G.; Sinyashin, O. G. *J. Organomet. Chem.* **2005**, *690*, 2416–2425; (b) Budnikova, Y. H.; Tazeev, D. I.; Gryaznova, T. V.; Sinyashin, O. G. *Russ. J. Electrochem.* **2006**, *42*, 1127–1133; (c) Budnikova, Y. H.; Krasnov, S. A.; Graznova, T. V.; Tomilov, A. P.; Turigin, V. V.; Magdeev, I. M.; Sinyashin, O. G. *Phosphorus Sulfur Silicon Relat. Elem.* **2008**, *183*, 513–518.
54. Schoeller, W. W. *Phys. Chem. Chem. Phys.* **2009**, *11*, 5273–5280.
55. Milyukov, V. A.; Budnikova, Y. H.; Sinyashin, O. G. *Russ. Chem. Rev.* **2005**, *74*, 781–805.
56. Krossing, I. In *Molecular Clusters of the Main Group Elements*; Driess, M., Nöth, H., Eds.; Wiley-VCH: Weinheim, 2004; pp 209–229.
57. Power, M. B.; Barron, A. R. *Angew. Chem. Int. Ed Engl.* **1991**, *30*, 1353–1355.
58. (a) Kettle, S. F. A. *Theor. Chim. Acta* **1966**, *4*, 150–154; (b) Schmidtke, H. H. *Theor. Chim. Acta* **1968**, *9*, 199–209; (c) Joitham, R. W. *Chem. Soc. Rev.* **1973**, *2*, 457–474; (d) Gimarc, B. M. *Molecular Structure and Bonding. The Qualitative Molecular Orbital Approach*. Wiley: New York, 1979.
59. For the assignment of orbitals see: (a) Guest, M. F.; Hillier, I. H.; Saunders, V. R. *J. Chem. Soc. Faraday Trans. 2* **1972**, *68*, 2070–2074; (b) Hillier, I. H.; Saunders, V. R. *J. Chem. Soc. Chem. Commun.* **1970**, 1233–1234.
60. Schoeller, W. W.; Staemmler, V.; Rademacher, P.; Niecke, E. *Inorg. Chem.* **1986**, *25*, 4382–4385.
61. For the photoelectron spectrum of P<sub>4</sub> see: (a) Brundle, C. R.; Kuebler, N. A.; Robin, M. B.; Basch, H. *Inorg. Chem.* **1972**, *11*, 20–25; (b) Evans, S.; Joachim, P. J.; Orchard, A. F.; Turner, D. W. *Int. J. Mass Spectrom. Ion Phys.* **1972**, *9*, 41–52; (c) Hart, R. R.; Robin, M. B.; Kuebler, N. A. *J. Chem. Phys.* **1965**, *42*, 3631–3638.
62. (a) Bourissou, D.; Guerret, O.; Gabbai, F. P.; Bertrand, G. *Chem. Rev.* **1999**, *100*, 39–92; (b) Hahn, F. E.; Jahnke, M. C. *Angew. Chem. Int. Ed.* **2008**, *47*, 3122–3172.
63. Nyíri, K.; Szilvasi, T.; Veszpremi, T. *Dalton Trans.* **2010**, *39*, 9347–9352.
64. (a) Hinchley, S. L.; Morrison, C. A.; Rankin, D. W. H.; Macdonald, C. L. B.; Wiacek, R. J.; Voigt, A.; Cowley, A. H.; Lappert, M. F.; Gundersen, G.; Clyburne, J. A. C.; Power, P. P. *J. Am. Chem. Soc.* **2001**, *123*, 9045–9053; (b) Hinchley, S. L.; Morrison, C. A.; Rankin, D. W. H.; Macdonald, C. L. B.; Wiacek, R. J.; Cowley, A. H.; Lappert, M. F.; Gundersen, G.; Clyburne, J. A. C.; Power, P. P. *Chem. Commun.* **2000**, 2045–2046.
65. Bezombes, J.; Hitchcock, P. B.; Lappert, M. F.; Nycz, J. E. *Dalton Trans.* **2004**, 499–501.
66. Cossairt, B. M.; Cummins, C. C. *New J. Chem.* **2010**, *34*, 1533–1536.
67. Ozin, G. A. *J. Chem. Soc. A* **1970**, 2307–2310.
68. (a) Schleyer, P. V.; Maerker, C.; Dransfeld, A.; Jiao, H.; Hommes, N. *J. Am. Chem. Soc.* **1996**, *118*, 6317–6318; (b) Hirsch, A.; Chen, Z.; Jiao, H. *Angew. Chem. Int. Ed.* **2001**, *40*, 2834–2838.
69. Cossairt, B. M.; Cummins, C. C.; Head, A. R.; Lichtenberger, D. L.; Berger, R. J. F.; Hayes, S. A.; Mitzel, N. W.; Wu, G. *J. Am. Chem. Soc.* **2010**, *132*, 8459–8465.
70. (a) Jamieson, J. C. *Science* **1991**, *139*, 1291–1292; (b) Ahuja, R. *Phys. Status Solidi B* **2003**, *235*, 282–287; (c) Kikegawa, T.; Iwasaki, H. *Acta Crystallogr.* **1983**, *B39*, 158–164.
71. Brown, A.; Rundqvist, S. *Acta Crystallogr.* **1965**, *19*, 684–685.
72. Chang, K. J.; Cohen, M. L. *Phys. Rev. B* **1986**, 6177–6186.
73. Lange, S.; Schmidt, P.; Nilges, T. *Inorg. Chem.* **2007**, *46*, 4028–4035.
74. Qi, L.; Hu, X.; Chen, H.; Mao, Y. Faming Zhuanli Shenqing Gongkai Shuomingshu. Patent CN 1,481,040, 2004, 6 pp.
75. (a) Haser, M.; Treutler, O. *J. Chem. Phys.* **1995**, *102*, 3703–3712; (b) Pfitzner, A.; Freudenthaler, E. *Angew. Chem. Int. Ed Engl.* **1995**, *34*, 1647–1649; (c) Pfitzner, A.; Braeu, M. F.; Zweck, J.; Brunklaus, G.; Eckert, H. *Angew. Chem. Int. Ed.* **2004**, *43*, 4228–4230; (d) Hartl, H. *Angew. Chem. Int. Ed Engl.* **1996**, *34*, 2637–2638.
76. Ruck, M.; Hoppe, D.; Wahl, B.; Simon, P.; Wang, Y.; Seifert, G. *Angew. Chem. Int. Ed.* **2005**, *44*, 7616–7619.
77. Boecker, S.; Häser, M. *Z. Anorg. Allg. Chem.* **1995**, *621*, 258–286.
78. Winchester, R. A. L.; Whitty, M.; Shaffer, M. S. P. *Angew. Chem. Int. Ed.* **2009**, *48*, 3616–3619.
79. Trofimov, B. A.; Malysheva, S. F.; Gusarova, N. K.; Belogorlova, N. A.; Kuimov, V. A.; Sukhov, B. G.; Tarasova, N. P.; Smetannikov, Y. V.; Vilesov, A. S.; Sinegovskaya, L. M.; Arsen'ev, K. Y.; Likhoshvai, E. V. *Dokl. Chem.* **2009**, *427*, 153–155; Boecker, S.; Häser, M. *Z. Anorg. Allg. Chem.* **1995**, *621*, 258–286.
80. Häser, M.; Schneider, U.; Ahlrichs, R. *J. Am. Chem. Soc.* **1992**, *114*, 9559–9661.
81. Warren, D. S.; Gimarc, B. M. *J. Am. Chem. Soc.* **1992**, *114*, 5378–5385.
82. Jutzi, P.; Kroos, R.; Müller, A.; Penk, M. *Angew. Chem. Int. Ed Engl.* **1989**, *28*, 600–602.
83. (a) Goldberg, N.; Schwarz, H. *Acc. Chem. Res.* **1994**, *27*, 347–352; (b) Schalley, C. A.; Hornung, G.; Schröder, D.; Schwarz, H. *J. Chem. Soc. Rev.* **1998**, *27*, 91–104.
84. (a) Seifert, G.; Jones, R. O. *J. Chem. Phys.* **1992**, *96*, 2951–2964; (b) Jones, R. O.; Seifert, G. *J. Chem. Phys.* **1992**, *96*, 7564–7572.
85. Schröder, D.; Schwarz, H.; Wulf, H. S.; Jutzi, P.; Reiher, M. *Angew. Chem. Int. Ed.* **1999**, *38*, 3513–3515.
86. Hollemann, A. F.; Wiberg, N. *Lehrbuch der Anorganischen Chemie*, 102 ed.; DeGruyter: Berlin, 2007.
87. Sharfe, S.; Kraus, F.; Stegmaier, S.; Schier, A.; Fässler, T. *Angew. Chem. Int. Ed.* **2011**, *50*, 3630–3670.
88. Kaulzlarich, S. M., Ed.; In *Chemistry, Structure, and Bonding of Zintl Phases and Ions*; VCH: New York, 1996.
89. Mooser, E.; Pearson, W. B. *Phys. Rev.* **1956**, *101*, 1608–1609.
90. (a) Häser, M. *Systematik der Phosphorgerüste, eine theoretische Untersuchung*. Habilitationsschrift: Karlsruhe, 1996; (b) Böcker, S.; Häser, M. *Z. Anorg. Allg. Chem.* **1995**, *621*, 258–286.
91. (a) Scherer, O. J. *Angew. Chem. Int. Ed Engl.* **1985**, *24*, 924–943; (b) Scherer, O. J. *Angew. Chem. Int. Ed Engl.* **1990**, *29*, 1104–1122.
92. Manriquez, V.; Hönl, W. H.; von Schnering, H.-G. *Z. Anorg. Allg. Chem.* **1986**, *539*, 95–109.
93. Hönl, W.; von Schnering, H. G.; Schmidpeter, A.; Burget, G. *Angew. Chem. Int. Ed Engl.* **1984**, *23*, 817–818.
94. Fritz, G.; Hoppe, K. D.; Hönl, W.; Weber, D.; Mujica, C.; Manriquez, V.; von Schnering, H. G. *J. Organomet. Chem.* **1983**, *249*, 63–80.
95. Fritz, G.; Schneider, H. W.; Hönl, W.; von Schnering, H.-G. *Z. Anorg. Allg. Chem.* **1988**, *43*, 561–565.
96. Tebbe, K. F.; Feher, V.; Baudler, V. *Z. Kristallogr.* **1985**, *170*, 180–181.
97. Kraus, F.; Korber, N. *Chem. Eur. J.* **2005**, *11*, 5945–5959.
98. Korber, N.; Daniels, J. *Helv. Chim. Acta* **1996**, *79*, 2083–2084.
99. Korber, N.; von Schnering, H.-G. *Chem. Ber.* **1996**, *129*, 155–162.
100. Korber, N.; Daniels, J. *Acta Crystallogr. Sect. C* **1996**, *52*, 2454–2456.
101. Korber, N.; Daniels, J. *J. Chem. Soc. Dalton Trans.* **1996**, 1653–1658.
102. Korber, N.; Daniels, J. *Z. Anorg. Allg. Chem.* **1999**, *625*, 189–191.
103. Korber, N. *Phosphorus Sulfur Silicon Relat. Elem.* **1997**, *125*, 339–342.
104. Korber, N.; Daniels, J. *Z. Anorg. Allg. Chem.* **1996**, *622*, 1833–1838.
105. Kraus, F.; Hanauer, T.; Korber, N. *Inorg. Chem.* **2006**, *45*, 1117–1123.
106. Korber, N.; Richter, F. *Chem. Commun.* **1996**, 2023–2024.
107. Korber, N.; Daniels, J.; von Schnering, H.-G. *Angew. Chem. Int. Ed Engl.* **1996**, *35*, 1107–1113.
108. Dai, F. R.; Xu, L. *Chin. J. Struct. Chem.* **2007**, *26*, 45–49.
109. Hanauer, T.; Aschenbrenner, J. C.; Korber, N. *Inorg. Chem.* **2006**, *45*, 6723–6727.

110. Miluykov, V.; Kataev, A.; Sinyashin, O.; Lönnecke, P.; Hey-Hawkins, E. *Z. Anorg. Allg. Chem.* **2006**, *632*, 1728–1730.
111. Kraus, F.; Aschenbrenner, J. C.; Korber, N. *Angew. Chem. Int. Ed Engl.* **2003**, *42*, 4030–4033.
112. Knettel, D.; Reil, M.; Korber, N. *Z. Naturforsch.* **2001**, *56b*, 965–969.
113. Baudler, M.; Winzek, P. *Z. Anorg. Allg. Chem.* **1999**, *625*, 417–422.
114. Korber, N.; von Schnering, H.-G. *J. Chem. Soc. Chem. Commun.* **1995**, 1713–1714.
115. Aschenbrenner, J. C.; Korber, N. *Z. Anorg. Allg. Chem.* **2004**, *630*, 31–32.
116. Dai, F.-R.; Xu, L. *Inorg. Chim. Acta* **2006**, *359*, 4265–4273.
117. Korber, N.; Daniels, J. *Inorg. Chem.* **1997**, *36*, 4906–4908.
118. Korber, N.; Aschenbrenner, J. *J. Chem. Soc. Dalton Trans.* **2001**, 1665–1676.
119. (a) Kraus, F.; Aschenbrenner, J. C.; Korber, N. *Angew. Chem.* **2003**, *115*, 4162–4165; (b) Kraus, F.; Hanauer, T.; Korber, N. *Angew. Chem. Int. Ed.* **2005**, *44*, 7200–7204; (c) Hanauer, T.; Kraus, F.; Reil, M.; Korber, N. *Monatsh. Chem.* **2006**, *137*, 147–156; (d) Kraus, F.; Hanauer, T.; Korber, N. *Inorg. Chem.* **2006**, *45*, 1117–1123; (e) Kraus, F.; auf der Günne Schmedt, J.; DiSalle, B. F.; Korber, N. *Chem. Commun.* **2006**, *2*, 218–219.
120. (a) Igau, A.; Baccireddo, A.; Grützmacher, H.; Pritzkow, H.; Bertrand, G. *J. Am. Chem. Soc.* **1989**, *111*, 6853–6854; (b) Grützmacher, H.; Pritzkow, H. *Angew. Chem. Int. Ed.* **1991**, *30*, 709–710; (c) Loss, S.; Widauer, C.; Grützmacher, H. *Angew. Chem. Int. Ed.* **1999**, *38*, 3329–3331.
121. Kraus, F.; Aschenbrenner, J. C.; Klamroth, T.; Korber, N. *Inorg. Chem.* **2009**, *48*, 1911–1919.
122. Jutzi, P.; Meyer, U. *Phosphorus Sulfur Silicon Relat. Elem.* **1988**, *40*, 275–277.
123. Thelen, V.; Schmidt, D.; Nieger, M.; Niecke, E.; Schoeller, W. W. *Angew. Chem. Int. Ed Engl.* **1996**, *35*, 313–314.
124. Baudler, M.; Hahn, J. *Z. Naturforsch.* **1990**, *45b*, 1139–1141.
125. Fox, A. R.; Wright, R. J.; Rivard, E.; Power, P. P. *Angew. Chem. Int. Ed.* **2005**, *44*, 7729–7733.
126. Wiberg, N. *Coord. Chem. Rev.* **1997**, *163*, 217–252.
127. (a) Lerner, H.-W.; Bolte, M.; Karaghiosoff, K.; Wagner, M. *Organometallics* **2004**, *23*, 6073–6076; (b) Wiberg, N.; Woerner, A.; Lerner, H.-W.; Karaghiosoff, K.; Fenske, D.; Baum, G.; Dransfeld, A.; von Rague Schleyer, P. *Eur. J. Inorg. Chem.* **1998**, *6*, 833–841; (c) Wiberg, N.; Wörner, A.; Lerner, H.-W.; Karaghiosoff, K.; Nöth, H. *Z. Naturforsch.* **1998**, *53B*, 1004–1014; (d) Wiberg, N.; Wörner, A.; Nöth, H.; Karaghiosoff, K. In *Organosilicon Chemistry II*; Auner, N., Weis, J., Eds.; VCH: Weinheim, 1996; p 195; (e) Kovács, I.; Baum, G.; Fritz, G.; Fenske, D.; Wiberg, N.; Schuster, H.; Karaghiosoff, K. *Z. Anorg. Allg. Chem.* **1993**, *619*, 453–460.
128. Yao, S. Tris(trimethylsilyl) Stabilized Phosphorus and Lead Clusters. Ph.D. Thesis, Johannes Gutenberg – University of Mainz, 2005
129. Lerner, H.-W.; Wagner, M.; Bolte, M. *Chem. Commun.* **2003**, 990–991.
130. Wolf, R.; Finger, M.; Limburg, C.; Willis, A. C.; Wild, S. B.; Hey-Hawkins, E. *Dalton Trans.* **2006**, 831–837.
131. Uhl, W.; Benter, M. *J. Chem. Soc. Dalton Trans.* **2000**, 3133–3135.
132. Üffing, C.; von Hänisch, C.; Schnöckel, H. *Z. Anorg. Allg. Chem.* **2000**, *626*, 1557–1560.
133. Beswick, M. A.; Choi, N.; Hopkins, A. D.; McPartlin, M.; Mosquera, M. E. G.; Rathby, P. R.; Rothenberger, A.; Stalke, D.; Wheatley, A. J.; Wright, D. S. *Chem. Commun.* **1998**, 2485–2486.
134. (a) Issleib, K.; Krech, K. *Chem. Ber.* **1965**, *98*, 2545–2550; (b) Fluck, E.; Issleib, K. *Z. Anorg. Allg. Chem.* **1965**, *339*, 274–280; (c) Issleib, K.; Krech, K. *Chem. Ber.* **1966**, *99*, 1310–1315; (d) Issleib, K.; Hoffmann, M. *Chem. Ber.* **1966**, *99*, 1320–1324; (e) Issleib, K.; Rockstroh, Ch.; Duchek, I.; Fluck, E. *Z. Anorg. Allg. Chem.* **1968**, *360*, 77–87; (f) Issleib, K.; Krech, K. *J. Prakt. Chem.* **1969**, *311*, 463–471.
135. Baudler, M.; Gruner, C.; Fürstberg, G.; Kloth, B.; Saykowski, F.; Özer, U. *Z. Anorg. Allg. Chem.* **1978**, *446*, 169–176.
136. Schmidpeter, A.; Burget, G. *Phosphorus Sulfur Silicon Relat. Elem.* **1985**, *22*, 323–335.
137. (a) Fritz, G.; Stoll, K. *Z. Anorg. Allg. Chem.* **1986**, *538*, 78–112; (b) Fritz, G.; Biastoch, R.; Stoll, K.; Vaahs, T.; Hanke, D.; Schneider, H. W. *Phosphorus Sulfur Silicon Relat. Elem.* **1987**, *30*, 385–388.
138. Stein, D.; Dransfeld, A.; Flock, M.; Rügger, H.; Grützmacher, H. *Eur. J. Inorg. Chem.* **2006**, 4157–4167.
139. (a) Geier, J.; Rügger, H.; Wörle, M.; Grützmacher, H. *Angew. Chem. Int. Ed.* **2003**, *42*, 3951–3954; (b) Geier, J.; Harmer, J.; Grützmacher, H. *Angew. Chem. Int. Ed.* **2004**, *43*, 4093–4097.
140. Wolf, R.; Schisler, A.; Lönnecke, P.; Jones, C.; Hey-Hawkins, E. *Eur. J. Inorg. Chem.* **2004**, 3277–3286.
141. Wolf, R.; Hey-Hawkins, E. *Z. Anorg. Allg. Chem.* **2006**, *632*, 727–734.
142. Wolf, R.; Gómez-Ruiz, S.; Reinhold, J.; Böhlmann, W.; Hey-Hawkins, E. *Inorg. Chem.* **2006**, *45*, 9107–9113.
143. Wolf, R. Synthese, Struktur und Reaktivität phosphorreicher Hauptgruppen- und Übergangsmetallverbindungen. Ph.D. Thesis, University of Leipzig, Leipzig, 2005
144. Baker, R. J.; Jones, C.; Mills, D. P.; Murphy, D. M.; Hey-Hawkins, E.; Wolf, R. *Dalton Trans.* **2006**, 64–72.
145. Herrero, R.; Gómez-Ruiz, S.; Dávalos, J. Z.; Hey-Hawkins, E. *C. R. Chimie* **2010**, *13*, 1185–1190.
146. Schisler, A.; Lönnecke, P.; Huniar, U.; Ahlrich, R.; Hey-Hawkins, E. *Angew. Chem. Int. Ed Engl.* **2001**, *40*, 4217–4219.
147. Schisler, A.; Lönnecke, P.; Gelbrich, T.; Hey-Hawkins, E. *Dalton Trans.* **2004**, 2895–2898.
148. Feldmann, K.-O.; Fröhlich, R.; Weigand, J. *J. Chem. Commun.* **2012**, *48*, 4296–4298.
149. (a) Niecke, E.; Rüger, R.; Krebs, B. *Angew. Chem. Int. Ed Engl.* **1982**, *21*, 544; (b) Jurkschat, K.; Mugge, C.; Tzschach, A.; Uhlig, W.; Zschunke, A. *Tetrahedron Lett.* **1982**, *23*, 1345; (c) Mazieres, M. R.; Rauzy, K.; Bellan, J.; Sanchez, M.; Pfister-Guillouzo, G.; Senio, A. *Phosphorus Sulfur Silicon Relat. Elem.* **1993**, *76*, 45.
150. Riegel, S. D.; Burford, N.; Lumsden, M. D.; Decken, A. *Chem. Commun.* **2007**, 4668–4670.
151. (a) Schmidpeter, A.; Lochschmidt, S.; Sheldrick, W. S. *Angew. Chem. Int. Ed.* **1982**, *21*, 63–64; (b) Schmidpeter, A.; Lochschmidt, S.; Sheldrick, W. S. *Angew. Chem. Int. Ed.* **1985**, *24*, 226–227; (c) Ellis, B.; Carlesimo, M.; Macdonald, C. *Chem. Commun.* **2003**, 1946–1947; (d) Kilian, P.; Slawin, A. M. Z.; Woollins, J. D. *Dalton Trans.* **2006**, 2175–2183; (e) Schmidpeter, A.; Lochschmidt, S.; Karaghiosoff, K.; Sheldrick, W. S. *Chem. Commun.* **1985**, 1447–1448; (f) Schmidpeter, A.; Lochschmidt, S. *Inorg. Synth.* **1990**, *27*, 253–258; (g) Ellis, B. D.; MacDonald, C. L. B. *Inorg. Chem.* **2006**, *45*, 6864–6875.
152. David, G.; Niecke, E.; Nieger, M.; Radseck, J.; Schoeller, W. W. *J. Am. Chem. Soc.* **1994**, *116*, 2191–2192.
153. (a) Niecke, E.; Nieger, M.; Reichert, F. *Angew. Chem. Int. Ed.* **1988**, *27*, 1715–1716; (b) Burford, N.; Clyburne, J. A. C.; Bakshi, P. K.; Cameron, T. S. *Organometallics* **1995**, *14*, 1578–1585; (c) Burford, N.; Cameron, T. S.; Clyburn, J. A. C.; Eichele, K.; Robertson, K. N.; Serda, S.; Wasylishen, R. E.; Whitla, W. A. *Inorg. Chem.* **1996**, *35*, 5460–5467; (d) Burford, N.; Spinney, H. A.; Ferguson, M. J.; McDonald, R. *Chem. Commun.* **2004**, 2696–2697.
154. (a) Rovnanik, P.; Kapička, L.; Taraba, J.; Cerník, M. *Inorg. Chem.* **2004**, *43*, 2435–2442; (b) Meisel, M.; Lönnecke, P.; Grimmer, A. R.; Wulff-Molder, D. *Angew. Chem. Int. Ed.* **1997**, *36*, 1869–1870.
155. Blättner, M.; Nieger, M.; Ruban, A.; Schoeller, W. W.; Niecke, E. *Angew. Chem. Int. Ed.* **2000**, *39*, 2768–2771.
156. Kaukorat, T.; Ernst, L.; Schmutzler, R. *Polyhedron* **1990**, *9*, 1463–1466.
157. Weigand, J. J.; Burford, N.; Mahnke, D.; Decken, A. *Inorg. Chem.* **2007**, *46*, 7689–7691.
158. Huynh, K.; Lough, A. J.; Manners, I. *J. Am. Chem. Soc.* **2006**, *128*, 14002–14003.
159. (a) Weiss, R.; Engel, S. *Synthesis* **1991**, 1077–1079; (b) Weiss, R.; Engel, S. *Angew. Chem. Int. Ed.* **1992**, *31*, 216–217.
160. Weigand, J. J.; Feldmann, K.-O.; Echterhoff, A. K. C.; Ehlers, A.; Lammertsma, K. *Angew. Chem. Int. Ed.* **2010**, *49*, 6178–6181.
161. Heuer, L.; Ernst, L.; Schmutzler, R.; Schomburg, D. *Angew. Chem. Int. Ed.* **1989**, *28*, 1507–1509.
162. Weigand, J. J.; Burford, N.; Decken, A.; Schulz, A. *Eur. J. Inorg. Chem.* **2007**, 4868–4872.
163. Schultz, C. W.; Parry, R. W. *Inorg. Chem.* **1976**, *15*, 3046–3050; Thomas, M. G.; Schultz, C. W.; Parry, R. W. *Inorg. Chem.* **1977**, *16*, 994–1001; Kopp, R. W.; Bond, A. C.; Parry, R. W. *Inorg. Chem.* **1976**, *15*, 3042–3046; Shagvaleev, F. Sh.; Zykova, T. V.; Tarasova, R. I.; Sitdikova, T. Sh.; Moskva, V. V. *Zh. Obshch. Khim.* **1990**, *60*, 1775–1779.
164. (a) Burford, N.; Cameron, T. S.; LeBlanc, D. J.; Losier, P.; Sereida, S.; Wu, G. *Organometallics* **1997**, *16*, 4712–4717; (b) Burford, N.; Cameron, T. S.; Ragogna, P. J.; Ocampo-Mavarez, E.; Gee, M.; McDonald, R.; Wasylishen, R. E. *J. Am. Chem. Soc.* **2001**, *123*, 7947–7948; (c) Burford, N.; Ragogna, P. J.; McDonald, R.; Ferguson, M. J. *Am. Chem. Soc.* **2003**, *125*, 14404–14410.
165. (a) Abrams, M. B.; Scott, B. L.; Baker, R. T. *Organometallics* **2000**, *19*, 4944–4956; (b) Slattery, J. M.; Fish, C.; Green, M.; Hooper, T. N.; Jeffery, J. C.; Kilby, R. J.; Lynam, J. M.; McGrady, J. E.; Pantazis, D. A.; Russell, C. A.; Williams, C. E. *Chem. Eur. J.* **2007**, *13*, 6967–6974; (c) Burford, N.; Cameron, T. S.; Ragogna, P. J.; Ocampo-Mavarez, E.; Gee, M.; McDonald, R.; Wasylishen, R. E. *J. Am. Chem. Soc.* **2001**, *123*, 7947–7948; (d) Gee, M.; Wasylishen, R. E.; Ragogna, P. J.; Burford, N.; McDonald, R. *Can. J. Chem.* **2002**, *80*, 1488–1500; (e) Gonsior, M.; Krossing, I.; Müller, L.; Raabe, I.; Jansen, M.; van Wüllen, L. *Chem. Eur. J.* **2002**, *8*, 4475–4492; (f) Burford, N.;



- Herbert, D. E.; Ragogna, P. J.; McDonald, R.; Ferguson, M. J. *J. Am. Chem. Soc.* **2004**, *126*, 17067–17073.
166. Burford, N.; Losier, P.; Sereda, S. V.; Cameron, T. S.; Wu, G. *J. Am. Chem. Soc.* **1994**, *116*, 6474–6475.
167. (a) Cowley, A. H. *Polyhedron* **1984**, *3*, 389–432; (b) Cowley, A. H. *Acc. Chem. Res.* **1984**, *17*, 386–392; (c) Norman, N. C. *Polyhedron* **1993**, *12*, 2431–2446; (d) Power, P. P. *Chem. Rev.* **1999**, *99*, 3463–3503; (e) Fischer, R. C.; Power, P. P. *Chem. Rev.* **2010**, *110*, 3877–3923.
168. (a) Yoshifuji, M.; Shima, I.; Inamoto, N.; Hirotsu, K.; Higuchi, T. *J. Am. Chem. Soc.* **1981**, *103*, 4587–4589; (b) Yoshifuji, M. *J. Chem. Soc. Dalton Trans.* **1998**, 3343–3349; (c) Weber, L. *Chem. Rev.* **1992**, *92*, 1839–1906.
169. Loss, S.; Widauer, C.; Grützmaier, H. *Angew. Chem. Int. Ed.* **1999**, *38*, 3329–3331.
170. Nenajdenko, V. G.; Shevchenko, N. E.; Balenkova, E. S.; Alabugin, I. V. *Chem. Rev.* **2003**, *103*, 229–282.
171. (a) Schomburg, D.; Bettermann, G.; Ernst, L.; Schmutzler, R. *Angew. Chem. Int. Ed.* **1985**, *24*, 975–976; (b) Alder, R. W.; Ganter, C.; Harris, C. J.; Orpen, A. G. *Chem. Commun.* **1992**, 1170–1172; (c) Alder, R. W.; Ganter, C.; Harris, C. J.; Orpen, A. G. *Chem. Commun.* **1992**, 1172–1174; (d) Weigand, J. J.; Riegel, S. D.; Burford, N.; Decken, A. *J. Am. Chem. Soc.* **2007**, *129*, 7969–7976; (e) Somisara, D. M. U. K.; Buhl, M.; Lebl, T.; Richardson, N. V.; Slawin, A. M. Z.; Woollins, J. D.; Kilian, P. *Chem. Eur. J.* **2011**, *17*, 2666–2677.
172. (a) Nikitin, E. V.; Romakhin, A. S.; Zagumennov, V. A.; Babkin, Yu. A. *Electrochim. Acta* **1997**, *42*, 2217–2224; (b) Romakhin, A. S.; Palyutin, F. M.; Ignat'ev, Y. A.; Nikitin, E. V.; Kargin, Yu. M.; Litvinov, I. A.; Naumov, V. A. *Bull. Russ. Acad. Sci.* **1990**, *39*, 585–589.
173. Krossing, I. *J. Chem. Soc. Dalton Trans.* **2002**, 500–512.
174. Burford, N.; Dyker, C. A.; Decken, A. *Angew. Chem. Int. Ed.* **2005**, *44*, 2364–2367.
175. Green, M.; Russell, C. A.; Lynam, J. M.; Copsey, M. C.; Jeffery, J. C.; Slattery, J. M.; Swain, A. C. *Angew. Chem. Int. Ed.* **2003**, *42*, 2778–2782.
176. Romanenko, V. D.; Rudzevich, V. L.; Rusanov, E. B.; Chernega, A. N.; Senio, A.; Sotiropoulos, J.-M.; Pfister-Guillouzo, G.; Sanchez, M. *J. Chem. Soc. Chem. Commun.* **1995**, 1383–1385.
177. Burford, N.; Dyker, C. A.; Lumsden, M.; Decken, A. *Angew. Chem. Int. Ed.* **2005**, *44*, 6196–6199.
178. Hahn, J.; Baudler, M.; Kruger, C.; Tsay, Y.-H. *Z. Naturforsch. B* **1982**, *37*, 797–805.
179. Ellis, B.; Macdonald, C. L. B. *Acta Cryst.* **2006**, *E62*, m1869–m1870.
180. (a) Lochschmidt, S.; Schmidpeter, A. *Z. Naturforsch.* **1985**, *40*, 765–773; (b) Schmidpeter, A. *Angew. Chem. Int. Ed.* **1986**, *25*, 253–254; (c) Boon, J. A.; Byers, H. L.; Dillon, K. B.; Goeta, A. E.; Longbottom, D. A. *Heteroatom Chem.* **2000**, *11*, 226–231; (d) Barnham, R. J.; Deng, R. M. K.; Dillon, K. B.; Goeta, A. E.; Howard, J. A. K.; Puschmann, H. *Heteroatom Chem.* **2001**, *12*, 501–510; (e) Boyall, A. J.; Dillon, K. B.; Monks, P. K.; Potts, J. C. *Heteroatom Chem.* **2007**, *18*, 609–612; (f) Dillon, K. B.; Monks, P. K. *Dalton Trans.* **2007**, 1420–1424; (g) Norton, E. L.; Szekeley, K. L. S.; Dube, J. W.; Bomben, P. G.; Macdonald, C. L. B. *Inorg. Chem.* **2008**, *47*, 1196–1203.
181. (a) Schmidpeter, A.; Lochschmidt, S.; Karaghiosoff, K.; Sheldrick, W. S. *Chem. Commun.* **1985**, 1447–1448; (b) Dillon, K. B.; Olivey, R. J. *Heteroatom Chem.* **2004**, *15*, 150–154; (c) Dillon, K. B.; Monks, P. K.; Olivey, R. J.; Karsch, H. H. *Heteroatom Chem.* **2004**, *15*, 464–467; (d) Dillon, K. B.; Goeta, A. E.; Howard, J. A. K.; Monks, P. K.; Shepherd, H. J.; Thompson, A. L. *Dalton Trans.* **2008**, 1144–1149; (e) Konstatin Karaghiosoff, 'Heterophosphole', Ph.D. Thesis, LMU Munich, 1976.
182. Burford, N.; Phillips, A. D.; Spinney, H. A.; Lumsden, M.; Werner-Zwanziger, U.; Ferguson, M. J.; McDonald, R. *J. Am. Chem. Soc.* **2005**, *127*, 3921–3927.
183. (a) Dyker, C. A.; Burford, N.; Lumsden, M. D.; Decken, A. *J. Am. Chem. Soc.* **2006**, *128*, 9632–9633; (b) Carpenter, Y.-Y.; Dyker, C. A.; Burford, N.; Lumsden, M. D.; Decken, A. *J. Am. Chem. Soc.* **2008**, *130*, 15732–15741.
184. Boyall, A. J.; Dillon, K. B.; Howard, J. A. K.; Monks, P. K.; Thompson, A. L. *Dalton Trans.* **2007**, 1374–1376.
185. Lochschmidt, S.; Muller, G.; Huber, B.; Schmidpeter, A. *Z. Naturforsch. B* **1986**, *41*, 444–454.
186. Kilian, P.; Slawin, A. M. Z.; Woollins, J. D. *Dalton Trans.* **2006**, 2175–2183.
187. Dyker, C. A.; Burford, N.; Menard, G.; Lumsden, M. D.; Decken, A. *Inorg. Chem.* **2007**, *46*, 4277–4285.
188. Weigand, J. J.; Burford, N.; Davidson, R. J.; Cameron, T. S.; Seelheim, P. *J. Am. Chem. Soc.* **2009**, *131*, 17943–17953.
189. Dyker, C. A.; Riegel, S. D.; Burford, N.; Lumsden, M. D.; Decken, A. *J. Am. Chem. Soc.* **2007**, *129*, 7464–7474.
190. Weigand, J. J.; Burford, N.; Decken, A. *Angew. Chem. Int. Ed.* **2006**, *45*, 6733–6737.
191. Bihlmeier, A.; Gonsior, M.; Raabe, I.; Trapp, N.; Krossing, I. *Chem. Eur. J.* **2004**, *10*, 5041–5051; (b) Krossing, I. *J. Chem. Soc. Dalton Trans.* **2002**, 500–512; (c) Gonsior, M.; Krossing, I.; Müller, L.; Raabe, I.; Jansen, M.; van Wüllen, L. *Chem. Eur. J.* **2002**, *8*, 4475–4492.
192. Weigand, J. J.; Burford, N.; Decken, A. *Eur. J. Inorg. Chem.* **2008**, 4343–4347.
193. Holthausen, M. H.; Feldmann, K.-O.; Schulz, S.; Hepp, A.; Weigand, J. J. *Inorg. Chem.* **2012**, *51*, 3374–3387.
194. Holthausen, M. H.; Weigand, J. J. *J. Am. Chem. Soc.* **2009**, *131*, 14210–14211.
195. Holthausen, M. H.; Richter, C.; Hepp, A.; Weigand, J. J. *Chem. Commun.* **2010**, 46, 6921–6923.
196. Donat, M.; Conrad, E.; Jerabek, P.; Frenking, G.; Fröhlich, R.; Burford, N.; Weigand, J. J. *Angew. Chem. Int. Ed.* **2012**, *51*, 2964–2967.

This page intentionally left blank

## 1.05 Catenated Compounds – Group 15 (As, Sb, Bi)

HJ Breunig, Universität Bremen, Bremen, Germany

Cl Raț, Babeș-Bolyai University, Cluj-Napoca, Romania

© 2013 Elsevier Ltd. All rights reserved.

1.05.1	Introduction	151
1.05.2	Dipnicogen Compounds	152
1.05.3	Monocycles (RE) <sub>n</sub> (E = As, Sb, Bi)	158
1.05.4	Catena Tri- and Tetra-Pnicogen Compounds and Extended Chains (RE) <sub>x</sub> (E = As, Sb, Bi)	163
1.05.5	Heteromonocycles with Pnicogen–Pnicogen Bonds	163
1.05.6	Neutral Homoatomic Organometallic Pnicogen Polycycles (R <sub>n</sub> E <sub>m</sub> ) (E = As, Sb, Bi; n < m)	164
1.05.7	Heteroatomic Polycycles with Pnicogen–Pnicogen Bonds	166
1.05.8	Cationic Species with Pnicogen–Pnicogen Bonds	166
1.05.9	Extended Ribbons in Bismuth Subhalides	168
1.05.10	Anionic Catenated Species of As, Sb, and Bi	168
1.05.11	Ligand-Free Pnicogen Cluster Anions with Heteroatoms	172
1.05.12	Neutral Adducts with Dative Pnicogen–Pnicogen Bonds	173
1.05.13	Catena Species in Complexes and Clusters	173
1.05.14	Naked Neutral E <sub>n</sub> Species (E = As, Sb, Bi)	174
1.05.15	Conclusion	175
References		175

### 1.05.1 Introduction

The scope of this chapter is to give an overview on the developments in the field of catenated As, Sb, and Bi compounds since the year 2000. Syntheses, properties, and reactions including coordination chemistry are reviewed.

Catenated compounds are known as both organometallic and purely inorganic derivatives of the heavy pnicogen elements with element–element bonds. They include dimers, linear or branched chains of variable lengths, or bicyclic or polycyclic (cluster) compounds. Catenation occurs mainly in the three-bonded state of As, Sb, or Bi. Examples of four-bonded species with an E–E bond, for example, adducts R<sub>3</sub>E–EX<sub>3</sub> (E = As, Sb, Bi), or related species are less numerous.

To control catenation of three-bonded pnicogen atoms, the valences, which are not involved in element–element bonding, have to be blocked. This can be achieved, for instance, by monovalent substituents or by negative charges. The latter approach leads to catena anions, which frequently are encountered in Zintl anions of polypnicogen species, for example, dimers, E<sub>2</sub><sup>4–</sup>, rings E<sub>6</sub><sup>6–</sup>, or extended chains ∞E<sup>–</sup> (E = As, Sb, Bi). One fascinating aspect of the chemistry of catenated pnicogen compounds involves the structural relationships between the purely inorganic and the organometallic catena species. In some cases, there are also close chemical relations, that is, inorganic catena species can be used as starting materials for organometallic catena compounds, and vice versa. The Zintl concept of assigning negative charges to substituent-free pnicogen atoms is particularly useful for pnicogen derivatives of the most electropositive metals, for example, alkali-metal or earth alkali-metal pnictides. Pnicogen catenates are, however, also encountered in pnicogen-rich alloys with other metals.

Not only negative charges or substituents are useful for the stabilization of catena species. Linear and branched As, Sb, and Bi catenates, with or without substituents, are frequently incorporated in frameworks with other elements or in solid-state materials.

It is useful to consider the relationship between the pnicogen catenates and the modifications of the elements. Single-bonded dimers, linear or branched chains, as well as isolated or fused six-membered rings can be considered as sections of the stable modifications of the elements, such as gray arsenic, antimony, and bismuth, which consist of two-dimensional arrays of puckered six-membered rings. However, many examples are known, such as three-, four-, or five-membered rings or many polycyclic species that cannot be cut out of the metallic lattice of the element. In addition, the comparison with the pnicogen clusters, which exist in the gas phase, and, in the case of As<sub>4</sub>, in the condensed phase, as metastable modifications is useful. As<sub>4</sub> is also a reagent for the synthesis of catenates of arsenic and the E<sub>4</sub> tetrahedra are models for tetrahedral pnicogen transition metal clusters.

Catena species in which alkyl or aryl groups are bonded to the element have been known since the earliest days of organometallic chemistry. Furthermore, compounds with bonds of pnicogen centers to organometallic groups, for example, organosilyl or stannyl groups, belong to this family. Catenated organometallic compounds include dipnicogen (E = As, Sb, Bi, R = monovalent substituent) compounds of the type R<sub>2</sub>EER<sub>2</sub>, linear chains of the type R<sub>2</sub>E(ER)<sub>n</sub>ER<sub>2</sub>, or branched-chain compounds, and mono cycles (RE)<sub>n</sub>. Neutral polycycles R<sub>n</sub>E<sub>m</sub> (n < m) (clusters) result when the number of pnicogen atoms (E) is smaller than the number of substituents. Cationic organometallic species are obtained when positively charged substituents are added formally to neutral catena species, for example, reaction of R<sup>+</sup> with R<sub>2</sub>EER<sub>2</sub> gives [R<sub>3</sub>EER<sub>2</sub>]<sup>+</sup>.

Negatively charged catena compounds result when one substituent of a neutral chain species is formally removed as a cation and is thus replaced by a negative charge. Removal of  $R^+$  from  $R_2EER_2$ , for instance, gives  $[R_2EER]^-$ .

Organometallic dimers with well-defined double bonds between the pnictogen compounds of the type  $RE=ER$  (i.e., diarsenes, distibenes, and dibismutenes) are reviewed in **Chapter 1.12**. However, in clusters or inorganic catena species, the bond order often is less well-defined, and a large range of pnictogen–pnictogen bond lengths from values indicating triple bonds to values typical for weak pnictogen–pnictogen interactions are encountered. Such weak interactions with bond lengths similar to van der Waals contact distances also occur frequently in the solid-state structures of organometallic catena species of the heavy and soft elements antimony and bismuth. Catenation usually is related to unusual electron-rich low oxidation states of the elements (e.g., +2 for  $R_2E$ , +1 for  $RE$ ,  $\pm 0$  for substituent-free  $E$ ,  $-1$  for  $E^-$ , and  $-2$  for  $E^{2-}$  moieties) and intermolecular interactions extending the normal valence occur frequently. Typical Zintl ions, for example,  $E_7^{3-}$ , are considered in **Chapter 1.09**. In this chapter, mainly molecular species with single bonds between the pnictogen atoms are considered.

The stability of catenated compounds depends on various factors. One of them is the energy of the pnictogen–pnictogen single bond. The values for the single-bond energies ( $\text{kJ mol}^{-1}$ ), N–N 159, P–P 205, As–As 146, and Sb–Sb 128 were reported.<sup>1</sup> For the bond dissociation energy in the cluster  $Bi_2-Bi$ , a value of 92 ( $\text{kJ mol}^{-1}$ ) was reported.<sup>2</sup> These values clearly show that among the heavier pnictogen elements the most stable homonuclear single bonds are formed between phosphorus or arsenic atoms, and that Sb–Sb and Bi–Bi bonds are weaker. Also, the bonds from Sb or Bi to groups or atoms that frequently are used to block and control the valences of these heavier pnictogen compounds are rather weak. Consequently, catena species of the heavier pnictogen atoms often are highly reactive species, and frequently the substitution pattern at the pnictogen centers is changed during reactions, that is,  $R_2E$  centers can become  $RE$  or  $E$  centers ( $E=As, Sb, Bi$ ) by migration or elimination of substituents. This behavior often makes it difficult to control the reactions but offers the possibility of catena species to rearrange the pnictogen skeleton and to adapt to given or emerging new environments. Recent examples for such arrangements are the formation of unusual  $(RSb)_3Sb$  or  $(RSb)_2Sb_7$  species in reactions of distibines  $R_2Sb-SbR_2$  with a titanocene source.<sup>3</sup> Sterical protection by bulky aryl or silyl groups can provide efficient stabilization of catena species for the heavy pnictogen elements. There are, however, limitations. With sterically demanding groups  $R$ , it is possible that, instead of homocyclic catena-species *cyclo*-( $RE$ ) $_n$  ( $n > 2$ ) with pnictogen–pnictogen single bonds, the doubly bonded dimers  $RE=ER$  ( $E=As, Sb, Bi$ ) are preferable.

Previous overviews of catenated As, Sb, and Bi compounds were included in books,<sup>4–11</sup> review articles,<sup>12–29</sup> and annual reports.<sup>30–36</sup>

### 1.05.2 Dipnictogen Compounds

The first dipnictogen compound reported was Cadet's fuming liquid, described already by Louis Cadet de Gassicourt in 1760. Later, Bunsen found out that this liquid contained the

organometallic species tetramethyldiarsane  $Me_2As-AsMe_2$ , named cacodyl (malodor), as well as other components. An excellent overview of the chemistry of tetramethyldiarsane highlighting the early achievements of Cadet and Bunsen was published by Seyferth.<sup>37</sup>

More recently, not only diarsanes with other substituents but also several distibanes and dibismuthanes including the methylated compounds  $Me_2E-EMe_2$  ( $E=Sb, Bi$ ) have been synthesized and investigated. Motivation for the investigations on distibanes and dibismuthanes since the 1980s has arisen from the observation of unusual color effects, that is, bathochromic shifts on crystallization and the formation of extended linear chains in the crystals. In fact, the  $R_2E-ER_2$  molecules of these so-called thermochromic distibanes and dibismuthanes  $R_2E-ER_2$  ( $E=Sb, Bi$ ;  $R=Me, Me_3Si, Me_3Ge, Me_3Sn$ ;  $R_2=Me_2C_4H_2$ ) are aligned through close intermolecular  $Sb\cdots Sb$  or  $Bi\cdots Bi$  contacts to  $E-E\cdots E-E\cdots E$  chains with alternating single bonds and intermolecular contacts between the pnictogen atoms. The work in this field has been summarized in several review articles.<sup>11,13,17</sup> Little recent work in the field has been reported. Applications of organometallic dipnictogen compounds include their use as reagents and ligands or as As, Sb, or Bi sources for electronic materials.  $RE-ER$  units also are frequently incorporated in clusters or transition metal complexes. Although some of them can be considered as derivatives of  $RE=ER$  species, their bond lengths frequently exceed the values for typical double bonds.

Inorganic substituent-free dipnictogen compounds exist as ions  $E_2^{n-}$  ( $E=As, Sb, Bi$ ;  $n=4$ ) in solid phases or as  $E_2$  units in complexes and clusters. Dipnictogen compounds  $R_2E-ER_2$  ( $E=As, Sb, Bi$ ) frequently are synthesized by reductive methods, for example, reactions of  $R_2EX$  ( $X=Cl, Br, I$ ) with hydrides, alkali metals, or magnesium. However, oxidative coupling reactions with formation of pnictogen–pnictogen bonds are also used.

An example for reduction with hydrides is the synthesis of  $R(H)Sb-Sb(H)R$  ( $R=(Me_3Si)_2CH$ ), the first organodistibane with Sb–H bonds, which is formed in good yield by reaction of  $RSbCl_2$  with  $LiAlH_4$ . A probable intermediate is  $RSb(H)Cl$ , which reacts with  $RSbH_2$  with elimination of  $HCl$  to give  $R(H)Sb-Sb(H)R$ . The deuterium analogue  $R(D)Sb-Sb(D)R$  is formed from  $RSbCl_2$  and  $LiAlD_4$ . The structure of *meso*- $R(H)Sb-Sb(H)R$  was determined both by x-ray crystallography and by neutron diffraction. Crystals contain the distibane molecules in the *meso* form. The Sb–Sb bond length is 2.8304(8) Å. Nuclear magnetic resonance (NMR) studies reveal that *meso*- $R(H)Sb-Sb(H)R$  takes part in equilibria with formation of  $RSbH_2$ ,  $D,L-R(H)Sb-Sb(H)R$  and tristibane  $R(H)Sb-SbR-Sb(H)R$ .<sup>38,39</sup>

Tetramesityldibismuthane  $Mes_2Bi-BiMes_2$  ( $Mes=2,4,6-Me_3C_6H_2$ ) is obtained by the reaction of  $Mes_2BiCl$  and  $LiBH_4$  or  $LiAlH_4$  in diethylether in the temperature range between  $-70$  and  $-30$  °C and decomposition of the initially formed  $Mes_2BiH$  above 0 °C. The red crystals of  $Mes_2Bi-BiMes_2$  consist of centrosymmetric molecules in the *trans* conformation. The value of the Bi–Bi bond length is 3.087(3) Å.<sup>40</sup>

A convenient synthetic method for distibanes is the reaction of diorganoantimony chlorides or bromides with magnesium filings activated by 1,2-dibromoethane in tetrahydrofuran at or above ambient temperatures. Tetraisobutyldistibine  $R_2Sb-SbR_2$  ( $R=Bu^t$ ) is formed as a yellow viscous liquid by reduction of  $R_2SbBr$  with  $Mg$ .<sup>41</sup>

In an analogous way, the reduction of  $R(\text{Ph})\text{SbCl}$  ( $R = (\text{Me}_3\text{Si})_2\text{CH}$ ) with Mg gives the sterically congested unsymmetric distibane *meso*- $R(\text{Ph})\text{Sb-Sb}(\text{Ph})R$  a yellow crystalline compound. The crystals of *meso*- $R(\text{Ph})\text{Sb-Sb}(\text{Ph})R$  ( $R = (\text{Me}_3\text{Si})_2\text{CH}$ ) are composed of molecules in the *trans* conformation. The dihedral angle  $\Phi = \text{lp-Sb-Sb-lp}$  (lp = assumed orientation of the lone pair of electrons at antimony) is  $137.42(2)^\circ$ . It deviates considerably from the ideal value of  $180^\circ$ , which is observed in many distibanes with smaller substituents including tetraphenyldistibane. The value for the Sb-Sb bond length for *meso*- $R(\text{Ph})\text{Sb-Sb}(\text{Ph})R$  is  $2.844(1)\text{ \AA}$ .<sup>42</sup>

Dibismuthanes with small alkyl groups such as methyl, ethyl, or propyl groups are thermally unstable. They decompose at room temperature even in an inert atmosphere, with formation of elemental bismuth and trialkyl bismuthanes. Tetraaryl dibismuthanes, for example,  $\text{Ph}_2\text{Bi-BiPh}_2$ , are thermally more stable. Additional stabilization is achieved with pendant arm ligands  $2-(\text{Me}_2\text{NCH}_2)\text{C}_6\text{H}_4$  (one arm), or  $2,6-(\text{Me}_2\text{NCH}_2)_2\text{C}_6\text{H}_3$  (two arms) where bonding to the pnictogen atom is performed not only through normal covalent pnictogen carbon bonds but also through additional dative bonds from the pendant amino groups to the pnictogen centers. When these additional dative bonds are taken into account, the organic ligands can be considered as bidentate or tridentate, although the dative bonds are relatively weak and are involved in dynamic processes in solution. Recently, these pendant arm ligands were used as protecting groups for otherwise labile catena species of antimony or bismuth.

Protection through ligands with one pendant arm is achieved in the dibismuthane  $R_2\text{Bi-BiR}_2$  ( $R = 2-(\text{Me}_2\text{NCH}_2)\text{C}_6\text{H}_4$ ), a dark-red crystalline compound which is formed from  $R_2\text{BiCl}$  and Mg in tetrahydrofuran at  $-40^\circ\text{C}$ . The dibismuthane exhibits an antiperiplanar conformation in the crystalline state with three of the four pendant ligands coordinated to the bismuth atoms. The value for the Bi-Bi bond length is  $3.0657(5)\text{ \AA}$ .<sup>43</sup>

Ligands with two pendant arms stabilize the red crystalline dibismuthane  $R_2\text{Bi-BiR}_2$  ( $R = 2,6-(\text{Me}_2\text{NCH}_2)_2\text{C}_6\text{H}_3$ ), which is formed from  $R_2\text{BiCl}$  and Mg. Crystals obtained from toluene or diethylether contain three different forms of the dibismuthane, which in all forms adopts the *trans* conformation; however, the dihedral angles and the types of coordination of the pendant dimethylaminomethyl arms are different. One of the structures of  $R_2\text{Bi-BiR}_2$  ( $R = 2,6-(\text{Me}_2\text{NCH}_2)_2\text{C}_6\text{H}_3$ ) is shown in Figure 1. The Bi-Bi bonds are exceptionally long. They lie between  $3.0992(6)$  and  $3.2092(8)\text{ \AA}$ . NMR spectra show that in solution the substituents are equivalent. Apparently, the solid-state structures are not preserved in solution and dynamic processes occur.<sup>44</sup>

Chloro-tetraethyl-arsole and -stibole  $(\text{EtC})_4\text{E-Cl}$  ( $\text{E} = \text{As}, \text{Sb}; \text{Et} = \text{C}_2\text{H}_5$ ) react with Ca, Sr, or Ba with formation of the corresponding diarsanes or distibanes, that is, octaethyl-diarsolyl and distibolyl,  $(\text{EtC})_4\text{E-E}(\text{CEt})_4$ , as viscous liquids. Further reduction with Mg or Ca gives the corresponding anionic species, that is, tetraethylarsolide or stibolide  $(\text{EtC})_4\text{E}^-$ .<sup>45</sup>

The bicyclic distibane  $[(\text{Bu}^t\text{P})_3\text{Sb-Sb}(\text{PBU}^t)_3]_2$  is obtained by reaction of  $\text{Sb}(\text{NMe}_2)_3$  with  $\text{Bu}^t\text{P}(\text{H})\text{Li}$  through initial formation of the  $[(\text{Bu}^t\text{P})_3\text{Sb}]^-$  anions. The structure of  $[(\text{Bu}^t\text{P})_3\text{Sb-Sb}(\text{PBU}^t)_3]_2$  is shown in Figure 2.<sup>46</sup>

Tetramesityldistibane is formed as a component of crystals of the composition  $(\text{Cp}_2\text{TiCl})_2 \cdot 2\text{Mes}_2\text{Sb-SbMes}_2$  in a reaction

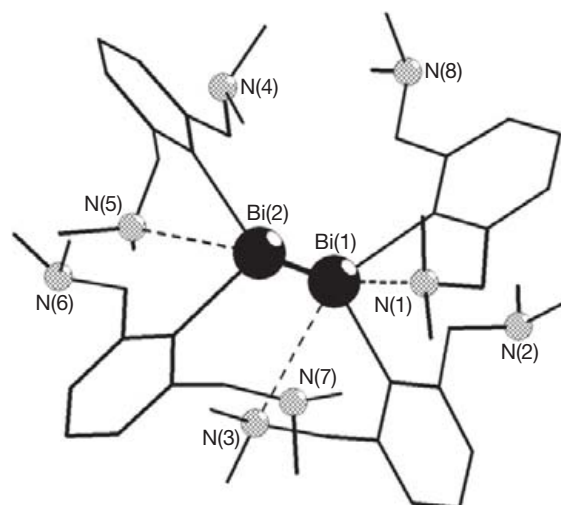


Figure 1 Structure of the central core of  $R_2\text{Bi-BiR}_2$  ( $R = 2,6-(\text{Me}_2\text{NCH}_2)_2\text{C}_6\text{H}_3$ ).<sup>44</sup> Hydrogen atoms are omitted for clarity.

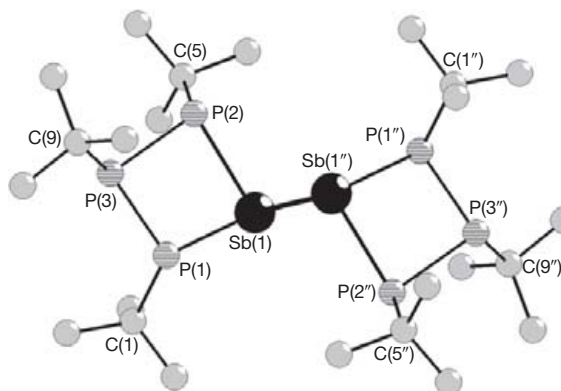


Figure 2 Structure of  $[(\text{Bu}^t\text{P})_3\text{Sb-Sb}(\text{PBU}^t)_3]_2$ .<sup>46</sup> Hydrogen atoms are omitted for clarity.

between  $\text{Cp}_2\text{Ti}(\text{Me}_3\text{SiC}\equiv\text{SiMe}_3)$ ,  $\text{Mes}_2\text{SbH}$ , and traces of  $\text{NH}_4\text{Cl}$ . The geometrical parameters of tetramesityldistibane are similar in the pure compound and in the adduct. The value of the Sb-Sb bond length is  $2.8589(8)\text{ \AA}$ .<sup>47</sup>

The ferrate  $\text{K}_2[\text{Fe}(\text{CO})_3(\text{PPh}_3)]$  reacts with  $\text{Ph}_2\text{SbCl}$  by metal-assisted reductive Sb-Sb coupling to give the distibane complex *trans*- $[\text{Fe}(\text{CO})_3(\text{PPh}_3)-(\text{Ph}_2\text{Sb-SbPh}_2)]$ . The distibane ligand is terminally  $\eta^1$ -coordinated *trans* to the phosphane ligand. The  $\text{Ph}_2\text{Sb-SbPh}_2$  ligand differs by approximately  $4^\circ$  from the *trans* conformation. The Sb-Sb bond length in the complex is  $2.8282(7)\text{ \AA}$ , which is slightly shorter than that of the free  $\text{Ph}_2\text{Sb-SbPh}_2$  ( $2.844(1)\text{ \AA}$ ).<sup>48</sup>

Catalytic dehydrocoupling with formation of tetraphenyldiarsane  $\text{Ph}_2\text{As-AsPh}_2$  occurs when benzene solutions of  $\text{Ph}_2\text{AsH}$  are heated in the presence of  $\text{N}(\text{CH}_2\text{CH}_2\text{NSiMe}_3)_3\text{ZrAsPh}_2$ .<sup>49</sup>

An exceptional inorganic bismuth compound with a Bi-Bi bond is bismuth(II) trifluoroacetate  $\text{Bi}_2(\text{O}_2\text{CCF}_3)_4$ , which is formed by oxidation of elemental bismuth with Ag or Hg trifluoroacetates, by reduction of bismuth(III) trifluoroacetate with Zn or by a comproportionation between Bi and Bi ( $\text{O}_2\text{CCF}_3$ )<sub>3</sub>. The crystal structure is shown in Figure 3.



It consists of  $\text{Bi}_2(\text{O}_2\text{CCF}_3)_4$  molecules with a dinuclear paddle-wheel shape. The Bi–Bi bond distances are averaged to 2.9462 (3) Å. The compound is volatile and exists in vapor phase up to 220 °C. The solution chemistry is quite limited: the bismuth (II) trifluoroacetate is decomposed by the majority of common solvents, but it can be stabilized by aromatic systems, for example, as adducts,  $\text{Bi}_2(\text{O}_2\text{CCF}_3)_4 \cdot (\text{C}_6\text{H}_5\text{Me})$  and  $\text{Bi}_2(\text{O}_2\text{CCF}_3)_4 \cdot (1,4\text{-C}_6\text{H}_4\text{Me}_2)_2$ . In the structures of the adducts, the bismuth(II) centers exhibit weak  $\eta^6$ -coordination to aromatic rings.<sup>50</sup>

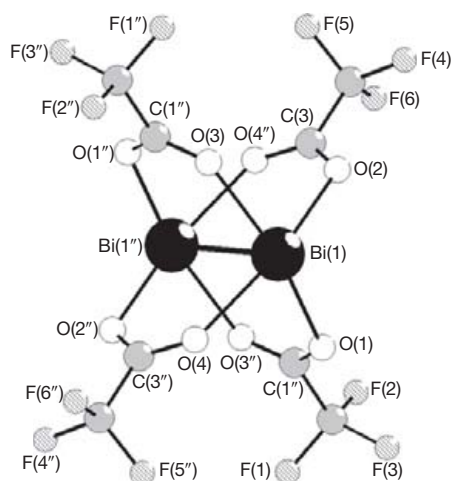
Heating  $\text{Bi}_2(\text{O}_2\text{CCF}_3)_4$  and  $\text{M}_2(\text{O}_2\text{CCF}_3)_4$  (M = Rh, Ru) in the solid state gives the mixed species  $[\text{BiM}(\text{O}_2\text{CCF}_3)_4]$ .<sup>51</sup>

Oxidative coupling processes lead to the formation of tetraacyldiarsanes.<sup>52</sup> Tetrabenzoyldiarsane  $\text{R}_2\text{As–AsR}_2$  (R = Ph (O)C) is formed from  $\text{Ph}(\text{HO})\text{C}=\text{As–C}(\text{O})\text{Ph}$  and  $\text{Hg}[\text{N}(\text{SiMe}_3)_2]_2$ . The value for the As–As bond length is 2.4254(6) Å. It is likely that initially the intermediate  $[\text{Hg}\{\text{As}[\text{C}(\text{O})\text{Ph}]_2\}_2]$  forms, which is unstable at room temperature and decomposes to give the diarsane via an oxidative coupling reaction involving a simultaneous elimination of elemental mercury.<sup>52</sup>

Another example for a tetraacyldiarsane formed by oxidative coupling is the compound  $[\text{Mes}(\text{O})\text{C}]_2\text{As–As}[\text{C}(\text{O})\text{Mes}]_2$  (Mes = 2,4,6-Me<sub>3</sub>C<sub>6</sub>H<sub>4</sub>). The coupling occurs in the reaction of lithium arsenadonate  $\text{LiAs}[\text{C}(\text{O})\text{Mes}]_2$  and  $\text{TaCl}_5$ . The value for the As–As bond length is 2.4300(8) Å.<sup>53</sup> For both tetraacyldiarsanes, the As–C and As–As bond lengths are typical for single bonds and all the C–O distances are in the localized double-bond range.

Oxidative coupling occurs also in the formation of tetramesityldistibane,  $\text{Mes}_2\text{Sb–SbMes}_2$  (Mes = 2,4,6-Me<sub>3</sub>C<sub>6</sub>H<sub>2</sub>) from the bis(stibido) complex  $\text{CpCp}^*\text{Hf}(\text{SbMes}_2)_2$  (Cp\* = Me<sub>5</sub>C<sub>5</sub>) by reactions with oxidants (I<sub>2</sub> and O<sub>2</sub>) or donors (carbon monoxide and diphenylacetylene) or by thermolysis.<sup>54</sup> Tetramesityldistibane was previously obtained by the reaction of  $\text{Mes}_2\text{SbBr}$  with magnesium in tetrahydrofuran.<sup>55</sup>

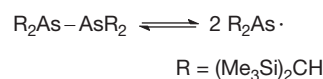
Tetranepentylidibismuthane  $\text{R}_2\text{Bi–BiR}_2$  (R = Me<sub>3</sub>CCH<sub>2</sub>) and elemental bismuth are products of the thermal decomposition of *cyclo*-(R<sub>2</sub>Bi)<sub>n</sub> (n = 3, 5) at room temperature. The reaction can be described as disproportionation of Bi(I) in the cyclobismuthane giving Bi(II) in the dibismuthane and Bi(0) in the element. Tetranepentylidibismuthane is an orange-red, air-sensitive solid.<sup>56</sup>



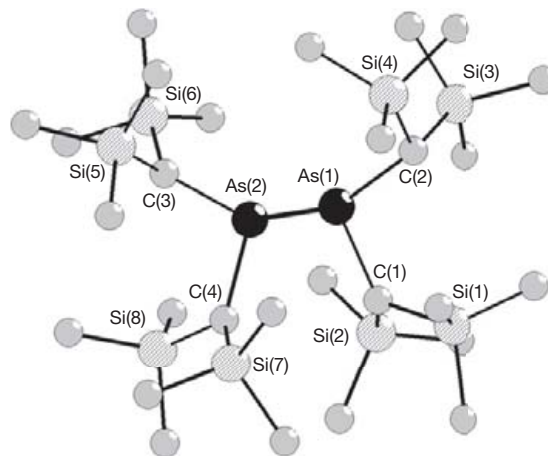
**Figure 3** Structure of  $\text{Bi}_2(\text{O}_2\text{CCF}_3)_4$ .<sup>50</sup>

The ‘jack-in-the-box’ diarsane  $\text{R}_2\text{As–AsR}_2$  (R = (Me<sub>3</sub>Si)<sub>2</sub>CH) is unusual because it exists only in the solid state, whereas the two  $\text{R}_2\text{As}$  radicals spring apart upon release from the solid state by melting, dissolution, or evaporation. The driving force for this dissociation is probably the decrease of steric tension between the bulky substituents in the [(Me<sub>3</sub>Si)<sub>2</sub>CH]<sub>2</sub>As group during the transition from the congested diarsane to the arsinyl radical (**Scheme 1**). The diarsane is obtained by reduction of  $\text{R}_2\text{AsI}$  with Li metal. The solid-state structure of  $\text{R}_2\text{As–AsR}_2$  (R = (Me<sub>3</sub>Si)<sub>2</sub>CH) features the presence of eight independent molecules in the asymmetric unit. However, each molecule adopts a *syn, anti* conformation. There are large distortions of the ligands attached to arsenic. The As–As bond lengths average 2.587 Å (2.576(2) to 2.592(2) Å range) and are approximately 0.1 Å longer than those reported for other diarsines (Cambridge Structural Database average, 2.455 Å; range, 2.417–2.489 Å). The structure of one of the diarsane molecules is shown in **Figure 4**.<sup>57</sup>

Although the Bi–Bi bond is weaker than the As–As bond, the corresponding dibismuthane  $\text{R}_2\text{Bi–BiR}_2$  (R = (Me<sub>3</sub>Si)<sub>2</sub>CH) shows no tendency for dissociation in solution. Apparently, there is less steric tension between the bulky alkyl substituents in the dibismuthane than in the diarsane, and the driving force for dissociation with formation of  $\text{R}_2\text{Bi}$  radicals is not sufficient.  $\text{R}_2\text{Bi–BiR}_2$  is a dark-red crystalline solid, which is formed by elimination of H<sub>2</sub> from  $\text{R}_2\text{BiH}$  at room temperature. The solid is stable at room temperature for a long time but in solution decomposition with formation of (R<sub>2</sub>Bi)<sub>n</sub> and R<sub>3</sub>Bi occurs. The crystal structure of  $\text{R}_2\text{Bi–BiR}_2$  (R = (Me<sub>3</sub>Si)<sub>2</sub>CH) consists of molecules in the near *trans* conformation. The value for the Bi–Bi bond length is 3.0534(13) Å. Attempts to prepare  $\text{R}_2\text{Sb–SbR}_2$  (R = (Me<sub>3</sub>Si)<sub>2</sub>CH) in a similar way, by decomposition of the corresponding stibine, failed.  $\text{R}_2\text{SbH}$  (R = (Me<sub>3</sub>Si)<sub>2</sub>CH) is stable up to 100 °C.<sup>58</sup>



**Scheme 1** Dissociation of the ‘jack-in-the-box’ diarsane  $\text{R}_2\text{As–AsR}_2$ .



**Figure 4** Structure of  $\text{R}_2\text{As–AsR}_2$  (R = (Me<sub>3</sub>Si)<sub>2</sub>CH).<sup>57</sup> Hydrogen atoms are omitted for clarity.



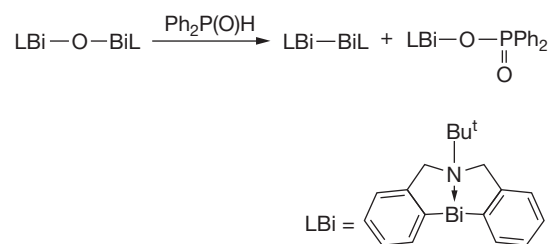
Very efficient protection of dibismuth species is achieved with very bulky silyl groups such as the diphenyl(*tert*-butyl) silyl group. Both redox and metathesis processes occur in reactions of BiBr<sub>3</sub> with Li(THF)<sub>3</sub>SiPh<sub>2</sub>Bu<sup>t</sup> in a 1:3 molar ratio to give (Bu<sup>t</sup>Ph<sub>2</sub>Si)<sub>2</sub>Bi–Bi(SiPh<sub>2</sub>Bu<sup>t</sup>)<sub>2</sub>. This dibismuthane is a dark-red crystalline compound that is thermally very stable. Heating under reflux at 100 °C for 3 h does not lead to disproportionation into elemental bismuth and (Bu<sup>t</sup>Ph<sub>2</sub>Si)<sub>3</sub>Bi or to dissociation into corresponding radicals. The effective steric protection of the bismuth centers is probably one of the main reasons for the stability of this compound. The Si<sub>2</sub>Bi–BiSi<sub>2</sub> core is in the semi-eclipsed conformation. Although there is considerable steric strain in the molecule, the Bi–Bi distance (3.006(8) Å) is relatively short.<sup>59</sup>

In crystals of (Bu<sup>t</sup>Ph<sub>2</sub>Si)<sub>2</sub>Bi–Bi(SiPh<sub>2</sub>Bu<sup>t</sup>)<sub>2</sub> there are no short intermolecular Bi···Bi contacts, whereas the trimethylsilyl derivative (Me<sub>3</sub>Si)<sub>2</sub>Bi–Bi(SiMe<sub>3</sub>)<sub>2</sub> is thermochromic and the solid-state structure contains extended bismuth chains.<sup>11</sup> Recently, calculations were performed on Me<sub>2</sub>Bi–BiMe<sub>2</sub> and (H<sub>3</sub>Si)<sub>2</sub>Bi–Bi(SiH<sub>3</sub>)<sub>2</sub>, two model compounds for thermochromic dibismuthanes. According to density functional theory (DFT)-optimized geometries of the systems *n*[(H<sub>3</sub>Si)<sub>2</sub>Bi–Bi(SiH<sub>3</sub>)<sub>2</sub>] (*n*=1–3), the closed-shell attraction between intermolecular Bi centers in the chain provides a moderate elongation of the intramolecular Bi–Bi bond in the dibismuthane unit and a shortening of the intermolecular Bi···Bi contacts. According to MP4(SDQ) computations, such oligomerization is carried out by intermolecular interaction of s lone pairs that are bound together and p-type orbitals of the Bi–Bi bonds in the bismuth chain. An increase in the number of (H<sub>3</sub>Si)<sub>2</sub>Bi–Bi(SiH<sub>3</sub>)<sub>2</sub> molecules per chain results in a decrease in the highest occupied molecular orbital–lowest unoccupied molecular orbital (HOMO–LUMO) gap and leads to a bathochromic shift. TD-PBE0 computations suggest that the lowest energy electron transition is metal–metal charge transfer. In addition, the attractive contributions in the chain [(H<sub>3</sub>Si)<sub>2</sub>Bi–Bi(SiH<sub>3</sub>)<sub>2</sub>]···[(H<sub>3</sub>Si)<sub>2</sub>Bi–Bi(SiH<sub>3</sub>)<sub>2</sub>] with silyl groups outweigh the repulsion of the Bi···Bi centers, whereas for the methyl-substituted bismuth chain the repulsive van der Waals force dominates. This fact makes the rectangular oligomerization model more preferred for *n*[Me<sub>2</sub>Bi–BiMe<sub>2</sub>] (*n*=2), while for *n*[(H<sub>3</sub>Si)<sub>2</sub>Bi–Bi(SiH<sub>3</sub>)<sub>2</sub>] chain formation is favored in the gas phase.<sup>59</sup> Nevertheless, the chain formation is observed in solid tetramethyldibismuthane.<sup>11</sup>

Another method for an effective protection of dibismuth species is the use of ligands of the type RN(CH<sub>2</sub>C<sub>6</sub>H<sub>4</sub>)<sub>2</sub>, which coordinate strongly through two carbon atoms, forming Bi–C bonds, and in addition through dative bonds from nitrogen to bismuth. Therefore, these ligands can be viewed as tridentate.

Examples are the thermally stable dibismuthanes LBi–BiL, with LBi = RN(CH<sub>2</sub>C<sub>6</sub>H<sub>4</sub>)<sub>2</sub>Bi (R = Me, Bu<sup>t</sup>, Oct<sup>t</sup>), which are formed by reactions of the corresponding organobismuth oxides LBi–O–BiL with phosphorus compounds such as Ph<sub>2</sub>P(O)H or, more efficiently, 9,10-dihydro-9-oxa-10-phospha-phenantrene-10-oxide. A reaction path leading to LBi–BiL is given in Scheme 2.

The thermal stability of the dibismuthanes LBi–BiL is remarkable. For example, LBi–BiL, LBi = Oct<sup>t</sup>N(CH<sub>2</sub>C<sub>6</sub>H<sub>4</sub>)<sub>2</sub>Bi, melts at 181–182 °C and no appreciable decomposition was



**Scheme 2** Synthesis of the dibismuthane LBi–BiL.

observed on heating in boiling toluene for 10 h. The structures were determined by x-ray diffraction. The values for the Bi–Bi bond lengths range from 3.0547(2) to 3.0707(3) Å.<sup>60</sup>

A 1,2-dichlorodiarlyldibismuthane is formed in the reaction of the sterically encumbered arylbismuth dichloride RBiCl<sub>2</sub> (R = 2,6-(2,6-Pr<sup>i</sup><sub>2</sub>C<sub>6</sub>H<sub>3</sub>)<sub>2</sub>C<sub>6</sub>H<sub>3</sub>) with KSi(SiMe<sub>3</sub>)<sub>3</sub>. Instead of silylation at bismuth reduction occurs and the dibismuthane R(Cl)Bi–Bi(Cl)R forms. The solid-state molecular structure shows the mixed-substituted dibismuthane with a Bi–Bi single bond length of 3.0232(4) Å. The aryl and chlorine substituents adopt strictly *trans* arrangements in the anti-periplanar conformation of the dibismuthane.<sup>61</sup>

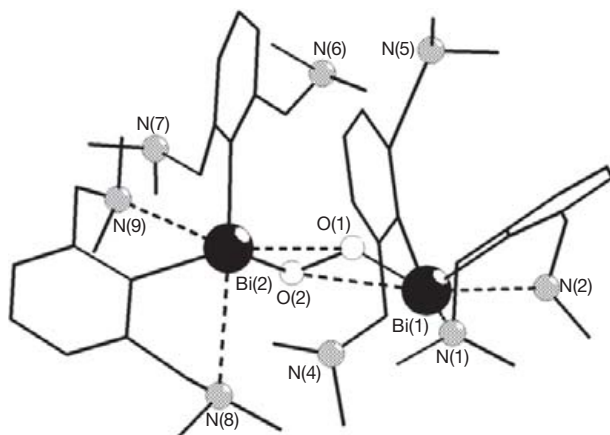
Many dipnicogen compounds are very air sensitive. For instance, the exposure of tetramethyldistibane to excess air leads to self-ignition, but with excess distibane the monoxide Me<sub>2</sub>SbOSbMe<sub>2</sub> or the acid Me<sub>2</sub>Sb(O)OH forms. Controlled air oxidation is equally performed when air is slowly introduced into the yellow solutions of tetraaryldistibanes R<sub>2</sub>Sb–SbR<sub>2</sub> (R = Ph, *o*-Tol, *p*-Tol) and the colorless oxides (R<sub>2</sub>Sb)<sub>2</sub>O are obtained as crystalline samples. Further oxidation leads to anhydrides of aryl stibinic acids of the type (R<sub>2</sub>Sb)<sub>4</sub>O<sub>6</sub>.<sup>62</sup>

The dibismuthanes LBi–BiL with LBi = RN(CH<sub>2</sub>C<sub>6</sub>H<sub>4</sub>)<sub>2</sub>Bi (R = Me, Bu<sup>t</sup>, Oct<sup>t</sup>) are also less air sensitive in the solid state, while in solution they quickly react with air oxygen to form the monoxide LBi–O–BiL.<sup>60</sup>

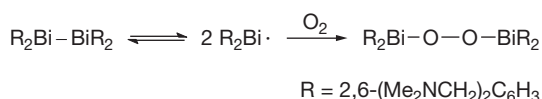
It has been well documented in older literature that reactions of distibanes and dibismuthanes R<sub>2</sub>E–ER<sub>2</sub> with dichalogenides RE′–E′R occur readily in an inert atmosphere, with quantitative formation of the mixed compounds R<sub>2</sub>E–E′R (E = Sb, Bi; E′ = S, Se, Te). A recent result is the formation of the thiolate LBi–SAr from ArS–SAr (Ar = aryl group) and LBi–BiL, respectively.<sup>60</sup>

Still, little is known of the mechanisms that are involved in the oxidation processes of the dipnicogen compounds. One possible mechanism involves insertion of dioxygen into the pnictogen–pnictogen bond. An example where the resulting peroxide was in fact isolated is the reaction of the dibismuthane with the two arm ligands R<sub>2</sub>Bi–BiR<sub>2</sub> (R = 2,6-(Me<sub>2</sub>NCH<sub>2</sub>)<sub>2</sub>C<sub>6</sub>H<sub>3</sub>), which with air gives the peroxide R<sub>2</sub>Bi–O–O–BiR<sub>2</sub>, probably via homolytic dissociation of the dibismuthane with formation of R<sub>2</sub>Bi· radicals that react with the dioxygen.<sup>44</sup> The structure of this peroxide, in which the dioxygen bridge adopts a close to ‘side-on’ coordination, is shown in Figure 5.

In addition to the insertion of dioxygen, further oxidation processes occur in which the organic substituents are involved. One of the pendant arms is transformed into an amine oxide and another is oxidized to a carboxyl group. It is very likely that the peroxide is involved in the unusual oxidizing processes of



**Figure 5** Structure of the central core of  $R_2BiO_2BiR_2$  ( $R = 2,6-(Me_2NCH_2)_2C_6H_3$ ).<sup>44</sup> Hydrogen atoms are omitted for clarity.



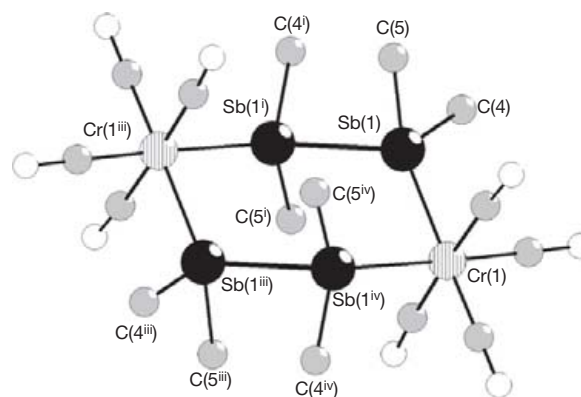
**Scheme 3** Possible reaction paths leading to the peroxide  $R_2BiO_2BiR_2$ .

the ligands that occur at room temperature and that it has potential as an oxidating agent in organic syntheses. The oxidation processes of  $R_2Bi-BiR_2$  ( $R = 2,6-(Me_2NCH_2)_2C_6H_3$ ) are shown in **Scheme 3**.<sup>44</sup>

Reduction of organometallic dipnicogen compounds occurs with group 1 or with group 2 metals. Recent examples are the diarsenic and diantimony species octaethyl-diarsolyl and distibolyl  $(EtC)_4E-E(CEt)_4$  ( $E = As, Sb; Et = C_2H_5$ ), which react with Mg and  $MgCl_2$  or Ca and  $CaCl_2$  with fission of the pnictogen–pnictogen bond and formation of magnesium or calcium chloride tetraethyl arsolide or stibolide  $(EtC)_4EMCl$  ( $M = Mg, Ca$ ), respectively. In the absence of the earth alkaline metal dihalides, no reaction is observed. For the larger metals, strontium and barium, the reduction of the  $(EtC)_4E-E(CEt)_4$  succeeds also in tetrahydrofuran without the addition of the halides and halogen-free metallocene complexes of Sr and Ba with  $\eta^5$ -coordinated tetraethylarsolide or stibolide ligands of the type  $[(EtC)_4E]_2M$  ( $E = As, Sb; M = Sr, Ba$ ) result.<sup>45</sup>

It is well known that tetraorganodiaranes and distibanes can be incorporated as intact donor ligands into transition metal carbonyl complexes and into adducts with main group element acceptors. Complexes with the weaker donors, tetraorganodibismuthanes, are known as adducts with group 13 metal Lewis acids of type  $R_3M$  ( $M = Al, In$ ).

A recent example of a transition metal carbonyl complex of a distibane ligand with a known crystal structure is the complex  $(CO)_4Cr(Me_2Sb-SbMe_2)_2Cr(CO)_4$ , which contains two bridging distibane ligands between chromium centers. The distibane complex was formed in a reaction between the tristibane  $2,6-Me_2C_6H_3Sb(SbMe_2)_2$  and  $Cr(CO)_4$ (norbornadiene). A polymer  $[(CO)_4Cr(Me_2Sb-SbMe_2)]_n$  is formed in the direct reaction between  $Cr(CO)_4$ (norbornadiene) and  $Me_2Sb-SbMe_2$ . The Sb–Sb bond length in the crystal structure of  $(CO)_4Cr(Me_2Sb-SbMe_2)_2Cr(CO)_4$  is 2.8157(11) Å. The structure is shown in **Figure 6**.<sup>63</sup>



**Figure 6** Structure of  $(CO)_4Cr(Me_2Sb-SbMe_2)_2Cr(CO)_4$ . Hydrogen atoms are omitted for clarity.<sup>63</sup>

The related complex with one tetramethyldistibane bridge, that is,  $(CO)_5CrMe_2Sb-SbMe_2Cr(CO)_5$ , has also been characterized by single-crystal x-ray crystallography. A remarkable feature is the substantial deviation from the ideal antiperiplaric (*trans*) conformation adopted by the free tetramethyldistibane. The value for the Sb–Sb bond length is 2.8097(9) Å, which is shorter than in noncoordinated crystalline  $Me_2Sb-SbMe_2$  (2.862(2) Å).<sup>64</sup>

Reactions of the distibanes  $R_2Sb-SbR_2$  ( $R = Me, Et, Me_3SiCH_2, 2-(Me_2NCH_2)C_6H_4, Me_3Si$ ) with the titanocene source  $Cp_2Ti(Me_3SiC\equiv SiMe_3)$  give various products. The most straightforward reaction leads to paramagnetic dimers  $(R_2SbTiCp_2)_2$  ( $R = Me, Et, Me_3Si$ ), probably with the insertion of a titanocene molecule into the Sb–Sb bond of a distibane followed by addition of a second titanocene molecule. The transannular antimony–antimony distances in these dimers  $(R_2SbTiCp_2)_2$  ( $R = Me, Sb \cdots Sb 3.4491(11) \text{ \AA}, R = Me_3Si, Sb \cdots Sb 3.7145(4) \text{ \AA}$ ) are shorter than the sum of the van der Waals radii of two antimony atoms ( $\Sigma_{vdw}(Sb, Sb) 4.4 \text{ \AA}$ ).<sup>47</sup> It is likely that in the case of the reactions of the distibanes  $R_2Sb-SbR_2$  ( $R = Me_3SiCH_2, 2-(Me_2NCH_2)C_6H_4$ ) with  $Cp_2Ti(Me_3SiC\equiv SiMe_3)$  dimers of the type  $(R_2SbTiCp_2)_2$  also form initially. Further reactions with rearrangement of the antimony skeleton and loss or migration of organic groups lead to the larger antimony titanium clusters  $(Cp_2Ti)_3(R_3Sb_4)$  or  $(Cp_2Ti)_5(R_2Sb_9)$ . Incorporated into the clusters are the catena Sb species of the types  $(RSb)_3Sb$  or  $(RSb)_2Sb_7$ .<sup>3</sup> The  $(RSb)_3Sb$  fragment represents a star-like geometry with three RSb units bonded to a central naked antimony atom and Sb–Sb bond lengths of 2.8267(4) Å. The central  $(RSb)_2Sb_7$  framework is composed of a tricyclic Sb<sub>7</sub> unit and two exocyclic RSb groups. The Sb–Sb bond lengths lie in the range 2.773(4)–2.850(3) Å. The formation of the TiSb clusters represents the successive construction of an antimony framework that can serve as model for the thermal decomposition of organoantimony compounds with Sb–Sb bonds.

The distibanes  $R_2Sb-SbR_2$  ( $R = Me_3SiCH_2, 2-(Me_2NCH_2)C_6H_4$ ) are thermally stable in the absence of catalysts. They decompose only at very high temperatures with formation of elemental antimony and other products. The rearrangement processes leading to clusters are probably favored by the presence of the paramagnetic titanocene complex species. A function of the titanocene groups is to bind and protect the

polyantimony species sterically.<sup>3,47</sup> An overview of the reactions between distibanes and the titanocene source is given in **Scheme 4**.

Fission of the Sb–Sb bonds occurs in reactions of distibanes  $R_2Sb-SbR_2$  ( $R = Et, Pr^i, Me_3SiCH_2$ ) with  $Fe_2(CO)_9$ , and multinuclear complexes composed of  $R_2Sb$  units and  $Fe(CO)_4$  or  $Fe(CO)_3$  fragments result. However, the pendant arm distibane  $R_2Sb-SbR_2$  ( $R = 2-(Me_2NCH_2)C_6H_4$ ) reacts with  $Fe_2(CO)_9$ , resulting in the formation of the stibinidene complex  $RSb[Fe(CO)_4]_2$ , which is stabilized through the close intramolecular coordination of the pendant dimethylamino group on the antimony center.<sup>65</sup>

$R(H)Sb-Sb(H)R$  ( $R = (Me_3Si)_2CH$ ) reacts with  $W(CO)_5$  (tetrahydrofuran) to give the crystalline isomers *meso*- and *D, L*- $(CO)_5W[R(H)Sb-Sb(H)R]W(CO)_5$ . The Sb–Sb bond lengths are 2.833(1) Å for the *meso*-form and 2.842(1) Å for the *D, L*-form. Heating the distibane complexes results in the evolution of  $H_2$  and formation of the distibene complex (*trans*- $RSb=SbR$ ) $W(CO)_5$ . The Sb–Sb bond length in the distibene complex is 2.7413(9) Å.

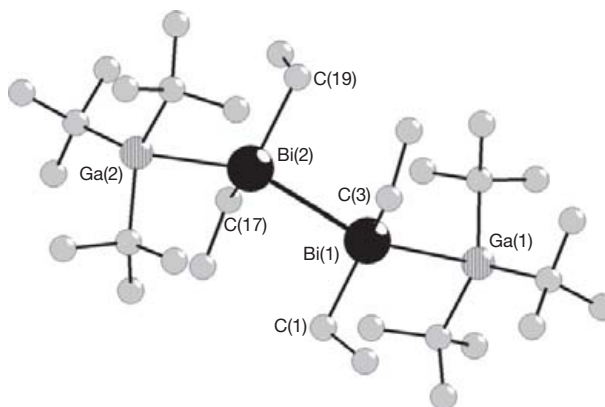
Reaction of  $R(H)Sb-Sb(H)R$  with MeI and diazidobutyronitrile results in the substitution of hydrogen by methyl groups with formation of the methylated distibane  $R(Me)Sb-Sb(Me)R$  as a mixture of the *meso*- and *D, L*-isomers.<sup>39</sup>

Tetraalkyldistibanes  $R_2Sb-SbR_2$  ( $R = Pr^i, Bu^i$ ) react with  $Bu^t_3M$  ( $M = Al, Ga$ ) at  $-30^\circ C$ , with the formation of the Lewis acid–base adducts  $Bu^t_3M(R_2Sb-SbR_2)MBu^t_3$  ( $M = Al, R = Pr^i, Bu^i; M = Ga, R = Pr^i, Pr^i$ ). The aluminum adducts  $Bu^t_3Al(R_2Sb-SbR_2)AlBu^t_3$  ( $R = Pr^i, Bu^i$ ) are stable in solution, whereas the gallium derivatives  $Bu^t_3Ga(R_2Sb-SbR_2)GaBu^t_3$  ( $R = Pr^i, Bu^i$ ) undergo a Sb–Sb bond-breakage reaction with the subsequent formation of the heterocycles  $[(Bu^t_2GaSbR)_2]_2$ . The Sb–Sb bond lengths in  $Bu^t_3Al(R_2Sb-SbR_2)AlBu^t_3$  ( $R = Pr^i, 2.839(1) \text{ \AA}; R = Bu^i, 2.822(5) \text{ \AA}$ ) are almost identical to those of pure distibanes, for example,  $Me_2Sb-SbMe_2$  (2.862(2)–2.838(1) Å). The most significant structural change of the distibane moiety due to the adduct formation is the increase of the

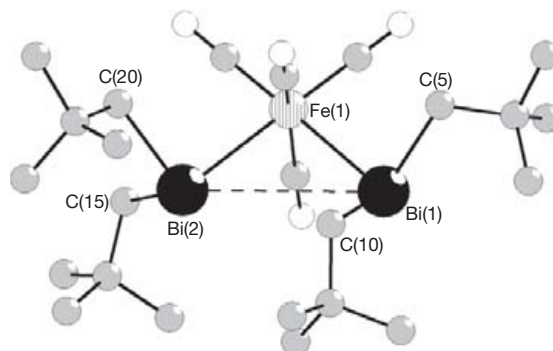
degree of pyramidalization of the central Sb atoms. The sums of the C–Sb–C and C–Sb–Sb bond angles observed for  $Bu^t_3Al(R_2Sb-SbR_2)AlBu^t_3$  ( $R = Pr^i, 292.2^\circ; R = Bu^i, 290.6^\circ$ ) are significantly increased compared with uncomplexed distibanes such as  $Me_2Sb-SbMe_2$  (283.1°), resulting from an increase in p character of the former Sb electron lone pair and an increase in s character of the former Sb–C and Sb–Sb bonding electron pairs. Similar reactions occur also between  $R_2Sb-SbR_2$  ( $R = Me, Et$ ) and  $R_3M$  ( $M = Al, Ga, In; R = Me, Pr^i, Pr^i, Bu^i$ ) yielding adducts  $R_3M(R_2Sb-SbR_2)MR_3$ . The adducts are unstable in solution toward the formation of heterocycles of the type  $(R_2SbMR_2)_n$  ( $n = 2, 3$ ).<sup>66–68</sup>

The adducts  $Bu^t_3M(Et_2Bi-BiEt_2)M^iBu_3$  ( $M = Al, Ga$ ) are formed from  $Et_2Bi-BiEt_2$  and  $M^iBu_3$  at  $-78^\circ C$  in *n*-pentane. These adducts are exceptional as complexes with intact dibismuthane ligands. The gallium compound is stable at  $-30^\circ C$  for weeks, whereas the aluminum compound decomposes under these conditions. In the crystal, both adducts adopt a staggered conformation with the  $MBu^t_3$  groups in *trans* positions. The structure of  $Bu^t_3Ga(Et_2Bi-BiEt_2)GaBu^t_3$  is shown in **Figure 7**. The value for the Bi–Bi bond length is 2.983(1) Å.<sup>69</sup>

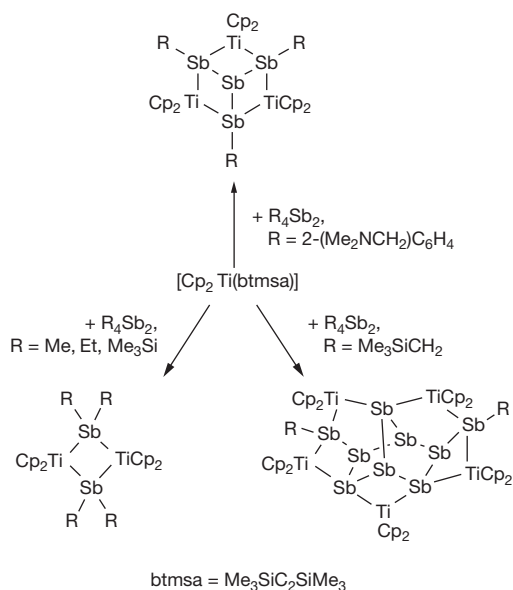
The reaction of the dibismuthane  $R_2Bi-BiR_2$  ( $R = Me_3CCH_2$ ) with  $Fe_2(CO)_9$  leads to the fission of the Bi–Bi bond and formation of  $(R_2Bi)_2Fe(CO)_4$ .<sup>70</sup> The structure of  $(R_2Bi)_2Fe(CO)_4$  is shown in **Figure 8**. With a Bi–Bi distance of 3.9581(10) Å, the complex is better described as an octahedral iron complex with



**Figure 7** Structure of  $Bu^t_3Ga(Et_2Bi-BiEt_2)GaBu^t_3$ .<sup>69</sup> Hydrogen atoms are omitted for clarity.



**Figure 8** Structure of  $(R_2Bi)_2Fe(CO)_4$  ( $R = Me_3CCH_2$ ).<sup>70</sup> Hydrogen atoms are omitted for clarity.



**Scheme 4** Reactions between distibanes and a titanocene source.

two  $R_2Bi$  ligands in *cis* positions. The alternative description, that is, an  $Fe(CO)_4$  complex with dibismuthane ligand 'side-on' coordinated through the electrons of the Bi–Bi bond, enjoys less support from the geometric parameters, although this type of coordination should lead to considerable elongation of the Bi–Bi  $\sigma$  bond.

### 1.05.3 Monocycles $(RE)_n$ (E = As, Sb, Bi)

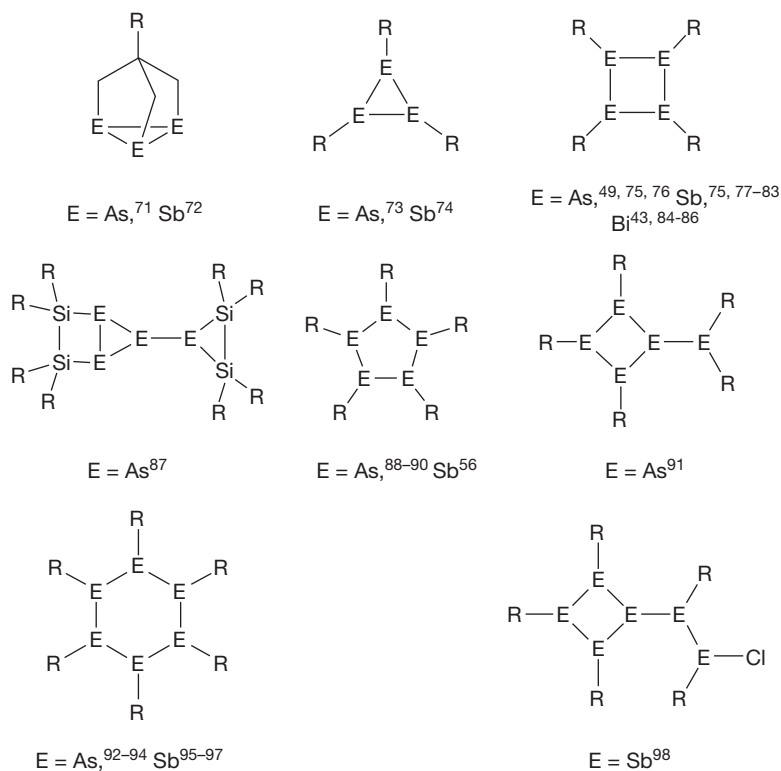
An overview of the types of monocycles with structures established by single-crystal x-ray crystallography, including rings with the size  $n = 3-6$  and monocycles with pnictogen  $R_2E^-$ ,  $RE(Cl)^-$ ,  $RE^-$  groups as substituents, is given in Scheme 5.

For arsenic and antimony, the three-membered rings (triarsiranes and tristibiranes) are well established, but no tribismirane with a known crystal structure has been reported, although three-membered bismuth rings exist in solution. Generally, the formation of three-membered rings is less favored because the geometry of these trimers requires  $E_3$  (E = As, Sb, Bi) angles close to  $60^\circ$  and *cis*-positions for the substituents. However, this difficulty can be overcome by the use of appropriate substituents, such as the bis(trimethylsilyl)methyl group. The asymmetrical shape of this group is particularly suitable for three-membered rings because it combines sterical protection in the ring periphery with little sterical tension inside the ring. Larger rings with an even number of ring members, allowing the formation of all-*trans* isomers, are more favorable. It is therefore not surprising that four-membered rings are known for As, Sb, and Bi, with bulky substituents adopting a trigonal cone symmetry, as in the case of the tertiary butyl group or

tertiary silyl or stannyl groups  $R_3M$  (R =  $Me_3Si$ ,  $Me_3Sn$ , M = Si, Sn). Five-membered rings with arsenic are well known, but only one five-membered antimony homocycle, namely, *cyclo*-(RSb) $_5$  (R =  $Me_3CCH_2$ ), was characterized by crystallography, though five-membered antimony rings were frequently detected in solution. Crystals of a five-membered ring were also obtained for  $(Me_3SiCH_2Sb)_5$ ; however, disorder phenomena hindered the complete crystallographic characterization. This ring was, however, fully characterized in the coordination sphere of a transition metal carbonyl complex.

Six-membered rings with known crystal structures were already repeatedly reported in the older literature for As and Sb. Phenyl- or tolyl-groups favor the formation of *cyclo*-hexamers in the crystalline state. In solution, the *cyclo*-hexamers  $(RSb)_6$  participate in ring–ring equilibria with pentamers. Six-membered bismuth rings (hexabismuthanes) are still unknown and represent a challenge for future work. Recent approaches for the syntheses of bismuth rings imply the use of extremely bulky ligands that favor more the formation of smaller rings or dimers with Bi=Bi double bonds. Isolated homocycles with more than six members are not known as crystalline species. However, the nine-membered arsenic ring  $(MeAs)_9$  was stabilized as a ligand in the complex  $(MeAs)_9Cr_2(CO)_6$ .<sup>5</sup>

Common methods for the syntheses of monocycles  $(RE)_n$  (E = As, Sb, Bi) include reduction of organopnictogen dihalides with magnesium or other metals, elimination of  $H_2$  from  $REH_2$ , or reactions between pnictogen trihalides with lithium organyl or silyl reagents, which combine methathesis and reduction.  $H_2$  elimination occurs readily at low temperatures with bismuthanes  $RBiH_2$ . For analogous reactions of primary stibanes  $RSbH_2$ , the use of catalysts is preferred.



Scheme 5 Types of monocycles with known crystal structures.



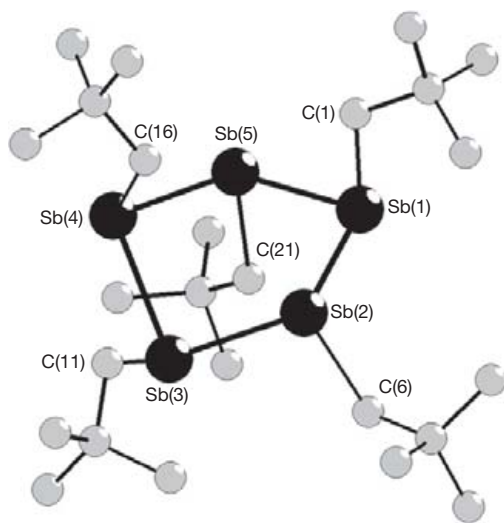
Examples for sterically less protected antimony rings are the isobutyl compounds  $cyclo\text{-(RSb)}_n$  ( $R = \text{Me}_2\text{CHCH}_2$ ,  $n = 4, 5$ ), which are obtained from  $\text{RSbBr}_2$  and Mg in tetrahydrofuran. In benzene solutions, the five-membered ring is the dominant species.<sup>41</sup>

Dehalogenation of  $\text{RSbBr}_2$  ( $R = \text{Me}_3\text{CCH}_2$ ) with Mg gives  $cyclo\text{-(RSb)}_n$  ( $n = 4, 5$ ). Equilibria between the four-membered and the five-membered rings favor the smaller ring at higher temperature and dilution. The crystal structure of  $(\text{RSb})_5$  ( $R = \text{Me}_3\text{CCH}_2$ ) is shown in Figure 9. The structure contains the five-membered antimony ring in a close to envelope conformation. The Sb–Sb bond lengths range from 2.812(3) to 2.820(3) Å. The neopentyl substituents adopt a maximum of *trans* positions.<sup>56</sup>

Protection of cyclic structures is also achieved with potentially bidentate or tridentate pendant arm ligands that can be coordinated to the pnictogen atoms not only through normal  $\sigma$ -bonds with carbon, but also through dative bonds from nitrogen.

Stabilization by a potentially bidentate (one-arm ligand) is achieved in the *cyclo*-stibane  $(\text{RSb})_4$  ( $R = 2\text{-(Me}_2\text{NCH}_2\text{)C}_6\text{H}_4$ ) that is formed by reduction of  $\text{RSbCl}_2$  with Mg in tetrahydrofuran or with Na in liquid ammonia. Crystals of the cyclostibane consist of folded four-membered  $\text{R}_4\text{Sb}_4$  rings with the organic substituent in the all-*trans* configuration. All pendant amino groups are coordinated to the antimony centers. Probably due to steric strain in the ring, the Sb–Sb bond lengths differ, ranging between 2.8474(5) and 2.8605(4) Å.  $(\text{RSb})_4$  ( $R = 2\text{-(Me}_2\text{NCH}_2\text{)C}_6\text{H}_4$ ) belongs to the family of sterically protected antimony rings that do not easily participate in ring–ring equilibria.<sup>77</sup>

The four-membered cycle  $(\text{RSb})_4$  ( $R = 2,6\text{-(Me}_2\text{NCH}_2\text{)}_2\text{C}_6\text{H}_3$ ) with a potentially tridentate (two arm) ligand is obtained by reduction of  $\text{RSbCl}_2$  with  $\text{K[B(Bu}^t\text{)}_3\text{H]}$ , probably via intermediate formation of  $\text{RSbH}_2$ .  $(\text{RSb})_4$  ( $R = 2,6\text{-(Me}_2\text{NCH}_2\text{)}_2\text{C}_6\text{H}_3$ ) is a folded  $\text{Sb}_4$  ring similar to the analogue with the one-arm substituent ( $R = 2\text{-(Me}_2\text{NCH}_2\text{)C}_6\text{H}_4$ ). Six of the eight amino groups in the crystal structure of  $(\text{RSb})_4$



**Figure 9** Crystal structure of  $(\text{RSb})_5$  ( $R = \text{Me}_3\text{CCH}_2$ ).<sup>56</sup> Hydrogen atoms are omitted for clarity.

( $R = 2,6\text{-(Me}_2\text{NCH}_2\text{)}_2\text{C}_6\text{H}_3$ ) are weakly coordinated to antimony atoms.<sup>83</sup>

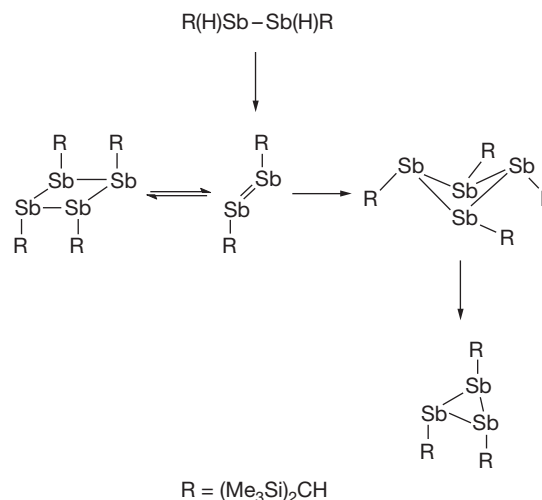
Functionalized cyclotriarsanes  $(\text{RAs})_3$  ( $R = \text{HB(3,5-Me}_2\text{pz)}_3(\text{CO})_2\text{M}\equiv\text{C-}$ ) are obtained from arsaalkenes and  $\text{Au(CO)Cl}$ .<sup>73</sup>

The tritibirane  $cyclo\text{-R}_3\text{Sb}_3$  ( $R = (\text{Me}_3\text{Si})_2\text{CH}$ ) is formed by reduction of  $\text{RSbCl}_2$  with  $\text{Li}_3\text{Sb}$ . The tritibirane forms also by photochemical ring contraction of  $cyclo\text{-(RSb)}_4$  or from the polycycle  $\text{R}_4\text{Sb}_8$ .<sup>39</sup>

The reaction of  $(\text{Me}_3\text{Si})_3\text{SiK-18-crown-6}$  with  $\text{SbCl}_3$  [3:1 equiv.] gives the *cyclo*-tetrastibane  $[(\text{Me}_3\text{Si})_3\text{SiSb}]_4$ . In this method, the silylation of the antimony center and the reduction are both affected by the silyl lithium reagent. The Sb–Sb bond lengths in the ring (average 2.86 Å) are at the upper end of the range seen for Sb–Sb distances in other  $\text{Sb}_4$  ring systems (2.75–2.88 Å) and the ring plane puckering angle is an average of 41.23°, which is at the lower end of the range of fold angles seen in these ring systems (which range from 76° to 36°). These observations are consistent with the  $[(\text{Me}_3\text{Si})_3\text{Si}]$  group being a very bulky group and as such the  $\text{Sb}_4$  ring is much closer to planarity than in other examples.<sup>79</sup>

The zirconocene complexes  $[\text{Cp}_2\text{Zr(H)Cl}]$  and  $[\text{Cp}_2\text{ZrMe}_2]$  ( $\text{Cp} = \text{cyclopentadienyl}$ ) react with  $\text{MesSbH}_2$  in  $\text{C}_6\text{D}_6$  to liberate  $\text{H}_2$  and produce the *cyclo*-tetrastibane  $cyclo\text{-(MesSb)}_4$  in high yield. The ring formation probably proceeds with a catalytic antimony–antimony bond coupling through stibinidene elimination from the zirconocene complexes.<sup>99</sup>

A source of four- and three-membered antimony rings is the distibane  $\text{R(H)Sb-Sb(H)R}$  ( $R = (\text{Me}_3\text{Si})_2\text{CH}$ ), which eliminates dihydrogen to form the distibene  $\text{RSb}=\text{SbR}$  as a probable intermediate. Rapid dimerization of the distibene leads to the unique *cis-trans* *cyclo*-tetrastibane  $cyclo\text{-(RSb)}_4$ . Structural features of this ring are a square planar  $\text{Sb}_4$  unit and two pairs of organic groups in *cis* positions above and below the plane of the antimony atoms. This result exemplifies the suitability of the  $(\text{Me}_3\text{Si})_2\text{CH}$  group for *cis* arrangements in Sb homocycles. Slow dimerization of  $\text{RSb}=\text{SbR}$  leads to all-*trans* *cyclo*- $(\text{RSb})_4$ . Photochemical ring contraction of this *cyclo*-tetrastibane gives the three-membered ring *cyclo*- $(\text{RSb})_3$ . The reactions are shown in Scheme 6.<sup>39</sup>



**Scheme 6** Reactions of the distibane  $\text{R(H)Sb-Sb(H)R}$ .

The reaction of  $\text{RSbCl}_2$  ( $\text{R} = (\text{Me}_3\text{Si})_2\text{CH}$ ) with Na–K alloy gives the rings  $\text{cyclo}-(\text{SbR})_n$  ( $n = 3, 4$ ) and the unique pentaalkylchlorohexastibane  $\text{Sb}_6\text{R}_5\text{Cl}$ . The structure of  $\text{Sb}_6\text{R}_5\text{Cl}$  consists of a monocyclic  $\text{Sb}_4\text{R}_3$  unit and a linear  $\text{Sb}_2\text{R}_2\text{Cl}$  unit.<sup>98</sup> The structure is depicted in Figure 10. The Sb–Sb bond lengths are in the range 2.837(1)–2.872(2) Å.

The cyclobismuthanes  $\text{cyclo}-(\text{RBi})_n$  ( $\text{R} = \text{Me}_3\text{CCH}_2$ ,  $\text{Me}_3\text{SiCH}_2$ ;  $n = 3, 5$ ) form by reaction of  $\text{RBiCl}_2$  with  $\text{LiAlH}_4$ , with intermediate formation of  $\text{RBiH}_2$ . Elimination of dihydrogen occurs readily with a color change to red when the solutions of the hydrides, which are prepared from  $\text{RBiCl}_2$  and  $\text{LiAlH}_4$  at  $-78^\circ\text{C}$ , are warmed above  $-30^\circ\text{C}$ . The rings represent cyclobismuthanes with less sterically demanding substituents. Their chemical behavior gives insight into the chemistry of bismuth ring systems that are not fixed in an environment of bulky substituents. It is remarkable that ring-ring equilibria in solution exist between the three-membered and the five-membered bismuth rings.<sup>56,100</sup> In contrast, the four-membered ring  $(\text{RBi})_4$  ( $\text{R} = (\text{Me}_3\text{Si})_2\text{CH}$ ) with the bis(trimethylsilyl)methyl group takes part in a ring-ring equilibrium with the three-membered ring.

A four-membered bismuth ring  $\text{cyclo}-(\text{RBi})_4$  with bulky silyl substituents ( $\text{R} = \text{Si}(\text{SiMe}_3)_3$ ) was obtained, along with R–R, from  $\text{LiR}$  and  $\text{BiBr}_3$ . The ring is thermally and photochemically remarkably stable, showing no tendency for dissociation. The ring consists of a folded  $\text{Bi}_4$  core and the silyl groups in *trans* positions. The Bi–Bi bonds lie in the narrow range 3.013(1)–3.028(1) Å.

The analogous ring  $(\text{Bu}^t_3\text{SiBi})_4$  is obtained from  $\text{Bu}^t_3\text{SiNa}$  and  $\text{BiBr}_3$  with  $\text{Bu}^t_3\text{Si}-\text{Si}^t\text{Bu}_3$  and anionic bismuth species as additional products. Also,  $(\text{Bu}^t_3\text{SiBi})_4$  is a folded tetrabismethane with the bulky silyl groups in *trans* positions. The Bi–Bi distances range from 3.013(1) to 3.038(2) Å.<sup>84,85</sup>

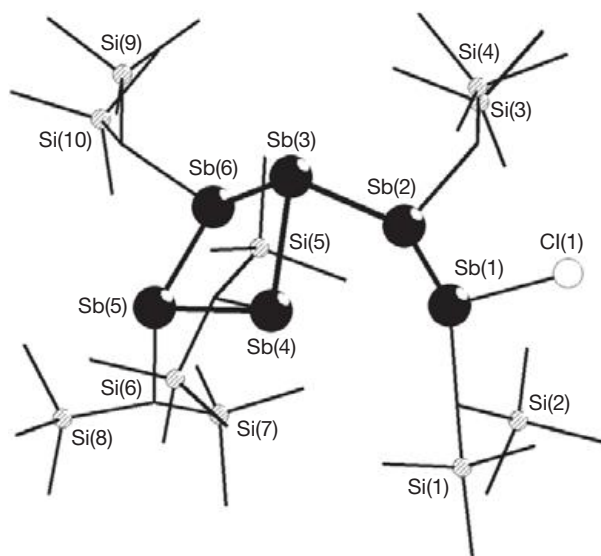
The pendant arm  $\text{cyclo}$ -bismuthanes  $\text{cyclo}-(\text{RBi})_n$  ( $\text{R} = 2-(\text{Me}_2\text{NCH}_2)\text{C}_6\text{H}_4$ ;  $n = 3, 4$ ) form by reduction of  $\text{RBiCl}_2$  with Na in liquid ammonia or by reaction of  $\text{R}_2\text{BiCl}$  with  $\text{LiAlH}_4$  in  $\text{Et}_2\text{O}$ . The latter method probably involves the intermediate

formation of  $\text{R}_2\text{BiH}$  and elimination of  $\text{RH}$ . The crystal structure determination of  $\text{cyclo}-(\text{RBi})_4$  reveals the intramolecular coordination of the pendant  $\text{Me}_2\text{NCH}_2$  groups to the bismuth atom. The structure of  $\text{cyclo}-(\text{RBi})_4$  ( $\text{R} = 2-(\text{Me}_2\text{NCH}_2)\text{C}_6\text{H}_4$ ) is shown in Figure 11. The Bi–Bi bond lengths lie in the range 3.0095(16)–3.0221(16) Å. The ring is folded, with  $\text{Bi}_3$ – $\text{Bi}_3$  dihedral angles of 107.9 and 109.4°. NMR analyses reveal that there is an equilibrium in solution between the four-membered ring and the three-membered bismuth ring  $\text{cyclo}-(\text{RBi})_3$  ( $\text{R} = 2-(\text{Me}_2\text{NCH}_2)\text{C}_6\text{H}_4$ ); however, only the four-membered ring is present in the crystalline phase. Crystals of the four-membered ring are stable at room temperature, but solutions decompose readily, with formation of the dibismuthane  $\text{R}_2\text{Bi}-\text{BiR}_2$  ( $\text{R} = 2-(\text{Me}_2\text{NCH}_2)\text{C}_6\text{H}_4$ ) and metallic bismuth.<sup>43</sup>

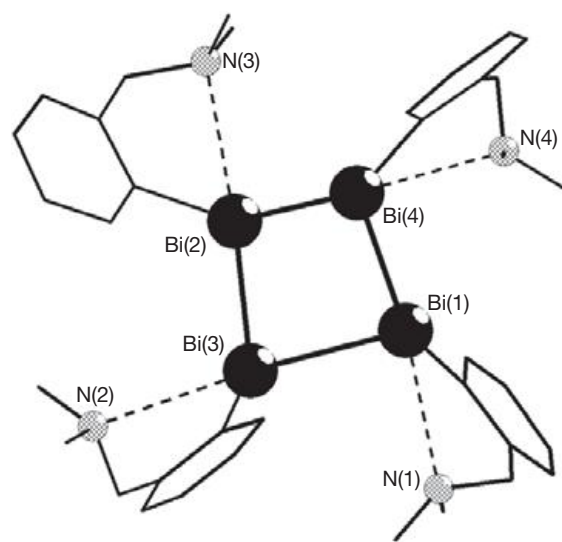
Various synthetic pathways lead to the arsenic four-membered ring  $(\text{MesAs})_4$  ( $\text{Mes} = 2,4,6-\text{Me}_3\text{C}_6\text{H}_2$ ), which is formed by reduction of  $\text{MesAsCl}_2$  with Mg in tetrahydrofuran by catalytic dehydrocoupling of  $\text{MesAsH}_2$  in the presence of zirconium complexes  $(\text{N}_3\text{N})\text{Zr}$  or  $(\text{N}_3\text{N})\text{ZrAsHMes}$  ( $\text{N}_3\text{N} = \text{N}(\text{CH}_2\text{CH}_2\text{NSiMe}_3)_3$ ) or by thermal decomposition of  $(\text{N}_3\text{N})\text{ZrAsHMes}$  via elimination of mesitylarsinidene  $\text{MesAs}$ .  $(\text{MesAs})_4$  is a folded four-membered ring with the mesityl substituents in *trans* positions. The average As–As bond length is 2.4843(6) Å.<sup>49</sup>

Monocycles  $(\text{RE})_n$  ( $\text{E} = \text{As, Sb, Bi}$ ) can be sources for mono or dipnicogen species or pnicogen chains. Such fragments are frequently trapped with suitable reagents including dienes or transition metal complexes. Complexes with intact  $\text{cyclo}-(\text{ER})_n$  ligands are known only for cyclo-arsanes and cyclo-stibanes. Upon complexation, cyclobismuthanes are transformed to  $\text{RBi}$ ,  $\text{RB}=\text{BiR}$ , or unsubstituted Bi ligands. Types of complexes with cycloarsanes and cyclostibanes as ligands are depicted in Scheme 7.

An example for the formation and trapping of a dipnicogen compound from a monocycle is the photolysis of tetrakis(trifluoromethyl)cyclotetraarsane  $(\text{F}_3\text{CAs})_4$  with formation of the diarsene  $\text{F}_3\text{CAs}=\text{AsCF}_3$ . The [4+2]-cycloaddition reaction

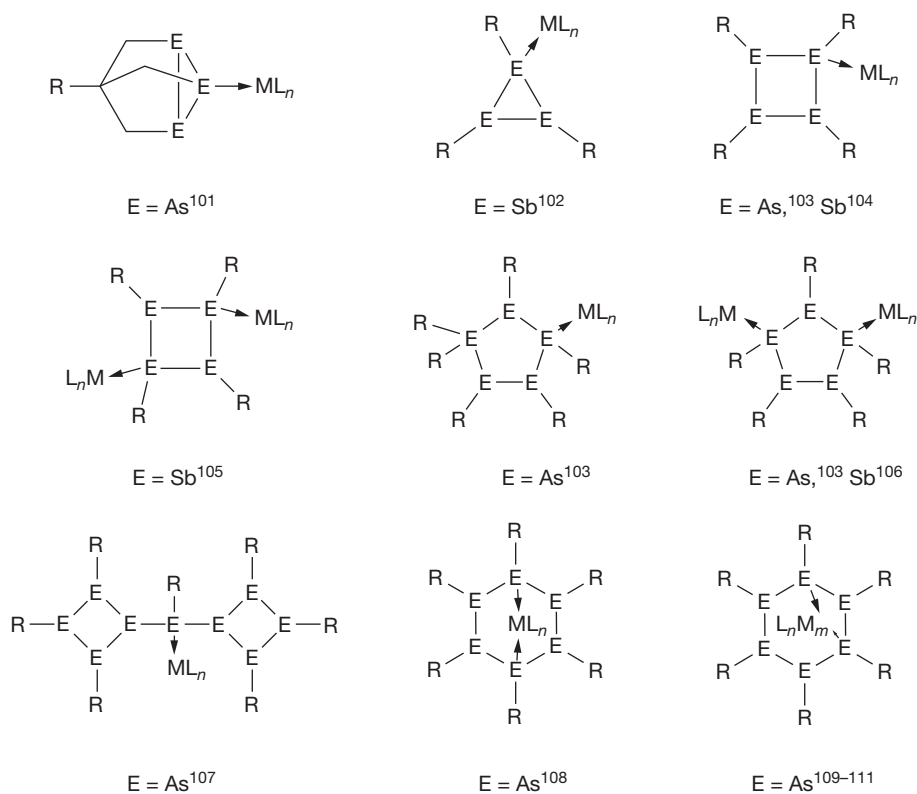


**Figure 10** Structure of  $\text{Sb}_6\text{R}_5\text{Cl}$  ( $\text{R} = (\text{Me}_3\text{Si})_2\text{CH}$ ).<sup>98</sup> Hydrogen atoms are omitted for clarity.

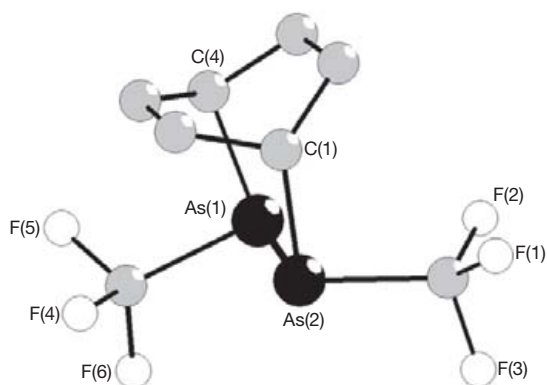


**Figure 11** Structure of  $\text{cyclo}-(\text{RBi})_4$  ( $\text{R} = 2-(\text{Me}_2\text{NCH}_2)\text{C}_6\text{H}_4$ ).<sup>43</sup> Hydrogen atoms are omitted for clarity.





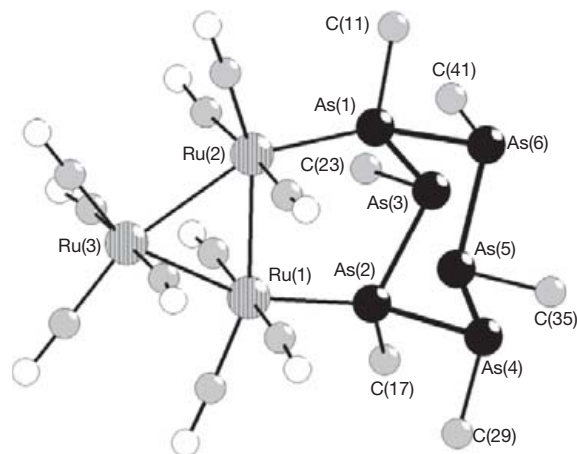
**Scheme 7** Types of complexes with *cyclo*-arsanes and *cyclo*-stibanes as ligands.



**Figure 12** Structure of the *cyclo*-adduct of  $F_3CAs=AsCF_3$  and cyclohexa-1,3-diene.<sup>112</sup> Hydrogen atoms are omitted for clarity.

of the diarsene with cyclohexa-1,3-diene gives the corresponding *cyclo*-adduct which contains the diarsene group in its *E*-configuration. The structure of the *cyclo*-adduct is shown in **Figure 12**. The value for the As–As bond length in the adduct is 2.427(3) Å.<sup>112</sup>

The cyclotetraarsane  $(F_3CAs)_4$  is also a precursor for the ‘side-on’ diarsene complex  $\eta^2-(F_3CAs=AsCF_3)(Ph_3P)_2Pd$ . The As–As bond length of 2.341(1) Å in the complex is the average of the single-bond value in  $(F_3CAs)_4$  (2.45 Å) and the double-bond value in  $Mes^*As=AsCH(SiMe_3)_2$  ( $Mes^*=2,4,6-Bu^t_3C_6H_2$ ) (2.22 Å), as expected for ‘side-on’ coordination. In comparison to the above-mentioned representatives, the bond



**Figure 13** Structure of  $[Ru_3\{\mu_2-cyclo-(PhAs)_6\}(CO)_{10}]$ .<sup>111</sup> For clarity, only the *ipso* carbon atoms (labeled) are shown.

length, due to less bulky substituents, is reduced by 0.03–0.05 Å.<sup>112</sup>

Coordination of an intact *cyclo*-hexaarsane occurs in the reaction of the sulfur-capped dicobalt–iron complex  $[Co_2Fe(\mu_3-S)(CO)_9]$  with *cyclo*-(PhAs)<sub>6</sub> in toluene at 70 °C to give  $[Co_2Fe(\mu_3-S)\{\mu_2-cyclo-(PhAs)_6\}(CO)_7]$  as the only product in good yield.<sup>110</sup>

Also, reaction of  $[Ru_3(CO)_{10}(NCMe)_2]$  with *cyclo*-(PhAs)<sub>6</sub> in toluene at ambient temperature results in coordination of the intact arsenic rings in the complex  $[Ru_3\{\mu_2-cyclo-(PhAs)_6\}(CO)_{10}]$  (**Figure 13**), in which rings adopt a chair conformation

and bridge metal–metal edges of a  $\text{Ru}_3$  core via two arsenic atoms in the 1,5-positions of the *cyclo*-hexaarsane ring. The average As–As–As angle of  $93.58^\circ$  in the arsenic ring is close to that in *cyclo*-(PhAs)<sub>6</sub> ( $91.08^\circ$ ). The As–As bond lengths lie in the range 2.456(2)–2.487(2) Å.

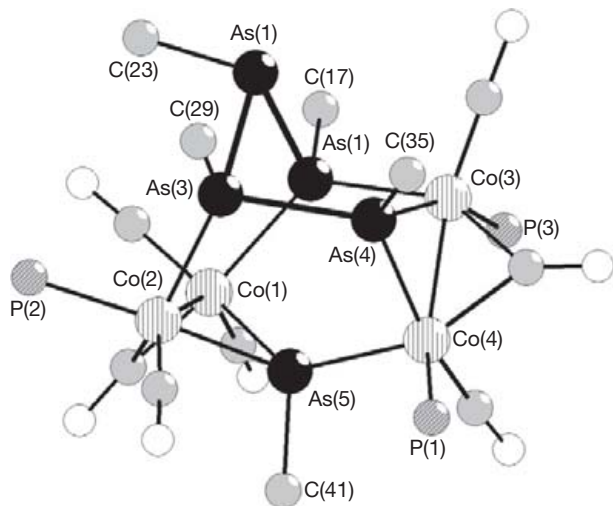
Conversely, treatment of  $[\text{Ru}_3(\text{CO})_{12}]$  with *cyclo*-(PhAs)<sub>6</sub> in toluene at elevated temperature results in fragmentation of the six-membered rings to afford  $[\text{Ru}_4(\mu_3\text{-AsPh})_2(\text{CO})_{13}]$ . Fragmentation of the *cyclo*-hexaarsane ring also occurs on reaction with  $[\text{Fe}_3(\text{CO})_{12}]$  in toluene at elevated temperature to furnish  $[\text{Fe}_3(\mu_3\text{-AsPh})_2(\text{CO})_9]$  as the sole product.<sup>111</sup>

*cyclo*-(AsPh)<sub>6</sub> reacts with  $[\text{Co}_2(\text{CO})_8]$  in toluene in a sealed tube at  $90^\circ\text{C}$  to give the cobalt cluster  $[\text{Co}_4(\text{AsPh-As}_4\text{Ph}_4)(\text{CO})_{10}]$ . Further thermolysis leads to  $[\text{Co}_4(\text{AsPh})_2(\text{As}_2\text{Ph}_2)(\text{CO})_{10}]$ , in which the tetraarsane chain has been cleaved to give the bridging PhAs–AsPh unit. Similar fragmentation of the As<sub>4</sub>Ph<sub>4</sub> chain occurs on treatment with  $[\text{Fe}_2(\text{CO})_9]$  in benzene, affording  $[\text{Co}_4(\text{AsPh})_2(\text{As}_2\text{Ph}_2)\text{Fe}(\text{CO})_4](\text{CO})_{10}$ . In contrast, reaction of  $[\text{Co}_4(\text{AsPh-As}_4\text{Ph}_4)(\text{CO})_{10}]$  with excess P(OMe)<sub>3</sub> gives  $[\text{Co}_4(\text{AsPh})(\text{As}_4\text{Ph}_4)(\text{CO})_7\{\text{P}(\text{OMe})_3\}_3]$ , in which the As<sub>4</sub>Ph<sub>4</sub> chain remains intact (Figure 14).<sup>113</sup>

Remarkable differences emerge in reactions of analogous cyclostibanes or cyclobismuthanes with Me<sub>3</sub>CCH<sub>2</sub> or Me<sub>3</sub>SiCH<sub>2</sub> substituents. *cyclo*-(RSb)<sub>5</sub> (R = Me<sub>3</sub>SiCH<sub>2</sub>) reacts with W(CO)<sub>5</sub>(tetrahydrofuran) to form  $\mu_2$ -*cyclo*-(RSb)<sub>5</sub>(W(CO)<sub>5</sub>)<sub>2</sub>, a complex where the intact antimony ring is preserved. The structure is shown in Figure 15.<sup>56,114</sup>

In contrast, the analogous bismuth rings *cyclo*-(RBi)<sub>n</sub> (R = Me<sub>3</sub>CCH<sub>2</sub>, Me<sub>3</sub>SiCH<sub>2</sub>; n = 3, 5) react with W(CO)<sub>5</sub>(tetrahydrofuran) to give the *cis*- and *trans*-isomers of 'side-on' dibismuthene complexes (RBi)<sub>2</sub>[W(CO)<sub>5</sub>]<sub>2</sub>. The structure of the complex with R = Me<sub>3</sub>SiCH<sub>2</sub> is shown in Figure 16. The Bi–Bi bond length in this complex (3.0024(7) Å) corresponds to the value of a Bi–Bi single bond.<sup>56,100</sup>

Reactions of *cyclo*-(RBi)<sub>n</sub> (R = Me<sub>3</sub>CCH<sub>2</sub>; n = 3, 5) with Fe<sub>2</sub>CO<sub>9</sub> lead to the four-membered heterocycle  $[\text{RBiFe}(\text{CO})_4]_2$ . The rings *cyclo*-(RBi)<sub>n</sub> (R = Me<sub>3</sub>SiCH<sub>2</sub>; n = 3, 5) are transformed to naked Bi<sub>2</sub> units on irradiation with ultraviolet (UV) light in



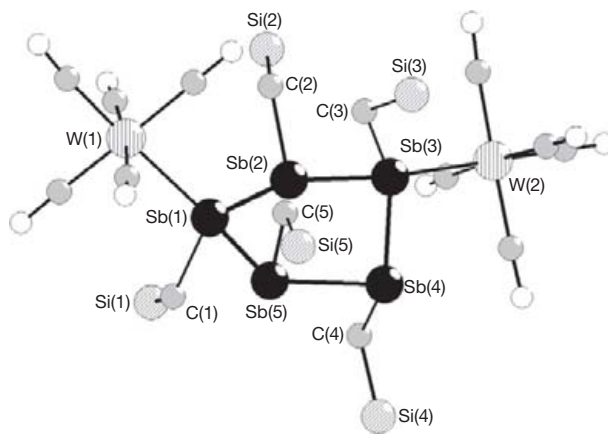
**Figure 14** Structure of  $[\text{Co}_4(\text{AsPh})(\text{As}_4\text{Ph}_4)(\text{CO})_7\{\text{P}(\text{OMe})_3\}_3]$ .<sup>113</sup> The methoxy and the phenyl (except *ipso* carbon atoms) groups are omitted for clarity.

the presence of  $\text{MeC}_5\text{H}_4\text{Mn}(\text{CO})_2$ (tetrahydrofuran) and the dibismuth complex  $(\text{Bi})_2[\text{Mn}(\text{CO})_2(\text{MeC}_5\text{H}_4)]_3$  forms.<sup>70,115</sup>

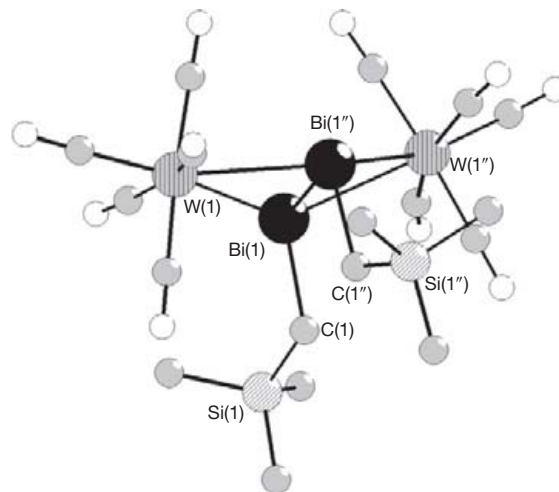
Closely related is the coordination chemistry for Sb- and Bi-homocycles with the pendant arm 2-(dimethylamino-methyl)phenyl ligand. Reactions of *cyclo*-(RE)<sub>n</sub> (R = 2-(Me<sub>2</sub>NCH<sub>2</sub>)C<sub>6</sub>H<sub>4</sub>; E = Sb, n = 4; E = Bi, n = 3, 5) with W(CO)<sub>5</sub>(tetrahydrofuran) give the analogous stibinidene and bismuthinidene complexes RE[W(CO)<sub>5</sub>]<sub>2</sub> (E = Sb, Bi), both of which are stabilized through the intramolecular coordination of the pendant dimethylamino group on the pnictogen centers.<sup>43,77</sup>

Copolymerization of *cyclo*-(MeAs)<sub>5</sub> with phenylacetylene occurs without any added catalyst or radical initiator at  $25^\circ\text{C}$  in chloroform to give an organoarsenic polymer having a methylarsine (MeAs) unit and a vinylbenzene unit alternating in the main chain,  $-\text{[AsMe-CH=CPh]}_n-$ .<sup>116</sup>

Analogous polymerization reactions between pentamethylcyclopentarsane or hexaphenylcyclohexaarsane with phenylacetylene or other acetylene derivatives also occur in the presence of a catalytic amount of 2,2-azobisisobutyronitrile (AIBN). Styrene and 2,3-dimethyl-1,3-butadiene can also be incorporated in the polymers.<sup>117–119</sup>



**Figure 15** Structure of  $\mu_2$ -*cyclo*-(RSb)<sub>5</sub>(W(CO)<sub>5</sub>)<sub>2</sub>.<sup>56</sup> Methyl groups are omitted for clarity.

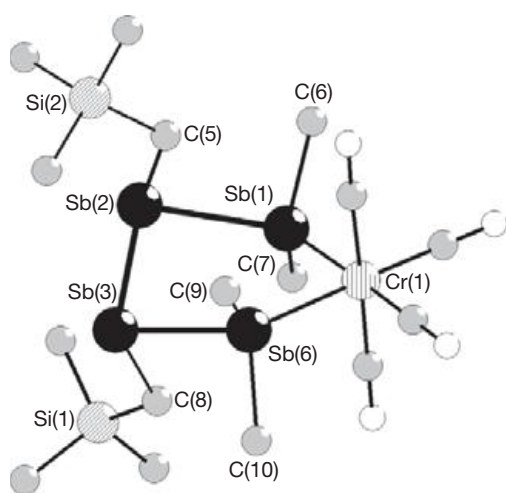


**Figure 16** Structure of  $(\text{Me}_3\text{SiCH}_2\text{Bi})_2[\text{W}(\text{CO})_5]_2$ .<sup>56</sup> Hydrogen atoms are omitted for clarity.

### 1.05.4 Catena Tri- and Tetra-Pnicogen Compounds and Extended Chains (RE)<sub>x</sub> (E = As, Sb, Bi)

Catena species of the type R<sub>2</sub>E(ER)<sub>n</sub>ER<sub>2</sub> (n = 1, 2) have recently been investigated for E = Sb. Unless protected by bulky substituents, these chain compounds exist in ring-chain equilibria with the homocycles (RE)<sub>n</sub> and dimers R<sub>2</sub>E–ER<sub>2</sub>. Tetrastibanes can be trapped from these mixtures with norbornadiene chromium tetracarbonyl. Examples include the tetrastibane complexes *cyclo*-[Cr(CO)<sub>4</sub>(R'<sub>2</sub>Sb–SbR–SbR–SbR'<sub>2</sub>)] (R' = Me, Ph; R = Me<sub>3</sub>SiCH<sub>2</sub>). The structure of *cyclo*-[Cr(CO)<sub>4</sub>(R'<sub>2</sub>Sb–SbR–SbR–SbR'<sub>2</sub>)] (R' = Me, R = Me<sub>3</sub>SiCH<sub>2</sub>) is shown in Figure 17.<sup>64,120</sup>

Mixtures of tri- and tetrastibanes of the types R<sub>2</sub>Sb(SbR')<sub>n</sub>SbR<sub>2</sub> (R = Mes, R' = Ph; R = Bu<sup>t</sup>, R' = Me), which under protection by terminal mesityl or *tert*-butyl groups are not



**Figure 17** Structure of *cyclo*-[Cr(CO)<sub>4</sub>(R'<sub>2</sub>Sb–SbR–SbR–SbR'<sub>2</sub>)] (R' = Me, R = Me<sub>3</sub>SiCH<sub>2</sub>).<sup>120</sup> Hydrogen atoms are omitted for clarity.

involved in ring-chain equilibria, were obtained as components of mixtures.<sup>64</sup>

Other examples of complexes with pnicogen-chain ligands are shown in Scheme 8.

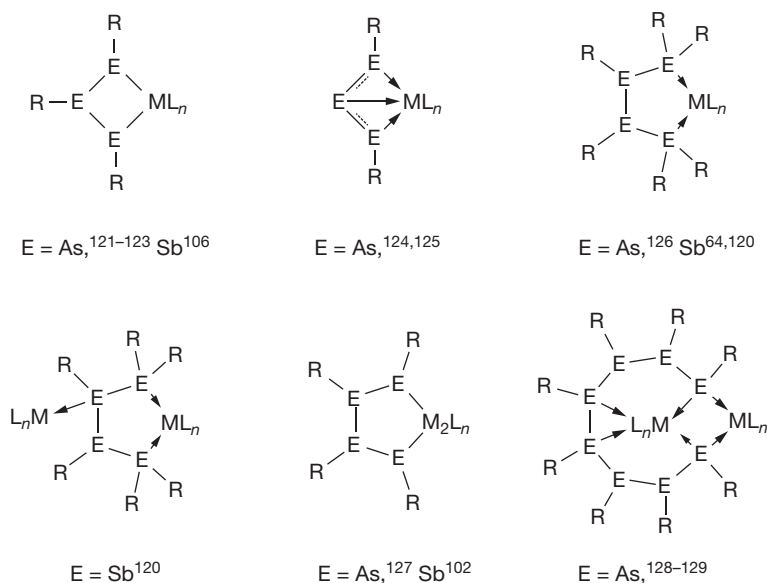
The first tristibane isolated in the pure state, that is, the *catena*-tristibane DmpSb(SbMe<sub>2</sub>)<sub>2</sub> (Dmp = 2,6-Mes<sub>2</sub>C<sub>6</sub>H<sub>3</sub>), was obtained from Me<sub>2</sub>Sb–SbMe<sub>2</sub> and DmpSbH<sub>2</sub>.<sup>130</sup>

A chain compound with three arsenic atoms [(k<sup>1</sup>-L)<sub>2</sub>As–As=As(k<sup>2</sup>-L)] is formed by the reaction of the potassium β-diiminate KL (L = [{N(Ar)C(H)}<sub>2</sub>CPh]<sup>−</sup>; Ar = 2,6-Pr<sup>i</sup><sub>2</sub>C<sub>6</sub>H<sub>3</sub>) with AsI<sub>3</sub> and reduction with KC<sub>8</sub>. The three arsenic atoms have the formal oxidation states +2, 0, and +1. The structure of [(k<sup>1</sup>-L)<sub>2</sub>As–As=As(k<sup>2</sup>-L)] is shown in Figure 18. The three As atoms are in a bent (ca. 90°) chain arrangement with the central As atom being two-coordinate and bonded only to the other As atoms. One terminal As atom is chelated by a single ligand L. The other terminal As atom bears two ligands L. The As–As bond lengths are As(1)–As(2) 2.3328(8), As(1)–As(3) 2.4139(9) Å.<sup>131</sup>

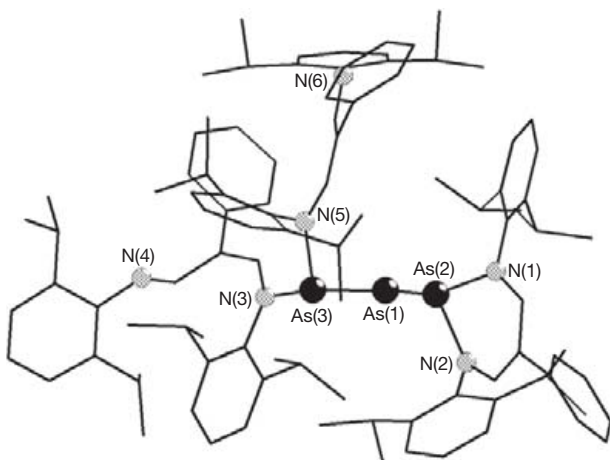
### 1.05.5 Heteromonocycles with Pnicogen–Pnicogen Bonds

Heteromonocycles of the type (RE)<sub>n</sub>Y<sub>m</sub> (E = As, Sb, Bi; Y = heteroatomic groups) are known, with various ring sizes and composition of the main group or transition metal complex fragment. In the case of three-membered heterocycles (RE)<sub>2</sub>Y (Y = transition metal complex fragment, ML<sub>n</sub> = transition metal complex fragment), an alternative description as complexes with 'side-on' coordinated double-bonded dipnicogen RE=ER ligands, as shown in Scheme 9, is sometimes possible.<sup>132</sup>

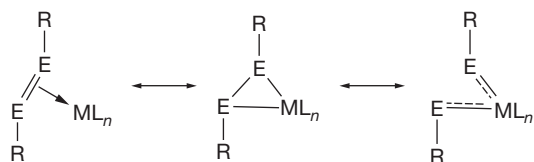
The ZrBi<sub>2</sub> heterocycle Cp<sub>2</sub>Zr(BiR)<sub>2</sub> (Cp = C<sub>5</sub>H<sub>5</sub>; R = 2,6-Mes<sub>2</sub>C<sub>6</sub>H<sub>3</sub>) is formed by the sodium metal reduction of Cp<sub>2</sub>ZrCl<sub>2</sub> with RBiCl<sub>2</sub>. The value for the Bi–Bi bond length (3.1442(7) Å) corresponds to the description of Cp<sub>2</sub>Zr(BiR)<sub>2</sub> as



**Scheme 8** Types of complexes with pnicogen-chains ligands.



**Figure 18** Structure of  $[(k^1-L)_2As-As=As(k^2-L)]$ .<sup>131</sup> Hydrogen atoms are omitted for clarity.



**Scheme 9** Bonding in complexes with side-on RE=ER ligands.

a heterocycle with a long Bi–Bi single bond and not as a dibismuthene complex.<sup>132</sup> In contrast, the relatively short Bi–Bi distance (2.8769(5) Å) in  $[(Rbi)_2[W(CO)_5]]$  ( $R = Me_3SiCH_2$ ) justifies the description as a dibismuthene complex.<sup>56</sup>

The three-membered  $TiSb_2$  heterocycle  $Cp_2Ti(SbR)_2$  ( $R = 2,6-Mes_2C_6H_3$ ) is the product of the reaction of  $Cp_2Ti(Me_3SiC\equiv CSiMe_3)$  and  $RSbH_2$ . The value for the Sb–Sb bond length in  $Cp_2Ti(SbR)_2$  (2.8642(6) Å) corresponds to a Sb–Sb single bond and consequently the complex is best described as a three-membered heterocycle with the bulky aryl groups *trans* to each other. The related ring complex  $(CO)_5W(SbR)_2$ , which is formed by photolysis of the precursor  $(CO)_5WSb(R)H_2$ , contains the  $RSb-SbR$  unit with a Sb–Sb distance of 2.758(6) Å. In both complexes, the Sb–Sb bonds are longer than in the free distibene  $RSb=SBR$  (2.65585(5) Å).<sup>133</sup> Nevertheless, the shorter distance in  $(CO)_5W(SbR)_2$  supports the description as a distibene complex because ‘side-on’ coordination of dipnicogen ligands usually leads to an elongation of the respective bond.<sup>134</sup> Related complexes are the iron dibismuth complexes  $[Fe(CO)_4(Bi_2R_2)]$  ( $R = 2,6-(2,6-Pr^i_2C_6H_3)_2C_6H_3$ , 2,6- $Mes_2C_6H_3$ ), which are formed from the terphenylbismuth dihalides  $RBiCl_2$  and  $Na_2[Fe(CO)_4]$ . Corresponding to the general trend, the Bi–Bi bond lengths in the iron dibismuth complexes (2.9432(2) and 2.9294(2) Å) are longer than Bi=Bi bonds in dibismuthenes and shorter than Bi–Bi single bonds in dibismuthanes.<sup>61</sup>

Protection with bulky aryl groups is applied also in the heterocycles  $(RE)_2Se$  and  $(RE)_2Te$  ( $E = Sb, Bi$ ;  $R = 2,6-bis[bis(trimethylsilyl)methyl]-4-[tris(trimethylsilyl)methyl]phenyl = Bbt$ ), which are formed by reactions of the distibene  $RSb=SBR$  or the dibismuthene  $RBi=BiR$  with elemental selenium or  $Bu^t_3P=Te$ . The values for the Sb–Sb bond (2.8833(6) Å) in the structure of

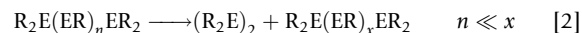
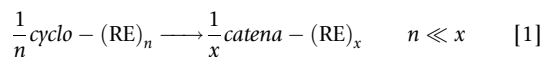
$(RSb)_2Te$  and the Bi–Bi bond (3.0388(3) Å) in  $(Rbi)_2Te$  correspond to pnictogen–pnictogen single bonds.<sup>135,136</sup>

In contrast, reactions of  $RSb=SBR$  or  $RBi=BiR$  with elemental sulfur  $S_8$  give five-membered heterocycles  $(RE)_2S_3$  ( $E = Sb, Bi$ ;  $R = Bbt$ ).<sup>135</sup>

A four-membered  $FeSb_3$  heterocycle  $(RSb)_3Fe(CO)_4$  ( $R = (Me_3Si)_2CH$ ) is formed by an insertion of the  $Fe(CO)_4$  fragment in the reaction of  $cyclo-(RSb)_3$  and  $Fe_2(CO)_9$ . The  $FeSb_3$  ring is folded with the alkyl groups in *trans* positions. There are close structural relations to the four-membered homocycle  $(RSb)_4$ .<sup>106</sup>

Dechlorofluorination of  $ArSb(F)C(Cl)=CR_2$  ( $CR_2 =$  fluorenylidene,  $Ar = 2,4,6$ -tri-*tert*-butylphenyl) by *tert*-butyl lithium leads to the four-membered heterocycle 3,4-bis(fluorenylidene)-1,2-distibacyclobutane. A probable intermediate is the stibaallene  $ArSb=C=CR_2$ , which dimerizes via the  $Sb=C$  bonds.<sup>137</sup>

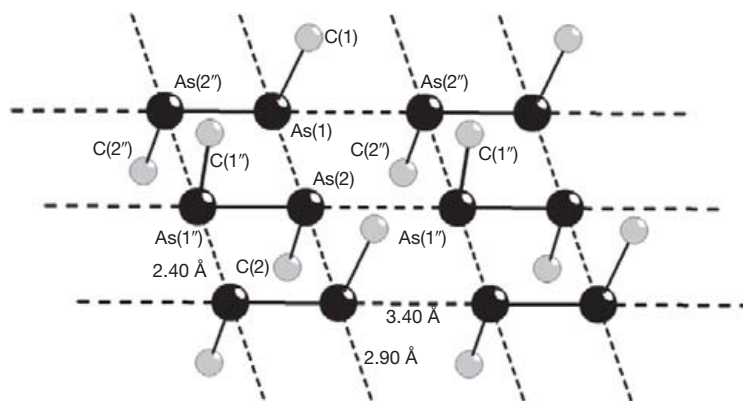
In older literature, there are numerous reports on polymeric materials of the type  $X(RE)_nX$  or  $(RE)_x$ . These polymeric species form by decomposition of  $REH_2$ , by reduction of  $REX_2$  ( $X = Cl, Br$ ), or by other methods. Usually, these materials are impure and not very well characterized. More clearly defined products result when homocycles  $cyclo-(RE)_n$  ( $n = 4, 5$ ,  $E = As, Sb$ ) are used as starting materials and the polymeric catena species form in ring-chain reactions (eqn [1]) or by removal of dipnicogen species from short chains (eqn [2]).



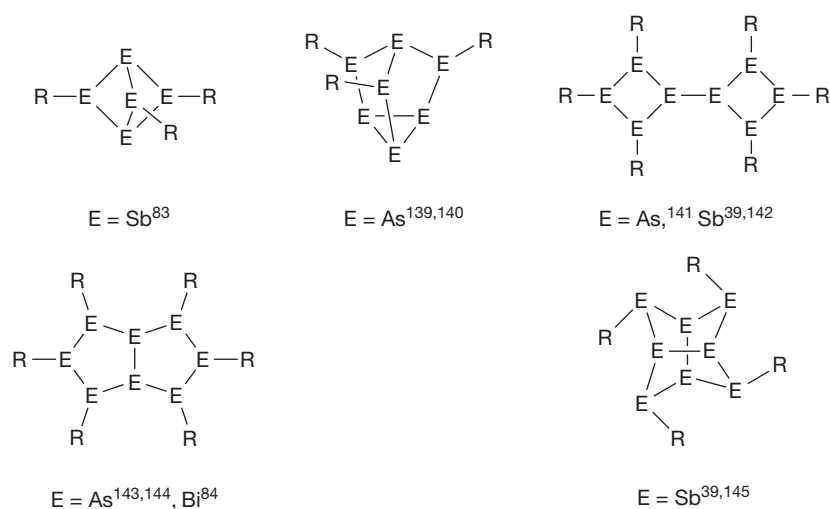
Both pathways were used to produce long-chain polymeric alkyl antimony species, but the structures are unknown. A unique structure for a catena pnictogen species is the famous ladder polymer catena-poly(methylarsenic), which is obtained from  $CH_3AsH_2$  and  $CH_3AsI_2$  as a purple-black crystalline precipitate after 400–600 days at 60 °C. The structure is shown in **Figure 19**. The horizontal distance in the ladder is a normal As–As single bond (ca. 2.4 Å) but the vertical distance is very long (2.9 Å).<sup>5</sup> Catena-poly(methylarsenic) represents a fascinating structure, an ideal for organometallic catena species, but the long reaction time makes it difficult to reproduce the synthesis. Attempts to obtain analogous crystalline arsenic or antimony chains have not been successful. In the arsenic systems, ring species generally form preferentially. Numerous polymeric alkyl or aryl antimony chains were prepared, but the samples were not suitable for single-crystal analyses.<sup>130</sup> Research in this field can be motivated by the expectation that Sb or Bi analogues of catena-poly(methylarsenic) should have interesting electrical properties. The arsenic polymer is likely an intrinsic semiconductor.<sup>5</sup>

### 1.05.6 Neutral Homoatomic Organometallic Pnictogen Polycycles ( $R_nE_m$ ) ( $E = As, Sb, Bi$ ; $n < m$ )

Structural types of organometallic polycycles ( $R_nE_m$ ) ( $n < m$ ) are depicted in **Scheme 10**. They are composed of cycles sharing corners or edges and represent combinations of naked pnictogens and pnictogens bearing substituents.



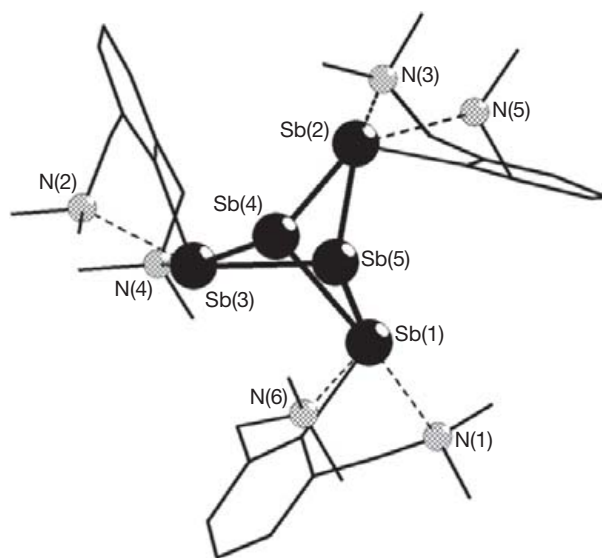
**Figure 19** Structure of catena-poly(methylarsenic),  $(\text{MeAs})_x$ .<sup>138</sup> The coordinates of the hydrogen atoms are not published.



**Scheme 10** Structural types of polycycles  $(\text{R}_n \text{E}_m)$  ( $n < m$ ).

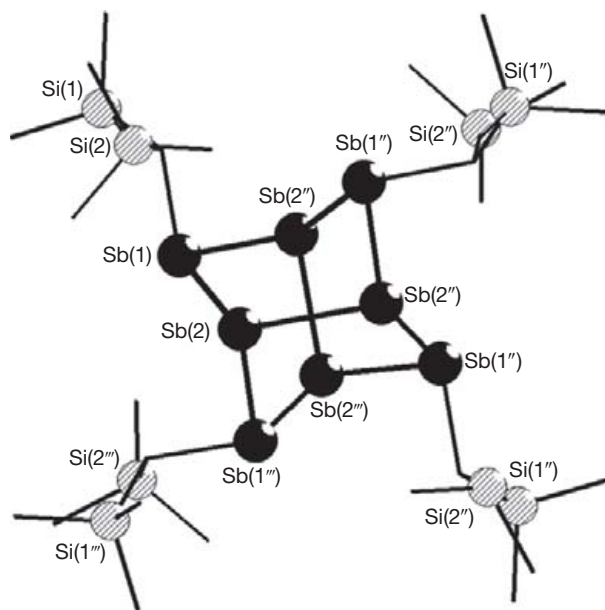
There are many examples for arsenic polycycles and, more recently, homocycles of antimony and bismuth were also synthesized. These neutral molecular clusters are often protected by very bulky substituents. Without sterical protection, decomposition occurs via intermolecular pnictogen–pnictogen contacts and formation of the elemental forms of the pnictogens. Synthetic pathways leading to polycycles are the reduction reactions of organopnictogen dihalides with partial removal of organic substituents or HCl elimination from  $\text{RSbH}_2$  and  $\text{SbCl}_3$ .

One example for the reductive pathway is the synthesis of the trigonal bipyramidal cluster  $\text{Sb}_5\text{R}_3$  ( $\text{R} = 2,6\text{-(Me}_2\text{NCH}_2)_2\text{C}_6\text{H}_3$ ), which is obtained together with  $\text{cyclo-(SbR)}_4$  by reduction of  $\text{RSbCl}_2$  with  $\text{K}[\text{B}(\text{Bu}^i)_3\text{H}]$  probably with intermediate formation of  $\text{RSbH}_2$  and elimination of  $\text{RH}$ . The cluster is sterically protected by the potentially tridentate N,C,N ligand with two pendant arm amino groups. The structure of  $\text{Sb}_5\text{R}_3$ , in which all the pendant amino groups are coordinated to antimony atoms, is shown in **Figure 20**. The Sb–Sb bond lengths lie in the range 2.8459(6)–2.8699(7) Å, which is typical for single bonds. The transannular Sb–Sb distances range from 3.6664(8) to 3.8558(7) Å. They are



**Figure 20** Structure of  $\text{Sb}_5\text{R}_3$  ( $\text{R} = 2,6\text{-(Me}_2\text{NCH}_2)_2\text{C}_6\text{H}_3$ ).<sup>83</sup> Hydrogen atoms are omitted for clarity.





**Figure 21** Structure of the  $Sb_8R_4$  ( $R = (Me_3Si)_2CH$ ).<sup>39</sup> Hydrogen atoms are omitted for clarity.

significantly shorter than the sum of van der Waals radii of two antimony atoms ( $\Sigma_{vdW}(Sb,Sb)$  4.52 Å). The geometry of the  $Sb_5$  framework is close to  $D_{3h}$ .<sup>83</sup>

The polycycle  $R_4Sb_8$  ( $R = (Me_3Si)_2CH$ ) is formed from  $RSbH_2$ ,  $SbCl_3$ , and pyridine or by reduction of  $RSbCl_2$ . The crystal structure of  $R_4Sb_8 \cdot 2$  tetrahydrofuran consists of stacks of  $R_4Sb_8$  molecules. The structure of the polycycle resembles the structure of the arsenic sulfide realgar  $As_4S_4$  with naked Sb atoms in the place of the As atoms and  $RSb$  units replacing the sulfur atoms.  $R_4Sb_8$  can also be described as a  $Sb_4$  tetrahedron where four Sb–Sb bonds are bridged by  $RSb$  units. The Sb–Sb bond lengths lie in the range 2.7980(4)–2.8592(5) Å. In the crystal, there are stacks of the cluster molecules with disordered tetrahydrofuran molecules in holes between the stacks. The polycycle is an air- and light-sensitive compound. Exposure to light leads to photochemical ring contraction with formation of the tritibirane *cis-trans* *cyclo*- $R_3Sb_3$ .<sup>39</sup> The structure of the  $Sb_8R_4$  molecule is depicted in **Figure 21**.

Another  $Sb_8$  cluster protected by a bulky silyl group,  $Sb_8R_6$  ( $R = Bu^t_3Si$ ), is obtained from  $RNa$  and  $SbCl_3$  in a reaction where silylation and reduction of antimony is combined. The structure contains two  $Sb_4$  rings connected through a Sb–Sb bond. The four-membered  $Sb_4$  cycles are folded. The bulkiness of the tri(*tert*-butyl)silyl substituents is also reflected in the wide Sb–Sb–Si angles with an average value of 105.5°. The average Sb–Sb bond length (2.854 Å) corresponds to a normal Sb–Sb single bond. The structure of  $Sb_8R_6$  ( $R = Bu^t_3Si$ ) is shown in **Figure 22**.<sup>142</sup>

A bicyclic bismuth compound with sterical protection by a bulky stannyl group is the  $Bi_8$  cluster  $Bi_8R_5$  ( $R = (Me_3Si)_3Sn$ ), which was obtained together with the distannane  $[(Me_3Si)_3Sn]_2$  from  $LiR$  and  $BiBr_3$ . The structure of the octabismuthane consists of two considerably folded five-membered bismuth rings with a common edge. The stannyl groups on neighboring bismuth

atoms are in *trans* positions. The Bi–Bi bond lengths lie between 2.972(2) and 3.019(2) Å, in the range of Bi–Bi single bonds (**Figure 23**).<sup>84</sup>

### 1.05.7 Heteroatomic Polycycles with Pnicogen–Pnicogen Bonds

There are also several molecular heteroatomic polycyclic compounds with protection by bulky silyl substituents known. Examples are the cage compounds  $[Sb_4(PSiMe_2R)_4]$  and  $[Sb_4(AsSiPr^i_3)_4]$ , which are formed by reactions of  $Me_2RSiPLi_2$  ( $R = CMe_2Pr^i$ ) or  $Pr^i_3SiAsLi_2$  with  $SbCl_3$  in a 3:2 molar ratio, respectively. The structures feature  $Sb_4E_4$  ( $E = P, As$ ) clusters which are composed of five-membered heterocycles sharing edges. The structures can be considered as derived from a tetrahedral  $Sb_4$  unit where four of the six Sb–Sb edges are bridged by  $PSiMe_2R$  or  $AsSiPr^i_3$  groups. They are closely related to the antimony cage  $Sb_8R_4$  ( $R = CH(SiMe_3)_2$ ), mentioned above. The Sb–Sb bond lengths in  $[Sb_4(PSiMe_2R)_4]$  (2.879(1) Å) and  $[Sb_4(AsSiPr^i_3)_4]$  (2.884(2) and 2.890(2) Å) are in the usual range for single bonds. The structure of  $[Sb_4(AsSiPr^i_3)_4]$  is shown in **Figure 24**.<sup>146</sup>

The bicyclic bismuth compound  $[Bi_2(PSiPh_2Bu^t)_4]$ , exhibiting a Bi–Bi single bond, is formed from  $Li_2PSiPh_2Bu^t$  with  $BiCl_3$ . The structure of  $[Bi_2(PSiPh_2Bu^t)_4]$  is shown in **Figure 25**. It is constructed of five-membered  $P_3Bi_2$  and three-membered  $PBi_2$  rings sharing a common bridgehead. The value for the Bi–Bi bond length is 2.942(2) Å.<sup>147</sup>

An As–As unit exists in the bicyclic complex  $[(dppe)Ni(As)_2Si^tBu(R)]$  formed from  $[(dppe)Ni(AsH)_2Si^tBu(R)]$  ( $R = 2,4,6$ -triisopropylphenyl,  $dppe = 1,2$ -bis(diphenylphosphino)ethane) through intramolecular dehydrogenation. The  $SiAs_2Ni$  skeleton is puckered with a torsion angle of 74.2(4)°. <sup>148</sup>

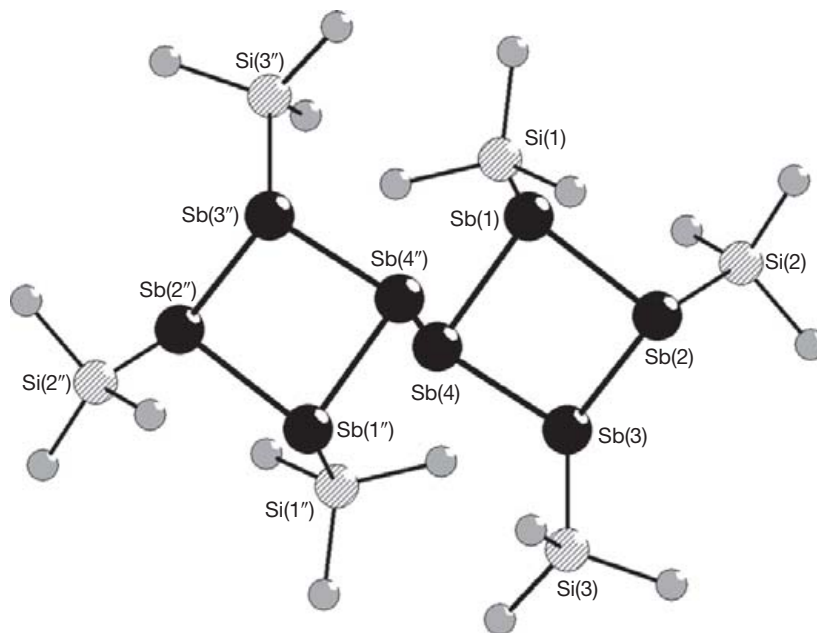
### 1.05.8 Cationic Species with Pnicogen–Pnicogen Bonds

Cationic catenated species with pnicogen atoms bearing substituents of the types  $R_3E-ER_2^+$ ,  $R_3E-ER_3^{2+}$ , and  $R_2E-ER_2-ER_2^+$  ( $E = As, Sb$ ) are known. In these cationic organometallic chain compounds, the pnicogen atoms are four coordinate. One recent example is the hexamethyldiarsonium dication which exists in the triflate  $[(Me_3As-AsMe_3)]^{2+}[(OSO_2CF_3)_2]^-$ , which is formed from  $PCL_3$ ,  $Me_3As$ , and  $Me_3SiOSO_2CF_3$ . The diarsonium cation adopts the eclipsed conformation. The value of the As–As bond length 2.4109(3) Å corresponds to a single bond.<sup>149</sup>

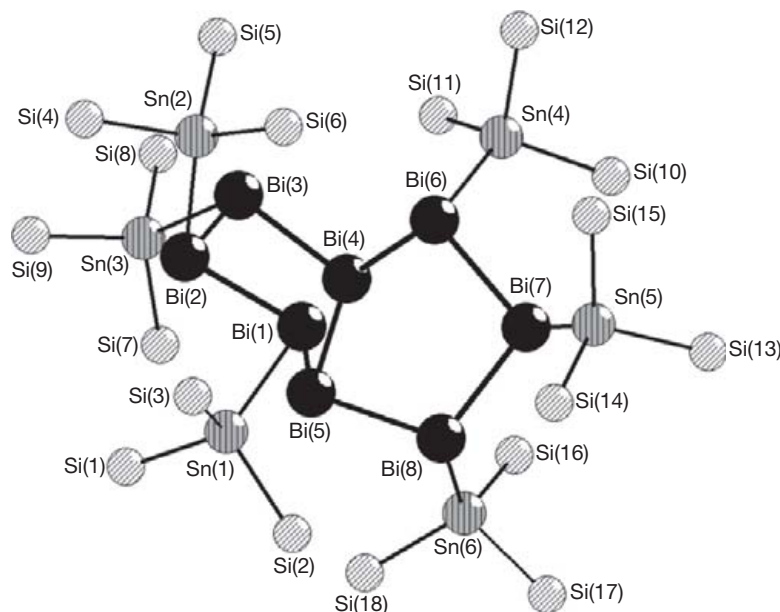
The formation of ligand-free polycationic clusters is a well-known feature of bismuth and, to a lesser extent, of antimony and arsenic. Examples for bismuth polycations are  $Bi_5^+$ ,  $Bi_3^{3+}$ ,  $Bi_6^{2+}$ ,  $Bi_8^{2+}$  and  $Bi_9^{5+}$ , and  $Bi_{10}^{4+}$ . A known polycation of antimony is  $Sb_8^{2+}$ . Also, mixed cationic species with a combination of pnicogen atoms and heteroatoms in cluster frameworks are known for As, Sb, and Bi, as in the examples  $As_3Se_4^+$  or  $[Bi_{10}Au_2]^{6+}$ . Heteroatoms can also reside in the cluster centers as in  $[Au@Bi_{10}]^{5+}$  or  $[Pd@Bi_{10}]^{4+}$ .<sup>150,151</sup>

Known routes for the synthesis of bismuth polycations include the high-temperature reaction of melts containing bismuth and  $BiX_3$  ( $X = Cl, Br, I$ ), and, in some cases,  $AlX_3$ ,





**Figure 22** Structure of  $\text{Sb}_8\text{R}_6$  ( $\text{R} = \text{Bu}^t_3\text{Si}$ ).<sup>142</sup> Hydrogen atoms are omitted for clarity.

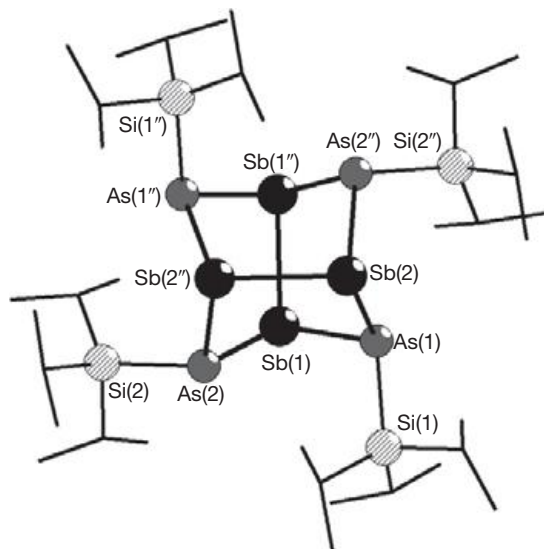


**Figure 23** Structure of  $\text{Bi}_8\text{R}_5$  ( $\text{R} = (\text{Me}_3\text{Si})_3\text{Sn}$ ).<sup>84</sup> Methyl groups are omitted for clarity.

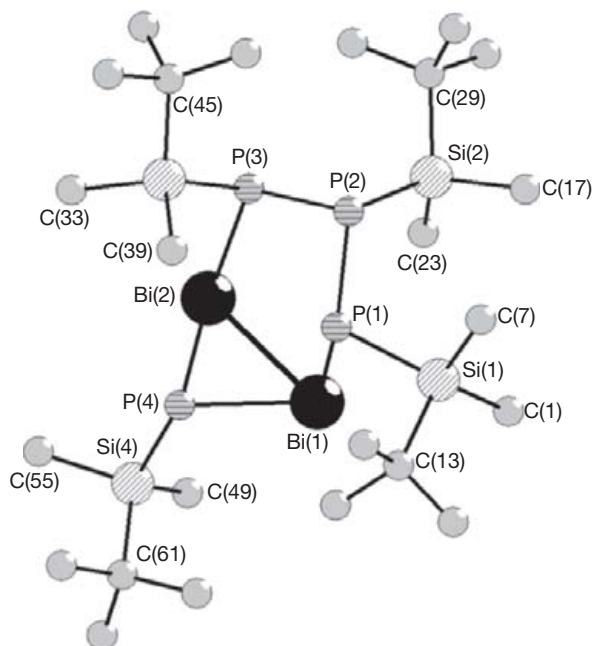
oxidation of bismuth by  $\text{AsF}_5$  or  $\text{SbF}_5$  in liquid  $\text{SO}_2$  and the reduction of  $\text{BiX}_3$  in  $\text{GaX}_3$ -benzene media. The  $\text{Bi}_5^{3+}$  polycation is obtained as tetrachloridoaluminate in crystals of  $\text{Bi}_5(\text{AlCl}_4)_3$ , which are formed by reaction between elemental bismuth,  $\text{BiCl}_3$ , and  $\text{AlCl}_3$  and can be isolated from the ionic liquid  $[\text{BMIM}]\text{Cl}/\text{AlCl}_3$  ( $\text{BMIM} = 1$ -*n*-butyl-3-methylimidazolium).<sup>152</sup>  $\text{Bi}_6^{2+}$  polycations are a constituent of  $\text{Bi}_6[\text{PtBi}_6\text{Cl}_{12}]$  formed by melting reactions of Bi with Pt and  $\text{BiCl}_3$ . The  $\text{Bi}_6^{2+}$  cation, a *nido* cluster, has the shape of a distorted octahedron with an opened edge.<sup>153</sup>  $\text{E}_8^{2+}$  polycations ( $\text{E} = \text{Sb}, \text{Bi}$ ) adopt the square-antiprismatic geometry ( $D_{4d}$  symmetry) consistent with the Wade rules.  $\text{Sb}_8^{2+}$

polycations exist in the salt  $\text{Sb}_8(\text{GaCl}_4)_2$ , formed by reduction of a solution of  $\text{SbCl}_3$  in  $\text{GaCl}_3$ -benzene by a solution of  $\text{Ga}^+(\text{GaCl}_4)^-$  in  $\text{GaCl}_3$ -benzene.<sup>154</sup>  $\text{Bi}_8^{2+}$  cations and polymeric bromooxotantalate(V) anions exist in  $\text{Bi}_8[\text{Ta}_2\text{O}_2\text{Br}_7]_2$ , which is formed by a trace of  $\text{H}_2\text{O}$  in a reaction of Bi,  $\text{BiBr}_3$ , and  $\text{TaBr}_5$  at 570 K.<sup>155</sup>  $\text{E}_8^{2+}$  polycations ( $\text{E} = \text{Sb}, \text{Bi}$ ) exist also in the salts  $\text{E}_8[\text{GaBr}_4]_2$ .<sup>156</sup>

$\text{Bi}_9^{5+}$  polycations have the shape of tri-capped trigonal prisms. Various examples are known.  $\text{Bi}_9^{5+}$  ions embedded in a chloridobismuthate(III) framework exist in the black crystals of the bismuth subchloride  $\text{Bi}_7\text{Cl}_{10}$ , which is formed by slow cooling of stoichiometric mixtures of Bi and  $\text{BiCl}_3$  from 500 °C



**Figure 24** Structure of  $[\text{Sb}_4(\text{AsSiPr}_3)_4]$ .<sup>146</sup> Hydrogen atoms are omitted for clarity.



**Figure 25** Structure of  $\text{Bi}_2(\text{PSiPh}_2\text{Bu})_4$ .<sup>147</sup> Only *ipso* carbon atoms of the phenyl groups are represented. Hydrogen atoms are omitted for clarity.

to ambient temperature. In another subchloride  $\text{Bi}_6\text{Cl}_7$  there are  $\text{Bi}_9^{5+}$  cations surrounded by chloridobismuthate(III) anions  $\text{Bi}_3\text{Cl}_{14}^{5-}$ .<sup>157</sup>

Another example for the existence of the  $\text{Bi}_9^{5+}$  cluster cation is  $\text{Ag}_3\text{Bi}_{14}\text{Br}_{21} = (\text{Bi}_9^{5+})[\text{Ag}_3\text{Bi}_3\text{Br}_{15}]^{3-}[\text{Bi}_2\text{Br}_6]^{2-}$ , a black crystalline compound obtained from a stoichiometric melt of Ag, Bi, and  $\text{BiBr}_3$ .<sup>158</sup>  $\text{Bi}_9^{5+}$  polycations are also present in the bismuth-rich bromidostannate  $\text{Bi}_{18}\text{Sn}_7\text{Br}_{24} = (\text{Bi}_9^{5+})_2[\text{Sn}_7\text{Br}_{24}]^{10-}$ , which is obtained from a melt of bismuth, tin, and  $\text{BiBr}_3$ .<sup>159</sup> Both  $\text{Bi}_9^{5+}$  and  $\text{Bi}^+$  ions form the cationic part in the salt  $\text{Bi}(\text{Bi}_9)[\text{NbCl}_6]$ , which formed from Bi,  $\text{BiCl}_3$ , and  $\text{NbCl}_5$ .<sup>155</sup>

Several cationic clusters have recently been investigated which are composed of pnictogen (As, Sb, and Bi) atoms with element–element bonds and heteroatoms. The heteroatoms can be incorporated in the cluster framework or reside in the center of closed pnictogen clusters.

An example for a cationic cluster framework composed of arsenic and selenium atoms is the structure of the cation in  $(\text{As}_3\text{Se}_4)[\text{AlCl}_4]$ , which can be derived from the  $\text{As}_3\text{Se}$  tetrahedron with three edges bridged by Se atoms. The compound is formed by reaction of arsenic,  $\text{AsCl}_3$ , and  $\text{AlCl}_3$  with selenium.<sup>160</sup>

A cluster containing bismuth and gold is the cation in the salt-like compound  $[\text{Bi}_{10}\text{Au}_2](\text{SbBi}_3\text{Br}_9)_2$ , which is obtained by cooling a melt of the metals and  $\text{BiBr}_3$ . There is an icosahedral cation  $[\text{Bi}_{10}\text{Au}_2]^{6+}$  where bismuth–gold interactions are involved. The cation can be interpreted as a  $[\text{Bi}_{10}]^{4+}$  polycation capped by two  $\text{Au}^+$  cations. The anion contains covalent bonds between bismuth and antimony.<sup>161,162</sup>

Examples for pnictogen polycations where heteroatoms are included in the cluster framework are the noble-metal-centered polycations  $[\text{Au}@\text{Bi}_{10}]^{5+}$  and  $[\text{Pd}@\text{Bi}_{10}]^{4+}$ . Both cations have the shape of pentagonal antiprisms ( $D_{5d}$  symmetry) and contain interstitial Au or Pd atoms. The cations are embedded in the framework of complex chloridobismuthate or halogenido-bismuthate(III)-stannate(II) anions.<sup>150,151</sup>

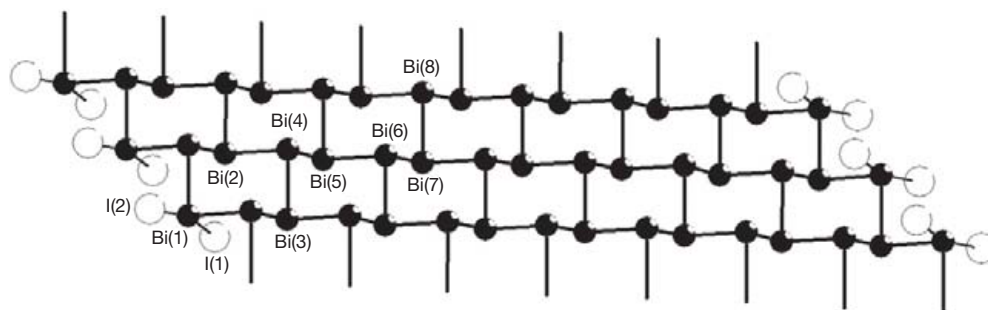
### 1.05.9 Extended Ribbons in Bismuth Subhalides

Low-dimensional extended structures are exemplified by the subvalent bismuth iodides (bismuth in an oxidation state lower than +3) and their derivatives. Earlier examples are bismuth monoiodide and bismuth monobromide. Compounds belonging to the  $\text{Bi}_m\text{I}_4$  ( $m = 14, 16, 18$ ) family of low-dimensional subhalides feature one-dimensional bismuth ribbons of varying width, terminated by iodine atoms. The interior of the ribbons contains only bismuth–bismuth bonds. The arrangements of the bismuth atoms in the bismuth subiodides and in the pure metal, which is composed of folded bismuth hexagons, are similar, and, in fact, the subiodides can be viewed as slices of the metal layers terminated by iodine atoms. The width of the ribbons is reflected in the stoichiometry of the respective subiodide.<sup>163</sup>

One example for a bismuth subhalide is the compound  $\text{Bi}_{16}\text{I}_4$ , which is formed by high-temperature synthesis. The structure is composed of six-membered bismuth rings with iodine atoms on the polymer edges. Two iodine atoms are bonded to each edge-bismuth atom. The width of the ribbon, that is, 16 bismuth atoms, corresponds to the overall stoichiometry. The ribbons are packed into parallel two-dimensional blocks (Figure 26), which are further packed into a three-dimensional lattice. The bismuth–bismuth bond lengths in  $\text{Bi}_{16}\text{I}_4$  lie in the range 3.0334(9)–3.0722(12) Å.<sup>163</sup>

### 1.05.10 Anionic Catenated Species of As, Sb, and Bi

Anionic catena species of the heavy pnictogens are known both with and without substituents. Anions with organo-substituted pnictogen atoms are often derived from neutral organometallic catena species. Substituent-free catena species usually belong to the family of Zintl anions with element–element bonds and



**Figure 26** Section including three formula units in the structure of  $\text{Bi}_{16}\text{I}_4$ .<sup>163</sup>

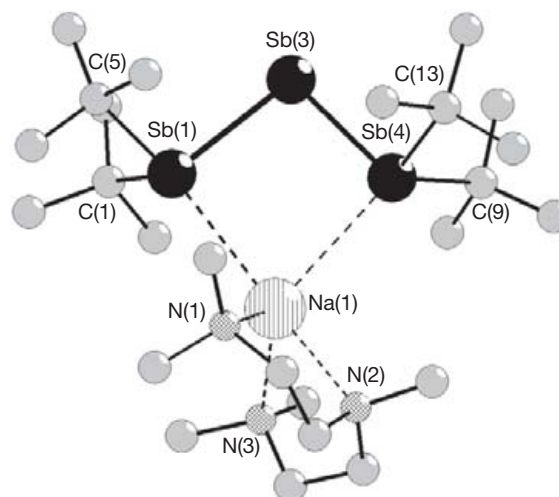
localized negative charges on the elements. Zintl phases are characterized by the presence of covalently bonded anion structures similar to those found in the pure element. There are interesting relations between the organometallic species and the corresponding Zintl anions where pnictogen atoms bear negative charges instead of organic groups. For example, the dipnictogen species  $\text{R}_2\text{E}-\text{ER}_2$  ( $\text{E} = \text{As}, \text{Sb}, \text{Bi}$ ) can be compared with the Zintl anions  $[\text{E}-\text{E}]^{4-}$ .

The remarkable triply charged anion  $[\text{PhSb}_2]^{3-}$  is formed as ammoniate  $[\text{Cs}_6(\text{PhSb}_2)_2] \cdot 11\text{NH}_3$  by reaction of cesium and triphenylantimony in liquid ammonia in a molar ratio of 5:1. The length of the single Sb–Sb bond in  $[\text{PhSb}_2]^{3-}$  is 2.8198(7) Å, similar to the corresponding bond in  $\text{Ph}_4\text{Sb}_2$  (2.844(1) Å), but considerably shorter than the values obtained for the Zintl anion  $\text{Sb}_2^{4-}$  in densely packed ionic solids, for example, in  $\text{Cs}_4\text{Sb}_2$ , the Sb–Sb distance is 2.923(2) Å. This shortening of the single bond in  $[\text{PhSb}_2]^{3-}$  may probably result from a reduced repulsion between the Sb atoms which have lesser charge than in  $\text{Sb}_2^{4-}$ . The Sb–Sb bond length in the  $[\text{Sb}_3\text{Ph}_4]^-$  (2.761(1) Å) is even shorter. In the crystal of  $[\text{Cs}_6(\text{PhSb}_2)_2] \cdot 11\text{NH}_3$ , there are close contacts between the Sb atoms and the  $\text{Cs}^+$  cations. The structure of the  $[\text{PhSb}_2]^{3-}$  anion is approximately planar.<sup>164</sup>

Black crystals of the Sb–Sb-bonded dimer  $\{\text{Li}(\text{tmEDA})\}_4 \cdot \{\{\text{C}_6\text{H}_4\text{P}_2\text{Sb}-\text{SbP}_2\text{C}_6\text{H}_4\}\}$  are obtained by lithiation of 1,2-( $\text{PH}_2$ )<sub>2</sub> $\text{C}_6\text{H}_4$  with  $\text{Bu}^n\text{Li}$  in  $\text{Me}_2\text{NCH}_2\text{CH}_2\text{NMe}_2$  (TMEDA) followed by reaction with  $\text{Sb}(\text{NMe}_2)_3$  in toluene. In the solid-state structure of the dimeric tetraanion the two  $[1,2-\text{C}_6\text{H}_4\text{P}_2\text{Sb}]^{2-}$  radicals are associated in a cisoid (cofacial) arrangement. The Sb–Sb distance (2.9711(3) Å) is only slightly greater than a Sb–Sb single bond.<sup>165</sup>

Mono anionic  $\text{Sb}_2$  or  $\text{Sb}_3$  species  $\text{Bu}_2\text{Sb}(\text{Bu}^t)\text{Sb}^-$  or  $(\text{Bu}^t)_2\text{Sb})_2\text{Sb}^-$  are formed from *cyclo*- $\text{Bu}_4\text{Sb}_4$  and alkali metals (Li, Na, and K). The structure of  $\text{Li}(\text{TMEDA})_2(\text{Bu}_2\text{Sb})_2\text{Sb}$  contains well-separated anions. In the structure of  $\text{Na}(\text{TMEDA})(\text{THF})(\text{Bu}_2\text{Sb})_2\text{Sb}$  the anion is coordinated through the terminal Sb atoms to the Na centers (Figure 27). The values for the Sb–Sb bond lengths (2.7542(8) and 2.7631(10) Å) are shorter than the single bond lengths of distibanes.<sup>166–168</sup>

Substituent-free ('naked') anionic catena species result when antimony or bismuth is alloyed with electropositive metals and many types of anionic sublattices form where the bond often lies at the boundary between the metallic and the ionic-covalent state. The majority of these anionic networks obey Zintl–Klemm electron counting rules. On the other hand, there are also networks built from the heavier pnictogens



**Figure 27** Structure of  $\text{Na}(\text{TMEDA})(\text{THF})(\text{Bu}_2\text{Sb})_2\text{Sb}$ .<sup>167</sup> Hydrogen atoms are omitted for clarity.

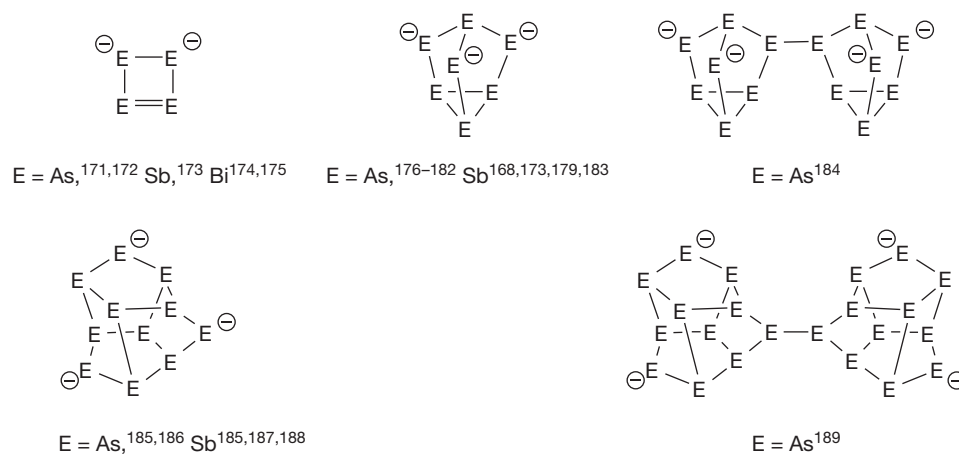
which show an unusual, nonclassical local coordination such as two-dimensional square sheets, whose bonding schemes can be explained by the concept of 'hypervalent bonding' proposed by Hoffmann.<sup>169</sup>

Examples for formal anions following the Zintl concept in solids composed of pnictogens and electropositive metals include the catena species  $\text{Sb}_2^{4-}$ ,  $\text{Bi}_2^{2-}$ ,  $\text{Bi}_3^{3-}$ ,  $\text{As}_4^{2-}$ ,  $\text{As}_6^{4-}$ ,  $\text{Sb}_6^{8-}$ ,  $\text{As}_7^{3-}$ ,  $\text{Sb}_7^{3-}$ ,  $(\text{As}^-)_{\infty}$ ,  $(\text{Sb}^-)_{\infty}$ , and others. These anionic species are incorporated in the crystal lattice together with the cationic part of the lattice. More isolated dimeric or polymeric anions result when the cations are coordinated with crown ether or cryptate ligands. An excellent overview of the earlier literature, with focus on the bonding in polyanionides, has been presented in review articles.<sup>169,170</sup> More recent developments are reviewed here.

Selected examples of naked pnictogen anions deposited in Cambridge Structural Database are shown in Scheme 11.

Formal  $\text{Sb}_2^{4-}$  (Zintl) anions with the shape of  $\text{Sb}_2$  dumbbells exist in intermetallic compounds  $\text{TiSb}_2$  and  $\text{VSb}_2$ . The distance between the Sb atoms is in the range of the reported single-bond values of 2.853 Å. Both compounds may formally be described as  $\text{M}^{4+}[\text{Sb}_2]^{4-}$  ( $\text{M} = \text{Ti}, \text{V}$ ) in the Zintl concept.<sup>190</sup> Also,  $\text{Cs}_4\text{Sb}_2$  contains the anion  $\text{Sb}_2^{4-}$  with Sb–Sb 2.923 Å.<sup>191</sup>

There are two types of compounds with formal  $\text{Bi}_2^{2-}$  dianions, one with a double bond and the stoichiometry  $\text{A}_2\text{Bi}_2$



**Scheme 11** Examples of naked pnictogen anions with known crystal structures.

(A = alkali metal) and one with an extra delocalized electron and the stoichiometry  $A_3\text{Bi}_2$ . In the latter, the bond order is between a single and a double bond.

An isolated dibismuthide anion  $\text{Bi}_2^{2-}$  exists in  $(\text{K-crypt})_2\text{Bi}_2$ , which is produced from ethylenediamine solutions of crypt and  $\text{K}_3\text{Bi}_2$  or  $\text{K}_5\text{In}_2\text{Bi}_4$ , the latter formed by heating stoichiometric mixtures of the elements. The Bi–Bi distance is 2.8377(7) Å corresponding to a double bond. Unlike the paramagnetic  $\text{O}_2$ , the ground state of  $\text{Bi}_2^{2-}$  in  $(\text{K-crypt})_2\text{Bi}_2$  is singlet (shown by electron paramagnetic resonance (EPR)) with paired electrons in an antibonding orbital.<sup>192,193</sup>

A coordinated dibismuthide anion  $\text{Bi}_2^{2-}$  exists in  $[\text{Cs}(18\text{-crown-6})]_2\text{Bi}_2 \cdot 7\text{NH}_3$ . The compound was prepared by solvating  $\text{Cs}_5\text{Bi}_4$  together with excess 18-crown-6 in liquid ammonia. The anion coordinates ‘side-on’ to the central cesium cations of two  $[\text{Cs}(18\text{-crown-6})]$  complexes, resulting in a neutral, molecular  $[\text{Cs}(18\text{-crown-6})]_2\text{Bi}_2$  complex. The Bi–Bi bond length is 2.8635(4) Å, which is considerably shorter than the values for Bi–Bi single bonds.<sup>194</sup>

There are also dimers of bismuth in crystals of  $A_3\text{Bi}_2$  (A = K, Rb, Cs). In  $\text{Cs}_3\text{Bi}_2$  the Bi–Bi distance is 2.976(2) Å. This distance is clearly longer than what might be expected for a double bond in a neat solid (2.90 Å). Based on magnetic measurements, the structure is described as containing  $\text{Bi}_2^{2-}$  dimers with an extra delocalized electron over the structure. The elongation of the Bi–Bi bond is caused by the extra electron delocalized over the cations and the antibonding states of the dimer.<sup>193</sup>

Bent trimers of  $\text{Bi}_3^{3-}$  can be ‘fished out’ from solutions of  $\text{K}_5\text{Bi}_4$  in ethylenediamine and crypt (crypt = hexaoxa-diazabicyclo-hexacosane) with the help of (mesitylene) $M(\text{CO})_3$  (M = Cr or Mo), which is used as the ‘bait.’ They form trigonal bipyramidal closo clusters of  $[\text{Bi}_3\text{M}_2(\text{CO})_6]^{3-}$ , where the M(CO)<sub>3</sub> fragments are equatorial. The clusters are isoelectronic and isostructural with the  $[\text{Bi}_3]^{3+}$  ion. The Bi–Bi bond lengths in the clusters lie in the range 2.954(1)–3.005(1) Å. The species  $[\text{Bi}_3\text{M}_2(\text{CO})_6]^{3-}$  can be viewed also in a ‘noncluster’ way, that is, without delocalized bonding. Thus, they can be described as made of bent  $[\text{Bi}_3]^{3-}$  molecules coordinated to two neutral M(CO)<sub>3</sub> moieties. The trimer  $[\text{Bi}_3]^{3-}$  is isovalent and isostructural with ozone,  $\text{O}_3$ , where the average bond order is 1.5 per

bond. The Bi–Bi distances are relatively short and lie between the single bond length of 3.02 Å and the double bond length of 2.8377(7) Å observed for the naked diatomic molecule  $[\text{Bi}=\text{Bi}]^{2-}$ .<sup>195</sup>

The  $\text{As}_4^{2-}$  dianion exists in  $(\text{K}@18\text{-crown-6})_2\text{As}_4$ . The structure features a triple-decker-like coordination of the cyclo-tetraarsenide anion between two crown ether-coordinated potassium cations. Calculations reveal that  $\text{As}_4^{2-}$  shows electron delocalization primarily through the lone pairs of electrons.<sup>172</sup>

The compounds  $\text{K}_5\text{As}_4$ ,  $\text{A}_5\text{Sb}_4$  (A = K, Rb), and  $\text{A}_5\text{Bi}_4$  (A = K, Rb, Cs) contain zigzag tetramers of  $\text{E}_4^{4-}$  (E = As, Sb, Bi) and also multiple bonding. Like  $\text{K}_3\text{Bi}_2$ , they belong to the class of ‘metallic salts,’ due to the extra alkali-metal cation and the corresponding ‘extra’ electron delocalized over the structure. All six compounds are metallic and show temperature-independent paramagnetism due to a delocalized electron from the extra alkali-metal cation in the formula. At low temperatures (around 9.5 K) and low magnetic fields, the bismuthides become superconducting. The E–E distances in the tetramers (e.g.,  $\text{K}_5\text{As}_4$  2.446(2) Å,  $\text{K}_5\text{Sb}_4$  2.818(3) Å, and  $\text{K}_5\text{Bi}_4$  3.046(3) Å) are shorter than known single bonds for the corresponding element. For the arsenide and the antimonides, they are also shorter than in helical chains of  $(\text{As}^-)_\infty$  and  $(\text{Sb}^-)_\infty$  in the compounds  $\text{AE}$  (A = alkali metal, E = As, Sb; no compound of the type  $\text{ABi}$  is known), with bond lengths in the ranges of 2.47–2.50 and 2.83–2.88 Å, respectively, or in the dimers of  $\text{Sb}_2^{4-}$  in  $\text{Cs}_4\text{Sb}_2$  (Sb–Sb, 2.92 Å) or in hexamers of  $\text{Sb}_6^{8-}$  in  $\text{Ba}_4\text{Sb}_6$  (Sb–Sb, 2.86–3.00 Å).<sup>196</sup>

The gaseous pentapnictogen anions  $\text{E}_5^-$  (E = As, Sb, Bi) are produced by laser vaporization of the corresponding element targets in the presence of helium carrier gas. Studies using photoelectron spectroscopy and *ab initio* calculations reveal that the ground state of the  $\text{E}_5^-$  (E = As, Sb, Bi) ions is the aromatic cyclic  $D_{5h}$  structure with a low-lying  $C_{2v}$  isomer.<sup>197</sup>

Hexameric pnictogen anions were recently studied for arsenic, and hexaarsenides exist in the compounds  $\text{M}_4\text{As}_6$  (M = Rb, Cs). Upon solvation in liquid ammonia, these hexaarsenides form heptaarsenide  $\text{As}_7^{3-}$ , tetradecaarsenide  $[(\text{As}_7)_2]^{4-}$ , and the cyclo-tetraarsenide  $\text{As}_4^{2-}$  as crystalline products. From  $\text{Rb}_4\text{As}_6$  in liquid ammonia the ammoniate  $\{\text{Rb}(18\text{-crown-6})\}_2\text{Rb}_2\text{As}_6 \cdot 6\text{NH}_3$  forms, which contains the hexaarsenide



ring  $\text{As}_6^{4-}$  as anionic part. The ring has a chair conformation with As–As bond lengths in the range 2.399(4)–2.415(3) Å, and bond angles close to 120°. In the crystal structure, four Rb atoms coordinate to the arsenic ring.<sup>198</sup>

Pnicogen cluster ions containing seven pnicogen atoms are exemplified by the well-known  $\text{Sb}_7^{3-}$  anion, which has the common nortricyclane structure and is isostructural and iso-electronic to  $\text{P}_4\text{S}_3$ .  $\text{Sb}_7^{3-}$  exists in (crypt-Na) $_3\text{Sb}_7$ , (crypt-K) $_3\text{Sb}_7$ , and  $\text{Rb}_3\text{Sb}_7$ . It forms also the anionic part of  $\text{Cs}_3\text{Sb}_7$ , which is obtained from the elements. In all these compounds, the structure of the anion is very similar. A general feature is that the bond lengths between the Sb(0) atoms [ $\text{Cs}_3\text{Sb}_7$ , 2.856(2)–2.908(1) Å] are longer than the bonds between Sb(0) and  $\text{Sb}^-$  atoms [ $\text{Cs}_3\text{Sb}_7$ , 2.728(1)–2.798(1) Å].<sup>191</sup>

Eight pnicogen atoms forming a polyanion are represented by the  $\text{S}_8$ -like anion  $\text{Sb}_8^{8-}$ , which exists in the ammoniate  $[\text{K}_{17}(\text{Sb}_8)_2(\text{NH}_2)] \cdot 17.5\text{NH}_3$ . The compound is formed by reduction of antimony with potassium in liquid ammonia. The ammoniate contains crown-shaped  $\text{Sb}_8^{8-}$  Zintl anions analogous to  $\text{S}_8$ . In the crystal structure of  $[\text{K}_{17}(\text{Sb}_8)_2(\text{NH}_2)] \cdot 17.5\text{NH}_3$ , there are nearly identical  $[\text{Sb}_8]^{8-}$  rings with Sb–Sb bond lengths between 2.847(2) and 2.872(3) Å and a mean value of 2.861 Å.<sup>199</sup>

Extended linear pnicogen (As, Sb, Bi) chains are known in alkali-metal pnictides of the composition AE (A = alkali metal, E = As, Sb, Bi). A recently studied example is  $\beta\text{-CsSb}$  where the anionic part of the structure consists of helical antimony chains. The structure of the chain is shown in Figure 28. The distances Sb–Sb (2.855–2.878(2) Å) are similar to the values for  $\alpha\text{-CsSb}$  (2.844(3) and 2.863 Å),  $\text{KSb}$  (2.829 and 2.852 Å),  $\alpha\text{-RbSb}$  (2.852 and 2.864 Å), and  $\beta\text{-RbSb}$  (2.838(1) and 2.862 Å). They correspond very well to Sb–Sb single bond lengths in tetraorganano distibanes or other organometallic catena species.<sup>200,201</sup>

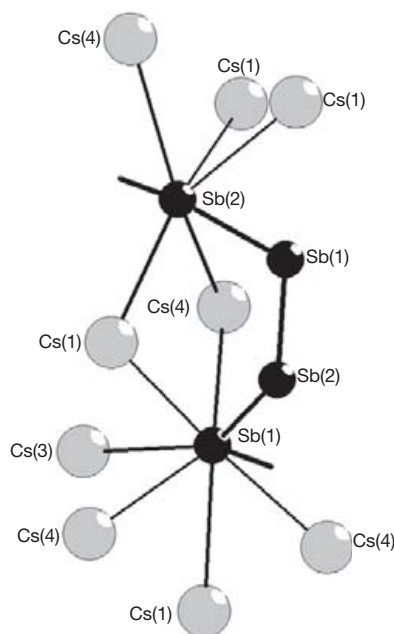


Figure 28 Section of the structure of  $\beta\text{-CsSb}$ .<sup>200</sup>

Short Sb–Sb bonds in linear antimony chains exist also in  $(\text{Zr},\text{V})_{13}\text{Sb}_{10}$ ,  $(\text{Zr},\text{V})_{11}\text{Sb}_8$ , and  $(\text{Zr},\text{Ti})\text{Sb}_{13}$ . The Sb–Sb interactions in these chains can be described as half bonds, and the Sb atoms as being in the  $-2$  state, although the bond lengths (between 2.80 and 2.90 Å) correspond to single bond distances. Related antimony chains with Sb–Sb distances ( $>3.06$  Å) and nonclassical (hypervalent) bonding have been discussed in the reviews of Hoffmann.<sup>169,202</sup> Antimony chains with Sb–Sb interactions of 3.10 and 3.25 Å exist in the antimonides  $\text{Ti}_5\text{Sb}_8$  and  $\text{Zr}_{11}\text{Sb}_{18}$ .<sup>203,204</sup> Structures of metallic antimonides  $(\text{M}',\text{Ti})_5\text{Sb}_8$  ( $\text{M}' = \text{Zr}, \text{Hf}, \text{Nb}, \text{and Mo}$ ) contain three-dimensional extended Sb networks with intermediate Sb–Sb bond lengths (starting at 3.16 Å). They are prepared from the melt of mixtures of Ti,  $\text{TiSb}_2$ , and  $\text{M}'\text{Sb}_2$ .<sup>205</sup> A mixed chain containing antimony and titanium atoms occurs in the nonstoichiometric compound  $\text{Ti}_{11-x}\text{Sb}_{8-y}$ . There are short bonds of alternating 2.76 and 2.84 Å. The chain consists mainly of Sb atoms (i.e., 87% Sb and 13% Ti).<sup>202</sup>

Ribbons composed of polyanion antimony anions exist in the rubidium antimonide  $\text{RbSb}_2$ . There are  $[\text{Sb}_2]^-$  ribbons forming the anionic part of this electron-precise Zintl compound.  $\text{RbSb}_2$  is formed from elemental rubidium and antimony. In accordance with the ribbon-shaped antimonide anions, the compound crystallizes as extremely thin needles of dark-metallic luster. The crystal structure shows fused six-membered rings of two- and three-bonded Sb atoms forming ribbons, which can be interpreted as sections of the elemental structure of antimony (Sb–Sb: 2.819(5) and 2.860(9) Å, respectively). The structure of  $\text{RbSb}_2$  is closely related to that of  $\text{KSb}_2$ , which exhibits identical antimony anions.<sup>206</sup> Puckered layers composed of 5- and 28-membered rings of two- and three-bonded antimony atoms form the anionic part of the cesium polyanion  $\text{Cs}_5\text{Sb}_8$ . A section of the layer anion is shown in Figure 29.<sup>200</sup>

Two- and three-dimensionally infinite antimony polyanions exist in the phases  $\text{Pr}_{9-x}\text{Sb}_{21-y}$  and  $\text{Ho}_2\text{Sb}_5$ . The structure of  $\text{Pr}_{9-x}\text{Sb}_{21-y}$  contains a two-dimensionally infinite polyanion with interatomic distances in the range 2.98–3.07 Å. In the structure of  $\text{Ho}_2\text{Sb}_5$ , there is a three-dimensional network of antimony atoms with Sb–Sb distances in the range 2.83–3.33 Å.<sup>207</sup>

Anionic bismuth chains and sheets are part of the hypervalent binary phase  $\text{EuBi}_2$ , which is formed from high-temperature solid-state reactions of the pure metal elements. The structure of  $\text{EuBi}_2$  features one-dimensional Bi-zigzag anionic chains and two-dimensional Bi-square sheets. It can be described as  $\text{Eu}^{2+}(\text{Bi}^-)$  chain ( $\text{Bi}^-$ ) square. Within the Bi-chain, the Bi–Bi distance (3.2244(16) Å) corresponds to an elongated Bi–Bi single bond. Within the two-dimensional Bi-square sheet, the Bi–Bi distance (3.3442(7) Å) is larger than that of a single bond and corresponds to a 'hypervalent' Bi–Bi bond. Similar square Sb sheets exist in  $\text{EuSb}_2$  and  $\text{BaZnSb}_2$ .<sup>208</sup>

Planar anionic layers composed of six- and four-membered bismuth rings with three- and four-bonded Bi, which are separated by Ba atoms, exist in the phase  $\text{Ba}_2\text{Bi}_3$ . Single crystals of  $\text{Ba}_2\text{Bi}_3$  are obtained by reacting stoichiometric amounts of pure elements (with a slight excess of barium). The stoichiometric amount of Ba, Sb, and Bi under similar reaction conditions gives  $\text{Ba}_2\text{BiSb}_2$ . In the mixed compound, there is strict site preference with Sb occupying only the three-bonded sites.  $\text{Ba}_2\text{Bi}_3$  can be described neither by the classical Zintl concept

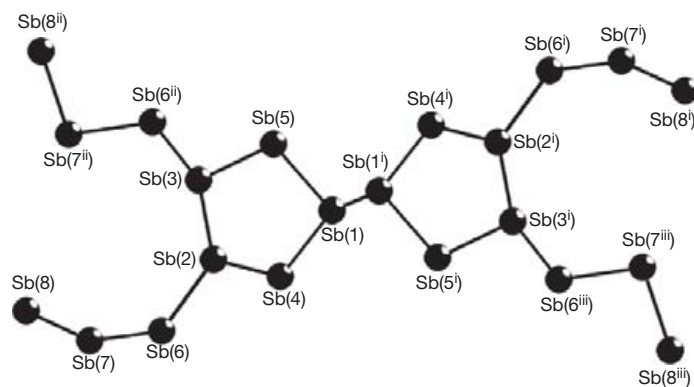


Figure 29 Section of the anionic layer in  $\text{Cs}_5\text{Sb}_8$ .<sup>200</sup>

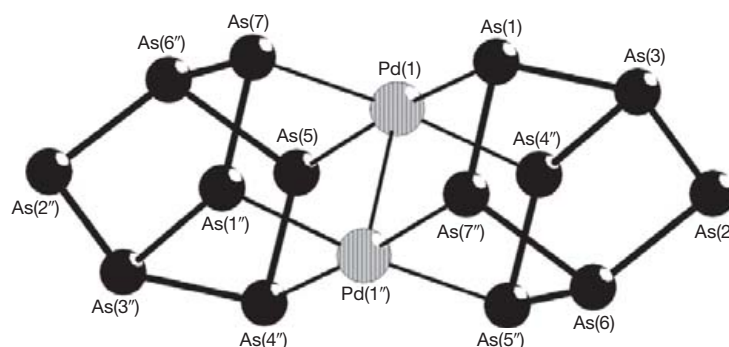


Figure 30 Structure of the anion  $[\text{Pd}_2\text{As}_{14}]^{4-}$ .<sup>210</sup>

nor with the extended electron counting rules for two-dimensional nets, which have been introduced by Hoffmann.<sup>169,170</sup> The anionic network of  $\text{Ba}_2\text{Bi}_3$  can be rationalized as  $(\text{Ba}^{2+})_2[\text{Bi}_3]^{3-}(\text{e}^-)$ . Bonding distances suggest that the extra electron fills Bi–Bi antibonding states. The densities of states obtained from TB-LMTO-ASA calculations show metallic character for both compounds. The Bi–Bi bond lengths in  $\text{Ba}_2\text{Bi}_3$  are 3.247(6) and 3.380(2) Å. They are longer than that of elemental bismuth (3.072 Å). The Sb–Sb distance in  $\text{Ba}_2\text{BiSb}_2$  is (3.098 Å).<sup>209</sup>

### 1.05.11 Ligand-Free Pnictogen Cluster Anions with Heteroatoms

A cluster composed of nickel and antimony is the paramagnetic anion  $[\text{Ni}_5\text{Sb}_{17}]^{4-}$ , which is obtained as a dark-brown crystalline  $[\text{K}(2,2,2\text{-crypt})]^+$  salt by reaction of  $\text{K}_3\text{Sb}_7$  and  $\text{Ni}(\text{COD})_2$  (COD = cyclooctadiene) in the presence of 2,2,2-cryptand in ethylenediamine. The structure consists of a Ni (*cyclo*- $\text{Ni}_4\text{Sb}_4$ ) ring unit in a  $\text{Sb}_{13}$  bowl. It resembles the structure of  $[\text{Pd}_7\text{As}_{16}]^{4-}$  where a Pd (*cyclo*- $\text{Pd}_4\text{As}_4$ ) ring is positioned in a  $\text{Pd}_2\text{As}_{12}$  bowl. In  $[\text{Ni}_5\text{Sb}_{17}]^{4-}$  there are 12 Sb–Sb single bonds (bond lengths 2.816(4)–2.928(4) Å) and 12 additional Sb–Sb contacts in the range 3.095(2)–3.176(2) Å, which correspond to partial or secondary Sb–Sb bonds. DFT calculations suggest an  $S = 3/2$  ground state which may explain the absence

of a room-temperature EPR signal. There are also similarities to  $\text{M}(\text{cyclo-E}_8)^{n-}$  ( $\text{M} = \text{Mo}, \text{Nb}, \text{Cr}, \text{E} = \text{As}, \text{Sb}; n = 2, 3$ ).<sup>210,211</sup>

A different structure consisting of Zintl  $\text{As}_7^{3-}$  anions connected through a  $\text{Pd}_2$  linker was found in the anion  $[\text{Pd}_2\text{As}_{14}]^{4-}$  (Figure 30).<sup>210</sup>

Reactions of ethylenediamine solutions of  $\text{K}_5\text{Bi}_4$  with  $\text{Ni}(\text{PPh}_3)_2(\text{CO})_2$  give closo clusters, for example, the pentagonal bipyramidal  $[\text{Bi}_3\text{Ni}_4(\text{CO})_6]^{3-}$ , the dodecahedral  $[\text{Bi}_4\text{Ni}_4(\text{CO})_6]^{2-}$ , and the Ni-centered or empty icosahedral  $[\text{Ni}_x@(\text{Bi}_6\text{Ni}_6(\text{CO})_8)]^{4-}$ . The counterions are potassium cations coordinated by 2,2,2-crypt or 18-crown-6 ether.<sup>212</sup> Another example of a heteroatomic naked cluster with a monocapped square-antiprismatic geometry was found in  $(\text{Na-crypt})_3[\text{In}_4\text{Bi}_5]$ .<sup>213</sup> In the  $[\text{In}_4\text{Bi}_5]^{3-}$  anion, the indium atoms are located in the five bonded positions (Figure 31).

A ligand-free 20-atom intermetalloid cluster is the anion of  $\text{K}(2,2,2\text{-crypt})_5[\text{Zn}_9\text{Bi}_{11}] \cdot 2\text{en} \cdot \text{tol}$  (en = ethylenediamine, tol = toluene). The cluster is obtained from en solutions of  $\text{K}_5\text{Bi}_4$ ,  $\text{ZnPh}_2$ , 2,2,2-crypt and toluene.<sup>214</sup>

An  $\text{As}_{20}$  dodecahedral (fullerene) cage is a component of the ion-skin-like  $[\text{As}@(\text{Ni}_{12}@\text{As}_{20})]^{3-}$  ion that was prepared from  $\text{As}_7^{3-}$  and  $\text{Ni}(\text{COD})_2$  (COD = cyclooctadiene) in ethylenediamine and isolated as the  $\text{Bu}_4\text{P}^+$  salt. The anion contains an icosahedral  $[\text{Ni}_{12}(\mu_{12}\text{-As})]^{3-}$  fragment that resides at the center of the  $\text{As}_{20}$  dodecahedral (fullerene) cage to give the  $[\text{As}@(\text{Ni}_{12}@\text{As}_{20})]^{3-}$  cluster with  $I_h$  point symmetry.<sup>215</sup> The cluster ions  $[\text{As}@(\text{Ni}_{12}@\text{As}_{20})]^{3-}$  and  $[\text{Sb}@(\text{Pd}_{12}\text{Sb}_{20})]^{3-}$  are also the objective of a density functional study.<sup>216</sup>



A group of compounds containing lanthanides in frameworks of polyanions of As or Sb named lanthanide-filled skutterudites were studied due to useful thermoelectric applications. Skutterudite is the name of a  $\text{CoAs}_3$ -based mineral that was first extensively mined as a source of cobalt and nickel in the region of Skutterud, Norway. The chemical composition of the lanthanide-filled skutterudites with As or Sb polyanions is given by  $\text{LnM}_4\text{E}_{12}$ , where Ln are the lanthanides La, Ce, Pr, Nd, Sm, Eu, Gd, Tb, Yb; M = Fe, Co, Ni, Ru, Os, and E = As, Sb. Some of the lanthanide skutterudites have excellent thermoelectric properties above room temperature and this increased the interest in these materials for thermoelectric applications. The rattling of the Ln atom, which is located in a cage of As or Sb atoms, leads to an effective scattering of the phonons, thus causing the extraordinarily low thermal conductivity. The electronic structure of the lanthanide-filled skutterudites can be understood within the framework of the Zintl concept.<sup>205,217,218</sup>

The heterocubane dianion  $[\text{As}_6\text{I}_8]^{2-}$  is present in  $[\text{PPh}_4]_2[\text{As}_6\text{I}_8]$  and  $[\text{Ph}_2\text{P}(\text{O})\text{CH}_2\text{CH}_2\text{P}(\text{OH})\text{Ph}_2]_2[\text{As}_6\text{I}_8](2\text{CH}_2\text{Cl}_2)$ , two compounds formed by oxidation of the arsenic(I) reagent (dppe)AsI (dppe = 1,2-bis(diphenylphosphino)-ethane).  $[\text{As}_6\text{I}_8]^{2-}$  is composed of an  $\text{As}_6\text{I}_6$  ring arranged in a chair conformation (with each terminal iodine ligand in an equatorial position) and two iodide anions that cap each face of the ring.<sup>219</sup> The structure of dianion  $[\text{As}_6\text{I}_8]^{2-}$  is depicted in Figure 32.

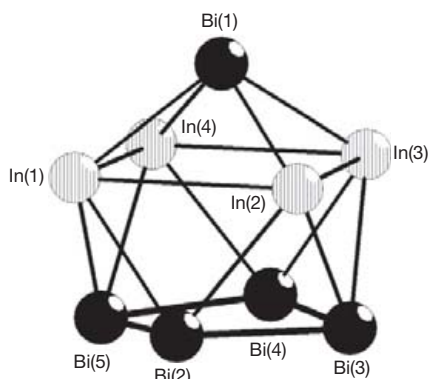


Figure 31 Structure of the  $[\text{In}_4\text{Bi}_5]^{3-}$  anion.<sup>213</sup>

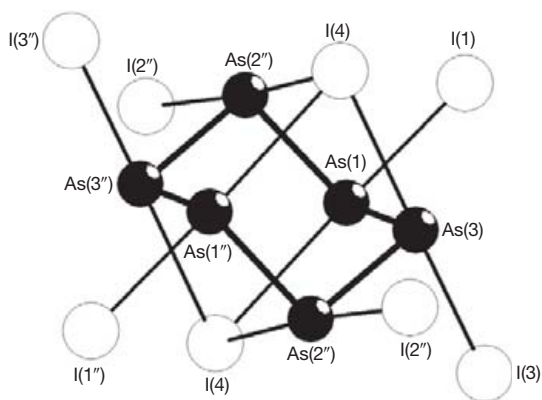


Figure 32 The structure of the  $[\text{As}_6\text{I}_8]^{2-}$  dianion.<sup>219</sup>

$\text{As}_{12}\text{Se}_4^{4-}$  is a selenoarsenate anion which consists of a central  $\text{As}_{12}$  cage with four exo-bonded, formally negatively charged Se atoms that exist in the compound  $[\text{Co}(\text{NH}_3)_6]_2\text{As}_{12}\text{Se}_4 \cdot 12\text{NH}_3$  formed by the reaction of  $\text{As}_4\text{Se}_4$  with a solution of sodium in liquid ammonia and subsequent precipitation with  $\text{CoBr}_2$ .<sup>220</sup>

### 1.05.12 Neutral Adducts with Dative Pnicogen–Pnicogen Bonds

Dative As–As bonds exist in the Lewis acid–base adducts  $\text{PhMe}_2\text{As–AsPhI}_2$ ,  $\text{PhMe}_2\text{As–AsMeI}_2$ , and  $\text{PhMeEtAs–AsMeI}_2$  which form from the components.<sup>221</sup> The tertiary arsine-stabilized arsenium salts,  $[\text{R}_3\text{As–AsMePh}]\text{OTf}$  ( $\text{R}_3\text{As} = \text{Ph}_3\text{As}$ ,  $\text{Me}_2\text{PhAs}$ ,  $[2-(\text{MeOCH}_2)\text{C}_6\text{H}_4]\text{Ph}_2\text{As}$ , and  $[2-(\text{MeOCH}_2)\text{C}_6\text{H}_4]\text{Me}_2\text{As}$ ), are formed by chloride abstraction from chloromethylphenylarsine with trimethylsilyl triflate in the presence of the arsine.<sup>222</sup>  $\text{As}_3$  units combined through dative bonds exist in the complexes  $\text{AsX}_3[0\text{-C}_6\text{H}_4(\text{AsMe}_2)_2]$  ( $\text{X} = \text{Br}, \text{I}$ ).<sup>223</sup>

### 1.05.13 Catena Species in Complexes and Clusters

Pnicogen–pnictogen-bonded species are frequently formed from mononuclear pnicogen reagents during cluster building reactions with metal halides or other reagents.

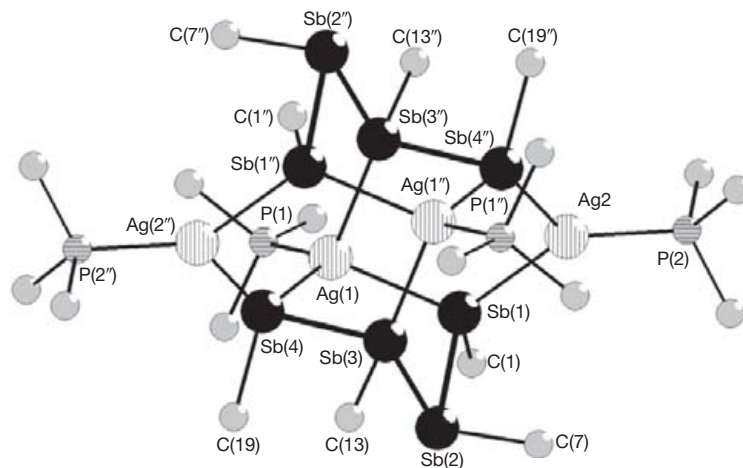
Reactions of  $\text{AsPh}(\text{SiMe}_3)_2$ ,  $\text{CuSCN}$ , and  $\text{PRR}'_2$  give the compounds  $\text{Cu}_4(\text{AsPh}_4)_2(\text{PRR}'_2)_4$  ( $\text{R}, \text{R}' = \text{Pr}^n, \text{Et}; \text{R} = \text{Me}, \text{R}' = \text{Pr}^n$ ) which contain  $(\text{As}_4\text{Ph}_4)^{2-}$  chains as constituent.<sup>224</sup>

The reaction of  $\text{CuCl}$ ,  $\text{LiAs}(\text{SiMe}_3)_2$  and  $[\text{dppb} = \text{bis}(\text{diphenylphosphino})\text{butane}]$  leads to the formation of ionic cluster complexes containing As–As bonded fragments. Depending on the reaction conditions one can isolate the salts  $[\text{Cu}_8\text{As}_3(\text{AsSiMe}_3)_2(\text{dppb})_4]^+ [\text{Cu}\{\text{As}_2(\text{SiMe}_3)_2\}\{\text{As}_4(\text{SiMe}_3)_4\}]_2^-$  or  $[\text{Cu}_8\text{As}_3(\text{AsSiMe}_3)_2(\text{dppb})_4]^+ [\text{Cu}\{\text{As}(\text{SiMe}_3)_2\}_2]_2^-$ .<sup>225</sup>

Reaction of  $\text{LiSb}(\text{SiMe}_3)_2$ ,  $\text{CuCl}$ , and  $[\text{dppm} = \text{bis}(\text{diphenylphosphino})\text{methane}]$  leads to the neutral cluster  $[\text{Cu}_{10}(\text{Sb}_3)_2(\text{SbSiMe}_3)_2(\text{dppm})_6]$ .<sup>225</sup>

The stibanes  $\text{PhSb}(\text{SiMe}_3)_2$  or  $\text{Sb}(\text{SiMe}_3)_3$  react with silver nitrate and phosphanes to give the silver antimony compounds  $[\text{Ag}_{12}\{\text{Sb}(\text{SiMe}_3)_2\}_6(\text{PPR}'_3)_6]$  with a distorted triangular antiprism of antimony atoms bearing  $\text{SiMe}_3$  groups,  $[\text{Ag}_4(\text{Sb}_4\text{Ph}_4)_2(\text{PPR}'_3)_4]$  containing  $[(\text{PhSb})_4]^{2-}$  anions and  $[\text{Ag}_4(\text{Sb}_6\text{Ph}_6)_2(\text{PBU}^n)_4]$ , where  $[(\text{PhSb})_6]^{2-}$  anions are incorporated in the cluster structure.<sup>226</sup> The structure of  $\text{Ag}_4(\text{Sb}_4\text{Ph}_4)_2(\text{PPR}'_3)_4$  is shown in Figure 33.

$[\text{Pb}_4(\text{SbR})_6]$  ( $\text{R} = \text{Pr}^i\text{Si}$ ) was obtained by the reaction of  $\text{RSb}(\text{SiMe}_3)_2$  with  $\text{PbCl}_2$  in  $\text{Et}_2\text{O}$ . The  $\text{Pb}_4\text{Sb}_6$  cage structure can be described as a  $\text{Pb}_4\text{Sb}_4$  heterocube where two  $\text{SbR}$  edges are replaced by  $(\text{RSb–SbR})$  units.<sup>227</sup> A  $\text{ClSb–SbCl}$  unit exists in the cation  $[\{\text{CyP}\}_4]_2(\text{ClSb–SbCl})]^{2+}$  which is formed in reactions of  $(\text{CyP})_4$  with stibonium cations  $[\text{R}_2\text{Sb}^+]$ ,  $\text{R} = \text{Cl}, \text{Ph}$ .<sup>228</sup> Dibismuth ligands of the types  $\text{PhBi–BiPh}$  and  $\text{Bi–BiPh}_2$  exist in  $\text{Re}_4(\text{CO})_{16}(\text{BiPh}_2)_2(\text{BiPhBiPh})$  and  $\text{Re}_4(\text{CO})_{16}(\text{BiPh}_2)_2(\text{BiBiPh}_2)$ , two complexes that form by thermal and photolytic reactions of the six-membered heterocycle  $[\text{Re}(\text{CO})_4(\text{BiPh}_2)]_3$ .<sup>229</sup>



**Figure 33** Structure of  $\text{Ag}_4(\text{Sb}_4\text{Ph}_4)_2(\text{PPr}_3)_4$ .<sup>226</sup> Only the *ipso* and methylene carbon atoms are represented. The hydrogen atoms of the methylene groups are omitted for clarity.

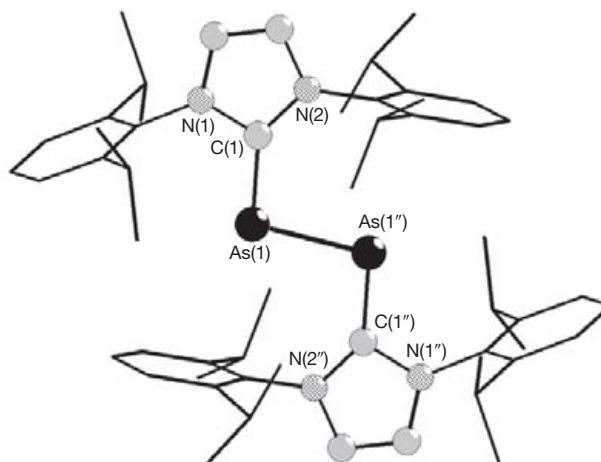
$(\text{PPh}_4)_2[\text{Bi}_{10}\text{Cu}_{10}(\text{SPh})_{24}] \cdot 0.5\text{DME}$  is formed from  $\text{Bi}(\text{SPh})_3$ ,  $\text{CuSPh}$ ,  $\text{PPh}_4\text{Cl}$ , and  $\text{PhSSiMe}_3$  in 1,2-dimethoxyethane. The most striking structural motif within the cluster ion is the  $\text{Bi}_{10}$  unit, which consists of two connected  $\text{Bi}_5$  chains.<sup>230</sup>

#### 1.05.14 Naked Neutral $E_n$ Species ( $E = \text{As}, \text{Sb}, \text{Bi}$ )

The neutral oligomers  $E_n$  ( $E = \text{As}, \text{Sb}, \text{Bi}; n \geq 2$ ) are highly reactive species that exist in the gas phase in vapors of the elements or can be generated by decomposition of organometallic precursors. The most stable species is yellow arsenic  $\text{As}_4$ , which can be used as an arsenic reagent also in condensed phase. In contrast,  $\text{Sb}_4$  and  $\text{Bi}_4$  aggregate on condensation from the gas phase, with formation of the stable (semi)metallic modifications of antimony and bismuth which are much less reactive. The  $E_n$  species with As–As, Sb–Sb, and Bi–Bi bonds exist however in stable compounds as building blocks in clusters, as ligands in complexes, or with protection of suitable donors. Coordination compounds containing ‘naked’  $\text{As}_n$ ,  $\text{Sb}_n$ , or  $\text{Bi}_n$  as components are also well known.

$E_n$  species can also be stabilized on special surfaces or in channels of zeolites and they are objectives of theoretical studies.  $\text{Sb}_4$  molecules exist on the surface of a  $\text{MoS}_2$  crystal and a  $\text{AuSb}_2$  surface.<sup>231</sup> Distorted cubic clusters  $\text{Sb}_8$  are formed in channels of the zeolite ZSM-11 Å.<sup>232</sup> Ligand-free neutral and anionic  $E_3$  ( $E = \text{As}, \text{Sb}, \text{Bi}$ ) species were studied with theoretical methods (CCSD(T), B3LYP-DFT).<sup>233</sup> Fullerene-like  $\text{As}_n$  cages for sizes 4, 8, 20, 28, 32, 36, and 60, wherein each As atom is threefold coordinated, were examined in a density functional study. All the cages studied are energetically stable with respect to isolated arsenic atoms, but only  $\text{As}_{20}$  is energetically stable against dissociation into  $\text{As}_4$ .<sup>234</sup>

Complexes containing the dinitrogen analogue  $E_2$  ( $E = \text{As}, \text{Sb}, \text{Bi}$ ) molecules as ligands are well known. The naked  $E_2$  ligands are ‘side-on’ coordinated through the electrons of the triple bond to 16 electron complex fragments. Precursor for the  $\text{Bi}_2$  ligand is the cyclobismuthane *cyclo*-( $\text{Me}_3\text{SiCH}_2\text{Bi}$ ) $_n$  ( $n = 3-5$ ) that reacts photochemically with  $[\text{Mn}(\text{CO})_3\text{C}_5\text{H}_4\text{CH}_3]$  to form  $[\text{Bi}_2[\text{Mn}(\text{CO})_2\text{C}_5\text{H}_4\text{CH}_3]_3]$ .<sup>70</sup> A complex where the  $\text{As}_2$  unit is

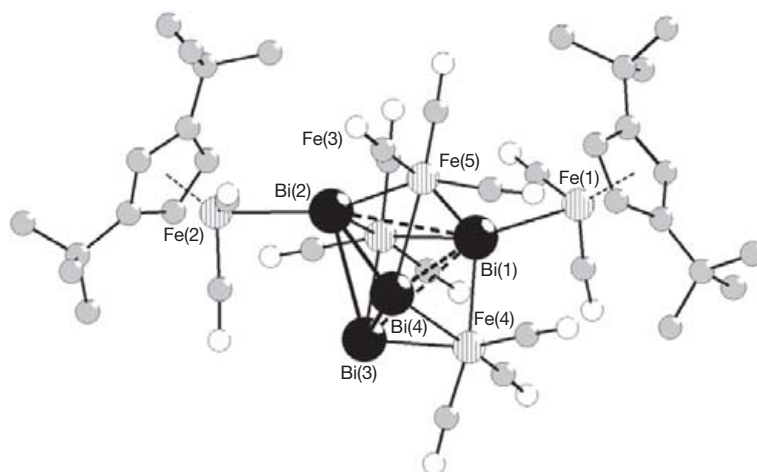


**Figure 34** Structure of  $\text{L-As-As-L}$  ( $\text{L} = \text{C}\{\text{N}(2,6\text{-Pr}'_2\text{C}_6\text{H}_3)\text{CH}\}_2$ ).<sup>235</sup> Hydrogen atoms are omitted for clarity.

protected by a carbene ligand is the compound  $\text{L-As-As-L}$  ( $\text{L} = \text{C}\{\text{N}(2,6\text{-Pr}'_2\text{C}_6\text{H}_3)\text{CH}\}_2$ ), which is formed by reduction of  $\text{L-AsCl}_3$  with potassium/graphite. The structure of  $\text{L-As-As-L}$  is shown in **Figure 34**. The molecule adopts a *trans*-bent geometry around the As–As bond. The As–As distance 2.442(1) Å corresponds to an As–As single bond.<sup>235</sup>

The tetrahedral  $\text{MoAs}_3$  clusters  $\text{Cp}^*\text{Mo}(\text{CO})_2\text{As}_3$  react with  $\text{CuX}$  ( $X = \text{Cl}, \text{Br}, \text{I}$ ) to give  $\text{Cu}_2\text{X}_2$  bridged complexes  $[\text{Cp}^*\text{Mo}(\text{CO})_2\text{As}_3\text{CuX}]_2$ .<sup>236</sup> Reactions of the Sb–Sb cluster species  $[\{\text{CpMo}(\text{CO})_2\}_2(\text{Sb}_2)]$  with  $\text{CuX}$  ( $X = \text{Br}, \text{Cl}, \text{I}$ ) produce oligomers or polymers of the general formula  $[\{\text{CpMo}(\text{CO})_2\}_2(\text{Sb}_2)(\text{CuX})]_n$ . With  $X = \text{Cl}, \text{Br}$  halogen-bridged dimers and with  $X = \text{I}$ , a linear polymer forms.<sup>237</sup> The reaction of  $[\text{Me}_5\text{C}_5\text{Fe}(\eta^5\text{-As}_5)]$  with  $\text{Cu(I)}$  halides  $\text{CuX}$  ( $X = \text{Cl}, \text{Br}, \text{I}$ ) leads to the formation of polymers that are built up by the  $\pi$ -coordination of the *cyclo*- $\text{As}_5$  ring to  $(\text{CuX})_n$  moieties.<sup>26</sup>

The complex  $[\text{Bi}_4\{\mu_3\text{-Fe}(\text{CO})_3\}_3\{\text{Fe}(\text{CO})_2\text{Cp}''\}_2]$ , ( $\text{Cp}'' = \text{Bu}'_2\text{C}_5\text{H}_3$ ), formed from  $[\text{Fe}(\text{CO})_4]^{2-}$  and  $[\text{Cp}''(\text{CO})_2\text{Fe}]\text{BiCl}_2$ , contains a distorted-tetrahedral  $\text{Bi}_4$  cluster core in which three of the faces are capped by  $\text{Fe}(\text{CO})_3$  moieties (**Figure 35**). The Bi–Bi distances around the basal face



**Figure 35** Structure of  $[\text{Bi}_4\{\mu_3\text{-Fe}(\text{CO})_3\}_3\{\text{Fe}(\text{CO})_2\text{Cp}\}_2]$ .<sup>238</sup> Hydrogen atoms are omitted for clarity.

(3.0893(11)–3.1949(12) Å) are systematically shortened by 0.2–0.4 Å relative to the other three Bi–Bi distances to the apical Bi atom (3.4226(10)–3.5298(9) Å).<sup>238</sup>

### 1.05.15 Conclusion

Developments in the field of catenated As, Sb, and Bi compounds since the year 2000 are reviewed. Catena species comprise dipnicogen compounds, oligomeric pnictogen compounds with structures of linear or branched chains or bicyclic or polycyclic (cluster) arrangements as well as polymeric species with extended structures in indefinite chains or strips. Catenation occurs both in organometallic or purely inorganic neutral or ionic pnictogen species. Element–element bonds in catenated As, Sb, Bi bonds range from weak intermolecular or interatomic interactions to well established single or multiple bonds. Chemical and physical properties of catenated species as well as structural aspects are included in the review.

### References

- Holleman, A. F.; Wiberg, E.; Wiberg, N. *Lehrbuch der Anorganischen Chemie*, 102nd ed.; de Gruyter: Berlin, 2007.
- Luo, Y. *Comprehensive Handbook of Chemical Bond Energies*. CRC Press: Boca Raton, 2007.
- Breunig, H. J.; Lork, E.; Moldovan, O.; Rat, C. I.; Rosenthal, U.; Silvestru, C. *Dalton Trans.* **2009**, 5065–5067.
- Breunig, H. J.; Wagner, R. In *Comprehensive Organometallic Chemistry III*; Crabtree, R. H.; Mingos, D. M. P., Eds.; Elsevier: Oxford, 2007; Vol. 3, Chapter 16, pp 905–929.
- Rheingold, A. L., Ed.; In *Homoatomic Rings Chains and Macromolecules of Main-group Elements*; Elsevier: Amsterdam, 1977.
- Haiduc, I.; Sowerby, D. B. In *The Chemistry of Inorganic Homo and Heterocycles*; Haiduc, I., Sowerby, D. B., Eds.; Academic Press: London, 1987; pp 701–711.
- Breunig, H. J. In *Encyclopedia of Inorganic Chemistry*, 2nd ed.; King, R. B., Ed.; Wiley: Chichester, 2005; Chapter IA012.
- Breunig, H. J. In *Encyclopedia of Inorganic Chemistry*, 2nd ed.; King, R. B., Ed.; Wiley: Chichester, 2005; Chapter IA011.
- Norman, N. C., Ed.; In *The Chemistry of Arsenic, Antimony and Bismuth Compounds*; Blackie Academic and Professional: London, 1998.
- Suzuki, H.; Matano, Y., Eds.; In *Organobismuth Chemistry*; Elsevier: Amsterdam, 2001.
- Patai, S., Ed.; In *The Chemistry of Organic Arsenic, Antimony and Bismuth Compounds*; Wiley: Chichester, 1994.
- Whitmire, K. H. *Adv. Organomet. Chem.* **1998**, *42*, 1–145.
- Breunig, H. J. *Z. Anorg. Allg. Chem.* **2005**, *631*, 621–631.
- Breunig, H. J.; Ghesner, I. *Adv. Organomet. Chem.* **2003**, *49*, 95–131.
- Breunig, H. J.; Balazs, L. *Organometallics* **2004**, *23*, 304–310.
- Balazs, L.; Breunig, H. J. *Coord. Chem. Rev.* **2004**, *248*, 603–621.
- Breunig, H. J.; Roesler, R. *Chem. Soc. Rev.* **2000**, *29*, 403–410.
- Breunig, H. J.; Roesler, R. *Coord. Chem. Rev.* **1997**, *163*, 33–53.
- Silvestru, C.; Breunig, H. J.; Althaus, H. *Chem. Rev.* **1999**, *99*, 3277–3328.
- DiMaio, A. J.; Rheingold, A. L. *Chem. Rev.* **1990**, *90*, 169–190.
- Dove, M. F. A.; Sowerby, D. B. *Coord. Chem. Rev.* **1988**, *85*, 289–423.
- Ellis, B. D.; Macdonald, C. L. B. *Coord. Chem. Rev.* **2007**, *251*, 936–973.
- Green, M.; Francis, M. D. In *Organometallic Chemistry*; The Royal Society of Chemistry: Cambridge, 2004; Vol. 31, pp 191–208.
- Green, M.; Jones, C. In *Organometallic Chemistry*; The Royal Society of Chemistry: Cambridge, 2002; Vol. 30, pp 159–171.
- Green, M.; Jones, C. In *Organometallic Chemistry*; The Royal Society of Chemistry: Cambridge, 2001; Vol. 29, pp 153–169.
- Krauss, H.; Balazs, G.; Bodensteiner, M.; Scheer, M. *Chem. Sci.* **2010**, *1*, 337–342.
- Scheer, M.; Gregoriades, L. J.; Merkle, R.; Johnson, B. P.; Dielmann, F. *Phosphorus, Sulfur Silicon Relat. Elem.* **2008**, *183*, 504–508.
- Scherer, O. J. *Acc. Chem. Res.* **1999**, *32*, 751–762.
- Scherer, O. J. *Angew. Chem. Int. Ed. Engl.* **1985**, *24*, 924–943.
- Lynam, J. M. *Annu. Rep. Prog. Chem., Sect. A: Inorg. Chem.* **2009**, *105*, 140–154.
- Lynam, J. M. *Annu. Rep. Prog. Chem., Sect. A: Inorg. Chem.* **2008**, *104*, 112–123.
- Lynam, J. M. *Annu. Rep. Prog. Chem., Sect. A: Inorg. Chem.* **2007**, *103*, 104–115.
- Burrows, A. D. *Annu. Rep. Prog. Chem. Sect. A: Inorg. Chem.* **2004**, *100*, 95–111.
- Burrows, A. D. *Annu. Rep. Prog. Chem., Sect. A: Inorg. Chem.* **2003**, *99*, 83–99.
- Burrows, A. D. *Annu. Rep. Prog. Chem., Sect. A: Inorg. Chem.* **2002**, *98*, 77–91.
- Burrows, A. D. *Annu. Rep. Prog. Chem., Sect. A: Inorg. Chem.* **2001**, *97*, 81–93.
- Seyferth, D. *Organometallics* **2001**, *20*, 1488–1498.
- Balazs, G.; Breunig, H. J.; Lork, E.; Offermann, W. *Organometallics* **2001**, *20*, 2666–2668.
- Balazs, G.; Breunig, H. J.; Lork, E.; Mason, S. *Organometallics* **2003**, *22*, 576–585.
- Balazs, L.; Breunig, H. J.; Lork, E. *Z. Naturforsch. B: J. Chem. Sci.* **2005**, *60*, 180–182.
- Balazs, L.; Balazs, G.; Breunig, H. J.; Ghesner, I.; Lork, E. *Polyhedron* **2003**, *22*, 1719–1723.
- Balazs, L.; Breunig, H. J.; Silvestru, C.; Varga, R. *Z. Naturforsch. B: J. Chem. Sci.* **2005**, *60*, 1321–1323.

43. Balazs, L.; Breunig, H.; Lork, E.; Silvestru, C. *Eur. J. Inorg. Chem.* **2003**, 1361–1365.
44. Balazs, L.; Breunig, H. J.; Lork, E.; Soran, A.; Silvestru, C. *Inorg. Chem.* **2006**, *45*, 2341–2346.
45. Westerhausen, M.; Gueckel, C.; Piotrowski, H.; Mayer, P.; Warchhold, M.; Noeth, H. Z. *Anorg. Allg. Chem.* **2001**, *627*, 1741–1750.
46. Bashall, A.; Garcia, F.; Lawson, G. T.; McPartlin, M.; Rothenberger, A.; Woods, A. D.; Wright, D. S. *Can. J. Chem.* **2002**, *80*, 1421–1427.
47. Breunig, H. J.; Moldovan, O.; Nema, M.; Rosenthal, U.; Rat, C. I.; Varga, R. A. *J. Organomet. Chem.* **2011**, *696*, 523–526.
48. Lorenz, I.-P.; Rudolph, S.; Piotrowski, H.; Polborn, K. *Eur. J. Inorg. Chem.* **2005**, 82–85.
49. Roering, A. J.; Davidson, J. J.; MacMillan, S. N.; Tanski, J. M.; Waterman, R. *Dalton Trans.* **2008**, 4488–4498.
50. Dikarev, E. V.; Li, B. *Inorg. Chem.* **2004**, *43*, 3461–3466.
51. Dikarev, E. V.; Gray, T. G.; Li, B. *Angew. Chem. Int. Ed.* **2005**, *44*, 1721–1724.
52. Jones, C.; Junk, P. C.; Steed, J. W.; Thomas, R. C.; Williams, T. C. *J. Chem. Soc. Dalton Trans.* **2001**, 3219–3226.
53. Jones, C.; Williams, T. C. *J. Organomet. Chem.* **2004**, *689*, 1648–1656.
54. Waterman, R.; Tilley, T. D. *Inorg. Chem.* **2006**, *45*, 9625–9627.
55. Ates, M.; Breunig, H. J.; Soltani-Neshan, A.; Tegeler, M. Z. *Naturforsch. B: Chem. Sci.* **1986**, *41*, 321–326.
56. Balazs, G.; Balazs, L.; Breunig, H. J.; Lork, E. *Organometallics* **2003**, *22*, 2919–2924.
57. Hinchley, S. L.; Morrison, C. A.; Rankin, D. W. H.; Macdonald, C. L. B.; Wiacek, R. J.; Voigt, A.; Cowley, A. H.; Lappert, M. F.; Gundersen, G.; Clyburne, J. A. C.; Power, P. P. *J. Am. Chem. Soc.* **2001**, *123*, 9045–9053.
58. Balazs, G.; Breunig, H. J.; Lork, E. *Organometallics* **2002**, *21*, 2584–2586.
59. Monakhov, K. Y.; Zessin, T.; Linti, G. *Eur. J. Inorg. Chem.* **2010**, 322–332.
60. Shimada, S.; Maruyama, J.; Choe, Y.-K.; Yamashita, T. *Chem. Commun.* **2009**, 6168–6170.
61. Wolf, R.; Fischer, J.; Fischer, R. C.; Fettingner, J. C.; Power, P. P. *Eur. J. Inorg. Chem.* **2008**, 2515–2521.
62. Breunig, H. J.; Krueger, T.; Lork, E. *J. Organomet. Chem.* **2002**, *648*, 209–213.
63. Breunig, H. J.; Lork, E.; Moldovan, O.; Rat, C. I. *Acta Crystallogr., Sect. C: Cryst. Struct. Commun.* **2007**, *63*, m548–m549.
64. Breunig, H. J.; Ghesner, I.; Ghesner, M. E.; Lork, E. *J. Organomet. Chem.* **2003**, *677*, 15–20.
65. Breunig, H.; Lork, E.; Moldovan, O.; Rat, C. Z. *Anorg. Allg. Chem.* **2010**, *636*, 1090–1094.
66. Kuczkowski, A.; Schulz, S.; Nieger, M.; Saarenketo, P. *Organometallics* **2001**, *20*, 2000–2006.
67. Kuczkowski, A.; Fahrenholz, S.; Schulz, S.; Nieger, M. *Organometallics* **2004**, *23*, 3615–3621.
68. Schuchmann, D.; Kuczkowski, A.; Fahrenholz, S.; Schulz, S.; Floerke, U. *Eur. J. Inorg. Chem.* **2007**, 931–935.
69. Kuczkowski, A.; Schulz, S.; Nieger, M. *Angew. Chem. Int. Ed.* **2001**, *40*, 4222–4225.
70. Balazs, L.; Breunig, H. J.; Lork, E. Z. *Anorg. Allg. Chem.* **2004**, *630*, 1937–1940.
71. Thiele, G.; Zoubek, G.; Lindner, H. A.; Ellermann, J. *Angew. Chem. Int. Ed. Engl.* **1978**, *17*, 135–136.
72. Ellermann, J.; Kock, E.; Burzlaff, H. *Acta Crystallogr., Sect. C: Cryst. Struct. Commun.* **1985**, *41*, 1437–1439.
73. Weber, L.; Dembeck, G.; Loenneke, P.; Stammer, H.-G.; Neumann, B. *Organometallics* **2001**, *20*, 2288–2293.
74. Breunig, H. J.; Roesler, R.; Lork, E. *Organometallics* **1998**, *17*, 5594–5595.
75. Mundt, O.; Becker, G.; Wessely, H.-J.; Breunig, H. J.; Kischkel, H. Z. *Anorg. Allg. Chem.* **1982**, *486*, 70–89.
76. Mandel, N.; Donohue, J. *Acta Crystallogr., Sect. B: Struct. Crystallogr. Cryst. Chem.* **1971**, *27*, 476–480.
77. Opris, L. M.; Silvestru, A.; Silvestru, C.; Breunig, H. J.; Lork, E. *Dalton Trans.* **2004**, 3575–3585.
78. Ates, M.; Breunig, H. J.; Ebert, K.; Guelec, S.; Kaller, R.; Draeger, M. *Organometallics* **1992**, *11*, 145–150.
79. Garcia, F.; Hopkins, A. D.; Kowenicki, R. A.; McPartlin, M.; Tesa, Y. *Dalton Trans.* **2004**, 2051–2052.
80. Ates, M.; Breunig, H. J.; Guelec, S.; Offermann, W.; Haerberle, K.; Draeger, M. *Chem. Ber.* **1989**, *122*, 473–478.
81. Berlitz, T. F.; Sinning, H.; Lorberth, J.; Mueller, U. *Private Commun.* **1992**, CCDC, Cambridge (refcode: SOWDUD).
82. Kekia, O. M.; Jones, R. L.; Rheingold, A. L. *Organometallics* **1996**, *15*, 4104–4106.
83. Dostal, L.; Jambor, R.; Ruzicka, A.; Holecek, J. *Organometallics* **2008**, *27*, 2169–2171.
84. Linti, G.; Koestler, W. Z. *Anorg. Allg. Chem.* **2002**, *628*, 63–66.
85. Linti, G.; Koestler, W.; Pritzkow, H. *Eur. J. Inorg. Chem.* **2002**, 2643–2647.
86. Breunig, H. J.; Roesler, R.; Lork, E. *Angew. Chem. Int. Ed.* **1998**, *37*, 3175–3177.
87. Tan, R. P.; Comerlato, N. M.; Powell, D. R.; West, R. *Angew. Chem. Int. Ed. Engl.* **1992**, *31*, 1217–1218.
88. Burns, J. H.; Waser, J. *J. Am. Chem. Soc.* **1957**, *79*, 859–864.
89. Wells, R. L.; Kwag, C.-Y.; Purdy, A. P.; Mcphail, A. T.; Pitt, C. G. *Polyhedron* **1990**, *9*, 319–327.
90. Rheingold, A. L.; Kekia, O. M.; Strong, J. B. *Main Group Chem.* **1997**, *2*, 31–35.
91. Mast, K.; Scherer, O. J.; Wolmershauser, G. *Private Commun.* **2003**, CCDC, Cambridge (refcode: GUXDOS).
92. Hedberg, K.; Hughes, E. W.; Waser, J. *Acta Cryst.* **1961**, *14*, 369–374.
93. Rheingold, A. L.; Sullivan, P. J. *Organometallics* **1983**, *2*, 327–331.
94. Marx, M. B. L.; Pritzkow, H.; Keppler, B. K. Z. *Anorg. Allg. Chem.* **1997**, *623*, 75–78.
95. Breunig, H. J.; Haerberle, K.; Draeger, M.; Severengiz, T. *Angew. Chem. Int. Ed. Engl.* **1985**, *24*, 72–73.
96. Breunig, H. J.; Soltani-Neshan, A.; Haerberle, K.; Draeger, M. Z. *Naturforsch. B: J. Chem. Sci.* **1986**, *41*, 327–333.
97. Breunig, H. J.; Ebert, K. H.; Guelec, S.; Probst, J. *Chem. Ber.* **1995**, *128*, 599–603.
98. Balazs, G.; Breunig, H. J.; Lork, E. Z. *Anorg. Allg. Chem.* **2003**, *629*, 637–640.
99. Waterman, R.; Tilley, T. D. *Angew. Chem. Int. Ed.* **2006**, *45*, 2926–2929.
100. Balazs, L.; Breunig, H. J.; Lork, E. *Angew. Chem. Int. Ed.* **2002**, *41*, 2309–2312.
101. Ellermann, J.; Lindner, H. A.; Schossner, H.; Thiele, G.; Zoubek, G. Z. *Naturforsch. B: J. Chem. Sci.* **1978**, *33*, 1386.
102. Balazs, G.; Breunig, H. J.; Lork, E. Z. *Anorg. Allg. Chem.* **2003**, *629*, 1937–1942.
103. Jibril, I.; Frank, L.-R.; Zsolnai, L.; Evertz, K.; Huttner, G. *J. Organomet. Chem.* **1990**, *393*, 213–225.
104. Breunig, H. J.; Roesler, R.; Lork, E. Z. *Anorg. Allg. Chem.* **1999**, *625*, 1619–1623.
105. Breunig, H. J.; Pawlik, J. Z. *Anorg. Allg. Chem.* **1995**, *621*, 817–822.
106. Balazs, G.; Breunig, H. J.; Lork, E. Z. *Anorg. Allg. Chem.* **2001**, *627*, 1855–1858.
107. Mast, K.; Scherer, O. J.; Wolmershaeuser, G. Z. *Anorg. Allg. Chem.* **1999**, *625*, 1475–1478.
108. Rheingold, A. L.; Fountain, M. E. *Organometallics* **1986**, *5*, 2410–2413.
109. De Silva, R. M.; Mays, M. J.; Davies, J. E.; Raithby, P. R.; Rennie, M. A.; Shield, G. P. *J. Chem. Soc. Dalton Trans.* **1998**, 439–446.
110. De Silva, R. M.; Mays, M. J.; Raithby, P. R.; Solan, G. A. *J. Organomet. Chem.* **2002**, *642*, 237–245.
111. De Silva, R. M.; Mays, M. J.; Solan, G. A. *J. Organomet. Chem.* **2002**, *664*, 27–36.
112. Grobe, J.; Karst, A.; Krebs, B.; Laege, M.; Wuertwein, E.-U. Z. *Anorg. Allg. Chem.* **2006**, *632*, 599–608.
113. De Silva, R. M.; Mays, M. J.; Raithby, P. R.; Solan, G. A. *J. Organomet. Chem.* **2001**, *625*, 245–254.
114. Balazs, G.; Breunig, H. J. Phosphorus, *Sulfur Silicon Relat. Elem.* **2001**, *169*, 301–304.
115. Breunig, H. J.; Balazs, L.; Philipp, N.; Soran, A.; Silvestru, C. Phosphorus, *Sulfur Silicon Relat. Elem.* **2004**, *179*, 853–857.
116. Umeyama, T.; Naka, K.; Chujo, Y. *Macromolecules* **2004**, *37*, 5952–5958.
117. Naka, K.; Umeyama, T.; Chujo, Y. *J. Am. Chem. Soc.* **2002**, *124*, 6600–6603.
118. Umeyama, T.; Naka, K.; Nakahashi, A.; Chujo, Y. *Macromolecules* **2004**, *37*, 1271–1275.
119. Umeyama, T.; Naka, K.; Chujo, Y. *Macromolecules* **2004**, *37*, 3623–3629.
120. Breunig, H. J.; Ghesner, I.; Lork, E. *Organometallics* **2001**, *20*, 1360–1364.
121. Werner, H.; Paul, W.; Zolk, R. *Angew. Chem. Int. Ed. Engl.* **1984**, *23*, 626–627.
122. Werner, H.; Paul, W.; Wolf, J.; Steinmetz, M.; Zolk, R.; Mueller, G.; Steigelmann, O.; Riede, J. *Chem. Ber.* **1989**, *122*, 1061–1066.
123. Mercado, P.; DiMaio, A.-J.; Rheingold, A. L. *Angew. Chem. Int. Ed. Engl.* **1987**, *26*, 244–245.
124. Weber, L.; Bayer, P.; Braun, T.; Stammer, H.-G.; Neumann, B. *Organometallics* **2006**, *25*, 1786–1794.
125. Harper, J. R.; Fountain, M. E.; Rheingold, A. L. *Organometallics* **1989**, *8*, 2316–2320.
126. Jones, R. A.; Whittlesey, B. R. *Organometallics* **1984**, *3*, 469–475.
127. Gatehouse, B. M. *J. Chem. Soc. D* **1969**, 948–949.
128. Rheingold, A. L.; Fountain, M. E.; DiMaio, A. J. *J. Am. Chem. Soc.* **1987**, *109*, 141–148.
129. Elmes, P. S.; Gatehouse, B. M.; Lloyd, D. J.; West, B. O. *J. Chem. Soc. Chem. Commun.* **1974**, 953–954.



130. Breunig, H. J.; Lork, E.; Moldovan, O.; Rat, C. I. *J. Organomet. Chem.* **2008**, *693*, 2527–2534.
131. Hitchcock, P. B.; Lappert, M. F.; Li, G.; Protchenko, A. V. *Chem. Commun.* **2009**, 428–429.
132. Wang, Y.; Quillian, B.; Yang, X.-J.; Wei, P.; Chen, Z.; Wannere, C. S.; Schleyer, P. v.R.; Robinson, G. H. *J. Am. Chem. Soc.* **2005**, *127*, 7672–7673.
133. Twamley, B.; Sofield, C. D.; Olmstead, M. M.; Power, P. P. *J. Am. Chem. Soc.* **1999**, *121*, 3357–3367.
134. Breunig, H. J.; Borrmann, T.; Lork, E.; Rat, C. I.; Rosenthal, U. *Organometallics* **2007**, *26*, 5364–5368.
135. Sasamori, T.; Mieda, E.; Tokitoh, N. *Bull. Chem. Soc. Jpn.* **2007**, *80*, 2425–2435.
136. Sasamori, T.; Mieda, E.; Takeda, N.; Tokitoh, N. *Angew. Chem. Int. Ed.* **2005**, *44*, 3717–3720.
137. Baiget, L.; Ranaivonjatovo, H.; Escudie, J.; Nemes, G. C.; Silaghi-Dumitrescu, I.; Silaghi-Dumitrescu, L. *J. Organomet. Chem.* **2005**, *690*, 307–312.
138. Daly, J. J.; Sanz, F. *Helv. Chim. Acta* **1970**, *53*, 1879–1883.
139. Scherer, O. J.; Puettmann, M. *Angew. Chem. Int. Ed. Engl.* **1979**, *18*, 679–680.
140. Honle, W.; Wolf, J.; von Schnering, H. G. Z. *Naturforsch. B: J. Chem. Sci.* **1988**, *43*, 219.
141. Von Haenisch, C.; Fenske, D. Z. *Anorg. Allg. Chem.* **1997**, *623*, 1040–1042.
142. Westerhausen, M.; Weinrich, S.; Mayer, P. Z. *Anorg. Allg. Chem.* **2003**, *629*, 1153–1156.
143. Froehlich, R.; Tebbe, K.-F. Z. *Kristallogr. Kristallgeom. Kristallphys. Kristallchem.* **1981**, *154*, 277.
144. Froehlich, R.; Tebbe, K.-F. Z. *Kristallogr. Kristallgeom. Kristallphys. Kristallchem.* **1982**, *158*, 255.
145. Breunig, H. J.; Roesler, R.; Lork, E. *Angew. Chem. Int. Ed. Engl.* **1997**, *36*, 2237–2238.
146. Nikolova, D.; von Haenisch, C. *Eur. J. Inorg. Chem.* **2005**, 378–382.
147. von Haenisch, C.; Nikolova, D. *Eur. J. Inorg. Chem.* **2006**, 4770–4773.
148. Driess, M.; Franke, F.; Pritzkow, H. *J. Organomet. Chem.* **2002**, *643–644*, 468–478.
149. Conrad, E.; Burford, N.; McDonald, R.; Ferguson, M. J. *Inorg. Chem.* **2008**, *47*, 2952–2954.
150. Dubenskyy, V.; Ruck, M. Z. *Anorg. Allg. Chem.* **2004**, *630*, 2458–2462.
151. Wahl, B.; Erbe, M.; Gerisch, A.; Kloo, L.; Ruck, M. Z. *Anorg. Allg. Chem.* **2009**, *635*, 743–752.
152. Ahmed, E.; Koehler, D.; Ruck, M. Z. *Anorg. Allg. Chem.* **2009**, *635*, 297–300.
153. Hampel, S.; Ruck, M. Z. *Anorg. Allg. Chem.* **2006**, *632*, 1150–1156.
154. Lindsjoe, M.; Fischer, A.; Kloo, L. *Angew. Chem. Int. Ed.* **2004**, *43*, 2540–2543.
155. Beck, J.; Hilbert, T. *Eur. J. Inorg. Chem.* **2004**, 2019–2026.
156. Kuznetsov, A. N.; Popovkin, B. A.; Stahl, K.; Lindsjoe, M.; Kloo, L. *Eur. J. Inorg. Chem.* **2005**, 4907–4913.
157. Hampel, S.; Schmidt, P.; Ruck, M. Z. *Anorg. Allg. Chem.* **2005**, *631*, 272–283.
158. Wahl, B.; Ruck, M. Z. *Anorg. Allg. Chem.* **2008**, *634*, 2873–2879.
159. Wahl, B.; Ruck, M. Z. *Anorg. Allg. Chem.* **2010**, *636*, 337–342.
160. Beck, J.; Schlueter, S.; Zotov, N. Z. *Anorg. Allg. Chem.* **2005**, *631*, 2450–2456.
161. Wahl, B.; Kloo, L.; Ruck, M. *Angew. Chem. Int. Ed.* **2008**, *47*, 3932–3935.
162. Wahl, B.; Ruck, M. Z. *Anorg. Allg. Chem.* **2008**, *634*, 2267–2275.
163. Lindsjoe, M.; Kloo, L.; Kuznetsov, A.; Popovkin, B. *Eur. J. Inorg. Chem.* **2008**, 5196–5202.
164. Wiesler, K.; Korber, N. *Polyhedron* **2005**, *24*, 1565–1568.
165. Garcia, F.; Less, R. J.; Naseri, V.; McPartlin, M.; Rawson, J. M.; Wright, D. S. *Angew. Chem. Int. Ed.* **2007**, *46*, 7827–7830.
166. Breunig, H. J.; Ghesner, M. E. *Phosphorus, Sulfur Silicon Relat. Elem.* **2004**, *179*, 971–972.
167. Breunig, H. J.; Ghesner, M. E.; Lork, E. *J. Organomet. Chem.* **2002**, *660*, 167–172.
168. Breunig, H. J.; Ghesner, M. E.; Lork, E. Z. *Anorg. Allg. Chem.* **2005**, *631*, 851–856.
169. Papoian, G. A.; Hoffmann, R. *Angew. Chem. Int. Ed.* **2000**, *39*, 2408–2448.
170. Papoian, G.; Hoffmann, R. *J. Am. Chem. Soc.* **2001**, *123*, 6600–6608.
171. Hanauer, T.; Kraus, F.; Reil, M.; Korber, N. *Monatsh. Chem.* **2006**, *137*, 147–156.
172. Kraus, F.; Hanauer, T.; Korber, N. *Inorg. Chem.* **2006**, *45*, 1117–1123.
173. Critchlow, S. C.; Corbett, J. D. *Inorg. Chem.* **1984**, *23*, 770–774.
174. Kuznetsov, A. N.; Faessler, T. F. Z. *Anorg. Allg. Chem.* **2002**, *628*, 2537–2541.
175. Cisar, A.; Corbett, J. D. *Inorg. Chem.* **1977**, *16*, 2482–2487.
176. Bashall, A.; Bond, A. D.; Hopkins, A. D.; Kidd, S. J.; McPartlin, M.; Steiner, A.; Wolf, R.; Woods, A. D.; Wright, D. S. *J. Chem. Soc. Dalton Trans.* **2002**, 343–351.
177. Hanauer, T.; Grothe, M.; Reil, M.; Korber, N. *Helv. Chim. Acta* **2005**, *88*, 950–961.
178. Korber, N.; von Schnering, H. G. Z. *Kristallogr. New Cryst. Struct.* **1997**, *212*, 85.
179. Bashall, A.; Beswick, M. A.; Choi, N.; Hopkins, A. D.; Kidd, S. J.; Lawson, Y. G.; Mosquera, M. E. G.; McPartlin, M.; Raithby, P. R.; Wheatley, A. A. E. H.; Wood, J. A.; Wright, D. S. *J. Chem. Soc. Dalton Trans.* **2000**, 479–486.
180. Castleman, A. W.; Khanna, S. N.; Sen, A.; Reber, A. C.; Qian, M.; Davis, K. M.; Peppernick, S. J.; Ugrinov, A.; Merritt, M. D. *Nano Lett.* **2007**, *7*, 2734–2741.
181. Huebler, K.; Becker, G. Z. *Anorg. Allg. Chem.* **1998**, *624*, 483–496.
182. Driess, M.; Merz, K.; Pritzkow, H.; Janoschek, R. *Angew. Chem. Int. Ed. Engl.* **1996**, *35*, 2507–2510.
183. Adolphson, D. G.; Corbett, J. D.; Meryman, D. J. *J. Am. Chem. Soc.* **1976**, *98*, 7234–7239.
184. Hanauer, T.; Aschenbrenner, J. C.; Korber, N. *Inorg. Chem.* **2006**, *45*, 6723–6727.
185. Hanauer, T.; Korber, N. Z. *Anorg. Allg. Chem.* **2006**, *632*, 1135–1140.
186. Belin, C. H. E. *J. Am. Chem. Soc.* **1980**, *102*, 6036–6040.
187. Garcia, F.; Less, R. J.; Naseri, V.; McPartlin, M.; Rawson, J. M.; Sancho Tomas, M.; Wright, D. S. *Chem. Commun.* **2008**, 859–861.
188. Bolle, U.; Tremel, W. *J. Chem. Soc. Chem. Commun.* **1992**, 91–93.
189. Haushalter, R. C.; Eichhorn, B. W.; Rheingold, A. L.; Geib, S. J. *J. Chem. Soc. Chem. Commun.* **1988**, 1027–1028.
190. Armbruster, M.; Schnelle, W.; Schwarz, U.; Grin, Y. *Inorg. Chem.* **2007**, *46*, 6319–6328.
191. Hirschle, C.; Roehr, C. Z. *Anorg. Allg. Chem.* **2000**, *626*, 1992–1998.
192. Xu, L.; Bobev, S.; El-Bahraoui, J.; Sevov, S. C. *J. Am. Chem. Soc.* **2000**, *122*, 1838–1839.
193. Gascoin, F.; Sevov, S. C. *J. Am. Chem. Soc.* **2000**, *122*, 10251–10252.
194. Hanauer, T.; Korber, N. Z. *Anorg. Allg. Chem.* **2004**, *630*, 2532–2534.
195. Xu, L.; Ugrinov, A.; Sevov, S. C. *J. Am. Chem. Soc.* **2001**, *123*, 4091–4092.
196. Gascoin, F.; Sevov, S. C. *Inorg. Chem.* **2001**, *40*, 5177–5181.
197. Zhai, H.-J.; Wang, L.-S.; Kuznetsov, A. E.; Boldyrev, A. I. *J. Phys. Chem. A* **2002**, *106*, 5600–5606.
198. Kraus, F.; Hanauer, T.; Korber, N. *Angew. Chem. Int. Ed.* **2005**, *44*, 7200–7204.
199. Reil, M.; Korber, N. Z. *Anorg. Allg. Chem.* **2007**, *633*, 1599–1602.
200. Emmerling, F.; Hirschle, C.; Roehr, C. Z. *Anorg. Allg. Chem.* **2002**, *628*, 559–563.
201. Hirschle, C.; Emmerling, F.; Rohr, C. *Acta Crystallogr., Sect. C: Cryst. Struct. Commun.* **2001**, *57*, 501–502.
202. Bobev, S.; Kleinke, H. *Chem. Mater.* **2003**, *15*, 3523–3529.
203. Zhu, Y.; Kleinke, H. Z. *Anorg. Allg. Chem.* **2002**, *628*, 2233.
204. Elder, I.; Lee, C.-S.; Kleinke, H. *Inorg. Chem.* **2002**, *41*, 538–545.
205. Kleinke, H. *Inorg. Chem.* **2001**, *40*, 95–100.
206. Petri, D.; Roehr, C. Z. *Anorg. Allg. Chem.* **2008**, *634*, 1724–1728.
207. Schmidt, T.; Altmeyer, R. O.; Jeitschko, W. *J. Solid State Chem.* **2003**, *173*, 259–272.
208. Sun, Z.-M.; Mao, J.-G. *J. Solid State Chem.* **2004**, *177*, 3752–3756.
209. Ponou, S.; Faessler, T. F. *Inorg. Chem.* **2004**, *43*, 6124–6126.
210. Moses, M. J.; Fettinger, J.; Eichhorn, B. *J. Am. Chem. Soc.* **2002**, *124*, 5944–5945.
211. Moses, M. J.; Fettinger, J. C.; Eichhorn, B. W. *Inorg. Chem.* **2007**, *46*, 1036–1038.
212. Goicoechea, J. M.; Hull, M. W.; Sevov, S. C. *J. Am. Chem. Soc.* **2007**, *129*, 7885–7893.
213. Xu, L.; Sevov, S. C. *Inorg. Chem.* **2000**, *39*, 5383–5389.
214. Goicoechea, J. M.; Sevov, S. C. *Angew. Chem. Int. Ed.* **2006**, *45*, 5147–5150.
215. Moses, M. J.; Fettinger, J. C.; Eichhorn, B. W. *Science* **2003**, *300*, 778–780.
216. Zhao, J.; Xie, R.-H. *Chem. Phys. Lett.* **2004**, *396*, 161–166.
217. Sales, B. C. *Science* **2002**, *295*, 1248–1249.
218. Sales, B. C. In *Handbook on the Physics and Chemistry of Rare Earths*; Gschneidner, K. A. Jr., Bünzli, J.-C. G., Pecharsky, V. K., Eds.; North-Holland: Amsterdam, 2003; Vol. 33, pp 1–34.
219. Ellis, B. D.; Macdonald, C. L. B. *Inorg. Chem.* **2004**, *43*, 5981–5986.
220. Grothe, M.; Korber, N. Z. *Anorg. Allg. Chem.* **2003**, *629*, 399–402.
221. Petrie, S.; Stranger, R.; Rae, A. D.; Willis, A. C.; Zhou, X.; Wild, S. B. *Organometallics* **2006**, *25*, 164–171.
222. Kilah, N. L.; Weir, M. L.; Wild, S. B. *Dalton Trans.* **2008**, 2480–2486.
223. Hill, N. J.; Levason, W.; Reid, G. *J. Chem. Soc. Dalton Trans.* **2002**, 1188–1192.
224. Besinger, J.; Fenske, D. Z. *Anorg. Allg. Chem.* **2001**, *627*, 1487–1494.
225. Besinger, J.; Treptow, J.; Fenske, D. Z. *Anorg. Allg. Chem.* **2002**, *628*, 512–515.
226. Fenske, D.; Rothenberger, A.; Wieber, S. *Eur. J. Inorg. Chem.* **2007**, 648–651.
227. Traut, S.; von Haenisch, C. *Chem. Commun.* **2010**, *46*, 1538–1540.



228. Conrad, E.; Burford, N.; Werner-Zwanziger, U.; McDonald, R.; Ferguson, M. J. *Chem. Commun.* **2010**, *46*, 2465–2467.
229. Adams, R. D.; Pearl, W. C. *Inorg. Chem.* **2009**, *48*, 9519–9525.
230. Ahlrichs, R.; Eichhoefer, A.; Fenske, D.; May, K.; Sommer, H. *Angew. Chem. Int. Ed.* **2007**, *46*, 8254–8257.
231. Kaiser, B.; Stegemann, B.; Bernhardt, T. M.; Rademann, K. *Z. Anorg. Allg. Chem.* **2002**, *628*, 2187.
232. Lapshin, A.; Shepelev, Y.; Smolin, Y.; Vasil'eva, E. *Russ. J. Inorg. Chem. Transl. Zh. Neorg. Khim.* **2007**, *52*, 1657–1661.
233. Choi, H.; Park, C.; Baeck, K. K. *J. Phys. Chem. A* **2002**, *106*, 5177–5187.
234. Baruah, T.; Pederson, M. R.; Zope, R. R.; Beltran, M. R. *Chem. Phys. Lett.* **2004**, *387*, 476–480.
235. Abraham, M. Y.; Wang, Y.; Xie, Y.; Wei, P.; Schaefer, H. F.; Schleyer, P.v.R.; Robinson, G. H. *Chem. Eur. J.* **2010**, *16*, 432–435.
236. Gregoriades, L. J.; Krauss, H.; Wachter, J.; Virovets, A. V.; Sierka, M.; Scheer, M. *Angew. Chem. Int. Ed.* **2006**, *45*, 4189–4192.
237. Ly, H. V.; Parvez, M.; Roesler, R. *Inorg. Chem.* **2006**, *45*, 345–351.
238. Groer, T.; Scheer, M. *Organometallics* **2000**, *19*, 3683–3691.

## 1.06 Catenated Sulfur Compounds

PF Kelly and RSP King, Loughborough University, Loughborough, UK

© 2013 Elsevier Ltd. All rights reserved.

<b>1.06.1</b>	<b>Background and Scope</b>	179
<b>1.06.2</b>	<b>Neutral Systems: The Allotropes of Sulfur</b>	180
1.06.2.1	The Gas-Phase Allotropes – S <sub>2</sub> , S <sub>3</sub> , and S <sub>4</sub>	180
1.06.2.2	Forms of S <sub>8</sub> and the Effects of Pressure upon This Allotrope	181
1.06.2.2.1	Forms at ambient pressure, and biologically produced S <sub>8</sub>	181
1.06.2.2.2	The effects of pressure upon S <sub>8</sub>	182
1.06.2.2.3	Polymerization of S <sub>8</sub>	183
1.06.2.3	The Smaller Rings – S <sub>6</sub> and S <sub>7</sub>	183
1.06.2.4	The Larger Rings S <sub>9</sub> –S <sub>20</sub> : Preparation and Structure	183
1.06.2.5	Reactivity of S <sub>8</sub> and the Larger Rings	185
1.06.2.5.1	Complexes of intact rings	185
1.06.2.5.2	Oxides of the cyclic allotropes	186
<b>1.06.3</b>	<b>Homoatomic Cations of Sulfur</b>	187
1.06.3.1	General Introduction	187
1.06.3.2	Preparation and Structure of Solid-State Sulfur Cations	187
1.06.3.2.1	The preparation and structure of salts of [S <sub>4</sub> ] <sup>2+</sup>	187
1.06.3.2.2	The preparation and structure of salts of [S <sub>8</sub> ] <sup>2+</sup>	187
1.06.3.2.3	The preparation and structure of salts of [S <sub>19</sub> ] <sup>2+</sup>	188
1.06.3.3	Bonding Within Sulfur Cations	188
1.06.3.4	Sulfur Cations in Solution	189
1.06.3.5	Sulfur Cations in the Gas Phase	190
1.06.3.6	Sulfur Cations within Zeolite Hosts	190
<b>1.06.4</b>	<b>Polysulfide Anions</b>	190
1.06.4.1	Free Polysulfide Anions	190
1.06.4.2	Polysulfides as Ligands	191
<b>1.06.5</b>	<b>Conclusion</b>	192
<b>References</b>		194

### 1.06.1 Background and Scope

While the range of different-sized fullerenes may well exceed the range of molecular forms of sulfur, it is still fair to say that sulfur is unique in terms of its diversity of allotropes. This is clearly testament to the element's remarkable propensity for homoatomic catenation; even if we were to ignore the rarer allotropes and just focus on S<sub>8</sub>, sulfur's preeminence would still be guaranteed, thanks to the fact that – uniquely among the solid elements – it appears in a naturally occurring catenated discrete molecular form (i.e., volcanic sulfur). It follows that our long history of interaction with the element has seen us influenced – either wittingly or unwittingly – by the modifications imposed upon its reactivity by this catenation. The very fact that the word sulfur itself stems from Latin (*cf.* Sanskrit as sometimes claimed)<sup>1</sup> reveals the historical nature of such interactions, and even moving into the age of true chemical understanding, the element continued to play a part in development of the science of chemistry *per se*. Thus, in a very real sense, the history and chemistry of the element are inextricably bound to its propensity for catenation. If we then consider the other allotropes, we find that the element is

unique in another aspect, namely the way in which specific allotropes may be generated by structured, systematic synthetic methodologies. This contrasts markedly with elements such as carbon and phosphorus (see **Chapter 1.04**) for which allotrope formation tends to be directed by brute force (albeit often backed up by exquisite experimental prowess) rather than pure guile.

In terms of the remit of this chapter, its prime aim is to highlight just what is possible in terms of units containing only sulfur atoms. In part, this stems from the astonishing range of compounds in which, alongside other elements, multiple sulfur atoms are present, linked by sulfur–sulfur bonds. It would be impossible to do justice to all such compounds, but it is important to note that catenated sulfur units play a key role in numerous important organic species (including many natural products) and within systems bearing other main group elements. In many cases, we find systems with a very high sulfur 'content'; a good example comes with the sulfimides such as S<sub>7</sub>NH, in which a crown structure analogous to S<sub>8</sub> is seen, save for replacement of one S by NH (for information on these and other sulfur–nitrogen species bearing sulfur chain units, see the recent monolog by Chivers<sup>2</sup>). Other examples include the

sulfanes ( $\text{H}_2\text{S}_x$ ) and sulfur chlorides ( $\text{S}_x\text{Cl}_2$ ) which can both exhibit long sulfur chains; while both are alluded to here as synthetic reagents, detailed accounts of their chemistry must be sought elsewhere.<sup>3</sup> The recent treatise on p-block rings and polymers by Chivers and Manners is also an excellent resource for many main group systems bearing catenated sulfurs.<sup>4</sup> A caveat to our self-imposed restriction comes in the case of metal sulfide complexes, which we will touch on (more by way of illustration of what is possible rather than any attempt at a comprehensive review) and in examples of systems wherein the ring structure of an allotrope is retained upon reaction. Specifically in the latter case, we will look at the coordination chemistry of the intact rings, and the formation of oxides of the allotropes such as  $\text{S}_8\text{O}$ .

In terms of the timescale of results reported here, the primary aim is to address work that has happened since 2000; this not only reflects the need to illustrate the fact that advances continue, even with such a long-studied element, but also acknowledges the appearance of Steudel's magisterial two-volume compendium of the state of play in 2003, to which readers requiring more in-depth information on the element are directed.<sup>5</sup> However, the fact remains that many of the key advances in the formation of new molecular species occurred during the decade or so prior to that; thus, it is impossible to summarize the broad sweep of species and reactions without looking further back. Ultimately, the aim here is to try to highlight not only the diversity of forms that the element can exhibit but also areas where ongoing research is being most keenly undertaken. In order to do this, the species in question are looked at in three broad classifications: neutral systems, cations, and anions. As an aside it should be noted that all the 'ball and stick' illustrations of molecular structures herein have been generated from the raw X-ray data by the authors (using the mercury crystal structure visualization program).

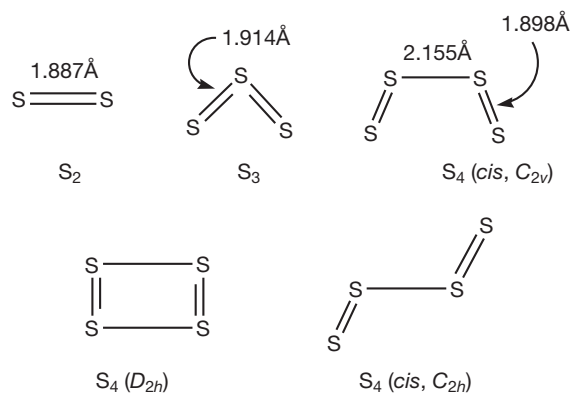
## 1.06.2 Neutral Systems: The Allotropes of Sulfur

### 1.06.2.1 The Gas-Phase Allotropes – $\text{S}_2$ , $\text{S}_3$ , and $\text{S}_4$

The composition of sulfur vapor has been the subject of numerous studies, employing a wealth of spectroscopic and spectrometric techniques. Allotropes  $\text{S}_x$  with the values  $x=2-8$  can all be detected, with the exact ratios of species being dependent upon the precise conditions. A good illustration of the presence of various species in sulfur vapor comes with the 'trapping' of  $\text{S}_8$ ,  $\text{S}_6$ , and  $\text{S}_2$  within zeolite  $\text{NaX}$  "(for zeolites see [Chapters 4.05](#) and [5.05](#)) when the latter is heated with the element.<sup>6</sup> Although the smaller systems  $\text{S}_2$ ,  $\text{S}_3$ , and  $\text{S}_4$  may, on the face of it, appear to have less relevance than the common solid-state allotrope  $\text{S}_8$ , a number of studies and observations have shown that they can in fact have a high degree of pertinence to natural scenarios and thus cannot safely be ignored. This is certainly becoming ever truer as we learn more about the chemistry of the harsher environments found in the solar system. Thus, in 1999<sup>7</sup> (and again in 2003<sup>8</sup>) data from the Hubble Space Telescope provided evidence for the presence of  $\text{S}_2$  in the volcanic plume emitted from the Jovian satellite Io's volcano *Pele*. This in turn allows the conclusion that dimerization of the latter to  $\text{S}_4$  occurs on the solid surface of the moon, a fact which manifests itself as the spectacular characteristic red

coloration observed around the base of such plumes.<sup>9</sup> Indeed, the fact that the *Galileo* spacecraft visiting that moon between 1996 and 2001 also observed localized red deposits near likely volcanic sites strongly indicates that the appearance and influence of these small allotropes are widespread on this far-off world, and any assessment of surface chemistry has to take them into account.<sup>8</sup> This was demonstrated even more spectacularly not far from Io when Jupiter itself presented evidence of  $\text{S}_2$  formation in a spectacular one-off event in 1994. In many ways, this event could justifiably be called the largest-scale inorganic chemistry 'experiment' ever observed in real time, and was initiated by the collision of comet Shoemaker-Levy 9 with the gas giant. Ultraviolet (UV) reflection spectrum revealed the presence of  $\text{S}_2$  in the resulting 'scar' in the cloud belt. A few days later, it could still be detected; a few weeks later, it was gone. Any doubts as to the scale of these events are surely dispelled by the calculation that the observations were consistent with the production of a hundred million tons of disulfur during the collision!<sup>10</sup>

Given that  $\text{S}_3$  has also been implicated in the atmospheric chemistry of Venus (e.g., via new analysis of data from the Soviet *Venera* missions<sup>11</sup>) and that  $\text{S}_2$  has been studied in the context of lightning-induced chemistry within storm clouds on Saturn,<sup>12</sup> it follows that we can be sure that many more roles for these transient species will be found in the further-flung regions of the solar system.<sup>13</sup> Closer to home spatially – though certainly not temporally – the vapor-phase sulfur allotropes may well have played a much more significant role in Earth's ancient atmospheric chemistry than they do now. Key to such suggestions is the observation in 2000 that the sulfide and sulfates present in extremely old rocks (in the order of 2.5 billion years) exhibit the so-called sulfur isotope mass-independent fractionation (S-MIF).<sup>14</sup> In essence, this means that sulfur cycles not affected by mass-dependent processes such as evaporation or kinetic isotope effects predominated, or at least they did until the collapse of methane levels in the later Archean period.<sup>15</sup> While photodissociation of primordial  $\text{SO}_2$  has been mooted as one of the origins for this S-MIF effect, the possibility that gas-phase reactions such as the combination of  $\text{S}_2$  with sulfur radicals to give  $\text{S}_3$  are key has also been raised. Thus, it may well be that these transient and apparently rare species played a significant role. Investigation into the overall role of sulfur in atmospheric evolution is very much ongoing, with its importance stemming from the fact that the results are not simply limited to an understanding of the 'history' of the element itself but also provide important clues to the understanding of other constituents of the early atmosphere, such as oxygen levels.<sup>16</sup> Such work constitutes an excellent example of the way in which ostensibly simple inorganic chemistry can cross over into other areas such as geology and the origin of life, with the studies often necessitating advanced calculation methods. By way of illustration, the humblest reaction in this area, namely the combination of two sulfur atoms (generated, e.g., within volcanic eruptions) to form  $\text{S}_2$ , might appear 'trivial' but in fact has been the subject of many computational studies. The most recent of these used quasiclassical trajectory calculations to come up with a rate constant of  $4.19 \times 10^{-33} \text{ cm}^6 \text{ molecule}^{-2} \text{ s}^{-1}$  for the argon-partnered recombination.<sup>17</sup> Clearly, much more work is still required to get the full story; a very recent and extremely



**Figure 1** The structures of  $S_2$ ,  $S_3$ , and  $S_4$  (n.b. bond orders shown are approximate), together with the  $D_{2h}$  isomer of the latter, which forms during its automerization, and the putative *trans* isomer.

comprehensive review of the area of atmospheric sulfur by Johnston is recommended for those requiring further information.<sup>18</sup> Away from atmospheric concerns it is worth noting that the reaction of  $R_3MSSMR_3$  (where  $M = Si$  or  $Ge$ ) with  $Ph_3PBr_2$  acts as a source of ' $S_2$ ' insofar as the intermediate formed undergoes Diels–Alder adduct formation with dienes in the manner expected for the putative disulfur. In the absence of the diene, this species oligomerizes to  $S_8$ .<sup>19</sup>

While the structure of violet-colored  $S_2$  is, of course, simply diatomic, the arrangements with  $S_3$  and  $S_4$  have been the subject of continuing investigation, particularly in the latter case. Although a V-shape for  $S_3$  with  $C_{2v}$  symmetry analogous to ozone (hence the term 'thiozone' which is often used) has been acknowledged for some time, computational<sup>20</sup> and spectroscopic<sup>21,22</sup> studies continue in an effort to fully elucidate bonding and reactivity. Identifying the structure(s) associated with  $S_4$  has proved more problematic, however. Multiple isomers can be envisaged for this compound, and the number of different theoretical studies alone runs into the dozens. However, recent consensus from both experimental (e.g., via rotational spectroscopy)<sup>22,23</sup> and theoretical<sup>24–26</sup> studies confirms the long-held view that an open chain  $C_{2v}$  structure is the most stable arrangement, with automerization occurring via a rectangular  $D_{2h}$  transition state (Figure 1). Indeed, this structural conclusion mirrors that of matrix-isolation techniques performed back in 1992 by Andrews and Hassanzadeh.<sup>27</sup> Earlier work such as this also hinted at isomerization induced photothermally<sup>28</sup> or by microwave discharge<sup>27</sup> that might involve the *trans* isomer (i.e., of  $C_{2h}$  symmetry). More recent studies have backed this up,<sup>24</sup> though to what extent this possibility has been fully dealt with is unclear.

### 1.06.2.2 Forms of $S_8$ and the Effects of Pressure upon This Allotrope

#### 1.06.2.2.1 Forms at ambient pressure, and biologically produced $S_8$

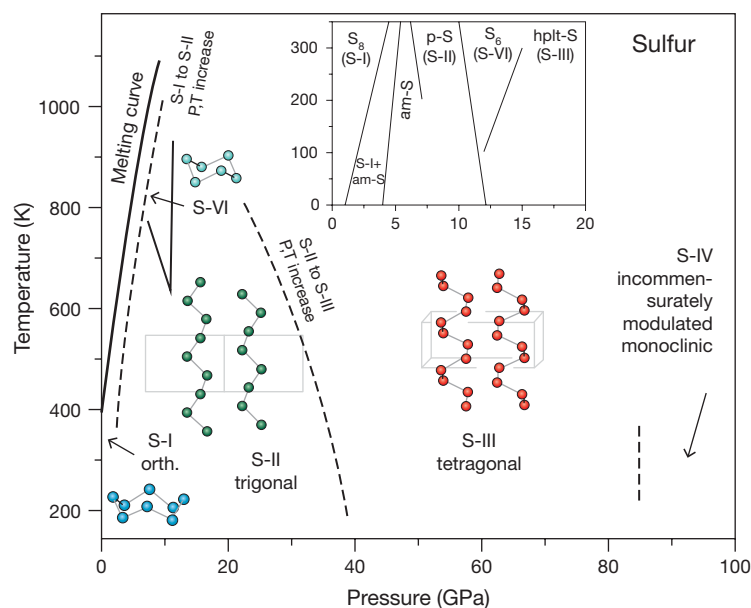
The fact that the primary stable allotrope of sulfur consists of a crown  $S_8$  unit has been known for almost a century now (thanks in no small part to pioneering crystallographic studies by the great Bragg<sup>29</sup>). The conversion of this orthorhombic ( $\alpha$ ) form to a monoclinic ( $\beta$ ) analog at around 96 °C is also well

documented in standard inorganic textbooks<sup>30</sup> and needs no further comment here, save to note that the effect is primarily one of intermolecular packing rather than any change in the intramolecular bonding arrangement. While this means that for most purposes elemental sulfur in commercial laboratory samples can simply be thought of as consisting of the  $S_8$  crown form, there are important considerations/caveats to be borne in mind. The first is that as this is the most stable of all allotropes of the element, this also means that it is the least reactive and indeed recent years have seen work on the reactivity of specific alternative allotropes. The other point of note is that, strictly speaking, such samples are not actually exclusively composed of  $S_8$ , even though it is by far and away the primary component. Other allotropes such as  $S_7$  can be shown to be present and it has even been suggested that such 'impurities' play a role in determining the characteristic color of commercial samples.<sup>31</sup> So not only is referring to such samples as ' $S_8$ ' inaccurate, but also, in fact, purification of the latter is quite time consuming; a recommended route consists of extraction (toluene or dichloromethane) and cooling, followed by meticulous thermal treatment and then distillation. As noted by Stuedel, even commercially available super-high-purity material tends to rank this only on the amount of metallic contaminant present rather than other forms of sulfur. Returning to the subject of color, as Figure 2 shows, cooling commercial samples to liquid nitrogen reversibly 'bleaches' the color; if the material is irradiated with X-rays at this temperature, then a red color develops, consistent with the formation of the smaller allotropes.<sup>32</sup> Again this effect is reversible and the familiar yellow color reappears on warming.

In contrast to the  $\alpha$  and  $\beta$  forms, it is only relatively recently that studies have fully confirmed the structure of the third form of  $S_8$ . This monoclinic ( $\gamma$ , or 'nacreous') polymorph can be generated in the laboratory (e.g., by the reaction of pyridine with  $CuSSCOEt$ ) or found in nature (as the mineral rosickyite), and X-ray crystallography has confirmed earlier suggestions of a so-called 'sheared penny roll' packing arrangement of the crown units.<sup>33</sup> Away from the lab, a fascinating aspect of this form of sulfur has emerged during work on geological biosignatures. These are the traces of minerals whose sources can be shown to be biogenic and whose appearance indicates the presence of life, either now or in the past; and, of course, the preservation of such signatures could have immense implications in future investigations into the history of life on Earth and elsewhere. The presence of rosickyite as a geological material has recently been shown to be just such a biosignature; in studies upon evaporate basins in Death Valley (the nearest natural model for the surface of Mars that we possess), Douglas reports that the mineral is constantly replenished by a cycle of microbial attack on gypsum deposits, followed by bacterial reoxidation of the resulting sulfide to this form of elemental sulfur.<sup>34</sup> That the presence of a sulfur allotrope could betray such a complex interplay of primitive life and chemical/geological conditions serves yet again to highlight the importance and ubiquitous nature of the element. Such conclusions are bolstered by the fact that elemental sulfur can appear directly associated with/in microorganisms. A good example comes in the case of *Thiomargarita namibiensis*, which is the largest bacterium thus far discovered (with individual cells up to 0.75 mm in size).<sup>35</sup> Not only are cells large enough to be



**Figure 2** Contrast in the color of elemental sulfur immediately after removal from liquid nitrogen temperatures (left) and after warming to ambient (right).



**Figure 3** Phase diagram for the various forms of sulfur at high pressure. Adapted from Degtyareva, O.; Hernandez, E. R.; Serrano, J.; Somayazulu, M.; Mao, H.-K.; Gregoryanz, E.; Hemley, R. J. *J. Chem. Phys.* **2007**, *126*, 084503.

visible to the naked eye, but also this is aided by the presence of sulfur globules within the cells. Subsequent to its discovery, XANES was employed to show that the sulfur was present as  $S_8$ .<sup>36</sup> In other cases, Raman spectroscopy has been employed to ascertain the form of the element. In a particularly elegant recent example, Himmel and coworkers demonstrated the use of Raman spectroscopy on living samples of the nematode *Eubostrichus diana* (preparative techniques required for X-ray studies would kill biological materials) which possesses a matted coat of symbiotic sulfur-oxidizing bacteria. These bacteria generate granules of sulfur in the course of their metabolism and the Raman studies were able to map the three intense bands associated with  $S_8$  in exquisite detail.<sup>37</sup>

#### 1.06.2.2.2 The effects of pressure upon $S_8$

While the standard notion of sulfur existing as  $S_8$  crowns is readily appreciated at even basic levels of chemistry, the effect of pressure upon  $S_8$  is not only often neglected in basic accounts of the element, but also complicated enough to mean that work on its full elucidation is still very much ongoing. In

part, this apparent gap in our knowledge is due to the fact that work in this area is not simple, requiring as it does very specialist techniques and expertise. The other reason why full elucidation of the effect of pressure on the element is taking so long is that it is in fact a far from straightforward story. To summarize (and simplify), it now appears that the following sequence of phases can be obtained starting with  $S_8$  and ramping up the pressure.

The first transformation appears upon heating at pressures of  $\sim 3$  GPa. This form, often referred to as S-II, now exhibits a structure in which the rings have opened up to form spiraling chains within a trigonal structure. As shown in **Figure 3**, we see triangular arrangements generating three atoms per turn of the spiral, making a structure quite analogous to that of the standard allotropes of selenium or tellurium (see **Chapter 1.07**).<sup>38</sup>

The fate of this form depends upon the parameters of the subsequent experiment; if taken back down to ambient temperature, it remains stable at pressures as high as 36 GPa. If, however, it is taken beyond this pressure, a new form, S-III, is



generated. This form also appears directly from standard  $S_8$  if such pressures are applied at ambient temperature. As shown in Figure 3, S-III retains the chain structure of S-II, but it is now tetragonal, exhibiting squared units resulting in four atoms per turn of the spiral.<sup>38</sup> An intermediate, triclinic phase (S-V) has also recently been reported to form as pressure decreases.<sup>39</sup>

On the other hand, if instead of cooling, S-II is heated to beyond 650 K, and subjected to at least 7 GPa pressure, an entirely different transformation takes place. Now, remarkably, chains are eschewed once more in favor of a molecular ring, in this case containing six sulfur atoms.<sup>40</sup> This form – S-VI – mirrors the  $S_6$  allotrope which, as we will see below, can be prepared at ambient temperatures. As with  $S_6$  prepared under ambient conditions, this material is rhombohedral in crystal form. It is fascinating to consider that although 114 years separate the work of Engel who first prepared  $S_6$  and Crapanzano et al. who definitively identified S-VI, and though the contrast in the complexity of the experiments could not be more marked (the action of HCl upon an ice-cold saturated solution of thiosulfate and X-ray diffraction studies upon sulfur at 7.2 GPa/950 K, respectively), they are nevertheless inextricably linked by a common outcome.

Application of still higher pressure results in metallic forms of the element, and recent work has confirmed the onset of S-IV (with a body-centered monoclinic arrangement) at 83 GPa and of rhombohedral S-V at 153 GPa.<sup>41</sup> A useful overall phase diagram summarizing these changes has recently been generated by Degtyareva et al.<sup>42</sup>

#### 1.06.2.2.3 Polymerization of $S_8$

The polymerization of sulfur has been the subject of many studies and key results in the full elucidation of its complicated story were obtained many decades ago; to a large extent, therefore, current interest tends to center on problems such as the high-pressure phases. The area has been extensively reviewed by Steudel and Eckert<sup>43</sup> and succinctly covered by Greenwood and Earnshaw<sup>30</sup>; to briefly summarize, if the molten element is quenched by rapid cooling the resulting ‘plastic’ sulfur can be crystallized by the stretching of filaments. This product contains  $\gamma$   $S_8$  and an infinite chain helical polymer; slower cooling of melts or sublimation of the element allows the isolation of two other polymeric forms, one termed ‘laminar’ sulfur, thanks to the presence of a ‘cross-graining’ effect of perpendicular chains.

#### 1.06.2.3 The Smaller Rings – $S_6$ and $S_7$

As already noted, both these allotropes of sulfur are found naturally in various circumstances and the specific (albeit unwitting) synthesis of  $S_6$  as far back as the end of the nineteenth century has also been alluded to. An excellent method of preparation of either of these stems from the ability of the sulfide complex  $TiCp_2S_5$  to act as a source of the  $[S_5]^{2-}$  unit; given that this material is a commercially available, easily handled, red crystalline solid, it follows that it is more amenable than using the troublesome sulfanes ( $H_2S_x$ ). In addition to Engel’s original route,  $S_6$  can also be prepared from the reaction of iodide with disulfur dichloride followed by the appropriate purification and recrystallization.<sup>44</sup>

As Figure 4 shows,  $S_6$  and  $S_7$  both exhibit chair conformations. In the case of  $S_6$ , all S–S bond lengths are identical and there appears to be only one known polymorph

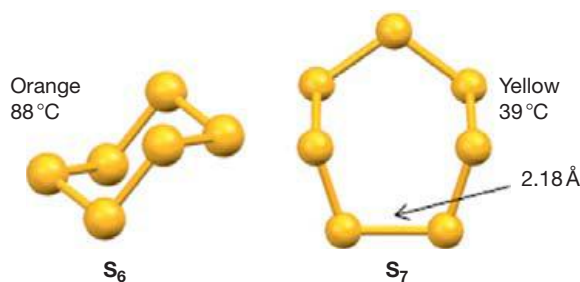


Figure 4 The structures, appearance, and melting points of  $S_6$  and  $S_7$ .

(rhombohedral) and in fact this is the densest form of the element.<sup>45</sup> The stability of this arrangement is attested to by the fact that as noted above this molecular structure forms upon application of high pressure to elemental sulfur and also by the fact that chair-shaped units of  $S_6$  have been observed within zeolitic structures exposed to sulfur vapor.<sup>6</sup> Detailed studies by Steudel et al. have, however, shown that other molecular structures such as the  $D_{3h}$  prism are lower in energy than the energy required for ring opening of  $S_6$ , a result which might have implications for reactivity of this allotrope.<sup>46</sup>

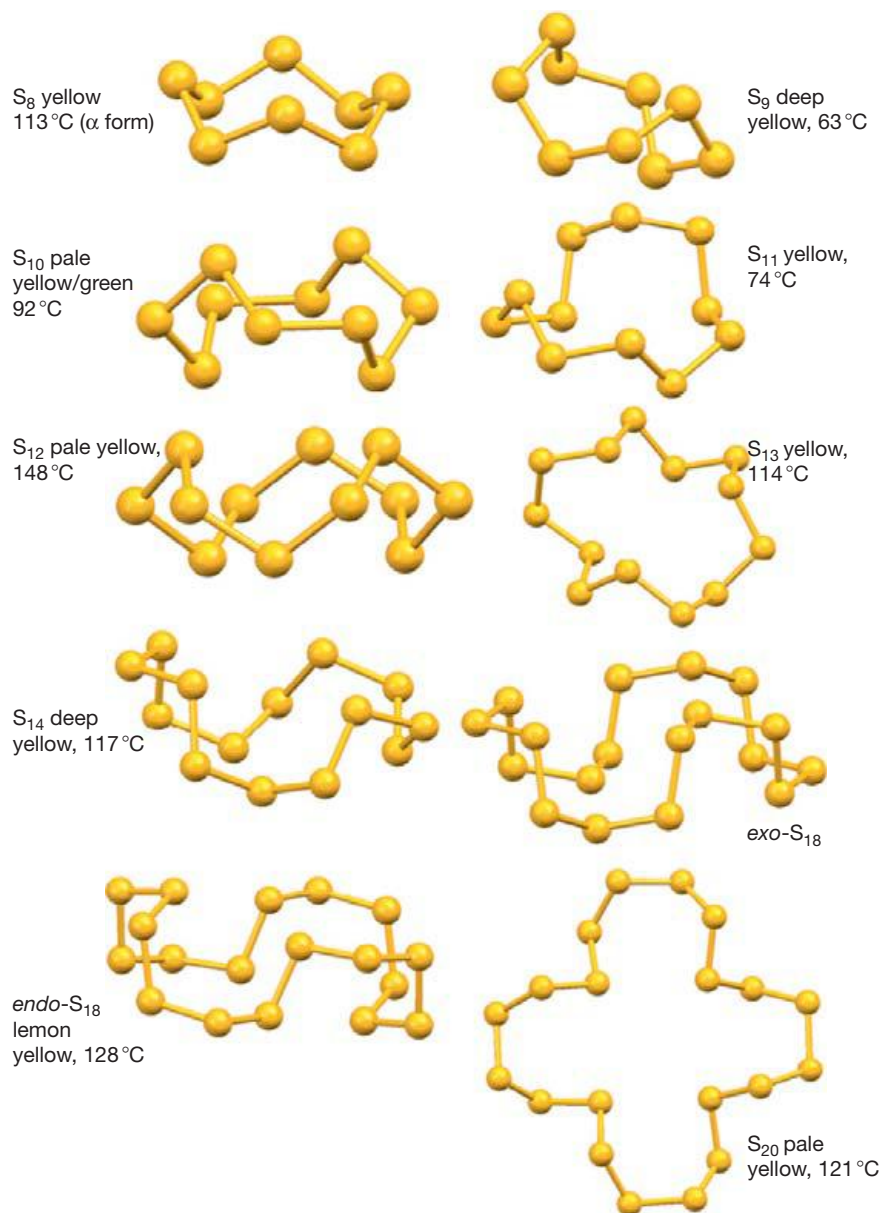
In the case of  $S_7$  the fundamental molecular unit shows much greater variation in bond lengths than  $S_6$ , with one bond markedly longer than the others,<sup>47</sup> although spectroscopy reveals an averaging of the bonds via a pseudorotation effect in solution.<sup>48</sup> Another contrast to  $S_6$  comes with the fact that this allotrope can exhibit four different polymorphs ( $\alpha$ – $\delta$ ), though as with  $S_8$  the differences between such forms hinge on intermolecular packing effects rather than substantial changes to the molecular dimensions. Isolation of the individual forms can be brought about by the specific crystallization technique employed; for example, the  $\alpha$  form results when solutions in toluene or  $CH_2Cl_2$  are rapidly cooled.<sup>49</sup>

Both  $S_6$  and  $S_7$  ultimately revert to  $S_8$  at ambient temperatures, with  $S_7$  being the less stable of the two (with decomposition beginning within minutes at these temperatures). The higher reactivity (i.e., lower stability) of  $S_7$  has been attributed to the aforementioned long S–S bond within the structure; in contrast, studies by Steudel suggest that  $S_6$  can be stored for a number of days at room temperature without decomposition.<sup>50</sup>

Direct reactions of these two allotropes are limited, though they can be taken through to oxides in which the ring structure is maintained (*vide infra*). An important reaction in which the ring structure is not preserved is chlorination to give  $S_4Cl_2$ , itself a useful precursor to other allotropes. Reaction of  $S_6$  with *trans*-cyclooctene has been shown to result in the corresponding episulfide.<sup>51</sup> Although not a ‘reaction’ per se, the co-crystallization of  $S_6$  and  $S_{10}$  results in a system consisting of alternating layers of the two molecular forms.<sup>52</sup> This has been claimed as the only example of an allotrope of an element consisting of different-sized molecules, though it should be noted that co-crystallization of  $C_{60}$  and  $C_{70}$  has been reported, for example, which also fits that bill.<sup>53</sup>

#### 1.06.2.4 The Larger Rings $S_9$ – $S_{20}$ : Preparation and Structure

Figure 5 reveals the known structures of the larger annular allotropes. Perhaps the most significant feature of the structures shown comes in the case of  $S_{18}$  which, as it shows, can – uniquely among the cyclic allotropes – display two different



**Figure 5** The structures, appearance, and melting points of the larger annular allotropes (thermal properties of *exo-S*<sub>18</sub> do not appear to have been reported). Note that in addition to these, the lemon-yellow-colored allotrope *S*<sub>15</sub> has also been prepared, though its structure has not been confirmed by X-ray crystallography.

molecular forms; these are usually designated *endo* (orthorhombic) and *exo* (monoclinic).<sup>54</sup> In addition to the differences apparent in **Figure 5**, the average bond length within the *exo* form is markedly larger than in its counterpart, including one very long bond of 2.103 Å. As shown in **Figure 5**, these differ by molecular variation, which does not occur in the other rings, though different packing arrangements allow the possibility of crystallizing two polymorphs of *S*<sub>9</sub>. One of these ( $\alpha$ ) has been fully characterized by X-ray crystallography; while there appears to be no absolute confirmation of the structure of the  $\beta$  form by this technique, Raman spectroscopy suggests its molecular structure matches that of the  $\alpha$  form.<sup>55</sup> Another point of note that is that the structure of *S*<sub>15</sub> has yet to be unambiguously confirmed by X-ray crystallography;

spectroscopy and calculation both lend credence to a ring structure however.<sup>56</sup>

Small amounts of many of these species will be present in commercial samples of sulfur, in sulfur melts, etc., and so can in that sense be thought of as ‘naturally occurring.’ In practice, however, probing their structure and chemistry has necessitated the development of ingenious routes to each. In the case of *S*<sub>9</sub> this is best achieved by the reaction of TiCp<sub>2</sub>S<sub>5</sub> with S<sub>4</sub>Cl<sub>2</sub> (itself best prepared, as noted above, by chlorination of *S*<sub>6</sub>). In a recent study, Harpp et al. noted a 21% yield for this technique after recrystallization of the product from CS<sub>2</sub>/*n*-pentane.<sup>57</sup> A variation on this reaction recommended by Stuedel involves utilizing S<sub>4</sub>(SCN)<sub>2</sub> which can be prepared in purer form than the dichloride.<sup>56</sup> As with *S*<sub>7</sub>, *S*<sub>9</sub> is light- and

temperature-sensitive and a typical storage protocol involves keeping it in the dark at  $-40\text{ }^{\circ}\text{C}$ .

While  $\text{S}_{10}$  can result from the decomposition of sulfur oxides (*vide infra*), the most logical preparation again utilizes  $\text{TiCp}_2\text{S}_5$ , this time in the reaction with  $\text{SO}_2\text{Cl}_2$ . The titanocene complex also acts as a precursor to  $\text{S}_{11}$  via reaction with  $\text{S}_6\text{Cl}_2$  and to  $\text{S}_{12}$  as a side product of the reaction with  $\text{SCL}_2$ . Harpp's recent study noted an 8% yield for the latter which is in agreement with Steudel's earlier work<sup>57</sup>; smaller yields result from the reaction of sulfanes with  $\text{S}_2\text{Cl}_2$  or by extraction of rapidly quenched liquid sulfur (which also generates  $\text{S}_8$ ,  $\text{S}_7$ ,  $\text{S}_{18}$ , and  $\text{S}_{20}$ ). Unlike most of the rarer allotropes,  $\text{S}_{12}$  exhibits high stability.

Perhaps the two most elegant examples of sulfur allotrope formation (and thus maybe of directed, systematic synthesis of allotropes of any element) come with the use of  $\text{S}_8\text{Cl}_2$ . This is tricky to prepare, but, once formed, it reacts with the aforementioned titanocene complex to give the expected  $\text{S}_{13}$ <sup>58</sup> and with another metal sulfide complex  $\text{Zn}(\text{TMEDA})\text{S}_6$ <sup>59</sup> to give  $\text{S}_{14}$ . This zinc species was first prepared in 1995 by Rauchfuss and coworkers,<sup>60</sup> utilizing the fact that the amine moderates the normally violent reaction between the elements (leading to the quip in the paper's title that the reaction is 'sans explosion!') and just as the titanocene species acts as a stable source of  $[\text{S}_5]^{2-}$ , this yellow material acts as a source of  $[\text{S}_6]^{2-}$  during the formation of  $\text{S}_{14}$ .

The reaction of  $\text{TiCp}_2\text{S}_5$  with  $\text{SO}_2\text{Cl}_2$ , which generates  $\text{S}_{10}$ , also produces a low yield of  $\text{S}_{15}$ <sup>56</sup> while, as already alluded to,  $\text{S}_{18}$  can be isolated from quenched melts of the element – a technique which also yields  $\text{S}_{20}$ . The latter also forms in the  $\text{TiCp}_2\text{S}_5/\text{SO}_2\text{Cl}_2$  reaction, with Harpp's recent study generating it in 5% yield as a side product in their accumulation of  $\text{S}_{10}$ .

### 1.06.2.5 Reactivity of $\text{S}_8$ and the Larger Rings

Given the problems in generating pure samples of the larger annular allotropes (other than  $\text{S}_8$ ), it is maybe no surprise that little work has been done on their individual chemistries beyond assessment of basic properties such as thermal stability. Harpp and coworkers have looked at their ability to act as sulfur-transfer agents. The first such study looked at the reaction of  $\text{S}_{10}$  with 1,3-dienes and with strained olefins and were able to demonstrate that they progressed under milder conditions than with  $\text{S}_8$ .<sup>61</sup> In the case of the dienes, cyclic di- and tetra-sulfides form; in the case of strained systems, cyclic trisulfides are the result. The follow-up work revealed similar reactivity for  $\text{S}_{12}$  and  $\text{S}_{20}$  (with additional pentasulfide products in the olefin case), with  $\text{S}_9$  reacting similarly but with lower yields.<sup>57</sup> Overall, the conclusion of such studies was that of those allotropes,  $\text{S}_{10}$  was the most effective source of sulfur units.

#### 1.06.2.5.1 Complexes of intact rings

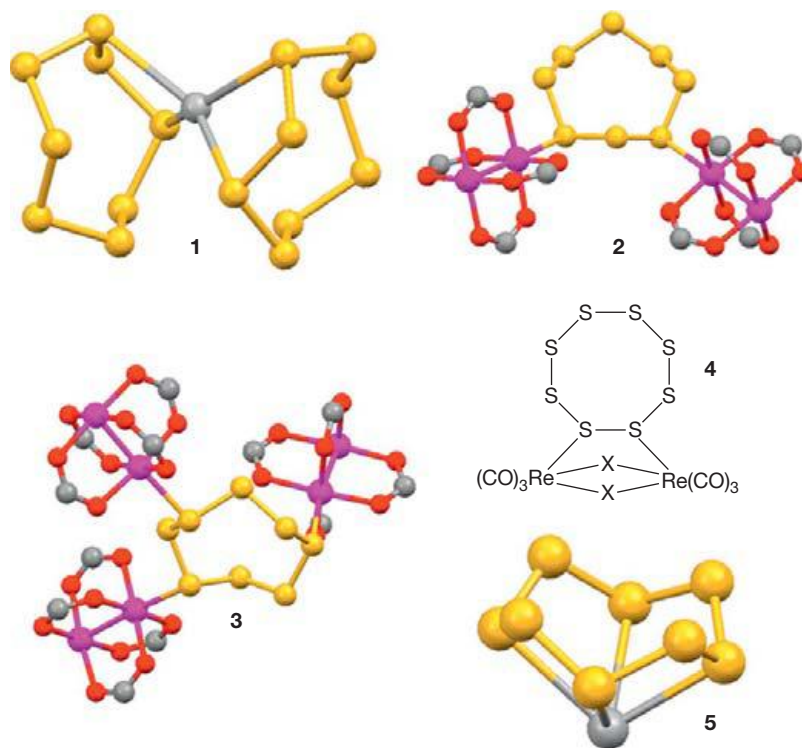
Given that the neutral allotropes of sulfur have no shortage of lone pairs, they could reasonably be expected to coordinate to metal centers, especially since the weak Lewis basicity of the sulfurs would be enhanced by a chelate effect if more than one sulfur was involved in coordination. Unfortunately, this situation rarely occurs, and reaction with transition metal centers almost inevitably results in reduction and breaking of the ring

to give a wide variety of (poly)sulfide ligands. Some examples of these are provided in a later section. Just a handful of examples of complexes of intact rings are known, even though it is almost 30 years since the first report of such a species. This groundbreaking example came in the form of a salt of the  $[\text{Ag}(\text{S}_8)_2]^+$  cation **1**, formed in the reaction of  $\text{Ag}[\text{AsF}_6]$  with  $\text{S}_8$  in liquid  $\text{SO}_2$  (as solvent).<sup>62</sup>

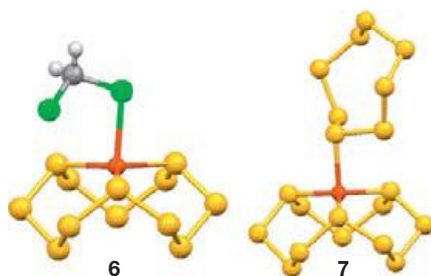
As **Figure 6** shows, this product contains two  $\text{S}_8$  crowns bound (via relatively long bonds of 2.744 and 2.802 Å) to the central silver atom through the 1,3 atoms of both rings. Although this result clearly indicated the potential for ring coordination, it was not until 2001 that a further unequivocal advance was made in the form of the rhodium complexes  $\text{Rh}_2(\text{O}_2\text{CCF}_3)_4(\text{S}_8)$  **2** and  $[\text{Rh}_2(\text{O}_2\text{CCF}_3)_4]_3(\text{S}_8)_2$  **3** which form in the high-temperature solid-state reaction of the element with  $\text{Rh}_2(\text{O}_2\text{CCF}_3)_4$ .<sup>63</sup> In the first of these, the  $\text{S}_8$  unit again coordinates in 1,3 fashion, but now to two different metal centers, resulting in a zigzag 1-D chain. In the second example, each crown coordinates in 1,3,6 fashion to three different rhodium atoms, resulting in a quite complex overall architecture. In both examples, as in the previously mentioned silver case, the  $\text{S}_8$  units effectively retain the crown motif exhibited by the uncoordinated allotrope. At around the same time as this work, and building upon earlier results, an example of a rhenium complex of  $\text{S}_8$  was reported.<sup>64</sup> The reaction of  $\text{Re}_2\text{Br}_2(\text{CO})_6(\text{THF})_2$  with  $\text{S}_8$  in  $\text{CS}_2$  generated  $\text{Re}_2\text{Br}_2(\text{CO})_6(\text{S}_8)$  **4** in which the sulfur unit was postulated to be acting as a bridge via 1,2 coordination. This was not confirmed by X-ray crystallography, however, due to the instability of the complex in solution (excess THF, e.g., effectively shifting the equilibrium back to the starting materials and precipitating sulfur). Again in 2002, Krossing and coworkers were able to advance the chemistry of silver complexes by showing that by a judicious choice of counterion, salts of the  $[\text{Ag}(\text{S}_8)]^+$  cation **5** could also be generated, with the silver now bearing just the one crown ligand, with a 1,3,5,7 tetradentate mode of coordination.<sup>65</sup>

The most recent results in this area are perhaps the most intriguing, as they pave the way for a wide variety of new systems. Again this stems from the laboratory of Krossing, and the reaction of a salt of the  $[\text{Cu}(1,2\text{-F}_2\text{C}_6\text{H}_4)_2]^+$  cation with excess sulfur in a mixture of  $\text{CH}_2\text{Cl}_2$  and  $\text{CS}_2$ .<sup>66</sup> The key to the reaction is the use of the large weakly coordinating anion  $[\text{Al}(\text{OC}(\text{CF}_3)_3)_4]^-$ , making this system a potent source of 'Cu<sup>+</sup>'. This allows the isolation of two products containing novel cations:  $[\text{Cu}(\text{S}_{12})(\text{CH}_2\text{Cl}_2)]^+$  **6** and  $[\text{Cu}(\text{S}_{12})(\text{S}_8)]^+$  **7**. In both cases, the  $\text{S}_{12}$  ligand exhibits a 1,5,9 tridentate coordination mode and appears undistorted with respect to the structure of the uncoordinated allotrope. What makes the  $[\text{Cu}(\text{S}_{12})(\text{S}_8)]^+$  structure even more noteworthy is the fact that, in addition to the unique  $\text{S}_{12}$  ligand, it also exhibits the first example of a monodentate  $\text{S}_8$  ligand and also constitutes the first example of a complex in which two modifications of an element are bound to a metal atom. The isolation of these compounds clearly hints at the possibility of wide-ranging coordination chemistry for other sulfur allotropes (**Figure 7**).

Finally, in this area it should be noted that the interaction of  $\text{S}_8$  with a large range of metal centers has been investigated by mass spectrometry. For example, the work of Dance et al. has revealed that laser ablation of metals in the ion trap of a



**Figure 6** Complexes bearing the  $S_8$  ring coordinated intact (note in the case of **2** and **3** only the immediate coordination environment of one sulfur ring is displayed and that the structure of **4** has not been confirmed by x-ray crystallography).



**Figure 7** Structures of complexes of the intact  $S_{12}$  allotrope.

Fourier transform ion cyclotron resonance mass spectrometer followed by interaction with sulfur vapor results in  $[MS_x]^+$  ( $x=2-16$ ).<sup>67</sup> In related work, calculations have suggested that coordination of  $S_7$  to  $Li^+$  would result in the former acting as a tetradentate ligand.<sup>68</sup> Such results indicate that a rich chemistry awaits elucidation. In a note of caution, however, it should be borne in mind that in some compounds such as  $WCl_6S_8$ ,<sup>69</sup> which at first glance would appear to contain annular ligands, in fact have the sulfur units only weakly coordinating to outer atoms of the central molecule rather than the metal itself. Reference 65 lists a number of further examples of such compounds.

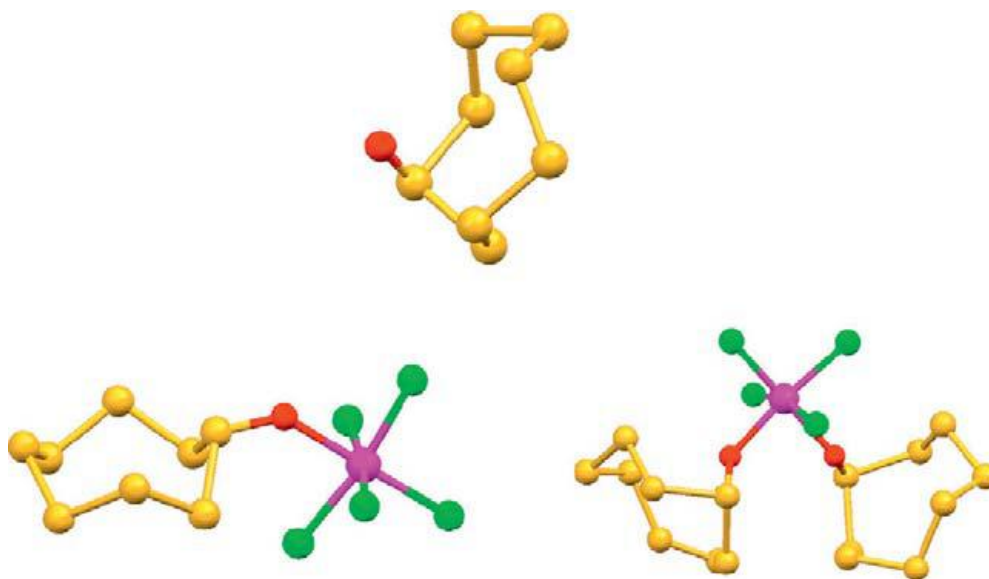
#### 1.06.2.5.2 Oxides of the cyclic allotropes

Reactions of any of the five allotropes  $S_x$  ( $x=6-10$ ) with  $CF_3CO_3H$  in  $CH_2Cl_2$  at low temperature result in the formation of  $S_xO$  in which the cyclic structure is retained with one of

the sulfur atoms now oxidized via formation of a  $S=O$  double bond. Additionally, in the case of  $S_6O$ , Ishii and Yamashita have recently shown that it can be generated *in situ* by the reaction of  $TiCp_2S_5$  with  $SOCl_2$  (in  $CS_2$  at low temperature and in the absence of light).<sup>51</sup> The material is unstable in solution at ambient temperatures and can be crystallized in two forms which may represent different orientations of the  $S=O$  bond, though this has yet to be confirmed by X-ray crystallography. If an excess of the oxidizing agent is used, then the dioxide  $S_6O_2$  can be obtained; a more unexpected reaction occurs, however, when the monoxide reacts with the Lewis acid  $SbCl_5$ . The product in this case is  $S_{12}O_2 \cdot 2SbCl_5$ , which consists of a 12-membered sulfur ring coordinated to the antimonies via the two oxygens.<sup>70</sup> This product is rendered all the more strange by the fact that free  $S_{12}O_2$  is not yet known.

The product from  $S_7$  shows the expected arrangement and this material can also be further oxidized to  $S_7O_2$ ; the latter also forms in the oxidation (via excess acid) reaction of  $S_8$ , possibly via the higher oxide  $S_8O_3$ .<sup>71</sup> If the stoichiometric reaction is performed,  $S_8O$  results and this material can coordinate to antimony<sup>72</sup> and tin<sup>73</sup> centers in the complexes  $S_8O \cdot SbCl_5$  and  $(S_8O)_2 \cdot SnCl_4$ ; as expected, the ligands coordinate through the oxygen atoms (Figure 8). Cyclic structures have been postulated for  $S_9O$  and  $S_{10}O$  through spectroscopy, though this has not been confirmed by X-ray work. In terms of reactivity of the oxides, studies beyond the aforementioned acid/base reactions are limited, though Ishii has investigated the ability of  $S_6O$  to react with alkenes and act as a sulfur source.<sup>51</sup>





**Figure 8** The structures of  $S_8O$ ,  $S_8O \cdot SbCl_5$ , and  $(S_8O)_2 \cdot SnCl_4$ .

### 1.06.3 Homoatomic Cations of Sulfur

#### 1.06.3.1 General Introduction

The relatively high electron affinity (electronegativity value of 2.58 on the Pauling scale) of sulfur ensures it is an effective electron acceptor; thus, many anionic sulfur species of the type  $[S_n]^{2-}$  (and their relevant derivatives) are known (*vide infra*). In contrast, the number of homopolyatomic sulfur cations is very limited. This is largely due to the high first ( $999 \text{ kJ mol}^{-1}$ ) and second ( $2252 \text{ kJ mol}^{-1}$ ) ionization energies which in turn result in highly reactive, thermodynamically stable cation salts, requiring both specialist reaction conditions and experimental design. Given this, it is perhaps ironic that while the oxidation of sulfur to homopolyatomic cations is the least developed of our sections (at least in terms of the raw number of species isolated), the practical/observational chemistry behind it is as old as anything the others have to offer. In fact, this dates back over two centuries ago to Bucholz's observations on the dissolution of sulfur in oleum.<sup>74</sup> Understandably, elucidation of the nature of the colored species obtained in such reactions posed challenges to investigators; indeed, this is still a research area that is being addressed, but a general understanding of the role of sulfur cations is now agreed upon. Key development between the late 1960s and 1980s helped advance our knowledge of the area significantly, resulting in the syntheses of examples with weakly basic antimonite and fluoroarsenate anions. The first isolable solid-state sulfur cation salt,  $[S_8][AsF_6]_2$ , was structurally characterized by Gillespie and coworkers in 1971 and found to contain discrete  $S_8^{2+}$  and  $AsF_6^-$  ions in a monoclinic crystal system.<sup>75</sup> Passmore et al. reported the synthesis and crystal structure of two  $[S_4]^{2+}$  hexafluoroarsenate compounds,  $[S_7]_4[S_4][AsF_6]_6$  and  $[S_4][AsF_6]_2$ , in 1980, with the  $[S_4]^{2+}$  cation exhibiting square planar geometry in both systems.<sup>76</sup> Gillespie and coworkers first prepared and characterized the structure of  $[S_{19}][AsF_6]_2$ , in the same year, and showed the irregular  $[S_{19}]^{2+}$  cation consisted of two seven-membered rings linked through a five-atom sulfur chain.<sup>77</sup>

The understanding of sulfur cation solutions is less clear than their condensed phase counterparts, with the observation that the former typically contain increased quantities of at least two radical cations  $[S_n]^+$  ( $n \geq 4$ ): one as a probable consequence of dissolved  $[S_5]^{+78}$  and the other tentatively assigned as  $[S_7]^+$ .<sup>79</sup> More recent work has centered upon further examples, namely  $[S_6]^{2+}$ ,<sup>80</sup> square planar  $[S_4]^+$ ,<sup>80</sup>  $[n-S_4]^{2+}$ ,<sup>81</sup> and  $[S_4]^{4+}$ .<sup>81</sup>

#### 1.06.3.2 Preparation and Structure of Solid-State Sulfur Cations

It is immediately apparent that the synthesis of sulfur cation salts requires the use of strong oxidizing agents in weakly basic solvents, such as HF,  $HSO_3F$ , and liquid  $SO_2$ .<sup>82</sup> One of the most commonly employed oxidizing systems is thus the  $MF_5$ /liquid  $SO_2$  combination (where  $M = As$  or  $Sb$ ). Crystalline samples of all three sulfur cation salts have been characterized by means of X-ray diffraction (see Chapter 5.01), vibrational and UV-visible (vis) spectroscopy, and elemental analysis (see Ref. 83 for an overview).

##### 1.06.3.2.1 The preparation and structure of salts of $[S_4]^{2+}$

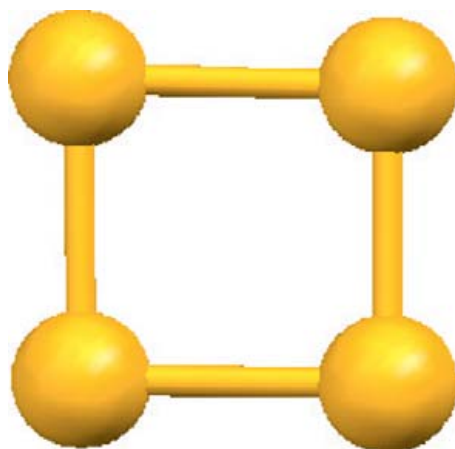
Synthesis of  $[S_4]^{2+}$  salts (22 valence electrons,  $D_{4h}$  symmetry) requires the presence of a trace amount of halogen to act as a catalyst or 'facilitator' to the reaction.<sup>84</sup> All known  $[S_4]^{2+}$  salts are colorless, with the exception of  $[S_4][SO_3F]_2$  which is pale yellow.<sup>85</sup>

In the solid state, the  $[S_4]^{2+}$  cation is a  $D_{4h}$  symmetric homocycle that adopts a regular square planar structure, much like the  $S_2N_2$  heterocycle,<sup>86</sup> with bond lengths that approximate to  $2 \text{ \AA}$ . The positive charge, as determined through analysis of the solid-state anion contacts, is delocalized almost uniformly over the entire cation (Figure 9).<sup>87</sup>

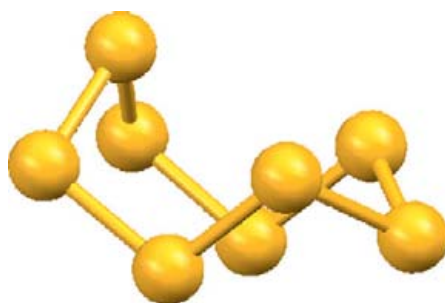
##### 1.06.3.2.2 The preparation and structure of salts of $[S_8]^{2+}$

Until observations by Passmore et al. in 2000, salts of the  $[S_8]^{2+}$  cation were always reported to be dark blue in color.





**Figure 9** The structure of the  $[S_4]^{2+}$  cation.



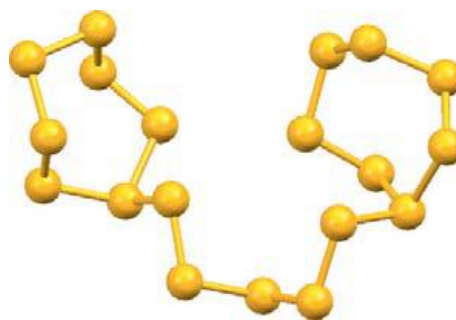
**Figure 10** The structure of the  $[S_8]^{2+}$  cation.

The latter study, however, reported the isolation of bulk samples of red single crystals of  $[S_8][AsF_6]_2$  and analogous crystals that appeared red in transmitted light but blue under reflected light, both identical by X-ray diffraction (Figure 10).<sup>88</sup>

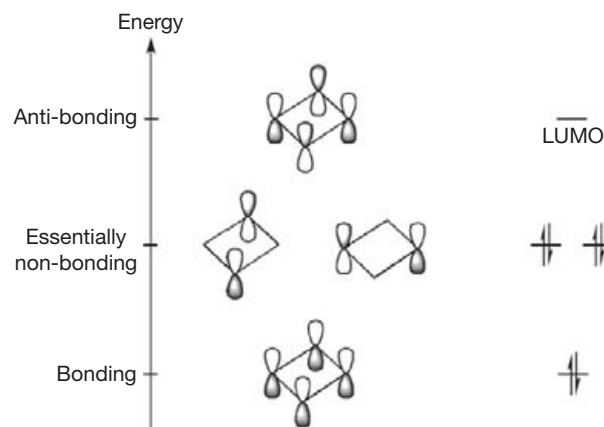
The  $C_s$  symmetric  $[S_8]^{2+}$  cation is homocyclic in the solid state and adopts an *exo-endo*-type conformation with three weak transannular contacts. As in the case of the smaller  $[S_4]^{2+}$  moiety, the positive charge is delocalized almost equally over the entire cation.<sup>88</sup> Although the S–S bond length around the ring ( $\sim 2.04$  Å) is only slightly shorter than those found in the neutral  $S_8$  molecule (2.06 Å), the structure of  $[S_8]^{2+}$  differs from the crown-shaped  $S_8$  allotrope as a result of transannular bonding effects. The cross-ring distance in solid-state  $S_8^{2+}$  cations is approximately 2.86 Å, which compares to 4.68 Å in  $S_8$ , and is indicative of weak transannular bonding between adjacent atoms (van der Waals distance  $\sim 3.7$  Å). Ring distortion occurs as a result of the cross-ring bonding, creating bond angles ranging from  $91.5^\circ$  to  $104.3^\circ$ , in comparison to  $107.9^\circ$  as found in the  $S_8$  system. Accordingly, an *exo-endo*-type conformation results which is intermediate between that of  $S_8$  and *endo-endo*  $S_4N_4$ ,<sup>89</sup> owing to the distortion created by transannular bonding, coupled with nonbonded repulsions.

### 1.06.3.2.3 The preparation and structure of salts of $[S_{19}]^{2+}$

Salts containing the  $[S_{19}]^{2+}$  cation are typically dark orange red/brown in color. Two known examples have been isolated and characterized by means of single-crystal X-ray diffraction.<sup>77,90</sup> The first of these,  $[S_{19}][AsF_6]_2$ , revealed two seven-membered



**Figure 11** The structure of the  $[S_{19}]^{2+}$  cation.



**Figure 12** Molecular orbitals of  $\pi$  symmetry within  $[S_4]^{2+}$ . Adapted from Brownridge, S.; Krossing, I.; Passmore, J.; Jenkins, H. D. B.; Roobottom, H. K. *Coord. Chem. Rev.* **2000**, *197*, 397–481.

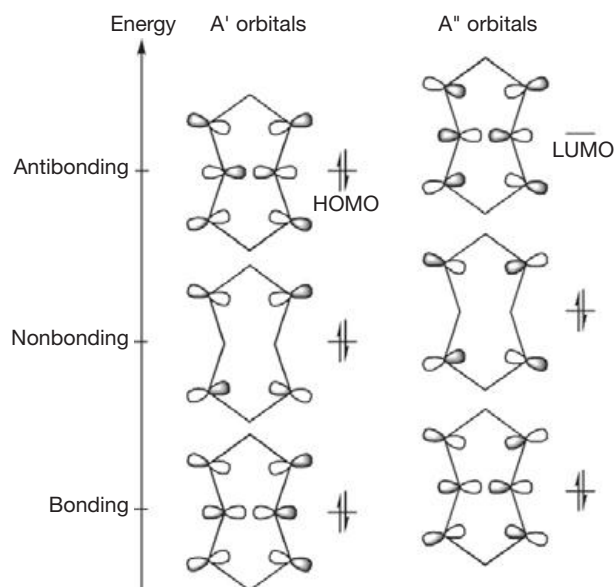
sulfur rings linked by a penta-sulfur bridge, thus necessitating two triply coordinated sulfur atoms.<sup>77</sup> In this particular system, differences between the two rings were highlighted: one of the rings exhibits a boat-type conformation, the other disordered with both a major chair (80%) and a minor boat (20%) conformation (Figure 11).

Subsequent analysis of the  $[SbF_6]^-$  salt showed that the structure was not isomorphous with the previous example, exhibiting a completely ordered  $[S_{19}]^{2+}$  cation.<sup>90</sup> It is noteworthy that the S–S distances around the cation adopt an alternating short–long bond length and the three-coordinate sulfur atoms have the longest S–S bond length of all those reported within the sulfur cation homocycles.

### 1.06.3.3 Bonding Within Sulfur Cations

The  $[S_4]^{2+}$  cation is an aromatic  $6\pi$  electron species in which the four  $3p_z$  atomic orbitals combine (Figure 12) to form one  $\pi$ -bonding, two nonbonding, and one antibonding vacant  $\pi^*$  molecular orbital. Both calculations (see Chapters 9.01 and 9.02)<sup>91</sup> and experimental evidence (indicating a decreased S–S bond distance in  $[S_4]^{2+}$  salts)<sup>87</sup> give support to the notion that one  $\pi$  bond is delocalized around the entire homocycle, creating a bond order of 1.25.

The nature of the bonding within the  $[S_8]^{2+}$  cation has been the subject of numerous investigations. Although the

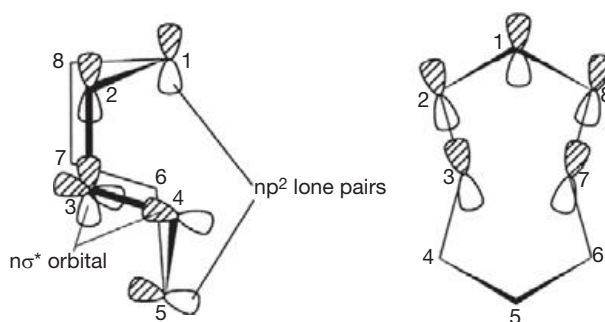


**Figure 13**  $\pi$  and  $\pi^*-\pi^*$  bonding molecular orbitals in  $[\text{S}_8]^{2+}$ . Adapted from Cameron, T. S.; Deeth, R. J.; Dionne, I.; Du, H.; Jenkins, H. D. B.; Krossing, I.; Passmore, J.; Roobottom, H. K. *Inorg. Chem.* **2000**, *39*, 5614–5631.

geometrical structure of the dication may be accounted for through consideration of an intermediate state between crown-like  $\text{S}_8$  (*exo-exo*) and cage-like  $\text{S}_4\text{N}_4$  (*endo-endo*), the unexpected cross-ring transannular bonds and charge delocalization around the entire homocycle may not. Initial comparisons were made between the structure of  $[\text{Se}_2\text{I}_4]^{2+}$  and the six central sulfur atoms of  $[\text{S}_8]^{2+}$ , whereby bonding was thought to be the result of an intracationic  $\pi^*-\pi^*$  bond interaction. In 2000, Cameron et al. confirmed that the S–S transannular bonds are the result of a weakly bonded  $\pi^*-\pi^*$  interaction of the partially vacant 3p orbitals within the central six sulfur atoms of the ring (Figure 13).<sup>88</sup>

The positive charge within the dication is delocalized across all atoms, including the two apical sulfur atoms (average 0.25), thereby decreasing Coulomb repulsion. The charge delocalization is achieved by donation of  $3p^2$  lone-pair electrons in the adjacent, and empty,  $3\sigma^*$  orbitals. Accordingly, charge delocalization may be considered as a progression from the classically expected  $[\text{S}_8]^{2+}$  crown-like structure, whereby positive charge is found at two discrete positions (tricoordinate atoms), to a partially shared intermediate state with each of the six central atoms occupying one third of the positive charge, and finally resulting in a uniformly distributed charge delocalization with each sulfur atom sharing 0.25 of the charge density (Figure 14).<sup>88</sup>

For many years, the cation now known to be  $[\text{S}_{19}]^{2+}$  was mistakenly identified as  $[\text{S}_{16}]^{2+}$ .<sup>82,92</sup> These conclusions were reached, in part, via analytical data of the red solid obtained from reaction of sulfur with  $\text{AsF}_5$  in anhydrous HF and cryoscopic measurements which all supported the formulation of an  $[\text{S}_{16}][\text{AsF}_6]_2$  salt. Initial attempts made to crystallize this material for X-ray structure determination were unsuccessful, and it was not until Gillespie and coworkers successfully managed to isolate single, red needle-like crystals in 1980 that a



**Figure 14** Charge delocalization in  $[\text{S}_8]^{2+}$  by a  $3p^2$  to  $3\sigma^*$  interaction. Reproduced from Cameron, T. S.; Deeth, R. J.; Dionne, I.; Du, H.; Jenkins, H. D. B.; Krossing, I.; Passmore, J.; Roobottom, H. K. *Inorg. Chem.* **2000**, *39*, 5614–5631.

decisive single-crystal structure was obtained (as illustrated previously in Figure 11).<sup>77</sup>

To date, however, a thorough bonding motif has not been elucidated for the  $[\text{S}_{19}]^{2+}$  cation, nor have chemical calculations of this intricate system been conclusively investigated. The alternating bond length around both seven-membered sulfur rings, which decreases with increasing distance from the tricoordinate sulfur atoms, may be addressed through consideration of both the bondings within  $[\text{S}_8]^{2+}$ , as discussed above, and that associated with  $\text{S}_7$  itself.<sup>93</sup> Within the  $[\text{S}_{19}]^{2+}$  dication, the two tricoordinate sulfur atoms are thought to be the only atoms within the homocycle to possess a  $3s^2$  lone-pair orbital, but no  $3p^2$  lone-pair orbital. Accordingly, and as illustrated for  $[\text{S}_8]^{2+}$ , the localized positive charge that formally resides on these two sulfur atoms may be delocalized through several  $3p^2$  to  $3\sigma^*$  interactions. Electron density is consequently transferred to the neighboring antibonding  $3\sigma^*$  orbitals of the adjacent bonds, inducing a net bond lengthening in the bonds around the tricoordinate sulfur atoms. The delocalization of electron density progresses around each of the seven-membered rings through the formation of additional  $3p^2$  to  $3\sigma^*$  interactions. This effect is brought about by the formation of induced positive charges on adjacent sulfur atoms that are located next to the tricoordinate chalcogen atoms.

### 1.06.3.4 Sulfur Cations in Solution

The variation in solution color (brown, green, or blue) obtained by dissolving elemental sulfur in oleum implies that the chemistry of sulfur in solution is less than straightforward. While the original discoverers of this reaction so many years ago<sup>74</sup> clearly could not have been expected to even begin elucidating the true chemistry involved, the complexity of the system means that even in the age of modern understanding this poses a challenge. Thus, the species responsible for these colors have been the focus of several studies using experimental techniques such as UV/Vis spectroscopy,<sup>77</sup> electron spin resonance (ESR),<sup>78</sup> magnetic measurements,<sup>75,82,92</sup> and magnetic circular dichroism.<sup>94</sup> The solvent polarity used to examine the dissolved sulfur dication salts was shown to affect the composition of the sulfur species present in the solution itself. Typically, dissociation products (radical cations) of the dication salts were found to be present in higher

concentrations within less polar solvents (such as  $\text{SO}_2$ ), compared to more polar solvents, such as fluorosulfuric acid, which favor the dications.

Early ESR and magnetic investigations highlighted the presence of numerous radical monocationic species  $[\text{S}_n]^+$  present within solution, that exist in equilibrium with the condensed phase  $[\text{S}_8]^{2+}$  and  $[\text{S}_{19}]^{2+}$  dications (pure  $[\text{S}_4]^{2+}$  solutions are ESR silent). Initial findings suggested the intense blue color, often associated with  $[\text{S}_8]^{2+}$  salts, was attributable to the  $[\text{S}_4]^+$  radical cation (in equilibrium with  $[\text{S}_8]^{2+}$  in solution). Several years later, however,  $[\text{S}_5]^+$  was the only radical (mono)cation to be unambiguously identified from solution via experimental ESR analysis of 91.8%  $^{33}\text{S}$ -enriched sulfur in 65% oleum.<sup>78</sup> In 2004, however, Crossing and Passmore presented evidence in support of a previously unknown solution-phase species as being responsible for this blue color.<sup>80</sup> The  $[\text{S}_6]^{2+}$  dication, with  $10\pi$  electrons, was predicted to be an important solution-phase species, observed computationally, in  $\text{S}_8^{2+}$  dication solutions. Calculated thermochemical data suggest that  $[\text{S}_8]^{2+}$  dissociates in solution to an equilibrium mixture of *ca.* 0.5  $[\text{S}_6]^{2+}$  and  $[\text{S}_5]^+$ . Thus, the blue color of associated solutions is thought to be caused by HOMO-LUMO  $\pi^*-\pi^*$  electronic transition transitions within this putative  $[\text{S}_6]^{2+}$  cation.<sup>80,95</sup>

### 1.06.3.5 Sulfur Cations in the Gas Phase

The presence of sulfur (radical)cations  $[\text{S}_n]^+$  (where  $n=2-8$ ) within the gas phase has been known for many years, with basic thermodynamic properties having been explored. Despite the structural properties of  $[\text{S}_2]^+$  having been ascertained,<sup>96</sup> experimental data relating to structural information of the larger monocationic species are missing. In the case of  $[\text{S}_2]^+$ , the relatively short S-S bond length of 1.825 Å is highly indicative of dominant  $\pi$ -bonding.<sup>97</sup> The structural properties of other potential sulfur monocations ( $\text{S}_3^+ - \text{S}_7^+$ ) have been investigated computationally.<sup>80,98</sup> Owing to repulsion of the two positive charges within  $[\text{S}_n]^{2+}$  species, the dications readily dissociate within the vapor phase, yielding  $[\text{S}_x]^+$  and  $[\text{S}_y]^+$  radical monocations, through a phenomenon referred to as Coulomb explosion.

### 1.06.3.6 Sulfur Cations within Zeolite Hosts

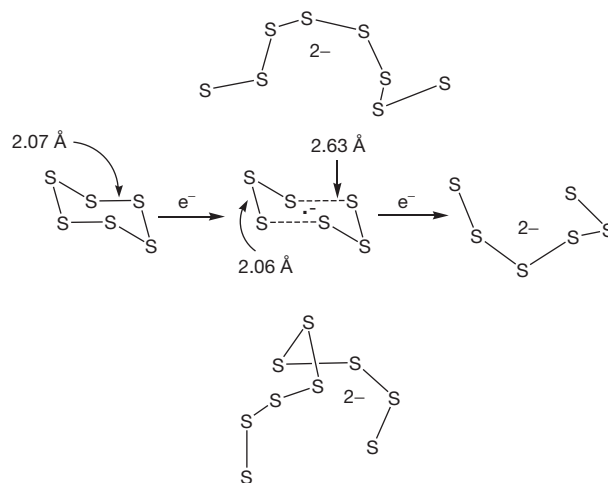
A decade or so ago, Crossing proposed that the experimental development and access to new sulfur cations in the solid state were only a matter of time, suggesting that by using large and weakly coordinating anions, such as  $[\text{Al}(\text{OR})_4]^-$ , new synthetic routes to mono- or dication salts could be conceived.<sup>99</sup> Since then, however, these condensed phase materials have eluded experimental synthesis as 'free' species. However, Kim and co-workers have isolated two new polyatomic cations of sulfur via sulfur disproportionation within a zeolite host.<sup>81</sup> This research focused on the ability of zeolites (see Chapter 5.05), with their regular cavity and channel structures, to offer a somewhat unique medium in which clusters could assemble and be stabilized. By fully dehydrating the  $\text{Cd}_{46}\text{-X}$  system, through prolonged vacuum pumping at 450 °C, it became possible to introduce sulfur vapor to individual  $\text{Cd}_{46}\text{-X}$  crystallites. X-Ray studies performed upon the resulting yellow material revealed the presence of sulfur anions and two new tetrasulfur cations:

$[\text{S}_4]^{4+}$  and  $[\text{n-S}_4]^{2+}$ . Within each  $\text{Cd}_{46}\text{-X}$  supercage (an interconnected set of sodalite  $\beta$ -cages, creating a large 12-ring window), 12 sulfide ions coordinate to one  $\text{Cd}^{2+}$  ion, and can be essentially considered as individual neutral  $\text{CdS}$  molecules. The tetrahedral  $[\text{S}_4]^{4+}$  cation occupies, and is stabilized within, two of the eight anionic sodalite cavities per unit cell, with a S-S bond length of 2.17(2) Å. Each of the supercage units also hosts the electron-deficient  $[\text{n-S}_4]^{2+}$  zigzag cluster (torsion angle =  $\tau$  114(8)°). This novel dication isomer covalently bridges two of the zeolite framework oxygen atoms and exhibits ionic interaction with neighboring sulfide ions. It becomes important, in this instance, to consider the ability of the negatively charged zeolite framework to provide a suitable host environment for both isolation and stabilization of these new sulfur cations. Moreover, it highlights the potential experimental means of synthesising other homopolyatomic cations (not only of sulfur, but also of other chalcogen analogs) and in turn helping in the better understanding of this fascinating class of compounds.

## 1.06.4 Polysulfide Anions

### 1.06.4.1 Free Polysulfide Anions

Figure 15 provides three different, though related, insights into the chemistry of chain-structured polysulfides via recent (or relatively recent) observations. The first pertains to the question of what happens when one of the neutral annular allotropes undergoes reduction. In the case of  $\text{S}_8$ , electrochemical reduction in DMF proceeds via an initially formed cyclic monoanion, through an open monoanion and finally onto the chain-structured dianion  $[\text{S}_8]^{2-}$  shown.<sup>100</sup> Insight into potential intermediates in this reaction can be gleaned from the other structures shown in Figure 15; here we see the  $[\text{S}_6]^-$  anion which occurs within the salt  $[\text{PPh}_4][\text{S}_6]$  and forms as orange/red crystals in the reaction of  $\text{H}_2\text{S}$  with a mixture of  $\text{Me}_3\text{SiN}_3$  and  $[\text{PPh}_4]\text{N}_3$ .<sup>101</sup> X-Ray crystallography reveals its structure to be a chair arrangement wherein two  $\text{S}_3$  fragments



**Figure 15** (Top) The structure of  $[\text{S}_8]^{2-}$ ; (middle) comparison of the structures of  $\text{S}_6$ ,  $[\text{S}_6]^-$ , and  $[\text{S}_6]^{2-}$ ; (bottom) the structure of the  $[\text{S}_9]^{2-}$  anion.

have been joined by two long S–S linkages (2.63 Å compared to 2.06 Å within the  $S_3$  units; note also the comparison in length to the bonds within the neutral  $S_6$  ring). Finally, K [PPh<sub>2</sub>BH<sub>3</sub>] reacts with sulfur to generate a salt of the fully reduced  $[S_6]^{2-}$  and as Figure 15 shows this is now a fully open chain structure; in contrast, the related reagent K [SPPH<sub>2</sub>BH<sub>3</sub>] generates a salt of  $[S_9]^{2-}$ , again exhibiting an open chain structure as shown.<sup>102</sup>

This set of results confirms three key things about the reduction of sulfur: (1) it proceeds via partially reduced rings within which we see bond weakening compared to the parent ring to give (2) open chain dianions whose (3) chain lengths vary with the reducing agent. From these three ‘rules’ springs a massive body of chemistry. Apart from those mentioned thus far, chains  $[S_x]^{2-}$  wherein  $x=2-5$  and 7 are also known, making the series complete up to  $x=9$ . A large range of materials will bring about such reductions and such products have been extensively documented.<sup>103</sup> A feature of such anions is their ability to act as sources of radical anions of the type  $[S_x]^-$ , to which they decompose in solution. An excellent example comes in the form of  $[S_3]^-$  which is the blue chromophore in the mineral lapis lazuli, prized as a pigment by artists for centuries. Even though it is now almost four decades since Chivers’ identification of this species as the active color center,<sup>104</sup> the last few years have seen continued efforts to probe its properties via X-ray absorption spectroscopy,<sup>105</sup> Raman spectroscopy,<sup>106</sup> and computational techniques,<sup>107</sup> while very recent work has revealed this anion to be far more ubiquitous than previously imagined (see Section 1.06.5). Just to show how challenging work on such systems can be, it was only in 2011 that electron paramagnetic resonance (EPR) (see Chapter 9.13) observation of the smaller  $[S_2]^-$  within related ‘green ultramarine’ was finally achieved; although Raman spectroscopy had previously revealed its presence, this was the first characterization via the unpaired electron.<sup>108</sup>

From a technological point of view, a full evaluation of the speciation of polysulfides in solution is an important aspect of the complete understanding of all the redox processes going on within group 1 metal–sulfur batteries. Free sulfides may even play a biological role; this has been discussed recently in the context of the beneficial properties of garlic, alongside organic polysulfide systems.<sup>109</sup>

#### 1.06.4.2 Polysulfides as Ligands

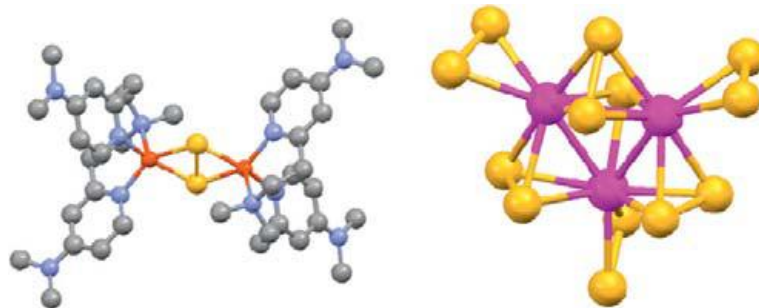
The prime remit of this chapter was to look at, for want of a better phrase, ‘naked’ sulfur compounds, i.e., systems

containing just sulfur. When looking at sulfides it is, however, impossible to do justice to the structural diversity they can promote without briefly considering the coordination complexes they can generate.<sup>110</sup> Polysulfides can act as mono-, bi-, and tridentate ligands in both homoleptic and heteroleptic systems, as well as provide bridging moieties between two, or more, transition or p-block metal atoms. Moreover, through appropriate chain-length alteration and the provision of multiple coordination sites, polysulfides have the capacity to bind (or ‘glue’) metal aggregates together, as shown in the  $[Cu_6(S_4)_3(S_5)]^{2-}$  system.<sup>111</sup> Here, we see more examples, looking at complexes of the known free polysulfides ( $[S_n]^{2-}$   $n=2-9$ ) in ascending order of polysulfide chain length.

There is an assortment of complexes with different types of coordinated  $[S_2]^{2-}$  ligands (the smallest polysulfide unit). The breadth of structural chemistry exhibited by this group of polysulfido complexes results from an extension of the fundamental structural coordination type (side-on) to an ‘end-on’ *cis* and *trans* (double) bridging coordination, through use of the sulfur lone pair. Two examples of  $[S_2]^{2-}$  complexes are shown in Figure 16, with one resulting from recent work on the synthesis and reactivity of a  $\{Cu_2S_2\}$  core with a bound side-on  $\mu-\eta^2:\eta^2-S_2^{2-}$  unit.<sup>112</sup> This particular compound proved to be capable of exhibiting the first examples of a sulfur atom-transfer reaction from a Cu–S moiety to various substrates. It should be noted, however, that despite the apparent simplicity of the ligands, all is not necessarily cut and dried when it comes to describing the bonding in some of these compounds. The heated debate on the presence or absence of a sulfur–sulfur bond within one such copper complex (with a seemingly credible S–S distance of 2.73 Å) is testimony to this – and rather ironic given sulfur’s general propensity for catenation!<sup>113</sup>

Examples of complexes of  $[S_3]^{2-}$  ligand have been known for some time, a good example being  $Ti(MeCp)_2(S_3)$ , which contains a nonplanar four-membered  $TiS_3$  ring (Figure 17).<sup>115</sup>

Numerous examples and structural characterization of complexes containing the  $[S_4]^{2-}$  ligand exist. Typically within these compounds, the  $S_4^{2-}$  anion acts as a bidentate ligand and adopts either an ‘envelope’ or a ‘half-chair’-type conformation. Metal atoms that coordinate tetrahedrally tend to favor the half-chair conformation (as seen in  $[Ni(S_4)_2]^{2-}$ ),<sup>116</sup> whereas those that coordinate in a square-pyramidal manner often depict the envelope conformation (as found for  $[Mo_2S_{10}]^{2-}$ ).<sup>117</sup> In contrast to this very well known bidentate behavior, it was only in 1997 that an example of  $[S_4]^{2-}$  acting as monodentate ligand was finally observed; this came when Bensch and Dürichen prepared and characterized the novel



**Figure 16** The structure of  $[(CuL)_2-(S_2)]^{2+}$  (left,  $L=N,N$ -bis[2-[2-( $N,N'$ -4-dimethylamino)pyridyl]ethyl] methylamine)<sup>112</sup> and  $Mo_3(S_2)_6$  (right).<sup>114</sup>



ternary niobium polysulfide,  $K_4Nb_2S_{14}$ .<sup>118</sup> In this particular compound, the  $[Nb_2S_{14}]^{4-}$  anion plays host to numerous polysulfide bonding arrangements with terminal monosulfide  $S^{2-}$ ,  $\eta^2-(S_2)^{2-}$ ,  $\eta^1-S_2^{2-}$  and terminal  $[S_4]^{2-}$  bonding units present around the two Nb centers (Figure 18).

As already noted, the  $[S_5]^{2-}$  anion is present in  $TiCp_2S_5$ ,<sup>119</sup> a compound which has proved an exceptionally useful synthon. The  $TiS_5$  ring adopts the chair conformation in both solid state (as is typical for all  $MS_5$  moieties within mononuclear complexes) and solution. Recently, Hossain and Matsumoto reported the room-temperature synthesis of the first known tridentate chelating  $S_5^{2-}$  ligand, found within the ruthenium complex,  $Ru(P(OE)_3)_3S_5$  (E=Me and Et).<sup>120</sup> In these systems, the bicyclic  $RuS_5$  units essentially have three- and five-membered polysulfide rings around the central Ru atom (see Figure 19).

Since 2000, substantial work by Bensch and coworkers has resulted in the synthesis and characterization of several novel polysulfide-containing metal complexes that incorporate a

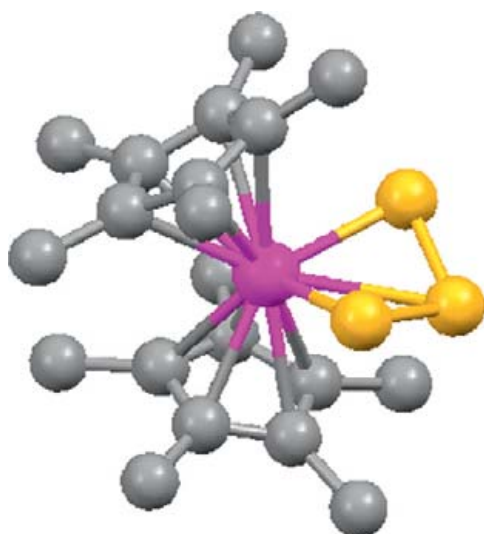


Figure 17 The structure of  $Ti(MeCp)_2(S_3)$ .

pentasulfide unit both as a linker chain moiety<sup>121</sup> or as bidentate ligands that form homocycles in the chair conformation with the relevant metal center.<sup>122</sup> In 2011, Jambor et al. reported the preparation of the heptathiadistannabicyclo [1.1.5]nonane,  $[{\{2,6-(Me_2NCH_2)_2C_6H_3\}Sn(\mu-S)}_2(\mu-S_5)]$ .<sup>123</sup> This intriguing compound, prepared via oxidation of intramolecularly coordinated distannyne by  $S_8$ , was shown to possess one pentasulfide and two monosulfide bridges between the two  $\{2,6-(Me_2NCH_2)_2C_6H_3\}Sn$  moieties (Figure 19).

Many complexes containing the bidentate  $[S_6]^{2-}$  ligand are known; typical examples include the  $[M(S_6)_2]^{2-}$  complexes (M=Zn, Cd, Hg).<sup>124</sup> The tetraphenylphosphonium salt of  $[MnS_{11}]^-$  also possesses a bidentate  $S_6^{2-}$  ligand that is bound, along with a bidentate  $S_5^{2-}$  ligand, to a tetrahedrally coordinated Mn center.<sup>116</sup> The fascinating structure of  $[Et_4N]_3[Cu_3(S_6)_3]$  arises through bridging interactions by one end of each of the  $S_6$  chelates, affording a  $Cu_3S_3$  ring.<sup>125</sup>  $S_6$  rings are also found in compounds such as the tricoordinate copper(I),  $[Cu_2S_{20}]^{4-}$  complex, which features two  $CuS_6$  rings that are linked by an octasulfur chain (Figure 20).<sup>126</sup>

An  $[S_6]^{2-}$  chain may be found within the structure of the extremely sulfur-rich  $[Bi_2S_{34}]^{4-}$  anion, first prepared in 1986 by Müller and coworkers.<sup>127</sup> Within this anion, the two bismuth atoms are linked, as mentioned, via the  $[S_6]^{2-}$  chain, and coordinated to two bidentate  $[S_7]^{2-}$  ligands. Tridentate  $[S_7]^{2-}$  ligands are seen in the ruthenium and osmium complexes,  $M(PMe_3)_3S_7$ <sup>128</sup> (Figure 21).

The  $[S_9]^{2-}$  ligand is found in the structurally fascinating  $[AuS_9]^{2-}$  anion (first reported in 1984 by Strähle and Marbach)<sup>129</sup> which simply and elegantly highlights (Figure 22) both the catenating and coordinating properties of sulfur. The analogous silver complex can also be prepared.<sup>130</sup>

### 1.06.5 Conclusion

There is no getting away from sulfur. This fact was well illustrated during the final stages of the completion of this chapter, with the publication of fascinating results from three quite

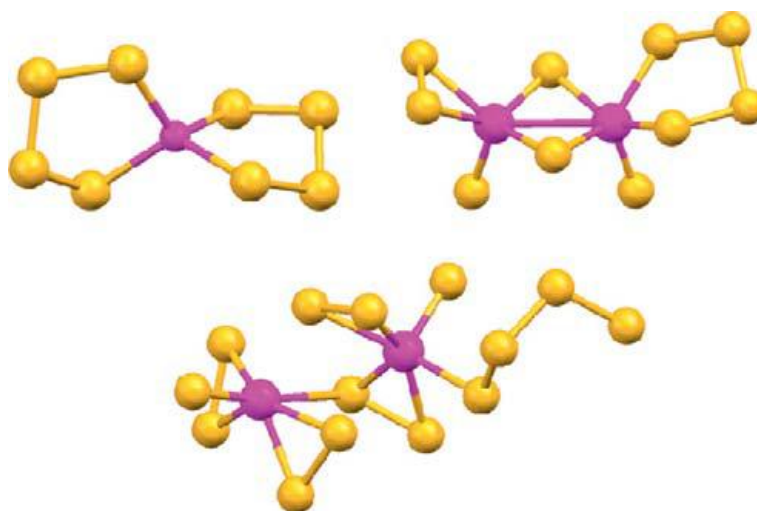
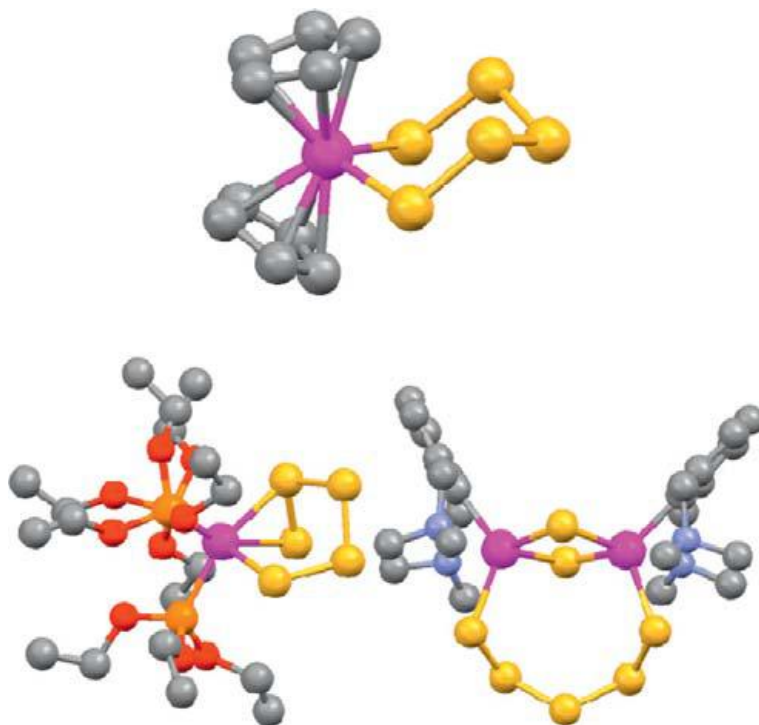
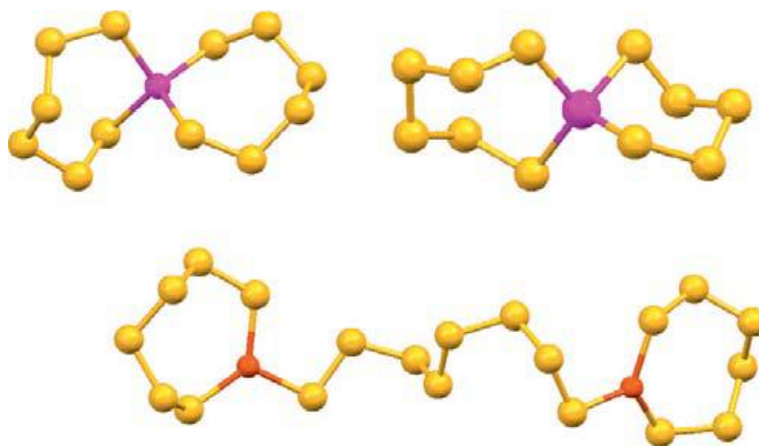


Figure 18 The structures of the  $[Ni(S_4)_2]^{2-}$  (top left),  $[Mo_2S_{10}]^{2-}$  (top right), and  $[Nb_2S_{14}]^{4-}$  (bottom) anions.





**Figure 19** The structures of  $\text{TiCp}_2\text{S}_5$  (top),  $\text{Ru}(\text{P}(\text{OEt})_3)_3\text{S}_5$  (bottom left), and  $[(2,6\text{-}(\text{Me}_2\text{NCH}_2)_2\text{C}_6\text{H}_3)\text{Sn}(\mu\text{-S})]_2(\mu\text{-S}_5)$  (bottom right).

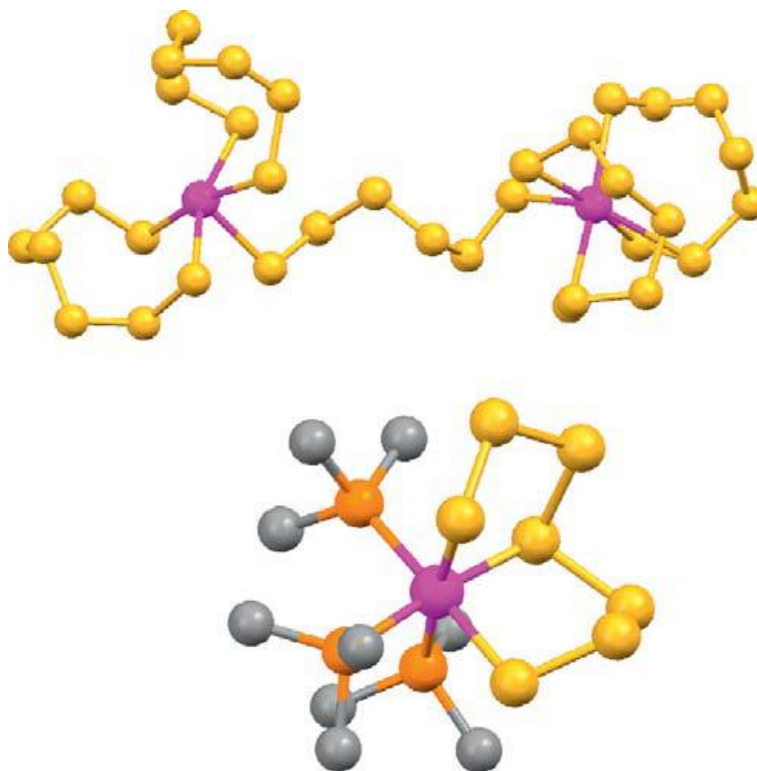


**Figure 20** The structures of  $[\text{Hg}(\text{S}_6)_2]^{2-}$  (top left),  $[\text{MnS}_{11}]^-$  (top right), and  $[\text{Cu}_2\text{S}_{20}]^{4-}$  (bottom).

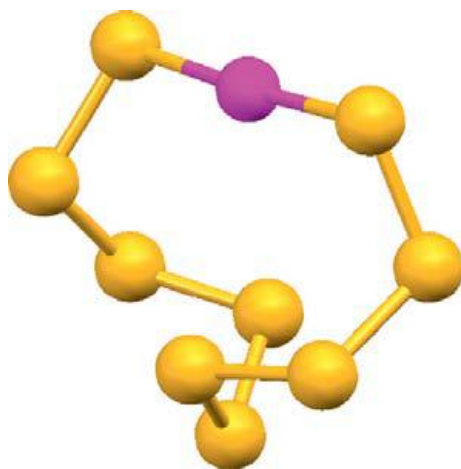
different spheres of investigation. As already alluded to, the  $[\text{S}_5]^-$  anion has now been shown (using in situ Raman spectroscopy) not only to be stable in aqueous solutions at elevated temperatures and pressure, but also, in fact, to be the primary form of the element in such circumstances.<sup>131</sup> This observation clearly has many implications for our understanding of the geological role of sulfur; it is not just on Earth that aspects of this role are being elucidated. Millions of miles away, the *MESSENGER* spacecraft in orbit around Mercury recently revealed the presence of high sulfur levels on the planet's surface via X-ray spectrometer measurements.<sup>132</sup> Again, this observation has significant implications for our quest to understand planetary formation and evolution. In contrast, rather than looking out into the depths of space, the third recent

observation we have chosen to highlight peered back into the far depths of Earth's history. The result was the identification of microfossils of cells living three and a half billion years ago in what is now Western Australia. They sit alongside pyrite crystals – telltale signs of the sulfur-based metabolism of these most ancient of bugs.<sup>133</sup>

However, even away from such exotica, the importance of sulfur to industry and technology ensures that there will be continued interest in all aspects of its chemistry. Within the specific remit of this chapter, it is fair to say that the pioneering and astonishingly thorough work of Ralf Steudel in the decades preceding the turn of the millennium has resulted in an understanding of the structural properties of annular allotropes that surely needs relatively little in the way of further



**Figure 21** The structures of the [Bi<sub>2</sub>S<sub>34</sub>]<sup>4-</sup> anion (top) and Os(PEt<sub>3</sub>)<sub>3</sub>S<sub>7</sub> (bottom).



**Figure 22** The structure of the [AuS<sub>9</sub>]<sup>-</sup> anion.

embellishment. It may well be that more attention is now paid to the chemistry of the individual allotropes, and Krossing's isolation of the first complexes of intact S<sub>12</sub> hints at a wealth of untapped potential. Even if such products do not prove to be of direct practical use, they must provide some insight into how the element reacts with metal centers, acting as maybe a snapshot of the very first stage of such interactions.

While the importance of sulfides to technology (such as power sources) means that they are much studied and will continue to be so, it may well be that it is with the cations that the more fundamental breakthroughs lie in wait.

Certainly, the list of known cations is relatively sparse. However, it is the smallest allotropes that have, perhaps, some of the greatest potential for future work. Though they may be unstable, transient species in everyday terms, S<sub>2</sub>, S<sub>3</sub>, and S<sub>4</sub> will have had – as we have seen – a significant part to play in the atmospheric chemistry of the early Earth, and continue to do so in alien environments elsewhere in our solar system. Given that understanding atmospheric chemistry and history is a key priority for those attempting to pin down the origin of life on Earth (and indeed to discover life elsewhere) it follows that these ostensibly minor players in sulfur's drama may yet prove to have starring roles.

## References

1. Kelly, P. F. *Chem. World* **2004**, *1*, 64.
2. Chivers, T. *A Guide to Chalcogen-Nitrogen Chemistry*. World Scientific Publishing: Singapore, 2005.
3. For example, in the case of the sulfanes see Steudel, R. *Top. Curr. Chem.* **2003**, *231*, 99–125.
4. Chivers, T.; Manners, I. *Inorganic Rings and Polymers of the p-Block Elements*. RSC Publishing: Cambridge, 2009.
5. Steudel, R., Ed. *Top. Curr. Chem.* **2003**, *230*; **2003**, *231*.
6. Lapshin, A. E.; Vasil'eva, E. A. *Glass Phys. Chem.* **2008**, *34*, 742–748.
7. Spencer, J. R.; Jessup, K. L.; Yelle, R.; Ballester, G. E.; McGrath, M. A. *Science* **2000**, *24*, 1208–1210.
8. Jessup, K. L.; Spencer, J.; Yelle, R. *Icarus* **2007**, *192*, 24–40.
9. Dalton, J. B.; Cruikshank, D. P.; Stephan, K.; McCord, T. B.; Coustenis, A.; Carlson, R. W.; Coradini, A. *Space Sci. Rev.* **2010**, *153*, 113–154.
10. Noll, K. S.; McGrath, M. A.; Trafton, L. M.; Atreya, S. K.; Caldwell, J. J.; Weaver, H. A.; Yelle, R. V.; Barnett, C.; Edgington, S. *Science* **1995**, *267*, 1307–1313.

11. Maiorov, B. S.; Ignat'ev, N. I.; Moroz, V. I.; Zasova, L. V.; Moshkin, B. E.; Khatuntsev, I. V.; Ekonomov, A. P. *Solar Syst. Res.* **2005**, *39*, 267–282.
12. Baines, K. H.; Delitsky, M. L.; Momary, T. W.; Brown, R. H.; Burattini, B. J.; Clark, R. N.; Nicholson, P. D. *Planet. Space Sci.* **2009**, *57*, 1650–1658.
13. Lyons, J. R. *J. Sulf. Chem.* **2008**, *29*, 269–279.
14. Farquhar, J.; Bao, H.; Thieme, M. *Science* **2000**, *289*, 756–758.
15. Zahnle, K.; Claire, M.; Catling, D. *Geobiology* **2006**, *4*, 271–283.
16. Pavlov, A. A.; Kasting, J. F. *Astrobiology* **2002**, *2*, 27–41.
17. Du, S.; Francisco, J. S.; Shepler, B. C.; Peterson, K. A. *J. Chem. Phys.* **2008**, *128*, 204306.
18. Johnston, D. T. *Earth Sci. Rev.* **2011**, *106*, 161–183.
19. Steliou, K.; Gareau, Y.; Harpp, D. N. *J. Am. Chem. Soc.* **1984**, *106*, 799–801.
20. Peterson, K. A.; Lyons, J. R.; Francisco, J. S. *J. Chem. Phys.* **2006**, *125*, 084314.
21. McCarthy, M. C.; Thorwith, S.; Gottlieb, C. A.; Thaddeus, P. *J. Am. Chem. Soc.* **2004**, *126*, 4096–4097.
22. Thorwith, S.; McCarthy, M. C.; Gottlieb, C. A.; Thaddeus, P.; Gupta, H.; Stanton, J. F. *J. Chem. Phys.* **2005**, *123*, 054326.
23. McCarthy, M. C.; Thorwith, S.; Gottlieb, C. A.; Thaddeus, P. *J. Chem. Phys.* **2004**, *121*, 632–635.
24. Wong, M. W.; Steudel, R. *Chem. Phys. Lett.* **2003**, *379*, 162–169.
25. Matus, M. H.; Dixon, D. A.; Peterson, K. A.; Harkless, J. A. W.; Francisco, J. S. *J. Phys. Chem. A* **2007**, *127*, 174305.
26. Ramírez-Solís, A.; Jolibois, F.; Maron, L. *J. Phys. Chem. A* **2010**, *114*, 12378–12383.
27. Hassanzadeh, P.; Andrews, L. *J. Phys. Chem.* **1992**, *96*, 6579–6585.
28. Boumediene, M. S.; Corset, J.; Picquenard, E. *J. Raman Spectrosc.* **1999**, *30*, 463.
29. Bragg, W. H. *Proc. Royal Soc.* **1914**, *89*, 575–580.
30. Greenwood, N. N.; Earnshaw, A. *Chemistry of the Elements*, 2nd ed.; Butterworth-Heinemann: Oxford, 1997; pp 654–656.
31. Steudel, R.; Echert, B. *Top. Curr. Chem.* **2003**, *230*, 6.
32. Nelson, R. M.; Smythe, W. D.; Hapke, B. W.; Cohen, A. *J. Icarus* **1990**, *85*, 326–334.
33. Gallacher, A. C.; Pinkerton, A. A. *Acta Cryst.* **1993**, *C49*, 125–126.
34. Douglas, S. *Planet. Space Sci.* **2004**, *52*, 223–227.
35. Schulz, N. H.; Brinkhoff, T.; Ferdelman, T. G.; Hernández Mariné, M.; Teske, A.; Jørgensen, B. B. *Science* **1999**, *284*, 493–495.
36. Prange, A.; Chauvistre, R.; Modrow, H.; Hormes, J.; Truper, H. G.; Dahl, C. *Microbiology* **2002**, *148*, 267–276.
37. Himmel, D.; Maurin, L. C.; Gros, O.; Mansot, J.-L. *Biol. Cell* **2009**, *101*, 43–45.
38. Degtyareva, O.; Gregoryanz, E.; Somayazulu, M.; Dera, P.; Mao, H.-K.; Hemley, R. *J. Nature Mat.* **2005**, *4*, 152–156.
39. Hejny, C.; Lundegaard, L. F.; Falconi, S.; McMahon, M. I.; Hanfland, M. *Phys. Rev. B* **2005**, *71*, 020101.
40. Crapanzano, L.; Crichton, W. A.; Monaco, G.; Bellissent, R.; Mezouab, M. *Nature Mat.* **2005**, *4*, 560–562.
41. Degtyareva, O.; Gregoryanz, E.; Somayazulu, M.; Dera, P.; Mao, H.-K.; Hemley, R. *J. Phys. Rev. B* **2005**, *71*, 214104.
42. Degtyareva, O.; Hernandez, E. R.; Serrano, J.; Somayazulu, M.; Mao, H.-K.; Gregoryanz, E.; Hemley, R. *J. Chem. Phys.* **2007**, *126*, 084503.
43. Steudel, R.; Echert, B. *Top. Curr. Chem.* **2003**, *230*, 40–49.
44. Mausle, H.-J.; Steudel, R. *Z. Anorg. Allg. Chem.* **1980**, *463*, 27–31.
45. Steidel, J.; Pickardt, J.; Steudel, R. *Z. Naturforsch. Part B* **1978**, *33*, 1554–1555.
46. Wong, M. W.; Steudel, Y.; Steudel, R. *J. Chem. Phys.* **2004**, *121*, 5899–5907.
47. Steudel, R.; Steidel, J.; Pickardt, J.; Schuster, F.; Reinhardt, R. *Z. Naturforsch. Part B* **1980**, *35*, 1378–1383.
48. Steudel, R.; Papavassiliou, M.; Seppelt, K. *Z. Naturforsch. Part B* **1988**, *43*, 245–247.
49. Steudel, R.; Schuster, F. *J. Mol. Struct.* **1978**, *44*, 143–157.
50. Bartlett, P. D.; Lohaus, G.; Weis, C. D. *J. Am. Chem. Soc.* **1958**, *80*, 5064–5066.
51. Ishii, A.; Yamashita, R. *J. Sulfur Chem.* **2008**, *29*, 303–308.
52. Steudel, R.; Steidel, J.; Sandow, T.; Schuster, F. *Z. Naturforsch. Part B* **1978**, *33*, 1198–1200.
53. Dorset, D. L. *J. Phys. Chem.* **1996**, *100*, 16706–16710.
54. Schmidt, M.; Wilhelm, E.; Debaerdemaker, T.; Hellner, E.; Kutoglu, A. *Z. Anorg. Allg. Chem.* **1974**, *405*, 153–162.
55. Steudel, R.; Bergemann, K.; Buschmann, J.; Luger, P. *Inorg. Chem.* **1996**, *35*, 2184–2188.
56. Strauss, R.; Steudel, R. *Z. Naturforsch. Part B* **1988**, *43*, 1151–1155.
57. Zysman-Colman, E.; Leste-Lassere, P.; Harpp, D. H. *J. Sulfur Chem.* **2008**, *29*, 309–326.
58. Sandow, T.; Steidel, J.; Steudel, R. *Angew. Chem. Int. Ed.* **1982**, *21*, 794.
59. Steudel, R.; Schumann, O.; Buschmann, J.; Luger, P. *Angew. Chem. Int. Ed.* **1998**, *37*, 2377–2378.
60. Verma, A. K.; Rauchfuss, T. B.; Wilson, S. R. *Inorg. Chem.* **1995**, *34*, 3072–3078.
61. Leste-Lassere, P.; Harpp, D. H. *Tet. Lett.* **1999**, *40*, 7961–7964.
62. Roesky, H. W.; Thomas, M.; Schimkowiak, J.; Jones, P. G.; Pinkert, W.; Sheldrick, G. M. *J. Chem. Soc. Chem. Commun.* **1982**, 895–896.
63. Cotton, F. A.; Dikarev, E. V.; Petrukhina, M. A. *Angew. Chem. Int. Ed.* **2001**, *40*, 1521–1523.
64. Bacchi, A.; Baratta, W.; Calderazzo, F.; Marchetti, F.; Pelizzi, G. *Inorg. Chem.* **2002**, *41*, 3894–3900.
65. Cameron, T. S.; Deeken, A.; Dionne, I.; Fang, M.; Krossing, I.; Passmore, J. *Chem. Eur. J.* **2002**, *8*, 3386–3401.
66. Santiso-Quinones, G.; Bruckner, R.; Knapp, C.; Dionne, I.; Passmore, J.; Krossing, I. *Angew. Chem. Int. Ed.* **2009**, *48*, 1133–1137.
67. Dance, I.; Fisher, K.; Willett, G. *Angew. Chem. Int. Ed. Engl.* **1995**, *34*, 201–203.
68. Wong, M. W.; Steudel, Y.; Steudel, R. *Inorg. Chem.* **2005**, *44*, 8908–8915.
69. Cotton, F. A.; Kibala, P. A.; Sandor, R. B. W. *Acta Crystallogr.* **1989**, *C45*, 1287–1289.
70. Steudel, R.; Steidel, J.; Pichardt, J. *Angew. Chem. Int. Ed. Engl.* **1980**, *19*, 325–326.
71. Steudel, R.; Sandow, T. *Angew. Chem. Int. Ed. Engl.* **1978**, *17*, 611–612.
72. Steudel, R.; Sandow, T.; Steidel, J. *J. Chem. Soc. Chem. Commun.* **1980**, 180–181.
73. Steudel, R.; Steidel, J.; Sandow, T. *Z. Naturforsch. Part B* **1986**, *41*, 951–957.
74. Bucholz, C. F. *Gehler's neues J. Chem.* **1804**, *3*, 7.
75. Davies, C. G.; Gillespie, R. J.; Park, J. J.; Passmore, J. *Inorg. Chem.* **1971**, *10*, 2781–2784.
76. Passmore, J.; Sutherland, G.; White, P. S. *J.C.S. Chem. Comm.* **1980**, 330–331.
77. Burns, R. C.; Gillespie, R. J.; Sawyer, J. F. *Inorg. Chem.* **1980**, *19*, 1423–1432.
78. Low, H. S.; Beaudet, R. A. *J. Am. Chem. Soc.* **1976**, *98*, 3849–3852.
79. Passmore, J.; Sutherland, G.; Taylor, P.; Whidden, T. K.; White, P. S. *Inorg. Chem.* **1981**, *20*, 3839–3845.
80. Krossing, I.; Passmore, J. *Inorg. Chem.* **2004**, *43*, 1000–1011.
81. Song, M. K.; Kim, Y.; Seff, K. *J. Phys. Chem. B* **2003**, *107*, 3117–3123.
82. Gillespie, R. J.; Passmore, J.; Ummat, P. K.; Vaidya, O. C. *Inorg. Chem.* **1971**, *10*, 1327–1332.
83. Brownridge, S.; Krossing, I.; Passmore, J.; Jenkins, H. D. B.; Roobottom, H. K. *Coord. Chem. Rev.* **2000**, *197*, 397–481.
84. Murchie, M. P.; Passmore, J.; Sutherland, G. W.; Kapoor, R. *Dalton. Trans.* **1992**, 503–508.
85. Burns, R. C.; Gillespie, R. J. *Inorg. Chem.* **1982**, *21*, 3877–3886.
86. Cohen, M. J.; Garito, A. F.; Heeger, A. J.; MacDiarmid, A. G.; Mikulski, C. M.; Saran, M. S.; Kleppinger, J.; Samuel, E. *J. Am. Chem. Soc.* **1976**, *98*, 3844–3848.
87. Cameron, T. S.; Roobottom, H. K.; Dionne, I.; Passmore, J.; Jenkins, H. D. B. *Inorg. Chem.* **2000**, *39*, 2042–2052.
88. Cameron, T. S.; Deeth, R. J.; Dionne, I.; Du, H.; Jenkins, H. D. B.; Krossing, I.; Passmore, J.; Roobottom, H. K. *Inorg. Chem.* **2000**, *39*, 5614–5631.
89. de Lucia, M. L.; Coppens, P. *Inorg. Chem.* **1978**, *17*, 2336–2338.
90. Faggiani, R.; Gillespie, R. J.; Sawyer, J. F.; Vekris, J. E. *Acta Cryst.* **1989**, *C45*, 1847–1853.
91. Krossing, I.; Passmore, J. *Inorg. Chem.* **1999**, *38*, 5203–5211.
92. Gillespie, R. J.; Passmore, J. *J. Chem. Soc. D. Chem. Commun.* **1969**, 1333–1334.
93. See, for example, Steudel, R. *Top. Curr. Chem.* **1981**, *102*, 149.
94. Stephens, P. J. *J. Chem. Soc. D. Chem. Commun.* **1969**, 1496–1497.
95. Li, J.; Liu, C.-W.; Lu, J.-X. *Mol. Struct. Theochem.* **1993**, *223*–231.
96. Lias, S. G.; Bartmess, J. E.; Liebman, J. F.; Holmes, J. L.; Levin, R. D.; Mallard, W. G. *J. Phys. Chem. Ref. Data* **1988**, *17*(Suppl. 1), 1–861.
97. Brabharan, K.; Coxon, J. A. *J. Mol. Spectr.* **1988**, *128*, 540–553.
98. Chen, M. D.; Liu, M.; Liu, J. W.; Zhang, Q. E.; Au, C. T. *J. Mol. Struct. (THEOCHEM)* **2002**, *582*, 205–212.
99. Krossing, I. *Chem. Eur. J.* **2001**, *7*, 490–502.
100. Levillain, E.; Gaillard, F.; Leghie, P.; Demortier, A.; Lelieur, J. P. *J. Electroanal. Chem.* **1997**, *420*, 167–177.
101. Neumuller, B.; Schmick, F.; Kirmse, R.; Voigt, A.; Diefenbach, A.; Bickelhaupt, F. M.; Dehnicke, K. *Angew. Chem. Int. Ed.* **2000**, *39*, 4580–4582.
102. Dornhaus, F.; Bolte, M.; Wagner, M.; Lerner, H. W. *Z. Anorg. Allg. Chem.* **2007**, *633*, 425–428.
103. Steudel, R. *Top. Curr. Chem.* **2003**, *231*, 127–152.
104. Chivers, T. *Nature* **1974**, *252*, 32–33.
105. Flett, M. E.; Liu, X. *Spectrochim. Acta B* **2010**, *65*, 75–79.
106. Lede, B.; Demortier, A.; Gobeltz-Hauteceur, N.; Lefieur, J.-P.; Picquenard, E.; Duhayon, C. *J. Raman Spectrosc.* **2007**, *38*, 1461–1468.

107. Linguerri, R.; Komih, N.; Fabian, J.; Rosmus, P. *Zeit. Phys. Chemie* **2008**, *222*, 163–176.
108. Raulin, K.; Gobeltz, N.; Vezin, H.; Touati, N.; Ledé, B.; Moissette, A. *Phys. Chem. Chem. Phys.* **2011**, *13*, 9253–9259.
109. Münchber, U.; Anwar, A.; Mecklenburg, S.; Jacob, C. *Org. Biomol. Chem.* **2007**, *5*, 1505–1518.
110. For a more wide ranging review see Takeda, N.; Tokitoh, N.; Okazaki, R. *Top. Curr. Chem.* **2003**, *231*, 153–202.
111. Müller, A.; Römer, M.; Bögge, H.; Krickemeyer, E.; Bergmann, D. *J. Chem. Soc. Chem. Commun.* **1984**, 348–349.
112. Helton, M. E.; Maiti, D.; Zakharov, L. V.; Rheingold, A. L.; Porco, J. A.; Karlin, K. D. *Angew. Chem. Int. Ed.* **2006**, *45*, 1138–1141.
113. Alvarez, S.; Hoffmann, R.; Mealli, C. *Chem. Eur. J.* **2009**, *15*, 8358–8373, together with follow up correspondence: Berry, J. F. *Chem. Eur. J.* **2010**, *16*, 2719–2724; Alvarez, S.; Ruiz, E. *Chem. Eur. J.* **2010**, *16*, 2726–2728.
114. Diemann, E.; Müller, A.; Aymonino, P. *J. Z. Anorg. Allg. Chem.* **1981**, *479*, 191–198.
115. Bird, P. H.; McCall, J. M.; Shaver, A.; Siriwardane, U. *Angew. Chem. Int. Ed. Engl.* **1982**, *21*, 384–385.
116. Coucouvanis, D.; Patil, P. R.; Kanatzidis, M. G.; Detering, B.; Baenziger, N. C. *Inorg. Chem.* **1985**, *24*, 24–31.
117. Draganjac, M.; Simhon, E.; Chan, L. T.; Kanatzidis, M. G.; Baenziger, N. C.; Coucouvanis, D. *Inorg. Chem.* **1982**, *21*, 3321–3332.
118. Bensch, W.; Dürichen, P. *Inorg. Chim. Acta* **1997**, *261*, 103–107.
119. Epstein, E. F.; Bernal, I. J. *Organomet. Chem.* **1971**, *26*, 229–245.
120. Hossain, M. M.; Matsumoto, K. *Inorg. Chem.* **2000**, *39*, 247–250.
121. Bensch, W.; Stoll, P. *Acta Cryst.* **2003**, *E59*, i4–i6.
122. Bensch, W.; Wu, Y. *J. Solid State Chem.* **2007**, 2166–2174.
123. Bouška, M.; Dostál, L.; Růžička, A.; Beneš, L.; Jambor, R. *Chem. Eur. J.* **2011**, *17*, 450–454.
124. Müller, A.; Schimanski, J.; Schimanski, U. *Angew. Chem. Int. Ed. Engl.* **1984**, *23*, 159–160.
125. Müller, A.; Schimanski, U. *Inorg. Chim. Acta* **1983**, *77*, L187–L188.
126. Müller, A.; Baumann, F.-W.; Bögge, H.; Römer, M.; Krickemeyer, E.; Schmitz, K. *Angew. Chem. Int. Ed. Engl.* **1984**, *23*, 632–633.
127. Müller, A.; Zimmermann, M.; Bögge, H. *Angew. Chem. Int. Ed. Engl.* **1986**, *25*, 273.
128. Gotzig, J.; Rheingold, A. L.; Werner, H. *Angew. Chem. Int. Ed. Engl.* **1984**, *23*, 814–815.
129. Marbach, G.; Strähle, J.; Werner, H. *Angew. Chem. Int. Ed. Engl.* **1984**, *23*, 246–247.
130. Müller, A.; Krickemeyer, E.; Zimmermann, M.; Römer, M.; Bögge, H.; Penk, M.; Schmitz, K. *Inorg. Chim. Acta* **1984**, *90*, L69–L71.
131. Pokrovski, G. S.; Dubrovinsky, L. S. *Science* **2011**, *331*, 1052–1054.
132. [www.nasa.gov/mission\\_pages/messenger/media/NewsConference20110616.html](http://www.nasa.gov/mission_pages/messenger/media/NewsConference20110616.html).
133. Wacey, D.; Kilburn, M. R.; Saunders, M.; Cliff, J.; Brasier, M. D. *Nature Geosci.* **2011**, <http://dx.doi.org/10.1038/NGEO1238>.

## 1.07 Catenated Compounds – Group 16 (Se, Te)

RS Laitinen and R Oilunkaniemi, University of Oulu, Oulu, Finland

© 2013 Elsevier Ltd. All rights reserved.

<b>1.07.1</b>	<b>Introduction</b>	197
<b>1.07.2</b>	<b>Elemental Selenium and Tellurium and Related Mixed Chalcogen Systems</b>	199
1.07.2.1	Polymeric Selenium and Tellurium Allotropes	199
1.07.2.2	Selenium- and Tellurium-Containing Chalcogen Rings	200
1.07.2.2.1	General	200
1.07.2.2.2	Homocyclic selenium molecules	200
1.07.2.2.3	Homocyclic tellurium molecules	200
1.07.2.2.4	Selenium and tellurium rings in metal complexes	202
1.07.2.2.5	Heterocyclic chalcogen molecules	202
<b>1.07.3</b>	<b>Selenium- and Tellurium-Containing Ions</b>	205
1.07.3.1	Polyatomic Selenium and Tellurium Cations	205
1.07.3.1.1	General	205
1.07.3.1.2	$E_4^{2+}$	206
1.07.3.1.3	$E_6^{n+}$ ( $n=2, 4$ )	206
1.07.3.1.4	$E_8^{n+}$ ( $n=2, 4$ )	207
1.07.3.1.5	$E_n^{2+}$ ( $n>8$ )	209
1.07.3.2	Polyatomic Selenium–Halogen and Tellurium–Halogen Cations	209
1.07.3.2.1	General	209
1.07.3.2.2	Selenium–chlorine and selenium–bromine cations	210
1.07.3.2.3	Selenium–iodine and tellurium–iodine cations	210
1.07.3.3	Anions	212
1.07.3.3.1	General	212
1.07.3.3.2	Acyclic polyselenides and polytellurides	213
1.07.3.3.3	Cyclic polyselenides and polytellurides	213
1.07.3.3.4	Extended polytelluride networks	215
<b>1.07.4</b>	<b>Catenated Main Group Polyselenides and -tellurides</b>	216
1.07.4.1	Selenium and Tellurium Halogenides	216
1.07.4.2	Group 15 Polyselenides and -tellurides	219
1.07.4.3	Group 14 Polyselenides and -tellurides	223
1.07.4.4	Group 13 Polyselenides and -tellurides	226
<b>1.07.5</b>	<b>Transition Metal Complexes</b>	228
<b>1.07.6</b>	<b>Conclusion</b>	228
<b>References</b>		229

### 1.07.1 Introduction

The characteristic feature in the chemistry of group 16 elements sulfur, selenium, and tellurium is their propensity to form molecular species containing cumulated homo- and heteronuclear chalcogen–chalcogen bonds, which leads to rich chemistry involving a large number of homo- and heteronuclear, both cyclic and acyclic polychalcogen molecules<sup>1–3</sup> and ions,<sup>3–6</sup> main group compounds and ions,<sup>7–12</sup> and transition metal complexes<sup>13–17</sup> that contain polychalcogen ligands. Illustrative examples of compounds containing cumulated chalcogen–chalcogen bonds are shown in **Table 1**.

The structural chemistry of catenated polysulfur compounds is particularly extensive (see **Chapter 1.06**). That of related selenium and tellurium species is more limited, though it is developing very rapidly. Although the molecular structures of the selenium- and tellurium-containing species are often similar to those of the analogous sulfur compounds,

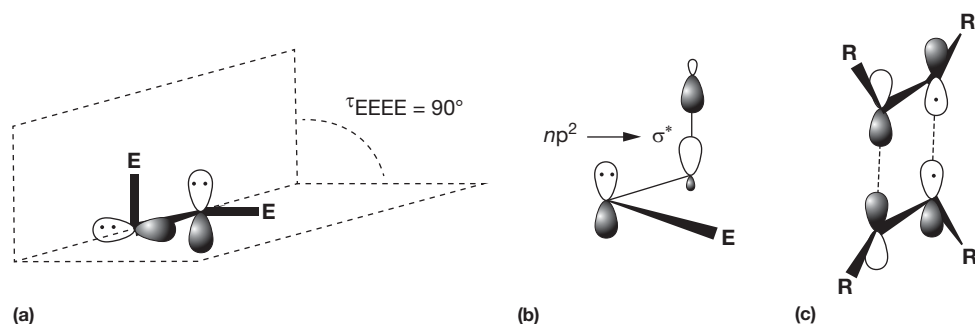
there are pronounced differences among the three chalcogen elements. For instance, selenium and tellurium have a weaker ability to form homocyclic molecules than sulfur, and the polymeric trigonal chains of selenium and tellurium are the most stable forms of the two elements. By contrast, polymeric sulfur is unstable and the thermodynamically stable form of the element at NTP consists of cyclooctasulfur molecules. Decreasing propensity to form  $\pi$ -bonds<sup>18</sup> and the formation of secondary bonding interactions<sup>19</sup> in heavier chalcogens seem to play an important role in explaining the structural differences.

The structural features of the chalcogen–chalcogen chains can be explained by three types of interactions. Without steric effects, the unstrained chalcogen–chalcogen bond adopts a torsional angle near 90°. This can be explained by the minimized repulsion of  $np$  lone pairs of the adjacent atoms (see **Figure 1(a)**). The second lone pair occupies the valence  $ns$  orbital and has no stereochemical consequences.

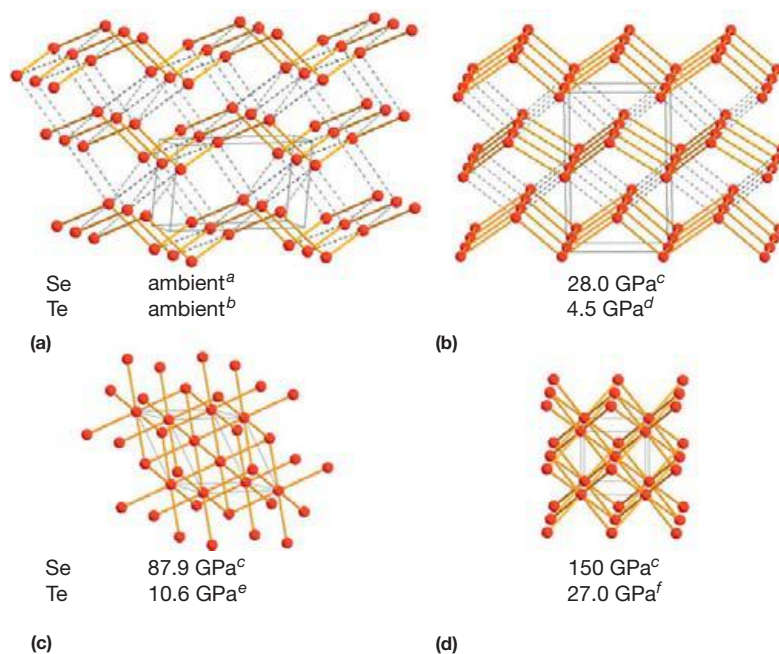


**Table 1** Illustrative examples of the catenation in selenium and tellurium species

Molecular species		Cations	Anions
<i>Selenium and tellurium allotropes and interchalcogen species</i>			
<i>Acyclic</i>			
$\text{Se}_{\infty}$ , $\text{Te}_{\infty}$ , $(\text{Se}_n\text{S}_m)_{\infty}$ , $(\text{Te}_n\text{S}_m)_{\infty}$ , $(\text{Te}_n\text{Se}_m)_{\infty}$ , $(\text{Te}_n\text{Se}_m\text{S}_p)_{\infty}$	<i>Cyclic</i>	$\text{Me}_3\text{Se}_3^+$	<i>Acy</i> $\text{Se}_5^{2-}$ , $\text{Te}_5^{2-}$
$\text{Se}_8$ , $\text{Se}_7\text{S}_{8-n}$ , $\text{Te}_7\text{S}_{8-n}$ , $\text{Te}_7\text{Se}_{8-n}$		$(\text{mes}^*)_5\text{Te}_3^+$	$\text{Ph}_3\text{Te}_3^-$
$\text{Se}_6(\text{N}^t\text{Bu})_2$		<i>Hon</i>	
$\text{Te}_3(\text{C}(\text{SiMe}_3)_3)_2$		$\text{Se}_8^{2+}$	
$[\text{TiCp}_2\text{Se}_5]$ , $[\text{TiCp}_2\text{Se}_n\text{S}_{5-n}]$		<i>clc</i>	
$[\text{Fe}(\text{C}_5\text{H}_4\text{E})_2\text{E}]$ (E, E' = S, Se, Te)		$\text{Se}_6\text{I}_2^{2+}$ , $\text{Te}_6\text{I}_2^{2-}$	$\text{Te}_8^{2-}$
		$\text{Ph}_2\text{Se}_6^{2+}$	$[\text{HgTe}_7^-]$
			$\text{MeC}(\text{O})\text{C}(\text{Se})\text{Se}_5$
		<i>Het</i>	
		$\text{Te}_3\text{S}_6^{2+}$	
			$\text{Te}_2\text{Se}_6^{2+}$



**Figure 1** (a) The minimized repulsion of the  $np$  lone pairs of adjacent chalcogen atoms leads to a torsional angle of approximately  $90^\circ$ . (b) The hyperconjugative  $np^2 \rightarrow \sigma^*$  interaction results often in the alternation of chalcogen–chalcogen bond lengths. (c) The  $\pi^*-\pi^*$  interaction between two  $R_2E_2^+$  stabilizes the square-planar  $(RE)_4^{2+}$  cation.



**Figure 2** Well-characterized selenium- and tellurium-allotropes as a function of pressure. (a) hexagonal polymorph, (b) monoclinic-orthorhombic polymorph, (c) rhombohedral polymorph ( $\beta$ -Po structure), (d)  $bcc$ -polymorph. <sup>a</sup>Keller et al.<sup>20</sup> <sup>b</sup>Adenis et al.<sup>21</sup> <sup>c</sup>Akashima et al.<sup>23</sup> <sup>d</sup>Aoki et al.<sup>24</sup> <sup>e</sup>Aoki et al.<sup>24</sup> and Jamieson and McWhan.<sup>25</sup> <sup>f</sup>Parthasarathy and Holzappel.<sup>26</sup>

The  $np$  lone pairs are often involved in hyperconjugative  $np^2 \rightarrow n\sigma^*$  interactions (see [Figure 1\(b\)](#)) that explain significant bond length alternations in molecules like  $S_7$  (see [Section 1.07.2.2.2](#)) and can also be utilized to justify the bonding and structures of many ionic and electronically neutral polychalcogen species (see, for instance, [Section 1.07.3.2](#)).

Partially occupied  $\pi^*$  orbitals of two chalcogen fragments can also overlap and lead to attractive  $\pi^*-\pi^*$  interactions, as shown in [Figure 1\(c\)](#).  $(EtTe)_4^{2+}$  is a typical example of an ion exhibiting such interactions (see [Section 1.07.4.1](#)). The observed bond length differences in  $S_2I_4^{2+}$  and  $Se_2I_4^{2+}$  can also be explained by invoking  $\pi^*-\pi^*$  interactions (see [Section 1.07.3.2.3.1](#)).

This chapter explores the selenium and tellurium bond catenation in different chemical environments. The emphasis is on the structures and bonding of the different species, but the synthetic aspects will be discussed, where appropriate. The rapidly growing research material precludes the fully comprehensive treatment of the subject, but the basic theme will be pursued by providing illustrative examples throughout the chapter.

## 1.07.2 Elemental Selenium and Tellurium and Related Mixed Chalcogen Systems

### 1.07.2.1 Polymeric Selenium and Tellurium Allotropes

Hexagonal  $\alpha$ -selenium and tellurium are the thermodynamically stable allotropes of the elements. They are isostructural and are composed of a network of trigonal helical chains, as shown in [Figure 2\(a\)](#). The Se–Se bond length is  $2.350 \text{ \AA}$ <sup>20</sup> and the Te–Te bond length is  $2.835 \text{ \AA}$ ,<sup>21</sup> both corresponding closely to single bond lengths. The closest interchain distances are  $3.463$ <sup>20</sup> and  $3.4912 \text{ \AA}$ ,<sup>21</sup> respectively. As seen from [Figure 2\(a\)](#), the closest interchain contacts expand the coordination around each atom into a distorted octahedron. This kind of secondary bonding interactions has originally been proposed by Allcock.<sup>19</sup> They are expectedly weaker in selenium (the van der Waals' radii of selenium and tellurium are  $1.80$  and  $2.20 \text{ \AA}$ , respectively).

Both selenium and tellurium have several high-pressure allotropes, although complete information on their high-pressure

behavior is still rather vague. In the case of both elements, there are several modifications, which have been proposed,<sup>22</sup> but only three distinct high-pressure phases seem to have been unambiguously isolated and structurally characterized for both selenium<sup>23</sup> and tellurium<sup>24–26</sup> (see **Figure 2(b)–2(d)**). Recently, however, even the structures of the two lowest high-pressure forms have been questioned and incommensurate crystal structures have been suggested instead.<sup>27</sup> It can be seen from **Figure 2** that as the pressure increases, the packing becomes more efficient and approaches and finally reaches the body-centered cubic structure.

The electrical properties of both selenium and tellurium depend on pressure. Whereas the ambient, trigonal forms of both elements are semiconducting, all high-pressure polymorphs exhibit metallic conductivity.<sup>28,29</sup> In addition, both the high-pressure polymorphs of both elements are superconducting.<sup>30,31</sup> The transition temperature seems to increase as a function of pressure and is in the range of 2.5–4.3 K up to 15 GPa and is ~6.5 K in the range 15–18 GPa.<sup>31</sup>

Research activity has been boosted by the observation that mixed selenium–tellurium system shows enhanced conducting and photoconducting properties compared to those of selenium.<sup>32</sup> The indexing of x-ray powder diagrams in terms of a hexagonal unit cell indicates an almost linear variation in the lattice constants as a function of the elemental composition.<sup>33</sup> These results can be interpreted by the statistical distribution of tellurium and selenium atoms in the helical chain that is shown in **Figure 2**.

### 1.07.2.2 Selenium- and Tellurium-Containing Chalcogen Rings

#### 1.07.2.2.1 General

Sulfur is known to exhibit a wide variety of cyclic molecular forms of different ring sizes.<sup>1–3</sup> The existence of analogous selenium rings is limited to Se<sub>8</sub>,<sup>34–38</sup> Se<sub>7</sub>,<sup>39</sup> and Se<sub>6</sub>.<sup>40</sup> There are only a few reports on homocyclic tellurium molecules.

The chemical and structural similarity of the three chalcogen elements has led to investigations on the structures and properties of the binary and ternary systems.<sup>2</sup> Heterocyclic selenium sulfides form an extensive binary system that bridges the properties of an electrical insulator (sulfur) and a semiconductor (selenium). The heterocyclic tellurium-containing species are much sparser, and therefore very little is known about their properties.

The preparation of homo- and heterocyclic chalcogen rings has been summarized in several reviews (for instance, see Studel and Eckert, 2003<sup>1</sup> and Laitinen et al., 1994<sup>2</sup>). Some of the reactions yield pure stoichiometric products, but in most cases the reactions afford mixtures of different molecular species.

Chalcogen ring molecules are conveniently produced from the melts of the elements or element mixtures by quenching the equilibrium melt in liquid nitrogen or in an ice bath followed by extraction using nonpolar solvents (for details, see Laitinen et al., 1994<sup>2</sup> and references therein).

Transition metal chalcogenides of the type [TiCp<sub>2</sub>E<sub>5</sub>] (E=S, Se) and [TiCp<sub>2</sub>(μ-E<sub>2</sub>)<sub>2</sub>TiCp<sub>2</sub>] (E=S, Se, Te; Cp=C<sub>5</sub>H<sub>5</sub><sup>−</sup> or its alkyl-substituted derivatives) are useful reagents for the preparation of homo- and heterocyclic chalcogen rings. In

particular, the reactions of [TiCp<sub>2</sub>S<sub>5</sub>] with S<sub>n</sub>Cl<sub>2</sub> afford a large number of homocyclic sulfur ring molecules S<sub>n+5</sub> (see **Chapter 1.06**). In a similar fashion, [TiCp<sub>2</sub>Se<sub>5</sub>] reacts with Se<sub>2</sub>Cl<sub>2</sub> and SeCl<sub>2</sub> to afford Se<sub>7</sub> and Se<sub>6</sub>.<sup>39,41,42</sup> In CS<sub>2</sub> both quickly equilibrate to form a mixture of Se<sub>8</sub>, Se<sub>7</sub>, and Se<sub>6</sub>.<sup>43</sup> The reactions of [TiCp<sub>2</sub>S<sub>5</sub>] with Se<sub>2</sub>Cl<sub>2</sub><sup>44</sup> or SeCl<sub>2</sub>,<sup>42</sup> and those of [TiCp<sub>2</sub>Se<sub>5</sub>] with S<sub>n</sub>Cl<sub>2</sub> (n=1, 2)<sup>39,45,46</sup> afford heterocyclic selenium sulfides, as do the reactions of [TiCp<sub>2</sub>Se<sub>n</sub>S<sub>5−n</sub>] mixtures with sulfur or selenium chlorides.<sup>46</sup> Dinuclear [TiCp<sub>2</sub>(μ-E<sub>2</sub>)<sub>2</sub>TiCp<sub>2</sub>] (E=S, Se, Te) also react with chalcogen chlorides to form chalcogen rings in a similar fashion.<sup>41,47</sup>

#### 1.07.2.2.2 Homocyclic selenium molecules

Three monoclinic polymorphs are known for Se<sub>8</sub>.<sup>34–38</sup> They all consist of puckered crown-shaped Se<sub>8</sub> ring molecules, which are similar to those of the three known crystallographic modifications of S<sub>8</sub>.<sup>48–52</sup> The bond parameters in all three cyclic selenium modifications are near to those expected for single bonds (see **Table 2**).

The structures of monoclinic α- and β-Se<sub>8</sub> depend on temperature. In both polymorphs, the individual bond lengths in the two low-temperature structures<sup>35,37</sup> are significantly shorter than the corresponding bonds in the room-temperature structures.<sup>33,35</sup> In the case of α-Se<sub>8</sub>, the ring becomes more distorted from the ideal D<sub>4d</sub> symmetry, as the temperature is lowered.<sup>35</sup> Similar distortion is not so evident in monoclinic β-Se<sub>8</sub>.<sup>37</sup>

The intermolecular interactions in all three monoclinic polymorphs are stronger than those in S<sub>8</sub>. In monoclinic γ-Se<sub>8</sub>,<sup>38</sup> the shortest intermolecular contact is shorter than in any modifications of S<sub>8</sub>.<sup>48–52</sup> The packing of Se<sub>8</sub> molecules in the three monoclinic polymorphs is shown in **Figure 3**.

Recently, a fourth monoclinic polymorph has been reported for Se<sub>8</sub>.<sup>56</sup> However, it is in fact identical to monoclinic α-Se<sub>8</sub>,<sup>34,35</sup> if the transformation from the standard setting P2<sub>1</sub>/c to P2<sub>1</sub>/n is carried out. Any differences in metric parameters are due to differences in the temperature of the crystal structure determination.

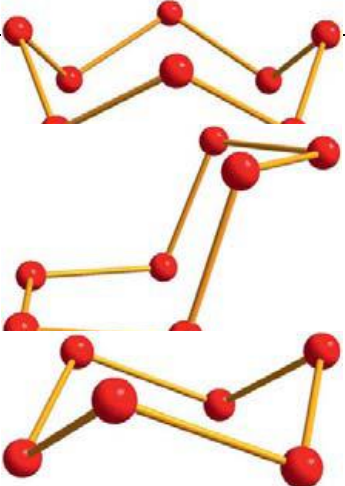
The crystal structure of Se<sub>7</sub> is unknown, but its Raman spectrum<sup>39</sup> is similar to that of γ- and δ-S<sub>7</sub><sup>57</sup> indicating a similar structure. The molecular Se<sub>7</sub> ring in two ionic products, [Na(12-crown-4)]<sub>2</sub>(Se<sub>8</sub>)·(Se<sub>7</sub>)<sup>53</sup> and (NEt<sub>4</sub>)<sub>2</sub>(Se<sub>5</sub>)·(½Se<sub>6</sub>Se<sub>7</sub>),<sup>54</sup> shows a conformation and bond length alternation similar to those in S<sub>7</sub>.<sup>58,59</sup>

The bond length alternation can be rationalized in terms of the p lone-pair repulsion of the two central atoms in the planar four-atomic fragment and of the hyperconjugational interaction of these lone pairs to the σ\* orbitals of the bonds connecting the fragment to the rest of the molecule,<sup>57</sup> as shown schematically in **Figure 4**.

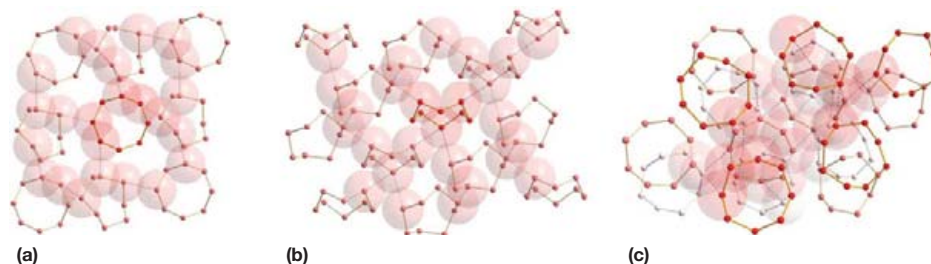
#### 1.07.2.2.3 Homocyclic tellurium molecules

The evidence for homocyclic tellurium rings is very sparse.<sup>2,3</sup> The presence of the Te<sub>8</sub> ring molecule in zeolites has been suggested based on conductivity measurements and Raman spectroscopy.<sup>60,61</sup> The treatment of [TiCp<sub>2</sub>(μ-Te<sub>2</sub>)<sub>2</sub>TiCp<sub>2</sub>] with Te<sub>2</sub>Cl<sub>2</sub> in CS<sub>2</sub> results in the observation of a single resonance at 869 ppm in the <sup>125</sup>Te NMR spectrum.<sup>62</sup> This resonance is in the region that could be expected for Te<sub>8</sub> (cf. 611.5 ppm for Se<sub>8</sub><sup>63</sup>).

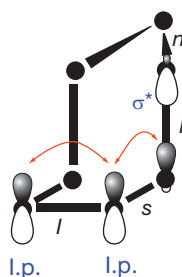
**Table 2** Homocyclic selenium molecules

Molecule		$r_{\text{SeSe}} (\text{\AA})$	$\alpha_{\text{SeSeSe}} (^{\circ})$	$\tau_{\text{SeSeSeSe}} (^{\circ})$	Ref.
Se <sub>8</sub>	$\alpha\text{-Se}_8^a$	2.291(1)–2.327(1)	103.15(4)–107.88(5)	95.80(5)–106.89(5)	35
	$\beta\text{-Se}_8^b$	2.301(1)–2.324(1)	104.60(5)–106.97(5)	98.21(6)–104.27(6)	37
	$\gamma\text{-Se}_8^c$	2.325(2)–2.344(2)	103.26(8)–109.08(8)	98.15(9)–107.23(9)	38
Se <sub>7</sub>	$[\text{Na}(12\text{-crown-}4)_2(\text{Se}_6)\cdot(\text{Se}_7)]^c$	2.281(6)–2.440(8)	99.6(2)–110.3(3)	1.6(3), 69.9(2)–114.0(3)	53
	$(\text{NEt}_4)_2(\text{Se}_5)\cdot(\frac{1}{2}\text{Se}_6, \text{Se}_7)^c$	2.324(7)–2.409(7)	101.1(2)–108.3(2)	4.6(3), 73.7(3)–111.7(3)	54
	$[\text{Re}_2(\mu\text{-I})_2(\mu\text{-Se}_7)(\text{CO})_6]\cdot\frac{1}{2}\text{C}_7\text{H}_{16}^c$	2.309(3)–2.558(3)	99.33(10)–104.28(9)	4.3(1), 77.9(1)–114.2(1)	55
Se <sub>6</sub>	$\text{Se}_6^c$	2.356(9)	101.1(3)	76.2(4)	40
	$(\text{NEt}_4)_2(\text{Se}_5)\cdot(\frac{1}{2}\text{Se}_6, \text{Se}_7)^c$	2.319(7)–2.419(7)	97.3(2)–105.8(2)	71.5(3)–77.9(3)	54

<sup>a</sup>*T* = 120 K.<sup>b</sup>*T* = 150 K.<sup>c</sup>r.t.



**Figure 3** Packing of molecules in monoclinic (a)  $\alpha$ -Se<sub>8</sub>,<sup>35</sup> (b)  $\beta$ -Se<sub>8</sub>,<sup>37</sup> and (c)  $\gamma$ -Se<sub>8</sub>.<sup>38</sup>



**Figure 4** Lone-pair interaction and bond length alternation in heptachalcogen ring molecules.  $l$  = long,  $s$  = short,  $n$  = normal single bond.<sup>57</sup>

#### 1.07.2.2.4 Selenium and tellurium rings in metal complexes

Structural information of the Te<sub>8</sub> ring comes from Cs<sub>3</sub>Te<sub>22</sub><sup>64</sup> in which the crown-shaped puckered Te<sub>8</sub> rings are found between the [Te<sub>4</sub>Te<sub>4/2</sub>]<sub>2∞</sub><sup>3-</sup> layer anions (see **Figure 5**). The Te–Te distances in the ring are 2.787–2.818 Å, the bond angles 99.32–101.12°, and the torsional angles 106.53–106.95°. Cs<sub>4</sub>Te<sub>28</sub> also contains a Te<sub>8</sub> ring in a related layered two-dimensional (2D) polytelluride lattice.<sup>65</sup> In a similar fashion, the related selenium phase, Cs<sub>3</sub>Se<sub>22</sub>, has been shown to contain a cyclooctaselenium ring molecule between the cesium selenide layers.<sup>66</sup>

The Te<sub>6</sub> ring has also been stabilized as [(AgI)<sub>2</sub>Te<sub>6</sub>] (see **Figure 6(a)**)<sup>67</sup> and [Re<sub>6</sub>Te<sub>10</sub>Cl<sub>6</sub>(Te<sub>6</sub>)].<sup>68</sup> Despite coordination to the metal, they both show bond parameters that are expected for the isolated Te<sub>6</sub> ring (bond lengths 2.729–2.760 Å<sup>67</sup> and 2.762–2.900 Å<sup>68</sup>; bond angles 95.9–100.2°<sup>67</sup> and 92.2–100.2°<sup>68</sup>; torsion angles 78.5–82.0°<sup>67</sup> and 75.2–87.0°<sup>68</sup>) on the basis of bond parameters from Se<sub>6</sub><sup>40</sup> (see **Table 2**).

The reaction of elemental tellurium and iridium and tellurium tetrachloride in a sealed, evacuated ampoule at 250 °C for 7 days afforded black crystals of [{Ir(TeCl<sub>4</sub>)(TeCl<sub>3</sub>)<sub>2</sub>(Te<sub>10</sub>)] containing a novel type of electrically neutral tellurium cage molecule Te<sub>10</sub> (see **Figure 6(b)**).<sup>69</sup> The molecule consists of two nearly linear 3c–4e bonding arrangements bridging the two four-membered rings. The ten-atomic cage is considered to be formally uncharged (Te<sup>+0.50</sup>)<sub>4</sub>(Te<sup>0</sup>)<sub>4</sub>(Te<sup>-</sup>)<sub>2</sub>.<sup>69</sup>

The heating of ruthenium, indium, tellurium, and tellurium tetrachloride or ruthenium, tellurium, and tellurium tetrachloride at 300 °C afforded shiny black [Ru(Te<sub>9</sub>)]InCl<sub>4</sub> and [Ru(Te<sub>8</sub>)]Cl<sub>2</sub>, respectively.<sup>70</sup> A similar reaction involving rhodium, tellurium, and tellurium tetrachloride yielded [Rh(Te<sub>6</sub>)]Cl<sub>3</sub>. All complexes are 1D coordination polymers with the uncharged tellurium rings acting as bridging bis-tridentate ligands.

Selenium forms several complexes, which contain homocyclic ring molecules as a ligands.<sup>71–74</sup> In addition to [(AgI)<sub>2</sub>(Se<sub>6</sub>)], which is isomorphic with [(AgI)<sub>2</sub>(Te<sub>6</sub>)],<sup>67</sup> the coordination of Se<sub>6</sub> ring with Ag<sup>+</sup> has recently been demonstrated to form isolated [Ag(Se<sub>6</sub>)Ag]<sup>2+</sup> ions or close-packed stacked arrays of Se<sub>6</sub> molecules with Ag<sup>+</sup> residing in the octahedral holes depending on the size of the counterion.<sup>71</sup> Solvothermal reactions also lead to solid phases containing Se<sub>6</sub><sup>72,75</sup> or Se<sub>8</sub><sup>72,76,77</sup> ring molecules. In addition to x-ray structures, these phases have been characterized by vibrational spectroscopy,<sup>72,76</sup> solid-state NMR spectroscopy,<sup>75</sup> and thermal analysis.<sup>76</sup>

The Se<sub>7</sub> ring molecule has been isolated as a bridging ligand in the dinuclear rhenium complex [Re<sub>2</sub>(μ-1)<sub>2</sub>(μ-Se<sub>7</sub>)(CO)<sub>8</sub>].<sup>55</sup> Despite the coordination to the dinuclear Re center, the molecules show the four coplanar atoms and the bond length alternation well established for S<sub>7</sub>.<sup>58,59</sup> Very recently, [Rh<sub>2</sub>Se<sub>9</sub>Cl<sub>6</sub>] was prepared from RhCl<sub>3</sub>·4H<sub>2</sub>O and Se<sub>2</sub>Cl<sub>2</sub>.<sup>73</sup> It was found to contain the Se<sub>9</sub> ring as a bridging ligand between two Rh centers (see **Figure 7**) in a similar fashion to the Te<sub>9</sub> ring in [Ru(Te<sub>9</sub>)]InCl<sub>4</sub>.<sup>70</sup> Similarly, homocyclic dodeca-selenium molecule was observed as a bridging ligand in the dinuclear [Ag<sub>2</sub>Se<sub>12</sub>]<sup>2+</sup> containing a weakly coordinating counteranion [Al{OC(CF<sub>3</sub>)<sub>3</sub>}<sub>4</sub>]<sup>-</sup> or [AlF{OC(C<sub>5</sub>F<sub>10</sub>)(C<sub>6</sub>F<sub>5</sub>)<sub>3</sub>}<sub>3</sub>].<sup>74</sup> The Se<sub>12</sub> molecule shows a similar conformation and analogous bond parameters to S<sub>12</sub>.<sup>2</sup>

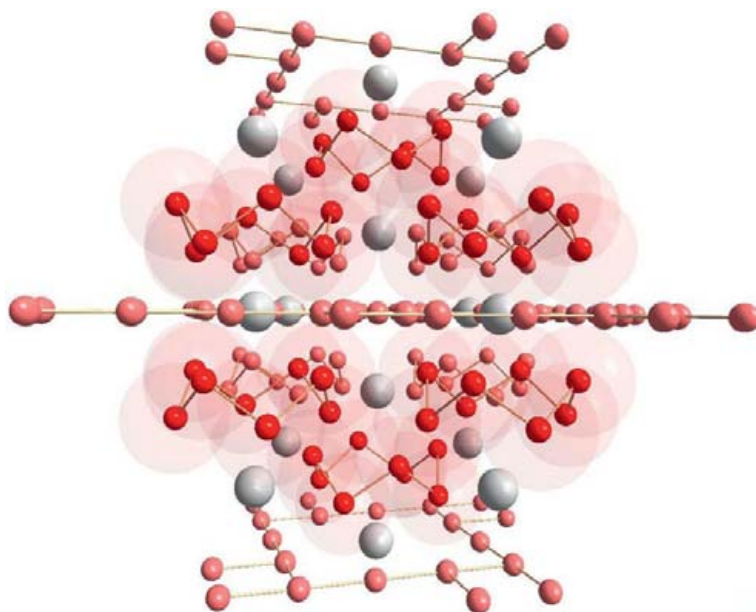
#### 1.07.2.2.5 Heterocyclic chalcogen molecules

##### 1.07.2.2.5.1 Selenium sulfides

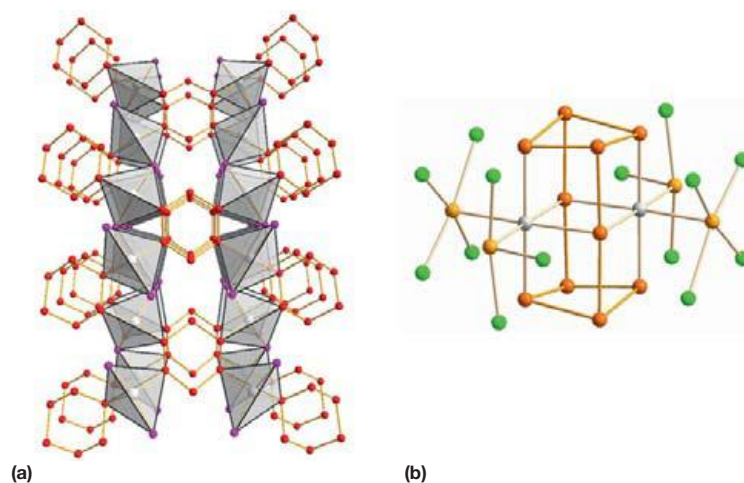
The similarity of sulfur and selenium is reflected by a complicated binary system between the two elements. With the exception of the condensation reactions of [TiCp<sub>2</sub>E<sub>5</sub>] or [TiCp<sub>2</sub>(μ-E<sub>2</sub>)<sub>2</sub>TiCp<sub>2</sub>] (E = S, Se) with sulfur and selenium chlorides (see **Section 1.07.2.2.1**), most synthetic routes produce mixtures of various selenium sulfides.<sup>2</sup> The eight-membered Se<sub>*n*</sub>S<sub>8–*n*</sub> species are the most abundant and most stable molecular species, although heterocyclic selenium sulfides of other ring sizes can also be formed.

All known crystal structures of heterocyclic selenium sulfides are disordered.<sup>39,45,78–83</sup> It has therefore not been possible to calculate accurate bond parameters or identify individual molecular species. Vibrational spectroscopy provided the first indications that selenium sulfides are present in the various mixtures.<sup>84,85</sup> The normal coordinate calculations enabled the assignment of the Raman spectra of 1,2-Se<sub>2</sub>S<sub>5</sub>,<sup>86,87</sup> 1,2,3,4,5-Se<sub>5</sub>S<sub>2</sub>,<sup>39,87</sup> 1,2,3-Se<sub>3</sub>S<sub>5</sub>,<sup>82</sup> 1,2,5,6-Se<sub>4</sub>S<sub>4</sub>,<sup>83</sup> and Se<sub>7</sub>S<sup>45</sup> and identification of the molecular species.





**Figure 5** Crystal structure of  $\text{Cs}_3\text{Te}_{22}$  layers consisting of puckered  $\text{Te}_8$  rings between the  $[\text{Te}_4\text{Te}_{4/2}]_{2\infty}^{3-}$  layer anions.<sup>64</sup>

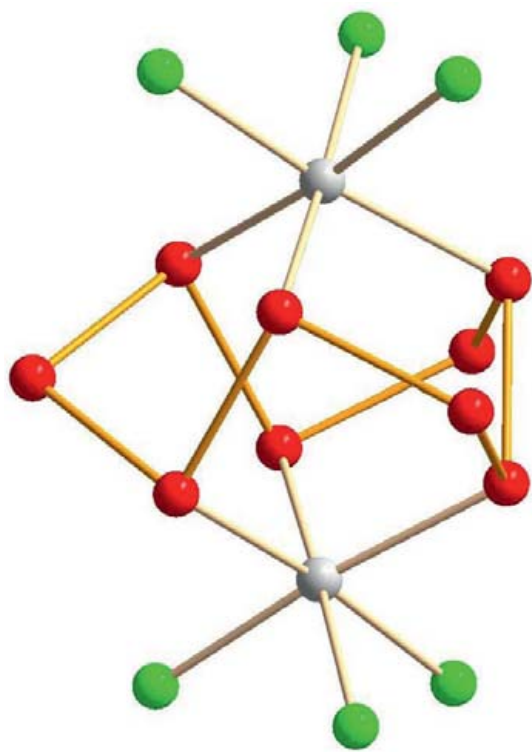


**Figure 6** (a) The  $\text{Te}_6$  molecule stabilized as  $[(\text{AgI})_2(\text{Te}_6)]$ .<sup>67</sup>  $[(\text{AgI})_2(\text{Se}_6)]$  is isomorphic with the tellurium analog. (b) The novel uncharged  $\text{Te}_{10}$  cage stabilized as  $[(\text{Ir}(\text{TeCl}_4)(\text{TeCl}_3))_2(\text{Te}_{10})]$ .<sup>69</sup> Tellurium atoms in the  $\text{Te}_{10}$  molecule are depicted in orange, those in the  $\text{TeCl}_4$  and  $\text{TeCl}_3$  fragments in light orange, chlorine atoms in green, and iridium in light gray.

$^{77}\text{Se}$  NMR spectroscopy is the most powerful technique to date to identify individual heterocyclic selenium sulfides in mixtures of complicated composition.<sup>63,88,89</sup> The spectral assignment is based on the combined information from the natural-abundance samples and from the samples of the same chemical composition but involving selenium enriched with  $^{77}\text{Se}$ -isotope (enrichment 92%).<sup>63</sup> Due to the low natural abundances of the  $^{77}\text{Se}$ -isotope in the natural-abundance selenium, the coupling can only be observed by the appearance of small satellites that are often lost in the background. Full coupling information is only obtained with the enrichment of the  $^{77}\text{Se}$ -isotope.

The assignment of the  $^{77}\text{Se}$  chemical shifts to individual molecules is exemplified in **Figure 8** by the NMR spectrum of

the  $\text{CS}_2$  solution that was prepared from the quenched sulfur-selenium melt containing 30% of  $^{77}\text{Se}$ -enriched selenium (enrichment 92%) and 70% of sulfur. In addition to the resonances shown in the figure, there are eight resonances in the spectrum, which appear as singlets even in the  $^{77}\text{Se}$ -enriched sample.<sup>63</sup> These singlets were assigned to  $\text{Se}_7$ , all isomers of  $\text{Se}_2\text{S}_6$ , 1,2,5,6- $\text{Se}_4\text{S}_4$ ,  $\text{Se}_8$ , and  $\text{Se}_6$  on the basis of the trends in the chemical shifts deduced from unambiguously identified molecular species.<sup>41,63</sup> The assignments were later verified by DFT calculations of  $^{77}\text{Se}$  chemical shifts.<sup>90</sup> Sulfur-rich  $\text{Se}_7$  and 1,2- $\text{Se}_6\text{S}_2$  are the main components in the mixture even when the initial selenium content is high. Other major components are 1,2,3- $\text{Se}_3\text{S}_5$ , 1,2,3,4- $\text{Se}_4\text{S}_4$ , 1,2,3,4,5- $\text{Se}_5\text{S}_3$ , 1,2,3,4,5,6- $\text{Se}_6\text{S}_2$ , and  $\text{Se}_8$ <sup>63</sup> in agreement with the deductions from earlier



**Figure 7** The bridging electrically neutral homocyclic  $\text{Se}_9$  ligand in  $[\text{Rh}_2\text{Se}_9\text{Cl}_6]$ .<sup>73</sup> Selenium is depicted in red, chlorine in green, and rhodium in light gray.

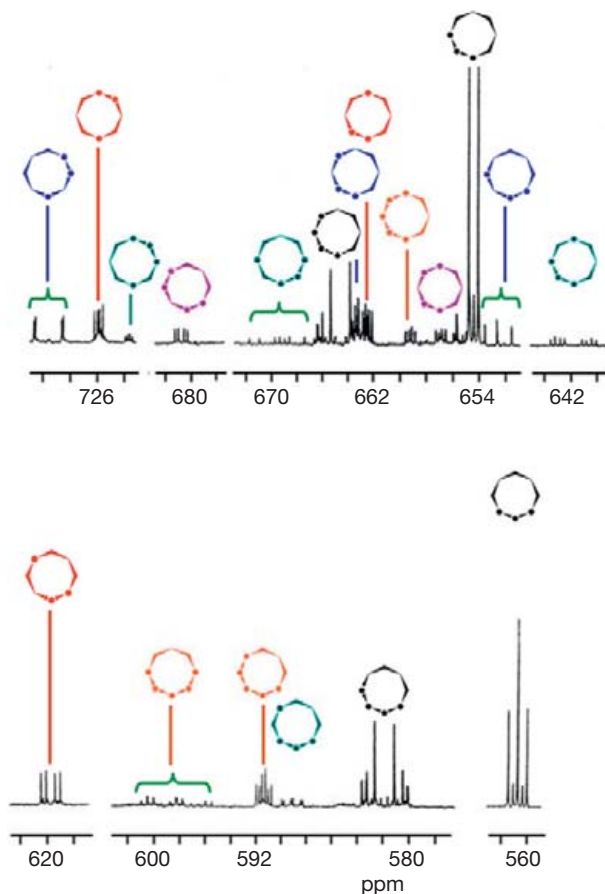
vibrational analysis<sup>84</sup> that the number of homonuclear Se–Se or S–S bonds is maximized in the eight-membered rings.

$^{77}\text{Se}$  NMR spectroscopy can also be utilized to monitor interconversion reactions that take place between the different chalcogen rings in solution. This is exemplified in **Figure 9** for the reaction of  $[\text{TiCp}_2\text{Se}_5]$  and  $\text{S}_2\text{Cl}_2$ .<sup>91</sup> It can be seen that the initial fluxional seven-membered 1,2,3,4,5- $\text{Se}_5\text{S}_2$  ring decomposes into 1,2,3,4- $\text{Se}_4\text{S}_2$  and 1,2,3,4,5,6- $\text{Se}_6\text{S}_2$ . Similar interconversion has been shown to take place between  $\text{Se}_7$ ,  $\text{Se}_6$ , and  $\text{Se}_8$ <sup>43</sup> and 1,2- $\text{Se}_2\text{S}_5$ ,  $\text{SeS}_5$ , and 1,2,3- $\text{Se}_3\text{S}_5$ .<sup>82,86</sup>

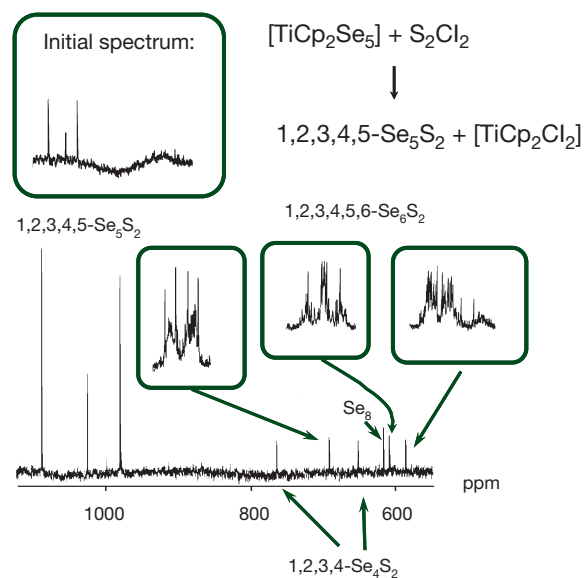
#### 1.07.2.2.5.2 Tellurium-containing chalcogen rings

The formation of  $\text{Te}_n\text{S}_{8-n}$  rings in sulfur–tellurium melt has been deduced by mass spectrometry,<sup>92</sup> Mössbauer spectrometry,<sup>93</sup> and  $^{125}\text{Te}$  NMR spectrometry.<sup>94</sup> The disordered crystal structure of the phase prepared from  $\text{H}_2\text{S}$  and  $\text{TeCl}_4$  was deduced to contain a mixture of ring molecules  $\text{S}_8$ ,  $\text{TeS}_7$ , and  $\text{Te}_2\text{S}_6$ <sup>95</sup> with a conformation similar to that in  $\text{TeS}_7\text{X}_2$  ( $\text{X}=\text{Cl}, \text{Br}$ ).<sup>96</sup> Nagata et al.<sup>97,98</sup> have reported that the seven- and eight-membered selenium-rich selenium telluride heterocycles have conformations which are similar to the analogous sulfur, selenium, and selenium sulfide ring molecules.<sup>39,53,54,58,59</sup>

$^{125}\text{Te}$  and  $^{77}\text{Se}$  NMR spectroscopic characterization of sulfur–tellurium and sulfur–selenium–tellurium melts at 145 °C using both natural-abundance selenium and tellurium and  $^{77}\text{Se}$ -enriched and  $^{125}\text{Te}$ -enriched isotopes has indicated that the sulfur-rich binary molten mixture contains  $\text{TeS}_7$  and 1,2-, 1,3-, and 1,4-isomers of  $\text{Te}_2\text{S}_6$ .<sup>94</sup> In addition, 1,2-, 1,3-, 1,4-, and 1,5- $\text{TeSe}_6$  rings have been detected in the ternary melt



**Figure 8**  $^{77}\text{Se}$  NMR spectrum of the  $\text{CS}_2$  solution of quenched sulfur–selenium melt containing 30 mol.% of selenium enriched in  $^{77}\text{Se}$ -isotope (enrichment 92%).<sup>63</sup> The different  $\text{Se}_n\text{S}_{8-n}$  species have been color-coded. The colored circles indicate selenium atoms and the empty corners sulfur atoms.



**Figure 9** The natural-abundance  $^{77}\text{Se}$  NMR spectrum of the reaction mixture of  $[\text{TiCp}_2\text{Se}_5]$  and  $\text{S}_2\text{Cl}_2$  recorded after 1 day of decomposition.<sup>91</sup> The uppermost inset is the spectrum recorded at the beginning of the reaction. The lower insets are resonances of the  $^{77}\text{Se}$ -enriched 1,2,3,4,5,6- $\text{Se}_6\text{S}_2$  (enrichment 92%).

(1.5 mol.% of both tellurium and selenium and 97 mol.% of sulfur).<sup>94</sup> The <sup>125</sup>Te NMR spectrum has been recorded at 145 °C for the melt containing selenium enriched in the <sup>77</sup>Se isotope and tellurium enriched in the <sup>125</sup>Te isotope (in both cases the enrichment is 92%) and is shown in Figure 10.

Tellurium-containing chalcogen rings are also formed by following the preparative routes known for other chalcogen rings (see Laitinen et al., 1994<sup>2</sup> and references therein). The most important processes have been summarized below (Scheme 1).<sup>47</sup>

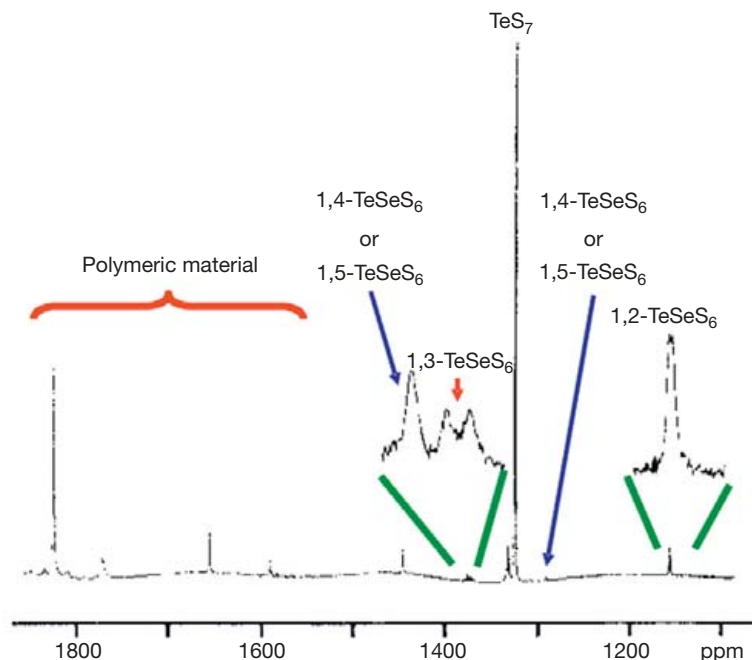
An ab initio molecular orbital (MO) study of eight-membered sulfur-rich tellurium selenium sulfide rings has shown that the most stable species contain Se–Te bonds.<sup>47</sup> 1,2,8-TeSe<sub>2</sub>S<sub>5</sub> was deduced to be the most stable of the isomers. The formation of this species was indeed observed in the reaction of (Me<sub>3</sub>Si)<sub>2</sub>Te with ClSeS<sub>5</sub>SeCl.<sup>47</sup>

## 1.07.3 Selenium- and Tellurium-Containing Ions

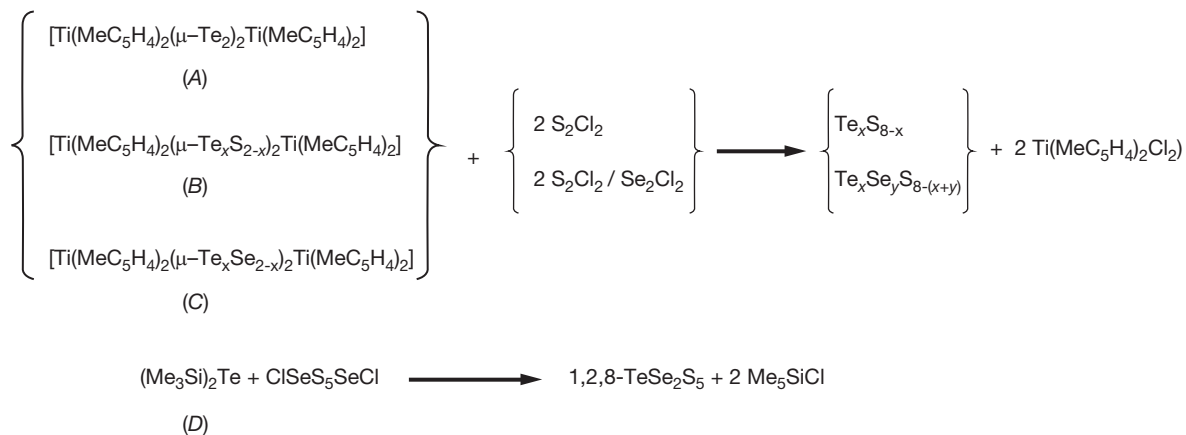
### 1.07.3.1 Polyatomic Selenium and Tellurium Cations

#### 1.07.3.1.1 General

It has been known since the late eighteenth and beginning of nineteenth century that like sulfur, elemental selenium and tellurium can be dissolved in oleum with the formation of intensively colored solutions. With the advent of modern instrumental techniques, it is now well established that all three chalcogen elements form homopolyatomic cations with weakly coordinating anions in such strongly oxidizing media.<sup>3–5</sup> In addition to oleum, the synthetic routes involve super acids, acidic melts, or SO<sub>2</sub> and related aprotic solvents. Suitable oxidizing agents comprise strong main group Lewis acids such as AlCl<sub>3</sub>, AsF<sub>5</sub>, SbCl<sub>5</sub>, and BiCl<sub>5</sub>, and transition



**Figure 10** <sup>125</sup>Te NMR spectrum of ternary sulfur–selenium–tellurium melt containing 1.5 mol.% of both <sup>77</sup>Se-enriched selenium and <sup>125</sup>Te-enriched tellurium (enrichment in both cases 92%) recorded at 145 °C. Adapted from Chivers, T.; Laitinen, R. S.; Schmidt, K. J.; Taavitsainen, J. *Inorg. Chem.* **1993**, *32*, 337–340, with permission. Copyright 1993 American Chemical Society.



**Scheme 1** Formation of tellurium-containing heterocyclic chalcogen ring molecules.

metal halides such as  $\text{MF}_6$  ( $\text{M}=\text{W}, \text{Re}, \text{Os}, \text{Ir}, \text{Pt}$ ),  $\text{MCl}_6$  ( $\text{M}=\text{V}, \text{W}, \text{Zr}, \text{Hf}, \text{Nb}, \text{Ta}, \text{Re}$ ),  $\text{VOCl}_3$ ,  $\text{NbOCl}_3$ , and  $\text{WOCl}_4$ . Very recently, the use of chemical vapor transport methods<sup>4</sup> and ionic liquids<sup>99</sup> in the syntheses of the cations has been suggested. The known homopolynuclear selenium and tellurium cations are summarized in Table 3.

### 1.07.3.1.2 $\text{E}_4^{2+}$

Like  $\text{S}_4^{2+}$  (see Chapter 1.06),  $\text{Se}_4^{2+}$  and  $\text{Te}_4^{2+}$  are  $6\pi$  electron square-planar dications that can be described as mostly aromatic with the formal bond order of 1.25.<sup>100</sup> However, all three cations have been found to show significant singlet diradical character in their electronic structures.<sup>101</sup> The diradical character increases in the order  $\text{S}_4^{2+} < \text{Se}_4^{2+} < \text{Te}_4^{2+}$ . The diradical nature is manifested in the computational prediction of different molecular properties. This is well exemplified by comparing the theoretical computation of <sup>77</sup>Se NMR chemical

**Table 3** Homopolynuclear selenium and tellurium cations for which the solid-state structures are known (see Krossing, 2007,<sup>3</sup> Brownridge et al., 2000,<sup>4</sup> Beck, 1997<sup>5</sup> and references therein)

Chalcogen framework	Homopolychalcogen cations	Heteropolychalcogen cations
4	$\text{Se}_4^{2+}, \text{Te}_4^{2+}, (\text{Te}_4)_n^{2n+}$	$\text{Se}_x\text{S}_{4-x}^{2+}, \text{Te}_2\text{S}_2^{2+}$
6	$\text{Te}_6^{2+}, \text{Te}_6^{4+}$	$\text{Te}_3\text{S}_3^{2+}, \text{Te}_2\text{Se}_4^{2+}$
7	$\text{Te}_7^{2+}$	
8	$\text{Se}_8^{2+}, \text{Te}_8^{2+}, \text{Te}_8^{4+}$	$\text{Te}_2\text{Se}_6^{2+}$
10	$\text{Se}_{10}^{2+}, (\text{Te}_{10})_n^{2n+}$	$\text{Te}_2\text{Se}_8^{2+}$
17	$\text{Se}_{17}^{2+}$	
$\infty$	$(\text{Te}_7)_n^{2n+}, (\text{Te}_8)_n^{2n+}$	

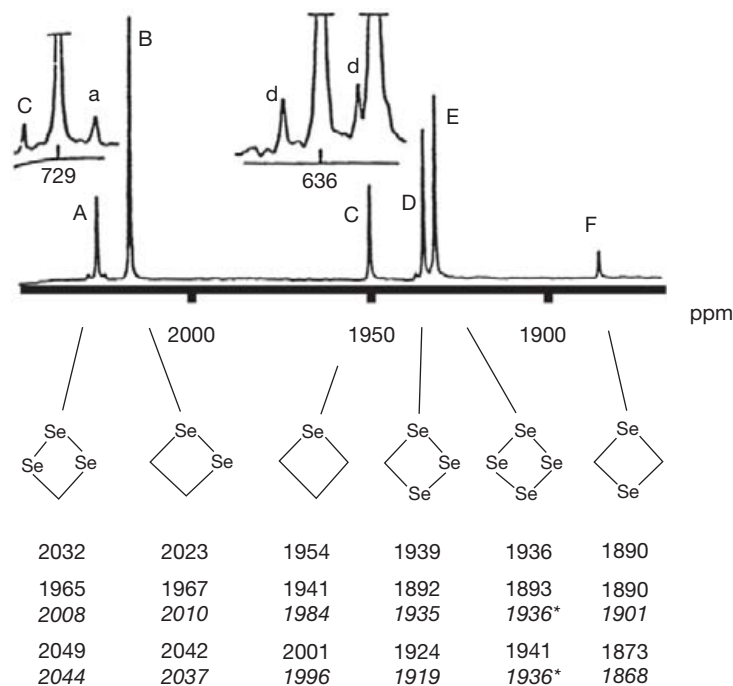
shifts for different  $\text{Se}_n\text{S}_{4-n}^{2+}$  ( $n=1-4$ ) cations<sup>101</sup> for which experimental spectroscopic data and the tentative assignment of the resonances to different species have been reported.<sup>102</sup> Multiconfigurational ab initio methods or pure density functionals are needed to compute the chemical shifts with sufficient accuracy to enable the full verification of the tentative assignment (see Figure 11).<sup>101</sup>

Numerous structures containing different counterions have been determined by x-ray crystallography.<sup>3-5</sup> The bond lengths in each cation depend on the nature of the counterions. This is exemplified by  $\text{Te}_4^{2+}$ , the bond length of which spans a range of 2.660–2.695 Å. The halogen atoms of the counterions bridge the Te–Te edges of the square-planar cation, as illustrated in Figure 12 by  $(\text{Te}_4)[\text{WCl}_6]_2$ .<sup>103</sup> The bond lengthening is caused by the transfer of electron density from the halogen into the  $\sigma^*$  orbital of the cation, and therefore the more basic anions give rise to longer bonds.<sup>5</sup>

Unlike  $\text{S}_4^{2+}$  and  $\text{Se}_4^{2+}$ , the  $\text{Te}_4^{2+}$  cation shows a propensity for extended structures. In  $(\text{Te}_4)(\text{Te}_{10})[\text{Bi}_2\text{Cl}_8]_2$ ,<sup>104</sup> the four-membered rings are linked together through 1,3-positions (see Figure 13). The formal  $\text{Te}_{10}^{2+}$  cation in the structure can be conceived to consist of another stack of polymeric four-membered rings surrounded by two polymeric tellurium helical chains.

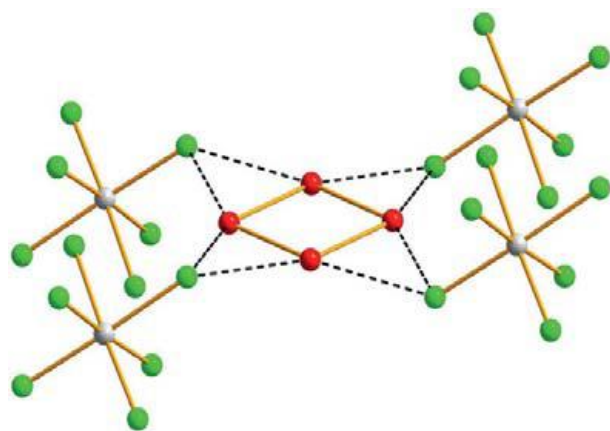
### 1.07.3.1.3 $\text{E}_6^{n+}$ ( $n=2, 4$ )

There are four known hexachalcogen cations:  $\text{Te}_6^{4+}$ ,<sup>105,106</sup>  $\text{Te}_6^{2+}$ ,<sup>107,108</sup>  $\text{Te}_3\text{S}_3^{2+}$ ,<sup>109</sup> and  $\text{Te}_2\text{Se}_4^{2+}$ .<sup>110</sup> Their structures are shown in Figure 14. They cannot be described in terms of electron precise Lewis structures. The structural relationships, however, can be rationalized by applying the electron-accounting principles presented by Gillespie.<sup>111</sup>

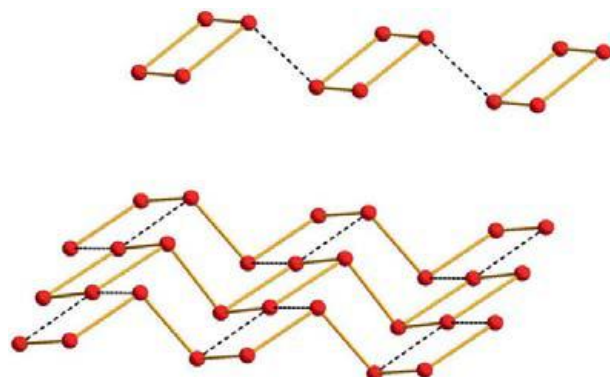


**Figure 11** The <sup>77</sup>Se NMR spectrum of the mixture of  $\text{Se}_n\text{S}_{4-n}^{2+}$  ions in  $\text{SO}_2$ . Reprinted from Collins, M. J.; Gillespie, R. J.; Sawyer, J. F.; Schrobilgen, G. J. *Inorg. Chem.* **1986**, *25*, 2053–2057, with permission. Copyright 1986 American Chemical Society.<sup>102</sup> <sup>a</sup>The assignments of experimental resonances have tentatively been made by Collins et al.<sup>102</sup> <sup>b</sup>The [22,16]-CAS/cc-pVTZ and BPW91/cc-pVTZ calculations of the <sup>77</sup>Se chemical shifts are according to Tuononen et al.<sup>101</sup> Two sets of chemical shifts are reported for both methods. The upper line in each case represents values relative to  $\text{Me}_2\text{Se}$ . The lower line of data shown in italics has been referenced with respect to  $\text{Se}_4^{2+}$  (marked with\*).

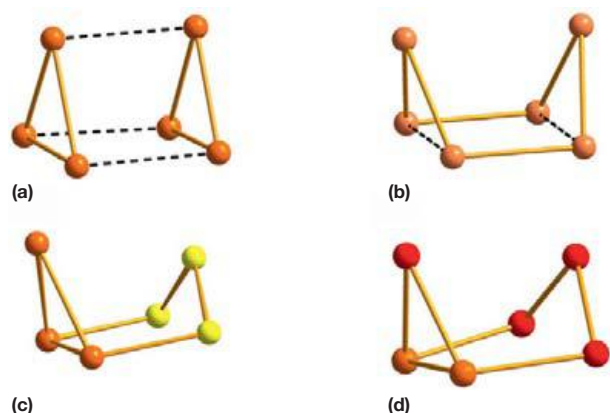




**Figure 12** The cation–anion interactions in  $(\text{Te}_4)[\text{WCl}_6]_2$ .<sup>103</sup> Tellurium atoms are depicted in red, chlorine in green, and tungsten in gray.



**Figure 13** The structure of the cation in  $(\text{Te}_4)(\text{Te}_{10})[\text{Bi}_2\text{Cl}_8]_2$ .<sup>104</sup>



**Figure 14** (a) The structure of the  $\text{Te}_6^{4+}$  cation.<sup>105,106</sup> (b) The structure of  $\text{Te}_6^{2+}$  cation.<sup>107,108</sup> (c) The structure of the  $\text{Te}_3\text{S}_3^{2+}$  cation.<sup>109</sup> (d) The structure of  $\text{Te}_2\text{Se}_4^{2+}$  cation.<sup>110</sup> Tellurium atoms are depicted in orange, selenium in red, and sulfur in yellow.

$\text{Te}_6^{6+}$  is a hypothetical cation containing 30 valence electrons. It fulfills the relationship  $e = 5n$  in which  $n$  is the number of atoms and  $e$  is the number of valence electrons. According to Gillespie,<sup>111</sup> this species is therefore an electron-precise classical cluster and appears as a trigonal prism in which each framework atom is connected to three other framework atoms with single bonds and in addition contains one lone pair of electrons.

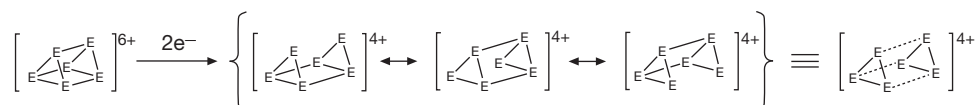
Upon addition of two electrons into  $\text{Te}_6^{6+}$ , a 32-electron cation,  $\text{Te}_6^{4+}$ , is formed. It is an elongated trigonal prism (see **Figure 14(a)**), the structure of which has been established experimentally by x-ray diffraction a long time ago.<sup>105,106</sup> The bonds at the triangular face show approximately single bond lengths (2.662–2.679 Å), but those at the rectangular face are significantly longer (3.062–3.172 Å). According to the electron accounting,<sup>111</sup> it is expected that one bond in  $\text{Te}_6^{6+}$  would be broken by the addition of two electrons. The observed elongated trigonal prism can be rationalized by considering the three resonance structures of  $\text{Te}_6^{4+}$  shown in **Scheme 2**.

These observations are in accordance with the suggestion by Passmore<sup>112</sup> that the characteristic features in homopolychalcogen cations involve the delocalization of the positive charge over all atoms leading to bond length alternations, the presence of  $n p_\pi - n p_\pi$  bonds ( $n \geq 3$ ) and long intracationic transannular interactions, as well as four-center two electron, and six-center two electron bonds. The DFT calculations with local density approximation show that  $\text{Te}_6^{4+}$  can indeed be considered as a dimer of two  $\text{Te}_3^+$  fragments through  $6c-2e$   $\pi^* - \pi^*$  bonds as depicted in **Figure 15**.<sup>113</sup> The elongated  $D_{3h}$  structure is the ground state of the cation with the extra electron pair causing the simultaneous elongation of the three bonds parallel to the  $C_3$  axis.

$\text{E}_6^{2+}$  is a 34-electron cation. The addition of two electron pairs into the classic  $\text{E}_6^{6+}$  cage should lead to the cleavage of two bonds.<sup>111</sup> The crystal structure determinations of  $\text{Te}_6^{2+}$ <sup>107,108</sup> show, however, that one bond is delocalized between two different triangular faces (the relevant Te–Te distances are 3.209–3.382 Å<sup>107,108</sup>) and only one bond is completely missing (see **Figure 14(b)**). The DFT calculations on the MO interactions again support this bonding description.<sup>114</sup> It is only in the case of hybrid  $\text{Te}_3\text{S}_3^{2+}$ <sup>109</sup> and  $\text{Te}_2\text{Se}_4^{2+}$ <sup>110</sup> cations that the expected,<sup>111</sup> more open structure is seen, as shown in **Figure 14(c)** and **14(d)**, respectively.

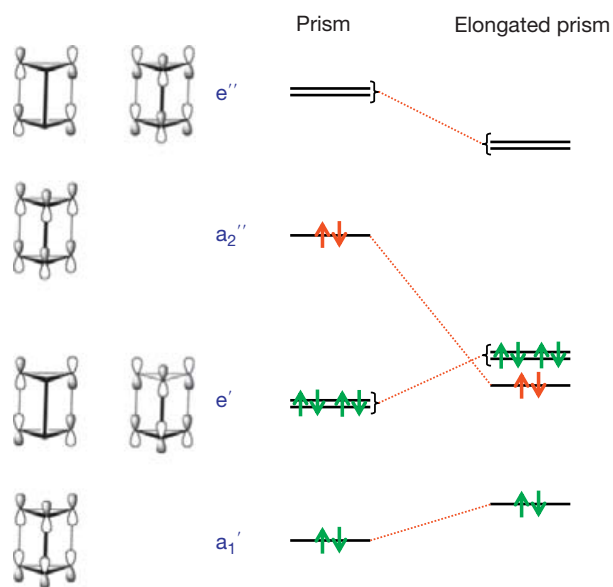
#### 1.07.3.1.4 $\text{E}_8^{n+}$ ( $n=2, 4$ )

$\text{Se}_8^{2+}$  is isostructural with  $\text{S}_8^{2+}$  (see **Chapter 1.06**). The solid-state structure shows three weak transannular interactions, which can be derived from the classical 40-electron  $\text{E}_8^{8+}$  cubane cage,<sup>111</sup> as shown in **Figure 16**. Deductions from the recent DFT study of the structures, bonding, and energetics of different  $\text{E}_8^{2+}$  ( $\text{E}=\text{S}, \text{Se}, \text{Te}$ ) cations<sup>114</sup> are consistent with the concept of three weak transannular interactions and the observed slight bond length alternation, as shown in **Figure 17**. It can be seen from the figure that while the orders of the endocyclic bonds show very little variation around the bond order of one, the 1,5-transannular interaction increases in the order  $\text{S}_8^{2+} < \text{Se}_8^{2+} < \text{Te}_8^{2+}$  (see



**Scheme 2** The addition of two electrons to the classical 30  $e^-$  cluster  $\text{Te}_6^{6+}$  to form  $\text{Te}_6^{4+}$ , a 32  $e^-$  elongated trigonal prism.





**Figure 15** BP88/TZ(d,p) molecular orbitals of the intertriangular  $\sigma$ -bonding and antibonding orbitals of the  $\text{Te}_6^{4+}$  prism.<sup>113</sup> The electrons depicted in green represent those in the highest occupied molecular orbitals of the electron-precise  $\text{Te}_6^{6+}$  prism (30 electrons). The two extra electrons (depicted in red) to form the observed  $\text{Te}_6^{4+}$  cation occupy the  $a_2''$  orbital, which is stabilized by the elongation of the prism.

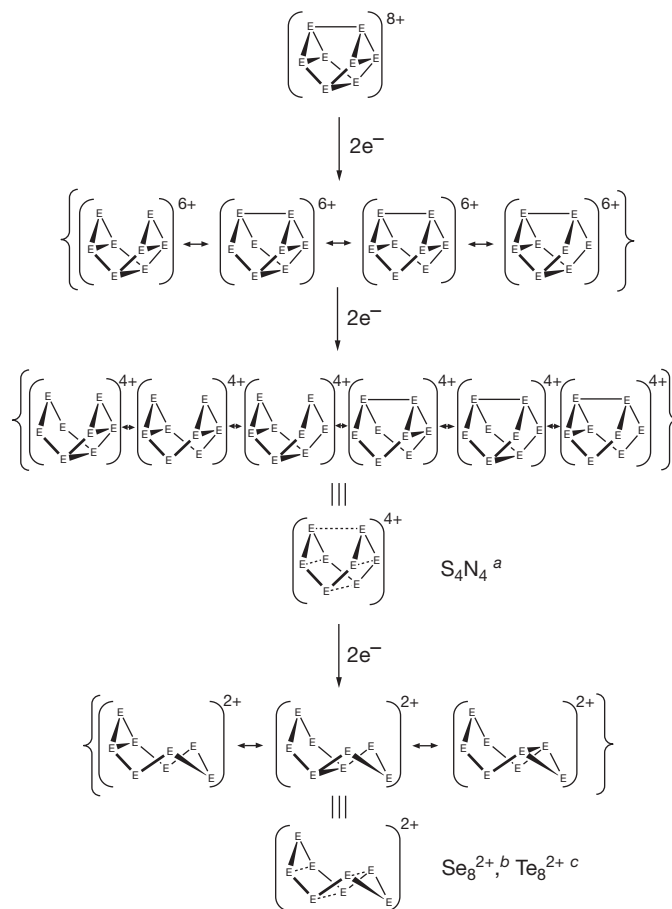
interaction marked as B in **Figure 17**).<sup>4,5</sup> An even more pronounced bicyclic nature is found in the  $\text{Te}_8^{2+}$  cation in  $(\text{Te}_8)[\text{WCl}_6]_2$ <sup>115</sup> (see **Figure 18(a)**). The transannular bond is only 2.993 Å and approaches the single bond length.

The  $\text{Te}_8^{2+}$  cation has also been found to show a bicyclo [2,2,2]octane structure<sup>5</sup> similar to that observed in  $\text{Te}_2\text{S}_6^{2+}$ <sup>116</sup> (see **Figure 18(b)**).

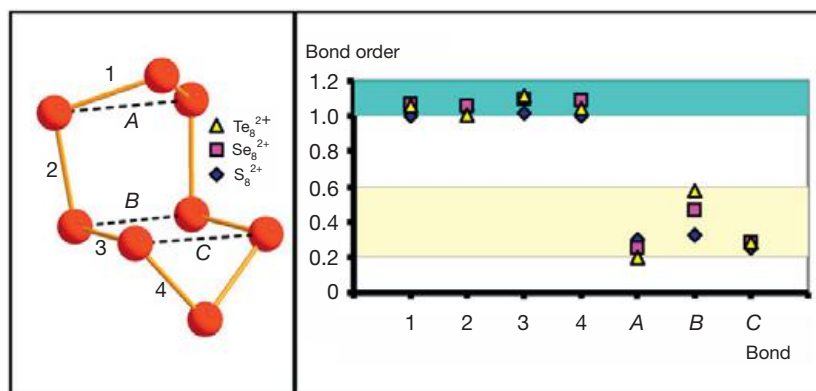
While the structure of the  $\text{Te}_8^{2+}$  cation in  $(\text{Te}_8)[\text{WCl}_6]_2$  can also be derived from the classic 40-electron cuneane cage by adding six electrons and breaking three bonds (see **Figure 16**), that in  $(\text{Te}_6)(\text{Te}_8)[\text{WCl}_6]_4$  is derived from the cube that is another classic 40-electron cage (see **Figure 19**).<sup>110</sup> The  $\text{Te}_8^{4+}$  cation in  $(\text{Te}_8)[\text{VOCl}_4]_2$ <sup>120</sup> is another isomer of the  $\text{Te}_8^{n+}$  cation, the structure of which is also based on the cube. It can be considered as a dimer of two  $\text{Te}_4^{2+}$  cations. In the solid state this  $(\text{Te}_4)_2^{2+}$  dimer shows significant association (see **Figure 20**).

The lengths of the long bonds within the  $(\text{Te}_4)_2^{4+}$  dimer are 3.010 Å and the contacts between the dimers 3.594 Å.<sup>120</sup> Evoking the Pauling equation for the bond orders,<sup>118</sup> it can be concluded that the sum of the bond orders of the weak bonds for one  $\text{Te}_8^{4+}$  unit is almost exactly 2 in accordance with the expectations for the 44-electron cage.<sup>111</sup> Crossing and Passmore<sup>100</sup> have explained these weak bonds in terms of  $5p^2 \rightarrow \sigma^*$  interactions.

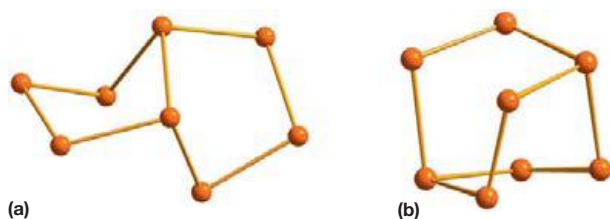
The  $\text{Se}_8^{2+}$  cation has been characterized by <sup>77</sup>Se NMR spectroscopy in  $\text{SO}_2$  solution using both natural-abundance



**Figure 16** Structural relationships between the  $\text{E}_8^{8+}$  (40 valence electrons) classical cage and other species derived from it by successive addition of electrons. Illustrative examples: <sup>a</sup>DeLucia and Coppens,<sup>117</sup> <sup>b</sup>Krossing,<sup>3</sup> Brownridge et al.,<sup>4</sup> and Beck.<sup>5</sup> <sup>c</sup>Beck.<sup>115</sup>



**Figure 17** Pauling bond orders<sup>118</sup> based on structural data of E<sub>8</sub><sup>2+</sup> (E = S,<sup>100</sup> Se,<sup>106</sup> Te<sup>119</sup>).



**Figure 18** The Te<sub>8</sub><sup>2+</sup> cation in (a) (Te<sub>8</sub>)[WCl<sub>6</sub>]<sub>2</sub><sup>106</sup> and (b) (Te<sub>6</sub>)(Te<sub>8</sub>)[WCl<sub>6</sub>]<sub>4</sub>.<sup>5</sup>

selenium and <sup>77</sup>Se-isotope-enriched selenium in the preparation of the sample and provided for full <sup>77</sup>Se–<sup>77</sup>Se coupling information.<sup>121,122</sup> The ZORA NMR calculations of the <sup>77</sup>Se chemical shifts using the rPBE GGA functional and a large QZAP basis set and involving explicit solvent molecules<sup>122</sup> agreed with the observed spectroscopic data but led to a slightly modified assignment of the resonances.

### 1.07.3.1.5 E<sub>n</sub><sup>2+</sup> (n > 8)

Both selenium and tellurium show a number of higher nuclearity polyatomic cations. The crystal structure of Se<sub>10</sub><sup>2+</sup> has been elucidated from several salts.<sup>123–125</sup> The cation is isostructural with Te<sub>2</sub>Se<sub>8</sub><sup>2+</sup><sup>116,126</sup> (see **Figure 21**).

The structure of this 58-electron cation can be derived from one of the alternative classical ten-atom 50-electron cages (**Scheme 3**).<sup>111</sup>

The structure and geometry of Se<sub>10</sub><sup>2+</sup> have been explored by DFT methods involving the PBE0 functional and the cc-pVTZ basis set.<sup>122</sup> The experimental bond parameters could be reproduced well by the computations. The structural features have been discussed in terms of 4p<sup>2</sup> → σ\* and 4p<sup>2</sup> → 4p<sup>2</sup> interactions within the cation.<sup>4</sup>

It has been shown by <sup>77</sup>Se NMR spectroscopy that in SO<sub>2</sub> solution Se<sub>10</sub><sup>2+</sup> is fluxional undergoing a complicated exchange process even at low temperature.<sup>121</sup> Consequently, only two resonances are observed even using the <sup>77</sup>Se-enriched selenium with relative intensities varying as a function of temperature. It was also concluded on the basis of significant differences between the electronic spectra in the solid (Se<sub>10</sub>)[AsF<sub>6</sub>]<sub>2</sub> and that recorded for the dissolved material that Se<sub>10</sub><sup>2+</sup> does not retain its solid-state structure in solution.<sup>121</sup>

The largest known discrete selenium cation, Se<sub>17</sub><sup>2+</sup><sup>127,128</sup>, consists of two seven-membered rings with similar conformations as in S<sub>7</sub> ring molecules.<sup>58,59</sup> The ring fragments are linked together by a Se<sub>3</sub> bridge (see **Figure 22(a)**). There is expectedly marked bond length alternation in this dication. The bonds from the two three-coordinate selenium atoms are long and the adjacent bonds are short. Normal single bond lengths are observed only for bonds further removed from the three-coordinate selenium. This bond length alternation can again be explained by charge delocalization through the 4p<sup>2</sup> → σ\* interactions involving the p lone pair of electrons of the selenium atoms bound to the three-coordinate selenium (see **Figure 22(b)**).

Two polymeric forms of (Te<sub>8</sub>)<sub>n</sub><sup>2+</sup> have been synthesized and characterized. They both contain six-membered rings in a boat conformation that are linked together by Te<sub>2</sub> fragments in 1,4-positions.<sup>129,130</sup> The main difference between the two isomers is the relative orientations of adjacent ring fragments (see **Figure 23(a)** and **23(b)**).

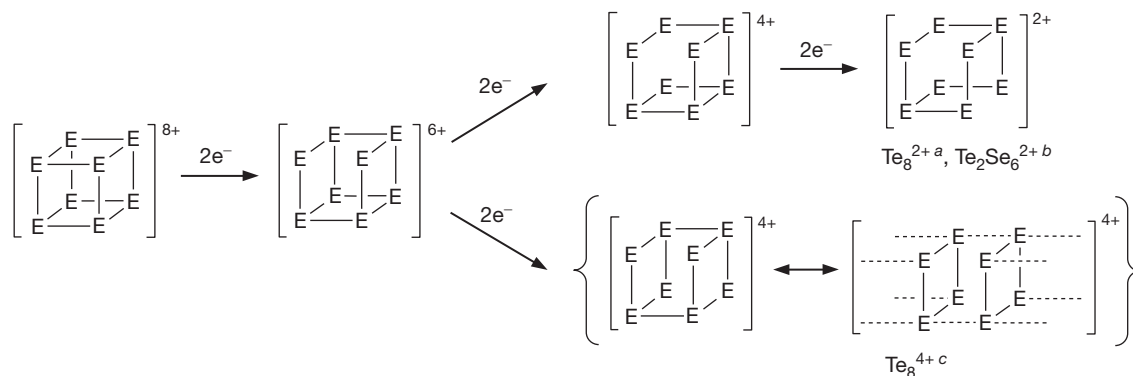
Other polymeric homonuclear tellurium cations have also been recently prepared, as shown in **Figure 24**. They are all based on repeating (Te<sub>7</sub>)<sub>n</sub><sup>2+</sup> units.

## 1.07.3.2 Polyatomic Selenium–Halogen and Tellurium–Halogen Cations

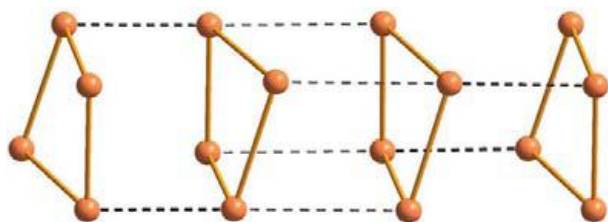
### 1.07.3.2.1 General

In addition to the chemistry of polyselenium and polytellurium cations, the recent decades have also seen rapid development in that of chalcogen–halogen cations.<sup>12</sup> In particular, selenium–iodine cations have grown from nonexistence to show a rich variety of species.<sup>12,133,134</sup> The species for which the structure in the solid state is known are listed in **Table 4**. Only those cations, which have chalcogen–chalcogen bonds, are shown.

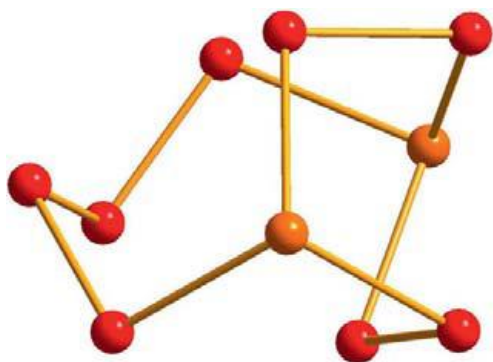
Many chalcogen–halogen cations may be prepared by the reaction of elemental chalcogen and halogen in appropriate molar ratios with AsF<sub>5</sub> or other suitable strong Lewis acids in SO<sub>2</sub>.<sup>12,122,134</sup> In some cases, other synthetic routes have also been successfully realized. (Se<sub>2</sub>I<sub>4</sub>)[Sb<sub>2</sub>F<sub>11</sub>], (Se<sub>3</sub>X<sub>3</sub>)[MF<sub>6</sub>] (M = As, Sb, X = Cl, Br), and (Se<sub>9</sub>Cl)[SbCl<sub>6</sub>] are prepared by the reaction of elemental selenium with (I<sub>2</sub>)[Sb<sub>2</sub>F<sub>11</sub>],<sup>135</sup> (SeCl<sub>3</sub>)



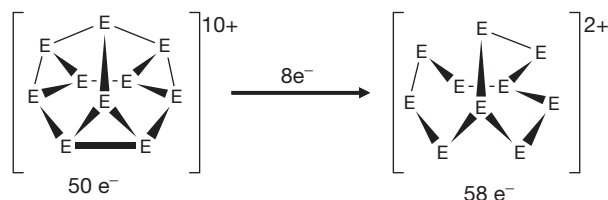
**Figure 19** Structural relationships between the classic 40 electron cube and cations derived from it. <sup>a</sup>Beck<sup>5</sup>. <sup>b</sup>Collins et al.<sup>116</sup>. <sup>c</sup>Beck and Bock.<sup>120</sup>



**Figure 20** Structure of the  $\text{Te}_8^{4+}$  cation in  $(\text{Te}_8)[\text{VOCl}_4]_2$ .<sup>108</sup>



**Figure 21** The structure of the  $\text{Te}_2\text{Se}_8^{2+}$  cation in  $(\text{Te}_2\text{Se}_8)[\text{AsF}_6]_2 \cdot \text{SO}_2$ .<sup>126</sup> Selenium atoms are depicted in red and tellurium in orange.



**Scheme 3** Derivation of the structure of  $\text{E}_{10}^{2+}$  from a classical  $\text{E}_{10}^{8+}$  cluster.

$[\text{MF}_6]$ ,<sup>134</sup> and  $(\text{NO})[\text{SbCl}_6]$  in  $\text{SO}_2$ ,<sup>136</sup> respectively.  $(\text{Se}_4\text{I}_4)[\text{AsF}_6]$  can be made by treating  $(\text{Se}_4)[\text{AsF}_6]$  with iodine,<sup>137</sup> and  $[\text{Te}_{15}\text{X}_4]_n[\text{MOX}_4]_{2n}$  ( $\text{M}=\text{Mo}, \text{W}$ ;  $\text{X}=\text{Cl}, \text{Br}$ ) by the reactions of  $\text{Te}_2\text{Br}$  with  $\text{MoOBr}_3$ ,  $\text{TeCl}_4$  with  $\text{MoNCl}_2/\text{MoOCl}_3$ , and  $\text{Te}$  with  $\text{WBr}_5/\text{WOBr}$ .<sup>138</sup>

### 1.07.3.2.2 Selenium–chlorine and selenium–bromine cations

The structure of  $\text{Se}_3\text{X}_3^+$  ( $\text{X}=\text{Cl}, \text{Br}$ ) is exemplified by  $\text{Se}_3\text{Cl}_3^+$  in **Figure 25(a)** and that of  $\text{Se}_3\text{Br}_3^+$  is shown in **Figure 25(b)**. Both cations show marked bond length alternation. Klapötke and Passmore have discussed the bond length alternation in terms of maximized intracationic  $\text{X} \cdots \text{Se}$  contacts, charge delocalization, and  $\pi$  bonding.<sup>12</sup>

In contrast to the discrete selenium–halogen cations, tellurium–chlorine and tellurium–bromine cations  $(\text{Te}_{15}\text{X}_4)^{n+}$  show polymeric structures that are related with that of the tellurium subhalide  $\text{Te}_2\text{Br}$ .<sup>138</sup> The crystal structure, however, is disordered with one tellurium atom showing the site occupation factor of only 0.75.

A preliminary natural-abundance <sup>77</sup>Se NMR study of the soluble products of the reaction of  $(\text{Se}_4)[\text{AsF}_6]_2$  and bromine in liquid  $\text{SO}_2$  exhibited resonances attributable to 1,1,4,4- $\text{Se}_4\text{Br}_4^{2+}$  and  $\text{Se}_7\text{Br}^+$ . These assignments are supported by calculated <sup>77</sup>Se chemical shifts.<sup>122</sup>

### 1.07.3.2.3 Selenium–iodine and tellurium–iodine cations

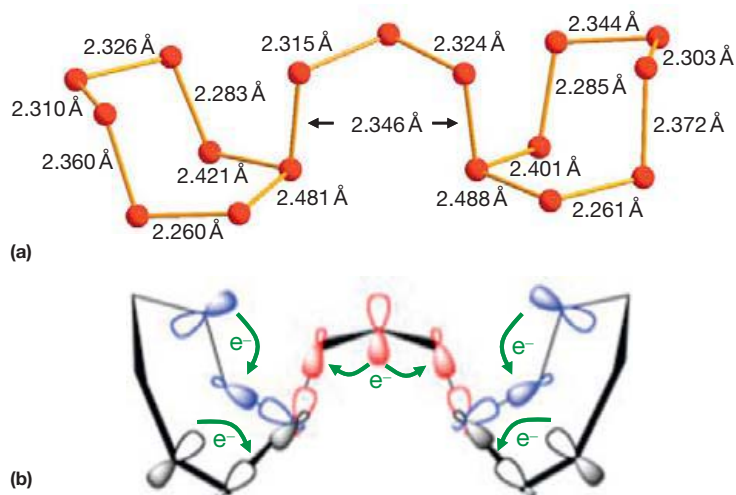
#### 1.07.3.2.3.1 $\text{Se}_2\text{I}_4^{2+}$

The structures and conformations of  $\text{Se}_2\text{I}_4^{2+}$  and  $\text{S}_2\text{I}_4^{2+}$  resemble each other, but there are key differences in interatomic distances that also reflect the differences in their bonding (see **Figure 26**).

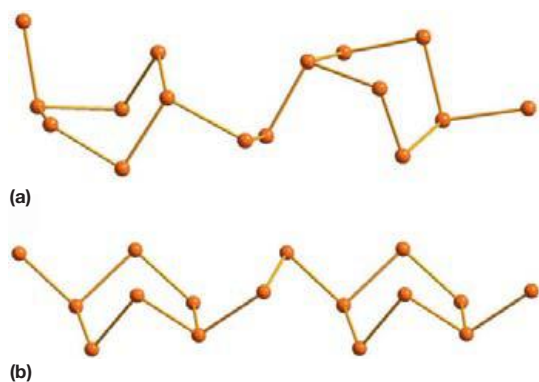
The bonding in  $\text{S}_2\text{I}_4^{2+}$  can be described in terms of mutually perpendicular  $4c-2e \pi^*-\pi^*$  bonds,<sup>140-142</sup> whereas that in  $\text{Se}_4\text{I}_4^{2+}$  consists of two  $\text{SeI}_2^+$  fragments joined by  $6c-2e \pi^*-\pi^*$  bonds<sup>140,142</sup> (see **Figure 27**). Recently, Brownridge et al.<sup>142</sup> have reported a detailed analysis to account for the structural differences. These factors are summarized in **Figure 27** and are related to the strong S–S  $\pi$  bond compared to the weak S–I  $\sigma$  bond and the additional stabilization from increased delocalization of the positive charge in  $\text{S}_2\text{I}_4^{2+}$  that is missing in  $\text{Se}_2\text{I}_4^{2+}$ .

#### 1.07.3.2.3.2 $\text{E}_6\text{I}_2^{2+}$ ( $\text{E}=\text{Se}, \text{Te}$ )

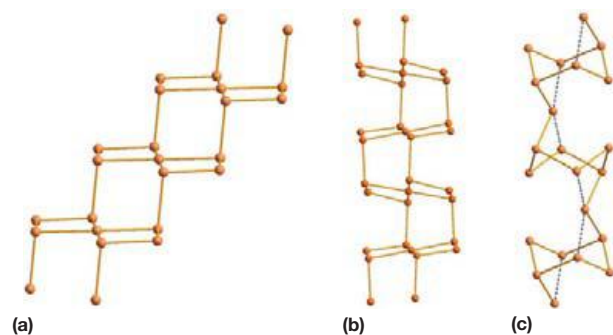
The structures of  $\text{Se}_6\text{I}_2^{2+}$  and  $\text{Te}_6\text{I}_2^{2+}$  are expectedly similar<sup>143,107</sup> and can be described as distorted cubes (see **Figure 28**). In a similar fashion to other polychalcogen cations, the positive charge of the three-coordinate chalcogen atom is delocalized and leads to bond length alternation. The relevant orbital interactions are shown in **Figure 28(b)**.



**Figure 22** (a) The structure of the  $\text{Se}_{17}^{2+}$  cation in  $(\text{Se}_{17})[\text{WCl}_6]_2$  indicating the Se–Se bond lengths.<sup>127,128</sup> (b)  $4p^2 \rightarrow \sigma^*$  interactions rationalizing the bond length alternations (for more details, see Brownridge et al.<sup>4</sup>).



**Figure 23** The structures of  $(\text{Te}_8^{2+})_n$  in (a)  $(\text{Te}_8)[\text{Bi}_4\text{Cl}_{14}]$ <sup>129</sup> and (b)  $(\text{Te}_8)[\text{U}_2\text{Br}_{10}]$ .<sup>130</sup>



**Figure 24** The structure of  $(\text{Te}_7^{2+})_n$  in (a)  $(\text{Te}_7)[\text{Be}_2\text{Cl}_6]$ ,<sup>104</sup> (b)  $(\text{Te}_7)[\text{NbOCl}_4]\text{Cl}$ ,<sup>131</sup> and (c)  $(\text{Te}_7)[\text{AsF}_6]_2$ .<sup>132</sup>

A related polymeric cation  $(\text{Se}_6\text{I})_n^{n+}$  has been isolated as a hexafluoroarsenate salt and its crystal structure has been determined.<sup>144</sup> The six-membered  $\text{Se}_6$  ring is in the chair conformation like in  $\text{Se}_6\text{I}_2^{2+}$  (see Figure 28(a)). Two bridging iodine atoms in 1,4-positions link the rings into a polymeric zigzag chain.

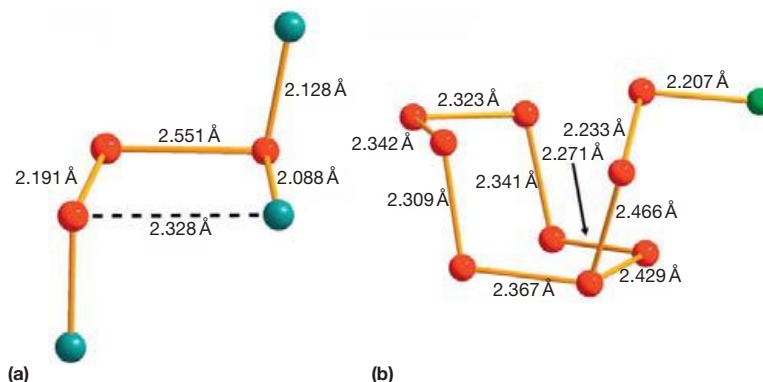
When solid  $(\text{Se}_6\text{I}_2)_2[\text{AsF}_6]_2 \cdot 2\text{SO}_2$  is dissolved into liquid  $\text{SO}_2$ , a complicated equilibrium is set up.<sup>122</sup> The composition

**Table 4** Polychalcogen selenium- and tellurium-halogen cations that have been structurally characterized by x-ray diffraction

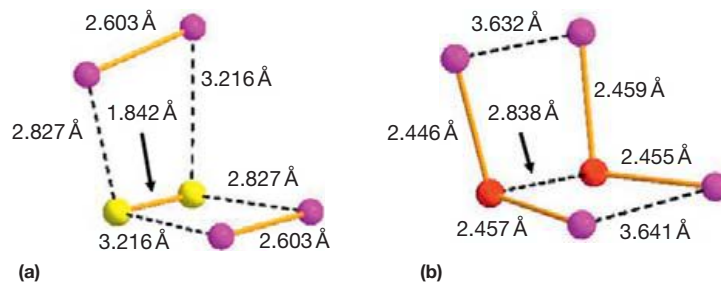
	<i>Cl</i>	<i>Br</i>	<i>I</i>
Se	$\text{Se}_3\text{Cl}_3^+$ , $\text{Se}_9\text{Cl}^+$	$\text{Se}_3\text{Br}_3^+$	$\text{Se}_2\text{I}_2^{2+}$ , $\text{Se}_4\text{I}_4^{2+}$ , $(\text{Se}_6\text{I})_n^{n+}$ , $\text{Se}_6\text{I}_2^{2+}$
Te	$(\text{Te}_{15}\text{Cl}_4)_n^{2n+}$	$(\text{Te}_{15}\text{Br}_4)_n^{2n+}$	$\text{Te}_6\text{I}_2^{2+}$

of the equilibrium mixture was studied by  $^{77}\text{Se}$  NMR spectroscopy at  $-70^\circ\text{C}$  using both natural-abundance and enriched  $^{77}\text{Se}$ -isotope samples (enrichment 92%). Some of the resonances in Figure 29 were due to known species ( $\text{Se}_6\text{I}_2^{2+}$ ,  $\text{Se}_4\text{I}_4^{2+}$ , and  $\text{SeI}_3^+$ ,<sup>112,137</sup>  $\text{Se}_4^{2+}$ ,<sup>102,145</sup> as well as  $\text{Se}_8^{2+}$  and  $\text{Se}_{10}^{2+}$ <sup>121</sup>). The unknown 22 resonances were assigned on the basis of homonuclear  $^{77}\text{Se}$ - $^{77}\text{Se}$  COSY NMR spectrum, selective irradiation experiments, and spectral simulation.<sup>121</sup> Because the  $^{77}\text{Se}$ -enrichment is 92%, several isotopomers of a given cation have a significant abundance and need to be considered in the simulation. This is exemplified for  $\text{Se}_6\text{I}_2^{2+}$  in Figure 30.

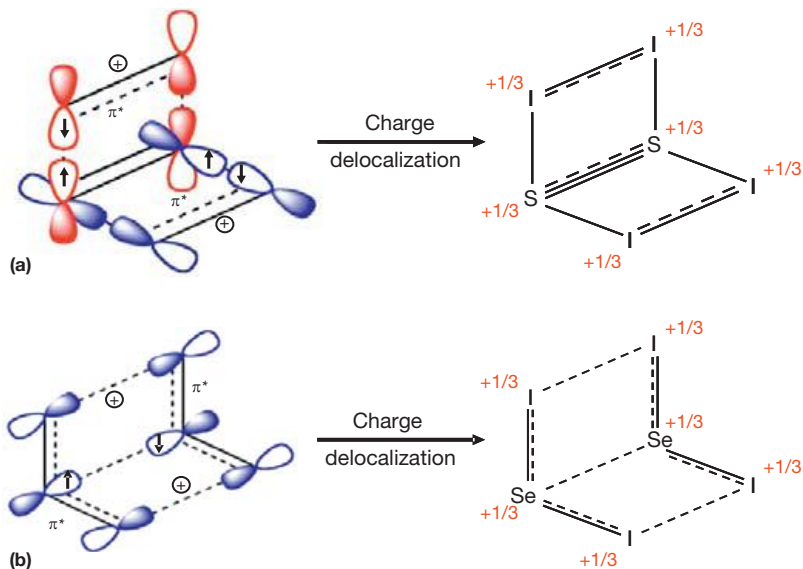
It was inferred that the 22 resonances are due to five cationic species, and the simulations provided for their spin systems. This information was combined with the trends in the chemical shifts, with iodine, selenium, and charge balances, as well as with ZORA chemical shift predictions, which employ the rPBE GGA functional and large QZ4P basis sets, an implicit conductor-like screening model, and a small number of explicit solvent molecules to include solvent effects.<sup>122</sup> All information available is consistent with the assignment of the unknown resonances to acyclic 1,1,2- $\text{Se}_2\text{I}_3^+$ , 1,1,6,6- $\text{Se}_6\text{I}_4^{2+}$ , and 1,1,6- $\text{Se}_6\text{I}_3^+$ , as well as to cyclic  $\text{Se}_7\text{I}^+$  and  $(4\text{-Se}_7\text{I})_2\text{I}^{3+}$  (see Figure 31). It is interesting to note that upon evaporation of the  $\text{SO}_2$  from solution, the solid material contains only  $(\text{Se}_6\text{I}_2)[\text{AsF}_6]_2 \cdot 2\text{SO}_2$  indicating that the dissociation of  $\text{Se}_6\text{I}_2^{2+}$  is reversible.<sup>122</sup> Volume-based thermodynamics calculations show that nonsolvated  $(\text{Se}_6\text{I}_2)[\text{AsF}_6]_2$  is not thermodynamically stable, disproportionating to  $(\text{Se}_4\text{I}_4)[\text{AsF}_6]_2(\text{s})$  and  $(\text{Se}_8)[\text{AsF}_6]_2(\text{s})$  (estimated  $\Delta G^\circ = -17 \pm 15 \text{ kJ mol}^{-1}$  at 298 K).<sup>122</sup>



**Figure 25** The structures of the cations in (a)  $(\text{Se}_3\text{X}_3)[\text{MF}_6]$  ( $\text{X} = \text{Cl}, \text{Br}; \text{M} = \text{As}, \text{Sb}$ ) as exemplified by  $\text{Se}_3\text{Cl}_3^+$ <sup>134</sup> and (b)  $(\text{Se}_9\text{Cl})[\text{SbCl}_6]^+$ .<sup>136</sup> Selenium atoms are depicted in red, chlorine in green, and Cl/Br atoms in turquoise.



**Figure 26** The structure of the cation in (a)  $(\text{S}_2\text{I}_4)[\text{AsF}_6]^+$ <sup>139</sup> and (b)  $(\text{Se}_2\text{I}_4)[\text{AsF}_6]^+\cdot\text{SO}_2$ .<sup>140</sup> Sulfur atoms are depicted in yellow, selenium in red, and iodine in violet.



**Figure 27** (a)  $\text{S}_2\text{I}_4^{2+}$ : Interaction of  $\pi^*$  orbitals of  $\text{S}_2$  with those of two  $\text{I}_2^+$  in mutually perpendicular planes with subsequent charge delocalization. The bond orders: S–S 2.33; I–I 1.33.<sup>141,142</sup> (b)  $\text{Se}_2\text{I}_4^{2+}$ : Interaction of two  $\pi^*$   $\text{SeI}_2^+$  SOMOs with subsequent charge delocalization. The bond orders: Se–Se  $\ll 1$ , Se–I 1.25.<sup>140,142</sup>

### 1.07.3.3 Anions

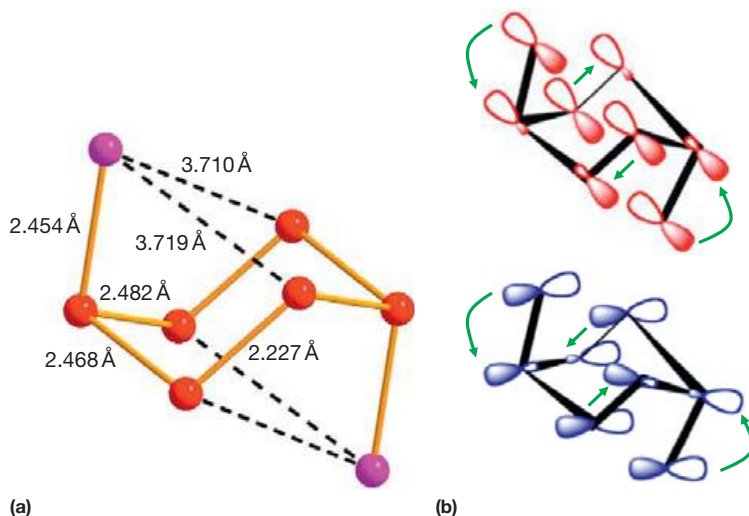
#### 1.07.3.3.1 General

Polyselenide and polytelluride anions show a rich and diverse structural chemistry that is both similar to and different from the related polysulfides. In addition to acyclic polychalcogenides, both selenium and tellurium also form polycyclic species. Their synthetic and structural chemistry as well as ligand

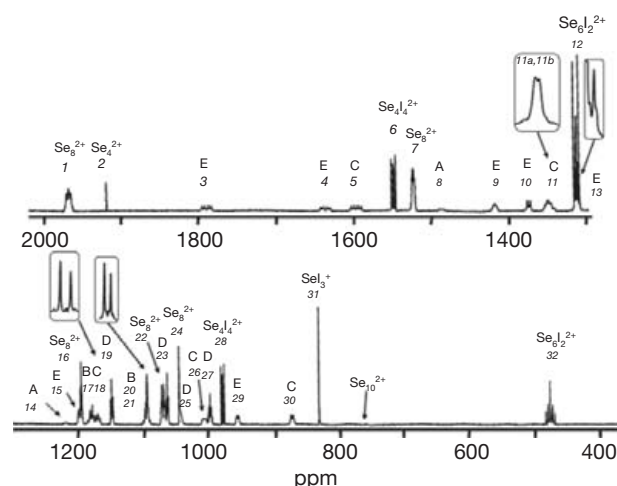
properties and applications have recently been reviewed several times (for some recent reviews, see Graf et al., 2009,<sup>6</sup> Sheldrick, 2007,<sup>146</sup> and Smith and Ibers, 2000<sup>147</sup>).

The usual preparation of the materials involves direct high-temperature combination of the elements, solution reactions involving chalcogen elements and alkali metal carbonates, solvothermal reactions, or oxidation–reduction reactions with





**Figure 28** (a) The crystal structure of the  $\text{Se}_6\text{I}_2^{2+}$  cation in  $(\text{Se}_6\text{I}_2)[\text{AsF}_6]_2 \cdot 2\text{SO}_2$ .<sup>143</sup> The  $\text{Te}_6\text{I}_2^{2+}$  cation in  $(\text{Te}_6\text{I}_2)[\text{WCl}_6]_2$ <sup>107</sup> shows a similar conformation and similar bond length alternation. Selenium atoms are depicted in red and iodine in violet. (b) The bond length alternation can be explained by two parallel  $4p^2 \rightarrow \sigma^*$  electron transfers.<sup>122</sup>



**Figure 29** The  $^{77}\text{Se}$  NMR spectrum of the  $\text{SO}_2(\text{l})$  solution of the dissociation equilibrium of  $\text{Se}_6\text{I}_2^{2+}$  at  $-70^\circ\text{C}$  using selenium enriched in the  $^{77}\text{Se}$ -isotope (enrichment 92%).<sup>122</sup> The insets represent portions of the spectrum recorded for the natural-abundance sample. Reprinted (adapted) from Brownridge, S.; Calhoun, L.; Jenkins, H. D. B.; Laitinen, R. S.; Murchie, M. P.; Passmore, J.; Pietikäinen, J.; Rautiainen, J. M.; Sanders, J. C. P.; Schrobilgen, G. J.; Suontamo, R. J.; Tuononen, H. M.; Valkonen, J. U.; Wong, C.-M. *Inorg. Chem.* **2009**, *48*, 1938-1959, with permission. Copyright 2009 American Chemical Society.

Lewis acids.<sup>148,149</sup> These methods have mostly been applied to alkali metal or alkaline earth metal selenides and tellurides that can then serve as precursors to other chalcogenides. The presence of a large organic cation or the encapsulating agent such as the crown ether complex of an alkali metal leads to the stabilization of otherwise unstable anions.

Tellurium shows more diverse polyanion chemistry than sulfur and selenium due to increasing importance of hyperconjugation and secondary bonding, when going down group 16 (see Sheldrick, 2007<sup>146</sup> and Kanatzidis, 1999,<sup>148</sup> and

references therein). In contrast to polysulfides and polyselenides, polytelluride anions can exhibit charges that deviate from  $-2$ .

#### 1.07.3.3.2 Acyclic polyselenides and polytellurides

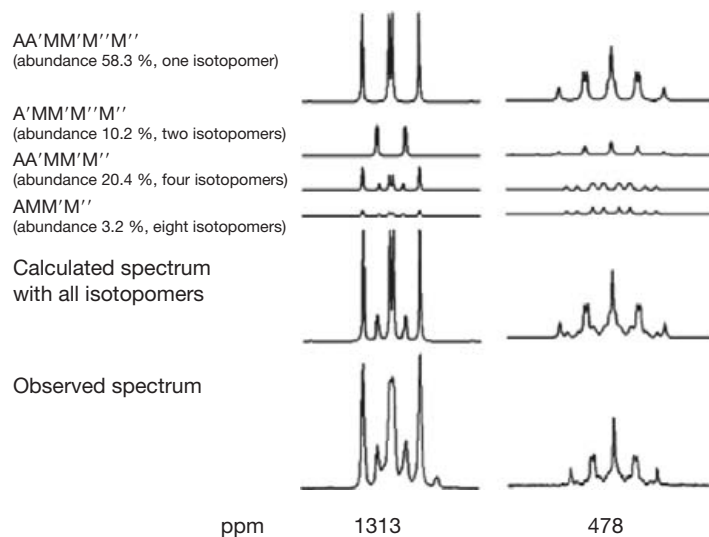
The x-ray structures have been determined for several acyclic polyselenides and -tellurides  $\text{E}_n^{2-}$  ( $n=2-9$  for selenium and 2-6, 8, 12, 13 for tellurium). Shorter polychalcogenides occur as binary alkali metal or alkaline earth metal salts, but longer chains require bulkier counterions for stabilization.<sup>146</sup> These may comprise alkali or alkaline earth metals encapsulated with crown ethers or cryptates, or large noncoordinating monocations such as  $\text{Et}_4\text{N}^+$ ,  $\text{Ph}_4\text{P}^+$ , and  $[\text{Ph}_3\text{PNPPH}_3]^+$ . Typical structures of the open-chain polyselenides  $\text{Se}_3^{2-} - \text{Se}_9^{2-}$  are shown in Figure 32. Discrete polytelluride anions show similar structures. Since the monoatomic counterions have a significant effect on the bond parameters of the polychalcogenides, the examples in Figure 32 have been selected from salts containing bulky polyatomic cations.

The conformations of the polyselenide and polytelluride chains vary depending on the counterions.<sup>6,146-149</sup> In addition to changes in the numerical values of torsional angles, there is a possibility for isomerism in the case of  $\text{E}_n^{2-}$  chains with  $n \geq 5$  depending on the signs of the torsional angle. Longer chain polyselenides and -tellurides, however, tend to adopt helical conformations to mimic the hexagonal polymeric chains of the stable allotropic form of the elements,<sup>20,21</sup> as can be seen in Figure 32.

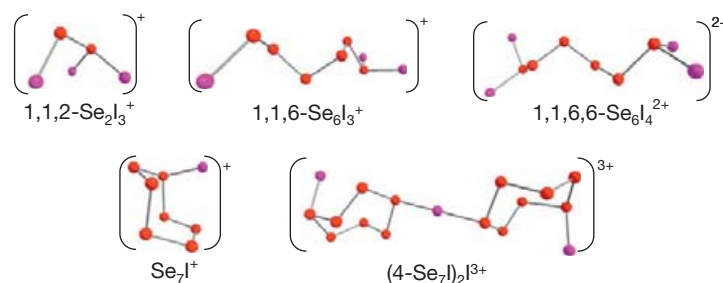
Dodecatelluride  $\text{Te}_{12}^{2-}$ <sup>158</sup> and tridecatelluride  $\text{Te}_{13}^{2-}$ <sup>159</sup> anions are the longest reported acyclic polyselenides and -tellurides. The structure of the latter is shown in Figure 33.

#### 1.07.3.3.3 Cyclic polyselenides and polytellurides

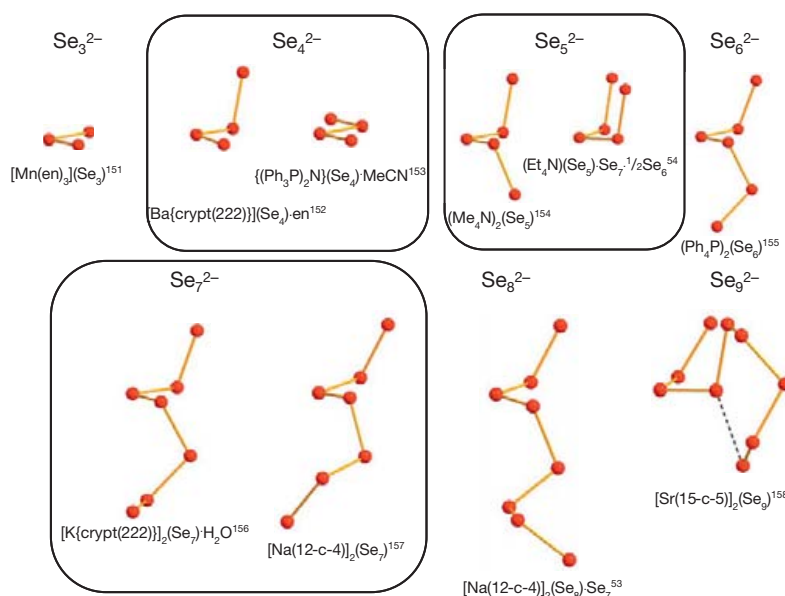
Sheldrick<sup>146</sup> has noted that the importance of hypervalent 3c-4e bonding increases when going down group 16. While  $\text{Se}_9^{2-}$  can be regarded as having an open-chain structure (see Figure 32),<sup>157</sup> it has a short intrachain contact of 2.953 Å that indicates an incipient tendency toward ring formation. A



**Figure 30** The simulated and observed  $^{77}\text{Se}$  NMR chemical shifts of  $\text{Se}_6\text{I}_2^{2+}$  using a sample prepared from selenium enriched in the  $^{77}\text{Se}$ -isotope (enrichment 92%).<sup>122</sup> The observed resonance at 1313 ppm overlaps a resonance due to another cationic species. Reprinted (adapted) from Brownridge, S.; Calhoun, L.; Jenkins, H. D. B.; Laitinen, R. S.; Murchie, M. P.; Passmore, J.; Pietikäinen, J.; Rautiainen, J. M.; Sanders, J. C. P.; Schrobilgen, G. J.; Suontamo, R. J.; Tuononen, H. M.; Valkonen, J. U.; Wong, C.-M. *Inorg. Chem.* **2009**, *48*, 1938-1959, with permission. Copyright 2009 American Chemical Society.



**Figure 31** The species assigned to the 22  $^{77}\text{Se}$  NMR resonances observed from dissociation of  $\text{Se}_6\text{I}_2^{2+}$  in  $\text{SO}_2(\text{l})$  solution.<sup>122</sup> Selenium atoms are depicted in red and iodine in violet.



**Figure 32** Structures of selected acyclic polyselenides containing weakly coordinating counter-cations [12-c-4 = 12-crown-4; 15-c-5 = 15-crown-5].

similar, though stronger, transannular distance (2.460 Å) is observed in a nominally bicyclic  $\text{Se}_{10}^{2-160}$  (see Figure 34). Other cyclic polyselenide anions comprise  $\text{Se}_{11}^{2-54}$  and  $\text{Se}_{16}^{4-161}$  and are also shown in Figure 34 together with two known spirocyclic polytellurides.  $\text{Te}_7^{2-}$  has been isolated as a  $[\text{Re}_6\text{Te}_8](\text{Te}_7)$  salt<sup>162</sup> and  $\text{Te}_8^{2-}$  has been characterized in  $[\text{K}(15\text{-crown-5})_2]_2(\text{Te}_8)$ .<sup>163</sup>

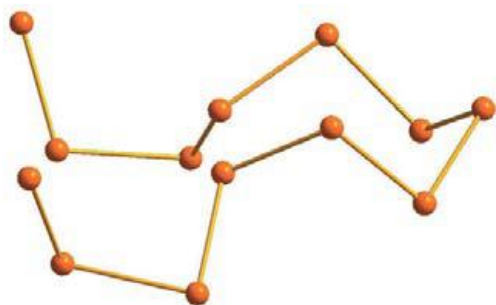


Figure 33 The molecular structure of  $\text{Te}_{13}^{2-159}$ .

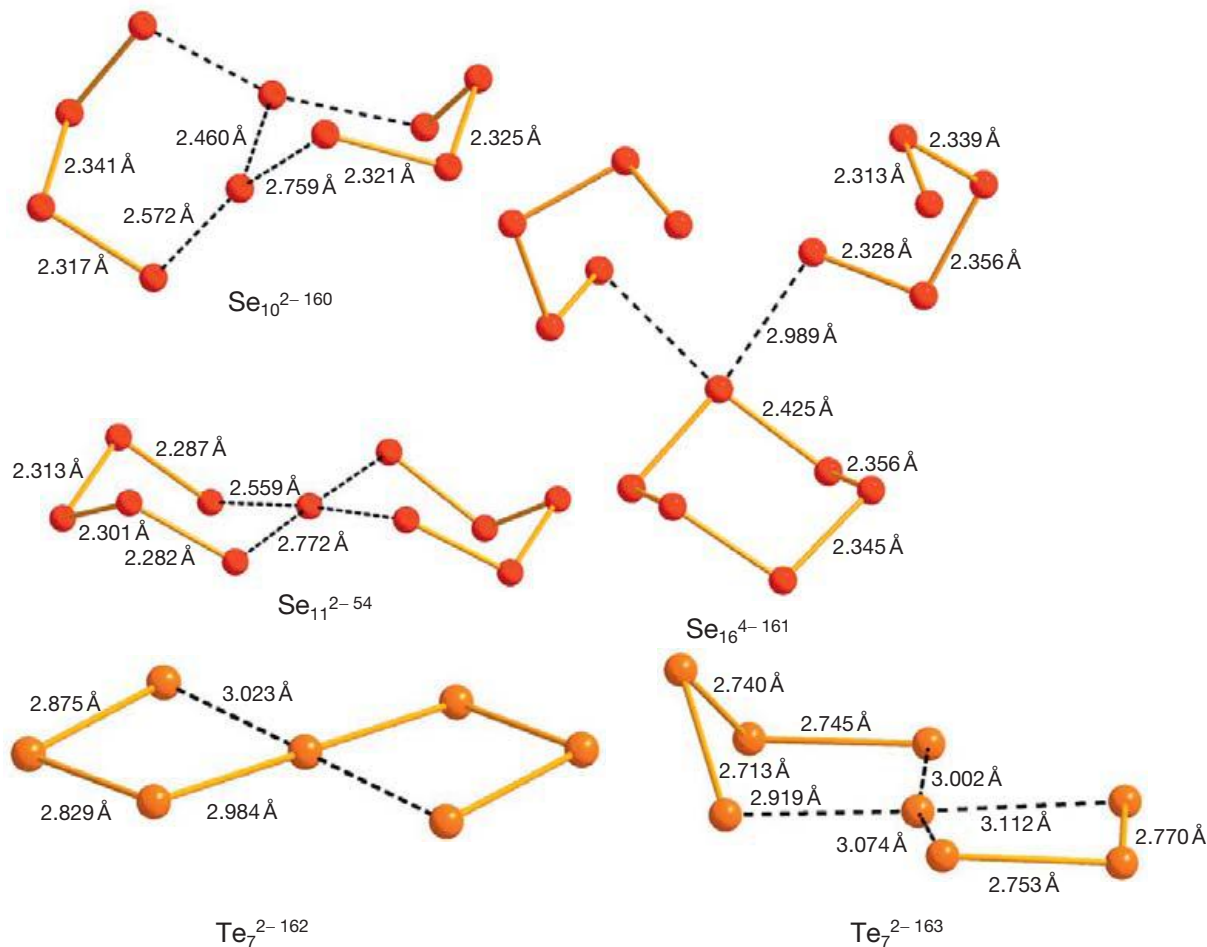
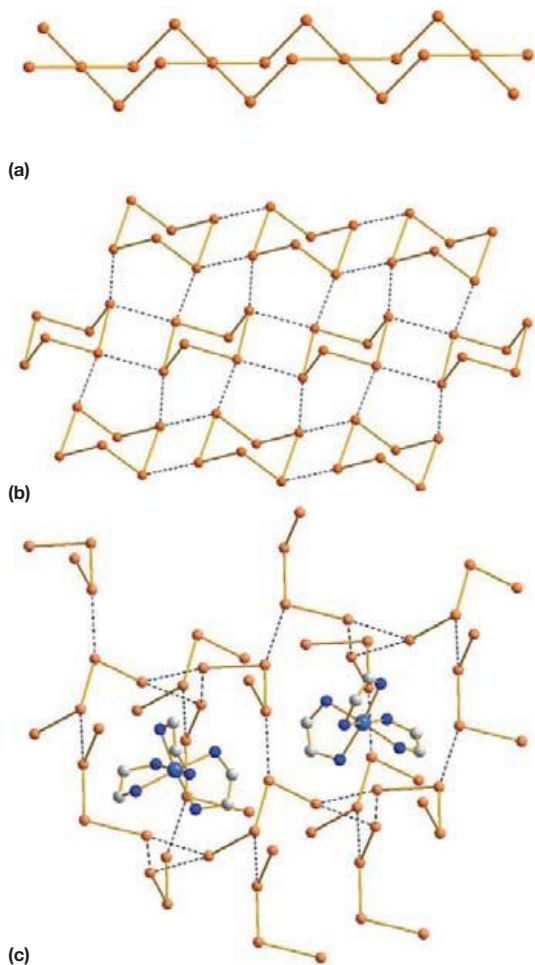


Figure 34 Examples of cyclic polyselenide and polytelluride anions.

#### 1.07.3.3.4 Extended polytelluride networks

The propensity of polychalcogenide anions to form extended structures increases down group 16. Polysulfides are discrete acyclic  $\text{S}_n^{2-}$  anions, polyselenides show only a few structures with an extended anionic network, as exemplified by  $\text{Cs}_3\text{Se}_{16}$ ,<sup>66</sup> but polytellurides exhibit rich structural variety that obscures the deceptively simple stoichiometry of the polytelluride salts. Sheldrick<sup>146</sup> has summarized the structural and bonding features in polytellurides, which can contain classical bent  $\text{TeTe}_2^{2-}$ , linear  $\text{TeTe}_2^{4-}$ , T-shaped  $\text{TeTe}_3^{4-}$ , and square-planar  $\text{TeTe}_4^{6-}$  units involving 3c–4e bonds of formal bond order of 0.5. In addition, the fragments can be linked together by weak secondary  $\text{Te}\cdots\text{Te}$  bonds.<sup>19</sup> These interactions result in the formation of 1D, 2D, and 3D networks, as exemplified in Figure 35.

$\text{Rb}_2\text{Te}_5$  exhibits a continuous spirocyclic chain  $(\text{Te}_3)_n^{2-164}$  that can be thought to consist of square-planar  $\text{TeTe}_4$  units stacked together (see Figure 35(a)). The charge of the polytellurides can deviate from  $-2$ . This is exemplified by  $\text{RbTe}_6$ <sup>165</sup> that is shown in Figure 35(b). It consists of  $\text{Te}_6$  rings that are linked together into a 2D network by two pairs of  $\text{Te}\cdots\text{Te}$  contacts. Interestingly,  $[\text{Cr}(\text{en})_3]\text{Te}_6$  has been reported to contain a polymeric  $\text{Te}_6^{3-}$  anion.<sup>166</sup> Considering the  $\text{Te}\text{--}\text{Te}$



**Figure 35** The structures of (a)  $(\text{Te}_5)_n^{2-}$  in  $\text{Rb}_2\text{Te}_5$ ,<sup>164</sup> (b)  $(\text{Te}_6)_n^-$  in  $\text{RbTe}_6$ ,<sup>165</sup> and (c)  $[\text{Cr}(\text{en})_3]_2(\text{Te}_4)_3$ .<sup>166</sup>

distances in the 3D network of the anion, the formula of the complex is best described as  $[\text{Cr}(\text{en})_3]_2(\text{Te}_4)_3$  in which case each tetratelluride carries the charge  $-2$  (see **Figure 35(c)**).

Particularly interesting structures of  $\text{Cs}_3\text{Te}_{22}$ <sup>64</sup> and  $\text{Cs}_4\text{Te}_{28}$ <sup>65</sup> have been discussed above (see **Section 1.07.2.2.4**).

## 1.07.4 Catenated Main Group Polyselenides and -tellurides

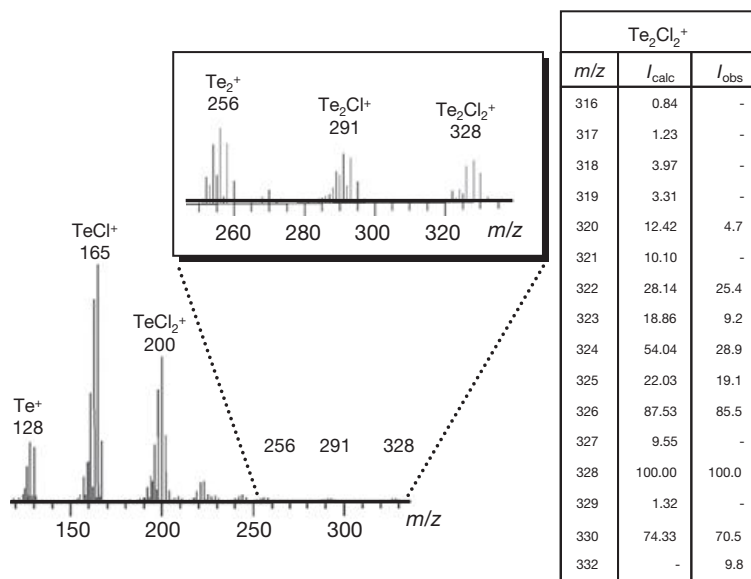
### 1.07.4.1 Selenium and Tellurium Halogenides

Diselenium dichlorides and dibromides are a well-characterized class of reagents, the structures of which have been known for a long time.<sup>167,168</sup> They are dark brown liquids that undergo facile disproportionation into a small amount of  $\text{SeX}_2$  and  $\text{Se}_n\text{X}_2$  ( $n=3, 4$ ).<sup>169</sup> The interconversion reaction of a mixture of  $\text{Se}_2\text{Cl}_2$  and  $\text{Se}_2\text{Br}_2$  affords  $\text{Se}_2\text{ClBr}$ .<sup>169</sup> In a similar fashion, a mixture of  $\text{Se}_2\text{Cl}_2$  and  $\text{S}_2\text{Cl}_2$  yields an equilibrium mixture containing  $\text{SeSCl}_2$ .<sup>170,171</sup>

Both  $\text{Se}_2\text{Cl}_2$  and  $\text{Se}_2\text{Br}_2$  are open-chain X–Se–Se–X compounds in a gauche conformation (the torsional angles are  $87.43^\circ$  and  $85.00^\circ$ , respectively).<sup>167</sup> They are useful reagents in a number of synthetic applications.

Ditellurium dichloride  $\text{Te}_2\text{Cl}_2$  and dibromide  $\text{Te}_2\text{Br}_2$  can be prepared in moderate yields by reducing elemental tellurium with  $\text{LiBHET}_3$  in tetrahydrofuran (THF) with a subsequent treatment with  $\text{TeX}_4$  ( $X=\text{Cl}, \text{Br}$ ).<sup>62</sup> Both are dark brown liquids that decompose rapidly. In  $\text{CS}_2$  solution, they, however, are rather stable. The molecular species were identified by electron impact mass spectroscopy (see **Figure 36**). The reaction of  $\text{Te}_2\text{Cl}_2$  and  $[\text{TiCp}_2\text{S}_5]$  or  $[\text{TiCp}_2\text{Se}_5]$  expectedly affords 1,2- $\text{Te}_2\text{S}_5$  and 1,2- $\text{Te}_2\text{Se}_5$ , respectively, which were identified by  $^{77}\text{Se}$  and  $^{125}\text{Te}$  NMR spectroscopy.<sup>62</sup>

Tellurium forms subhalides that do not find analogs with lighter chalcogen elements.<sup>172,173</sup> The main characterized



**Figure 36** EI mass spectrum of  $\text{Te}_2\text{Cl}_2$ . The fragmentation and their isotopic distributions indicate the expected composition of the species. Reproduced from Pietikäinen, J.; Laitinen, R.S. *J. Chem. Soc., Chem. Commun.* **1998**, 2381–2382, with permission of The Royal Society of Chemistry (RSC).



species are  $\text{Te}_3\text{Cl}_2$ ,  $\text{Te}_2\text{X}$  ( $\text{X}=\text{Cl}, \text{Br}, \text{I}$ ), and two polymorphs of  $\text{TeI}$ . The general method of preparation involves the heating of the elements at 200–300 °C with subsequent homogenization, annealing, quenching, and extraction to remove the excess tellurium tetrahalogenide.<sup>174–178</sup> Single crystals of  $\text{Te}_2\text{I}$ , and  $\alpha$ - and  $\beta$ - $\text{TeI}$  can be produced by hydrothermal methods in concentrated aqueous hydroiodic acid.<sup>176–178</sup> Crystals of stable  $\text{Te}_3\text{Cl}_2$ ,  $\text{Te}_2\text{Br}$ , and  $\alpha$ - $\text{TeI}$  can also be grown from the melt.<sup>173</sup> The reduction of tellurium tetrabromide and tetraiodide by the corresponding tin dihalogenide affords tellurium subbromides and -iodides.<sup>178,174</sup>

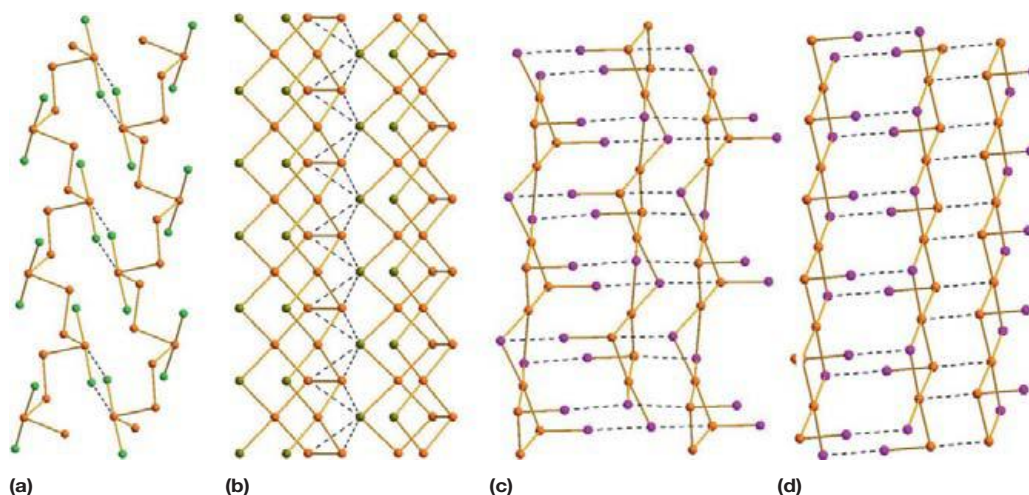
Kniep and Rabenau<sup>173</sup> and Xu<sup>12</sup> have noted the structural relationship between all subhalides and hexagonal tellurium.  $\text{Te}_3\text{Cl}_2$  contains a continuous twisted tellurium chain with every third tellurium atom bonded to two chlorine atoms in axial positions of the trigonal bipyramidal coordination environment (see **Figure 37(a)**).<sup>174</sup> The Te–Te bonds within the

chain are approximate single bonds. The chains are connected by secondary  $\text{Te}\cdots\text{Cl}$  contacts.<sup>174,178</sup>

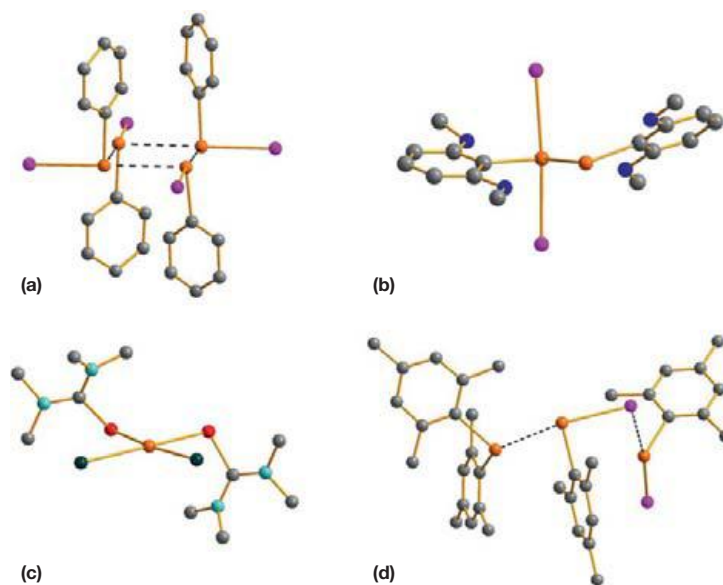
$\text{Te}_2\text{Cl}$ ,  $\text{Te}_2\text{Br}$ , and  $\text{Te}_2\text{I}$  show mutually similar structures containing fused  $\text{Te}_6$  rings in the boat conformation (see **Figure 37(b)**). The ring fragments are also connected together by two halogen bridges in 1- and 4-position.<sup>178,174</sup> The polymeric chains are linked together by very weak  $\text{Te}\cdots\text{Br}$  and  $\text{Te}\cdots\text{I}$  secondary bonds.

$\text{TeI}$  has two different polymorphs.  $\alpha$ - $\text{TeI}$  is composed of infinite chains of  $\text{Te}(\text{TeI})_2(\text{TeI}_2)$  units containing a slightly puckered four-membered  $\text{Te}_4$  ring (see **Figure 37(c)**).<sup>178</sup> One tellurium atom is bound to two iodine atoms that also exhibit the  $\text{Te}\cdots\text{I}$  secondary bonding contacts to the adjacent unit. Other  $\text{Te}\cdots\text{I}$  and  $\text{I}\cdots\text{I}$  secondary bonds also link adjacent  $[\text{Te}(\text{TeI})_2(\text{TeI}_2)]_n$  chains together.

$\beta$ - $\text{TeI}$  is a slightly different polymer, the structure of which is related to that of  $\text{Te}_2\text{X}$  (see **Figure 37(d)**).<sup>178</sup> It consists of

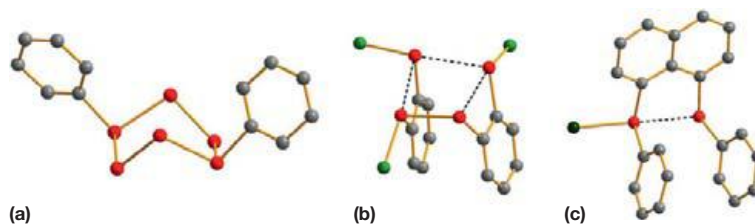


**Figure 37** (a) The structure of  $\text{Te}_3\text{Cl}_2$ ,<sup>174</sup> (b)  $\text{Te}_2\text{X}$  ( $\text{X}=\text{Cl}, \text{Br}, \text{I}$ ),<sup>174,178</sup> (c)  $\alpha$ - $\text{TeI}$ ,<sup>178</sup> and (d)  $\beta$ - $\text{TeI}$ .<sup>178</sup> Tellurium atoms are depicted in orange, chlorine in bright green, bromine in dark green, and iodine in violet.

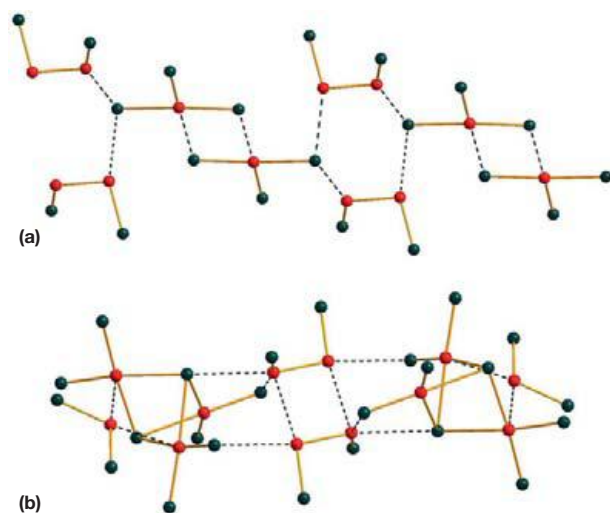


**Figure 38** The structures of (a)  $(\text{PhTeI})_4$ ,<sup>181</sup> (b)  $\{(\text{MeO})_2\text{C}_6\text{H}_3-2,6\}\text{TeI}_2\text{Te}\{\text{C}_6\text{H}_3(\text{OMe})_2-2,6\}$ ,<sup>183</sup> (c)  $\{(\text{Me}_2\text{N})_2\text{CSe}\}_2\text{TeCl}_2$ ,<sup>186</sup> and (d)  $(\text{mes})_2\text{TeTe}(\text{mes})$ .<sup>188</sup> Tellurium atoms are depicted in orange, selenium in red, oxygen in dark blue, nitrogen in light blue, and carbon in dark gray.





**Figure 39** The structures of the cations in (a)  $(\text{Se}_6\text{Ph}_2)[\text{AsF}_6]_2 \cdot \text{SO}_2$ ,<sup>190</sup> (b)  $(\text{C}_6\text{H}_4(\text{SeCl}))_2(\text{Se}_2\text{Cl})[\text{SbCl}_6]\text{MeCN}$ ,<sup>191</sup> and (c)  $((\text{C}_6\text{H}_5)_2(\text{C}_{10}\text{H}_6)\text{Se}_2\text{Br})$  ( $\text{Br}_3$ ).<sup>192</sup> Selenium atoms are depicted in red, chlorine in bright green, bromine in dark green, and carbon in dark gray.



**Figure 40** Structures of some extended polyselenium–halogen anions from the crystal structures of (a)  $(\text{Ph}_4\text{P})_2[\text{Se}_2\text{Br}_4] \cdot 2\text{Se}_2\text{Br}_2$ <sup>193</sup> and (b)  $(\text{Me}_4\text{N})_4[\text{Se}_3\text{Br}_8]_2 \cdot 2\text{SeBr}_2 \cdot 2\text{Se}_2\text{Br}_2$ .<sup>194</sup> Selenium atoms are depicted in red and bromine in dark green.

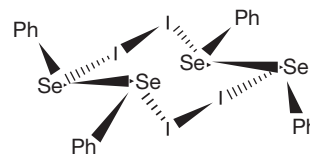
four-membered spirocyclic  $(\text{Te}_3\text{I}_2)_n$  fragments with one exocyclic and one endocyclic iodine atom. The polymeric chains are linked together by  $\text{Te} \cdots \text{Te}$  and  $\text{I} \cdots \text{I}$  secondary bonding interactions also in this species.

The optical, electrical, and thermodynamic properties of tellurium subhalides have attracted considerable research interest for some time.<sup>175</sup> For instance,  $\alpha$ -Tel has been suggested to find applications as solid electrolytes in galvanic cells.

In addition to binary halogenides, selenium and tellurium also form a number of catenated compounds and ions, which contain additional main group elements in addition to halogens. Some examples of molecular compounds comprise  $(\text{PhEX})_4$  ( $\text{E} = \text{Se}, \text{X} = \text{Cl}, \text{Br}; \text{E} = \text{Te}, \text{X} = \text{I}$ ),<sup>179–182</sup> mixed valence aryltellurenyl halogenides,<sup>183,184</sup> as well as thio- and selenourea adducts of  $\text{TeX}_2$  ( $\text{X} = \text{Cl}, \text{Br}, \text{I}, \text{SCN}, \text{SeCN}$ ),<sup>185–187</sup> and an adduct of  $(\text{mes})_2\text{Te}$  with two molecules of  $(\text{mes})\text{Tel}$  (see **Figure 38**).<sup>188</sup>

The  $(\text{REX})_4$  ( $\text{E} = \text{Se}, \text{Te}$ ) tetramer, which is exemplified by  $(\text{PhTeI})_4$  in **Figure 38(a)**, is formed in the halogenation reaction of  $\text{PhEPh}$ .<sup>179–182</sup> The close  $\text{Se} \cdots \text{Se}$  and  $\text{Te} \cdots \text{Te}$  contacts of the four-membered rings in  $(\text{PhEX})_4$  can be considered to be due to secondary bonding  $p^2 \rightarrow \sigma^*(\text{E}-\text{I})$  interactions. The approximate average bond orders of 0.38 and 0.57 can be estimated for the  $\text{Se}_4$ <sup>179,180</sup> and  $\text{Te}_4$ <sup>181,182</sup> rings, respectively, based

on the interatomic distances and Pauling's equation.<sup>117</sup> Interestingly, the reaction of  $\text{PhSePh}$  with  $\text{I}_2$  did not afford the  $(\text{PhSeI})_4$  tetramer, but a dimeric charge-transfer complex  $\text{Ph}_2\text{Se}_2 \cdot \text{I}_2$ .<sup>189</sup>



In addition to electrically neutral molecules, main group chalcogen–halogen species can also form ions. Selenium– and tellurium–halogen cations have been discussed above (see **Sections 1.07.3.2.2** and **1.07.3.2.3**). Some related cations with ions containing organic groups have been presented in **Figure 39**.

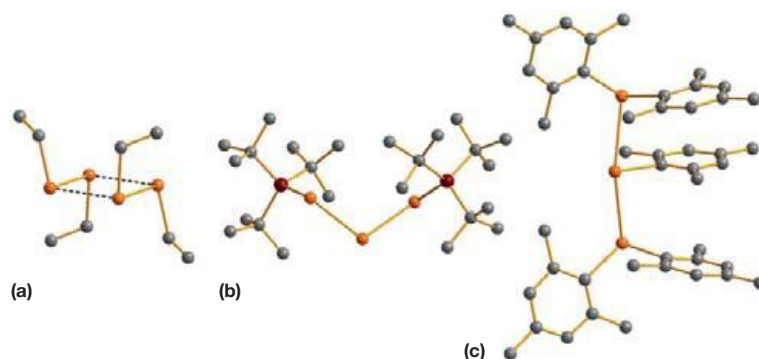
The formation of extended selenium–halogen anions has recently been reported, as exemplified in **Figure 40**.

The anion shown in **Figure 40(a)** can be conceived to be composed of  $[\text{Se}_2\text{Br}_6]^{2-}$  anions that are linked into a continuous chain by two  $\text{Se}_2\text{Br}_2$  molecules involving secondary bonding interactions.<sup>193</sup> Similarly, in  $(\text{Me}_4\text{N})_4[\text{Se}_3\text{Br}_8]_2 \cdot 2\text{SeBr}_2 \cdot 2\text{Se}_2\text{Br}_2$ , two  $[\text{Se}_3\text{Br}_8]^{2-}$  anions are linked into dimers by secondary bonding interactions involving two  $\text{Se}_2\text{Br}_2$  molecules (see **Figure 40(b)**).<sup>194</sup> The weak  $\text{Br} \cdots \text{Br}$  and  $\text{Se} \cdots \text{Br}$  interactions involving  $\text{SeBr}_2$  join the dimers into continuous chains.

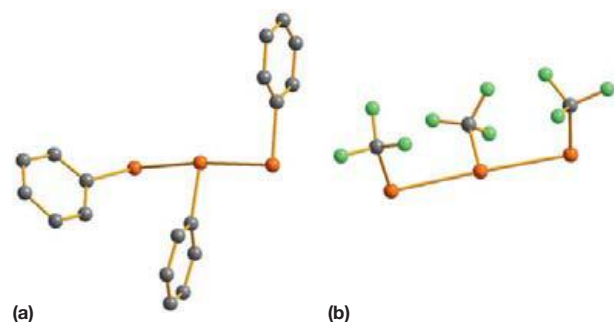
The information for organic polytellurium ions is sparser than that for organic polyselenium ions. One-electron oxidation of dialkyl ditellurides can be carried out with nitrosyl trifluoromethyl sulfonate  $(\text{NO})(\text{O}_3\text{SCF}_3)$ .<sup>195</sup> The radical  $(\text{RTe})_2 \cdot^+$  cations thus formed dimerize to form rectangular  $(\text{RTe})_4^{2+}$  (see **Figure 41(a)**). Dialkyl diselenides can also be oxidized in a similar fashion.

The long  $\text{Te} \cdots \text{Te}$  contact of 3.284 Å in  $(\text{EtTe})_4^{2+}$  is due to  $\pi^* - \pi^*$  interaction.<sup>195</sup> Consequently, the  $\text{Te}-\text{Te}$  bond of 2.653 Å in the  $(\text{RTe})_2 \cdot^+$  fragment is shorter than the single bond. The  $\text{Te}-\text{Te}$  bond in the  $\{(\text{tBu}_3\text{P})_2\text{Te}_3\}^+$  cation is also slightly shorter than the single bond (see **Figure 41(b)**).<sup>196</sup> By contrast, the  $\text{P}-\text{Te}$  bond is weak. Kuhn et al.<sup>196</sup> have deduced that the bonding is best described as tri(*tert*-butyl)phosphane coordinated to a  $\text{Te}_3^{2+}$  cation.

$\{(\text{mes})_2\text{Te}\}_2\text{Te}(\text{mes})\{[\text{SbF}_6]\}$  (see **Figure 41(c)**) has been obtained by the reaction of  $\{(\text{mes})_2\text{TeTe}(\text{mes})\}[\text{SbF}_6]$  with  $(\text{mes})_2\text{Te}$  ( $\text{mes} = \text{mesityl}, 2,4,6\text{-Me}_3(\text{C}_6\text{H}_2)$ ).<sup>197</sup> The two elongated  $\text{Te}-\text{Te}$  bonds of 2.979 and 3.049 Å in the  $\text{R}_2\text{Te}-\text{Te}(\text{R})-\text{TeR}_2^+$  cation can be understood in terms of the  $3c-4e$  bonding. Alternatively, the central tellurium of the cation can be



**Figure 41** Structure of (a)  $(\text{EtTe})_4^{2+}$  in  $(\text{EtTe})_4(\text{O}_3\text{SCF}_3)$ ,<sup>195</sup> (b)  $({}^t\text{Bu}_3\text{P})_2\text{Te}_3^+$  in  $\{({}^t\text{Bu}_3\text{P})_2\text{Te}_3\}[\text{SbF}_6]$ ,<sup>196</sup> and (c)  $[(\text{mes})_2\text{Te}]_2\text{Te}(\text{mes})^+$  in  $\{[(\text{mes})_2\text{Te}]_2\text{Te}(\text{mes})\}[\text{SbF}_6]\cdot\text{CH}_2\text{Cl}_2$ .<sup>197</sup> Tellurium atoms are depicted in orange, phosphorus in dark brown, and carbon in dark gray.



**Figure 42** The structure of (a)  $\{(\text{PhTe})_2\text{TePh}\}^-$ <sup>198,199</sup> and (b)  $\{(\text{CF}_3\text{Te})_2\text{TeCF}_3\}^-$ .<sup>200</sup> Tellurium atoms are depicted in orange, fluorine in light green, and carbon in dark gray.

considered as a five-electron pair  $\text{AX}_3\text{E}_2$  system with a trigonal bipyramidal arrangement of electron pairs. The two long Te–Te bonds are in the axial positions.

Recently, the preparation and crystal structures of several species containing the tritelluride anion  $\{\text{RTeTe}(\text{R})\text{TeR}\}^-$  have been reported (see **Figure 42**).<sup>198–200</sup> Like in the case of the  $\{\text{R}_2\text{TeTe}(\text{R})\text{TeR}_2\}^+$  cation, the axial Te–Te bonds form a 3c–4e system. Consequently, the axial Te–Te bonds of  $\sim 3.0$  Å are rather long.

#### 1.07.4.2 Group 15 Polyselenides and -tellurides

While selenium–nitrogen and tellurium–nitrogen chemistry is not as developed or as extensive as sulfur–nitrogen chemistry (see **Chapter 1.06**), they have seen rapid progress over the last decades (for recent detailed reviews on chalcogen–nitrogen chemistry, see Chivers, 2005,<sup>10</sup> Martin and Ragnogna, 2011,<sup>201</sup> and Chivers et al., 2007<sup>202</sup>). Some typical compounds containing catenated Se–Se bonds are shown in **Figure 43**.

Dipiperidino tetraselane (**Figure 43(a)**) and dimorpholino tetraselane have been prepared by heating black selenium powder with piperidine or morpholine in the presence of  $\text{Pb}_3\text{O}_4$ .<sup>203</sup> The Se–Se bond lengths imply normal single bonds and all Se–Se torsional angles are near  $90^\circ$  ( $76.4$ – $88.5^\circ$ ).

Cyclic selenium imide derivatives have been prepared from  $(\text{Me}_3\text{Si})({}^t\text{Bu})\text{NLi}$ . Its reaction with  $\text{Se}_2\text{Cl}_2$  affords  $\text{Se}_6(\text{N}^t\text{Bu})_2$  (see **Figure 43(b)**)<sup>204</sup> and that with  $\text{SeOCl}_2$

yields  $\text{Se}_9(\text{N}^t\text{Bu})_6$  (**Figure 43(c)**).<sup>204</sup> The latter species was later prepared in better yields by treatment of  ${}^t\text{BuNH}_2$  with an equimolar mixture of elemental selenium and selenium tetrachloride.<sup>205</sup> The reaction of  $(\text{Me}_3\text{Si})({}^t\text{Bu})\text{NLi}$  and  $\text{SeCl}_4$  results in the formation of  $\text{Se}_3(\text{N}^t\text{Bu})_2$ .<sup>209</sup> It was identified only by NMR spectroscopy, but the related  $\text{Se}_3(\text{NAd})_2$  ( $\text{Ad}$  = adamantyl) has been obtained as a crystalline solid by the reaction of  $\text{AdNH}_2$  and  $\text{SeCl}_2$ , and its crystal structure could be determined (**Figure 43(d)**).<sup>205</sup>

The Se–Se bond lengths of  $2.331$ – $2.333$  Å and the torsional angle of  $73.6$ – $99.5^\circ$  in the cyclic imide derivatives  $\text{Se}_6(\text{N}^t\text{Bu})_2$  and  $\text{Se}_9(\text{N}^t\text{Bu})_6$ <sup>204</sup> indicate single bonds. The Se–Se bond of  $2.404$  Å in  $\text{Se}_3(\text{NAd})_2$ <sup>205</sup> is somewhat longer due to a smaller torsional angle of  $46.7^\circ$ .

The  $\text{Se}_2\text{N}_2\text{CH}$  dimer has been prepared from 1,3,5-triazine according to **Scheme 4**.<sup>206</sup>

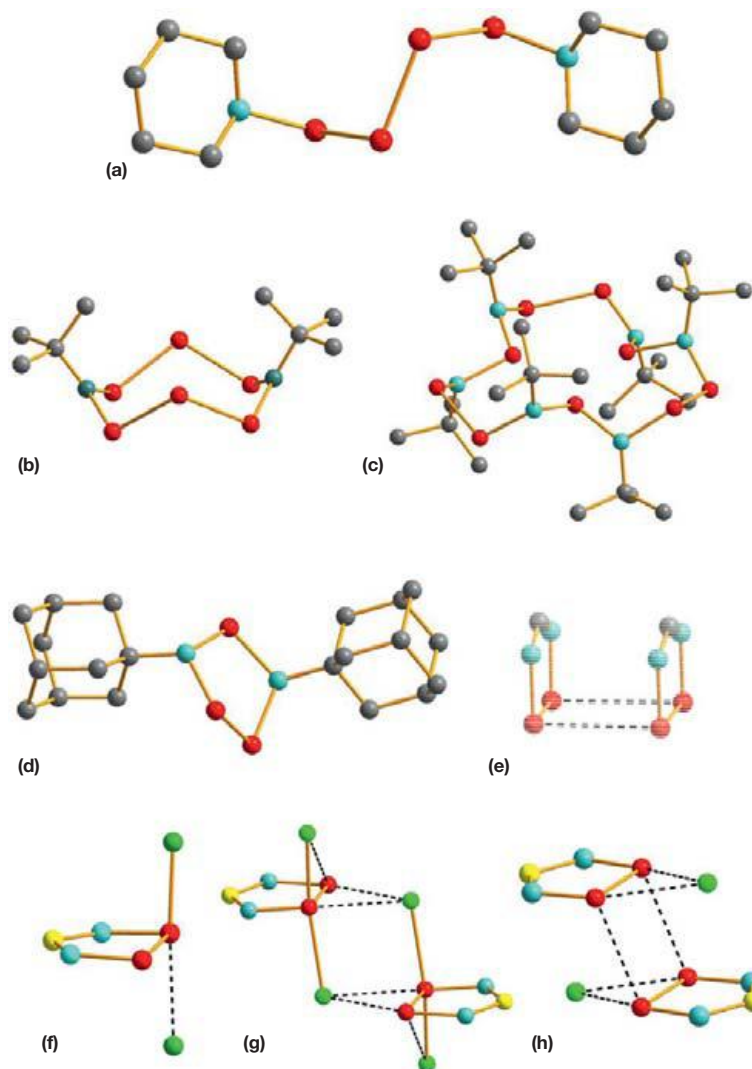
In the solid state, the dimer  $(\text{HCN}_2\text{Se}_2)_2$  is diamagnetic, with a residual spin density of 0.01%. The material exhibits three orders of magnitude higher single-crystal conductivity than the other monofunctional selenium-based radical dimers.<sup>210</sup>

$\text{Se}(\text{NSO})_2$  is a versatile reagent for a number of chalcogen–nitrogen species, as shown in **Scheme 5**.<sup>207,211</sup> It can be prepared by the reaction of  $\text{Me}_3\text{SiNSO}$  and  $\text{Se}_2\text{Cl}_2$ .

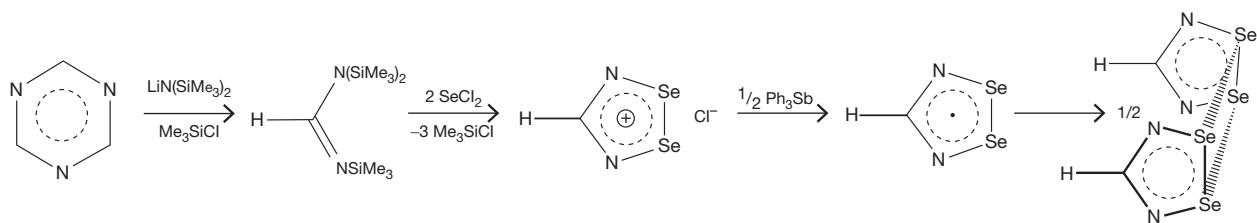
With the reaction of  $\text{POCl}_3$ ,  $\text{Se}(\text{NSO})_2$  yields molecular  $\text{SeCl}_2(\text{SeNSN})$  (see **Figure 43(g)**). With  $\text{MF}_5$  in  $\text{SO}_2(\text{l})$  solution followed by the reaction with  $\text{Cl}_2$ , the ionic isomer  $\{\text{SeCl}(\text{SeNSN})\}\text{Cl}$  is formed (see **Figure 43(f)**).<sup>207</sup>

The product distribution in the reaction of  $\{(\text{Me}_3\text{Si})_2\text{N}\}_2\text{S}$  and  $\text{SeCl}_4$  depends on the reaction conditions. In carbon disulfide at  $-70^\circ\text{C}$ , only  $1,5\text{-Se}_2\text{S}_2\text{N}_4$  is formed,<sup>212</sup> but at ambient temperature in either  $\text{CS}_2$  or dichloromethane, the reaction affords  $\sim 75\%$   $1,5\text{-Se}_2\text{S}_2\text{N}_4$  and  $25\%$   $\{(\text{Se}_2\text{SN}_2)\text{Cl}\}_2$ , and in dioxane at  $50^\circ\text{C}$ , the product mixture is reversed containing  $\sim 70\%$   $\{(\text{Se}_2\text{SN}_2)\text{Cl}\}_2$  and  $30\%$   $1,5\text{-Se}_2\text{S}_2\text{N}_4$ .<sup>208</sup> This is consistent with the proposal of Haas et al.<sup>207</sup> that  $1,5\text{-Se}_2\text{S}_2\text{N}_4$  is an intermediate in the formation of the  $\text{Se}_2\text{SN}_2$  ring upon treatment of  $\text{Se}(\text{NSO})_2$  with Lewis acids (see **Scheme 5**).<sup>207</sup>

Catenated tellurium–nitrogen species are very rare.  $\text{TeCl}_2(\text{TeNSN})$  is analogous to the corresponding selenium compound.<sup>213</sup> It can be converted to a  $\{\text{ClTe}(\text{TeNSN})\}^+$  cation by the reaction with  $\text{AsF}_5$  (see **Scheme 6**). Another example is  $(\text{Te}_2\text{S}_2\text{N}_4)[\text{AsF}_6]$  that contains a cyclic cation with a transannular TeTe single bond.<sup>214</sup>



**Figure 43** Some typical selenium–nitrogen compounds containing Se–Se bonds. (a)  $\text{Se}_4(\text{NC}_5\text{H}_{10})_2$ .<sup>203</sup> (b)  $\text{Se}_6(\text{N}^t\text{Bu})_2$ .<sup>204</sup> (c)  $\text{Se}_9(\text{N}^t\text{Bu})_6$ .<sup>204</sup> (d)  $\text{Se}_3(\text{NAd})_2$  (Ad = adamantyl).<sup>205</sup> (e)  $\text{Se}_2\text{N}_2\text{CH}$  dimer.<sup>206</sup> (f)  $(\text{SeCl}(\text{SeNSN})\text{Cl})\text{Cl}$ .<sup>207</sup> (g)  $\text{SeCl}_2(\text{SeNSN})$ .<sup>207</sup> (h)  $(\text{SN}_2\text{Se}_2\text{Cl})_2$ .<sup>208</sup> Selenium atoms are depicted in red, sulfur in yellow, nitrogen in light blue, chlorine in green, and carbon in dark gray.

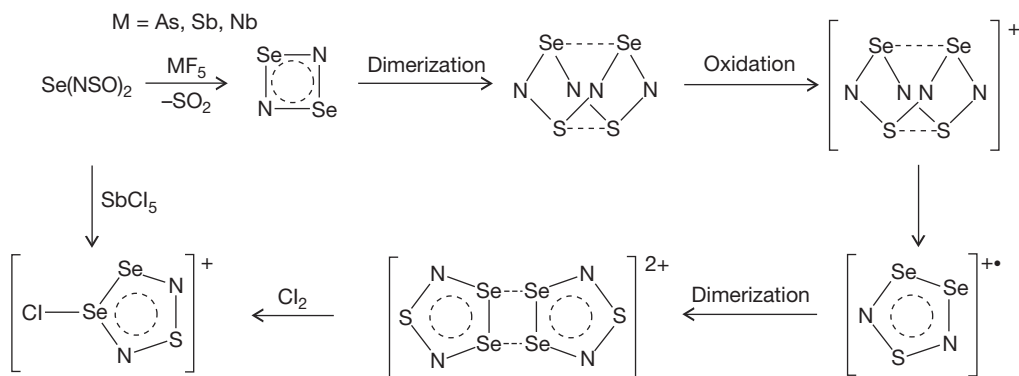


**Scheme 4** The preparation of the  $\text{Se}_2\text{N}_2\text{CH}$  dimer from 1,3,5-triazine.

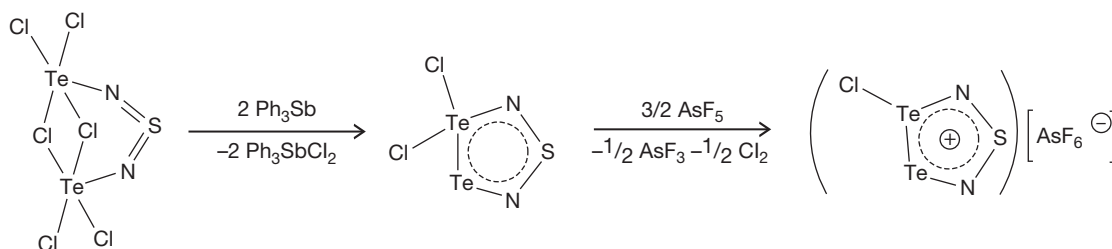
Whereas several binary phosphorus, arsenic, antimony, and bismuth selenides and tellurides are known, only  $\text{P}_2\text{Se}_5$  contains chalcogen–chalcogen bonds (see [Figure 44\(a\)](#)).<sup>215</sup> A number of phosphoryl polyselenides and -tellurides have been prepared and characterized. The metrical parameters of the chalcogen–chalcogen bonds indicate strainless single bonds (see [Figure 44\(b\)](#) and [44\(c\)](#)).

$(\text{PhPSe})_2\text{Se}_2$ , the so-called Woollins' reagent,<sup>218</sup> has proved to be a useful synthon in the development of macrocyclic organoselenium chemistry.<sup>219</sup> Structures of some typical examples are shown in [Figure 45](#).

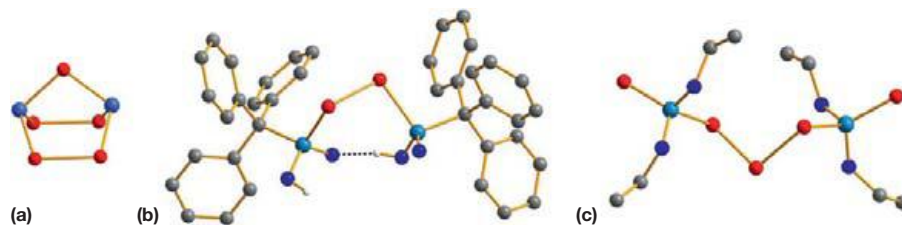
The diselenides shown in [Figure 45](#) are prepared by treating the Woollins' reagent with a diol that yields bis(diselenophosphonic) acids quantitatively. The reaction with primary alkyl



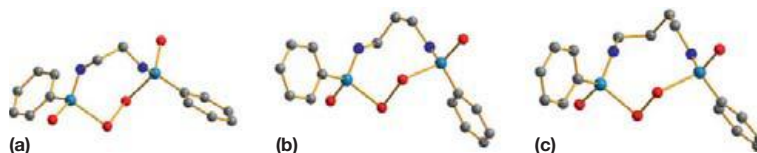
**Scheme 5** Preparation of cyclic chalcogen–nitrogen species from  $\text{Se}(\text{NSO})_2$ .



**Scheme 6** The conversion of  $\text{TeCl}_2(\text{TeNSN})$  to a  $[\text{ClTe}(\text{TeNSN})]_p$  cation by treatment with  $\text{Ph}_3\text{Sb}$  and  $\text{AsF}_5$ .



**Figure 44** Molecular structures of (a)  $\text{P}_2\text{Se}_5$ ,<sup>215</sup> (b)  $\{(\text{Ph}_3\text{C})\text{P}(\text{O})(\text{OH})_2\}_2\text{Se}_2$ ,<sup>216</sup> and (c)  $\{(\text{EtO})_2\text{P}(\text{Se})\}_2\text{Se}_3$ .<sup>217</sup> Selenium atoms are depicted in red, oxygen in dark blue, phosphorus in light blue, and carbon in dark gray.



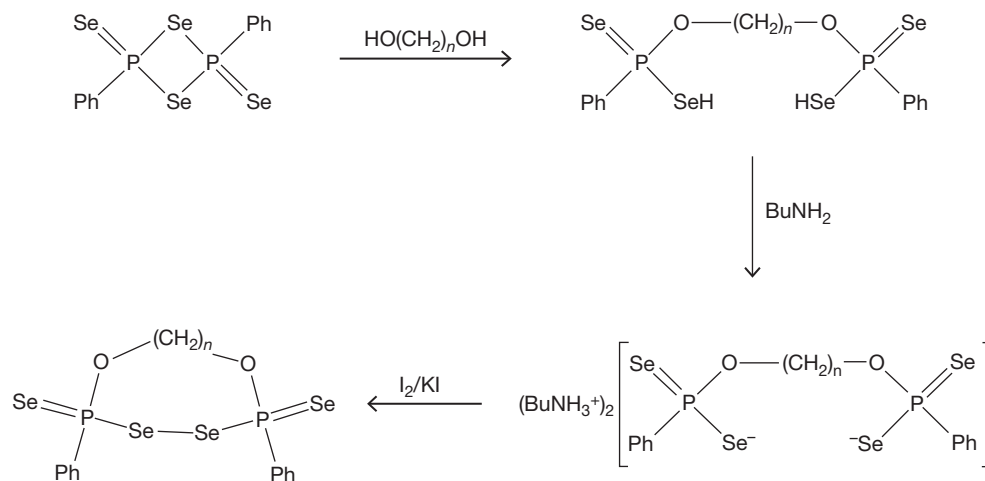
**Figure 45** Molecular structures of  $(\text{Ph}(\text{Se})\text{P})_2[\mu\text{-O}_2(\text{CH}_2)_n](\mu\text{-Se}_2)$ . (a)  $n = 2$ , (b)  $n = 3$ , and (c)  $n = 4$ .<sup>220</sup> Selenium atoms are depicted in red, oxygen in dark blue, phosphorus in light blue, and carbon in dark gray.

amines converts them into alkylammonium salts. The oxidation with  $\text{I}_2/\text{KI}$  affords the macrocyclic diselenides (see **Scheme 7**), the structures of which are shown in **Figure 45**.

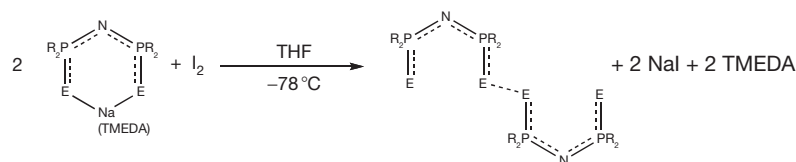
Dichalcogenoimidodiphosphinates  $(\text{EPR}_2\text{NPR}_2\text{E})^-$  ( $\text{E} = \text{S}, \text{Se}, \text{Te}$ ;  $\text{R} = {}^i\text{Pr}, {}^t\text{Bu}$ ) have been shown to be versatile reactants for the preparation of new types of catenated selenium and tellurium species.<sup>221,222</sup> While the sulfur- and selenium-containing anions can be prepared by the deprotonation of  $\text{EPR}_2\text{N}(\text{H})\text{PR}_2\text{E}$ , which is obtained by prolonged reflux of  $(\text{R}_2\text{P})_2\text{NH}$  with elemental sulfur or selenium in toluene, the

related tellurium-containing anions are best obtained as sodium salts from  $\text{Na}\{\text{R}_2\text{PNPR}_2\}$  and elemental tellurium in hot toluene containing tetramethylethylenediamine (TMEDA). This procedure has recently been extended also for the lighter congeners of tellurium.<sup>222</sup> One-electron oxidation of the sodium salts by iodine in THF affords unprecedented molecular dimers (see **Scheme 8**):

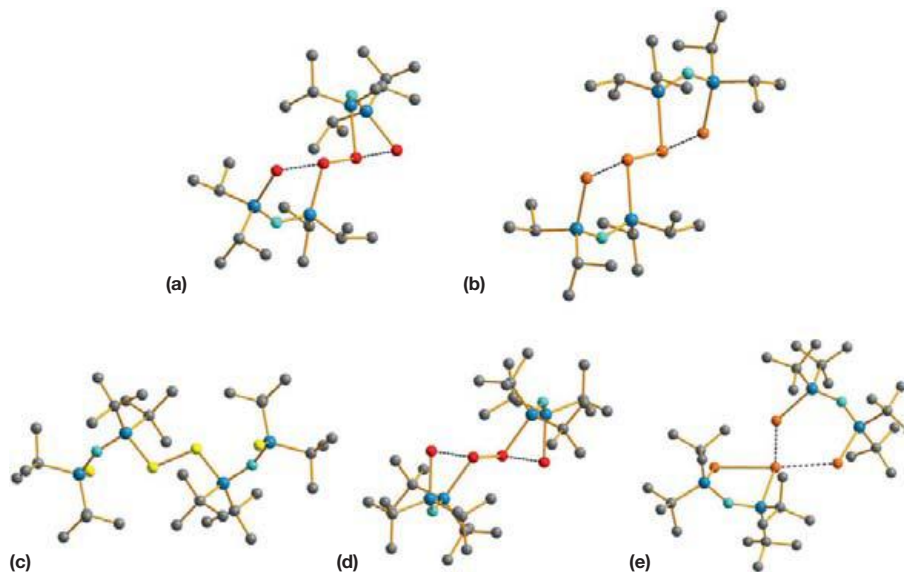
The molecular structures of  $(\text{EPR}_2\text{NPR}_2\text{E})_2$  ( $\text{E} = \text{S}, \text{Se}, \text{Te}$ ;  $\text{R} = {}^i\text{Pr}, {}^t\text{Bu}$ ) dimers are shown in **Figure 46**. The formal chalcogen–chalcogen bond between the monomers is elongated



**Scheme 7** Macrocyclic diselenides from Woollins' reagent.



**Scheme 8** One electron oxidation of Na(TMDEA)(EPR<sub>2</sub>NPR<sub>2</sub>E) by iodine to form novel (EPR<sub>2</sub>NPR<sub>2</sub>E)<sub>2</sub> (E = S, Se, Te).



**Figure 46** Molecular structures of (a) (Se<sup>i</sup>Pr<sub>2</sub>N<sup>i</sup>Pr<sub>2</sub>Se)<sub>2</sub>,<sup>222</sup> (b) (Te<sup>i</sup>Pr<sub>2</sub>N<sup>i</sup>Pr<sub>2</sub>Te)<sub>2</sub>,<sup>224</sup> (c) (SP<sup>t</sup>Bu<sub>2</sub>NP<sup>t</sup>Bu<sub>2</sub>S)<sub>2</sub>,<sup>222</sup> (d) (SeP<sup>t</sup>Bu<sub>2</sub>NP<sup>t</sup>Bu<sub>2</sub>Se)<sub>2</sub>,<sup>222</sup> and (e) the contact ion pair {TeP<sup>t</sup>Bu<sub>2</sub>N}<sup>+</sup>{(TeP<sup>t</sup>Bu<sub>2</sub>N)<sup>-</sup>.<sup>222</sup> Selenium atoms are depicted in red, tellurium in orange, sulfur in yellow, phosphorus in light blue, nitrogen in turquoise, and carbon in dark gray.

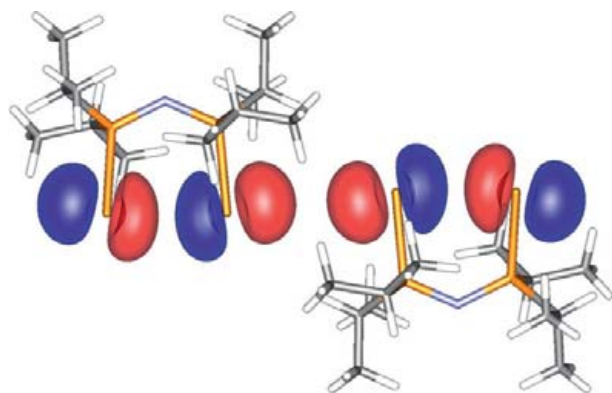
from the corresponding single bond in each molecule shown in **Figure 46(a)–46(d)**. The elongation increases in the order S–S (2%) < Se–Se (6%) < Te–Te (8%).<sup>222</sup> These elongations correspond to the respective Pauling bond orders of 0.97, 0.84, and 0.75. The opposite trend in the interactions between the terminal chalcogen–chalcogen bonds is observed. In the case of (SP<sup>t</sup>Bu<sub>2</sub>NP<sup>t</sup>Bu<sub>2</sub>S)<sub>2</sub> (**Figure 46(c)**), the terminal S··S

distance is 5.182 Å<sup>222</sup> indicating no interaction. The observed bond elongation of the middle S–S bond (2.104 Å) is probably only due to the p lone-pair repulsion as a consequence of the PSSP torsional angle of 180°.<sup>223</sup> The selenium and tellurium dimers (**Figure 46(a)**, **46(b)**, and **46(d)**) show Pauling bond orders in the terminal chalcogen–chalcogen interactions of 0.24 and 0.36, respectively, corresponding to the respective



distances of 3.329–3.355 and 3.464 Å.<sup>222</sup> In these two cases, all three chalcogen–chalcogen distances can be explained by the interaction between two  $(\text{EPR}_2\text{NPR}_2\text{Te})\cdot$  SOMOs, as exemplified in **Figure 47** by the model dimer  $(\text{Te}^i\text{Pr}_2\text{NP}^i\text{Pr}_2\text{Te})_2$ .<sup>224,225</sup>

The MO formed by the two SOMOs is bonding with respect to the middle bond but antibonding with respect to the terminal bonds. The interaction between the monomers is expected



**Figure 47** The bonding interaction between two  $(\text{Te}^i\text{Pr}_2\text{NP}^i\text{Pr}_2\text{Te})$  SOMOs.<sup>221,224,225</sup> Reproduced with permission from Chivers, T.; Konu, J., in Woollins, J. D.; Laitinen, R. S., Eds.; *Selenium and Tellurium Chemistry. From Small Molecules to Biomolecules and Materials*, Springer: Heidelberg, Dordrecht, London, New York, 2011, pp. 79–102. Copyright 2011 Springer.

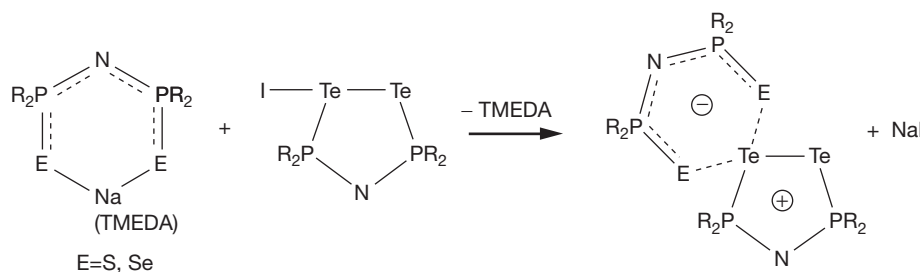
to be weaker for the tellurium dimer than for the selenium dimer.<sup>224</sup> As the overlap between the SOMOs increases, the middle E–E bond strengthens and the terminal interactions become weaker. This is consistent with the observed interatomic distances. The middle chalcogen–chalcogen bond shows a higher bond order in the selenium dimer than in the tellurium dimer. Conversely, the order of the terminal interactions is higher in the tellurium dimer than in the selenium dimer.

The DFT computations of Chivers et al.<sup>224</sup> yield the value of  $-80 \text{ kJ mol}^{-1}$  for the energy of dimerization of  $(\text{TeMe}_2\text{PNPMe}_2\text{Te})$ , which is clearly lower than the bond energy of the Te–Te bond of  $138 \text{ kJ mol}^{-1}$ .<sup>118</sup> This is in qualitative agreement with the estimated bond order of 0.75.

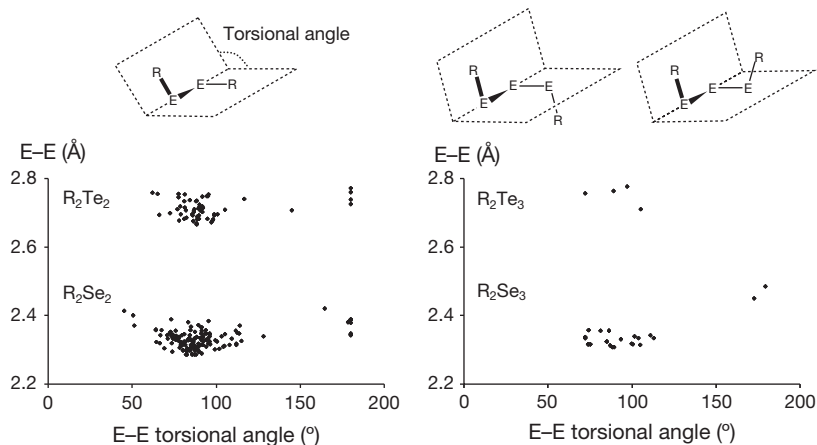
The geometry optimization of  $(\text{Te}^i\text{Bu}_2\text{NP}^i\text{Bu}_2\text{Te})_2$  predicts the middle Te–Te bond to be longer than in  $(\text{Te}^i\text{Pr}_2\text{NP}^i\text{Pr}_2\text{Te})_2$ .<sup>224</sup> In agreement with this observation, the repetition of the preparation shown in **Scheme 8** by using  $\{(\text{P}^i\text{Bu}_2\text{Te})\}(\text{TMEDA})\text{Na}$  instead of the isopropyl analog did not result in the formation of the dimer, but a contact ion pair involving the  $\{(\text{Te}^i\text{Bu}_2)_2\text{N}\}^+$  cation and  $\{(\text{Te}^i\text{Bu}_2)_2\text{N}\}^-$  anion (see **Figure 46(e)**).<sup>222</sup> Another route was later designed to prepare similar contact ion salts for other dichalcogenoimidodiphosphinates (see **Scheme 9**).<sup>226</sup>

### 1.07.4.3 Group 14 Polyselenides and -tellurides

A large number of organic di- and triselenides and tellurides are known. The Cambridge Crystallographic Database<sup>227</sup> shows 147 and 14 entries for open-chain di- and triselenides,



**Scheme 9** Preparation of dichalcogenoimidodiphosphinates.



**Figure 48** The chalcogen–chalcogen bond lengths as a function of the torsional angle in organic di- and tri-selenides and -tellurides (data taken from Cambridge Crystallographic Database.<sup>227</sup>)

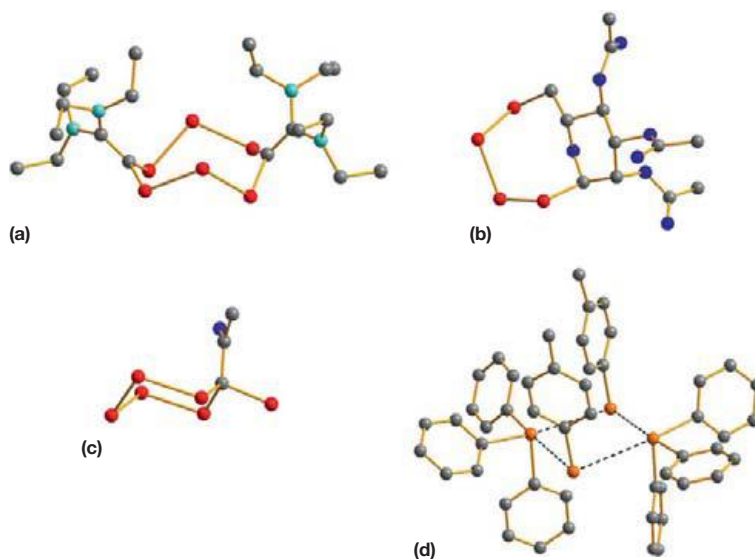
respectively, with organic substituents of varying complexity. In the case of related di- and tritellurides, there are 51 and 4 entries in the database, respectively. Both the Se–Se and Te–Te bonds in most compounds show quite normal single bond values with the torsional angle near  $90^\circ$ , as shown in Figure 48. However, there are a few species in which the torsional angle is near to or equal to  $180^\circ$ . In all these cases, the organic substituent is bulky and in many cases also electron withdrawing. However, no systematic factors could be inferred.

In addition to acyclic di- and trichalcogenides, also cyclic organic species have been prepared and characterized.<sup>227</sup> Their

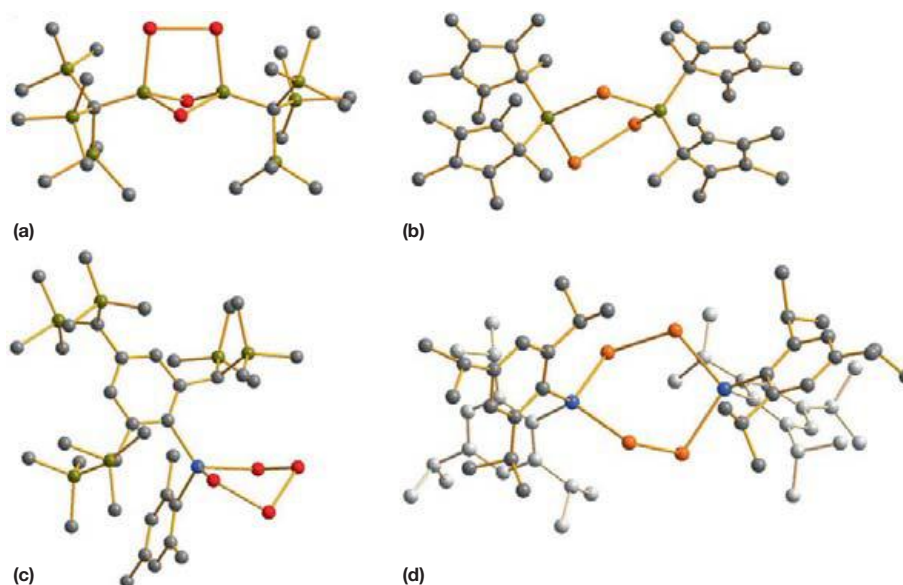
chalcogen–chalcogen bond parameters are in close agreement with those of dichalcogenides. Some examples are shown in Figure 49.

The molecular structure of  $\text{Se}_6 \{ \text{C}=\text{C}(\text{NEt}_2)_2 \}_2$  resembles that of  $\text{Se}_6(\text{N}^t\text{Bu})_2$ <sup>205</sup> (see Figure 43(b)). The compound is prepared from  $(\text{Et}_2\text{N})_2\text{C}=\text{CHCl}$  by refluxing with gray selenium in benzene for 5 h. The compound was reported to be a convenient reagent in an analogous manner to  $(\text{Et}_2\text{N})_2\text{C}=\text{CS}_2$ .<sup>228</sup>

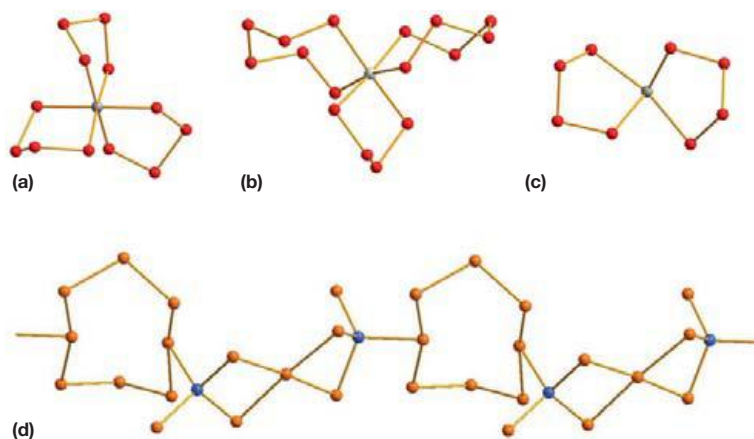
$\text{C}_5\text{H}_5\text{O}(\text{OAc})_3\text{Se}_4$  was obtained as a main product from mannose by treatment with  $(\text{Et}_4\text{N})_2\text{WSe}_2$ .<sup>229</sup> It is the first tetraselenide in which the  $\text{Se}_4$  fragment forms a cyclic



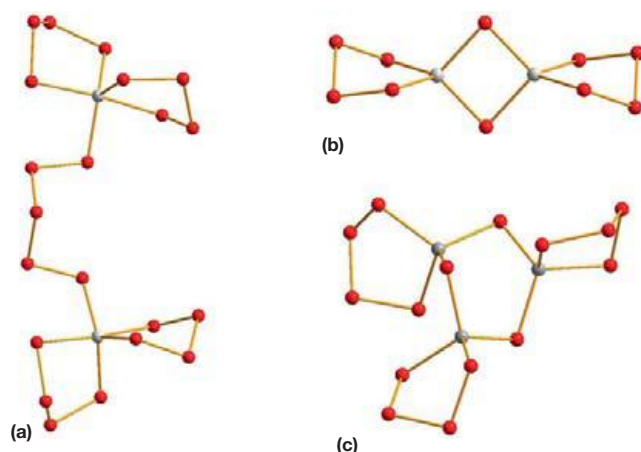
**Figure 49** Cyclic organic polyselenides and tellurides: (a)  $\text{Se}_6\{\text{C}=\text{C}(\text{NEt}_2)_2\}_2$ ,<sup>228</sup> (b)  $\text{C}_5\text{H}_5\text{O}(\text{OAc})_3\text{Se}_4$ ,<sup>229</sup> (c)  $[\text{Se}_5\text{C}(\text{Se})\text{COMe}]^-$  anion,<sup>230</sup> and (d)  $\{(\text{Ph}_3\text{Te})(\text{TeC}_6\text{H}_4\text{Me})\}_2$ .<sup>231</sup> Selenium atoms are depicted in red, tellurium in orange, oxygen in dark blue, nitrogen in turquoise, and carbon in dark gray.



**Figure 50** Crystal structures of (a) one molecule in the disordered crystal structure of  $\{(\text{Me}_3\text{Si})_3\text{CSi}_2(\mu\text{-Se})_2(\mu\text{-Se}_2)\}$ ,<sup>234</sup> (b)  $\{(\text{C}_5\text{Me}_5)_2\text{Si}_2(\mu\text{-Te})(\mu\text{-Te}_2)\}$ ,<sup>235</sup> (c)  $\{[(\text{Me}_3\text{Si})_2\text{C}]_3\text{C}_6\text{H}_2(\text{Me}_3\text{C}_6\text{H}_2)\text{GeSe}_4\}$ ,<sup>236</sup> and (d)  $\{(\text{Pr}_3\text{C}_6\text{H}_2)_2\text{Ge}_2(\mu\text{-Te})_2\}$ .<sup>237</sup> Selenium atoms are depicted in red, tellurium in orange, silicon in olive green, germanium in light blue, and carbon in gray.



**Figure 51** Polychalcogenidotin and -lead complexes: (a)  $[\text{Sn}(\text{Se}_4)_3]^{2-}$ ,<sup>244</sup> (b)  $[\text{Sn}(\text{Se}_4)(\text{Se}_6)_2]^{2-}$ ,<sup>245</sup> and (c)  $[\text{Pb}(\text{Se}_4)_2]^{2-}$ .<sup>244</sup> (d) The extended anionic network involving  $\text{GeTe}_2$ ,  $\text{Te}_8^{4-}$ , and  $\text{TeTe}_4^{6-}$ .<sup>243</sup> Selenium atoms are depicted in red, tellurium in orange, tin and lead in gray, and germanium in light blue.

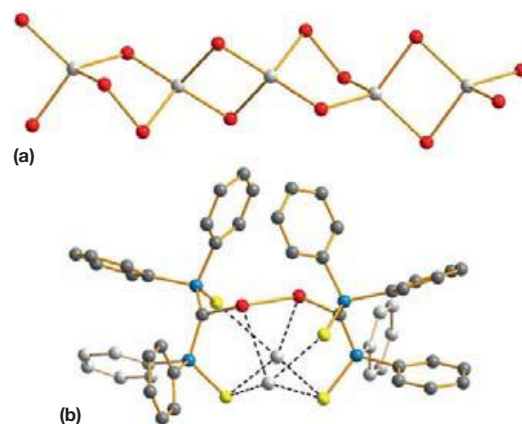


**Figure 52** The structure of (a)  $[\text{In}_2(\text{Se}_4)_4(\text{Se}_5)]^{4-}$ ,<sup>246,247</sup> (b)  $[\text{In}_2(\text{Se})_2(\text{Se}_4)]^{2-}$ ,<sup>247</sup> and (c)  $[\text{In}_3(\text{Se})_3(\text{Se}_4)_3]^{3-}$ .<sup>247</sup> Selenium atoms are depicted in red and indium in gray.

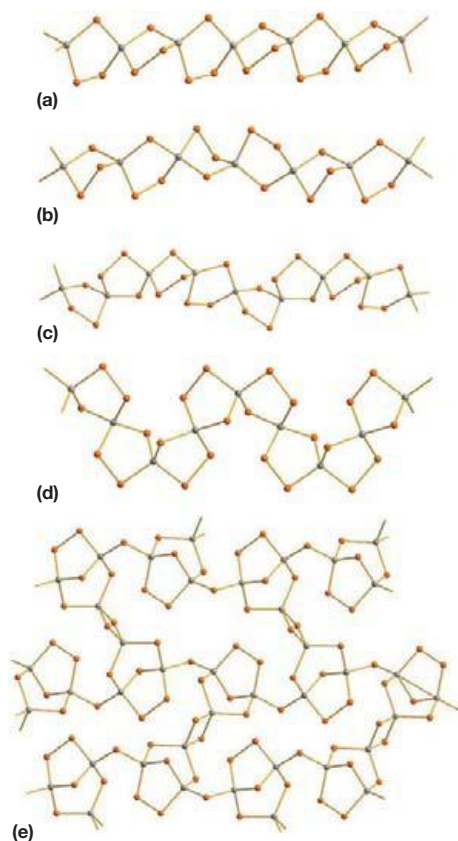
arrangement with the carbon backbone. The reaction of  $\text{K}_2\text{CO}_3$  with red selenium in acetone in the presence of  $\{(\text{Ph}_3\text{P})_2\text{N}\}\text{Cl}$  at  $23^\circ\text{C}$  afforded an ionic product  $\{(\text{Ph}_3\text{P})_2\text{N}\}\{\text{Se}_5\text{C}(\text{Se})\text{COMe}\}$  (see **Figure 49(c)**).<sup>230</sup> The anion shows two short contacts of 2.942 and 2.955 Å between the exocyclic selenium atom and the geminal endocyclic selenium atoms.

The triphenyltelluronium cation forms ion pairs with the arylchalcogenolate anions resulting in cyclic arrangements.<sup>231,232</sup>  $\{(\text{Ph}_3\text{Te})(\text{TeC}_6\text{H}_4\text{R})\}_2$  ( $\text{R}=\text{Me}, \text{OMe}$ )<sup>231</sup> (see **Figure 49(d)**) contains four-membered  $\text{Te}_4$  rings with the  $\text{Te}\cdots\text{Te}$  distances ranging 3.380–3.596 Å and  $\{(\text{Ph}_3\text{Te})(\text{SC}_6\text{H}_4\text{Cl})\}_4$ <sup>232</sup> consists of an eight-membered  $\text{Te}_4\text{S}_4$  ring with contacts ranging 3.024–3.639 Å.

The information on polyselenium and polytellurium species with heavier group 16 elements is much sparser than on those of carbon. Kückmann et al.<sup>233</sup> have reported the preparation and structure of acyclic  ${}^t\text{Bu}_2\text{RSiE-ESiR}^t\text{Bu}_2$  ( $\text{E}=\text{Se}, \text{Te}$ ;  $\text{R}={}^t\text{Bu}, \text{Ph}$ ) from  $\text{Na}(\text{ESiR}^t\text{Bu}_2)$ . The molecular structures of the four dichalcogenides are analogous to those in organic diselenides and ditellurides. Both the  $\text{Se-Se}$  and  $\text{Te-Te}$  bonds



**Figure 53** (a) The structure of polymeric  $[\text{In}_2(\text{Se})_3(\text{Se}_2)]^{2-}$  anion.<sup>249</sup> (b) The structure of  $\text{Tl}_2\{[(\text{SPh}_2\text{P})_2\text{Cl}_2\text{Se}_2]\}$ .<sup>250</sup> Selenium atoms are depicted in red, sulfur in yellow, indium in gray, phosphorus in light blue, thallium in light gray, and carbon in gray.



**Figure 54** Polymeric  $\text{In}_2\text{Te}_6^{2-}$  anions from  $\text{In}_2\text{Te}_3$  building blocks in (a)  $(\text{Ph}_4\text{P})_2[\text{In}_2\text{Te}_6]$ ,<sup>252</sup> (b)  $[\text{Zn}(\text{en})_3][\text{In}_2\text{Te}_6]$ ,<sup>252</sup> (c)  $\alpha$ - and (d)  $\beta$ - $[\text{Mo}_3(\text{en})_3(\mu_2\text{-Te}_2)_3(\mu_3\text{-Te})(\mu_2\text{-O})][\text{In}_2\text{Te}_6]$ ,<sup>252</sup> (e)  $[\text{Ga}(\text{en})_3][\text{In}_3\text{Te}_7]$ .<sup>254</sup> Tellurium atoms are depicted in orange and indium atoms in gray.

show approximate single bond lengths (2.368–2.390 and 2.724–2.740 Å, respectively). The torsional angle about the chalcogen–chalcogen bond is  $180^\circ$  in each molecule.

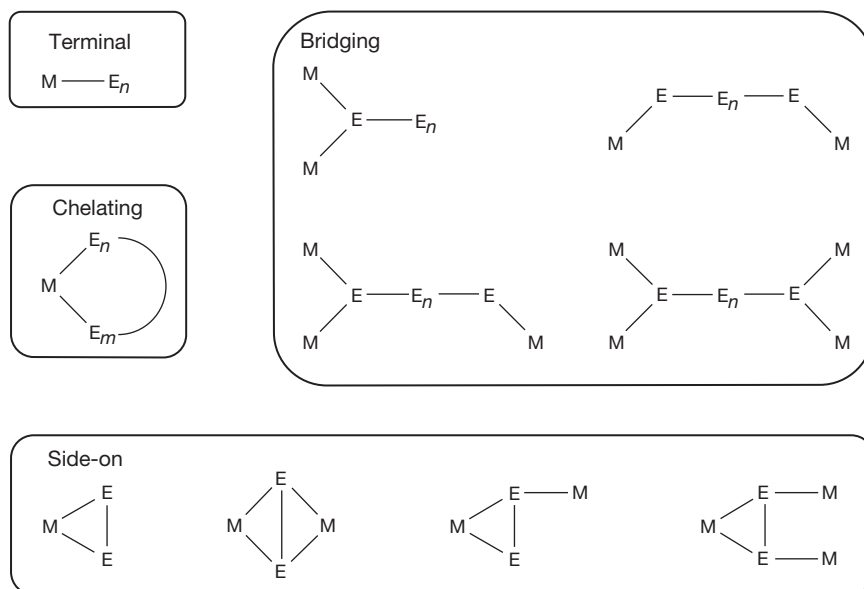
A few ring and cage compounds have been reported for silicon and germanium species containing diselenium and ditellurium moieties, as shown in **Figure 50**.

$\{(\text{Me}_3\text{Si})_3\text{CSi}\}_2(\mu\text{-Se})_2(\mu\text{-Se}_2)$  and  $\{[(\text{Me}_3\text{Si})_2\text{C}]_3\text{C}_6\text{H}_2\}(\text{Me}_3\text{C}_6\text{H}_2)\text{GeSe}_4$  could be isolated in small amounts by the reaction of  $(\text{Me}_3\text{Si})_3\text{CSiH}_2$  with elemental selenium.<sup>234</sup> Similarly,  $\{[(\text{Me}_3\text{Si})_2\text{C}]_3\text{C}_6\text{H}_2\}(\text{Me}_3\text{C}_6\text{H}_2)\text{GeSe}_4$  was obtained by lithiation of  $\text{R}_2\text{GeH}_2$  or  $\text{R}_2\text{GeCl}_2$  by  $^t\text{BuLi}$  followed by the reaction with selenium.<sup>236</sup> Trialkylphosphane telluride was utilized as the tellurium transfer reagent in the preparation of  $\{(\text{C}_5\text{Me}_5)_2\text{Si}\}_2(\mu\text{-Te})(\mu\text{-Te}_2)$ <sup>235</sup> and  $\{(\text{Pr}_3\text{C}_6\text{H}_2)_2\text{Ge}\}_2(\mu\text{-Te}_2)$ .<sup>237</sup>

Tin and lead are metallic elements. In addition to dinuclear species of the type shown in **Figure 50** for silicon and germanium,<sup>238–241</sup> they form complexes with polychalcogenides and extended anionic networks (see **Figure 51**), the formation, structures, and utilization of which have been reviewed by Sheldrick and Wachold with a special interest in the design of nanoporous materials with tailored properties.<sup>242</sup> Such extended phases can be exemplified by  $\{[\text{Ga}(\text{en})_3]_2(\text{Ge}_2\text{Te}_{15})\}_n$  that has recently been prepared by solvothermal methods.<sup>243</sup> The single-crystal x-ray structure was interpreted in terms of two interacting polytelluride anions: cross-shaped  $\text{TeTe}_4^{6-}$  anions and  $\text{Te}_8^{4-}$  rings (see **Figure 51(d)**). The material was found to be a p-type semiconductor at room temperature. It switches to an n-type semiconductor at 380 K.<sup>243</sup>

#### 1.07.4.4 Group 13 Polyselenides and -tellurides

The structural chemistry involving group 13 polychalcogenides is centered on indium, although some gallium and thallium species have also been reported. The reaction of  $\text{Na}_2\text{Se}_5$  and  $\text{InCl}_3$  in dimethylformamide in the presence of  $\text{R}_4\text{MX}$  ( $\text{R} = \text{Ph}$ ,  $\text{Pr}$ ,  $\text{Et}$ ;  $\text{M} = \text{P}$ ,  $\text{N}$ ;  $\text{X} = \text{Cl}$ ,  $\text{Br}$ ) afforded  $(\text{R}_4\text{M})_4[\text{In}_2(\text{Se}_4)_4(\text{Se}_5)]$



**Figure 55** Ligation modes of chalcogenido complexes of the transition metals. Adapted from Sheldrick, W. S., in Devillanova, F. A. (ed.), *Handbook of Chalcogen Chemistry*, RSC Publishing: Cambridge 2007, pp. 543–573.

(see Figure 52(a)) in good yields.<sup>246,247</sup> The hydrothermal reaction of  $\text{InCl}_3$  with  $\text{Na}_2\text{Se}_4$  in the presence of  $\text{R}_4\text{MX}$  and water at  $110^\circ\text{C}$  for 3 days yielded  $(\text{R}_4\text{M})_2[\text{InCl}_2(\text{Se})_2(\text{Se}_4)_2]$  (see Figure 52(b)). When the molar ratio of  $\text{InCl}_3$  and  $\text{Na}_2\text{Se}_5$  was changed to 1:2 and the reaction was carried out in acetonitrile in the presence of  $\text{Et}_4\text{NBr}$ ,  $(\text{Et}_4\text{N})_3[\text{In}_3(\text{Se})_3(\text{Se}_4)_3]$  (see Figure 52(c)) was formed. The reaction with thallium chloride resulted in the formation of the analogous salt.<sup>247</sup>

The reaction of elemental gallium, indium, or thallium with  $(\text{Ph}_4\text{P})_2\text{Se}_5$  and an excess of elemental selenium in a sealed, evacuated Pyrex tube at  $200^\circ\text{C}$  yielded red crystals of  $(\text{Ph}_4\text{P})[\text{M}(\text{Se}_6)_2]$  ( $\text{M}=\text{Ga}, \text{In}, \text{Tl}$ ), which exhibit an open layered framework.<sup>248</sup> These compounds have congruent melting points and transform into a glassy state upon cooling. The

materials recrystallize when subsequently reheated. The materials are also capable of ion-exchange reactions, which could lead to the possibility for generation of microporous materials.

A hydrothermal reaction involving elemental indium, selenium, and *trans*-1,4-diaminocyclohexane in water at  $170^\circ\text{C}$  for 10 days afford  $(\text{C}_6\text{H}_{16}\text{N}_2)[\text{In}_2(\text{Se})_3(\text{Se}_2)]$ , which contains polymeric  $[\text{In}_2(\text{Se})_3(\text{Se}_2)]^{2-}$  chains (see Figure 53(a)).<sup>249</sup> The optical bandgap of  $(\text{C}_6\text{H}_{16}\text{N}_2)[\text{In}_2(\text{Se})_3(\text{Se}_2)]$  was estimated to be 2.23 eV at room temperature.

The metathetical reaction of  $[\text{Li}(\text{TMEDA})]_2\{(\text{SPh}_2\text{P})_2\text{C}\}_2\text{Se}_2$  and  $\text{TlOEt}$  at a low temperature cleanly affords  $\text{Tl}_2\{(\text{SPh}_2\text{P})_2\text{C}\}_2\text{Se}_2$  in good yield.<sup>250</sup> The molecular structure is shown in Figure 53(b). The Se–Se bond length of 2.531 Å is significantly longer than the single bond, but it is near the Se–Se

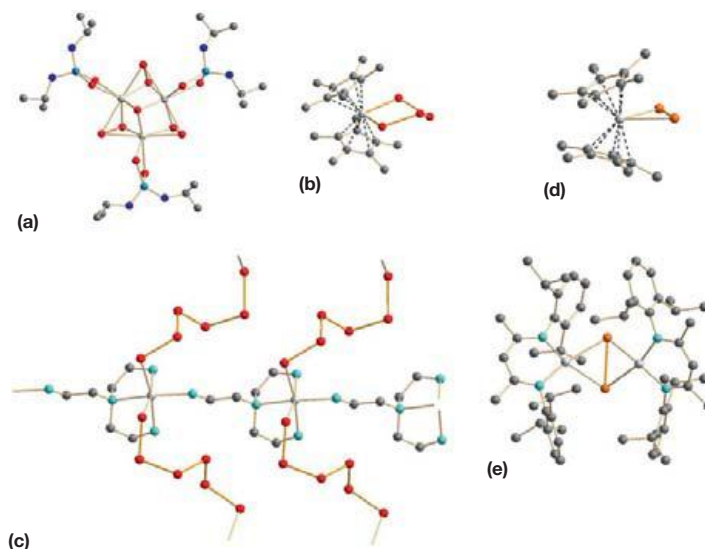
**Table 5** Transition metal complexes involving polyselenido and tellurido ligands in their different ligation modes

Ligation mode	Selenium		Tellurium	
	No <sup>a</sup>	Central atom	No <sup>a</sup>	Central atom
	6	Ag, Fe, Mo, Mn, Ti	3	Cr, Hg
	12	Ag, Fe, Mn, Mo, Ni, Re, Ru	5	Fe, Hg
	44	Ag, Au, Co, Cu, Hf, Hg, Mn, Mo, Nb, Ni, Pd, Rer, Ru, Ti, V, W, Y, Zr	28	Ag, Au, Co, Cr, Cu, Hg, Mn, Mo, Ni, Pt, Rh, Ti, V, W
	22	Ag, Co, Cr, Cu, Fe, Hg, Mn, Pd, Re, Rh, Ru	18	Ag, Au, Cr, Cu, Hg, Zn
	13	Co, Fe, Mn, Mo, Re	34	Ag, Cd, Co, Cr, Cu, Fe, Hg, Mn, Mo, Nb, Ru, W
	86	Ag, Au, Cd, Cu, Fe, Hf, Hg, Ir, Mn, Mo, Ni, Os, Pd, Pt, Re, Ti, V, W, Zn, Zr	20	Ag, Cd, Cr, Cu, Hg, Mo, Pd, W, Zn, Zr
	31	Cr, Cu, Ir, Mo, Nb, Ni, Os, Pt, V, W	15	Fe, Mo, Ni, Ta, Ti, Zr
	53	Cr, Fe, Hf, La, Mn, Mo, Nb, Ni, Ru, V, W	17	Cu, Fe, Mo, Nb, Ni, Pd, Pt, W
	8	Fe, Ir, Mn, Mo, Pd, Rh	1	Nb, Cr
	2	Cr, Fe, Mn	2	Fe, Mn, Re

<sup>a</sup>Number of complexes for which the crystal structure is known.

Data according to CSD, version 5.32, Cambridge Crystallographic Data Center 2011.





**Figure 56** (a) ( $\mu_3$ -Selenido)-tris( $\mu$ -diselenido)-tris( $O,O'$ -di-isopropylidisenophosphato)-trimolybdenum- $O,O'$ -diisopropylidisenophosphate,<sup>256</sup> (b) bis( $\eta^5$ -pentamethylcyclopentadienyl)tetraselenidomolybdenum,<sup>257</sup> (c) *catena*-[( $\mu$ -tris(2-aminoethyl)amine)-( $\mu$ -hexaselenido)dimanganese(ii)],<sup>258</sup> (d) bis( $\eta^5$ -pentamethylcyclopentadienyl) ditelluridomolybdenum,<sup>257</sup> and (e) ( $\mu_3$ -ditellurido)-bis( $N,N'$ -bis(2,6-diisopropylphenyl)pent-2-en-2-amino-4-imino)dinickel.<sup>259</sup> Selenium atoms are depicted in red, tellurium in orange, oxygen in dark blue, phosphorus in light blue, nitrogen in turquoise, carbon atoms in dark gray, and metal atoms in light gray.

bond of 2.508 Å observed in  $[\text{Li}(\text{TMEDA})]_2\{(\text{SPh}_2\text{P})_2\text{C}\}_2\text{Se}_2$ .<sup>251</sup> Their respective Pauling bond orders of 0.76 and 0.79 are close to the value 0.84 calculated for the bond order of the Se–Se bond in  $(\text{SePR}_2\text{NPR}_2\text{Se})_2$  with the observed elongation of 6%.<sup>222</sup> This is consistent with the conclusion that the long Se–Se bond is a consequence of the dimerization of the  $(\text{SPh}_2\text{P})_2\text{CSe}^-$  radical anion.<sup>250</sup>

The few known polymeric telluroindates have been prepared by solvothermal reactions.<sup>252–255</sup> The polymeric anions all have a formal composition  $\text{In}_2\text{Te}_6^{2-}$ , they are all composed of similar cyclic five-membered  $\text{TeInTeTeInTe}$  building blocks, but their overall structures differ considerably, as shown in Figure 54.

The interest in anionic indium or thallium networks comes from their thermal behavior. Thermogravimetry and differential scanning calorimetry studies have shown that they may provide a low-temperature route to binary chalcogenides of catalytic and electronic importance and therefore they may prove to be suitable precursors for fabrication of thin films.<sup>247,248</sup>

### 1.07.5 Transition Metal Complexes

Both anionic and molecular polyselenides and tellurides can coordinate to both hard and soft transition metal centers and they form complexes with most transition metals. They are flexible ligands and show terminal, side-on, bridging, and chelating coordination and can therefore be involved in a large number of mononuclear and polynuclear complexes.<sup>15–17,146</sup> The ligation modes are shown in Figure 55 and a summary of polyselenido and tellurido complexes for which crystal structures are known is shown in Table 5.

Some recent examples of the structures of the complexes are shown in Figure 56.

All bond parameters of chalcogen–chalcogen bonds in the chelating and bridging ligands (see Figure 56(b) and 56(c)) indicate normal single bonds. By contrast, the  $\text{E}_2^{2-}$  ( $\text{E}=\text{Se}, \text{Te}$ ) ligands that are coordinated side-on show bond lengths that are somewhat shorter than single bonds (the Se–Se bonds are in the range 2.314–2.336 Å in the complex in Figure 56(a) and the Te–Te bonds span the range of 2.696–2.699 Å in the complex in Figure 56(e)). The side-on donation involves the antibonding  $\pi^*$  orbital of the chalcogen–chalcogen bond and the coordination therefore strengthens the bond in question.

### 1.07.6 Conclusion

Catenation, that is, the tendency to form compounds containing cumulated chalcogen–chalcogen bonds, is a characteristic feature for group 16 elements sulfur, selenium, and tellurium. They all exhibit a large number of both cyclic and acyclic homo- and heterochalcogen molecules and ions. Many main group and transition metal compounds and ions also contain polychalcogen fragments. The structural chemistry of sulfur and polysulfides is particularly extensive, but while information of polyselenium and -tellurium chemistry is much sparser, recent years have seen rapid progress also in this area of chemistry.

The bonding, the geometrical features, and the intermolecular interactions can be described in terms of  $np^2$ – $np^2$  interactions, hyperconjugative  $np^2$ – $\sigma^*$  interactions, and  $\pi^*$ – $\pi^*$  interactions. The significance of the latter two interactions increases when going down group 16, and they play a major role in the so-called secondary bonding interactions. They also explain why the structures and properties of selenium and tellurium species differ from those of sulfur.

Binary chalcogenides are promising materials in many electronic devices. Active research interest is currently being

directed into synthesis and characterization of novel nonmetallic polychalcogen compounds, as well as toward transition metal complexes containing polychalcogenido ligands. The objective is to use these compounds as single-source precursors for the generation of thin films for electronic applications. Many polychalcogen compounds also find utility in organic and inorganic synthetic chemistry. The advances in selenium and tellurium chemistry benefit both fundamental and applied research.

## References

- Stuedel, R.; Eckert, B. *Topics Curr. Chem.* **2003**, *230*, 1–80.
- Laitinen, R. S.; Pekonen, P.; Suontamo, R. *Coord. Chem. Rev.* **1994**, *130*, 1–62.
- Krossing, I. In *Handbook of Chalcogen Chemistry*; Devillanova, F. A., Ed.; RSC Publishing: Cambridge, MA, 2007; pp 381–416.
- Brownridge, S.; Krossing, I.; Passmore, J.; Jenkins, H. D. B.; Rootbottom, H. K. *Coord. Chem. Rev.* **2000**, *197*, 397–481.
- Beck, J. *Coord. Chem. Rev.* **1997**, *163*, 55–70.
- Graf, C.; Assoud, A.; Mayasree, O.; Kleinke, H. *Molecules* **2009**, *14*, 3115–3131.
- Kanatzidis, M. G. *Comm. Inorg. Chem.* **1990**, *10*, 161–195.
- Drake, G. W.; Kolis, J. W. *Coord. Chem. Rev.* **1994**, *137*, 131–178.
- Okazaki, R. *Phosphorus Sulfur Silicon Relat. Elem.* **2001**, *168–169*, 41–50.
- Chivers, T. A *Guide to Chalcogen-Nitrogen Chemistry*; World Scientific Publishing: Hackensack, NJ, 2005; 318.
- Takeda, N.; Tokitoh, N.; Okazaki, R. In *Handbook of Chalcogen Chemistry*; Devillanova, F. A., Ed.; RSC Publishing: Cambridge, MA, 2007; pp 195–222.
- Xu, Z. In *Handbook of Chalcogen Chemistry*; Devillanova, F. A., Ed.; RSC Publishing: Cambridge, MA, 2007; pp 457–476.
- Draganjac, M.; Rauchfuss, T. B. *Angew. Chem. Int. Ed Engl.* **1985**, *24*, 742–757.
- Müller, A.; Diemann, E. *Adv. Inorg. Chem.* **1987**, *31*, 89–122.
- Kolis, J. W. *Coord. Chem. Rev.* **1990**, *105*, 195–219.
- Ansari, M. A.; Ibers, J. A. *Coord. Chem. Rev.* **1990**, *100*, 223–266.
- Roof, L. C.; Kolis, J. W. *Chem. Rev.* **1993**, *93*, 1037–1080.
- Chivers, T. J. *Chem. Soc. Dalton Trans.* **1996**, 1185–1194.
- Alcock, N. W. *Adv. Inorg. Chem. Radiochem.* **1972**, *15*, 1–58.
- Keller, R.; Holzapfel, W. B.; Schulz, H. *Phys. Rev. B* **1977**, *16*, 4404–4412.
- Adenis, C.; Langer, V.; Lindqvist, O. *Acta Crystallogr.* **1989**, *C45*, 941–942.
- Hejny, C.; McMahon, M. I. *Phys. Rev. B* **2004**, *70*, 184109/1–184109/5 and references therein.
- Akahama, Y.; Kobayashi, M.; Kawamura, H. *Phys. Rev. B* **1993**, *47*, 20–26 and references therein.
- Aoki, K.; Shimomura, O.; Minomura, S. J. *Phys. Soc. Japan* **1980**, *48*, 551–556.
- Jamieson, J. C.; McWhan, D. B. J. *Chem. Phys.* **1965**, *43*, 1149–1152.
- Parthasarathy, G.; Holzapfel, W. B. *Phys. Rev. B* **1988**, *37*, 8499–8501.
- Hejny, C.; McMahon, M. I. *Phys. Rev. Lett.* **2003**, *91*, 215502/1–215502/4.
- Bridgman, P. W. *Proc. Am. Acad. Arts Sci.* **1952**, *81*, 165–251.
- Bundy, F. P.; Dunn, K. J. *J. Chem. Phys.* **1979**, *71*, 1550–1558.
- Bundy, F. P.; Dunn, K. J. *Phys. Rev. B* **1980**, *22*, 3157–3164.
- Bundy, F. P.; Dunn, K. J. *Phys. Rev. Lett.* **1980**, *44*, 1623–1626.
- Misra, R.; Goel, S.; Tripathi, S. K.; Agnihotri, A. K.; Kumar, A. *Physica B* **1990**, *167*, 195–199.
- Smith, K. W.; Smith, S. D.; Badesha, S. S. J. *Am. Chem. Soc.* **1984**, *106*, 7247–7248.
- Cherin, P.; Unger, P. *Acta Crystallogr. Sect. B* **1972**, *28*, 313–317.
- Maaninen, A.; Konu, J.; Laitinen, R. S.; Chivers, T.; Schatte, G.; Pietikäinen, J. *Inorg. Chem.* **2001**, *40*, 3539–3543.
- Marsh, R. E.; Pauling, L.; McCullough, J. D. *Acta Crystallogr.* **1953**, *6*, 71–75.
- Maaninen, T.; Konu, J.; Laitinen, R. S. *Acta Crystallogr. Sect. E* **2004**, *60*, o2235–o2237.
- Foss, O.; Janickis, V. J. *Chem. Soc. Dalton Trans.* **1980**, 624–627.
- Stuedel, R.; Papavassiliou, M.; Strauss, E.-M.; Laitinen, R. *Angew. Chem. Int. Ed Engl.* **1986**, *25*, 99–101.
- Miyamoto, Y. *Jpn. J. Appl. Phys.* **1980**, *19*, 1813–1819.
- Pekonen, P.; Taavitsainen, J.; Laitinen, R. S. *Acta Chem. Scand.* **1998**, *52*, 1188–1193.
- Pekonen, P.; Taavitsainen, J.; Laitinen, R. S., unpublished results.
- Stuedel, R.; Strauss, E.-M. *Z. Naturforsch.* **1981**, *36b*, 1085–1088.
- Stuedel, R.; Papavassiliou, M.; Jensen, D.; Seppelt, K. *Z. Naturforsch.* **1988**, *43b*, 245–247.
- Stuedel, R.; Papavassiliou, M.; Baumgart, F. *Z. Naturforsch.* **1991**, *46b*, 1674–1678.
- Pekonen, P.; Laitinen, R. S.; Hiltunen, Y. *J. Chem. Soc. Dalton Trans.* **1992**, 2885–2887.
- Taavitsainen, J.; Laitinen, R. S. *Main Group Chem.* **1999**, *3*, 59–67.
- Coppens, P.; Yang, Y. W.; Blessing, R. H.; Cooper, W. F.; Larsen, F. K. *J. Am. Chem. Soc.* **1977**, *99*, 760–766.
- Rettig, S. J.; Trotter, I. *Acta Crystallogr. Sect. C* **1987**, *43*, 2260–2262.
- Templeton, L. K.; Templeton, D. H.; Zalkin, A. *Inorg. Chem.* **1976**, *15*, 1999–2001.
- Goldsmith, L. M.; Strouse, C. E. *J. Am. Chem. Soc.* **1977**, *99*, 7580–7589.
- Watanabe, Y. *Acta Crystallogr. Sect. B* **1974**, *30*, 1396–1401.
- Staffel, R.; Müller, U.; Ahle, A.; Dehnicke, K. *Z. Naturforsch.* **1991**, *46b*, 1287–1292.
- Dietz, J.; Müller, U.; Müller, V.; Dehnicke, K. *Z. Naturforsch.* **1991**, *46b*, 1293–1299.
- Bacchi, A.; Baratta, W.; Calderazzo, F.; Marchetti, F.; Pelizzi, G. *Angew. Chem. Int. Ed Engl.* **1994**, *33*, 193–195.
- Cernosek, Z.; Ruzicka, A.; Holubova, J.; Cernokova, E. *Main Group Met. Chem.* **2007**, *30*, 231–233.
- Stuedel, R.; Schuster, F. J. *Mol. Struct.* **1978**, *44*, 143–157.
- Stuedel, R.; Reinhardt, R.; Schuster, F. *Angew. Chem. Int. Ed Engl.* **1977**, *16*, 715.
- Stuedel, R.; Steidel, J.; Pickardt, J.; Schuster, F.; Reinhardt, R. *Z. Naturforsch.* **1980**, *35b*, 1378–1383.
- Bogomolov, V. N.; Zadorozhnyi, A. I.; Petranovskii, V. P.; Fokin, A. V.; Kholodkevich, S. V. *JETP Lett.* **1979**, *29*, 373–375.
- Bogomolov, V. N.; Zadorozhnyi, A. I.; Pavlova, T. M.; Petranovskii, V. P.; Podkhaluzin, V. P.; Kholkin, A. L. *JETP Lett.* **1980**, *31*, 378–381.
- Pietikäinen, J.; Laitinen, R. S. *J. Chem. Soc. Chem. Commun.* **1998**, 2381–2382.
- Laitinen, R. S.; Pakkanen, T. A. *Inorg. Chem.* **1987**, *26*, 2598–2603.
- Sheldrick, W. S.; Wachhold, M. *Angew. Chem. Int. Ed Engl.* **1995**, *34*, 450–451.
- Sheldrick, W. S.; Wachhold, M. *J. Chem. Soc. Chem. Commun.* **1996**, *5*, 607–608.
- Kromm, A.; Sheldrick, W. S. *Z. Anorg. Allg. Chem.* **2009**, *632*, 191–194.
- Deiseroth, H.-J.; Wagener, M.; Neumann, E. *Eur. J. Inorg. Chem.* **2004**, 4755–4758.
- Mironov, Y. V.; Pell, M. A.; Ibers, J. A. *Angew. Chem. Int. Ed Engl.* **1996**, *35*, 2854–2856.
- Günther, A.; Heise, M.; Wagner, F. R.; Ruck, M. *Angew. Chem. Int. Ed.* **2011**, *50*, 9987–9990.
- Günther, A.; Isaeva, A.; Baranov, A. I.; Ruck, M. *Chem. Eur. J.* **2011**, 6382–6388.
- Aris, D.; Beck, J.; Decken, A.; Dionne, I.; Schmedt auf der Günne, J.; Hoffbauer, W.; Köchner, T.; Krossing, I.; Passmore, J.; Rivard, E.; Steden, F.; Wang, X. *Dalton Trans.* **2011**, *40*, 5865–5880 and references therein.
- Deiseroth, H.-J.; Reiner, C.; Schlosser, M.; Wang, X.; Ajaz, H.; Kienle, L. *Inorg. Chem.* **2007**, *46*, 8418–8425 and references therein.
- Demchenko, P. Yu.; Gkadyshvskii, R. E.; Volkov, S. V.; Yanko, O. G.; Kharkova, L. B.; Fokina, Z. A.; Fokin, A. A. *Chem. Commun.* **2010**, *46*, 4520–4522 and references therein.
- Köcher, T.; Trapp, N.; Engesser, T. A.; Lehner, A. J.; Röhr, C.; Riedel, S.; Knapp, C.; Scherer, H.; Krossing, I. *Angew. Chem. Int. Ed.* **2011**, *50*, <http://dx.doi.org/10.1002/anie.201104666> and references therein.
- Dickerson, C. A.; Fisher, M. J.; Sykora, R. E.; Albrecht-Schmitt, T. E.; Cody, J. A. *Inorg. Chem.* **2002**, *41*, 640–642.
- Goldbach, A.; Fayon, F.; Vosegaard, T.; Wachhold, M.; Kanatzidis, M. G.; Massiot, D.; Saboungi, M.-L. *Inorg. Chem.* **2003**, *42*, 6996–7000.
- Wachhold, M.; Kanatzidis, M. G. *J. Am. Chem. Soc.* **1999**, *121*, 4189–4195.
- Laitinen, R.; Niinistö, L.; Stuedel, R. *Acta Chem. Scand.* **1979**, *A33*, 737–747.
- Weiss, J. *Z. Anorg. Allg. Chem.* **1977**, *435*, 113–118.
- Calvo, C.; Gillespie, R. J.; Vekris, J. E.; Ng, H. N. *Acta Crystallogr. Sect. B* **1978**, *34*, 911–912.
- Boudreau, R. A.; Haendler, H. M. *J. Solid State Chem.* **1981**, *36*, 289–296.
- Laitinen, R.; Rautenberg, N.; Steidel, J.; Stuedel, R. *Z. Anorg. Allg. Chem.* **1982**, *486*, 116–128.
- Giolando, D. M.; Papavassiliou, M.; Pickardt, J.; Rauchfuss, T. B.; Stuedel, R. *Inorg. Chem.* **1988**, *27*, 2596–2600.
- Laitinen, R.; Stuedel, R. *J. Mol. Struct.* **1980**, *68*, 19–32.
- Eysel, H. H. *J. Mol. Struct.* **1982**, *78*, 203–213.
- Stuedel, R.; Strauss, E.-M. *Angew. Chem. Int. Ed Engl.* **1984**, *23*, 362–363.
- Laitinen, R.; Stuedel, R.; Strauss, E.-M. *J. Chem. Soc. Dalton Trans.* **1985**, 1869–1875.

88. Laitinen, R. S.; Pekonen, P.; Hiltunen, Y.; Pakkanen, T. A. *Acta Chem. Scand.* **1989**, *43*, 436–440.
89. Chivers, T.; Laitinen, R. S.; Schmidt, K. J. *Can. J. Chem.* **1992**, *70*, 719–725.
90. Komulainen, J.; Laitinen, R. S.; Suontamo, R. J. *Can. J. Chem.* **2002**, *80*, 1435–1443.
91. Pekonen, P.; Hiltunen, Y.; Laitinen, R. S.; Pakkanen, T. A. *Inorg. Chem.* **1991**, *30*, 3679–3682.
92. Cooper, R.; Culka, J. V. *J. Inorg. Nucl. Chem.* **1967**, *29*, 1877–1879.
93. Binnewies, M. Z. *Anorg. Allg. Chem.* **1976**, *422*, 43–46.
94. Chivers, T.; Laitinen, R. S.; Schmidt, K. J.; Taavitsainen, J. *Inorg. Chem.* **1993**, *32*, 337–340.
95. Pupp, M.; Weiss, J. Z. *Anorg. Allg. Chem.* **1978**, *440*, 31–36.
96. Weiss, J.; Pupp, M. *Angew. Chem.* **1970**, *82*, 447–448; Weiss, J.; Pupp, M. *Acta Crystallog. Sect. B* **1972**, *28*, 3653–3655; Weiss, J.; Pupp, M. *Angew. Chem. Int. Ed. Engl.* **1970**, *9*, 463–464.
97. Nagata, K.; Hayashi, H.; Miyamoto, Y. *Fukuoka Univ. Sci. Rep.* **1988**, *18*, 23–33.
98. Nagata, K.; Hayashi, H.; Miyamoto, Y. *Fukuoka Univ. Sci. Rep.* **1988**, *18*, 35–46.
99. Ahmed, E.; Ruck, M. *Coord. Chem. Rev.* **2011**, *255*, 2892–2903.
100. Krossing, I.; Passmore, J. *Inorg. Chem.* **1999**, *38*, 5203–5211 and references therein.
101. Tuononen, H. M.; Suontamo, R.; Valkonen, J.; Laitinen, R. S. *J. Phys. Chem. A* **2004**, *108*, 5670–5677.
102. Collins, M. J.; Gillespie, R. J.; Sawyer, J. F.; Schrobilgen, G. J. *Inorg. Chem.* **1986**, *25*, 2053–2057.
103. Beck, J. Z. *Naturforsch.* **1990**, *45b*, 413–416.
104. Beck, J.; Fischer, A.; Stankowski, A. Z. *Anorg. Allg. Chem.* **2002**, *628*, 2542–2548.
105. Burns, R. C.; Gillespie, R. J.; Luk, W.-C.; Slim, D. R. *Inorg. Chem.* **1979**, *18*, 3086–3094.
106. Collins, M. J.; Gillespie, R. J.; Sawyer, J. F. *Acta Crystallogr. Sect. C* **1988**, *44*, 405–409.
107. Beck, J. *Chem. Ber.* **1995**, *128*, 23–27.
108. Beck, J.; Bock, G. Z. *Anorg. Allg. Chem.* **1996**, *622*, 823–828.
109. Gillespie, R. J.; Luk, W. C.; Maharajh, E.; Slim, D. R. *Inorg. Chem.* **1977**, *16*, 892–896.
110. Burns, R. C.; Collins, M. J.; Eicher, S. M.; Gillespie, R. J.; Sawyer, J. F. *Inorg. Chem.* **1988**, *27*, 1807–1813.
111. Gillespie, R. J. *Chem. Soc. Rev.* **1979**, *8*, 315–352.
112. Passmore, J. In *Studies in Inorganic Chemistry*; Stedel, R., Ed.; Elsevier: Amsterdam, 1992; Vol. 14, pp 373–406.
113. Lyne, P. D.; Mingos, D. M. P.; Ziegler, T. J. *Chem. Soc. Dalton Trans.* **1992**, 2743–2747.
114. Cameron, T. S.; Deeth, R. J.; Dionne, I.; Du, H.; Jenkins, H. D. B.; Krossing, I.; Passmore, J.; Roobottom, H. K. *Inorg. Chem.* **2000**, *39*, 5614–5631 and references therein.
115. Beck, J. *Angew. Chem. Int. Ed Engl.* **1990**, *29*, 293–295.
116. Collins, M. J.; Gillespie, R. J.; Sawyer, J. F. *Inorg. Chem.* **1987**, *26*, 1476–1481.
117. DeLucia, M. L.; Coppens, P. *Inorg. Chem.* **1978**, *17*, 2336–2338.
118. Pauling, L. *The Nature of the Chemical Bond*, 3rd ed.; Cornell University Press: Ithaca, NY, 1960.
119. Beck, J.; Müller-Buschbaum, K. Z. *Anorg. Allg. Chem.* **1997**, *623*, 409–413.
120. Beck, J.; Bock, G. *Angew. Chem. Int. Ed Engl.* **1995**, *34*, 2559–2561.
121. Burns, R. C.; Collins, M. J.; Gillespie, R. J.; Schrobilgen, G. J. *Inorg. Chem.* **1986**, *25*, 4465–4469.
122. Brownridge, S.; Calhoun, L.; Jenkins, H. D. B.; Laitinen, R. S.; Murchie, M. P.; Passmore, J.; Pietikäinen, J.; Rautiainen, J. M.; Sanders, J. C. P.; Schrobilgen, G. J.; Suontamo, R. J.; Tuononen, H. M.; Valkonen, J. U.; Wong, C.-M. *Inorg. Chem.* **2009**, *48*, 1938–1959.
123. Burns, R. C.; Chan, W. L.; Gillespie, R. J.; Luk, W. C.; Sawyer, J. F.; Slim, D. R. *Inorg. Chem.* **1980**, *19*, 1432–1439.
124. Collins, M. J.; Gillespie, R. J.; Sawyer, J. F.; Schrobilgen, G. J. *Acta Crystallogr. Sect. C* **1986**, *42*, 13–16.
125. Beck, J.; Hilbert, T. Z. *Anorg. Allg. Chem.* **2000**, *626*, 837–844.
126. Boldrini, P.; Brown, I.; Gillespie, R. J.; Ireland, P. R.; Luk, W. C.; Slim, D. R.; Vekris, J. E. *Inorg. Chem.* **1976**, *15*, 765–770.
127. Beck, J.; Fischer, A. Z. *Anorg. Allg. Chem.* **1997**, *623*, 780–784.
128. Beck, J.; Wetterau, J. *Inorg. Chem.* **1995**, *34*, 6202–6204.
129. Beck, J.; Stankowski, A. Z. *Naturforsch.* **2001**, *56b*, 453–457.
130. Beck, J.; Fischer, A. Z. *Anorg. Allg. Chem.* **2002**, *628*, 369–372.
131. Beck, J.; Bock, G. Z. *Anorg. Allg. Chem.* **1994**, *620*, 1971–1975.
132. Drake, G. W.; Schimek, G. L.; Kolis, J. W. *Inorg. Chem.* **1996**, *35*, 1740–1742.
133. Klapötke, T.; Passmore, J. *Acc. Chem. Res.* **1989**, *22*, 234–240.
134. Brownridge, S.; Cameron, T. S.; Passmore, J.; Schatte, G.; Way, T. C. *J. Chem. Soc. Dalton Trans.* **1996**, 2553–2570.
135. Nandana, W. A. S.; Passmore, J.; White, P. S.; Wong, C.-M. *J. Chem. Soc. Chem. Commun.* **1982**, 1098–1099.
136. Faggiani, R.; Gillespie, R. J.; Kolis, J. W.; Malhotra, K. C. *J. Chem. Soc. Chem. Commun.* **1987**, 591–592.
137. Carnell, M. M.; Grein, F.; Murchie, M. P.; Passmore, J.; Wong, C.-M. *J. Chem. Soc. Chem. Commun.* **1986**, 225–227.
138. Beck, J.; Richter, J.; Pell, M. A.; Ibers, J. A. Z. *Anorg. Allg. Chem.* **1996**, *622*, 473–478.
139. Brownridge, S.; Cameron, T. S.; Du, H.; Knapp, C.; Koeppel, R.; Passmore, J.; Rautiainen, J. M.; Schnoekel, H. *Inorg. Chem.* **2005**, *44*, 1660–1671.
140. Nandana, W. A. S.; Passmore, J.; White, P. S.; Wong, C.-M. *Inorg. Chem.* **1990**, *29*, 3529–3538.
141. Passmore, J.; Sutherland, G. W.; Whidden, T. K.; White, P. S. *J. Chem. Soc. Chem. Commun.* **1980**, 289–290.
142. Brownridge, S.; Crawford, M.-J.; Du, H.; Harcourt, R. D.; Knapp, C.; Laitinen, R. S.; Passmore, J.; Rautiainen, J. M.; Suontamo, R. J.; Knapp, C.; Valkonen, J. *Inorg. Chem.* **2007**, *46*, 681–699.
143. Passmore, J.; White, P. S.; Wong, C. M. *J. Chem. Soc. Chem. Commun.* **1985**, 1178–1179.
144. Nandana, W. A. S.; Passmore, J.; White, P. S.; Wong, C. M. *J. Chem. Soc. Chem. Commun.* **1983**, 526–527.
145. Schrobilgen, G. J.; Burns, R. C.; Granger, P. J. *J. Chem. Soc. Chem. Commun.* **1978**, 957–958.
146. Sheldrick, W. S. In *Handbook of Chalcogen Chemistry*; Devillanova, F. A., Ed.; RSC Publishing: Cambridge, 2007; pp 543–573.
147. Smith, D. M.; Ibers, J. A. *Coord. Chem. Rev.* **2000**, *187*, 200–205.
148. Kanatzidis, M. G.; Das, B. K. *Comments Inorg. Chem.* **1999**, *21*, 29–51.
149. Kanatzidis, M. G.; Huang, S. P. *Coord. Chem. Rev.* **1994**, *130*, 509–621.
150. Wendland, F.; Nather, C.; Bensch, W. Z. *Naturforsch.* **2000**, *55b*, 871–876.
151. König, T.; Eisenmann, B.; Schafer, H. Z. *Anorg. Allg. Chem.* **1983**, *498*, 99–104.
152. Brese, N. E.; Randall, C. R.; Ibers, J. A. *Inorg. Chem.* **1988**, *27*, 940–943.
153. Barrie, P. J.; Clark, R. J. H.; Chung, D.-Y.; Chakrabarty, D.; Kanatzidis, M. G. *Inorg. Chem.* **1995**, *34*, 4299–4304.
154. Fenske, D.; Kraus, C.; Dehnicke, K. Z. *Anorg. Allg. Chem.* **1992**, *607*, 109–112.
155. Müller, V.; Dehnicke, K.; Fenske, D. Z. *Naturforsch.* **1991**, *46b*, 63.
156. Müller, V.; Ahle, A.; Frenzen, G.; Neumüller, B.; Dehnicke, K.; Fenske, D. Z. *Anorg. Allg. Chem.* **1993**, *619*, 1247–1256.
157. Müller, V.; Grebe, C.; Müller, U.; Dehnicke, K. Z. *Anorg. Allg. Chem.* **1993**, *619*, 416–420.
158. Warren, C. J.; Haushalter, R. C.; Bocarsly, A. B. *J. Alloys Comp.* **1996**, *233*, 23–29.
159. Sheldrick, W. S.; Wachhold, M. *Chem. Commun.* **1996**, 607–608.
160. Fenske, D.; Kräuter, G.; Dehnicke, K. *Angew. Chem. Int. Ed Engl.* **1990**, *29*, 390–391.
161. Sheldrick, W. S.; Braunbeck, H. G. Z. *Naturforsch.* **1989**, *44b*, 1397–1401.
162. Klaiber, F.; Petter, W.; Hulliger, F. *J. Solid State Chem.* **1983**, *46*, 112–120.
163. Schreiner, B.; Dehnicke, K.; Maczek, K.; Fenske, D. Z. *Anorg. Allg. Chem.* **1993**, *619*, 1414–1418.
164. Boettcher, P.; Kretschmann, U. *J. Less-Common Metals* **1983**, *95*, 81–91.
165. Sheldrick, W. S.; Schaal, B. Z. *Naturforsch.* **1994**, *49*, 993–996.
166. Reisner, C.; Tremel, W. *J. Chem. Soc. Chem. Commun.* **1997**, 387–388.
167. Kniep, R.; Korte, L.; Mootz, D. Z. *Naturforsch.* **1983**, *38b*, 1–6.
168. Katryniok, D.; Kniep, R. *Angew. Chem. Int. Ed Engl.* **1980**, *19*, 645.
169. Lamoureux, M.; Milne, J. *Can. J. Chem.* **1989**, *67*, 1936–1941.
170. Milne, J. *J. Chem. Soc. Chem. Commun.* **1991**, 1048–1049.
171. Stedel, R.; Plinke, B.; Jensen, D.; Baumgart, F. *Polyhedron* **1991**, *10*, 1037–1048.
172. Krebs, B.; Ahlers, F.-P. *Adv. Inorg. Chem.* **1990**, *35*, 235–317.
173. Kniep, R.; Rabenau, A. *Top. Curr. Chem.* **1983**, *111*, 145–192.
174. Kniep, R.; Mootz, D.; Rabenau, A. Z. *Anorg. Allg. Chem.* **1976**, *422*, 17–38.
175. Rabenau, A.; Rau, H. Z. *Anorg. Allg. Chem.* **1973**, *395*, 273.
176. Bauhofer, W.; Kniep, R. *Mater. Res. Bull.* **1973**, *8*, 989.
177. Rabenau, A.; Rau, H.; Eckerlin, P. *Angew. Chem. Int. Ed Engl.* **1967**, *6*, 706.
178. Rabenau, A.; Rau, H.; Rosenstein, G. *Angew. Chem. Int. Ed Engl.* **1970**, *9*, 802–803.
179. Barnes, N. A.; Godfrey, S. M.; Halton, R. T. A.; Mushtaq, I.; Parsons, S.; Pritchard, R. G.; Sadler, M. *Polyhedron* **2007**, *26*, 1053–1060.
180. Barnes, N. A.; Godfrey, S. M.; Halton, R. T. A.; Mushtaq, I.; Pritchard, R. G.; Sarwar, S. *Dalton Trans.* **2006**, 1517–1523.
181. Lang, E. S.; Fernandez, R. M., Jr.; Silveira, E. T.; Abram, U.; Vazquez-Lopez, E. M. Z. *Anorg. Allg. Chem.* **1999**, *625*, 1401–1404.

182. Boyle, P. D.; Cross, W. I.; Godfrey, S. M.; McAuliffe, C. A.; Pritchard, R. G.; Sarwar, S.; Sheffield, J. M. *Angew. Chem. Int. Ed Engl.* **2000**, *39*, 1796–1798.
183. de Oliveira, G. M.; Faoro, E.; Lang, E. S. *Inorg. Chem.* **2009**, *48*, 4607–4609.
184. Beckmann, J.; Hesse, M.; Poleschner, H.; Seppelt, K. *Angew. Chem. Int. Ed.* **2007**, *46*, 8277–8280.
185. Eide, J.; Foss, O.; Maartmann-Moe, K.; Maberg, O.; Scheie, O. *Acta Chem. Scand.* **1987**, *41A*, 67–76.
186. Foss, O.; Henjum, J.; Maartmann-Moe, K.; Maroy, K. *Acta Chem. Scand.* **1987**, *41A*, 77–86.
187. Foss, O.; Maartmann-Moe, K. *Acta Chem. Scand.* **1987**, *41A*, 121–129.
188. Copolovici, L.; Silvestru, C.; Lippolis, V.; Varga, R. A. *Acta Crystallogr. Sect C* **2007**, *63*, o528–o529.
189. Kubiniok, S.; du Mont, W.-W.; Pohl, S.; Saak, W. *Angew. Chem. Int. Ed Engl.* **1988**, *27*, 431–433.
190. Faggiani, R.; Gillespie, R. J.; Kolis, J. W. *J. Chem. Soc. Chem. Comm.* **1987**, 592–593.
191. Heckmann, G.; Wolmershauser, G. *Chem. Ber.* **1993**, *126*, 1071–1076.
192. Knight, F. R.; Fuller, A. L.; Buhl, M.; Slawin, A. M. Z.; Woollins, J. D. *Inorg. Chem.* **2010**, *49*, 7577–7596.
193. Janickis, V.; Necas, M. Z. *Anorg. Chem.* **2008**, *634*, 905–910.
194. Janickis, V.; Necas, M. Z. *Anorg. Allg. Chem.* **2010**, *636*, 818–823.
195. Müller, B.; Poleschner, H.; Seppelt, K. *Dalton Trans.* **2008**, 4424–4427.
196. Kuhn, N.; Schumann, H.; Boese, R. *Chem. Commun.* **1987**, 1257–1258.
197. Jeske, J.; du Mont, W.-W.; Jones, P. G. *Angew. Chem. Int. Ed.* **1997**, *36*, 2219–2221.
198. Hillier, A. C.; Liu, S.-Y.; Sella, A.; Elsegood, M. R. *J. Angew. Chem. Int. Ed.* **1999**, *38*, 2745–2747.
199. Witthaut, D.; Kirschbaum, K.; Conrad, O.; Giolando, D. M. *Organometallics* **2000**, *19*, 5238–5240.
200. Fischer, H. T. M.; Naumann, D.; Tyrre, W. *Chem. Eur. J.* **2006**, *12*, 2515–2519.
201. Martin, C. D.; Ragogna, P. J. *Ann. Rep. Prog. Chem. Sect. A* **2011**, *107*, 110–124.
202. Chivers, T.; Laitinen, R. S. In *Handbook of Chalcogen Chemistry*; Devillanova, F. A., Ed.; RSC Press: Cambridge, MA, 2007; pp 223–285.
203. Foss, O.; Janickis, V. *J. Chem. Soc. Dalton Trans.* **1980**, 620–623.
204. Roesky, H. W.; Weber, K.-L.; Bats, J. W. *Chem. Ber.* **1984**, *117*, 2686–2692.
205. Maaninen, T.; Tuononen, H. M.; Schatte, G.; Suontamo, R.; Valkonen, J.; Laitinen, R.; Chivers, T. *Inorg. Chem.* **2004**, *43*, 2097–2104.
206. Cordes, A. W.; Glarum, S. H.; Haddon, R. C.; Hallford, J.; Hicks, R. G.; Kennepohl, D. K.; Oakley, R. T.; Palstra, T. T. M.; Scott, S. R. *J. Chem. Soc. Chem. Commun.* **1992**, 1265–1266.
207. Haas, A.; Kasproski, J.; Angermund, K.; Betz, P.; Kruger, C.; Tsay, Y.-H.; Werner, S. *Chem. Ber.* **1991**, *124*, 1895–1906.
208. Maaninen, A.; Konu, J.; Laitinen, R. S.; Chivers, T.; Schatte, G.; Pietikainen, J.; Ahlgren, M. *Inorg. Chem.* **2001**, *40*, 3539–3543.
209. Herberhold, M.; Jellen, W. Z. *Naturforsch.* **1986**, *41b*, 144–148.
210. Cordes, A. W.; Haddon, R. C.; Hicks, R. G.; Oakley, R. T.; Palstra, T. T. M. *Inorg. Chem.* **1992**, *31*, 1802–1808.
211. Haas, A. *J. Organomet. Chem.* **2002**, *646*, 80–93.
212. Maaninen, A.; Laitinen, R. S.; Chivers, T.; Pakkanen, T. A. *Inorg. Chem.* **1999**, *38*, 3450–3454.
213. Haas, A.; Kasproski, J.; Pryka, M. *J. Chem. Soc. Chem. Commun.* **1992**, 1144–1145.
214. Haas, A.; Pryka, M. *J. Chem. Soc. Chem. Commun.* **1994**, 391–392.
215. Blachnik, R.; Lonneck, P.; Boldt, K.; Engelen, B. *Acta Crystallogr. Sect. C* **1994**, *50*, 659–661.
216. Gushwa, A. F.; Belabassi, Y.; Montchamp, J. L.; Richards, A. F. *J. Chem. Cryst.* **2009**, *39*, 337.
217. Bereau, V.; Ibers, J. A. *Acta Crystallogr. Sect. C* **2000**, *56*, 584.
218. Gray, I. P.; Bhattacharyya, P.; Slawin, A. M. Z.; Woollins, J. D. *Chem. Eur. J.* **2005**, *11*, 6221–6227.
219. Hua, G.; Fuller, A. M.; Slawin, A. M. Z.; Woollins, J. D. *Polyhedron* **2011**, *30*, 805–808 and references therein.
220. Hua, G.; Li, Y.; Slawin, A. M. Z.; Woollins, J. D. *Angew. Chem. Int. Ed.* **2008**, *47*, 2857–2859 and references therein.
221. Chivers, T.; Konu, J. In *Selenium and Tellurium Chemistry. From Small Molecules to Biomolecules and Materials*; Woollins, J. D., Laitinen, R. S., Eds.; Springer: Heidelberg, 2011; pp 79–102.
222. Ritch, J. S.; Chivers, T.; Eisler, D. J.; Tuononen, H. J. *Chem. Eur. J.* **2007**, *13*, 4643–4653.
223. Steudel, R. Z. *Naturforsch.* **1983**, *38b*, 543–545.
224. Chivers, T.; Eisler, D. J.; Ritch, J. S.; Tuononen, H. M. *Angew. Chem. Int. Ed.* **2005**, *44*, 4953–4956.
225. Tuononen, H. M., personal communication.
226. Robertson, S. D.; Chivers, T.; Tuononen, H. M. *Inorg. Chem.* **2009**, *48*, 6755–6762.
227. CSD, version 5.32, Cambridge Crystallographic Data Center 2011.
228. Nakayama, J.; Akiyama, I.; Sugihara, Y.; Nishio, T. *J. Am. Chem. Soc.* **1998**, *120*, 10027–10031.
229. Sivapriya, K.; Suguna, P.; Chandrasekaran, S. *Tetrahedron Lett.* **2007**, *48*, 2091–2095.
230. Chivers, T.; Parvez, M.; Peach, M.; Vollmerhaus, R. *J. Chem. Soc. Chem. Commun.* **1992**, 1539–1540.
231. Jeske, J.; du Mont, W.-W.; Jones, P. G. *Angew. Chem. Int. Ed.* **1996**, *35*, 2653–2655.
232. Wieber, M.; Lang, S.; Graf, N. *Phosphorus Sulfur Silicon Relat Elem.* **1993**, *85*, 31.
233. Kückmann, T. L.; Hermsen, M.; Bolte, M.; Wagner, M.; Lerner, H.-W. *Inorg. Chem.* **2005**, *44*, 3449–3458.
234. Yoshida, H.; Kabe, Y.; Ando, W. *Organometallics* **1991**, *10*, 27–29.
235. Jutzi, P.; Mohrke, A.; Müller, A.; Bogge, H. *Angew. Chem. Int. Ed Engl.* **1989**, *28*, 1518–1519.
236. Tokitoh, N.; Matsumoto, T.; Okazaki, R. *Tetrahedron Lett.* **1992**, *33*, 2531–2534.
237. Ramaker, G.; Saak, W.; Haase, D.; Weidenbruch, M. *Organometallics* **2003**, *22*, 5212–5216.
238. Saito, M.; Hashimoto, H.; Tajima, T.; Ikeda, M. *J. Organomet. Chem.* **2007**, *692*, 2729–2735.
239. Matsuhashi, Y.; Tokotoh, N.; Okazaki, R.; Goto, M.; Nagase, S. *Organometallics* **1993**, *12*, 1351–1358.
240. Tokitoh, N.; Matsuhashi, Y.; Okazaki, R. *Tetrahedron Lett.* **1991**, *32*, 6151–6154.
241. Saito, M.; Hashimoto, H.; Tajima, T. *Acta Crystallogr. Sect E* **2010**, *66*, m885–m886.
242. Sheldrick, W. S.; Wachold, M. *Coord. Chem. Rev.* **1998**, *176*, 211–322.
243. Zhang, Q.; Malliakas, C. D.; Kanatzidis, M. G. *Inorg. Chem.* **2009**, *48*, 10910–10912.
244. Banda, R. M. H.; Cusick, J.; Scudder, M. L.; Craig, D. C.; Dance, I. G. *Polyhedron* **1989**, *8*, 1995–1998.
245. Lehman, S. E., Jr.; Schimek, G. L.; Cusick, J. M.; Kolis, J. W. *Inorg. Chim. Acta* **1997**, *260*, 173–181.
246. Kanatzidis, M. G.; Dhingra, S. *Inorg. Chem.* **1989**, *28*, 2024–2026.
247. Dhingra, S. S.; Kanatzidis, M. G. *Inorg. Chem.* **1993**, *32*, 1350–1362.
248. Dhingra, S.; Kanatzidis, M. G. *Science* **1992**, *258*, 1769–1772.
249. Ewing, S. J.; Powell, A. V.; Vaqueiro, P. *J. Solid State Chem.* **2011**, *184*, 1800–1804.
250. Risto, M.; Chivers, T.; Konu, J. *Dalton Trans.* **2011**, *40*, 8238–8246.
251. Konu, J.; Chivers, T.; Tuononen, H. M. *Chem. Eur. J.* **2010**, *16*, 12977–12987.
252. Wang, C.; Haushalter, R. C. *Inorg. Chem.* **1997**, *36*, 3806–3807.
253. Li, J.; Chen, Z.; Emge, T. J.; Proserpio, D. M. *Inorg. Chem.* **1997**, *36*, 1437–1442.
254. Chen, Z.; Li, J.; Proserpio, D. M.; Huang, Z.-X. *Acta Chim. Sinica* **2000**, *58*, 835.
255. Zhou, J.; Daia, J.; Biana, G.-O.; Lia, C.-Y. *Coord. Chem. Rev.* **2009**, *253*, 1221–1247.
256. Liu, C. W.; Fang, C.-S.; Chuang, C.-W.; Lobana, T. S.; Liaw, B.-J.; Wang, J.-C. *J. Organomet. Chem.* **2007**, *692*, 1726–1734.
257. Shin, J. H.; Churchill, D. G.; Bridgewater, B. M.; Pang, K.; Parkin, G. *Inorg. Chim. Acta* **2006**, *359*, 2942–2955.
258. Kromm, A.; Sheldrick, W. S. *Z. Anorg. Allg. Chem.* **2007**, *633*, 529–532.
259. Yao, S.; Xiong, Y.; Zhang, X.; Schlagen, M.; Schwarz, H.; Milsman, C.; Driess, M. *Angew. Chem. Int. Ed.* **2009**, *48*, 4551–4554.

This page intentionally left blank



## 1.08 Catenated Compounds – Group 17 – Polyhalides

L Kloo, KTH Royal Institute of Technology, Stockholm, Sweden

© 2013 Elsevier Ltd. All rights reserved.

1.08.1	Introduction	233
1.08.2	The Triiodide Ion	233
1.08.2.1	The Bonding in Trihalide Ions	235
1.08.2.2	Bonding Trends in Trihalides	236
1.08.3	Polyiodides	237
1.08.4	New Trends in Polyiodide Chemistry	240
1.08.4.1	Structural Confinement	240
1.08.4.2	Metal–Iodide/Iodine Compounds	241
1.08.5	Liquids and Solvent Effects	242
1.08.6	Polybromides – An Emerging Branch of Polyhalide Chemistry	242
1.08.7	Other Polyhalides	244
1.08.8	Applications	245
1.08.8.1	Optical Applications	245
1.08.8.2	X-Ray Contrast Agents	245
1.08.8.3	Triiodide Detection	245
1.08.8.4	Doping of Polymers and Carbons	245
1.08.8.5	Electrolytes	246
1.08.9	Conclusion	247
	Acknowledgment	247
	References	247

### 1.08.1 Introduction

The concept of catenation can be traced to organic chemistry, which essentially is based on the ability of the element carbon to make strong carbon–carbon bonds. Catenation originates from the Greek word for chain, and through its origin from organic chemistry it also implicates that the chains are formed through covalent bonds between the elements involved. This is certainly a characteristic of the organic C–C chains, but it is not so obvious for polyhalides, which will be discussed later. Although carbon chemistry is the most prolific example, catenation is an inherent property of many of the p-block elements. For instance, the lighter pnictogens form tetrahedral  $P_4$  and  $As_4$  molecules and various polymers, sulfur forms ring-shaped  $S_8$  molecules and polymeric species, the chemistry of selenium and tellurium contains many examples of chain structures,<sup>1</sup> etc. Interestingly enough, the tendency to catenation appears to decrease down the groups 14–16, but for the group 17, the halogens, the tendency is the opposite. The reasons can be understood on the basis of the different type of chemical bonding, which will be discussed later in this overview.

There are a few comprehensive reviews on polyiodides in the literature, of which one is fairly recent.<sup>2–5</sup> These reviews offer a rather complete overview of the literature and focus on the aspect of structural chemistry. The objective of the present overview is not to ‘top up’ on published work since 2003; rather, the objective is to use the vast body of information to highlight the fundamental properties of polyiodides in particular and polyhalides in general. The chapter also aims to identify some recent directions of research and some important applications of polyhalides. The polyhalides included in this

work are essentially negatively charged. Also positively charged polyhalogen species exist, but that is a much smaller, less active, and recently reviewed area of research.<sup>4</sup> Therefore, such species are not included in this overview.

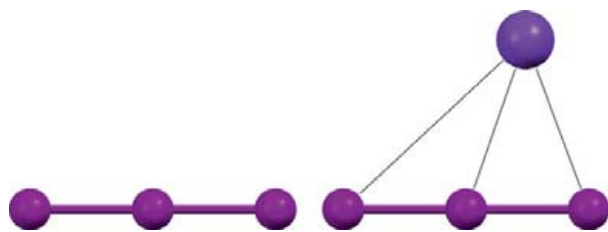
### 1.08.2 The Triiodide Ion

Formally, the group 17 concatenation starts with the well-known  $X_2$  molecules. However, these are thoroughly handled by all textbooks on fundamental, descriptive inorganic chemistry, and consequently we will regard the trihalides as the lowest representatives of concatenated polyhalides. The most extensively studied trihalide is the triiodide ion,  $I_3^-$ . Several hundreds of crystal structures are known. In 2003, we obtained about 500 crystalline triiodide compounds in a search of the Cambridge Structural Database, and since then another 50 or so have been added to the list. Very little new is learned from the additional structures, and the most exciting insights and applications emerge from low-dimensional structures of interacting triiodide ion (*vide infra*). Most likely, most of the triiodide compounds have emerged by accident, in the line of chemical synthesis of completely different molecular targets, often through reactions involving the oxidation by iodine.

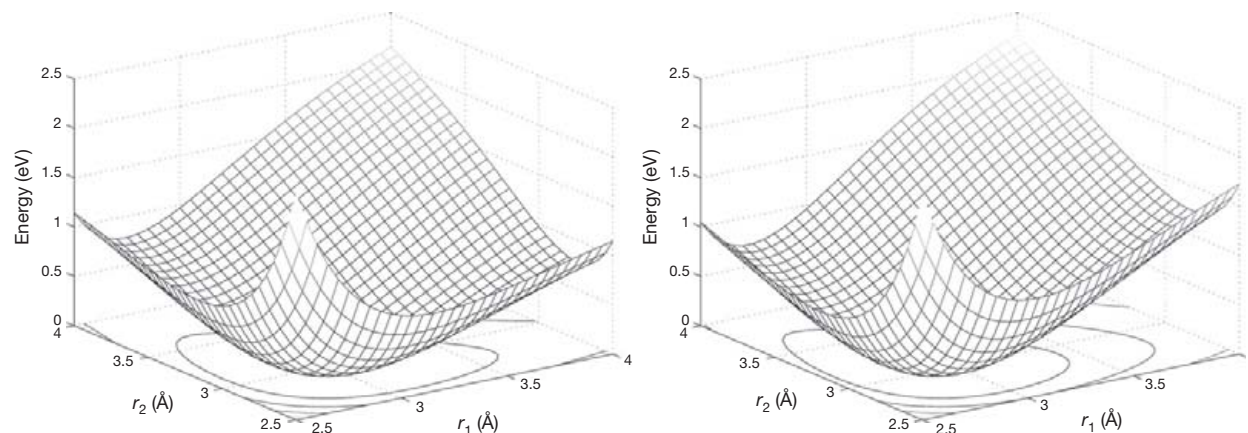
In **Figure 1**, the typical structures of a triiodide ion are shown. If interacting weakly with the surrounding ions or molecules, a centrosymmetric structure is normally observed. Upon stronger interaction with cations or, in particular, hydrogen-bonding components of the compounds, the triiodide is most commonly linearly distorted. However, a few features of the new triiodide structures deserve some attention.

For instance, in the structures of tetrahydrothiophene derivatives, pairs of triiodides interacting at a fairly long distance of 3.79 Å can be observed.<sup>7</sup> These may be regarded as dimer models of long-chain triiodide structures. Reis and coworkers isolated two closely placed (at 3.63 Å) triiodide ions in a host-guest structure and asked the question whether they were packed so closely by the host or were directly interacting.<sup>8</sup> Their conclusion was that the triiodide ions indeed are interacting, and at an unusually short intermolecular distance. Chains of triiodide ions are for instance found in quinoline derivatives with the shortest intermolecular I–I distance of 3.80 Å,<sup>9,10</sup> as a side product in the chemistry of bispyridyls with a distance of 3.69 Å.<sup>11</sup> Model systems for the very old application of iodine/iodide-containing solutions, starch tinting, still offer new insights. In the isolation of a helical sugar, Saenger and coworkers found triiodides in the channels at as short intermolecular distances as 3.66 Å.<sup>12</sup> It is also notable that it is not uncommon that double salts of iodide and triiodides with the same cation are formed.<sup>13–16</sup> Such compounds can be quite stable, and, as discussed in the section on applications, can constitute a problem because of low solubility.<sup>17</sup> An interesting case of polymorphism was discussed by Dance and coworkers showing that crystallization from different solvents in a reproducible way may give different crystal forms of a phosphonium triiodide compound.<sup>18</sup>

The chains of triiodide ions may be regarded as a link to applications. Such compounds are special in the sense that they do not fit into the simple coordination chemistry model of iodine solvation of ions described for the polyiodides below. Instead, the triiodide ions tend to interact end-on along chains at fairly long distances, typically around 4 Å. A few examples are



**Figure 1** A centrosymmetric and a non-centrosymmetric triiodide ion, the latter with a cation coordinated. Data taken from Svensson and Kloo.<sup>6</sup>



**Figure 2** Potential energy surfaces of linear distortion of the triiodide ion for the centrosymmetric and non-centrosymmetric configurations. Data taken from Svensson and Kloo.<sup>6</sup>

given below, and considering the applications noted at the end of this chapter, it is notable that the stacking, structural confinement, of triiodide ions is a unique and important phenomenon in polyiodide chemistry. Lu and coworkers reported two-dimensional sheets of triiodide ions, albeit the inter-triiodide distances appear rather long.<sup>19</sup> A crystal engineering approach afforded chains of triiodides using long-chain diammonium cations.<sup>20</sup> The inter-triiodide contacts observed are 4.13–4.17 Å. Using a substituted tetrathiafulvalene, an anisotropic organic metal was formed, containing both stacked fulvalene molecules and chains of triiodide ions along the plane of stacking.<sup>21</sup> The inter-triiodide distances found are around 3.90 Å.

In the crystalline solids, the triiodide ion most typically exists in two forms: either linear and centrosymmetric or non-centrosymmetric (Figure 1). Most commonly, the triiodide ion is slightly linearly distorted. One very important factor controlling the level of distortion is cation coordination. A cation is often found in the position indicated in Figure 1 (right). The degree of polarization determines the degree of distortion. In addition, in solution, most notably for strongly donating solvents, similar effects can be observed, in particular, when the solvent molecules interact with the triiodide ion *via* hydrogen bonding. The strongly polarized hydrogen atom as donor can be regarded as mimicking the effect of a cation. The reason for this facile linear distortion is the extremely low energy required; see Figure 2, in which the flat one-dimensional potential energy surfaces are shown for a centrosymmetric and non-centrosymmetric triiodide ion. In contrast, angular distortions are much more rarely observed in solid structures, since the energy required for bending distortions is considerably higher. This difference can be traced to the  $\sigma$ -type of bonding involving the valence p-orbitals, as discussed below.

The extremely low energy required to pull the terminal iodine atom far away from the remaining I<sub>2</sub> unit can directly be connected to the special form of electrical conductivity observed in many polyiodide compounds – the Grotthuss mechanism of conductivity.<sup>22</sup> Initially, the mechanism was used to explain the conductivity properties of water through hopping protons. It is equally well applied to polyiodides, where the hopping units instead are the iodide ions. This phenomenon is discussed in more detail later and in the light of polyiodide bonding.

In the ideal case, the linear and centrosymmetric triiodide ion has D<sub>∞h</sub> symmetry. The consequence in terms of group

**Table 1** Typical vibration characteristics of a centrosymmetric, linear triiodide ion<sup>6</sup>

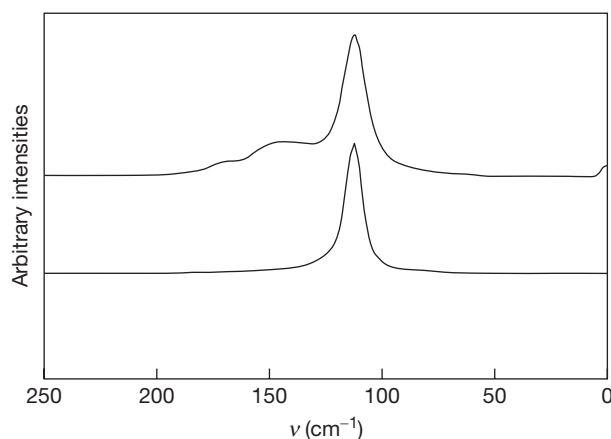
Modes of vibration	Typical frequency (cm <sup>-1</sup> )	Selection rules
Symmetric stretch ( $\Sigma_g^+$ )	110	Raman active
Asymmetric stretch ( $\Sigma_u^+$ )	145	IR active
Bending ( $\Pi_u$ )	75	IR active

theory is that it exhibits four normal vibration modes: the symmetrical stretch ( $\Sigma_g^+$  symmetry,  $\nu_1$ ), the asymmetrical stretch ( $\Sigma_u^+$  symmetry,  $\nu_3$ ), and the doubly degenerate bending modes ( $\Pi_u$  symmetry,  $\nu_2$ ). The combination of comparatively weak I–I bonding (bond order of 0.5), extremely flat potential energy surface of linear distortion, and the high atom mass of iodine make the frequencies of the vibration modes quite low.

This of course has some consequences. First, the vibrational modes are not readily observable using a standard experimental setup for infrared (IR) spectroscopy with a typical cutoff at about 200 or 400 cm<sup>-1</sup>. One needs optics (primarily IR source, beamsplitter, and detector) for far-IR spectroscopy. Second, because of the low energy of vibrational excitation, one should be aware that all modes typically are highly excited at ambient temperatures. Since excitation of vibrational modes affects the vibrational amplitudes, this again has implications for the shape of the potential energy surface and, as a consequence, also the Grotthuss mechanism of conductivity mentioned above. The technical challenges together with the fact that the triiodide modes of vibration render small changes in the molecular dipole moment typically give rather weak and broad bands in IR spectra. IR spectroscopy is a feasible but not optimal technique for the study of triiodide and polyiodide compounds. Instead, the large polarizability of the triiodide ion makes it highly suitable for Raman spectroscopic studies. Typically, the vibrational bands, allowed by symmetry, come out very strongly and one can obtain excellent Raman spectra even at very low concentrations in solution. However, surface-absorbed triiodide or polyiodide species still require an extra boost in sensitivity, such as from Raman-enhanced spectroscopy, to be detectable. The characteristics of the triiodide vibrational modes are shown in **Table 1**.

In the ideal state, only the symmetrical stretch mode will be observed in a Raman spectrum of a triiodide compound or solution. However, many factors can disturb the ideal local symmetry. Such factors involve the formation of higher polyiodides in solution, the coordination of cations, or solvation by strongly donating solvents. In such cases, the formally Raman-forbidden vibrational modes will also appear in the Raman spectra, sometimes together with extra features from loosely bound I<sub>2</sub> units. The two types of triiodide Raman spectra are shown in **Figure 3**. The very simple and easily interpreted Raman spectra can become complex very quickly and make interpretation far from nonambiguous. Nevertheless, Raman spectroscopy is one of the most informative experimental techniques available for the study of polyiodide chemistry.

In this context, it is appropriate to mention two other related phenomena concerning triiodide chemistry. As noted above, from the structural and spectroscopic properties, the expected chemical dissociation of a triiodide ion is into I<sup>-</sup> and I<sub>2</sub> fragments. This has one important implication: I<sup>-</sup> as donor to I<sub>2</sub> is

**Figure 3** Raman spectra of a centrosymmetric and a symmetry-broken triiodide ion, as represented by molten (Et<sub>3</sub>S)I<sub>3</sub> (top) and solid (Me<sub>3</sub>S)I<sub>3</sub> (bottom). Data taken from Svensson and Kloo.<sup>6</sup>

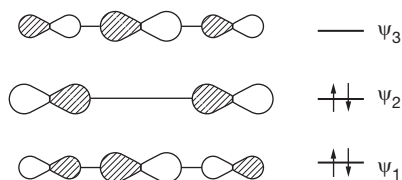
readily exposed to competition. Thus, many donors can out-compete I<sup>-</sup> if present in sufficient concentration. Typical competitors involve other halide anions, –N, –P, or –S functionalities of various molecules, and chemistry is full of compounds containing –X–I–I units.<sup>23</sup> A practical example, where this can become a problem, can be taken from the electrolyte chemistry of dye-sensitized solar cells (DSCs). Part of the reason why an ionic-liquid-based electrolyte requires higher iodine concentration can be traced to an inherent interaction between the ionic-liquid cation and I<sub>2</sub> lowering the effective concentration of triiodide in solution and thus reducing conversion efficiencies.<sup>24</sup> This type of chemistry is not within the scope of the present overview, but represents a characteristic phenomenon of iodine chemistry that should be kept in mind. Consequently, some of the main features of polyiodides can also be observed in related areas of chemistry. The other phenomenon relates to photochemistry. It should be noted that photodissociation of the triiodide ion instead typically renders the ion I<sub>2</sub><sup>-</sup> and the highly reactive radical I<sup>•</sup>.<sup>25</sup> A recent study in gas phase reveals a rather complex, nonadiabatic dissociation with several possible dissociation channels, although the I<sub>2</sub><sup>-</sup> + I<sup>•</sup> ones display the highest yields.<sup>26</sup> Referring to the section of solvent effects below, hydrogen-bonding solvents are indicated to influence product branching in the dissociation channels. In electrochemical applications, the I<sub>2</sub><sup>-</sup> ion frequently appears as an important intermediate in the redox reactions involving the iodide and triiodide ions.<sup>27–30</sup> Photodissociation studies of the triiodide ion in ionic liquids showed effects of bimolecular reactions resulting in both triiodide recombination and inter-I<sub>2</sub><sup>-</sup> reactions, depending on the nature of the ionic-liquid system.<sup>31</sup> A K-edge extended x-ray absorption fine structure (EXAFS) analysis of the triiodide ion in various solvents displayed a centrosymmetric triiodide ion with varying I–I bond lengths, albeit it was noted that large vibrational amplitudes blurred the next-neighbor correlations.<sup>32</sup>

### 1.08.2.1 The Bonding in Trihalide Ions

The established scheme of bonding in the triiodide ion was provided by Pimentel and Rundle in the early 1950s.<sup>33,34</sup> On the basis of molecular-orbital theory involving only the

iodine atom 5p-orbitals, three molecular orbitals (MOs) can be derived (see Figure 4). The bonding formalism is analogous to that of the 1s-orbitals of the simple  $\text{H}_3^-$  ion, allowing for a bit more complex symmetry consequences when involving the p-orbitals in  $\text{I}_3^-$ . Essentially, the three 5p-orbitals form one bonding, one nonbonding, and one antibonding MO. The 5p-orbitals are expected to house four valence electrons, thus filling the bonding and nonbonding MOs. This simple bonding scheme carries more information than noted at first sight, since it also explains the role of the triiodide ion in donor/acceptor type of complexes; more about this is discussed in the section on polyiodides. As a consequence of the bonding scheme, electrostatically the triiodide ion can be approximated as having  $-1/2$  charge on the terminal iodine atoms and close to zero charge on the central one.

Novoa and coworkers extended the bonding scheme to both the other homoatomic trihalides and later to some interhalogen trihalide species using correlated methods of theory.<sup>36,37</sup> All four trihalide ions,  $\text{F}_3^-$ ,  $\text{Cl}_3^-$ ,  $\text{Br}_3^-$ , and  $\text{I}_3^-$ , were found to be stable with respect to dissociation into the  $\text{X}^-$  and  $\text{X}_2$  fragments. The stability was found to increase down the group 17, in accordance with experiment. In addition, the interaction with a cation ( $\text{K}^+$ ) was investigated and the structural consequences in terms of symmetry lowering deduced. The same trend was found for the  $\text{X}_3^-$  series in solution and gas phase with respect to the formation of  $\text{X}^-$  and  $\text{X}_2$ .<sup>38</sup> However, it was also noted that the level of theoretical treatment significantly influences the results. Hoffmann and coworkers have studied both the bonding characteristics of various combinations of trihalides, homogenous and interhalogen ones, and found a similar pattern as Novoa et al. The site preference in interhalogen trihalide ions was also scrutinized and found to be the largest for chlorine.<sup>39</sup> In a later study, the amount of s,p-mixing was investigated in p-block triatomic molecules and ions. Antibonding effects from s,p-mixing and electron-pair repulsion tend to be larger further to the left in the p-block.<sup>35</sup> The bonding effects of the terminal binding of one and two  $\text{I}^-$  to a central  $\text{I}_2$  unit have been thoroughly investigated by Mealli and coworkers.<sup>40</sup> In a calculational study of a large series of interhalogen trihalide ions, Kikuchi et al. found that, in accordance with experiment, the terminal position of the most electronegative (lightest) element in group 17 promotes stability, whereas polar solvents flatten the potential energy surface enhancing  $\text{X}^- + \text{X}_2$  dissociation.<sup>41</sup> Kloos et al. made a thorough study of the bonding contributions to I–I bonding in the triiodide ion and larger polyiodides. It is clear that the triiodide ion, in addition to covalent interaction, is also stabilized by secondary types of interaction, such as induction, dispersion, as well as ion quadrupole ( $\text{I}_2$  has a strong quadrupolar moment).<sup>42</sup> It has been argued that a valence-bond (VB)



**Figure 4** The p-orbital bonding scheme proposed by Pimentel. Reproduced from Munzarova, M. L.; Hoffmann, R. *J. Am. Chem. Soc.* **2002**, *124*, 4787–4795.

formalism better describes the bonding in trihalide ions, as compared to the established (3c,4e)-MO scheme of Pimentel. The main argument is that dissociation barriers and states are better described by VB theory.<sup>43</sup>

Molecular dynamics and other studies in different solvents show that hydrogen-bonding solvents induce a symmetry breaking for the triiodide in solution.<sup>44–48</sup> Such effects must have a consequence for the recorded vibrational spectra, as noted in the experimental studies described above. In additional simulation studies also solvent-induced shifts of the peak wavenumbers have been determined.<sup>48–50</sup> As previously noted, solvent effects are of importance in the photodissociation of the triiodide ion. The results from high-level multi-configurational calculations indicate significant effects of solvent interaction on the structure and spectroscopic response of  $\text{I}_3^-$ .<sup>51</sup> One study has suggested that solvent effects give rise to a bent triiodide ion, although such a structural distortion is not necessary to explain the experimentally observed properties.<sup>52</sup>

### 1.08.2.2 Bonding Trends in Trihalides

The general conclusion from the body of calculational studies on trihalide systems is that the  $\sigma$ -bonded valence p-orbital interaction scheme of Pimentel is a good first approximation for all the  $\text{X}_3^-$  systems in group 17. Moving down the group, secondary bonding contributions become increasingly important. At the same time, atom–atom distances increase down the group. In view of the coordination chemistry approach described below, the  $\text{X}^- - \text{X}_2$  interaction within the trihalide ions represents a suitable model system for the understanding of the tendency to polyhalide formation, for example, catenation. In order to get a crude estimate of this tendency, some simple model calculations on the  $\text{X}_3^-$  ion were made using a long-range-corrected B3LYP functional together with the Stuttgart/Dresden effective-core potential and triple-zeta valence basis sets to, on a more uniform basis, obtain a few characteristic bonding parameters of the homogenous trihalide ion. The calculational results are given in Table 2 and are graphically represented in Figure 5.<sup>53,54</sup>

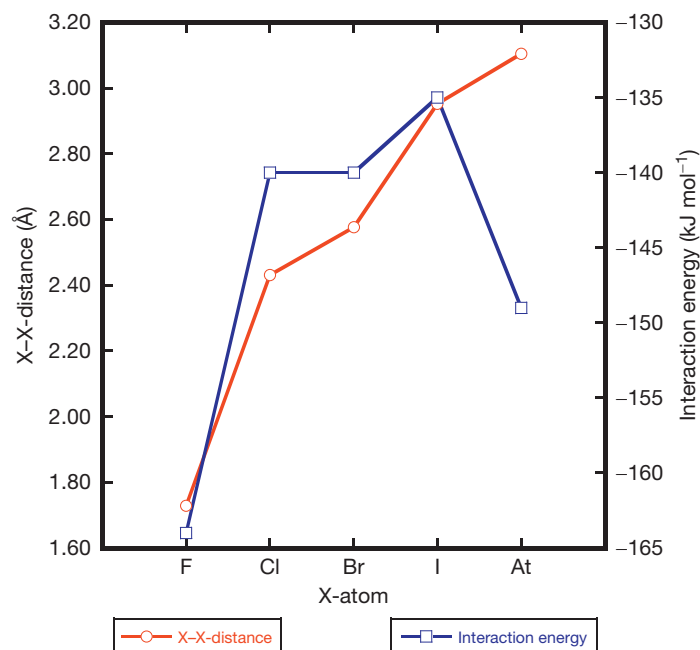
The results are at first sight a bit surprising, since interaction energies alone would suggest that polyfluoride chemistry should be the richest, although the interaction energies between the  $\text{X}_2$  and  $\text{X}^-$  fragments differ surprisingly little. It is clear that the issue requires a deeper analysis. More insight is obtained from the potential energy surfaces (PESs) of the linear  $\text{X}_2$  and  $\text{X}^-$  interaction.

The PESs of linear distortion shown in Figure 6 offer a couple of important observations. The width of the potential energy

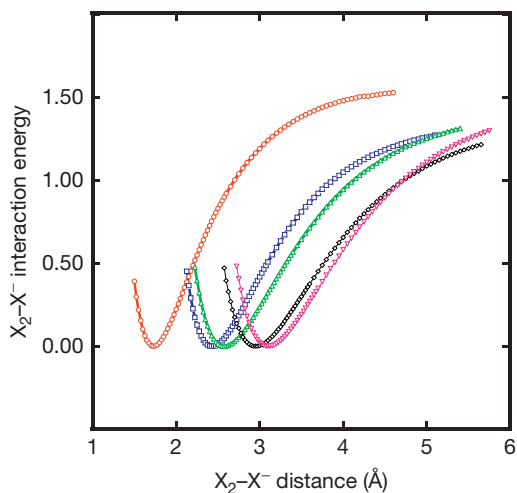
**Table 2** Calculational results for the homoatomic trihalide ions of  $D_{\infty h}$  symmetry

$\text{X}_3^-$ ion	X–X distance (Å)	Symmetrical stretch vibration ( $\text{cm}^{-1}$ )	Asymmetrical stretch vibration ( $\text{cm}^{-1}$ )	$\text{X}_2-\text{X}^-$ interaction energy ( $\text{kJ}^{-1} \text{mol}^{-1}$ )
$\text{F}_3^-$	1.729	483	555	–164
$\text{Cl}_3^-$	2.431	256	323	–140
$\text{Br}_3^-$	2.577	165	182	–140
$\text{I}_3^-$	2.952	116	138	–135
$\text{At}_3^-$	3.105	84	106	–149





**Figure 5** Graphical representation of the bond distances and interaction energies shown in Table 2.



**Figure 6** Potential energy curves for linear distortion in the  $X_3^-$  trihalide ions; from  $F_3^-$  furthest to the left to  $At_3^-$  furthest to the right; the conformation with the lowest total energy is set to zero in all systems.

wells are also numerically specified in Table 3. As expected, the X–X distance increases down the group 17. However, the increase is nonlinear and can be described as periodic. There is a large increase between the F–F and Cl–Cl distances, whereas the Br–Br one is only marginally longer than the Cl–Cl distance. In the same way, there is a fairly large increase in X–X distance between  $Br_3^-$  and  $I_3^-$  but small between  $I_3^-$  and  $At_3^-$ . Going from lighter to heavier systems, one can also note that the PES wells become flatter, more extended, and that the PESs increase less quickly with increasing X–X separation; see also PES well widths given in Table 2. This effect emerges from both more extended covalent interaction and an increasing influence from intermolecular interaction, such as induction and dispersion. In

**Table 3** Width of the potential energy well of the PES shown in Figure 6.

$X_3^-$ ion	Well width at 0.026 eV (kT at 298 K) (Å)	Well width at 0.4 eV (Å)
$F_3^-$	0.14	0.64
$Cl_3^-$	0.19	0.80
$Br_3^-$	0.23	0.98
$I_3^-$	0.24	1.04
$At_3^-$	0.24	0.99

summary, the heavier the element, the ‘stickier’ the interaction between the  $X_2$  and the  $X^-$  fragments becomes. In this context it is also notable that the periodic behavior cannot be directly traced to any fundamental physical property, such as polarizability and dipolar moment, etc. However, this effect peaks at iodine. In fact, the PES of  $I_3^-$  crosses that of  $At_3^-$  at longer distances (at about 4.7 Å) highlighting the very special properties of the element iodine. In this respect, the extensive polyiodide chemistry can be attributed to the strong long-distance attractive forces in iodine – stronger than any of its group 17 congeners, rather than the I–I interaction energy *per se*. Thus, the tendency to catenation is expected to be the strongest for iodine. Moreover, since the influence of covalent bonding is significant, probably the chains formed should be regarded as a true case of catenation. However, the case is less clear for the lighter elements.

### 1.08.3 Polyiodides

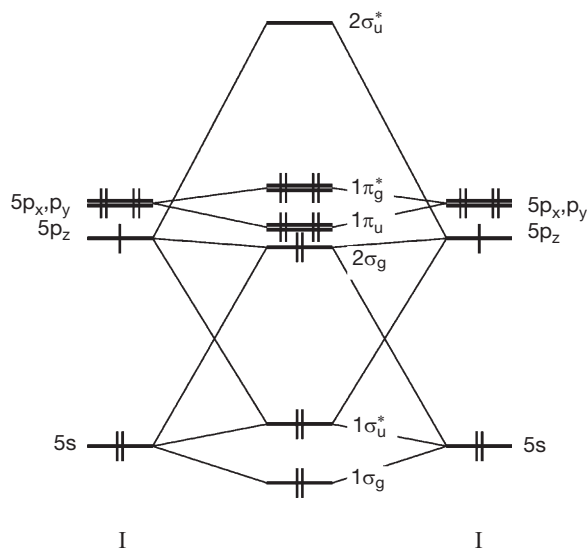
As compared to its group members, iodine is unique in the tendency to form extended, catenated structures, so-called polyiodides. Just as for the  $I_3^-$  ion, the bonding in the neutral, diatomic  $I_2$  molecule can as a first approximation be described



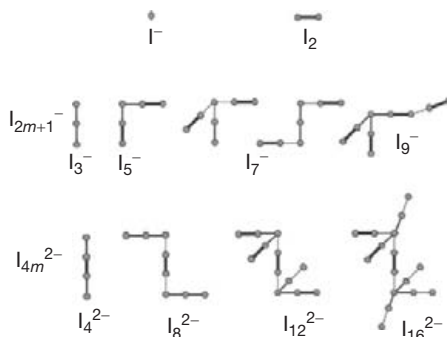
as the result of  $\sigma$ -interaction between the iodine 5p-orbitals forming a single bond. The bonding scheme of  $I_2$  is shown in Figure 7. This means that the  $\sigma$ -antibonding orbital ( $2\sigma_u^*$  MO in Figure 7) is available for accepting electron density, and thus  $I_2$  readily acts as an electron acceptor, a Lewis acid.

In this aspect, it is notable that the polyiodides typically are made from only three fundamental building blocks: the  $I^-$  and  $I_3^-$  ions and the neutral molecule  $I_2$ . Essentially, all polyiodide structures, with very few exceptions, can be rationalized in terms of these three fragments<sup>4</sup> (Figure 8). Thus, in the polyiodide structures, the ions will act as donors and typically the I–I bond distance in the  $I_2$  fragment is elongated as a consequence of the population of its  $\sigma$ -antibonding orbital. In classical coordination chemistry terms, the interaction can be regarded as a simple solvation, where the neutral molecule  $I_2$  solvates the anions  $I^-$  and  $I_3^-$ . This is a useful concept, since it also explains the ready exchange of the anions for others, for instance, like in the metal-iodide/iodine systems described later.

In this perspective, either the solvating power of  $I_2$  must be unique or the donor capacity of the iodide anion donors



**Figure 7** The p-orbital bonding scheme of  $I_2$ . Data taken from Svensson and Kloof.<sup>4</sup>



**Figure 8** A few polyiodide structures that can be visualized in terms of  $I_2$  solvation of the iodide ions. Reproduced from Walbaum, C.; Pantenburg, I.; Meyer, G. Z. Naturforsch. B 2010, 65, 1077–1083.

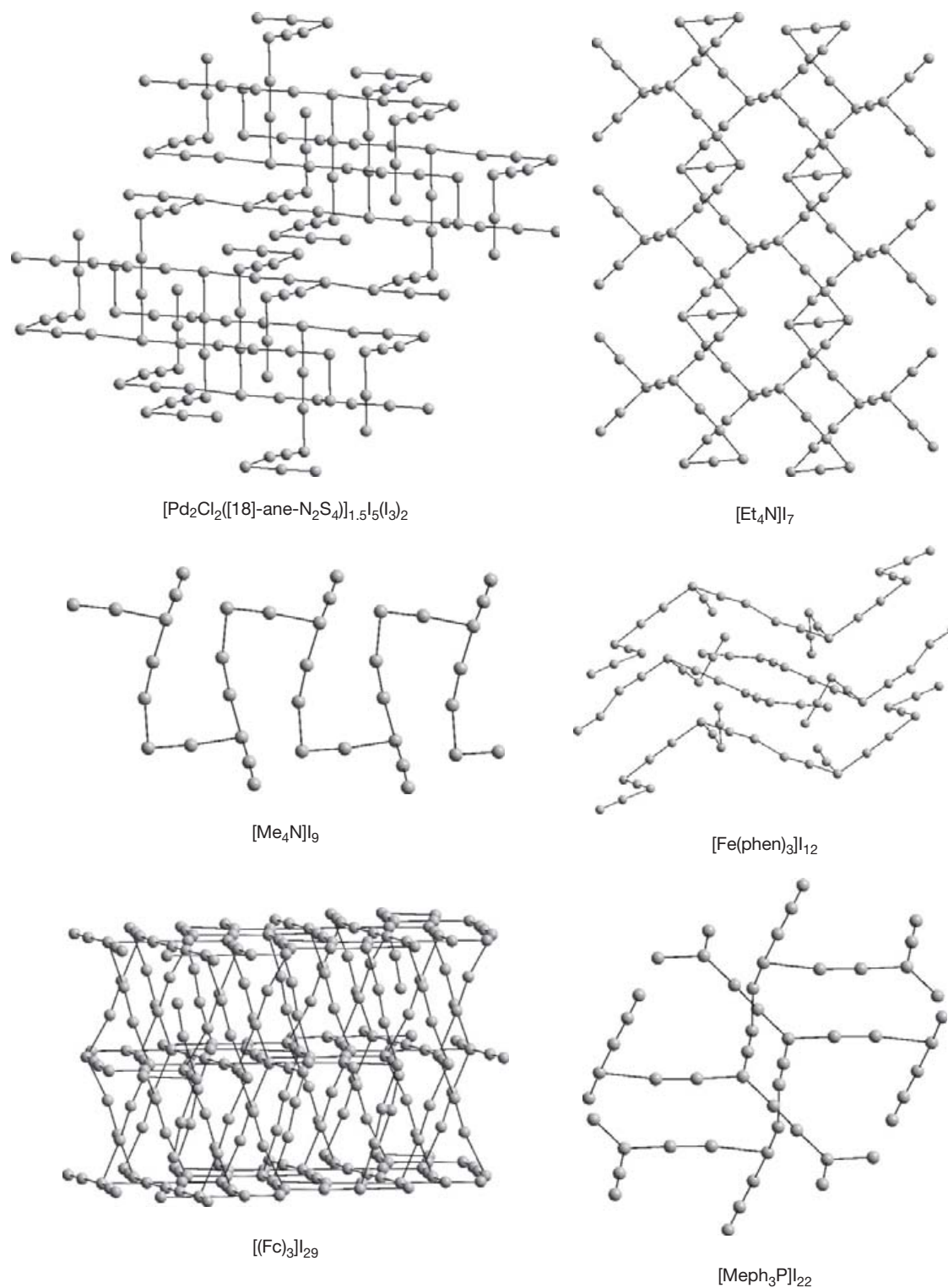
exceptional. Judging from the results in Table 2, the  $I_2 \cdots I^-$  interaction itself does not stand out in strength in comparison with the other halogen–halide interactions. Instead, it is the strong attractive interaction at longer ( $>3 \text{ \AA}$ ) distances that generates the rich polyiodide chemistry (*vide supra*) – a few nice highlights are given in Figure 9.

Nevertheless, the model of solvation justifies the typically used formalism in rationalizing polyiodide structures. For instance, the examples shown in Figure 9 can all be broken down into the three fundamental building blocks of polyiodides, in spite of the complexity indicated by the stoichiometry. A striking feature is the seemingly boundary less width of the I–I contact ranging from that in the  $I_2$  molecule (about  $2.7 \text{ \AA}$ ) up to over  $4 \text{ \AA}$ . A statistical analysis of I–I–I contacts showed a rather continuous distribution<sup>42</sup> (Figure 10). There are clear maxima in I–I–I contacts corresponding to intramolecular distances ( $I_2$  and  $I_3^-$ ) and essentially packing distances ( $>4 \text{ \AA}$ ). However, all distances in between are also well represented and it is clear that the intermolecular I–I bond must be very flexible. This phenomenon is also obvious in the attempts to rationalize the polyiodide structures to fit into the simple three-fragment solvation model described above; the assignment of an I–I contact in the range  $3.0\text{--}3.6 \text{ \AA}$  is sometimes far from unambiguous. The distance distributions also have implications for the Grotthuss mechanism of conduction; the transfer of an iodide ion from one polyiodide fragment to another is essentially continuous. The assignment of a specific proton in water to a specific neighboring water molecule oxygen atom can be problematic, just like the assignment of a specific iodide to a neighboring iodine molecule.

The bonding in polyiodides can be regarded as a logical extension from the bonding scheme in the simple  $I_3^-$  ion, visualized as a solvated iodide ion of  $I_2 \cdots I^-$  type. Consequently, a pentaiodide ion can be regarded as a  $(I_2)_2 \cdots I^-$  interaction, a heptaiodide ion as a  $(I_2)_3 \cdots I^-$ , etc. In relation to the region of difficult bonding assignment between 3 and  $4 \text{ \AA}$ , it is clear that the interaction energy can be partitioned into several different contributions. The partitioned potential energy surface is shown in Figure 11.

A few characteristics can immediately be noted. First, covalent bonding extends quite far and is significant out to at least  $5 \text{ \AA}$ . Second, also dispersion, induction, and ion-quadrupolar interactions contribute significantly in the  $3\text{--}4 \text{ \AA}$  region. For instance, at an I–I distance of  $3.5 \text{ \AA}$ , the attractive contributions, in terms of contribution to the total interaction energy, can be partitioned as follows: 52% covalent, 26% dispersion, 12% induction, and 11% ion-quadrupolar interaction. With this in mind, a Grotthuss mechanism of ionic conductivity becomes essentially inevitable. In addition, the reason for the ‘sticky’ character of the long-distance I–I interactions becomes clear.

In this context, it is appropriate to discuss the bonding in chains of  $I_3^-$  ions. Although the intermolecular, attractive forces of iodine-containing species appears to be significant even at the typical  $I_3^- \cdots I_3^-$  distances of about  $4 \text{ \AA}$ , the repulsive force of the negative charges on the terminal iodine atoms is expected to dominate. From an MO perspective, the interaction cannot be explained with a simple donor–acceptor formalism. The chains of triiodides, for instance, found in the herpaphite compound,<sup>56</sup> are thus not expected to be bound. However,



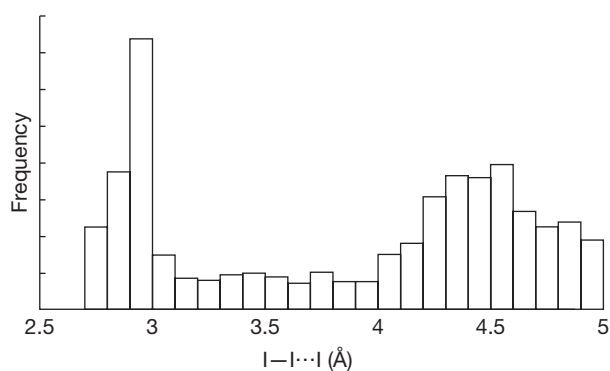
**Figure 9** Some large polyiodide fragments that can be broken down into the three fundamental building blocks  $\text{I}^-$ ,  $\text{I}_2$ , and  $\text{I}_3$ . This figure is based on structural data taken from Svensson and Kloo.<sup>4</sup>

such a view is too simplified in this case. Essentially, all known structures of chains of triiodide ions fall into one of two categories: the triiodides are confined into a host structure, where triiodide–host interactions are significant, or they

contain bridging cations linking the negatively charged ions together. Consequently, chains of triiodide ions are found in structures, where the surrounding components of the compound place the triiodide ions together at distances balancing

the electrostatically repulsive force of the anions. Macroscopically, such an anisotropic arrangement gives anisotropic physical properties.

In the last 10 years, more than 100 new polyiodide structures have been published in refereed journals. Many of these repeat known structural features and conform to the expected bonding pattern. However, a few new structures call for special attention and the field as such appears to follow a few new directions highlighted below. An interesting comparison between polytellurides and polyiodides was recently published by Devillanova et al., in which systematization in terms of few structural building blocks proved more difficult in polytellurides.<sup>57</sup> Lee and colleagues made a very thorough structural and theoretical study of aromatic, organic-polyiodide systems, rating the different types of interactions in such systems.<sup>58</sup> The iodine-iodine interactions were deduced to be the strongest, and thus implicitly the most important structure-directing interaction. Sulfur-containing organic molecules, or ligands in metal-containing systems, appear as a successful strategy to form new and



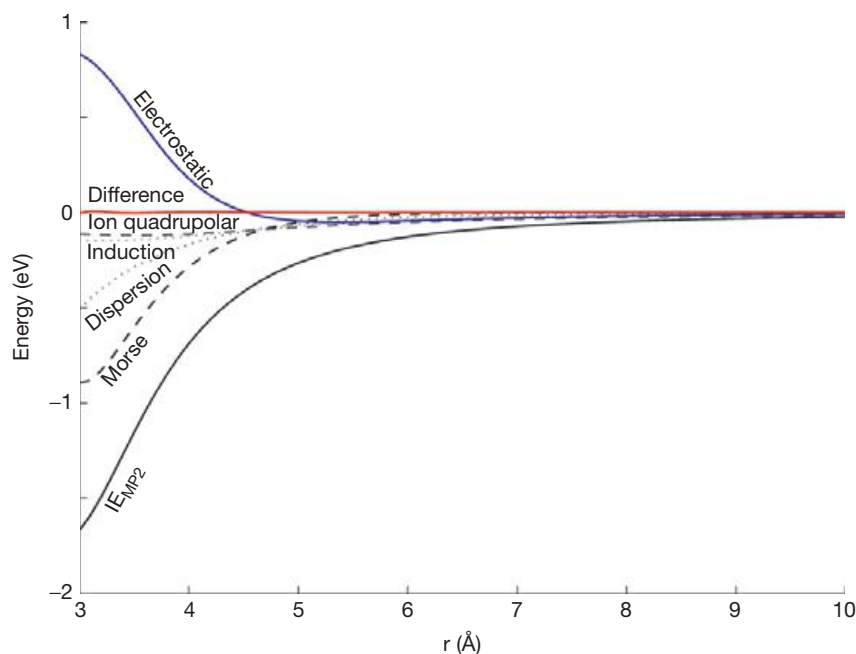
**Figure 10** Distance distribution of I-I distances in an  $I_3$  unit as derived from the Cambridge Structural Database. Data taken from Kloo et al.<sup>42</sup>

interesting polyiodide frameworks. Such an example is the quasi-cubic structure using a dipyrityldisulfide derivative (see **Figure 12**),<sup>59</sup> or substituted tetrathiafulvalenes of interesting inherent electrical properties,<sup>60</sup> or thiacyclanonanes as ligands to group-10 metal ions give rise to a rich structural polyiodide chemistry.<sup>61</sup> Of course, polyiodide structures can be described in different ways, as exemplified by the iodine-rich cryptand compound of Pantenburg and coworkers denoted as a mixed  $I_5^-$  and  $I_8^{2-}$  compound, where the anions can be further broken down into the three fundamental building blocks.<sup>62</sup> In another compound, cohabiting  $I_3^-$  and  $I_5^-$  ions were found.<sup>63</sup> Beryllium(II) is a less common cation to be used, but in one such compound a mixture between  $I_3^-$  and  $I_4^{2-}$  was determined.<sup>64</sup>

## 1.08.4 New Trends in Polyiodide Chemistry

### 1.08.4.1 Structural Confinement

Intercalation of iodide with iodine into a solid zeolite host appears to form various I-I-bonded species, as judged from vibrational spectroscopic and EXAFS data.<sup>65</sup> Yan and coworkers used hydrogen-bonded nucleotide bases to form supramolecular entities with ribbon-like structures as a consequence, including a formal  $I_{14}^{2-}$  entity of  $[(I_3^-)_2 \cdot 4I_2]$  type.<sup>66</sup> Lu and Schauss used a metal-organic framework to confine pentaiodide ions with intermolecular contacts of 3.56 Å and of  $[(I^-)_2 \cdot 2I_2]$  type.<sup>67</sup> Helical, metal-ligand systems were also used by both Dance with coworkers and Schröder et al. to template new polyiodide compounds.<sup>68–70</sup> A similar approach has been used by Devillanova and coworkers, isolating a series of polyiodides with high  $I_2$  content.<sup>71</sup> The use of the secondary interactions of cations with long aliphatic chains, self-assembling into low-dimensional structures known from basic colloidal chemistry, is another strategy producing confined polyiodides.<sup>20,72</sup> A similar strategy was used by different groups in a series of polyiodide compounds

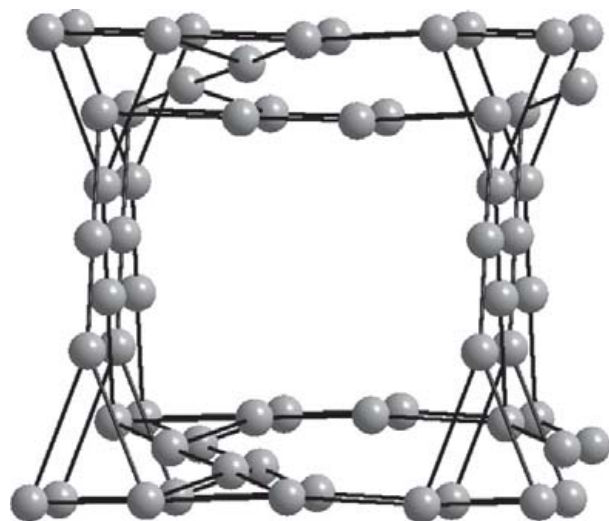


**Figure 11** Bonding contributions to the I-I bond in  $I_3^-$ . Data taken from Kloo et al.<sup>42</sup>



and was denoted dimensional caging.<sup>73–75</sup> Some beautiful structures of confined polyiodides are shown in **Figure 13**.

Of course, this type of structural confinement has strong ties with both the very old application of polyiodide systems to tint starch and other potential applications within mainly optics and electronics. With this in mind, structural confinement using



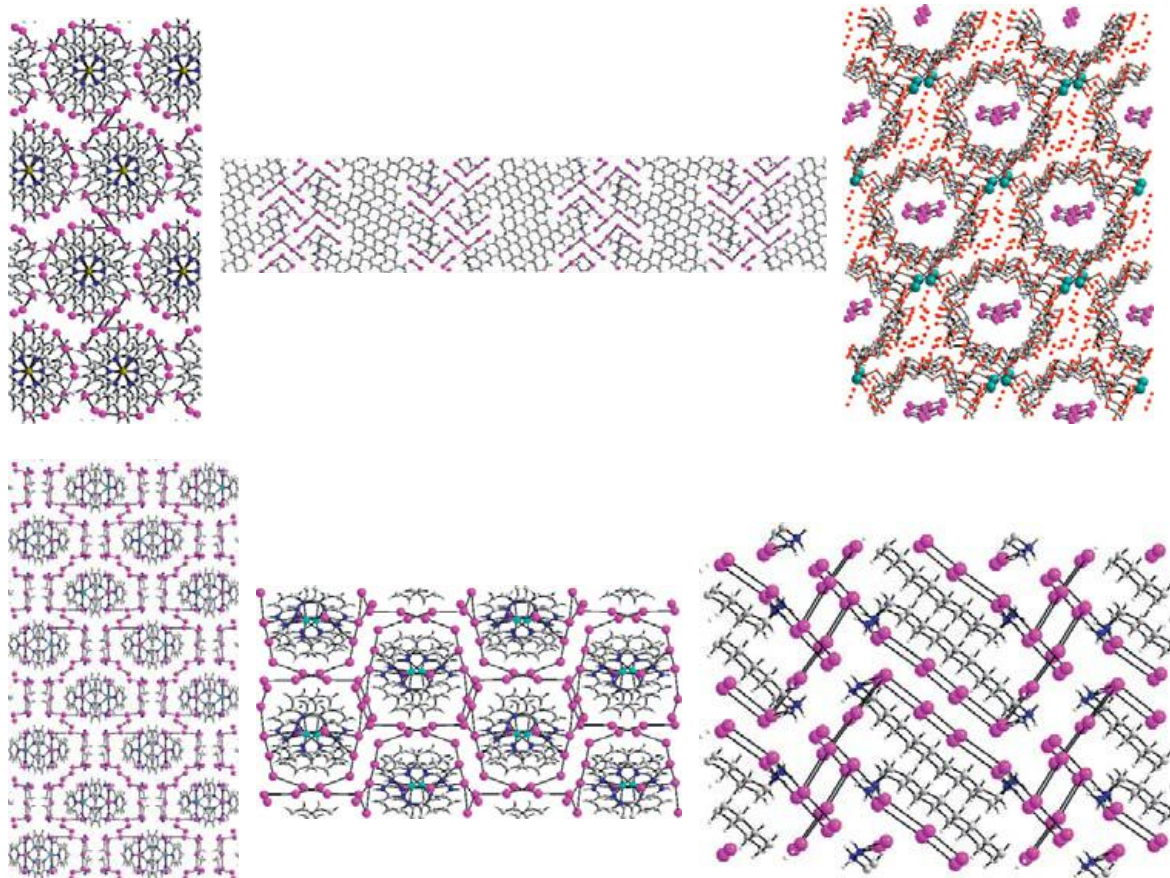
**Figure 12** The pseudo-cubic structure described by Devillanova et al. This figure is based on structural data taken from Aragoni et al.<sup>59</sup>

various carbohydrate systems is rather frequent, using, for instance, xylene or cyclodextrins.<sup>76–81</sup> However, most commonly, characterization is based on spectroscopic observations and the exact assignment of polyiodide units must in some cases be regarded as models to explain experimental results. However, crystal structure data render considerably higher credibility to the models in more disordered systems.<sup>82</sup>

#### 1.08.4.2 Metal-Iodide/Iodine Compounds

As discussed in the section on polyiodides, metal-halide complexes can be regarded as halide donors with respect to the diatomic halogen molecules. Normally, the donation capacity is lower than for a noncoordinated halide ion. The aspect of donor capacity was well illustrated in the work by Tsipis and Karipidis, where the donor strength essentially follows that shown in **Table 2** for the trihalides – the lighter the element, the larger the electron donation to the  $X_2$  unit.<sup>83</sup> It is pertinent to note that metal-halide/halogen compounds normally are regarded as different from polyhalides with metal-complex cations in that the former type has a halide ion directly coordinated to the metal ion. The metal ion, coordination center, does not necessarily have to be homoleptic, but the interaction with a halogen  $X_2$  molecule or other polyhalide fragment takes place via a coordinated halide ion.

Some early work included complex gold iodides as the iodide/triiodide 'substitute'.<sup>84,85</sup> Because of the highly similar



**Figure 13** Examples of new polyiodide structures in confined environments (see main text).

coordination chemistry of gold and iodine, this is not unexpected.<sup>4,85</sup> However, there are quite a number of compounds of this type. Typically, the halide ligands are bridged by I<sub>2</sub> or other halogen/interhalogen molecules (*vide infra*). As compared to the ‘pure’ polyhalides, the weaker metal–halide donor ability tends to give thermally rather unstable compounds. One exception are compounds isolated with a mercury–hexamethylenetetramine complex.<sup>86</sup>

Guloy reported a selection of new gold(I)/gold(III) complex compounds, containing I<sub>3</sub><sup>−</sup> and other halides in layered, perovskite-like structures.<sup>87,88</sup> It is normally rather difficult to isolate the I<sub>3</sub><sup>−</sup> analog AuI<sub>2</sub><sup>−</sup> from iodine-rich reaction media because of oxidation to gold (III), typically as AuI<sub>4</sub><sup>−</sup>. In these examples, the oxidation is only partial, retaining gold in the +I oxidation state. Ligand tuning, namely phosphane-ligand tuning, was used to address this problem by Schmidbaur and co-workers.<sup>89</sup> Several gold(I) compounds were isolated as phosphane gold(I)iodides, some bridged by I<sub>2</sub> at iodide–iodine distances of 3.44–3.65 Å. Also, triiodides of gold(III) compounds were isolated. Dimeric Pd(II)-halide structures are quite stable, and Pantenburg and Meyer have isolated a compound with an I<sub>2</sub>-bridged Pd<sub>2</sub>I<sub>6</sub><sup>2−</sup> complex, and with an iodide–iodine distance as short as 3.32 Å.<sup>90</sup> By reacting CuI with I<sub>2</sub>, Chen and colleagues obtained a similar I<sub>2</sub>-bridged Cu<sub>2</sub>I<sub>6</sub><sup>4−</sup> complex.<sup>91</sup> The iodide–iodine distance in this compound is even shorter, 3.02 Å, raising the question whether it should be regarded as a bridging I<sub>2</sub> molecule or rather as a coordinated, asymmetric, triiodide ion. Janiak and coworkers used a copper (I)-iodide-based inorganic starch model to obtain a series of confined polyiodide compounds.<sup>92</sup> Because of structural disorder, the nature of the captured, linear polyiodide entities is not fully clarified. Relating to the perovskite structures, Mercier et al. isolated a low-dimensional lead-iodide structure, where the metal-iodide ribbons are linked by I<sub>2</sub> molecules at an iodide–iodine distance of 3.51 Å.<sup>93</sup> A similar layered structure with intercalated triiodide ions was described by Chen and co-workers, rendering an optical semiconductor material.<sup>94</sup> Manganese(III) captured in a phthalocyanine ligand was shown to be bridged by I<sub>2</sub> via an asymmetrically bound, terminal iodide ligand.<sup>95</sup> The iodide–iodine bond length is 3.42 Å. As a curiosity, the Al<sub>13</sub><sup>−</sup> cluster can be regarded as a superhalide ion forming ‘polyiodides,’ as verified by mass spectrometry and calculations.<sup>96</sup> Not too different in character is the extremely iodine-rich W<sub>15</sub>I<sub>47</sub> compound consisting of W<sub>5</sub>I<sub>8</sub><sup>n−</sup> (with *n* somewhere between 1 and 3) and iodides/triiodides.<sup>97</sup> A few examples from this class of compounds are shown in Figure 14.

The gold–iodine system was subjected to a high-level calculational study in which the equatorial interaction of I<sub>2</sub> and AuI<sub>2</sub><sup>−</sup> was deduced to be of predominantly closed-shell type and containing contributions from secondary interactions at long distance, making a direct oxidative addition of I<sub>2</sub> to form gold(III) less plausible.<sup>98</sup> In previous studies, the AuI<sub>2</sub><sup>−</sup> ion was found to be remarkably similar to the I<sub>3</sub><sup>−</sup> ion in terms of internal and external coordination.<sup>85</sup>

### 1.08.5 Liquids and Solvent Effects

In an early and thorough study using liquid x-ray scattering and vibrational spectroscopy, Bengtsson et al. showed that

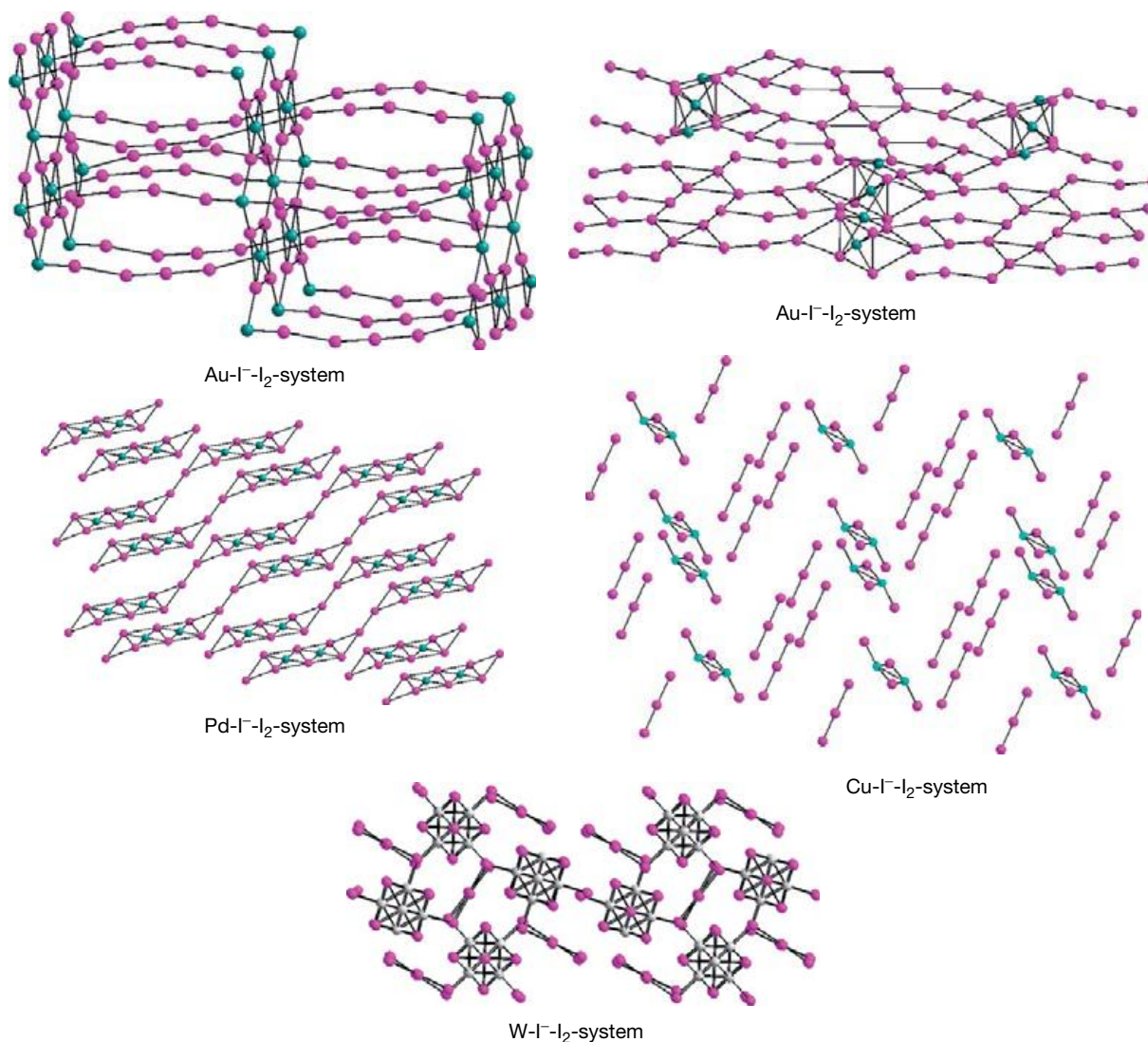
sulfonium iodide ionic liquids with added iodine essentially can be described in terms of iodine-solvated triiodide ions.<sup>99</sup> The liquid local structure has resemblance to the known solid polyiodide structures, but even more to the nearest-neighbor structure of solid iodine. When the iodine:iodide ratio is increased, on average the connectivity from the triiodide ions to the solvating iodine increases. This strongly correlates with an increase in conductivity with increasing iodine content.<sup>100</sup>

In the last 10 years, a clear increase in polyiodide studies in ionic liquids can be observed. This is to a large extent caused by the use of such electrolyte media in DSCs.<sup>101</sup> A few examples of more fundamental character are given in this section, and the DSCs will be handled more thoroughly in the section on applications. In a comparison of different electrochemical techniques for the determination of triiodide ion-diffusion constants in ionic-liquid mixtures, it was concluded that the transport was non-Stokesian, that is, of Grotthuss type.<sup>102</sup> A schematic view of the Grotthuss mechanism of conductivity is shown in Figure 15. In addition, microelectrodes appear to give the most accurate and reproducible results, also emphasized by later studies.<sup>103</sup> In ionic-liquid iodides with added iodine, the formation of polyiodides was concluded on the basis of combined electrochemical and vibrational spectroscopic investigations.<sup>104</sup> A related study revealed the formation of polyiodide species in solution as soon as the cation:iodide ratio was increased above 1 by the addition of iodine.<sup>105</sup> The formation of polyiodides was also correlated to an increase in conductivity attributed, once again, to a Grotthuss type of charge transport. A very recent study employing terahertz spectroscopy, also including effects of ion pairing, concludes that the Grotthuss mechanism can enhance conductivity by as much as 50% in rather viscous ionic-liquid media.<sup>106</sup>

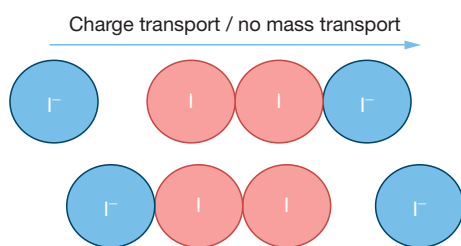
### 1.08.6 Polybromides – An Emerging Branch of Polyhalide Chemistry

The chemistry of triiodides in particular and also other polyiodides or iodide–iodine complexes is very extensive. In contrast, the corresponding compounds of the other halides are very rare. Among tribromides, only a few structures are known experimentally.<sup>107–111</sup> An outstretched tribromide can be assigned in a complex structure reported by Kornath and Blecher, in which the two Br–Br distances are about 3.10 and 2.54 Å, respectively.<sup>112</sup> Devillanova et al. isolated a Br<sub>4</sub><sup>2−</sup> bromide of [(Br<sup>−</sup>)<sub>2</sub>·Br<sub>2</sub>] type.<sup>113</sup> It seems that most knowledge about these compounds is derived from the analogy to triiodide ions together with theoretical comparisons, as described above. However, there is an increasing amount of attention devoted to this type of chemistry. A Br<sub>10</sub><sup>2−</sup> unit – in analogy to the polyiodide formalism it can be described as [(Br<sub>3</sub><sup>−</sup>)<sub>2</sub>·2Br<sub>2</sub>] – is reported by Cunningham and coworkers.<sup>114</sup> Along with some tribromide structures, Knop and coworkers also revealed the existence of a Br<sub>8</sub><sup>2−</sup> chain of the type [(Br<sub>3</sub><sup>−</sup>)<sub>2</sub>·Br<sub>2</sub>].<sup>109</sup> The subsequent theoretical study clearly indicates that the corresponding polybromides are more weakly bound than their polyiodide congeners. A theoretical study at the density-functional level showed that Br<sub>3</sub><sup>−</sup>, Br<sub>4</sub><sup>2−</sup>, and Br<sub>5</sub><sup>−</sup> all are analogous to their heavier relatives in terms of structural units.<sup>115</sup> Using a dithiolene compound, Devillanova and coworkers isolated a two-dimensional



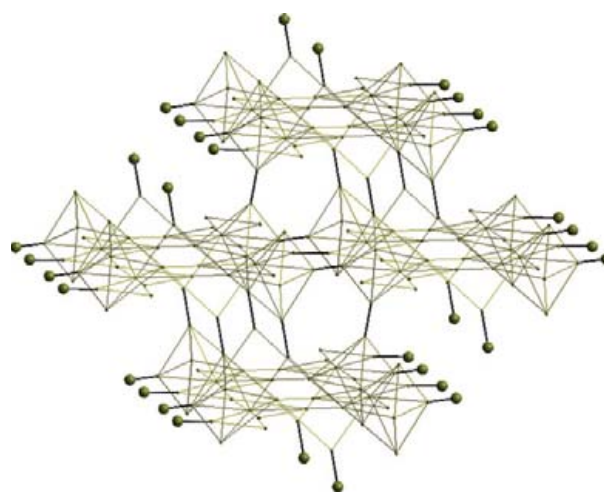


**Figure 14** Examples of new metal-iodide/iodine structures (see main text).



**Figure 15** A schematic view of the Grotthuss mechanism of conduction.

polybromide network of the type  $[(\text{Br}^-)_2 \cdot 3\text{Br}_2]$ .<sup>116</sup> Also more systematic studies of the formation of polybromide species in solution and solid phases have been reported on the basis of spectroscopy and calculations.<sup>117</sup> Just as for polyiodides, Raman spectroscopy is highly informative.<sup>118</sup> Also a three-dimensional network of the type  $[(\text{Br}^-)_2 \cdot 9\text{Br}_2]$  has been reported (see [Figure 16](#)).<sup>119</sup> In analogy to iodine-bridged metal iodides,



**Figure 16** The network structure of  $\text{Br}_{20}^{2-}$  deciphered as  $[(\text{Br}^-)_2 \cdot 9\text{Br}_2]$ . This figure is based on structural data taken from Wolff et al.<sup>119</sup>

bromine-bridged metal-bromide complexes have also been isolated. Such an example is  $[(\text{Me}_3\text{P})\text{AuBr}_3]$  bridged by a stoichiometric amount of  $\text{Br}_2$ .<sup>120</sup> In the same article, a gold(I) diphosphane compound containing a  $\text{Br}_3^-$  anion and a  $\text{Br}_2$  molecule is also reported. This is unusual, since the presence of an oxidizing agent, such as  $\text{Br}_2$  or  $\text{I}_2$ , typically renders gold (III) compounds. Heaton and coworkers isolated a few quite  $\text{Br}_2$ -rich platinum(IV) complexes analogous to many metal-iodide/iodine compounds.<sup>121</sup>

It is often claimed that the thermal stability of polybromides is lower than that of the corresponding polyiodides, based on the expected lower interaction energy of an ionic unit, such as  $\text{Br}^-$  or  $\text{Br}_3^-$ , with  $\text{Br}_2$ .<sup>109,114</sup> Consequently, it is expected that polybromides much more readily lose  $\text{Br}_2$  and decompose. In this perspective, it is notable that the most bromine-rich compound known is the formal  $\text{Br}_{20}^{2-}$ <sup>119</sup> clearly exceeding the  $X_2/X^-$  ratio of the most iodine-rich compound known so far,  $\text{I}_{29}^{3-}$ .<sup>122</sup> A general reflection is that  $\text{Br}_2$  appears to be the structure-forming unit rather than polybromide ions, in contrast to the polyiodide structures, where the triiodide ion is much more common in polyiodide structures. This hypothesis gains some support from the very recently published  $\text{Br}_9^-$  compound that is of  $[(\text{Br}^-)_4\text{Br}_2]$  type.<sup>123</sup>

### 1.08.7 Other Polyhalides

The existence of polychlorides is by far even more rare than polybromides. It seems that only a few trichloride compounds have been isolated in the solid state.<sup>124–126</sup> The crystallographically determined trichloride ions are linear and slightly asymmetric, 2.23 and 2.31 Å, and 2.25 and 2.34 Å, respectively. The symmetrical stretch vibration is reported to be about  $270\text{ cm}^{-1}$ , whereas the data given for asymmetrical stretch vibration differ a bit. However, it appears that the wavenumber is equal or lower than for the symmetrical stretch vibration, which is rather uncommon and different from what is observed for the triiodide ion. It is also different from the calculated results for a centrosymmetric  $\text{Cl}_3^-$ , as reported in Table 2. Evans and Lo also suggested the formation of a pentachloride ion on the basis of vibrational spectroscopic data.<sup>124</sup> A nuclear quadrupolar resonance (NQR) spectroscopic study on less well-characterized trichloride salts shows that they are centrosymmetric and adequately described by the Pimentel bonding scheme proposed for triiodides.<sup>127</sup> This investigation was later followed up by a calculational study.<sup>128</sup> Just as for polyiodides, vibrational spectroscopy is a useful tool for the characterization of trichloride compounds.<sup>129</sup> The formation of trichloride in the gas phase has been proposed,<sup>130</sup> and more or less well-defined polychlorides have been used as chlorination agents in organic chemistry.<sup>131</sup> Thus, the major knowledge on polychlorides can be extracted from calculational studies (*vide supra*) and experimental data, as well as examples of catenation, are limited.

The polyfluoride chemistry appears even more limited than the polychloride one. After some early work on matrix-isolated trifluorides, mainly theoretical investigations have been reported.<sup>132,133</sup> Mass spectrometry has been used to identify  $\text{F}_3^-$  in gas phase.<sup>134</sup> Mass spectrometry was also used

to determine the dissociation energies of  $\text{F}_3^-$  into  $\text{F}^- + \text{F}_2$  ( $98\text{ kJ mol}^{-1}$  – in close agreement with high-level theory) and  $\text{F} + \text{F}_2^-$  ( $27\text{ kJ mol}^{-1}$ ).<sup>135</sup> Failed reactions aimed at trifluorides in solution have been reported.<sup>136</sup> The symmetrical stretch vibration of  $\text{F}_3^-$  is assigned to a peak at about  $460\text{ cm}^{-1}$ . Some rather early high-level calculations on the  $\text{F}_3^-$  ion identified it as a challenging calculational task because of significant multiconfigurational character. A symmetrical stretch frequency, as compared to experiment, was determined by Ault and colleagues, and an F–F bond distance of 1.74 Å was obtained.<sup>137</sup> Later studies have shown hybrid density-functional methods to give reasonable results for the trifluoride ion in alkali-metal systems.<sup>138</sup> Also for the trifluoride ion, Braida et al. used a VB method to get a deeper insight into the bonding properties. Part of the stability of  $\text{F}_3^-$  was attributed to a lone-pair stretching instability of the  $\text{F}_2$  fragment, a property transferable also to the heavier analogs.<sup>139</sup> The old low-temperature work of Ault et al. was very recently revisited and combined with calculations at coupled-cluster level. The latter study was extended to tetra- and pentafluoride ions as well, essentially rediscovering the structural pattern known from polyiodide chemistry.<sup>140</sup> However, the main contribution to the  $\text{F}_3^- - \text{F}_2$  bonding was assigned to electrostatic interaction. Covalent catenation in polyfluoride systems may thus be questioned.

Astatine has a story of its own – and a very short one. Because of the inherent characteristics of radioactivity and rare appearance, experimental studies are limited. No studies on a triastatide or any polyastatide ions have been found in literature. More strangely, the system does not seem to have been investigated theoretically either. A simple presumption regarding a triastatide ion would be that it is even more inclined to polyhalide formation through ‘sticky’ long-range At–At bonding. However, this is not necessarily the case. In the theoretical studies on period-7 elements in relation to their lighter congeners, a periodic behavior is often identified rather than a monotonous change down a group, a phenomenon attributed to relativistic effects in superheavy elements.<sup>141</sup> The calculational results shown in Table 3 indicate that polyastatides are stable polyhalide units, and the results in Figure 6 that the potential energy surface is more similar to polybromides than to polyiodides.

There is a large plethora of interhalogen compounds. Typically, the most electronegative, for example, lighter, element takes on the terminal positions, and the heavier group-17 element can be regarded as the coordination center.<sup>2</sup> Many of the interhalogen compounds can be described on the basis of classical coordination chemistry, where the central atom is surrounded by ligands. Also, a trihalide, such as  $\text{I}_3^-$ , can be visualized in such a way. Of course, quite a number of linear  $\text{XY}_2^-$  ions have been reported in literature. However, they contribute little new understanding to our previous discussion on trihalide bonding. On the basis of established textbook knowledge, stability increases as the central atom becomes heavier and the difference in weight between the coordination center and ligand becomes lower. This has also implications for the prospects of forming interhalogen types of polyhalides. The heavier elements are most prone to bind to polyhalide species, and since they typically are buried in the center of interhalogen molecules, there is little tendency to form larger entities.<sup>142</sup> Interestingly enough, nonbonded



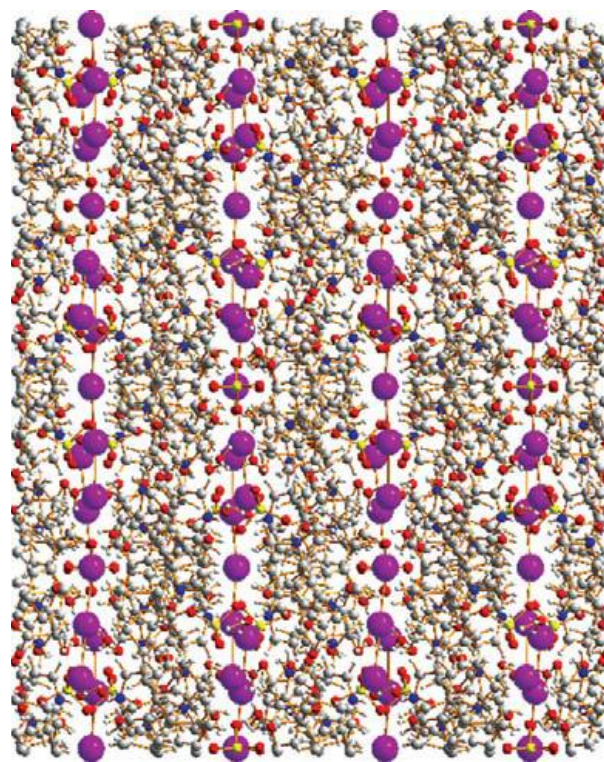
contacts in interhalogen compounds were recently used as an indicator to identify errors in crystal structure data.<sup>143</sup>

Having said this, however, a few examples of extended structures exist. For instance, the rather complex structure of  $I_3Br_4^-$  is pyramidal of the type  $[(Br^-) \cdot 3IBr]$  and with comparably short Br–Br contacts (3.36 Å) between the molecular units forming a chain-like structure.<sup>144</sup> This polyhalide ion and other interhalogen ions were subjected to a rather thorough diffraction, vibrational spectroscopic, and calculational investigation.<sup>145</sup> Parlow and Hartl isolated a series of iodine-bromide interhalogen ions, of which a V-shaped  $I_2Br_3^-$  and a two-dimensional layer of  $I_5Br_2^-$  composition are the most notable.<sup>146</sup> In these structures, the  $I_2Br^-$  ion, linked by Br<sub>2</sub> and I<sub>2</sub> in the structures, respectively, is claimed to be the fundamental structural unit. It is not unexpected that an extended structure is based on the I<sub>2</sub> bridging unit. A V-shaped  $I_2Cl_3^-$ , analogous to a pentaiodide, of the type  $[(Cl^-) \cdot 2ICl]$  has also been reported.<sup>147</sup> In this case, the ionic units are regarded as isolated, since intermolecular Cl–Cl contacts exceed the sum of the van der Waals radii. In a series of amide/thioamide compounds, the chlorine-containing  $I_2Cl_2^{2-}$ , analogous to  $I_4^{2-}$ , has been isolated, where the chloride ions take the terminal positions at the ends of the central I<sub>2</sub> unit.<sup>148</sup> In halogenated dithiols, IBr has been noted as a bridging unit.<sup>149</sup> In solution, it is clear that mixtures of the halides give rise to an extensive and quite complex situation with many coupled equilibria.<sup>150</sup> This was also a complication in attempts to use interhalogen systems as redox couples in DSCs, where the complex chemistry raises questions about the exact nature of the active redox agents in the electrolytes.<sup>151</sup>

## 1.08.8 Applications

### 1.08.8.1 Optical Applications

One of the oldest applications involving polyiodide chemistry is most likely in quantitative determination of redox-active components in solution – the iodometric titration. Very strongly associated with this method of analysis is the phenomenon of iodide/iodine tinting of starch, used as a universal indicator of iodine. Several studies have indicated the presence of polyiodide chains inside the carbohydrate helices as the origin of the intense color observed.<sup>152–155</sup> A rather recent study using L-edge x-ray absorption near-edge structure (XANES) data in comparison with model systems of known composition indicated the polyiodide chains in amylose to mainly consist of  $I_5^-$ .<sup>156</sup> It is amazing that the mineral herapathite was successfully used as light-polarizing material for decades until Kahr and coworkers very recently determined its structure.<sup>56</sup> The structure of herapathite is shown in Figure 17. A striking feature of this material is the chains of triiodide ions giving rise to its anisotropic optical properties. The inter-triiodide distances range from 3.74 to 3.81 Å. The remarkable linear dichroism of herapathite is described as originating from molecular transitions in the triiodide ions attributable to the confined linear arrangement.<sup>157</sup> The luminescent properties of metal–organic frameworks were shown to be affected by iodine enrichment, thus attributed to the confined polyiodide formation.<sup>158</sup>



**Figure 17** The linear triiodide chains in herapathite. This figure is based on structural data taken from Kahr et al.<sup>56</sup>

### 1.08.8.2 X-Ray Contrast Agents

A classical problem in crystallography, in particular for large molecules/unit cells, such as in protein crystallography, is the lack of phase information. One way to facilitate the crystallographic analysis is to introduce a heavy atom – a strong scatterer of x-rays – in a controlled way. Either comparably heavy cations, such as  $Cs^+$  or  $Gd^{3+}$ , or anions, such as the heavier halides, or Xe gas have been used. These elements are also known from medical x-ray imaging, where, of course, also biological availability must be taken into account. Recent studies have identified triiodide, for both chemical and physical reasons, to be a good candidate to treat the phasing problem.<sup>159</sup> Both  $I_3^-$  and  $I_5^-$  entities were found in the model systems studied.<sup>160</sup>

### 1.08.8.3 Triiodide Detection

Important advances in the development of a triiodide-selective electrochemical electrode/sensor have been made. One class of electrodes is based on a polyvinyl chloride (PVC) membrane incorporating an active, with respect to the triiodide ion, metal-complex or organic species.<sup>161–163</sup> The metal-complex-doped membranes often involve salen-like ligands.<sup>164,165</sup> The chemoluminescence has found an interesting application in the detection of the level of NO in human red blood cells.<sup>166</sup>

### 1.08.8.4 Doping of Polymers and Carbons

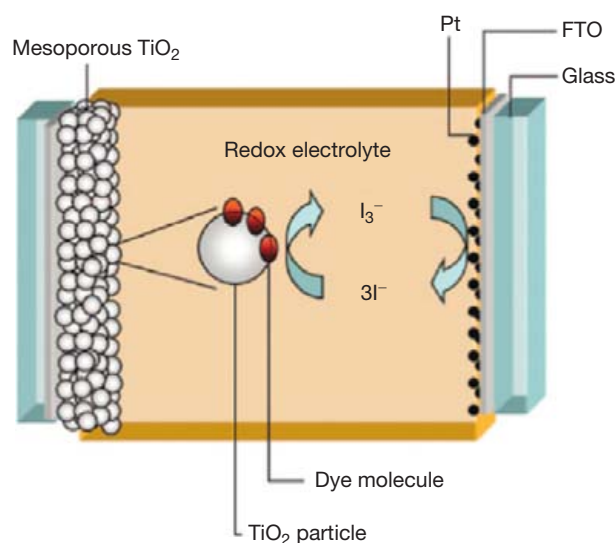
As already noted, the tetrathiafulvalene triiodide compound was found to exhibit low-dimensional metallic properties.<sup>21</sup>

One example of an iodine-doped superconducting organic system based on a selenium-based tetrathiafulvalene showed the presence of incommensurate  $I_3^-$  chains and a critical temperature of superconduction at about 8 K.<sup>167,168</sup> This is an interesting model system considering that iodine frequently is used to dope (partly oxidize) organic polymers in order to enhance hole-conducting properties. The interaction between iodine and carbon materials is also of interest in potential electronic applications. Carbon nanotubes doped with iodine were shown to host polyiodides of  $I_3^-$  or  $I_5^-$  type.<sup>169,170</sup> Shi et al. recently showed how hole doping levels, and thus the conducting character of the nanotubes, could be tuned by iodine and the changes could be correlated with the formation of different polyiodide species inside carbon nanotubes.<sup>171</sup> In a high-pressure study, the confined polyiodide species in the carbon nanotubes displayed an increasing linearization upon increasing pressure.<sup>172</sup> The carbon-iodide/polyiodide interface has a special interest because of, for instance, the development of supercapacitors.<sup>173</sup>

### 1.08.8.5 Electrolytes

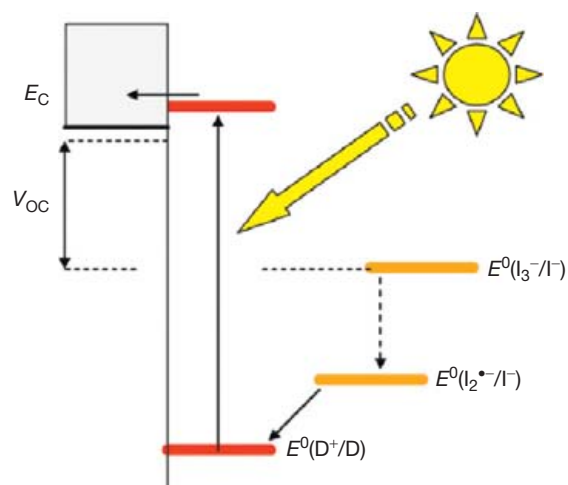
The zinc-bromine (flow) battery is a rather unusual type of battery, although with some advantages. The mixture of bromide and bromine in the electrolyte will inevitably lead to the formation of polybromides. Just as in many electrochemical devices, ionic liquids have emerged as attractive electrolyte media. In one such study, *in situ* IR spectroscopy identified polybromides at the carbon electrode material and the formation of  $Br_5^-$  was proposed.<sup>174</sup> More well known are the lithium-iodine batteries, which have found special applications, such as in pacemaker batteries, because of their typically very long-term and stable current output. A recent *in situ* combined electrochemical and Raman spectroscopic study showed the formation of  $I_3^-$  and  $I_5^-$  at the anode.<sup>175</sup>

One of the strongest boosts of polyiodide chemistry in relation to redox-active electrolytes can be attributed to the growing



**Figure 18** A schematic view of the DSC, including an  $I^-/I_3^-$ -based electrolyte. Reproduced from Hagfeldt, A.; Boschloo, G.; Sun, L.; Kloo, L.; Pettersson, H. *Chem. Rev.* **2010**, *110*, 6595–6663.

interest in DSCs. Ever since the remarkable improvement described by Grätzel and O'Regan in 1991,<sup>176,177</sup> redox-active electrolytes based on the iodide/triiodide ( $I^-/I_3^-$ ) system have prevailed. The schematic view in **Figure 18** shows the central role of the liquid redox electrolyte in the photoelectrochemical cell. Recent developments strive to avoid iodine in such electrolytes, mainly because of its unwanted photochemistry and corrosive nature setting limits to the DSC stability.<sup>178–180</sup> Nevertheless, the  $I^-/I_3^-$  system seems to represent a compromise between wanted and unwanted side reactions that is difficult to outperform. In a simplified view, the redox activity of the iodine-based system undergoes two essential reactions. The triiodide ions are reduced at the DSC counter-electrode forming iodide ions. This is a two-electron process, highly facilitated by catalyzing platinum particles adsorbed onto the conducting glass substrate constituting the counter-electrode. These diffuse to the working electrode (photoanode), where the iodide ions efficiently regenerate the sensitizing dye.<sup>27,29,181</sup> The two-electron process is here divided in space and time, allowing for a quick electron transfer to the dye. This very property of the iodine system also retards one of the most problematic side reactions, the unwanted back transfer of energy-rich photoelectrons from the working electrode to the electrolyte triiodide ions. This process becomes extremely slow, allowing the DSCs to reach high conversion efficiencies. Yanagida and coworkers have shown indications of efficient Grotthuss type of conduction in electrolytes based on ionic liquid crystals.<sup>182,183</sup> However, as noted above, double salts of iodide and triiodide appear to be quite stable, and it was shown that an unwanted precipitation in some working DSCs could be attributed to exactly such a compound, involving an additive aimed at blocking the loss of photoelectrons from the working electrode.<sup>17</sup> Solution chemistry sometimes gives unexpected reactions. Another concern regarding losses in conversion efficiencies using the  $I^-/I_3^-$ -redox couple is the observed overpotential with respect to dye regeneration. Efficient dye reduction of the system requires about 0.5 V too high voltage with respect to the necessary voltage for dye regeneration, of course with a reduction in photovoltage and efficiency



**Figure 19** The two-step redox chemistry of dye regeneration in DSCs. Reproduced from Boschloo, G.; Hagfeldt, A. *Accounts Chem. Res.* **2009**, *42*, 1819–1826.

as a consequence. However, Boschloo and colleagues recently found that the required overpotential can be traced to the two-electron character of the redox couple, showing that it is instead the  $I^-/I_2^-$  system that constitutes the driving force in dye regeneration, and thus the overpotential is just apparent.<sup>28</sup> Schematically, this is shown in Figure 19. Privalov and colleagues used density-functional theory to elucidate the electron-transfer mechanism of both organometallic and organic sensitizing dyes, strongly indicating an outer-sphere, two-step mechanism.<sup>29,181</sup> In an experimental study and overview, Meyer and coworkers arrived at a similar two-step mechanism, also highlighting the photoinduced formation of I–I bonds.<sup>184</sup> Ionic-liquid electrolytes have been used successfully in DSCs, although the main drawback can be attributed to the relatively high viscosity of such solvent media.<sup>101</sup> The high viscosities cause mass-transport problems at higher irradiation. In order to counteract this problem, typically 5–10 times higher concentration of iodine is used in ionic-liquid media as compared to organic solvent ones. This strategy reduces mass-transport limitations but introduces losses because of light absorption by the triiodide/polyiodide species in solution and higher losses because of recombination with triiodide in the electrolyte.<sup>24</sup> In summary, the polyiodide chemistry in DSCs offers benefits and drawbacks, but certainly calls for an understanding of the polyiodide chemistry.

### 1.08.9 Conclusion

An overview on polyhalide chemistry is provided with the aim to give explanations to the strong tendency for concatenation in the halogen group. The trihalide ion is used as a model for the understanding of the bonding conditions in polyhalide compounds. Special focus is given to the polyiodides. The emerging field of polybromides is also discussed in relation to polyiodides, and the application of polyhalides in the fields of optics, conducting polymers, and dye-sensitized solar cells is highlighted.

### Acknowledgment

Dr. Jan Rosdahl is acknowledged for the assistance in making the figures.

### References

- Beck, J. *Coord. Chem. Rev.* **1997**, *163*, 55–70.
- Wiebenga, E. H.; Havinga, E. E.; Boswijk, K. H., Eds.; In: Structures of Interhalogen Compounds and Polyhalides; Academic Press: New York, 1961; Vol. 3.
- Tebbe, K.-F., Ed.; In *Polyhalogen Cations and Polyhalide Anions*; Elsevier: Amsterdam, 1975.
- Svensson, P. H.; Kloo, L. *Chem. Rev.* **2003**, *103*, 1649–1684.
- Tebbe, K. F. *Beiträge zur Chemie und Strukturchemie der Polyiodide Komplexer Kationen*. Habilitation Thesis: Wilhelms-Universität Münster, 1975.
- Svensson, P. H.; Kloo, L. *J. Chem. Soc.-Dalton Trans.* **2000**, 2449–2455.
- Burykin, I. V.; Chernov'yants, M. S.; Aleshina, N. V. *Russ. Chem. Bull.* **2007**, *56*, 1390–1393.
- Meyer, M. K.; Graf, J.; Reiss, G. *J. Z. Naturforsch. B* **2010**, *65*, 1462–1466.
- Kazheva, O. N.; Aleksandrov, G. G.; D'Yachenko, O. A.; Chernov'yants, M. S.; Lykova, E. O.; Tolpygin, I. E.; Raskita, I. M. *Russ. J. Coord. Chem.* **2004**, *30*, 599–603.
- Kazheva, O. N.; Shilov, G. V.; D'Yachenko, O. A.; Chernov'yants, M. S.; Kirsanova, Y. A.; Lykova, E. O.; Tolpygin, I. E. *Russ. J. Inorg. Chem.* **2007**, *52*, 562–566.
- Niu, Y. Y.; Song, Y. L.; Zhang, N.; Hou, H. W.; Che, D. J.; Fan, Y. T.; Zhu, Y.; Duan, C. Y. *Eur. J. Inorg. Chem.* **2006**, 2259–2267.
- Nimz, O.; Gessler, K.; Uson, I.; Laettig, S.; Welfle, H.; Sheldrick, G. M.; Saenger, W. *Carbohydr. Res.* **2003**, *338*, 977–986.
- Chantrapromma, S.; Chanawanno, K.; Fun, H. K. *Acta Crystallogr. Sect. E Struct. Rep. Online* **2007**, *63*, O1554–O1556.
- Duarte-Ruiz, A.; Nunez-Dallos, N.; Garzon-Tovar, L.; Wurst, K.; Avella-Moreno, E.; Gomez-Baquero, F. *Chem. Commun.* **2011**, *47*, 7110–7112.
- Walbaum, C.; Pantenburg, I.; Meyer, G. *Z. Anorg. Allg. Chem.* **2009**, *635*, 1083–1085.
- Day, E. F.; Dean, N. S.; Franz, A. H. *Acta Crystallogr. C* **2006**, *62*, O571–O573.
- Fischer, A.; Pettersson, H.; Hagfeldt, A.; Boschloo, G.; Kloo, L.; Gorlov, M. *Sol. Energy Mater. Sol. C* **2007**, *91*, 1062–1065.
- Chow, H.; Dean, P. A. W.; Craig, D. C.; Lucas, N. T.; Scudder, M. L.; Dance, I. G. *New J. Chem.* **2003**, *27*, 704–713.
- Lu, J. Y.; Zhang, Y. P.; Cmaidalka, J. E. *CrystEngComm* **2002**, 213–214.
- Reiss, G. J.; Engel, J. S. *CrystEngComm* **2002**, 155–161.
- Bender, K.; Hennig, I.; Schweitzer, D.; Dietz, K.; Endres, H.; Keller, H. J. *Mol. Cryst. Liq. Cryst.* **1984**, *108*, 359–371.
- de Grotthuss, C. J. D. *Ann. Chim.* **1806**, 54–74.
- Pennington, W. T.; Hanks, T. W.; Arman, H. D. In *Halogen Bonding: Fundamentals and Applications*; Springer: Berlin, 2008; Vol. 126, pp 65–104.
- Yu, Z.; Gorlov, M.; Nissfolk, J.; Boschloo, G.; Kloo, L. *J. Phys. Chem. C* **2010**, *114*, 10612–10620.
- Hoops, A. A.; Gascooke, J. R.; Faulhaber, A. E.; Kautzman, K. E.; Neumark, D. M. *J. Chem. Phys.* **2004**, *120*, 7901–7909.
- Nakanishi, R.; Saitou, N.; Ohno, T.; Kowashi, S.; Yabushita, S.; Nagata, T. *J. Chem. Phys.* **2007**, *126*, 17.
- Farnum, B. H.; Gardner, J. M.; Meyer, G. *J. Inorg. Chem.* **2010**, *49*, 10223–10225.
- Boschloo, G.; Hagfeldt, A. *Acc. Chem. Res.* **2009**, *42*, 1819–1826.
- Privalov, T.; Boschloo, G.; Hagfeldt, A.; Svensson, P. H.; Kloo, L. *J. Phys. Chem. C* **2009**, *113*, 783–790.
- Baratz, A.; Ruhman, S. *Chem. Phys. Lett.* **2008**, *461*, 211–217.
- Nishiyama, Y.; Terazima, M.; Kimura, Y. *Chem. Phys. Lett.* **2010**, *491*, 164–168.
- Sakane, H.; Mitsui, T.; Tanida, H.; Watanabe, I. *J. Synchrotron. Radiat.* **2001**, *8*, 674–676.
- Pimentel, C. G. *J. Chem. Phys.* **1951**, *19*, 446–448.
- Hach, R. J.; Rundle, R. E. *J. Am. Chem. Soc.* **1951**, *73*, 4321–4324.
- Munzarova, M. L.; Hoffmann, R. *J. Am. Chem. Soc.* **2002**, *124*, 4787–4795.
- Novoa, J. J.; Mota, F.; Alvarez, S. *J. Phys. Chem.* **1988**, *92*, 6561–6566.
- Novoa, J. J.; Mota, F.; Whangbo, M. H.; Williams, J. M. *Inorg. Chem.* **1991**, *30*, 54–58.
- Ogawa, Y.; Takahashi, O.; Kikuchi, O. *Theochem.* **1998**, *424*, 285–292.
- Landrum, G. A.; Goldberg, N.; Hoffmann, R. *J. Chem. Soc. Dalton Trans.* **1997**, 3605–3613.
- Manca, G.; Ienco, A.; Mealli, C. *Cryst. Growth Des.* **2012**, *12*, 1762–1771.
- Ogawa, Y.; Takahashi, O.; Kikuchi, O. *Theochem.* **1998**, *429*, 187–196.
- Kloo, L.; Rosdahl, J.; Svensson, P. H. *Eur. J. Inorg. Chem.* **2002**, 1203–1209.
- Braida, B.; Hiberty, P. C. *J. Phys. Chem. A* **2008**, *112*, 13045–13052.
- Zhang, F. S.; Lynden-Bell, R. M. *Phys. Rev. Lett.* **2003**, *90*, 4.
- Margulis, C. J.; Coker, D. F.; Lynden-Bell, R. M. *J. Chem. Phys.* **2001**, *114*, 367–376.
- Margulis, C. J.; Coker, D. F.; Lynden-Bell, R. M. *Chem. Phys. Lett.* **2001**, *341*, 557–560.
- Zhang, F. S.; Lynden-Bell, R. M. *Eur. Phys. J. D* **2005**, *34*, 129–132.
- Zhang, F. S.; Lynden-Bell, R. M. *Phys. Rev. E* **2005**, *71*, 5.
- Zhang, F. S.; Lynden-Bell, R. M. *Mol. Phys.* **2003**, *101*, 1641–1649.
- Zhang, F. S.; Lynden-Bell, R. M. *J. Chem. Phys.* **2003**, *119*, 6119–6131.
- Sato, H.; Hirata, F.; Myers, A. B. *J. Phys. Chem. A* **1998**, *102*, 2065–2071.
- Kozłowski, T.; Vohringer, P. *Chem. Phys. Lett.* **2001**, *342*, 141–147.
- Frisch, M. J.; Trucks, G. W.; Schlegel, H. B.; Scuseria, G. E.; Robb, M. A.; Cheeseman, J. R.; Scalmani, G.; Barone, V.; Mennucci, B.; Petersson, G. A.; Nakatsuji, H.; Caricato, M.; Li, X.; Hratchian, H. P.; Izmaylov, A. F.; Bloino, J.; Zheng, G.; Sonnenberg, J. L.; Hada, M.; Ehara, M.; Toyota, K.; Fukuda, R.; Hasegawa, J.; Ishida, M.; Nakajima, T.; Honda, Y.; Kitao, O.; Nakai, H.; Vreven, T.; Montgomery, J. J. A.; Peralta, J. E.; Ogliaro, F.; Bearpark, M.; Heyd, J. J.; Brothers, E.; Kudin, K. N.; Staroverov, V. N.; Kobayashi, R.; Normand, J.; Raghavachari, K.; Rendell, A.; Burant, J. C.; Iyengar, S. S.; Tomasi, J.; Cossi, M.;



- Rega, N.; Millam, N. J.; Klene, M.; Knox, J. E.; Cross, J. B.; Bakken, V.; Adamo, C.; Jaramillo, J.; Gomper, R.; Stratmann, R. E.; Yazayev, O.; Austin, A. J.; Cammi, R.; Pomelli, C.; Ochterski, J. W.; Martin, R. L.; Morokuma, K.; Zakrzewski, V. G.; Voth, G. A.; Salvador, P.; Dannenberg, J. J.; Dapprich, S.; Daniels, A. D.; Farkas, Ö.; Foresman, J. B.; Ortiz, J. V.; Cioslowski, J.; Fox, D. J.; Gaussian 09, Revision A.02; Gaussian, Inc.: Wallingford CT, 2009.
54. The basis sets were all taken from the compilation of effective-core potentials with associated valence basis sets from the Institut für Theoretische Chemie, Stuttgart (<http://www.theochem.uni-stuttgart.de/>). The basis sets of Br, I and At were of triple-zeta quality, and slightly less expanded for F and Cl. Short characterization of the basis sets are as follows: F MWB2/(4s5p)/(2s3p); Cl MWB10/(4s5p)/(2s3p); Br MDF10/(10s11p9d1f)/(5s4p3d1f); I MDF28/(12s11p9d1f)/(5s4p3d1f); At MDF60/(12s11p8d1f)/(5s4p3d1f).
  55. Walbaum, C.; Pantenburg, I.; Meyer, G. *Z. Naturforsch. B* **2010**, *65*, 1077–1083.
  56. Kahr, B.; Freudenthal, J.; Phillips, S.; Kaminsky, W. *Science* **2009**, *324*, 1407.
  57. Aragoni, M. C.; Arca, M.; Devillanova, F. A.; Isaia, F.; Lippolis, V. *Phosphorus Sulfur Silicon Relat. Elem.* **2008**, *183*, 1036–1045.
  58. Lee, S.; Chen, B. L.; Fredrickson, D. C.; DiSalvo, F. J.; Lobkovsky, E.; Adams, J. A. *Chem. Mat.* **2003**, *15*, 1420–1433.
  59. Aragoni, M. C.; Arca, M.; Devillanova, F. A.; Hursthouse, M. B.; Huth, S. L.; Isaia, F.; Lippolis, V.; Mancini, A. *CrystEngComm* **2004**, *6*, 3.
  60. Dolder, S.; Liu, S. X.; Beurer, E.; Ouahab, L.; Decurtins, S. *Polyhedron* **2006**, *25*, 1514–1518.
  61. Blake, A. J.; Li, W. S.; Lippolis, V.; Parsons, S.; Schroder, M. *Acta Crystallogr. B* **2007**, *63*, 81–92.
  62. Link, C.; Pantenburg, I.; Meyer, G. *Z. Anorg. Allg. Chem.* **2008**, *634*, 616–618.
  63. Walbaum, C.; Pantenburg, I.; Meyer, G. *Z. Anorg. Allg. Chem.* **2008**, *634*, 1247–1248.
  64. Neumuller, B.; Dehnicke, K. *Z. Anorg. Allg. Chem.* **2010**, *636*, 515–517.
  65. Basch, A.; Hartl, M.; Behrens, P. *Microporous Mesoporous Mat.* **2007**, *99*, 244–250.
  66. Wang, Z. M.; Cheng, Y. J.; Liao, C. S.; Yan, C. H. *CrystEngComm* **2001**, *14*.
  67. Lu, J. Y.; Schauss, V. *Eur. J. Inorg. Chem.* **2002**, 1945–1947.
  68. Horn, C.; Scudder, M.; Dance, I. *CrystEngComm* **2001**, art. no.-1.
  69. Horn, C. J.; Blake, A. J.; Champness, N. R.; Garau, A.; Lippolis, V.; Wilson, C.; Schroder, M. *Chem. Commun.* **2003**, 312–313.
  70. Horn, C. J.; Blake, A. J.; Champness, N. R.; Lippolis, V.; Schroder, M. *Chem. Commun.* **2003**, 1488–1489.
  71. Aragoni, M. C.; Arca, M.; Demartin, F.; Devillanova, F. A.; Garau, A.; Isaia, F.; Lippolis, V.; Rizzato, S.; Verani, G. *Inorg. Chim. Acta* **2004**, *357*, 3803–3809.
  72. Reiss, G. J.; Engel, J. S. *Z. Naturforsch. B* **2004**, *59*, 1114–1117.
  73. Svensson, P. H.; Gorlov, M.; Kloo, L. *Inorg. Chem.* **2008**, *47*, 11464–11466.
  74. Abate, A.; Brischetto, M.; Cavallo, G.; Lahtinen, M.; Metrangolo, P.; Pilati, T.; Radice, S.; Resnati, G.; Rissanen, K.; Terraneo, G. *Chem. Commun.* **2010**, *46*, 2724–2726.
  75. Garcia, M. D.; Marti-Rujas, J.; Metrangolo, P.; Peinador, C.; Pilati, T.; Resnati, G.; Terraneo, G.; Ursini, M. *CrystEngComm* **2011**, *13*, 4411–4416.
  76. Yu, X. C.; Atalla, R. H. *Carbohydr. Res.* **2005**, *340*, 981–988.
  77. Papaioannou, J. C.; Ghikas, T. C. *Mol. Phys.* **2003**, *101*, 2601–2608.
  78. Papaioannou, J. C. *Mol. Phys.* **2004**, *102*, 95–99.
  79. Charalampopoulos, V. G.; Papaioannou, J. C.; Karayianni, H. S. *Solid State Sci.* **2006**, *8*, 97–103.
  80. Charalampopoulos, V. G.; Papaioannou, J. C.; Tampouris, K. E. *Solid State Ion.* **2007**, *178*, 793–799.
  81. Charalampopoulos, V. G.; Papaioannou, J. C.; Viras, K.; Karayianni, H. S.; Kakali, G. *Supramol. Chem.* **2010**, *22*, 499–510.
  82. Charalampopoulos, V. G.; Papaioannou, J. C.; Kakahlb, G.; Karayianni, H. S. *Carbohydr. Res.* **2008**, *343*, 489–500.
  83. Tsipis, A. C.; Karipidis, P. A. *Polyhedron* **2008**, *27*, 289–298.
  84. Lang, E. S.; Strähle, J. Z. *Anorg. Allg. Chem.* **1996**, *622*, 981–984.
  85. Svensson, P. H.; Rosdahl, J.; Kloo, L. *Chem. Eur. J.* **1999**, *5*, 305–311.
  86. Svensson, P. H.; Kloo, L. *Inorg. Chem.* **1999**, *38*, 3390–3393.
  87. Castro-Castro, L. M.; Guloy, A. M. *Angew. Chem. Int. Ed. Engl.* **2003**, *42*, 2771–2774.
  88. Castro-Castro, L. M.; Guloy, A. M. *Inorg. Chem.* **2004**, *43*, 4537–4539.
  89. Schneider, D.; Schier, A.; Schmidbaur, H. *Dalton Trans.* **2004**, 1995–2005.
  90. Walbaum, C.; Pantenburg, I.; Meyer, G. *Cryst. Res. Technol.* **2008**, *43*, 1183–1186.
  91. Li, H. H.; Chen, Z. R.; Liu, Y.; Liu, J. B.; Guo, L. Q.; Li, J. Q. *J. Mol. Struct.* **2009**, *934*, 112–116.
  92. Redel, E.; Rohr, C.; Janiak, C. *Chem. Commun.* **2009**, 2103–2105.
  93. Louvain, N.; Bi, W. H.; Mercier, N.; Buzare, J. Y.; Legein, C.; Corbel, G. *Dalton Trans.* **2007**, 965–970.
  94. Li, H. H.; Chen, Z. R.; Cheng, L. C.; Liu, J. B.; Chen, X. B.; Li, J. Q. *Cryst. Growth Des.* **2008**, *8*, 4355–4358.
  95. Janczak, J. *Acta Crystallogr. C* **2004**, *60*, M330–M332.
  96. Bergeron, D. E.; Roach, P. J.; Castleman, A. W.; Jones, N.; Khanna, S. N. *Science* **2005**, *307*, 231–235.
  97. Strobele, M.; Meyer, H. J. Z. *Anorg. Allg. Chem.* **2010**, *636*, 62–66.
  98. Mendizabal, F. *Theochem J. Mol. Struct.* **2010**, *955*, 71–74.
  99. Bengtsson, L. A.; Stegemann, H.; Holmberg, B.; Füllbier, H. *Mol. Phys.* **1991**, *73*, 283–296.
  100. Stegemann, H.; Schnittke, A.; Füllbier, H. *Electrochim. Acta* **1990**, *35*, 355–359.
  101. Gorlov, M.; Kloo, L. *Dalton Trans.* **2008**, 2655–2666.
  102. Zistler, M.; Wachter, P.; Wasserscheid, P.; Gerhard, D.; Hinsch, A.; Sastrawan, R.; Gores, H. J. *Electrochim. Acta* **2006**, *52*, 161–169.
  103. Wachter, P.; Schreiner, C.; Zistler, M.; Gerhard, D.; Wasserscheid, P.; Gores, H. J. *Microchim. Acta* **2008**, *160*, 125–133.
  104. Jovanovski, V.; Orel, B.; Jerman, I.; Hocevar, S. B.; Ogorevc, B. *Electrochem. Commun.* **2007**, *9*, 2062–2066.
  105. Jerman, I.; Jovanovski, V.; Vuk, A. S.; Hocevar, S. B.; Gaberscek, M.; Jesih, A.; Orel, B. *Electrochim. Acta* **2008**, *53*, 2281–2288.
  106. Thorsmolle, V. K.; Rothenberger, G.; Topgaard, D.; Brauer, J. C.; Kuang, D. B.; Zakeeruddin, S. M.; Lindman, B.; Gratzel, M.; Moser, J. E. *ChemPhysChem* **2011**, *12*, 145–149.
  107. Breneman, G. L.; Willett, R. D. *Acta Crystallogr.* **1967**, *23*, 334.
  108. Stroemme, K. O. *Acta Chem. Scand.* **1959**, *13*, 2089–2100.
  109. Robertson, K. N.; Bakshi, P. K.; Cameron, T. S.; Knop, O. Z. *Anorg. Allg. Chem.* **1997**, *623*, 104–114.
  110. Atwood, J. L.; Junk, P. C.; May, M. T.; Robinson, K. D. *J. Chem. Crystallogr.* **1994**, *24*, 243–245.
  111. Chekhlov, A. N. *Russ. J. Inorg. Chem.* **2008**, *53*, 1197–1202.
  112. Kornath, A.; Blecher, O. Z. *Anorg. Allg. Chem.* **2002**, *628*, 570–574.
  113. Aragoni, M. C.; Arca, M.; Devillanova, F. A.; Hursthouse, M. B.; Huth, S. L.; Isaia, F.; Lippolis, V.; Mancini, A.; Ogilvie, H. *Inorg. Chem. Commun.* **2005**, *8*, 79–82.
  114. Cunningham, C. W.; Burns, G. R.; McKee, V. *Inorg. Chim. Acta* **1990**, *167*, 135–137.
  115. Schuster, P.; Mikosch, H.; Bauer, G. *J. Chem. Phys.* **1998**, *109*, 1833–1844.
  116. Aragoni, M. C.; Arca, M.; Devillanova, F. A.; Isaia, F.; Lippolis, V.; Mancini, A.; Pala, L.; Slawin, A. M. Z.; Woollins, J. D. *Chem. Commun.* **2003**, 2226–2227.
  117. Chen, X. Y.; Rickard, M. A.; Hull, J. W.; Zheng, C.; Leugers, A.; Simoncic, P. *Inorg. Chem.* **2010**, *49*, 8684–8689.
  118. Burns, G. R.; Renner, R. M. *Spectrochim. Acta A Mol. Biomol. Spectrosc.* **1991**, *47*, 991–999.
  119. Wolff, M.; Meyer, J.; Feldmann, C. *Angew. Chem. Int. Ed. Engl.* **2011**, *50*, 4970–4973.
  120. Schneider, D.; Schuster, O.; Schmidbaur, H. *Dalton Trans.* **2005**, 1940–1947.
  121. Berkei, M.; Bickley, J. F.; Heaton, B. T.; Steiner, A. *Chem. Commun.* **2002**, 2080–2181.
  122. Tebbe, K.-F.; Buchem, R. *Angew. Chem. Int. Ed. Engl.* **1997**, *36*, 1345–1346.
  123. Haller, H.; Ellwanger, M.; Higelin, A.; Riedel, S. *Angew. Chem. Int. Ed. Engl.* **2011**, *50*, 11528–11532.
  124. Evans, J. C.; Lo, G. Y.-S. *J. Chem. Phys.* **1966**, *44*, 3638–3639.
  125. Bogaard, M. P.; Peterson, J.; Rae, A. D. *Acta Crystallogr. B* **1981**, *37*, 1357–1359.
  126. Chivers, T.; Richardson, J. F.; Smith, N. R. M. *Inorg. Chem.* **1985**, *24*, 2453–2458.
  127. Riedel, E. F.; Willett, R. D. *J. Am. Chem. Soc.* **1975**, *97*, 701–704.
  128. Riedel, E. F.; Willett, R. D. *Theor. Chim. Acta* **1976**, *42*, 237–246.
  129. Ault, B. S.; Andrews, L. J. *J. Chem. Phys.* **1976**, *64*, 4853–4859.
  130. Robbani, R.; Franklin, J. L. *J. Am. Chem. Soc.* **1979**, *101*, 764–765.
  131. Zelikman, V. M.; Tyurin, V. S.; Smirnov, V. V.; Zyk, N. V. *Russ. Chem. Bull.* **1998**, *47*, 1541–1546.
  132. Ault, B. S.; Andrews, L. J. *J. Am. Chem. Soc.* **1976**, *98*, 1591–1593.
  133. Ault, B. S.; Andrews, L. *Inorg. Chem.* **1977**, *16*, 2024–2028.
  134. Tuinman, A. A.; Gakh, A. A.; Hinde, R. J.; Compton, R. N. *J. Am. Chem. Soc.* **1999**, *121*, 8397–8398.
  135. Artau, A.; Nizzi, K. E.; Hill, B. T.; Sunderlin, L. S.; Wenthold, P. G. *J. Am. Chem. Soc.* **2000**, *122*, 10667–10670.
  136. Christe, K. O. *J. Fluor. Chem.* **1995**, *71*, 149–150.
  137. Heard, G. L.; Marsden, C. J.; Scuseria, G. E. *J. Phys. Chem.* **1992**, *96*, 4359–4366.
  138. Tozer, D. J.; Sosa, C. P. *Mol. Phys.* **1997**, *90*, 515–524.
  139. Braida, B.; Hiberty, P. C. *J. Am. Chem. Soc.* **2004**, *126*, 14890–14898.

140. Riedel, S.; Koechner, T.; Wang, X. F.; Andrews, L. *Inorg. Chem.* **2010**, *49*, 7156–7164.
141. Thierfelder, C.; Schwerdtfeger, P.; Koers, A.; Borschevsky, A.; Fricke, B. *Phys. Rev. A* **2009**, *80*, 022501-1–10.
142. Dove, M. F. A. *Coord. Chem. Rev.* **1988**, *85*, 504–522.
143. Serezhkin, V. V.; Prokaeva, M. A.; Pushkin, D. V.; Serezhkina, L. B. *Russ. J. Inorg. Chem.* **2009**, *54*, 1251–1260.
144. Minkwitz, R.; Berkei, M.; Ludwig, R. *Inorg. Chem.* **2001**, *40*, 25–28.
145. Aragoni, M. C.; Arca, M.; Devillanova, F. A.; Hursthouse, M. B.; Huth, S. L.; Isaia, F.; Lippolis, V.; Mancini, A.; Oglivie, H. R.; Verani, G. *J. Organomet. Chem.* **2005**, *690*, 1923–1934.
146. Parlow, A.; Hartl, H. *Z. Naturforsch. B* **1985**, *35*, 45–52.
147. Parlow, A.; Hartl, H. *Acta Crystallogr. B* **1979**, 1930–1933.
148. Parigoridi, I. E.; Corban, G. J.; Hadjidakou, S. K.; Hadjiliadis, N.; Kourkoumelis, N.; Kostakis, G.; Psycharis, V.; Raptopoulou, C. P.; Kubicki, M. *Dalton Trans.* **2008**, 5159–5165.
149. Sakbara, P. J.; Bricklebank, N.; Berridge, R.; Long, S.; Light, M. E.; Coles, S. J.; Hursthouse, M. B. *Dalton Trans.* **2000**, 3235–3236.
150. Olsson, L.-F. *Inorg. Chem.* **1985**, *24*, 1398–1405.
151. Gorlov, M.; Pettersson, H.; Hagfeldt, A.; Kloo, L. *Inorg. Chem.* **2007**, *46*, 3566–3575.
152. Reddy, J. M.; Knox, K.; Robin, M. B. *J. Chem. Phys.* **1964**, *40*, 1082–1089.
153. Teitelbaum, R. C.; Ruby, S. I.; Marks, T. J. *J. Am. Chem. Soc.* **1980**, *102*, 3322–3328.
154. Robin, M. B. *J. Chem. Phys.* **1964**, *40*, 3369–3377.
155. Teitelbaum, R. C.; Ruby, S. L.; Marks, T. J. *J. Am. Chem. Soc.* **1978**, *100*, 3215–3217.
156. Konishi, T.; Tanaka, W.; Kawai, T.; Fujikawa, T. *J. Synchrotron. Radiat.* **2001**, *8*, 737–739.
157. Liang, L.; Rulis, P.; Kahr, B.; Ching, W. Y. *Phys. Rev. B* **2009**, *80*, 5.
158. Liu, Q. K.; Ma, J. P.; Dong, Y. B. *Chem. Commun.* **2011**, *47*, 7185–7187.
159. Evans, G.; Bricogne, G. *Acta Crystallogr. D* **2002**, *58*, 976–991.
160. Evans, G.; Bricogne, G. *Acta Crystallogr. D* **2003**, *59*, 1923–1929.
161. Ganjali, M. R.; Emami, M.; Javanbakht, M.; Salavati-Niasari, M.; Shamsipur, M.; Yousefi, M. *Sens. Actuator B Chem.* **2005**, *105*, 127–131.
162. Ganjali, M. R.; Norouzi, P.; Shirvani-Arani, S.; Salavati-Niasari, M. *Bull. Korean Chem. Soc.* **2005**, *26*, 1738–1742.
163. Ganjali, M. R.; Moghaddamb, M. R.; Norouzi, P.; Shirvani-Arani, S.; Daneshgar, P.; Adib, M.; Sobhi, H. R. *Anal. Lett.* **2006**, *39*, 683–695.
164. Sadeghi, S.; Fathi, F.; Ali Esmaili, A.; Naeimi, H. *Sens. Actuator B Chem.* **2006**, *114*, 928–935.
165. Sadeghi, S.; Gafarzadeh, A.; Naeimi, H. *J. Anal. Chem.* **2006**, *61*, 677–682.
166. Rogers, S. C.; Khalatbari, A.; Gapper, P. W.; Frenneaux, M. P.; James, P. E. *J. Biol. Chem.* **2005**, *280*, 26720–26728.
167. Kawamoto, T.; Mori, T.; Terashima, T.; Uji, S.; Kitagawa, H.; Takimiya, K.; Takamori, A.; Otsubo, T. *J. Phys. IV* **2004**, *114*, 517–519.
168. Kawamoto, T.; Mori, T.; Uji, S.; Yamaura, J. I.; Kitagawa, H.; Takamori, A.; Takimiya, K.; Otsubo, T. *Phys. Rev. B* **2005**, *71*, 4.
169. Zhou, W. Y.; Xie, S. S.; Sun, L. F.; Tang, D. S.; Li, Y. B.; Liu, Z. Q.; Ci, L. J.; Zou, X. P.; Wang, G.; Tan, P.; Dong, X.; Xu, B.; Zhao, B. *Appl. Phys. Lett.* **2002**, *80*, 2553–2555.
170. Jung, Y.; Hwang, S. J.; Kim, S. J. *J. Phys. Chem. C* **2007**, *111*, 10181–10184.
171. Wang, Z. Y.; Wang, L.; Shi, Z. J.; Lu, J.; Gu, Z. N.; Gao, Z. X. *Chem. Commun.* **2008**, 3429–3431.
172. Alvarez, L.; Bantignies, J. L.; Le Parc, R.; Aznar, R.; Sauvajol, J. L.; Merlen, A.; Machon, D.; San Miguel, A. *Phys. Rev. B* **2010**, *82*, 7.
173. Lota, G.; Fic, K.; Frackowiak, E. *Electrochem. Commun.* **2011**, *13*, 38–41.
174. Kautek, W.; Conradi, A.; Fabjan, C.; Bauer, G. *Electrochim. Acta* **2001**, *47*, 815–823.
175. Weinstein, L.; Yourey, W.; Gural, J.; Amatucci, G. G. *J. Electrochem. Soc.* **2008**, *155*, A590–A598.
176. Hagfeldt, A.; Boschloo, G.; Sun, L.; Kloo, L.; Pettersson, H. *Chem. Rev.* **2010**, *110*, 6595–6663.
177. O'Regan, B.; Grätzel, M. *Nature* **1991**, *353*, 737–740.
178. Feldt, S. M.; Gibson, E. A.; Gabrielsson, E.; Sun, L.; Boschloo, G.; Hagfeldt, A. *J. Am. Chem. Soc.* **2010**, *132*, 16714–16724.
179. Wang, M.; Chamberland, N.; Breau, L.; Moser, J. E.; HumphryBaker, R.; Marsan, M.; Zakeeruddin, S. M.; Grätzel, M. *Nat Chem* **2010**, *2*, 385–390.
180. Tian, H.; Jiang, X.; Yu, Z.; Kloo, L.; Hagfeldt, A.; Sun, L. *Angew. Chem. Int. Ed. Engl.* **2011**, *49*, 11598–11620.
181. Nyhlen, J.; Boschloo, G.; Hagfeldt, A.; Kloo, L.; Privalov, T. *ChemPhysChem* **2010**, *11*, 1858–1862.
182. Yamanaka, N.; Kawano, R.; Kubo, W.; Kitamura, T.; Wada, Y.; Watanabe, M.; Yanagida, S. *Chem. Commun.* **2005**, 740–742.
183. Yamanaka, N.; Kawano, R.; Kubo, W.; Masaki, N.; Kitamura, T.; Wada, Y.; Watanabe, I.; Yanagida, S. *J. Phys. Chem. B* **2007**, *111*, 4763–4769.
184. Rowley, J. G.; Farnum, B. H.; Ardo, S.; Meyer, G. J. *J. Phys. Chem. Lett.* **2010**, *1*, 3132–3140.

This page intentionally left blank

## 1.09 Zintl Anions

S Gärtner and N Korber, University of Regensburg, Regensburg, Germany

© 2013 Elsevier Ltd. All rights reserved.

<b>1.09.1</b>	<b>Zintl Anions</b>	251
1.09.1.1	What is a Zintl Anion?	251
1.09.1.1.1	History	251
1.09.1.1.2	Definitions and concepts	252
1.09.1.1.3	Synthetic routes	253
1.09.1.2	Discrete Polyanions in Zintl Phases of Group 14 and Group 15 and Their Dissolution Behavior	254
1.09.1.2.1	Homoatomic polyanions of group 14 in solid state	255
1.09.1.2.2	Homoatomic polyanions of group 15 in solid state	256
1.09.1.2.3	Heteroatomic polyanions of group 14/15, group 14/16, and group 15/16 in solid state	257
1.09.1.2.4	Solid-state versus solution: similarities and discrepancies	257
1.09.1.3	Reactions of Zintl Anions	260
1.09.1.3.1	Oxidation of Zintl anions	260
1.09.1.3.2	Functionalization with exo-bonded main group elements	261
1.09.1.3.3	Reactions with transition metal complexes	263
<b>1.09.2</b>	<b>Conclusion</b>	266
<b>References</b>		266

### 1.09.1 Zintl Anions

#### 1.09.1.1 What is a Zintl Anion?

##### 1.09.1.1.1 History

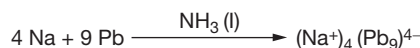
Zintl anions are a very interesting class of compounds, which have fascinated chemists for a long period of time and are still a matter of growing research interest all over the world. Their first experimental evidence was reported 120 years ago in 1891, when Joannis first observed a change in color by reacting the elements sodium and lead in liquid ammonia.<sup>1</sup> He probably could not have anticipated at that time that his observation would be the first step toward a completely new branch of inorganic chemistry, namely, ligand-free main group elements in negative oxidation states. Kraus reported in 1907 that the deep green Na–Pb solutions are electrolytes from which lead can be anodically deposited.<sup>2</sup> Furthermore, he showed that anionically dissolved lead can be precipitated through the addition of  $\text{Pb}^{2+}$  salts. This demonstrated the anionic, highly reduced character of the lead species in solution due to the comproportionation reaction with  $\text{Pb}^{2+}$ . About 40 years after Joannis' observation, Zintl et al. identified the reaction that was described by Joannis.<sup>3</sup> They assumed complete electron transfer from the electropositive element to the electronegative reaction partner. This assumption resulted in the formation of anionic species, which consisted of more than one atom, the so-called polyanions (Scheme 1).

The evaporation of ammonia resulted in an alloy that did not contain polyanions any more. As the x-ray structure determination of temperature labile compounds was not possible at that time, Zintl assumed the  $\text{Pb}_9^{4-}$  anion to be a  $[\text{Pb}^{4-}(\text{Pb}_8)]$  complex of a central  $\text{Pb}^{4-}$  atom and eight coordinating Pb atoms. The description of the correct geometry of the polyanion was not achieved until 1970, when the first crystal structure determination on the structurally related compound  $\text{Na}_4\text{Sn}_9\cdot 7\text{en}$  (en = ethylenediamine) was possible, which gave

monocapped square-antiprismatic-shaped anions.<sup>4</sup> Zintl was also responsible for the discovery of the possibility of dissolving alloys in liquid ammonia, for example  $\text{Na}_4\text{Pb}_9$ , which also contains polyanions precasted in the solid state. The dissolution of this material yielded the same solution as described in Scheme 1.

Five years later, Corbett and Edwards could show that the use of chelating ligands such as 18-crown-6 and [2.2.2]-cryptand yielded better solubility as well as better crystallization of compounds that contain homoatomic polyanions.<sup>5</sup> The possibility of reacting Zintl anions with transition metal complexes was first proved by NMR experiments by Rudolph et al. in 1983.<sup>6</sup> Five years later, the first crystal structure determination of a transition metal complex of a Zintl anion succeeded.<sup>7</sup> Another milestone in Zintl chemistry was the formation of transition metal-centered polyanionic compounds. These endohedral clusters are also called intermetallics and represent interesting models for doped materials.<sup>8,9</sup> Another recent development was the possibility of oxidative coupling of homoatomic clusters, which resulted in the formation of a new elemental modification.<sup>10</sup>

Besides the homoatomic polyanions, heteroatomic anionic species have also been investigated. The first anion of this type,  $\text{Sn}_2\text{Bi}_2^{2-}$ , was described in 1982.<sup>11</sup> A very recent research field is the doping by heavier homologs of the same group. This was shown for mixed Zintl phases and Zintl anions of the elements Ge/Sn and Si/Ge.<sup>12,13</sup> (For a review containing recent developments, see Scharfe et al.<sup>14</sup>) In Figure 1, milestones in Zintl anion chemistry from 1891 to date are given.



**Scheme 1** Zintl elucidated the chemical reaction described by Joannis: The dissolution of sodium in liquid ammonia in the presence of lead yields a salt, which contains homoatomic polyanions of lead.

Because of his remarkable contribution to the research on these polyanions, they are named after Eduard Zintl. This term was extended to one-, two-, and three-dimensional anionic partial structures of polar salt-like intermetallic solid-state materials, which are also commonly known as Zintl phases. It seems to be very useful to differentiate between Zintl anions and anionic partial structures of Zintl phases. Zintl anions are discussed in analogy with their historic origin while describing discrete, molecular anions, which are chemically stable outside a rigid solid-state network, that is, in solution, but not when the putatively anionic partial structure of an intermetallic alloy is designated.

### 1.09.1.1.2 Definitions and concepts

In the periodic system of the elements, there is a border between group 13 and group 14, which was described as the Zintl border. In combination with electropositive elements, this border separates typical intermetallic structures from salt-like structures that contain discrete anions. These anionic structures are interpretable by the generalized  $(8 - N)$  rule.

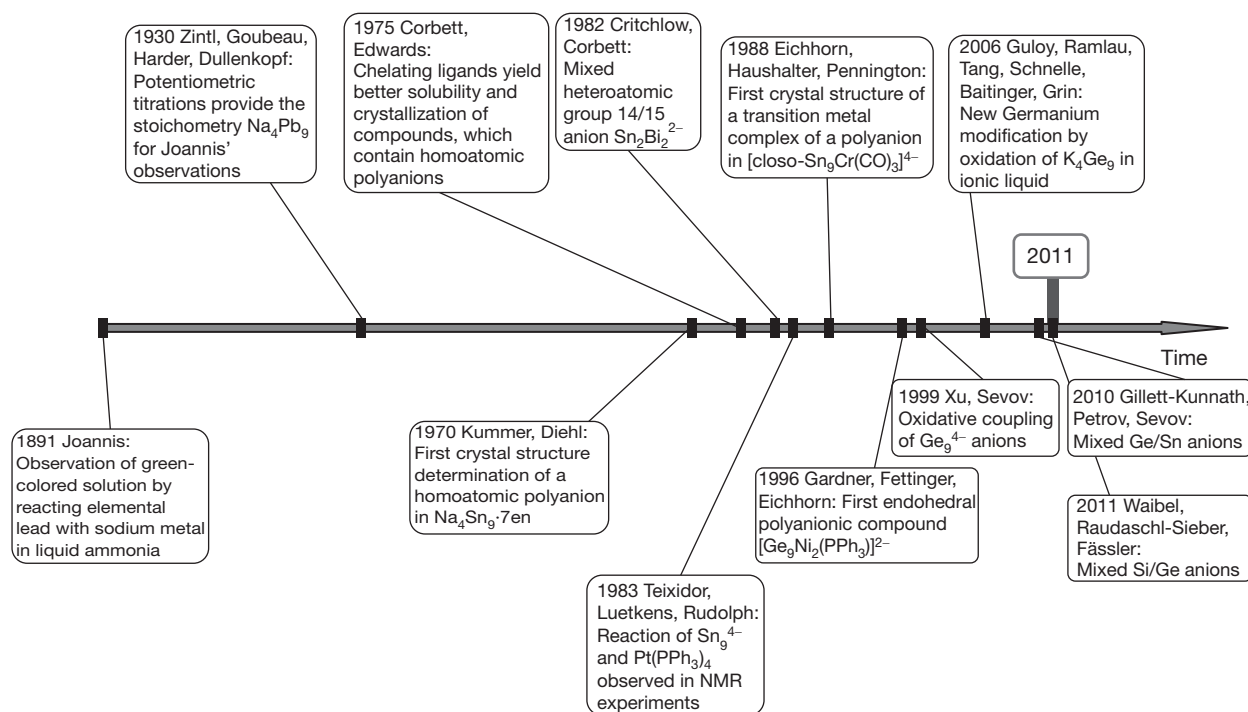
The generalized  $(8 - N)$  rule can be formulated like this: Take all valence electrons from electronegative ( $n_E$ ) and electropositive ( $n_M$ ) elements corresponding to the sum formula ( $M_mE_e$ ) and add them up. Divide the obtained number by the number of electronegative atoms in the sum formula. As a result, the valence electron concentration per anion atom  $N_E$  is obtained (eqn [1]). The subtraction of this number from eight gives the average number of element–element contacts (bonds) per anion atom  $b_e$  and predicts structures related to the isoelectronic element modifications of the neighbor

in the periodic table (Zintl–Klemm–Busmann concept) (eqn [2]):<sup>15,16</sup>

$$N_E = (mn_M + en_E)/e \quad [1]$$

$$b_e = (8 - N_E) \quad [2]$$

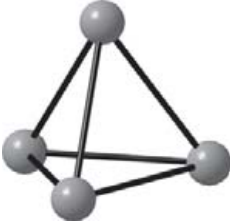

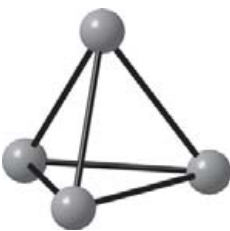


As mentioned before, discrete, zero-dimensional anions are very powerful starting materials in inorganic syntheses. These anions can be described in terms of the Zintl–Klemm–Busmann concept, which allows the formulation of electron-precise two-electron–two-center bonding within most of the cluster anions. Examples for these kinds of anions are given in Table 1. Besides these classical Zintl anions, which follow the Zintl–Klemm–Busmann concept, group 14 polyanions provide discrete molecular cluster anions, which are widely described using another concept originally established for borane chemistry. Nine-atom clusters of group 14 may be described by the Wade–Mingos–Williams rules,<sup>17–19</sup> which include the formulation of multicenter bonding. For  $\text{Ge}_9^{4-}$  anions, one can easily calculate the ideal shape of the cluster corresponding to the Wade–Mingos–Williams rules: The total amount of valence electrons adds up to 40, from which 18 electrons have to be subtracted due to nonparticipation in the cluster formation. This results in 22 electrons for the cluster bonding and a *nido* geometry ( $2n + 4$ ;  $n$  = number of cluster atoms), which points to a monocapped square-antiprismatic shape for a cluster consisting of nine atoms. In contrast, for silicon this bonding situation could not be confirmed in theoretical calculations.<sup>20</sup> The Wade–Mingos–Williams rules can be applied for the prediction of the shape of the cluster, but do not contribute to an understanding of the bonding situation in these anions. In this case, the application of the Zintl–Klemm–Busmann concept



**Figure 1** Milestones in Zintl anion chemistry from 1891 till date are summarized and give an idea about the (still growing) research topics in this fascinating field of inorganic chemistry. The literature for each milestone is given in the text.



**Table 1** Examples for Zintl anions, which can be described using electron-precise two-electron–two-center-bonding formulation

Compound	$N_E$	$b_e = 8 - N_E$	Anionic structure	
$K_4Si_4$	$[4_K + (4 \times 4_{Si})]/4_{Si} = 5$	3		The $Si_4^{4-}$ anion is built by threefold-bound silicon atoms. To every silicon atom, a formal charge of $-1$ can be assigned. This makes the anion isoelectronic to elemental phosphorus, and the similarity of the tetrahedral $Si_4^{4-}$ anion to white phosphorus is obvious.
$Ba_3Si_4$	$[(3 \times 2_{Ba}) + (4 \times 4_{Si})]/4_{Si} = 5.5$	2.5		Two threefold-bound and two twofold-bound atoms in $Si_4^{6-}$ result in an average value of Si—Si contacts of 2.5. To the twofold-bound atom, a formal charge of $-2$ can be assigned, whereas the charge of $-1$ corresponds to the threefold-bound atoms.
$(K@crypt)_2Sn_2Bi_2$	$[2_K + (2 \times 4_{Sn}) + 2 \times 5_{Bi}]/4_{Sn/Bi} = 5$	3		The $Bi_2Sn_2^{2-}$ anion consists of two threefold-bound tin atoms (formal charge $-1$ ) and two threefold-bound bismuth atoms (formal charge 0). Again, this anion is iso(valence)electronic to white phosphorus, and therefore the tetrahedral shape is intelligible.
$(K@crypt)_2Si_5$	$[2_K + (5 \times 4_{Si})]/5_{Si} = 4.4$	3.6		The $Si_5^{2-}$ anion is built by two threefold-bound and three fourfold-bound silicon atoms, which results in averaged 3.6 Si—Si contacts per atom. A formal charge of $-1$ can be assigned to the two apical atoms.
$K_3P_7$	$[3_K + 7 \times 5_P]/7_P = 5.43$	2.57		The $P_7^{3-}$ anion consists of four threefold-bound and three twofold-bound phosphorus atoms. This results in a $b_e$ value of 2.57. The formal charge assignment is $-1$ for the twofold-bound atoms and zero for the threefold-bound atoms.

seems to be much more reasonable, where we can formulate an electron-precise bonding situation (Figure 2).

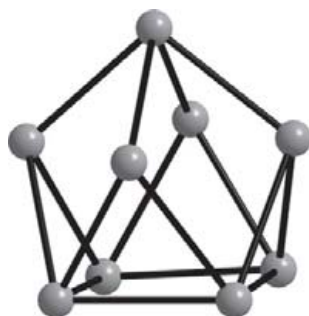
### 1.09.1.1.3 Synthetic routes

To obtain homoatomic polyanions in solution, there are different synthetic strategies. Besides the electrochemical generation, the relevancy of which is mainly historic at the moment, two main concepts are widely used, which have also been both described by Zintl et al. On the one hand, there is the low-temperature route. This procedure makes use of the solubility of electropositive metals in liquid ammonia.

The elements are placed in Schlenk tubes under an inert gas atmosphere, and dry liquid ammonia is condensed on the reaction mixture. The resulting solution, which is blue due to the presence of solvated electrons, is able to reduce the more electronegative elements across the Zintl border. After some storage time at temperatures below  $-33^\circ\text{C}$ , a change in color from blue to the characteristic color of the particular Zintl anions can be observed (Figure 3). This method is limited to the elements of group 14 (tin and lead), group 15 (phosphorus, arsenic, antimony, and bismuth), and group 16 (sulfur, selenium, and tellurium).<sup>15</sup> For the preparation of Zintl

anions of silicon and germanium in solution, this method has not succeeded so far.

On the other hand, there exists a much-used high-temperature route, where a Zintl phase that already includes discrete polyanions precast in solid state is dissolved in a

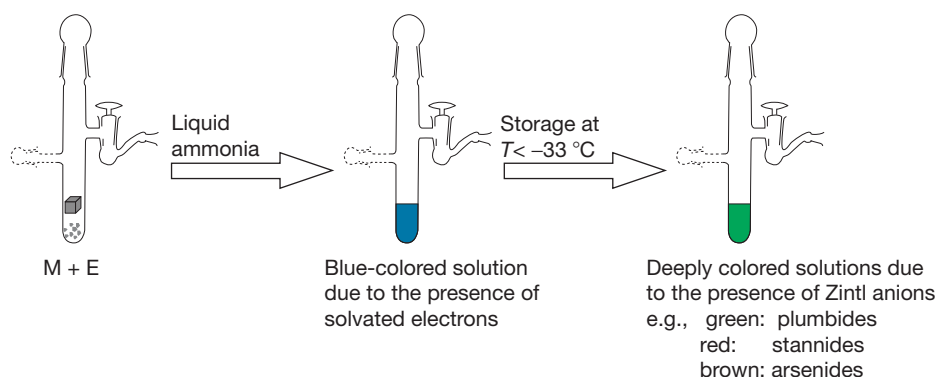


**Figure 2** Electron-precise description of the  $\text{Si}_9^{4-}$  anion results in five fourfold-bound and four threefold-bound silicon atoms. To the four threefold-bound atoms of the capped square, a charge of  $-1$  is assigned. This formulation is in accordance with the Zintl–Klemm–Busmann concept.

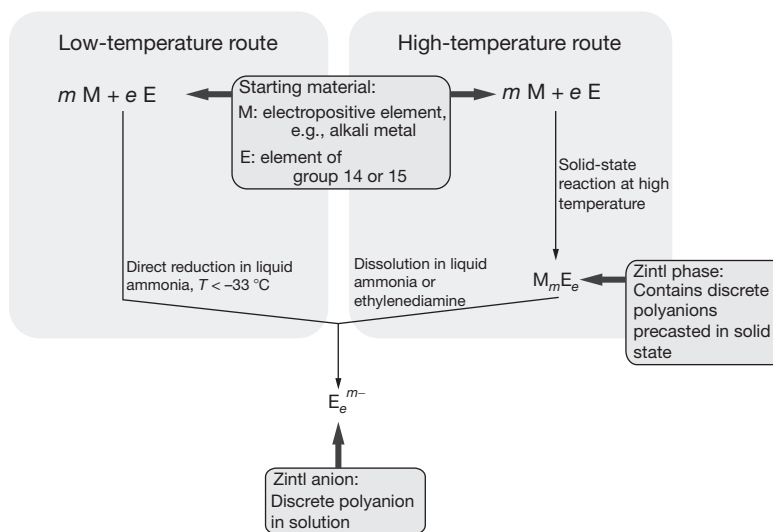
polar aprotic solvent such as liquid ammonia or ethylenediamine. Very rarely, solvents like DMF or pyridine are used. The Zintl phase is prepared in a classical solid-state reaction at high temperatures using the respective elements in stoichiometric amounts as starting materials. This method is especially important for the previously mentioned elements silicon and germanium, which cannot be directly reduced at low temperatures. **Figure 4** shows both preparation methods.

### 1.09.1.2 Discrete Polyanions in Zintl Phases of Group 14 and Group 15 and Their Dissolution Behavior

The presence of discrete polyanions in Zintl phases is very much dependent on the degree of reduction and the counter cation size. This is comprehensively described<sup>21</sup> for alkali and alkaline earth metal solid-state compounds of group 14 and group 15. There it was shown that homoatomic polyanions in Zintl phases of group 14 and group 15 fit like parts of a jigsaw puzzle concerning their counter cation sizes (**Figure 5**).



**Figure 3** Low-temperature route for the preparation of Zintl anions in liquid ammonia solution.



**Figure 4** Commonly used synthetic routes to obtain Zintl anions in liquid ammonia or ethylenediamine solution.

The focus in the following is on the different kinds of discrete anions one can find in solid-state materials without drawing special attention to cation size or bonding situations. Group 16 has been deliberately excluded from the considerations. A more complete summation of molecular anion-containing Zintl phases of group 14 and group 15 is given in Gärtner and Korber.<sup>21</sup> The combination of group 14 and group 15 elements results in heteroatomic polyanionic structures, which are also interpretable by the  $(8-N)$  rule. For a more detailed discussion of this kind of materials, consider Eisenmann and Cordier.<sup>22</sup>

### 1.09.1.2.1 Homoatomic polyanions of group 14 in solid state

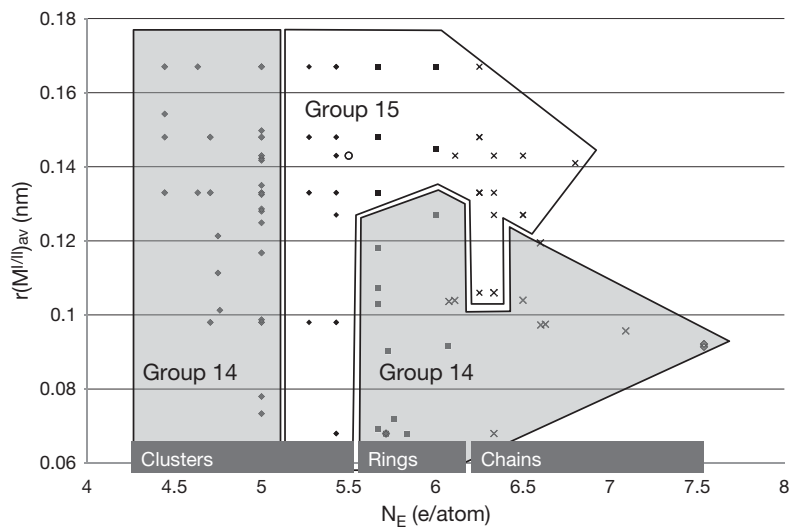
#### 1.09.1.2.1.1 Clusters

At a moderate degree of reduction of 4.4–5 electrons per anion atom, one can find three differently sized clusters of group 14 elements. The smallest cluster is represented by the tetrahedral-shaped  $E_4^{4-}$  anion, which is present, for example, in  $A_4E_4$  binary materials ( $A$ =alkali metal,  $E$ =group 14 element) (Figure 6(a)).<sup>23–28</sup> A second cluster species is the previously mentioned  $E_9^{4-}$  anion present in  $A_4E_9$ <sup>(29–32)</sup> or  $A_{12}E_{17}$ <sup>(33–36)</sup> binary materials. The ideal geometry of this kind of cluster is

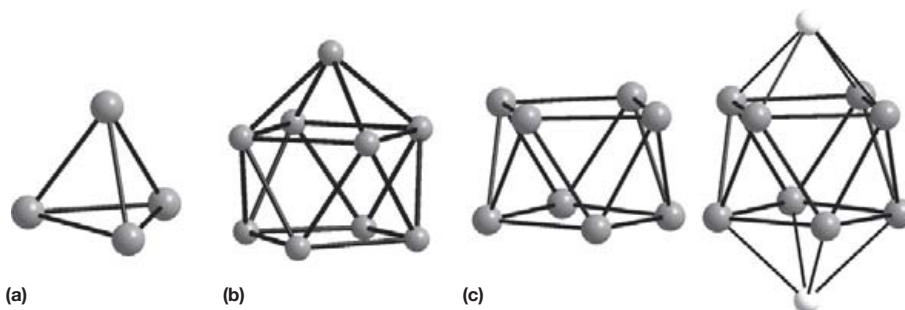
the monocapped square antiprism (point group  $C_{4v}$ ), which is also predicted for a 22-electron *nido*-cluster by the Wade–Mingos–Williams rules (Figure 6(b)). The shape of the nine-atom clusters is discussed more in detail in Section 1.09.1.2.4. With tin one more cluster has been found, the square-antiprismatic-shaped *arachno*  $Sn_8^{6-}$  anion. This anion is observed exclusively together with lithium cations that cap the square faces of the cluster, for example, in the material  $K_4Li_2Sn_8$  (Figure 6(c)).<sup>37</sup> If one takes the covalent interaction between tin and lithium into account, the  $[Li_2Sn_8]^{4-}$  anion can also be considered as a *closo*-cluster.

#### 1.09.1.2.1.2 $E_4^{6-}$ and rings

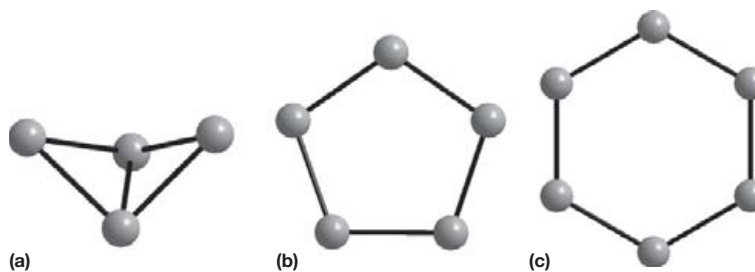
For an  $N_E$  value of 5.5  $e^-$  per atom, the butterfly-shaped  $E_4^{6-}$  anionic species is found in materials of the composition  $Ba_3Si_4$ <sup>(38)</sup> and  $\beta$ - $Ba_3Ge_4$ <sup>(39)</sup> (high-temperature phase,  $T > 630$  K; Figure 7(a)). In more electron-rich Zintl phases up to  $N_E=6$  per atom, anionic ring structures are observed. The chemical bonding in these rings is not trivial due to partial double-bonding and covalent interactions between electronegative and electropositive elements, which cannot be expressed in terms of the Zintl–Klemm–Busmann concept and the



**Figure 5** Zintl phases of alkali and alkaline earth metals that contain homoatomic polyanions of group 14 and group 15 fit together like parts of a jigsaw puzzle when mapped by their degree of reduction and their mean cation radii.



**Figure 6** Clusters of group 14 in Zintl phases. (a)  $E_4^{4-}$  ( $E$ =Si–Pb),<sup>23–28</sup> (b)  $E_9^{4-}$  ( $E$ =Si–Pb),<sup>29–36</sup> and (c)  $Sn_8^{6-}$ , respectively  $[Li_2Sn_8]^{4-}$ .<sup>37</sup>



**Figure 7** (a) Butterfly-shaped  $E_4^{6-}$  anion ( $E = \text{Si, Ge}$ ),<sup>38,39</sup> (b)  $E_5^{6-}$  rings ( $E = \text{Si-Pb}$ ),<sup>40-44</sup> and (c)  $E_6^{10-}$  rings ( $E = \text{Si, Ge}$ )<sup>45,46</sup> in Zintl phases.

**Table 2** Dense solid-state materials of group 14 which include chain-like polyanions in their crystal structures

Chain	Compound	Charge according to formula	Charge according to Zintl
Si <sub>3</sub>	Sr <sub>12</sub> Mg <sub>17.8</sub> Li <sub>2.2</sub> Si <sub>20</sub> <sup>(49)</sup>	-7.45	-8
Si <sub>6</sub>	Ba <sub>2</sub> Mg <sub>3</sub> Si <sub>4</sub> <sup>(50)</sup>	-14	-14
	Ba <sub>6</sub> Mg <sub>5.3</sub> Li <sub>2.7</sub> Si <sub>12</sub> <sup>(51)</sup>	-12.65	-14
	Ca <sub>8</sub> Li <sub>0.969</sub> Mg <sub>2.031</sub> Si <sub>8</sub> <sup>(52)</sup>	-13.03	-14
Si <sub>8</sub>	Sr <sub>11</sub> Mg <sub>2</sub> Si <sub>10</sub> <sup>(53)</sup>	-18	-18
Ge <sub>4</sub>	Ca <sub>7</sub> Ge <sub>6</sub> <sup>(54)</sup>	-8	-10
Ge <sub>6</sub>	Ca <sub>8</sub> Ge <sub>8</sub> Li <sub>1.18</sub> Mg <sub>1.82</sub> <sup>(52)</sup>	-12.82	-14
	Ba <sub>6</sub> Ge <sub>12</sub> Li <sub>3.1</sub> Mg <sub>4.9</sub> <sup>(55)</sup>	-12.45	-14
Sn <sub>3</sub>	Li <sub>7</sub> Sn <sub>3</sub> <sup>(56)</sup>	-7	-8
Sn <sub>4</sub>	Ca <sub>7</sub> Sn <sub>6</sub> <sup>(57)</sup>	-8	-10
Sn <sub>6</sub>	Li <sub>5</sub> Ca <sub>7</sub> Sn <sub>11</sub> <sup>(43)</sup>	-13	-14

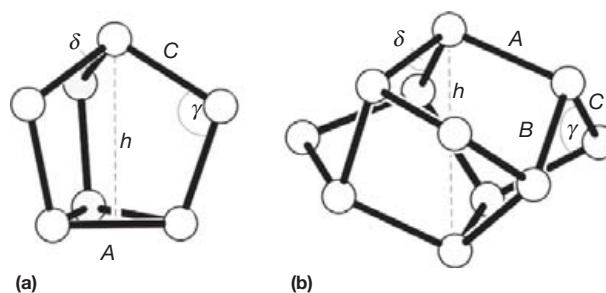
The charge assignment in these compounds is not trivial at all due to multiple bonding between the group 14 elements and covalent interactions between group 14 elements and electropositive metal.

(8 -  $N$ ) rule. The most common rings are the quasi-aromatic five-atom  $E_5^{6-}$  ( $E = \text{Si-Pb}$ ; **Figure 7(b)**)<sup>40-44</sup> and six-membered  $E_6^{10-}$  rings (**Figure 7(c)**).<sup>45,46</sup> Five-membered rings do not crystallize as sole anionic moiety but together with more reduced anions like mononuclear  $E^{4-}$ .  $E_6^{10-}$  rings are only reported for the elements silicon and germanium and represent the exclusive anionic moiety in compounds like Ba<sub>4</sub>Li<sub>2</sub>E<sub>6</sub>.<sup>45,46</sup>

In the alkaline earth metal compounds Ca<sub>7</sub>Mg<sub>7.5±δ</sub>Si<sub>14</sub> and SrSi derivatives of the six-membered rings are observed. In Ca<sub>7</sub>Mg<sub>7.5±δ</sub>Si<sub>14</sub> an Si<sub>6</sub> ring is described, where each corner additionally binds one silicon atom<sup>47</sup>; in SrSi, four corners are bound to additional silicon atoms.<sup>48</sup> Anyway, the charge assignment in these compounds is not trivial.

### 1.09.1.2.1.3 Chains

In even more reduced phases one can observe chains. Zintl phases containing these chains are interesting model compounds for the study of multiple bonding of heavier main group elements in the solid state, as well as the coordination behavior of differently charged main group element atoms in the same compound. The charge assignment in these compounds is not trivial at all due to multiple bonding between the group 14 elements and covalent interactions between group 14 elements and the electropositive metals (**Table 2**). Some of the compounds additionally contain more highly reduced anionic species like monoatomic  $E^{4-}$  anions.



**Figure 8** (a) Nortricyclane-like  $E_7^{3-}$  and (b) trishomocubane-like  $E_{11}^{3-}$  anions present in binary Zintl phases of alkali and alkaline earth metals.

## 1.09.1.2.2 Homoatomic polyanions of group 15 in solid state

### 1.09.1.2.2.1 Clusters

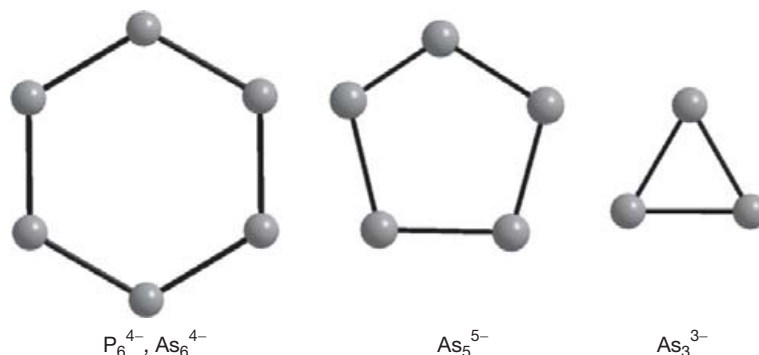
There are two distinct cluster species present in Zintl phases of group 15. The most common cluster species is observed, for example, in materials following the composition  $M_3E_7$  ( $A = \text{alkali metal}$ ;  $E = \text{P-Sb}$ ).<sup>58-60</sup> The shape of the cluster is nortricyclane like. Due to its  $C_{3v}$  point group symmetry, the anions feature three main distances ( $A, B, C$ ), where  $A > C > B$  and  $\delta > \gamma$  holds true (**Figure 8(a)**). The least reduced molecular polyanion of group 15 elements in binary solids is represented by the trishomocubane-like  $E_{11}^{3-}$  ( $E = \text{P, As}$ )<sup>61,62</sup> (**Figure 8(b)**).

### 1.09.1.2.2.2 Rings

An increased degree of reduction results in the formation of Zintl phases that contain ring-shaped polyanions. Up to now, six-, five-, and three-membered rings have been described. Phosphorus and arsenic compounds with heavy alkali metals which contain  $E_6^{4-}$  rings are known.<sup>63,64</sup> For these rings, aromaticity in terms of the Hückel concept was considered, which for phosphorus is however contradicted by the missing low field shift in <sup>31</sup>P MAS solid-state NMR spectra. Recent quantum chemical calculations demonstrated a slight distortion to a chair-like conformation. In contrast, for As<sub>5</sub><sup>5-(65)</sup> in envelope conformation and As<sub>3</sub><sup>3-(59)</sup> rings, where each atom formally carries one negative charge, the Zintl-Klemm-Busmann concept is perfectly applicable (**Figure 9**).

### 1.09.1.2.2.3 Chains

As in the case of highly reduced group 14 compounds, the analogous group 15 materials contain different chains of finite length. To stabilize group 15 chains in dense solid-state materials, larger cations are needed (radii above 0.106 nm)



**Figure 9** Homoatomic rings of group 15 elements that are present in Zintl phases.

compared to group 14 chains. One can distinguish between electron-precise chains, where two-electron–two-center bonding holds true and therefore the Zintl–Klemm–Busmann concept applies, and electron-deficient chains, where multiple element–element bonding as well as partial protonation is discussed. **Figure 10** shows chains of group 15 elements in perspective view to convey helical assemblies.

### 1.09.1.2.3 Heteroatomic polyanions of group 14/15, group 14/16, and group 15/16 in solid state

**Sections 1.09.1.2.1** and **1.09.1.2.2** dealt with homoatomic polyanions of group 14 and group 15 elements. Of course, the combination of elements of the two groups results in further polyanions in solid state.<sup>22</sup> Additionally, the combinations group 14/16 and group 15/16 are possible and also lead to heteroatomic polyanions.<sup>74</sup> These polyanions are also called chalcogenidometalates and are best described as complex polyanions structurally related to carbonate and phosphate anions. They are sometimes also described in terms of the Zintl–Klemm concept, but the focus here is on the consideration of Zintl anions in compounds, for which the description by Zintl is the most (perhaps only) feasible.

### 1.09.1.2.4 Solid-state versus solution: similarities and discrepancies

If one compares the structures of discrete polyanions of group 14 and group 15 found in Zintl phases (see **Sections 1.09.1.2.1** and **1.09.1.2.2**) with the compounds which crystallize from ammonia or ethylenediamine solutions prepared by the two routes given in **Section 1.09.1.1.3**, some similarities and discrepancies become evident. These similarities and discrepancies are presented in the next two subsections to demonstrate the nontrivial behavior of this class of compounds in solution, even without any additional reaction partner.

#### 1.09.1.2.4.1 Group 14 polyanions in solution

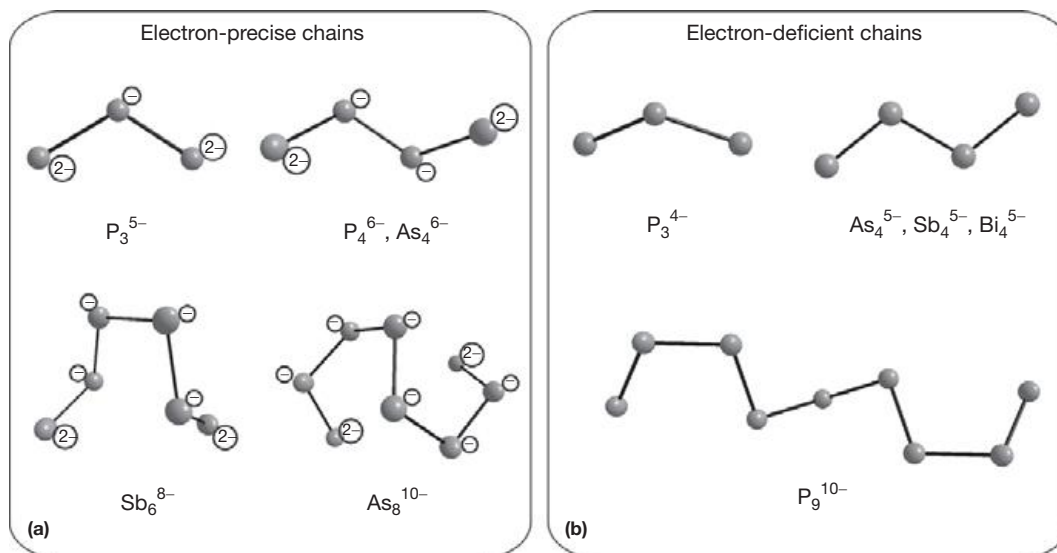
The most common cluster species of group 14 elements in solution is represented by the nine-atom species. This cluster type is nowadays well known from solid-state materials  $M_4E_9$  ( $M$ =alkali metal;  $E$ =Ge–Pb) or  $M_{12}E_{17}$  ( $M$ =alkali metal,  $E$ =Si–Pb),<sup>33</sup> which can be readily dissolved in ethylenediamine (Ge–Pb) or liquid ammonia (Si–Pb). Although both solvents are rather aprotic, the highly reduced clusters in solution may be subject to oxidation by solvent molecules. For the nine-atom cluster therefore, differently charged species are

present in solution: the highest reduced monocapped square-antiprismatic  $E_9^{4-}$ , known from solid state, the paramagnetic  $E_9^{3-}$  and the threefold-capped trigonal-prismatic-shaped  $E_9^{2-}$ .<sup>14</sup> The threefold-capped trigonal-prismatic geometry would correspond to a 20-electron *closo*-cluster according to the Wade–Mingos–Williams rules. Both geometries, with point group  $C_{4v}$  for the monocapped square antiprism and point group  $D_{3h}$  for the threefold-capped trigonal prism, have been shown to be very similar in energy;<sup>75</sup> ( $n = 2–4$ ) therefore their transformation barrier is very low. For  $Sn_9^{n-}$  clusters, a fluctuational behavior in solution is indicated by a single  $^{119}Sn$  singlet that shows two satellites due to coupling to  $^{117}Sn$ . The small coupling constant of  $\sim 250$  Hz is due to the averaging of one-bond, two-bond, and three-bond couplings one would expect for a static structure.<sup>76</sup> The transformation from monocapped square antiprism to the threefold-capped trigonal prism and vice versa is known as the diamond square process.<sup>77</sup> Here, one diagonal of the basal square of the antiprism is shortened until it features the same dimensions as the edge length of the capped square. The resulting polyhedron is the threefold-capped trigonal prism. The diamond square process is illustrated in **Figure 11**.

Of course,  $C_{4v}$  and  $D_{3h}$  are the point groups of the ideal symmetries of the underlying polyhedra. In reality, the crystallographic point group symmetry in most cases is  $C_1$ , which means there is no symmetry operation except identity. For explanation purposes, for the shape of the differently charged  $E_9^{n-}$  clusters ( $n = 2–4$ ), measures have been introduced to describe the degree of distortion from the ideal symmetries. For the monocapped square antiprism, the ratio of the diagonals of the basal square is taken into account. As there usually are two differently sized diagonals in real clusters, the convention was made to divide the length of the longer diagonal by the length of the shorter diagonal. The value of the ratio of diagonals is one for ideal  $C_{4v}$  geometry and greater than one for a distorted polyhedron. For the threefold-capped trigonal prism, the height-to-edge value is used to describe the degree of distortion from ideal  $D_{3h}$  symmetry. The  $h/e$  ratio is the quotient of the average value of the three heights and the average value of the six triangle edges of the threefold-capped trigonal prism.

The most common experimental route to obtain nine-atom clusters in solution is the dissolution of the corresponding Zintl phase of the desired element in the presence or absence of chelating ligands.<sup>20,78–81</sup> For tin and lead the direct reduction method also succeeds in providing this cluster species in





Chain	Compound	Electron precise
$P_3^{4-}$	$K_4P_3$ <sup>(66)</sup>	No
$P_3^{5-}$	$KBa_4P_5$ <sup>(67)</sup>	Yes
$P_4^{6-}$	$Sr_3P_4$ <sup>(68)</sup>	Yes
	$Ba_3P_4$ <sup>(68)</sup>	Yes
$P_9^{10-}$	$Ba_5P_9$ <sup>(69)</sup>	No
$As_4^{5-}$	$K_5As_4$ <sup>(70)</sup>	No
$As_4^{6-}$	$Ca_2As_3$ <sup>(71)</sup>	Yes
	$Sr_3As_4$ <sup>(72)</sup>	Yes
$As_8^{10-}$	$Ca_2As_3$ <sup>(71)</sup>	Yes
$Sb_4^{5-}$	$K_5Sb_4$ <sup>(61)</sup>	No
	$Rb_5Sb_4$ <sup>(70)</sup>	No
$Sb_6^{8-}$	$Ba_2Sb_3$ <sup>(73)</sup>	Yes
	$Sr_2Sb_3$ <sup>(73)</sup>	Yes
$Bi_4^{5-}$	$K_5Bi_4$ <sup>(70)</sup>	No
	$Rb_5Bi_4$ <sup>(70)</sup>	No
	$Cs_5Bi_4$ <sup>(70)</sup>	No

**Figure 10** (a) Electron-precise chains of group 15 elements with assigned formal charges. (b) Electron-deficient chains of group 15 elements. The table gives the compounds that include these anions, all of which are odd-electron (paramagnetic) species.

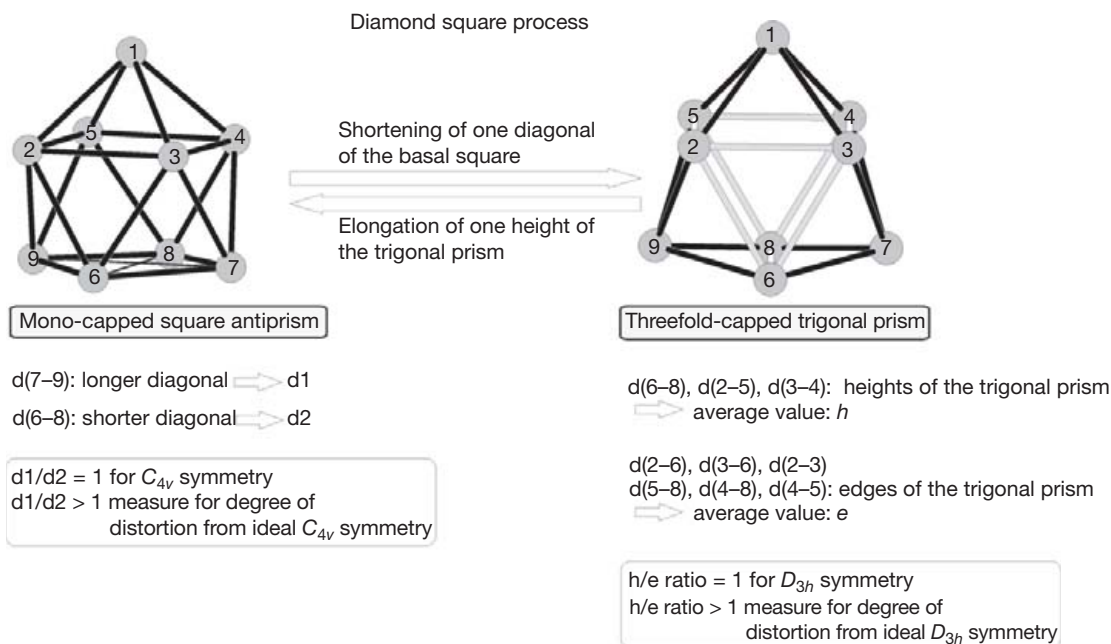
solution.<sup>82</sup> The case is different for silicon and germanium. For nine-atom clusters of these elements, only the dissolution route provides the favored result.

The tetrahedrally shaped  $E_4^{4-}$  anions have been observed only for tin and lead in solvate crystal structures of liquid ammonia.  $Pb_4^{4-}$  could be obtained by the high-temperature dissolution route, whereas  $Sn_4^{4-}$  has only been produced via the direct reduction method and not by dissolution of the analogous Zintl phase.<sup>83</sup> This shows that the two preparation methods to obtain Zintl anions do not necessarily lead to the same solutions. For silicon and germanium, no fourfold negatively charged tetrahedral four-atom cluster has been reported in solvate crystal structures. The existence of the anion  $[(MesCu)_2(\eta^3-Si_4)]^{4-}$  gives a hint that  $Si_4^{4-}$  anions may also be present in solution.<sup>84</sup>

In solvate structures, an additional homoatomic Zintl anion is present, for which no corresponding Zintl phase is known. The trigonal bipyramidal  $E_5^{2-}$  anion ( $E=Si-Pb$ ) is obtained in

dissolution experiments while using additional [2.2.2]-cryptand as a chelating ligand for the alkali metal cations.<sup>85–88</sup> The formation of this anion is not yet well understood. It is assumed that the responsible cluster in the solid for the formation of this anion is the tetrahedrally shaped  $E_4^{4-}$  anion, which cannot balance oxidation processes like the previously described nine-atom species and therefore reorganizes and enlarges.<sup>85</sup> In **Table 3**, the polyanions from Zintl phases and the two routes to obtain Zintl anions of group 14 in solution are compared.

The comparison of Zintl anions and the polyanions in Zintl phases clearly shows that the new cluster species  $E_5^{2-}$  is obtainable by dissolution of a Zintl phase. Furthermore, the solvent employed seems to play a major role for the stabilization of the highly reduced anions.  $E_4^{4-}$  anions have been reported only during the use of liquid ammonia, whereas the application of ethylenediamine results in many examples of oxidized nine-atom clusters. As silicide compounds are very sensitive toward oxidation, it is completely comprehensible



**Figure 11** The diamond square process describes the transformation from a monocapped square antiprism to a threefold-capped trigonal prism and vice versa. Both geometries are very similar in energy to  $E_9^{n-}$  ( $n=2-4$ ) clusters, therefore distorted variants of both border symmetries are found in real crystal structures.

**Table 3** The comparison of Zintl anions in solution of group 14 elements and Zintl phases containing homoatomic polyanions illustrates the similarities and discrepancies between solid state and solution and between the two different synthetic strategies to obtain the anions in solution

Zintl anion		Zintl phase	
Low-temperature route (direct reduction in $\text{NH}_3$ (l))	High-temperature route (dissolution of Zintl phase)	Solid-state reaction at high temperature	
$E_9^{4-}$ (Sn, Pb)	Zintl anion in ethylenediamine $E_9^{4-}$ (Ge-Pb) $E_9^{3-}$ (Si-Sn) $E_9^{2-}$ (Si, Ge)	Zintl anion in ammonia (l) $E_9^{4-}$ (Si-Pb) $E_9^{3-}$ (Ge)	Polyanion in Zintl phase $E_9^{4-}$ (Si-Pb)
$E_4^{4-}$ (Sn)	$E_5^{2-}$ (Ge-Pb)	$E_4^{4-}$ (Pb) $E_5^{2-}$ (Si-Pb)	$E_4^{4-}$ (Si-Pb)

For a recent review containing pertinent literature on homoatomic polyanions in solution, refer to Scharfe et al.<sup>14</sup>

that Zintl anions of this element are exclusively observed when liquid ammonia is used. Another conspicuous fact is that anionic rings and chains of group 14 elements have not yet been observed in solvate crystal structures at all. There seems to be a border for the stability of Zintl anions in solution at an  $N_E$  value of 5 for group 14 elements, which means a maximum charge of  $-1$  per anion atom.

#### 1.09.1.2.4.2 Group 15 polyanions in solution

From the Zintl phases, we know two different types of clusters,  $E_7^{3-}$  and  $E_{11}^{3-}$ .  $E_7^{3-}$  anions can be crystallized from solutions of liquid ammonia<sup>89,90</sup> or ethylenediamine<sup>91</sup> obtained by extraction of the corresponding Zintl phases; the direct reduction procedure also yields the same cage compounds.<sup>92</sup>  $P_{11}^{3-}$  and  $As_{11}^{3-}$  anions are observed after dissolving a corresponding Zintl phase in liquid ammonia<sup>93-95</sup> or ethylenediamine.<sup>96,97</sup> A further anion known from Zintl phases and also crystallizing from solution is represented by the ring-shaped  $As_6^{4-}$  anion, which could be obtained by dissolution of a Zintl phase.<sup>98</sup>

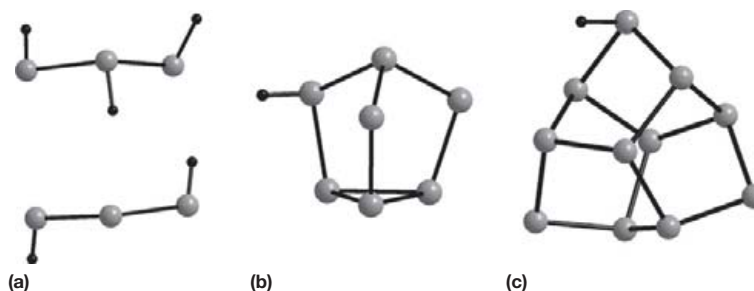
Besides the known polyanions from the solid state, the high-temperature route also provides access to new Zintl anions in solution, which are not known in Zintl phases up to now. The ring-shaped  $P_4^{2-}$ , for which the term lone-pair aromaticity was claimed, is obtainable by incongruent dissolution of the Zintl phase  $K_4P_6$  in liquid ammonia.<sup>99</sup> Whereas in dense solid-state materials evidence for  $Sb_{11}^{3-}$  anions is still missing, the dissolution method succeeded in crystallizing this anion and therefore proved its existence in solution.<sup>95,100</sup>

Using the low-temperature route, in which the elements or compounds of the element are directly reduced by a dissolved alkali metal, more new polyanions in solution have been synthesized. This method succeeded in preparing  $As_4^{2-}$  anions by directly reducing arsenic by elemental sodium.<sup>92,101</sup> Another experimental procedure to obtain  $P_4^{2-}$  anions in solution is the direct reduction of diphosphane by cesium.<sup>102</sup> Cyclic antimonides have not yet been reported in Zintl phases, but by applying the direct reduction method, the formation of  $Sb_5^{5-}$ <sup>(103)</sup> and  $Sb_8^{8-}$ <sup>(104)</sup> rings in solution could be proved.

**Table 4** Comparing Zintl anions in solution of group 15 elements and Zintl phases which contain homoatomic polyanions illustrates, as previously shown for group 14 elements, the similarities and discrepancies between solid state and solution and between the two different synthetic strategies

Zintl anion	Zintl phase	
Low-temperature route (direct reduction in $\text{NH}_3$ (l))	High-temperature route (dissolution of Zintl phase)	Solid-state reaction at high temperature
$\text{E}_4^{2-}$ (As)	Zintl anion in ethylenediamine	Zintl anion in ammonia (l)
$\text{E}_{14}^{4-}$ (P)	$\text{E}_7^{3-}$ (Sb)	$\text{E}_7^{3-}$ (P, As)
$\text{E}_5^{5-}$ (Sb)	$\text{E}_{11}^{3-}$ (P, As)	$\text{E}_{11}^{3-}$ (P–Sb)
$\text{E}_8^{8-}$ (Sb)	$\text{E}_4^{2-}$ (Sb)	$\text{E}_6^{4-}$ (As)
		$\text{E}_4^{2-}$ (P, As)
		$\text{As}_{14}^{4-}$
		Polyanion in Zintl phase
		$\text{E}_7^{3-}$ (P–Sb)
		$\text{E}_{11}^{3-}$ (P, As)
		$\text{E}_6^{4-}$ (P, As)

For a recent review containing pertinent literature on homoatomic polyanions in solution, refer to Scharfe et al.<sup>14</sup>



**Figure 12** Hydrogenpolyphosphides accessible from liquid ammonia solutions. (a)  $\text{P}_3\text{H}_3^{2-}$  in  $\text{K}_3(\text{P}_3\text{H}_2) \cdot 2.3\text{NH}_3$ ,<sup>108</sup> (b)  $\text{HP}_7^{2-}$  in  $[\text{K}(18\text{-crown-}6)]_2\text{HP}_7$ ,<sup>109</sup> (c)  $\text{HP}_{11}^{2-}$  in  $[\text{Sr}(\text{NH}_3)_8]\text{HP}_{11} \cdot \text{NH}_3$ .<sup>110</sup>

Furthermore, an anion consisting of two  $\text{P}_7$  units coupled by one single bond,  $\text{P}_{14}^{4-}$ , is obtainable by the low-temperature route, which can be explained by an oxidation of  $\text{P}_7^{3-}$  anions (for oxidation reactions see Section 1.09.1.3.1).<sup>105</sup> In Table 4, the polyanions from Zintl phases and the two routes to obtain Zintl anions in solution are compared.

Concerning polyphosphides,  $^{31}\text{P}$  NMR experiments of Baudler et al. in solution elucidated the presence of a great variety of Zintl anions.<sup>106,107</sup> The experiments also gave rise to protonated polyphosphides, the so-called hydrogen polyphosphides. Some of these hydrogen polyphosphides could also be crystallized from solution and may be regarded as the simplest form of derivatives of Zintl anions (Figure 12). The stability of the protonated species in solution is caused by the similar electronegativities of hydrogen and phosphorus, which results in a less polarized bond compared to group 14 hydrogen compounds. The protonation of group 14 or group 15 Zintl anions generally means an oxidation due to the higher electronegativity of hydrogen, compared to the heavier homologs of these groups.

The presence of the protonated phosphorus species in crystal structures indicates their stability in solution. This is in strong contrast to the group 14 Zintl anions, where no protonated species has been reported so far and detailed NMR investigations, similar to phosphorus chemistry, are still missing.

### 1.09.1.3 Reactions of Zintl Anions

In Section 1.09.1.2 the focus was on polyanions in the solid state and their dissolution behavior. It became evident that

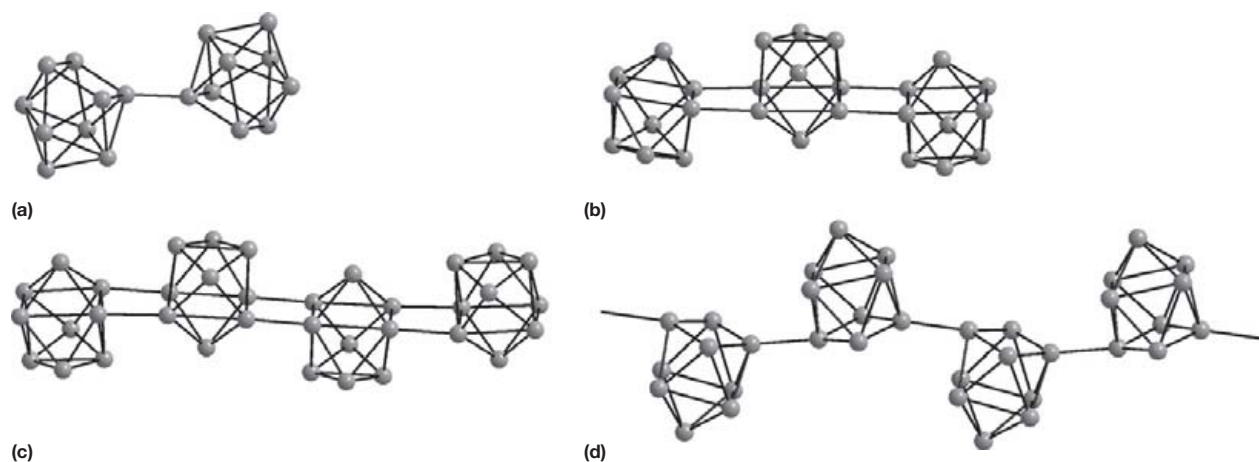
there are complex processes involved in dissolving the solid-state material and that even the chosen method to provide these Zintl anions in solution plays a major role concerning their availability in different solvents. These processes are not yet well understood and therefore straightforward syntheses are rare. Nevertheless, the most common and best understood cluster species  $\text{E}_9^{4-}$  (E=element of group 14) and  $\text{E}_7^{3-}$  (E=group 15) have been used in several reactions. The results of these sometimes more explorative than purposeful investigations are summarized in the following and should give an idea about the versatile reaction possibilities of Zintl anions rather than an exhaustive overview.

#### 1.09.1.3.1 Oxidation of Zintl anions

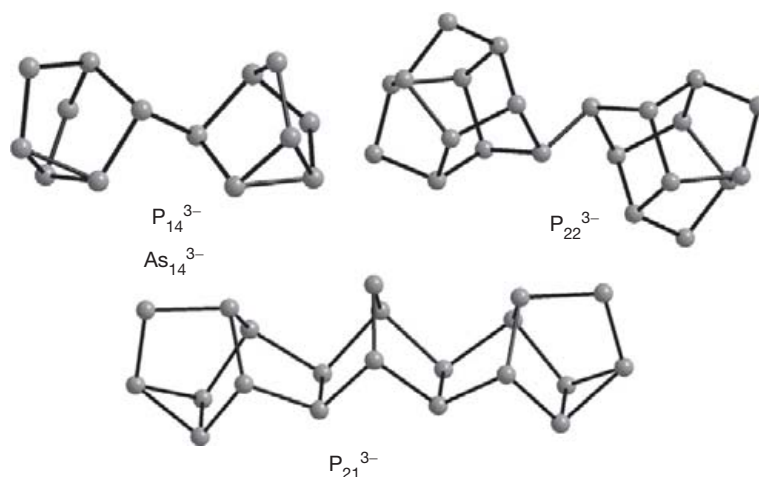
##### 1.09.1.3.1.1 Group 14

The oxidation of polyanions may lead to the formation of a bond between two or more monomers. Concerning group 14 elements, quite an impressive number of oligomers obtained from nine-atom clusters have been reported so far. The first dimer of a deltahedral Zintl anion of group 14 was synthesized in 1999 by dissolving a precursor Zintl phase of the nominal composition  $\text{Cs}_2\text{KGe}_9$  in ethylenediamine in the presence of [2.2.2]-cryptand.<sup>111</sup> This approach gave  $[\text{Ge}_9\text{-Ge}_9]^{6-}$  units, where two  $\text{Ge}_9$  clusters are linked by one single bond (Figure 13(a)).

A trimer of linked  $\text{Ge}_9$  clusters  $[\text{Ge}_9\text{Ge}_9\text{Ge}_9]^{6-}$  could be obtained by adding  $\text{Ph}_3\text{As}$  or  $\text{Ph}_3\text{P}$  or  $\text{GeI}_2$  to  $\text{Ge}_9^{4-}$  anion-containing solutions in ethylenediamine (Figure 13(b)),<sup>112,113</sup> and even tetramers  $[\text{Ge}_9\text{Ge}_9\text{Ge}_9\text{Ge}_9]^{8-}$ <sup>114</sup> could be crystallized from similar solutions, but without adding an oxidizing agent (Figure 13(c)). Further oxidation, again without intentional



**Figure 13** The oxidation of germanium clusters results in (a) dimeric  $[\text{Ge}_9\text{-Ge}_9]^{6-}$ , (b) trimeric  $[\text{Ge}_9=\text{Ge}_9=\text{Ge}_9]^{6-}$ , (c) tetrameric, and (d) polymeric  $\infty^1\{-[\text{Ge}_9]^{2-}\}$  units.



**Figure 14** Oxidatively coupled clusters of group 15 elements.

addition of an oxidizing agent, results in linear  $\infty^1\{-[\text{Ge}_9]^{2-}\}$  polymers (**Figure 13(d)**).<sup>115</sup> The ultimate goal in connecting Zintl clusters was achieved by Grin et al., who used an ionic liquid to oxidize  $\text{Ge}_9^{4-}$  clusters. This approach resulted in the formation of a guest-free germanium clathrate, and therefore a new elemental modification of germanium was born.<sup>10</sup> The experiments listed so far show that fourfold negatively charged nine-atom clusters of group 14 elements are very sensitive toward oxidation processes in solution. The oxidized radical clusters  $\text{E}_9^{3-}$  in solution compete with dimerization reactions, and this oxidation from  $\text{E}_9^{4-}$  to  $\text{E}_9^{3-}$  even takes place without intentionally adding an oxidizing component. Therefore, only slight impurities of water, obviously, are sufficient to oxidize the cluster that results in coupled cluster units.

#### 1.09.1.3.1.2 Group 15

Concerning group 15 clusters, there are also dimerization reactions of  $\text{P}_7^{3-}$  and  $\text{As}_7^{3-}$  observed in solution, which are, as was related above for the group 14-coupled clusters, not associated with the addition of an oxidizing agent and therefore show the sensitivity of the anions toward any impurity of the

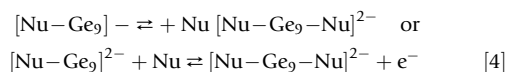
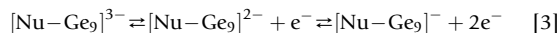
solvents.<sup>105</sup> In contrast, for the undecaphosphide anion  $\text{P}_{11}^{3-}$  a controlled oxidation by adding the mild oxidizing trihalogenide anion  $\text{Br}_2\text{I}^-$  at  $-70^\circ\text{C}$  in liquid ammonia resulted in the formation of the dimer  $\text{P}_{22}^{4-}$ .<sup>116</sup> The employment of the transition metal complex  $(\text{CHT})\text{Cr}(\text{CO})_3$  ( $\text{CHT}$  = cycloheptatriene) during dissolution experiments of  $\text{Li}_3\text{P}_7(\text{DME})_3$  in THF yielded a trimer of  $\text{P}_7$  units, where a central norbornane-like unit is connected to two heptaphosphanortricyclane cages (**Figure 14**).<sup>117</sup>

#### 1.09.1.3.2 Functionalization with *exo*-bonded main group elements

##### 1.09.1.3.2.1 Group 14

A further possible reaction route, besides the oxidation of the clusters, is their functionalization with *exo*-bonded main group element ligands.<sup>118</sup> In 2002, the first examples for functionalized  $\text{Ge}_9$  clusters were reported by Sevov et al.<sup>119</sup> While the employment of  $\text{Ph}_3\text{P}$  and  $\text{Ph}_3\text{As}$  results in the formation of oxidized  $\text{Ge}_9$  cage anions, which dimerize or trimerize in subsequent reactions,<sup>112</sup> the application of the heavier  $\text{Ph}_3\text{Pn}$  homologs  $\text{Ph}_3\text{Sb}$  and  $\text{Ph}_3\text{Bi}$  leaves  $\text{Ge}_9$  clusters with two *exo*-bonded ligands. The first step of the reaction was

interpreted as a nucleophilic attack of the nucleophile (Nu) at  $\text{Ge}_9^{2-}$ , which is in equilibria with solvated electrons:  $\text{Ge}_9^{4-} \rightleftharpoons \text{Ge}_9^{3-} + e^- \rightleftharpoons \text{Ge}_9^{2-} + 2e^-$ . Consequently, the substituted derivative  $[\text{Nu}-\text{Ge}_9]^{3-}$  is formed. The second step is not as perspicuous; it is assumed that  $[\text{Nu}-\text{Ge}_9]^{3-}$  units are now able to form equilibria with solvated electrons (eqn [3]). Due to change of the occupancy of the frontier orbital in  $[\text{Nu}-\text{Ge}_9]^-$  (empty and low-lying) or  $[\text{Nu}-\text{Ge}_9]^{2-}$  (half empty and low-lying) it is now available for a second nucleophilic attack (eqn [4]).

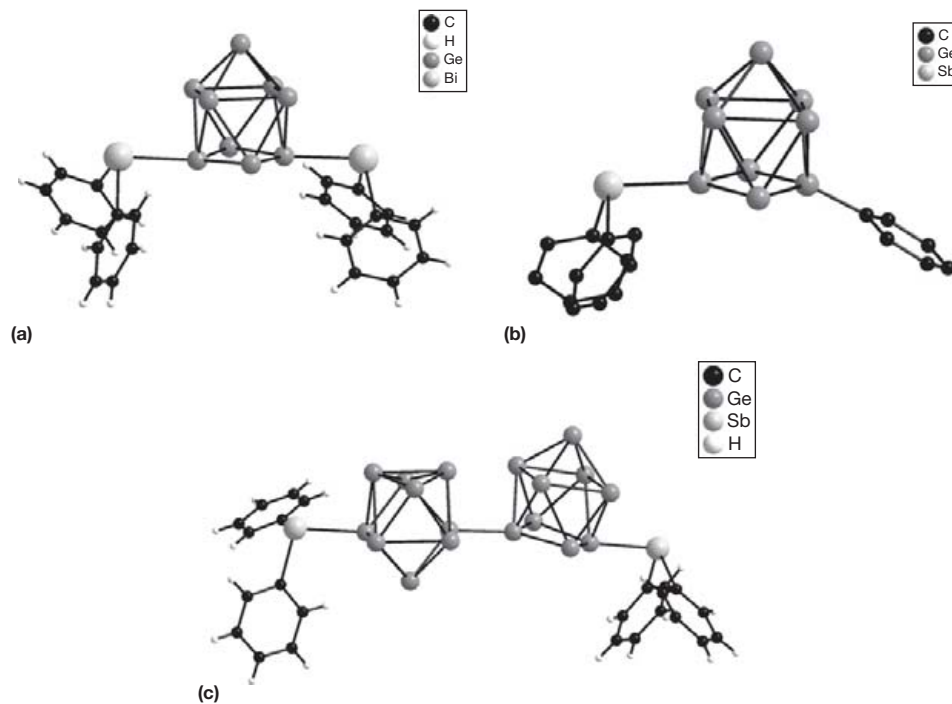


A more detailed investigation of the subsequent reactions shows the involvement of radical anions as intermediates.<sup>120</sup> As nucleophiles in these reactions, the  $\text{Ph}_2\text{Pn}^-$  anions as well as  $\text{Ph}^-$ , which are products of the reduction of  $\text{Ph}_3\text{Pn}$  by the highly reducing  $\text{Ge}_9^{4-}$  anions, have to be considered. Indeed, different types of exo-functionalized clusters have been described

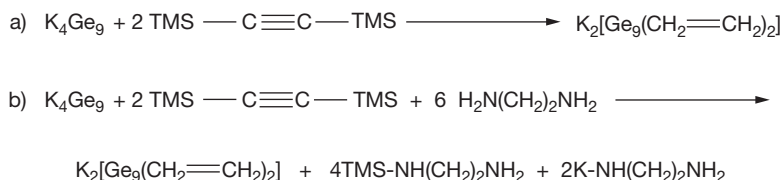
as, for example,  $[\text{Ph}_3\text{Bi}-\text{Ge}_9-\text{Ph}_3\text{Bi}]^{2-}$  and its isostructural compound  $[\text{Ph}_3\text{Sb}-\text{Ge}_9-\text{Ph}_3\text{Sb}]^{2-}$  (Figure 15(a))<sup>119</sup> and  $[\text{Ph}-\text{Ge}_9-\text{SbPh}_2]^{2-}$  (Figure 15(b)).<sup>121</sup> Functionalization reactions always compete with dimerisation of the cluster anions, and the existence of the anion  $[\text{Ph}_2\text{Sb}-\text{Ge}_9-\text{Ge}_9-\text{SbPh}_2]^{4-}$  gives an example of both reaction possibilities in one molecule (Figure 15(c)).<sup>121</sup>

Besides the functionalization with  $\text{PnPh}_3$ , similar reactions that used  $\text{Ph}_4\text{Sn}$  or  $\text{R}_3\text{TtCl}$  ( $\text{Tt} = \text{Ge}, \text{Sn}$ ;  $\text{R} = \text{Ph}, \text{Me}$ ) also succeeded in the crystallization of  $[\text{Ge}_9-\text{TtE}_3]^{3-}$ ,  $[\text{R}_3\text{Tt}-\text{Ge}_9-\text{TtE}_3]^{2-}$ , and  $[\text{R}_3\text{Tt}-\text{Ge}_9-\text{Ge}_9-\text{TtR}_3]^{4-}$  containing compounds.<sup>120</sup>

The best investigated reactions are the alkylation and alkenylation of  $\text{Ge}_9$ ,  $\text{Sn}_9$ , and  $\text{Ge}_9-x\text{Sn}_x$  clusters.<sup>12,122-124</sup> By using alkyl or alkenyl halides  $\text{RX}$ , where the halide can be located at primary, secondary, or tertiary carbon atoms, these clusters can be alkylated or alkenylated by nucleophilic substitution of the halide by the  $\text{E}_9^{4-}$  cluster. The vinylation of  $\text{Ge}_9$  clusters is also possible by reacting them with the trimethylsilyl (TMS) disubstituted acetylene. In the latter process, the formation of mono- and disubstituted species  $[\text{Ge}_9-(\text{CHCH}_2)]^{3-}$  and  $[\text{Ge}_9-(\text{CHCH}_2)_2]^{2-}$  may be controlled by adjusting the ratio of reagents (Scheme 2(a)).<sup>125</sup>

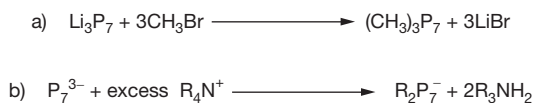


**Figure 15** Functionalization of  $\text{Ge}_9$  anions by exo-bonded main group element substituents. (a)  $[\text{Ph}_3\text{Sb}-\text{Ge}_9-\text{Ph}_3\text{Sb}]^{2-}$ , the isostructural anion  $[\text{Ph}_3\text{Bi}-\text{Ge}_9-\text{BiPh}_3]^{2-}$  is also known<sup>119</sup>; (b)  $[\text{Ph}_3\text{Sb}-\text{Ge}_9-\text{Ph}]^{2-}$ <sup>(121)</sup>;  $[\text{Ph}_3\text{Sb}-\text{Ge}_9-\text{Ge}_9-\text{SbPh}_2]^{4-}$ .<sup>121</sup>



**Scheme 2** (a) Unbalanced equation of the reaction of  $\text{Ge}_9^{4-}$  Zintl anions with TMS-substituted acetylene, yielding alkenylated  $\text{Ge}_9$  clusters. (b) Balanced equation for the vinylation of  $\text{Ge}_9$  clusters in ethylenediamine.





**Scheme 3** (a) Methylation of a  $\text{P}_7^{3-}$  cage anion. (b) Selective dialkylation of  $\text{P}_7^{3-}$  cage anions with the help of quaternary ammonium salts; R = Me, Et, nBu.

At the time of publication, the reaction (Scheme 2(a)) could not be balanced because it was unclear what happened to the TMS substituents and where the hydrogen for the hydrogenation of the triple bond came from. Recently it has been shown that the solvent ethylenediamine again plays a major role during this reaction, which involves the substituted solvent molecules  $\text{TMS-NH}(\text{CH}_2)_2\text{NH}_2$  formed by deprotonation of ethylenediamine and hydrogenation of the triple bond of the alkyne (Scheme 2(b)). For this reaction, acidic protons are indispensable; this could be shown by using pyridine as solvent, which did not yield the desired product. Only the addition of methanol to the pyridine solutions resulted in the same vinylated clusters that had been observed in ethylenediamine before.<sup>124</sup> The acidity of the used solvent is extremely important, and side reactions, which are often not trivial to determine, are often the driving force for successful chemical transformations.

#### 1.09.1.3.2.2 Group 15

Concerning group 15 clusters, similar functionalizations are possible, where the formally negatively charged phosphorus atoms attack an electrophilic center. One representative reaction is given below (Scheme 3(a)), where  $\text{Li}_3\text{P}_7$  is reacted with bromomethane in THF. In an  $\text{S}_{\text{N}}2$ -like reaction,  $\text{Me}_3\text{P}_7$  is formed and the salt LiBr is produced.<sup>126</sup>

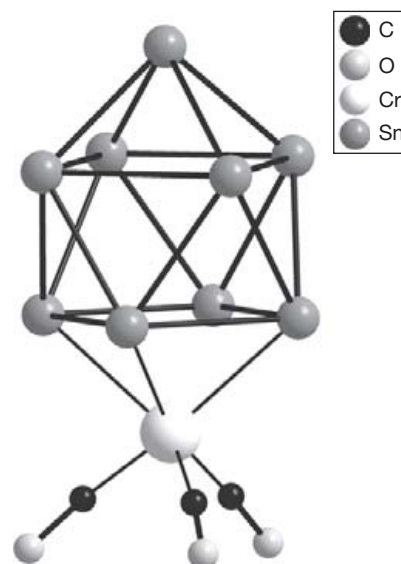
Partially alkylated cages can be synthesized by alkyl exchange; this reaction showed a distribution of compounds and pure partially alkylated polyphosphides could not be isolated by this method.<sup>127</sup> In subsequent works it could be demonstrated that the use of tetraalkylammonium salts in ethylenediamine yields exclusively dialkylated products (Scheme 3(b)).<sup>128</sup>

#### 1.09.1.3.3 Reactions with transition metal complexes

Besides the functionalization with main group element exo-bonded ligands (Section 1.09.1.3.2), the reactions of Zintl anions with transition metal complexes provide the possibility of testing their reactivity toward different kinds of reagents, as well as characterizing completely new classes of substances. Up to now, the employment of transition metal complexes in syntheses resulted in more than 70 (group 14) and more than 60 (group 15) compounds.<sup>14</sup> The versatile, often unpredictable, reactions of Zintl anions with selected transition metal complexes are illustrated in the following sections.

##### 1.09.1.3.3.1 Group 14

Mainly, there are three possible products that can be obtained by reacting a nine-atom group 14 element cluster in solution with a transition metal complex.



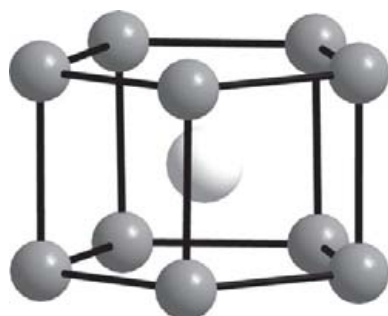
**Figure 16**  $[\text{Sn}_9\text{Cr}(\text{CO})_3]^{4-}$  complex with the shape of a ten-atom *closo*-cluster (bicapped square antiprism).<sup>129</sup>

1. The cluster anion acts as ligand toward the transition metal in a manner similar to that of the previously presented main group elements. Another possibility of exo-polyhedral transformation is that the basal noncapped square of the  $\text{E}_9^{4-}$  cluster is capped by the transition metal to form a 10-atom 22-electron *closo*-cluster (Figure 16).<sup>129</sup>
2. The transition metal is inserted into the cluster anion and the so-called endohedral complexes are formed, which sometimes cause a structural rearrangement of the cluster. The electronic structures of deltahedral clusters like  $[\text{Cu}@\text{E}_9]^{3-}$  (E = Sn, Pb),<sup>130</sup>  $[\text{Ni}@\text{Pb}_{10}]^{2-}$ , or  $[\text{M}@\text{Pb}_{12}]^{2-}$  (M = Ni, Pd, Pt)<sup>131</sup> can be rationalized by employing the Wade–Mingos–Williams rules. In  $[\text{Cu}@\text{E}_9]^{3-}$ , the central Cu atom is assigned a charge of +1 due to a spherical coordination environment, which accounts for a  $d^{10}$  configuration. In the case of  $[\text{Ni}@\text{Pb}_{10}]^{2-}$  and  $[\text{M}@\text{Pb}_{12}]^{2-}$  (M = Ni, Pd, Pt), the endohedral atom is regarded as electronically innocent. It has a formal charge of zero and does not interfere with the electron count of the cluster (Table 5).
3. Besides these regular-shaped deltahedral anions, the structure of which can be directly related to the number of electrons, there also exist unique clusters for germanium, which are highly symmetric but do not follow the Wade–Mingos–Williams rules. The first example of this class of intermetallics was the ten-atom pentagonal prismatic-shaped  $[\text{M}@\text{Ge}_{10}]^{3-}$  (M = Co, Fe) anion (Figure 17).<sup>132–134</sup>

Concerning the syntheses of transition metal compounds of Zintl anions, Fässler et al. could demonstrate that the reaction temperature presumably plays a major role in the formation of endohedral complexes. The reaction of  $\text{Sn}_9^{4-}$  anions with  $[\text{IrCl}(\text{COD})]_2$  (COD = 1,5-cyclooctadienyl) at room temperature in ethylenediamine yields the exo-bonded  $\text{Sn}_9\text{Ir}(\text{COD})$  complex. After stirring at 80 °C for 1 h, a compound could be crystallized from this solution, which contained endohedral  $[\text{Ir}@\text{Sn}_{12}]^{3-}$  anions (Figure 18). The formal oxidation

**Table 5** Endohedral cluster anions of group 14 elements

Endohedral cluster anion	Number of electrons $N_{VE}$	Number of main group element atoms $N_A$	Number of cluster bonding electrons $N_{CB} = N_{VE} - (2 \times N_A)$	Polyhedron according to Wade–Mingos–Williams rules
$[\text{Cu}@E_9]^{3-}$ <sup>(130)</sup>	40	9	22	<i>nido</i> ( $N_{CB} = 2N_A + 4$ ) monocapped square antiprism
$[\text{Ni}@Pb_{10}]^{2-}$ <sup>(131)</sup>	42	10	22	<i>closo</i> ( $N_{CB} = 2N_A + 2$ ) bicapped square antiprism
$[\text{M}@Pb_{12}]^{2-}$ <sup>(131)</sup>	50	12	26	<i>closo</i> ( $N_{CB} = 2N_A + 2$ ) icosahedron (bicapped pentagonal antiprism)

**Figure 17** No deltahedral shape: pentagonal prismatic-shaped  $[\text{M}@Ge_{10}]^{3-}$  anion ( $M = \text{Fe}, \text{Co}$ ).

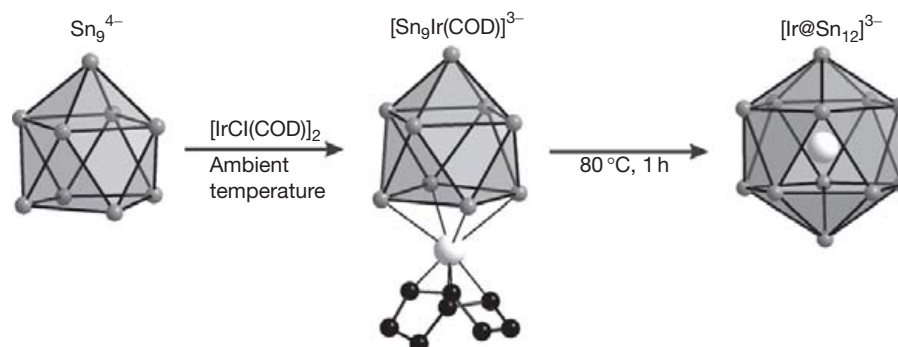
state of the iridium atom in these anions has to be  $-1$ , as the tin polyanion is considered to be a *closo*- $\text{Sn}_{12}^{2-}$  cluster and endohedral encapsulation is now well established for the  $d^{10}$  electronic configuration of transition metals. The step-by-step reaction clearly demonstrates that the Zintl anions first act as ligands toward the transition metal, and that in a subsequent reaction, the exo-bonded metal moves inside the cage anion under rearrangement of the cluster shape. This second step seems to be energetically not favored at ambient temperatures.<sup>135</sup>

As beautiful as this tuning of the reaction conditions and the desired product are, the behavior of the same complex toward

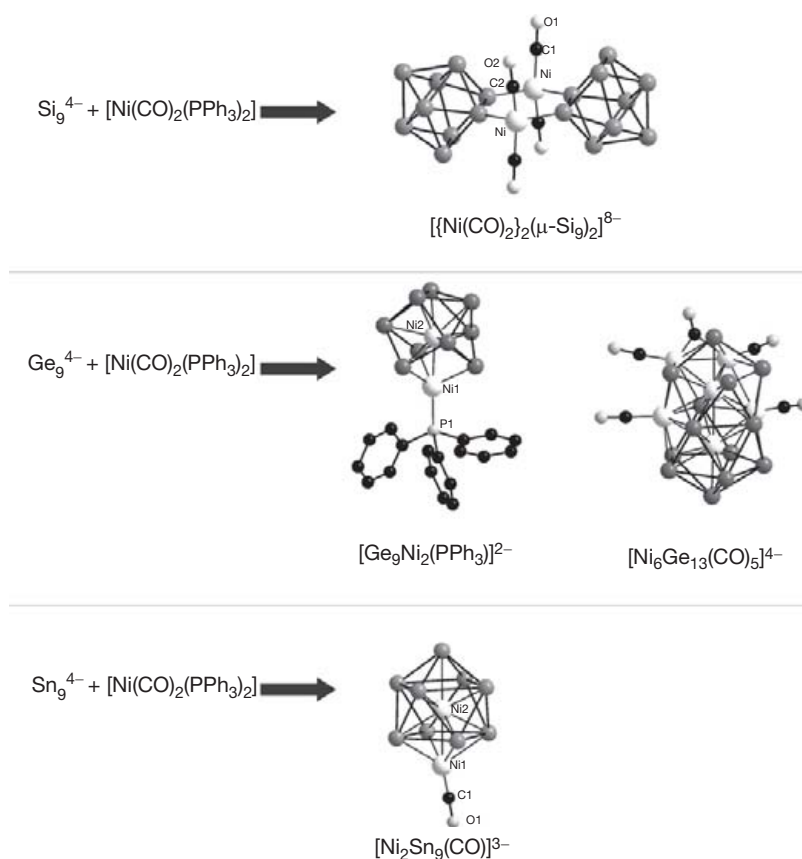
different group 14 clusters  $E_9^{4-}$  ( $E = \text{Si-Pb}$ ) often cannot be predicted at all. To demonstrate this, a closer look is taken at the reaction of the different tetrel clusters  $\text{Si}_9^{4-}$ ,  $\text{Ge}_9^{4-}$ , and  $\text{Sn}_9^{4-}$  with the  $\text{Ni}(\text{PPh}_3)_2(\text{CO})_2$  complex (Figure 19). In the case of  $\text{Si}_9^{4-}$ , the cluster acts as a bridging exo-ligand toward the  $\text{Ni}(\text{PPh}_3)_2(\text{CO})_2$  complex and the reaction can be understood as a classical ligand exchange of triphenylphosphane by  $\text{Si}_9^{4-}$ .<sup>136</sup> For  $\text{Ge}_9^{4-}$ , two different reaction products are described, both of which include endohedrally bound Ni atoms.<sup>137</sup> In one resulting cluster, the triphenylphosphane ligands remain at one Ni atom and no CO ligands are observed; in contrast, in the other cluster, the CO ligands remain. In both cases, the nine-atom cluster undergoes a rearrangement. Finally, for  $\text{Sn}_9^{4-}$  Zintl anions, the reaction results in a nine-atom cluster of which the shape still resembles the naked cluster but where one Ni atom is interstitially bound and additionally an  $\text{Ni}(\text{CO})$  fragment coordinates the noncapped square.<sup>138</sup>

#### 1.09.1.3.3.2 Group 15

The reaction behavior of group 15 Zintl anions toward transition metal complexes is quite as diverse as that of the group 14 clusters. The main difference that has to be noted is the absence of any endohedral clusters for group 15 anions till date. Three examples of how  $E_7^{3-}$  can be coordinated by transition metals in rational substitution reactions are given (Figure 20).



**Figure 18** Step-by-step synthesis of  $[\text{Ir}@\text{Sn}_{12}]^{3-}$  shows that at first the transition metal complex coordinates exohedrally under formation of the  $[\text{Sn}_9\text{Ir}(\text{COD})]^{3-}$  anion (COD = 1,5-cyclooctadienyl). In a subsequent reaction due to a rise in temperature to 80 °C, the  $[\text{Ir}@\text{Sn}_{12}]^{3-}$  anion is formed, in which an iridium atom with a formal oxidation state of  $-1$  is interstitially bound.

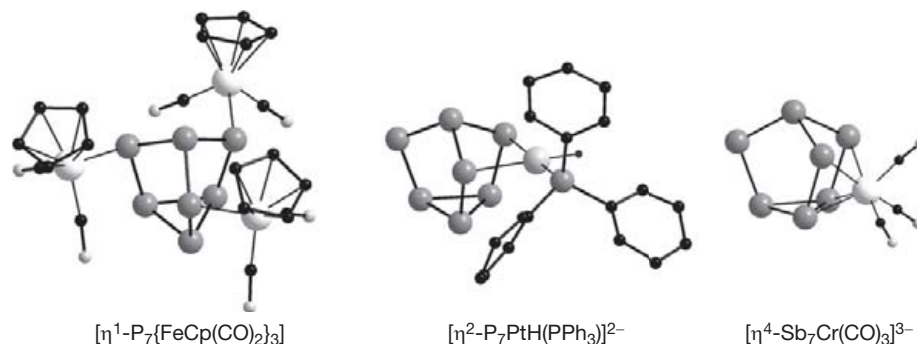


**Figure 19** Reaction of  $\text{E}_9^{4-}$  Zintl anions with  $\text{Ni}(\text{PPh}_3)_2(\text{CO})_2$  ( $\text{E} = \text{Si},^{136} \text{Ge},^{8,137} \text{Sn}^{138}$ ) gives completely different reaction products. This demonstrates the limited predictability for this kind of reaction.

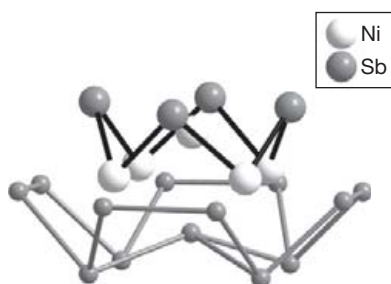
The twofold-bound, formally negatively charged atoms of the nortricyclane-like cage can coordinate transition metal complexes in an  $\eta^1$ -like style.  $\text{Li}_3\text{P}_7\cdot 3\text{DME}$  reacts with  $[\text{CpFe}(\text{CO})_2\text{Br}]$  to form  $[\eta^1\text{-P}_7\{\text{FeCp}(\text{CO})_2\}_3]$ ; the bromine atoms of the starting complex are thereby substituted by the negatively charged phosphorus atoms of the  $\text{P}_7^{3-}$  Zintl anion.<sup>139</sup>

Besides the  $\eta^1$ -like coordination, the transition metal can also be found  $\eta^2$ - or  $\eta^4$ -like bound. The coordination of two

negatively charged phosphorus atoms of the same cage anion results in  $\eta^2$ -coordination style. Solutions of  $\text{P}_7^{3-}$  in ethylenediamine react with  $\text{Pt}(\text{PPh}_3)_2(\text{C}_2\text{H}_4)$  and the  $[\eta^2\text{-P}_7\text{PtH}(\text{PPh}_3)]^{2-}$  anion is observed.<sup>140</sup> For the  $\eta^4$  mode, two negatively charged atoms and additionally two formally uncharged atoms of the basal triangle coordinate the transition metal. For instance, ethylenediamine solutions of  $\text{Sb}_7^{3-}$  anions react with  $\text{Cr}(\text{CO})_3(\text{mes})$  ( $\text{mes} = \text{mesitylene}$ ) to give the  $[\eta^4\text{-Sb}_7\text{Cr}(\text{CO})_3]^{3-}$  anion.<sup>141</sup>



**Figure 20**  $E_7^{3-}$  anions ( $E = \text{P-As}$ ) are able to coordinate in  $\eta^1$ ,  $\eta^2$ , and  $\eta^4$  mode to transition metal-central atoms.



**Figure 21** The  $[\text{Ni}_5\text{Sb}_{17}]^{4-}$  intermetalloid anion is accessible by reacting the Zintl anion  $\text{Sb}_7^{3-}$  with  $\text{Ni}(\text{COD})_2$  ( $\text{COD} = 1,5\text{-cyclooctadienyl}$ ).

The reaction of group 15 Zintl anions with transition metal complexes also provides the possibility of preparing huge intermetalloid clusters. By reacting  $\text{Sb}_7^{3-}$  Zintl anions with  $\text{Ni}(\text{COD})_2$  in ethylenediamine solution  $[\text{Ni}_5\text{Sb}_{17}]^{4-}$  anions could be crystallized. These anions consist of a  $\text{Ni}(\text{cyclo-Ni}_4\text{Sb}_4)$  ring, which is inside a  $\text{Sb}_{13}$  bowl (Figure 21).<sup>142</sup>

### 1.09.2 Conclusion

This chapter has introduced Zintl anions as a versatile and fascinating class of compounds, which offer different reaction possibilities. Their behavior with or without any additives in different solvents has been the subject of research for more than 120 years now, but their diverse reaction possibilities, as well as their frequently unpredictable behavior in solution, make this a highly topical and demanding field of research. Interesting challenges are the controlled oxidation-yielding oligomers and new elemental modifications, as well as the directed syntheses of different derivatives of Zintl anions. Furthermore, it would be very rewarding to investigate more highly reduced anionic species in solution, to broaden the range of available building blocks. It has to be seen if the border defined by a maximum charge of one negative charge per atom for dissolved polyanions can be transcended in the future of Zintl anions. For related chapters in this Comprehensive, we refer to Chapters 2.04 and 2.05.

### References

- Joannis, A. C. *C. R. Acad. Sci.* **1891**, 29, 795.
- Kraus, C. A. *J. Am. Chem. Soc.* **1907**, 29, 1557.
- Zintl, E.; Goubeau, J.; Dullenkopf, W. *Z. Phys. Chem.* **1931**, 154, 1.
- Kummer, D.; Diehl, L. *Angew. Chem. Int. Ed.* **1970**, 9, 895.
- Corbett, J. D.; Edwards, P. A. *Chem. Comm.* **1975**, 24, 984.
- Teixidor, F.; Luetkens, M. L.; Rudolph, R. W. *J. Am. Chem. Soc.* **1983**, 105, 149.
- Eichhorn, B. W.; Haushalter, R. C.; Pennington, W. T. *J. Am. Chem. Soc.* **1988**, 110, 8704.
- Gardner, D. R.; Fettinger, J. C.; Eichhorn, B. W. *Angew. Chem. Int. Ed.* **1996**, 35, 2852.
- Fässler, T. F.; Hoffmann, S. D. *Angew. Chem. Int. Ed.* **2004**, 43, 6242.
- Guloy, A. M.; Ramlau, R.; Tang, Z.; Schnelle, W.; Baitinger, M.; Grin, Y. *Nature* **2006**, 443, 320.
- Critchlow, S. C.; Corbett, J. D. *Inorg. Chem.* **1982**, 21, 3286.
- Gillett-Kunnath, M. M.; Petrov, I.; Sevov, S. C. *Inorg. Chem.* **2010**, 49, 721.
- Waibel, M.; Benda, B. B.; Wahl, B.; Fässler, T. F. *Chem. Eur. J.* **2011**, 17, 12928.
- Scharfe, S.; Kraus, F.; Stegmaier, S.; Schier, A.; Fässler, T. F. *Angew. Chem. Int. Ed.* **2011**, 50, 3630.
- Zintl, E.; Kaiser, H. *Z. Anorg. Allg. Chem.* **1933**, 211, 113.
- Kauzlarich, S. M. *Chemistry, Structure and Bonding of Zintl Phases and Ions*. VCH Publishers: New York, Weinheim, Cambridge, 1996.
- Wade, K. *Adv. Inorg. Radiochem.* **1976**, 18, 1.
- Mingos, D. M. P. *Nature* **1972**, 236, 99.
- Williams, R. E. *Chem. Rev.* **1992**, 92, 177.
- Joseph, S.; Suchenrunk, C.; Kraus, F.; Korber, N. *Eur. J. Inorg. Chem.* **2009**, 2009, 4641.
- Gärtner, S.; Korber, N. In *Zintl Ions Principles and Recent Developments*; Fässler, T. F., Ed.; Springer-Verlag: Berlin, 2011; Vol. 140, p 25.
- Eisenmann, B.; Cordier, G. In *Chemistry, Structure and Bonding of Zintl Phases and Ions*; Kauzlarich, S. M., Ed.; VCH Verlagsgesellschaft mbH: Weinheim, Germany, 1996; p 61.
- von Schnering, H. G.; Llanos, J.; Chang, J. H.; Peters, K.; Peters, E. M.; Nesper, R. *Z. Kristallogr. NCS* **2005**, 220, 324.
- von Schnering, H. G.; Schwarz, M.; Chang, J.-H.; Peters, K.; Peters, E.-M.; Nesper, R. *Z. Kristallogr. NCS* **2005**, 220, 525.
- Baitinger, M.; Grin, Y.; von Schnering, H. G.; Kniep, R. *Z. Kristallogr. NCS* **1999**, 214, 457.
- Grin, Y.; Baitinger, M.; Kniep, R.; von Schnering, H. G. *Z. Kristallogr. NCS* **1999**, 214, 453.
- Goebel, T.; Prots, Y.; Haarmann, F. *Z. Kristallogr. NCS* **2008**, 223, 187.
- Baitinger, M.; Peters, K.; Somer, M.; Carrillo-Cabrera, W.; Grin, Y.; Kniep, R.; von Schnering, H. G. *Z. Kristallogr. NCS* **1999**, 214, 455.
- Ponou, S.; Fässler, T. F. *Z. Anorg. Allg. Chem.* **2007**, 633, 393.
- Hoch, C.; Wendorff, M.; Röhr, C. *Acta Cryst. C* **2002**, 58, 145.
- Queneau, V.; Sevov, S. C. *Inorg. Chem.* **1998**, 37, 1358.
- Todorov, E.; Sevov, S. C. *Inorg. Chem.* **1998**, 37, 3889.
- Hoch, C.; Wendorff, M.; Röhr, C. *J. Alloys Compd.* **2003**, 361, 206.
- Carrillo-Cabrera, W.; Gil, R. C.; Somer, M.; Persil, O.; von Schnering, H. G. *Z. Anorg. Allg. Chem.* **2003**, 629, 601.
- von Schnering, H. G.; Baitinger, M.; Bolle, U.; Carrillo-Cabrera, W.; Curda, J.; Grin, Y.; Heinemann, F.; Llanos, J.; Peters, K.; Schmeding, A.; Somer, M. *Z. Anorg. Allg. Chem.* **1997**, 623, 1037.
- Queneau, V.; Todorov, E.; Sevov, S. C. *J. Am. Chem. Soc.* **1998**, 120, 3263.
- Bobev, S.; Sevov, S. C. *Angew. Chem. Int. Ed.* **2000**, 39, 4108.
- Aydemir, U.; Ormeci, A.; Borrmann, H.; Bohme, B.; Zurcher, F.; Uslu, B.; Goebel, T.; Schnelle, W.; Simon, P.; Carrillo-Cabrera, W.; Haarmann, F.; Baitinger, M.; Nesper, R.; von Schnering, H. G.; Grin, Y. *Z. Anorg. Allg. Chem.* **2008**, 634, 1651.

39. Zürcher, F.; Nesper, R. *Angew. Chem. Int. Ed.* **1998**, *37*, 3314.
40. Nesper, R.; von Schnering, H. G.; Curda, J. *Chem. Ber.* **1986**, *119*, 3576.
41. Nesper, R.; Curda, J.; von Schnering, H. G. *J. Solid State Chem.* **1986**, *62*, 199.
42. Frank, U.; Müller, W. Z. *Naturforsch.* **1975**, *30*, 313.
43. Todorov, I.; Sevov, S. C. *Inorg. Chem.* **2004**, *43*, 6490.
44. Todorov, I.; Sevov, S. C. *Inorg. Chem.* **2005**, *44*, 5361.
45. von Schnering, H. G.; Bolle, U.; Curda, J.; Peters, K.; CarrilloCabrera, W.; Somer, M.; Schultheiss, M.; Wedig, U. *Angew. Chem. Int. Ed.* **1996**, *35*, 984.
46. Bolle, U.; Carrillo-Cabrera, W.; Peters, K.; von Schnering, H. G. Z. *Kristallogr. NCS* **1998**, *213*, 689.
47. Nesper, R.; Currao, A.; Wengert, S. *Chem. Eur. J.* **1998**, *4*, 2251.
48. Eisenmann, B.; Schäfer, H.; Turban, K. Z. *Naturforsch. B* **1974**, *29*, 464.
49. Nesper, R.; Wengert, S. *Chem. Mon.* **1999**, *130*, 197.
50. Wengert, S.; Nesper, R. Z. *Anorg. Allg. Chem.* **1998**, *624*, 1801.
51. Wengert, S.; Nesper, R. *Inorg. Chem.* **2000**, *39*, 2861.
52. Zürcher, F.; Nesper, R. Z. *Kristallogr. NCS* **2001**, *216*, 507.
53. Currao, A.; Curda, J.; Nesper, R. Z. *Anorg. Allg. Chem.* **1996**, *622*, 85.
54. Palenzona, A.; Manfrinetti, P.; Fornasini, M. L. J. *Alloys Compd.* **2002**, *345*, 144.
55. Zürcher, F.; Nesper, R. Z. *Kristallogr. NCS* **2001**, *216*, 505.
56. Müller, W. Z. *Naturforsch. B* **1974**, *29*, 304.
57. Palenzona, A.; Manfrinetti, P.; Fornasini, M. L. J. *Alloys Compd.* **2000**, *312*, 165.
58. Meyer, T.; Hönle, W.; von Schnering, H. G. Z. *Anorg. Allg. Chem.* **1987**, *552*, 69.
59. Emmerling, F.; Röhr, C. Z. *Naturforsch. B* **2002**, *57*, 963.
60. Hirsche, C.; Röhr, C. Z. *Anorg. Allg. Chem.* **2000**, *626*, 1992.
61. von Schnering, H. G.; Somer, M.; Kliche, G.; Hönle, W.; Meyer, T.; Wolf, J.; Ohse, L.; Kempa, P. B. Z. *Anorg. Allg. Chem.* **1991**, *601*, 13.
62. Emmerling, F.; Röhr, C. Z. *Anorg. Allg. Chem.* **2003**, *629*, 467.
63. von Schnering, H. G.; Meyer, T.; Hönle, W.; Schmettow, W.; Hinze, U.; Bauhofer, W.; Kliche, G. Z. *Anorg. Allg. Chem.* **1987**, *553*, 261.
64. Hönle, W.; Krogull, G.; Peters, K.; von Schnering, H. G. Z. *Kristallogr. NCS* **1999**, *214*, 17.
65. Emmerling, F.; Petri, D.; Röhr, C. Z. *Anorg. Allg. Chem.* **2004**, *630*, 2490.
66. von Schnering, H. G.; Hartweg, M.; Hartweg, U.; Hönle, W. *Angew. Chem. Int. Ed.* **1989**, *28*, 56.
67. Derrien, G.; Tillard, M.; Manteghetti, A.; Belin, C. Z. *Anorg. Allg. Chem.* **2003**, *629*, 1601.
68. von Schnering, H. G.; Wittmann, M.; Sommer, D. Z. *Anorg. Allg. Chem.* **1984**, *510*, 61.
69. Eisenmann, B.; Rossler, U. Z. *Anorg. Allg. Chem.* **2003**, *629*, 459.
70. Gascoin, F.; Sevov, S. C. *Inorg. Chem.* **2001**, *40*, 5177.
71. Deller, K.; Eisenmann, B. Z. *Naturforsch. B* **1976**, *31*, 1023.
72. Deller, K.; Eisenmann, B. Z. *Naturforsch. B* **1977**, *32*, 1368.
73. Eisenmann, B.; Jordan, H.; Schäfer, H. Z. *Naturforsch. B* **1985**, *40*, 1603.
74. Sheldrick, W. S.; Wachhold, M. *Coord. Chem. Rev.* **1998**, *176*, 211.
75. Gupta, U.; Reber, A. C.; Clayborne, P. A.; Melko, J. J.; Khanna, S. N.; Castleman, A. W. *Inorg. Chem.* **2008**, *47*, 10953.
76. Rudolph, R. W.; Wilson, W. L.; Parker, F.; Taylor, R. C.; Young, D. C. *J. Am. Chem. Soc.* **1978**, *100*, 4629.
77. Guggenberger, L. J.; Muettterties, E. L. *J. Am. Chem. Soc.* **1976**, *98*, 7221.
78. Fässler, T. F. *Coord. Chem. Rev.* **2001**, *215*, 347.
79. Rosdahl, J.; Fässler, T. F.; Kloo, L. *Eur. J. Inorg. Chem.* **2005**, *14*, 2888.
80. Yong, L.; Hoffmann, S. D.; Fässler, T. F. *Inorg. Chim. Acta* **2006**, *359*, 4774.
81. Carrillo-Cabrera, W.; Aydemir, U.; Somer, M.; Kircali, A.; Fässler, T. F.; Hoffmann, S. D. Z. *Anorg. Allg. Chem.* **2007**, *633*, 1575.
82. Korber, N.; Fleischmann, A. *Dalton Trans.* **2001**, *4*, 383.
83. Wiesler, K.; Brandl, K.; Fleischmann, A.; Korber, N. Z. *Anorg. Allg. Chem.* **2009**, *635*, 508.
84. Waibel, M.; Kraus, F.; Scharfe, S.; Wahl, B.; Fässler, T. F. *Angew. Chem. Int. Ed.* **2010**, *49*, 6611.
85. Joseph, S.; Suchentrunk, C.; Korber, N. Z. *Naturforsch. B* **2010**, *B65*, 1059.
86. Suchentrunk, C.; Korber, N. *New J. Chem.* **2006**, *30*, 1737.
87. Somer, M.; Carrillo-Cabrera, W.; Peters, E. M.; Peters, K.; Kaupp, M.; von Schnering, H. G. Z. *Anorg. Allg. Chem.* **1999**, *625*, 37.
88. Edwards, P. A.; Corbett, J. D. *Inorg. Chem.* **1977**, *16*, 903.
89. Somer, M.; Hönle, W.; von Schnering, H. G. Z. *Naturforsch. B* **1989**, *44*, 296.
90. Korber, N.; von Schnering, H. G. *Chem. Ber.* **1996**, *129*, 155.
91. Diehl, L.; Khodadadeh, K.; Kummer, D.; Strahle, J. Z. *Naturforsch. B* **1976**, *31*, 522.
92. Hanauer, T.; Grothe, M.; Reil, M.; Korber, N. *Helv. Chim. Acta* **2005**, *88*, 950.
93. Korber, N.; Richter, F. *Chem. Comm.* **1996**, *17*, 2023.
94. Korber, N.; Daniels, J. Z. *Anorg. Allg. Chem.* **1996**, *622*, 1833.
95. Hanauer, T.; Korber, N. Z. *Anorg. Allg. Chem.* **2006**, *632*, 1135.
96. Dai, F. R.; Xu, L. *Chin. J. Struct. Chem.* **2007**, *26*, 45.
97. Belin, C. H. E. *J. Am. Chem. Soc.* **1980**, *102*, 6036.
98. Kraus, F.; Hanauer, T.; Korber, N. *Angew. Chem. Int. Ed.* **2005**, *44*, 7200.
99. Kraus, F.; Hanauer, T.; Korber, N. *Inorg. Chem.* **2006**, *45*, 1117.
100. Bolle, U.; Tremel, W. *Chem. Comm.* **1992**, *2*, 91.
101. Korber, N.; Reil, M. *Chem. Comm.* **2002**, *1*, 84.
102. Kraus, F.; Aschenbrenner, J. C.; Korber, N. *Angew. Chem. Int. Ed.* **2003**, *42*, 4030.
103. Korber, N.; Richter, F. *Angew. Chem. Int. Ed.* **1997**, *36*, 1512.
104. Reil, M.; Korber, N. Z. *Anorg. Allg. Chem.* **2007**, *633*, 1599.
105. Hanauer, T.; Aschenbrenner, J. C.; Korber, N. *Inorg. Chem.* **2006**, *45*, 6723.
106. Baudler, M.; Glinka, K. *Chem. Rev.* **1993**, *93*, 1623.
107. Baudler, M.; Glinka, K. *Chem. Rev.* **1994**, *94*, 1273.
108. Kraus, F.; Aschenbrenner, J. C.; Klamroth, T.; Korber, N. *Inorg. Chem.* **2009**, *48*, 1911.
109. Dai, F.-R.; Xu, L. *Inorg. Chim. Acta* **2006**, *359*, 4265.
110. Korber, N.; Daniels, J. *Inorg. Chem.* **1997**, *36*, 4906.
111. Xu, L.; Sevov, S. C. *J. Am. Chem. Soc.* **1999**, *121*, 9245.
112. Ugrinov, A.; Sevov, S. C. *J. Am. Chem. Soc.* **2002**, *124*, 10990.
113. Yong, L.; Hoffmann, S. D.; Fässler, T. F. Z. *Anorg. Allg. Chem.* **2005**, *631*, 1149.
114. Ugrinov, A.; Sevov, S. C. *Inorg. Chem.* **2003**, *42*, 5789.
115. Downie, C.; Tang, Z. J.; Guloy, A. M. *Angew. Chem. Int. Ed.* **2000**, *39*, 338.
116. Korber, N. *Phosphorus, Sulfur, Silicon* **1997**, *125*, 339.
117. Fritz, G.; Schneider, H. W.; Hönle, W.; von Schnering, H. G. Z. *Naturforsch. B* **1988**, *43*, 561.
118. Sevov, S. C.; Goicoechea, J. M. *Organometallics* **2006**, *25*, 5678.
119. Ugrinov, A.; Sevov, S. C. *J. Am. Chem. Soc.* **2002**, *124*, 2442.
120. Ugrinov, A.; Sevov, S. C. *Chem. Eur. J.* **2004**, *10*, 3727.
121. Ugrinov, A.; Sevov, S. C. *J. Am. Chem. Soc.* **2003**, *125*, 14059.
122. Hull, M. W.; Ugrinov, A.; Petrov, I.; Sevov, S. C. *Inorg. Chem.* **2007**, *46*, 2704.
123. Chapman, D. J.; Sevov, S. C. *Inorg. Chem.* **2008**, *47*, 6009.
124. Hull, M. W.; Sevov, S. C. *J. Am. Chem. Soc.* **2009**, *131*, 9026.
125. Hull, M. W.; Sevov, S. C. *Inorg. Chem.* **2007**, *46*, 10953.
126. Baudler, M.; Faber, W.; Hahn, J. Z. *Anorg. Allg. Chem.* **1980**, *469*, 15.
127. Fritz, G.; Harer, J.; Matern, E. Z. *Anorg. Allg. Chem.* **1983**, *504*, 38.
128. Charles, S.; Fettingler, J. C.; Eichhorn, B. W. *J. Am. Chem. Soc.* **1995**, *117*, 5303.
129. Kesani, B.; Fettingler, J.; Eichhorn, B. *Chem. Eur. J.* **2001**, *7*, 5277.
130. Scharfe, S.; Fässler, T. F.; Stegmaier, S.; Hoffmann, S. D.; Ruhland, K. *Chem. Eur. J.* **2008**, *14*, 4479.
131. Esenturk, E. N.; Fettingler, J.; Eichhorn, B. *J. Am. Chem. Soc.* **2006**, *128*, 9178.
132. Wang, J. Q.; Stegmaier, S.; Fässler, T. F. *Angew. Chem. Int. Ed.* **2009**, *48*, 1998.
133. Zhou, B. B.; Denning, M. S.; Kays, D. L.; Goicoechea, J. M. *J. Am. Chem. Soc.* **2009**, *131*, 2802.
134. Korber, N. *Angew. Chem. Int. Ed.* **2009**, *48*, 3216.
135. Wang, J.-Q.; Stegmaier, S.; Wahl, B.; Fässler, T. F. *Chem. Eur. J.* **2010**, *16*, 1793.
136. Joseph, S.; Hamberger, M.; Mutzbauer, F.; Hartl, O.; Meier, M.; Korber, N. *Angew. Chem. Int. Ed.* **2009**, *48*, 8770.
137. Esenturk, E. N.; Fettingler, J.; Eichhorn, B. *Polyhedron* **2006**, *25*, 521.
138. Kesani, B.; Fettingler, J.; Gardner, D. R.; Eichhorn, B. *J. Am. Chem. Soc.* **2002**, *124*, 4779.
139. Ahlrichs, R.; Fenske, D.; Fromm, K.; Krautscheid, H.; Krautscheid, U.; Treutler, O. *Chem. Eur. J.* **1996**, *2*, 238.
140. Charles, S.; Fettingler, J. C.; Bott, S. G.; Eichhorn, B. W. *J. Am. Chem. Soc.* **1996**, *118*, 4713.
141. Charles, S.; Eichhorn, B. W.; Rheingold, A. L.; Bott, S. G. *J. Am. Chem. Soc.* **1994**, *116*, 8077.
142. Moses, M. J.; Fettingler, J. C.; Eichhorn, B. W. *Inorg. Chem.* **2007**, *46*, 1036.



This page intentionally left blank